「探索金屬玻璃、泡沫金屬、金屬複合材料、陶瓷複合材料及相關加工技術的新產品及商機」項目

Program on "Exploring New Products and Business Opportunities of Metal Glass, Metal Foam, Metal Composite and Ceramic Composite and the Related Processing Technologies"

嶄新材料科技國際會議暨技術研討會紀要

Proceedings of "International Conference on New Materials Technologies cum 5 seminars"

Metal Matrix Composites
金屬基複合材料

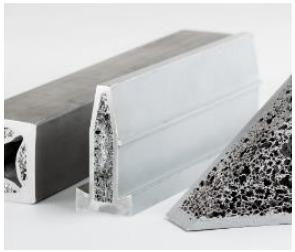

Metal Foam
金屬發泡

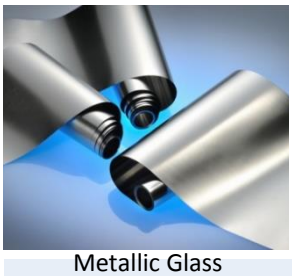

Metallic Glass
液態金屬

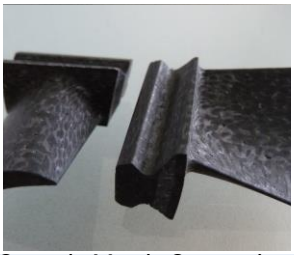

Ceramic Matrix Composites
陶瓷基複合材料

Joining Technology
接合技術

主辦機構：

HKPC Hong Kong Productivity Council 香港生產力促進局

資助機構：

創新科技署 Innovation and Technology Commission

贊助商：

GOA

工業支援機構：

FITMI 香港汽車零部件工業協會 Hong Kong Auto Parts Industry Association 鑄 HKMPTA MBC HONG KONG SAE INTERNATIONAL

在此刊物／活動內（或項目小組成員）表達的任何意見、研究成果、結論或建議，並不代表香港特別行政區政府創新科技署及一般支援計劃撥款資助專項基金評審委員會的觀點。

目錄

日期	活動	頁數
	嶄新材料科技技術總覽……	3
2018 年 1 月 29 日	**嶄新物料科技——優越功能帶來之商機國際會議**	
	「環球金屬碳纖複合材料發展、應用趨勢及新商機」……	17
	德國弗勞恩霍夫機床及成形技術研究所功能材質輕量化主管湯瑪士．協卡博士	
	「陶瓷基複合材料的新產品機遇及特點」……	65
	國立台灣大學材料科學與工程學系暨研究所特聘教授段維新教授	
	「利用電磁脈衝銲接技術達成高強度及品質銲接」……	103
	金屬工業研究發展中心正工程師兼銲接組副組長姜志華先生	
	「金屬發泡及開放式結構的應用和新機遇」……	139
	德國弗勞恩霍夫機床及成形技術研究所功能材質輕量化主管湯瑪士．協卡博士	
	「納米粒子為關鍵金屬部件帶來之理想特性」……	182
	澳洲斯威本科技大學校長劉建德教授	
	「金屬基複合材料的應用和最新發展」……	232
	香港理工大學工程及系統工程學系陳鏡昌教授	
	「先進激光輔助金屬成型技術及未來商機」……	330
	香港生產力促進局智能製造及材料科技部顧問陳偉倫博士	
2018 年 1 月 30 日	**利用金屬發泡技術顯著減少產品重量研討會**……	364
	德國弗勞恩霍夫機床及成形技術研究所功能材質輕量化主管湯瑪士．協卡博士	
2018 年 1 月 30 日	**陶瓷基複合材料在高溫和高效能要求環境下之用途研討會**……	591
	國立台灣大學材料科學與工程學系暨研究所特聘教授段維新教授	
2018 年 2 月 13 日	**低成本金屬部件局部補強專門接合技術研討會**……	776
	德國弗勞恩霍夫物料及光束技術研究所主管恩斯．史丹夫博士	
2018 年 4 月 3 日	**利用金屬基複合材料生產高韌度和強度部件研討會**……	1026
	國立台灣科技大學機械工程部黃崧任教授	
2018 年 4 月 13 日	**應用液態金屬微量化產品、生成薄膜及改變產品功能研討會**……	1221
	香港城市大學科學及工程學院特聘劉錦川教授	

嶄新材料技術總覽

1. 金屬基複合材料

金屬基複合材料種類有以下數種

1) 顆粒複合材料有微小分子、切斷纖維、小碎片、空心物料
2) 纖維複合材料有對齊方向、任意方向、編織層狀平行
3) 結構性複合材料則有層狀結構

金屬基複合材料設計

複合材料的設計有以下考量，分別為特性、設計參數、選材等。

複合材料特性考量有以下數點

1) 延伸性能
2) 溫度膨脹系數
3) 導熱性能
4) 強度
5) 硬化系數
6) 溫度及物理負載

設計參數有以下數點

1) 目標特性包括強度、導電、溫度或硬度等
2) 金屬基材包括鋁、鎂、鈦、鐵、鎳、鈷、銀等
3) 強化物料包括石墨、碳化硅、硼化碳、碳化鈦、硼化鈦等
4) 複合材料種類包括顆粒、長纖維、短纖維、層狀等
5) 材料及工藝成本
6) 製造工藝

選材方法跟從以下順序來進行

1) 性能指數是目標特性最大或最小化，例如輕巧(最大 E/ρ)或導熱(最大 λ/α)等
2) 選材圖表中找出在目標特性最大或最小限制所包涵之物料
3) 上下限計算則因應工藝參差的關係，個別物理參數會有上下限，而該上下限跟金屬基和強化材料有關

金屬基材料需計算上下限之常用參數，分別為

1) 密度
2) 強度係數
3) 強度
4) 比熱容值

5) 熱膨脹系數
6) 熱傳導系數

複合材料的生產工藝有以下數種

1) 擴散壓合法 (Diffusion Bonding)
2) 物理氣相沉積法 (Physical Vapour Deposition, PVD)
3) 攪拌鑄造法 (Stir Casting)
4) 擠壓鑄造法 (Squeeze Casting)
5) 壓力滲入法 (Gas Pressure Infiltration)
6) 壓鑄滲入法 (Pressure Die Infiltration)
7) 噴霧沉積法 (Spray Deposition)
8) 化學氣相沉積法 (Chemical Vapour Deposition, CVD)

金屬基複合材料有以下應用方案

1) 汽車及鐵路，例如汽車引擎部件、傳動系統、火車轉向架等
2) 溫度管理元件
3) 航空應用例如飛機引擎零部件
4) 工業應用

2. 金屬碳原素複合材料

金屬碳原素複合材料有以下五種

1) 金屬鑽石複合材料
2) 金屬石墨複合材料
3) 金屬碳纖維複合材料
4) 金屬納米管複合材料
5) 金屬富勒烯複合材料

金屬碳素複合材料主要用作散熱、吸震、補強用途，另外跟碳纖維也可以連接在一起作補強之用。

2.1. 金屬鑽石複合材料

為增加材料散熱特性，鑽石物料通常會加在本身導熱比較強的金屬，例如銅及銀等。

生產工藝	1) 銅鉻粉末和合成鑽石粉末混合 2) 用 1010 度和 45MPa 燒結，並快速加溫（600K/分）和降溫（1000K/分）
導熱性能	1) 最佳導熱性能在 1.07%鉻的時候，有 687Wm/K。然而因為含鉻的關係，在燒結的時候鉻碳的化合物會形成，並影響導熱性能。 2) 導熱性能會隨溫度變化 3) 轉用銀的導熱性能會比銅優勝

2.2. 金屬石墨複合材料

為增加導電材料剛性，石墨通常會加在比較柔軟的金屬，例如銅。

生產工藝	1) 金屬粉末和天然石墨粉末混合 2) 在高電壓並冷卻的狀態下加壓
分子結構	1) 非均向性結構 2) 金屬與碳化合物跟石墨成分與停留時間有關
物理特性	1) 導熱性能跟膨脹係數都並非均向 2) 垂直於熱壓方向的導熱性能跟石墨含量有關 3) 良好的吸震性能

2.3. 金屬納米管複合材料

生產工藝	1) 碳納米管跟金屬粉材混合作塊狀或粒狀 2) 經過熱壓或熱擠壓等熱處理

混合碳納米管的方法	1) 超音波分散法 2) 物理混合
物理特性	1) 碳納米管垂直於擠壓方向 2) 同軸於擠壓方向和經過熱處理後導熱較好 3) 經過熱處理後能增加伸張度 4) 混合均勻能提高韌性

3. 金屬玻璃結構

金屬玻璃跟普通金屬分別

普通金屬或合金	1) 晶體結構，不同生產製程，或不同成分之合金之下形成不同的晶體結構。 2) 冷卻速度較慢時成形，分子會重新排列 3) 固化時體積會收縮 4) 有位錯 5) 塑性變形時，晶體會隨其它晶體邊界滑動。
金屬玻璃	1) 無定型結構，沒有晶體 2) 極快冷卻速度時成形，分子來不及重新排列 3) 固態化時不會收縮，能精密控制大小 4) 沒有位錯 5) 金屬變形時只能隨剪切帶移動。

金屬玻璃物理其他物理特性

1) 超高韌性
2) 再過冷區域時延展性優異，超過 100 倍

金屬玻璃合金適用的生產製程有以下幾種

1) 傳統模具鑄造
2) 真空鑄造法
3) 內圓水紡法，用於生產線材
4) 熔紡法
5) 物理氣相沉積法（PVD）
6) 電鍍法

真空鑄造	1) 利用水冷銅模把熔化金屬高速降溫成形 2) 鑄造時利用惰性氣體充滿真空罩
內圓水紡法	1) 熔爐把金屬熔化 2) 熔化的金屬灌注到模具上 3) 圓形模具出口形成金屬線 4) 金屬線在有水道的金屬滾輪上立即降溫
熔紡法	1) 熔爐把金屬熔化 2) 熔化的金屬灌注到高速金屬滾輪上 3) 形成薄片並卷起包裝 傳統矽鋼薄片生產線距離約 1-2 公里，並因為需要回火的關係

	需要大量能源。相比之下金屬玻璃薄片生產線只需數十米，而且不需回火，能源消耗是傳統的大概四分之一。
物理氣相沉積法	1) 惰性氣體於高電壓之下被吸引到極高溫的金屬玻璃處 2) 金屬玻璃會氣化成霧並跑到目標金屬表面 3) 因為金屬本身特性，到目標金屬表面維持非晶狀態

金屬玻璃應用有以下範疇

1) 電機磁鐵
2) 運動產品
3) 醫療用品
4) 催化器
5) 彈簧
6) 感應器

金屬玻璃磁性特點

1) 良好軟磁性能
2) 硬磁性能
3) 磁致收縮效應

（當金屬玻璃受磁時可以變化長度和形成動能，相反可以將動能變為磁力。）

4) 磁製冷

（當金屬玻璃受磁時可以發熱，而退磁時則可以吸熱。）

4. 陶瓷基複合材料

陶瓷基複合材料種類有以下數類

1) 纖維複合材料有金屬纖維、陶瓷纖維
2) 碎片複合材料有陶瓷碎片
3) 板塊複合材料有陶瓷板塊

陶瓷基複合材料選材方法跟金屬基複合材料類同，都是分為以下三個步驟

1) 性能指數是目標特性最大或最小化，例如輕巧(最大 E/ρ)或導熱(最大 λ/α)等
2) 選材圖表中找出在目標特性最大或最小限制所包涵之物料
3) 上下限計算則因應工藝參差的關係，個別物理參數會有上下限，而該上下限跟陶瓷基和強化材料有關

陶瓷基複合材料生產工藝主要為粉末混合和其他新式方法

粉末混合	1) 傳統粉末混合燒結 2) 粉末混合加熱壓 3) 粉末混合加真空燒結 4) 粉末混合加熱等靜壓
其他新式方法	1) 熔化金屬滲透 2) 化學霧化滲透 3) 溶膠凝膠法

陶瓷機複合材料設計原則跟金屬基複合材料不同是介面要足夠強度承受重量，但不要過強，使其能在基材擴張前斷裂。經生產工序後處理之介面有以下要求

1) 停止基材裂縫擴張
2) 基材與複合材咬合

陶瓷基複合材料參數考慮有以下數點

1) 強度
2) 韌度
3) 韋氏(Weibull)參數
4) 抗裂能力
5) 蠕變阻力
6) 熱衝擊阻力

陶瓷複合材料特性

1) 各向異性隨複合材料方向

2) 比一般陶瓷更隔熱
3) 非常好的絕緣體

陶瓷基複合材料的應用
1) 飛機引擎零部件
2) 汽車零件
3) 電子設備

5. 金屬發泡技術

金屬發泡有以下種類，分別是

1) 開孔泡沫
2) 密閉泡沫
3) 球狀金屬發泡
4) 纖維結構
5) 籠狀結構
6) 一體化金屬結構

使用的金屬物料一般為鋁、銅、鐵、鎳、鋅、鎂等等

開孔泡沫

生產工藝	1) 聚合物泡沫成形 2) 金屬粉末黏附 3) 在聚合物泡沫支撐上形成塗層 4) 乾燥 5) 熱解聚合物泡沫 6) 金屬燒結
物料特性	1) 5-30%密度 2) 0.4-5.0mm 區間大小 3) 1-5% 原本金屬的導熱性能

密閉泡沫

生產工藝	1) 熔體冶金工藝 2) 粉末冶金工藝 3) 低壓泡沫鑄造工藝
物料特性	1) 5-30%密度 2) 0.4-5.0mm 區間大小 3) 1-5% 原本金屬的導熱性能

球狀金屬發泡

生產工藝	1) 在搞動的流動層將金屬球鍍上膠膜 2) 在壓鑄機床將金屬球倒模成型 3) 脫塑/燒結 4) 灌上錫和鑄造
物料特性	1) 5-30%密度 2) 0.4-5.0mm 孔隙大小

	3) 1-5% 原本金屬導熱性能

纖維結構

生產工藝	1) 採集熔池生成的纖維 2) 收集纖維 3) 加壓燒結 4) 機械加工
物料特性	1) 孔隙率 50-95% 2) 孔隙大小 10-250um 3) 纖維長度 3-50mm

籠狀結構

生產工藝	1) 鋼線原料放線 2) 將鋼線軋平 3) 經過螺旋滾輪成形 4) 結構生成

燒結金屬紙張

生產工藝	1) 造紙機將金屬紙張成型 2) 將部分金屬紙張折疊成波紋 3) 熱處理 (脫塑/燒結)
物料特性	1) 熱處理後的微結構 2) 未處理及燒結後的瓦楞紙結構

應用

1) 吸熱儲熱器
2) 催化器結構支撐
3) 吸音及吸震結構
4) 醫療移植件

6. 電磁脈衝焊接

電磁脈衝焊接原理

線圈產生短暫強力磁場	1) 外側工件加速靠近內側工件 2) 帶電流的線圈 (約 35 萬安培) 帶來勞侖茲力 (Lorentz Force)將金屬工件變形 3) 磁壓切線應力大於金屬片材降伏強度使工件塑性變形
高速度撞擊 (>200 m/s)	剪斷工件表面形成「衝擊波」
洗淨金屬表面和高衝壓	部件變形和連接

電磁脈衝接合是一個固態工序並適用於兩種不同合金金相的金屬接合

電磁脈衝焊接特點

1) 典型圓筒直徑介乎 10 至 80 毫米
2) 典型部件厚度介乎 0.5 至 3 毫米
3) 典型物料：銅、鋁、鋼、銅等等
4) 高能效且安全的工序
5) 能在毫秒內接合
6) 固態過程接合減少金屬間相
7) 不需焊料、焊接氣體和表面處理達致潔淨焊接

用光學和電子和透射電子顯微鏡來看接合部分橫切面的金相特性

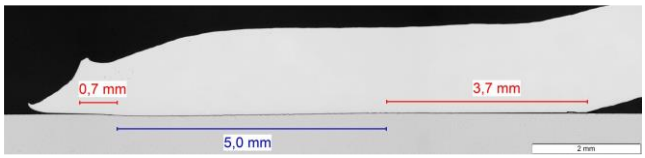

電磁脈衝焊接應用

1) 輕量化設計
2) 接合/焊接兩種不同物料

汽車工業	● 動力總成部件 ● 驅動軸
航空領域	● 鋁金屬接合 ● 鈦金屬接合
醫療	● 麻醉罐封密
建築/土木工程	● 水管接合

7. 雷射焊接

影響雷射焊接成果有以下因素

雷射的性質	1) 雷射生成媒介 2) 能源 3) 共振器 這三部分都會影響雷射的性質
金屬吸收雷射光的能力	一般來說波長越短吸收能力越強，但每一種金屬吸收雷射光能的起始波段都不一樣。只有起始波長或更短波長之光波才能將金屬有效熔解。

雷射焊接類型有以下幾種

1) 雷射熱傳導焊接

原理	1) 把激光射到金屬表面 2) 金屬表面開始氣化 3) 氣化金屬下層金屬熔化
特點	1) 焊接金屬厚度可達 20mm 2) 輕微焊接痕跡 3) 表面光滑 4) 焊接速度跟能量吸收成正比

2) 雷射多層焊接

原理	1) 焊枝深入焊接範圍 2) 把激光射到焊枝表面 3) 焊接範圍圍繞數圈把開口填滿
特點	1) 焊接金屬厚度可達 50mm 2) 焊接開口角度可減至三度以下 3) 焊接強度保持在原物料 90%以上 4) 可用於鋁材和鋼材

3) 雷射高頻率振動焊接

原理	1) 把小束雷射光射到金屬表面 2) 光束快速在金屬表面刻劃 3) 左右邊緣呈 8 字或圓圈並隨範圍移動
特點	1) 掃描頻率達數千 Hz 2) 增強熔池的穩定性 3) 減少焊接時金屬濺出

4)　高反射物料的雷射焊接

原理	因為一部分金屬反光能力較強，按目前雷射設備技術，使用515nm 波長綠光取代 1070nm 波長常用紅雷射光作焊接用途以增強穩定性。
特點	1) 可用於鋁材和銅 2) 適用於積層製造 3) 減少焊接雷射光束能耗 4) 未來可能有更短波長作焊接用途

活動一

嶄新物料科技——
優越功能帶來之商機國際會議

「環球金屬碳纖複合材料發展、應用趨勢及新商機」

「陶瓷基複合材料的新產品機遇及特點」

「利用電磁脈衝銲接技術達成高強度及品質銲接」

「金屬發泡及開放式結構的應用和新機遇」

「納米粒子為關鍵金屬部件帶來之理想特性」

「金屬基複合材料的應用和最新發展」

「先進激光輔助金屬成型技術及未來商機」

環球金屬碳纖複合材料發展、應用趨勢及新商機

由德國弗勞恩霍夫機床及成形技術研究所功能材質輕量化主管湯瑪士．協卡博士主講

METAL/ CARBON COMPOSITES DEVELOPMENT, APPLICATIONS AND NEW BUSINESS OPPORTUNITIES – POWDER METALLURGICAL APPROACH

Th. Hutsch[1], Th. Weißgärber[1], Th. Schubert B. Kieback[1]

[1] Fraunhofer Institute for Manufacturing Technology and Advanced Materials IFAM, Branch Lab Dresden, Winterbergstr. 28, D-01277 Dresden

GEFÖRDERT VOM

Bundesministerium für Bildung und Forschung

Contact: E-Mail: Thomas.Weissgaerber@ifam-dd.fraunhofer.de (head of department)
Thomas.Hutsch@ifam-dd.fraunhofer.de (research fellow)

© Fraunhofer IFAM Dresden

DRESDEN concept

Fraunhofer IFAM Branch Lab Dresden

Contact: Thomas.Weissgaerber@ifam-dd.fraunhofer.de (head of department), Thomas.Hutsch@ifam-dd.fraunhofer.de (research fellow)

Metal-Carbon composites at IFAM Dresden

passive cooling

- Metal-Diamond

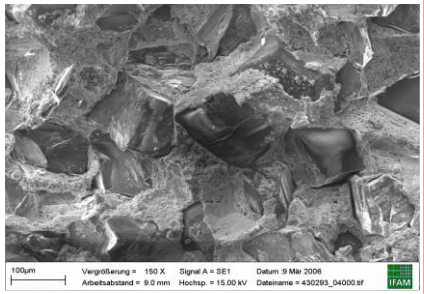

- Metal-Graphite

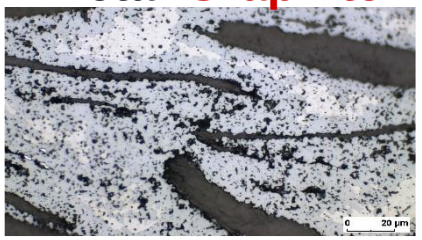

damping

- Metal-C-fibre

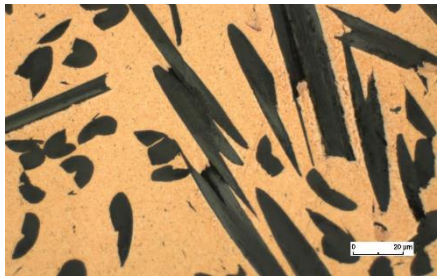

- Metal-Carbon Nanotube (CNT)

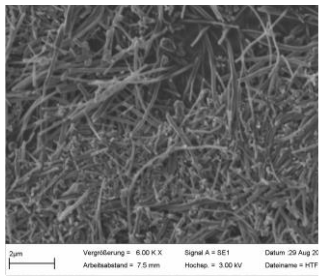

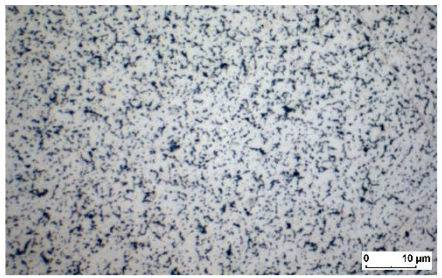

increase in strength

- Metal-Graphen
- Metal-Fullerene

load transfer

- Metal-FRP connection module

© Fraunhofer IFAM Dresden

DRESDEN concept

Fraunhofer IFAM Branch Lab Dresden

Contact: Thomas.Weissgaerber@ifam-dd.fraunhofer.de (head of department), Thomas.Hutsch@ifam-dd.fraunhofer.de (research fellow)

Motivation for composites

Diamond

- High thermal conductivity up to 1800 W/mK
- Low coefficient of thermal expansion (CTE), low density
- hard material

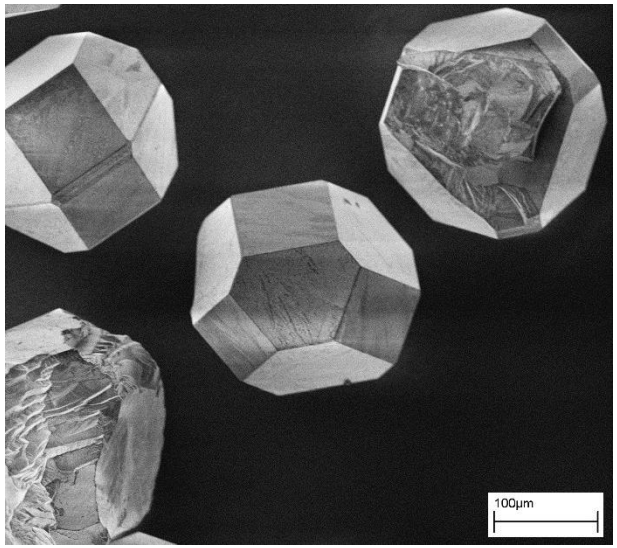

Syntethic diamond,
Diameter 20 – 120 µm

Graphite

- High thermal conductivity in two directions up to 2000 W/mK
- Low CTE, high damping capacity, self lubricant, low density
- Low cost

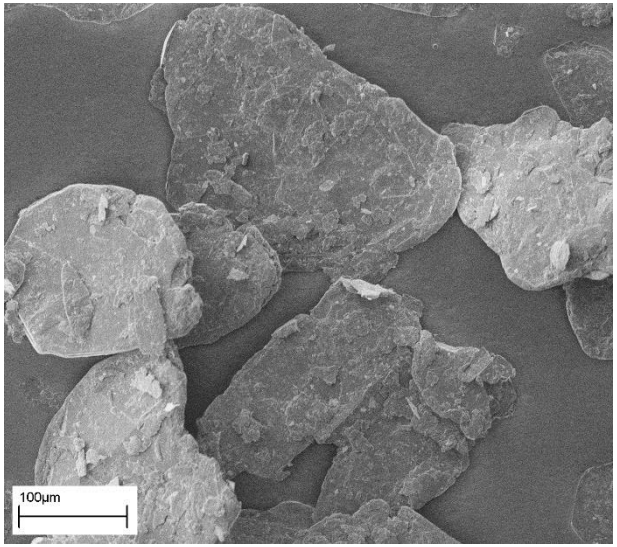

Natural Graphite-Flakes
Diameter: < 300 µm
Heigth: 3 – 15 µm

© Fraunhofer IFAM Dresden

DRESDEN concept

Fraunhofer IFAM Branch Lab Dresden

Contact: Thomas.Weissgaerber@ifam-dd.fraunhofer.de (head of department), Thomas.Hutsch@ifam-dd.fraunhofer.de (research fellow)

Metal-Carbon composites at IFAM Dresden

passive cooling

- Metal-Diamond

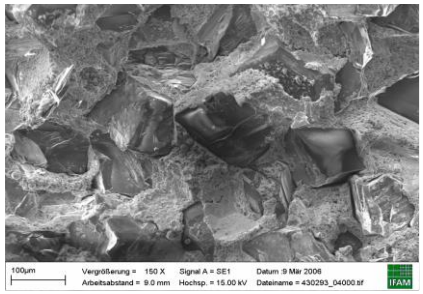

- Metal-Graphite

damping

- Metal-C-fibre

- Metal-Carbon Nanotube (CNT)

increase in strength

- Metal-Graphen
- Metal-Fullerene

load transfer

- Metal-FRP connection module

© Fraunhofer IFAM Dresden

DRESDEN concept

Fraunhofer IFAM Branch Lab Dresden

Contact: Thomas.Weissgaerber@ifam-dd.fraunhofer.de (head of department), Thomas.Hutsch@ifam-dd.fraunhofer.de (research fellow)

Thermal Conductivity Of PM Cu/Diamond Composites Depending On The Chromium Content – Prediction And Characterization

- Experimental

Cu + Cu(Cr)
powder

Tubular mixer

Spark Plasma Sintering

T_{sinter} = 1010°C; p = 45MPa;
heating rate = 600K/min;
cooling rate ca. 1000K/min

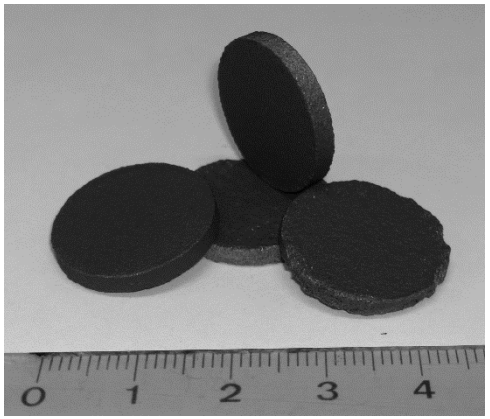

Sintered Bodies of a Cu(Cr)/ diamond composite with 60 vol.% diamond (diameter 20 mm, height ca. 2.8 mm)

Synthetic diamonds
(mesh 70/80, mesh 325/400)

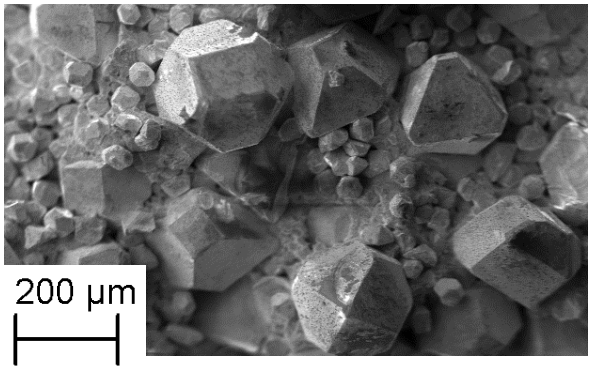

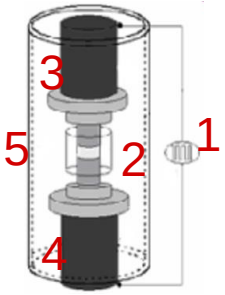

1 Pulsed electric generator
2 Press tool with sample
3 Upper die
4 Lower die
5 Cooled vacuum chamber

© Fraunhofer IFAM Dresden

DRESDEN concept

Fraunhofer IFAM Branch Lab Dresden

Contact: Thomas.Weissgaerber@ifam-dd.fraunhofer.de (head of department), Thomas.Hutsch@ifam-dd.fraunhofer.de (research fellow)

Thermal Conductivity Of PM Cu/Diamond Composites Depending On The Chromium Content – Prediction And Characterization

- Experimental Thermal conductivity

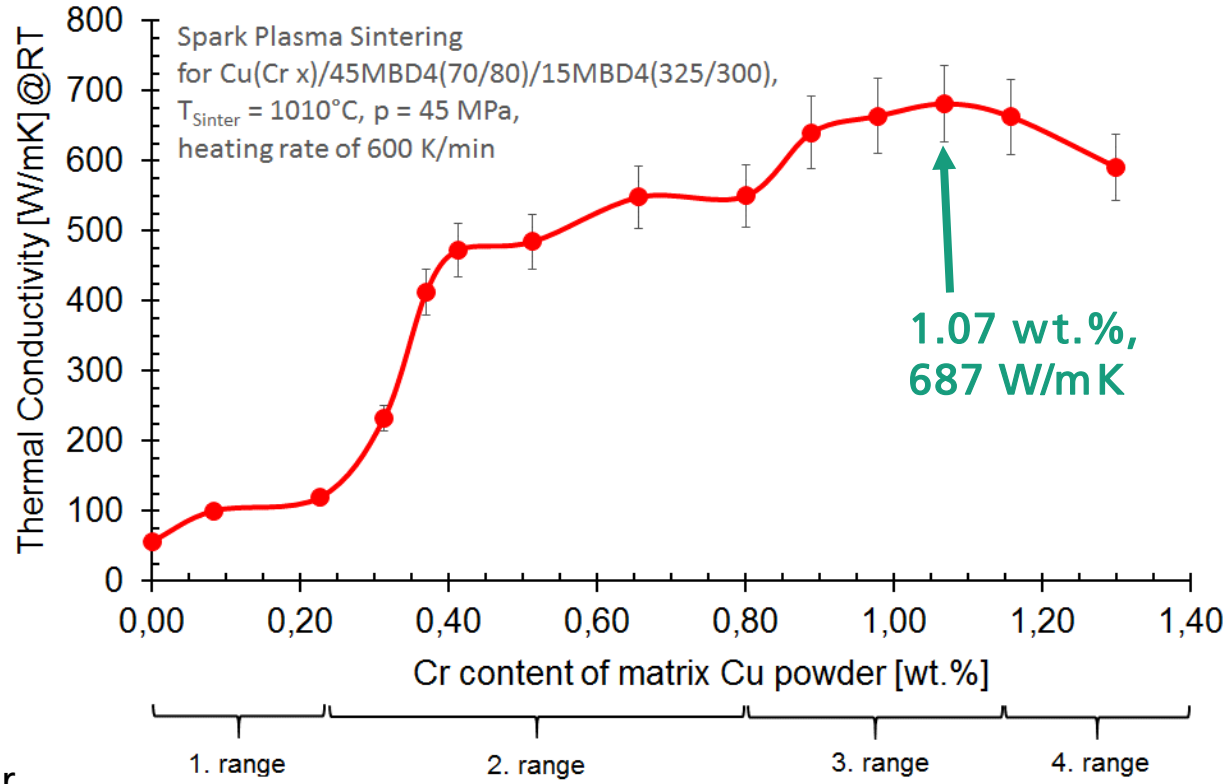

	1. range	2. range	3. range	4. range
Carbide layer thickness expectation	Nearly zero	Increasing	Good	Thickening carbide layer

© Fraunhofer IFAM Dresden

DRESDEN concept

Fraunhofer IFAM Branch Lab Dresden

Contact: Thomas.Weissgaerber@ifam-dd.fraunhofer.de (head of department), Thomas.Hutsch@ifam-dd.fraunhofer.de (research fellow)

Thermal Conductivity Of PM Cu/Diamond Composites Depending On The Chromium Content – Prediction And Characterization

- Prediction of the carbide layer thickness
  - Material factors
    - Solubility of Cr in Cu at sinter temperature to identify the reactive Cr content
    - Diffusion of Cr in Cu at applied heating rate & sinter temperature to identify the diffusion length of Cr
  - Geometric factors
    - Diamond fractions (particle size, volume content) to calculate the reactive surface area
    - Mathematical carbide layer thickness dependence on mean matrix Cr content to identify the best Cr content for aimed mean layer thickness (180 to 300 nm)

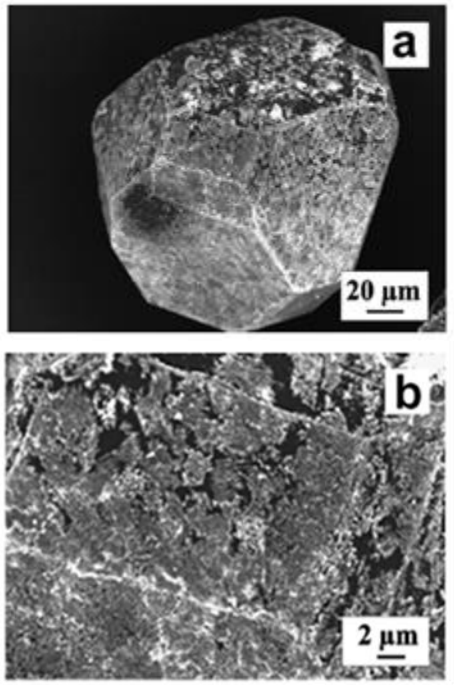

T. Schubert et al., Scripta Materialia, Vol. 58 (2008) pp 263-266

© Fraunhofer IFAM Dresden

DRESDEN concept

Fraunhofer IFAM Branch Lab Dresden

Contact: Thomas.Weissgaerber@ifam-dd.fraunhofer.de (head of department), Thomas.Hutsch@ifam-dd.fraunhofer.de (research fellow)

Thermal Conductivity Of PM Cu/Diamond Composites Depending On The Chromium Content – Prediction And Characterization

- Geometric factor – Mathematical carbide layer thickness dependence

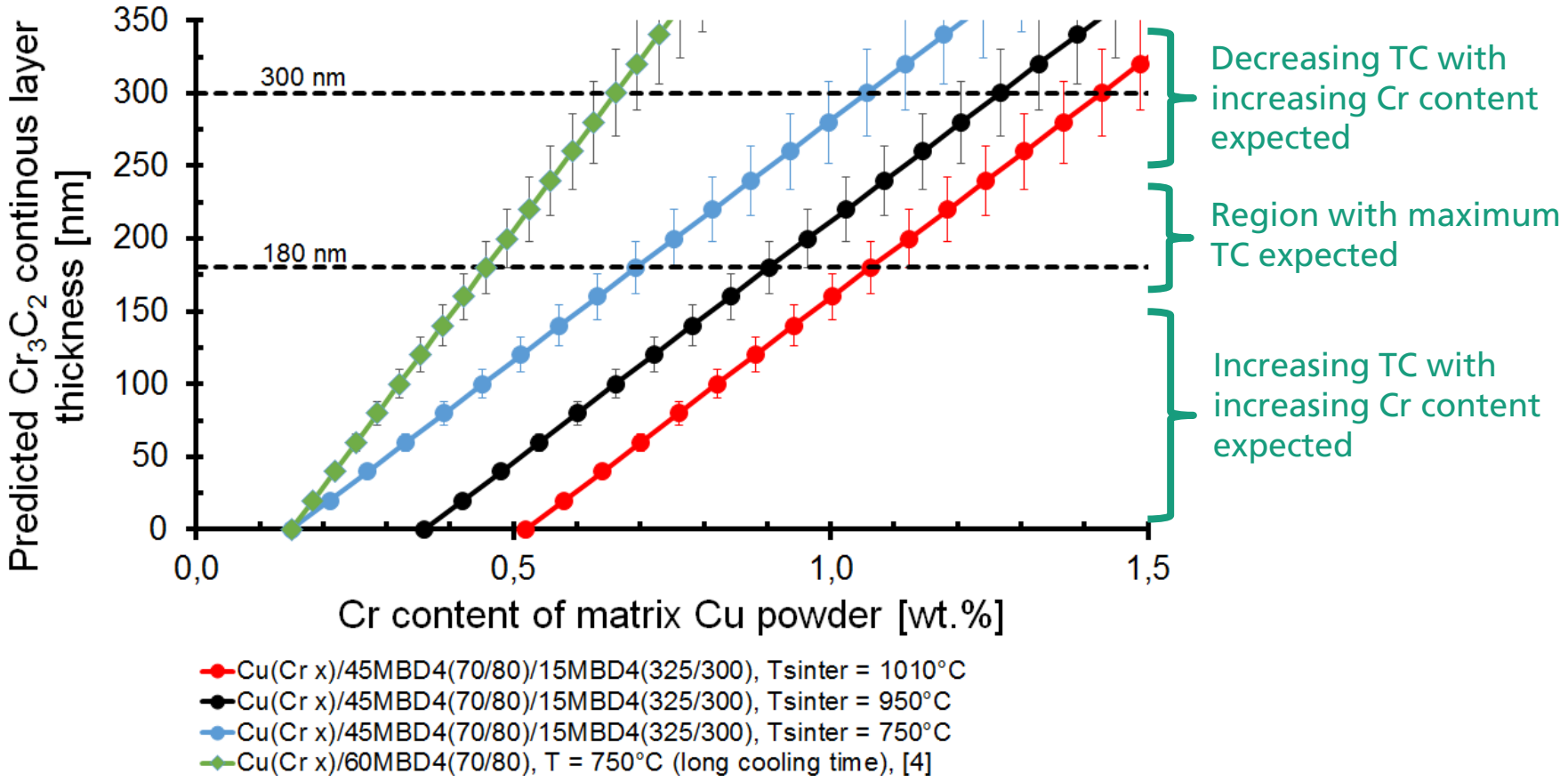

© Fraunhofer IFAM Dresden

DRESDEN concept

Fraunhofer IFAM Branch Lab Dresden

Contact: Thomas.Weissgaerber@ifam-dd.fraunhofer.de (head of department), Thomas.Hutsch@ifam-dd.fraunhofer.de (research fellow)

Thermal Conductivity Of PM Cu/Diamond Composites Depending On The Chromium Content – Prediction And Characterization

- Comparison of prediction and characterization

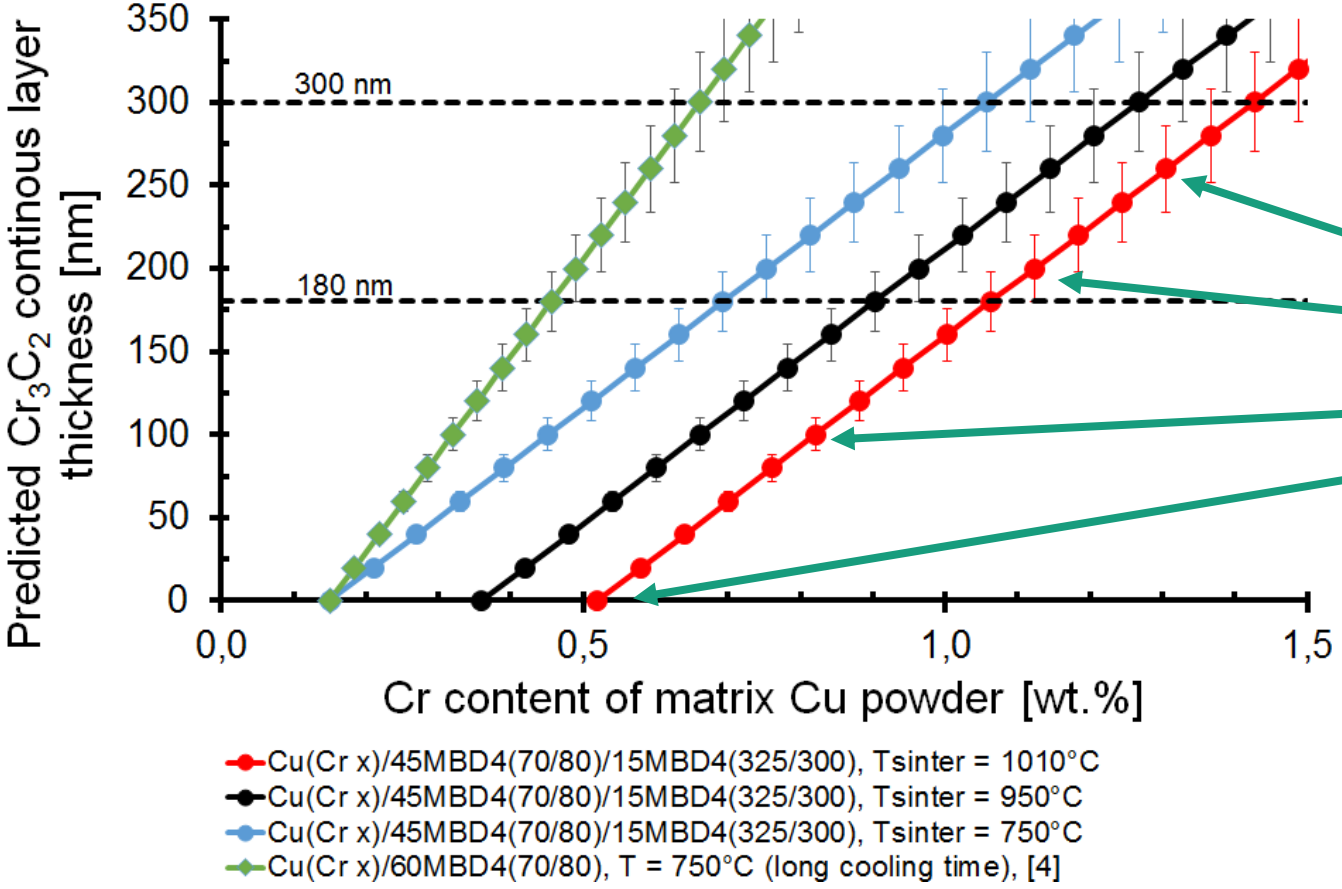

Experimental

Spark Plasma Sintering
for Cu(Cr x)/45MBD4(70/80)/15MBD4(325/300),
T_{Sinter} = 1010°C, p = 45 MPa,
heating rate of 600 K/min

602 W/mK @ Cr 1.3

687 W/mK @ Cr 1.07

565 W/mK @ Cr 0.8

484 W/mK @ Cr 0.41

- Sufficient way to predict the interesting Cr content to get high TC

© Fraunhofer IFAM Dresden

DRESDEN concept

Fraunhofer IFAM Branch Lab Dresden

Contact: Thomas.Weissgaerber@ifam-dd.fraunhofer.de (head of department), Thomas.Hutsch@ifam-dd.fraunhofer.de (research fellow)

Thermal Conductivity Of PM Cu/Diamond Composites Depending On The Chromium Content – Prediction And Characterization

- Temperature dependence of thermal conductivity

Spark Plasma Sintering
for Cu(Cr x)/45MBD4(70/80)/15MBD4(325/300),
T_{Sinter} = 1010°C, p = 45 MPa,
heating rate of 600 K/min

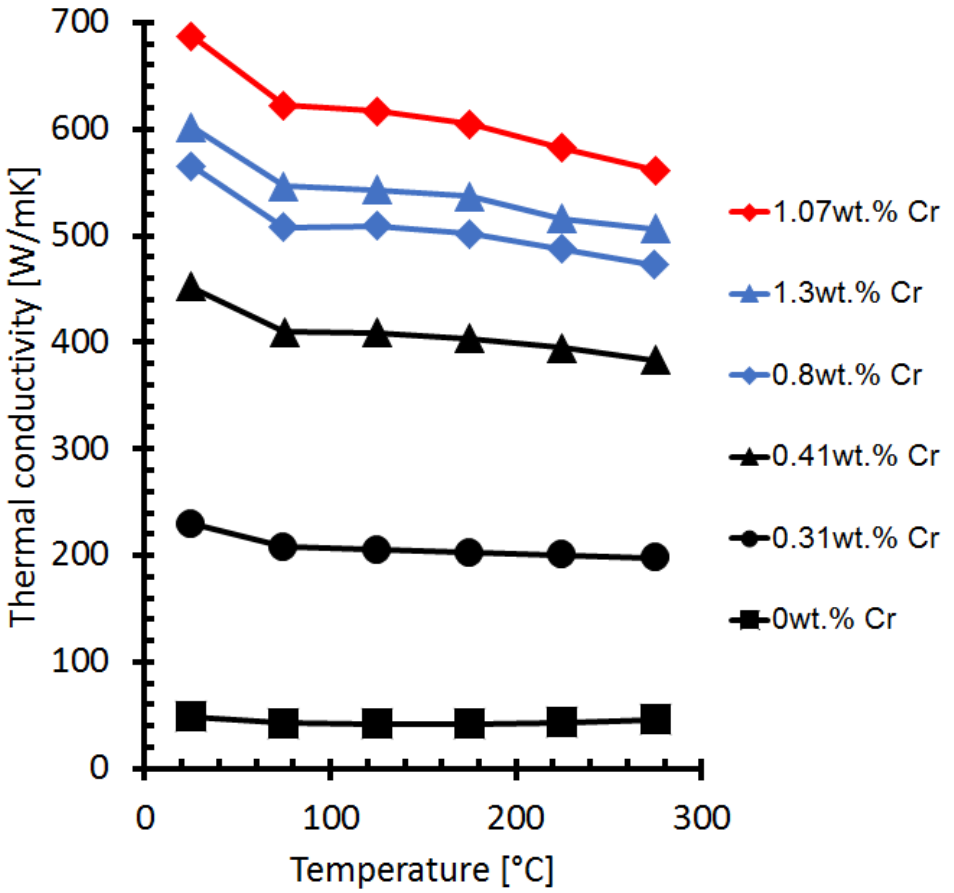

- TC @ RT for sample with 1.07wt.% Cr:
  after SPS: 687 W/mK
  after 275°C: 680 W/mK

© Fraunhofer IFAM Dresden

DRESDEN concept

Fraunhofer IFAM Branch Lab Dresden

Contact: Thomas.Weissgaerber@ifam-dd.fraunhofer.de (head of department), Thomas.Hutsch@ifam-dd.fraunhofer.de (research fellow)

Thermal management materials - overview

@ Raumtemperatur

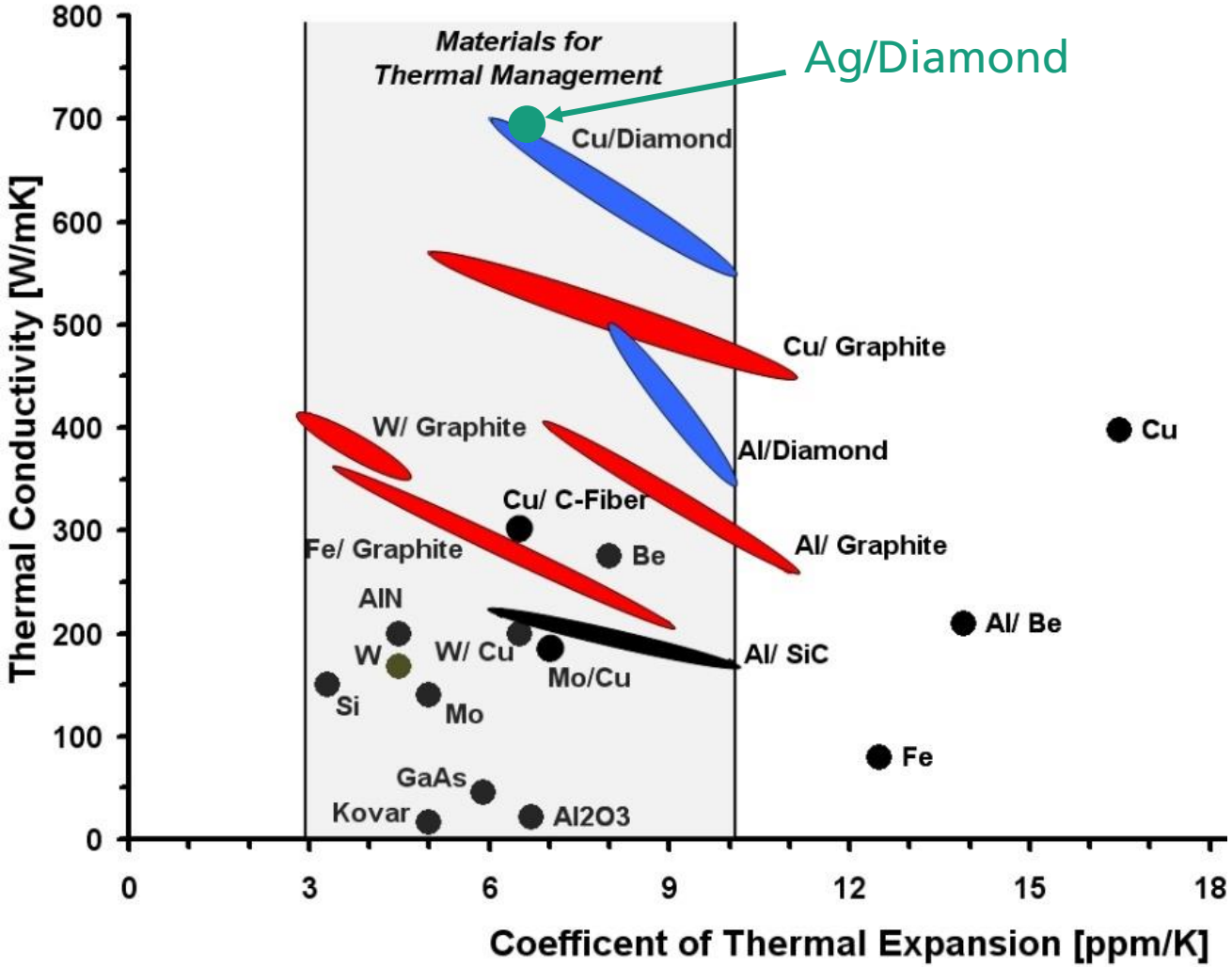

synthetic diamond
(quality MBD4)
d = 110 - 200 µm

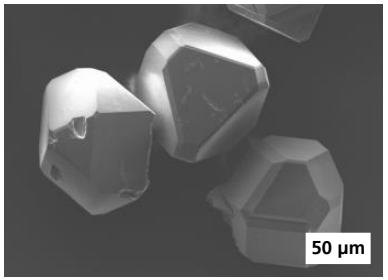

Natural graphite
Anisotropic flakes
d = 125µm

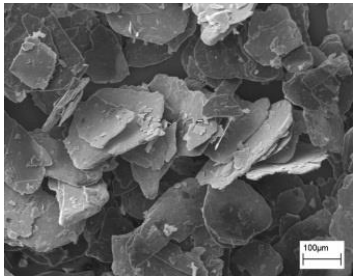

© Fraunhofer IFAM Dresden

DRESDEN concept

Fraunhofer IFAM Branch Lab Dresden

Contact: Thomas.Weissgaerber@ifam-dd.fraunhofer.de (head of department), Thomas.Hutsch@ifam-dd.fraunhofer.de (research fellow)

Carbon reinforced metal composites with tailored physical properties

- **Tailored properties and possible property combinations:**

	Metal-diamond composites
Properties, orientation	isotropic
Vol.% C [%]	up to 70
Thermal conductivity [W/mK]	up to 700
Thermal expansion [ppm/K @ RT]	5 to 10
Electrical conductivity [m/(Ohm*mm²]	higher 10
Damping	poor
Self lubricating	no
Maschine ability	poor

- **Applications in thermal management and electrical connector**

© Fraunhofer IFAM Dresden

DRESDEN concept

Fraunhofer IFAM Branch Lab Dresden

Contact: Thomas.Weissgaerber@ifam-dd.fraunhofer.de (head of department), Thomas.Hutsch@ifam-dd.fraunhofer.de (research fellow)

Metal-Carbon composites at IFAM Dresden

passive cooling

- Metal-Diamond

- Metal-Graphite

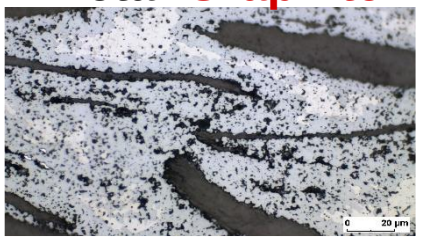

damping

- Metal-C-fibre

load transfer

- Metal-FRP connection module

- Metal-Carbon Nanotube (CNT)

increase in strength

- Metal-Graphen
- Metal-Fullerene

© Fraunhofer IFAM Dresden

DRESDEN concept

Fraunhofer IFAM Branch Lab Dresden

Contact: Thomas.Weissgaerber@ifam-dd.fraunhofer.de (head of department), Thomas.Hutsch@ifam-dd.fraunhofer.de (research fellow)

Metal/ graphite composite

- Experimental

Metal Powder
(Cu, Al, Fe, W & alloys)

Tubular mixer

Carbon
(natural graphite flakes)

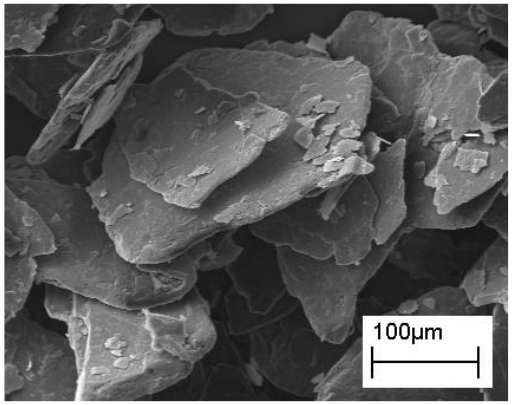

Consolidation

Spark Plasma Sintering

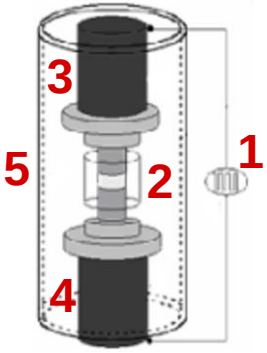

1 Pulsed electric generator
2 Press tool with sample
3 Upper die
4 Lower die
5 Cooled vacuum chamber

Composite

Metal-graphite composite

tungsten- 70 vol. %
graphite composite
(diameter 150 mm,
height 5 mm)

© Fraunhofer IFAM Dresden

DRESDEN concept

Fraunhofer IFAM Branch Lab Dresden

Contact: Thomas.Weissgaerber@ifam-dd.fraunhofer.de (head of department), Thomas.Hutsch@ifam-dd.fraunhofer.de (research fellow)

Metal-graphite composite

- Microstructure

two – dimensional orientation → anisotropic properties

a) Parallel and
b) Perpendicular to pressing direction

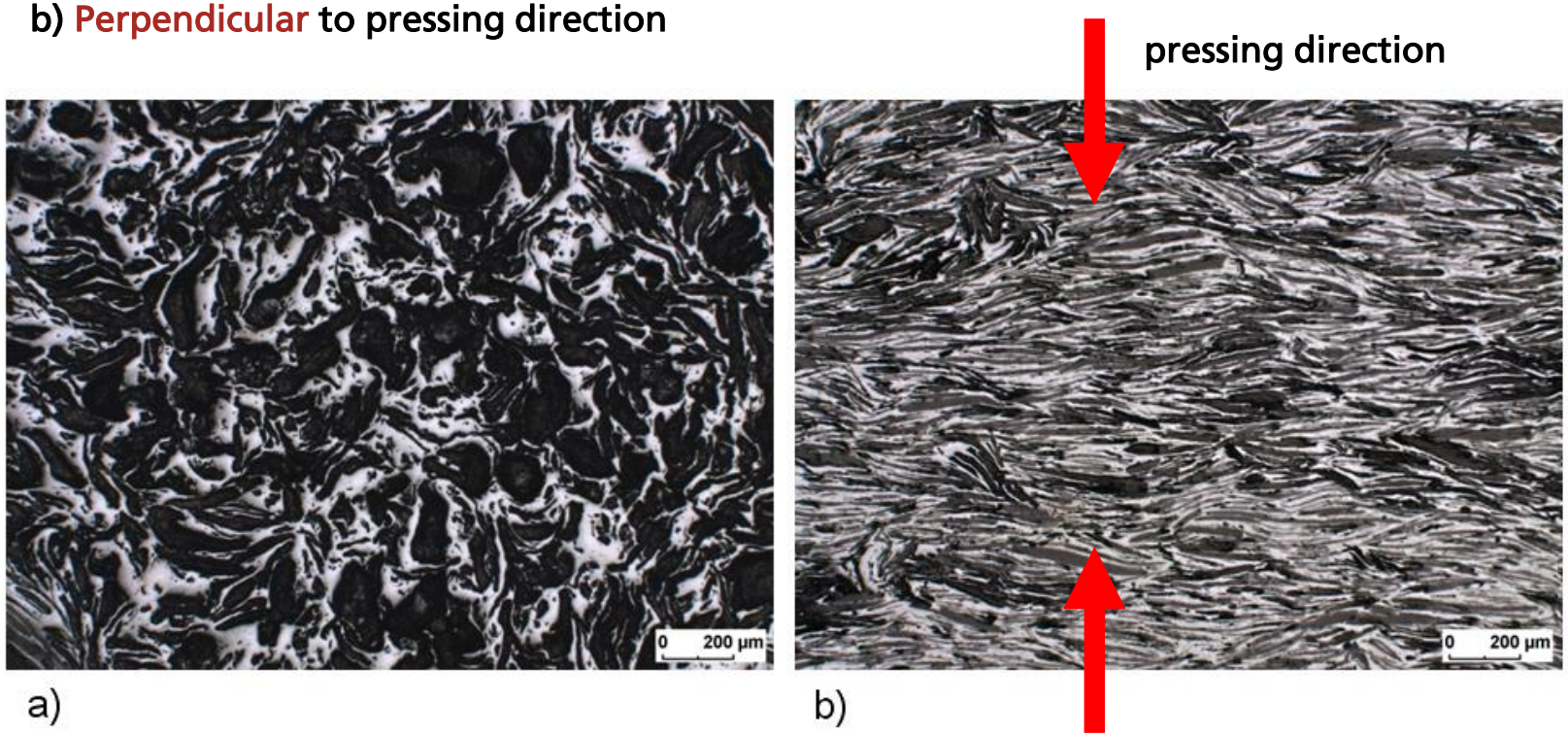

© Fraunhofer IFAM Dresden

DRESDEN concept

Fraunhofer IFAM Branch Lab Dresden

Contact: Thomas.Weissgaerber@ifam-dd.fraunhofer.de (head of department), Thomas.Hutsch@ifam-dd.fraunhofer.de (research fellow)

Metal-graphite composite

- Microstructure, carbide formation

Carbide formation controlled by composition metal + C, example: W + C

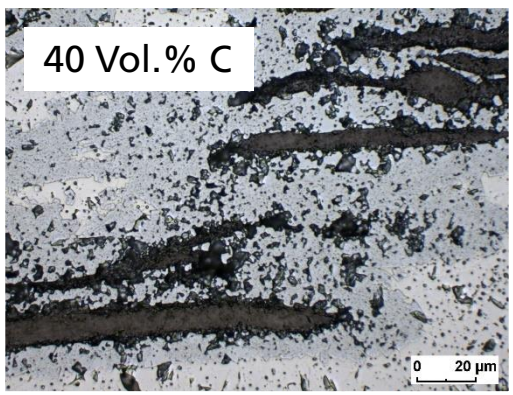

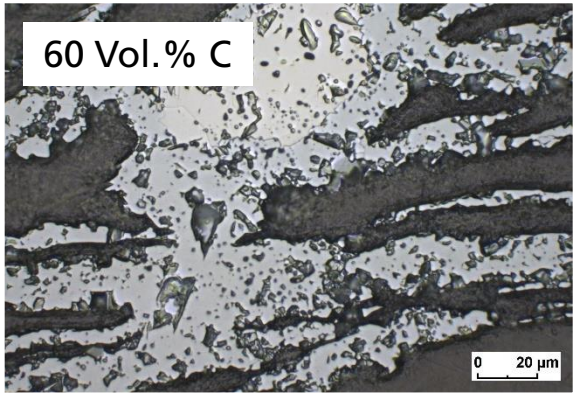

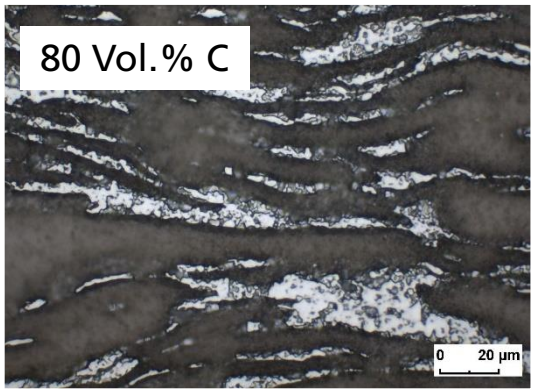

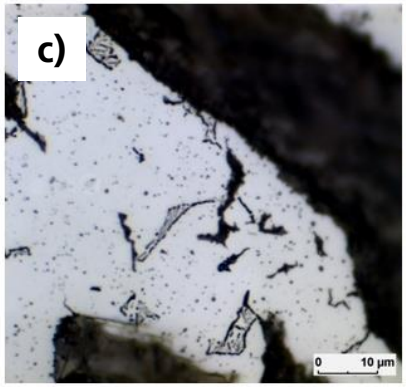

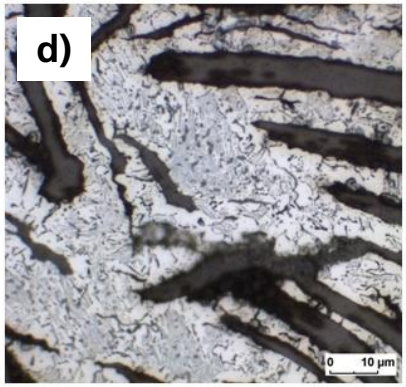

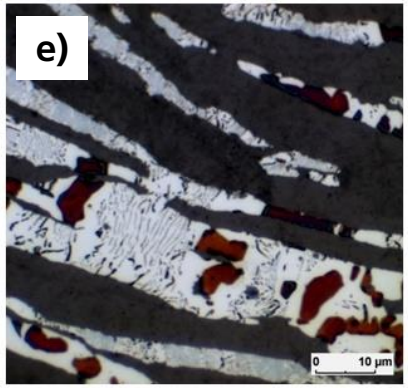

Control the carbide content upon the variation of dwell time
c) 10 s
d) 2 min
e) 20 min
Fe + 60 vol. % graphite etched with picric acid

© Fraunhofer IFAM Dresden

DRESDEN concept

Fraunhofer IFAM Branch Lab Dresden

Contact: Thomas.Weissgaerber@ifam-dd.fraunhofer.de (head of department), Thomas.Hutsch@ifam-dd.fraunhofer.de (research fellow)

Metal-graphite composite

- Thermo physical properties

Thermal conductivity

a) Parallel and

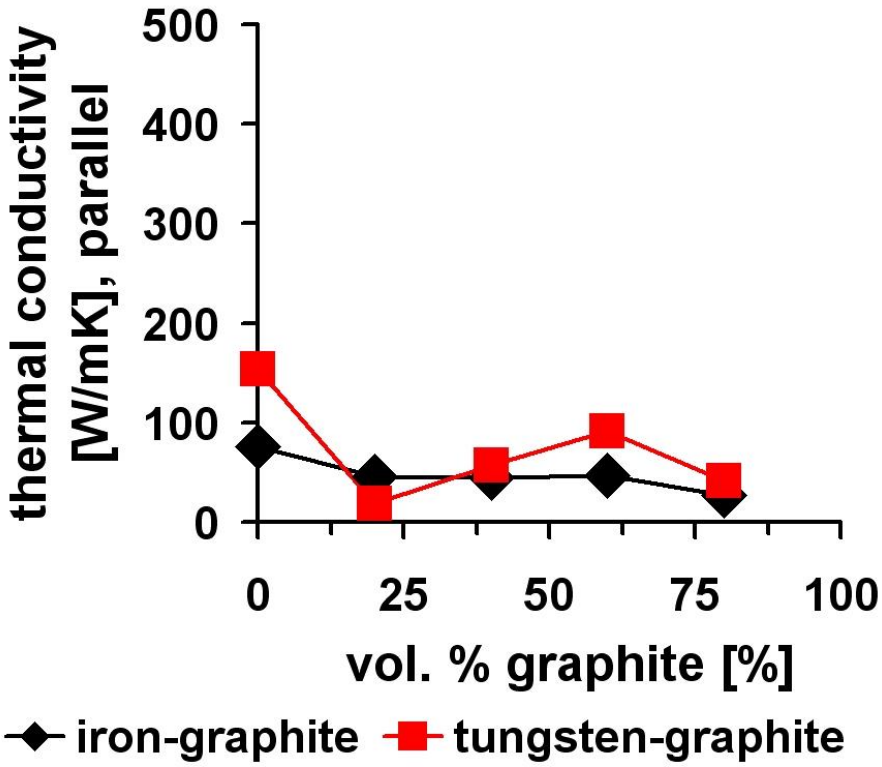

b) Perpendicular to pressing direction

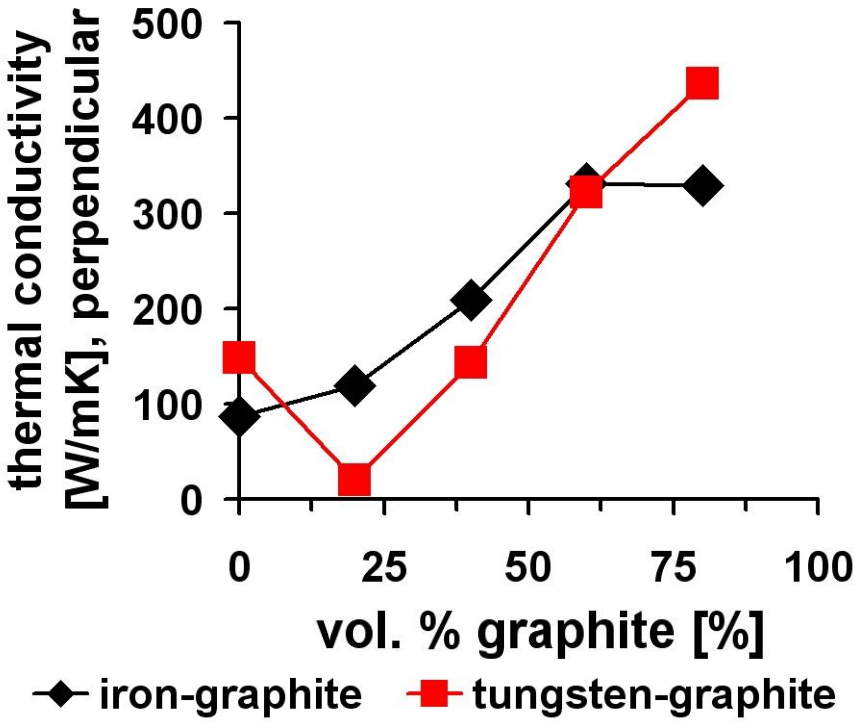

© Fraunhofer IFAM Dresden

DRESDEN concept

Fraunhofer IFAM Branch Lab Dresden

Contact: Thomas.Weissgaerber@ifam-dd.fraunhofer.de (head of department), Thomas.Hutsch@ifam-dd.fraunhofer.de (research fellow)

Metal-graphite composite

- Thermo physical properties

Physical CTE, example: tungsten with 70 vol.% graphite after 1000 cycles -20°C up to 200°C

a) Parallel and b) Perpendicular to pressing direction

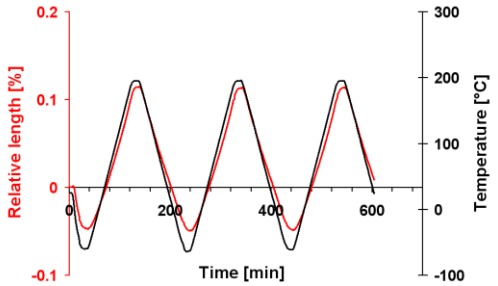

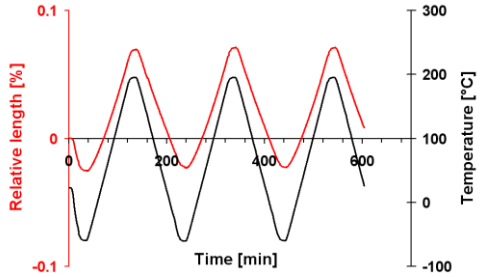

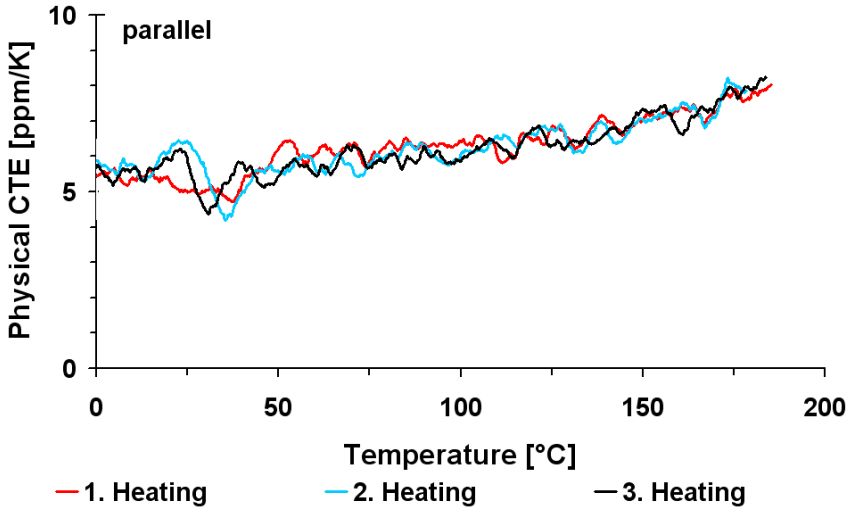

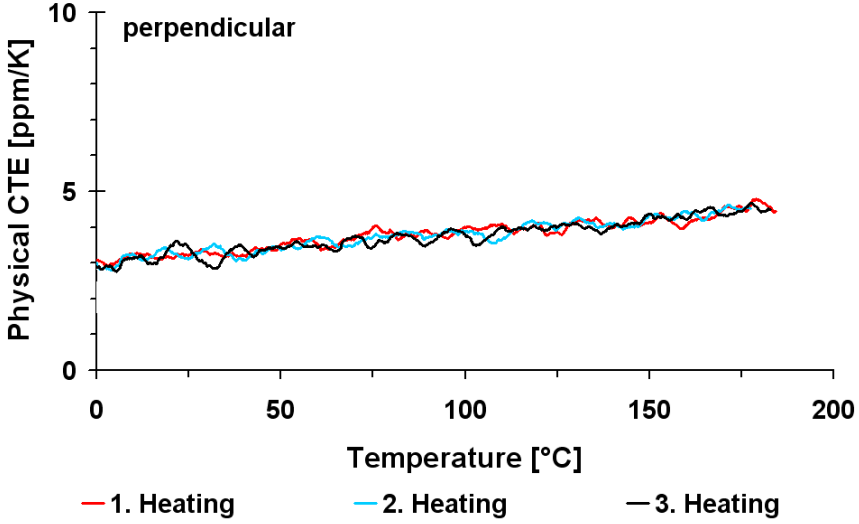

© Fraunhofer IFAM Dresden

DRESDEN concept

Fraunhofer IFAM Branch Lab Dresden

Contact: Thomas.Weissgaerber@ifam-dd.fraunhofer.de (head of department), Thomas.Hutsch@ifam-dd.fraunhofer.de (research fellow)

Thermal management materials - overview

@ Raumtemperatur

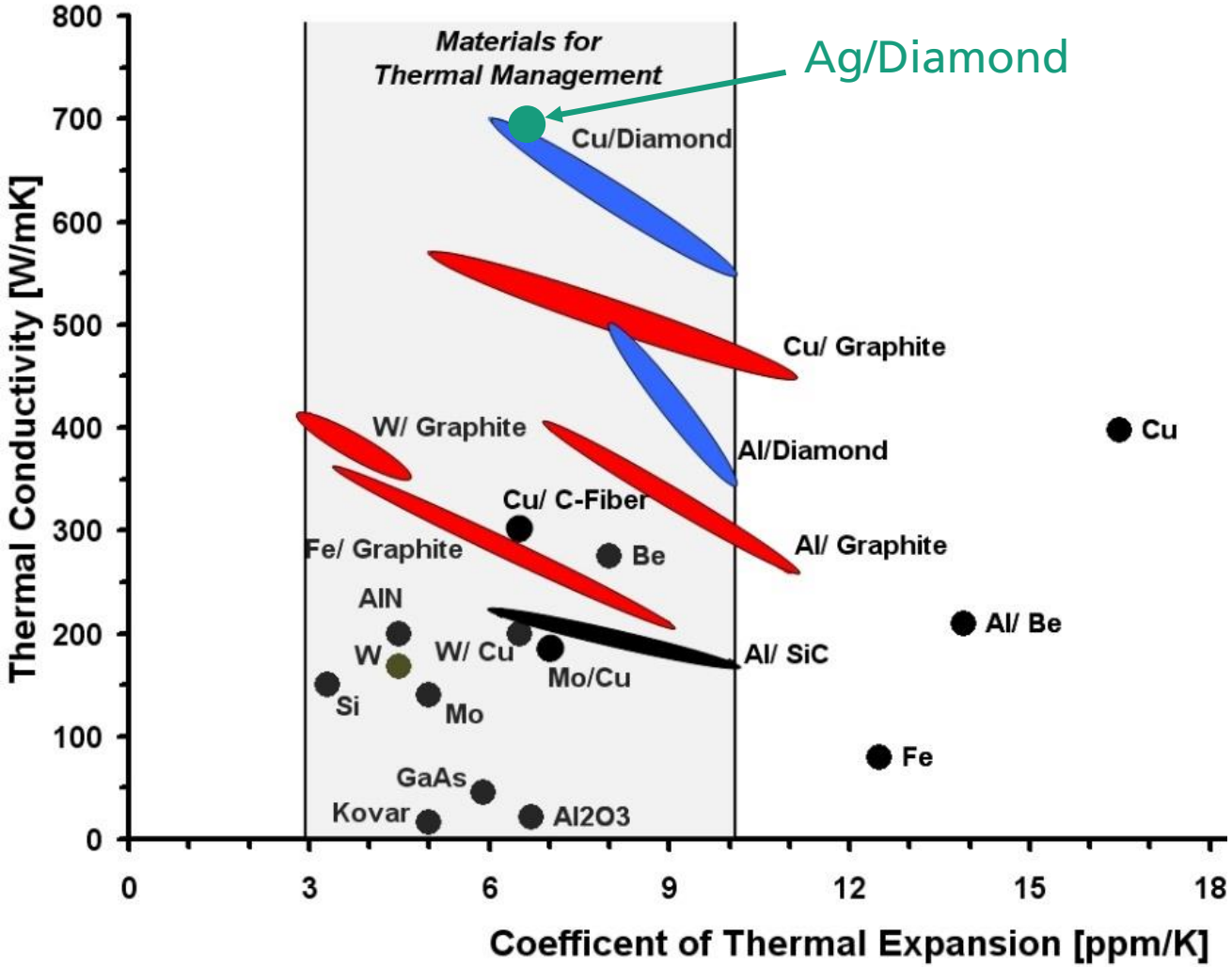

synthetic diamond
(quality MBD4)
d = 110 - 200 µm

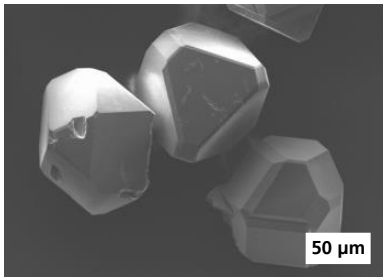

Natural graphite
Anisotropic flakes
d = 125µm

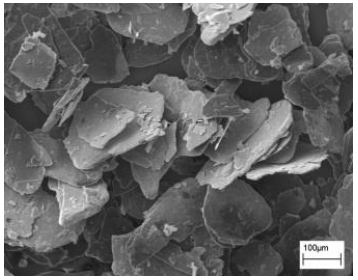

© Fraunhofer IFAM Dresden

DRESDEN concept

Fraunhofer IFAM Branch Lab Dresden

Contact: Thomas.Weissgaerber@ifam-dd.fraunhofer.de (head of department), Thomas.Hutsch@ifam-dd.fraunhofer.de (research fellow)

Metal-graphite composite

- Damping

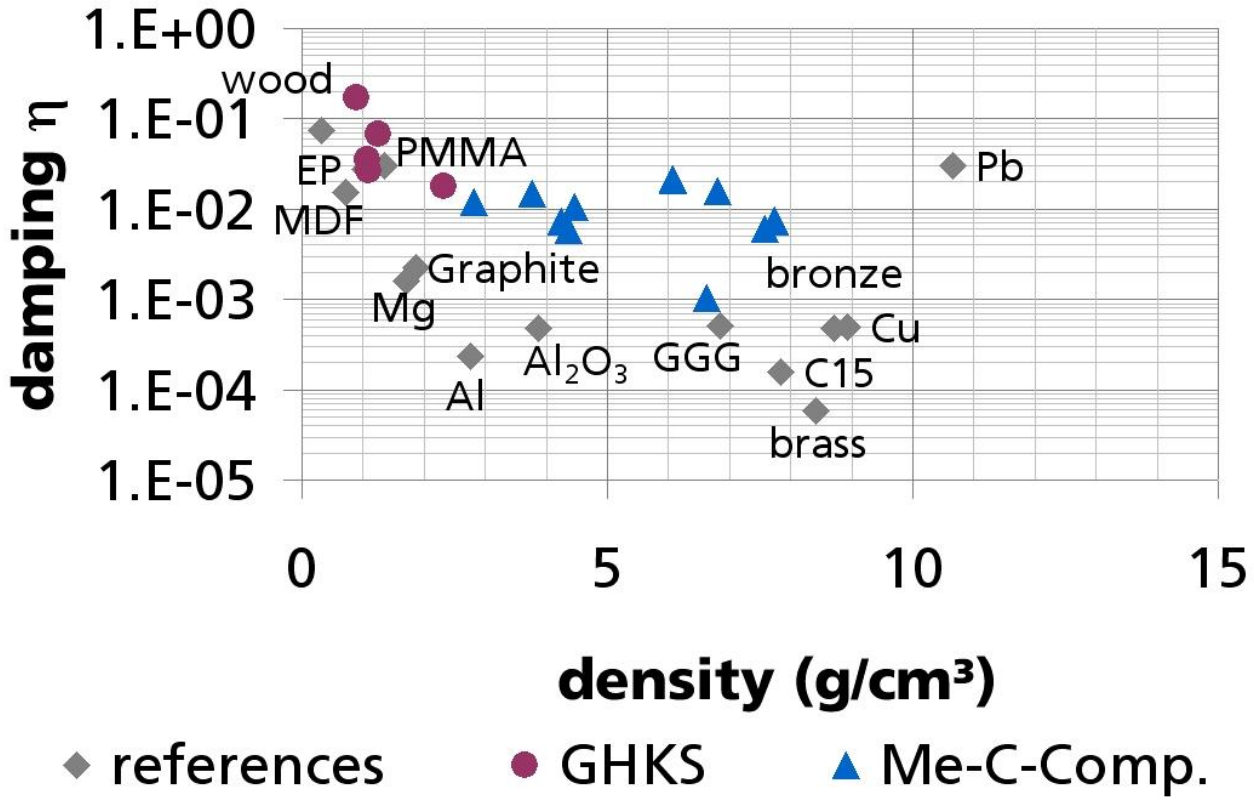

Me-C-Comp. → Metal-Graphite-Composite

GHKS → Particle filled hollow spheres

Mechanical damping capability can be combined with an elastic modulus in the range from 40 GPa up to 180 GPa depending on the graphite content and the microstructure.

© Fraunhofer IFAM Dresden

DRESDEN concept

Fraunhofer IFAM Branch Lab Dresden

Contact: Thomas.Weissgaerber@ifam-dd.fraunhofer.de (head of department), Thomas.Hutsch@ifam-dd.fraunhofer.de (research fellow)

Carbon reinforced metal composites with tailored physical properties

- **Tailored properties and possible property combinations:**

	Metal-diamond composites	Metal-graphite composites
Properties, orientation	isotropic	anisotropic, two-dimensional
Vol.% C [%]	up to 70	up to 90
Thermal conductivity [W/mK]	up to 700	up to 550
Thermal expansion [ppm/K @ RT]	5 to 10	3 to 10
Electrical conductivity [m/(Ohm*mm²]	higher 10	higher 5
Damping	poor	good
Self lubricating	no	good
Maschine ability	poor	good

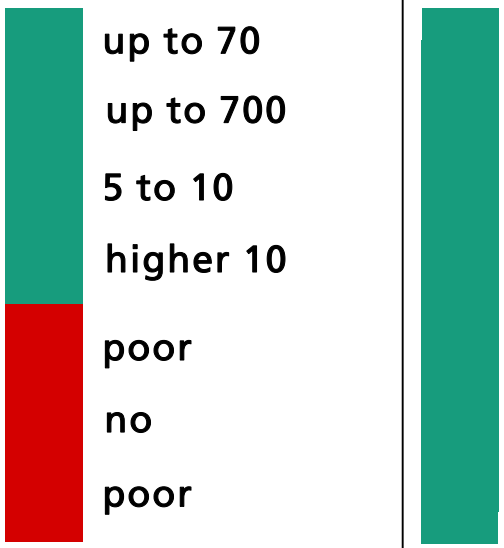

- **Applications in thermal management, passive dampers and electrical connector**

© Fraunhofer IFAM Dresden

DRESDEN concept

Fraunhofer IFAM Branch Lab Dresden

Contact: Thomas.Weissgaerber@ifam-dd.fraunhofer.de (head of department), Thomas.Hutsch@ifam-dd.fraunhofer.de (research fellow)

Metal-Carbon composites at IFAM Dresden

passive cooling

- Metal-Diamond

- Metal-Graphite

damping

- Metal-C-fibre

- **Metal-Carbon Nanotube (CNT)**

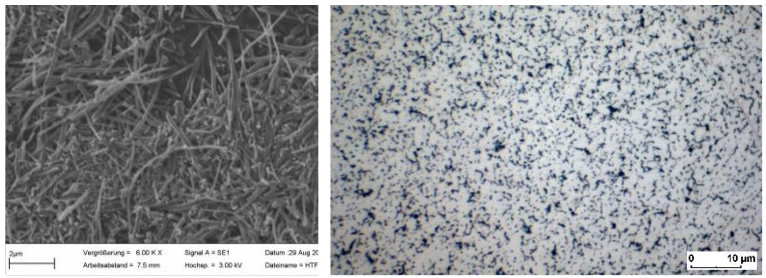

increase in strength

- Metal-Graphen
- Metal-Fullerene

load transfer

- Metal-FRP connection module

© Fraunhofer IFAM Dresden

DRESDEN concept

Fraunhofer IFAM Branch Lab Dresden

Contact: Thomas.Weissgaerber@ifam-dd.fraunhofer.de (head of department), Thomas.Hutsch@ifam-dd.fraunhofer.de (research fellow)

Raw materials

- Carbon nanotube (CNT) + metal powder

Pillow like aggregates

Pellet

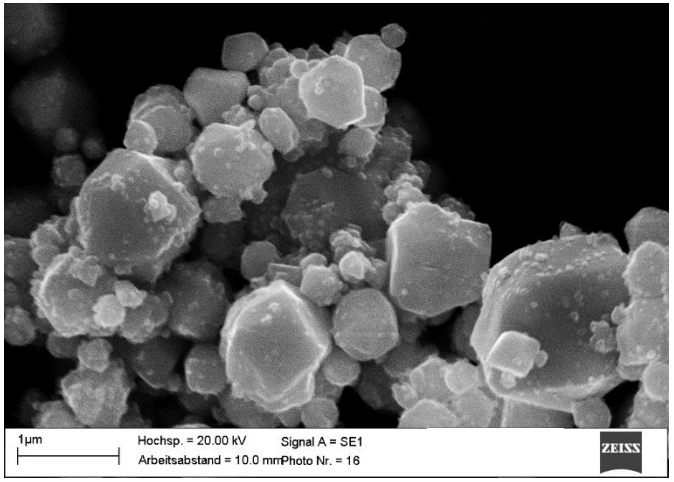

© Fraunhofer IFAM Dresden

DRESDEN concept

Fraunhofer IFAM Branch Lab Dresden

Contact: Thomas.Weissgaerber@ifam-dd.fraunhofer.de (head of department), Thomas.Hutsch@ifam-dd.fraunhofer.de (research fellow)

Metal/ CNT composite

- **Homogenious metal/ CNT mixtures**
  - **Heat treatment of mixtures**
  - **Consolidation (hot pressing, hot extrusion)**
  - **Heat treatment**
- **Composite**
  - **Characterization**
    (microstructure, mechanical properties, thermal expansion, electrical and thermal conductivity) depend on CNT (content, type) on example Cu/CNT

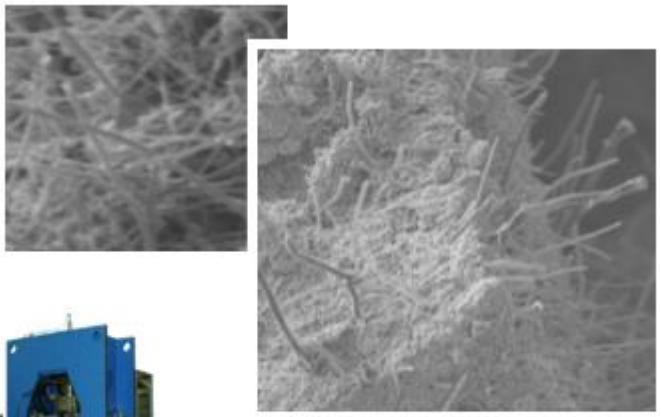

SPS

STP

© Fraunhofer IFAM Dresden

DRESDEN concept

Fraunhofer IFAM Branch Lab Dresden

Contact: Thomas.Weissgaerber@ifam-dd.fraunhofer.de (head of department), Thomas.Hutsch@ifam-dd.fraunhofer.de (research fellow)

Metal/ CNT composite

- Getting homogenious metal/ CNT mixtures

Dispersion in liquid state

Metal powder + CNT

Ultrasonic cavitation

Bildquelle: http://www.hielscher.com

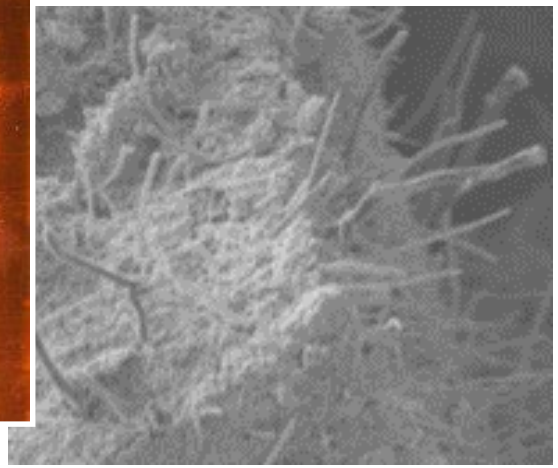

Mechanical dispersion

Al powder + CNT

Energy input
(milling time, rpm)

Homogenious metal/ CNT mixtures

© Fraunhofer IFAM Dresden

DRESDEN concept

Fraunhofer IFAM Branch Lab Dresden

Contact: Thomas.Weissgaerber@ifam-dd.fraunhofer.de (head of department), Thomas.Hutsch@ifam-dd.fraunhofer.de (research fellow)

Dispersion in liquid state – Pretreatment of CNT

- Schema

CNF + **Dispersion medium** (water, ethanol, …) + **Dispersion agent**

Ultrasonic support (intensity, time, volumen)

Dispersion of CNT (Devide in fractions)

1. Fraction:
Agglomerates, Growth catalyst particles, big carbon particle

2. Fraction:
pre-treated CNT

0,7g CNT
oben: raw CNT
unten: pre-treated CNT

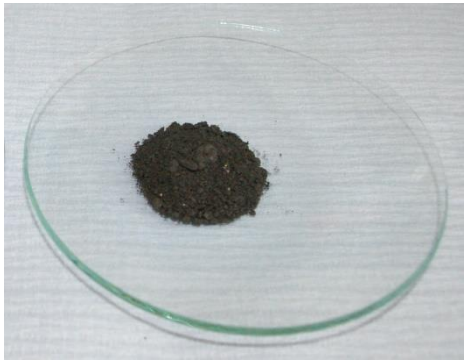

Advantage:
-Dispersion agent covers CNT after drying
-Redispersion possible, long time stable dispersions
-CNT functionalization of fraction possible
-Reduced transport volume

© Fraunhofer IFAM Dresden

DRESDEN concept

Fraunhofer IFAM Branch Lab Dresden

Contact: Thomas.Weissgaerber@ifam-dd.fraunhofer.de (head of department), Thomas.Hutsch@ifam-dd.fraunhofer.de (research fellow)

Dispersion in liquid state – Pretreatment of CNT

- Yield of pre-treated CNT

Examples	Yield [wt.%]
CNT Bayer, Baytubes C150P	20 bis 40
CNT IFW, MWCNT as grown	30 bis 40
CNT IFW, Fixbett + gereinigt	30 bis 50
CNT Future Carbon, MWCNT	30 bis 50
CNF IFW, Carbon Nanofibres	40 bis 60
CNF Electrovac, HTF150LHT	50 bis 65
CNT IFW, Aerosol	**80 bis 95**

→ Yield depend strongly on used CNT growth technique

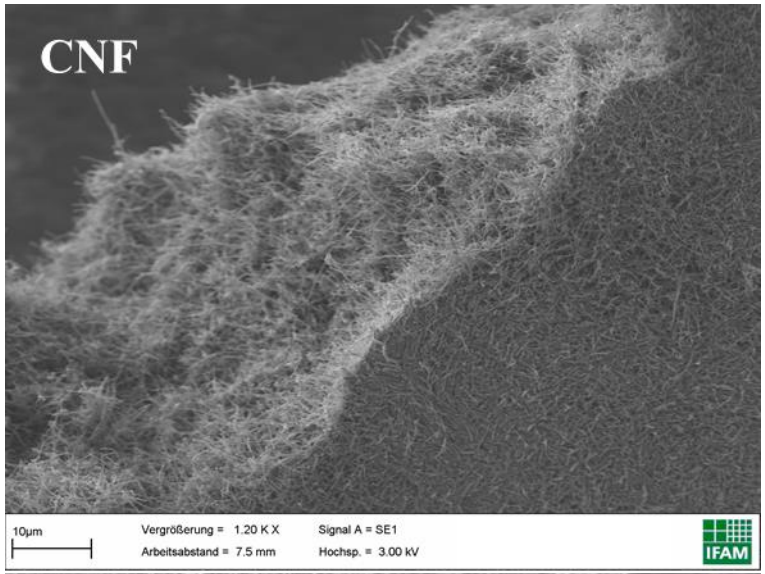

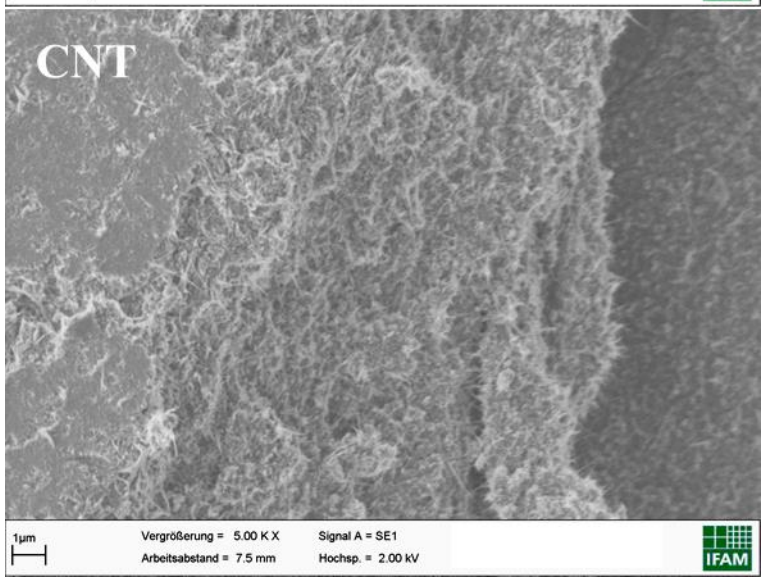

© Fraunhofer IFAM Dresden

DRESDEN concept

Fraunhofer IFAM Branch Lab Dresden

Contact: Thomas.Weissgaerber@ifam-dd.fraunhofer.de (head of department), Thomas.Hutsch@ifam-dd.fraunhofer.de (research fellow)

Characterization – microstructure, electrical conductivity

- After hot extrusion

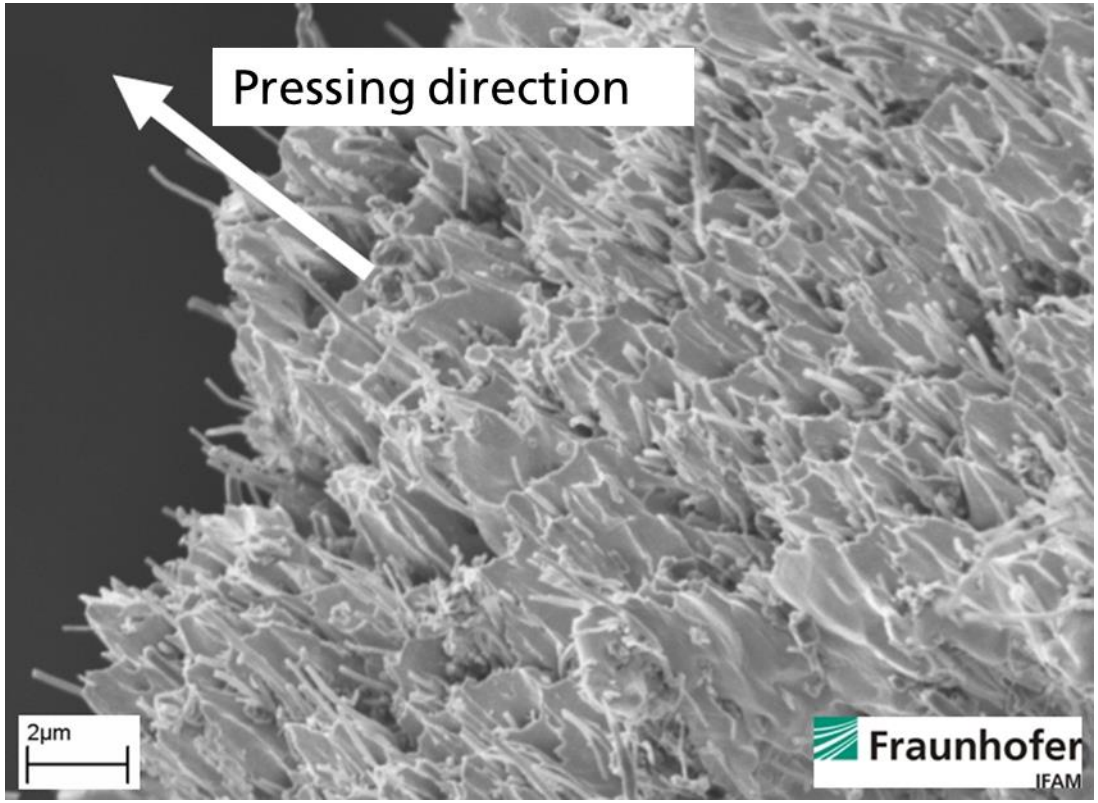

One-dimensional alignement

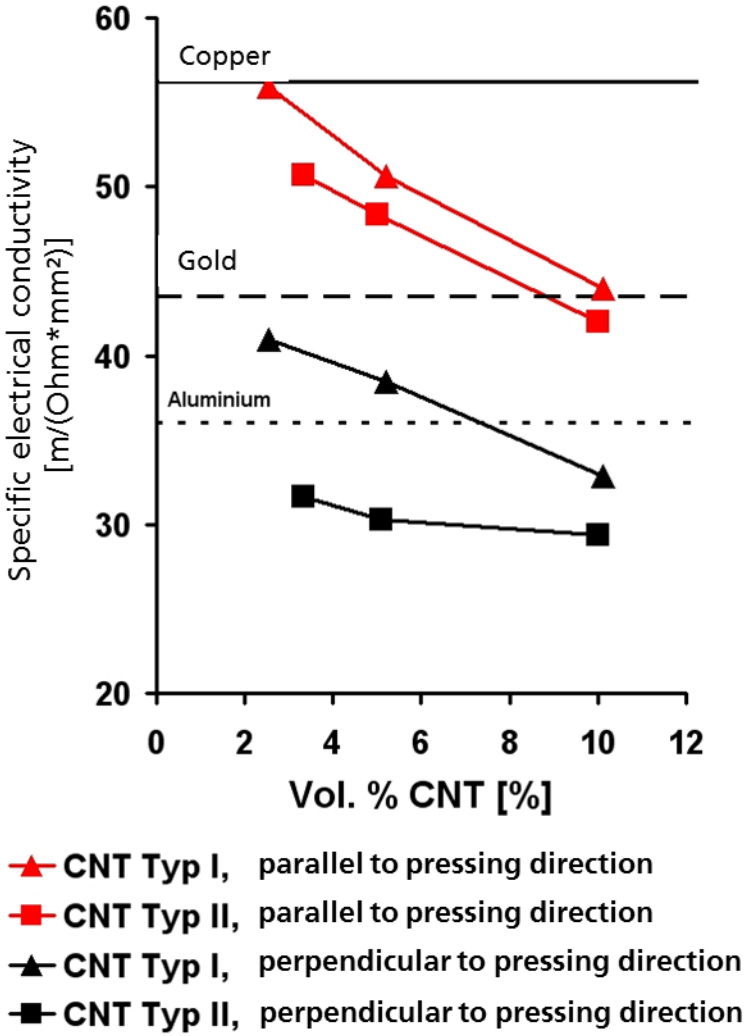

© Fraunhofer IFAM Dresden

DRESDEN concept

Fraunhofer IFAM Branch Lab Dresden

Contact: Thomas.Weissgaerber@ifam-dd.fraunhofer.de (head of department), Thomas.Hutsch@ifam-dd.fraunhofer.de (research fellow)

Characterization – thermo physical properties

- Thermal conductivity

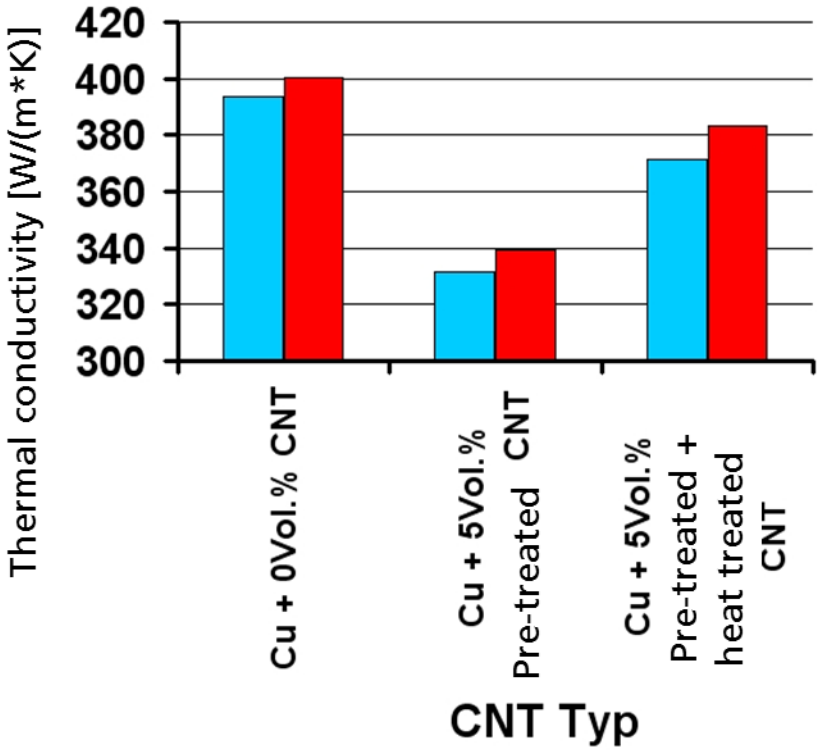

Heat treatment leads to a reorganisation of chemical bonds

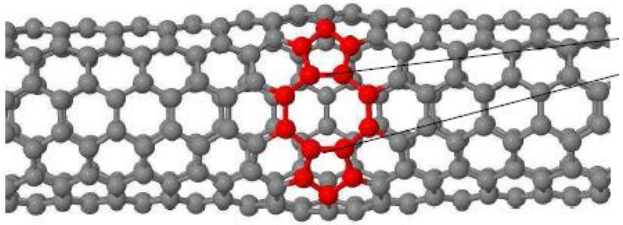

© Fraunhofer IFAM Dresden

Contact: Thomas.Weissgaerber@ifam-dd.fraunhofer.de (head of department), Thomas.Hutsch@ifam-dd.fraunhofer.de (research fellow)

Characterization – mechanical properties @ RT

- Effect of CNT dispersion

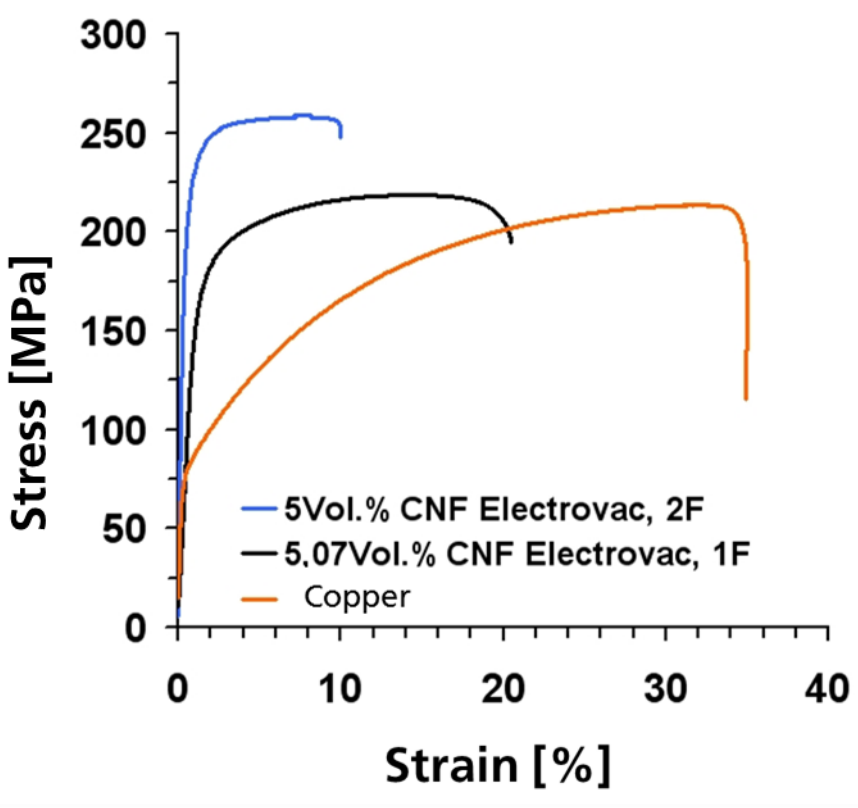

Homogenious dispersion is essential

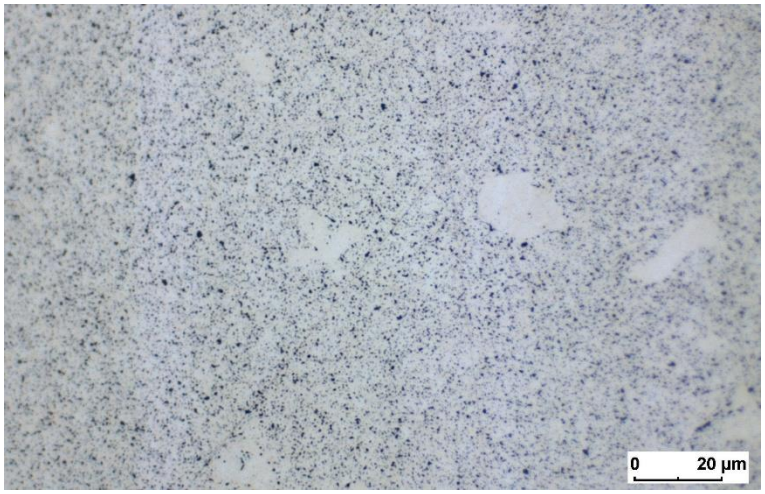

2F → 2.Fraction, pre-treated CNT
1F → 1.Fraction, rejected CNT

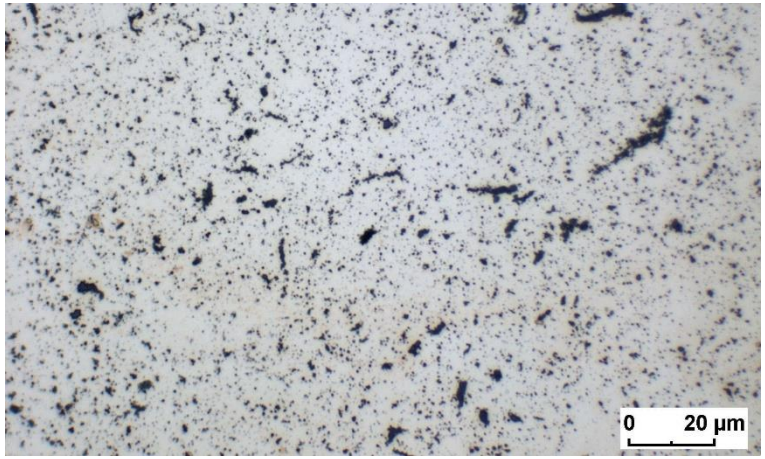

© Fraunhofer IFAM Dresden

DRESDEN concept

Fraunhofer IFAM Branch Lab Dresden

Contact: Thomas.Weissgaerber@ifam-dd.fraunhofer.de (head of department), Thomas.Hutsch@ifam-dd.fraunhofer.de (research fellow)

Characterization – mechanical properties @ RT

- Volume content (vol.%)

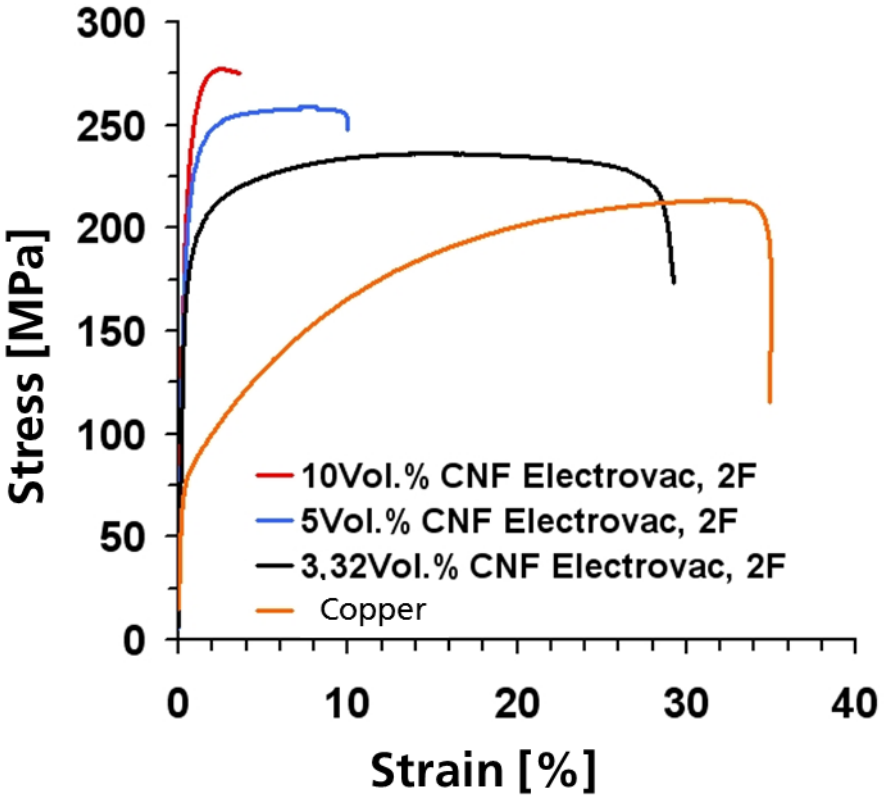

Vol.% ↑ → R_m ↑ and elongation ↓

- Heat treatment (WB)

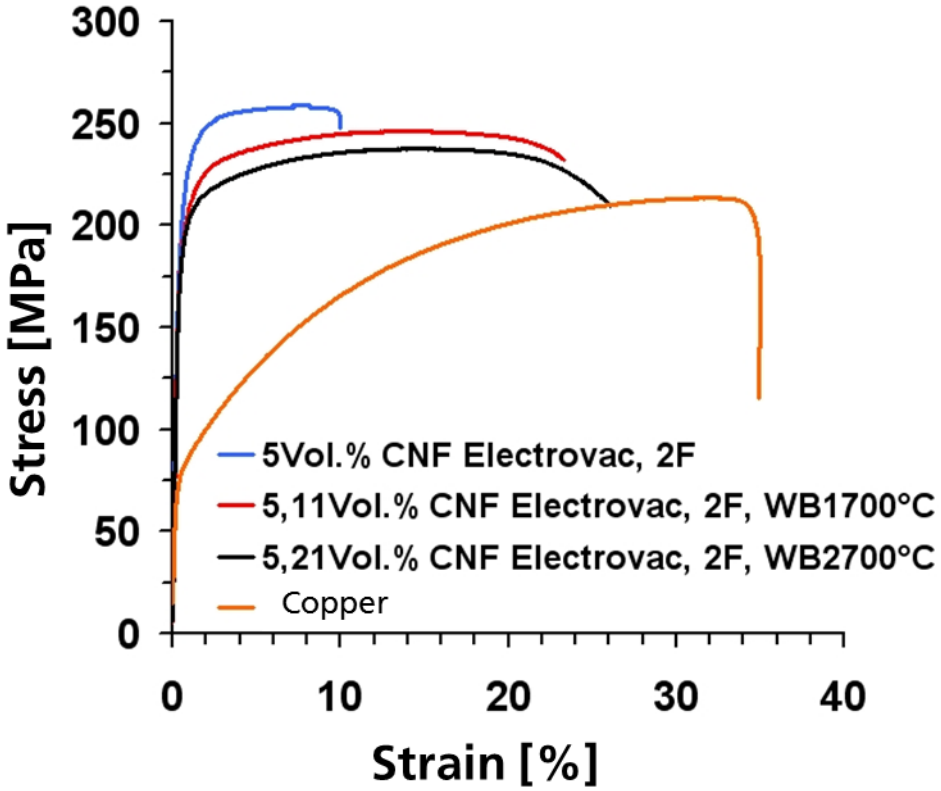

Temperature WB ↑ → R_m ↓ and elongation ↑
WB introduce shortening of CNT

© Fraunhofer IFAM Dresden

DRESDEN concept

Fraunhofer IFAM Branch Lab Dresden

Contact: Thomas.Weissgaerber@ifam-dd.fraunhofer.de (head of department), Thomas.Hutsch@ifam-dd.fraunhofer.de (research fellow)

Metal-Carbon composites at IFAM Dresden

passive cooling

- Metal-Diamond

- Metal-Graphite

damping

- Metal-C-fibre

- Metal-Carbon Nanotube (CNT)

increase in strength

- Metal-Graphen
- Metal-Fullerene

load transfer

- **Metal-FRP connection module**

© Fraunhofer IFAM Dresden

DRESDEN concept

Fraunhofer IFAM Branch Lab Dresden

Contact: Thomas.Weissgaerber@ifam-dd.fraunhofer.de (head of department), Thomas.Hutsch@ifam-dd.fraunhofer.de (research fellow)

METAL/ FRP CONNECTION MODULE & TFP REINFORCED METALS – A POWDER METALLURGICAL APPROACH

Thomas Hutsch

Contact: Thomas.Hutsch@ifam-dd.fraunhofer.de

Tel.: 0049-351-2537-396

[1] Fraunhofer Institute for Manufacturing Technology and Advanced Materials IFAM, Branch Lab Dresden, Winterbergstraße 28, 01277 Dresden, Germany

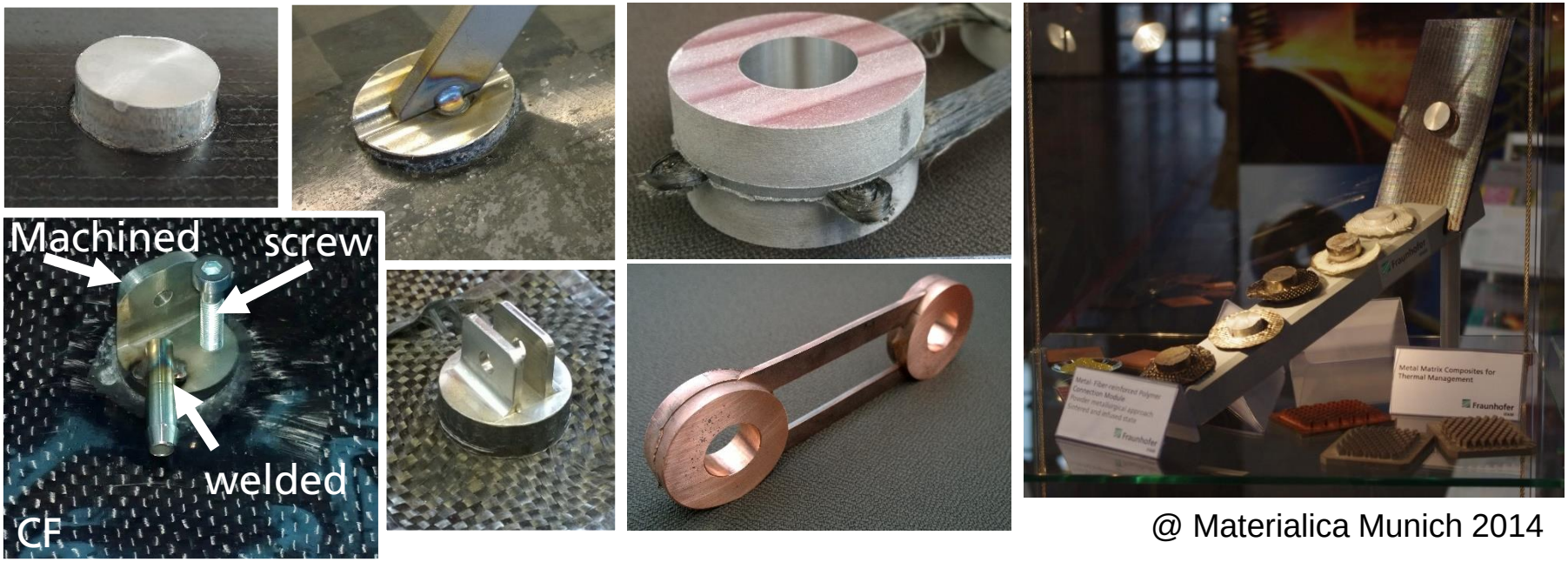

@ Materialica Munich 2014

© Fraunhofer IFAM Dresden

DRESDEN concept

Fraunhofer IFAM Branch Lab Dresden

Contact: Thomas.Weissgaerber@ifam-dd.fraunhofer.de (head of department), Thomas.Hutsch@ifam-dd.fraunhofer.de (research fellow)

Metal/ FRP Connection module – Motivation

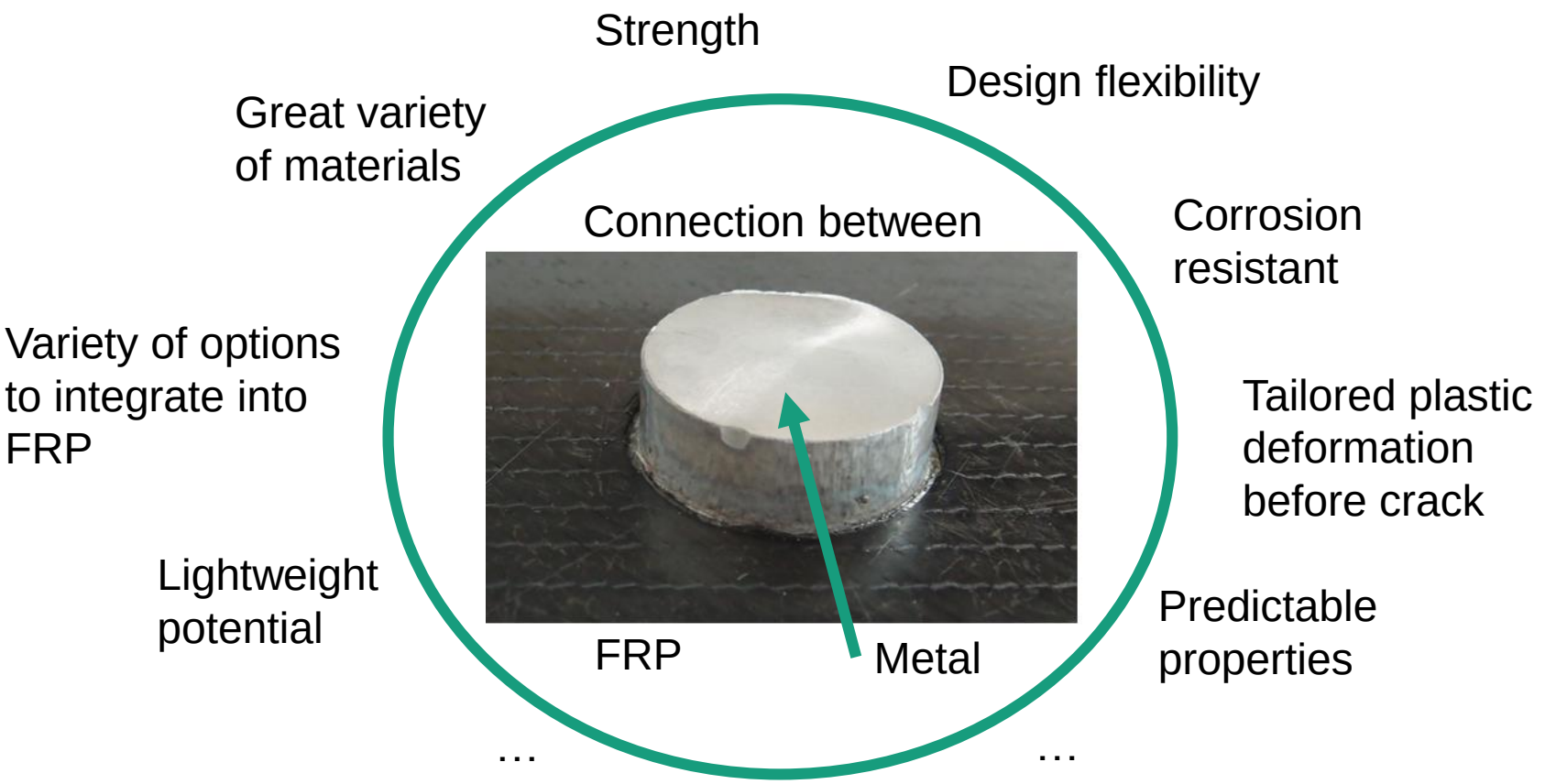

→ Powder Metallurgy offers great potential

© Fraunhofer IFAM Dresden

DRESDEN concept

Fraunhofer IFAM Branch Lab Dresden

Contact: Thomas.Weissgaerber@ifam-dd.fraunhofer.de (head of department), Thomas.Hutsch@ifam-dd.fraunhofer.de (research fellow)

Metal/ FRP Connection module – Consolidation

- Spark Plasma Sintering:

Filling	Sintering	Demolding

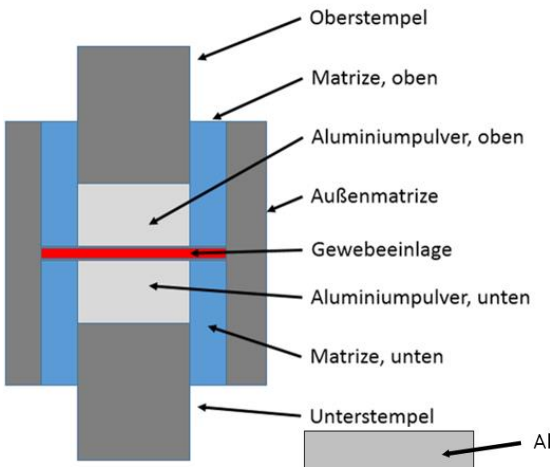

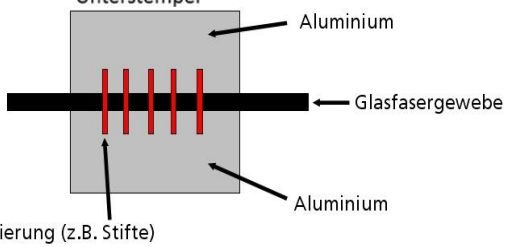

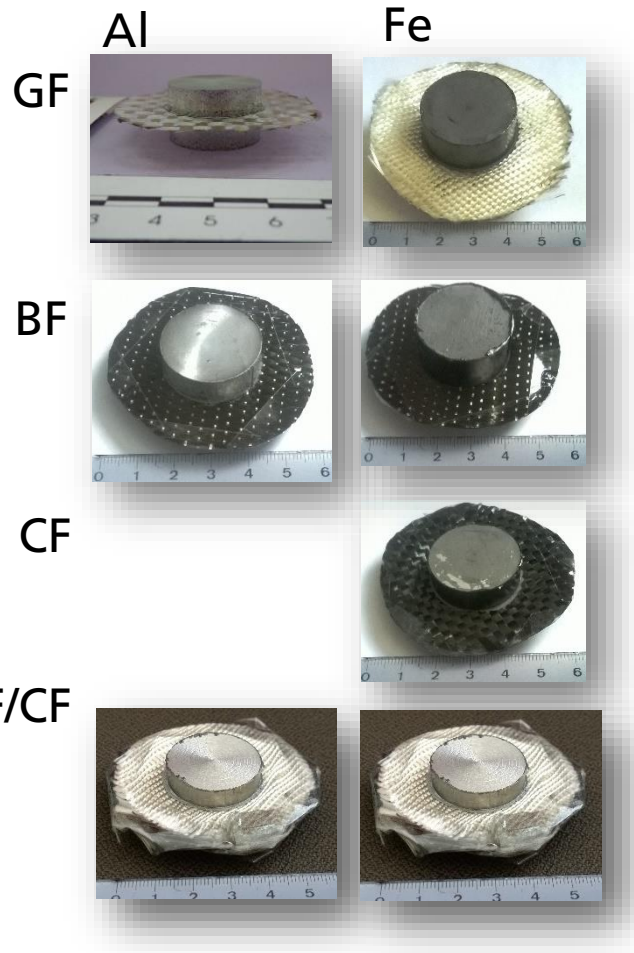

GF – Glas fiber BF – Basalt fiber CF – Carbon fiber

© Fraunhofer IFAM Dresden

DRESDEN concept

Fraunhofer IFAM Branch Lab Dresden

Contact: Thomas.Weissgaerber@ifam-dd.fraunhofer.de (head of department), Thomas.Hutsch@ifam-dd.fraunhofer.de (research fellow)

Metal/ FRP Connection module – Prediction of strength

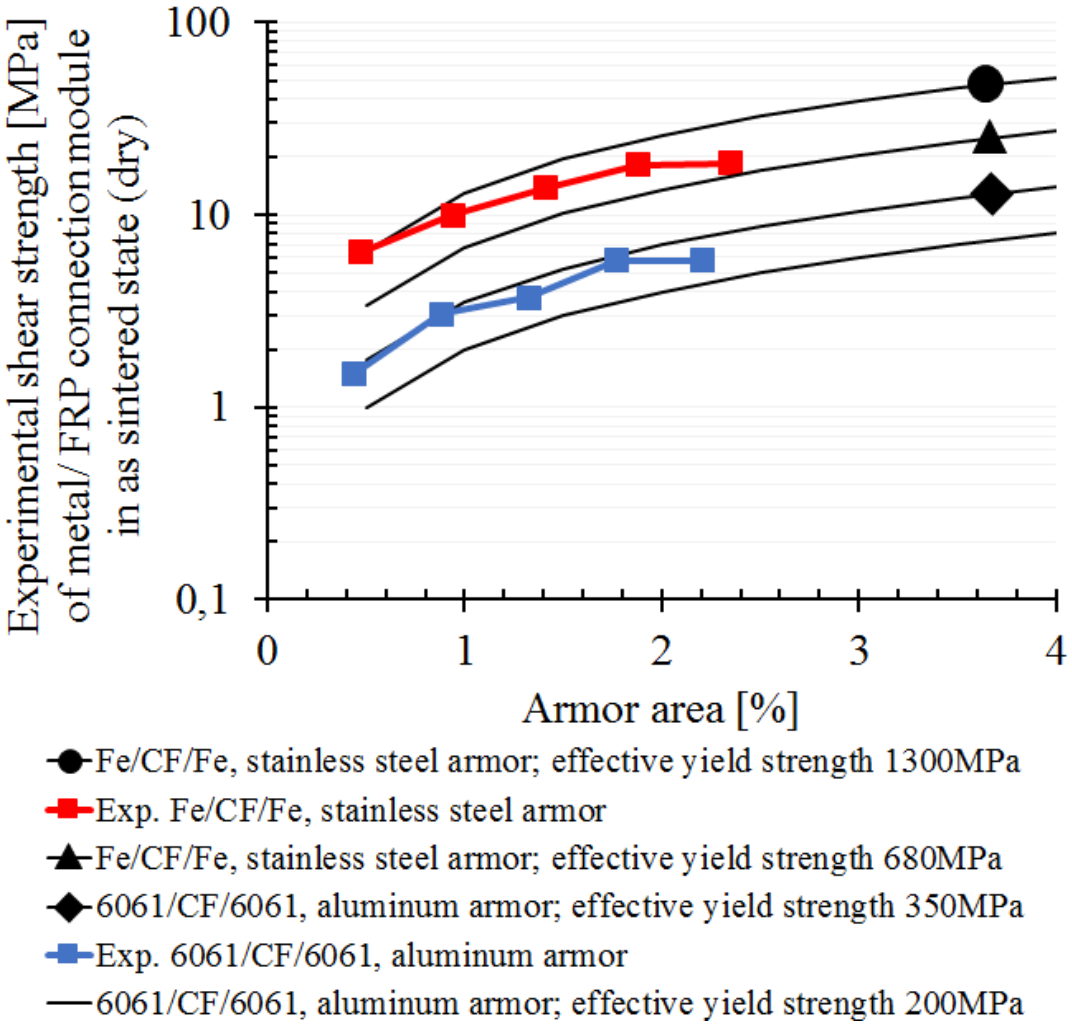

Computer tomography

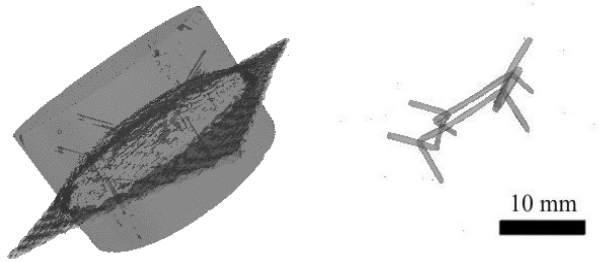

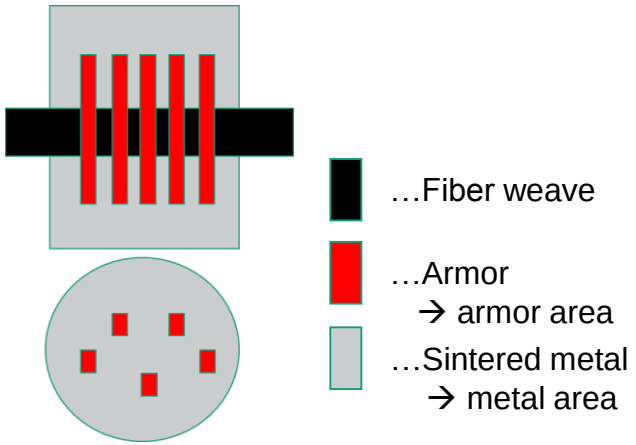

© Fraunhofer IFAM Dresden

DRESDEN concept

Fraunhofer IFAM Branch Lab Dresden

Contact: Thomas.Weissgaerber@ifam-dd.fraunhofer.de (head of department), Thomas.Hutsch@ifam-dd.fraunhofer.de (research fellow)

Metal/ FRP Connection module – Consolidation using Tailor Fiber Placement (TFP) preforms

- Experimental

Cu Powder

TFP

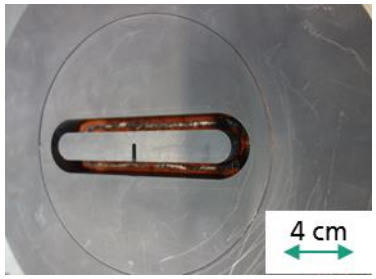

a) Cu coated b) raw

Spark Plasma Sintering

T_{sinter} ca. 680 °C (thermocouple in top stamp);
Holding time 1 min; p_{Sinter} = 30 MPa; heating rate = 100K/min;

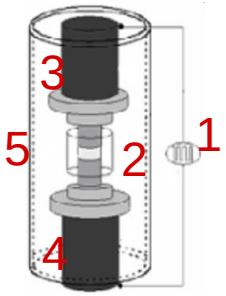

1 Electrical puls generator
2 Pressing tool with sample
3 Upper stamp
4 Lower stamp
5 Vacuum chamber

Sintered sample
copper reinforced with TFP

© Fraunhofer IFAM Dresden

DRESDEN concept

Fraunhofer IFAM Branch Lab Dresden

Contact: Thomas.Weissgaerber@ifam-dd.fraunhofer.de (head of department), Thomas.Hutsch@ifam-dd.fraunhofer.de (research fellow)

Metal/ FRP Connection module – Specific strength using Tailor Fiber Placement (TFP) preforms

- Tensile test of different setup

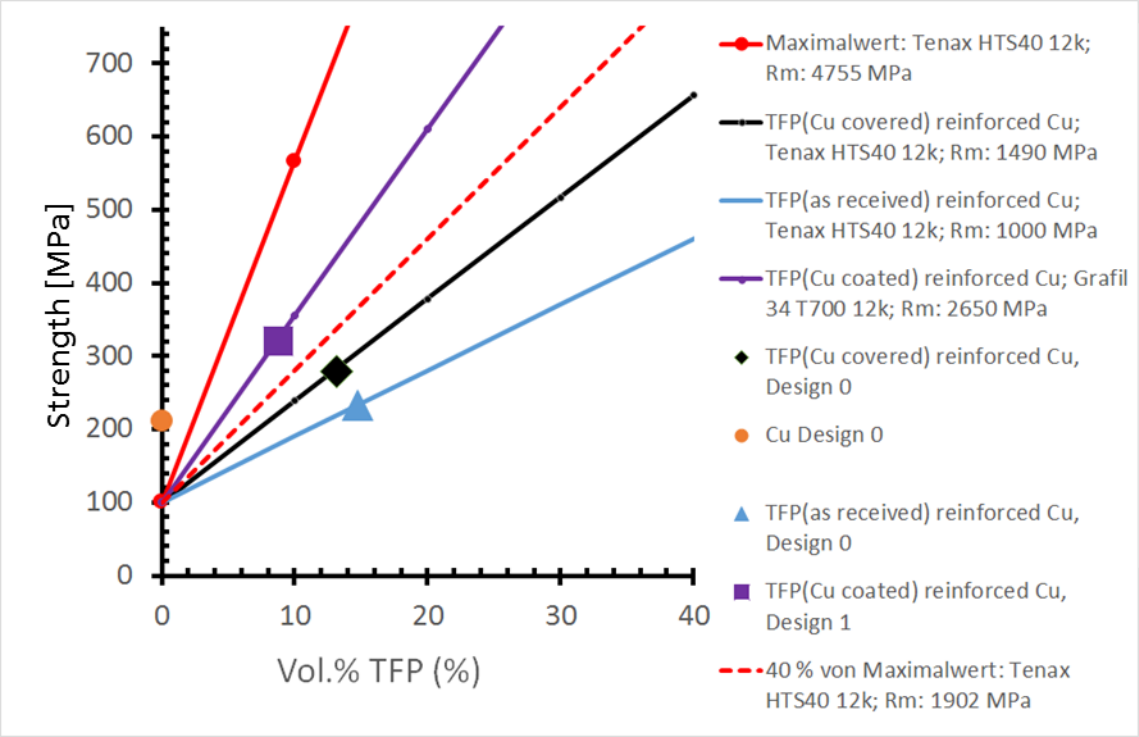

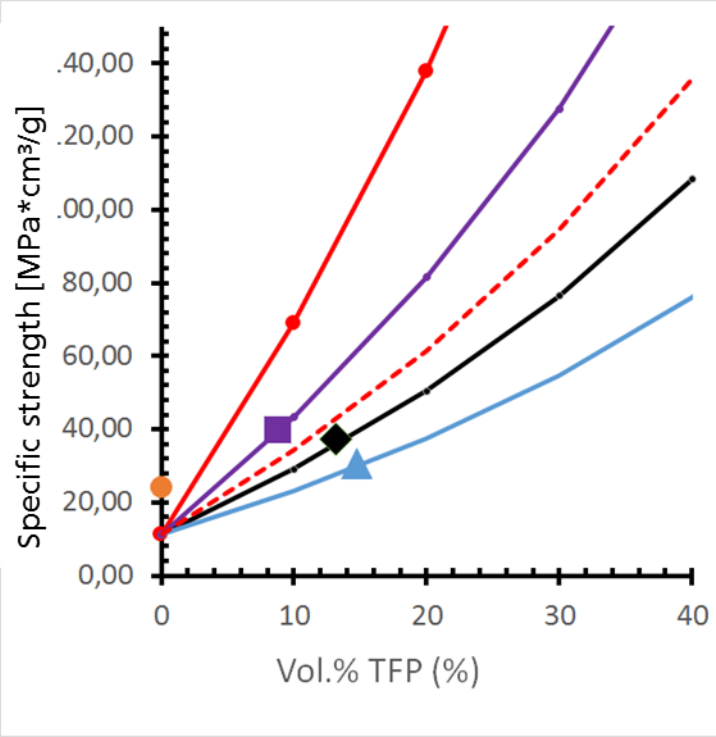

© Fraunhofer IFAM Dresden

DRESDEN concept

Fraunhofer IFAM Branch Lab Dresden

Contact: Thomas.Weissgaerber@ifam-dd.fraunhofer.de (head of department), Thomas.Hutsch@ifam-dd.fraunhofer.de (research fellow)

Metal/ FRP Connection module

- Options to connect Fiber reinforced plastics (FRP) using the connection module
  - Assembly by welding
  - Textil Fabric
  - Positive substance jointing
  - Adhesive bonding
  - Assembly by force fitting
  - Screwing
  - Shrink fitting
  - Rivetted bolt
  - …

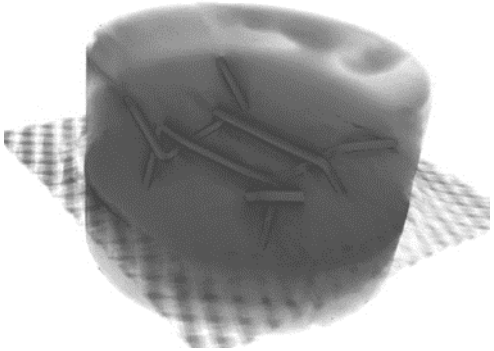

Computer tomography

Welded load transmission point in FRP

Tail plane mounting bracket in FRP

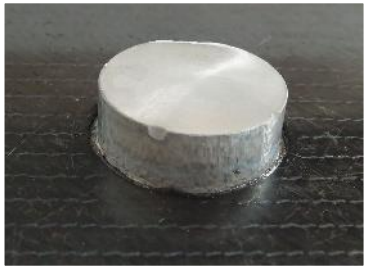

Textile joining to FRP

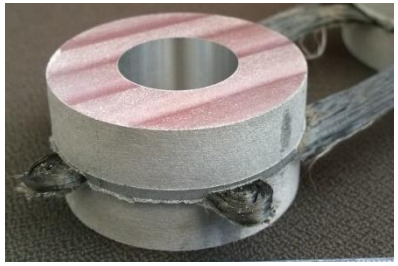

Load transfer elements with TFP reinforcement

According DIN 8593

© Fraunhofer IFAM Dresden

DRESDEN concept

Fraunhofer IFAM Branch Lab Dresden

Contact: Thomas.Weissgaerber@ifam-dd.fraunhofer.de (head of department), Thomas.Hutsch@ifam-dd.fraunhofer.de (research fellow)

Metal/ FRP Connection module – End use field

- Load transfer elements

Integration of TFP (tailored fiber placement) in metals like:
- Copper
- Titanium
- Stainless steel
- Aluminium
- Other on request

Local or full housing of the TFP with sintered metal

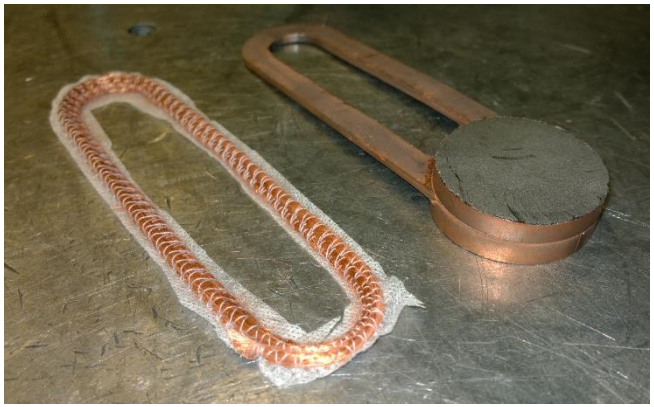

Use of raw or coated fibers for integration

Design of TFP according load

→ Adapted load transfer, increasing specific strength and temperature strength

© Fraunhofer IFAM Dresden

DRESDEN concept

Fraunhofer IFAM Branch Lab Dresden

Contact: Thomas.Weissgaerber@ifam-dd.fraunhofer.de (head of department), Thomas.Hutsch@ifam-dd.fraunhofer.de (research fellow)

Metal/ FRP Connection module – End use field

- Front wing mounting bracket

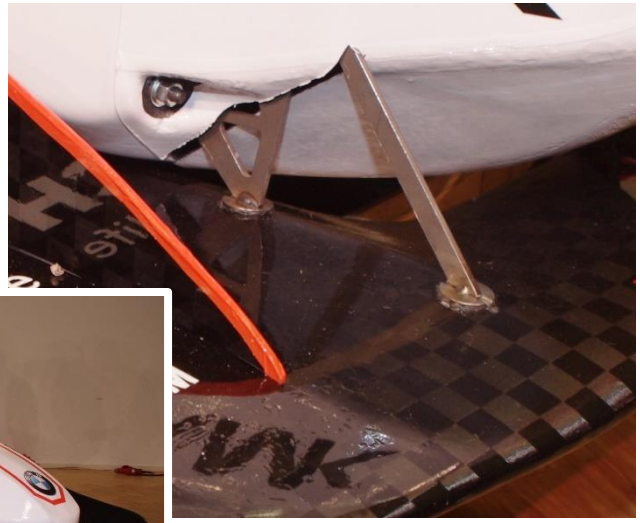

Load: Max. force x = -150 N,
Max. force y = +/- 100 N,
Max. force z = -375 N

x equal to driving direction

RollOut 2016

Solution:

Stainless steel:

- Connection (diameter 28 mm)
- Laminated front wing welded to the supporting structure

→ Advanced design potential and handling of CFK part like a steel sheet part

© Fraunhofer IFAM Dresden

DRESDEN concept

ELBFLORACEN Electric

Fraunhofer IFAM Branch Lab Dresden

Contact: Thomas.Weissgaerber@ifam-dd.fraunhofer.de (head of department), Thomas.Hutsch@ifam-dd.fraunhofer.de (research fellow)

Metal/ FRP Connection module – End use field

- Tail plane mounting bracket

RollOut 2016

Load: Max. force x = -150 N,
Max. force y = +/- 100 N,
Max. force z = -375 N

x equal to driving direction

Solution:

Stainless steel:

- Connection (diameter 28 mm)
- Sintered body machined before lamination process, screwed to supporting structure

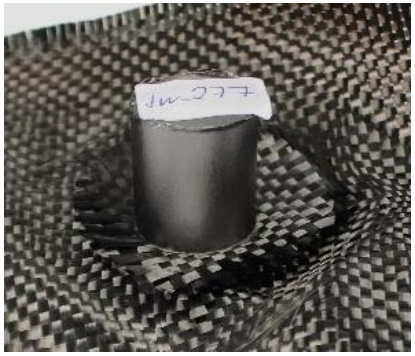

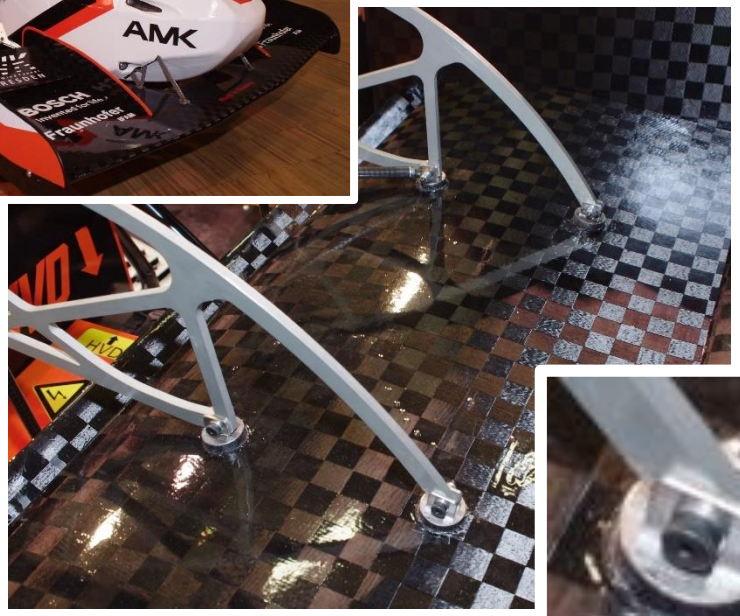

→ Advanced design potential and flexibility of mounting method

© Fraunhofer IFAM Dresden

DRESDEN concept

ELBFLORACEN Electric

Fraunhofer IFAM Branch Lab Dresden

Contact: Thomas.Weissgaerber@ifam-dd.fraunhofer.de (head of department), Thomas.Hutsch@ifam-dd.fraunhofer.de (research fellow)

Metal-Carbon composites at IFAM Dresden – Strong partner for development and prototype realization

passive cooling

- Metal-Diamond

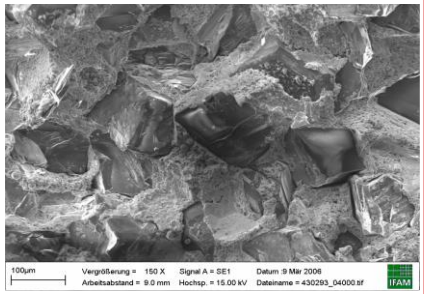

- Metal-Graphite

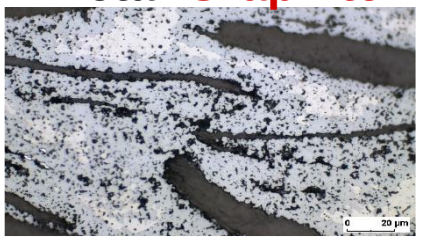

damping

- Metal-C-fibre

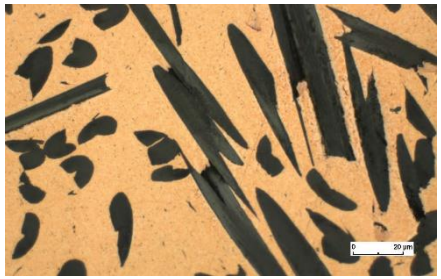

- Metal-Carbon Nanotube (CNT)

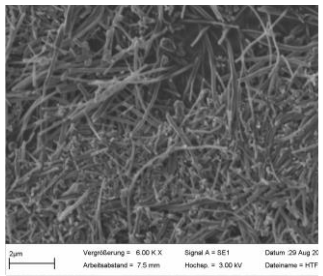

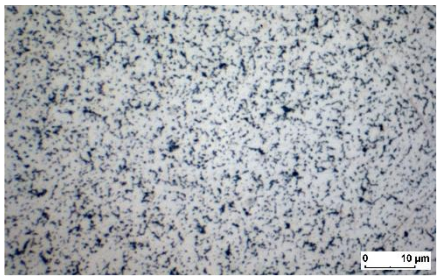

increase in strength

- Metal-Graphen
- Metal-Fullerene

load transfer

- Metal-FRP connection module

© Fraunhofer IFAM Dresden

DRESDEN concept

Fraunhofer IFAM Branch Lab Dresden

Contact: Thomas.Weissgaerber@ifam-dd.fraunhofer.de (head of department), Thomas.Hutsch@ifam-dd.fraunhofer.de (research fellow)

Metal-Carbon composites at IFAM Dresden – Strong partner for development and prototype realization

- Our offer

- Development and optimisation of the metal/ carbon composites regarding the needs of the application
  (for example: powder composition, consolidation method, shaping, integration in surounding processes)

- Characterisation in regarding mechanical, thermo-physical and electrical properties; X-ray diffraction; element analysis; fractography; metallography

- Planing and build up of prototypes

- Realisation of small batch series

- Technology transfer to customer

© Fraunhofer IFAM Dresden

DRESDEN concept

Fraunhofer IFAM Branch Lab Dresden

Contact: Thomas.Weissgaerber@ifam-dd.fraunhofer.de (head of department), Thomas.Hutsch@ifam-dd.fraunhofer.de (research fellow)

Thank you for your attention

The authors would like to thank the European Community and the German Federal Ministry of Education and Research for financial support of this project.

A part of this work has been performed within the framework of the Integrated European Project **"ExtreMat"** (contract NMP-CT-2004-500253).

Contact: E-Mail: Thomas.Weissgaerber@ifam-dd.fraunhofer.de (head of department)
Thomas.Hutsch@ifam-dd.fraunhofer.de (research fellow)

© Fraunhofer IFAM Dresden

DRESDEN concept

Fraunhofer IFAM Branch Lab Dresden

Contact: Thomas.Weissgaerber@ifam-dd.fraunhofer.de (head of department), Thomas.Hutsch@ifam-dd.fraunhofer.de (research fellow)

METAL/ CARBON COMPOSITES DEVELOPMENT, APPLICATIONS AND NEW BUSINESS OPPORTUNITIES – POWDER METALLURGICAL APPROACH

Th. Hutsch[1], Th. Weißgärber[1], B. Kieback[1]

[1] Fraunhofer Institute for Manufacturing Technology and Advanced Materials IFAM, Branch Lab Dresden, Winterbergstr. 28, D-01277 Dresden

GEFÖRDERT VOM

Bundesministerium für Bildung und Forschung

Thank you for your attention

Contact: E-Mail: Thomas.Weissgaerber@ifam-dd.fraunhofer.de (head of department)
Thomas.Hutsch@ifam-dd.fraunhofer.de (research fellow)

© Fraunhofer IFAM Dresden

DRESDEN concept

Fraunhofer IFAM Branch Lab Dresden

Contact: Thomas.Weissgaerber@ifam-dd.fraunhofer.de (head of department), Thomas.Hutsch@ifam-dd.fraunhofer.de (research fellow)

陶瓷基複合材料的新產品機遇及特點

由國立台灣大學材料科與工程系暨研究所特聘教授主講

International Conference on new materials technologies – The business opportunities arise from functionality excellence

New Product Opportunities and Features with Ceramic Composite Materials -

Composite Substrates with High Thermal Conductivity

Prof. Wei-Hsing Tuan
段維新 教授
National Taiwan University
國立臺灣大學

Jan. 29, 2018 @ HK

HKPC

1

Contents

- Background
- Demand on thermal dissipation
- Composite substrates
  - Bond ceramic to metal
    - Al_2O_3/Cu, AlN/Cu
  - Bond ceramic to graphite
    - Al_2O_3/AgCuTi/graphite, AlN/AgCuTi/graphite

Background

- Ceramic substrates
  - Al_2O_3
  - AlN
- Properties
  - Relatively low thermal conductivity
  - Electrical insulator
  - Electrical contact is needed

3

Background

- Demand on thermal dissipation
  - LED lighting
  - Power IC: IGBT
  - etc

4

Opportunities

- **Bonding ceramic to material with high thermal conductivity**
  - Thermal conductivity of Al_2O_3~24 W/mK
  - Thermal conductivity of AlN~200 W/mK
- **Bonding ceramics to copper**
  - Thermal conductivity of Cu ~ 400 W/mK
- **Bonding ceramics to graphite**
  - Thermal conductivity of graphite in x-y plane: 1000 W/mK

5

Bonding Copper to Ceramics -

Background and Objectives
Current status
Challenges
Application
Summary

Ref: Tuan & Lee, J. Euro. Ceram. Soc., 2014

6

Challenging area

- One important step toward integration
- Key step for the development of system

Objective
Joining metal to ceramics

- Many techniques to join metals to ceramics
  - Brazing
    - Ag-Cu tape
    - Ag-Cu-Ti tape
    - Mo-Mn paste
  - Diffusion bonding
    - External load is needed
  - ***Direct bonding copper (DBC)***

Advantages of using direct bonding copper (DBC)

- No brazing material is needed
- No external pressure is needed
- Bond Cu to many ceramics

9

Systems

- Bond copper to oxides
  - Cu-Al_2O_3
- Bond copper to nitrides
  - Cu-AlN
- Challenge

10

Wetting of Cu melt on Al_2O_3 : poor

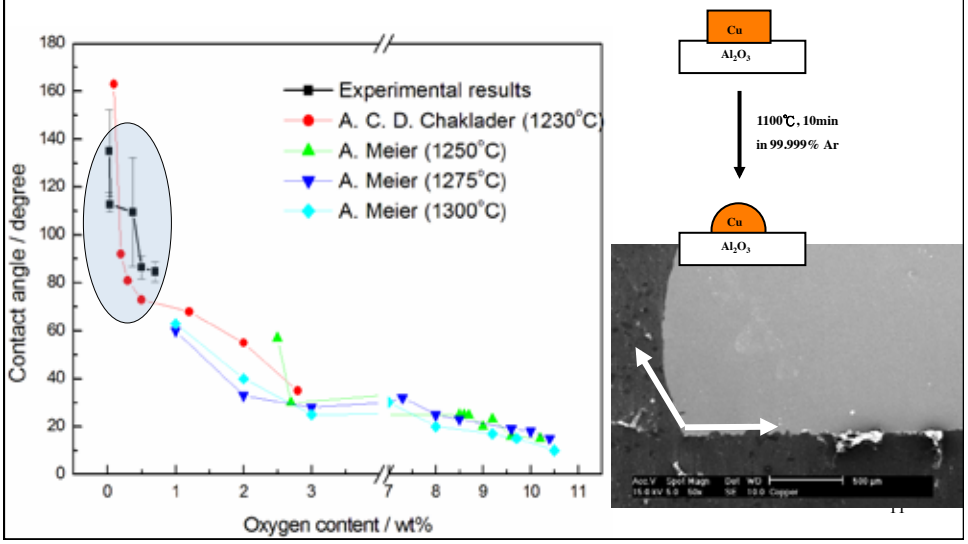

11

Key to the wetting: Oxygen

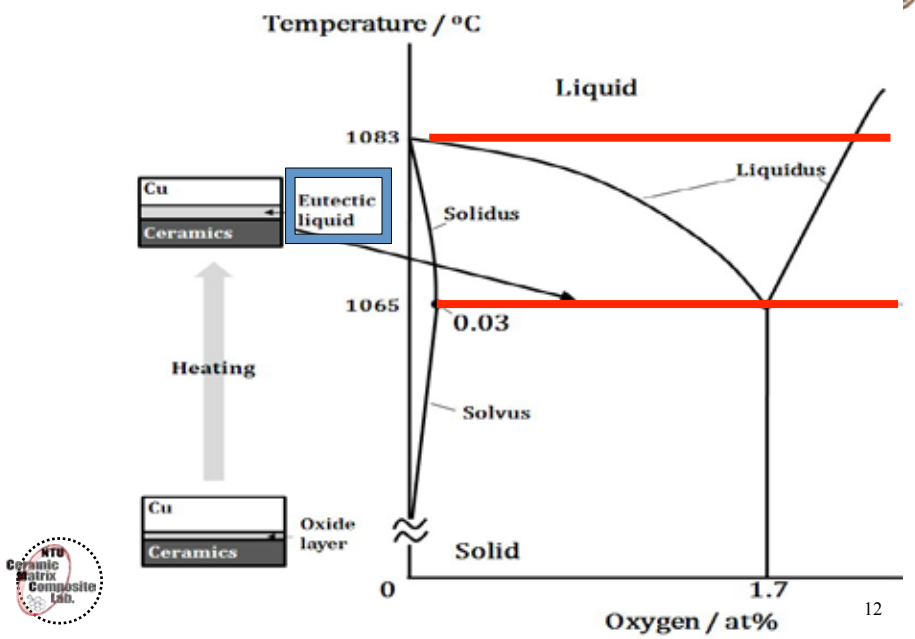

12

Processing of direct bond copper (DBC)

- Key to the success of DBC: oxygen
- Introduce oxygen through pre-oxidation
  - Temperature: 300°C to 1000°C
- Joining copper to oxides or nitrides
  - 1065°C to 1083°C

13

Al_2O_3/Cu substrate

- Direct bond copper (DBC) process
  - Pre-oxidation @ 300°C to 900°C
  - Bonding at 1075°C in nitrogen

14

Performance of Al_2O_3/Cu substrates

		Test methods or standard
Thermal conductivity	***>30 W/mK***	Laser flash method, ASTM E-1461
Breakdown voltage	> 3kV (AC)	ASTM 149-97a
Flexural strength	> 300 MPa	4-point bending
Interface energy release rate	*>30 J/m²*	4-point bending

15

Measurement of interface strength

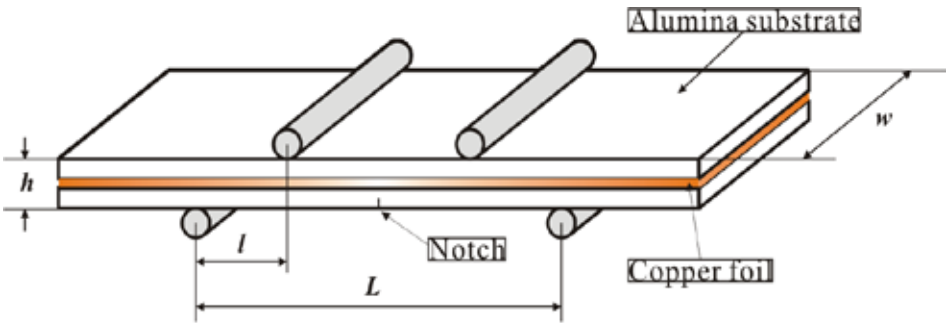

Cross-head rate: 0.001mm/sec

w=7mm, h=1.7mm, l=4.0mm and L=20mm

16

Load-displacement curve

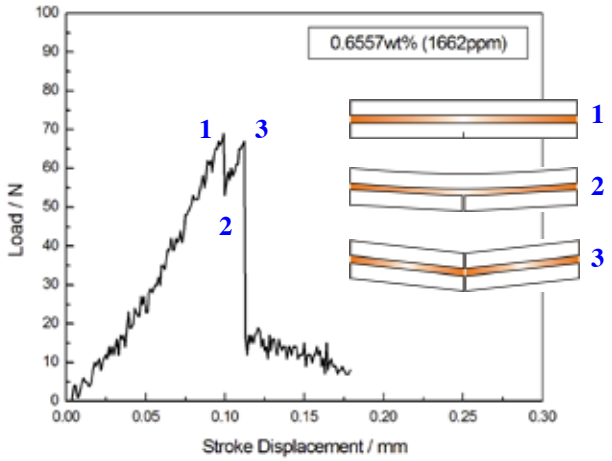

17

Microstructure at interface

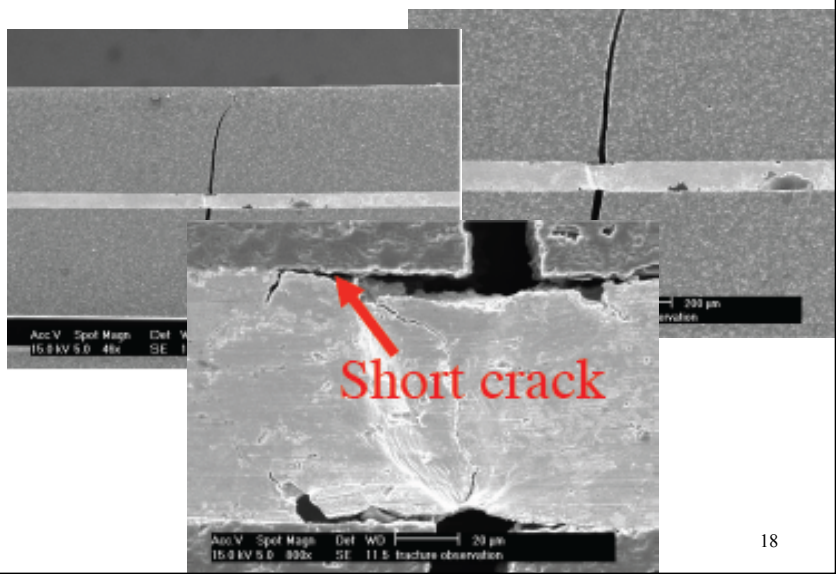

18

High interface strength

Interface energy release rate > 30 J/m^2

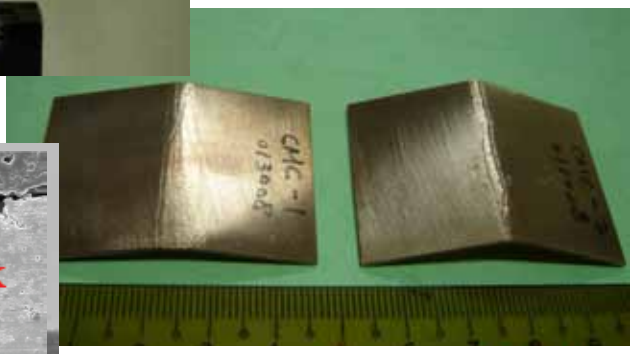

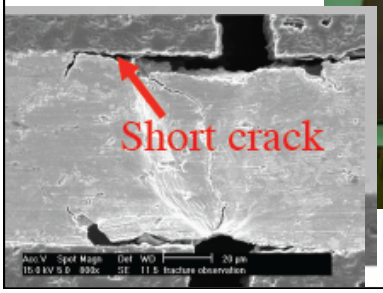

19

Processing of AlN/Cu substrate

- Pre-oxidation
  - Oxidation of AlN, 900°C-1450°C
  - Oxidation of Cu, 300°C-900°C
- Direct bonding, 1075°C

20

AlN/Cu bilayer

- Thermal conductivity in z-direction: 100 W/mK (flash method)

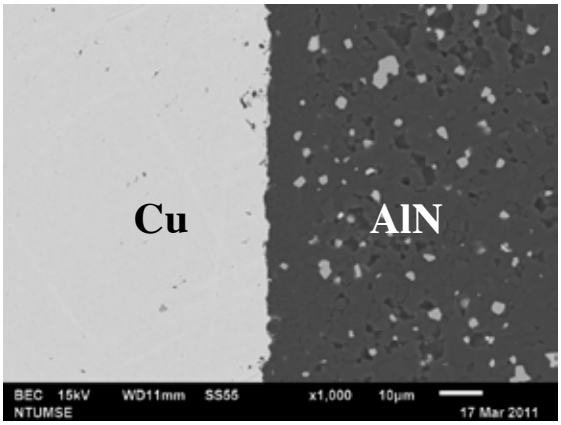

21

Interface for Al_2O_3/Cu substrate

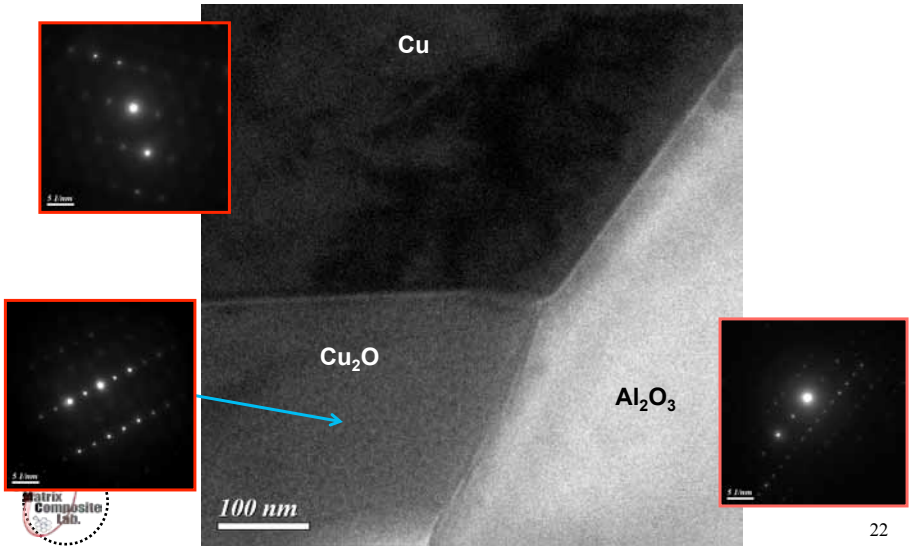

22

Results & Discussion

TEM analysis – Cu/Al_2O_3 interface

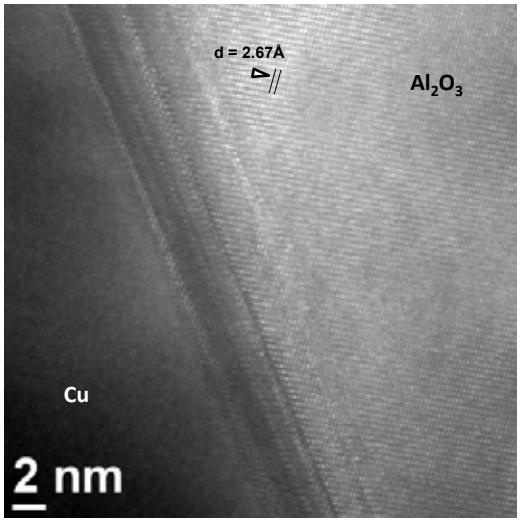

Results & Discussion

TEM analysis – Cu_2O/Al_2O_3 interface

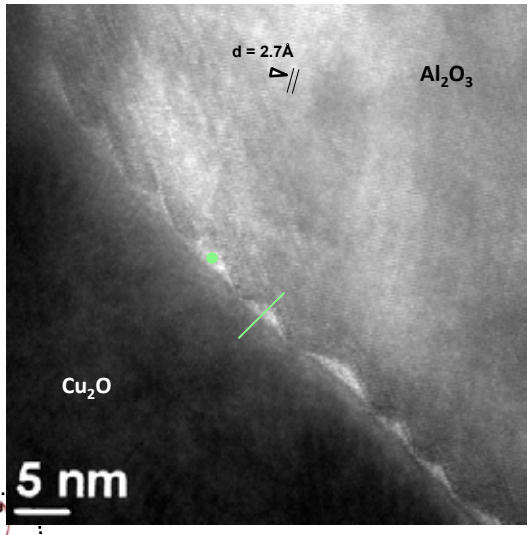

Ele.	At.%
Cu	28
Al	20
O	52

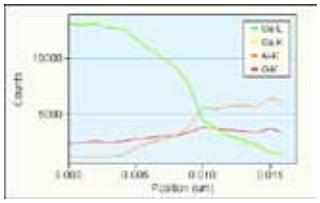

$Cu_2O + Al_2O_3 = 2CuAlO_2$

Why high thermal conductivity?

TEM analysis

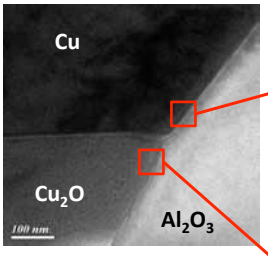

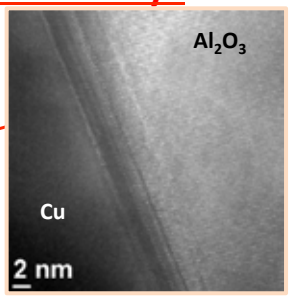

Low thermal resistance

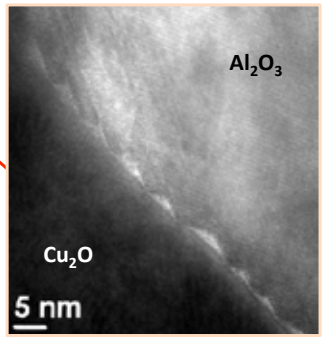

High thermal resistanc

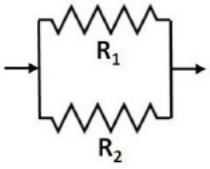

Current status

Good news:
Indeed, DBC is a straightforward process!

Bad news:
DBC is full of challenges !

HKPC

Challenges : Pores at interface

- Large pores are found at the Cu/ceramic interface
- Performance of DBC substrates is suffered
  - Bonding strength
  - Reliability

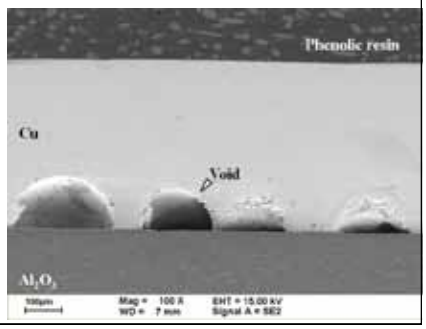

Pores at interface

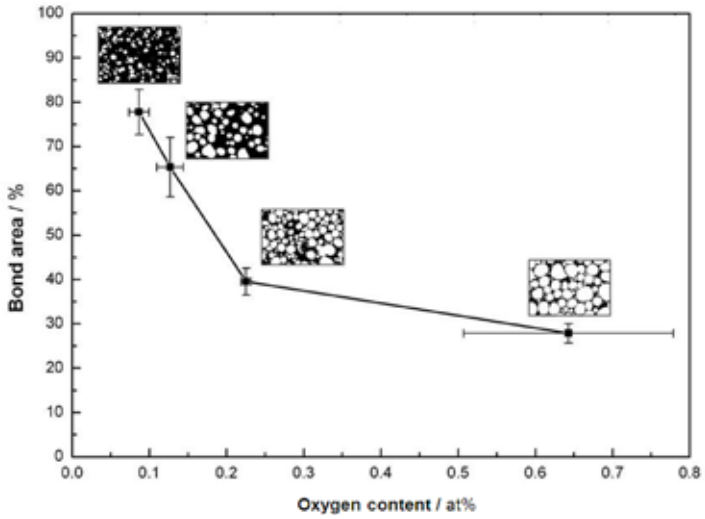

28

Interface engineering

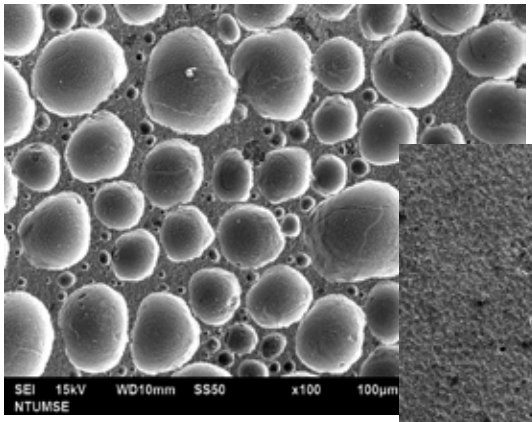

before

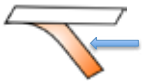

after

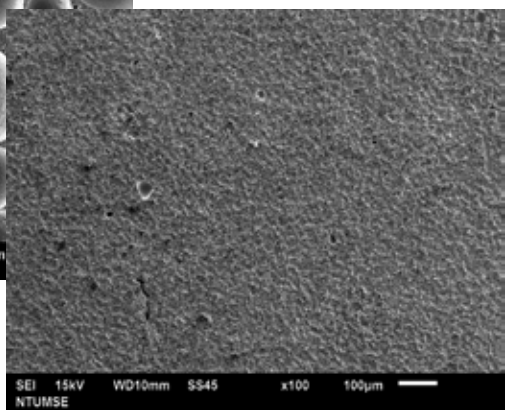

Reliability testing for sapphire/Cu bilayer (-55°C-155°C)

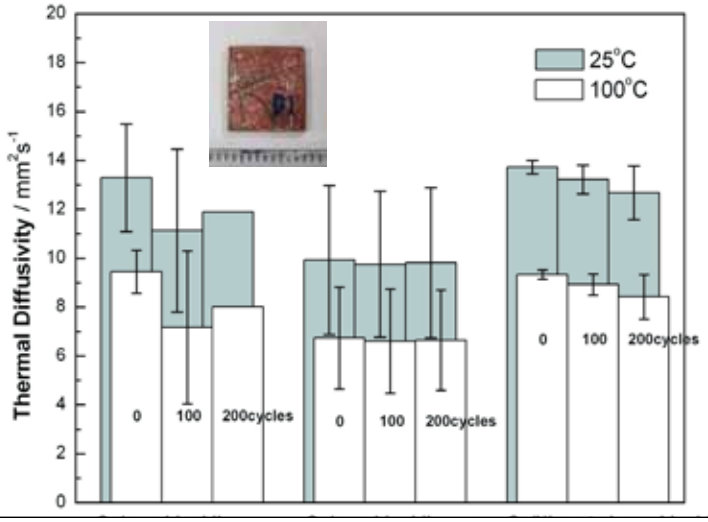

Summary for DBC

- Direct bonding copper (DBC) technique can be used to prepare
  - Al_2O_3/Cu substrate
  - AlN/Cu substrate
- Strong interface can be produced.

Summary for DBC

- The thermal conductivity of the DBC substrate is high as long as its interface is clean.
- The amount of oxygen is the key for the formation of pores at interface.

Patents

- 美國
- Method of manufacturing ceramic/metal composite structure, US 8,127,441 B2.
- Ceramic/metal composite structure and method of manufacturing the same, US 7,806,311 B2.
- Package assembly with heat dissipation structure, US 7,746,644 B2.
- Fully reflective and highly thermoconductive electronic module and method of manufacturing the same, US 8,304,660 B2.
- 中國
- 陶瓷/金屬複合結構之製造方法, CN 101439984B.
- 陶瓷/金屬複合結構及其製造方法, CN 101439983 B.
- 台灣
- 1. 陶瓷/金屬複合結構及其製造方法, I 335,792.
- 2. 陶瓷/金屬複合結構之製造方法, I 347,825.

33

Publication

ELSEVIER

Available online at www.sciencedirect.com

ScienceDirect

Journal of the European Ceramic Society 34 (2014) 4117–4130

www.elsevier.com/locate/jeurceramsoc

Review

Eutectic bonding of copper to ceramics for thermal dissipation applications – A review

Wei-Hsing Tuan*, Shao-Kuan Lee

Department of Materials Science & Engineering, National Taiwan University, Taipei 106, Taiwan

Received 3 April 2014; received in revised form 5 July 2014; accepted 8 July 2014

Available online 29 July 2014

34

Bonding Copper to graphite -

- Background and Objectives
- Current status
- Challenges
- Application
- Summary

Ref: Tuan & Lee, J. Euro. Ceram. Soc., 2014

35

Systems

- Bonding of graphite paper to ceramics
  - Al_2O_3-AgCuTi-graphite
  - AlN-AgCuTi-AlN
  - AlN-AgCuTi-graphite
- Properties
  - Mechanical property
  - Thermal property
- Summary

3

Graphene

- Excellent thermal conductor
  - Thermal conductivity > 5000 W/mK
- Size limit
- Hard to handle

37

Graphite paper

- Graphite in paper form
- Prepared by hot-pressing of polyimide
- Advantages
  - Width > 1 m
  - Thickness ~ 25 micrometer
  - Flexible and workable
- Applications
  - Heat spreader for mobile devices

38

Phase analysis for graphite paper

Highly anisotropic !

Thermal conductivity=?

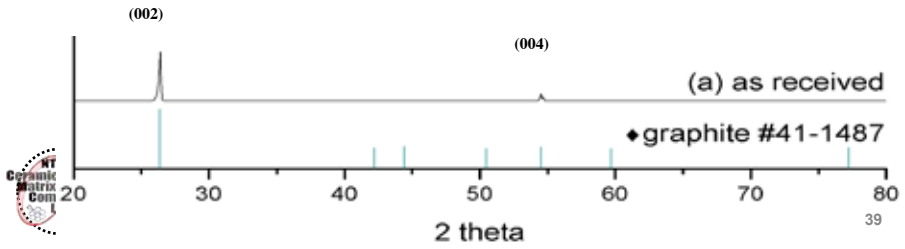

39

Characterization of graphite paper

- Graphite paper is thin !
- Preparation of bulk graphite by laminating graphite papers with a small amount resin
- To determine the thermal conductivity with a flash method

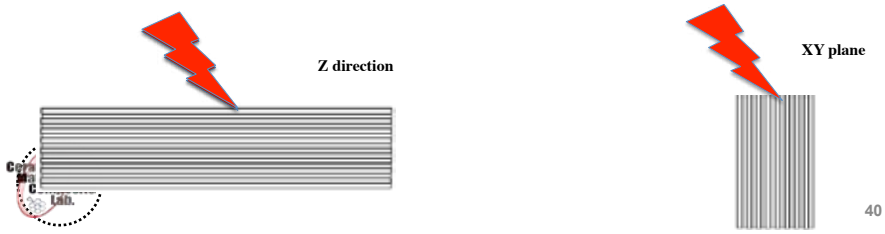

40

Thermal diffusivity of graphite paper

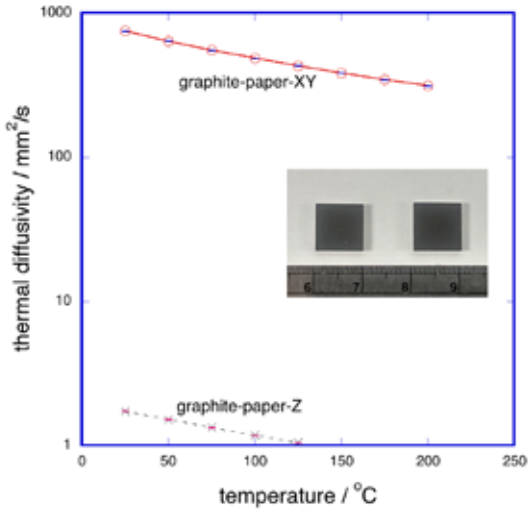

41

Heat capacity

- Heat capacity of graphite [ref]
  - XY direction: 0.64-0.71 J/gK
  - Z direction: 0.93 J/gK
- Thermal conductivity =
  - thermal diffusivity x heat capacity x density

Ref: S. Picard, D. Burns, P. Roger, Rapport BIPM-2006/01, International Bureau of Weights and Measures, France (2006).

42

Thermal conductivity of graphite paper

- Thermal conductivity of graphite paper along XY plane : 1050 W/mK
  - Higher than Ag, Cu, Al
- Thermal conductivity of graphite paper along Z direction : 2.4 W/mK
- Anisotropic
  - Excellent thermal conductor along XY plane
  - Thermal insulator along Z direction

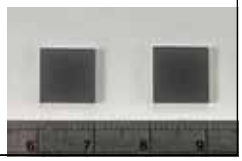

Graphite paper

- Dis-advantages
  - Rigidity is poor
  - Electrical insulation is poor
    - Electrical resistivity: 100~500 Ωcm
  - Not possible for high power devices

Objectives

- Improve the rigidity of graphite paper
  - By using a backing ceramic substrate
- High thermal conductivity
  - By using Al_2O_3 or AlN backing layers
- Raise the electrical resistance
  - By using Al_2O_3 or AlN backing layers

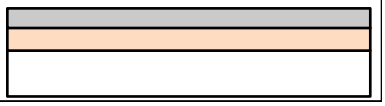

Bonding of graphite paper to ceramics
Using brazing technique

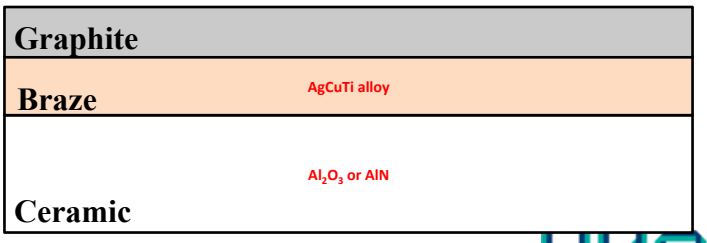

Materials

- Graphite paper
  - Prepared by hot-pressing polyimide
  - 25 micrometer
- Brazing foil
  - Ag-Cu-Ti alloy (68.8%Ag-26.7%Cu-4.5%Ti, Ticusil, Morgan Advanced Ceramics, Inc., USA)
  - 25 micrometer
- Alumina substrate
  - 96% Al_2O_3
- Aluminum nitride (AlN) substrate
  - $+Y_2O_3$

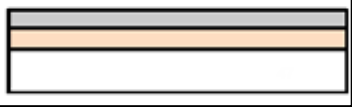

Experimental procedures

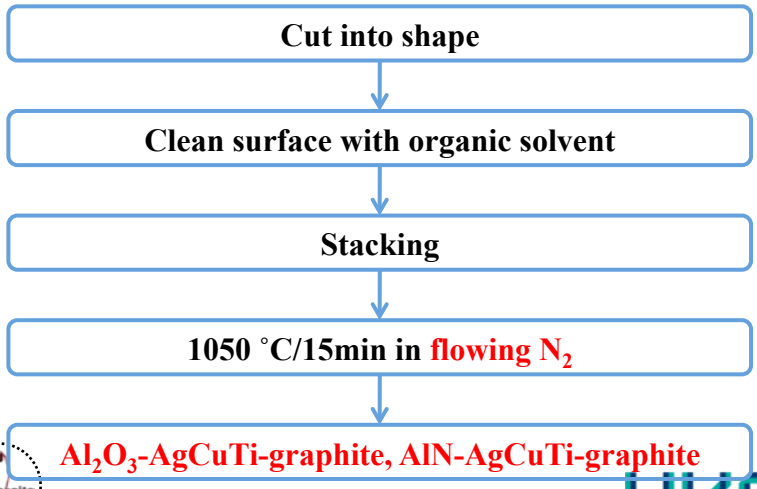

4

Unique features

- Brazing in flowing nitrogen
- At a slightly higher temperature
  - @ 1050 C

49

Al_2O_3-AgCuTi-graphite

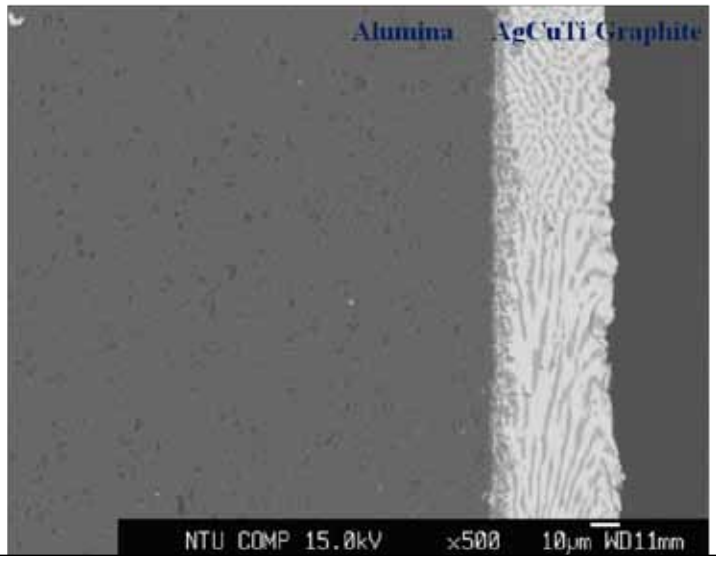

50

Al_2O_3-AgCuTi-graphite

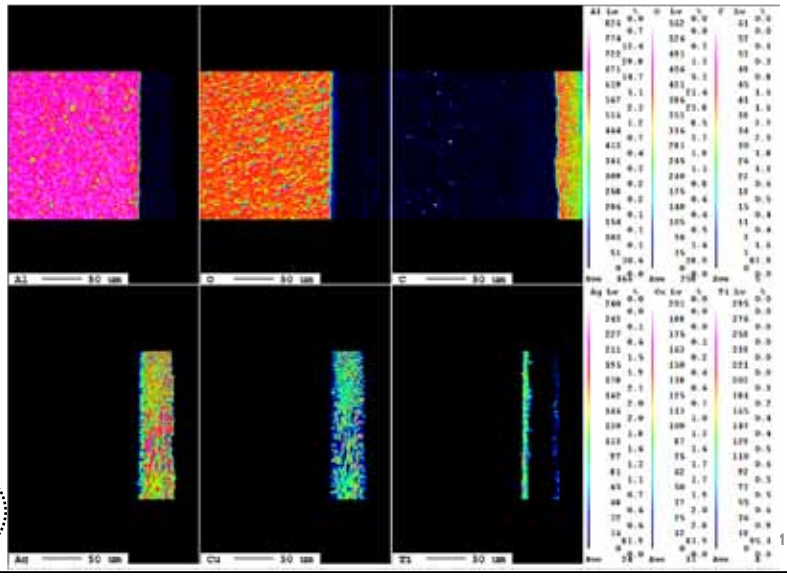

Distribution of Ti at interfaces

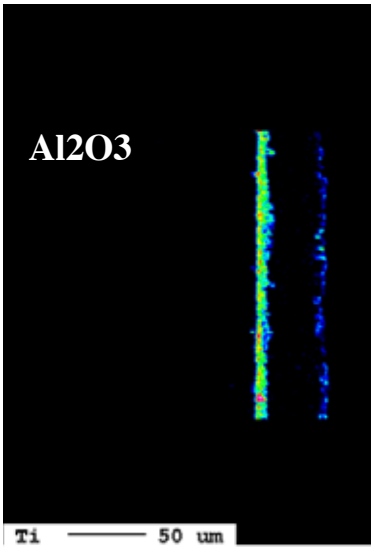

52

AlN-AgCuTi-AlN

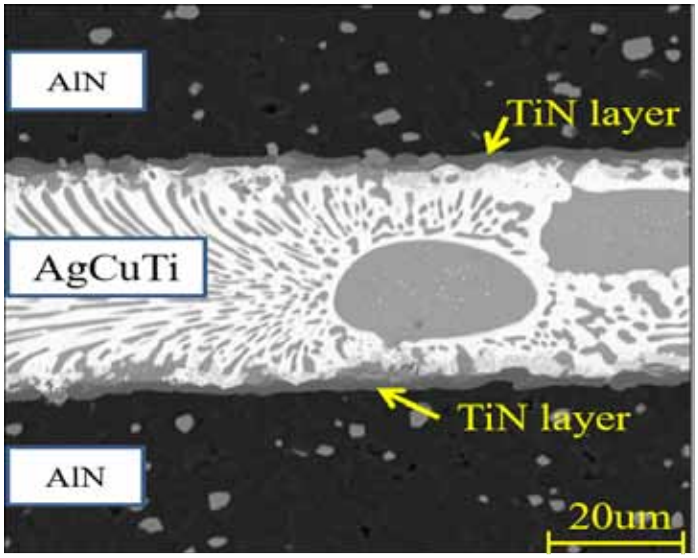

53

AlN-AgCuTi-AlN

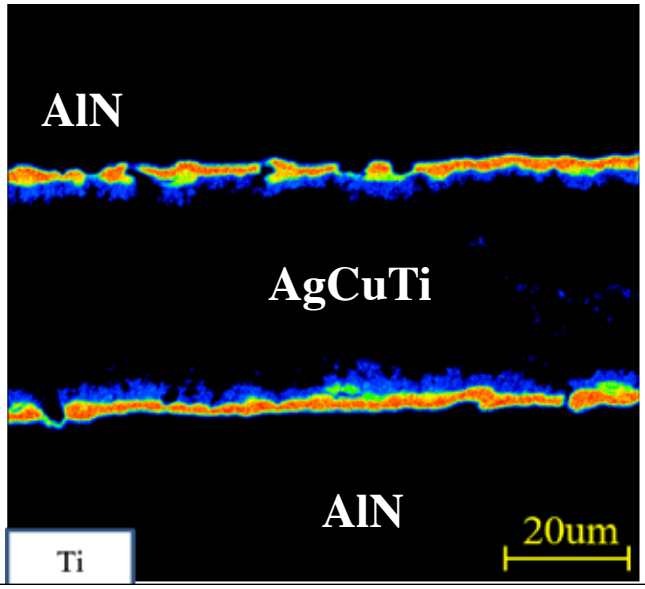

54

AlN-AgCuTi-AlN

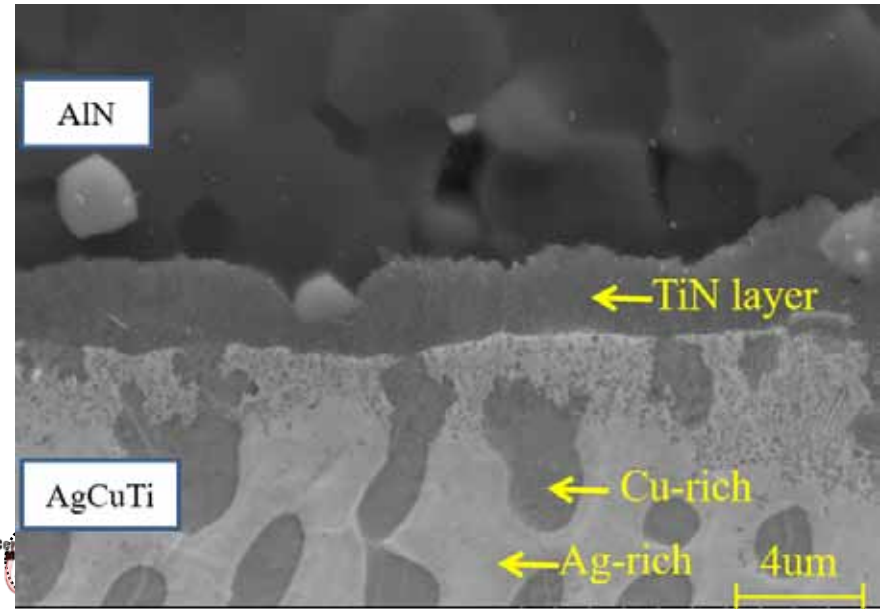

AlN-AgCuTi-graphite

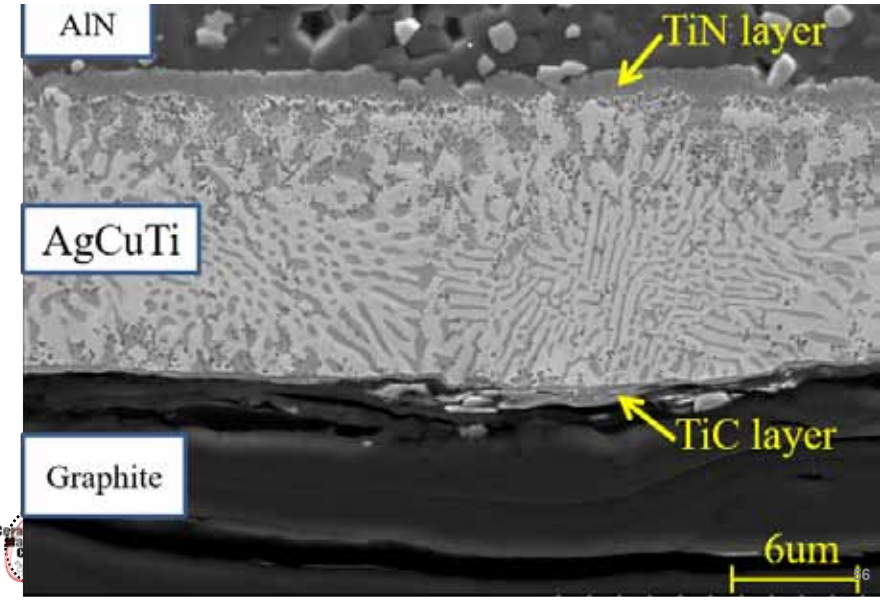

AlN-AgCuTi-graphite
EPMA mapping analysis

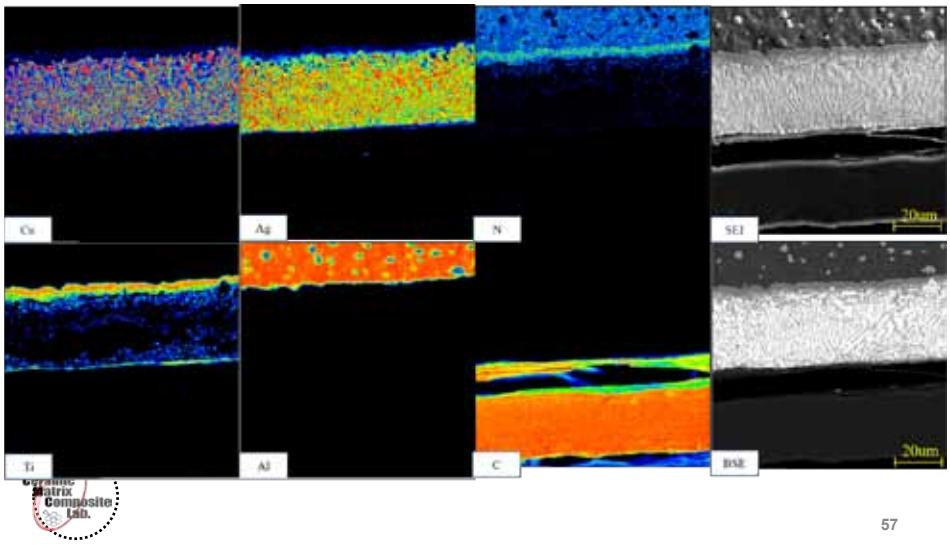

57

AlN-AgCuTi-graphite
EPMA mapping analysis

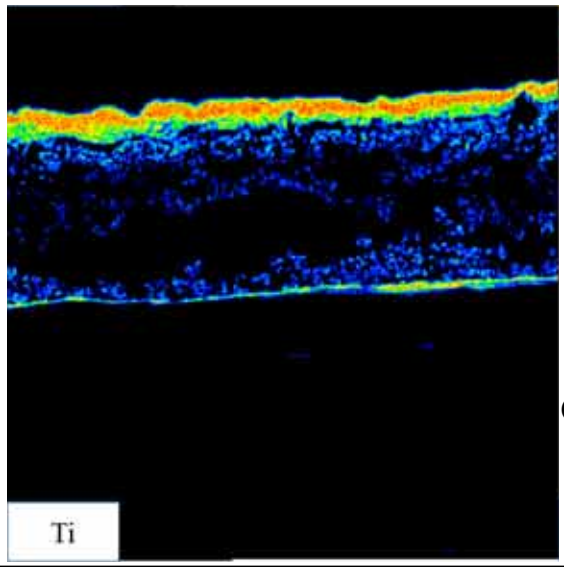

AlN

Graphite paper

58

AlN-AgCuTi-graphite

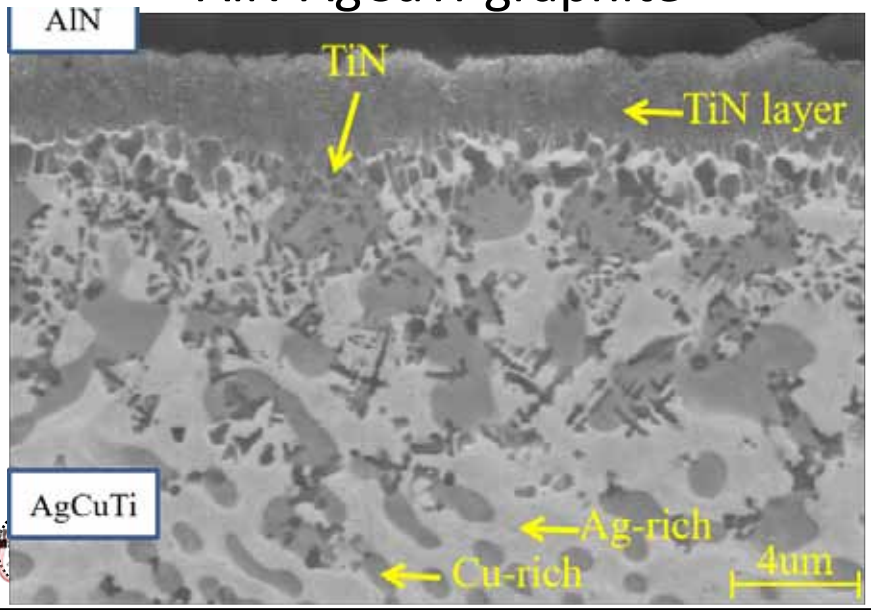

AlN-AgCuTi-graphite

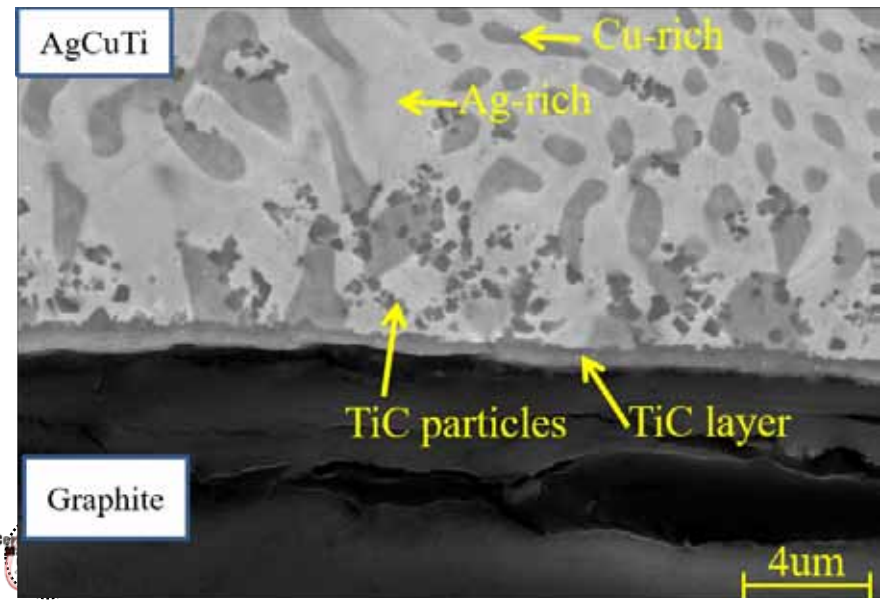

Characterization of AlN-graphite interface with XPS

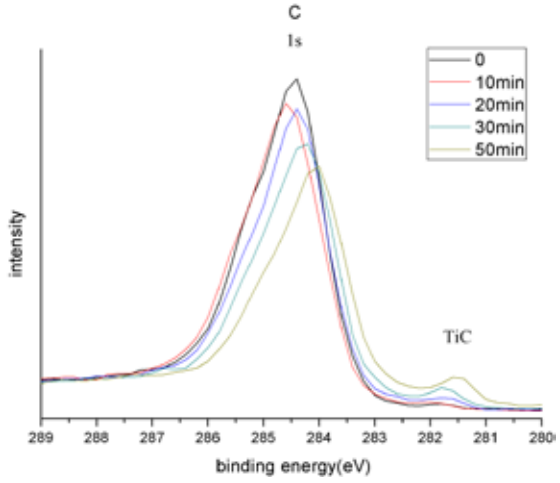

61

AlN substrate

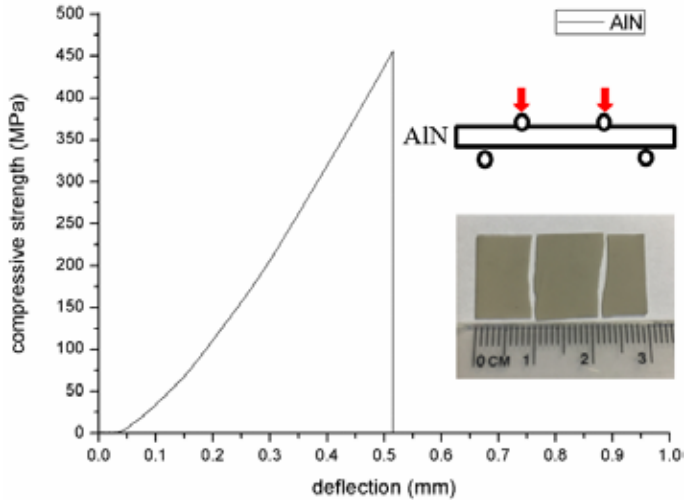

62

AlN-AgCuTi-AlN substrate

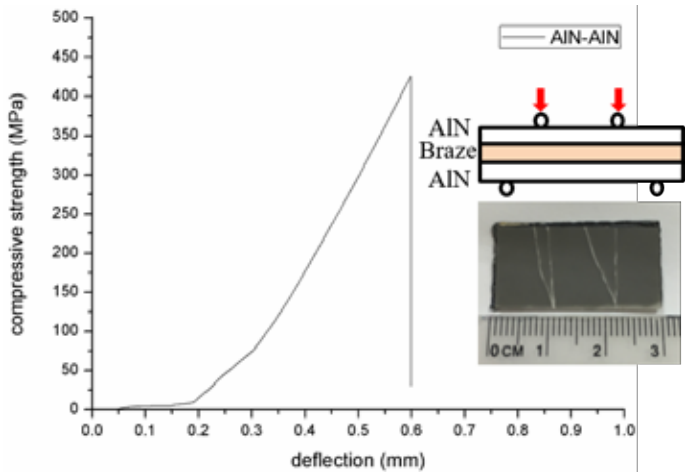

63

AlN-AgCuTi-graphite substrate

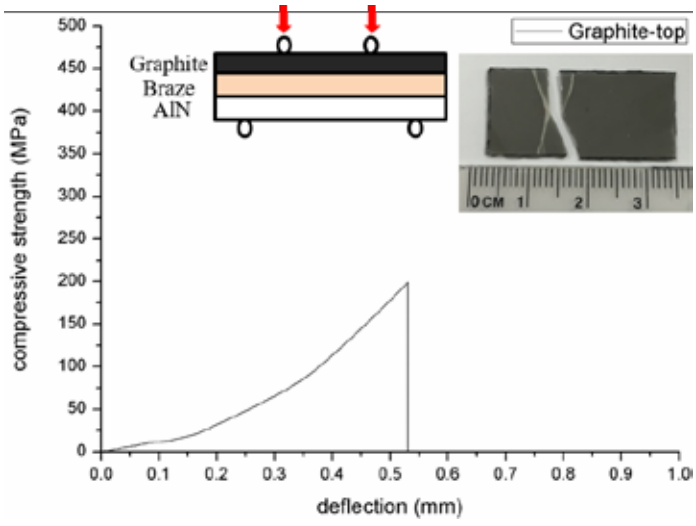

64

AlN-AgCuTi-graphite substrate

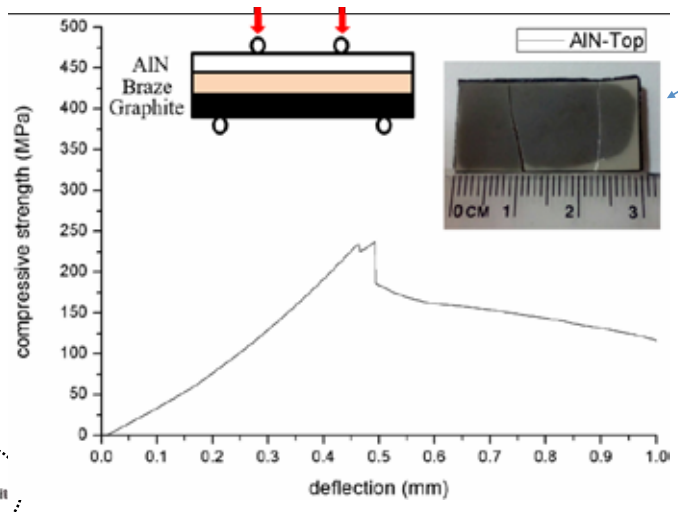

65

Al_2O_3-AgCuTi-graphite

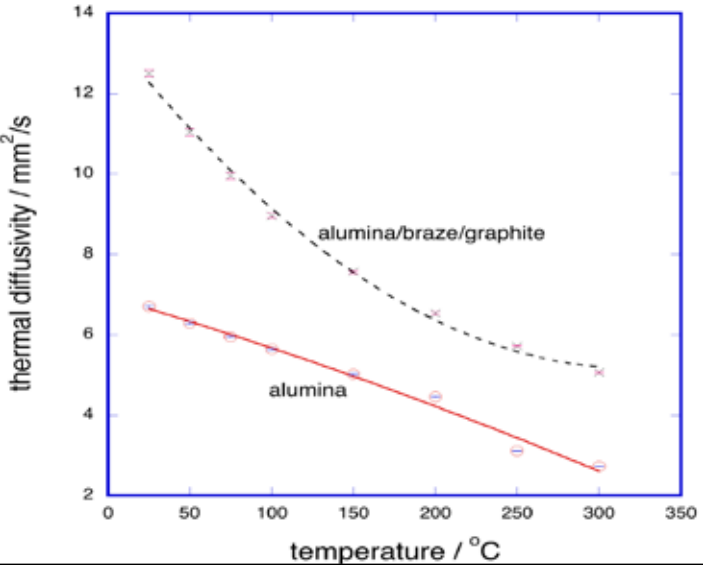

66

Thermal conductivity @ 25°C

	Density / g/cm³	Thermal diffusivity / mm²/s	Specific heat capacity / J/gK	Thermal conductivity / W/mK
AlN	3.45	50±0.8	0.73±0.02	**126±5**
AlN-AgCuTi-AlN	3.57	65±0.3	0.55±0.01	**127±3**
AlN-AgCuTi-graphite	3.56	100±16	0.50±0.04	**177±20**

67

Thermal conductivity for AlN-AgCuTi-graphite

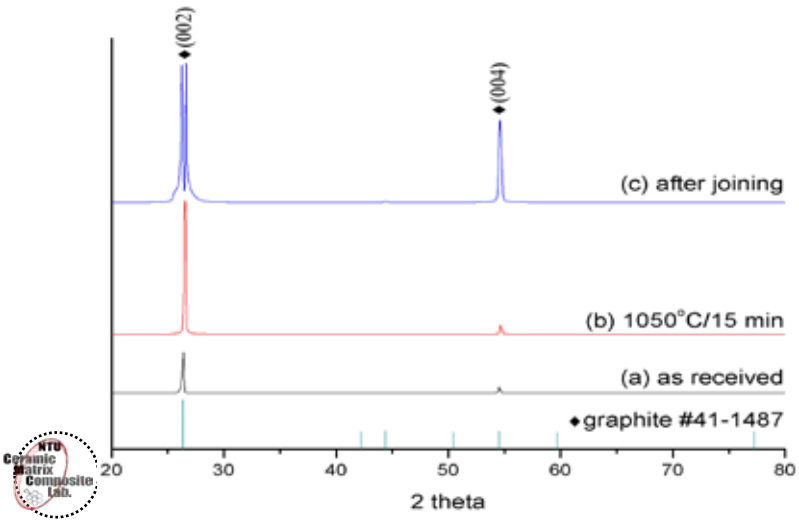

68

Electrical resistivity

	Thickness / μm	Electrical resistivity / Ωcm
Alumina	210	$4\sim5x10^{9}$
Ticusil	25	$3x10^{-10}$*
Graphite paper	25	100~500
Alumina/braze/graphite	**260**	**$7\ x10^{7} \sim 2x10^{10}$**

69

Application is challenging

- Advantages
  - Flexibility of graphite paper
  - Superb thermal conductivity along the planar direction

70

Summary for bonding ceramic to graphite

- Brazing technique can be used to bond Al_2O_3, AlN substrates to graphite paper.
- Thermal conductivity of AlN-AgCuTi-graphite substrate can reach 177 W/mK.
- The AlN-AgCuTi-graphite substrate is reliable in terms of thermal and failure characteristics.
- Applications need to be explored.

71

Acknowledgments

- Technical help from Dr. S. K. Lee, Dr. C.T. Yeh, Mr. T.T. Chou, Ms. Chun-Yu Lin
- Financial support from MOST, Taiwan

- References:

  - DBC: W. H. Tuan; S.K. Lee, J. Euro. Ceram. Soc., 2014
  - T. T. Chou, W.H. Tuan, H. Nishikawa, B.J. Weng, Advanced Engineering Materials (2017).
  - W.H. Tuan, Tsung-Te Chou, I-Cheng Kao, Shao-Yu Wang, Biing-Jyh Wen, J. European Ceramic Society, 38, 187 (2018)

72

Thank you for your attention

Thank you!
謝謝

利用電磁脈衝銲接技術達成高強度及品質銲接

由金屬工業研究發展中心正程師兼銲接組副長姜志華先生主講

International Conference on New Materials Technologies

嶄新材料科技國際會議暨技術研討會

High Strength & Quality Joining With Electromagnetic Forming

利用電磁脈衝銲接技術達成高强度及品質銲接

主辦單位:香港生產力促進局(HKPC)

受邀單位:金屬工業研究發展中心(MIRDC)

講　　師:金屬製程研發處 銲接組

姜 志 華

cwkg@mail.mirdc.org.tw

2018 年 1 月 29 日

大 綱

一、電磁脈衝銲接基本原理

二、電磁脈衝銲接技術特點

三、電磁脈衝異材銲接研究開發

四、電磁脈衝銲接應用例

五、結語

一、電磁脈衝銲接基本原理

當電場發生變化時，其磁場亦會發生變化，此時導體處於變化之磁場時，在導體中會產生渦電流，渦電流會產生感應磁場，伴隨電場發生變化之磁場與渦電流產生之感應磁場方向相反，且同性磁極相對，所以會產生互相排斥的電磁力，會使工件表面受電磁壓力之作用而發生變形(成形)，其電磁壓力大者，可使二待接合件產生銲接作用，右圖為金屬中心 (MIRDC)實銲研究之MPW Al/Cu銲件

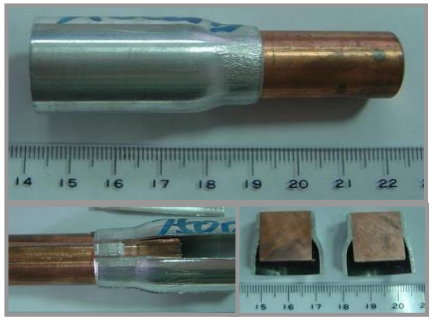

Al/Cu MPW銲件

Base concept of the welding of Al and Cu

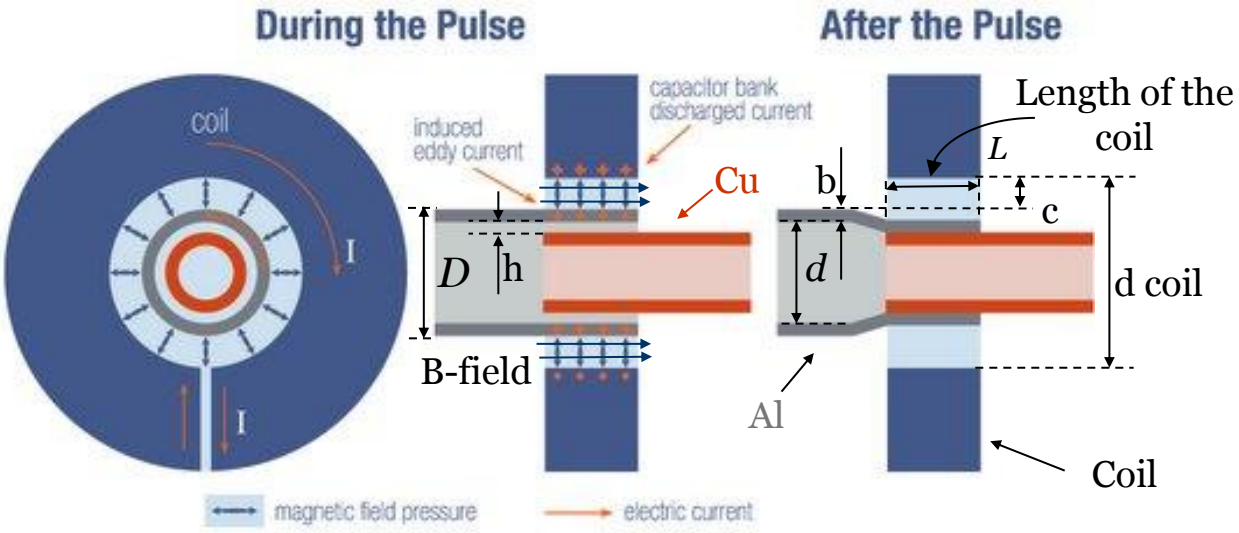

Ref. Fm. Training Company

一、電磁脈衝銲接基本原理(續)

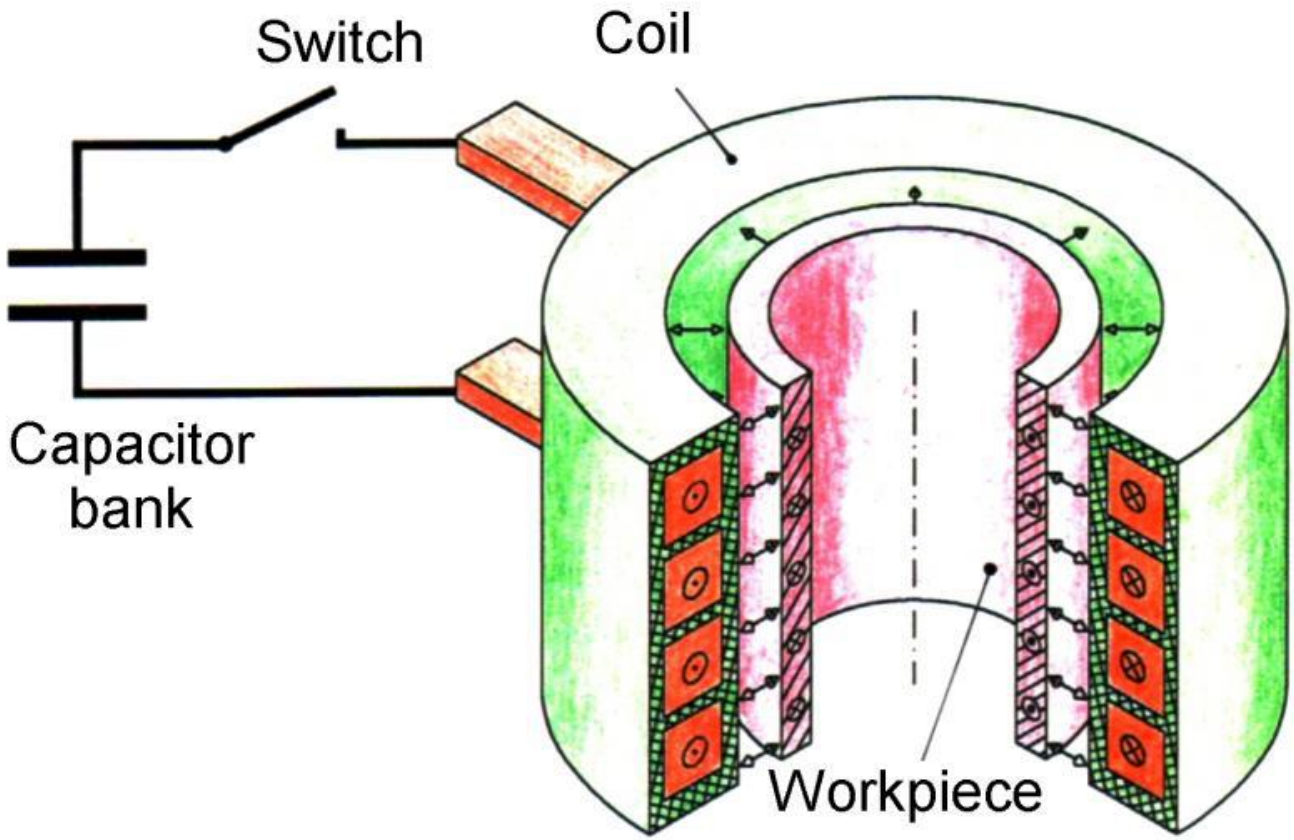

Ref. 4th International Conference on High Speed Forming – 2010

Interfacial Waves

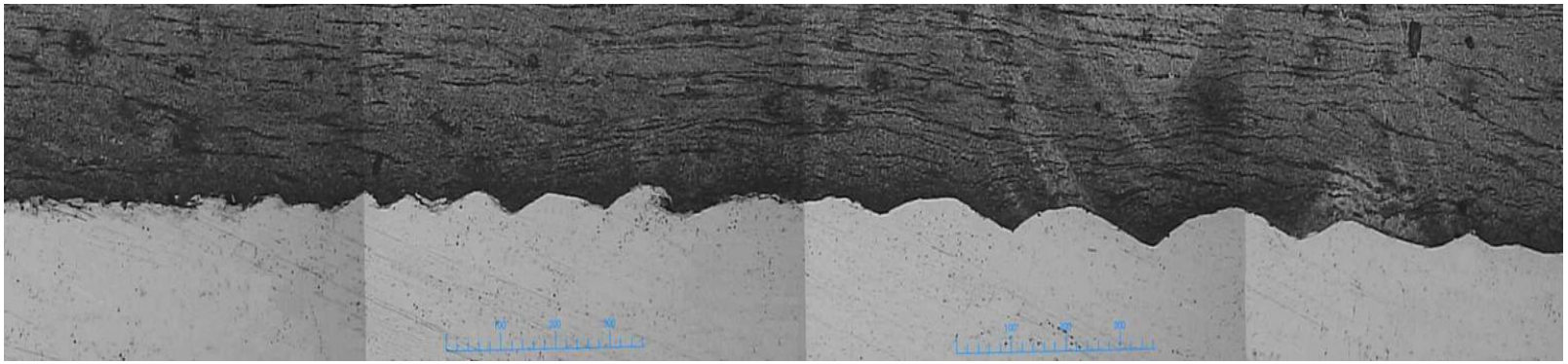

Cu-Cu Welded Interface

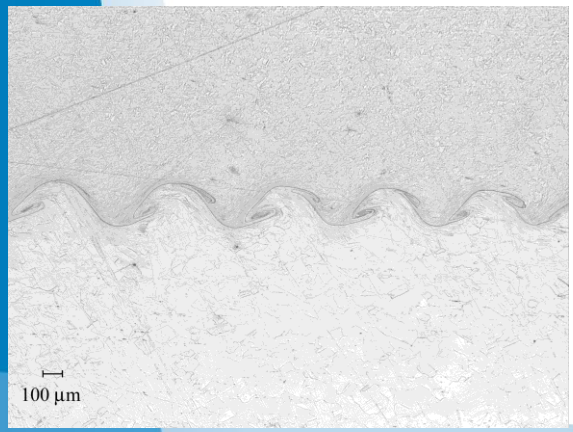

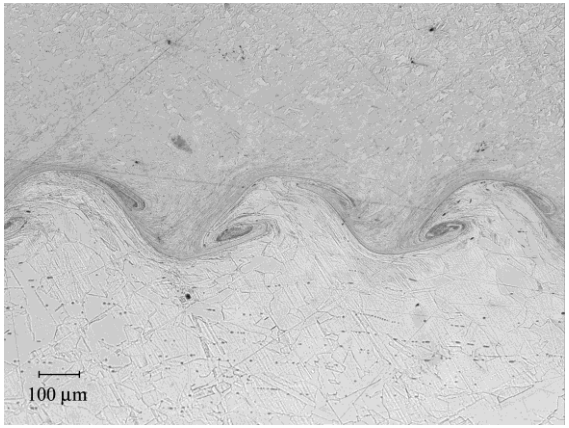

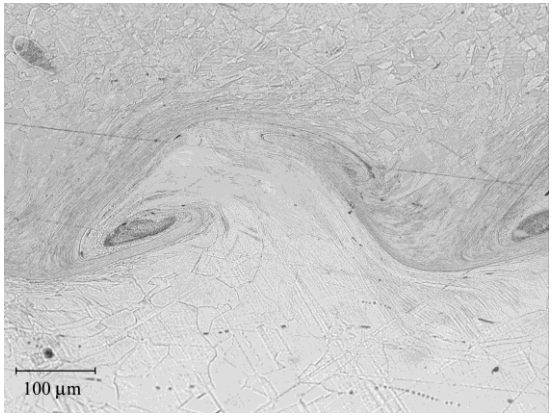

二、電磁脈衝銲接技術特點

(1)不須銲材、不須保護氣體
(2)銲接入熱量很低，類似於爆炸銲接
(3)適合於異種材料接合，適正參數條件銲道強度高於較弱母材
(4)非接觸式且銲接時間低於200μs，接合成本可節省50%以上
(5)傳統銲接無法施銲如Al 7075，應用電磁脈衝可施銲
(6)符合綠色環保製程等特點

三、電磁脈衝異材銲接研究開發

設備能量

◆電磁脈衝設備系統

油壓沖床與工作台車

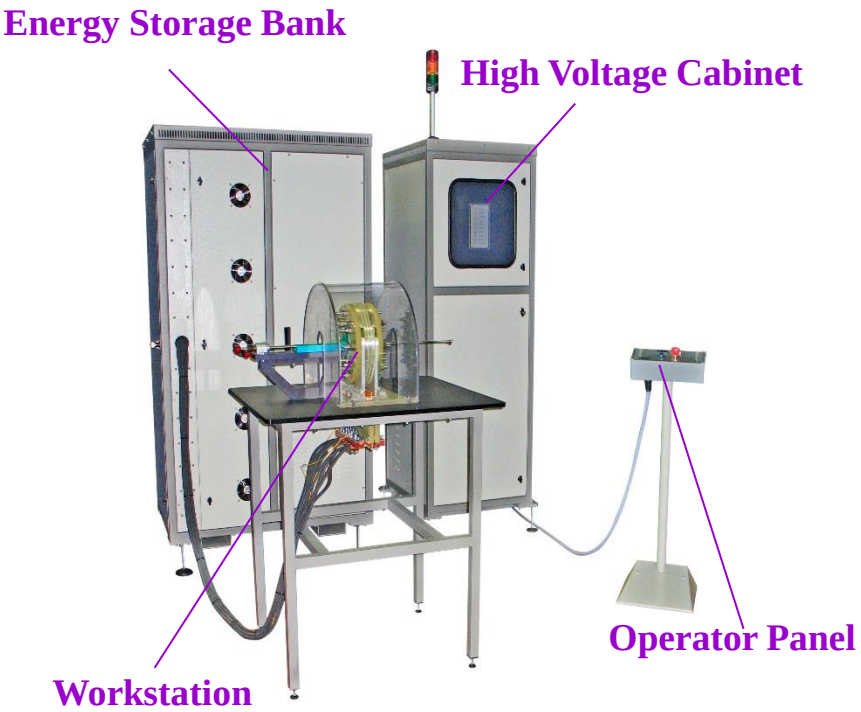

抽氣幫浦

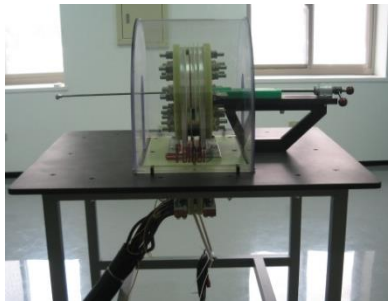

銲接線圈工作平台

電磁脈衝設備規格

設備電壓：三相220 V/60Hz

設備最大能量：25 KJ

最大工作電壓：9 KV

最大脈衝電流：600KA

工作頻率：28 KHz

設備能量(續)

電磁脈衝線圈開發種類

One-turn coils

Multi-turn coils ("Bitter")

Flat coil

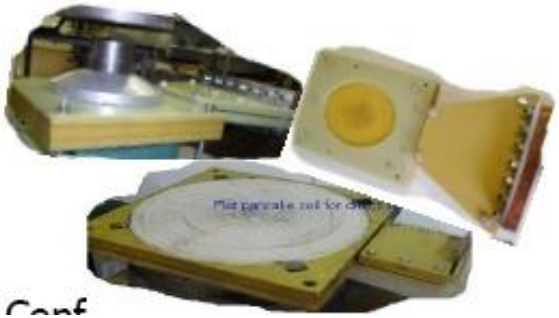

銲接線圈

成形線圈

異種金屬管MPW研究結果

鋁合金管母材機械性能

母 材	斷面面積 (mm^2)	降伏負荷 (kgf)	降伏強度 (kgf/mm^2)	平均降伏強度 (kgf/mm^2)	最高負荷 (kgf)	抗拉強度 (kgf/mm^2)	平均抗拉強度 (kgf/mm^2)
6061TD-b1	6.56	119	18.14	18.07	122	18.60	18.68
6061TD-b2	6.56	118	17.99		123	18.75	
6061T8-a1	6.56	200	30.49	30.11	216	32.93	32.63
6061T8-a2	6.56	195	29.73		212	32.32	
7005TD-c1	6.56	161	24.54	24.47	163	24.85	25.23
7005TD-c2	6.56	160	24.39		168	25.61	

中小管及中管銲件線切割抗剪試片尺寸圖

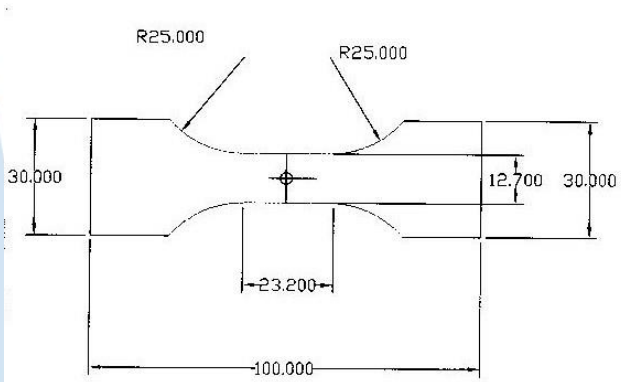

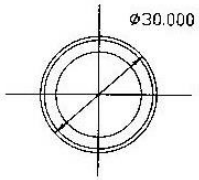

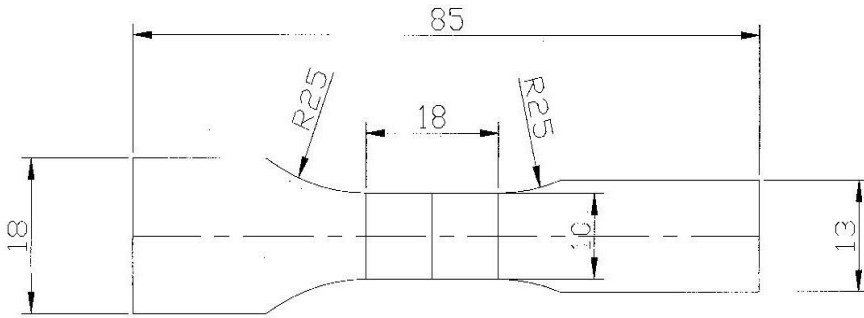

電磁脈衝銲接參數建立

A6061TD鋁合金/STKM11A鋼鐵及A6061TD鋁合金/SUS304不銹鋼管 (含Al/Cu管件接合)等組件之電磁脈衝銲接製程參數表(代表)，列如後。各銲接組件之搭接長度為10mm，間隙設計如前文所述。選用之電磁脈衝電壓自4500~8000V，其線圈輸出端資料，包括輸出端電壓、頻率及瞬間接合時間，以示波器擷取之，均如各表所列

6061TD/SUS304中小管電磁脈衝銲接參數表(代表)

編 號	材料及尺寸(mm)	間隙 (GAP mm)	搭接長度 (mm)	電壓 (V)	線圈輸入端示波器讀數			備 考
					Vo (V)	f (KHz)	T (μs)	
A61SUms-1	6061TD($25.48^{O.D}$x1.02^{t}x 45.37^{l})/ SUS304($19.40^{O.D}$x 50.12^{l})	2.02	10	4500	1.3	20	50	接合良好
A61SUms-2	6061TD($25.45^{O.D}$x1.05^{t}x 45.06^{l})/ SUS304($19.45^{O.D}$x 50.21^{l})	1.95	10	4500	1.3	20.833	48	〃
A61SUms-3	6061TD($25.45^{O.D}$x1.05^{t}x 44.82^{l})/ SUS304($19.41^{O.D}$x 50.06^{l})	1.96	10	4500	1.3	20.833	48	〃
A61SUms-4	6061TD($25.44^{O.D}$x1.08^{t}x 44.91^{l})/ SUS304($19.59^{O.D}$x 50.14^{l})	1.945	10	5000	1.4	19.231	52	〃
A61SUms-5	6061TD($25.64^{O.D}$x1.05^{t}x 45.04^{l})/ SUS304($19.42^{O.D}$x 50.05^{l})	2.06	10	5000	1.4	20.833	48	〃
A61SUms-6	6061TD($25.55^{O.D}$x1.10^{t}x 45.18^{l})/ SUS304($19.40^{O.D}$x 50.18^{l})	1.975	10	5000	1.4	20.833	48	〃

銲件抗剪性能試驗結果與討論

本研究選取之鋁合金外管(Faying Tube)，外管管徑分別為16.0mm$^{\Phi}$、25.4mm$^{\Phi}$及40.0mm$^{\Phi}$、厚度為1.0mm^{t}，其與鋼管或不銹鋼管所組配之管，吾等依序稱之為小管、中小管及中管。配合中心現有具電腦程式控制及繪圖功能之精密萬能試驗機(MTS拉伸試驗機)，小管銲件(外管16.0mm$^{\Phi}$之組件)，銲件量測尺寸後直接進行抗剪試驗，中小管 (外管25.4mm$^{\Phi}$之組件)及中管銲件(外管40.0mm$^{\Phi}$之組件)，則銲件先以線切割方式加工成拉伸試片後，再進行抗剪試驗(擇代表闡述)

電磁脈衝銲後銲件加工及抗剪試驗前外觀圖(代表)
圖左為A6061TD/STKM11A小管銲件
圖右為A7005TD/SUS304中小管銲件

A6061TD/STKM11A MPW管件在電壓7000V以上具銲接效應

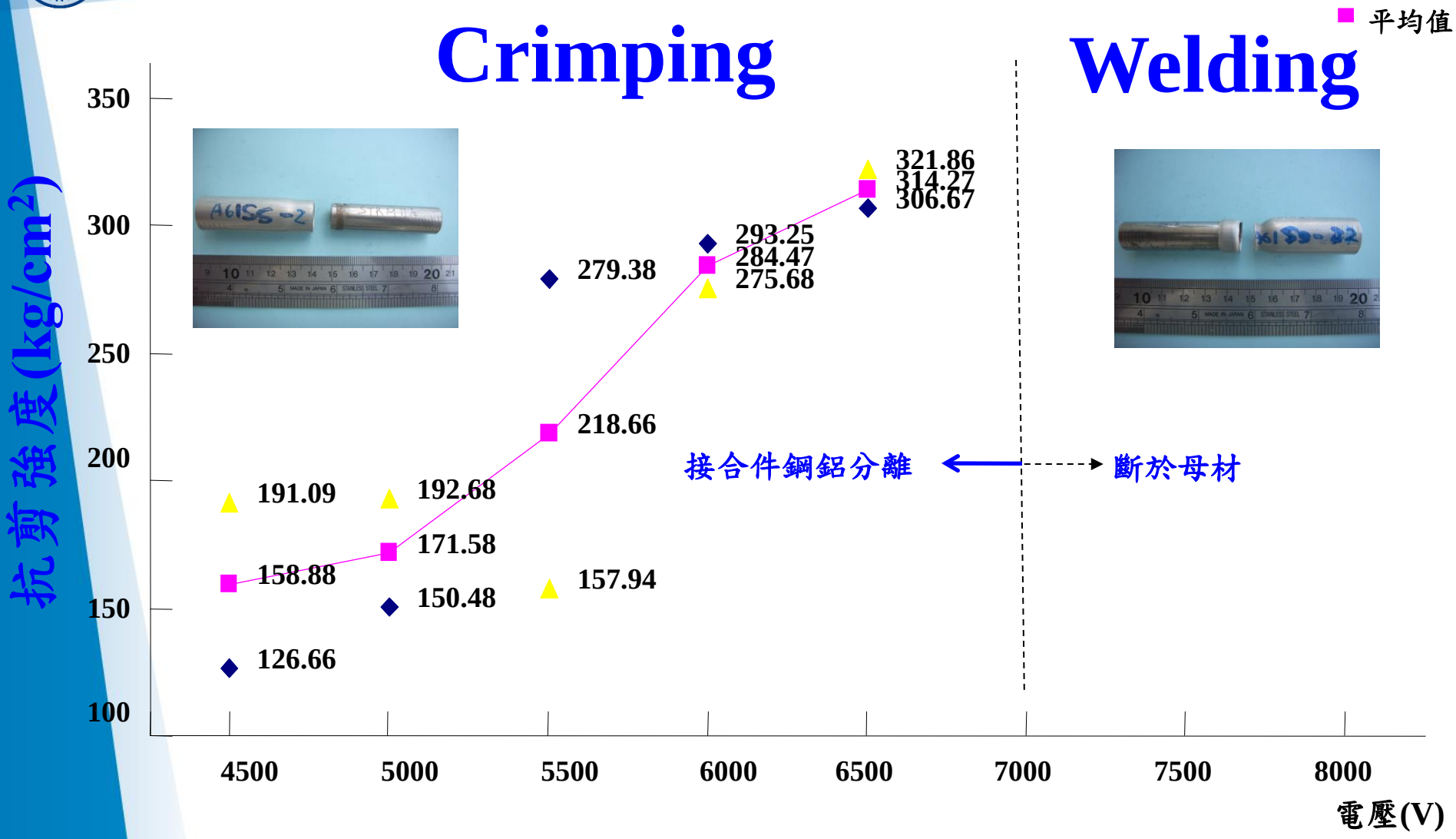

A6061TD/STKM11A電磁脈衝接合管件(小管)抗剪試驗結果(代表)

所有A6061T8/STKM11A MPW管件均屬Crimping試片

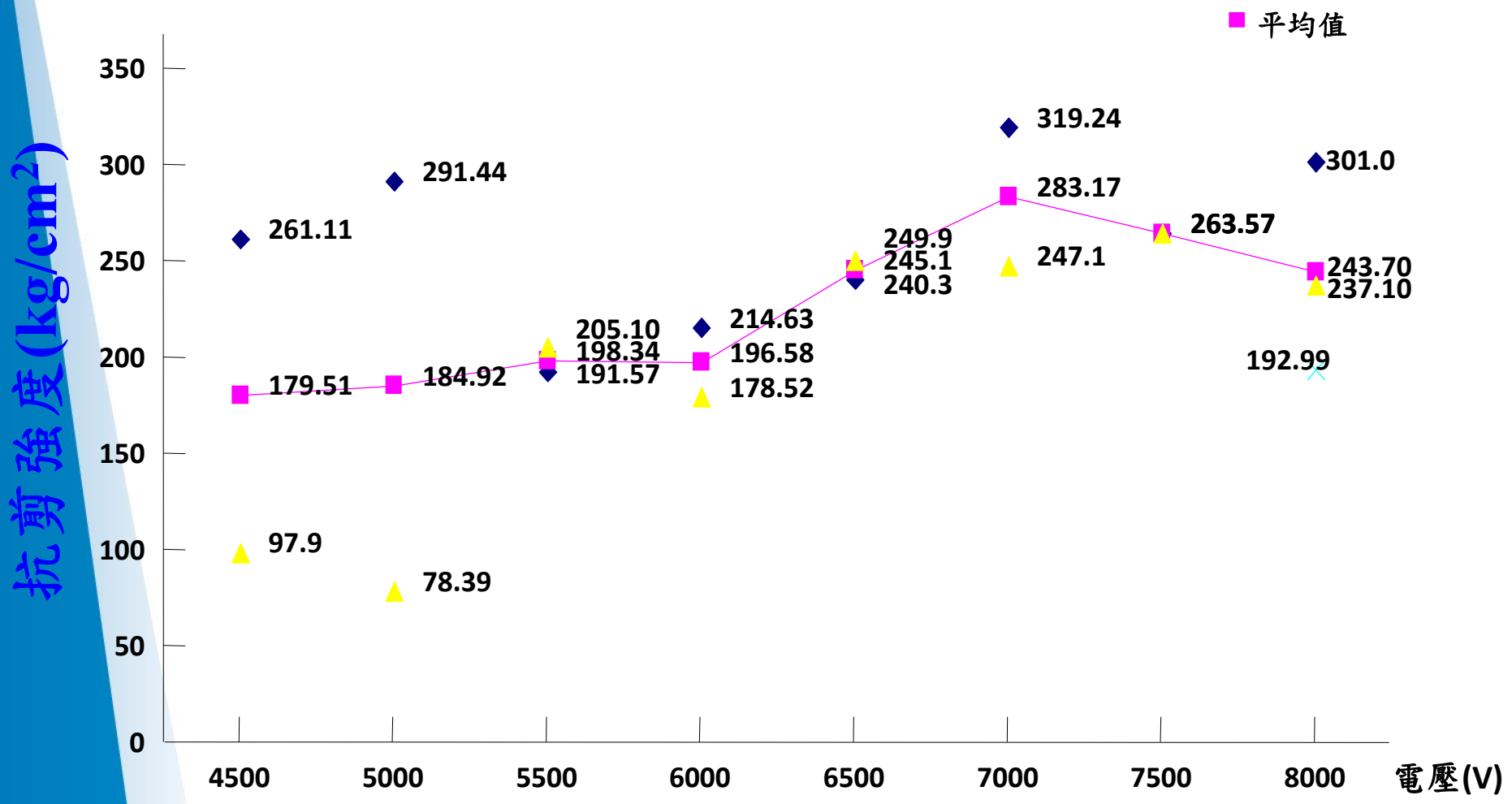

A6061T8/STKM11A電磁脈衝銲接管件(小管)抗剪試驗結果

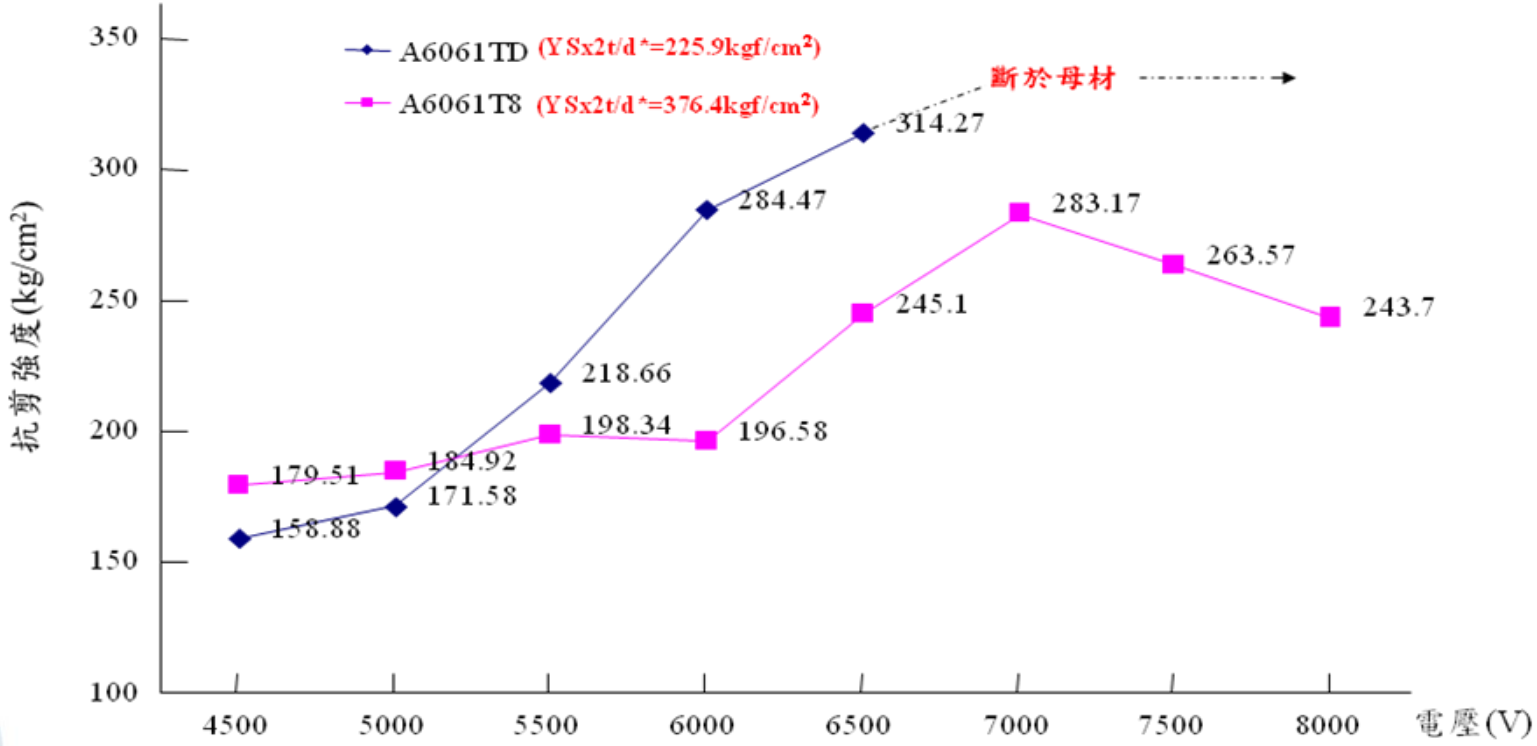

A6061TD/STKM11A 、A6061T8/STKM11A電磁脈衝接合管件平均抗剪強度比較圖

A6061TD、T8 16mm ϕ ×1.0mmt×50mml
STKM11A 12.7mm ϕ ×1.2mm×50mml

鋁/銅異材銲接例

STEP 1

STEP 2

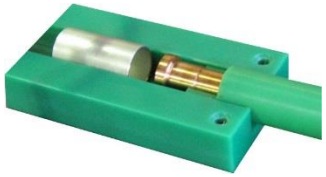

STEP 3

STEP 4

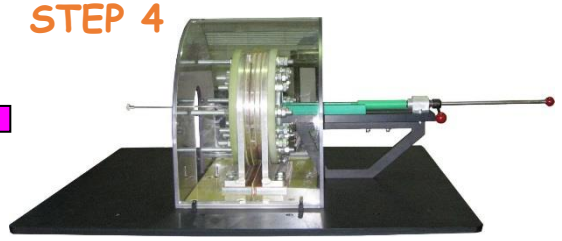

STEP 5

Welding & Crimping

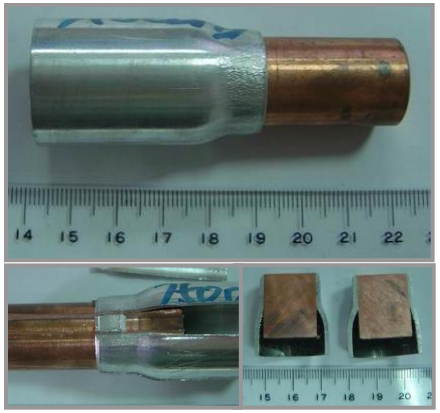

鋁/銅異材接合通過Peel Test

鋁/銅熱交換器

◆鋁/銅接合品質可達氣壓測漏 **7kg/cm²**

17

A6061F/Cu MPW界面分析

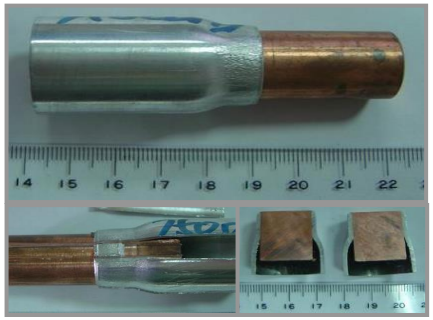

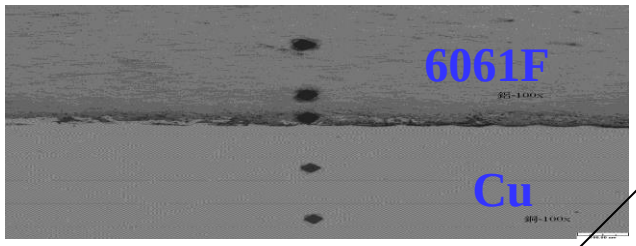

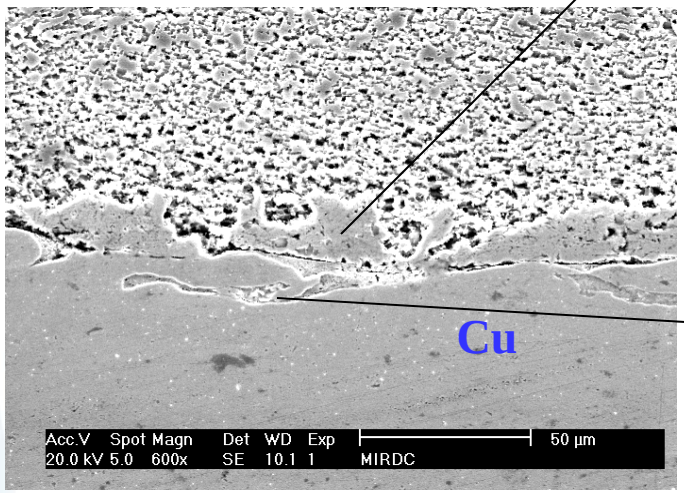

SEM

A6061F

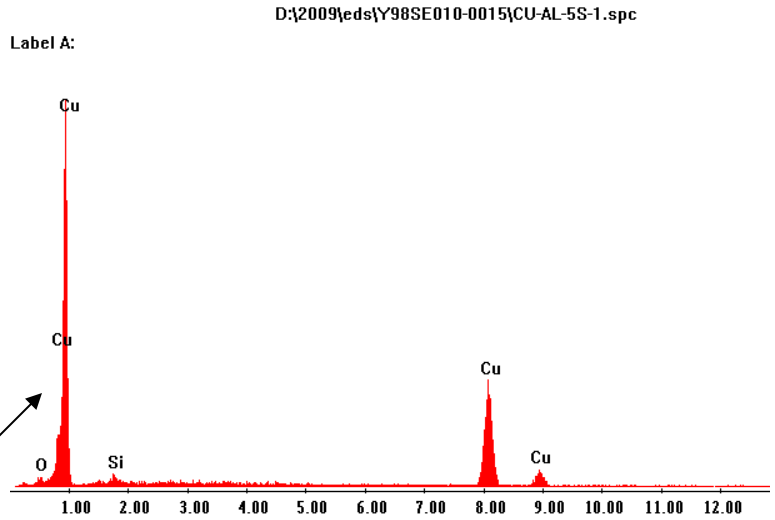

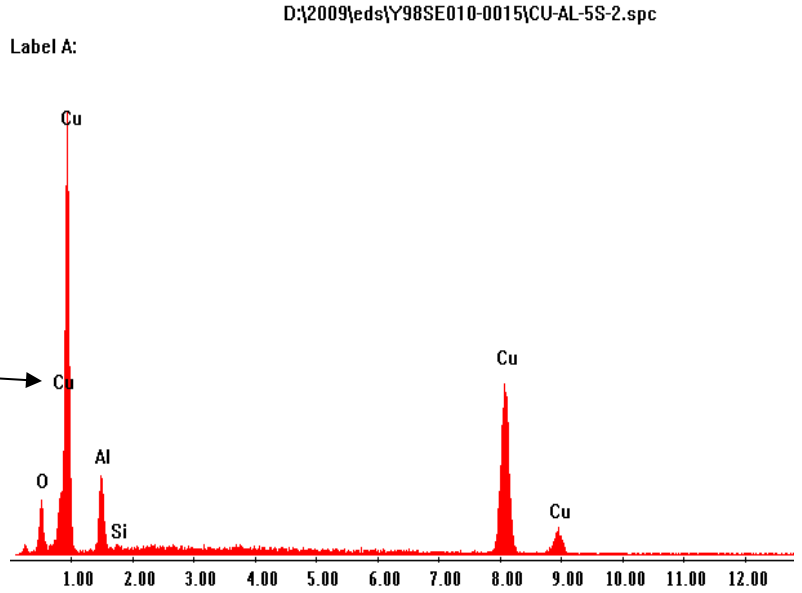

A6061F/Cu MPW界面及成份分析

A7005F/STKM11A MPW

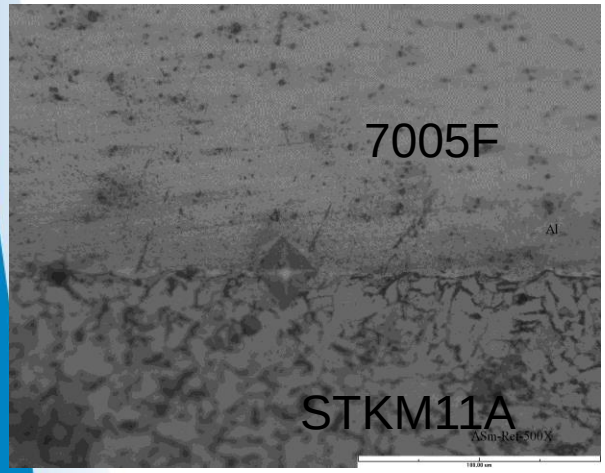

呈冶金鍵結界面

MPW銲件抗剪强度高、斷於鋁合金(鋁合金母材强度為24.8kg/mm^2)

實銲時間僅約56us，較等徑TIG銲(23.41s)快很多；異材銲接更為傳統電弧銲接所難以匹敵

A6061TD/SUS304管電磁脈衝銲件抗剪試驗後之外觀圖

適正銲接條件均斷於鋁合金母材(代表)

四、MPW應用例

Magnetic pulse systems can be used to perform the following product families:

Welding

Pulse Welded Al A/C Accumulator

Crimping

Forming

Stainless Steel Tray

Joining

Cutting & Perforating

Ref. Fm. Training Company

MPW應用例(續)

Aluminum Parts

Automotive Climate Control Elements

Filters

Dissimilar Metals

Driveshaft: Al-St, St-St

Earth Connector Al-St, Al-SS

Aluminum interfaces to Hydro Formed Steel

Al Power Cable to Copper, Brass or Al Connector

Stainless Steel Exhaust

Al Body Construction Elements

Ref. Fm. Training Company

MPW應用例(續)

◆鋁/銅 &鋁/鋼緊束(銅纜、鋼纜)

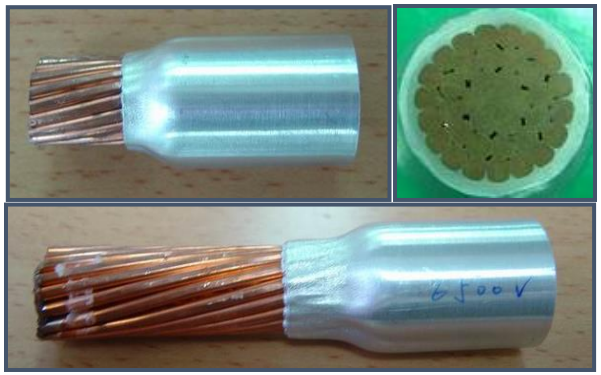

銅纜：Φ16mm

鋁管：6061-T6, t=1.5mm

鋼纜：Φ6mm

鋁管：6061-T6, t=3mm

◆金屬/非金屬緊束(纖維繩纜、鋼纜)

◆油壓製程：易造成繩纜表面纖維損傷因而斷裂。

◆電磁脈衝製程：可均勻受力，且材料快速塑性變形不易損傷繩纜表面纖維。

鋁合金6061-T6/纖維繩纜

不銹鋼/FRP

鋁/銅熱交換器及專利取得

鋁/銅熱交換器

◆鋁/銅接合品質可達氣壓測漏 7kg/cm^2

中華民國專利證書

發明第 I 387715 號

發明名稱：太陽能集熱器之管路結構及其管路之接合方法

專利權人：財團法人金屬工業研究發展中心

發明人：林典永、許宏旭、姜志華

專利權期間：自 2013年 3 月 1 日至 2029年12月21日止

上開發明業經專利權人依專利法之規定取得專利權

經濟部智慧財產局
局長 王美花

中華民國 102 年 3 月 1 日

五、結 語

1.MPW為固相銲接製程，銲件無明顯之熱影響區，適正之MPW銲接條件，可確立銲件呈冶金鍵結之界面，具優良之銲接品質

2.適正之接合設計及條件，銲件強度高，斷於較弱件母材

3.實銲速率甚快(約56us)，較傳統電弧銲接(TIG)快甚多

4.無需銲材、氣體、鎢棒、噴嘴等常用性耗材，對量產型製品，具長效性成本低減之優勢

5.MPW極適合異材之接合，傳統電弧銲接則難以匹敵

6.MPW為高度智能應用及發揮之製程，具開拓發展之潛力，目前圓形及異材接合應用具其優勢，板件接合先進國家發展中

簡報完畢　敬請指正

金屬工業研究發展中心
METAL INDUSTRIES
RESEARCH & DEVELOPMENT
CENTRE

附　件

集磁器設計注意事項

1.材料：高導電性與高強度，足以對抗脈衝時的負載與熱衝擊(常用的材料：鈹銅)
2.幾何：設計尺寸足以提高良好之效率
3.工件管徑
4.銲接區域
5.接合模式(weld/crimp)

6061TD/SUS304小管電磁脈衝銲接參數表(代表)

編 號	材料及尺寸(mm)	間隙 (GAP mm)	搭接長度 (mm)	電壓 (V)	線圈輸入端示波器讀數			備 考
					Vo (V)	f (KHz)	T (μs)	
A61SUs-7	6061TD($16.17^{O.D}$x1.19^{t} x50.12^{l})/ SUS304($9.97^{O.D}$x 50.26^{l})	1.91	10	5500	1.43	20	50	接合良好
A61SUs-8	6061TD($16.14^{O.D}$x1.14^{t} x50.25^{l})/ SUS304($9.96^{O.D}$x 50.14^{l})	1.95	10	5500	1.45	20	50	〃
A61SUs-9	6061TD($16.10^{O.D}$x1.11^{t}x 50.15^{l})/ SUS304($9.96^{O.D}$x 50.09^{l})	1.96	10	5500	1.5	20	50	〃
A61SUs-10	6061TD($16.01^{O.D}$x1.18^{t} x50.19^{l})/ SUS304($9.98^{O.D}$x 50.14^{l})	1.865	10	6000	1.6	20	50	〃
A61SUs-11	6061TD($16.01^{O.D}$x1.05^{t} x50.26^{l})/ SUS304($9.97^{O.D}$x 50.19^{l})	2	10	6000	1.6	19.608	51	〃
A61SUs-12	6061TD($16.24^{O.D}$x1.14^{t} x50.11^{l})/ SUS304($10.01^{O.D}$x 50.06^{l})	1.975	10	6000	1.6	20	50	〃

備註：鋁外管 、不銹鋼內棒

6061TD/SUS304中小管電磁脈衝銲接參數表(代表)

編 號	材料及尺寸(mm)	間隙 (GAP mm)	搭接長度 (mm)	電壓 (V)	線圈輸入端示波器讀數			備 考
					Vo (V)	f (KHz)	T (μs)	
A61SUms-1	6061TD($25.48^{O.D}$x1.02^{t}x 45.37^{l})/ SUS304($19.40^{O.D}$x 50.12^{l})	2.02	10	4500	1.3	20	50	接合良好
A61SUms-2	6061TD($25.45^{O.D}$x1.05^{t}x 45.06^{l})/ SUS304($19.45^{O.D}$x 50.21^{l})	1.95	10	4500	1.3	20.833	48	〃
A61SUms-3	6061TD($25.45^{O.D}$x1.05^{t}x 44.82^{l})/ SUS304($19.41^{O.D}$x 50.06^{l})	1.96	10	4500	1.3	20.833	48	〃
A61SUms-4	6061TD($25.44^{O.D}$x1.08^{t}x 44.91^{l})/ SUS304($19.59^{O.D}$x 50.14^{l})	1.945	10	5000	1.4	19.231	52	〃
A61SUms-5	6061TD($25.64^{O.D}$x1.05^{t}x 45.04^{l})/ SUS304($19.42^{O.D}$x 50.05^{l})	2.06	10	5000	1.4	20.833	48	〃
A61SUms-6	6061TD($25.55^{O.D}$x1.10^{t}x 45.18^{l})/ SUS304($19.40^{O.D}$x 50.18^{l})	1.975	10	5000	1.4	20.833	48	〃

7005TD/SUS304中小管電磁脈衝銲接參數表(代表)

編 號	材料及尺寸(mm)	間隙(GAP mm)	搭接長度(mm)	電壓(V)	線圈輸入端示波器讀數			備 考
					Vo (V)	f (KHz)	T (μs)	
7005TDSUms-13	7005TD(25.35$^{O.D}$x1.05^{t} x45.01^{l})/ SUS304(19.35$^{O.D}$x 50.07^{l})	1.95	10	6500	1.75	19.231	52	接合良好
7005TDSUms-14	7005TD(25.37$^{O.D}$x1.04^{t} x45.09^{l})/ SUS304(19.35$^{O.D}$x 50.01^{l})	1.97	10	6500	1.80	19.608	51	〃
7005TDSUms-15	7005TD(25.39$^{O.D}$x1.03^{t} x45.29^{l})/ SUS304(19.36$^{O.D}$x 50.04^{l})	1.98	10	6500	1.85	19.608	51	〃
7005TDSUms-16	7005TD(25.44$^{O.D}$x1.04^{t} x45^{l})/ SUS304(19.35$^{O.D}$x 49.92^{l})	2.005	10	7000	1.85	20.0	50	〃
7005TDSUms-17	7005TD(25.43$^{O.D}$x1.07^{t} x45.12^{l})/ SUS304(19.35$^{O.D}$x 49.97^{l})	1.97	10	7000	1.90	19.23	52	〃
7005TDSUms-18	7005TD(25.4$^{O.D}$x1.01^{t}x 45.17^{l})/ SUS304(19.35$^{O.D}$x 50.04^{l})	2.015	10	7000	1.90		19.608	〃

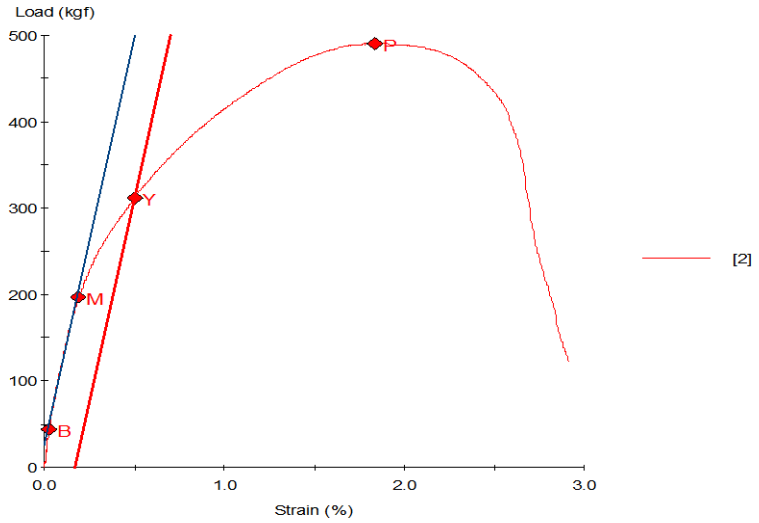

A7005T6/Cu MPW 銲件斷於 A7005T6鋁合金母材

Name	Value	Units
Thickness	11.81	mm
Width	12.57	mm
Area	148.45	mm^2
Modulus	6198	MPa
Load At Offset Yield	311	kgf
Stress At Offset Yield	2.1	kgf/mm^2
Peak Load	490	kgf
Peak Stress	3.3	kgf/mm^2

6061鋁管(下)/鈦64(上)試片接合處OM圖

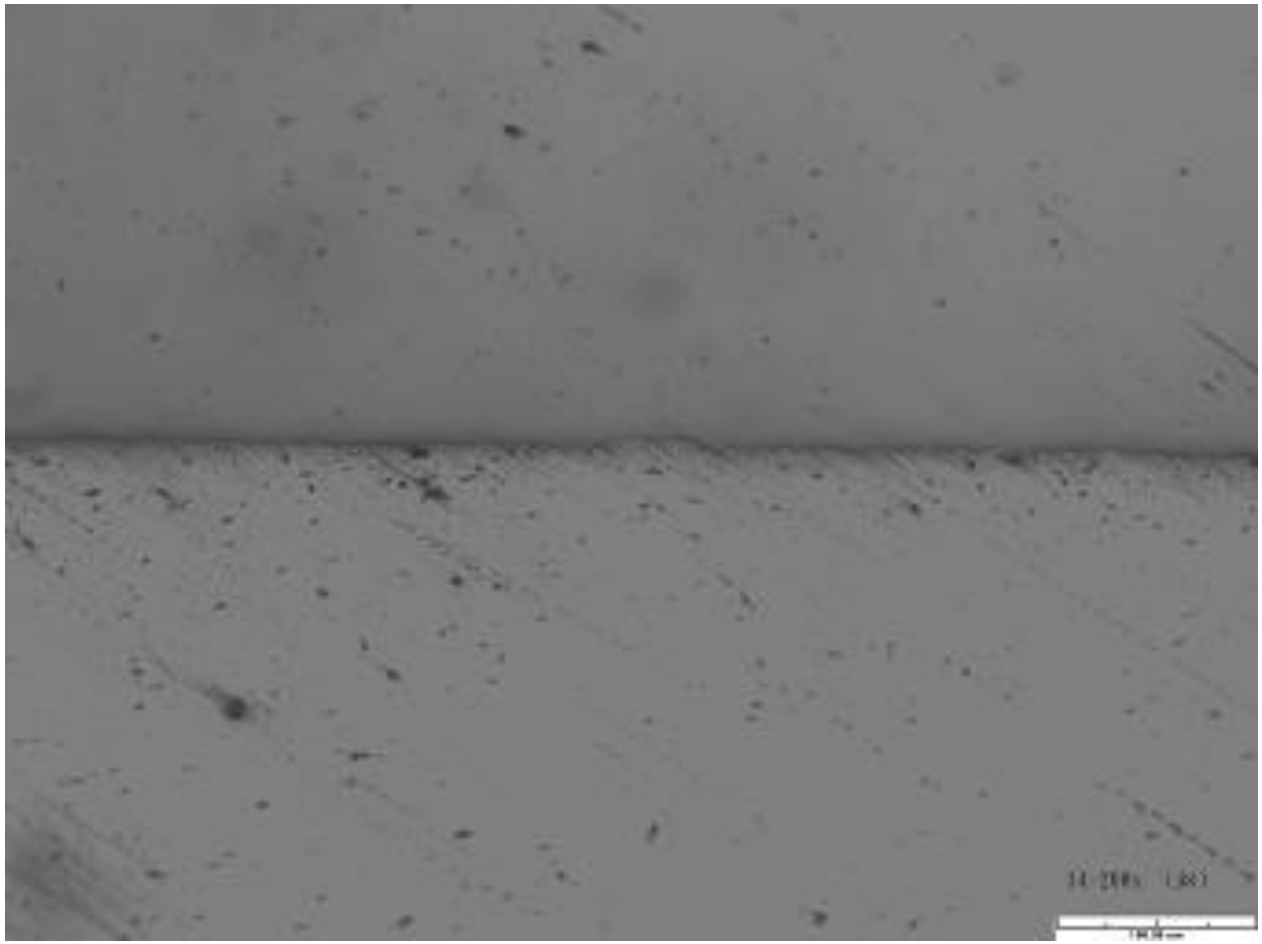

6061TD/SUS304中小管電磁脈衝銲接參數表(代表)

編 號	材料及尺寸(mm)	間隙 (GAP mm)	搭接長度 (mm)	電壓 (V)	線圈輸入端示波器讀數			備 考
					Vo (V)	f (KHz)	T (μs)	
A61SUms-1	6061TD($25.48^{O.D}$x1.02^{t}x 45.37^{l})/ SUS304($19.40^{O.D}$x 50.12^{l})	2.02	10	4500	1.3	20	50	接合良好
A61SUms-2	6061TD($25.45^{O.D}$x1.05^{t}x 45.06^{l})/ SUS304($19.45^{O.D}$x 50.21^{l})	1.95	10	4500	1.3	20.833	48	〃
A61SUms-3	6061TD($25.45^{O.D}$x1.05^{t}x 44.82^{l})/ SUS304($19.41^{O.D}$x 50.06^{l})	1.96	10	4500	1.3	20.833	48	〃
A61SUms-4	6061TD($25.44^{O.D}$x1.08^{t}x 44.91^{l})/ SUS304($19.59^{O.D}$x 50.14^{l})	1.945	10	5000	1.4	19.231	52	〃
A61SUms-5	6061TD($25.64^{O.D}$x1.05^{t}x 45.04^{l})/ SUS304($19.42^{O.D}$x 50.05^{l})	2.06	10	5000	1.4	20.833	48	〃
A61SUms-6	6061TD($25.55^{O.D}$x1.10^{t}x 45.18^{l})/ SUS304($19.40^{O.D}$x 50.18^{l})	1.975	10	5000	1.4	20.833	48	〃

34

金屬發泡及開放式結構的應用和新機遇

由德國弗勞恩霍夫機床及成形技術研究所功能材質輕量化主管湯瑪士主講

Cellular Metals in Dresden

Materials and Structures

Hollow Metal Spheres

Open Cell Foam

Sintered Metal Paper

3D Screen Printing

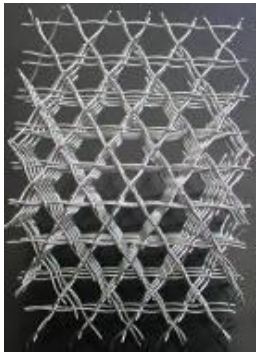

3d-Wire Structures

Fibre Structures

densities: 0,05-1,5 g/cm³
cell sizes: 5 µm-10 mm
porosities: 50-97 %

all sinterable materials:
Fe-, Ni-, Cu, Ti-Basis
Intermetallics

→ high energy absorption
→ sound absorption capabilities
→ damping
→ thermal insulation

© Fraunhofer IFAM Dresden

Cellular Metals

Manufacturing Processes

Foaming	Forming	Replication	Generation
Foaming Agent	Honey Comb	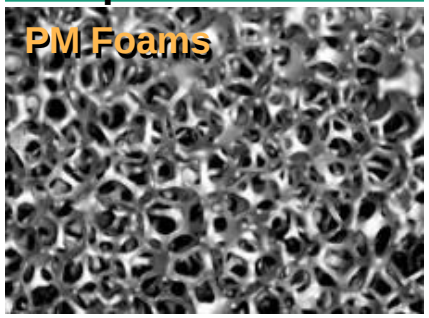 PM Foams	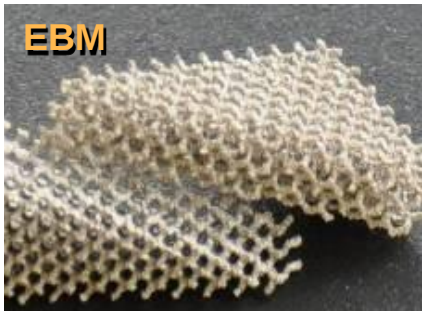 EBM
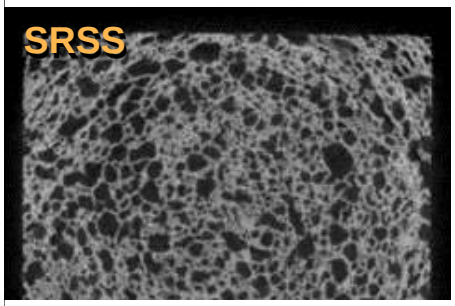 SRSS	Fibre Structures	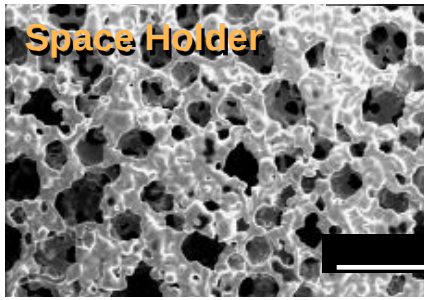 Space Holder	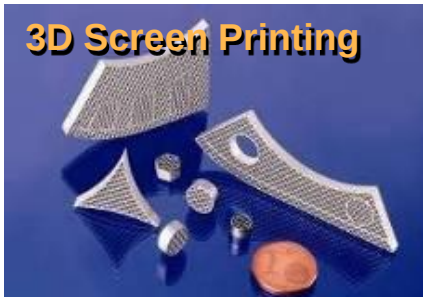 3D Screen Printing
Slurry Gelation	Hollow Spheres	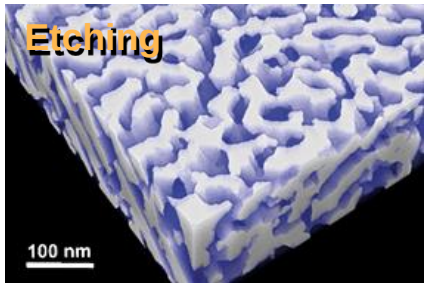 Etching	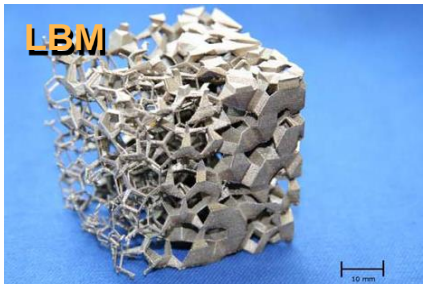 LBM

© Fraunhofer IFAM Dresden

Cellular Metals

Stakeholder in Germany

© Fraunhofer IFAM Dresden

Materials

Realized Materials

Realized Materials

Steel	unalloyed	C35, C45, C60
	ferritic	42CrMo4, 410L 430L, FeCrAlY
	austenitic	304L, 316L, AISI310, AISI314
Other	elements	Ni, Cu, Ti, Ta, Mo, Au, Ag
	alloys	Fe-Cu, Ni-Basis, Ti6Al4V
	intermetallics	$MoSi_2$, TiAl, NiTi, NiAl

© Fraunhofer IFAM Dresden

Technologies

Fibre Structures

Melt Extraction

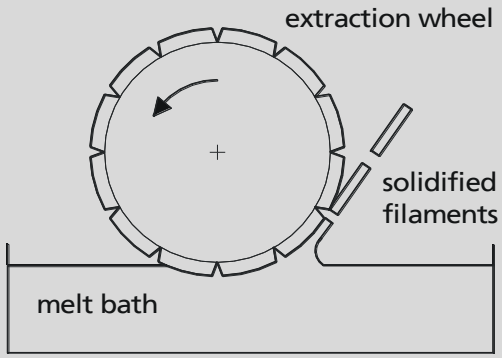

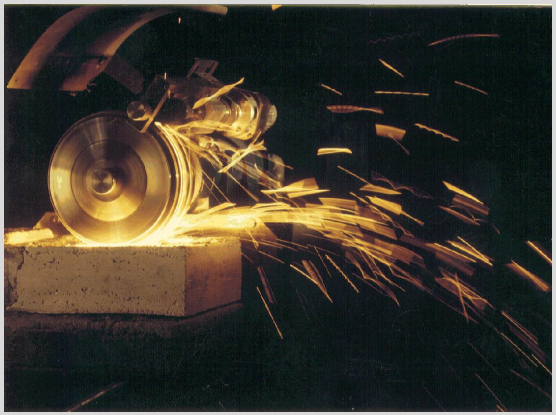

Fibre Deposition

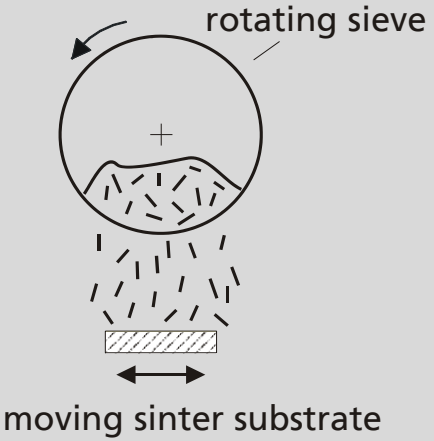

Sintering

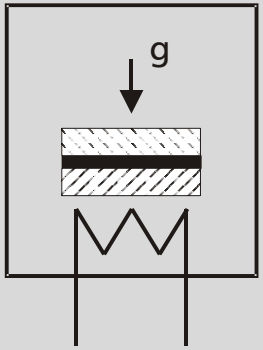

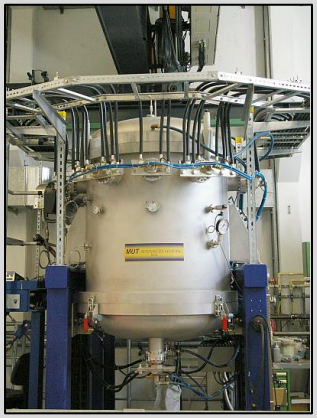

Machining

- cutting
- laser jet
- water jet
- erosion

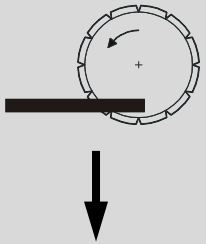

© Fraunhofer IFAM Dresden

Materials

Fibre Production by Melt Extraction

Properties of Metal Fibres

- All common metals and alloys (Al, Mg, Cu, Fe, Ni, Ti, Au, Pt, etc.)
- Intermetallics (FeAl, NiAl, TiAl)
- Fiber diameters ranging from 50 to 250 µm
- Fiber length ranging from 3 to 50 mm

© Fraunhofer IFAM Dresden

Properties

Metal Fibre Structures

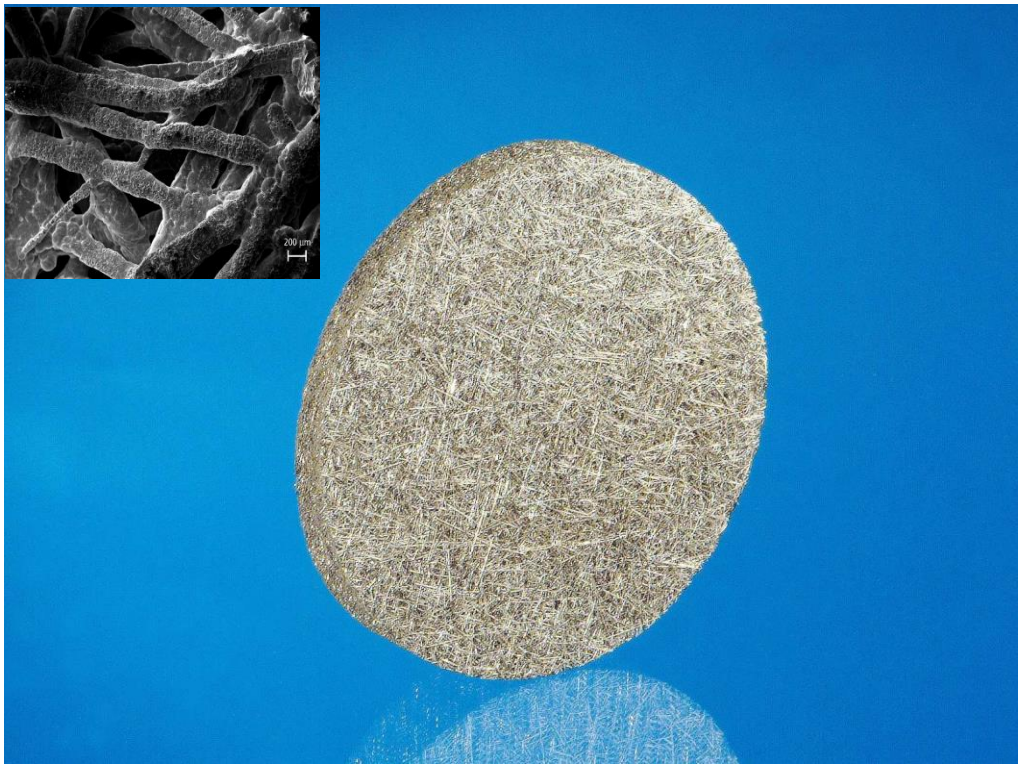

Properties of metal fibre structures

- sheets up to 600 x 1200 mm
- Rings with diameter up to 400 mm
- Open porosity 50 to 95 %
- pore sizes ca. 10 - 250 µm
- graded structures

© Fraunhofer IFAM Dresden

Technologies

Open Cell Metal Foams

Replication of polymeric foam

Schwartzwalder/Somers (US 3.090.094, 1961)

- shaped polymer foam
- metall-powder suspension
- coating of struts of polymer foam
- drying
- pyrolysis of PU foam
- sintering of metal

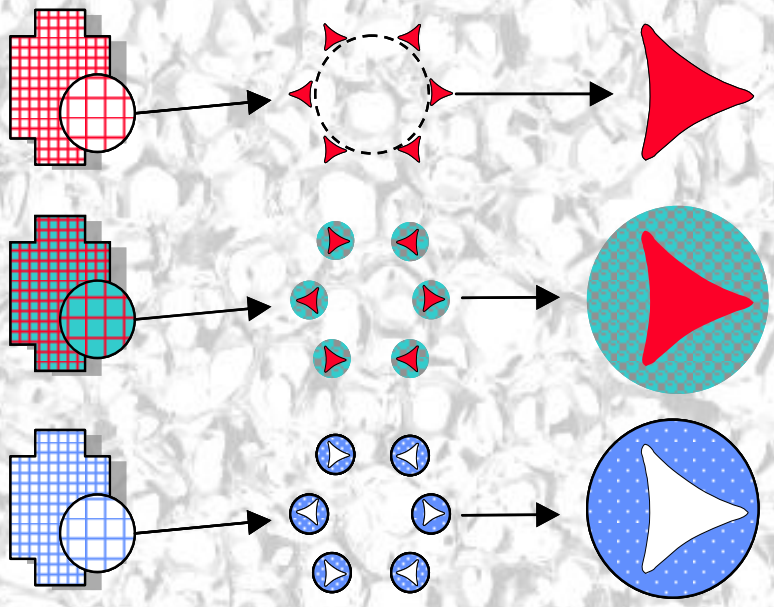

© Fraunhofer IFAM Dresden

Properties

Open Cell Metal Foam

metal powder + binder + suspension additives + water

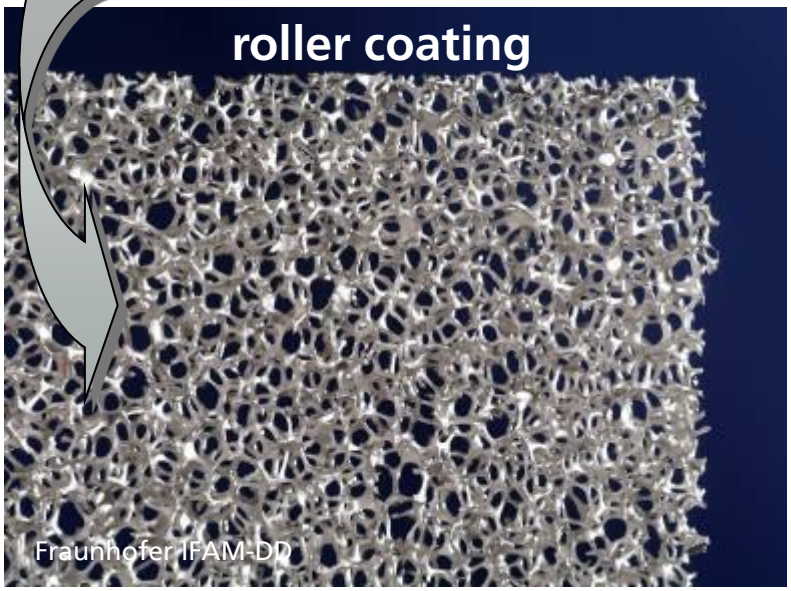

structural properties

density	5 - 30 % of basic material (adjustable)
cell sizes	0.4 – 5.0 mm
heat conductivity	ca. 1 – 5 % of basic material

adjustment of density by adjustment of coating mass

© Fraunhofer IFAM Dresden

Properties

Open Cell Metal Foam

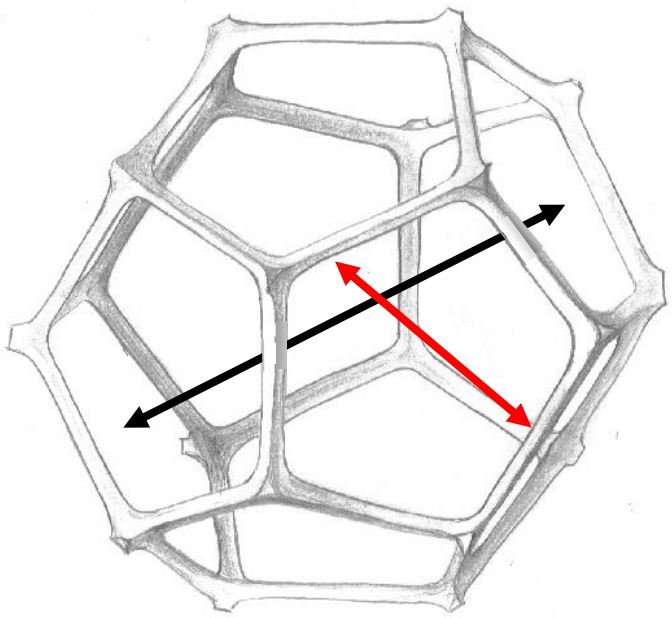

Structure

- Network of dodecahedron cells
- **cell size** = large diameter of cells
- **cell window** = small diameter of cells (appr. 1/3)
- Practically ideal porous organic structure

Cell size	cell width [mm]	surface [m²/m³]
ppi 10	4.5 - 5.0	400
ppi 20	2.0- 3.5	1100
ppi 30	1.8 - 2.0	1800
ppi 45	1.1 - 1.3	2800
ppi 60	0.7 - 0.8	3900
ppi 80	0.4 - 0.5	5300

© Fraunhofer IFAM Dresden

Open porous metals

- Open porous structures made from aluminium, zinc, copper, steel
- Production e.g. by means of
  - Casting with place-holder structures
  - Sintering of Cu-electroplated textiles
  - Printing
- Composites possible (ceramics, zeolites, PCM,…)

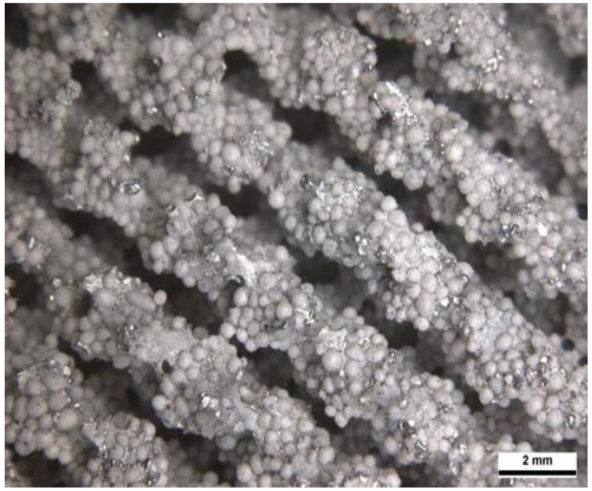

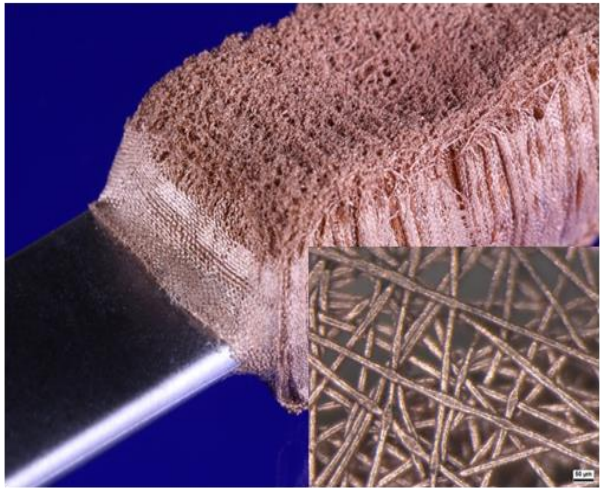

Joachim Baumeister, Fraunhofer Institute IFAM Bremen
Department of Powder Technology

Fraunhofer IFAM

Open porous metals

- Possible application fields
  - Thermochemical energy storage
  - Heat exchanger
  - Condenser/Evaporator

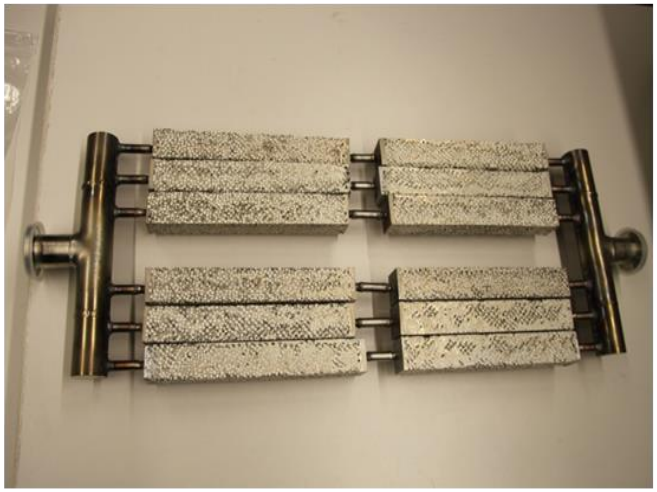

cast Al/zeolite composite heat exchanger

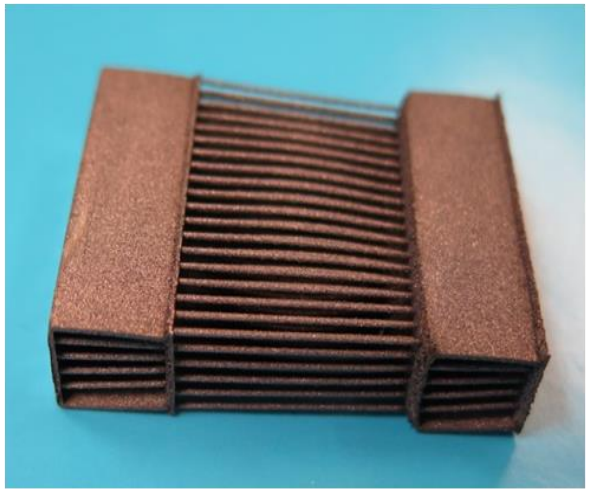

printed heat exchanger

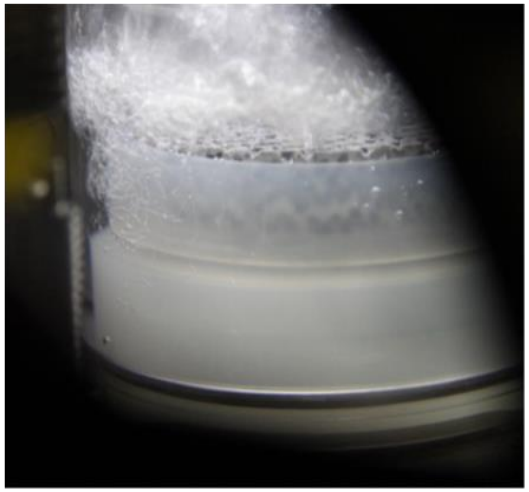

evaporator test

Joachim Baumeister, Fraunhofer Institute IFAM Bremen
Department of Powder Technology

Fraunhofer IFAM

Technologies

Hollow Metal Sphere Structures

Coating
Fluidised bed

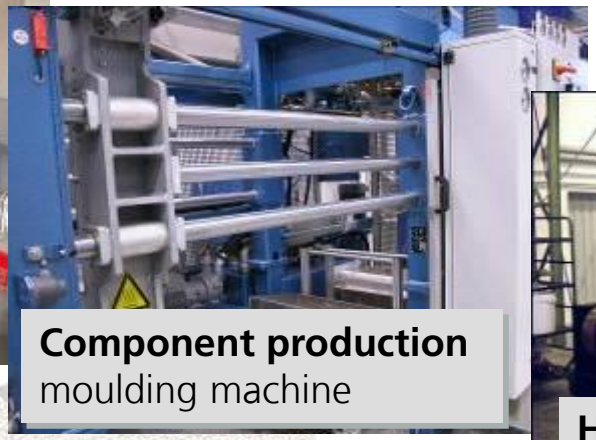

Component production
moulding machine

Heat treatment
debinding/sintering

Technology from established mass production processes

Coating technology from pharmaceutical industry	**Processing from packing industry**	**Sintering from metal injection moulding**

© Fraunhofer IFAM Dresden

hollomet®

Fraunhofer IFAM Branch Lab Dresden

Properties

Hollow Metal Sphere Structures

Suspension: metal powder, binder + additive + water

Structural propertoes

density	5 - 30 % of basic material (adjustable)
porosity	75 – 96 %
cell size	0.4 – 5.0 mm
heat conductivity	ca. 1 – 5 % of basic material

adjustment of density by adjustment of coating mass

© Fraunhofer IFAM Dresden

Properties

Hollow Metal Sphere Structures

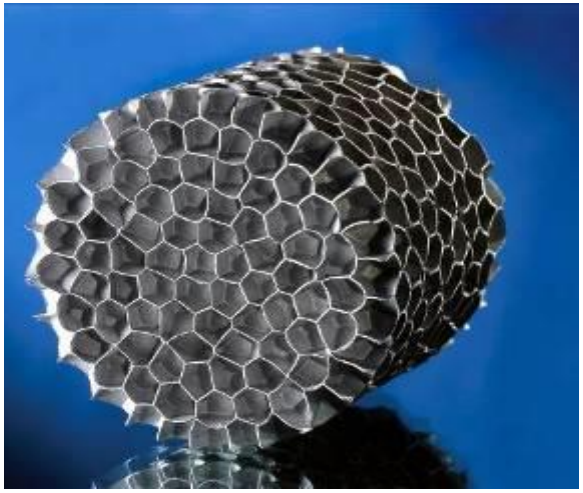

Closed cell honey comb

- high strength
- gas tight

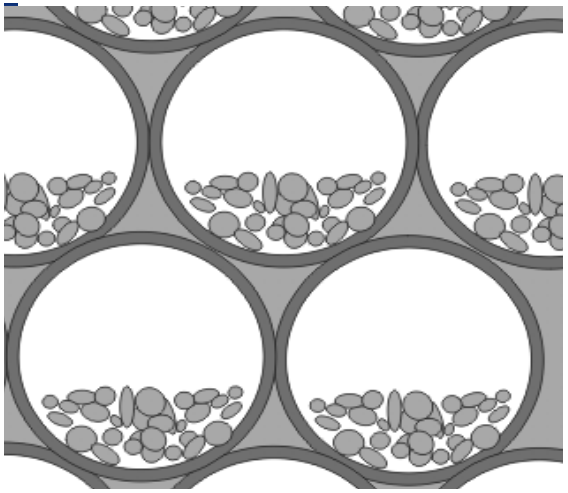

Particular filled structures

- high damping
- low mass

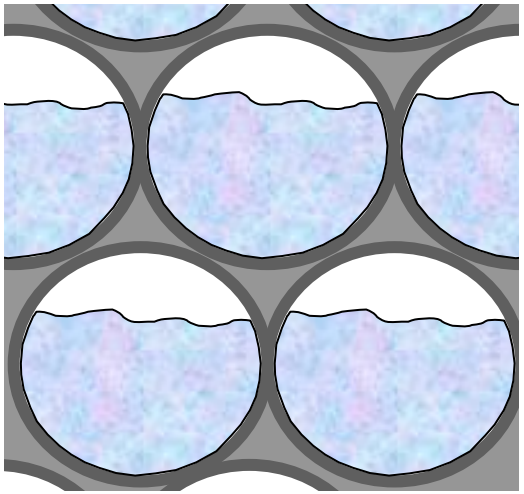

PCM-filled structures

- high thermal storage
- increased heat conductivity

© Fraunhofer IFAM Dresden

Properties

Porous Metal Paper

Porous Metal Paper - Microstructure after thermal treatment
(debinding and sintering)

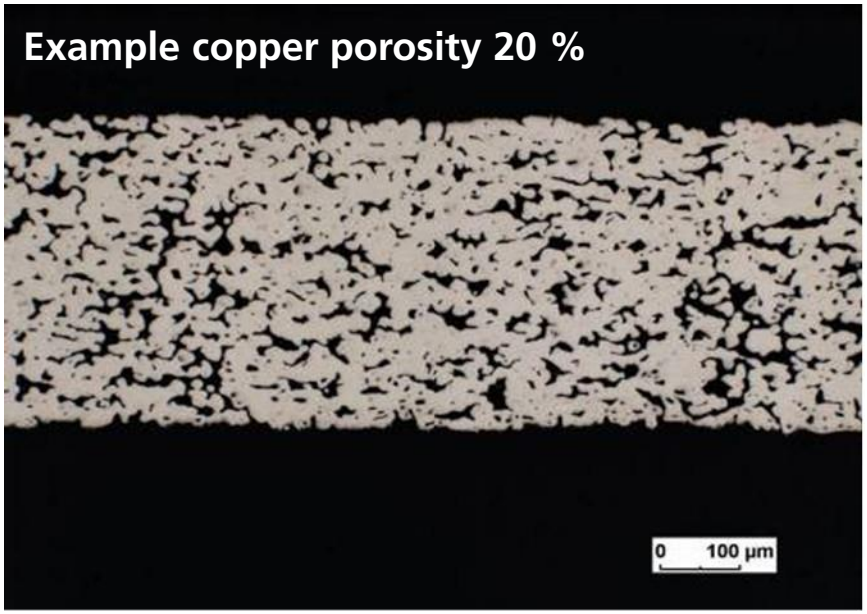

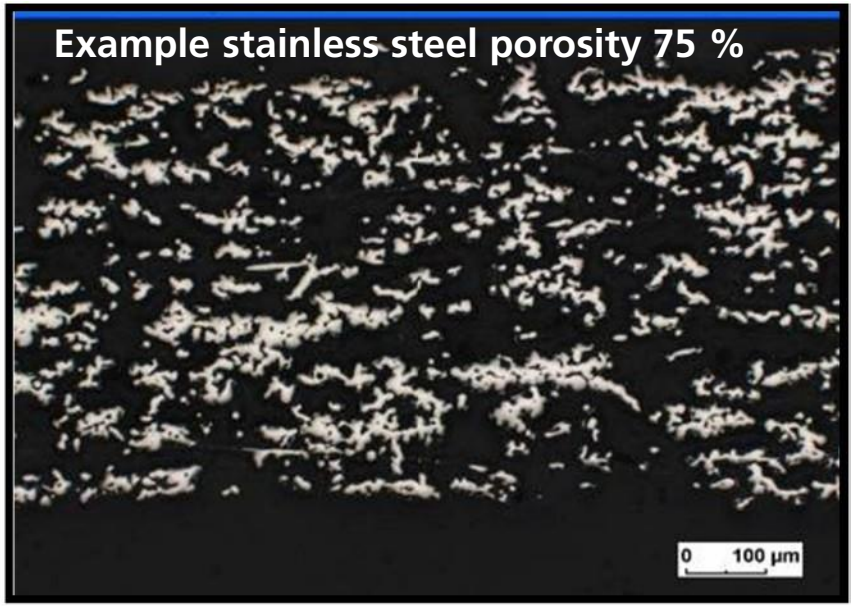

Variations with respect to pore size, morphology and porosity

© Fraunhofer IFAM Dresden

PTS THE PAPER TECHNOLOGY SPECIALISTS

Fraunhofer IFAM Branch Lab Dresden

Technologies

Porous Metal Paper

Metal Paper
Paper Machine

Component production
Corrugation

Heat treatment
debinding/sintering

Technology from established mass production processes

Paper Manufacturing Process	**Processing from corrugated board manufacturing industry**	**Sintering from metal injection moulding**

© Fraunhofer IFAM Dresden

PTS THE PAPER TECHNOLOGY SPECIALISTS

Fraunhofer IFAM Branch Lab Dresden

Properties

Porous Metal Paper

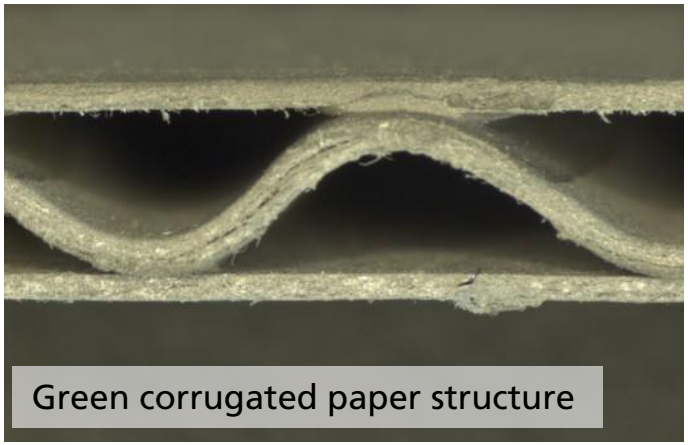

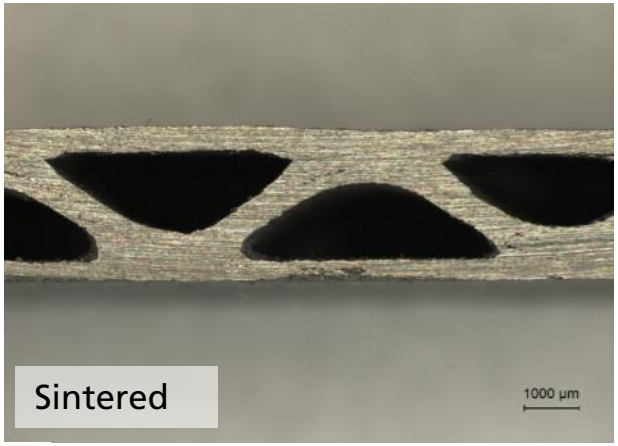

© Fraunhofer IFAM Dresden

PTS THE PAPER TECHNOLOGY SPECIALISTS

Fraunhofer IFAM Branch Lab Dresden

Technologies

3D Wire Structures

wire pay-off → leveller → forming → manufacturing of structures

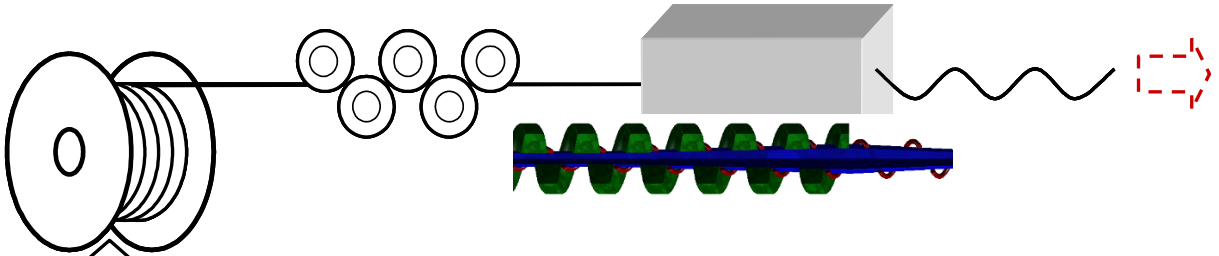

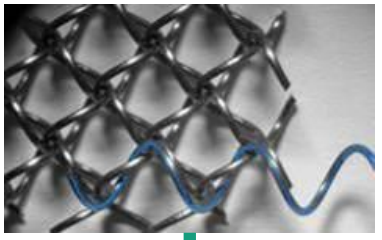

automated

manual

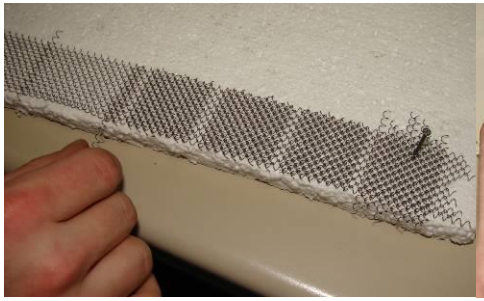

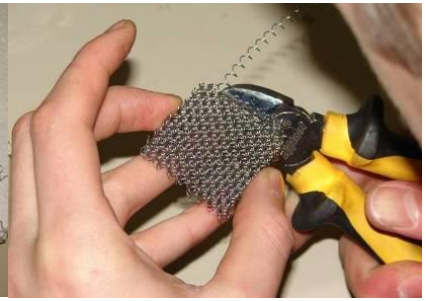

automated manufacturing test rig

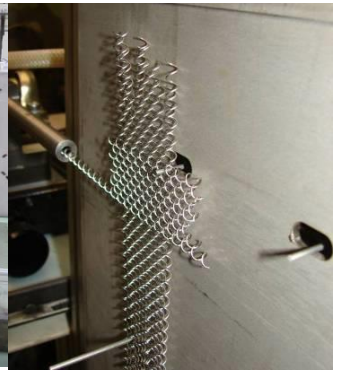

© Fraunhofer IFAM Dresden

KIESELSTEIN WIRE SOLUTIONS

Fraunhofer IFAM Branch Lab Dresden

Properties

3D Wire Structures

3D Wire Structures

- materials: steel, stainless, Cu, Al, Ti,
- cheap primary materials
- extremely low densities up to 0.05 g/cm³
- cell sizes 3, 5 10, 20 mm
- high specific strength

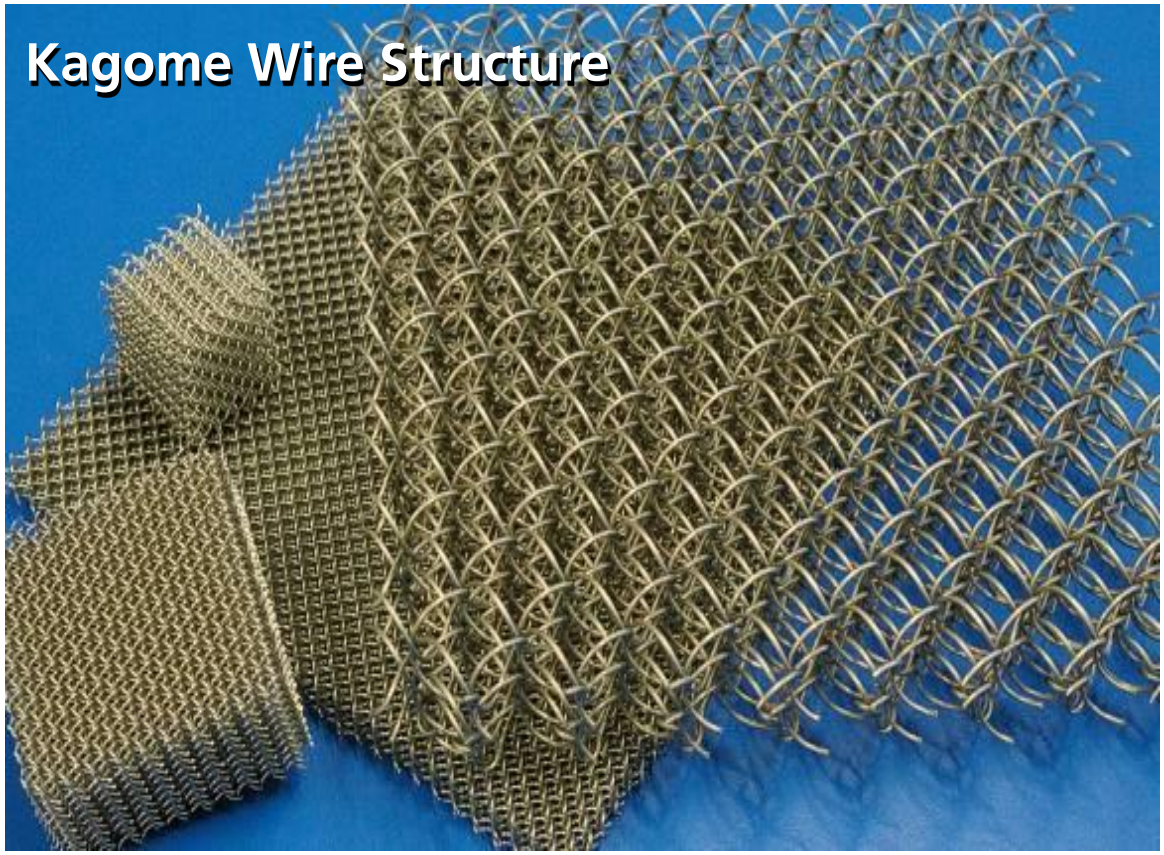

© Fraunhofer IFAM Dresden

Properties

3D Wire Structures

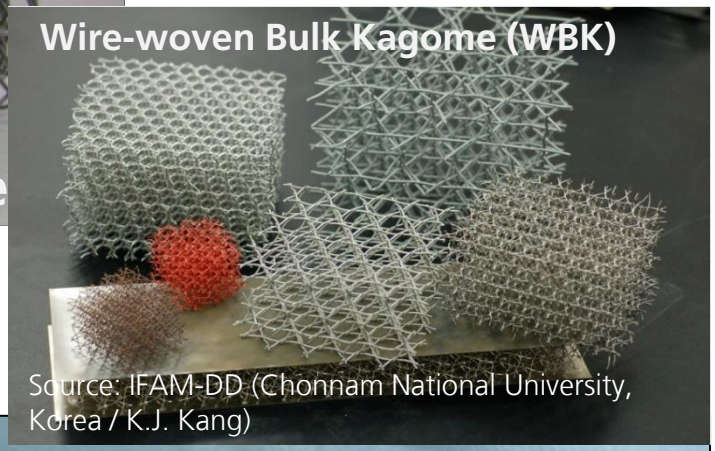

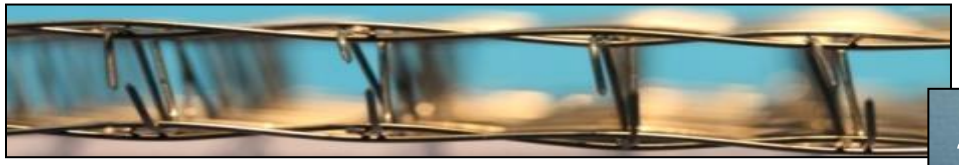

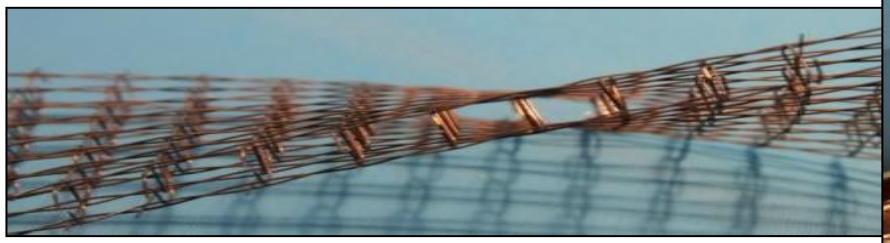

© Fraunhofer IFAM Dresden

Applications

PCM filled metal fibre heat exchanger

Main features:

- Stack of sintered AlCu5 fiber plates 200 x 200 x 200 mm³ (porosity 80 %)
- Tubes mechanically widened
- Filling with paraffine RT 42
- Storage capacity ~ 0,4 kWh

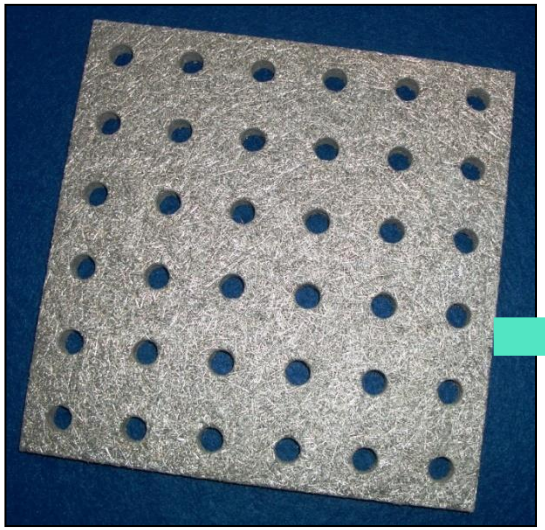

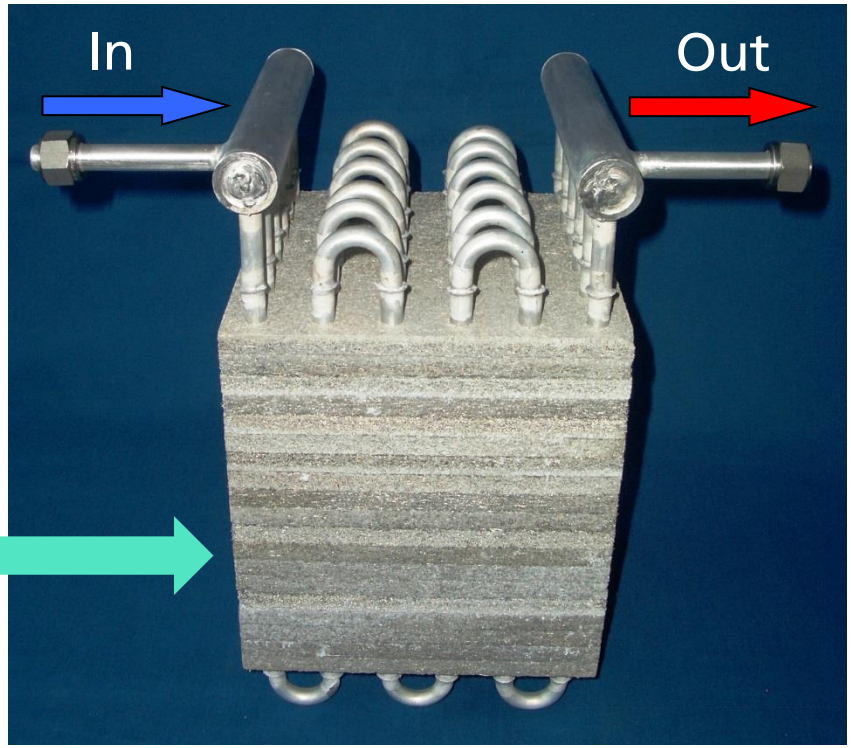

© Fraunhofer IFAM Dresden

Applications

Adsorption Heat Accumulator

- Adsorber made of thin zeolite layers (SorTech AG, Germany) on highly heat conducting network with high specific surface area (5.000 to 25.000 m^2/m^3)
- Lab test samples reach a power density of 4 kW/l with cycling times in the range of a few minutes; target value for real-life adsorber including heat exchanger architecture is > 0.5 kW/l

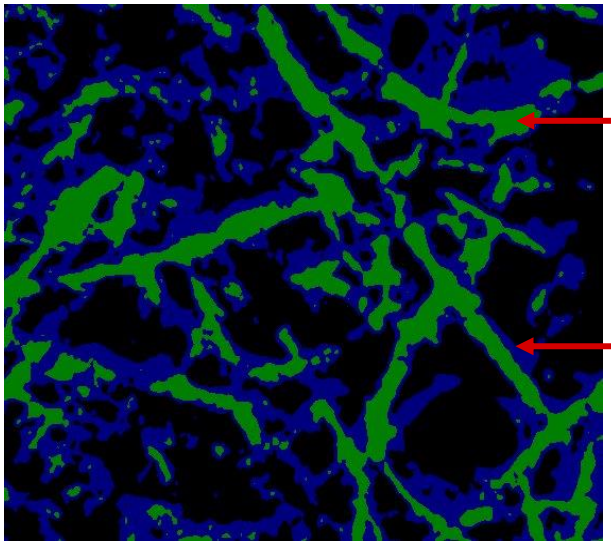

green: heat conducting AlCu5 fiber network

blue: zeolite layers

Tomography image courtesy of FhG ITWM

© Fraunhofer IFAM Dresden

Applications

Synthetic Bone Replacement

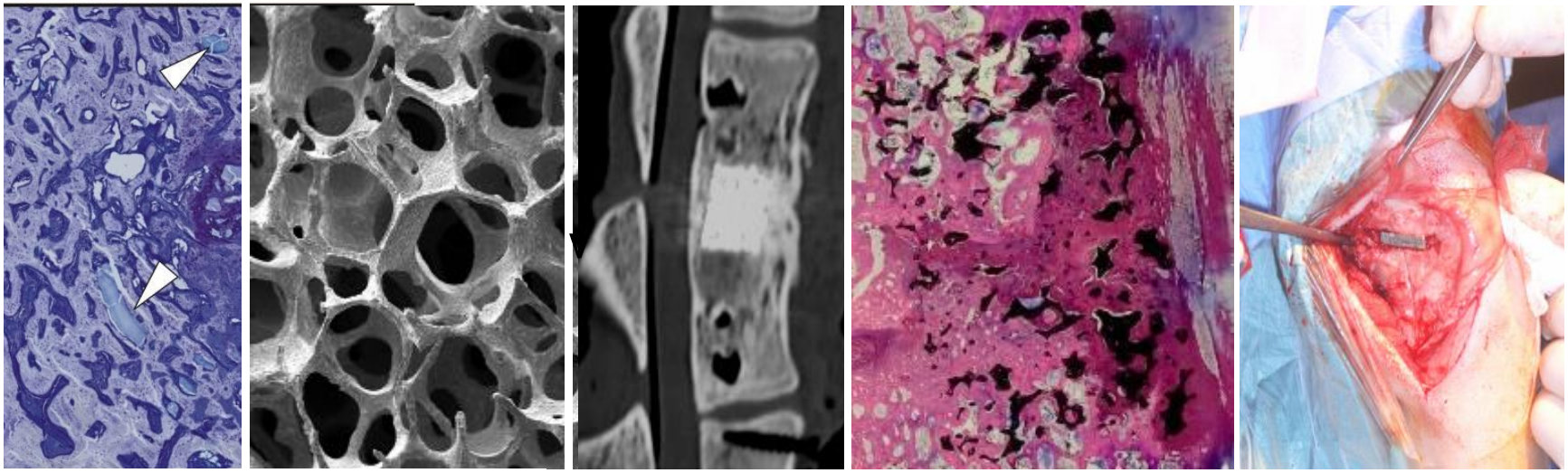

synthetic bone replacement

- Biomechanical adaption to bone properties
- Powder metallurgical technologies for manufacturing of cellular metals with adjustable stiffness
- interckonnecting pore structure
- osseointegration improves primary and secondary stability
- vascularisation needed for bone formation

CHARITÉ UNIVERSITÄTSMEDIZIN BERLIN

MHH Medizinische Hochschule Hannover

LMU

Fraunhofer IFAM Branch Lab Dresden

Applications

Biodegradable Bone Replacement Implants

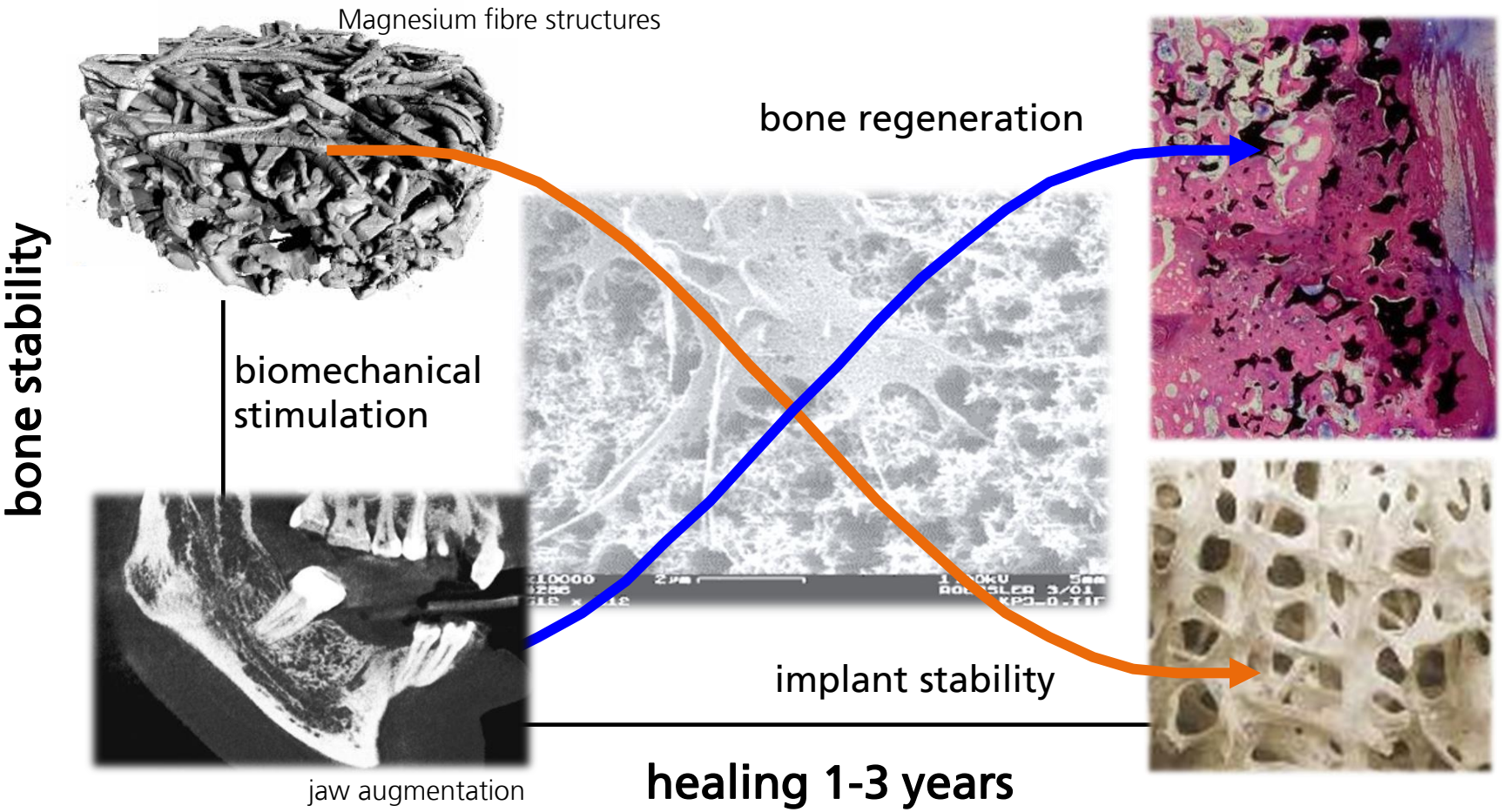

© Fraunhofer IFAM Dresden

Applications

Liquid Filtration

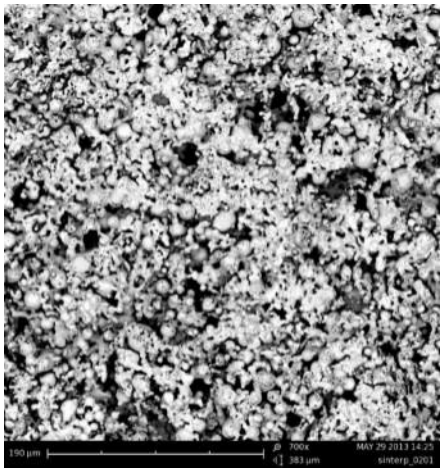

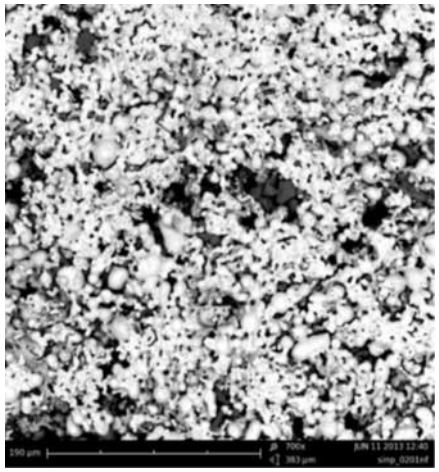

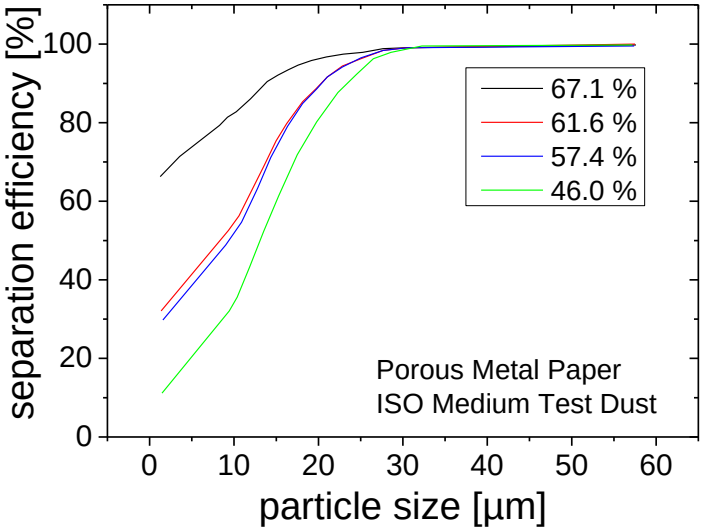

porosity [%]	cumulative efficiency [%]
67.1	88.3
61.6	70.7
57.4	59.4
46.0	71.9

Separation of Metal Paper

- Increased porosity enhances cumulative efficiency
- Mass related efficience is considerably higher

© Fraunhofer IFAM Dresden

Applications

Catalyst Support

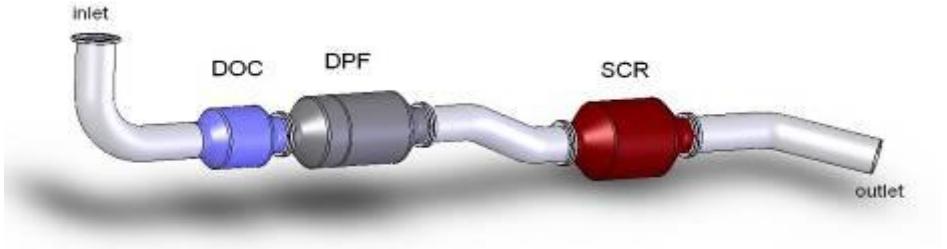

Benefits of cellular metals

- Cross flow
- Lowered need for noble metals
- Homogeneus temperature-distribution
- 30 % reduction of Pt: MFC 1.8 g, DOC (series) 2.6 g
- High strength (e.g. FeCrAl)

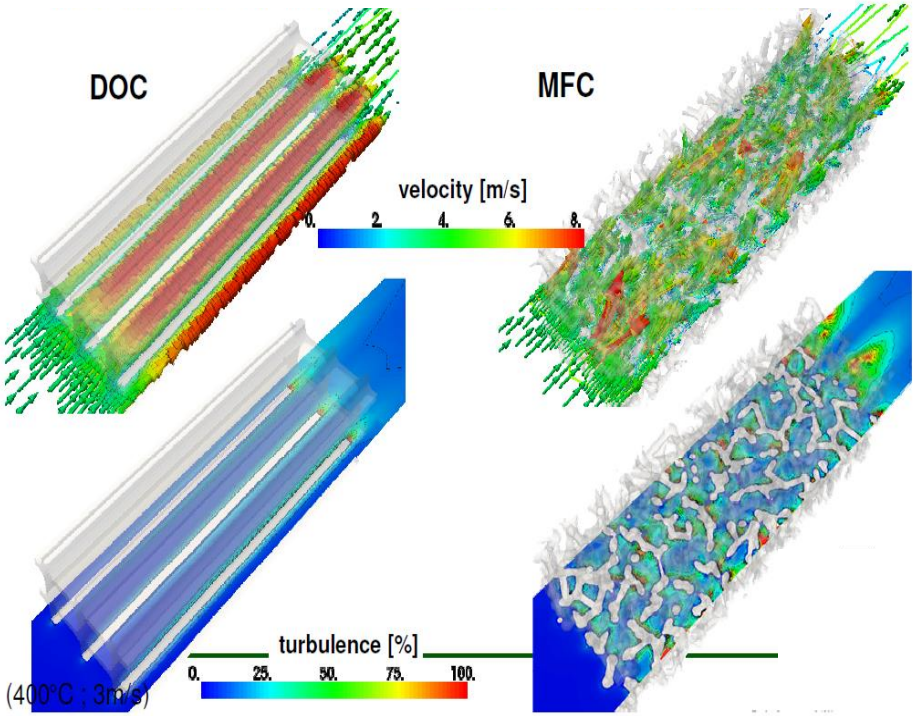

© Fraunhofer IFAM Dresden

Fraunhofer IFAM Branch Lab Dresden

Applications

Lightweight Tools für manufacturing of EPS

Increase of energy efficiency of moulding machine
Objective

- Reduction of energy consumption for heating/cooling
- Increase of energy efficiency by 30 %
- Reduction of mass by 50 %

Strategy

- Reduction of thermal mass by use of cellular metals with low heat capacity
- Realization of nozzleless surfaces

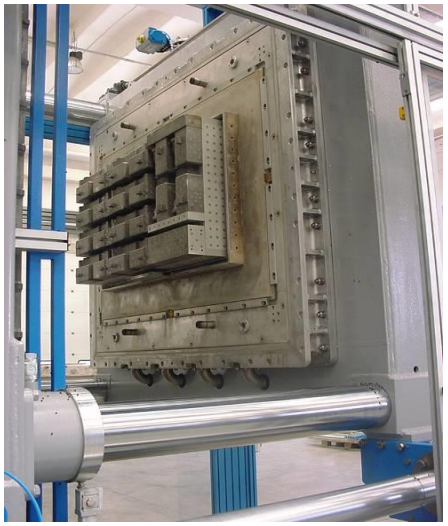

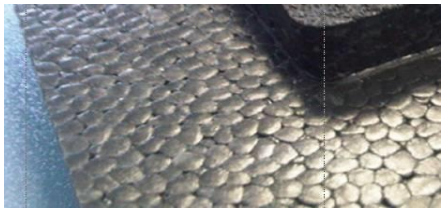

© Fraunhofer IFAM Dresden

RUCH NOVA PLAST

Fraunhofer IFAM Branch Lab Dresden

Applications

Crashbox

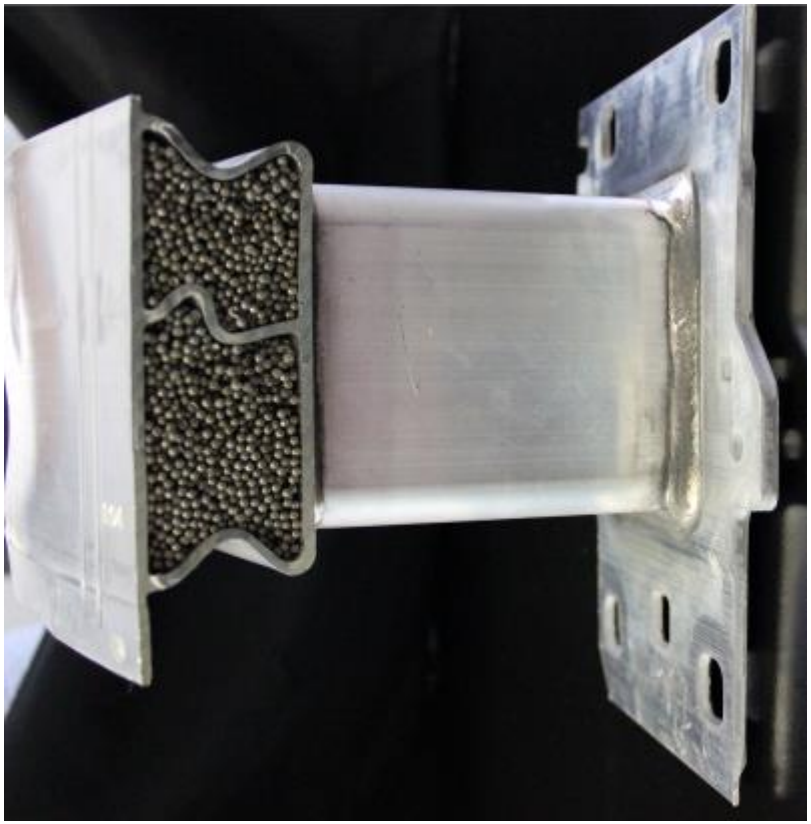

Cellular Metals in Crashbox

- Bonded hollow sphere structures
- Local increase of energy absorption capability
- lower wall thicknesses of profiles possible

Benefits

- lowered total mass
- lowered construction volume

© Fraunhofer IFAM Dresden

Idea of the Advanced Pore Morphology (APM) :

to separate the foaming step from the shaping step !!

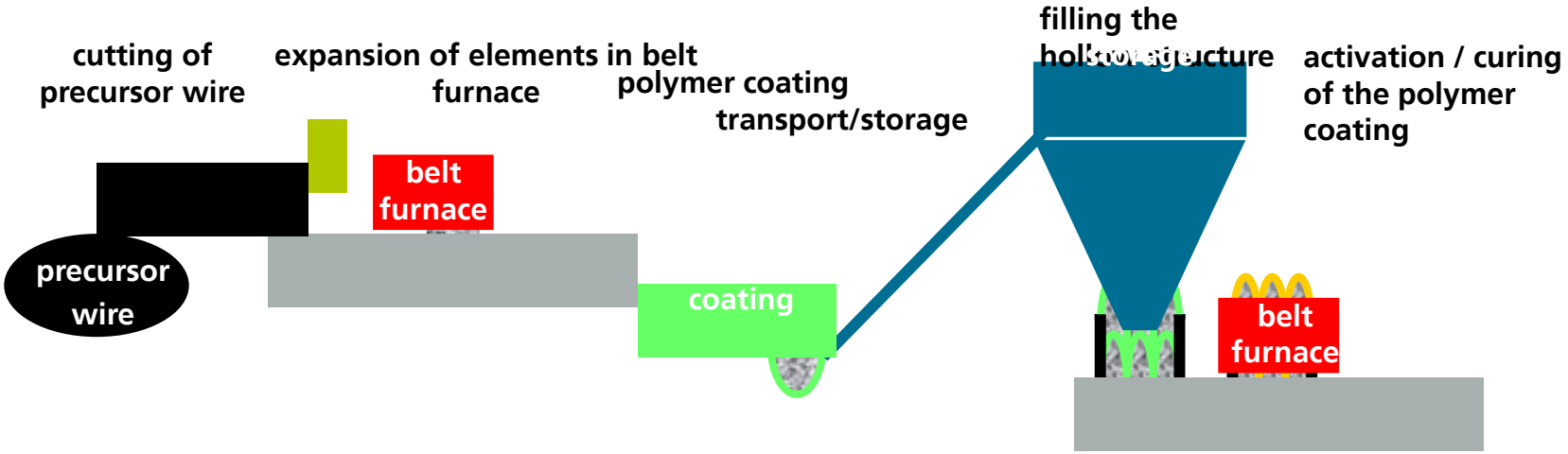

Joachim Baumeister, Fraunhofer Institute IFAM Bremen
Department of Powder Technology

Fraunhofer IFAM

APM Parts

APM foam parts

APM foam filled structures

APM sandwich structures

Joachim Baumeister, Fraunhofer Institute IFAM Bremen
Department of Powder Technology

Fraunhofer
IFAM

Mechanical properties of APM hybrid foams

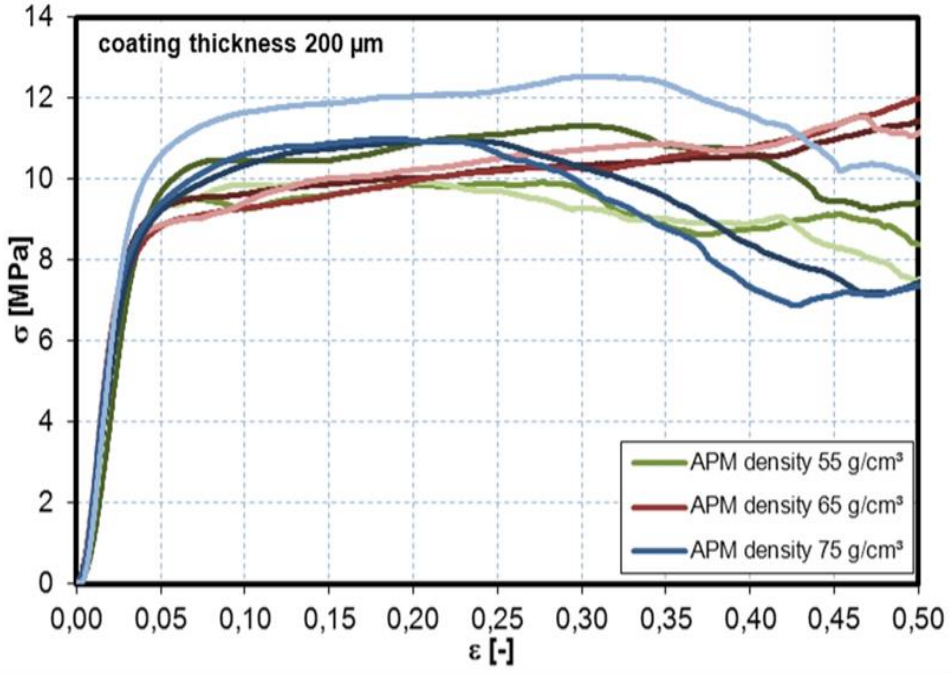

quasistatic tests ($d\varepsilon/dt \approx 0.004\ s^{-1}$)

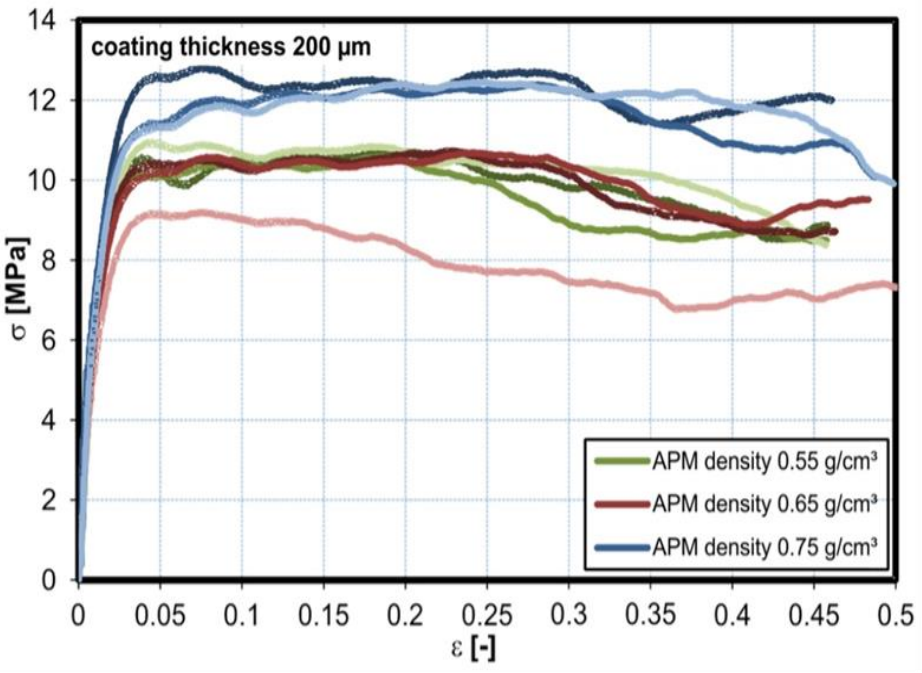

dynamic tests ($d\varepsilon/dt = 10\ s^{-1}$)

- ✓ strength similar to conventional aluminum foam of the same density
- ✓ no significant strain rate dependency of the properties

Joachim Baumeister, Fraunhofer Institute IFAM Bremen
Department of Powder Technology

Fraunhofer IFAM

Powder metallurgical metal foam production

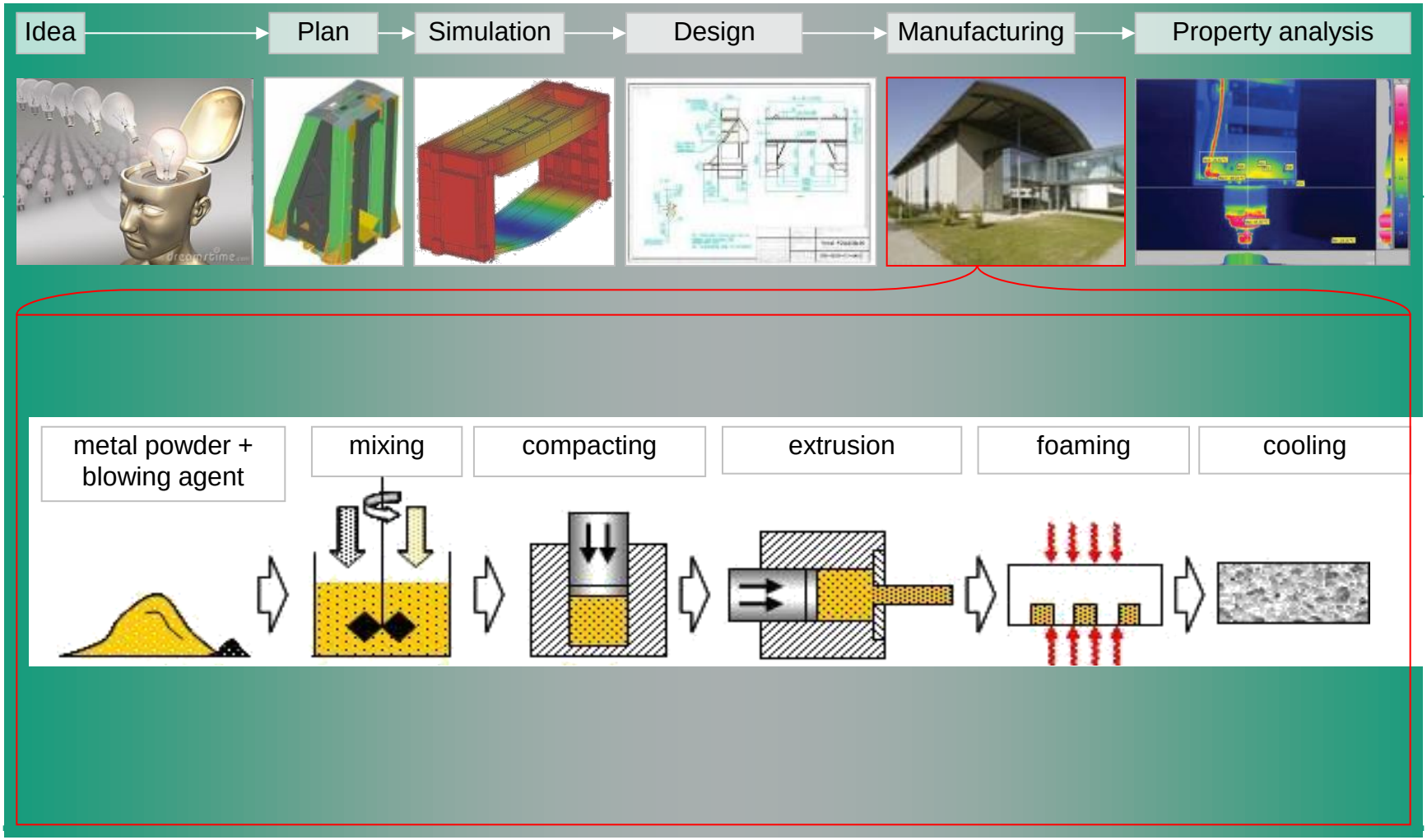

© Fraunhofer

Fraunhofer IWU

Aluminium 铝

Infrarot-
Strahler
红外线辐射器

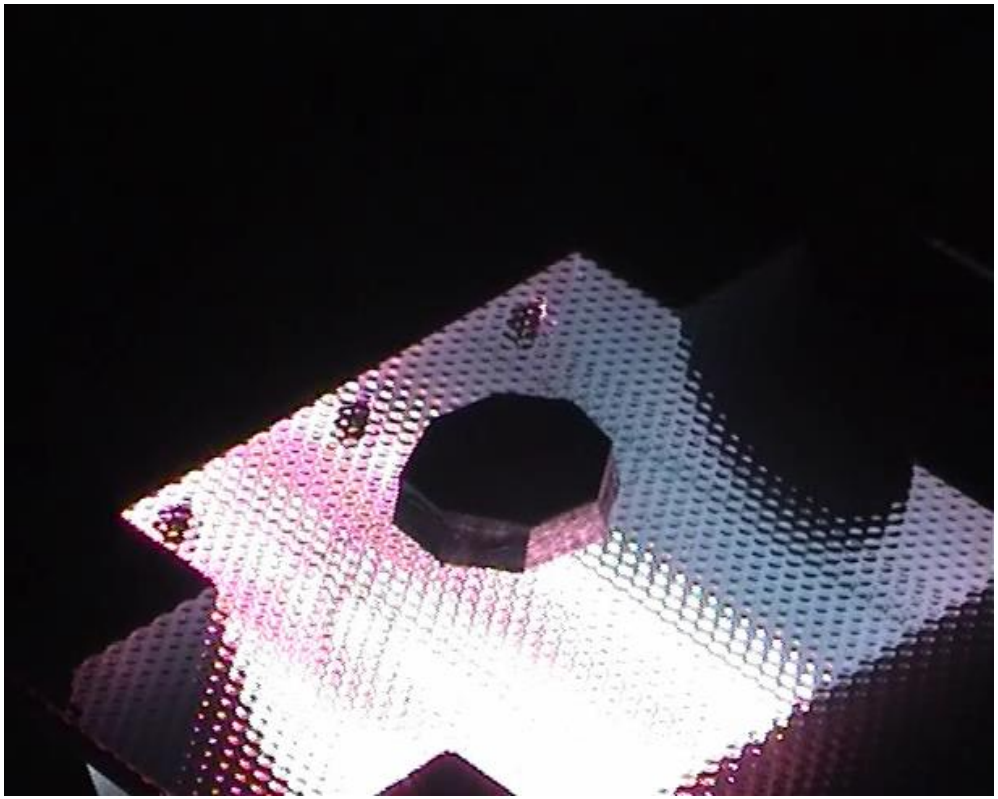

Quarzglas-
Platte
石英玻璃
板

Schäumvorgang 发泡程序

Infrarot-Schäumung 红外线发泡

© Fraunhofer

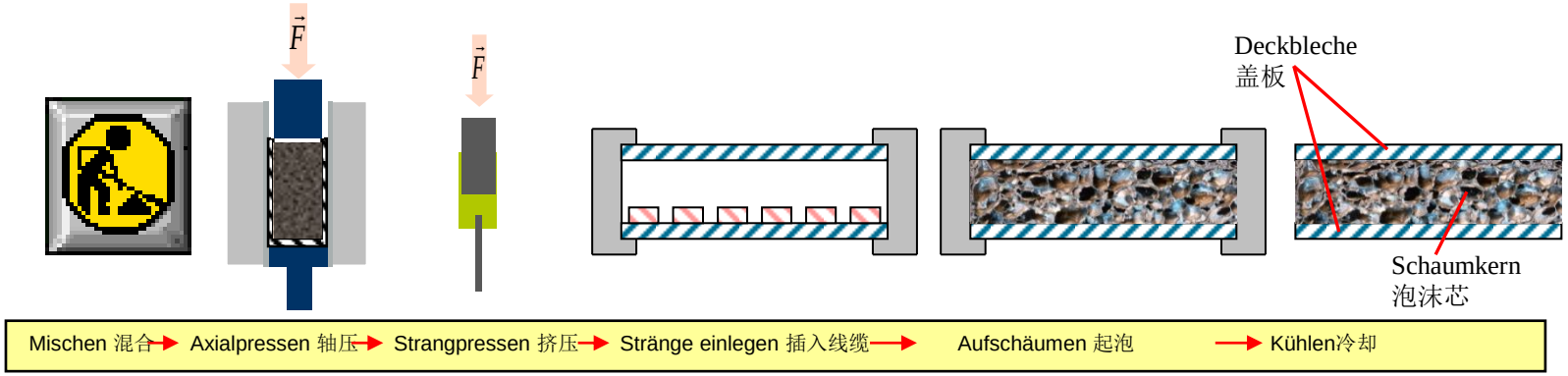

Herstellbare Größen 制造尺寸：

max. Fläche（最大面积）： **2500 x 1250 and 2200 x 1400 (3000 x 1500)**

max. Sandwichhöhe（最大夹层高度）： **50 (70)**

Deckblechdicke（盖板厚度）： **0,8 ... 10**

© Fraunhofer IFAM Dresden

Pulvermetallurgische Route – Sandwich 粉末冶金线路—夹层

Fraunhofer IWU

Werkstoffkennwerte des Aluminiumschaums 铝泡沫的原料特性值

Dichte 密度	0,5 - 0,9 g/cm³
Querkontraktion 横向收缩	0,31 - 0,34
E-Modul (0,7 g/cm³) 电子模块	约 6300 N/mm²
耐压强度 Druckfestigkeit (0,7 g/cm³)	约 15 N/mm²
导热性 Wärmeleitfähigkeit (0,7 g/cm³)	约 20 W/m·K
原料阻尼 Werkstoffdämpfung (0,7 g/cm³)	约 $4{,}5 \cdot 10^{-3}$

→ technologisch gut beherrschbar
可以实施良好的技术控制: 0,7 g/cm³

特性值$Kennwert_{Foam}$ =特性值$Kennwert_{Solid}$
$(\rho_{Foam}/\rho_{Solid})^n$, n = 1,7 bis（至） 2

Erfüllt die Brandschutzanforderungen nach DIN 4102
满足 DIN 4102标准的消防要求

Temperaturbeständigkeit bis ca. 500 ° C
耐受约500 ° C的高温

Hohes Energieabsorptionsvermögen
较高的能量吸收能力

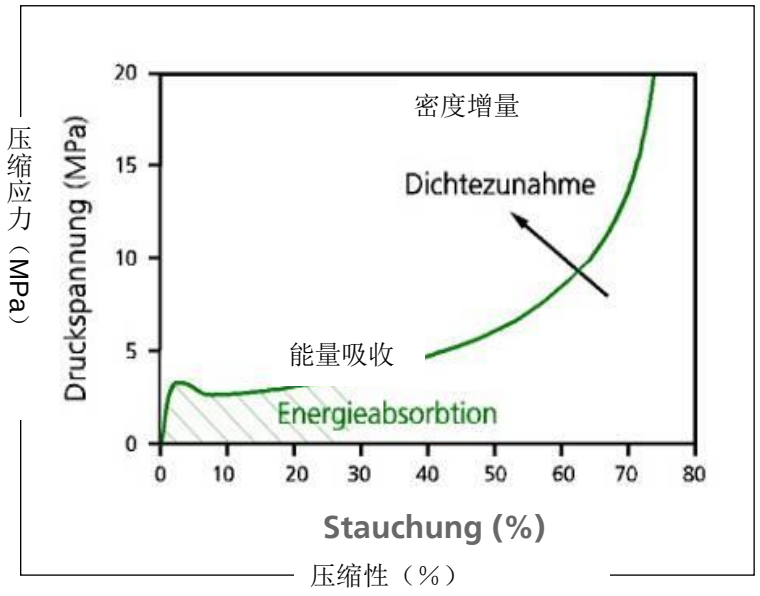

© Fraunhofer IFAM Dresden

Eigenschaften von Aluminium-schäumen 铝泡沫的特性

General Properties of aluminum foam

Powder metallurgical route

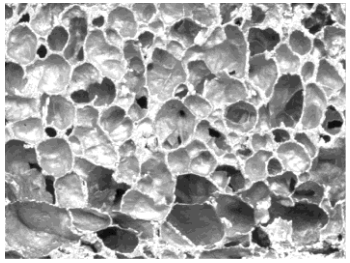

Aluminum foam = cellulare structure with cell walls

Parameter	Foam AlSiMg	Massive AlSi12Cu
Density	**0,3 - 0,9 g/cm³**	2,7 g/cm³
Poisson ratio	0,31 - 0,34	0,31 - 0,34
Modulus of elasticity (0,7 g/cm³)	ca. 6.300 N/mm²	ca. 70.000 N/mm²
compressive strength (0,7 g/cm³)	ca. 15 N/mm²	225-330 N/mm²
thermal conductivity (0,7 g/cm³)	ca. 20 W/(m · K)	135-147 W/(m · K)
Material damping (0,7 g/cm³)	**$4{,}5 \cdot 10^{-3}$**	k. A.

- Compliance with the fire protection requirements of German standard DIN 4102
- temperature resistant up to about 200 °C, short-term up to about 500 °C
- high energy absorption capacity

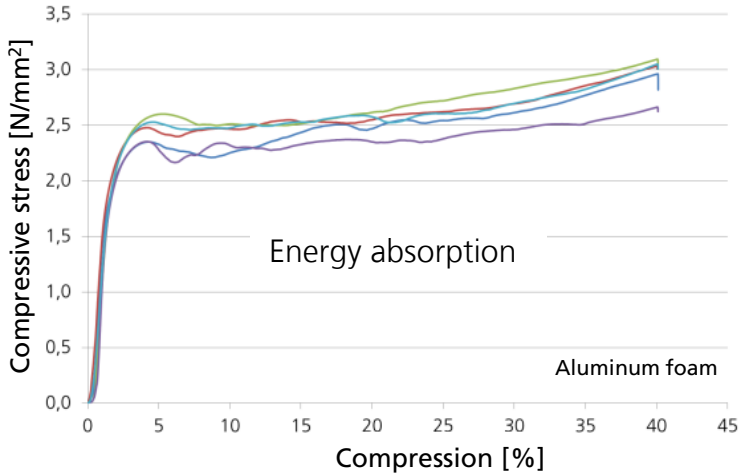

© Fraunhofer

Fraunhofer IWU

3-D-Formteile aus Aluminiumschaum
铝泡沫制成的三维立体模塑件

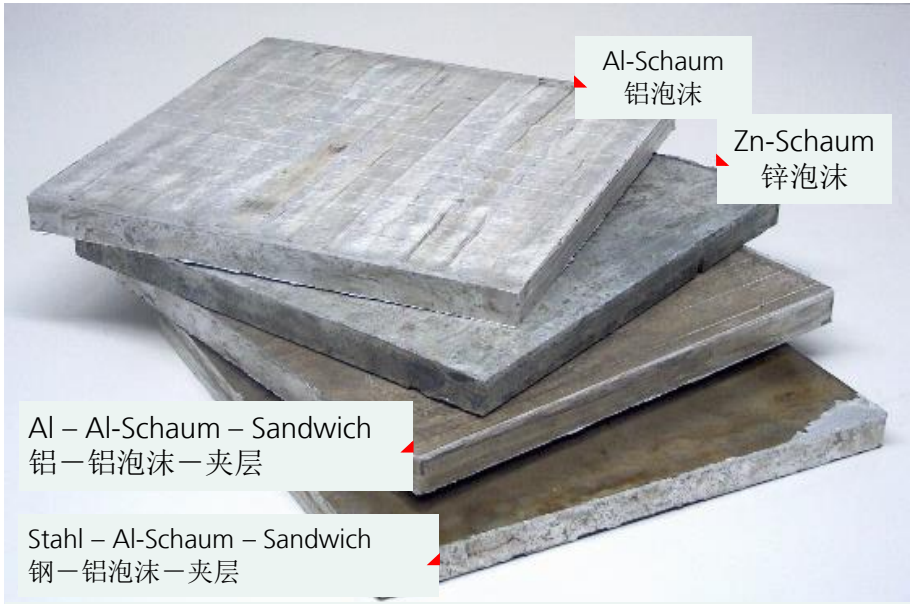

Metallschaum- und Sandwichplatten mit Metallschaum
金属泡沫板和带有金属泡沫的夹层板

ausgeschäumte Stahlprofile
充泡型钢剖面

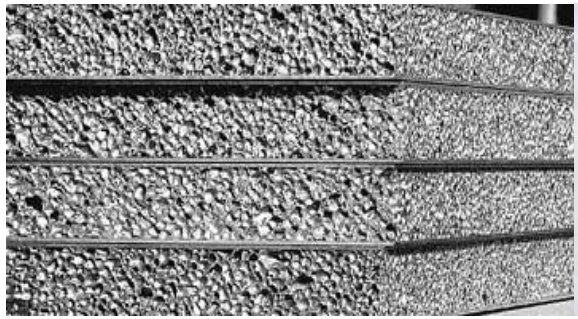

© Fraunhofer IFAM Dresden

Produktgeometrien – Beispiele 产品的几何图形实例

Fraunhofer IWU

AFS =

Aluminum foam-Sandwiches

Metallic bonding of aluminum foam with aluminum cover sheet

1 **2** **3** **4**

SAS =

Steel-Aluminum foam-Steel-Sandwiches

Metallic bonding of aluminum foam with steel cover sheet

钢板上铝泡沫的冶金接合

© Fraunhofer

1. Serienanwendung im Werkzeugmaschinenbau机床制造领域的首次批量应用

Fräsmaschine HPM 1850U für den Werkzeug- und Formenbau mit Stahl-Aluminiumschaum-Sandwiches

用于钢－铝泡沫夹层工具和模具制造的铣床HPM 1850U

HPM 1850U

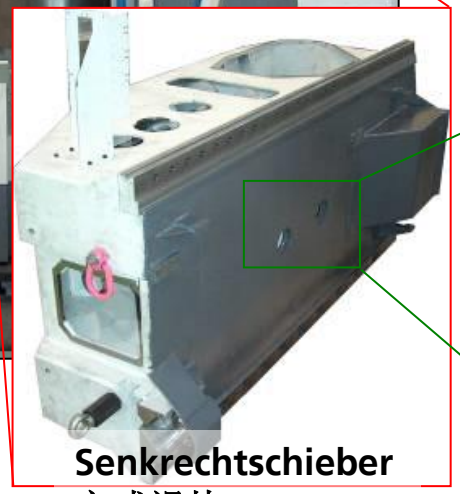

Senkrechtschieber
立式滑块

Mass reduction 28%
at same stiffness;
Very good damping

Machine tool with aluminium foam sandwiches in serial production
(about 15 pieces per year)

First Serial Production since 2004 !

Sandwich
夹层

1. geschäumte Baugruppe in Serie　发泡的串联模块

© Fraunhofer

Fraunhofer IWU

Application – Crash absorber and elements of stiffening

Source: Volkswagen AG; Fraunhofer IWU .

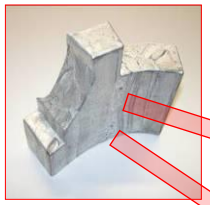

+ 10% torsional stiffness of the whole car body

Node area of D-pillar,
stiffening by Aluminium foam-cores.

Source: Alulight; Fraunhofer IWU.

Series - 3.000 pieces/year

+ Car-body stiffness

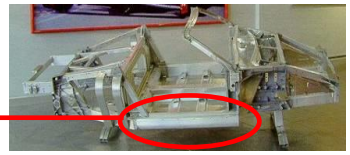

Reinforcing element of metal foam in a side-sillboard of Ferrari Spider 430.

Source: Fraunhofer IWU .

+ Crash absorption

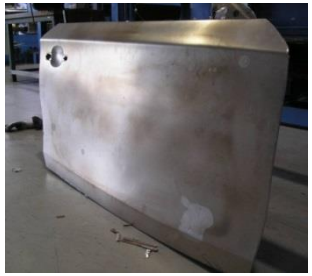

Concept door in aluminum-zinc foam sandwich construction and rear seat rest carrier.

+ Lightweight design

Series - 200.000 pieces/year

Metal foam-crash absorber in a baggage net of Audi Q7.

+ Crash absorption

Source: Alulight; Fraunhofer IWU.

© Fraunhofer

Fraunhofer IWU

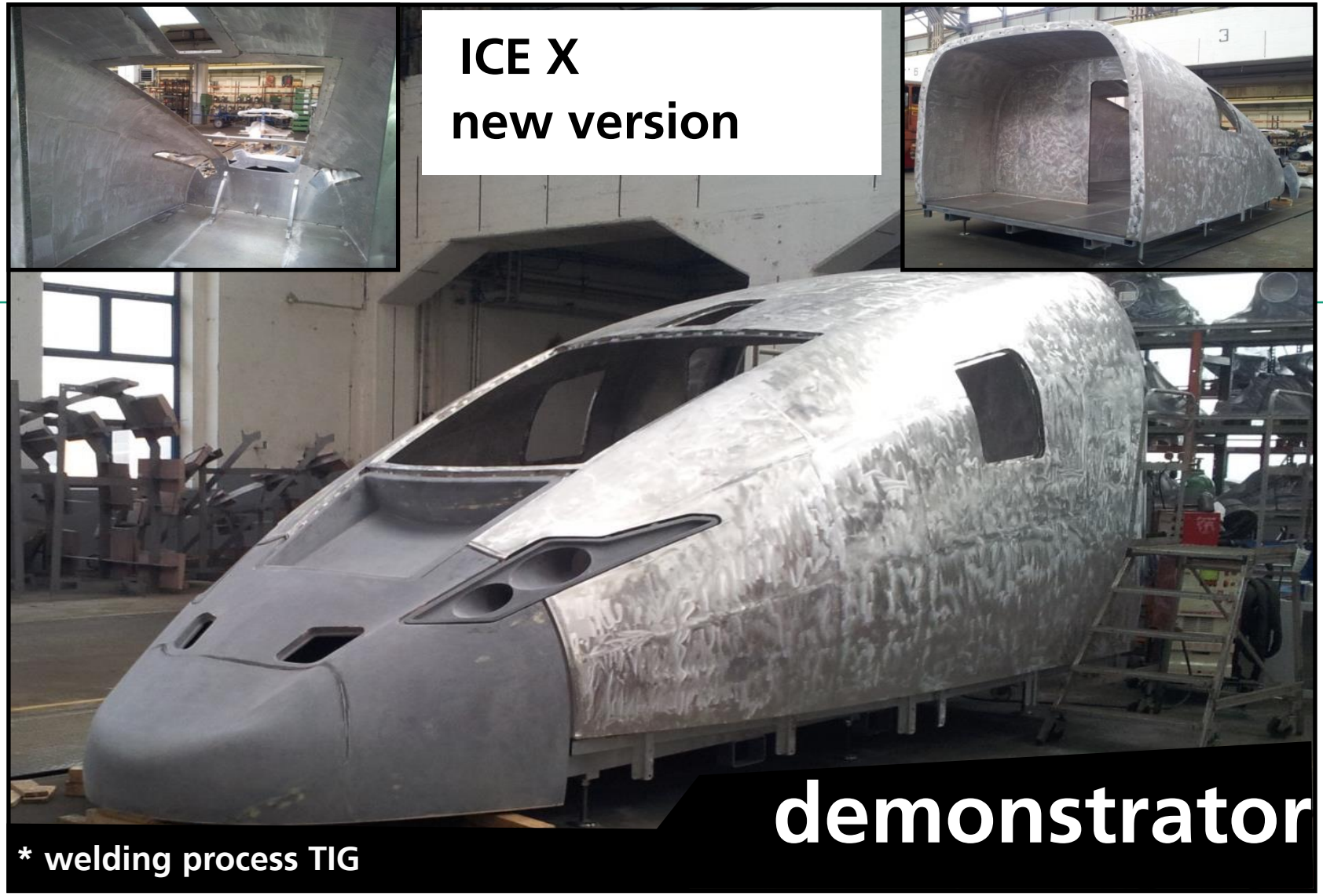

© Fraunhofer

Fraunhofer IWU

納米粒子為關鍵金屬部件帶來之理想特性

由澳洲斯威本科技大學校長劉建德教授主講

Enhancing the Properties of Lightweight Materials using Nano-particle

SWINBURNE UNIVERSITY OF TECHNOLOGY

Transforming Industries, Shaping Lives and Communities

SWINBURNE UNIVERSITY OF TECHNOLOGY

Transforming Industries, Shaping Lives and Communities

Swinburne University of Technology (now)
1908 Eastern Suburbs Technical College

SCIENCE
INNOVATION
TECHNOLOGY

Professor Alan Kin Tak Lau
(刘建德教授)

FIEAust FIMechE FIMMM FRAeS FHKIE FIED

Academician, European Academy of Sciences
(歐洲科學院院士)
Academician, European Academy of Sciences and Arts
(歐洲科學及藝術學院院士)
International Vice President of The Institution of Mechanical Engineers (IMechE)
(英國機械工程師學會國際副會長)
Independent Non-Executive Director of Kingsflair International (Holdings) Limited
(科勁國際集團獨立非執行董事)

Pro-Vice-Chancellor
(Research Performance and Development)
Swinburne University of Technology
Australia
(斯威本科技大学副校长(科研成果及发展))

KNOWING

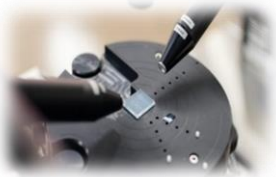

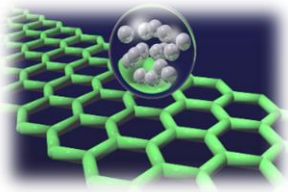

Micro-fabrication

Product Design and Development

Nano-materials

Data Science and Cybersecurity

Astrophysics and Physics

Solar Technology

Civil Engineering

Aviation

Bio-engineering and Neuroscience

KEY FOCUS AREAS

Funding received in 2017

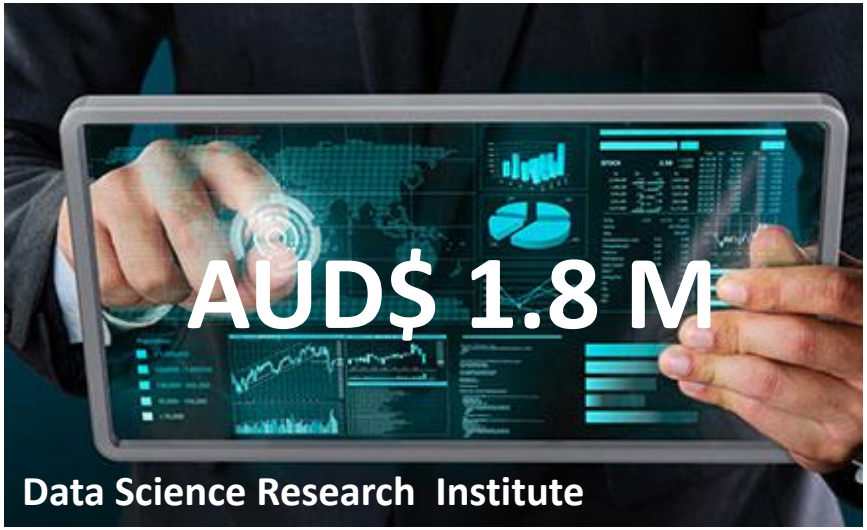

Swinburne Research is supported by 5 Research Institutes

Factory of the Future

Enhancing the Properties of Lightweight Materials

SWINBURNE UNIVERSITY OF TECHNOLOGY

Specialist Facilities

- Advanced Manufacturing and Design centre
- Advanced Technologies Centre
- ANEF-Vic Biointerface Engineering Hub
- Aviation Simulation Laboratory
- Chemistry and Biotechnology Laboratories
- Cisco Networking Laboratory
- Geotechnical Laboratory
- Hydraulics Laboratory
- Keck Observatory and Parkes Radio Telescope
- Micro-fabrication Laboratory
- Nano-fabrication Laboratory
- Neuroimaging Facility
- Smart Structures Laboratory
- Solar Facility
- Swinburne Supercomputers
- Ultrafast Micro-spectroscopy Facility
- Virtual Design Laboratory
- Virtual Reality Theatre

Swinburne Innovation Precinct

SWINBURNE UNIVERSITY OF TECHNOLOGY

Why Lightweight Materials and Structures Are So Important?

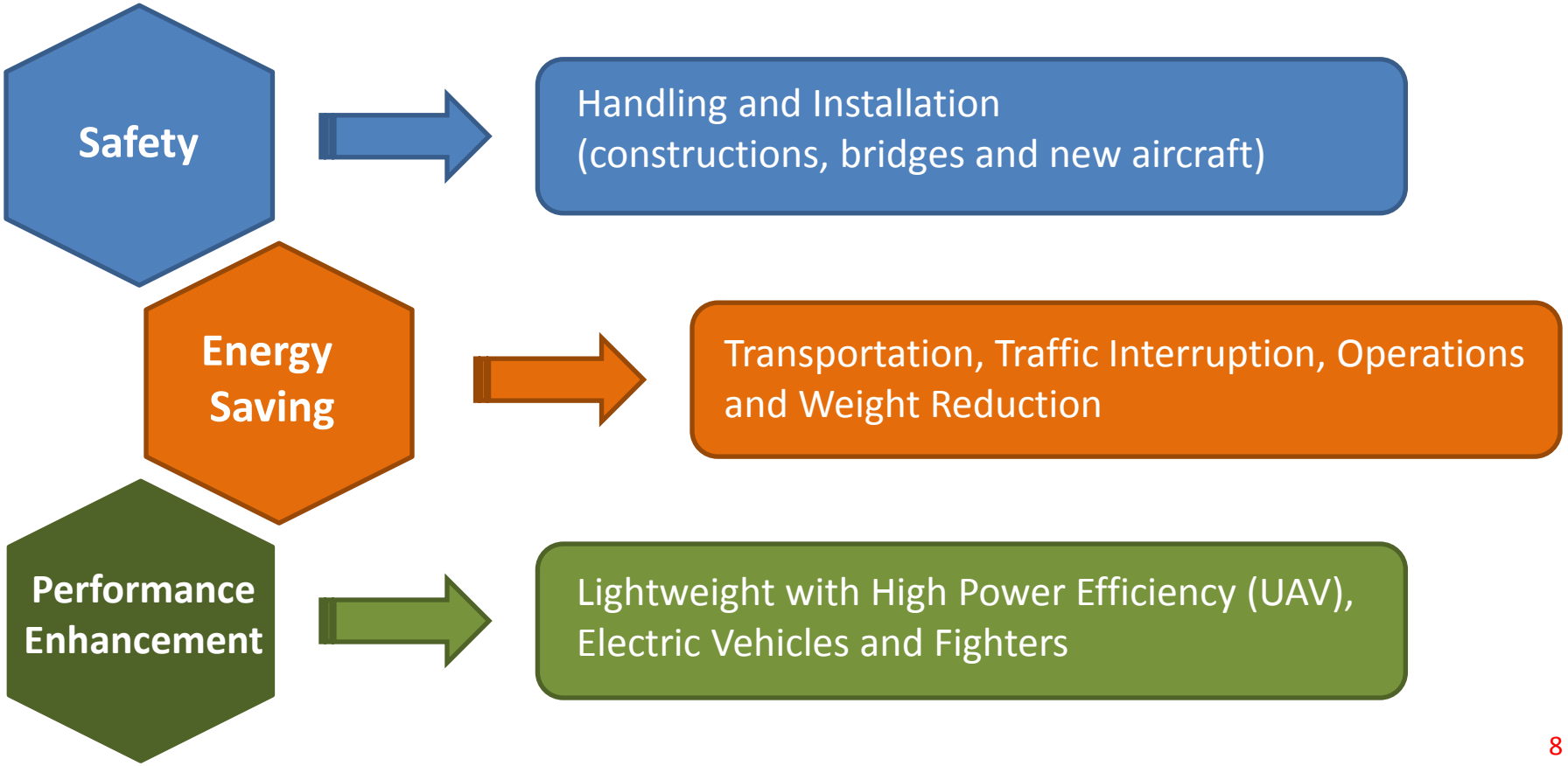

Enhancing the Properties of Lightweight Materials

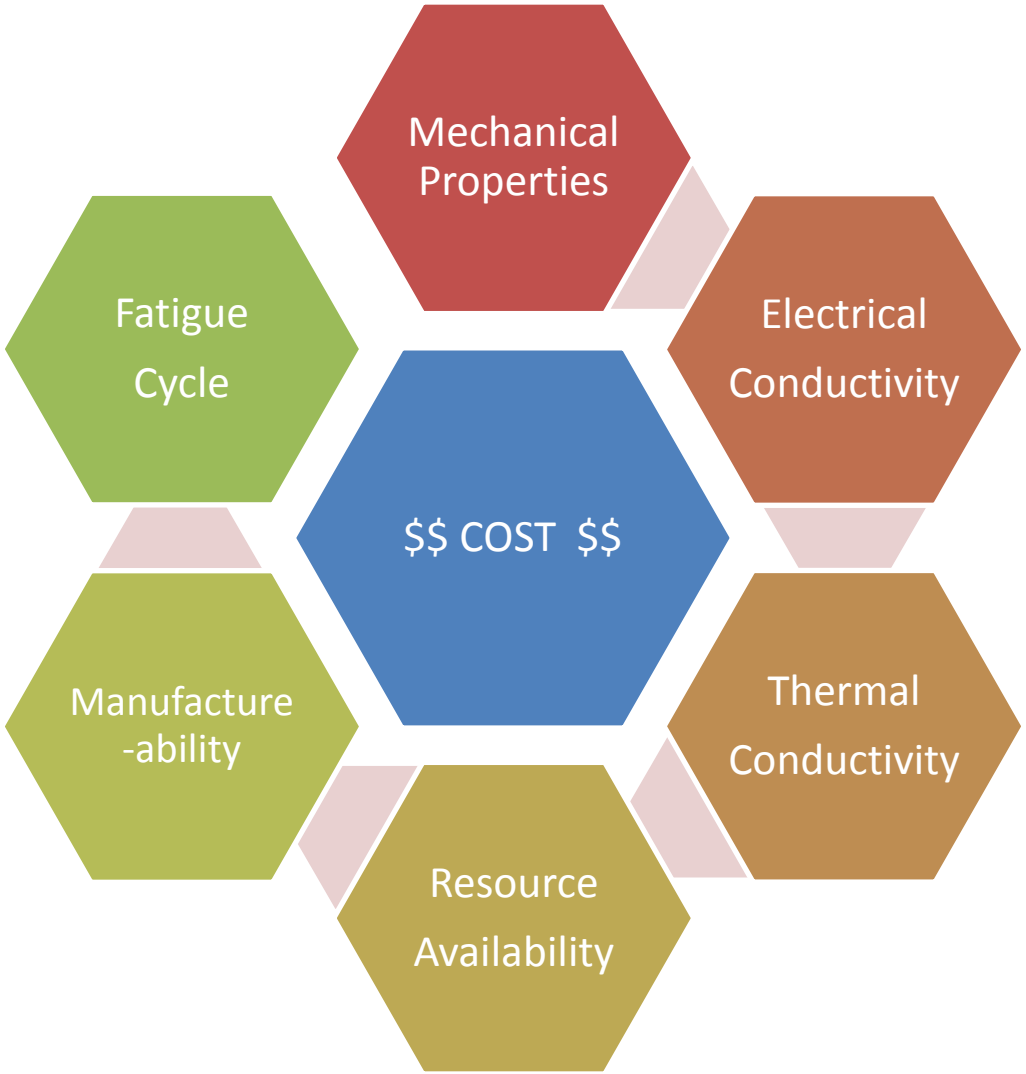

Commonly used lightweight materials

- Aluminium
- Magnesium
- Titanium
- Engineering polymers
- Structural Ceramics
- Composites

Enhancing the Properties of Lightweight Materials

SWINBURNE UNIVERSITY OF TECHNOLOGY

Automation of Composite Manufacture
自动化复合产品的制造

Civil Infrastructures
公共基础设施

3-D Printing Materials
用于轻质材料的3D打印技术

Smart Materials and Structures
智能材料及结构

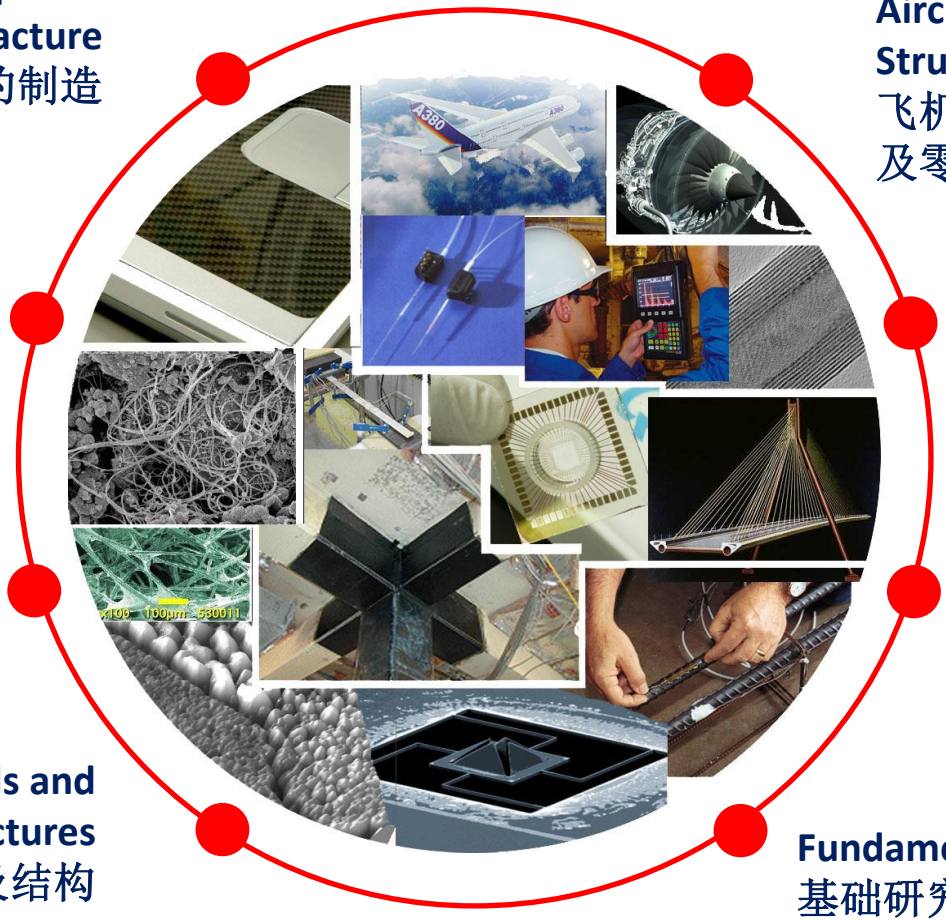

Aircraft and Aerospace Structural Components
飞机及太空工程材料及零部件 (铝合金面板修理)

Resin and Fibre Development
树脂和纤维开发

Biocomposites
生物材料

Fundamental Research
基础研究

Lightweight Materials Research in Swinburne

Enhancing the Properties of Lightweight Materials

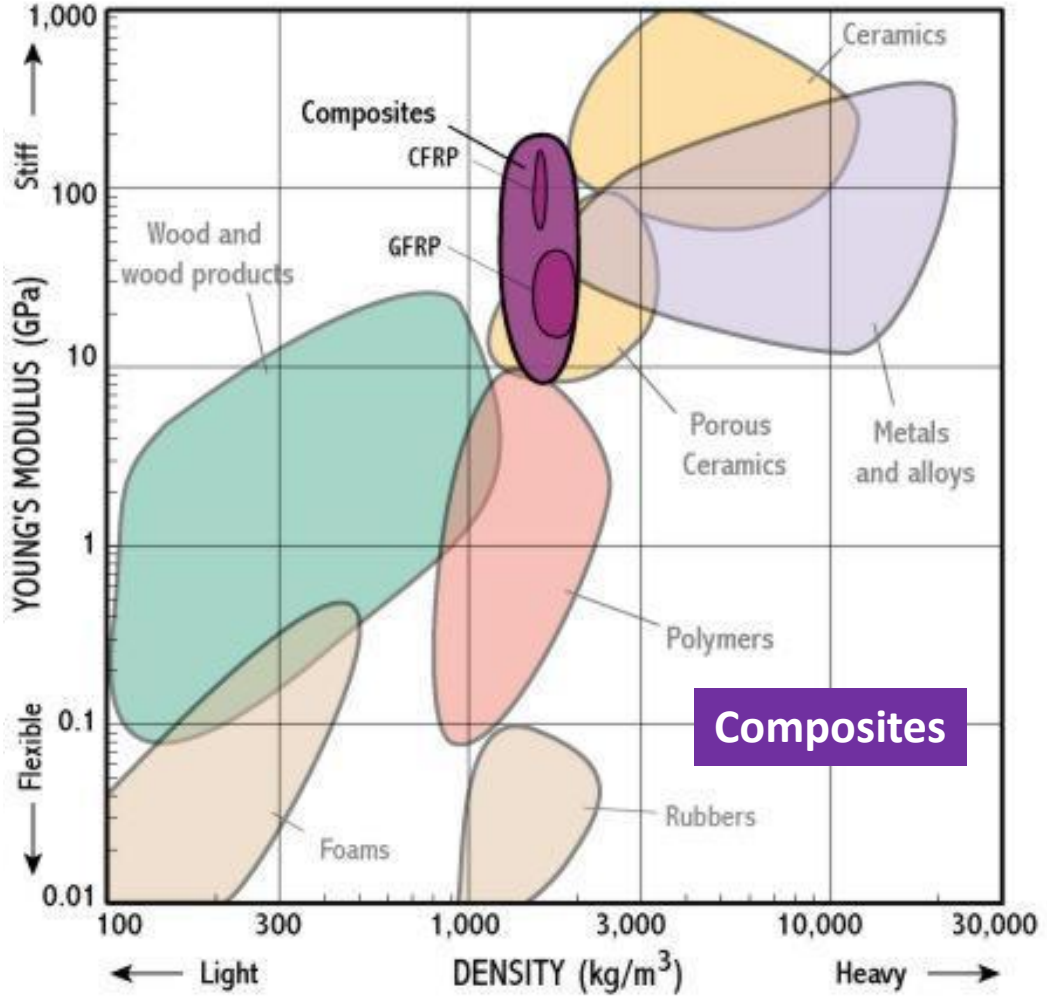

Aluminium Alloys

Advanced Composites

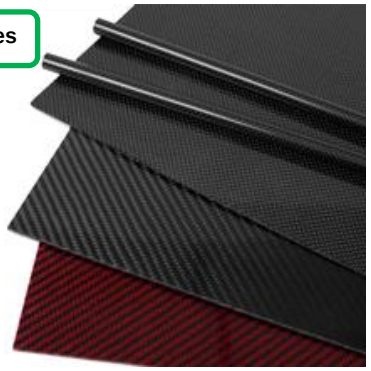

Enhancing the Properties of Lightweight Materials

SWINBURNE UNIVERSITY OF TECHNOLOGY

Jaguar XE

- Weight
- Strength
- Energy Absorbability

2015 Ford F-150 Aluminium body creates challenge for auto body shops

10 Best Cars with Aluminium Frames

Enhancing the Properties of Lightweight Materials

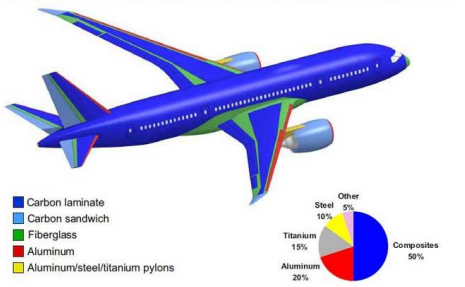

The C919 vertical tail — manufactured by AVIC Shenyang Aircraft Corporation (SAC, Liaoning, China) — comprises a vertical stabilizer and a rudder, made mostly of composite materials, except major attachment fittings which are titanium alloy. COMAC reports that composite materials have better fatigue resistance and corrosion resistance, which can greatly reduce the structural weight, improve the performance, lifetime, safety and maintainability of the aircraft and extend the time interval for field maintenance. All of this helps to reduce the aircraft operational maintenance cost and the life-cycle operating cost.

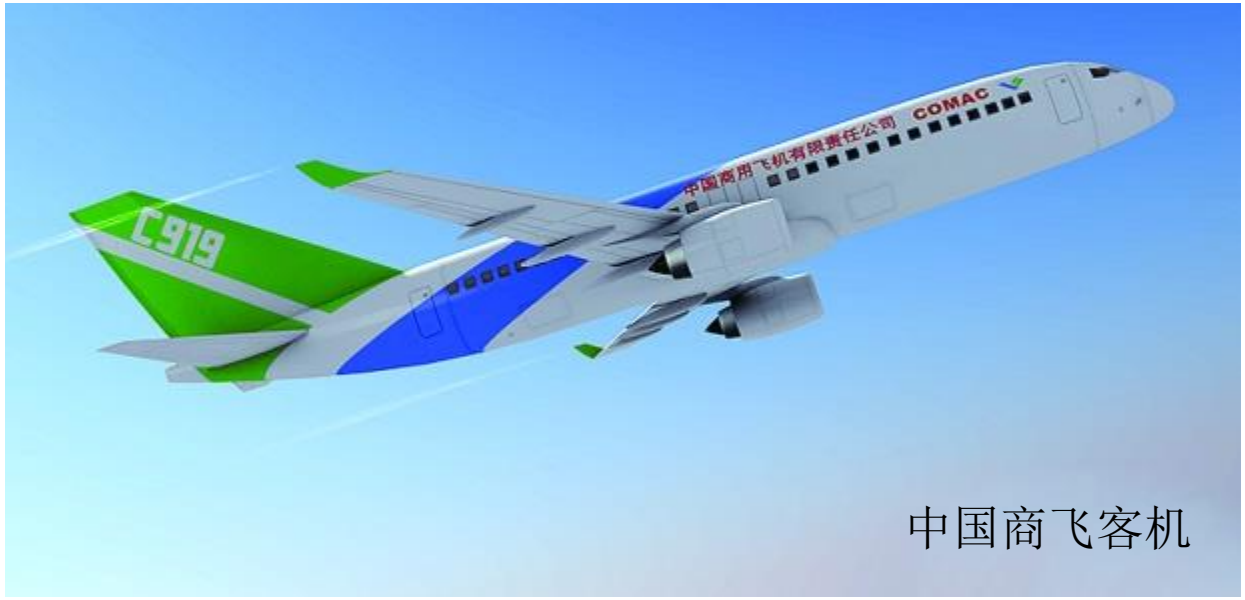

Enhancing the Properties of Lightweight Materials

Traditional Aluminum Structure

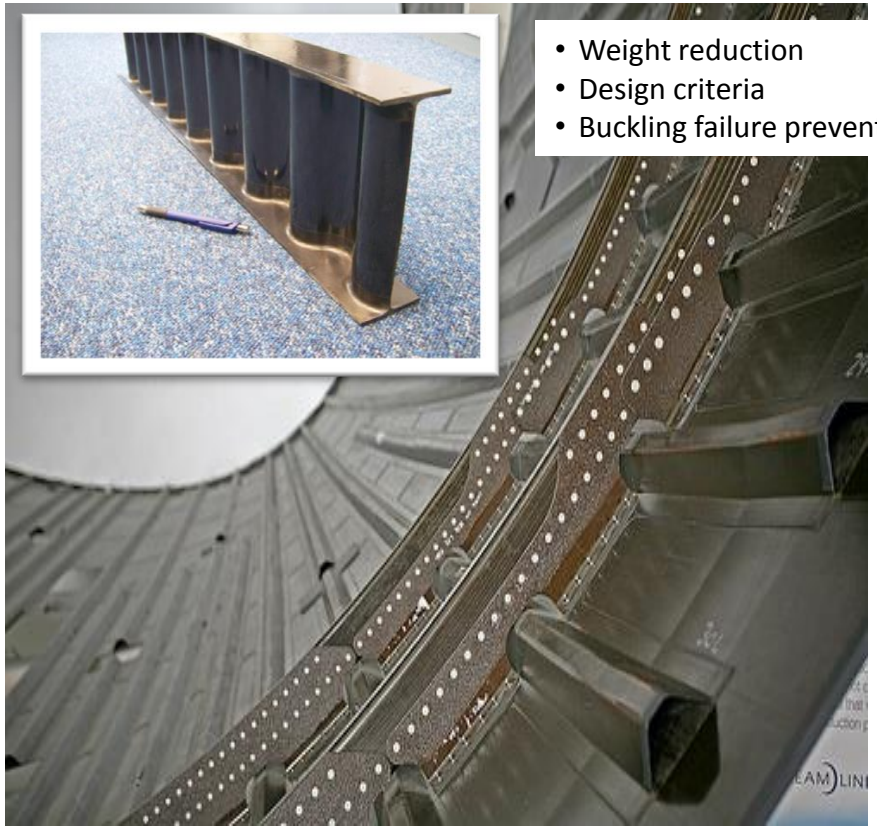

- Weight reduction
- Design criteria
- Buckling failure prevention

Carbon Fibre Composite Structure

Enhancing the Properties of Lightweight Materials

SWINBURNE UNIVERSITY OF TECHNOLOGY

At the harsh temperature environment, differential coefficients of thermal expansion (CTEs) between adherends and adhesive, may generate internal cracks that may cause a joined plate separates.

Debond at fibre/matrix interface
(Micro/nano scale level)

Delamination
(Micro/meso scale level)

Debond at the interface
(Meso/macro scale level)

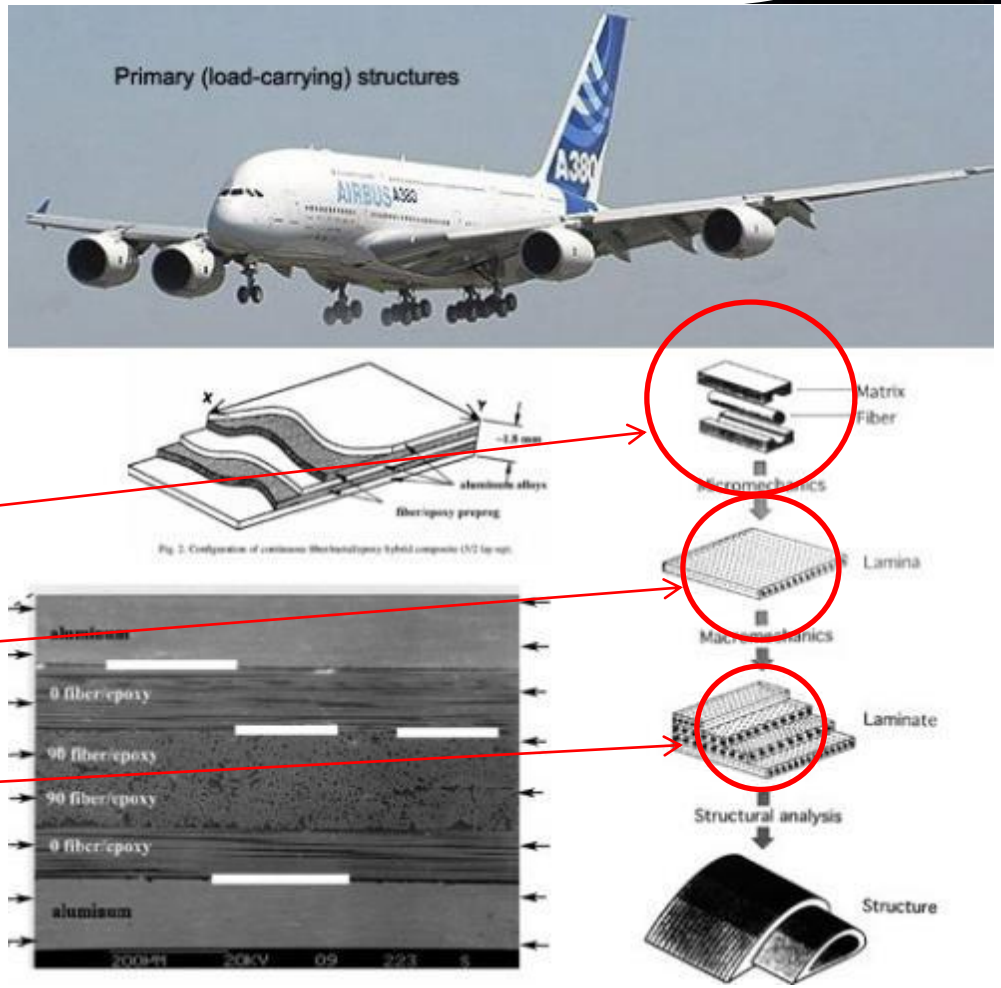

Typical Reinforcements for Engineering Materials

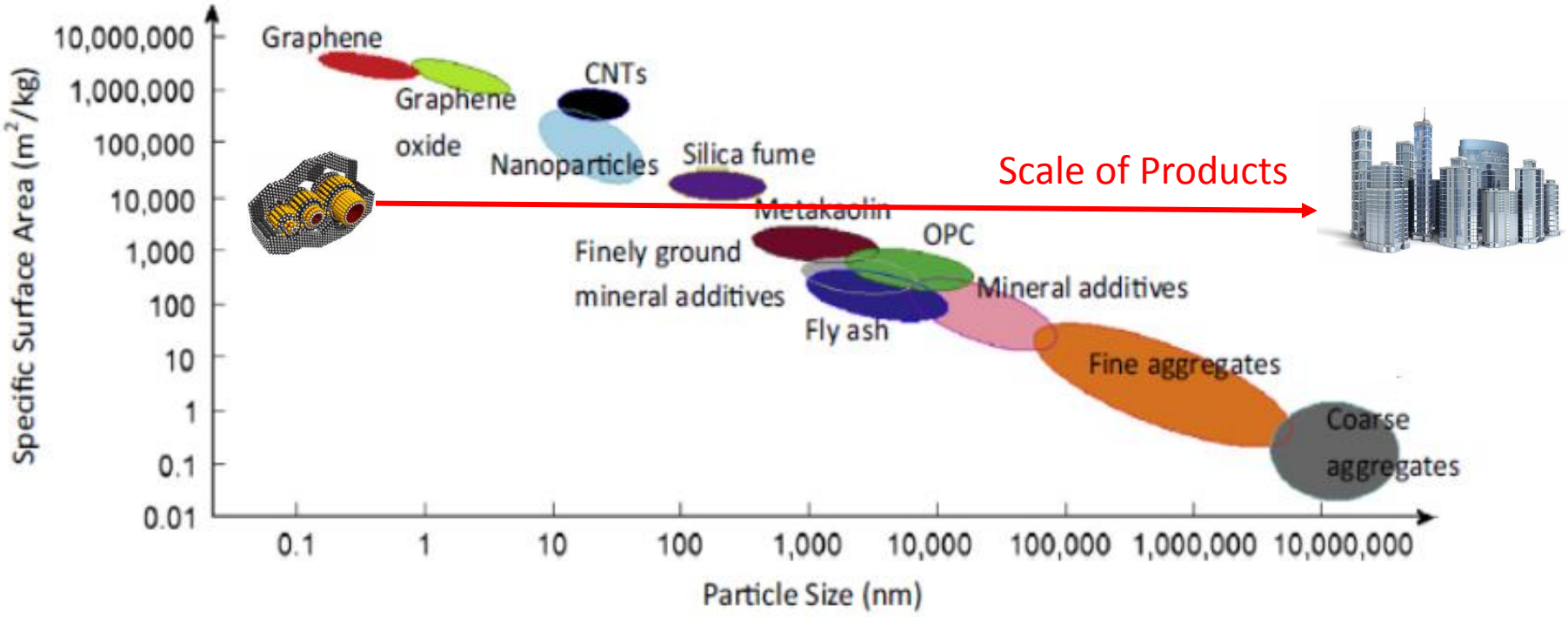

Sobolev K, Gutierrez MF. How nanotechnology can change the concrete world. Am Ceram Soc Bull. 2005; 84(11): 16-9

Nano-reinforcements

(加入纳米材料于纤维复合材料内用以改良其特性)

Layered Structures

- Nanoclays (Montmorillonite/layered silicates, MMT)
- Graphene layer

Tubular Structures

- Nanotubes (pure/modified, coiled, Multi-walled, Nanoclay-supported)

Particle-like Structures

- Silica, SiO
- Nanodiamond
- Nano-rubber
- Clusters (nanoclay and carbon black)
  - More realistic for large scale products

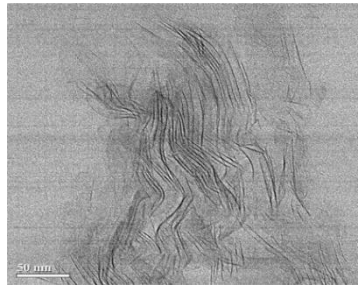

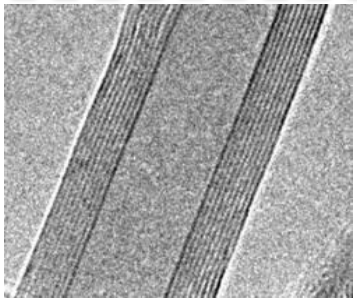

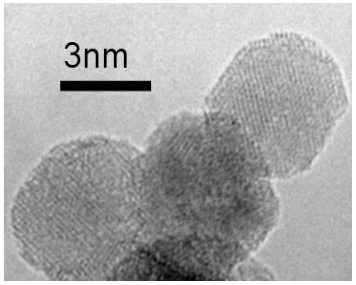

Enhancing the Properties of Lightweight Materials

< Low Temperature Environments >

- Properties Enhancement
  - Mechanical properties
  - Electrical and thermal conductivities
  - Flammability
  - Heat insulation
  - Sound proof and heat insulation
  - Energy storage
- Diffusivity/Barrier Properties
  - High pressure liquefied fuels
  - Food packaging
- Deploy-ability (on SMP)
  - Morphing wing structure
  - Space frame

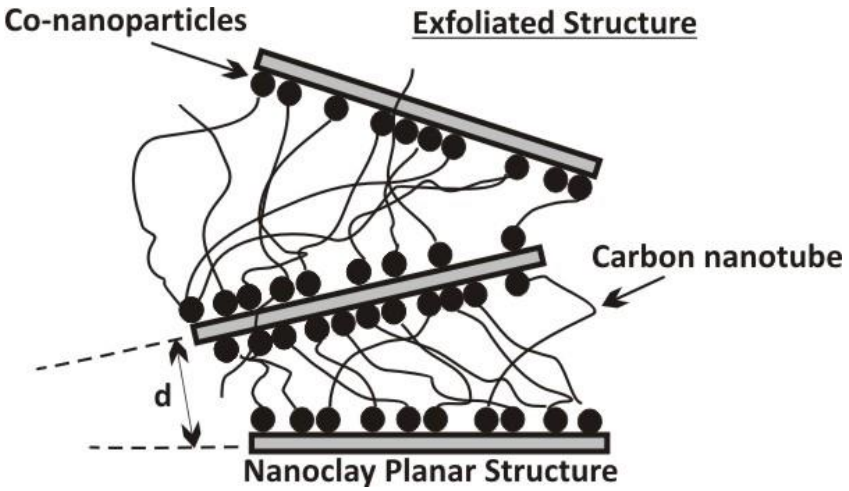

Normal Scale	Nano Scale
Opaque	Transparent
Inert material	A catalyst
Stable material	Combustible
Solids	Liquid
Insulator	Conductor

Enhancing the Properties of Lightweight Materials

< Low Temperature Environments >

- Nanotubes become well-known since the work done by Iijima (1991)
- High tensile modulus (1TPa) and strength (200 GPa)

- Interfacial bonding properties
  - Bare
  - Functionalized
  - Effectiveness
- Agglomeration of nanotubes
  - Single form
  - Entanglement
  - Dispersion
- Brittleness of Epoxy
- Alignment
- Effectiveness (for multi-walled types)

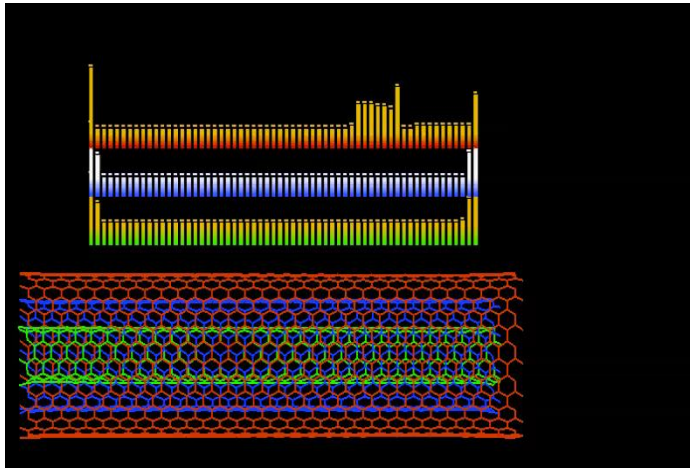

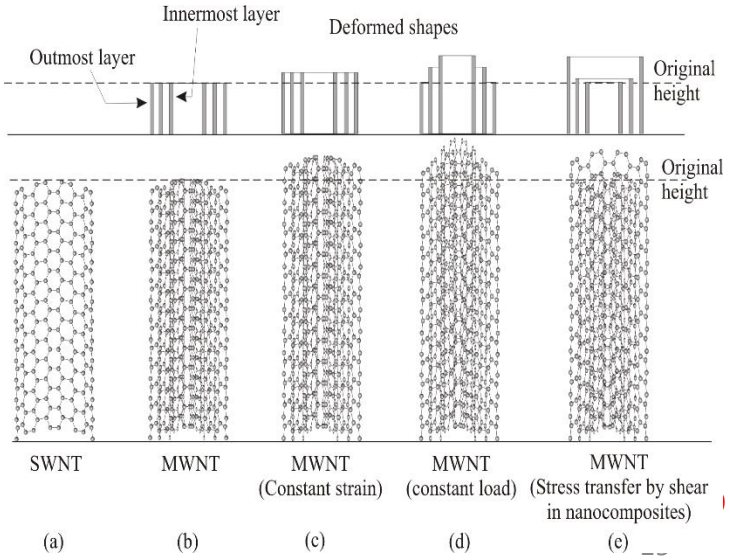

Lau et al. . Effectiveness of using Carbon Nanotubes as Nano-reinforcements for Advanced Composite Structures. Carbon, 2002; 40: 1605-1606.

Using Nanoparticle for Polymer-based Composites and Aluminium

- Mix carbon nanotubes with Aluminium
  - Nano-Al particle mixed with MWNTs (~ 5.0 Wt%), the size of mixed particle was about 50 nm (soaked in alcohol and sonicated)
  - The mixture was then compacted into a disk under
    - 1.5 GPa pressure at RT
    - 1 GPa for 30 mins
    - Then temperature increased from 260 to 480 Deg C
    - Nano-Al grains grew abnormally to about 800 nm

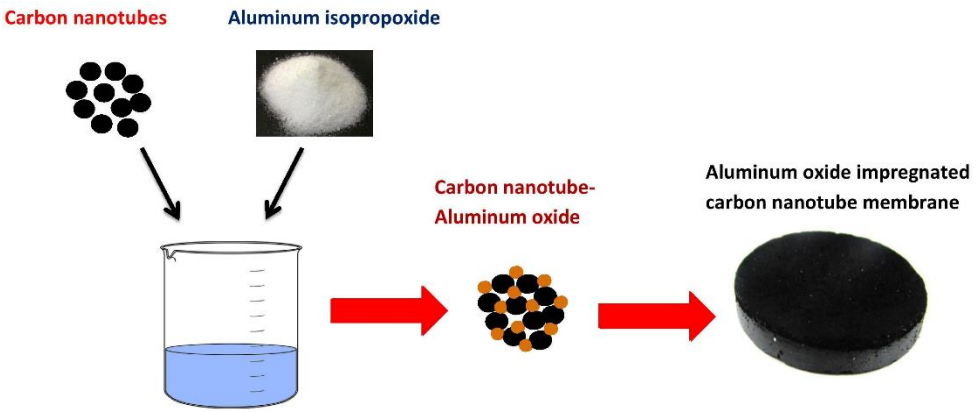

Enhancing the Properties of Lightweight Materials

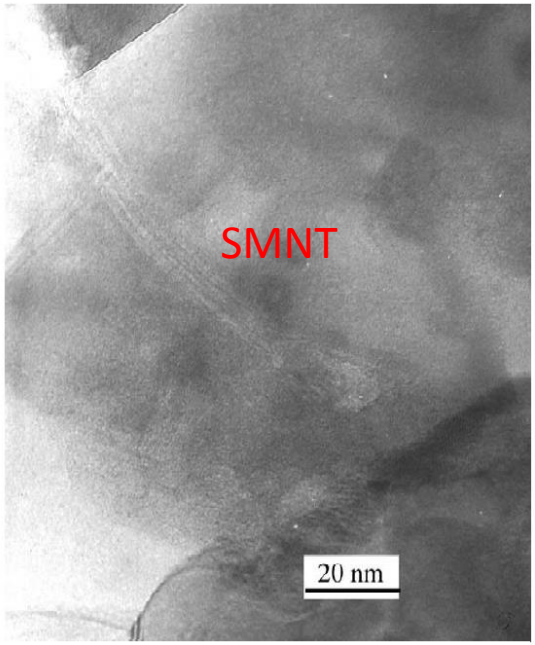

A bundle of carbon nanotubes is easily seen in the matrix without any damage at high pressure condition.

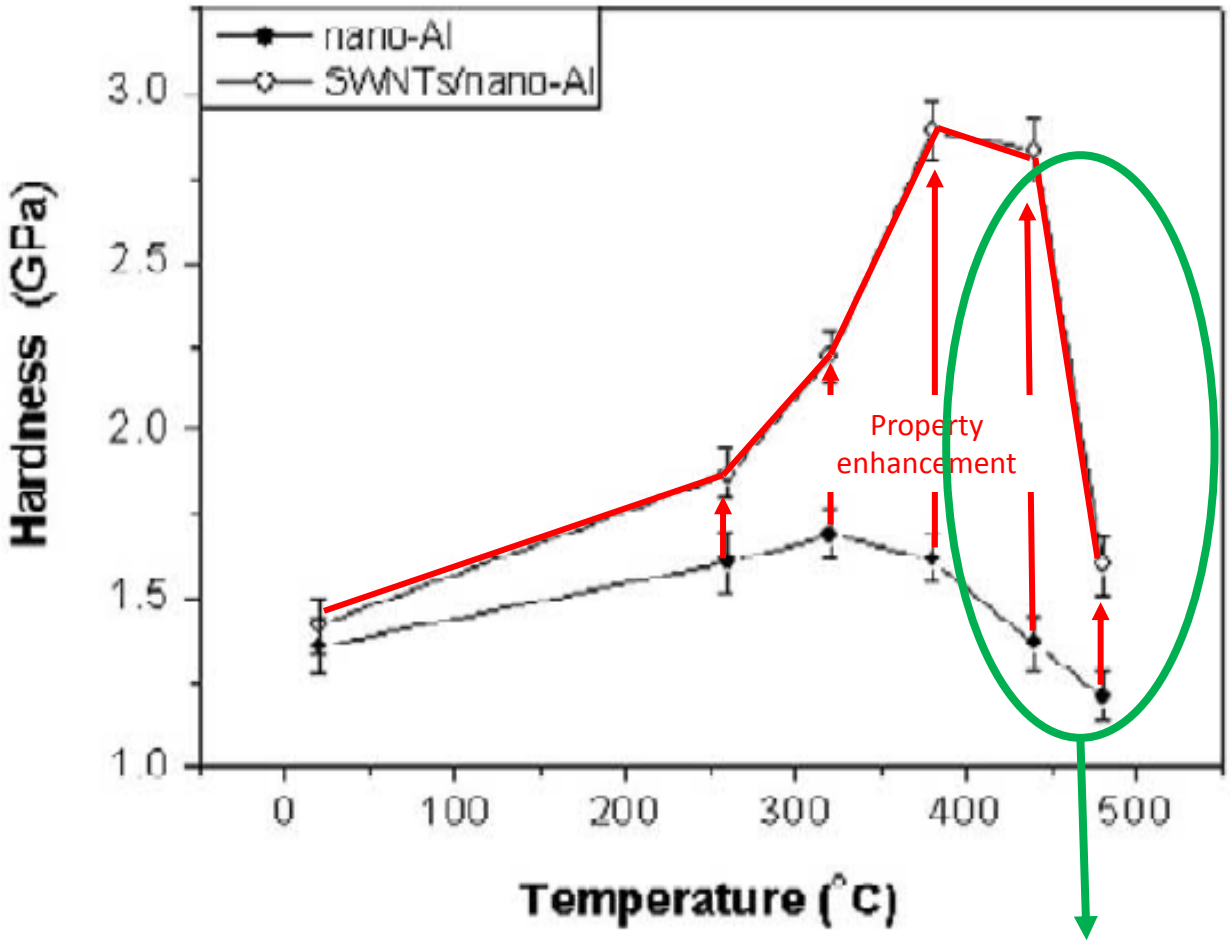

Grain growth of nano-Al matrix at high temperature

Zhong et al. Fabrication of nano-Al based composites reinforced by single-wall carbon nanotubes. Carbon. 2003; 41: 848-550.

Carbon nanotube/aluminium composites

- CNTs (SWNT and MWNT) were dispersed in ethanol and sonicated for 20 mins, then mixed with Al powders (200 mesh) by ball milling;
- The milled powder was compacted in a circular die with a load of 120 KN and then extruded to form samples for testing.

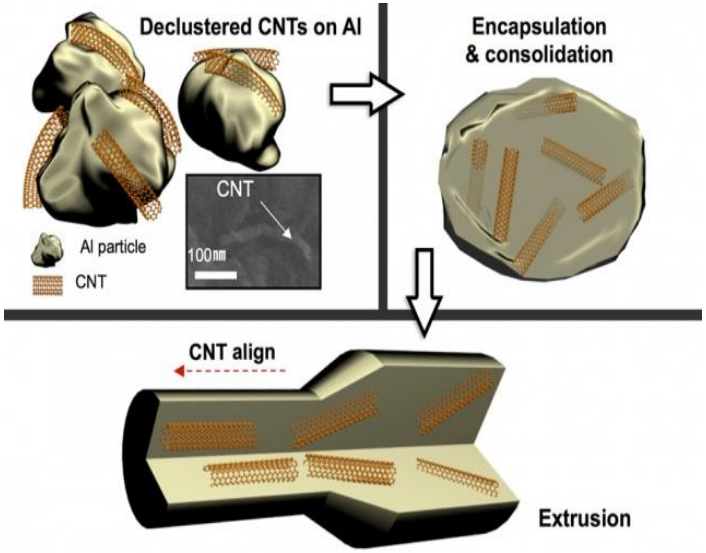

Comparison of theoretical and experimental data for MWNT/Al composite

MWNT % volume fraction	Shear lag Young's modulus, GPa	Experimental Young's modulus, GPa	Thermal mismatch yield strength, MPa	Experimental yield strength, MPa	Orowan looping yield strength, MPa	Experimental ultimate tensile strength, MPa
0.5	74.305	78.1	117.346	86	90.573	134
0.5 + K_2ZrF_6	74.305	75.20	117.346	93	90.573	150
2	87.376	85.85	197.346	99	101.145	138

George et al. Strength in carbon nanotube/aluminium (CNT/Al) composites. Script Materialia. 2005; 53: 115-11163.

Enhancing the Properties of Lightweight Materials

SWINBURNE UNIVERSITY OF TECHNOLOGY

Sintering Al_2O_3 – graphene composite

$Al(OH)_3$-graphene mixture was uni-axially pressed at 0.5 GPa and sintered in a dynamic hydrogen atmosphere for 2 hrs at 1000 C., to form pellets and then extruded to form samples.

In the figure, (A) shows graphite oxide prior exfoliation, (B) and (C) show the composites $Al(OH)_3$ – graphene and Al_2O_3-graophene are successfully exfoliated graphene oxide, where separate sheets could be clearly observed.

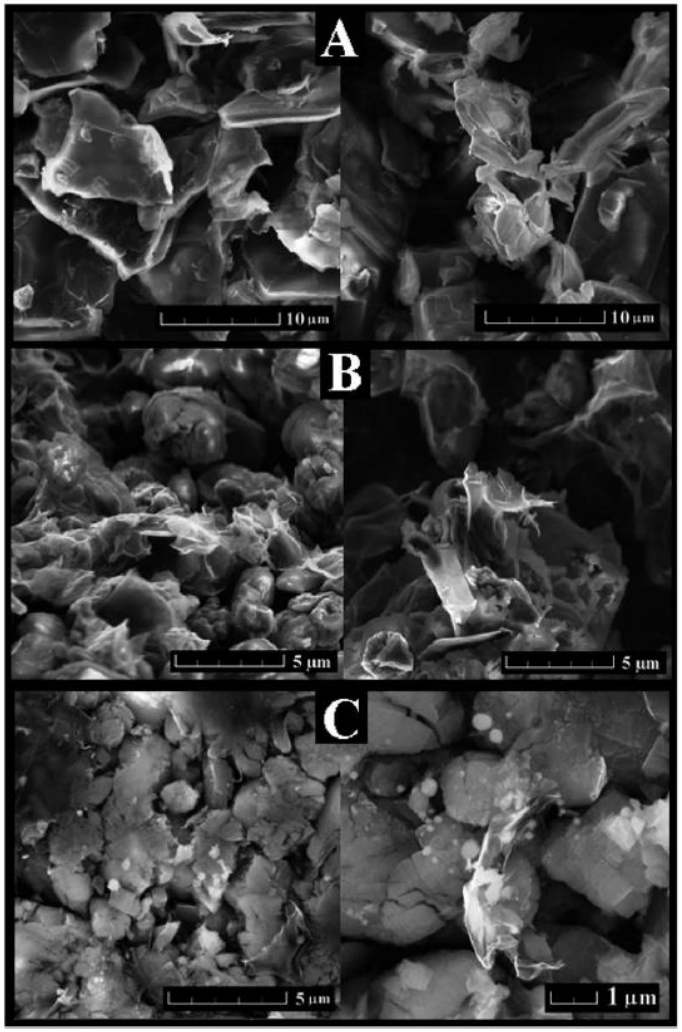

Jankovsky et al. Towards highly electrically conductive and thermally insulating graphene nanocomposites: Al2O3-graphene. Royal Society of Chemistry – RSC Advances. 2014; 4: 7418-7424.

Enhancing the Properties of Lightweight Materials

Only the concentration of 2.1 wt% of graphene was sufficient to obtain a reasonable value of electrical resistivity (765 ± 1.3 kΩcm). The resistivity of the sample with 1.5 wt% graphene was 35.2 ±0.4 MΩ and the resistivities of the other samples with lower concentrations were over 100 MΩ cm. Hence, the presence of graphene in the alumina–graphene composite has a significant effect on the electrical conductivity, with the percolation limiting concentration being about 2 wt% of graphene within the alumina.

The heat transfer by phonons is strongly influenced by many other factors such as the material porosity, grain boundaries and their size.

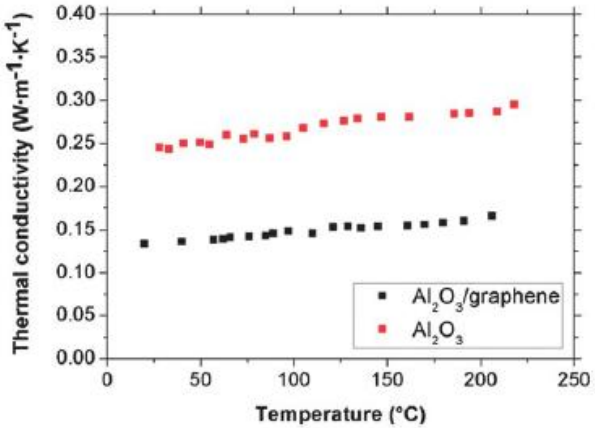

Fig. 10 Thermal conductivity of Al_2O_3–graphene and pure Al_2O_3 measured by LFA.

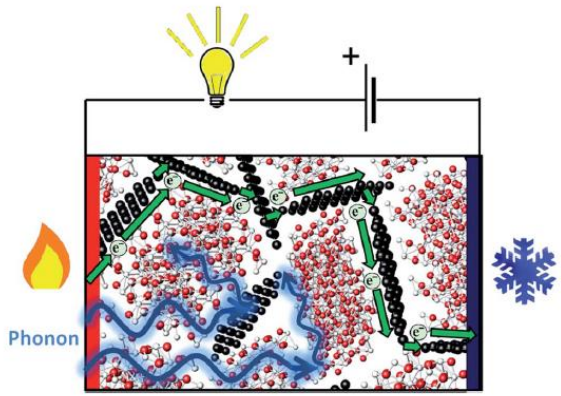

Fig. 9 A schematic drawing of the propagation of electric current and heat represented by phonons through the alumina–graphene composite material.

Factors:

- Conductivity of graphene
- Homogeneity (dispersion)

Thermal conductivity of typical aluminium = 237 W/(m·K)
Electrical resistivity = 28.2 MΩ·m (at 20 °C)

Enhancing the Properties of Lightweight Materials

SWINBURNE UNIVERSITY OF TECHNOLOGY

Hot-working of ball milling powder with MWCNTs (~ 20 nm in diameter and 5 micron in length)
Mix with Aluminium powder (150 micron in diameter).

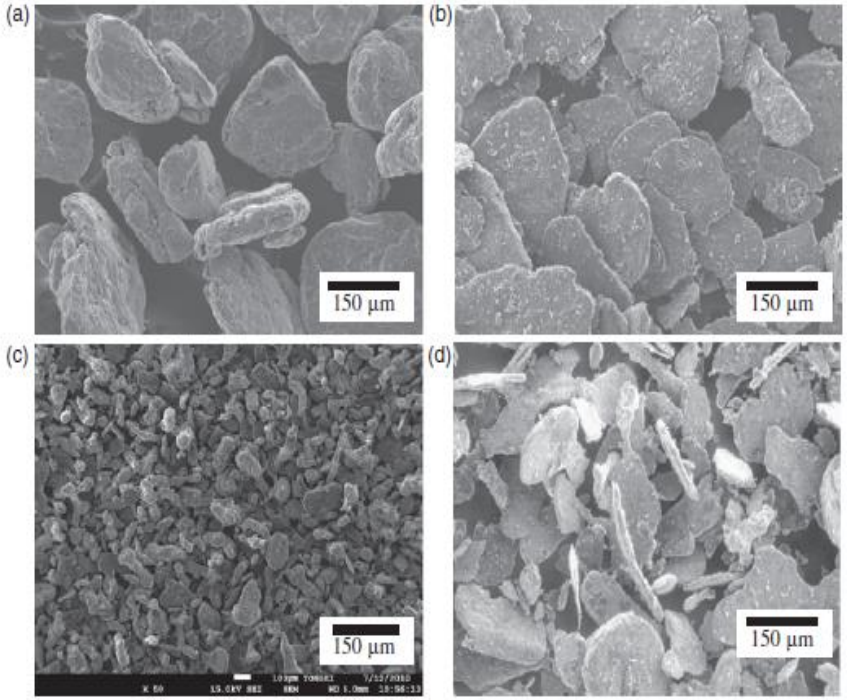

Figure 2. Scanning electron microscopy (SEM) images of Al-4 wt% multiwalled carbon nanotubes (MWCNTs) composite powders were fabricated by four different fabrication conditions; case (a) A, (b) B, (c) C, and (d) D.

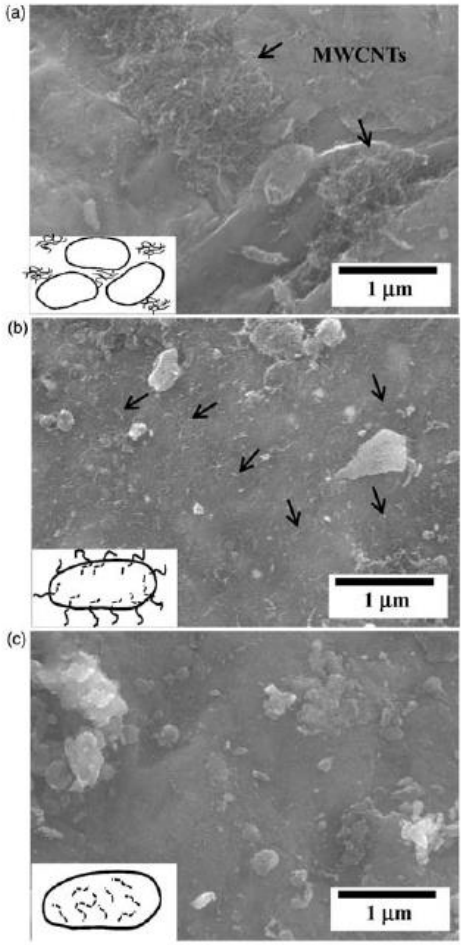

Figure 1. Scanning electron microscopy (SEM) images of the composite powders ball-milled at 100 r/min for (a) 1 h, (b) 2 h, and (c) 6 h, where schematic depictions representing each powder morphology are also provided in the inset of the image.

Enhancing the Properties of Lightweight Materials

Table 2. Electrical and thermal conductivities of the Al/MWCNT composites with different processing routes

Case	Electrical conductivity (E7 Sm^{-1})	Thermal conductivity (W/mK)
A	15.32	121
B	9.31	103
C	33.31	172
D	8.84	156

MWCNTs: multiwalled carbon nanotubes.

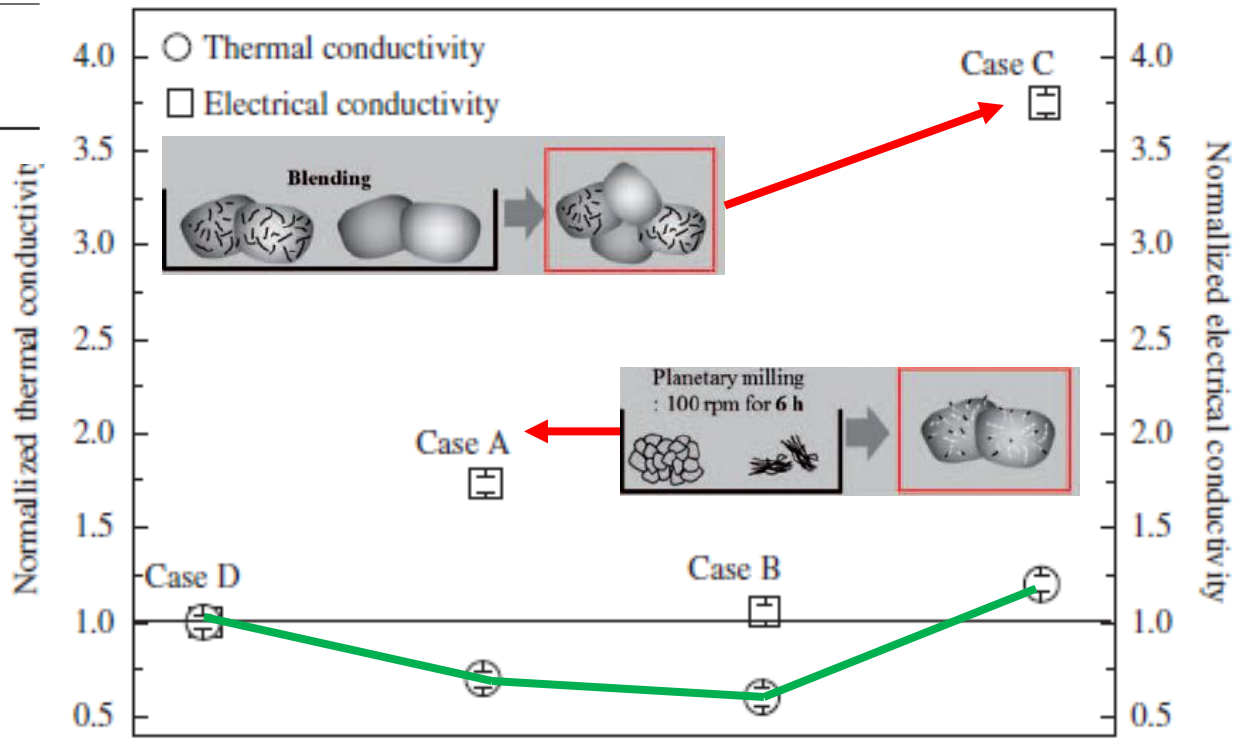

Figure 6. The ratio of electrical conductivity and thermal conductivity for Cases A to D.

Thermal conductivity

- Low heat transfer
- Small thermal deformation

Shin et al. Electrical and thermal conductivities of aluminium-based composites containing multi-walled carbon nanotubes. J. Composite Materials. 2012; 0: 1-8.

Enhancing the Properties of Lightweight Materials

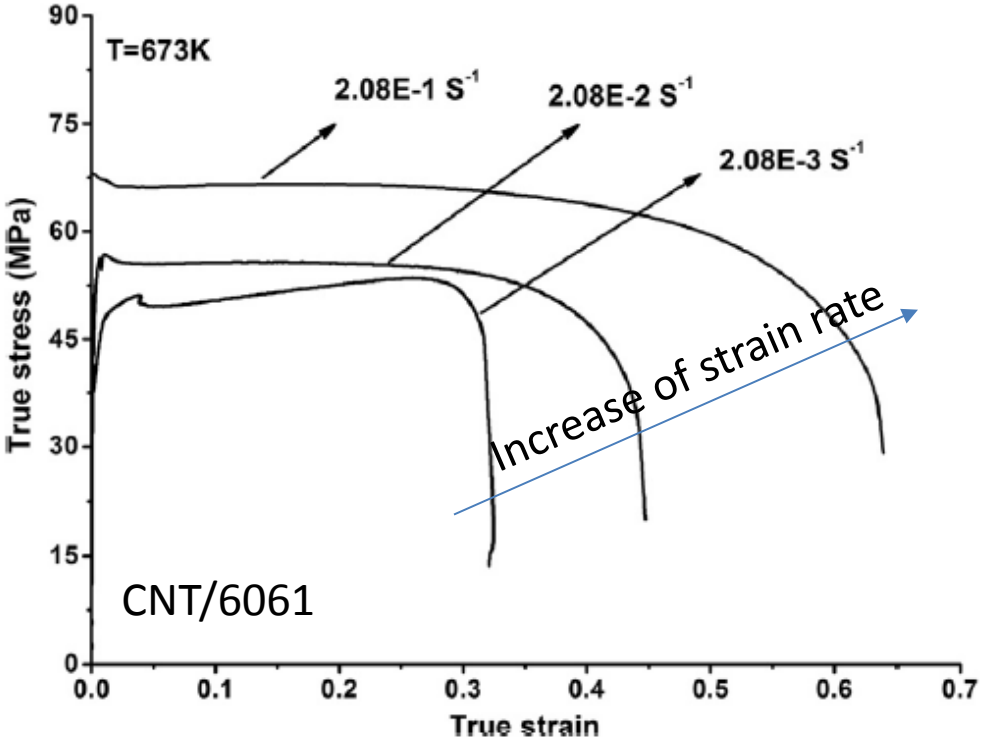

Fig. 3. True stress against true strain tested at 673 K at three different initial strain rates.

Fig. 3 shows the true stress-strain curves at 673 K. The peak tensile stress increases with increasing strain rate. All of the curves show well-behaved steady flow stress. According to Mishra et al. [7], this well behaved stress-strain curve is an indication that the deformation process is free of severe grain coarsening or necking.

1.5 wt % CNTs with 6061

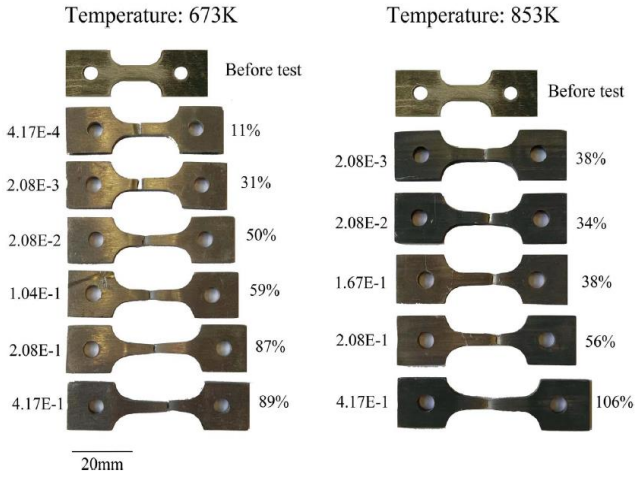

Fig. 2. Appearance of tensile specimens after deformation to failure at 673 K and 853 K.

Low temperature – block of movement
High temperature – liquid phase

Huang et al. Superplastic behaviour of carbon nanotube reinforced aluminium composites. Materials Sci & Engg A. 2017; 699: 55-61.

Enhancing the Properties of Lightweight Materials

SWINBURNE UNIVERSITY OF TECHNOLOGY

Table 1
Tensile properties of 1.5 wt.% CNT/Al composites and Al matrices.

Material	Milling regime	0.2% Offset yield strength (MPa)	Ultimate tensile strength (MPa)	Uniform elongation (%)	Total elongation (%)
Al	LSBM	185 ± 8	260 ± 6	7.1 ± 0.4	17.0 ± 1.6
	SSBM	206 ± 11	282 ± 5	6.5 ± 1.1	14.1 ± 0.4
	HSBM	251 ± 6	311 ± 6	4.0 ± 0.3	10.2 ± 1.8
1.5 wt.% CNT/Al	LSBM	293 ± 18	367 ± 2	3.2 ± 0.1	6.3 ± 0.4
	SSBM	326 ± 21	376 ± 3	3.9 ± 0.2	12.4 ± 1.3
	HSBM	384 ± 7	408 ± 1	1.5 ± 0.0	4.0 ± 0.3

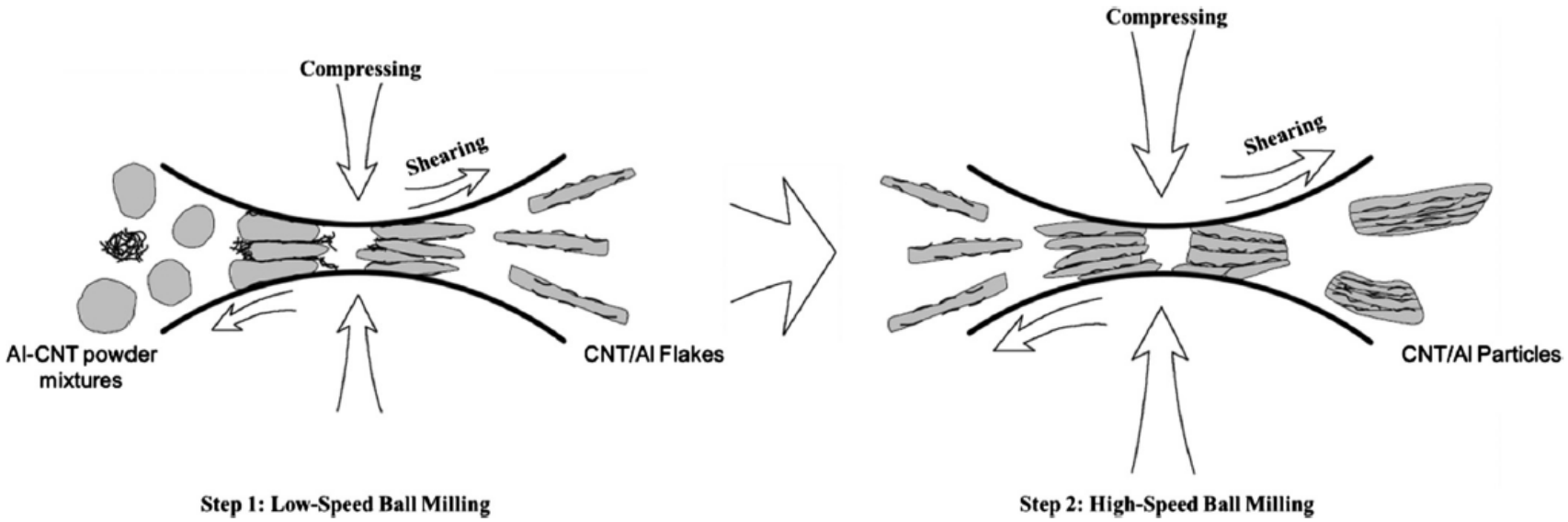

Fig. 9. Illustration of co-deformation/dispersion mechanisms of CNT/Al powders during SSBM.

Xu et al. Balanced strength and ductility in CNT/AL composites achieved by flake powder metallurgy via shift-speed ball milling. Composites part A. 2017. 96: 57-66.

Enhancing the Properties of Lightweight Materials

SWINBURNE UNIVERSITY OF TECHNOLOGY

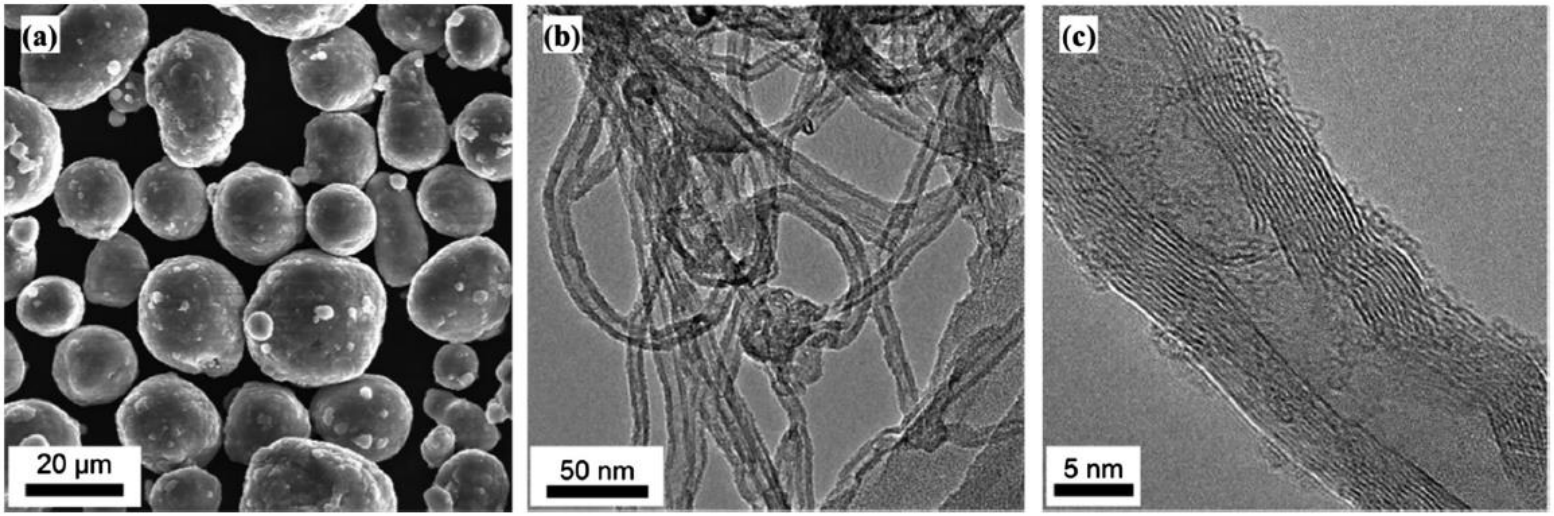

Fig. 1. (a) SEM image of the Al powders, (b) TEM and (c) HRTEM images of the multi-walled CNTs.

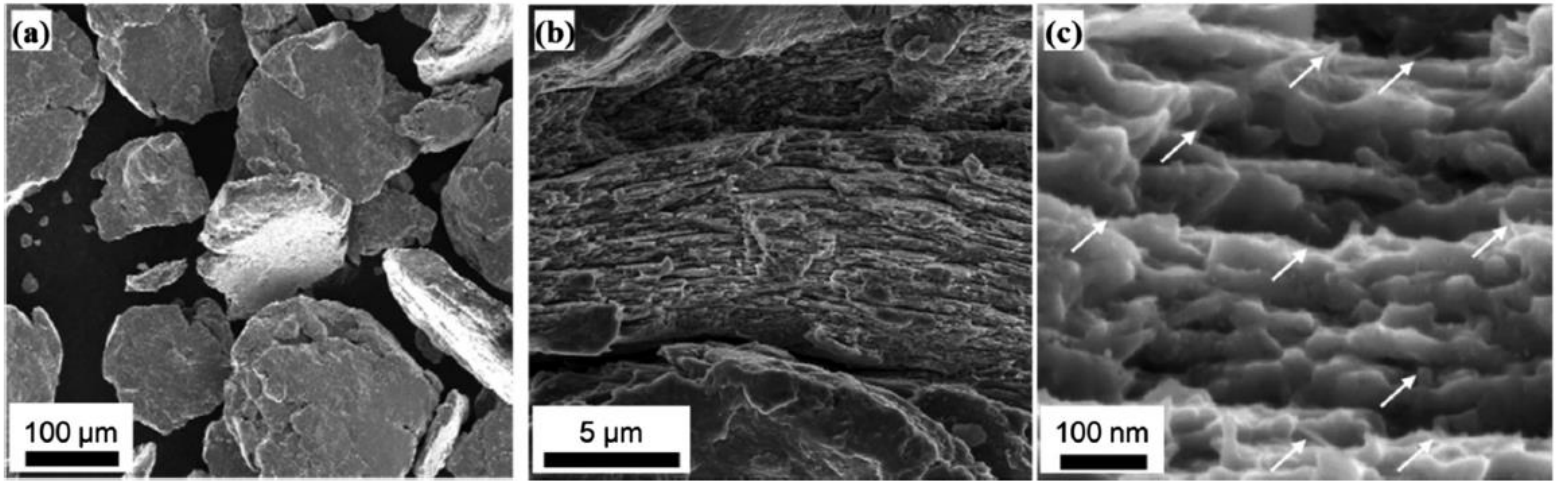

Fig. 4. SEM images of (a) CNT/Al particles obtained with SSBM, (b) and (c) the lamellar structured fracture surface of a CNT/Al particle obtained with SSBM. CNTs were pointed out by the white arrows.

Enhancing the Properties of Lightweight Materials

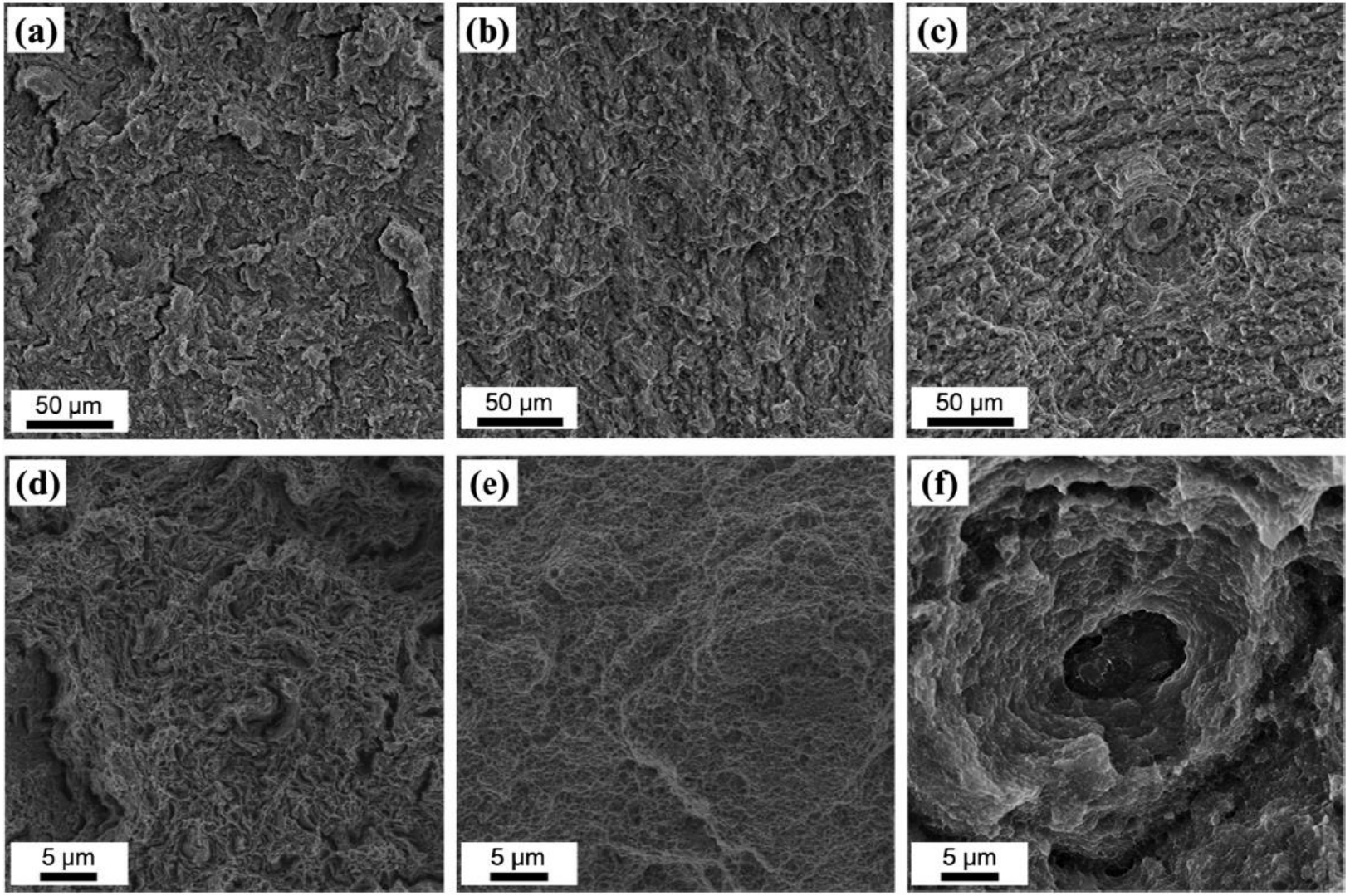

Fig. 8. Fractography of (a & d) LSBM, (b & e) SSBM and (c & f) HSBM CNT/Al.

SWINBURNE UNIVERSITY OF TECHNOLOGY

Nano-reinforcement for Polymer-based Composites

Enhancing the Properties of Lightweight Materials

< Low Temperature Environments for Polymer >

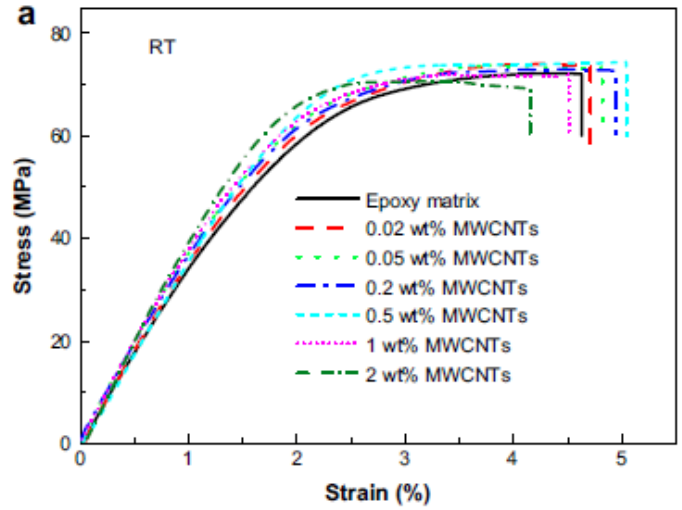

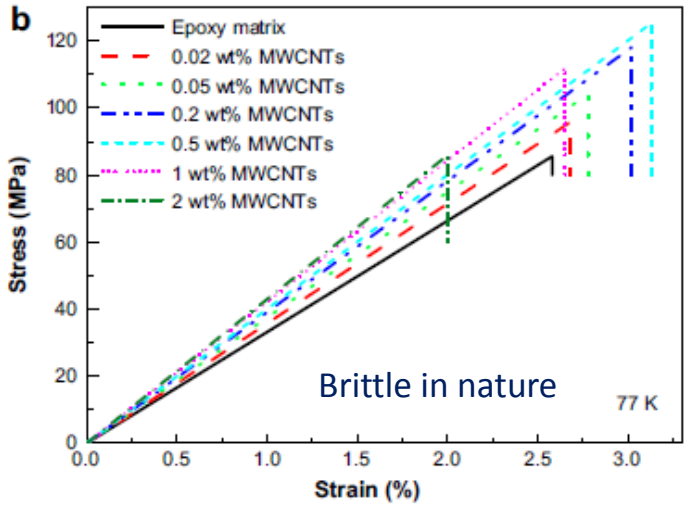

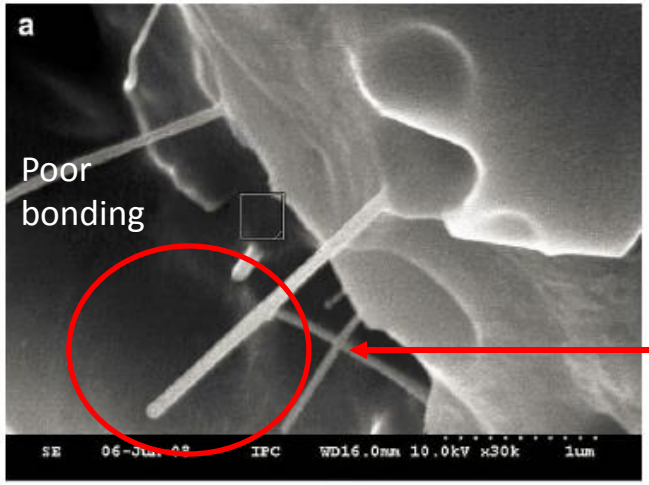

For Polymer-based composites

拙劣的粘连性能

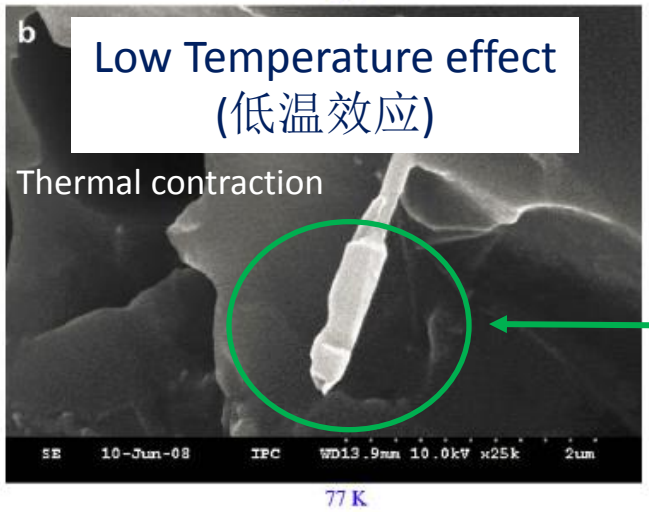

优质的粘连性能

a) At room temperature; b) At cryogenic environment

[*Chen et al. Polymer; 2009; 50: 4753-59*]

Enhancing the Properties of Lightweight Materials

< Low Temperature Environments >

The development of coiled carbon nanotubes is used to enhance their interfacial bonding properties to surrounding matrix. These nanotubes were prepared by catalytic chemical vapour deposition (CCVD) on finely divided Co nano-particles supported on silica gel under reduced pressure and lower gas flow rates.

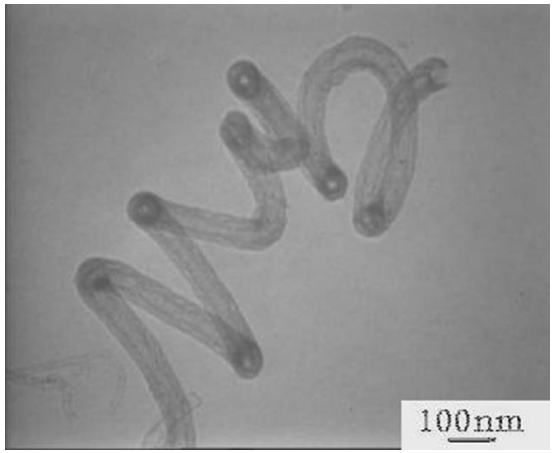

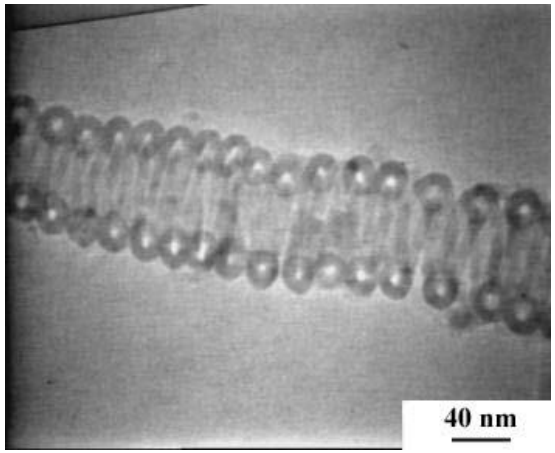

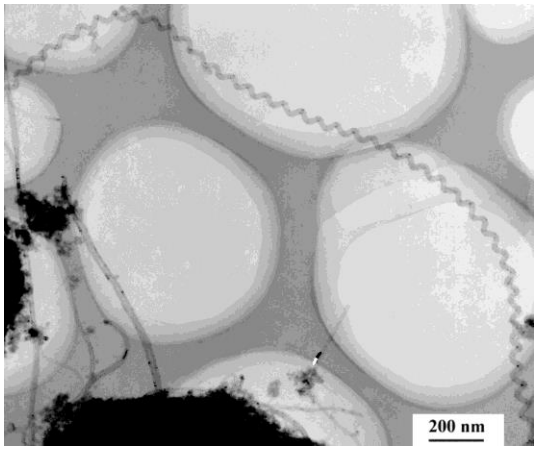

Li XF, **LAU KT** and Yin YS. Mechanical Properties of Epoxy-based Composites using Coiled Carbon Nanotubes. Comp. Sci. Tech. 2008; 68(14): 2876-2811.

Enhancing the Properties of Lightweight Materials

< Low Temperature Environments >

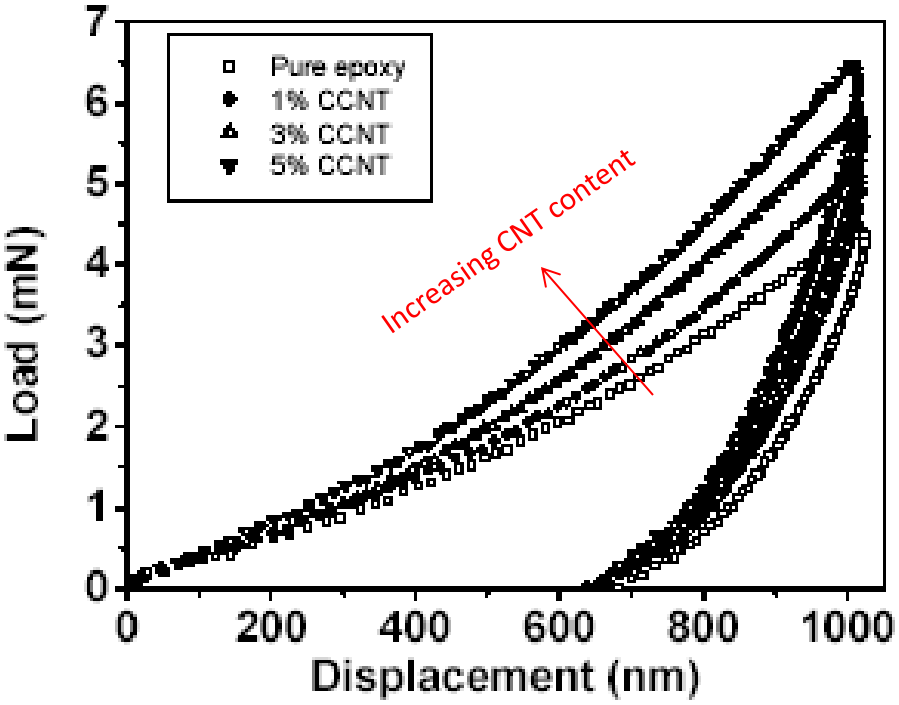

The load-displacement curves of indentations on the epoxy and its coiled nanotubes reinforced composites.

Wt. % of CCNTs	Hardness (GPa) RT	77K	Elastic Modulus (GPa) RT	77K
0	0.23	**0.31**	5	**7.1**
1	0.28	**0.36**	5.3	**7.5**
3	0.31	**0.38**	5.9	**7.9**
5	0.35	**0.41**	7	**8.9**

Improving the problem of agglomeration of nanotubes (non-functionalized)

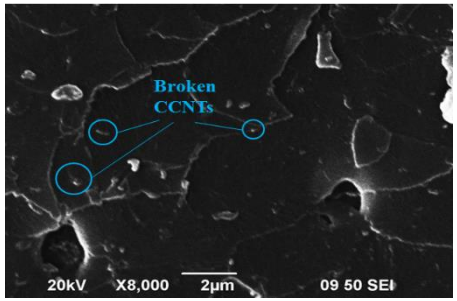

CCNT/epoxy composite

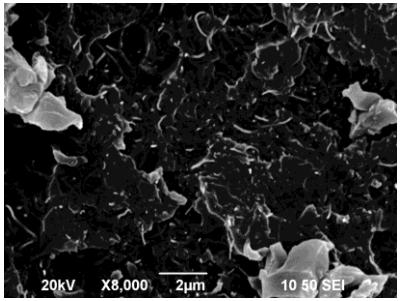

SWNT/epoxy composite

Enhancing the Properties of Lightweight Materials

< Low Temperature Environments and Repair-ability >

SWINBURNE UNIVERSITY OF TECHNOLOGY

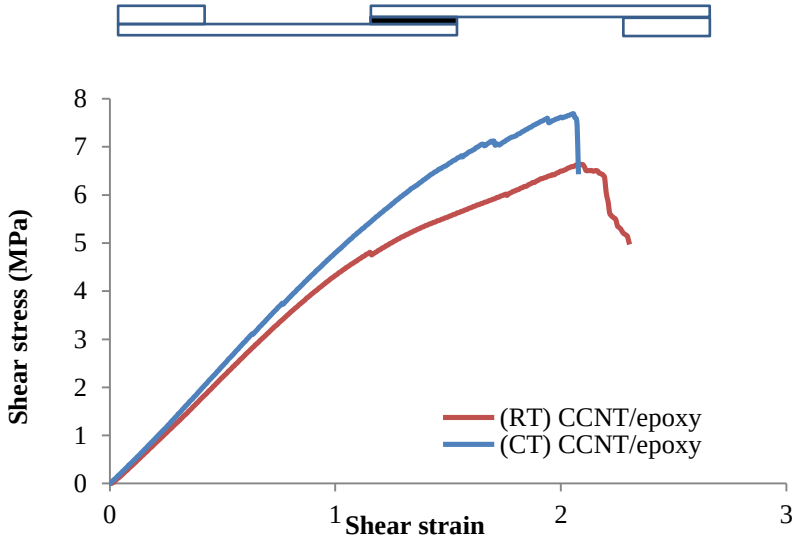

Lap Joint Shear Test

It provides an evidence that the CCNT does enhance the bonding strength of composite structures at low temperature environment. This result further assists the design of better adhesives for the purpose of new composite aircraft repair.

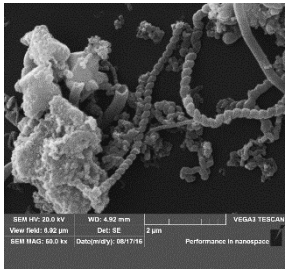

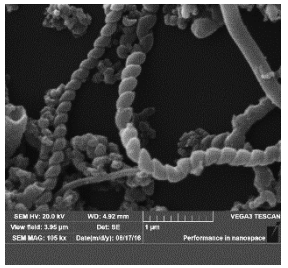

Pure Epoxy	MWNT/epoxy	CCNT/epoxy
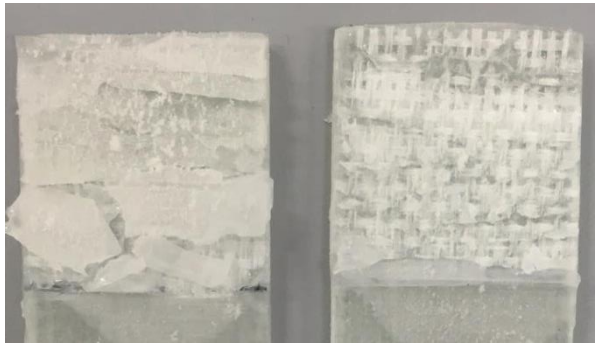	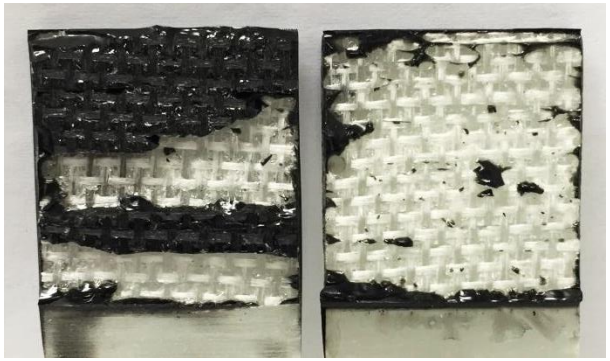	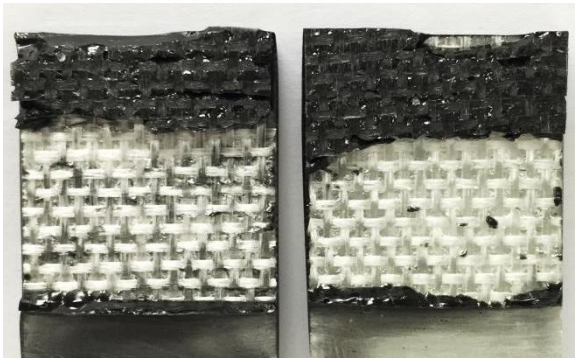

Enhancing the Properties of Lightweight Materials

< Low Temperature Environments for Polymer >

A representative volume element (RVE) of CNTs reinforced polymer composites was established to study the tensile behavior of SWCNT and DWCNT reinforced composites at RT and cryogenic temperature.

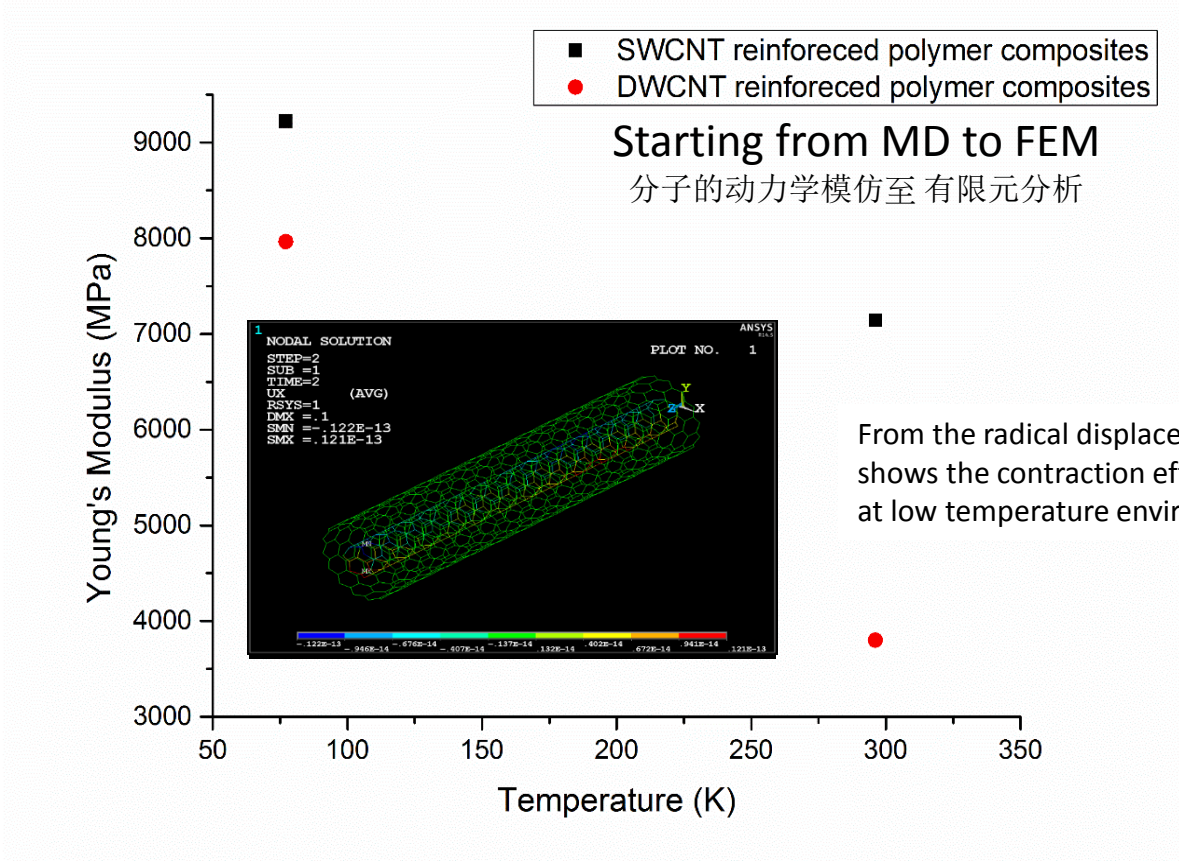

From the radical displacement curve, it shows the contraction effect does exist at low temperature environment

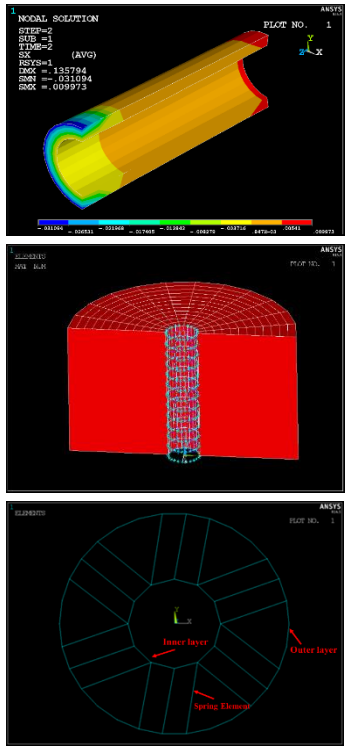

Jia ZM, Ma HL, Cheng LK and **Lau KT** Stress Transfer Properties of carbon Nanot8ibe Reinforced Polymer Composites at Low Temperature Environment. Composites part B: Engineering; 2016, in press.

Enhancing the Properties of Lightweight Materials

< Low Temperature Environments >

By using nanoclay as a support material to grow nanotubes on the surface of clay by reduced-pressure chemical vapor deposition (CVD) since clay itself is a good reinforcement for polymer composites with its high ion exchange capacity, high aspect ratio, ease of fabrication, and relatively low cost.

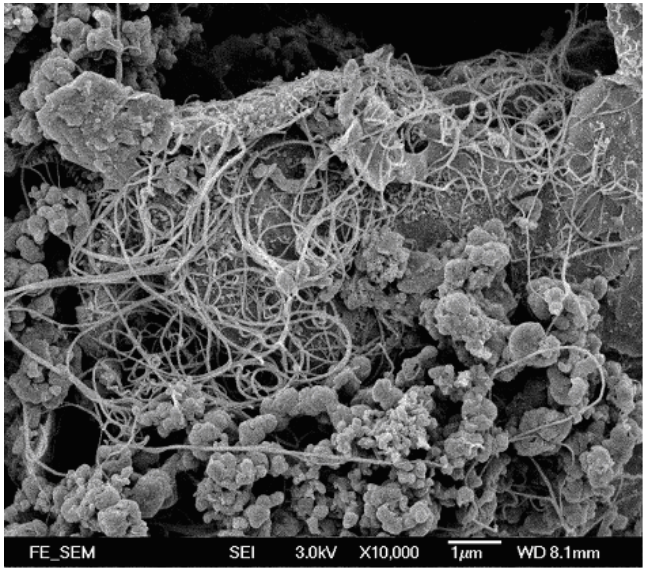

% NT-NC	硬度 Hardness (Hv) RT	77K
0	10.8	13
0.5	11.9	16.3
1	12.5	18.2
2	15.1	19.6
3	14.7	20

納米黏土支援納米碳管

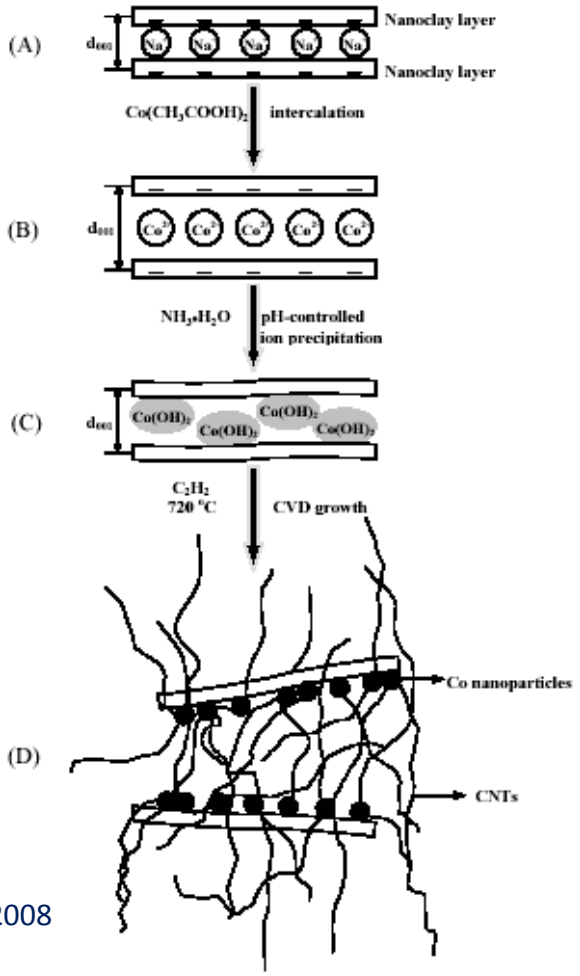

Schematic illustration of the growth of nanotubes from nanoclay layers (improvement of agglomeration)

Patent, Lau KT, 2008

Graphene

Comparison with multi-walled carbon nanotubes in modifying epoxy resin for enhancing cryogenic mechanical performance, the graphene nanosheets need less contents for maximizing the reinforcing efficiency due to larger surface areas.

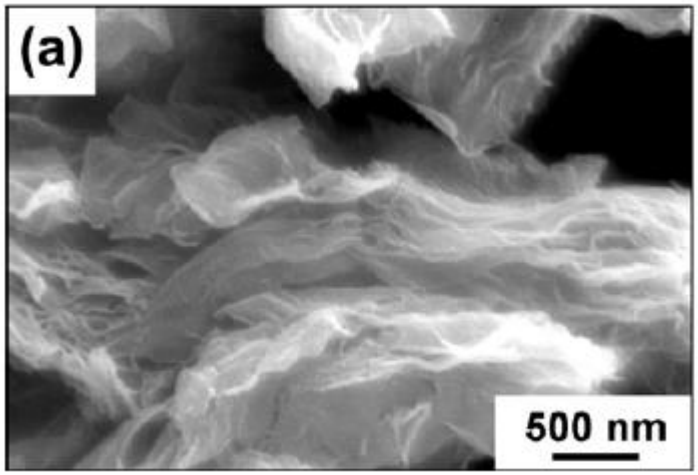

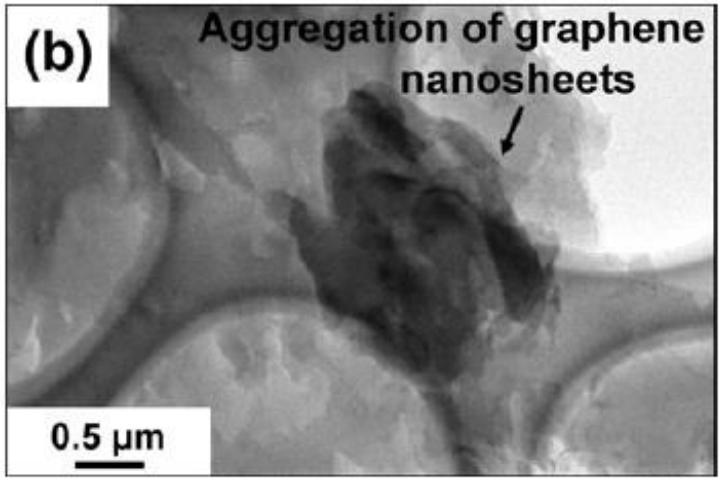

a) 0.1 wt%
b) 0.5 wt %

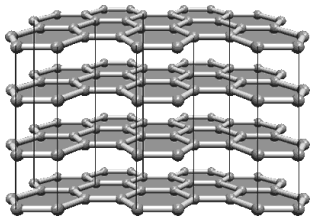

Comp. Sci. tech. 2012; 72: 1581-1587

Enhancing the Properties of Lightweight Materials

< Low Temperature Environments >

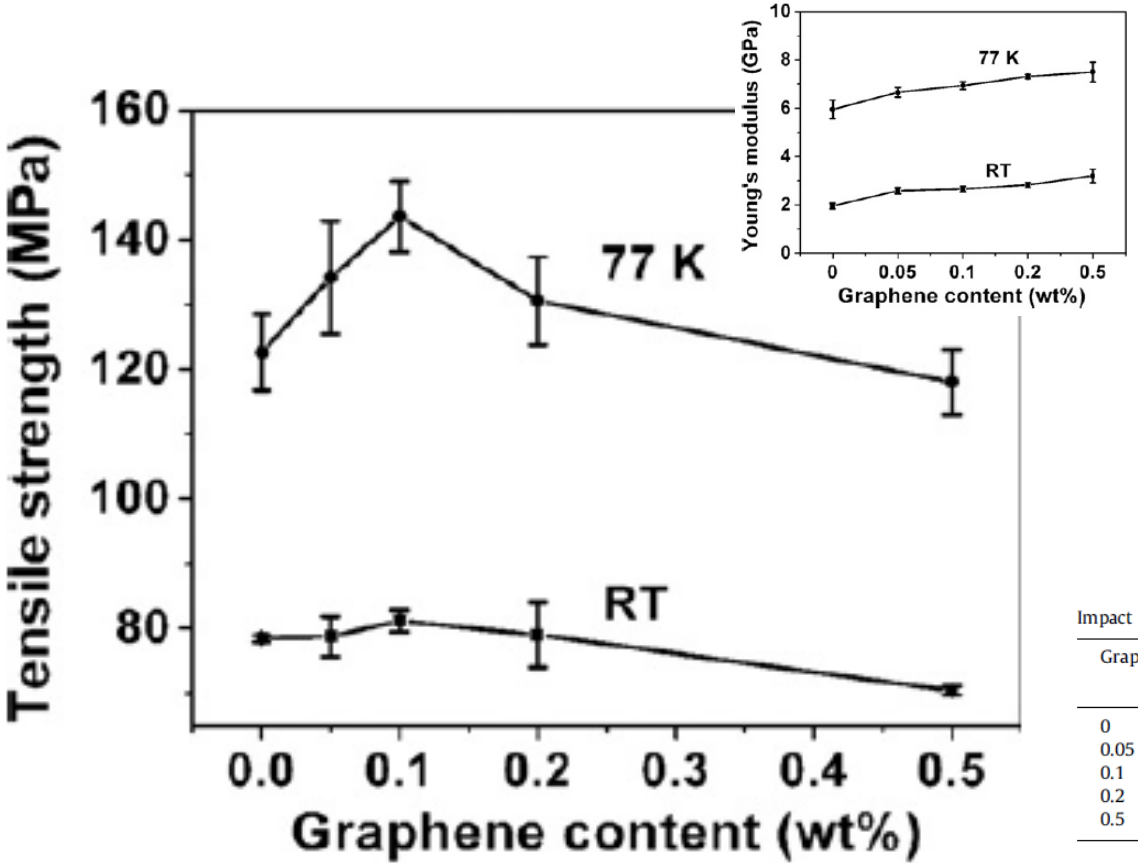

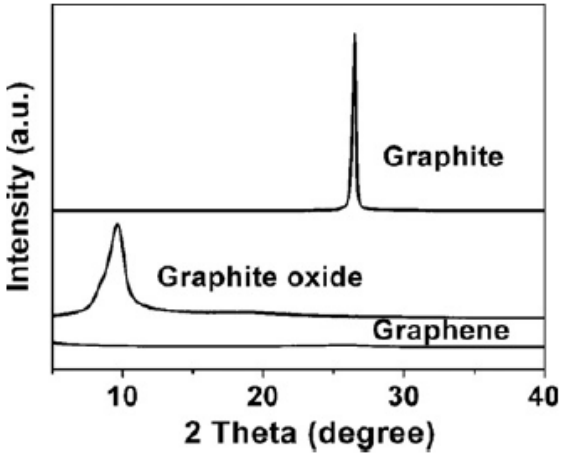

Impact strength at RT and 77 K of the epoxy matrix and the epoxy composites.

Graphene content (wt.%)	Impact strength (kJ/m^2)	
	RT	77 K
0	20.9 ± 1.9	17.7 ± 0.7
0.05	22.8 ± 2.7	19.3 ± 1.9
0.1	23.1 ± 2.3	21.9 ± 0.8
0.2	20.3 ± 2.6	18.4 ± 1.6
0.5	18.4 ± 1.2	17.7 ± 0.3

Reasons: High thermal stress due to the shrinkage of epoxy

(CTE of epoxy: 5.1 e-5/K and CTE of graphene: -7 e-6/K)

Enhancing the Properties of Lightweight Materials

< Low Temperature Environments >

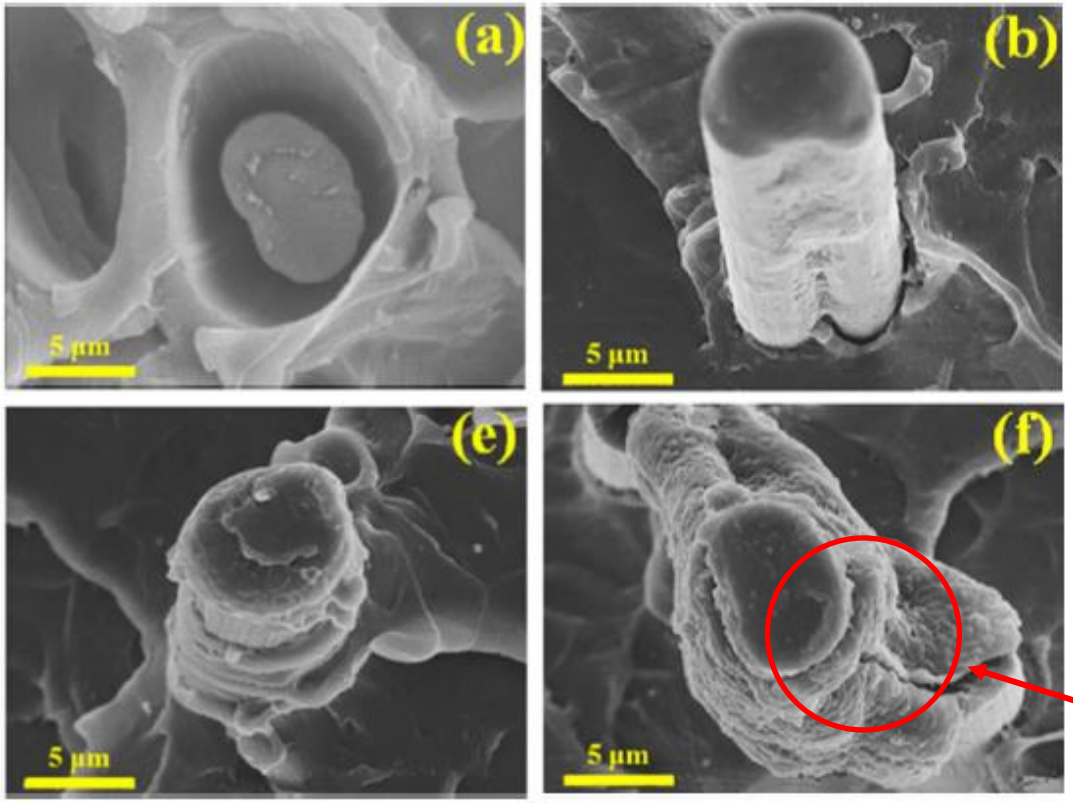

Tensile failure surface of a SCF/PES composite at room temperature (a) and 77K (b).

Tensile failure surface of a GO/SCF/PES composite at room temperature (e) and 77K (f).

GO/SCF/PES interface

The difference of coefficients of thermal expansion between carbon fibre and polymer-based resin may induce residual stress in a composite system.

Fei et al. greatly enhanced cryogenic mechanical properties of short carbon fibre/Polyethersulfone composites by graphene oxide coating. Composites part A. 2016; 89: 47-55.

Electrophoretic deposition (EDP) on carbon fabrics

- Negatively-charged GO (0.2 wt%)
- GO moves towards the positive electrode, where CF is placed
- Voltage, deposition time, concentration of solution
- Sonication

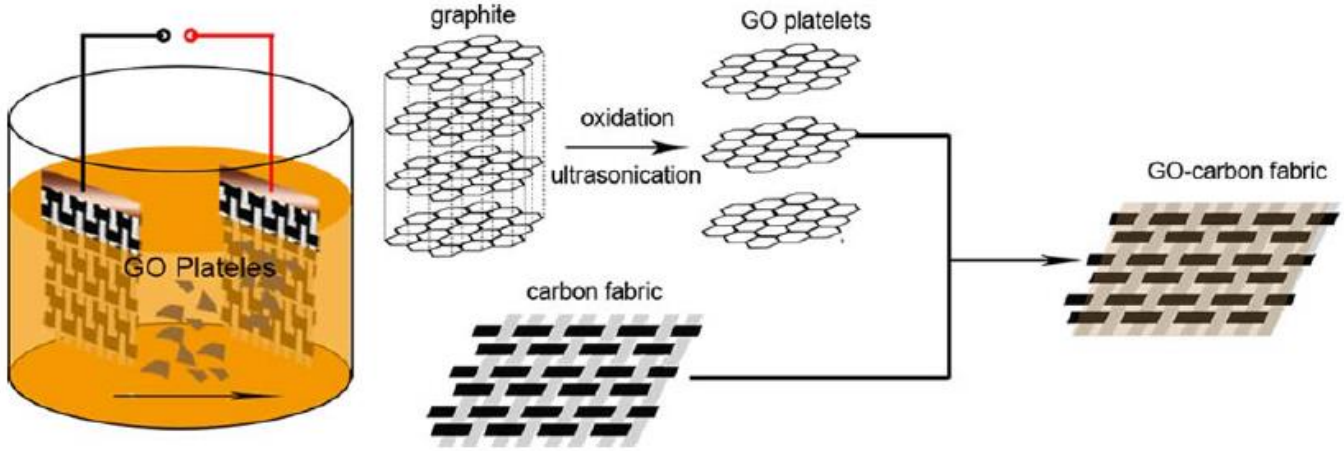

Hung PY, **Lau KT**, N Hameed and B Fox. "Surface modification of carbon fibre using graphene-related materials (GRMs) for multifunctional composites", In press. Composite Pt B. 2017.

Enhancing the Properties of Lightweight Materials

< Low Temperature Environments >

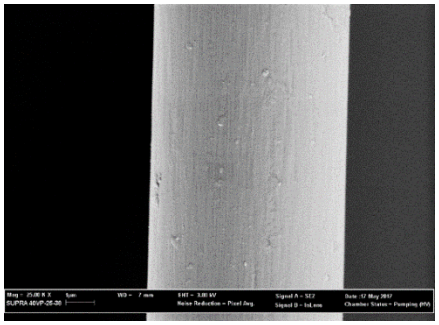

As- received CF
Plain, glass & clean surface

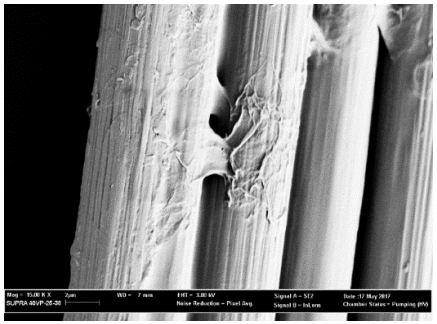

GO/CF
Wrinkled & hierarchical structure
Concave pits and convex hills covering the CF

High electrostatic attraction to GO
More GO attached on CF

GO/CFRP Composites

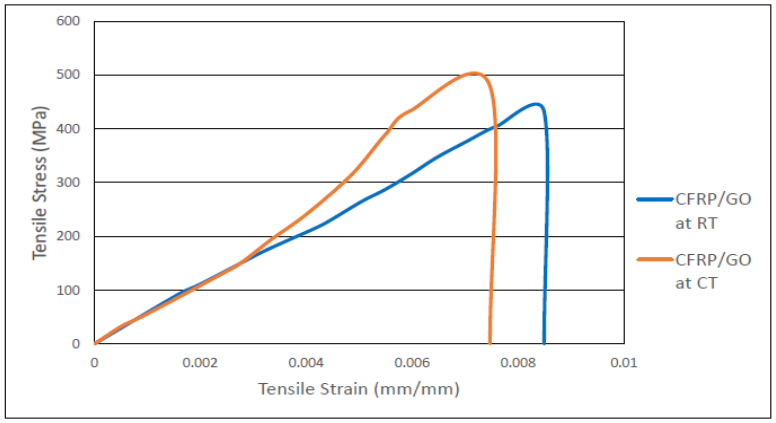

GO/CFRP at 298K

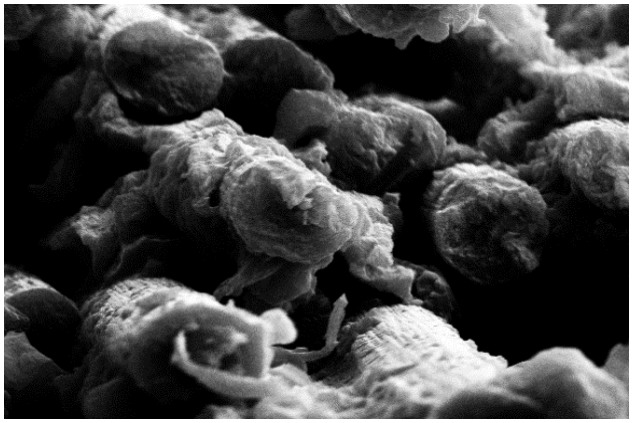

Sandwich panels with aluminum foam core

(碳纤维夹芯板，铝泡沫芯)

- Subject to impact (低速冲击) of an indenter at 3 m/s

Carbon fibre face sheets = 1.5 mm; Core = 25 mm

碳纤维面板

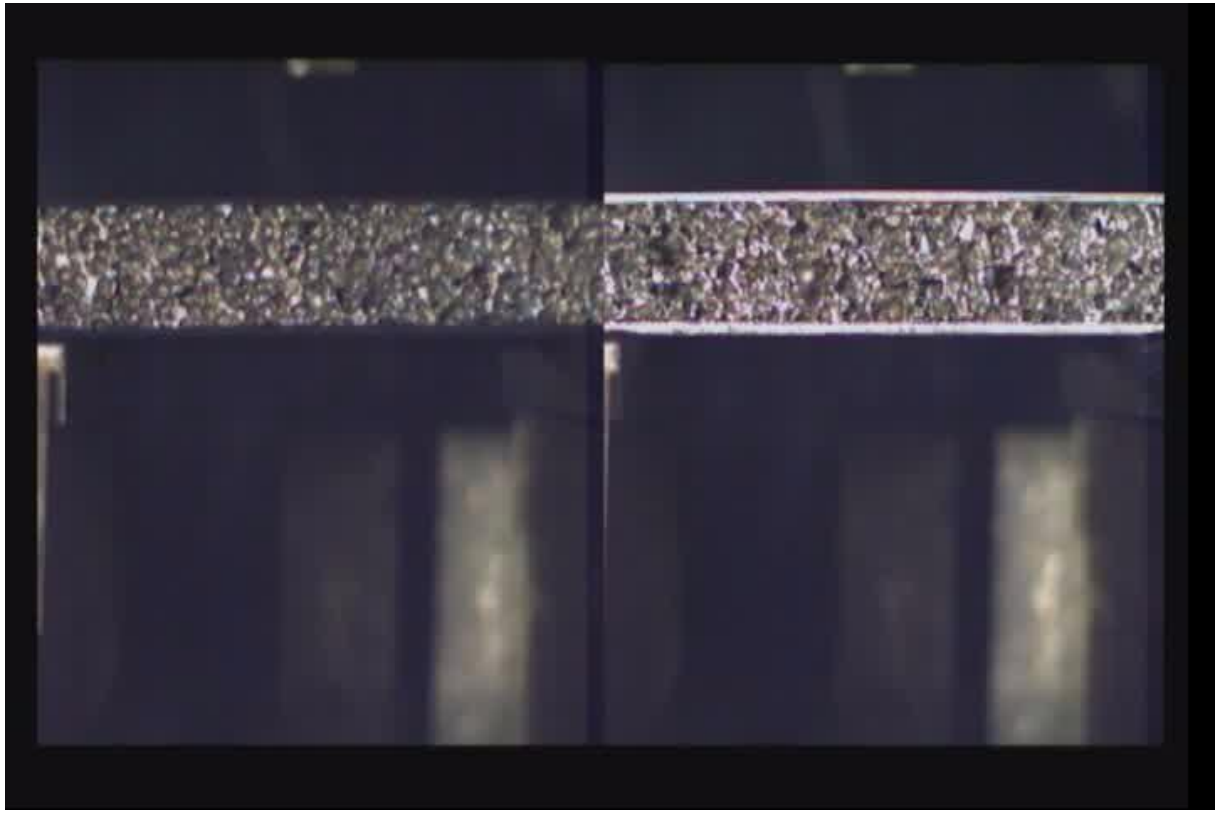

Aluminium face sheets (1.5 mm); Core = 25 mm

铝面板

Videos taken by Martin Vcelka and Dong Ruan

Enhancing the Properties of Lightweight Materials

SWINBURNE UNIVERSITY OF TECHNOLOGY

Research Partners in Lightweight Materials (Asia) - 2017

Enhancing the Properties of Lightweight Materials

SWINBURNE UNIVERSITY OF TECHNOLOGY

Acknowledgements (Composite and Lightweight Materials Research)

Professor Bronwyn Fox (Leader: Composites Research Group)

Professor Baohua Jia (Leader: Photonics Centre)

Dr. Tracy Dong Ruan

Dr. Nishar Hameed

Professor Guoxing LU (Leader: lightweight Materials

Professor Geoff brooks (Leader: Shandong JRC Research Group)

Dr. Yvonne Durandet

Professor Syed Masood (Leader: 3D Printing for Metals)

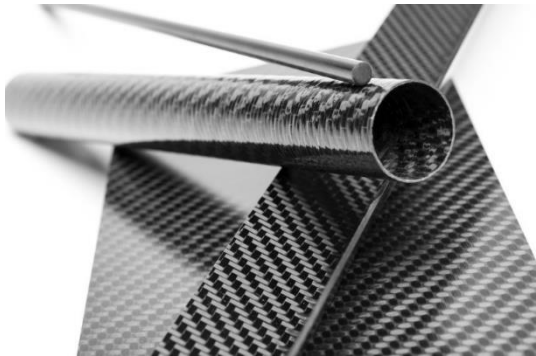

SWINBURNE UNIVERSITY OF TECHNOLOGY

Strategic Industry Partnerships (in the past 12 months ~ AUD$ 150m

- Wipro funded Chair in Artificial Intelligence
  - Plus 3 PhD scholarship ~ AUD$ 1.83 m
- Uniting Care funded Chair in Social Enterprise
  - AUD$ 1.73m
- CSIRO Lead Scientist
  - plus 3 RFs and 3 PhD scholarships ~ AUD$ 2m
- MAI funded Transport Innovation Centre
  - with 20 scholarships ~ AUD$ 5m
- "Imaging Intelligent Materials" funded Certifica Technologies
  - AUD$ 2m
- Secured AUD$ 135m investment for Siemens tc
- Communization on graphene projects (> AUD$

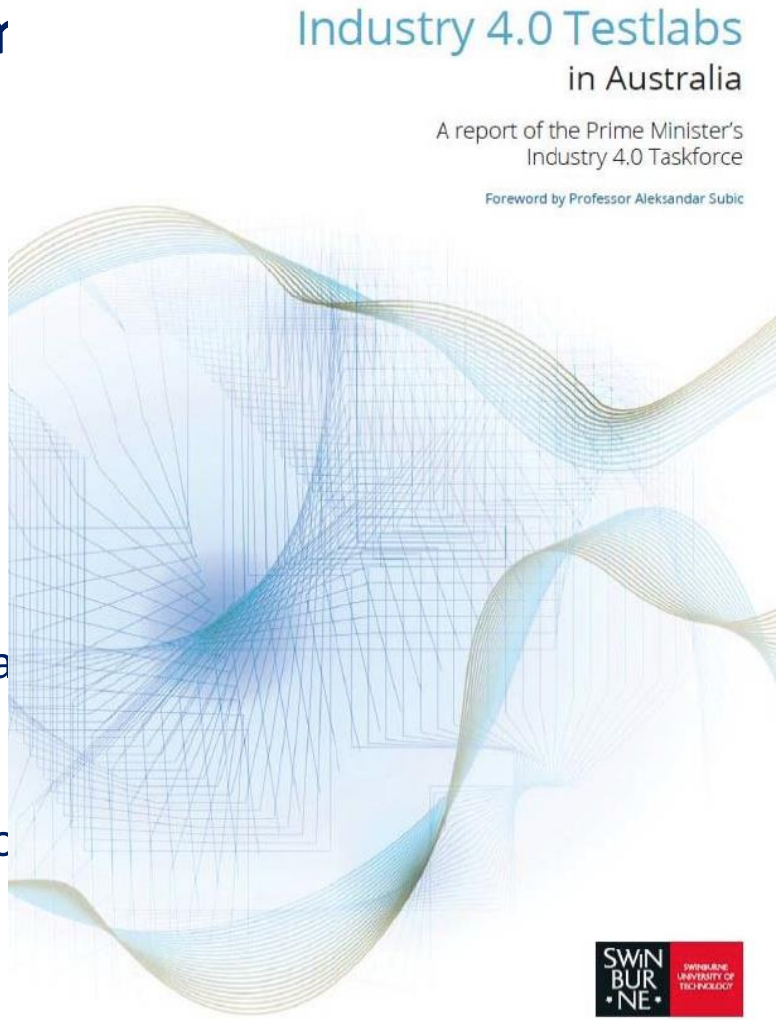

Enhancing the Properties of Lightweight Materials

SWINBURNE UNIVERSITY OF TECHNOLOGY

金雞獻瑞欽郅治，玉犬呈祥展宏猷

祝大家狗年事事如意
身體健康，心想事成

SWINBURNE
UNIVERSITY OF
TECHNOLOGY

THANKS

FOR YOUR ATTENTION

金屬基複合材料的應用和最新發展

由香港理工大學程及系統陳鏡昌教授主講

Latest development of Metallic Glasses and their applications

Prof. K. C. Chan

Advanced Manufacturing Technology Research Centre,
Dept. of Industrial and Systems Engineering,
The Hong Kong Polytechnic University

29 Jan. 2018

THE HONG KONG POLYTECHNIC UNIVERSITY
香港理工大學

Opening Minds • Shaping the Future
啟迪思維 • 成就未來

Overview

1. Introduction
2. Glass-forming ability of metallic glasses
3. Fabrication technologies
4. Mechanical properties and applications
5. Thermal-plastic formability and applications
6. Applications in catalysis
7. Applications in biomedicine
8. Magnetic properties and applications
9. Metallic glass coatings and applications
10. Conclusions

1. Introduction

Metallic glasses are solid metallic materials, usually alloys, but with a disordered atomic-scale (or "liquid-like"/"glass-like") structure.

Silicate glass
(optical transparency)

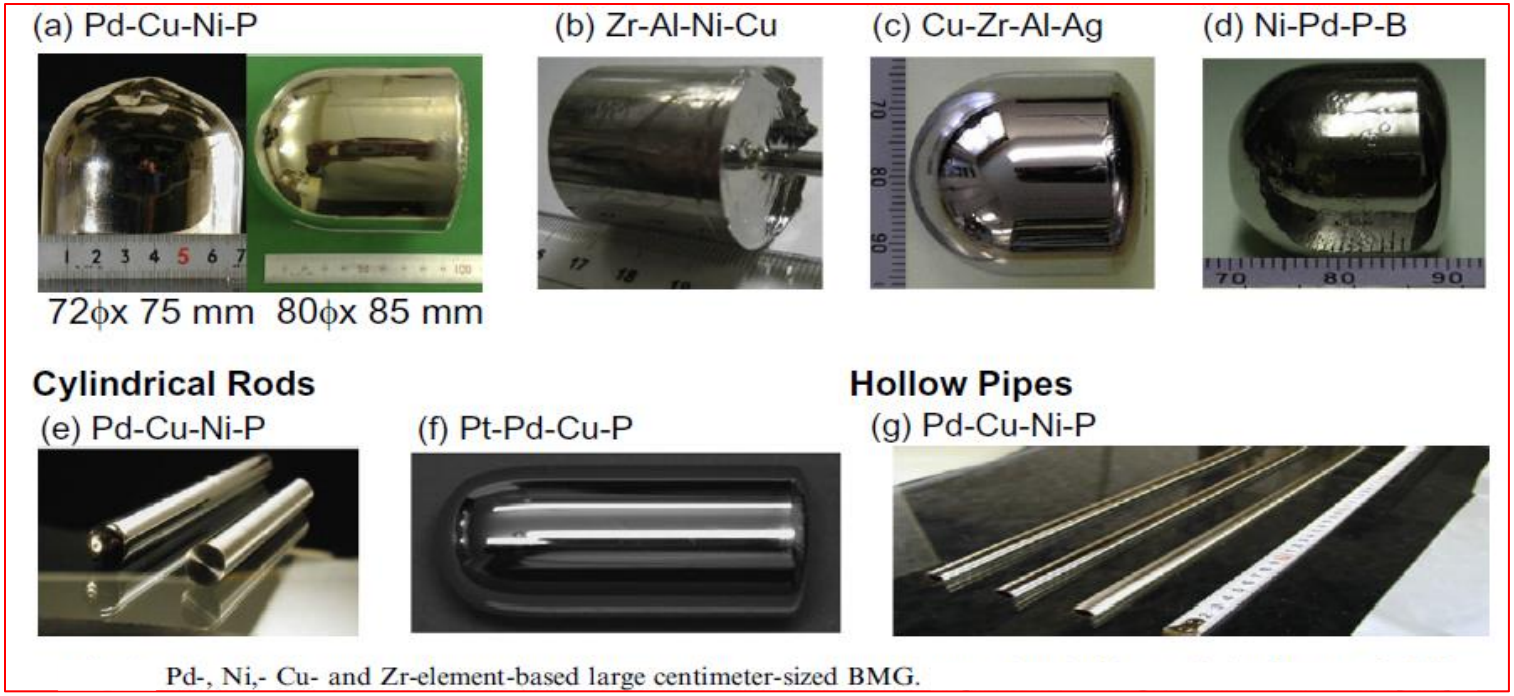

Metallic glass

Wang W H, et al. Materials Science and Engineering: R: Reports, 2004, 44(2): 45-89.

Examples of applications

Fe-based metallic glass

Thin, lightweight smartphone casings in the lab from Yale professor Jan Schroers

Zr-based metallic glass
$8400

Stainless steel
$2,500

Omega Seamaster Planet Ocean Liquidmetal watch-Limited edition

https://www.chrono24.com/omega/planet-ocean-liquidmetal-limited-edition--id7450408.htm

1.1 What is a metallic glass?

Schematic of structures

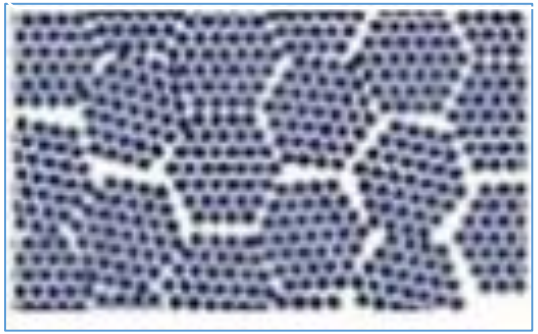

Polycrystalline

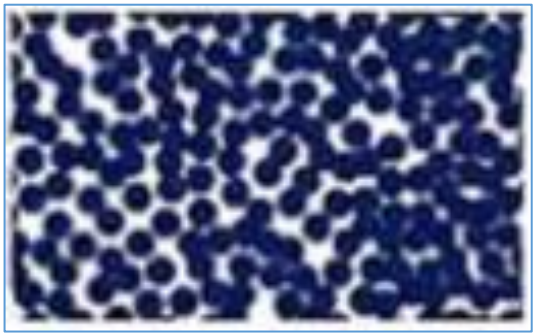

Liquid or Glass

Crystalline (traditional) metals

- Long-range order in lattices
- Crystal defects such as dislocations
- Phases and microstructures
- Grains and grain boundaries

Metallic glasses (amorphous metals/glassy metals)

- highly disordered with liquid-like atomic structures
- No crystal defects and microstructures

1) Schroers J, Johnson W L. Physical Review Letters, 2004, 93(25): 255506.
2) Spaepen F. Acta metallurgica, 1977, 25(4): 407-415.

Characterizations of amorphous structure using post-modern technologies

Crystalline metals (nanocrystalline Cu)

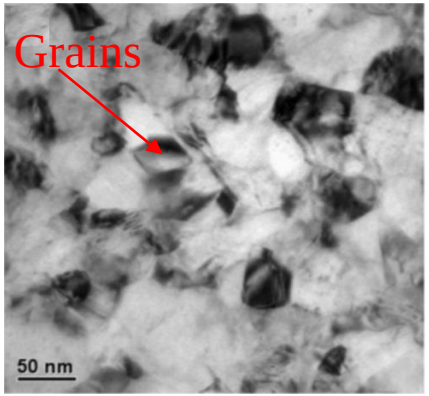

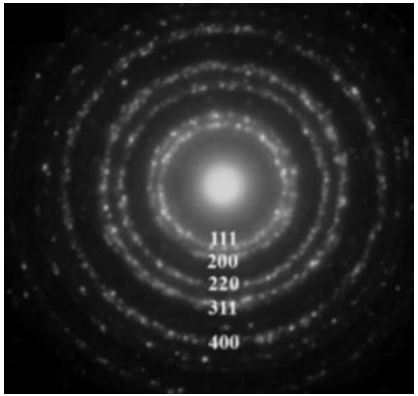

TEM ir

X-ray diffraction

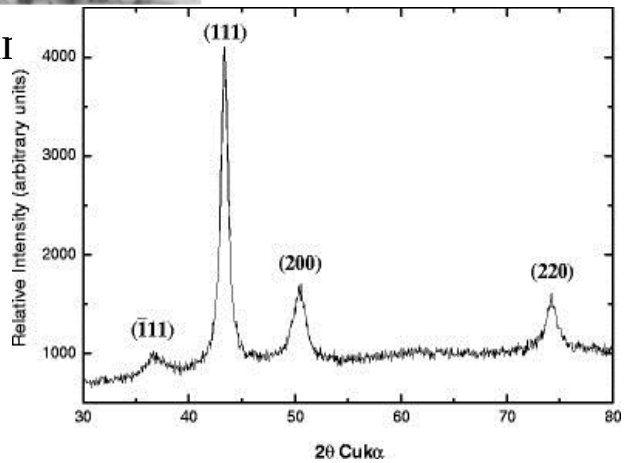

Metallic glasses ($Cu_{50}Zr_{50}$)

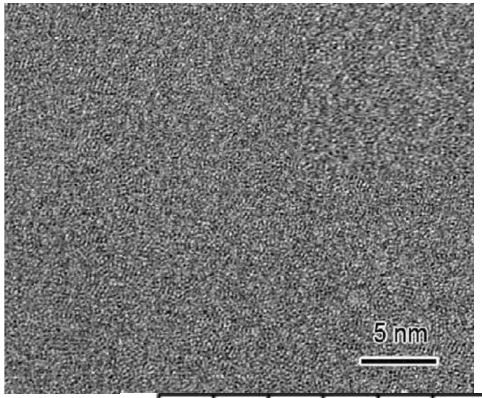

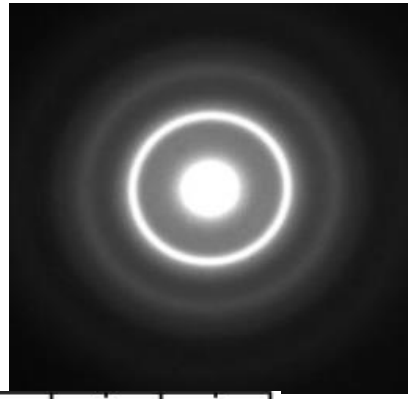

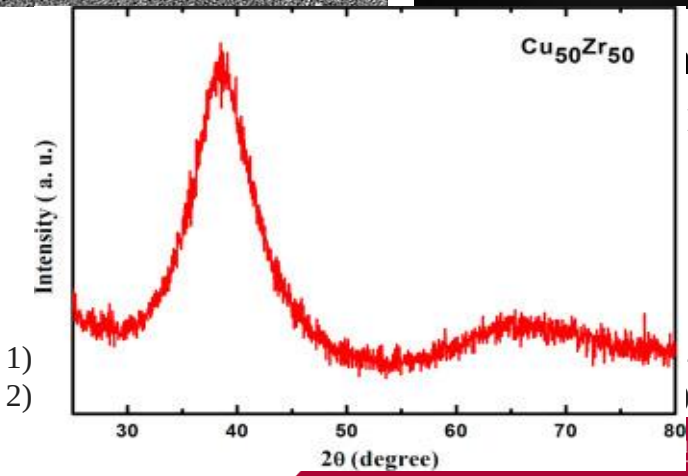

l

rn

1)
2)

-1533.
): 205501.

Outstanding mechanical proprieties

High strength and high elastic limits

Metallic glasses combine higher strength than crystalline metal alloys with the elasticity of polymers.

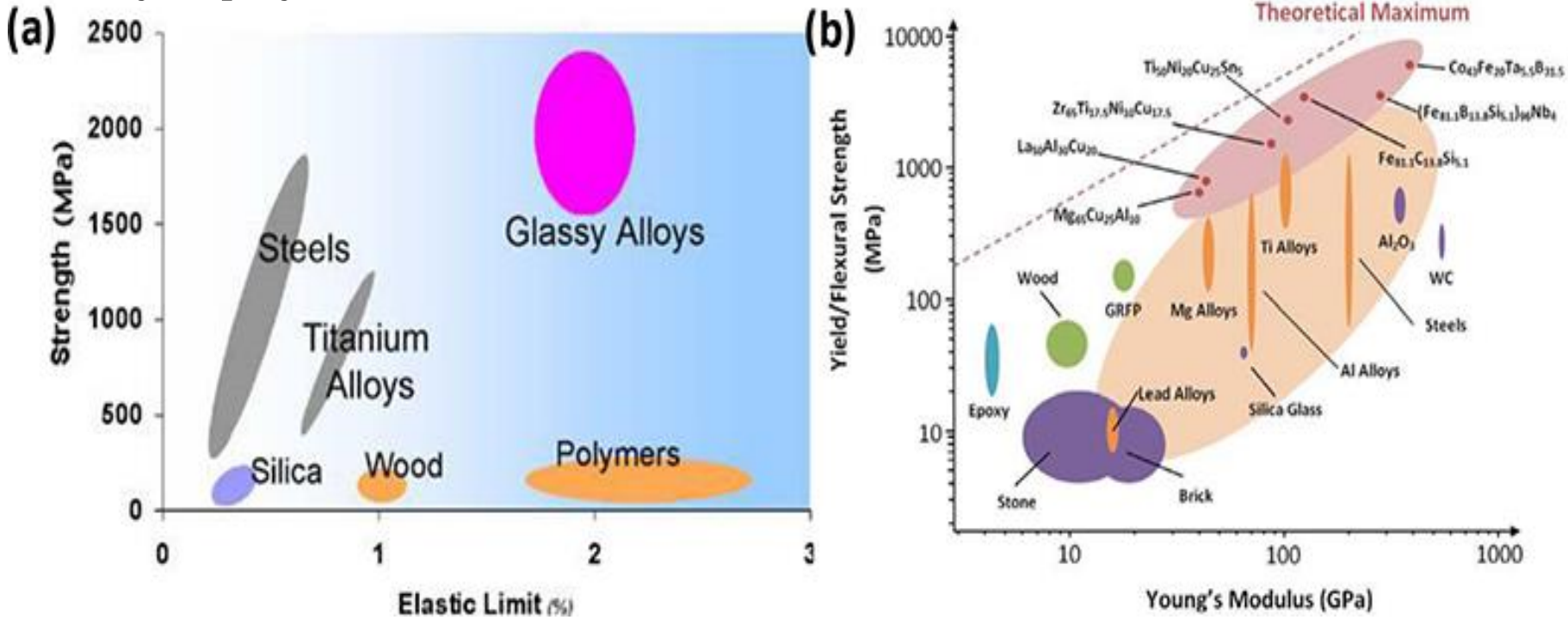

Axinte E. Materials & Design, 2012, 35: 518-556.

High hardness and wear resistance

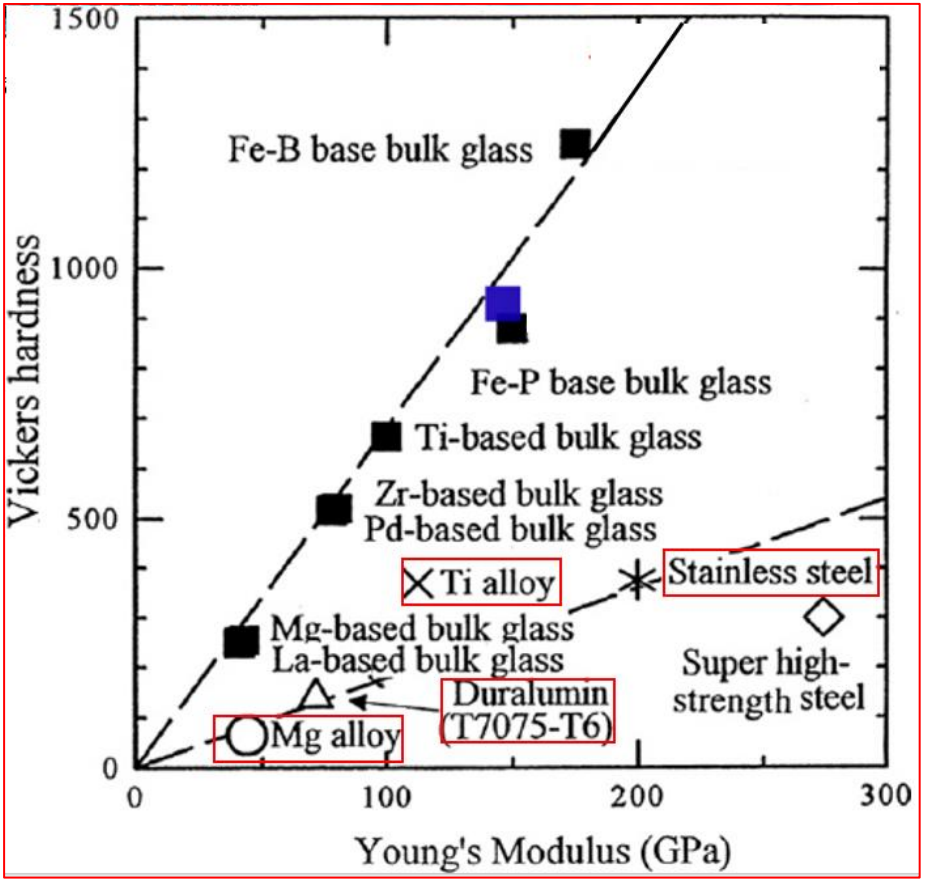

Relationship between Vickers hardness and Young's modulus for various BMGs

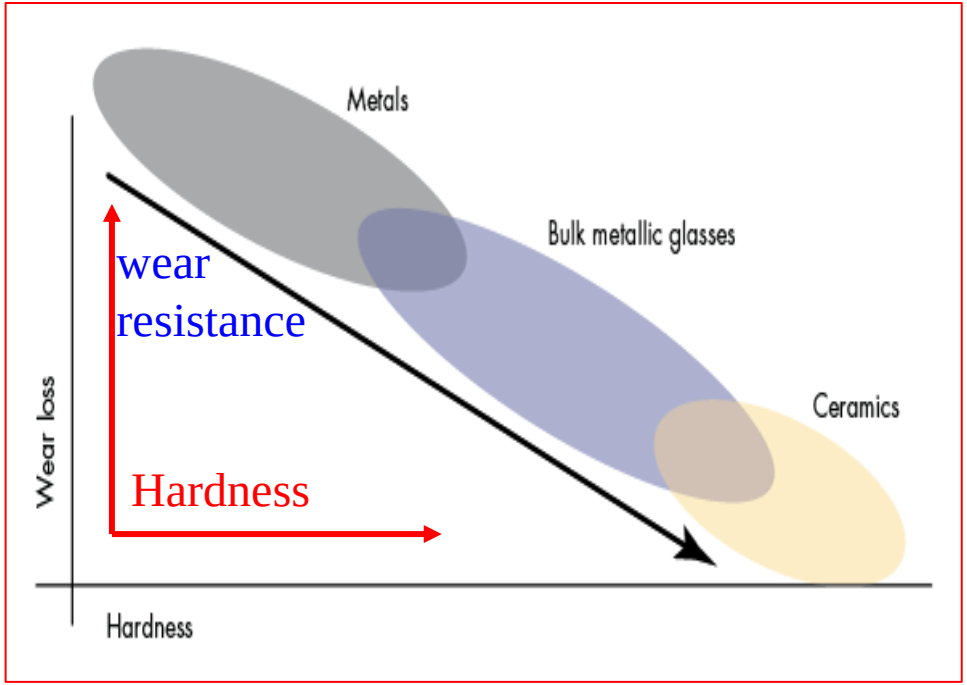

The hardness ranges of three types of materials

1. Wang W H, et al. Materials Science and Engineering: R: Reports, 2004, 44(2): 45-89.
2. Lu J, et al., Acta materialia, 2003, 51(12): 3429-3443.

Illustration of several types of metallic glasses

X-Based metallic glasses	Strength (GPa)	Elastic limit
Al-	0.8-1.5	~2 %
Zr-	1.7-2.0	
Ti-	1.8-2.6	
Cu-	1.9-2.5	
Ni-	2.7-3.1	
Fe/Co-	3.6-5.6	
steels	< 2.0	~0.65 %

An Al-based, $Al_{86}Ni_7Er_5Co_1La_1$, exhibits ultrahigh strength of up to ~1525 MPa, which is twice that of conventional crystalline aluminum alloys

The commercial amorphous alloy, Vitreloy 1 ($Zr_{41.2}Ti_{13.8}Cu_{12.5}Ni_{10}Be_{22.5}$), developed by *Liquidmetal Technologies*, can achieve a yield strength of over 1800 MPa, nearly twice the strength of conventional crystalline titanium alloys (Ti6Al4V is ~830 MPa) and about the strength of high-strength steels

1) Yin J, et al. Journal of Alloys and Compounds, 2015, 648: 276-279.
2) Schneider S, et al. Applied physics letters, 1996, 68(4): 493-495.

High fracture toughness

Material type	Material	K_{Ic} (MPa · $m^{1/2}$)
Metal	Aluminum alloy (7075)	24
	Steel alloy (4340)	50
	Titanium alloy	44–66
Ceramic/Silicate glass		0.2–5
Polymer		0.7–1.6
Metallic glass	Mg-based	2
	Zr-based	30-125
	Pd-based	200

Fracture toughness of various materials

1. Hofmann D C. Journal of Materials, 2013.
2. Gilbert C J, et al. Applied Physics Letters, 1997, 71(4): 476-478.

The first commercial amorphous alloy, Vitreloy 1 ($Zr_{41.2}Ti_{13.8}Cu_{12.5}Ni_{10}Be_{22.5}$), developed and sold by *Liquidmetal Technologies* since 2003.

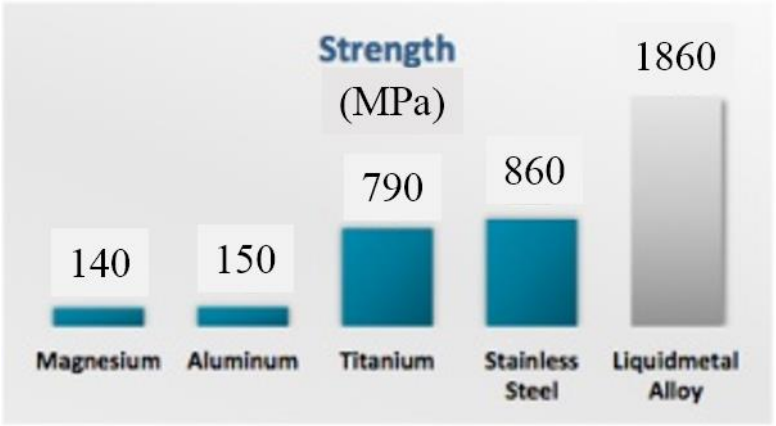

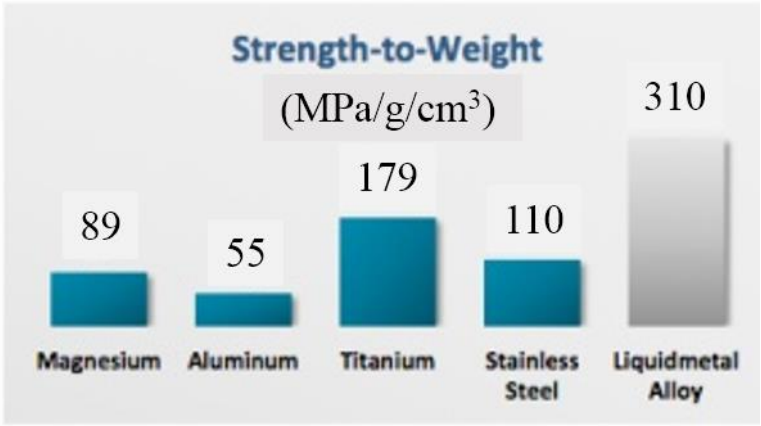

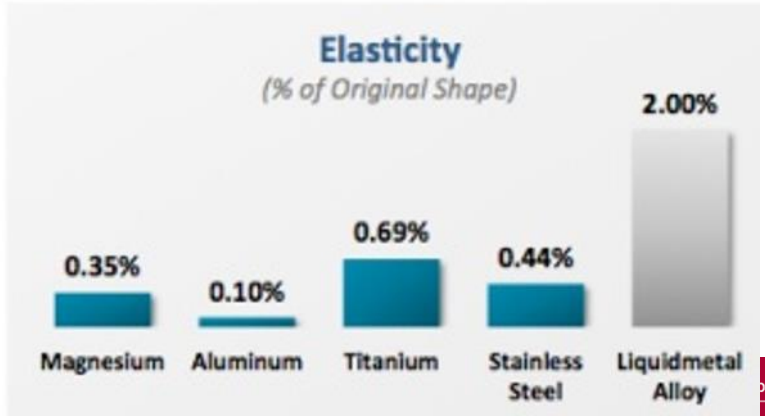

Data from the website of Liquidmetal Technologies

Overall properties of metallic glasses

- High elastic limit: ~ 2%
- High strength: > 2000 MPa
- low density: 2.5~6 g/cm^3 (high strength-to-weight ratio)
- High hardness: 600~1300 H_v
- High fracture toughness: > 70 MPa/m^2
- Good formability: > 1000%
- Superior corrosion resistance
- Good wear resistance
- Excellent soft magnetic properties: Fe-based metallic glasses
- Other interesting physical properties

Weak regions

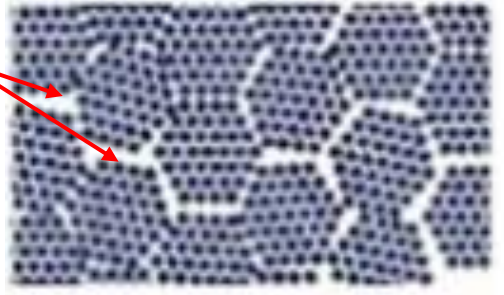

Polycrystalline alloys

Defect-free

Metallic glasses

1.2. Historical development of metallic glasses

1960 The first reported metallic glass was an Au-Si alloy produced at Caltech by Willens and Duwez. Early glass-forming alloys had to be cooled extremely rapidly (quenching on the order of 10^6 K/s) to avoid crystallization and could only be produced into ribbons, foils, or microwires.

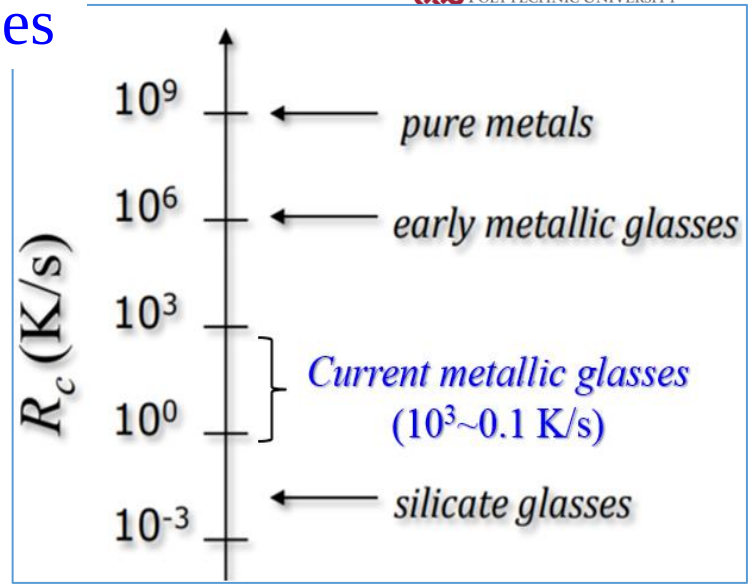

1969 Ternary Pd-Cu-Si alloys, were found by Chen to have critical cooling rates between 100 and 1000 K/s, which opened a new spectrum for investigating metallic glasses. Later, metallic glasses of bulk sizes continued to attract strong attention among many scientists.

1984 The Inoue group at Tohoku University, Japan reported a bulk metallic glass rod via water quenching in the composition of $La_{55}Al_{25}Ni_{20}$, which was the first metallic glass alloy reported without noble metal elements.

1989 Greer and Turnbull et al produced centimeter-sized Pd-Ni-P BMGs at a slow cooling rate of only 10 K/s.

1990 ↓ A wide variety of BMGs, including Mg-, Ca-, Zr-, Ti-, Fe-, Co-, Ni-, Nd-, Cu-, Pr-, W-, Ce-, Pt-based systems were subsequently developed at slow cooling rates, which is as low as 0.1 K/s and the maximum sizes reach ~80 mm in diameter ($Pd_{42.5}Cu_{30}Ni_{7.5}P_{20}$).

The key issues in the development of these amorphous alloys are to

1) Form large-sized amorphous alloys with high glass formability;
2) Improve ductility under unrestrained loading;
3) Look for practical mechanical and functional applications in various fields.

Development of BMGs

Splat-quenching Method

$Au_{75}Si_{25}$ film

Born 1960

Pol Duwez

Bulk samples (diameter/thickness >1 mm; Pd-Ni-P La-based etc.)

1980s

Turnbull et al.
Inoue et al.
.....

First commercial Zr-based BMG (Vitreloy 1, 1992)

Larger sizes (Pd-based, ~ 72 mm; Zr-based, ~ 20 mm)

1990s

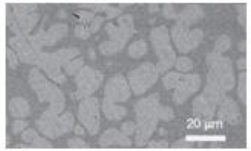

BMG composites (Particles; In-situ phases; Nanocrystals .....)

2000s

Shape-memory BMG composites (Phase transformation)

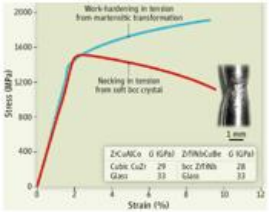

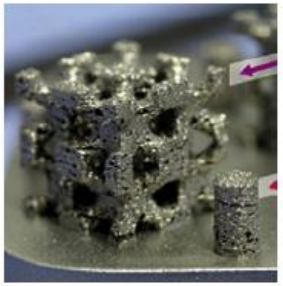

Selective Laser melting of BMGs

2010

2013

2017

Supra-nanometre-sized Dual-phase glass-crystal material

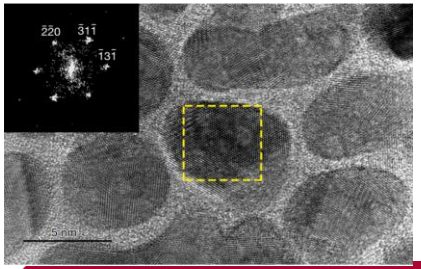

Time

2. Glass-forming ability of metallic glasses(quenching from the melt state)

The actual cooling rate should be larger than the critical cooling rate of a specific alloy ($R_a > R_c$).

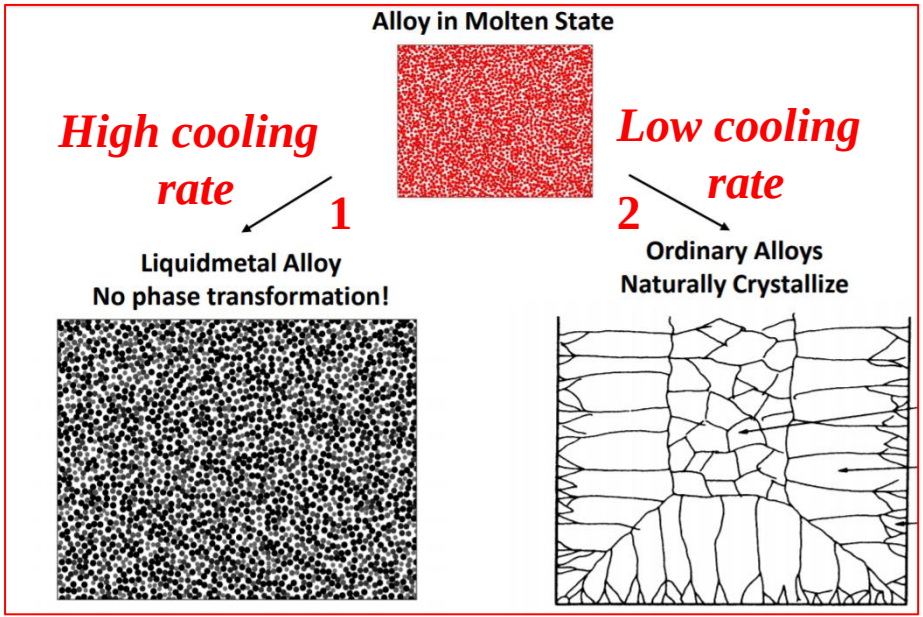

Schematic diagram of structural transformation when quenching a molten alloys from high temperature.

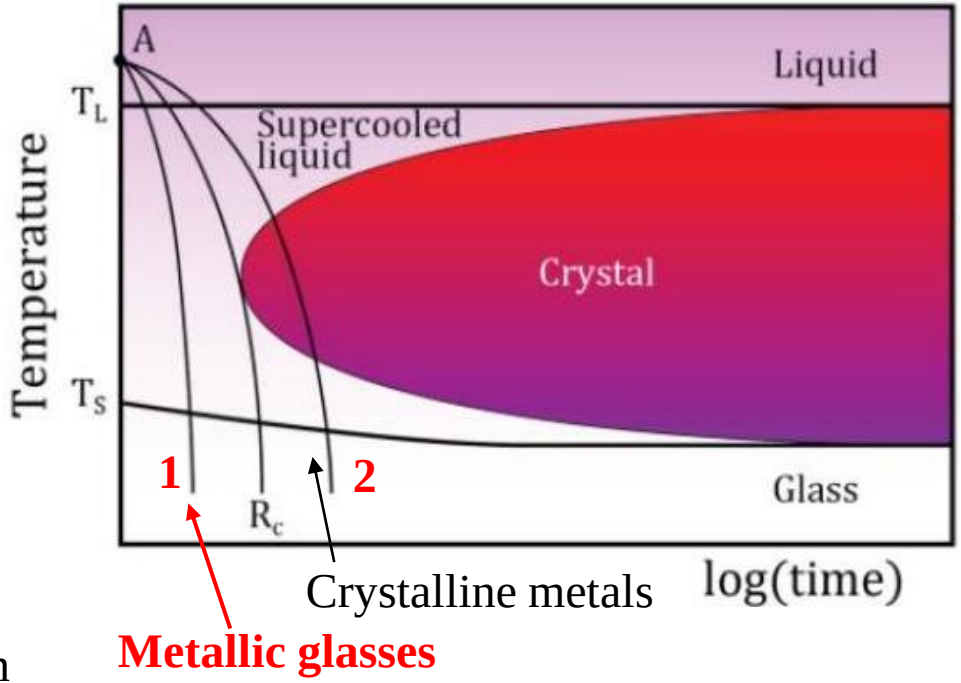

Cooling rate-dependent transformation

Axinte E. Materials & Design, 2012, 35: 518-556.

2.1. Strategies for composition design

Amorphous alloys are formed by exploiting a phenomenon called the "confusion effect". Such alloys contain so many different elements that upon cooling at sufficiently fast rates, the atoms simply cannot coordinate themselves into the equilibrium crystalline state before their mobility is stopped (i.e., crystallization is suppressed). In this way, the random disordered state of the atoms is retained.

Glass-forming criteria

Inoue et al. laid down the conditions for the formation of amorphous alloys:

(i) should have more than three constituent elements (the "confusion“ principle),

(ii) atomic size difference should be greater than 12% (to achieve high packing density and low free volume).

(iii) must possess a negative heat of mixing (to inhibit crystal nucleation and prolongs the time the molten metal stays in supercooled state).

2.2. Glass forming ability of various alloys

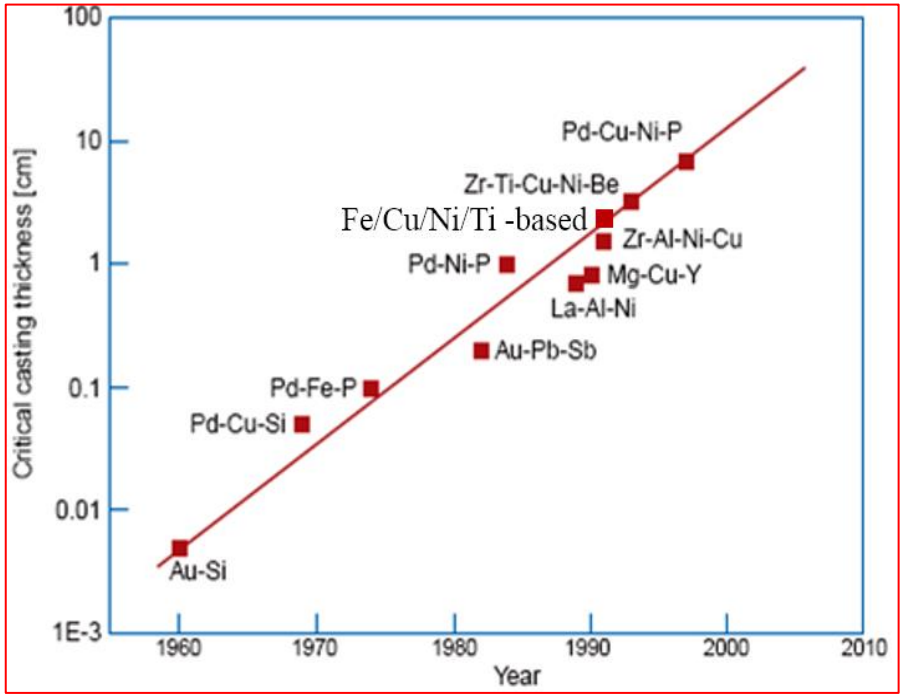

Critical casting diameter

compositions	t_{max}(mm)	Rc(k/sec)
Ln-Al-(Cu,Ni)	≅10	≃200
Mg-Al-(Cu,Ni)	≅10	≃200
Zr-Al-Cu,Ni)	≅30	1-10
Zr-Ti-Al-(Cu,Ni)	≅30	1-5
Zr-Ti-(Cu,Ni)-Be	≅30	1-5
Fe-(Al,Ga)-(P,C,B,Si)	≅3	≃400
Pd-Cu-Ni-P	≅75	0.1
Fe-(Co,Ni)-(Zr,Hf,Nb)-B	≃6	≃200
Ti-Ni-Cu-Sn	≅6	≅200

The critical casting thickness versus the year in which alloys were discovered. Over 40 years, the critical casting thickness has increased by more than three orders of magnitude.

1) Wu Z W, et al. Nature communications, 2015, 6: 6035.
2) Schroers J. Physics Today, 2014, 67(2): 11-11.

In addition to **direct cooling** from the melting liquid state, there are several other ways in which amorphous metals can be produced, including:

- From the vapour state (i.e., physical vapor deposition)
  - ➢ By condensing the vapour of the material onto a cold substrate.
- from the solid state (i.e., mechanical alloying/solid-state reaction)
  - ➢ By severely deforming the crystals (say a polycrystal) amorphous state can be obtained. Ball milling has been one of the popular examples for this method.
- from aqueous solution (i.e., electroplating/chemical plating)

Amorphous metals produced by these techniques are, strictly speaking, not glasses; however, materials scientists commonly consider amorphous alloys to be a single class of materials, regardless of how they are prepared.

3. Fabrication technologies

Metallic glasses can be fabricated into various shapes, such as in bulks, ribbons, micro/nano-wires, particles, films and even foams.

1) Rapid cooling of liquid alloys (bulks, ribbons, wires)
2) Mechanical alloying (bulks)
3) Powder metallurgy (bulks)
4) Physical vapor deposition/spraying (films)
5) Electroplating/chemical plating (films)
6) Gas atomization (particles)

bulks

ribbons

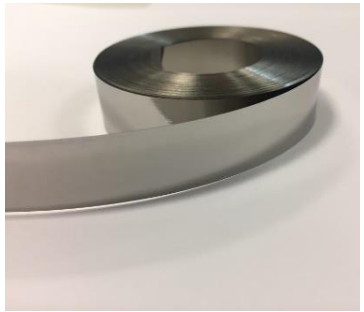

wires

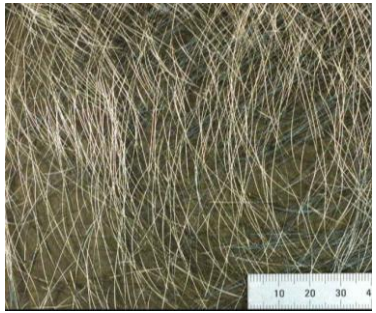

films/coating

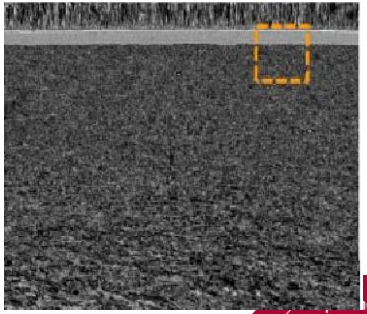

particles

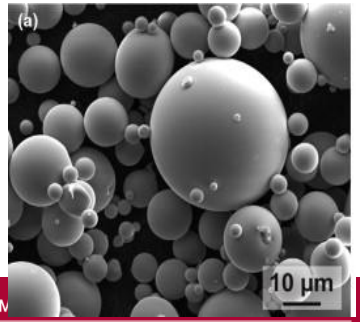

Rapid cooling of liquid alloys

Equivalent cooling rates of various fabrication technologies

Virtually, any metallic liquid can be turned into a glass if it is cooled quickly enough to avoid crystallization. The question is, how fast does the cooling need to be?

Annealing | Melt quenching | Copper mold Suction casting | Splat cooling | Melt Spinning | Thermal evaporation

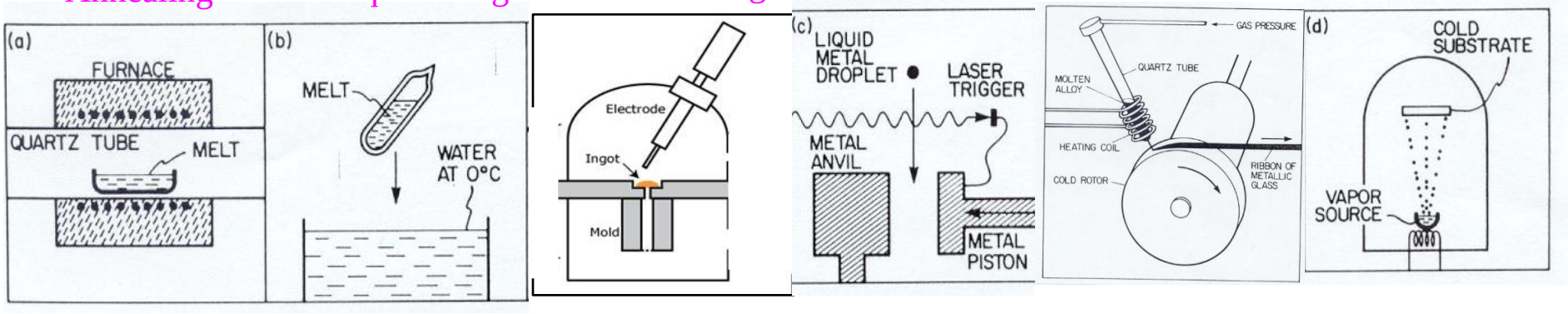

~ 10^{-3} K/s | ~ 10^{2} K/s | ~ 10^{3} K/s | ~ 10^{5} K/s | ~ 10^{7} K/s | ~ 10^{10} K/s

The maximum cooling rate of various fabrication approaches.

Wang W H, et al. Materials Science and Engineering: R: Reports, 2004, 44(2): 45-89.

3.1. Suction casting

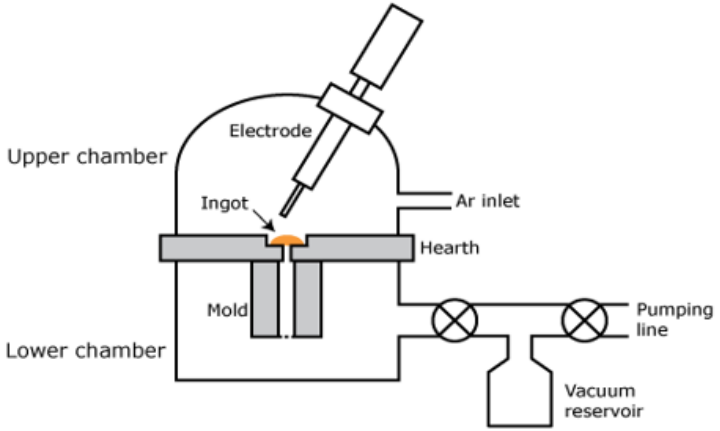

- Achieving high cooling rate using water-cooled copper molds
- The process is undertaken in Argon atmosphere inside a vacuum chamber.

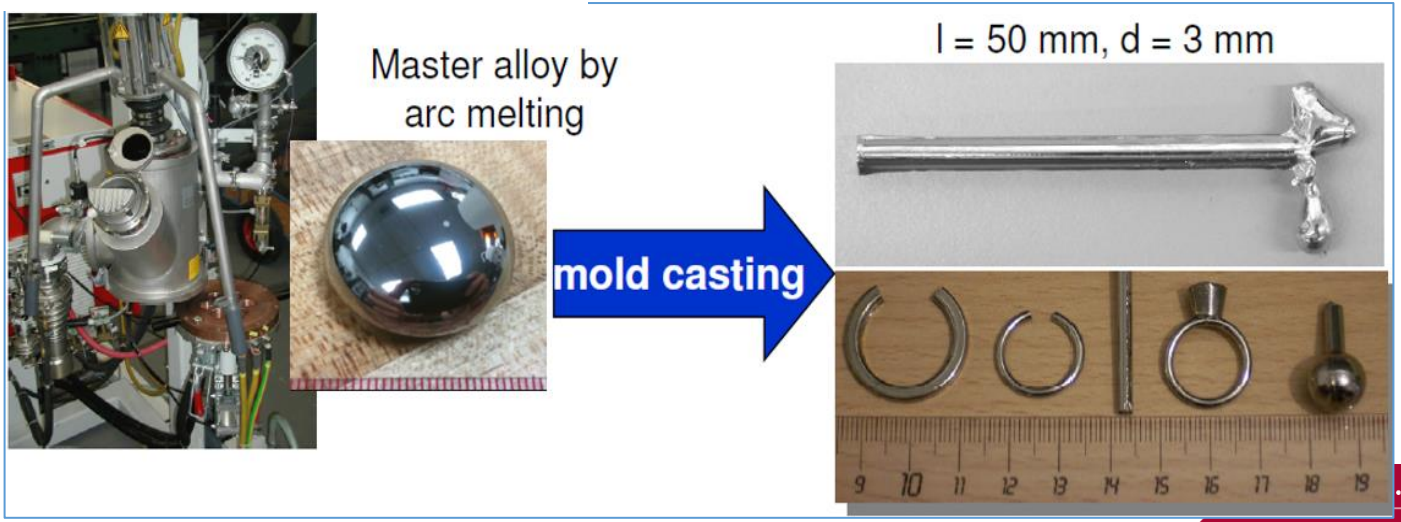

3.2. Mold casting

Raw Material	Raw Ingots	Mold	As Molded	End Components
		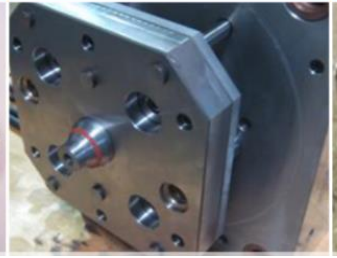		

Mold casting can produce high volumes of high precision, high strength parts with beautiful surface finish in a single step.

- Amazing Dimensional Accuracy, near that of the mold, only 0.2% shrinkage.
- Incredible Surface Finish, reflects the finish of the mold.
- Makes many complex metal component applications possible.

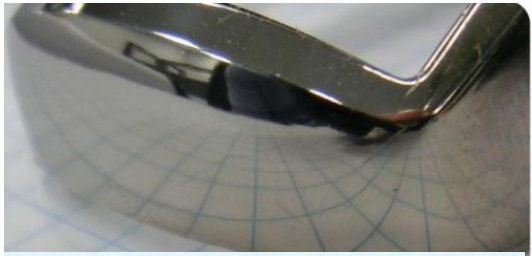

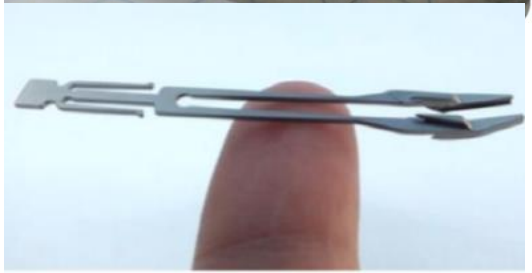

3.3. In-rotating-water spinning (rotating-water-bath casting)

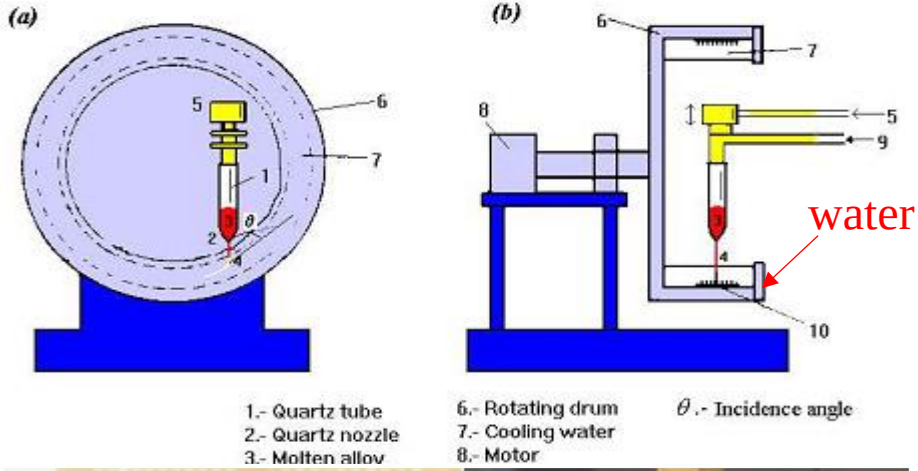

In-rotating-water spinning is popular technique for **making continuous Fe-/Co-based** amorphous alloy **microwires** (20~200 μm in diameter), in which the melt was ejected through the orifice into the rotating water layer.

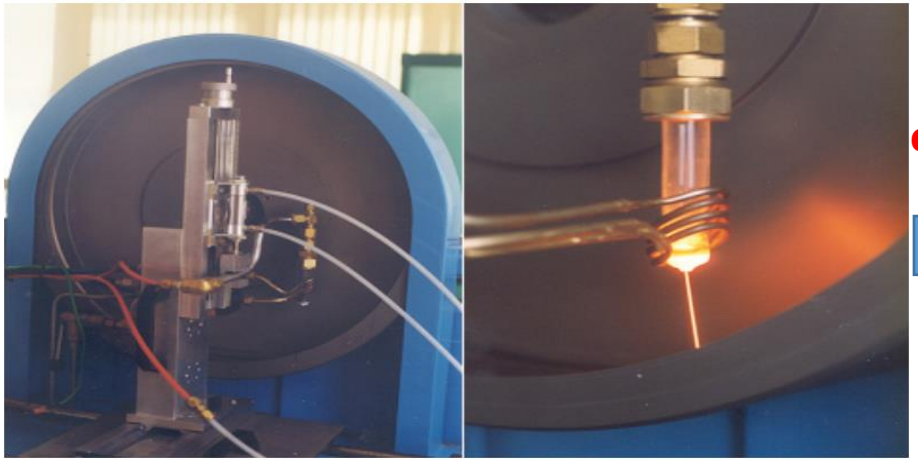

collection

In the

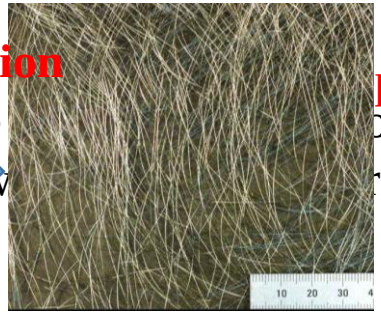

package

3.4 Melt Spinning

Melt spinning is popular technique for **making ribbons or foils** (5~50 µm-thick) which use molten material to flow from the nozzle in the form of a jet, which when comes in contact with cold rotating discs form a melt puddle.

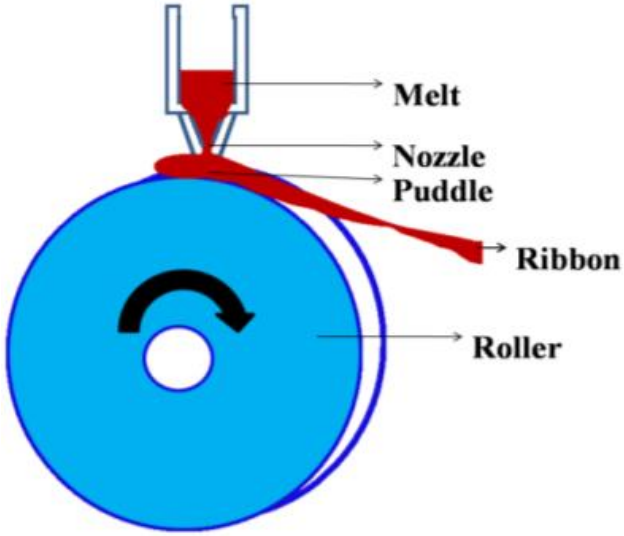

Schematic diagram of melt spinning technique

Setup

Ribbons

Properties & applications

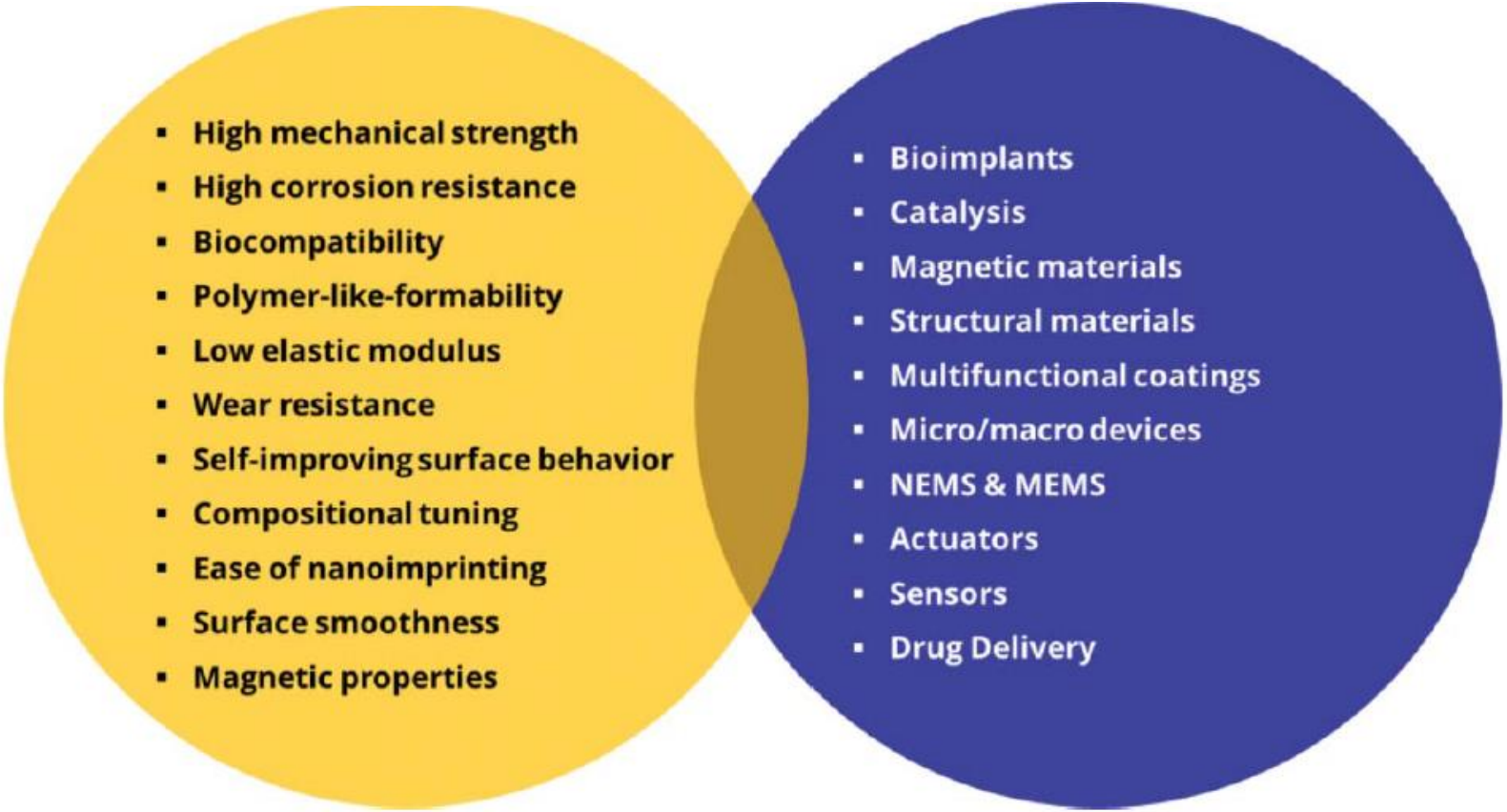

Some remarkable features exhibited by different metallic glass systems and their potential applications in various fields.

4. Mechanical properties and their applications

Overall properties of metallic glasses

- High elastic limit: ~ 2%
- High strength: > 2000 MPa
- low density: 2.5~6 g/cm^3 (high strength-to-weight ratio)
- High hardness: 550~1300 HV (304 stainless steel: <330 HV)
- Good wear resistance
- High fracture toughness: > 70 MPa/m^2
- Good formability: > 1000% (in supercooled liquid region)
- Superior corrosion resistance

Polycrystalline alloys

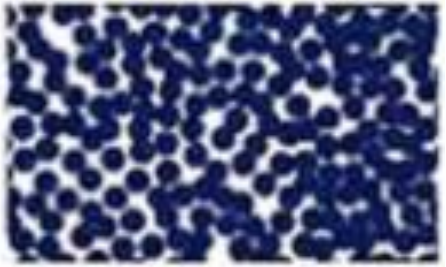

Metallic glasses

Drawbacks:

- Size limitations (The maximum is ~80 mm in diameter, Pd-based)
- Lack of ductility under tension and limited plasticity under compression at room temperature, which may affects service reliability as general structural materials.

Poor ductility of metallic glasses

As listed above, metallic glasses have many attractive mechanical properties that include high strength and elasticity, high hardness combined with excellent corrosion resistance. However, one major impediment in using MGs as structural materials are the lack of ductility in comparison with their crystalline counterparts.

In general, metallic glasses show a lack of ductility under tension and limited plasticity under compression.

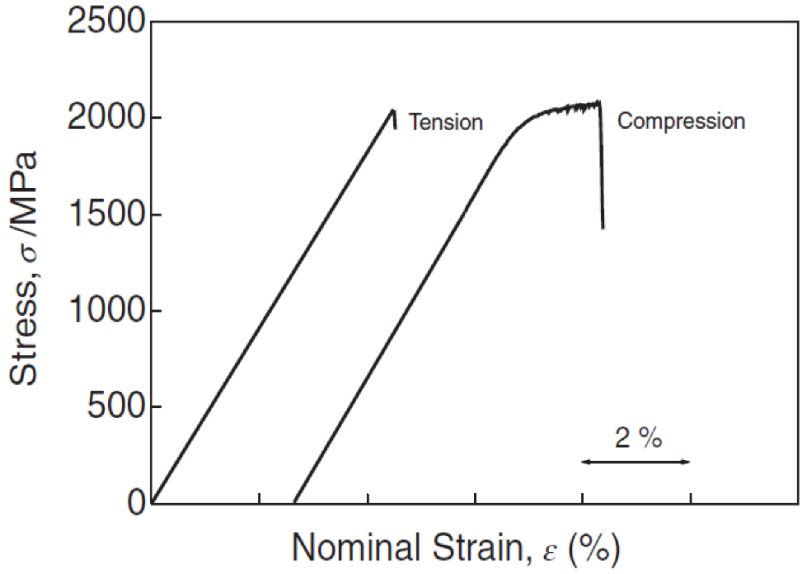

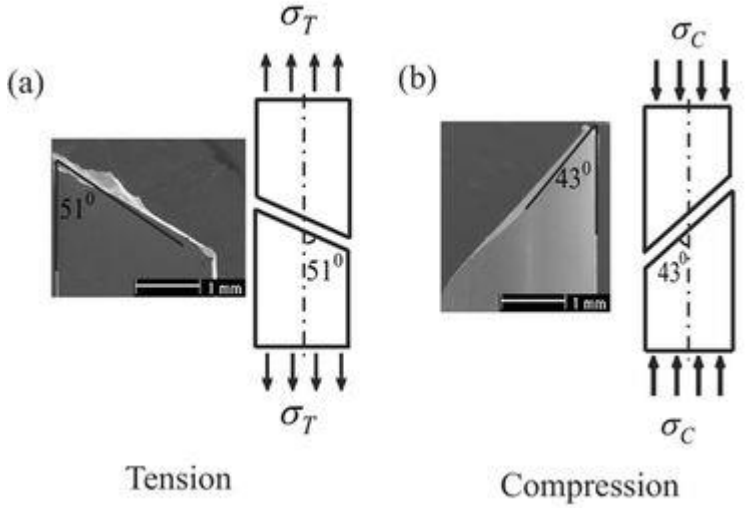

Schematic diagrams of fracture

The stress-strain curves of $Zr_{41.2}Ti_{13.8}Cu_{12.5}Ni_{10}Be_{22.5}$ under tension and compression

Strategies for plasticity improvements

A great deal of effort has been made in recent years to improve the plasticity of metallic glasses. Some monolithic MGs exhibiting obvious compressive plasticity were developed, possibly due to

- Composition design with a high Poisson's ratio with the relative ease of shearing over dilatation
- faster cooling with more free volume
- Minor alloying
- Reduced sample size (size effect)
- Metallic glass/crystalline composites
- Various pre-treatment methods, cold-rolling, surface shot-peening, high-pressure processing, surface mechanical attrition treatment

1) Minor alloying

$(Cu_{50}Zr_{50})_{100-x}Al_x$ (x=0-10) alloys were prepared by alloying $Cu_{50}Zr_{50}$ with the addition of Al.

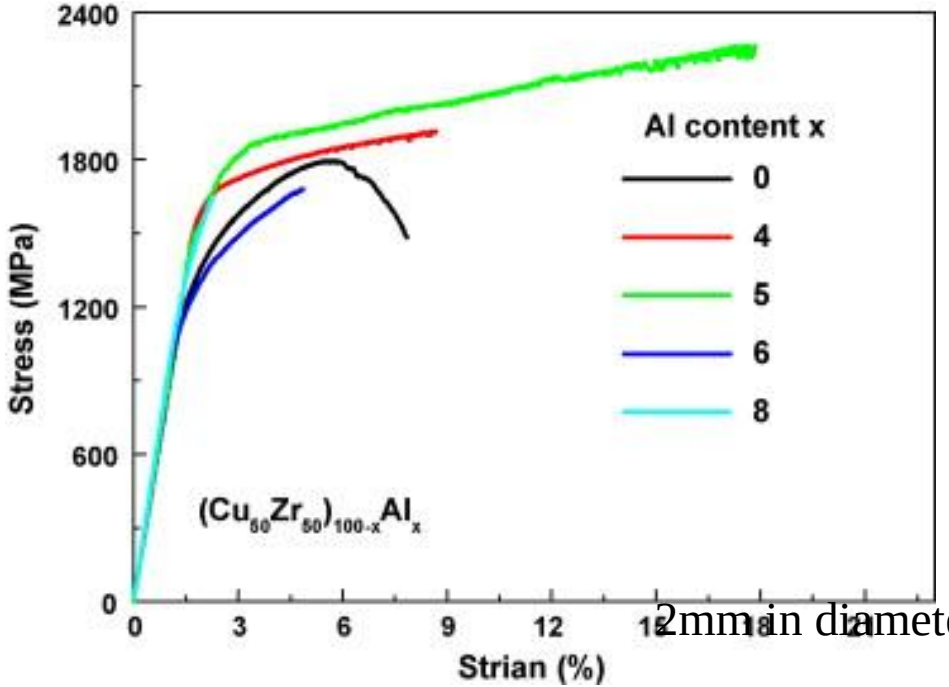

2mm in diameter

$Cu_{50}Zr_{50})_{100-x}Al_x$ shows a combination of highest strength and plasticity when x=5.

Stress-strain curves showing the different plastic flowability of the BMGs.

Yu P, Bai H Y. Materials Science and Engineering: A, 2008, 485(1): 1-4.

2) Pre-treatment

Case 1: cold rolling

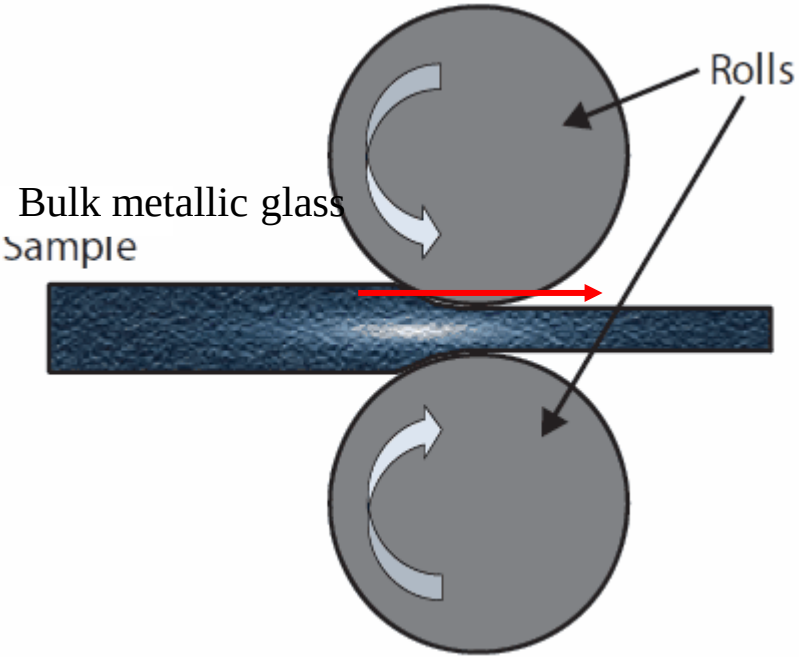

Schematic illustration of Cold Rolling

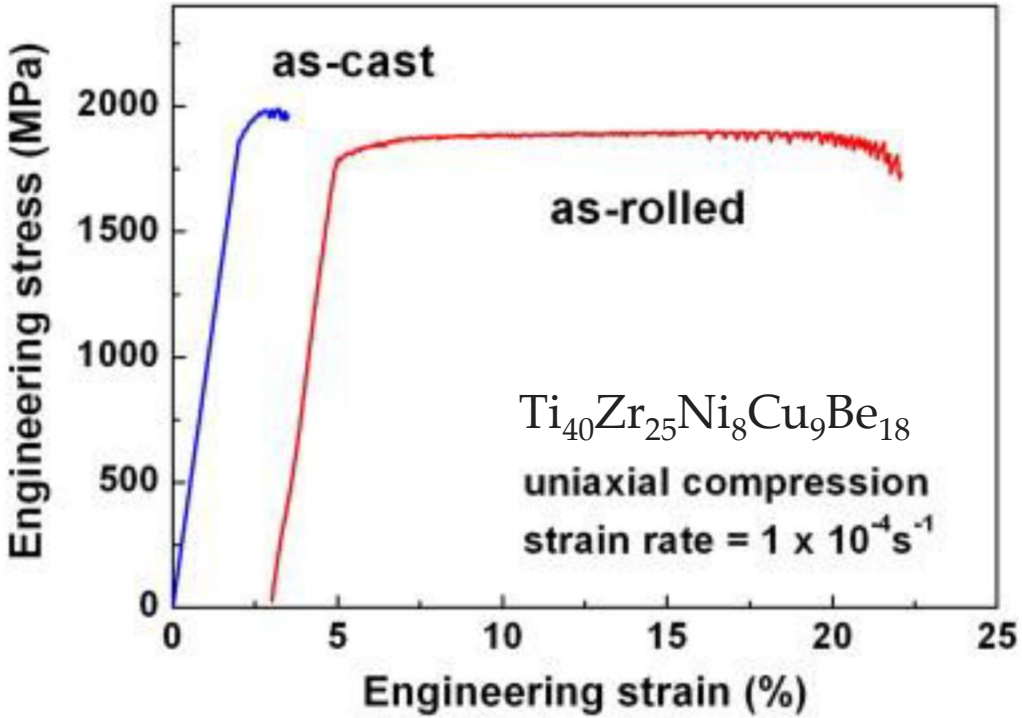

Compressive stress–strain curves of as-cast and cold-rolled BMG samples.

The compressive plastic strain can be dramatically improved from 1.5% to 14.5% with a 50% thickness reduction.

Park, J.M.; Kim, D.H.; Eckert, J. Intermetallics 2012, 29, 70–74.

2) Pre-treatment

Case 2: surface shot-peening

Induced surface residual stresses benefits the plasticity and strength.

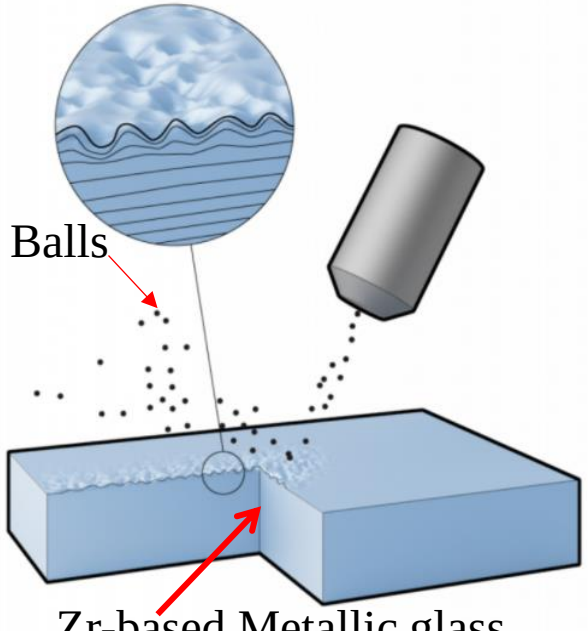

Zr-based Metallic glass, $Zr_{41.2}Ti_{13.8}Cu_{12.5}Ni_{10}Be_{22.5}$

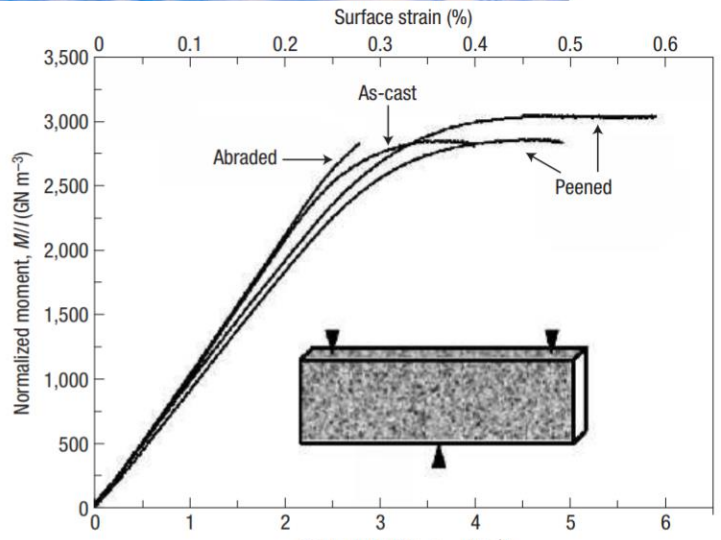

Effects of shot-peening on plasticity in three-point bending.

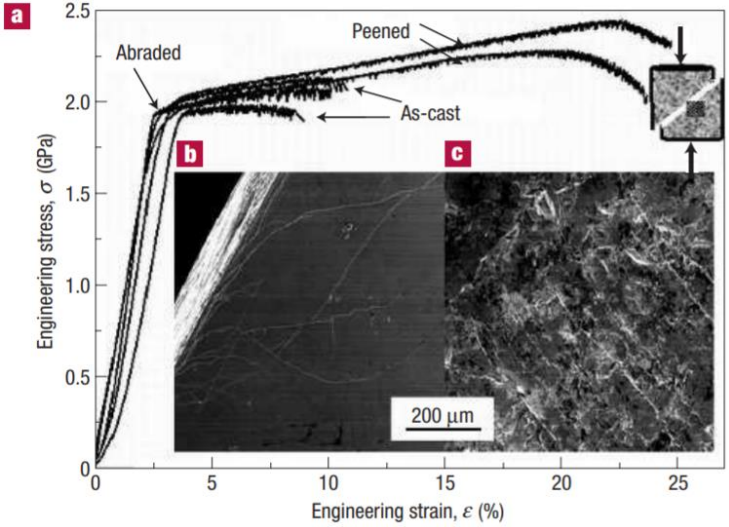

Effects of shot-peening on plasticity in uniaxial compression.

Zhang Y, et al. Nature materials, 2006, 5(11): 857-860.

3) Metallic glass matrix composites

Case 1: dendrite-reinforced bulk metallic glass composites

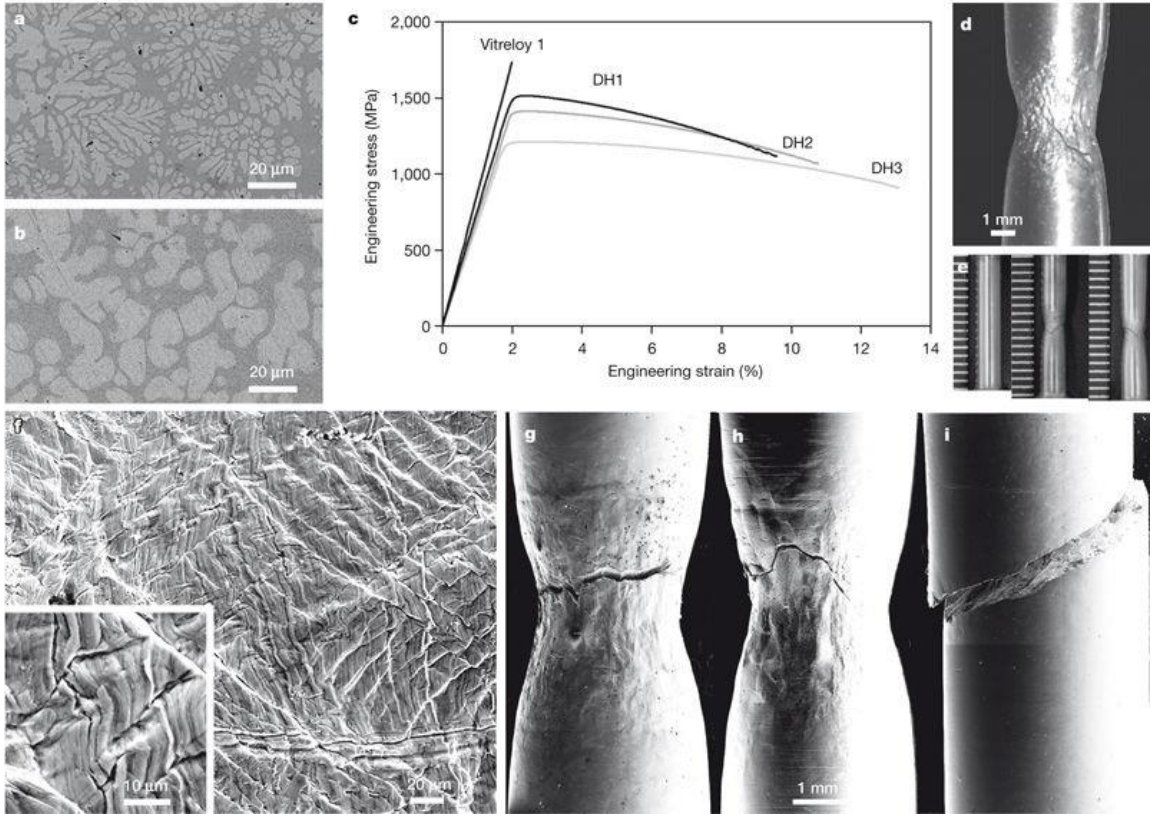

Alloy
$Zr_{36.6}Ti_{31.4}Nb_7Cu_{5.9}Be_{19..1}$ (DH1)
$Zr_{38.3}Ti_{32.9}Nb_{7.3}Cu_{6.2}Be_{15.3}$ (DH2)
$Zr_{39.6}Ti_{33.9}Nb_{7.6}Cu_{6.4}Be_{12.5}$ (DH3)
$Zr_{41.2}Ti_{13.8}Cu_{12.5}Ni_{10}Be_{22.5}$ (Vitreloy 1)
$Zr_{56.2}Ti_{13.8}Nb_{5.0}Cu_{6.9}Ni_{5.6}Be_{12.5}$ (LM 2)

- Tensile ductility ~ 10-14%
- K_{1C} up to ~170 MPa $m^{1/2}$

The inhomogeneous microstructure with isolated dendrites in a BMG matrix stabilizes the glass against the catastrophic failure associated with unlimited extension of a shear band and results in enhanced global plasticity and more graceful failure.

Hofmann D C, Nature, 2008, 451(7182): 1085-1089.

3) Metallic glass matrix composites

Case 2 : metastable B2 reinforced bulk metallic glass composites

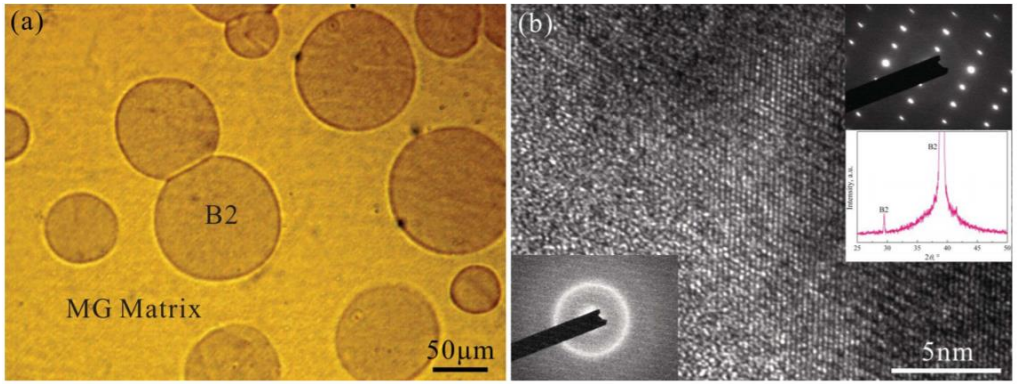

reversible B2↔B19’ phase transformation

OM and TEM imageS showing the microstructure of the B2-BMGC

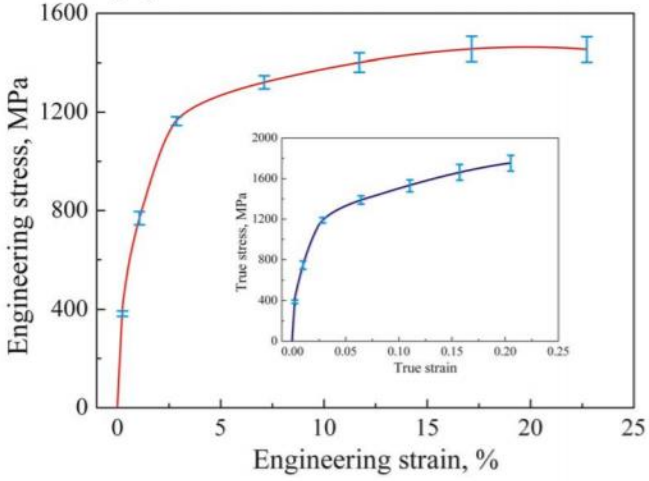

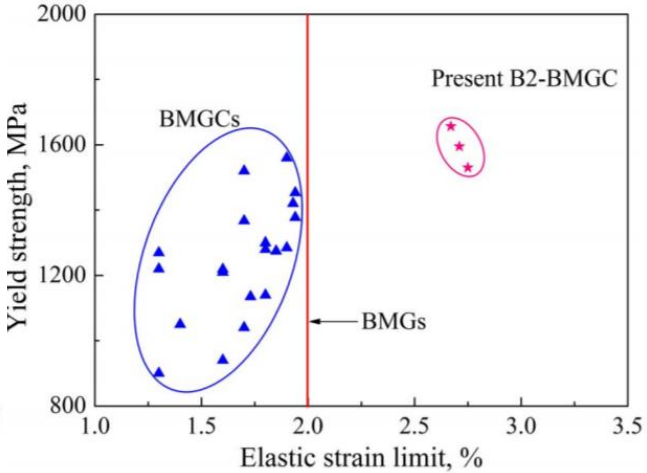

The bulk metallic glass composite can exhibit both a large elastic strain limit ~2.7% and high strength under tension

Wu F F, Chan K C, Jiang S S, et al. Scientific reports, 2014, 4: 5302.

4.3 Applications of mechanical properties

1) Electronic products

Use of advantages:

- High strength and hardness
- Mirror-like surfaces in one-step fabrication

iPhone

Turing Phone

https://hothardware.com/news/turing-announces-pre-orders-for-worlds-first-liquid-metal-frame-smartphone

Die casting produced pieces-LiquidMetal Technologies

2) Sports

Use of advantages:

- High strength-to-weight ratio
- High elastic limits
- High energy transfer efficiency

time 17s 81s 12s

Bouncing Ball Demonstration

Pieces from LiquidMetal Technologies

3) Biomedicine tools

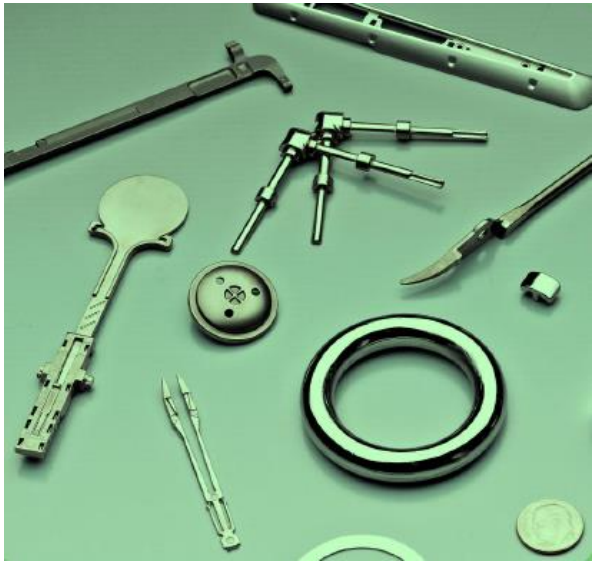

Zr-based metallic glass surgical tools

scalpel

Commercial products of BMGs-*LiquidMetal Technologies*

- Superior corrosion resistance
- Excellent wear resistance
- High hardness

4) Springs for engineering applications

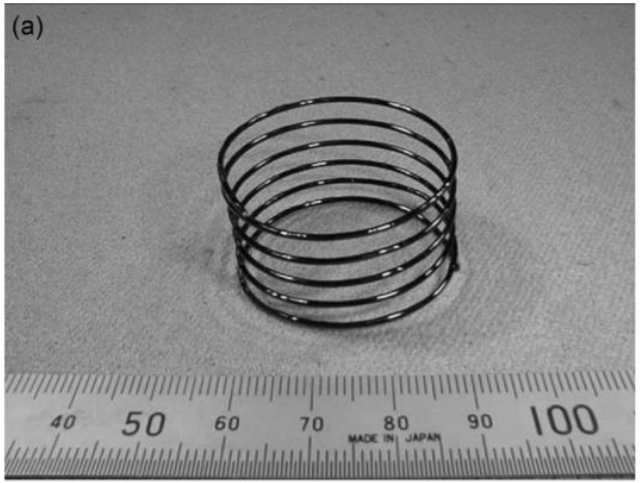

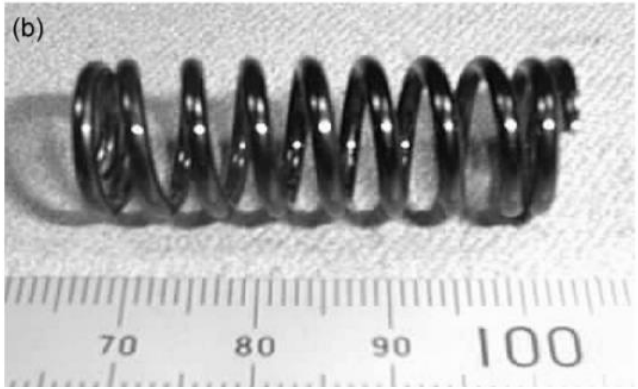

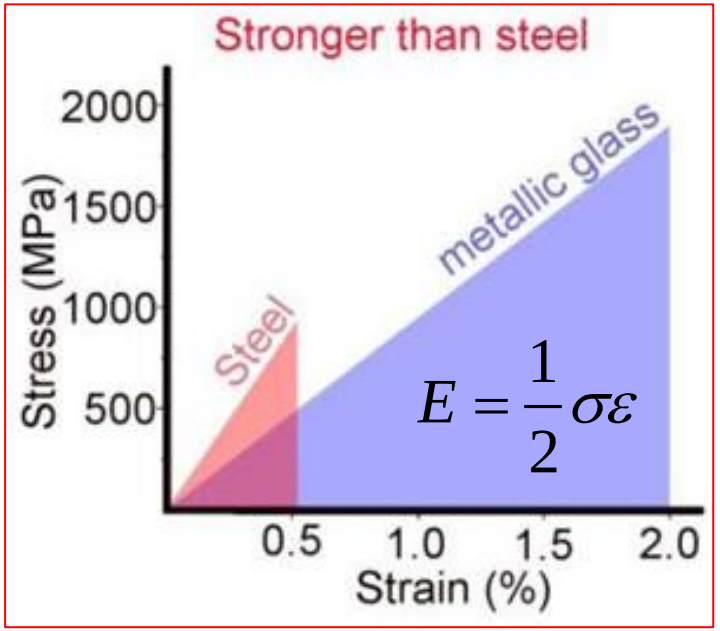

- High elastic energy storage
- High elastic limit

Ashby M F, Greer A L. Scripta Materialia, 2006, 54(3): 321-326.

5) Potential Sensors for industrial products

Examples

(1) Coriolis mass flowmeters
(2) Pressure sensors
(3) Strain gauges

Use of advantages:

- High elastic limits
- Low young's modulus
- High strength

Lower signal-to-noise ratio and higher sensitivity

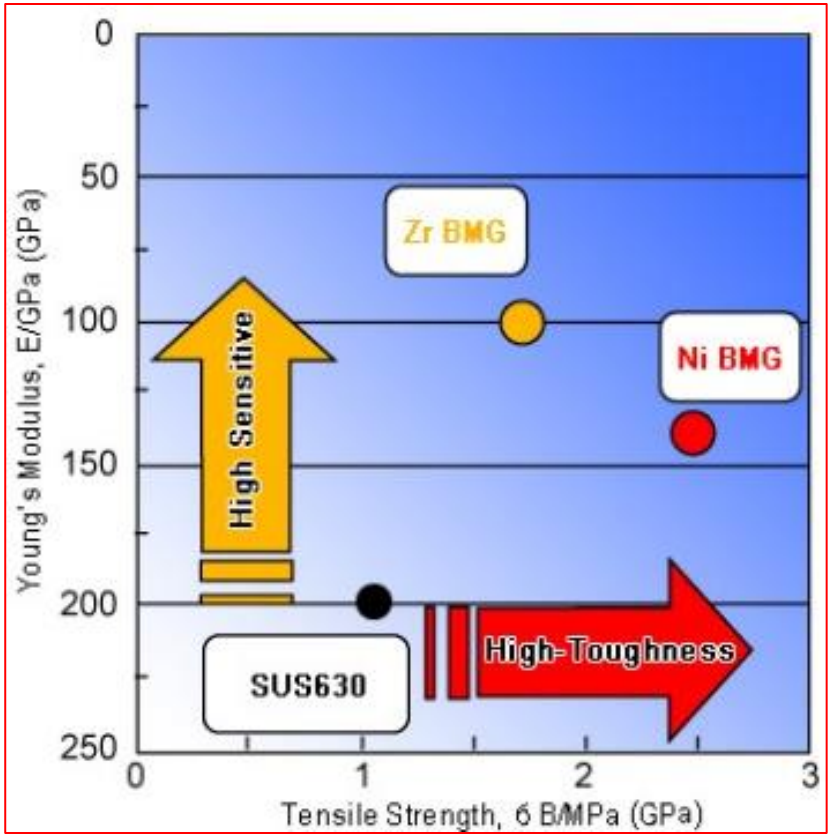

(1) Coriolis mass flowmeter (CMF)

Ma C, et al. Materials Science and Engineering: A, 2005, 407(1): 201-206.

Coriolis mass flowmeter (CMF) is known to be a unique flowmeter that can be used to directly measure the mass of fluid.

Sensitivity of Coriolis mass flowmeter $\delta_{\max} = \dfrac{4F_c l^3}{3\pi E(d_2^4 - d_1^4)}$

The equation indicates that δ_{max} is inversely proportional to Young's modulus, which means that a higher sensitivity can be obtained by using a sensor tube with a lower Young's modulus.

Ti-based glassy tubes have been applied to a CMF, and the prototype of the flowmeter exhibits 28.5 times higher sensitivity than that of the conventional one made of SUS630.

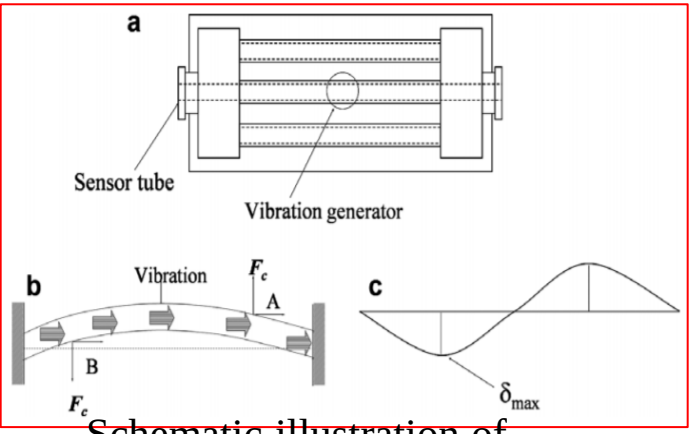

Schematic illustration of Coriolis mass flowmeter

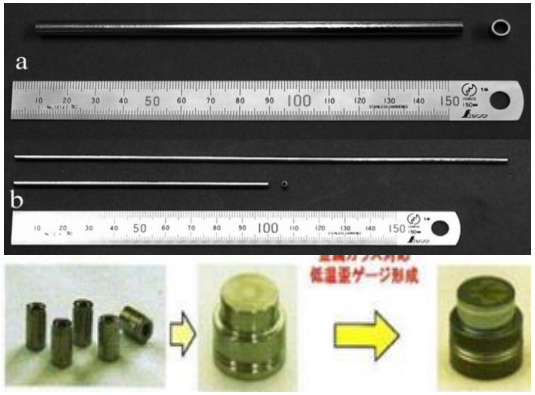

Ti-based alloy tube prepared by suction casting.

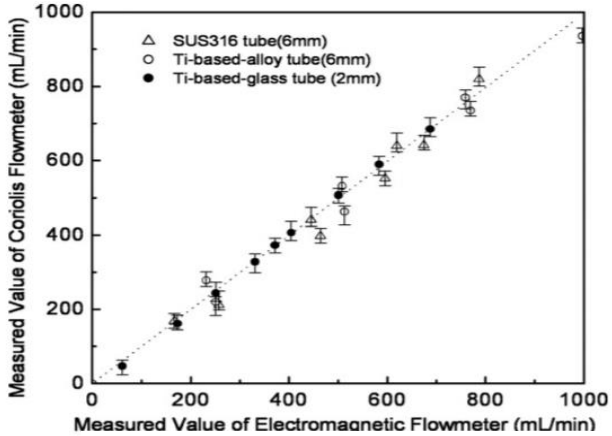

Comparison of sensitivity

(2) Pressure sensors

Nishiyama N, et al. Materials Science and Engineering: A, 2007, 449: 79-83.

$Zr_{55}Al_{10}Ni_5Cu_{30}$ glassy diaphragms are applied in pressure sensors. The prototype of pressure sensor with a Zr-based glassy diaphragm exhibits 3.8 times higher sensitivity than that of the sensor with the conventional SUS630 diaphragm.

Sensitivity of pressure sensor: $\varepsilon = \alpha \frac{Pa^2}{Et^2}$

where *a*, *P*, *a*, *E* and *t* are a constant, the applied pressure, the effective diameter of the diaphragm, Young's modulus, and the thickness of the diaphragm, respectively.

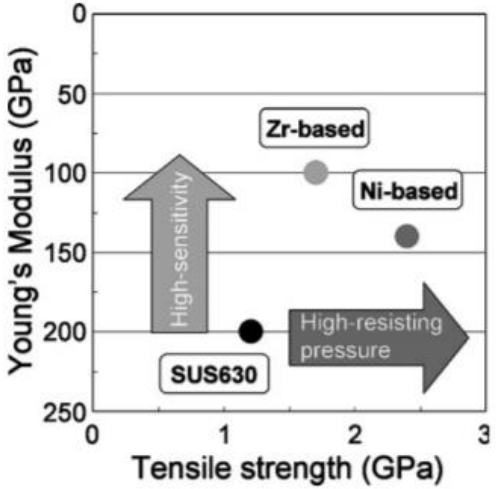

the advantage of MGs

Glassy diaphragms with deposited strain gauge.

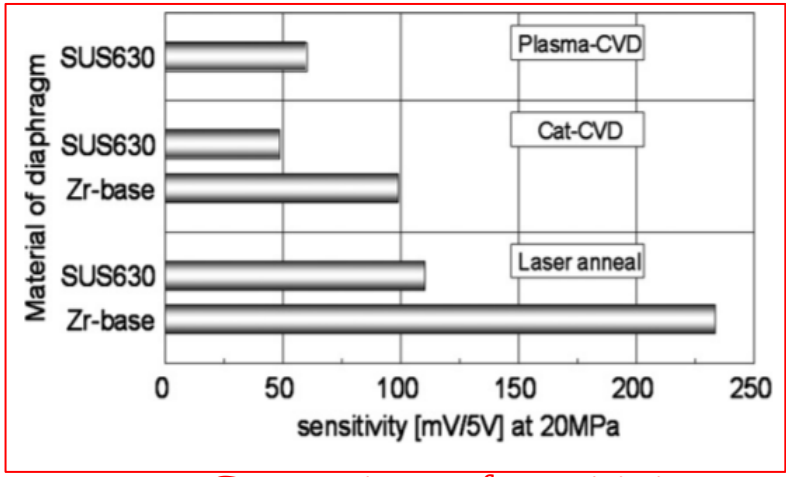

Comparison of sensitivity

(3) Electrical resistance strain gauges

Yi J, Huo L S, Zhao D Q, et al. SCIENCE CHINA Physics, Mechanics & Astronomy, 2012, 55(4): 609-613.

Electrical resistance strain gauges (SGs) are basic units many electromechanical transducers including load cells, pressure transducers, torque meters, accelerometers, force cells, displacement transducers and so forth.

Sensitivity of strain gauges: $\varepsilon = F/EA$

The strain limit of the metallic glass SG is 2.16%, which is remarkably high compared with that of the conventional foil SGs (0.26%~0.5%)

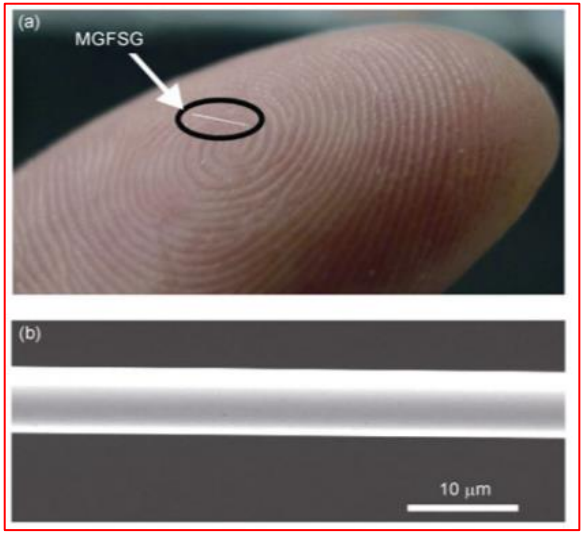

Morphology of the MGFSG.

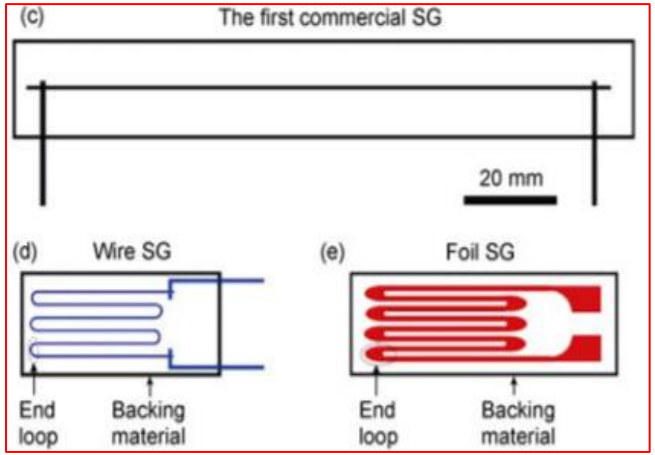

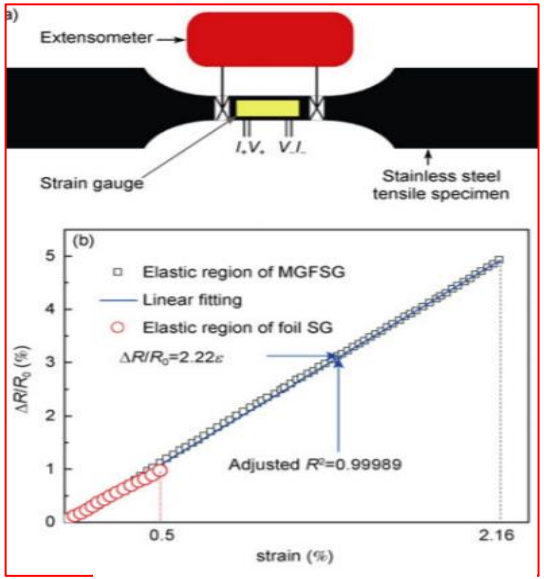

Performance properties of the MGFSG.

5. Thermal-plastic formability of metallic glasses and their applications

5. Thermal-plastic formability of metallic glasses and their applications

Introduction

In comparison with crystalline metals, the existence of a supercooled liquid region (SCLR) in metallic glasses is one of the most unique properties and is a consequence of their strong resistance to crystallization.

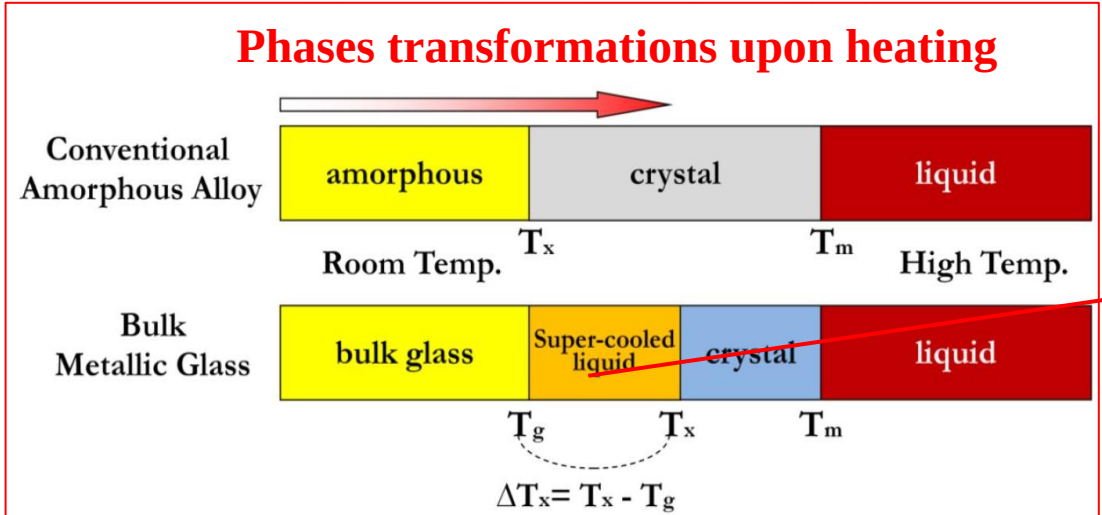

Fig. 2.3. A schematic diagram which illustrates the difference between convention amorphous alloys and bulk metallic glasses.

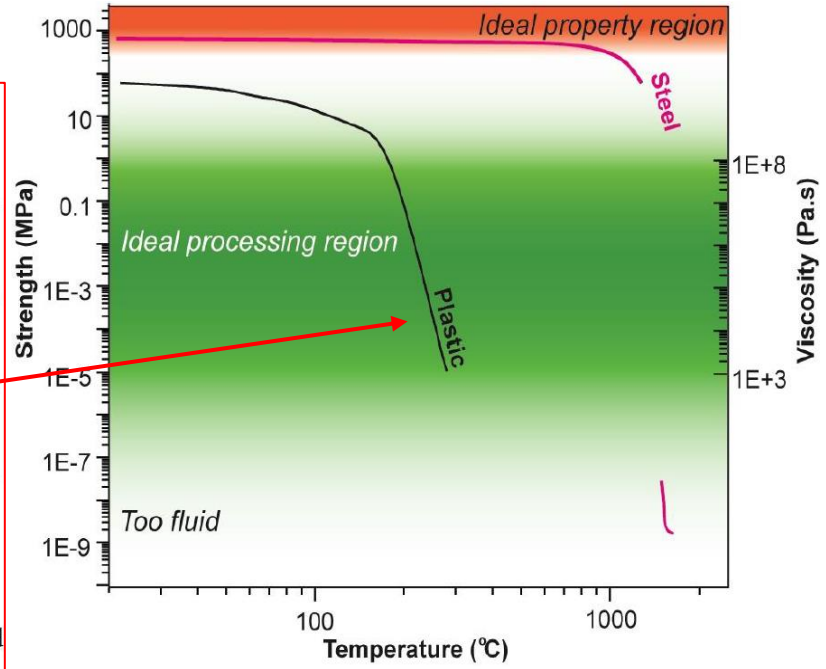

Schroers J. Advanced Materials, 2010, 22(14): 1566-1597.

5.1 Applied physics for processing metallic glasses

Amorphous metals exhibit unique softening behavior above their glass transition and this softening has been increasingly explored for thermoplastic forming of metallic glasses. It has been shown that metallic glasses can be patterned on extremely small length scales ranging from 10 nm to several millimeters.

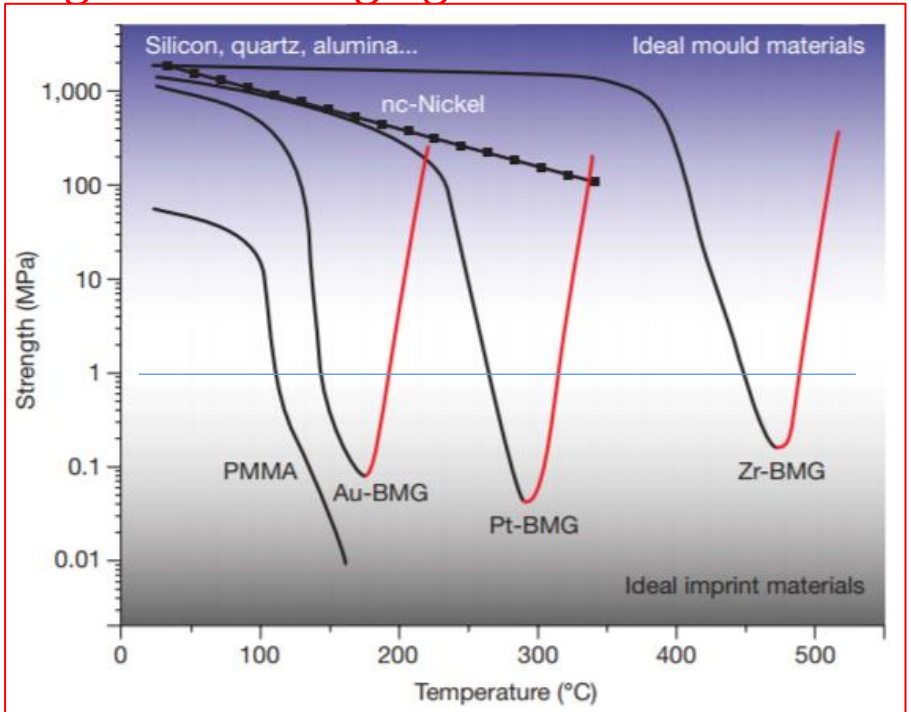

The materials are as strong and hard as cutting edge steels at room temperature, while with the ability to be re-formed like a plastic at in the SCLR (300~450℃).

Processing temperature:

PMMA(polymer) :	210-270 ℃
Al-MGs:	~270 ℃
Pt-MGs	~310 ℃
Zr-MGs:	~420 ℃
Silicate glass:	>850 ℃

5.2. Super-plasticity in the supercooled liquid region (SCLR)

$Zr_{55}Cu_{35}Al_{10}Ni_5$ metallic glass (Tg=410 ℃, Tx=494 ℃):

- A processing temperature around 430 ℃
- Thermal stability in the SCLR for 60 ~ 300 s
- A viscosity of 10^2 ~ 10^3 Pa-s

The superplastic deformation process of a Zr-based metallic glasses in the SCLR, displaying a maximum plastic strain ~1000% under tension.

Kawamura Y, et al. Scripta Materialia, 1997, 37(4): 431-436.

Blow molding of metallic glasses

5.3. Nanomoulding/imprinting for MEMS components

Khan M M, et al.Critical Reviews in Solid State and Materials Sciences. 2017: 1-36.

Principles:

Metallic glasses are heated to the supercooled liquid region (SCLR)

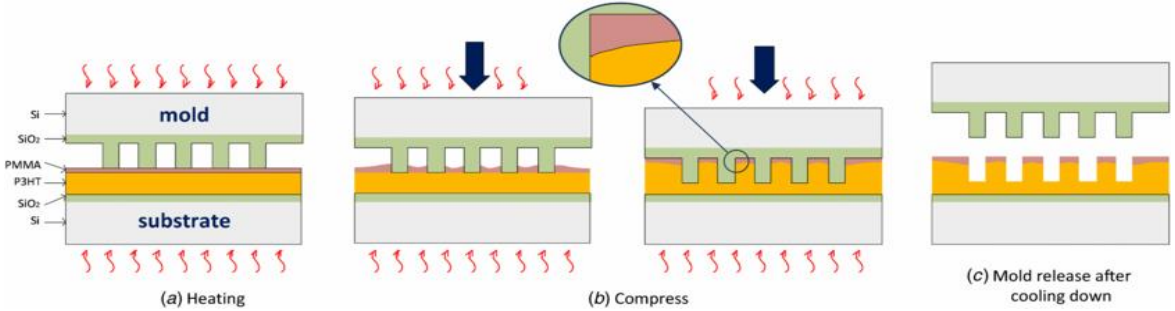

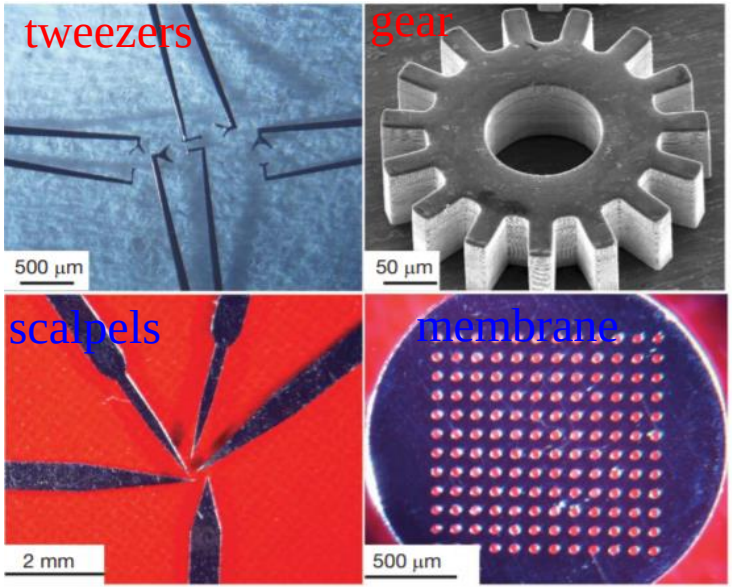

Microparts which were fabricated by hot embossing MG on an etched silicon wafer.

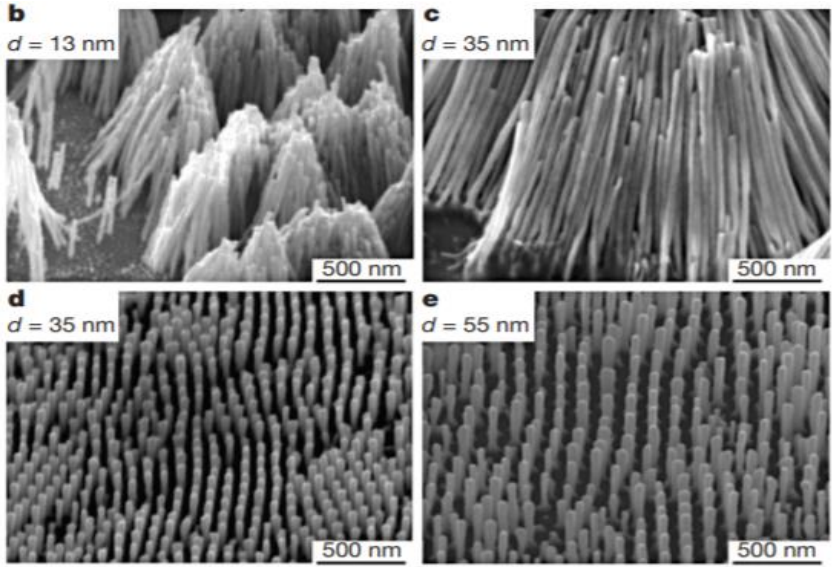

| Controlling the metallic glass molding on scales smaller than 100 nm.

5.3. Nanoimprint of gratings

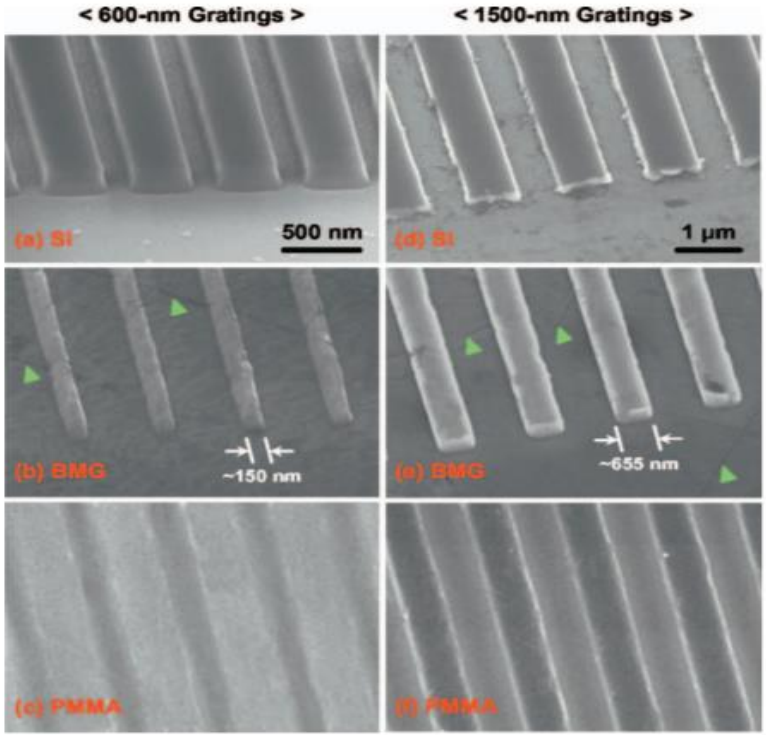

Metallic glass is a suitable material not only for imprinting nanostructured parts such as gratings, but also as a good die material for nanoimprints of conventional PMMA.

Chu J P, et al.. Applied physics letters, 2007, 90(3): 034101.

Nanoimprint of low reflectance surface

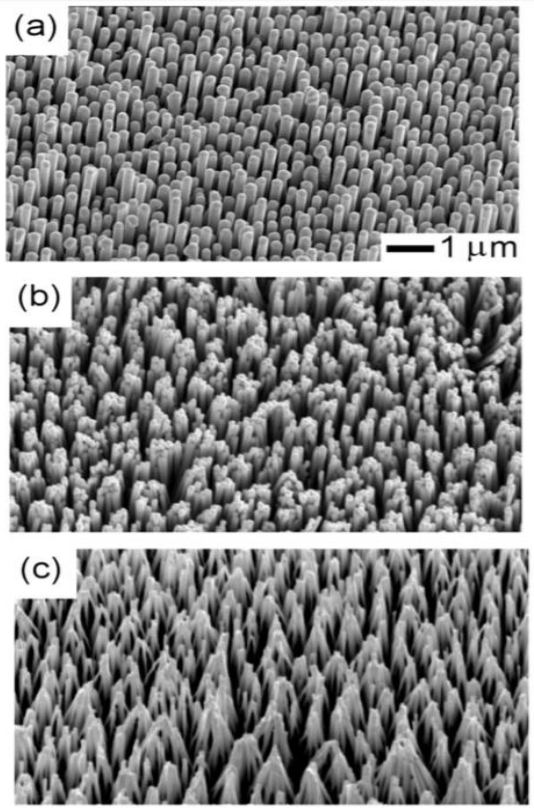

Nano-patterned Pt-MG

Diffuse reflectance is as low as 1.6%

Yanagishita T, et al. Applied physics express, 2009, 2(2): 022001.

Other examples

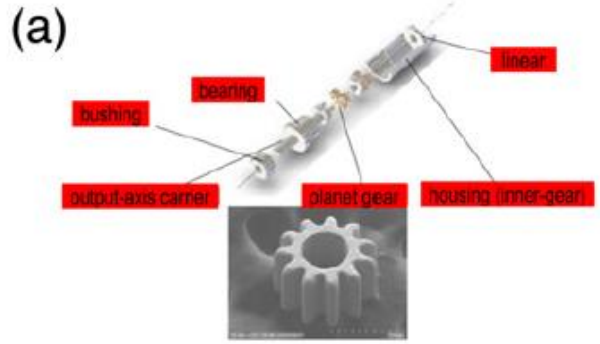

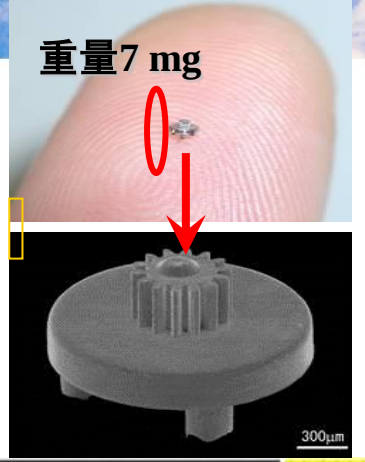

A promising material for micro-devices and micro-manufacture.

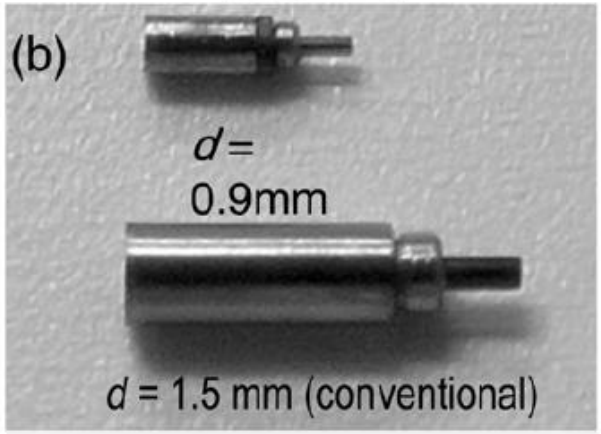

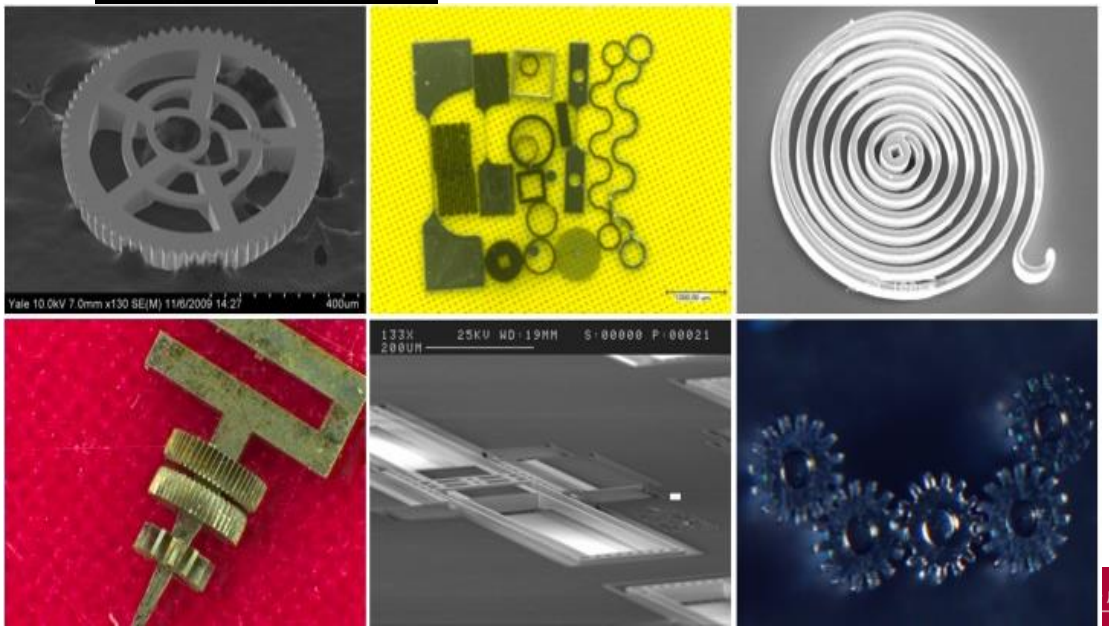

World's smallest geared-motors with d = 0.9 mm successfully constructed with metallic glass gears.

5.4. Nanoimprinting of surface with hydrophobicity and self-cleaning functions

Due to excellent thermoplastic formability in supercooled liquid region, metallic glasses can be easily fabricated with micro-nano scale hierarchical structured surfaces, which demonstrate super-hydrophobic feature, superior mechanical stability and corrosion resistance.

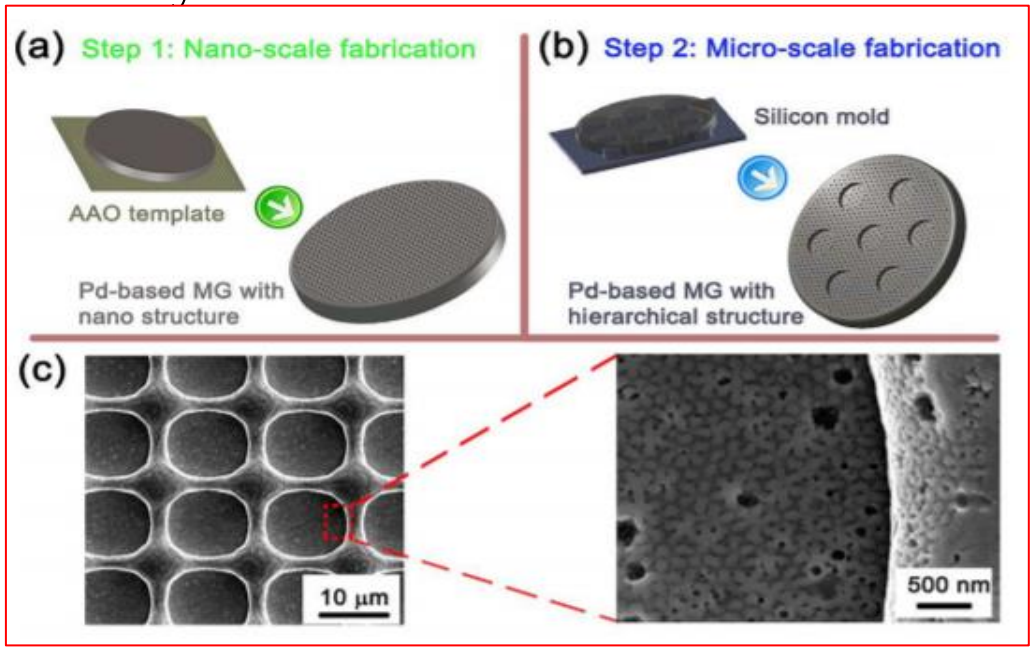

Schematic diagram of the fabrication of super-hydrophobic Pd-based metallic glass surface.

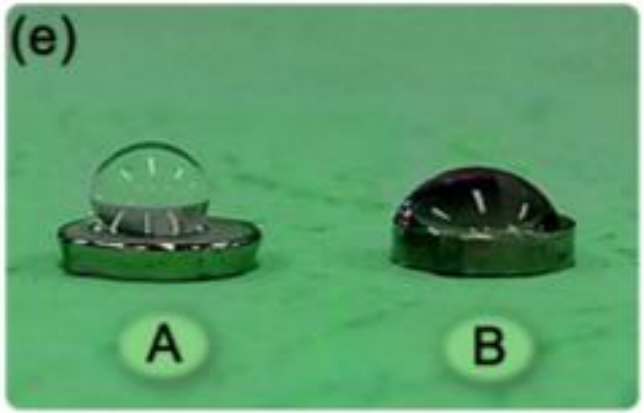

The photographs of water droplets on the two different surfaces, A: the micro-nano hierarchical surface and B: the polished one.

Ma J,, et al. Applied Physics Letters, 2014, 104(17): 173701

6. Applications in catalysis

6. Applications in catalysis

Introduction

Catalysis is the increase in the rate of a chemical reaction due to the participation of an additional substance called a catalyst, which is not consumed in the catalyzed reaction and can continue to act repeatedly.

Metallic glasses are indeed both catalytically active and unique selective!

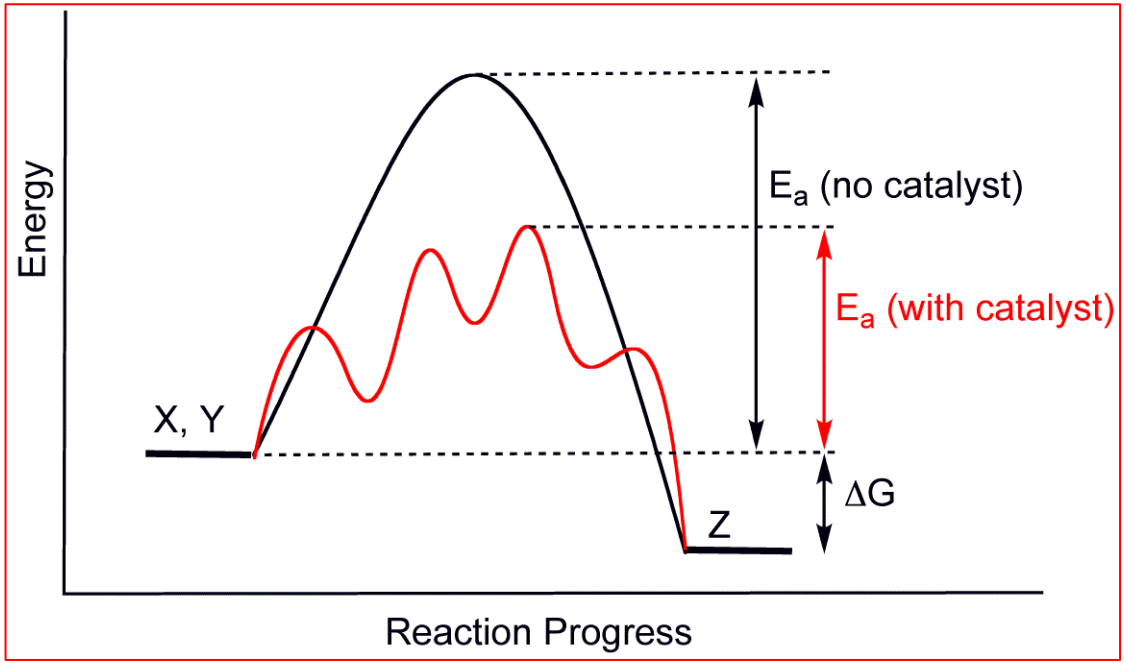

Brower et al., Nature, 2010, 301, 497-499

Case 1: MGs are active catalysts for Electrochemical Hydrogen Generation

Objectives of electrocatalysts: high efficiency, highly active and durable

Although conventional platinum (Pt)-based materials are found to be the most efficient for commercial electrocatalysts, the high cost and scarcity of Pt seriously impede its widespread applications.

$Pd_{40}Ni_{10}Cu_{30}P_{20}$ MG catalyst not only exhibits excellent electrocatalytic activity but also possesses unique self-stabilizing catalytic performance over a long-cycling life.

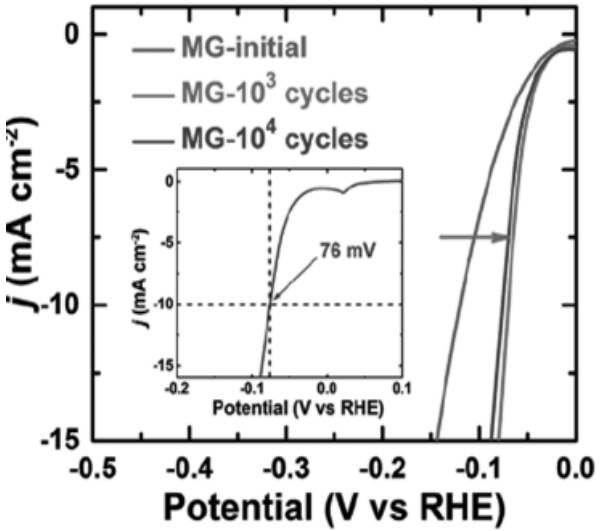

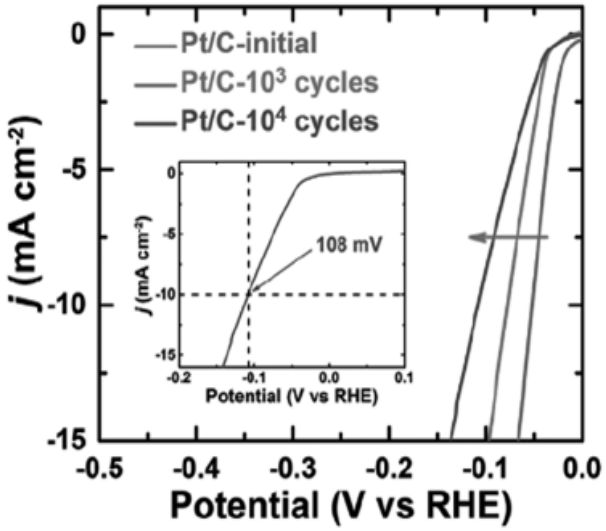

After 10 000 CV cycles, like other **crystalline catalysts**, the electrocatalytic activity of Pt/C **degrades**; in sharp contrast, that of the **MG exhibits an opposite trend**.

Hu et al. Adv. Mater. 2016, 28, 10293 – 10297

Case 1:

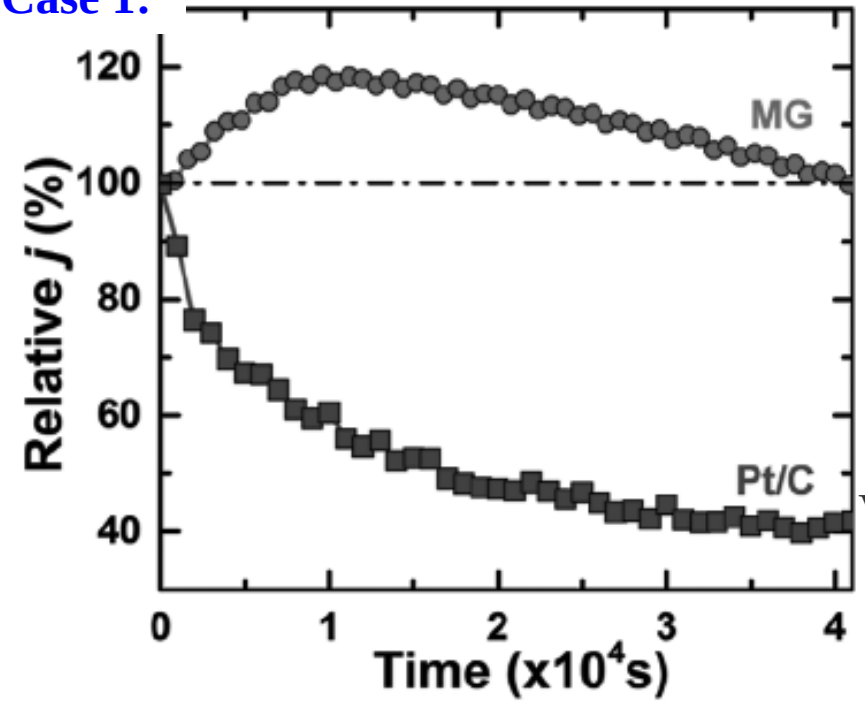

The efficiency of $Pd_{40}Ni_{10}Cu_{30}P_{20}$ MG catalyst **still retains 100%** after 40 000 s. While, the efficiency of **Pt/C** degrades seriously and **remains only 40%** of the initial value after 40 000 s.

Variations of efficiency versus time

The outstanding performance of the MG catalyst for HER can be attributed to the intrinsic chemical heterogeneity on the multi-compositional disordered surface which provides abundant types of active site and the selective dealloying of **Ni** element.

Case 2: $Fe_{72}Si_2B_{20}Nb_6$ metallic glass catalyst for methylene blue degradation

Catalysis has greatly enhanced removal of toxic pollutant combinations in effluents, such as dyes , heavy metals , phenols and nitrates.

- Porous surface structures were introduced to Fe-based ribbons.
- Porous surface structures improve azo-dye degradation efficiency.
- High porosity contributes to the catalytic activity improvement.

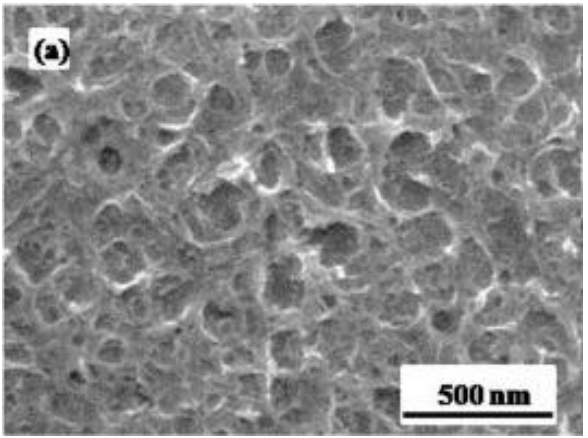

The surface morphology of ribbo
after etching treatment

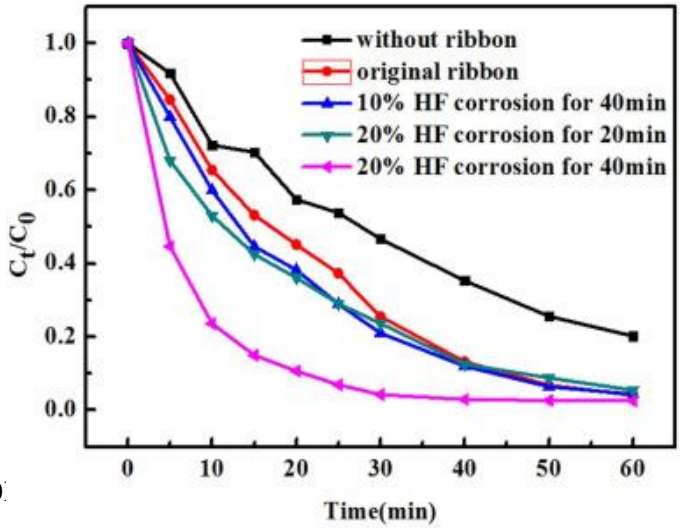

The degradation rate

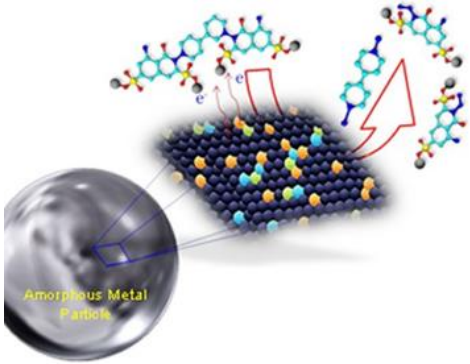

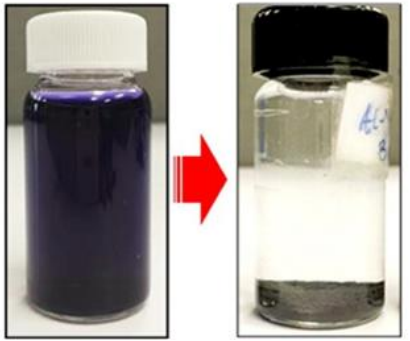

Z. Deng et al. Chemosphere 174 (2017) 76-81

Case 3: Synthesis of Nanoporous CuO network for oxidative degradation of methylene blue using dealloyed $Cu_{60}Zr_{35}Al_5$ glassy ribbon

glassy ribbon

Dealloying process

CuO nanostructures

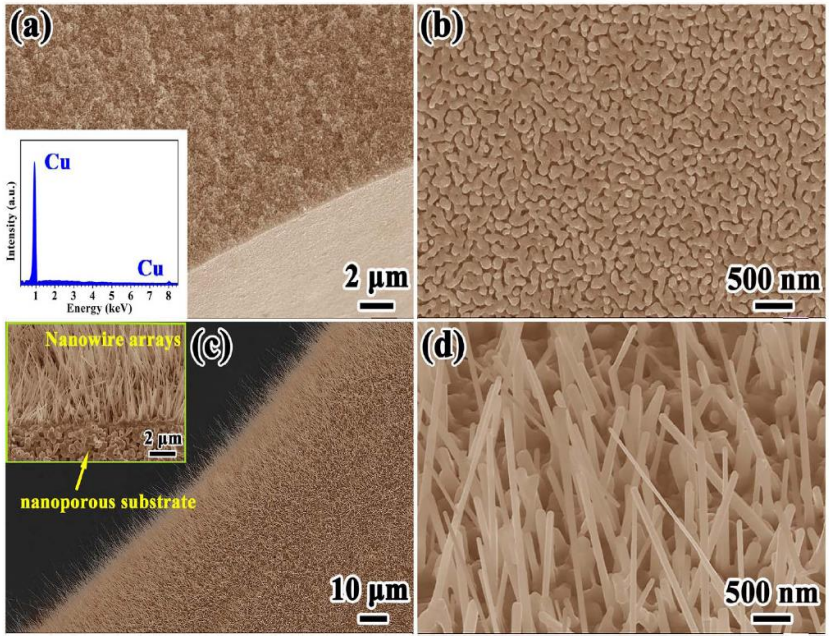

(a) Cross-sectional morphology of the dealloyed nanoporous Cu.
(b) Surface morphology of the nanoporous Cu.
(c) Overall SEM image of the freestanding CuO nanocomposite.
(d) Surface morphology of the as-prepared CuO nanocomposite.

Li et al. Corrosion Science 126 (2017) 37–43

Case 3

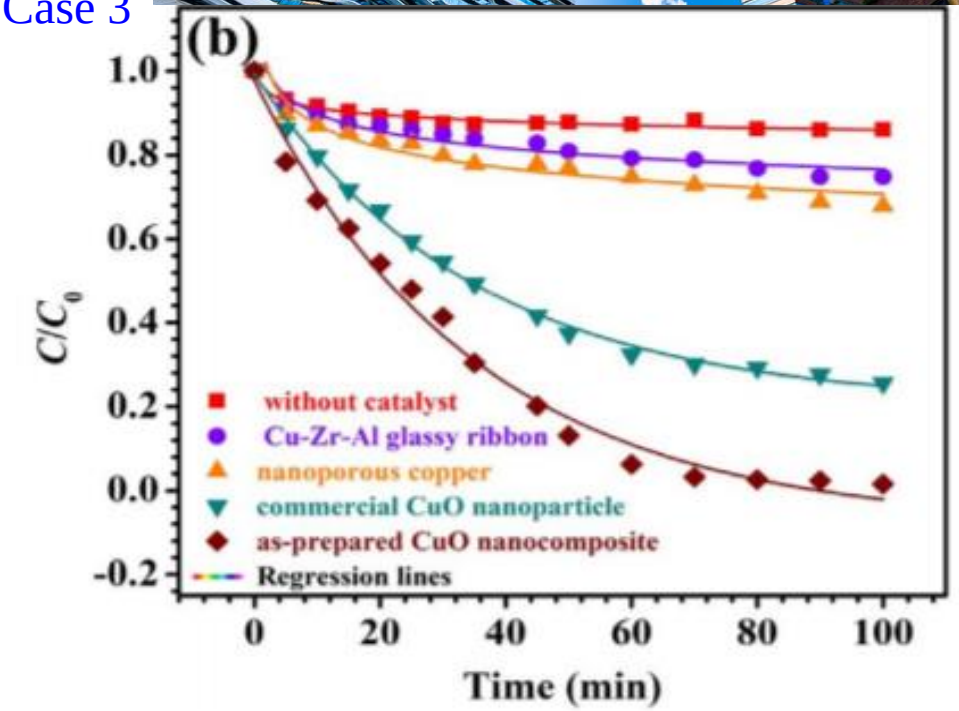

The normalized concentration of MB solution as function of reaction time in the presence of different catalysts at room temperature.

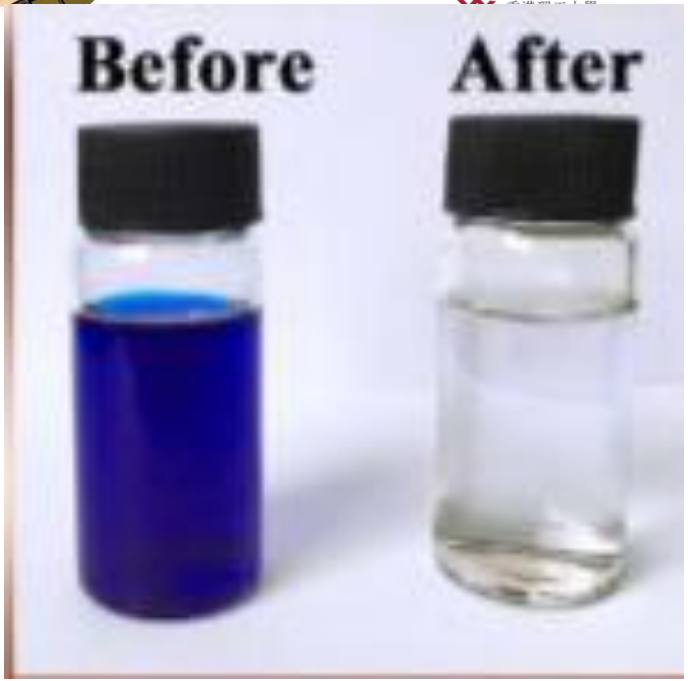

Appearance and color of the MB solution before and after the degradation treatment.

The as-synthesized monolithic hierarchical CuO nanocomposite exhibits superior oxidative degradation performance!

7. Applications in biomedicine

7.1. Biomedicine applications as biodegradable implants

Biodegradable Mg-, Ca- and Zn-MG are emerging as a new class of materials that can be used for wide range of applications where temporary implants are required.

Mg-based MG for biodegradable implants

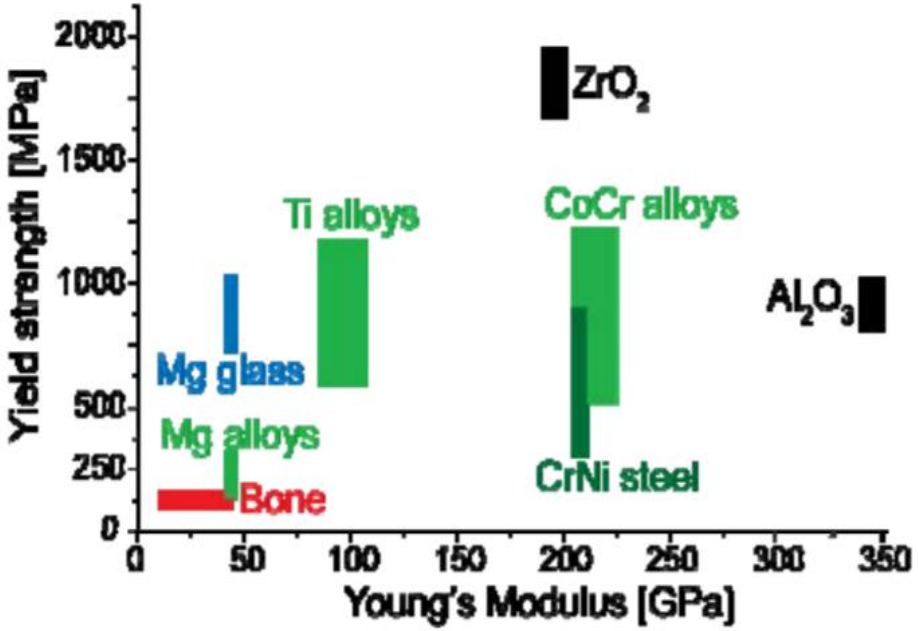

Advantages of Mg-based MG

- Young's modulus similar to bone
- Tailorable corrosion resistance via mirror alloying (no "phase-diagram limitations" in crystalline alloys)
- High biocompatibility
- Minimal or no degradation-induced H_2 formation ($Mg+2H_2O \rightarrow Mg(OH)_2+ H_2$)
- High strength (1-2 times higher than their crystalline counterparts)

In-vivo animal studies

Implantation of Mg-based MG in two tissues of domestic pigs.

- Mg-based MG do not show any in-vivo hydrogen evolution.
- Mg-based MG show better tissue healing reactions.

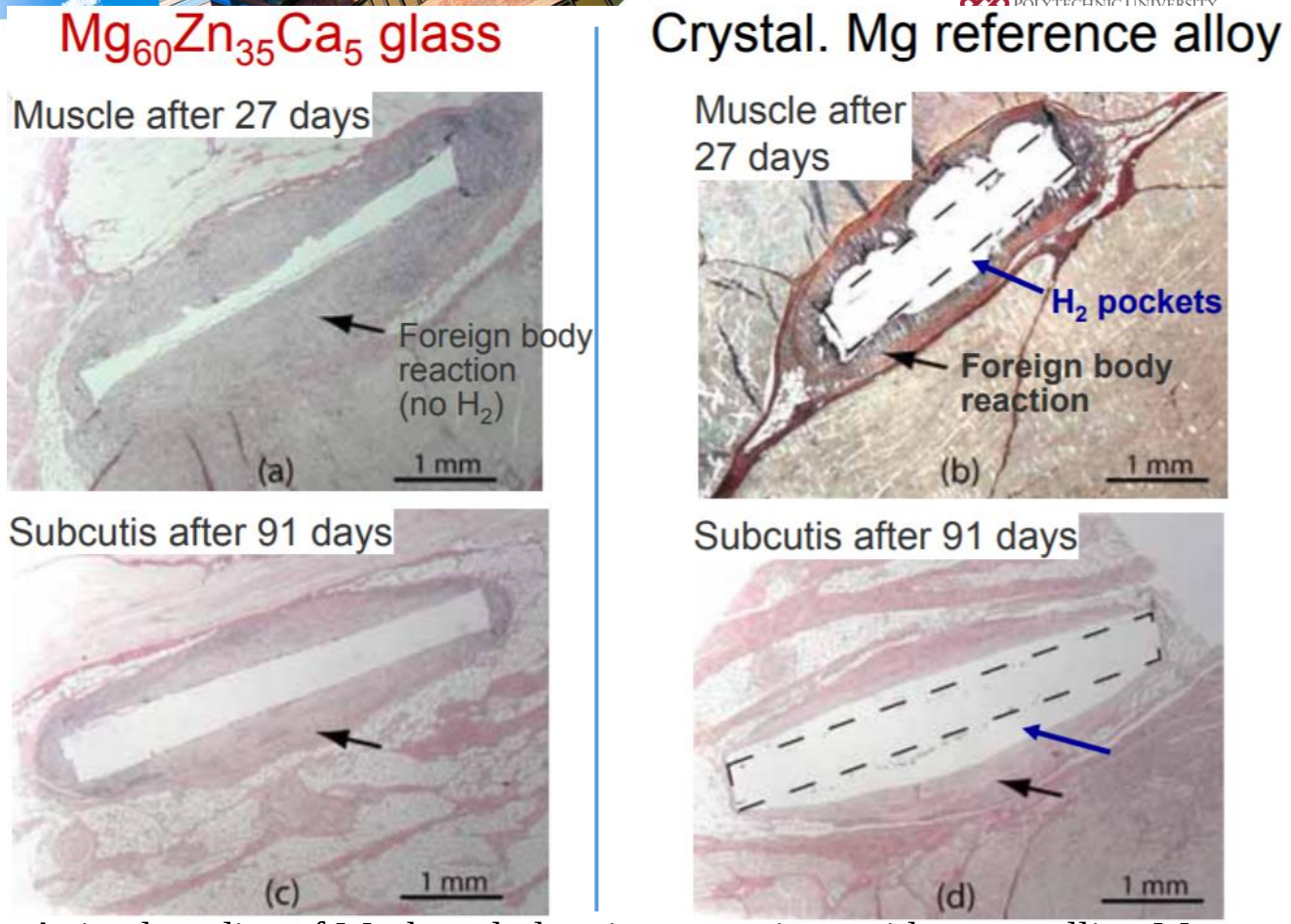

Animal studies of Mg-based glass in comparison with a crystalline Mg alloy reference sample.

8. Magnetic Properties and their applications

8. Magnetic Properties and their applications

Introduction

Since the first amorphous ferromagnetic alloy, $Fe_{80}P_{13}C_7$, was found by ***Duwez*** at Cal Tech in 1967, i.e., soon after the discovery of metallic glass, the magnetic properties among various compositions were exploited.

Magnetic-correlated properties in metallic glasses：

- Soft and hard magnetic properties (軟磁和硬磁性能)
- Magnetostriction (磁致伸縮效應)
- Magnetic refrigeration(磁制冷)

.

Type of ferromagnetic materials

Two categories:

a) Soft magnetic materials

- i.e., Fe: easily magnetized

If the external filed is removed, magnetism disappears

Criterion: H_c < 10A/m

Application: Transformers, motor cores

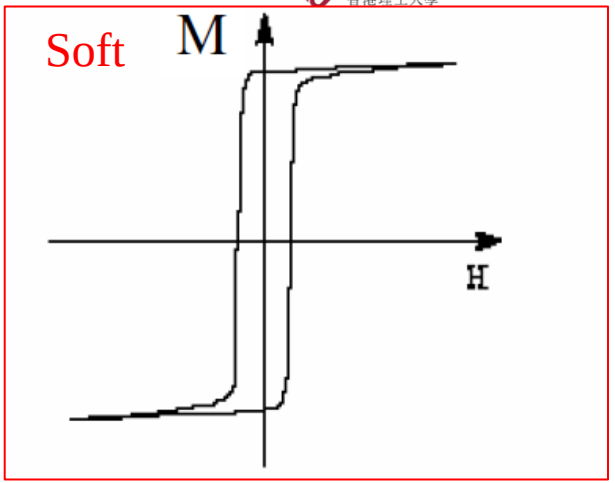

b) Hard magnetic materials

- i.e., Co and Ni : difficult to magnetize

If the external filed is removed, magnetism tend to be retained

Criterion: H_c > 100 A/m

Application: permanent magnets, memory devices and magnetic recording

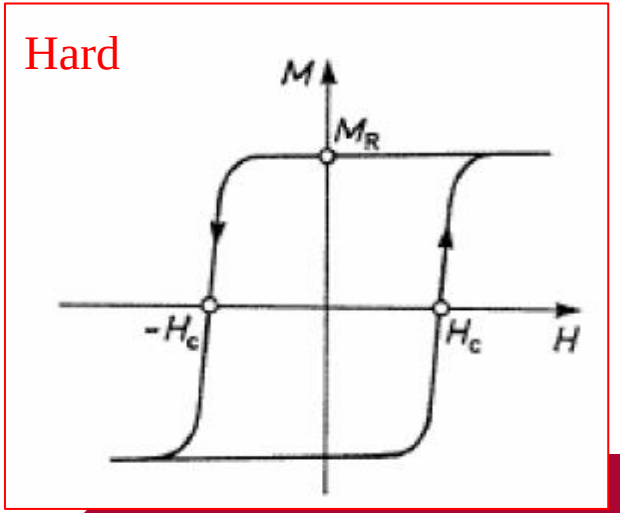

8.1. Soft Magnetic amorphous Alloys

Discovery history

Ferrous alloy systems – Soft Magnetic properties	Year
Fe–(Al,Ga)–(P,C,B,Si,Ge)	1995
Fe–(Nb-Mo)–(Al,Ga)–(P,B,Si)	1995
Co–(Al,Ga)–(P,B,Si)	1996
Fe–(Zr,Hf,Nb)–B	1996
Co–(Zr,Hf,Nb)–B	1996
Ni–(Zr,Hf,Nb)–B	1996
Fe–Co–Ln–B	1998
Fe–(Nb,Cr,Mo)–(C,B)	1999
Fe–(Cr,Mo,Ga)–(P,C,B)	1999
Co–Ta–B	1999
Fe–Ga–(P,B)	2000
Ni–Zr–Ti–Sn–Si	2001
Fe–Cr–Mo–(Y,Ln)–C–B	2004
Fe–Cr–Co–Mo–Mn–C–B–Y	2004
(Fe,Co)– B–Si–Nb	2006

Fe-, Ni-, and Co-based

List of metallic glasses displaying soft magnetic properties.

In comparison with traditional crystalline soft magnetic alloys, metallic glasses with crystalline soft magnetic property exhibit the following features:

- High saturation magnetization
- Low coercivity
- Narrow hysteresis loop
- High electrical resistivity and lower core loss

Soft magnetic properties have been exploited for applications in different fields such as cores, **transformers**, cantilevers, and sensors.

Transformers using amorphous alloy

Fe-Ni-P-B was the first metallic glassy ribbon exploited commercially for use in transformer cores due to its soft magnetic property and high electrical resistance, leading to low-core losses. With an amorphous core, this can be 70~80% lower than with traditional used crystalline silicon steels and Simple Payback ~ 2.5 Years!

Soft magnetic materials:

- High saturation magnetization
- Low coercivity
- High electrical resistivity

amorphous transformer core

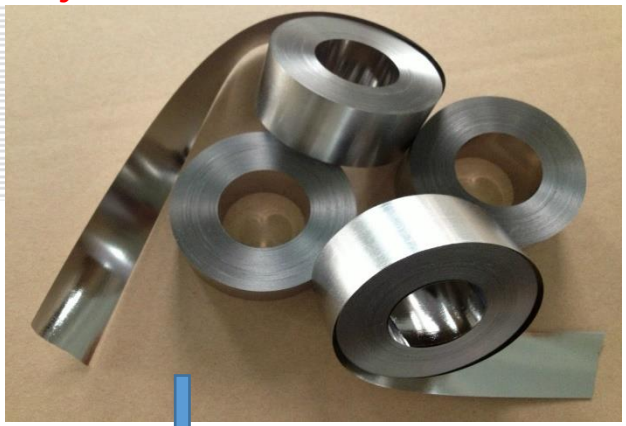

Thickness

Thickness 25μm

(1/10 of conventional materials)

Ribbon thickness is 1/10 of Silicon Steel's
[Silicon Steel:0.23mm, Amorphous Alloy:0.025mm]

100 thousand tons of Fe-based amorphous alloys for transformers in China last year.

Transformers using amorphous alloy

Material Characteristics Comparison

Higher electrical resistance, almost triple of Silicon steel's

[Silicon Steel:50 $\mu\Omega$-cm,

Amorphous Alloy:130 $\mu\Omega$-cm]

Material	Saturation flux density (T)	Electrical resistance ($\mu\Omega$-cm)	Iron loss (W/kg) (*1)	Thickness (mm)
Silicon steel(Crystalline)	2.03	50	0.440	0.23
Amorphous Alloy (Non-crystal line)	1.56	130	0.070	0.025

(*1) Estimated; 50Hz, flux density 1.3T

About the loss of transformers

The load loss and no load loss occur at the same time when the transformer is operated, the loss is a useless output chiefly converted into heat.

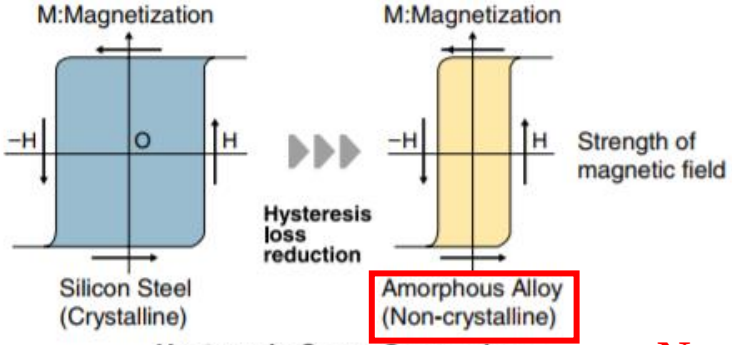

Hysteresis Curve Comparison

Hysteresis loss

By magnetic induction, magnetic domain rotates to have unified direction.

The loss caused by this movement is hysteresis loss.

Eddy current loss

When magnetic flux flows, eddy carrent flows to negate the flux.This eddy current cause loss proportional to the resistance.

Narrower hysteresis loop in metallic glasses profits into lower hysteresis energy losses.

8.2. Hard Magnetic amorphous Alloys

Hard magnetic materials (permanent magnets) retain their magnetism when removed from a magnetic field.

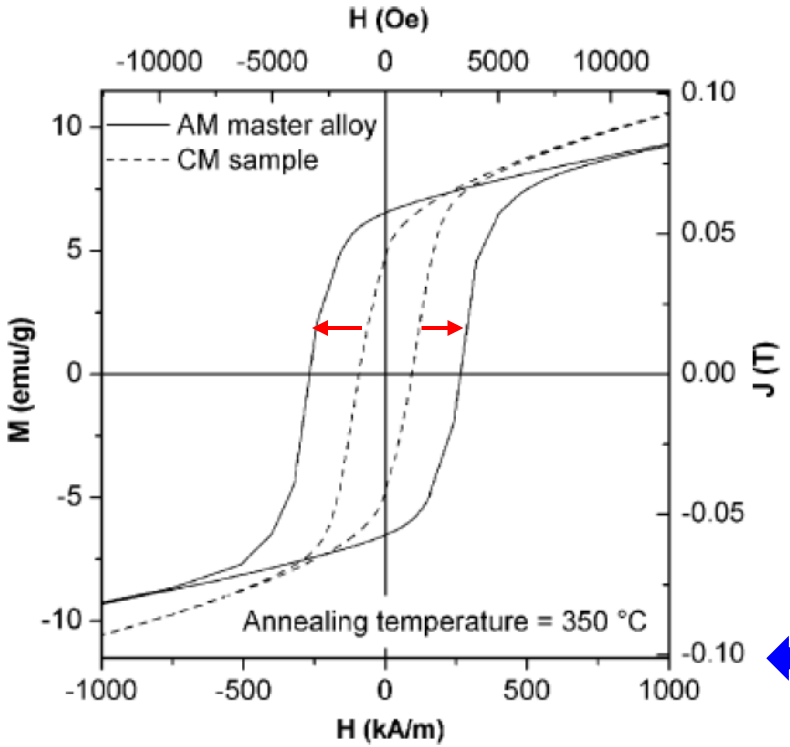

Nd-Fe-Al, Pr-Fe-Al, and Sm-Fe-Al are some of the amorphous systems with decent combination of both appreciable glass forming ability and hard magnetic properties.

Metallic glasses with hard magnetic properties used in potential applications in recording disks, actuators, and permanent magnetic motors, etc, would show a significant reduction in volume and weight and an improved efficiency.

Room temperature hysteresis loops of a $Nd_{70}Fe_{20}Al_{10}$ glassy and crystalline alloy.

E. Olivetti, et al., *J. Magn. Magn. Mater.* **2004**, *272–276*, e1949.

8.3. Magnetostriction

Magnetostriction (Magneto-elasticity), which was discovered in iron by J. P. Joule in 1842, is an intrinsic property of ferromagnetic materials in which their shape or dimensions change under a magnetic field.

Some metallic glasses possess magnetostriction-which expands their scope in the field of sensors, actuators and energy harvesting devices.

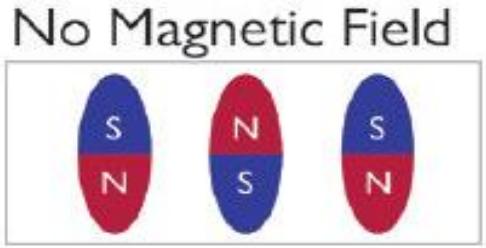

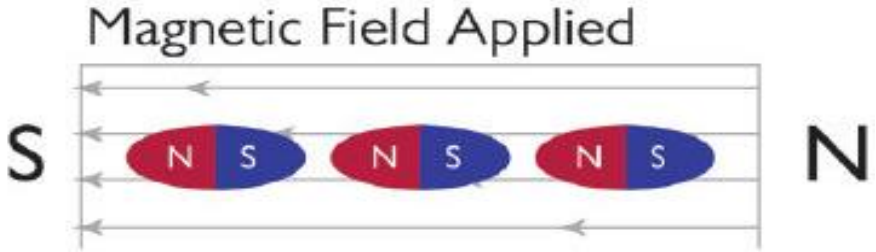

Magnetostrictive materials can convert magnetic energy into kinetic energy, or the reverse.

$Dy_{50}Co_{50}$ amorphous alloy

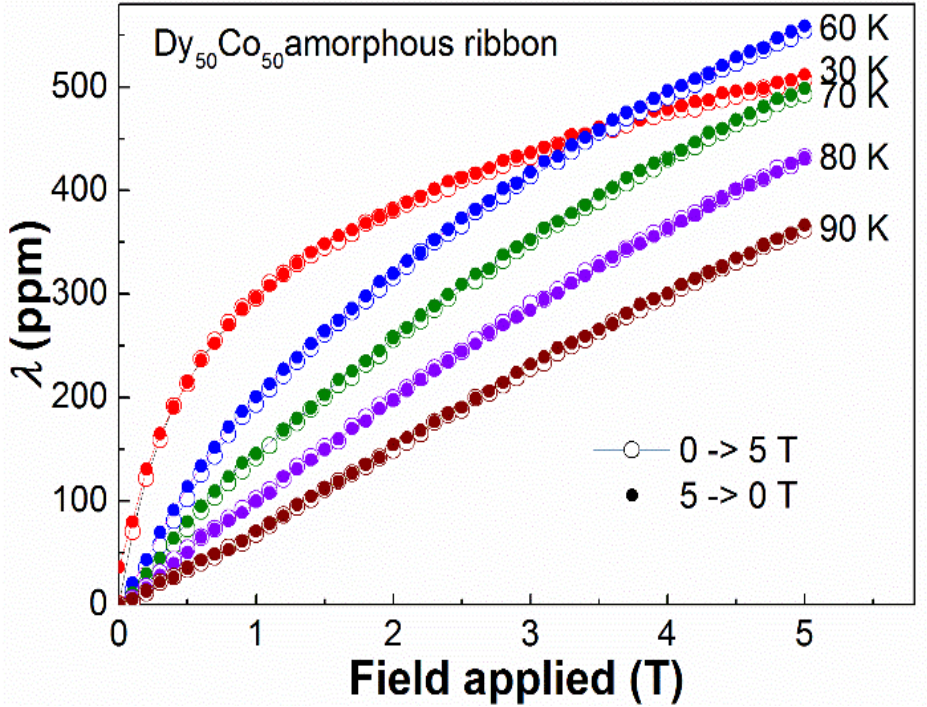

λ-H curves of the $Dy_{50}Co_{50}$ amorphous ribbon measured at 30 K, 60 K, 70 K, 80 K and 90 K from 0 to 5 T, and then from 5 to 0 T.

Metglas 2605SC

Another very common magnetostrictive composite is the amorphous alloy $Fe_{81}Si_{3.5}B_{13.5}C_2$ with its trade name Metglas 2605SC.

- High saturation-magnetostriction constant, λ, of about 20 microstrains.
- A low magnetic-anisotropy field strength (H_A<1kA/m) to reach magnetic saturation.

https://en.wikipedia.org/wiki/Magnetostriction

Application of Magnetostriction in metallic glasses

Case 1: Magnetostrictive $Fe_{70}Nb_5Si_5B_{20}$ metallic glass for force sensors

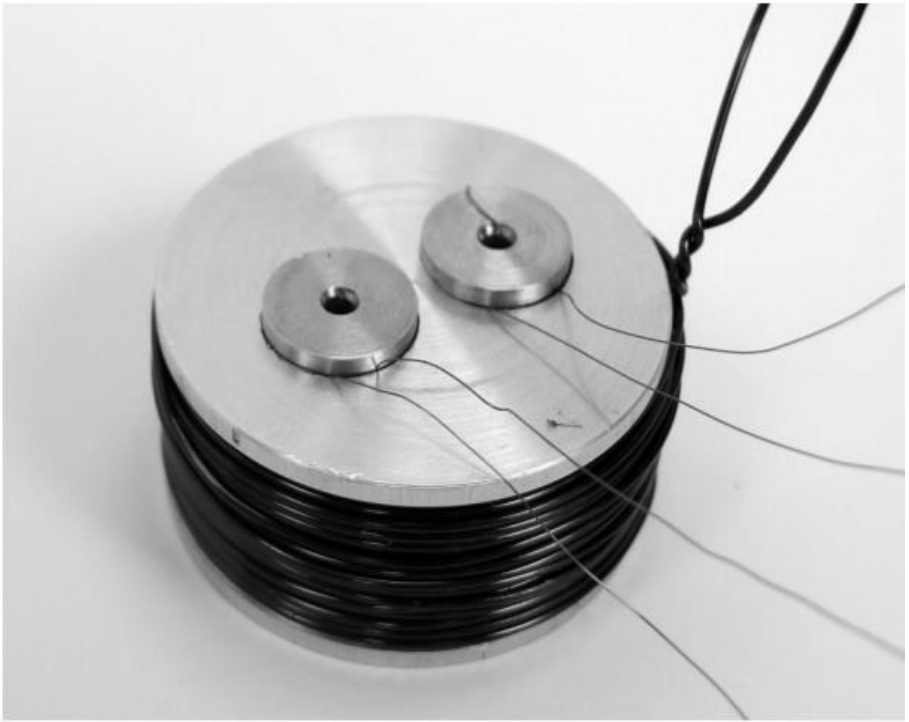

Magnetostrictive $Fe_{70}Nb_5Si_5B_{20}$ metallic glass for force sensors

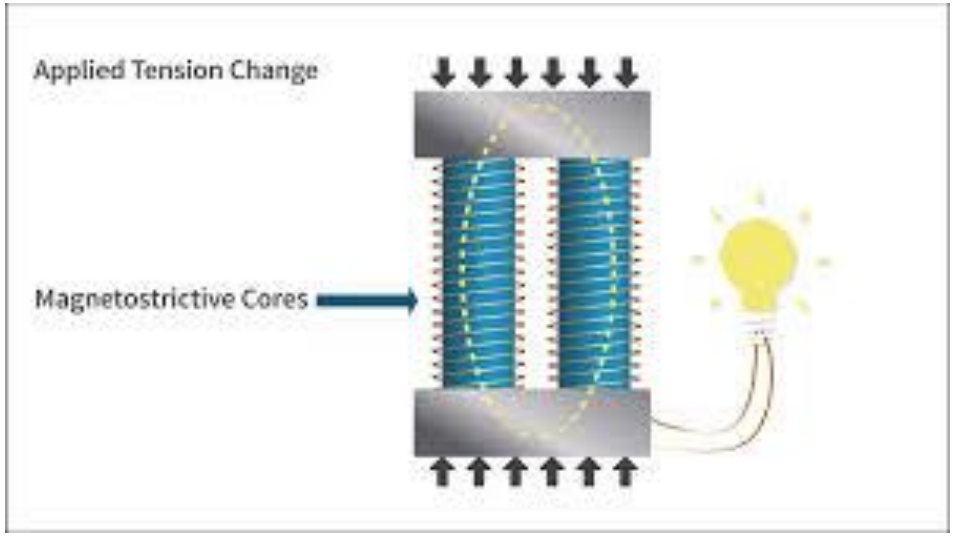

Operating principle of force sensors

Ferenc J, Kowalczyk M, Cieslak G, et al. IEEE Transactions on Magnetics, 2015, 50(4): 1-3.

Application of Magnetostriction in metallic glasses

Case 2: Energy-efficient magnetic MEMS

$Fe_{64}Co_{17}Si_7B_{12}$ has been used as a magnetostrictive material along with a piezoelectric element to fabricate a multiferroic magnetoelectric composite for energy harvesting.

Even a weak electromagnetic signal can deform the metallic glass cantilever because of high magnetostriction value ~ 25×10^{-6}.

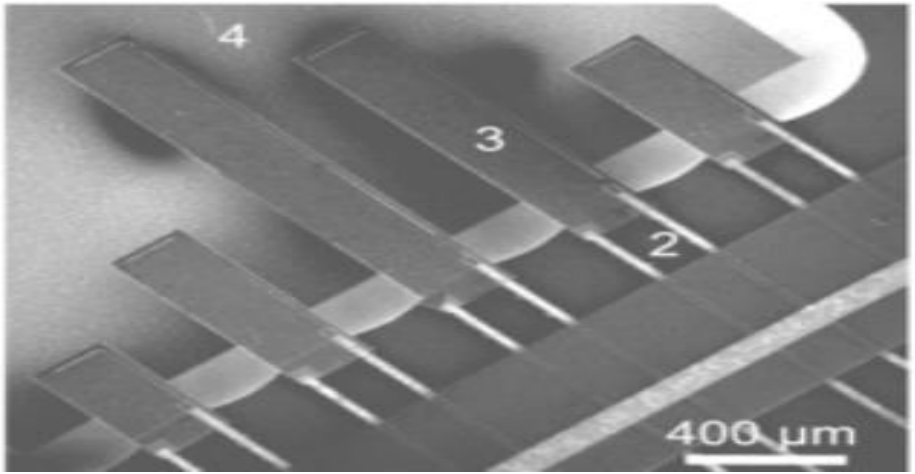

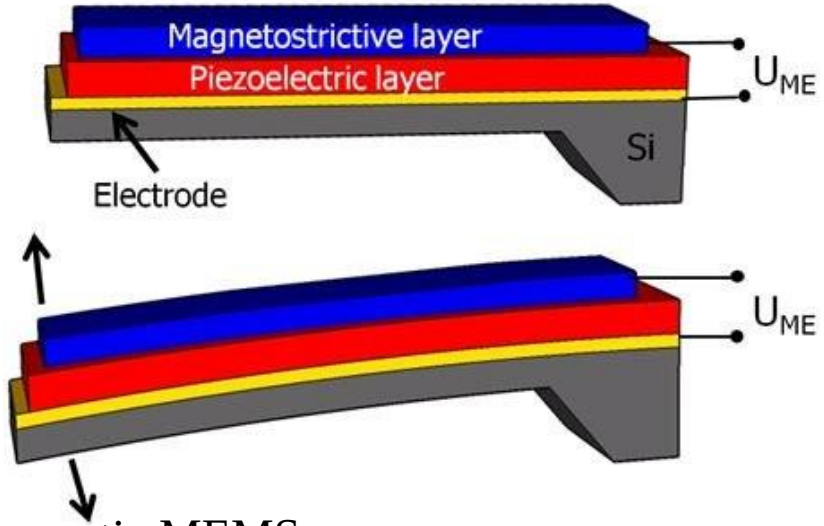

Energy-efficient magnetic MEMS

A. Lasheras, et al., Smart Mater. Struct. 24, 65024 (2015).

8.4. Magneto-caloric effect

Introduction

Magneto-caloric effect (MCE), discovered firstly in iron by Warburg, is the heat production or absorption of a magnetic material under a variation of magnetic field.

A magnetic solid **heats up when magnetized** and **cools down when demagnetized.**

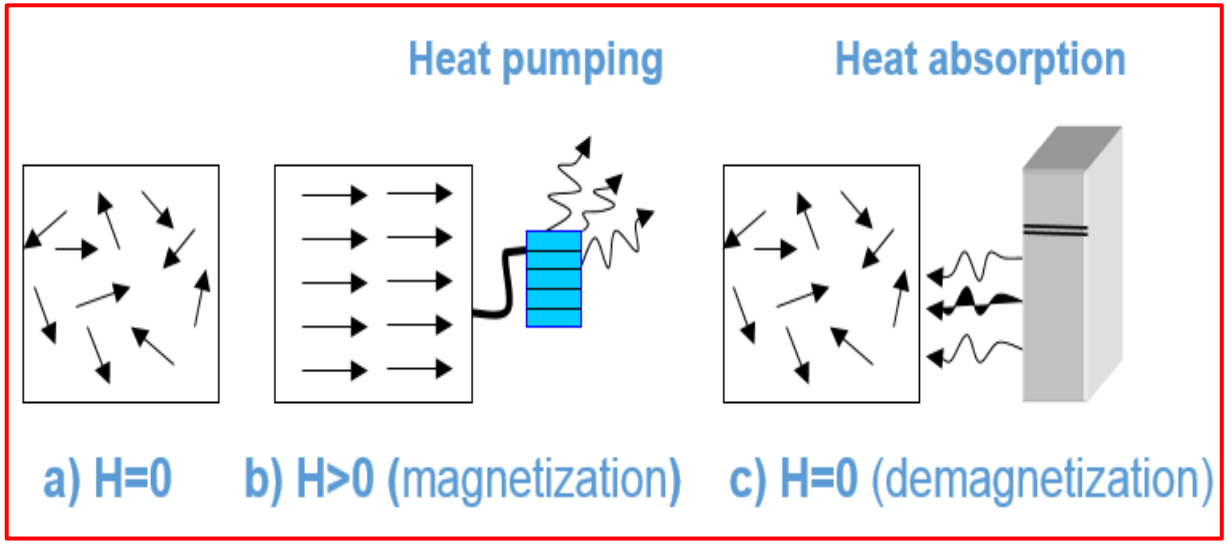

Magneto-caloric principles

Magnetic Refrigerator

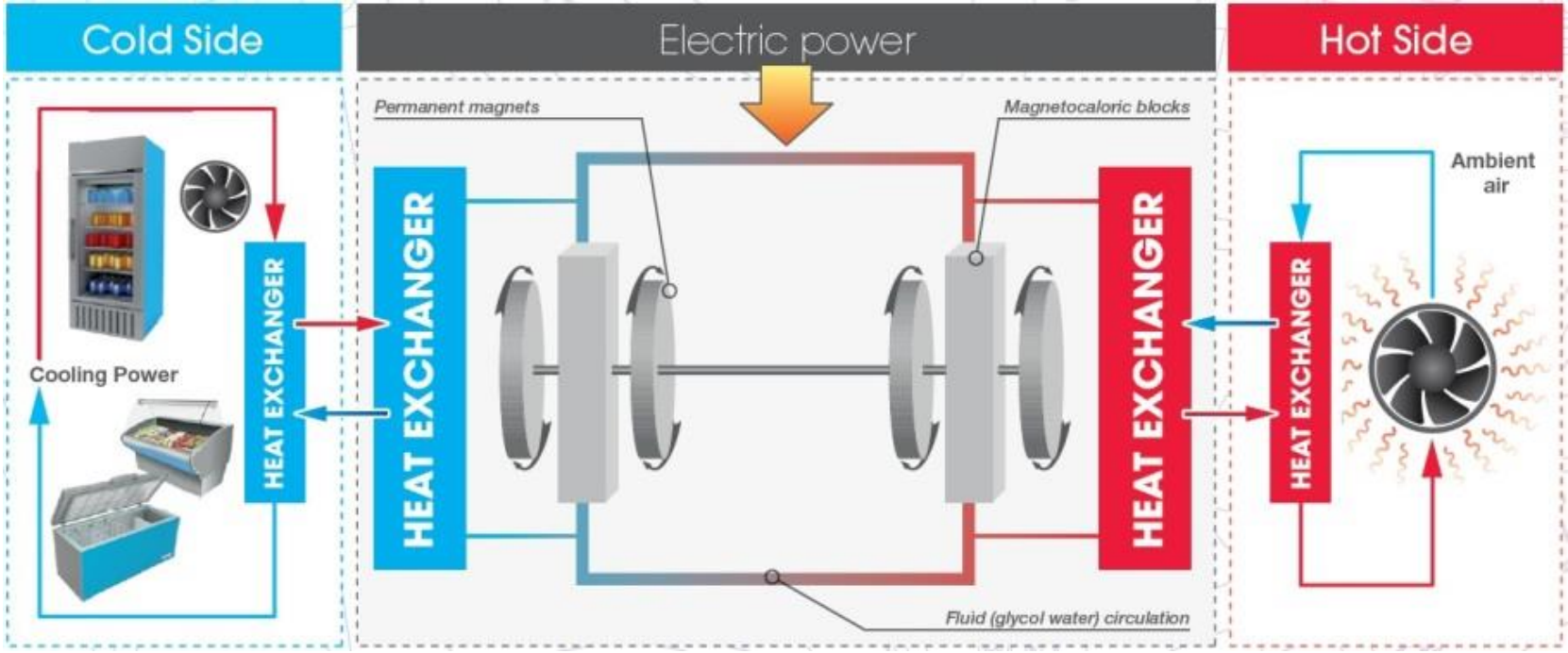

Operational Principles of Magnetic Refrigerator

Source: www.cooltech-applications.com

Magneto-caloric materials

Magneto-caloric materials

Alloys undergo a first-order magnetic transition

High but narrow magnetic entropy change peak

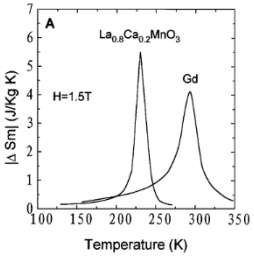

Crystalline
Gd-Si-Ge
La-Fe-Si
Ni-Mn-Ga
Mn-Fe-P-As
Mn-As-Sb

Alloys undergo a second-order magnetic transition

Broadened magnetic entropy change peak

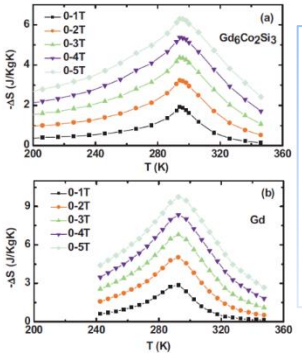

Crystalline
Gd, Gd-Co-Si

Amorphous
RE-TM glassy alloy
Fe-based glassy alloys

Magnetic Refrigerator

A real prototype of Magnetic Refrigerator

Source: www.cooltech-applications.com

Requirements for good magnetic refrigerants:

- Supply the maximum amount of over a wide temperature range;
- Nearly zero coercivity and low hysteresis lose;
- High electronic resistance and low eddy current loss;
- High corrosion resistance;
- Good mechanical properties and workability;
- Formability over a wide compositional range and tailorable magnetic properties.

→ Amorphous alloys

Background

Magnetocaloric effect (MCE)

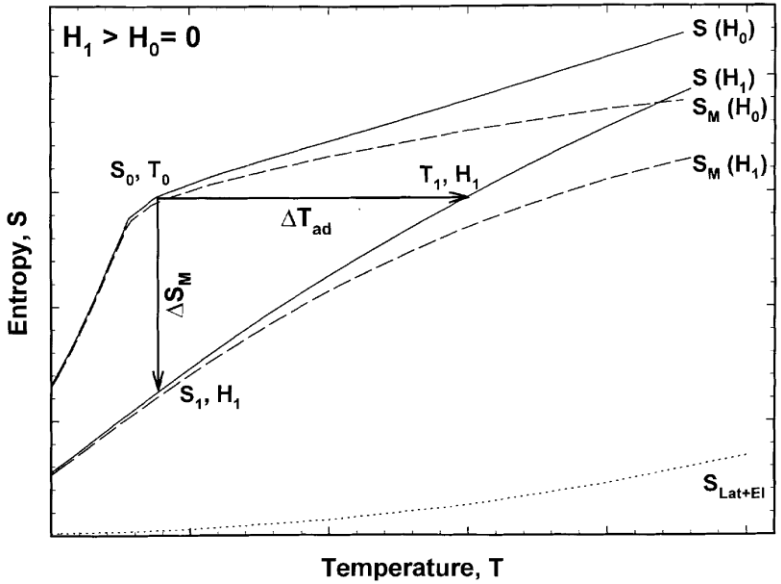

The entropy-temperature diagram for illustrating the MCE

(1) Magnetic entropy change (ΔS_M)

$$\Delta S_M(T,\Delta H)=\int_{H_1}^{H_2}\left(\frac{\partial M(T,H)}{\partial T}\right)_H dH$$

(2) Adiabatic temperature change (ΔT_{ad})

$$\Delta T_{ad}(T,\Delta H)=-\int_{H_1}^{H_2}\left(\frac{T}{C(T,H)}\right)_H\left(\frac{\partial M(T,H)}{\partial T}\right)_H dH$$

Background

Refrigeration capacity (RC)

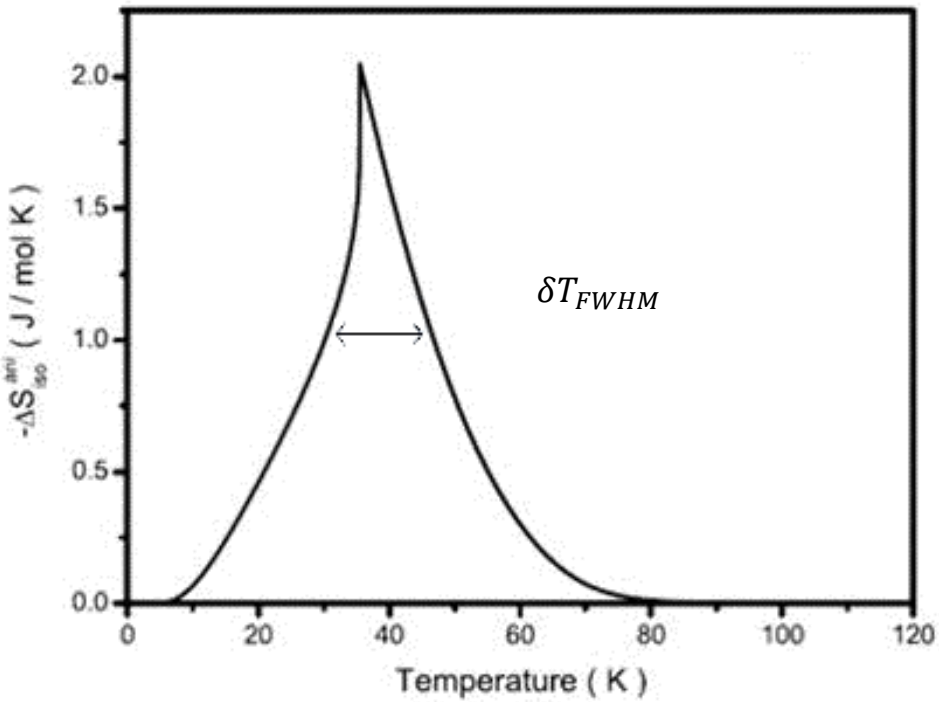

$$RC(\delta T, H_{max}) = \int_{T_{cold}}^{T_{hot}} \Delta S_M(T, H_{max}) dT$$

$$RC(\delta T, H_{max}) = \Delta S_M^{peak} \times \delta T_{FWHM}$$

Key challenge

- High magnetic entropy change peak
- Large refrigeration capacity

} At room temperature

Gd-based amorphous alloys

High ΔS_m^{peak}

Large *RC*

But

Much below room temperature

Fe-based amorphous alloys

Near room temperature

But

Low ΔS_m^{peak}

Low *RC*

Comparison of Gd-based and Fe-based amorphous alloys

Effect of microalloying on MCE of Gd-Co amorphous alloys

	T_C(K)		RC(Jkg^{-1})
$Gd_{50}Co_{50}$	267.5	4.6	686
$Gd_{50}Co_{48}Si_2$	244	5.3	684
$Gd_{50}Co_{45}Si_5$	214	5.87	734
$Gd_{50}Co_{45}Al_5$	197.5	6.64	764
$Gd_{50}Co_{48}Mn_2$	258	5.24	629
$Gd_{50}Co_{45}Mn_5$	244	5.49	612
$Gd_{50}Co_{48}Fe_2$	277	4.44	＞728
$Gd_{50}Co_{45}Fe_5$	291	3.64	＞659
$Gd_{50}Co_{48}Ni_2$	243	5.46	677
$Gd_{50}Co_{45}Ni_5$	230	5.55	705
$Gd_{50}Co_{48}Zn_2$	262	5.04	700
$Gd_{48}Co_{50}Zn_2$	260	5.02	＞700
$Gd_{50}Co_{48}Zr_2$	231	5.51	687
$Gd_{50}Co_{48}Nb_2$	242	5.3	640
$Gd_{50}Co_{45}Nb_5$	225	6.28	687

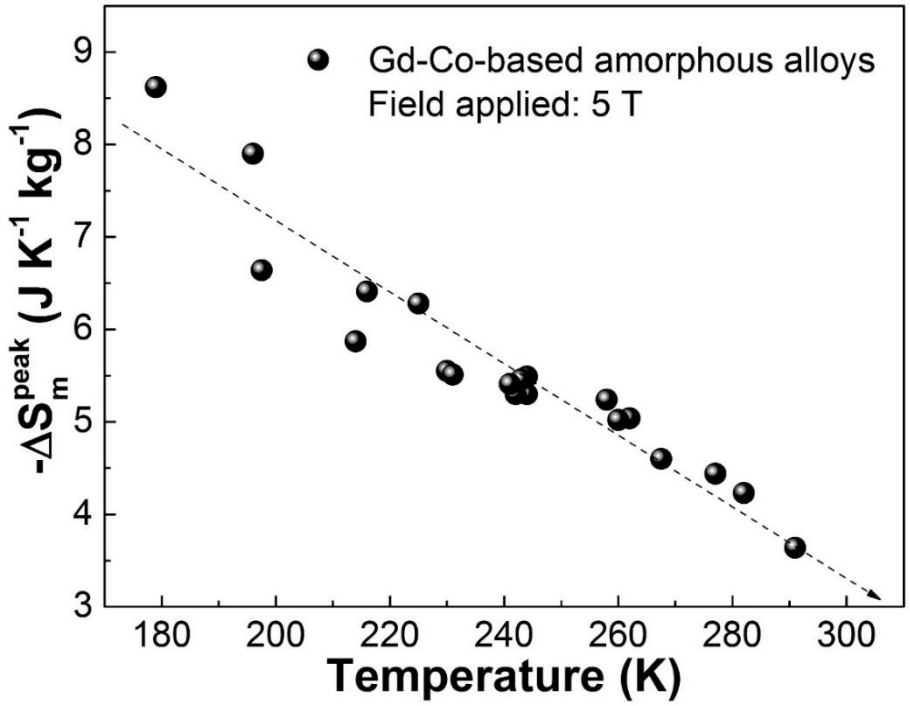

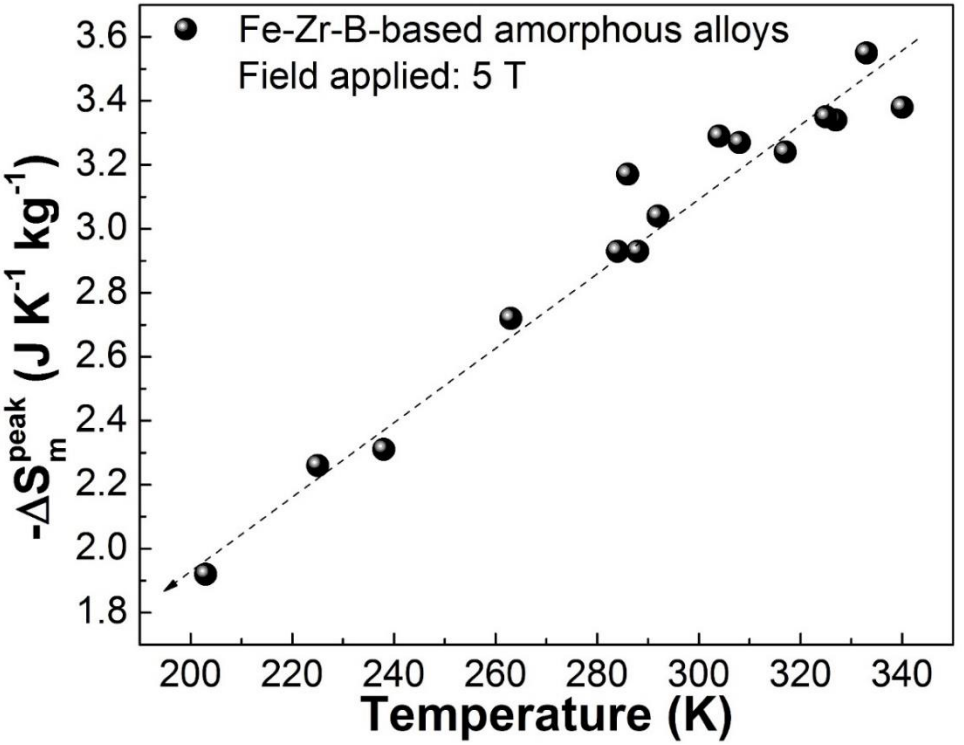

Refrigerant values of Gd-based and Fe-based amorphous alloys

Table-like magnetic entropy change

For magnetic refrigeration at room temperature, Eriksson cycle with cool storage processes and heat storage process have a higher efficiency than the others. When utilizing an Ericsson cycle, a specific table-like profile of the MCE, where $-\Delta S_m$ is a constant with respect to temperature in the cooling region, provides optimal efficiency.

Ericsson cycle

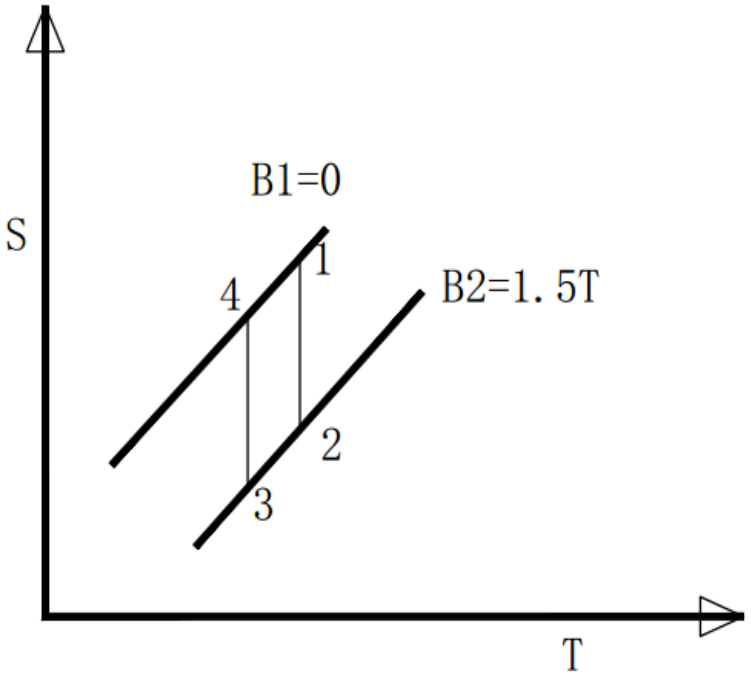

M-H curves of the amorphous hybrids: (a) sample 1, and (b) sample 2.

sample 1 = 70% (wt.%) $Gd_{50}Co_{48}Fe_2$ + 30% (wt.%) $Gd_{50}Co_{48}Mn_2$ amorphous ribbons;

sample 2 = 65% (wt.%) $Gd_{50}Co_{48}Fe_2$ + 25% (wt.%) $Gd_{50}Co_{45}Mn_5$ + 10% (wt.%) $Gd_{50}Co_{50}$ amorphous ribbons.

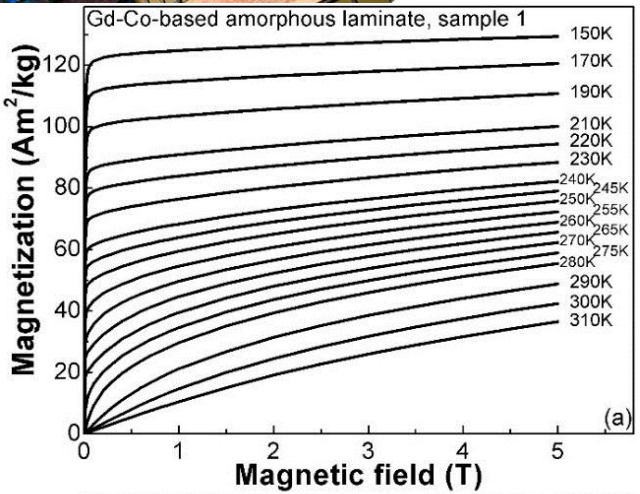

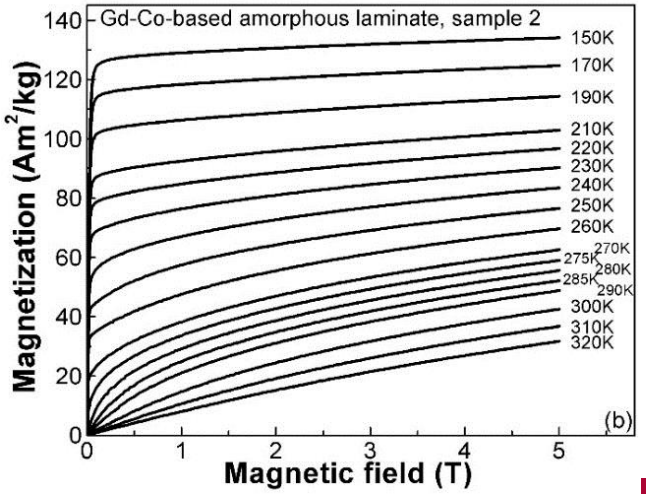

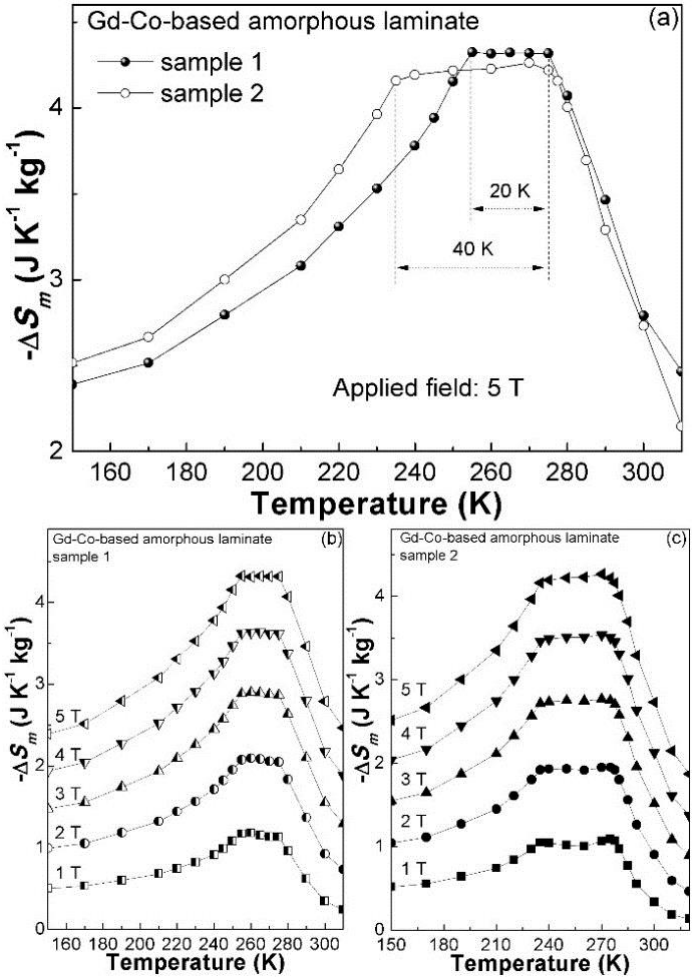

Table-like magnetic entropy change of amorphous hybrid samples within temperature range of about 20 K and 40 K, respectively, (b) the table-like magnetic entropy change of amorphous hybrid sample 1 under various fields, and (c) the table-like magnetic entropy change of amorphous hybrid sample 2 under various fields.

J. Alloy. Compd. 723, 197 (2017)

Fe-Zr-B-based amorphous composites with table-like magnetic entropy change near room temperature

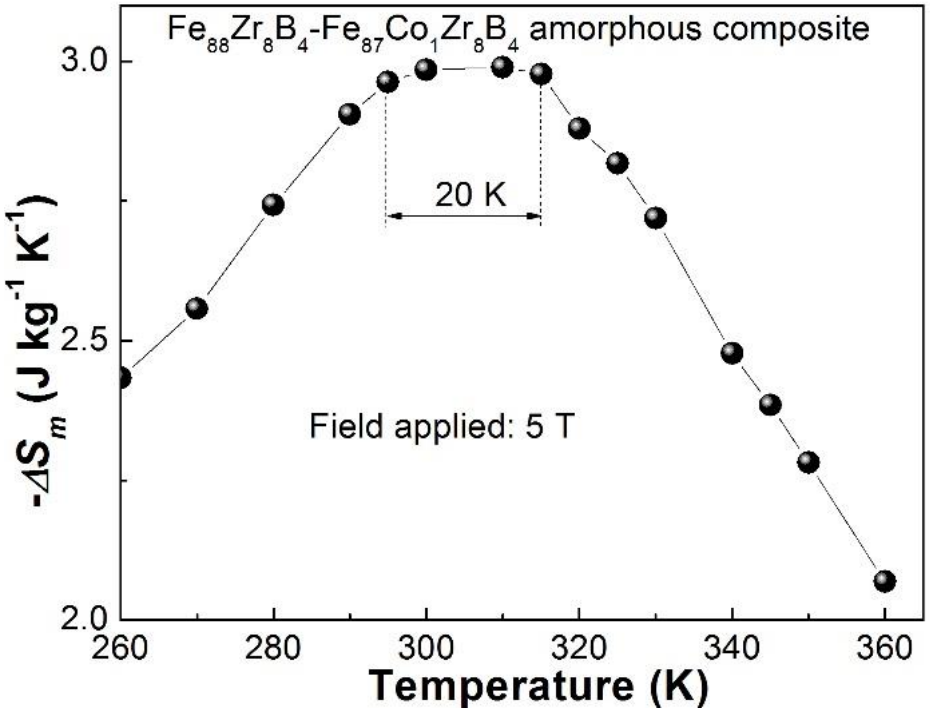

$-\Delta S_m$-T curve of an amorphous composite sample #1under a magnetic field of 5 T.

sample #1 = 57% (wt.%) $Fe_{88}Zr_8B_4$ + 43% (wt.%) $Fe_{87}Co_1Zr_8B_4$ amorphous ribbons

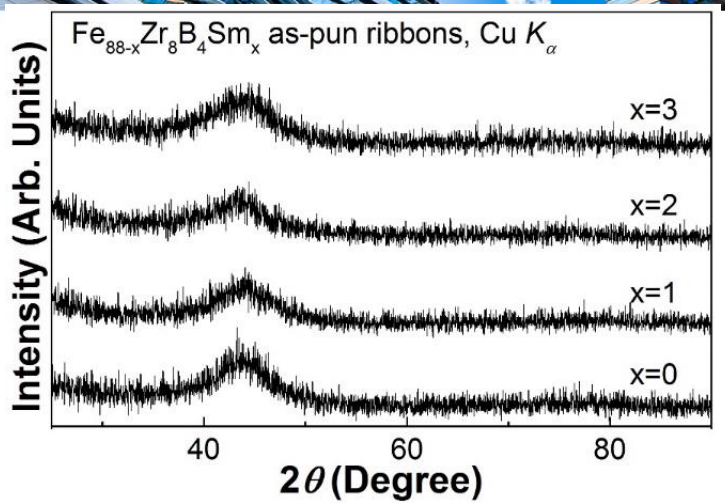

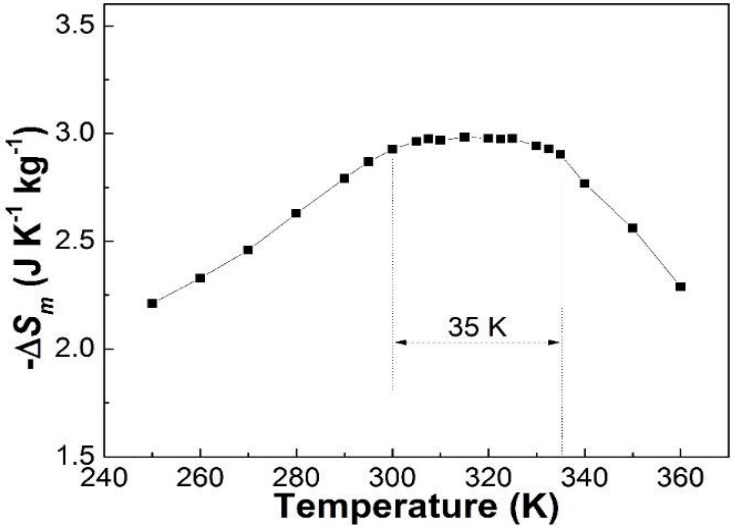

$-\Delta S_m$-T curve of an amorphous composite sample #2 under a magnetic field of 5 T.

sample #2 = 40% (wt.%) $Fe_{88}Zr_8B_4$ + 42% (wt.%) $Fe_{85}Zr_8B_4Sm_3$ + 18% (wt.%) $Fe_{87}Zr_8B_4Sm_1$ amorphous ribbons

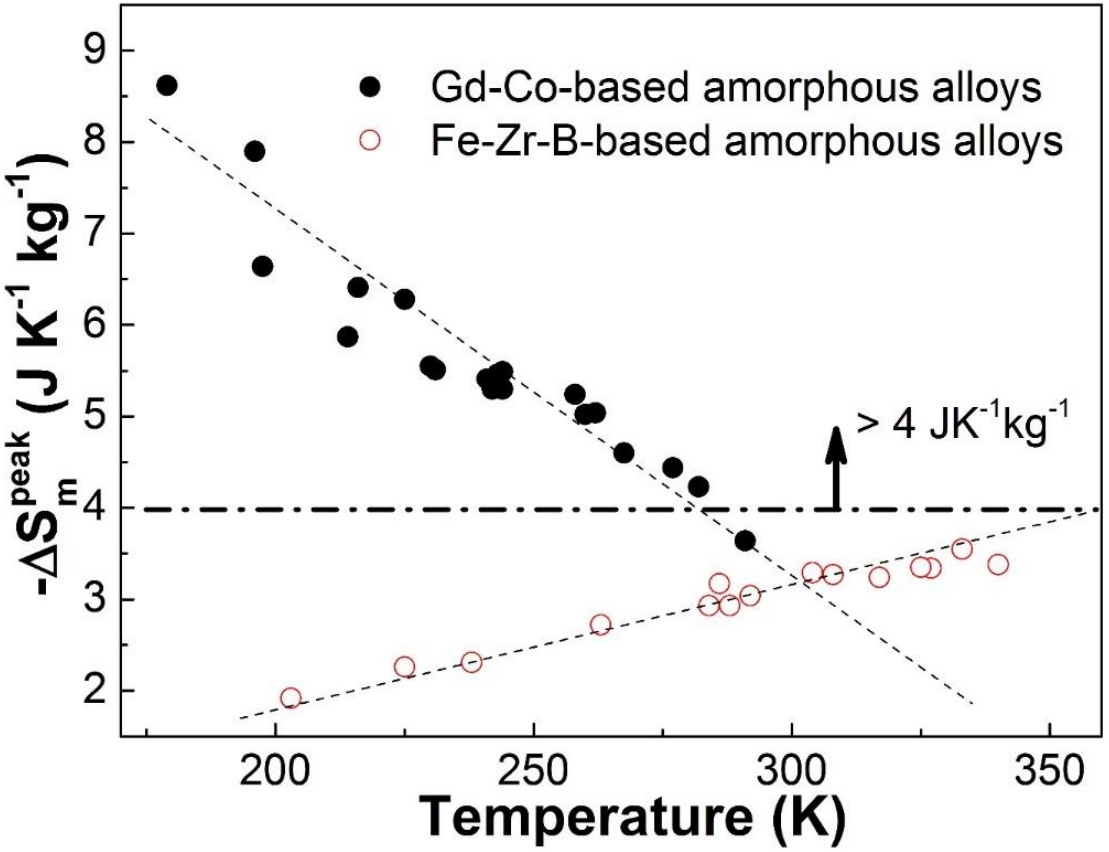

The aim of this project is to achieve table-like $-\Delta S_m$ with a maximum value larger than 4 $JK^{-1}kg^{-1}$ under a field of 5 T by means of:

1. Improve the $-\Delta S_m{}^{peak}$ of Fe-Zr-B-based amorphous alloys;
2. Achieving new amorphous alloys with higher $-\Delta S_m{}^{peak}$ near room temperature

9. Metallic glass films/coatings and their applications

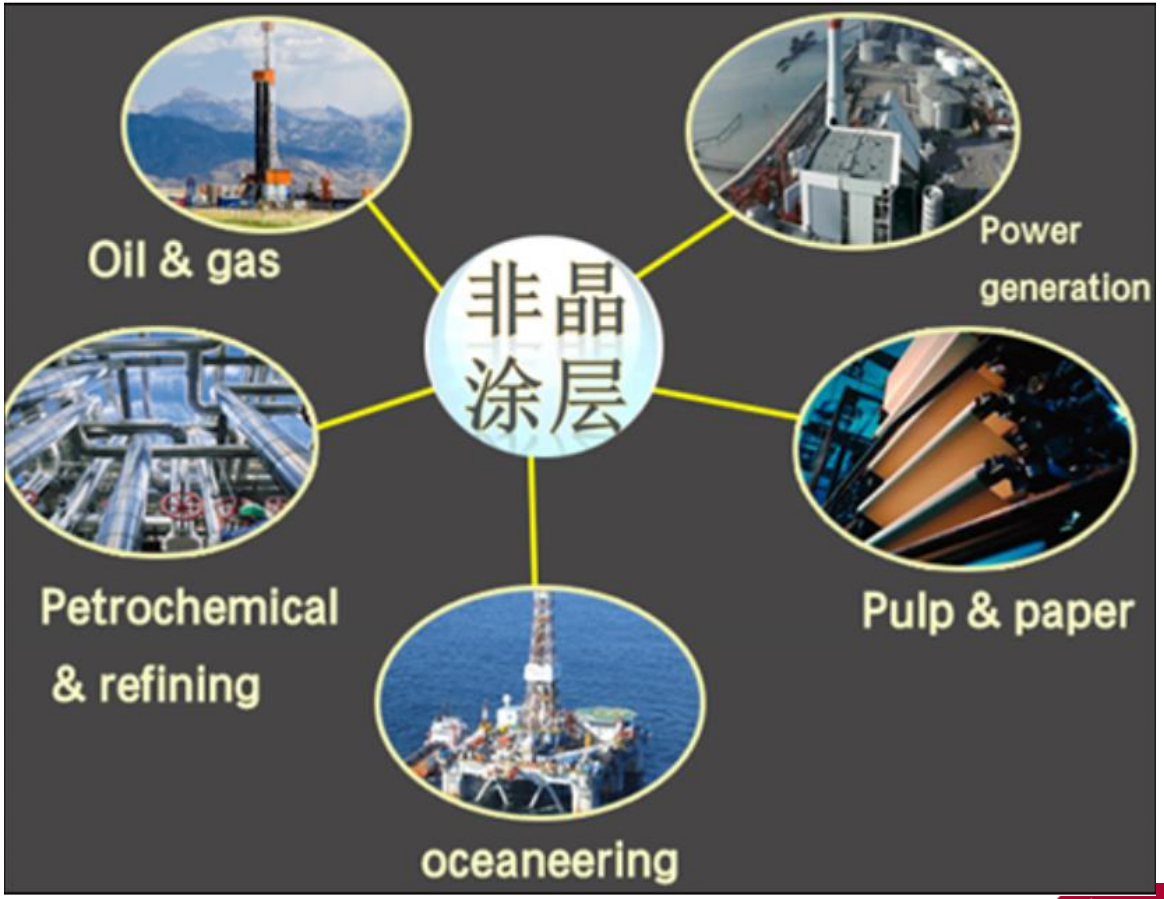

Film thickness:

100 nm ~ 20 um

Preparation approaches：

1) Sputter and evaporation deposition

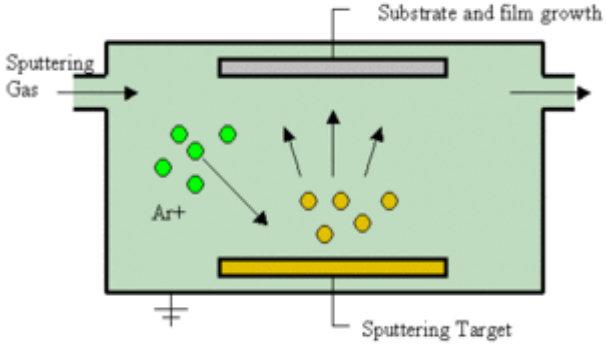

High effective cooling rate ~10^6K/s

Broad compositions

2) Electroplating/chemical plating

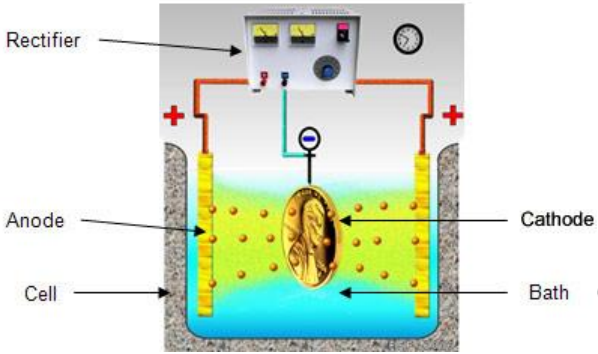

Limited to Ni-P/Co-P/ Ni-W/Ni-W-P, etc.

3) Cold spraying

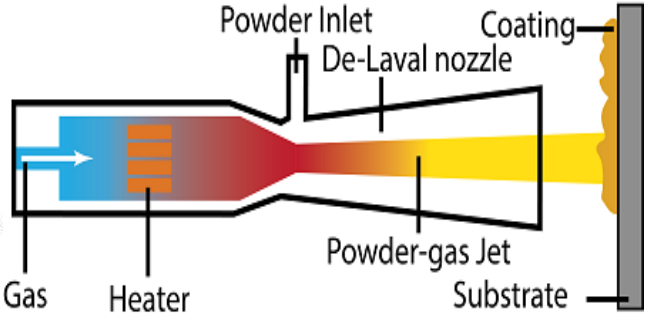

Supplied as gas atomized powders

Amorphous Coatings and Surfaces on Structural Materials

The absence of grain boundaries, the weak spots of crystalline materials, leads to better resistance to wear and corrosion. Amorphous metals, while technically glasses, are also much tougher and less brittle than oxide glasses and ceramics.

Using metallic glasses as the coatings for structural applications is an attractive way of taking advantage of their superior properties. metallic glasses can be synthesized as the coatings or subjected to surface modification to provide functionally superior surfaces.

9.1. Coatings for strength improvement

The yield strength and ultimate tensile strength of Ni substrate (6 mm in diameter) coated with 6 um thick Ni-P amorphous film via electroless plating was improved by 17% and 23%, respectively.

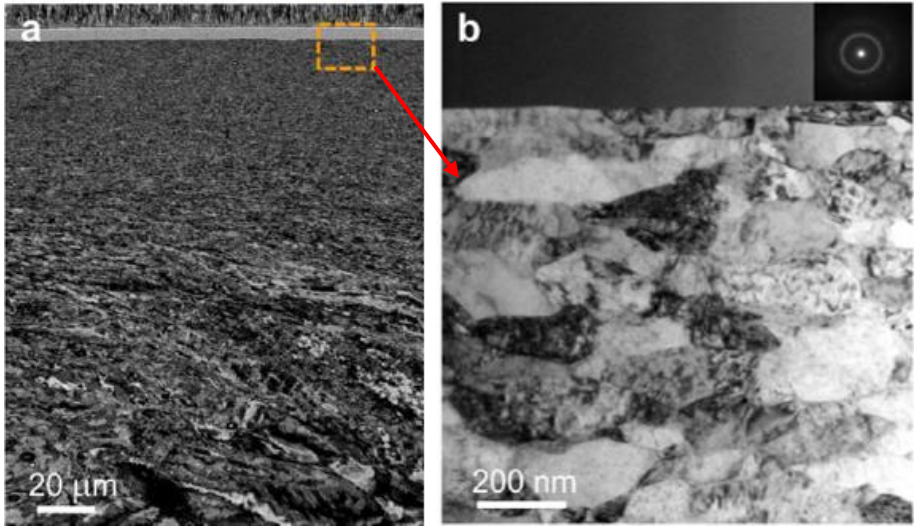

Microstructure of Ni substrate with Ni-P amorphous film.

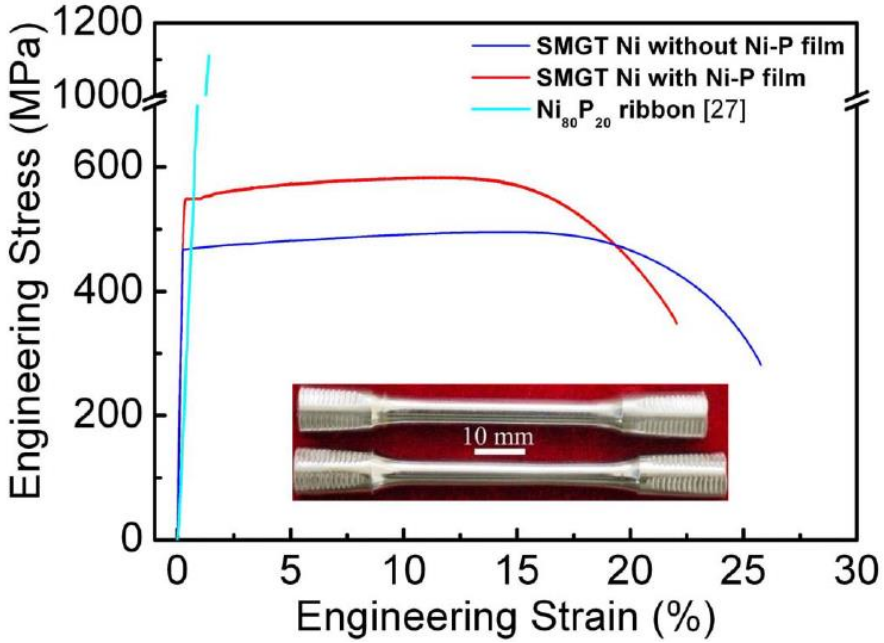

Lu X L, Lu Q H, Li Y, et al. Scientific reports, 2013, 3.

9.2. Coatings for improving fatigue-property of structural materials

Metallic glass coatings are ideal surface coating materials. It has been reported that applying metallic glass-forming metallic films to improve fatigue properties of many crystalline substrates such as 316 L stainless steel, Ti-, Ni- and Al-based alloys.

A 200-nm-thick Zr-based metallic glass coating and hard TiN films were deposited using magnetron sputtering on Ti–6Al–4V alloy, respectively. The effects of on the four-point fatigue property improvements were investigated.

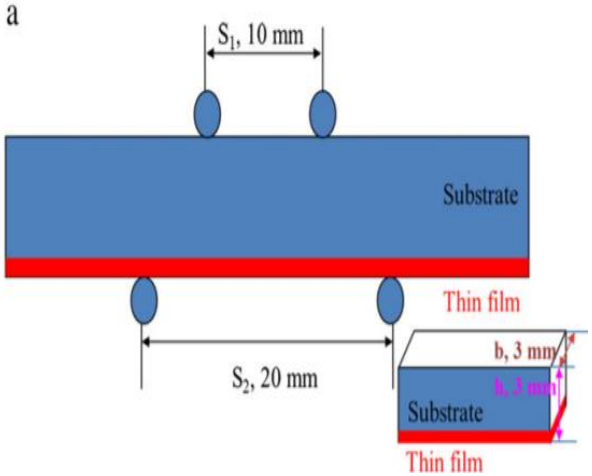

Four-point-bending for fatigue tests.

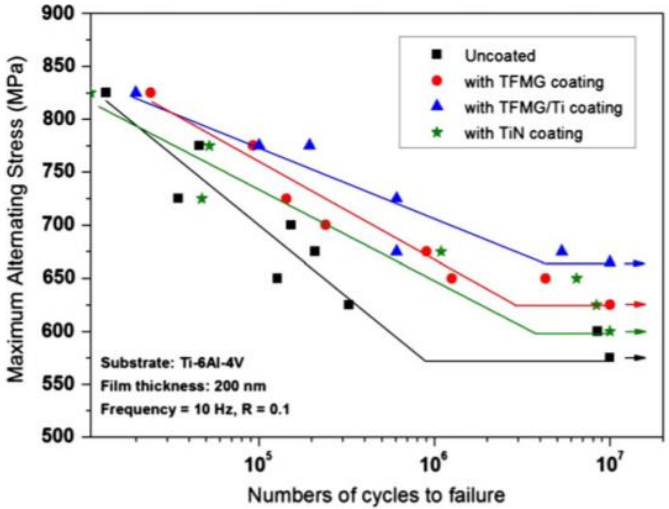

Stress versus number of fatigue cycles

The fatigue life was improved by ~4.5 times an ~17 times, and, by the TiN and metallic glass coating, respectively.

Chang Y Z, et al. Thin solid films, 2013, 544: 331-334.

9.3. Coatings for improving wear resistance

Fe-based thin film metallic glasses (TFMGs) with various thickness (125~745 nm) were deposited on glass and 304 stainless steel (SS) by using magnetron sputtering. Results of dry friction and wear tests against Si3N4 demonstrated that Fe-based TFMGs had lower friction coefficient and nearly three times higher wear resistance with respective to 304SS.

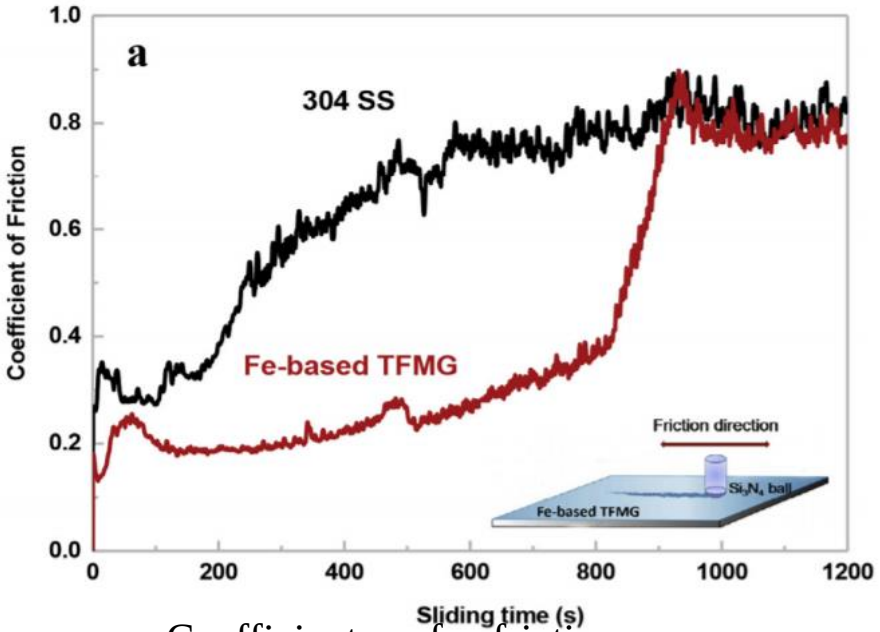

Coefficient of friction versus sliding time for the Fe-based TFMG

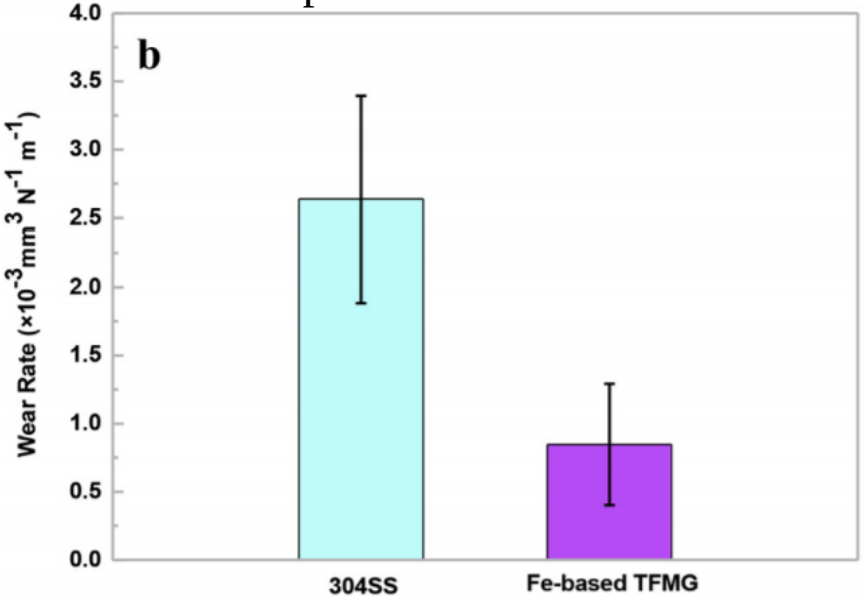

Wear rate for the Fe-based TFMG and the 304SS substrate.

Wu Y, Luo Q, Jiao J, et al. Metals, 2017, 7(4): 118.

9.4. Coatings for improving corrosion resistance

ting

Metallic glass has good corrosion resistance because metallic glass has homogeneous microstructure and does not have grain boundaries.

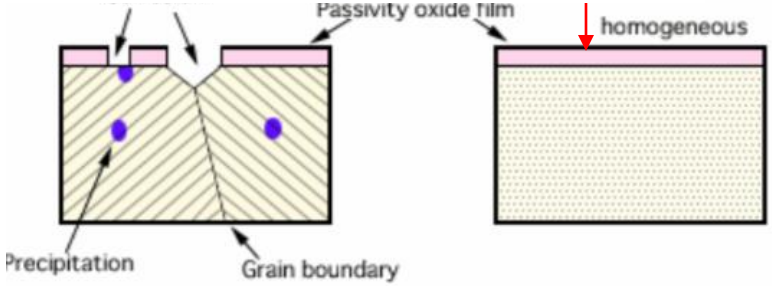

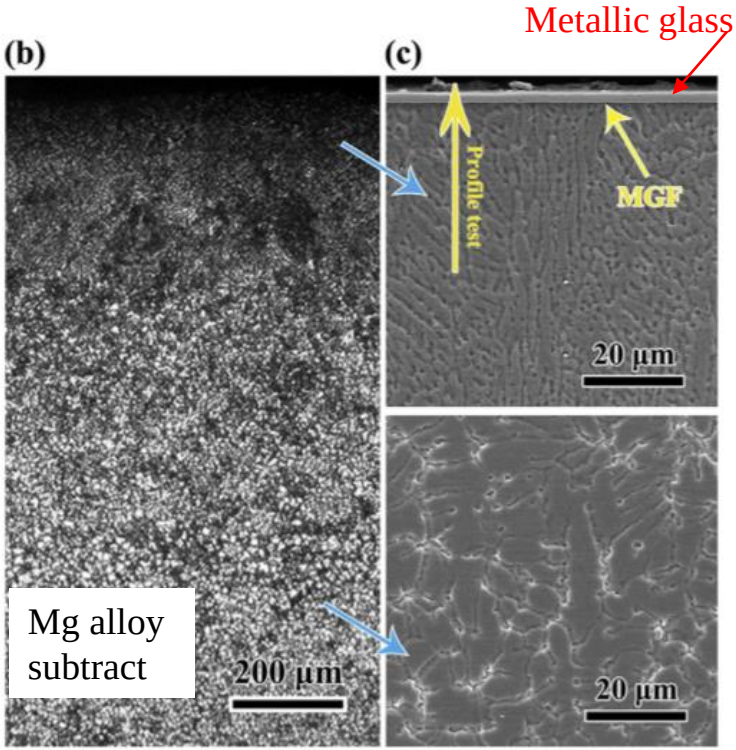

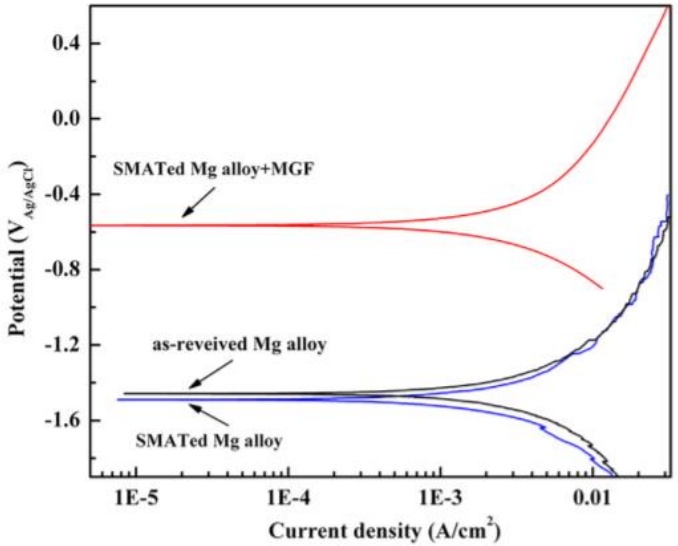

Fig. 4. Polarization curves for as-received Mg alloy, SMATed Mg, and SMATed Mg alloy with MGF deposition. i_{corr} values are 3.9×10^{-3} A/cm^2, 2.9×10^{-3} A/cm^2 and 7.8×10^{-4} A/cm^2 for the three samples; E_{corr} values are −1.46 V, −1.49 V and −0.65 V for the three samples respectively.

Metallic glass film deposited Mg alloy with superior corrosion resistance

Guo W, Zhang J, Wu Y, et al. Materials & Design, 2015, 78: 118-124

Limitations of metallic glasses

Notwithstanding the excellent properties exhibited by MGs, they also possess certain critical limitations that have put a damper on their widespread commercialization.

- complex fabrication routes that need tremendously high cooling rates, high material purity, expensive principal species, and sophisticated equipment. An economical and fast route may not be indispensable for MGs.

- The second issue is the size limitation. This issue is, mainly, a result of the first limitation since larger sizes result in low heat dissipation and make the formation of amorphous system increasingly difficult.

- The third issue is the instability at high temperature. Crystallization may occur during thermoplastic forming, that has rendered the MG system very special for a multitude of applications.

- The lack of ductility of most MGs is other major impediment in utilizing as general structural materials.

10. Conclusions

1) Metallic alloys are typically multicomponent systems so as to perturb the crystallization of the liquid melt and be vitrified using high cooling rates.

2) Due to their glassy structure, metallic glasses exhibit some outstanding properties like superior strength, good corrosion resistance, excellent wear resistance, and high elasticity as compared to their crystalline counterparts, and are finding applications in different fields such as in electronic products, sports and industrial sensors.

3) Metallic glass can improve the performance of many of the commercial devices as they can potentially replace the crucial elements such as catalysts, biomedicines, sensors, magnets, etc.

4) Metallic glass coatings have the potential to emerge as modern high-performance coatings, such as for improving wear/corrosion resistance and fatigue-property of structural materials.

先進激光輔助金屬成型技術及未來商機

由香港生產力促進局智能製造及材料科技部顧問陳偉倫博士主講

激光輔助成形技術

陳偉倫
智能製造及材料科技部
電話：（852）2788-5481
電子郵件：wailunchan@hkpc.org

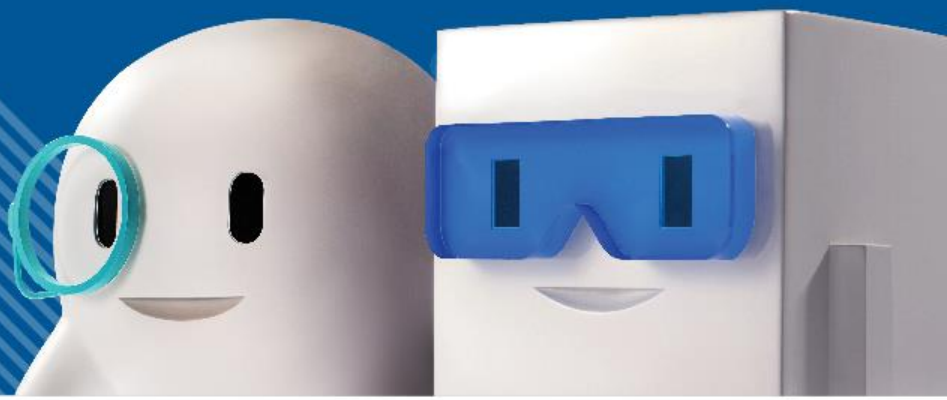

All-round Productivity Partner
全方位企業伙伴

輕量化設計

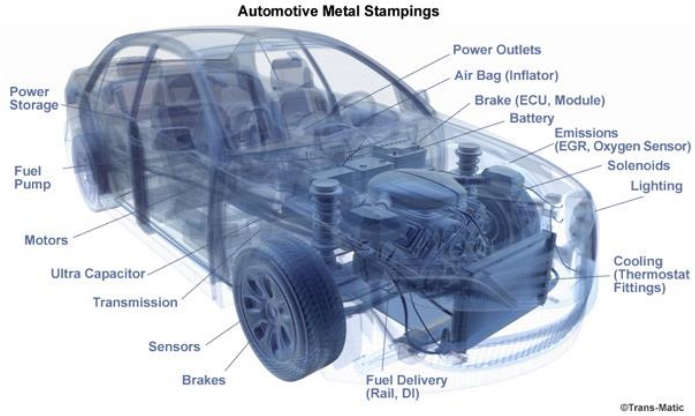

- 降低組件的重量可節約能源、提高速度、降低燃料成本和空氣污染
- 一架典型的客車約有65%的重量來自鋼和鐵
- 衝壓件已廣泛應用於汽車行業
- 材料具有高的強度 - 重量比可實現輕量化
- 減重(鈦， 高強度鋼：40%-50%）

技術難處

冷成形
- 高強度鋼和輕合金材料在室溫條件下成形性能較差
- 限制成形零件的幾何複雜性
- 模具疲勞壽命短
- 模具磨損快

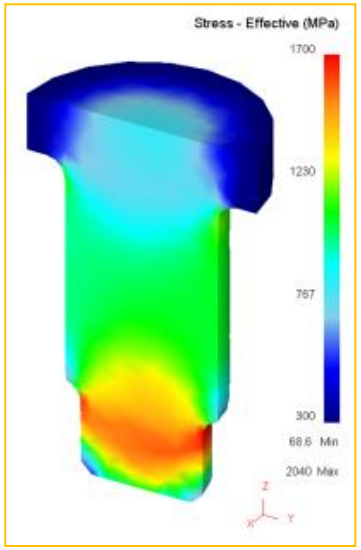

沖頭應力分佈

熱成形
- 成形件的表面品質和幾何精度差
- 難以控制小尺寸的工件冷卻速度
- 由於微觀結構的變化惡化成形件的機械性能
- 需要特別工具或機器來運輸加熱工件
- 生產週期長
- 能源浪費

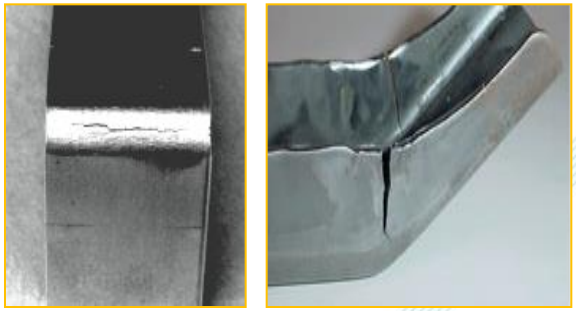

成形性能差

冷成形+退火
- 由於微觀結構的變化惡化成形件的機械性能
- 生產週期長

由機器人運輸加熱工件

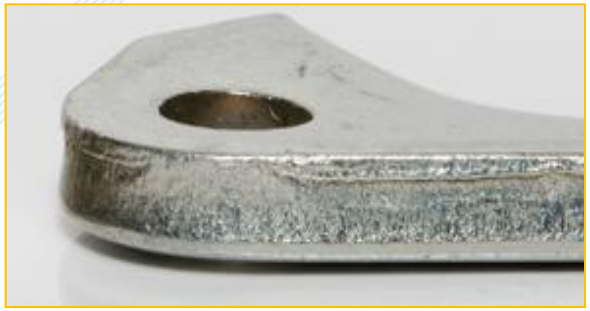

沖裁部件的表面光潔度差

激光輔助漸進成形

使用激光把關鍵成形區域加熱

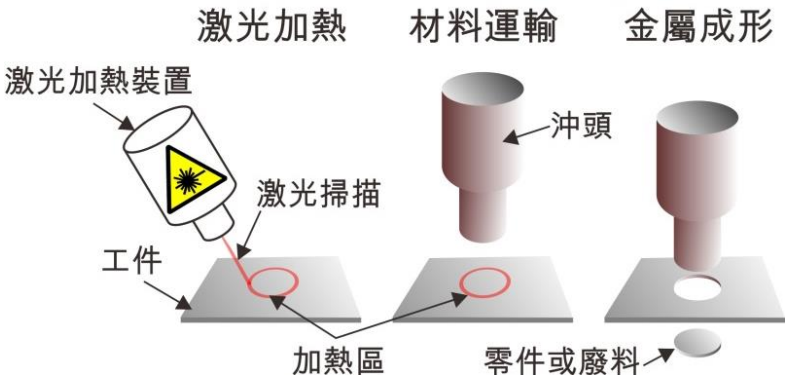

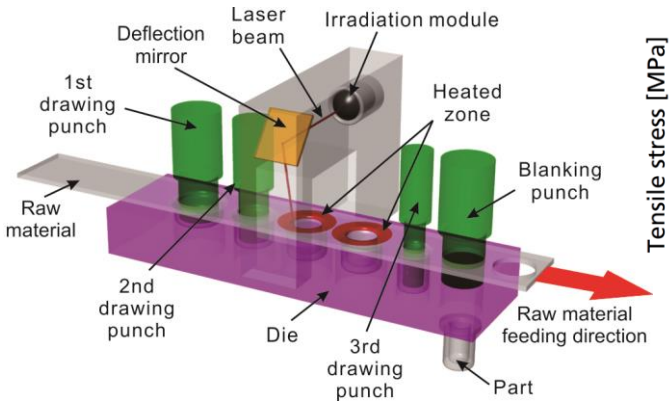

拉伸強度與溫度的關係

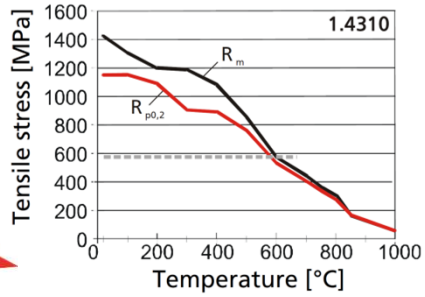

- 降低成形載荷
- 減少成形步驟
- 提升材料成形能力
- 提升模具壽命
- 可成形複雜零件的幾何形狀
- 增加了剪切光潔面面積
- 減少邊緣翹曲
- 增加長厚比
- 較大的板材厚度
- 可以降低因材料加熱所引至的尺寸變化
- 可避免嚴重氧化
- 可以控制局部材料流動。可以調整成形件的局部厚度，成形部件的剛度可以加強
- 避免加熱工件的運輸
- 能量直接吸收使週期時間短

激光輔助漸進成形

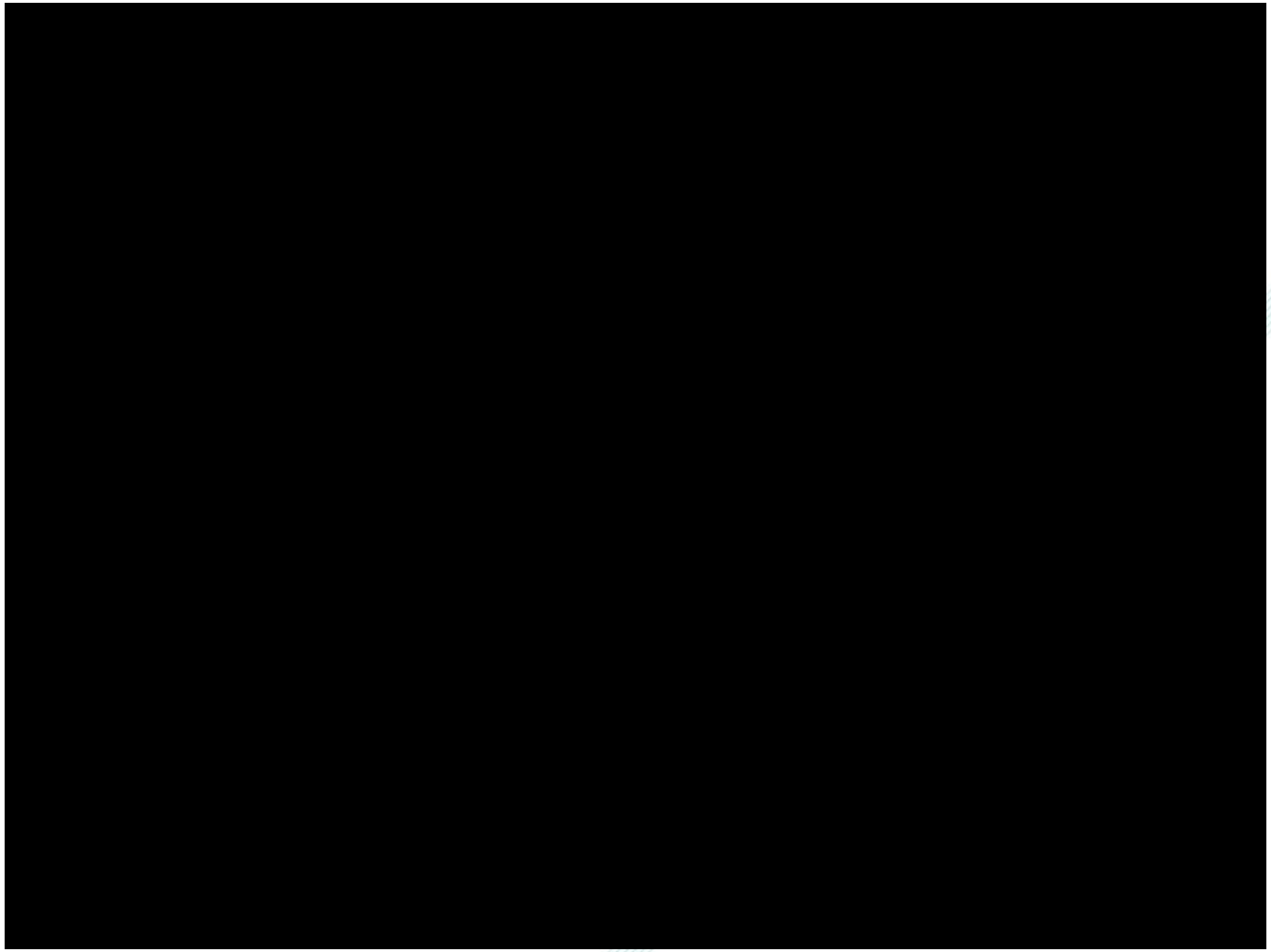

激光輔助漸進成形

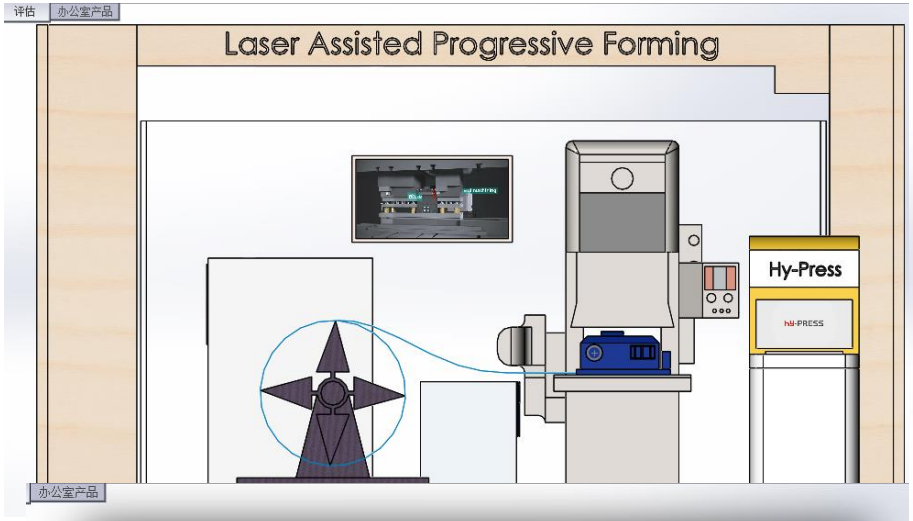

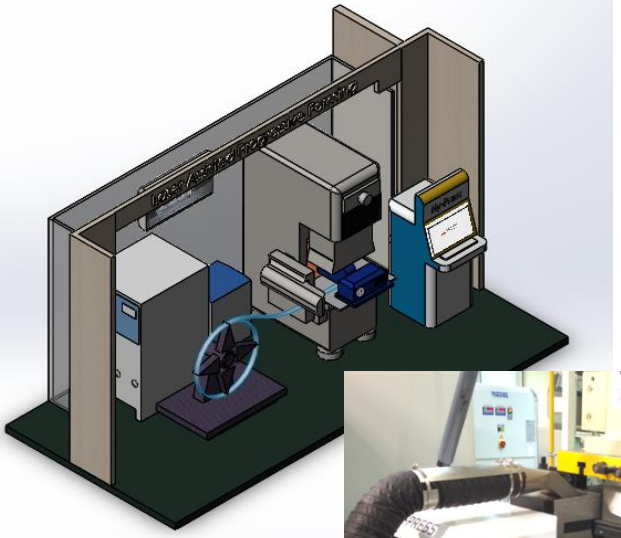

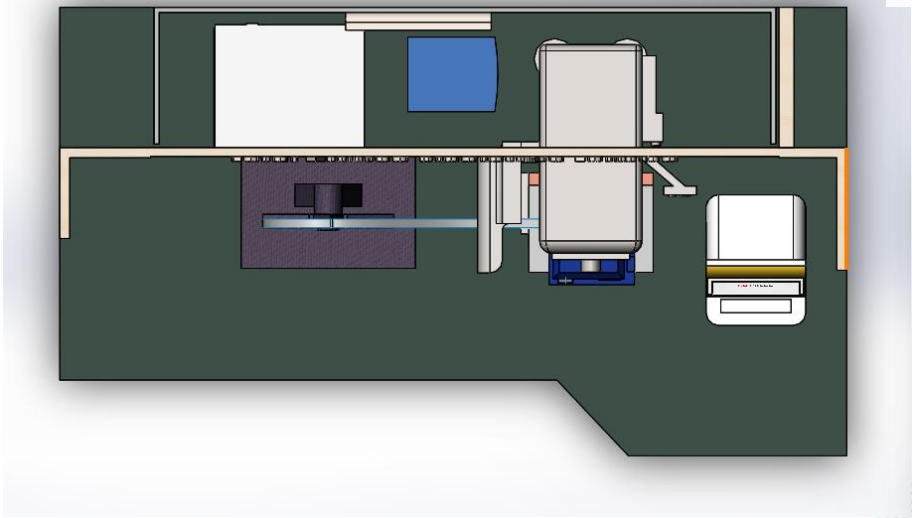

HKPC

激光輔助漸進成形

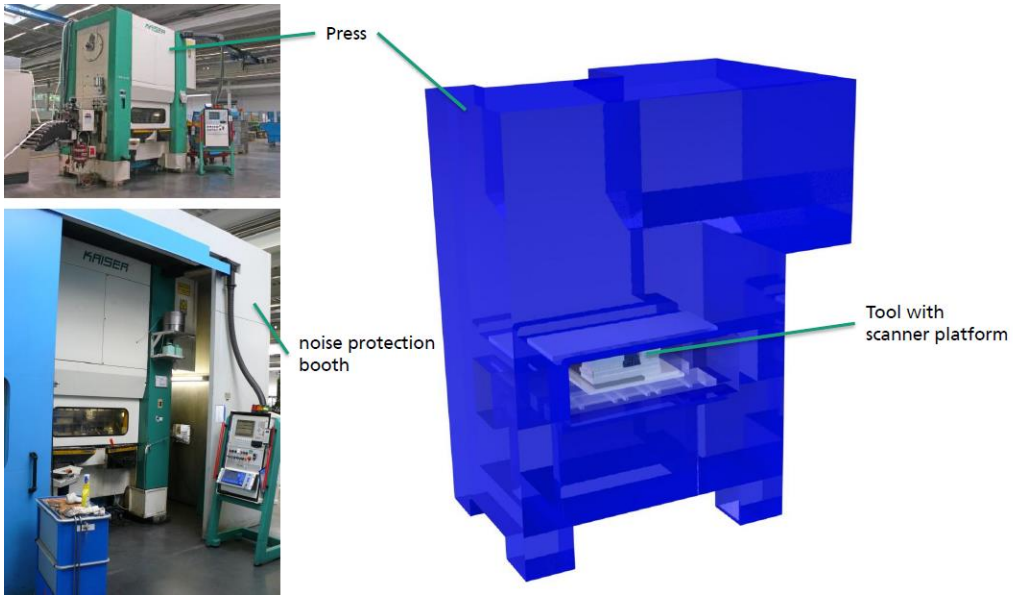

- 激光輔助成形技術可應用於傳統衝床（如：伺服衝床、液壓衝床）

- 優點：
  - 毋須改裝衝床
  - 可用現有的板金運送系統

- 改裝漸進模具，配置激光照射站

- 激光輔助金屬成形技術可應用於不同成形工藝
  - 彎曲
  - 深拉
  - 壓印
  - 剪切

激光輔助漸進成形

漸進成形模具

集成了光學及避震系統

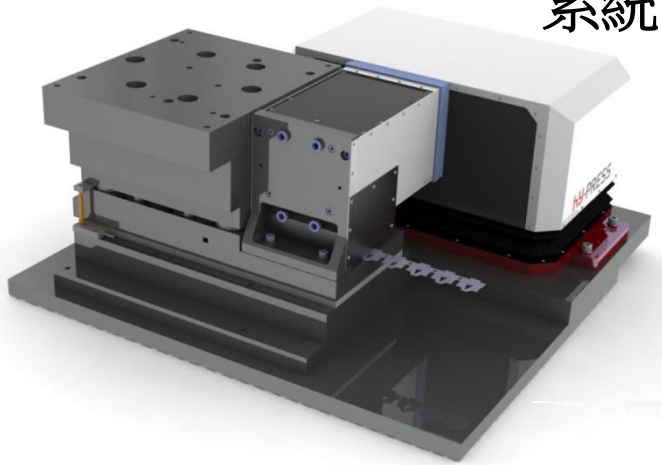

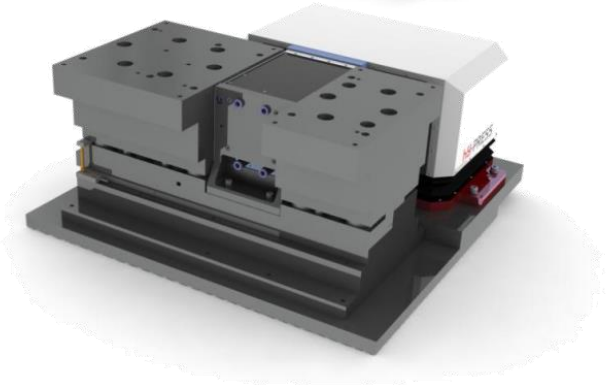

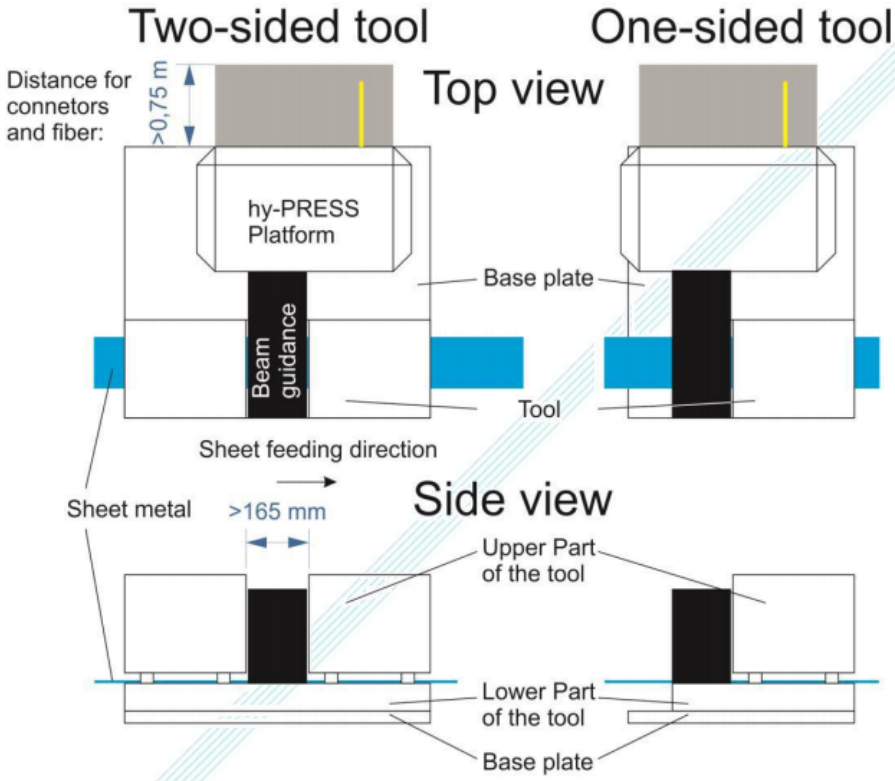

兩種結合方式，針對不同幾何特點之零件進行選擇。

工藝參數

主要激光變量：路徑軌跡、激光參數系列。
下表顯示激光輔助成形過程中主要調整的重要參數：

參數名稱	單位	參數意義
光斑速度	mm/s	激光光斑運動速度，設定值越高，激光光斑運動速度越快。
激光強度	%	激光的輸出功率。（激光在工作中通常不會採用100%的功率）
照射次數		激光掃描次數，激光將按照所編程路線多次往復運動，此參數代表激光往復次數。

案例

材料：彈簧鋼（1.4301）
板材厚度： 3mm
孔徑：6.5毫米

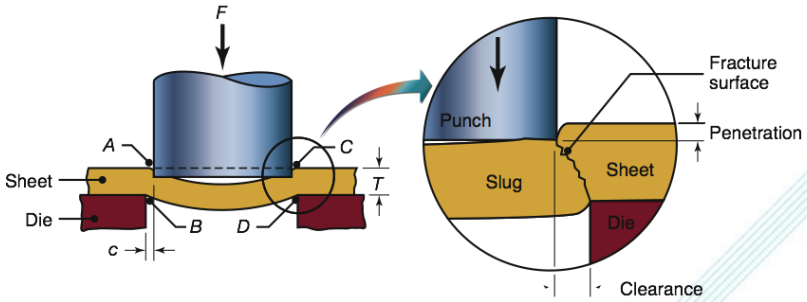

傳統剪切

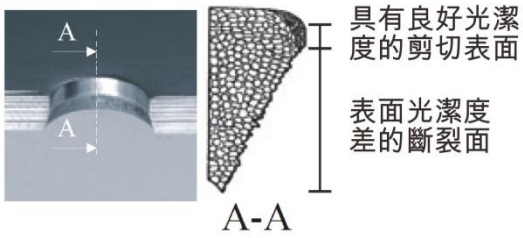

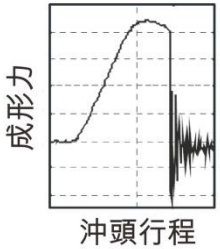

- 大斷面面積
- 在斷裂面的微裂紋可減弱部件強度
- 高切削力
- 模具磨損速度快

激光輔助剪切

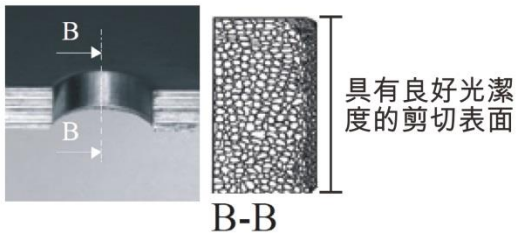

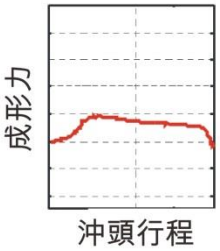

- 增加光潔剪切面面積(彈簧鋼可達100%光潔面積)
- 減少變形圓角（不銹鋼可減少60%）
- 降低沖裁力（超過60%）
- 提高機器和刀具壽命

HKPC

案例

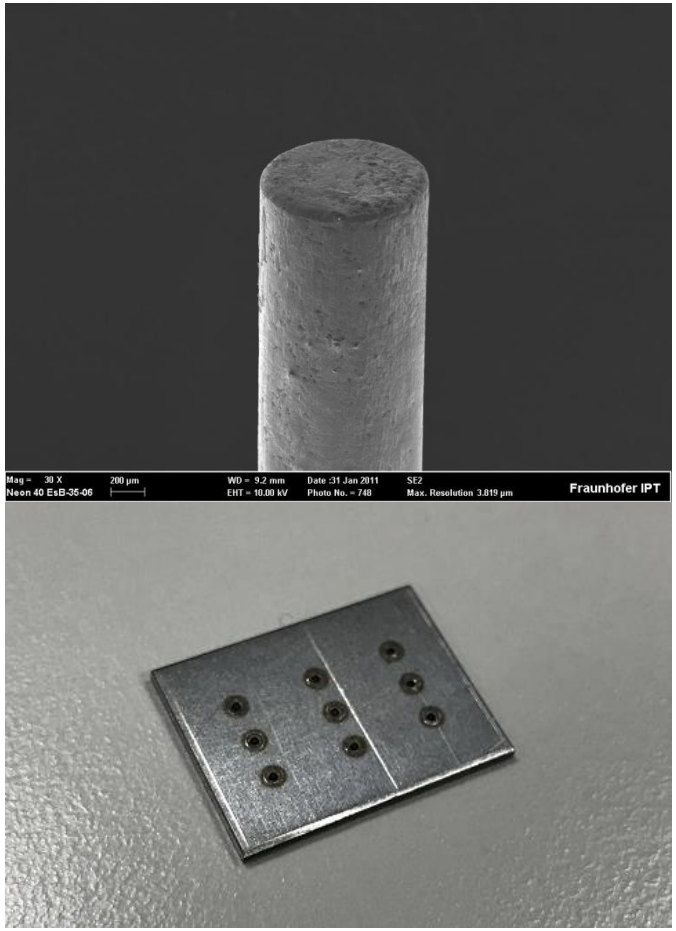

- 在1 mm厚的彈簧鋼板剪切1mm直徑的孔
- 降低成形力可延長刀具壽命

<u>模具</u>

- 直徑：1mm
- 材料：高速鋼無塗層
- 無潤滑油
- 沖件6000次
- 只有很少的磨損

案例

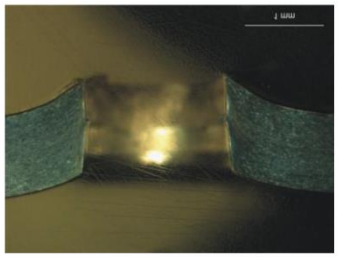

常溫下是
不可能的

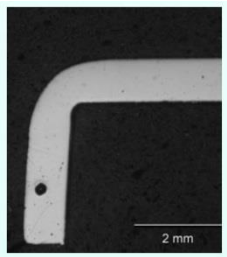

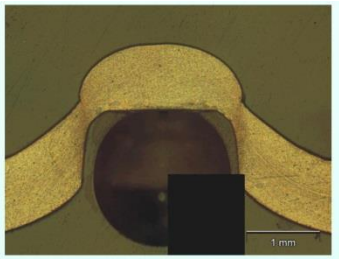

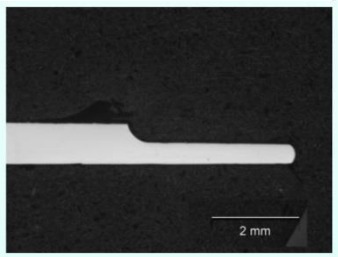

材料：彈簧鋼（1.4301）；板材厚度： 1mm ；拉伸強度：>1600（MPa）

- 高材料強度導致成形能力差
- 小的彎曲半徑無法實現
- 在一個成形工藝步驟中只能實較小拉伸比
- 只壓出較淺的紋

- 提高材料的成形性能
- 可實現小彎曲半徑
- 提高拉深比
- 增加壓紋深度
- 可實現複雜的部件幾何，更大的設計空間

案例

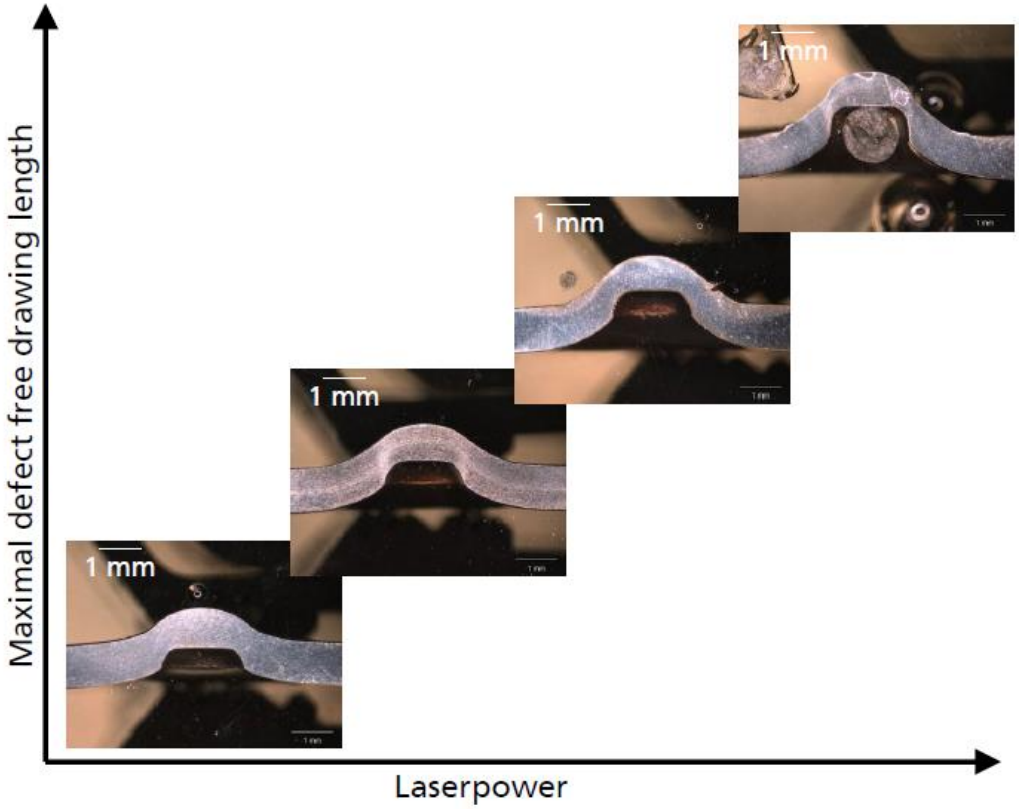

- 材料：彈簧鋼（**1.4301**）
  板材厚度： **1mm**
- 衝壓拉伸直徑：**2.3mm**
- 沒有激光可拉深度： **0.9mm**
- 有激光可拉深度： **2.0mm**
- 較佳的尺寸穩定性

案例

板料擠壓

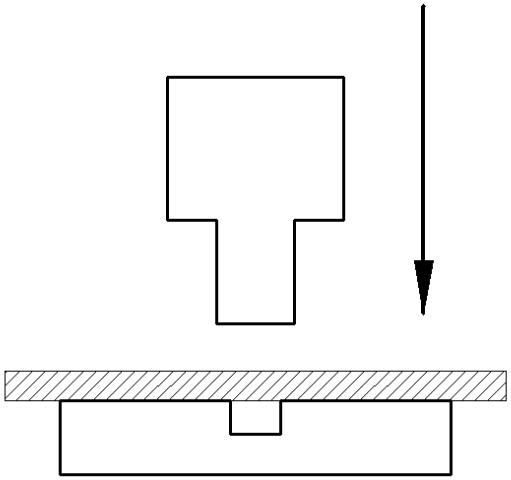

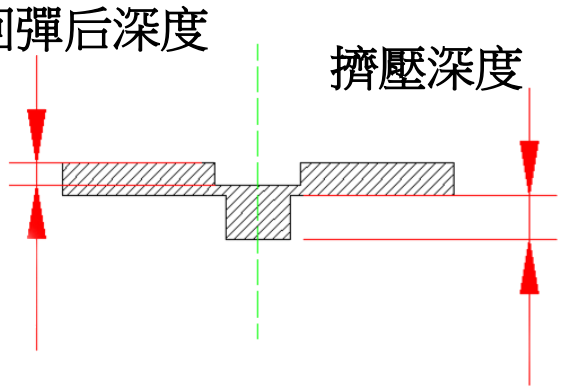

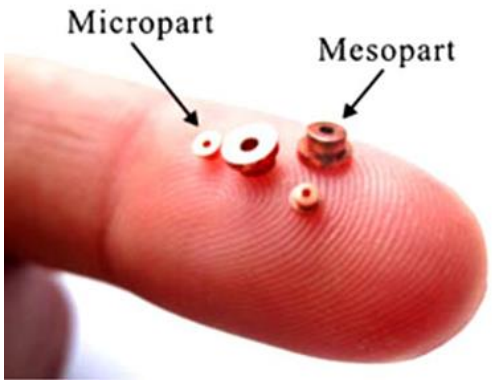

傳統加工

激光輔助

案例

翻邊成形

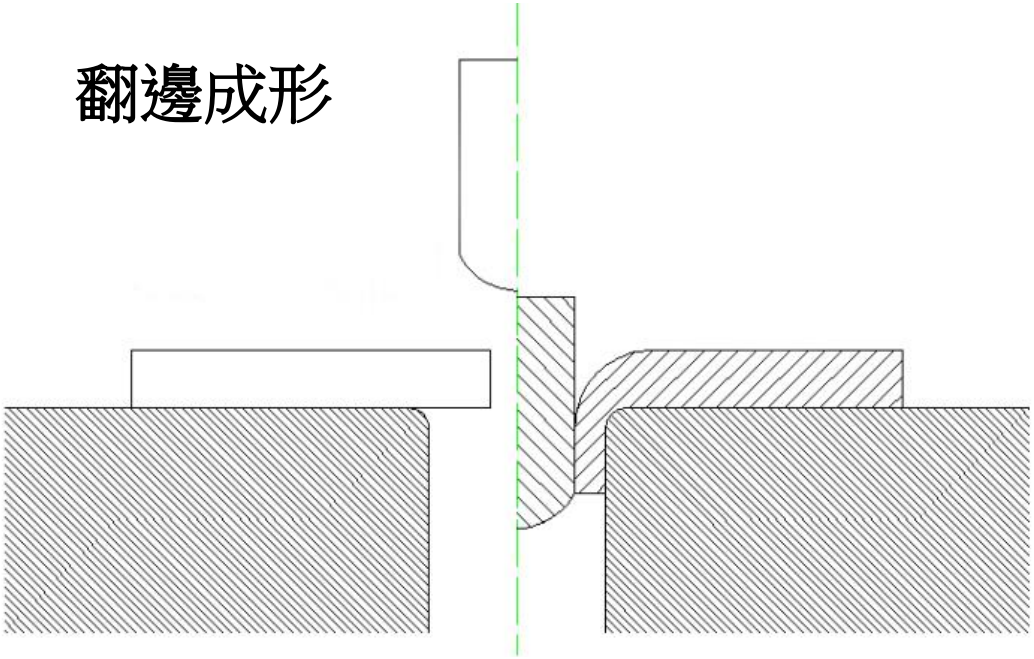

由於材料的流動性和成形性不足，在翻邊頂部或者底部的大變形區域通常會發生材料撕裂，零件不可成形。

傳統成形

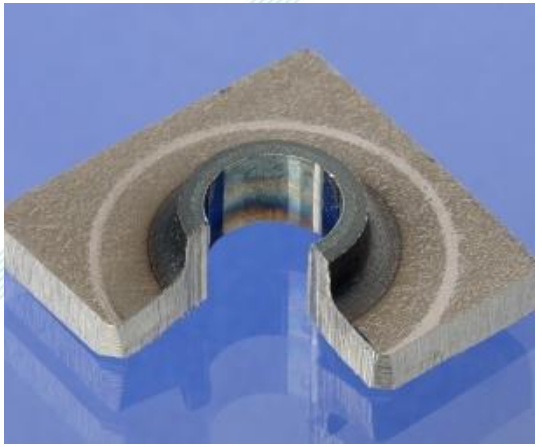

激光輔助成形

專利

相關技術已經申請/獲得下列專利：

1. 激光輔助沖壓高強度及輕量化零部件的方法及裝置 (China Invention Patent)
2. 激光輔助沖壓高強度及輕量化零部件的裝置 (China Utility Patent)
3. 激光輔助沖壓高強度及輕量化零部件的方法及裝置 (HK Short-term Patent)
4. 激光輔助沖壓高強度及輕量化零部件的方法及裝置 (HK Standard Patent)
5. 混合電磁感應及激光加熱的沖壓方法及其裝置 (China Invention Patent)
6. 混合電磁感應及激光加熱的沖壓裝置 (China Utility Patent)
7. 混合電磁感應及激光加熱的沖壓方法及其裝置 (HK Short-term Patent)
8. 混合電磁感應及激光加熱的沖壓方法及其裝置 (HK Standard Patent)

媒體

激光輔助成形製造
高強度及輕量化零部件

亮點：縮短工件加熱及冷却周期，避免熱工件的運輸問題 ・更好的尺寸精度及表面光潔度
・控制局部材料流動行爲 ・調整局部區域的厚度以及提高成形件的強度 ・可以減省運輸
壓生產步驟並提升效率20–40% ・增加模具壽命50%至數倍・節省材料及成本

香港生產力促進局材料及製造科技部

1.前言

在過去十年，人們對輕量化零部件的需求明顯增長。輕量化設計可實現經濟及環保駕駛。一般經驗法則告訴我們，每降低10%的車輛自身重量，耗油量能够降低高達8%，這意味一步減少二氧化碳的排放。現在的汽車制造商雖愈多花20歐元來減1公斤零部件重量。除了汽車行業外，其他行業如消費電子產品、醫療器材、家庭電器等產品要滿足市場對產品安全性及實際使用性的要求，也在積極量化方向發展。與其它金屬零件制造工藝相比，金屬成形工藝能够制造具有良好機械性能及表面光潔度的零部件，並且制造過程可實現低物耗及高產率等，而這些優勢是其它制造工藝如壓鑄、傳統金屬切削加工及粉末注射成形等不能達到的。因此，衝壓成形部件得已廣泛應用于各種產品。

2.應用高強度鋼和輕合金

應用輕合金材料是實現產品輕量化的方法之一。輕量化材料如鎂、鋁、鈦等已經在一些產品得到應用。在滿足同等性能情況下，與鋼材相比，鋁材能够減少30%–50%的重量，而鎂材能够減少40%–70%。除了使用輕合金材料之外，使用高強度鋼也能實現產品輕量化。保證產品擁有相同的剛度情況下，材料的強度越高，所需材料用量便可減少。相比傳統用電鍍鋅鋼及塗鋁鋼，用加彈簧鋼、貝氏體淬火鋼等高強度鋼制成的零部件厚度及重量能够減少一半。

重管高強度鋼及輕合金能够降低產品重量，但運用這類材料生產零件時却仍面臨挑戰。這類材料會顯著增加成形載荷，因此需要大型衝床進行生產。而且，成形載荷的增加會進一步加速了模具磨損、縮短了模具疲勞壽命，最終導致生產成本上升。同時，在常溫下，這類材料通常表現成形能力差，大變形區域易造成斷裂。這就限制了成形零件的幾何形狀。盡管現今可以結合多步工藝如先成形，後進火，再成形來制造形狀復雜的零件，但是成形期長，不利于生產。雖然傳統高溫成形工藝可提高材料的成形能力及降低成形載荷，但這方法會導致成形零件的表面質量變差，幾何形狀不精確，以及較長的生產周期。另外，當成形零件尺寸減少時，由于工件體積－面積比例(volume–to–surface ratio)變小，工件的成形溫度不易控制，溫度會在工件運送途中快速下降。

3.激光輔助成形加工技術

事實上，許多情況下我們紙需要在要求大變形的材料區域加溫即可避免很多成形問題。縮短加熱周期，精確控制溫度及加溫位置，以及避免熱工件的運輸是加工技術的關鍵。激光輔助成形技術可以滿足上述的條件。基本過程是，先用激光加熱工件待變形區域來提高其成形能力，然後透過成形模具使工件產生變形。由于以激光作爲熱源，因此溫度及能量易于控制，可實現材料局部加熱。該技術能够降低變形載荷（高達70%），簡化成形步驟，提高產量及改善模具壽命（可延長幾倍）。高强度能量激光及材料直接吸收能量遠可縮短整個工藝周期。與此同時，局部加熱能够降低工件尺寸變化和防止工件大面積氧化。此方法的另一個優勢在于能够實現定制熱處理板材（tailor heat–treated blank）來控制局部材料流動行爲，從而調整局部區域的厚度以及提高成形件的強度。學術界也展開了一些研究，發現鈦合金經過激光輔助成形後，其回彈性明顯降低（高達70%）。因此，激光在高強度鋼和輕合金的高溫成形加工方面的應用有着重大的發展前景。

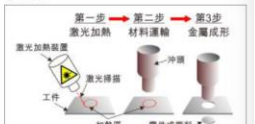

圖1: 激光輔助成形加工示意圖

圖2: 激光輔助成形技術可應用于許多不同種類高端值產品

4.案例

通過結合不同成形工藝如衝孔、深衝、彎曲及壓印等可以制成復雜的零件。運用傳統的衝孔工藝無法在厚度爲1mm的薄軍鋼上打出一個直徑爲1mm的孔，幾個同一至兩次衝壓後便會斷裂。然而，在激光輔助下，衝頭可以衝壓高强度鋼材超過6000次并帆有斷裂痕蹟（圖3）。在一般情況下激光輔助衝孔能够增加高亮度剪切面面積（圖4），衝件光滑程度與精密衝壓（fine blanking）近似，并且可降低成形載荷達70%以及延長刀具壽命達3倍。由于高强度鋼延展性差，其彎曲內徑必雖大于板材厚度。透過激光輔助彎曲加工，材料的成形能力明顯大大提升，通過該方法可實現傳統的彎曲內徑（圖5）。在深衝過程中，提高變形區域及周圍區域的材料流動性是十分必要的。在激光輔助下，材料的極限拉深比是傳統方法的兩倍（圖6）。傳統壓印不能够在高强度鋼壓痕十分之一的板材厚度，但在激光輔助下能够壓痕一半的厚度。因此，上述的激光輔助成形實驗結果表明該技術在高强度鋼和輕合金的成形加工方面的可行性。

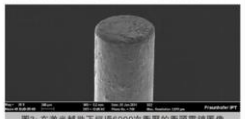
圖3: 在激光輔助下經過6000次衝壓的衝頭電鏡圖像
（德國Fraunhofer IPT 提供）

圖4: 傳統衝孔及激光輔助衝孔的對比
（德國Fraunhofer IPT 提供）

圖6: 傳統深衝及激光輔助深衝的對比
（德國Fraunhofer IPT 提供）

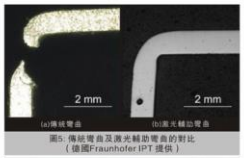

圖5: 傳統彎曲及激光輔助彎曲的對比
（德國Fraunhofer IPT 提供）

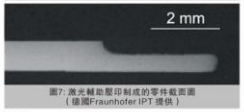

圖7: 激光輔助壓印制成的零件截面圖
（德國Fraunhofer IPT 提供）

5.結論

高强度–重量比(strength–to–weight ratio)材料，如鈦合金和高强度

下，這類材料

模具磨損快，

帶來產品表面

助成形技術可

工件特變形區

工件加熱及冷

局部加熱法能

同時能够實現

控制局部材料

成形件的强度

零件的生產成

高强度輕量化

促進傳統金屬

HKPC

類別的高增值

了解此項目中

事先生成 (852)

德國激光輔助漸進成形技術
提升輕量化金屬零件生產效率及品質

「輕量」是不少產品的其中一項重要要求，鎂輕強度高的金屬材料，例如：鋁合金、鎂合金、鈦合金、高强度鋼等，應用日趨廣泛，特別在汽車零部件、醫療設備、電子消費品、家庭電器等範疇。不過，傳統的沖壓成形技術應用於輕量化金屬以製造零部件時面對很多挑戰，包括：成形載荷過高，材料成形能力差等。

生產力局正與德國弗勞恩霍夫生產技術研究所（Fraunhofer Institute for Production Technology / IPT）合作，開發「激光輔助漸進成形技術」，在沖壓成形的過程中，於變形位置特別用激光加熱，既可降低成形載荷，亦可提升輕量化金屬的成形能力，有助提高生產效率20%至40%，延長模具壽命50%以上，以及節省材料及成本。

輕量化高強度材料 成形難度大

汽車零部件走向輕量化，有研究指出，車身重量每減輕10%，耗油量便可降低5%，減少二氧化碳排放，達致環保質駁。現在的汽車製造商願意多花20歐元，來減輕1公斤零部件重量，除了汽車之外，3C產品、醫療器材、家庭電器等也愈來愈講求輕量。

傳統的金屬成形工藝，相比壓鑄、切削加工、粉末注射成形等技術，產品無論在機械性能，表面光潔度或生產效益，也

設為優勢。不過，生產力局材料及製造科技部高級顧問黎偉華指出，輕量化方案常用的輕合金材料和高强度鋼，前者直接行金屬成形工藝（又稱「冷成形」），業界須克服成形載荷過高、材料成形能力差的挑戰，對產品品質、生產效率及模具保養，都造成不利影響。

最終業界一般會利用「熱成形」或「先冷成形、後退火，再冷成形」的方法，降低成形載荷及提升材料成形能力，但卻會衍生其他問題，包括：生產週期長、附容工件的機械性能、表面光潔度變差等。（詳見表一）

激光集中加熱 局部控制

解決工藝局限的關鍵，是集中加熱材料上需要變形的位置，達致局部控制的效果，而「激光」正是理想的局部加熱工具，黎偉華解釋：「激光能量集中，容易控制，板材加熱後提程高，是這種應用的不二之選。生產力局曾經嘗試用電腦考察時，發Fraunhofer IPT認識到『激光輔助漸進成形技術』的概念，有關這一步研究其可

表一：輕量化對金屬零部件製造的挑戰

冷成形問題	影響	一般解決方法的不足
成形載荷過高	• 需要大型沖床 • 加速模具磨損 • 縮短模具壽命，少於1,000次沖壓	熱成形 1. 表面光潔度變差 2. 尺寸精度差 3. 難以控制小型工件的冷却速度 4. 附容工件的機械性能 5. 生產週期長 先冷成形、後退火、再冷成形 1. 附容工件的機械性能 2. 生產週期長
材料成形能力差	• 變形位置容易斷裂 • 零件形狀設計受到限制	

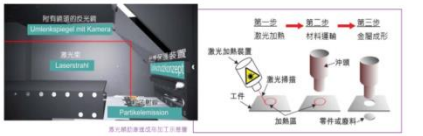

激光輔助漸進成形加工示意圖

行性，為香港企業引進這項新技術，促成了雙方今次的合作。」

按照Fraunhofer IPT的概念，最商可以用現有的沖床，在模具的適當位置，加裝激光加熱裝置，用以把工件特定部份加熱，然後在這熱力的輔助下進行沖壓，得出所需形狀的金屬零件。若多切的對，系統改裝的回本期約一年，視乎設備使用率而定。

成形載荷大降70%

通過激光的輔助，有助提升金屬成形技術的生產效率和經濟（詳見表二）。

生產效率方面，材料經過激光輔助加熱升溫之後，其成形載荷可大幅降低70%，由於激光能量直接加工件吸收，加熱和冷卻週期因而縮短，帶動生產效率提高，而成形後的工件仍產於常溫，避免壓縮熱工件的問題。另外，由於成形載荷降低的關係，減輕加壓對模具的磨損，延長模具壽命數倍，並節省模具的 維修保養時間及成本。

表二：「激光輔助漸進成形技術」的好處

生產效率	產品品質
• 降低70%成形載荷 • 能量直接吸收，縮短生產週期 • 生產效率倍增 • 避免壓縮熱工件的問題 • 延長模具壽命數倍 • 節省材料及成本 • 大量節省模具維修保養時間及成本	• 局部加熱，容易控制溫度和能量，工件尺寸更精準 • 可處理形狀複雜的零件 • 表面光潔度媲美精密衝件（Fine Blanking） • 可控制局部材料流動，調整成形件的局部厚度，加強工件剛度 • 減少撕裂個幼

至於產品品質，激光輔助最大的好處是，可以局部加熱工件，容易控制溫度和能量，工藝更精準和更重覆，可製造尺寸精準、形狀複雜的零件，利用這種方式提升材料的成形能力，工件的頻面光潔度可媲美成本高昂的精沖件（Fine Blanking）。

與德國科研機構合作開發

在「計劃」下，生產力局將獲德國Fraunhofer IPT提供的激光加熱裝置，開發激光輔助漸進成形技術，協助香港金屬製造業的核心能力。

雙方今次的合作，是生產力局首次與海外科研機構合作進行研究項目，黎偉華表示：「這種合作模式，對於本地的開發團隊而言，得到外國新設備的支持，研究工作不至於『足無措地，由零開始』，不但加快本地研發速度，更可減低風險，縮加科技商品化的成功機會，對於海外科研機構而言，合作亦成為他們開拓內地市場的機會，相信這種雙贏的合作模式，將為本局日後的科研工作開闢了新路向。」

「激光輔助漸進成形技術開發計劃」獲香港金屬製造業協會的支持，獲得三家先導企業資助應用該技術，王力生產新合金內部零部件，以電工製作參數和生產數據，掌握模具設計方法，並分析該項可行性。查詢：日本研究院制，查詢所需的相關資料包括《工藝指南》，供業界參考，有關該項及計劃的詳情，請聯絡黎偉華，電話：2788 5553，電郵：wwlai@hkpc.org，或鄭銘琳博士，電話：2788 5481，電郵：wwlinchan@hkpc.org。

HKPC

02

真空緊耦合超音速惰性氣體霧化

粉末冶金加工工藝

- 金屬注射成型
- 激光熔覆
- 粉末壓製成型
- 3D 金屬打印

① 創新性
② 定制化
③ 快速成型
④ 形狀複雜、一體化
⑤ 環保

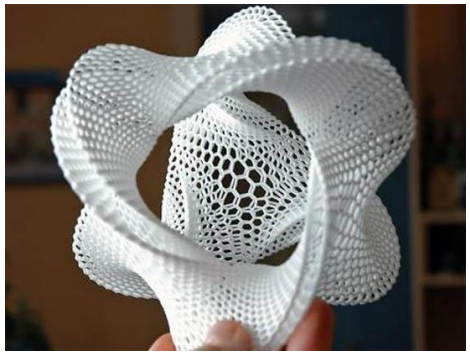

① 成本降低
② 越來越廣泛的應用

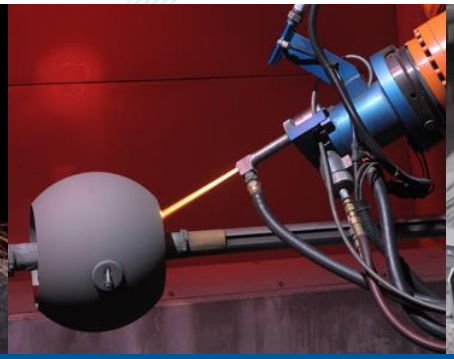

市場現狀

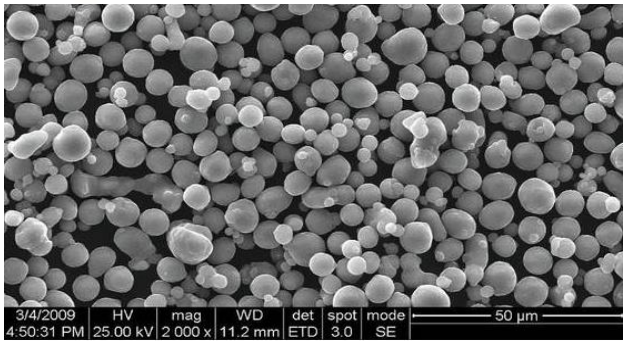

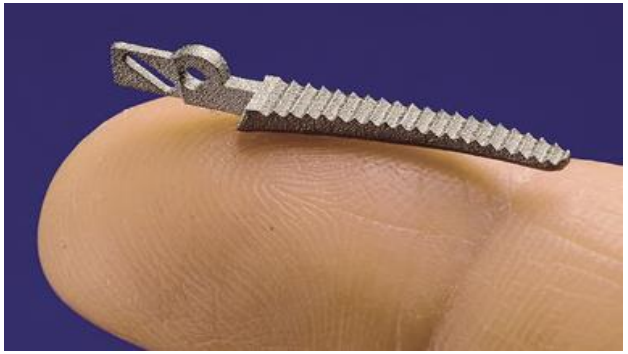

粉末

- 高質球形金屬粉末的市場需求上升
- 球形金屬粉末生產成本較高
- 現有氣霧化技術產量低且惰性氣體消耗量大

生產商

- 香港目前沒有金屬粉末生產商
- 大部分高質粉末來自進口（日本、德國）
- 運輸耗費人力及時間成本

霧化方法的比較

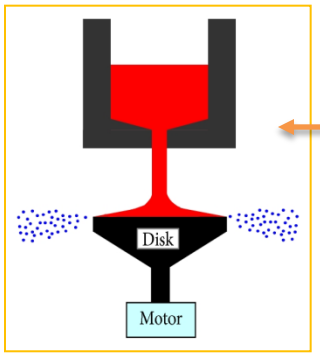

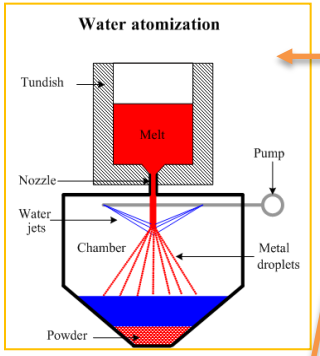

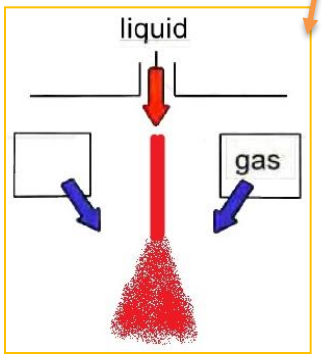

方式	粉末形狀	球形度	流動性	成本	顆粒大小
旋轉圓盤霧化	球狀	良好	良好	低	>35μm
水霧化	不規則形狀	N/A	較差	較低	>5μm
氣霧化	球狀	良好	良好	中等	>10μm

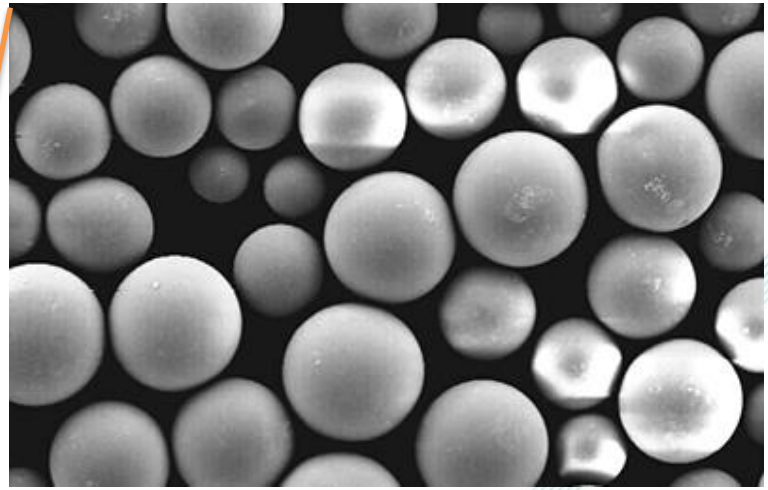

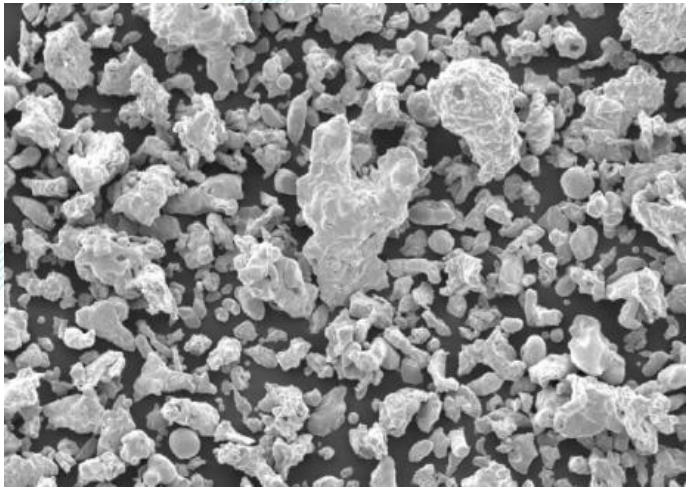

金屬粉末生產流程

1. 真空緊耦合超音速惰性氣體霧化系統
2. 粉末分級裝置
3. 攪拌機
4. 真空收集裝置

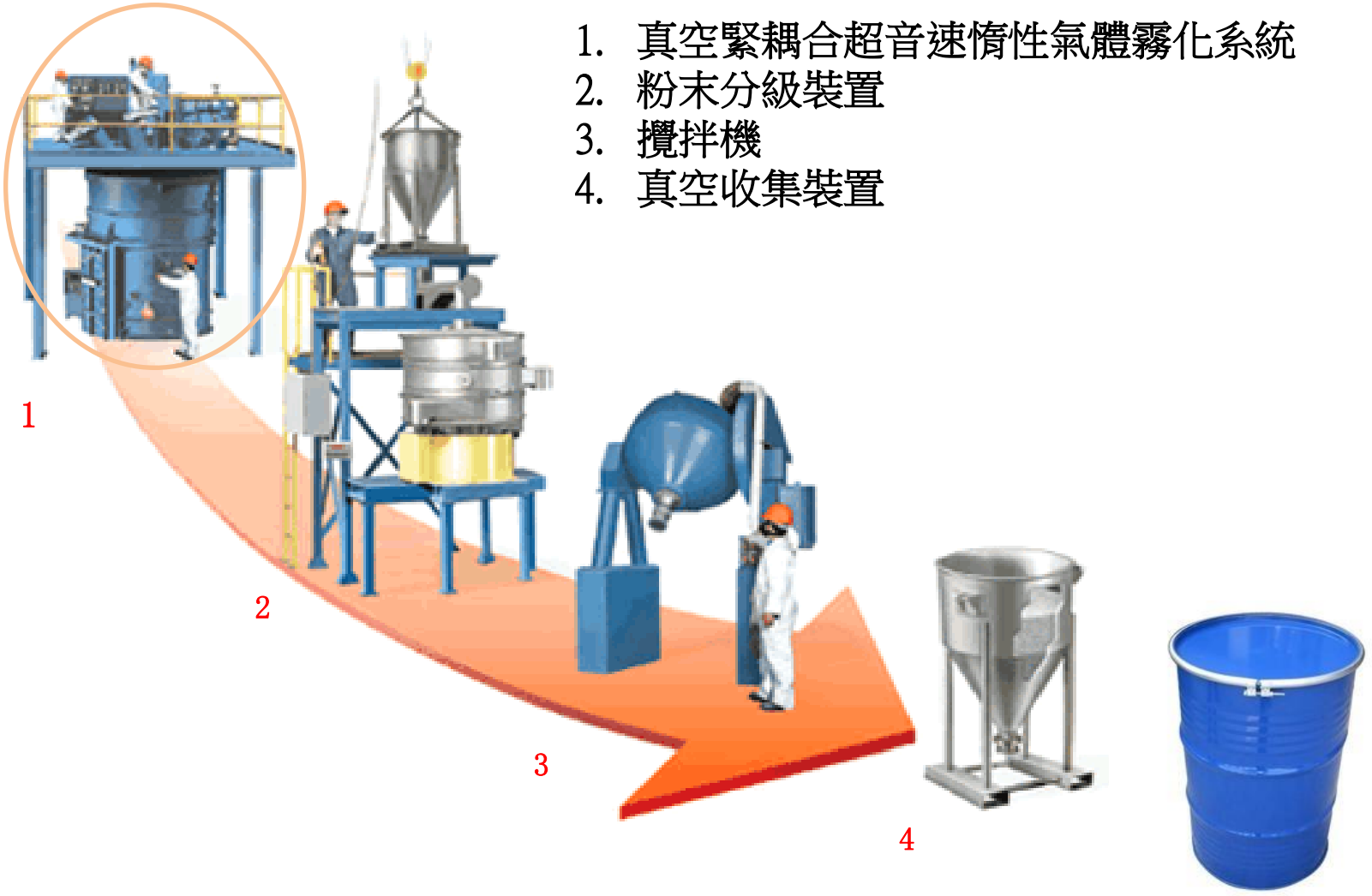

項目目的

1. 優化不銹鋼粉末生產過程
- 設計特殊氣霧化噴嘴
- 生產球形度和純度均較理想的粉末

2. 研究不同參數對系統的影響
- 成本：生產率，氣體消耗
- 質量：純度，粉末粒度分佈及球形度

3. 大力提高不銹鋼粉末的產率

項目意義

- 開拓高質粉末生產在本土的業務
- 幫助業務進入高增值粉末冶金行業，實現業務多元化
- 高質金屬粉末能夠直接從本地生產商購買
- 金屬粉末生產成本和售價能夠大大降低

真空緊耦合超音速惰性氣體霧化系統

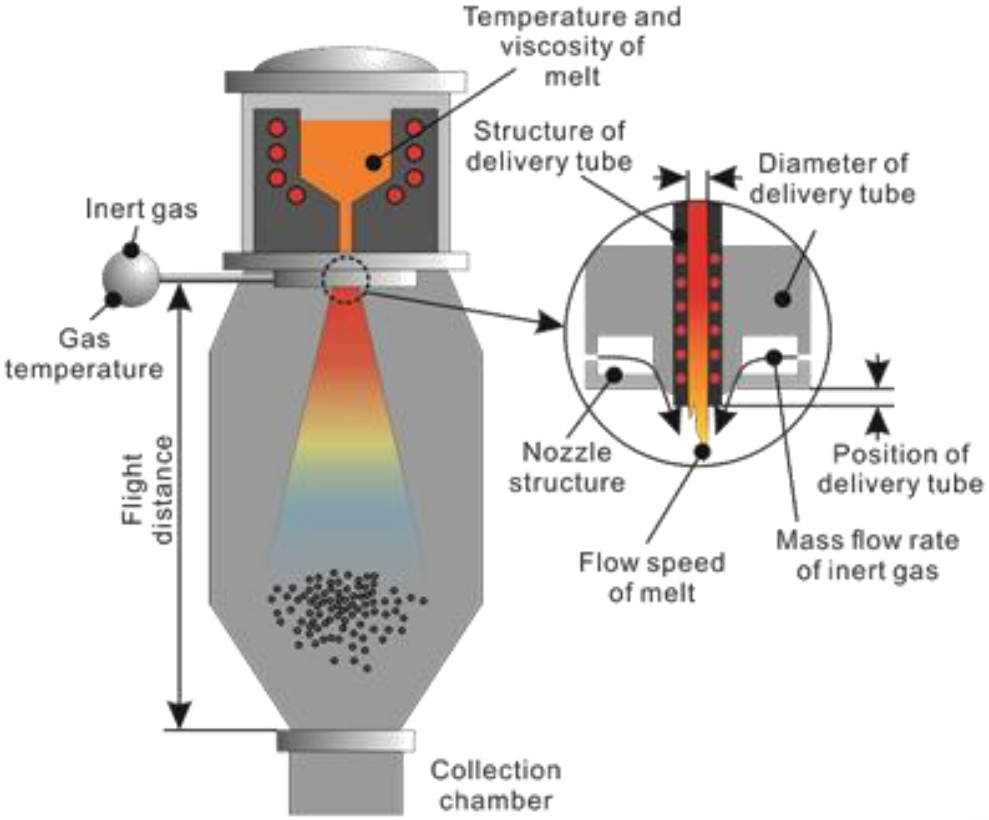

霧化系統設計

霧化過程

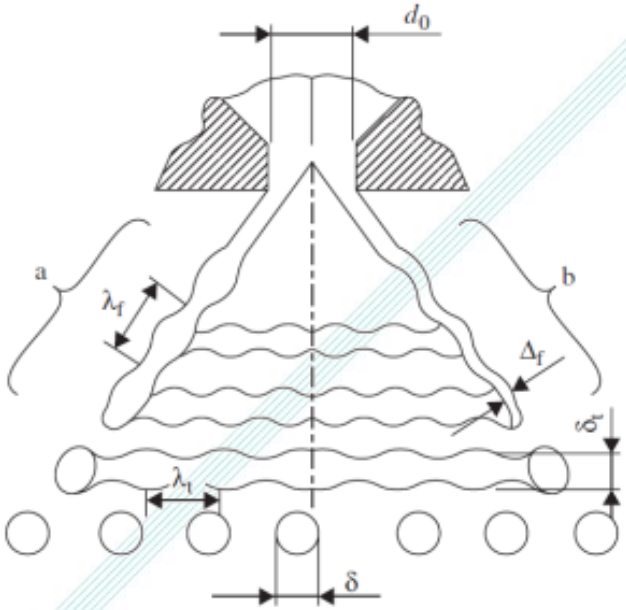

重要組成部分

- 熔煉系統
- 霧化系統

噴嘴設計

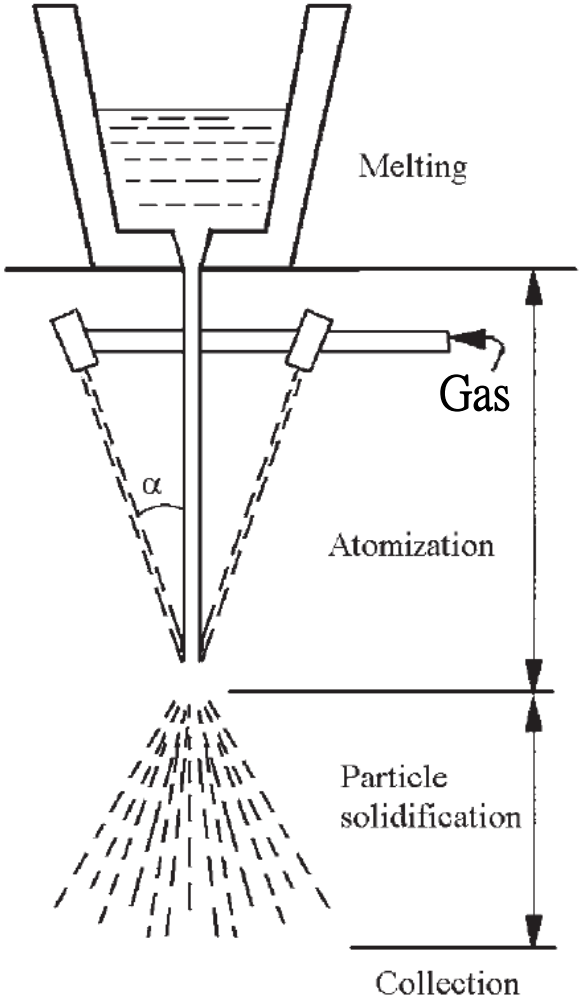

傳統噴嘴

- 氣體在接觸金屬溶液之前需移動較長距離
- 間接導致氣體的速度降低
- 霧化相同質量熔液時，消耗更多氣體

噴嘴設計

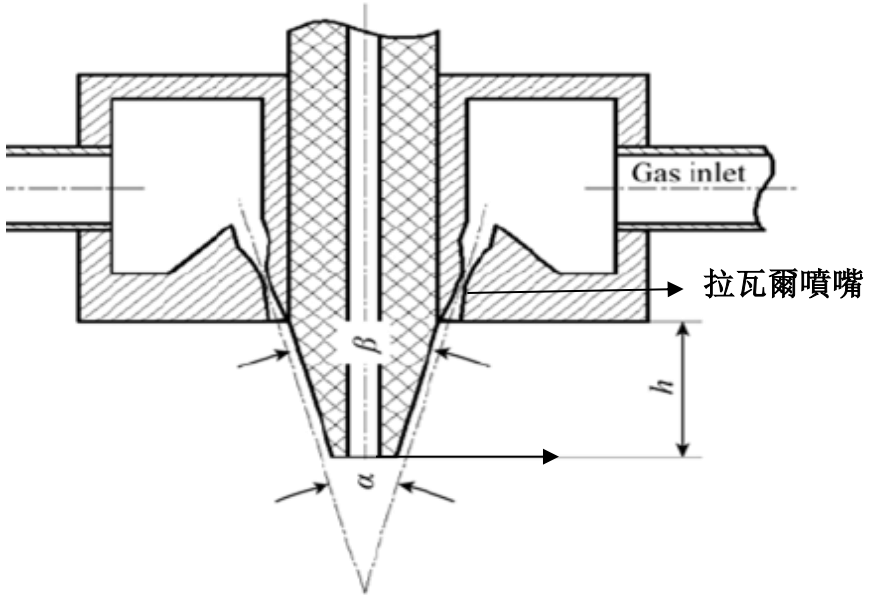

- 緊耦合
- 集成噴嘴和導流管
- 縮短氣體出口和熔體之間的距離
- 產生達到超音速的氣流
- 提高產量和質量
- 降低氣體消耗和生產成本

系統設計

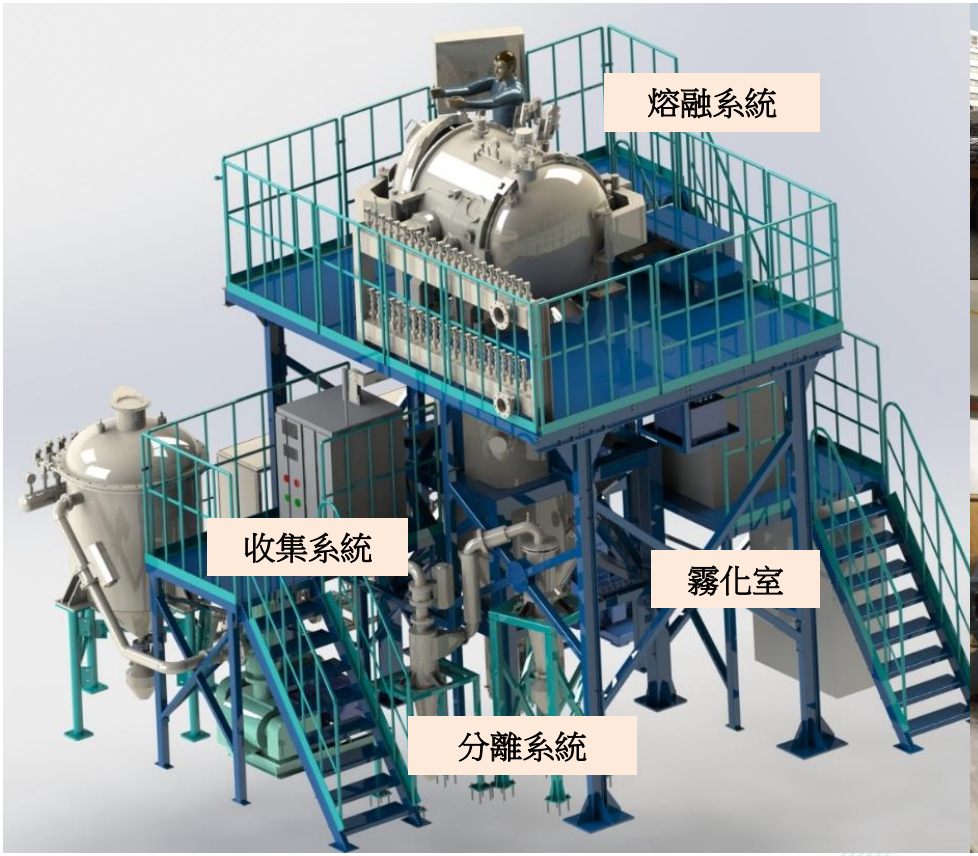

系統尺寸：長6.4m X寬6.3m X高5.9m

未來計劃

1. 提高系統熔煉能力

- 一個熔煉爐 → 兩個熔煉爐
- 熔煉和氣霧化同時進行

2. 提高氣體使用率和霧化率

- 預膜
- 提供旋流壓力 (a) / 離心力 (b)
- 增加熔融金屬和氣體的接觸面積

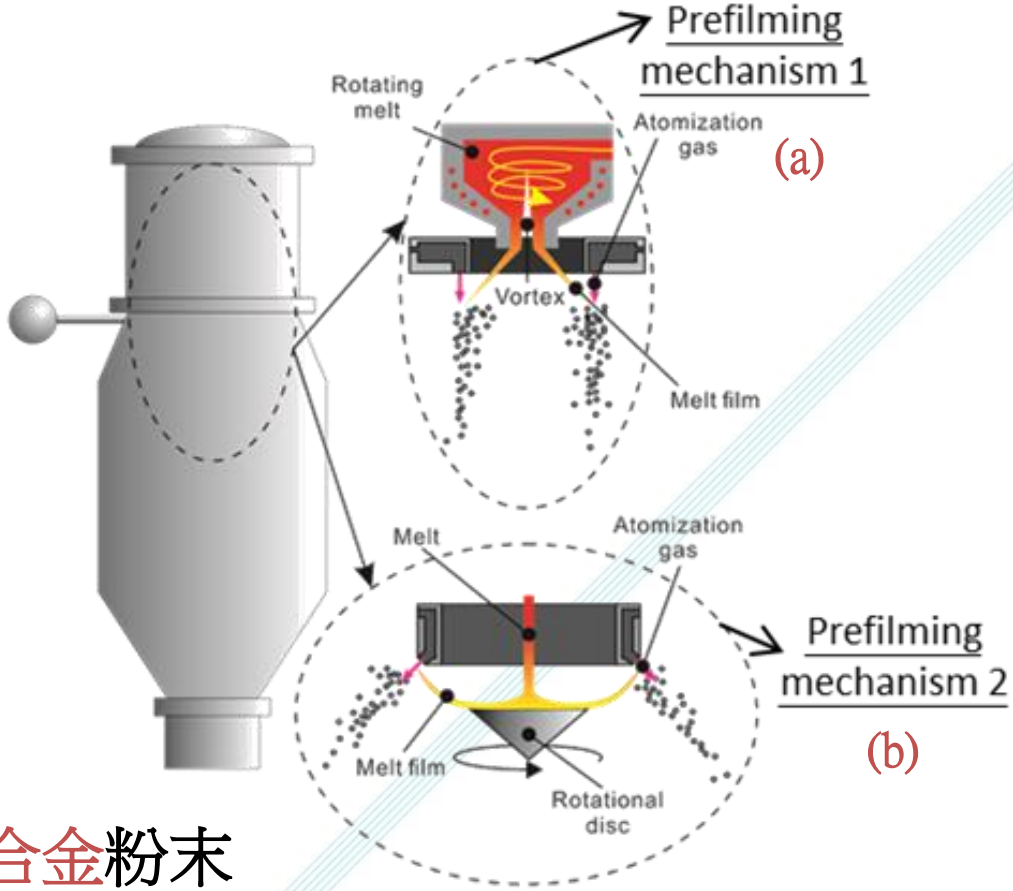

3. 無坩堝氣霧化系統熔煉鈦合金粉末

- 良好的強質比 & 生物相容性 & 合金記憶性…
- 滿足國內外市場不斷增長的對鈦合金粉末的需求

未來計劃

無坩堝氣霧化系統熔煉鈦合金粉末

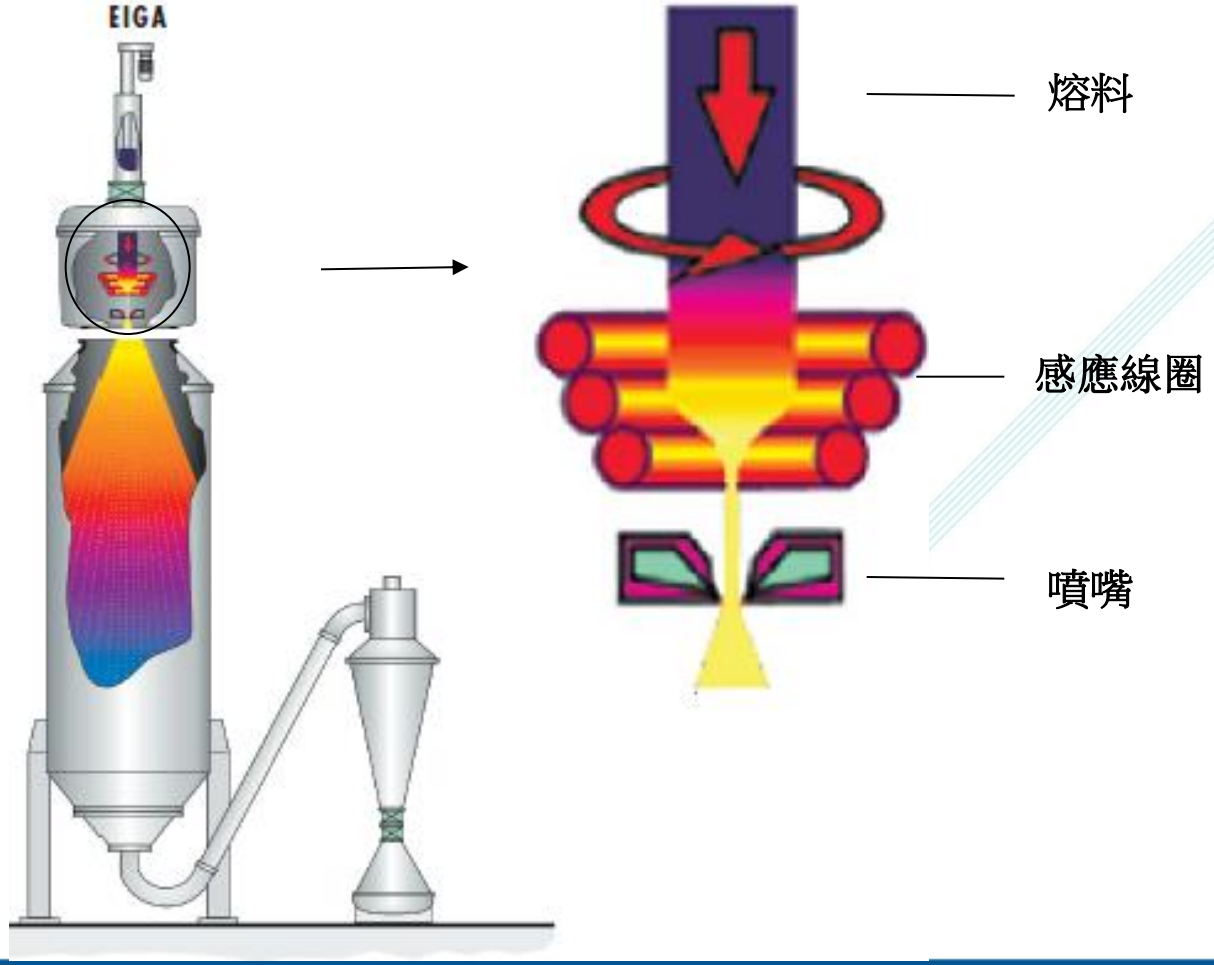

投資研發現金回贈計劃

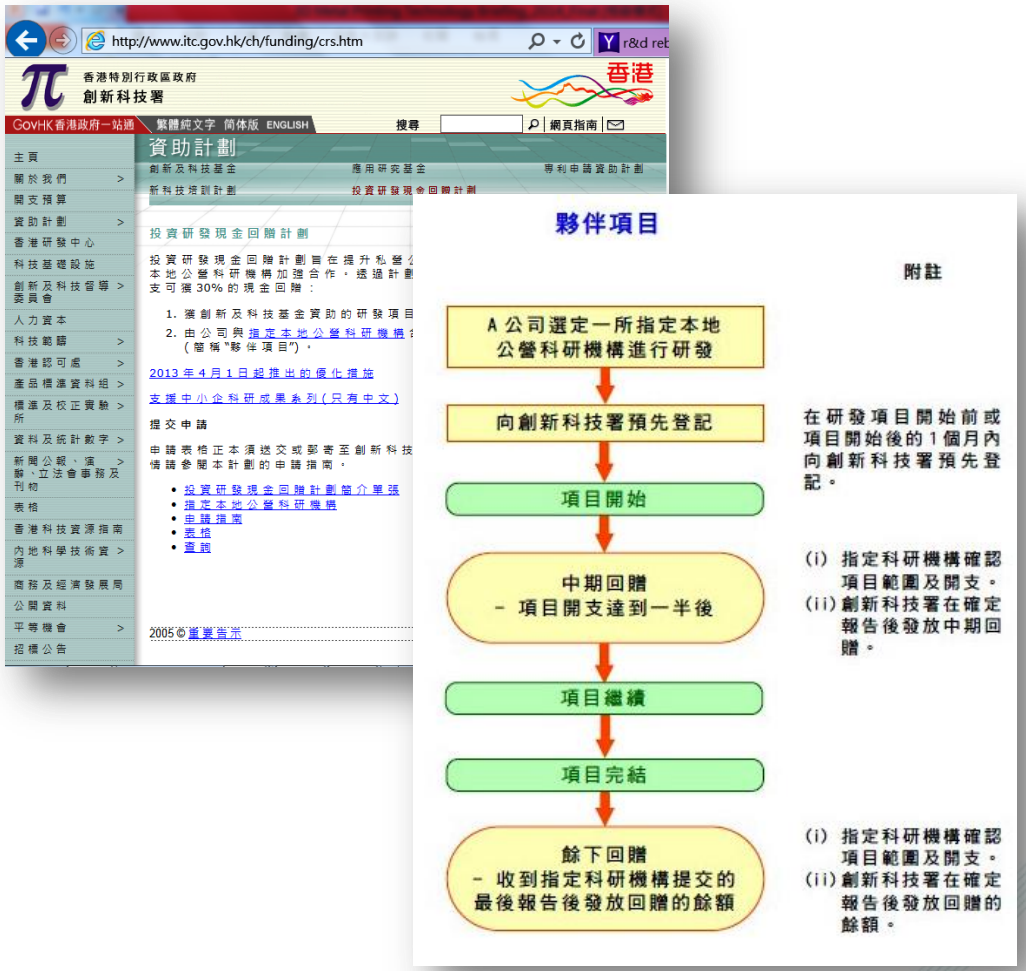

投資研發現金回贈計劃旨在提升私營公司的科研文化，並鼓勵他們與指定本地公營科研機構加強合作。透過計劃，公司在應用研發項目的開支可獲40%的現金回贈。

HKPC

創新及科技支援計畫

撥款向以產業為本及具商品化潛力的應用研發項目提供資助。

投資研發現金回贈計劃旨在提升私營公司的科研文化，並鼓勵他們與指定本地公營科研機構加強合作。計劃由創新科技署負責推行。

申請資格

公司若從事以下兩類應用研發項目，其開支可獲40%的現金回贈：

(1) 獲創新及科技基金資助的研發項目（簡稱"基金項目"），以及

(2) 由公司與指定本地公營科研機構合作，並由公司全費贊助的研發項目（簡稱"夥伴項目"）。

就夥伴項目而言，現金回贈將不適用於下列範疇：

✗ 沒有科研成份的產品改良/度身訂製和相關工作，普通的業務營運及商業活動，例如產品設計和一般系統自動化；以及

✗ 科技領域以外的研究項目，例如市場研究及管理研究。

申請程序

(1) 基金項目

(a) 就創新及科技基金的平台項目，公司在悉數繳付其承諾的贊助後可申請現金回贈。

(b) 就創新及科技基金下的合作項目(例如公司與基金各支付項目的一半開支)，公司可分兩期申請現金回贈，在研發開支超過該項目預期一半時申請中期現金回贈，待項目完成後再申請餘下回贈。

(2) 夥伴項目

(a) 公司委託指定科研機構進行應用研發項目後，在研發項目開始前應先向創新科技署預先登記其研發項目。

(b) 與上述(1)(b)類似，公司可分兩期申請現金回贈，申請時須提供指定科研機構的中期或最後項目報告。

申請表格正本須送交或郵寄至創新科技署投資研發現金回贈計劃組。申請須於有關研發項目完成後兩年內提交。

指定本地公營科研機構名單

(a)本地大學；

(b)創新及科技基金下成立的研發中心-

- 香港汽車零部件研發中心；
- 香港物流及供應鏈管理應用技術研發中心；
- 香港紡織及成衣研發中心；
- 納米及先進材料研發院；及
- 香港應用科技研究院；

(c) 香港生產力促進局；

(d) 職業訓練局；以及

(e) 香港生物科技研究院

投資研發現金回贈計劃的詳情、申請表格、申請指南，有關文件和指定科研機構的聯絡資料，可在 **http://crs.itc.gov.hk** 下載瀏覽。

詢問

香港添馬添美道二號
政府總部西翼二十一樓
創新科技署
投資研發現金回贈計劃組
電郵：crs-enquiry@itc.gov.hk
電話：3655 5725

例子

就一個100萬元的創新及科技基金的合作項目(例如公司與基金各贊助一半開支)，公司的實際開支大約只為25萬元(假設公司須繳付利得稅)：

	$
公司的研發支出	500,000
節省的利得稅*(16.5%)	(82,500)
現金回贈(40%)	(200,000)
現金回贈須繳付的稅項*(16.5%)	33,000
公司進行一個100萬元的研發項目的實際開支*	**$250,500**

*視乎公司是否須繳付利得稅。

二〇一六年二月

投資
研發
現金回贈計劃
Research and Development Cash Rebate Scheme
RESEARCH
DEVELOPMENT
π
創新科技署
Innovation and Technology Commission

例子

就一個100萬元的創新及科技基金的合作項目(例如公司與基金各贊助一半開支)，公司的實際開支大約只為25萬元(假設公司須繳付利得稅)：

	$
公司的研發支出	500,000
節省的利得稅*(16.5%)	(82,500)
現金回贈(40%)	(200,000)
現金回贈須繳付的稅項*(16.5%)	33,000
公司進行一個100萬元的研發項目的實際開支*	**$250,500**

*視乎公司是否須繳付利得稅。

HKPC

完

謝謝！

活動二

利用金屬發泡技術顯著減少產品重量研討會

由德國弗勞恩霍夫機床及成形技術研究所功能材質輕量化主管湯瑪士・協卡博士主講

THE FRAUNHOFER IWU

An Institute of the Fraunhofer-Gesellschaft

© Fraunhofer IWU
Prof. Neugebauer

IWP WERKZEUGMASCHINEN UND PRODUKTIONSPROZESSE

Fraunhofer IWU

The Fraunhofer-Gesellschaft
Locations in Germany

- 67 Institutes
- 23 000 employees, in majority scientists and engineers

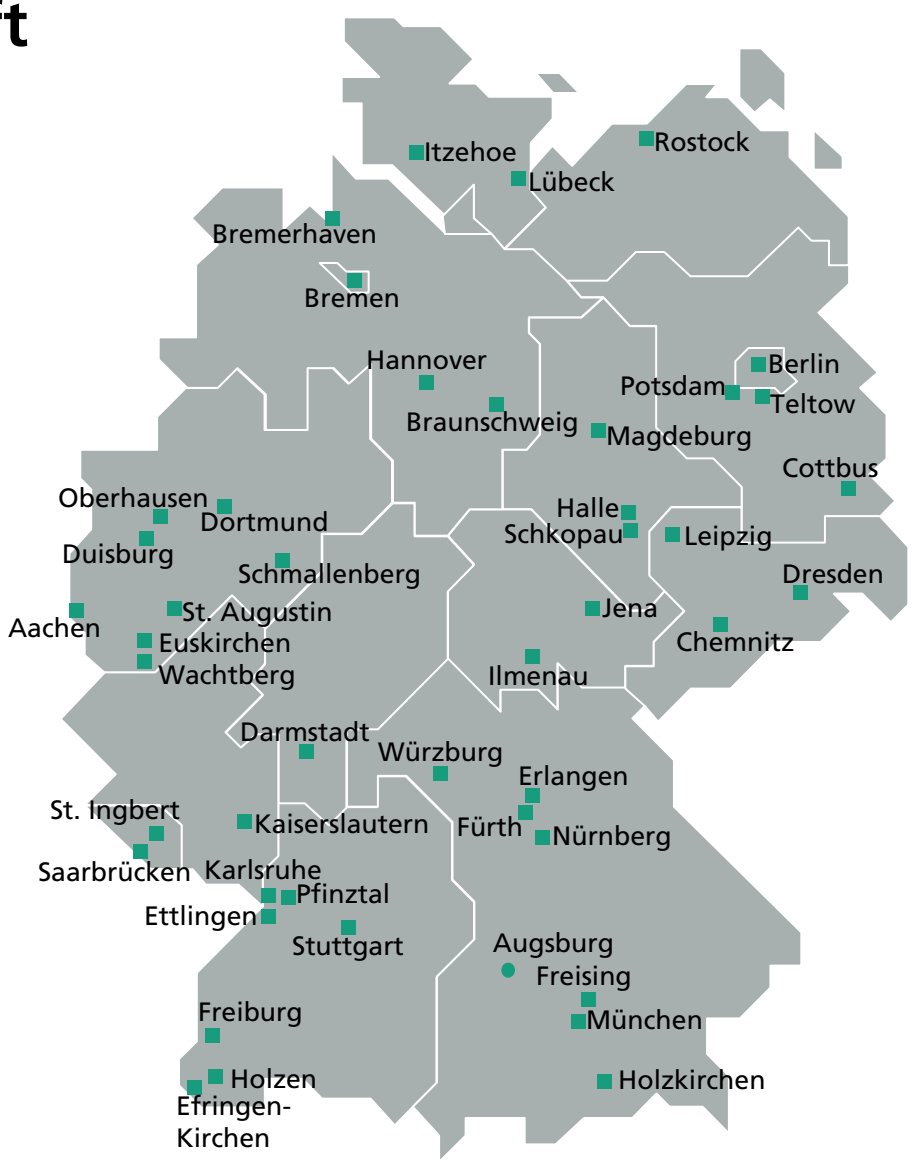

Archivierungsangaben

The Fraunhofer-Gesellschaft in Profile

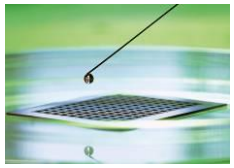
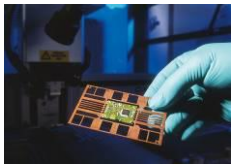
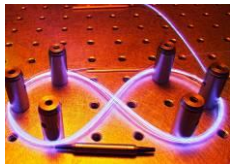

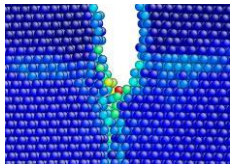

7 Groups:

- Information and Communication Technology
- Life Sciences
- Microelectronics
- Light & Surfaces
- Production
- Materials and Components – MATERIALS
- Defense and Security

Group Production
(founded 1998)

- IFF Magdeburg
- IML Dortmund
- IPA Stuttgart
- IPK Berlin
- IPT Aachen
- IWU Chemnitz / Dresden / Augsburg
- UMSICHT Oberhausen

Archivierungsangaben

IWP WERKZEUGMASCHINEN UND PRODUKTIONSPROZESSE

Fraunhofer IWU

Fraunhofer Research Units Worldwide

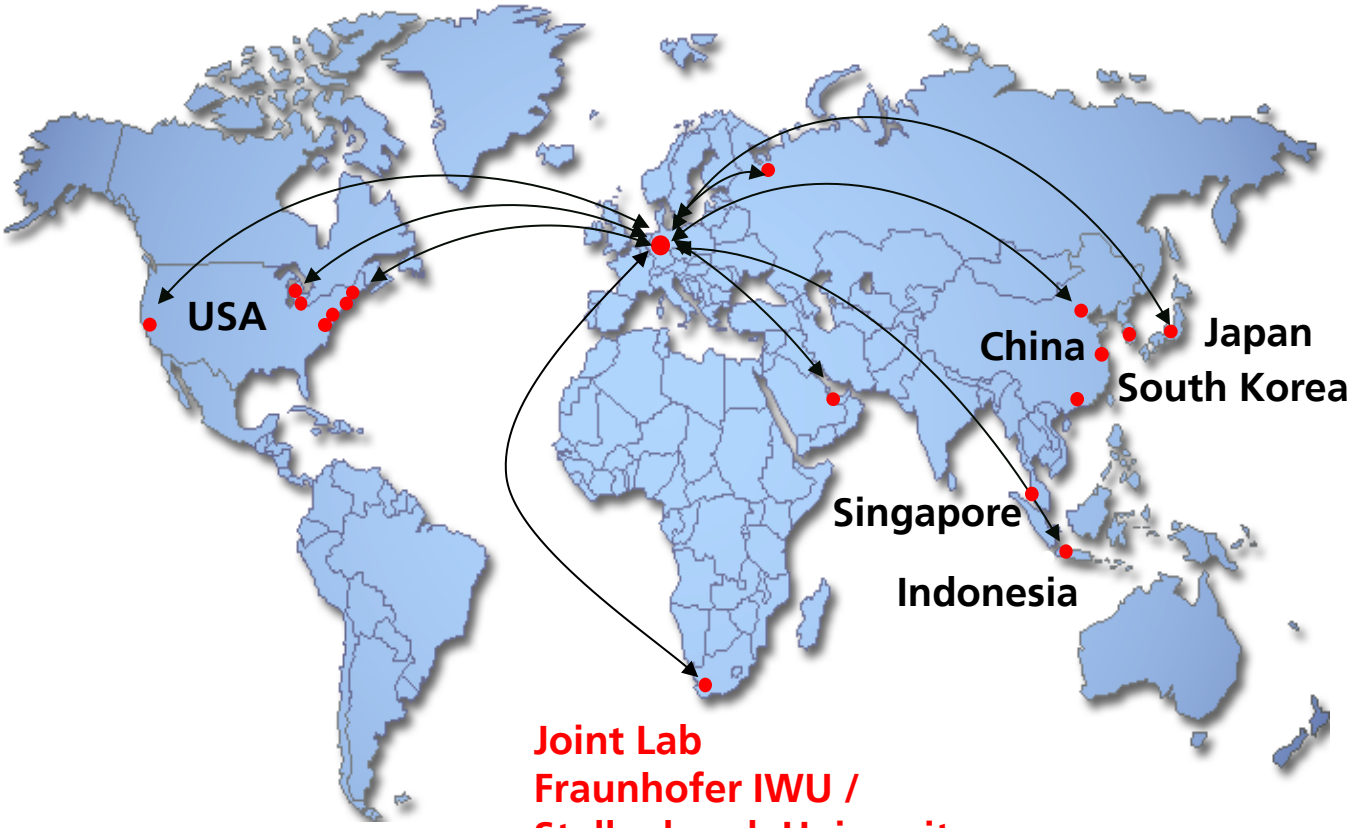

Archivierungsangaben

Institutional Network Production Engineering
Chemnitz – Dresden

Fraunhofer IWU
Chemnitz location

Fraunhofer IWU
Dresden location

IWP
TU Chemnitz

Archivierungsangaben

© Fraunhofer IWU

Structure and Regional Networks

Innovationscluster Mechatronischer Maschinenbau

PT PIESA

TR 39

eniPROD

SFB 692 HALS

Institutional Network Production Engineering Chemnitz – Dresden

Fraunhofer IWU Chemnitz
Prof. Neugebauer
Dr. Sterzing

- Forming Technology
- Production Systems
- Cutting and Precision Technique
- System Technology

Fraunhofer IWU Dresden
Prof. Neugebauer
Dr. Kunke

- Mechatronics
- Joining Technology
- Generative Technologies

Techn. Universität Chemnitz / IWP
Prof. Neugebauer
Dr. Koriath

- Virtual Reality
- Machine Tool Design
- Forming Technology
- Process Control Engineering

about 620 employees
> 40 million euro budget

about 60 employees
2,5 million euro third-party funds

Kompetenzzentrum Maschinenbau

VEMAS Verbundinitiative Maschinenbau Sachsen

MAINE

Archivierungsangaben

© Fraunhofer IWU
Prof. Neugebauer

IWP Werkzeugmaschinen und Produktionsprozesse

Fraunhofer IWU

THE FRAUNHOFER IWU
Core Competencies

© Fraunhofer IWU
Prof. Neugebauer

Core Competence
Machine Tools (1)

Machine tool and component design (forming and cutting)

- Machine tool concepts
- Design of function and accuracy determined components
- Development of handling equipment
- Parallel kinematic applications
- Determination of properties
- FEM calculation
- Optimization of thermal behavior

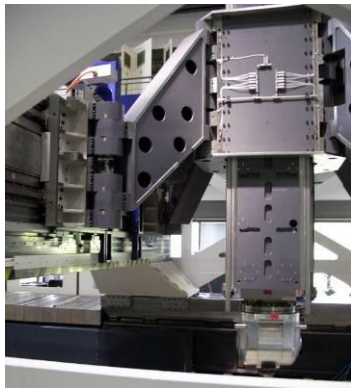

Archivierungsangaben

Core Competence
Machine Tools (2)

Lightweight design

- Structure optimization
- Metal foam applications
- Generative manufacturing of lightweight structures

Hydraulic systems

- Equipment and drives planning
- Hydraulic simulation
- Experimental testing

Archivierungsangaben

Core Competence
Mechatronics (1)

Machine tool control

- Mechatronic design
- Control of parallel kinematic machines, redundant machine tool axes
- Calibration methods
- Development and control of feed drive components

Data processing

- Video imaging
- Classification algorithms

Archivierungsangaben

IWP WERKZEUGMASCHINEN UND PRODUKTIONSPROZESSE

Fraunhofer IWU

Core Competencies
Mechatronics (2)

Adaptronics

- Application and optimization of active materials
- Design of sensor-actuator components
- Intelligent components
- Determination and optimization of acoustic bahavior
- Medical applications
- Generative manufacturing of adaptronic components and implants

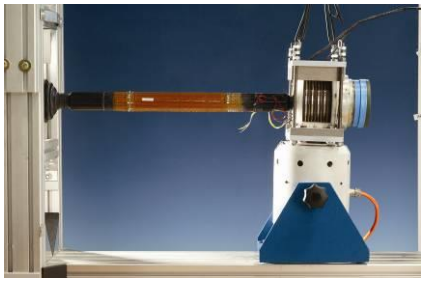

Archivierungsangaben

Core Competence
Cutting Technologies (1)

Process basis

- Modeling and simulation of cutting processes / optimization of cutting tools
- Design of modular tool systems
- Optimization of coating-substrate-systems
- Clamping of thinwalled workpieces

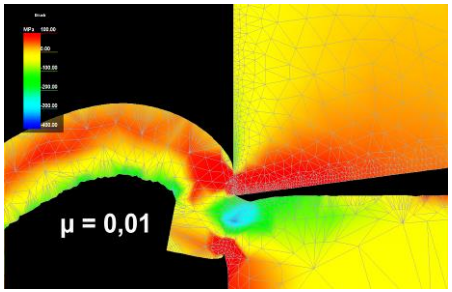

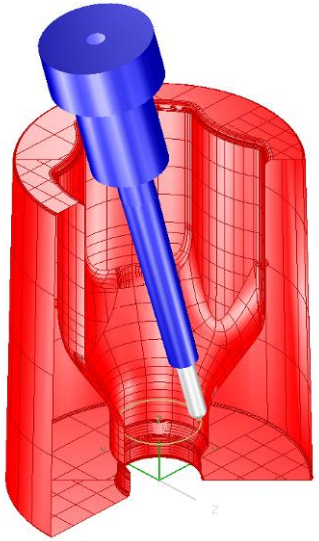

Experimental process and machine tool investigation

- Process monitoring
- Machine tool behavior

Archivierungsangaben

© Fraunhofer IWU

IWP WERKZEUGMASCHINEN UND PRODUKTIONSPROZESSE
Fraunhofer IWU

Core Competence
Cutting Technologies (2)

Process development

- Ultrasonic-assisted deep hole drilling
- Dry cutting (MQL)
- 5-axis milling, hard machining
- Optimization of process chains
- Process combinations / integration

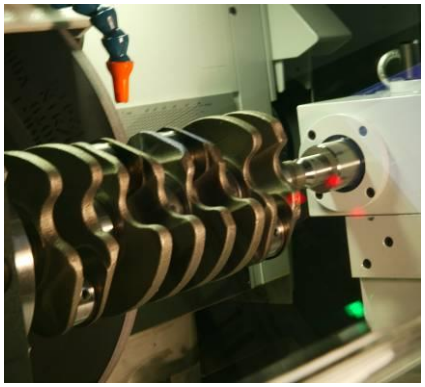

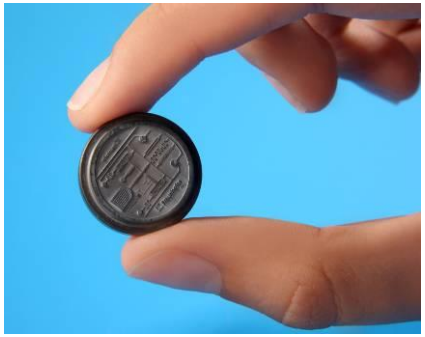

Micro and precision processing

- Development of components and technologies
- Tolls for microforming
- Microstructuring of surfaces
- Medical, optical and special automotive applications

Archivierungsangaben

© Fraunhofer IWU

IWP WERKZEUGMASCHINEN UND PRODUKTIONSPROZESSE

Fraunhofer IWU

Core Competence
Forming Technologies (1)

Sheet metal forming

- Controlled deep drawing process
- Hydroforming
- Forming at high velocities
- Fine blanking
- Development of technologies / tool concepts
- Generative technologies

Archivierungsangaben

IWP WERKZEUGMASCHINEN UND PRODUKTIONSPROZESSE

Fraunhofer IWU

Core Competence
Forming Technologies (2)

Bulk metal forming

- Forging
- Prototype forging die
- Cross rolling
- Spin extrusion
- High gear rolling

“interdisciplinary“

- Forming of alternative materials (highstrength steels and aluminum alloys, titanium, magnesium, patches…)
- Identification of specific forming parameters

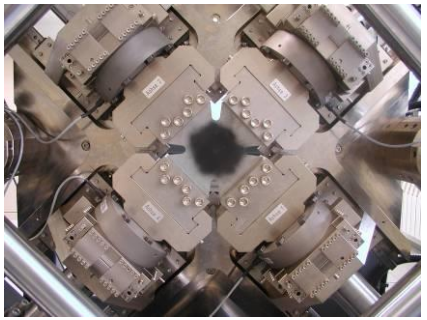

Archivierungsangaben

IWP WERKZEUGMASCHINEN UND PRODUKTIONSPROZESSE

Fraunhofer IWU

Core Competence
System TechnologY (1)

Facility and component design

- Concepts for joining and assembling systems
- Development and optimization of function determined components
- Development of handling systems

Joining technologies

- Thermal joining technologies
- Joining by forming (development, modification and integration of technologies)
- Process monitoring

Archivierungsangaben

Core Competence
System Technology (2)

Assembling technique

- Weak point analysis
- Process optimization
- Databasis

E-Services

- Production data management
- Teleservice
- Data mining

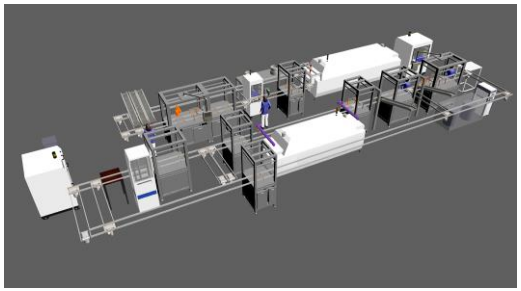

Archivierungsangaben

Global trend for metal carbon composites

Dr.-Ing. Thomas Hipke

Fraunhofer – IWU Chemnitz, Germany

Dipl.-Ing. Carsten Lies

© Fraunhofer IWU

IWP WERKZEUGMASCHINEN UND PRODUKTIONSPROZESSE

Fraunhofer IWU

Global trend for metal carbon composites

Mikro Scale

Makro Scale

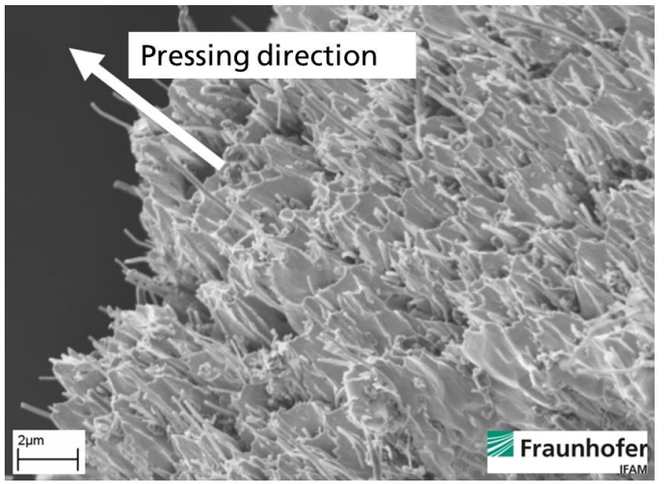

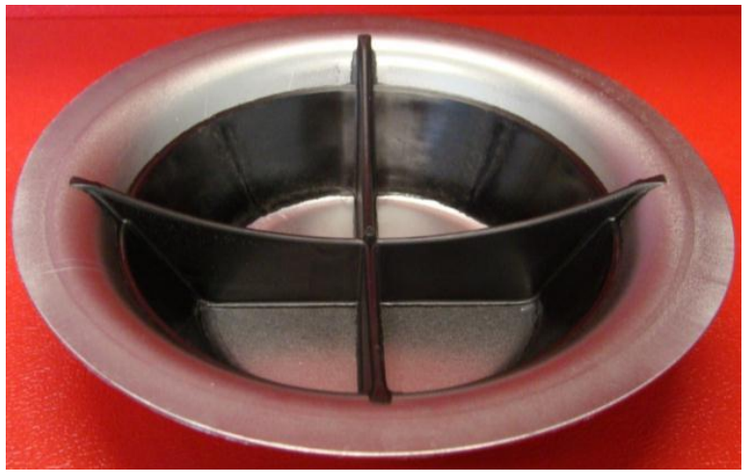

Dipl.-Ing. Carsten Lies

© Fraunhofer IWU

IWP WERKZEUGMASCHINEN UND PRODUKTIONSPROZESSE

Fraunhofer IWU

Lightweight Design by Hybrid Construction

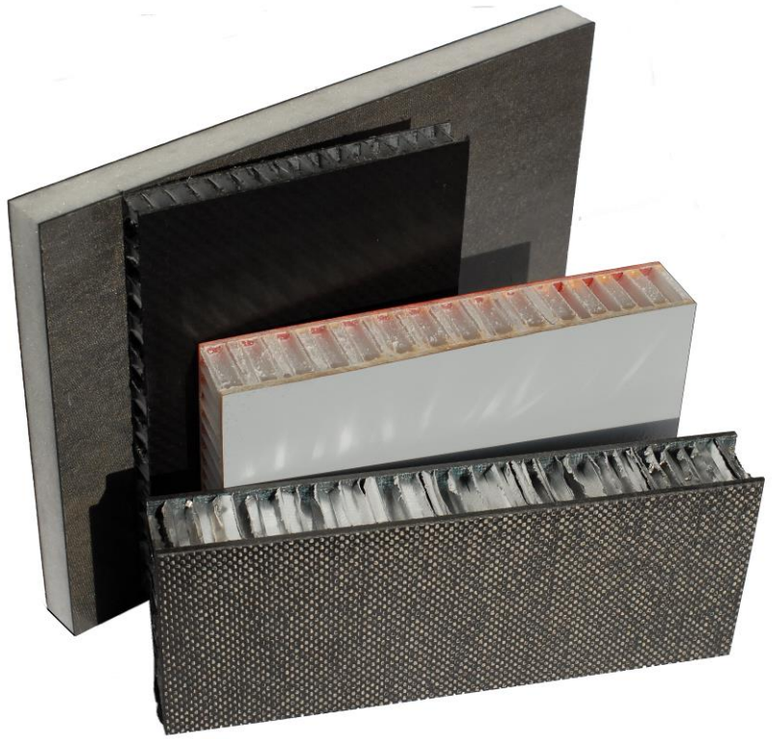

Dipl.-Ing. Carsten Lies

© Fraunhofer IWU

IWP WERKZEUGMASCHINEN UND PRODUKTIONSPROZESSE

Fraunhofer IWU

Why we need hybrid construction????

Metals: cheep, very common, stiff and strength

FRP: very good light weight behaviour, corrosion resistent

Well designed combination will bring the best results!

“The right material on the right place”

Dipl.-Ing. Carsten Lies

© Fraunhofer IWU

Applications – Machine Tool Systems / Plant Engineering

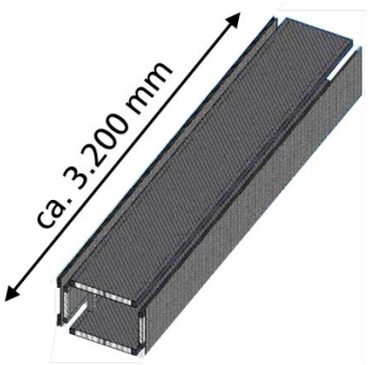

- 50 % mass
+ 100 % stiffness

crossbeam of a laser-cutting device

CFRP – machine slides and cross beam

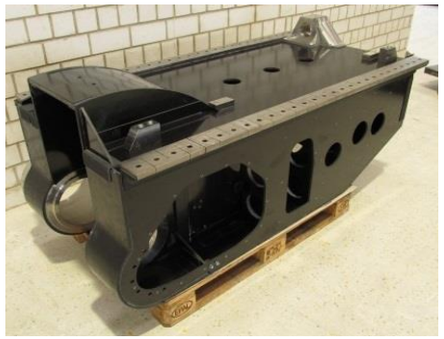

z-slide of a milling machine
1800 mm x 890mm x 760 mm

- 64 % mass

z-slide of a milling machine for
high dynamic machining
1.160 mm x 440 mm x 280 mm

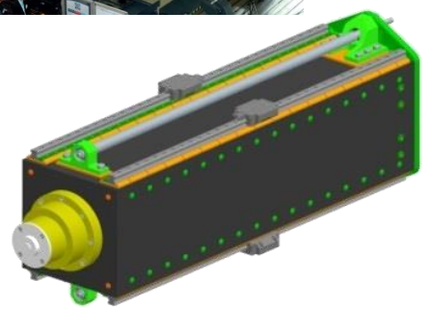

- 25 % mass
+ 150 % stiffness

Dipl.-Ing. Carsten Lies

© Fraunhofer IWU

IWP WERKZEUGMASCHINEN UND PRODUKTIONSPROZESSE

Fraunhofer IWU

Applications – Automotive Engineering

FRP/Metal – merge technologies

hydroforming and injection molding

deep drawing, injection molding and forming using molten plastic

CFRP/Metal – structural components

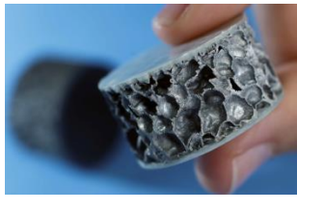

lightweight rim and wishbone made of CFRP

CFRP – equipment for body construction

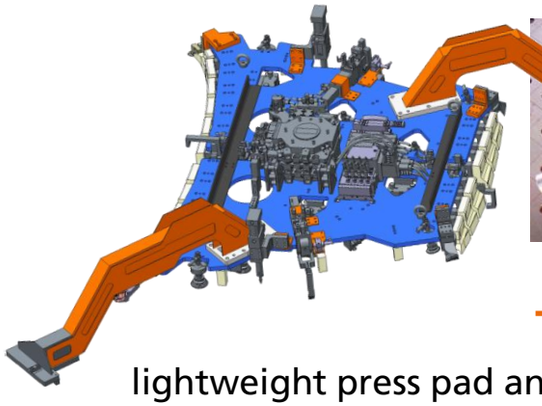

- 50 % mass

lightweight press pad and welding arm made of CFRP

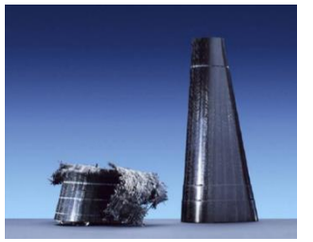

+ significant mass reduction

+ energy absorption

Dipl.-Ing. Carsten Lies

© Fraunhofer IWU

IWP WERKZEUGMASCHINEN UND PRODUKTIONSPROZESSE

Fraunhofer IWU

Approach: Combination of CFRP, GFRP and metal foam

FhG-IWU offers

- Design and simulation of complete assemblies
- Technology development
- Manufacturing and testing of demonstrators

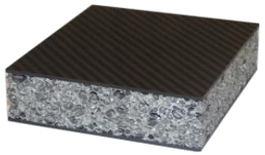

e.g.: CFRP – based frame for future electric car

- Up to 50% of saved weight
- Hybrid construction Aluminum/CFRP for high crash safety
- High exposure by low weight

knot reinforcement by aluminum foam

frame made of CFRP-profiles

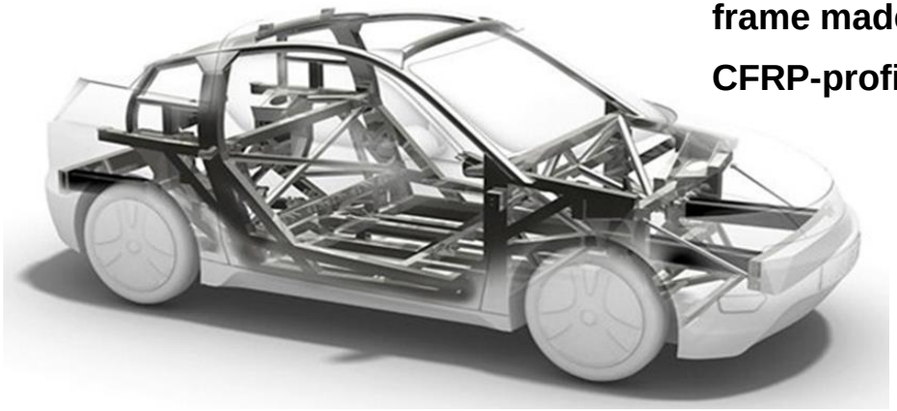

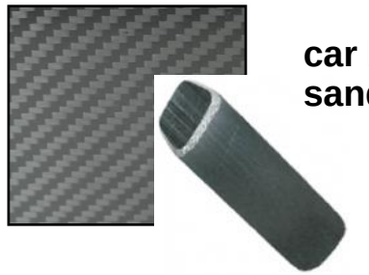

car body floor made of CFRP-sandwiches and profiles

Dipl.-Ing. Carsten Lies

© Fraunhofer IWU

Research Highlights

Aluminum Foam – PUR - Sandwiches

→ lightweight material for highest requirements

→ material combination of an aluminum foam core and polyurethane cover sheets with glass or carbon fiber reinforcements

load platform of the KULAN lightweight vehicle

front hood of a utility car

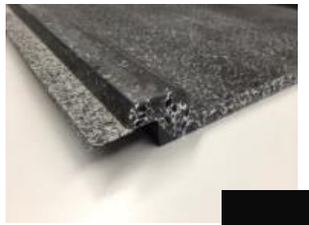

lightweight design and shape flexibility

Examples of Applications:

- floor panels for light utility cars
- hoods/covers for vehicles
- reinforced components

* … in cooperation with PESTEL PUR-Kunststofftechnik

Dipl.-Ing. Carsten Lies

© Fraunhofer IWU

IWP WERKZEUGMASCHINEN UND PRODUKTIONSPROZESSE

Fraunhofer IWU

Hybrid door

- **Integral concept in combination of a door frame and the mounting device**
- **Using of natural fibers for the outer shell**

Conventional

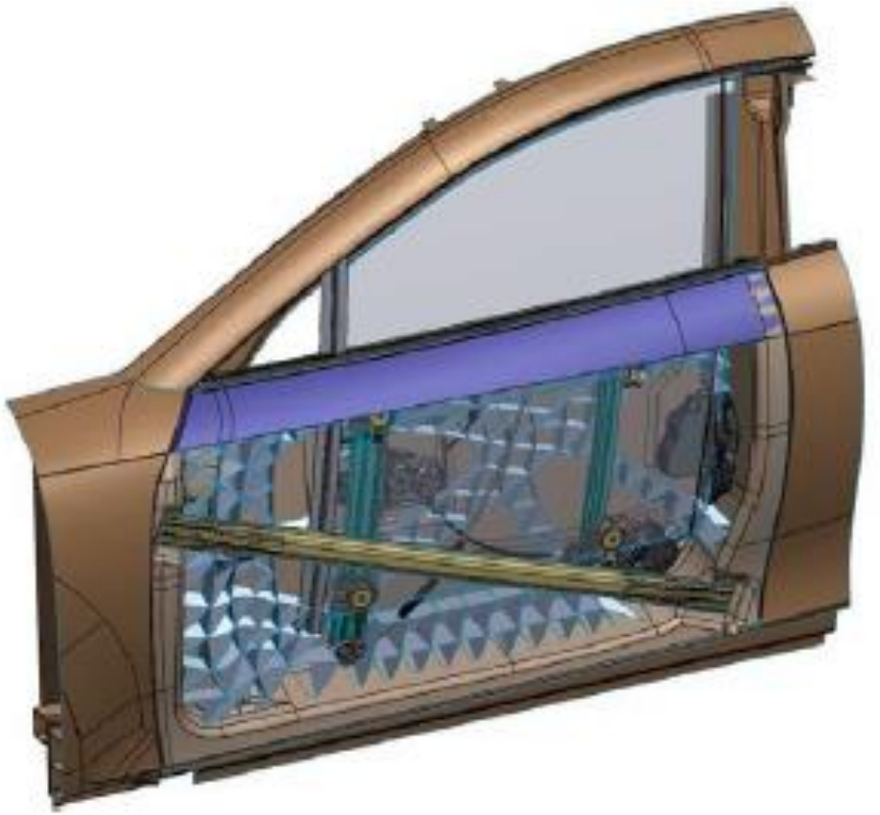

new design

Dipl.-Ing.

© Fraunhofer IWU

IWP WERKZEUGMASCHINEN UND PRODUKTIONSPROZESSE

Fraunhofer IWU

Hybrid door

Integrated metallic joining elements

Rips made from long fiberreinforced thermoplast

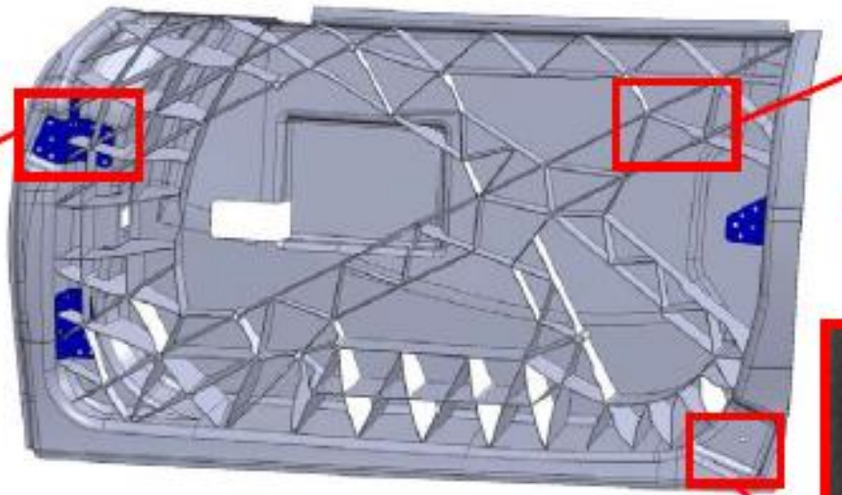

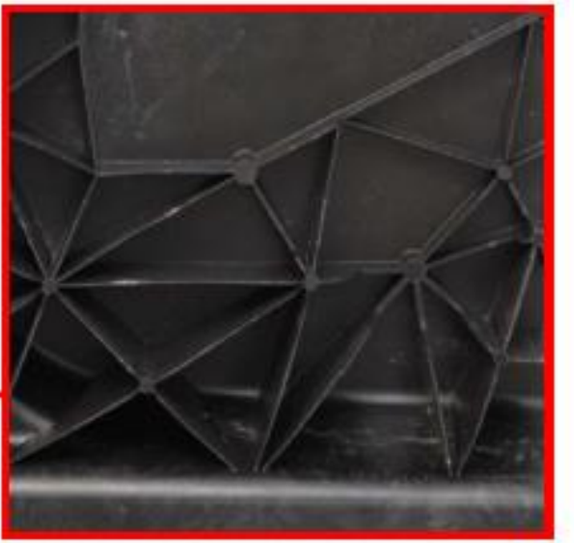

Shell made from natural fibers composites

Dipl.-Ing. Carsten Lies

© Fraunhofer IWU

IWP WERKZEUGMASCHINEN UND PRODUKTIONSPROZESSE

Fraunhofer IWU

3D Hybrid

Investigation of innovative Steel-Carbonfiber-Hybrid-Structures for using in the car body

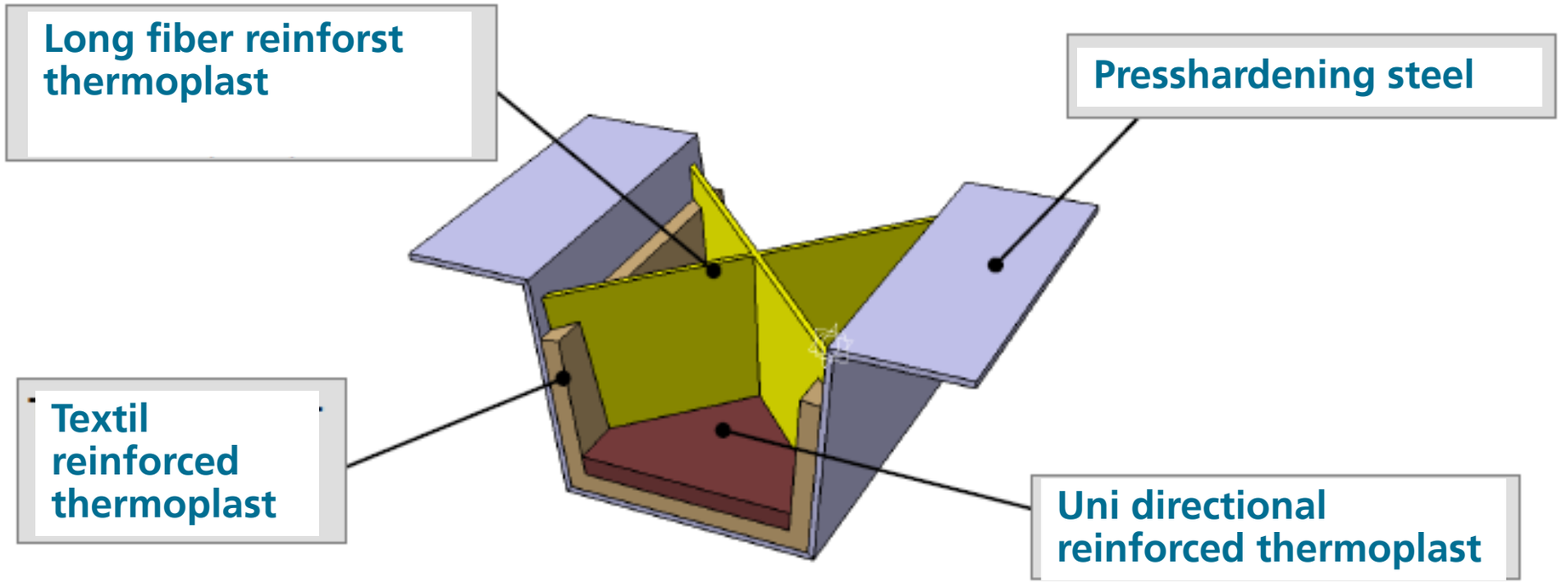

© Fraunhofer IWU

IWP WERKZEUGMASCHINEN UND PRODUKTIONSPROZESSE

Fraunhofer IWU

InEco

InEco – project (German consortium)

Partner

ThyssenKrupp

Institut für Leichtbau und Kunststofftechnik

LZS

DEKRA

FES GmbH Fahrzeug-Entwicklung Sachsen

Gefördert aus Mitteln der Europäischen Union und des Freistaates Sachsen.

Europa fördert Sachsen.
EFRE
Europäischer Fonds für regionale Entwicklung

SAB Sächsische AufbauBank

Dipl.-Ing. Carsten Lies

© Fraunhofer IWU

IWP Werkzeugmaschinen und Produktionsprozesse

Fraunhofer IWU

InEco

Targets:

- Development of new combinations between steel and carbon fibers for leight weight design
- Research on new high strength steels and korresponding CFRP with development of the joining technology
- Development of automated manufacturing technologies for the CFRP and for the compound
- Prototypical manufactruing of components of the in Eco car
- Technology transfer of all results into the industry

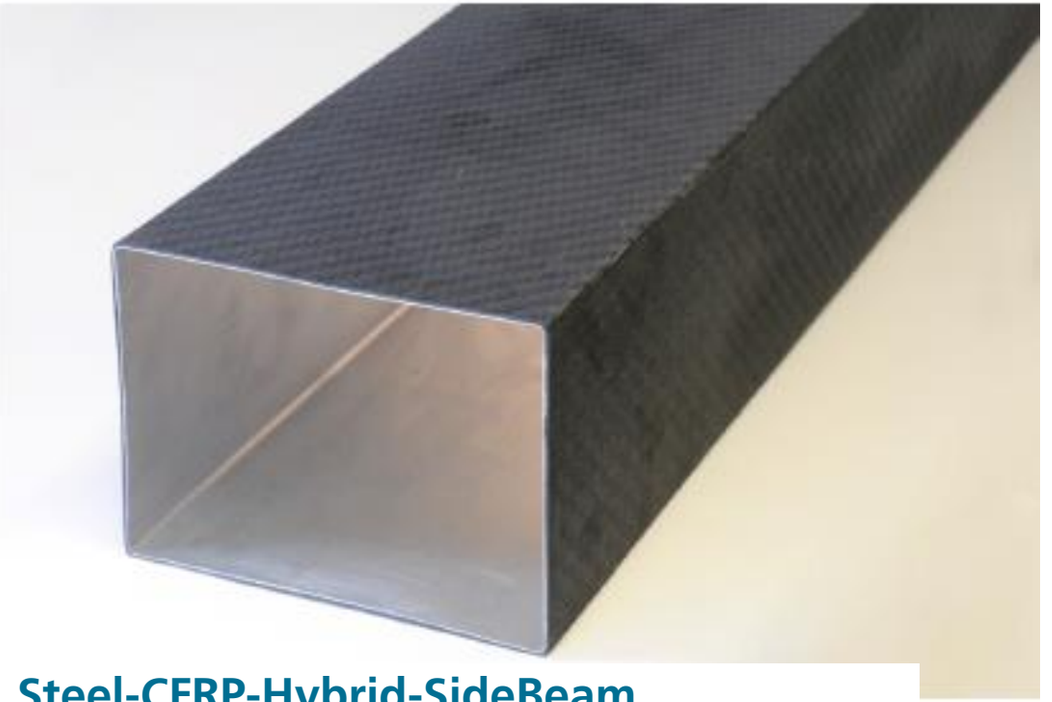

Steel-CFRP-Hybrid-SideBeam

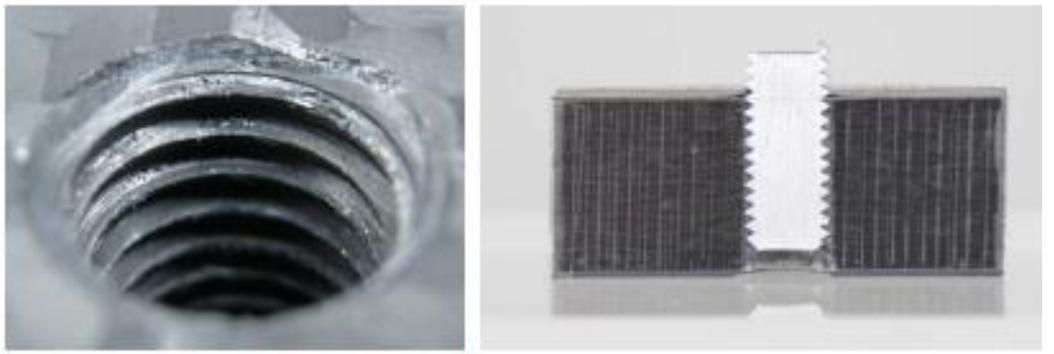

Hybrid joining technology

Dipl.-Ing. Carsten Lies

© Fraunhofer IWU

IWP WERKZEUGMASCHINEN UND PRODUKTIONSPROZESSE

Fraunhofer IWU

CRP-aluminium-riveting

Prinziple

- Cutting CRP and joining by deformation in aluminium

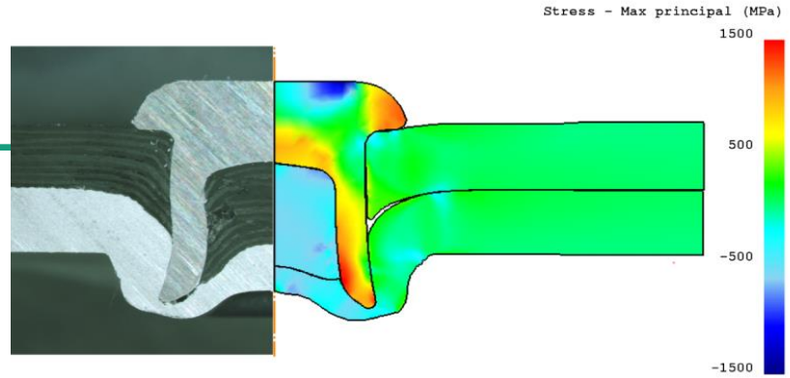

Comparison between experimental and simulated section

Possible Applications

- Reinforment details of passenger car's with CRP

Benefits

- Fixation until curing of adhesive
- Avoiding destruction of all carbon fibers with Crown Rivet
- Mixed compounds

Boundary conditions

- Lap joint
- Access from both sides
- In case of access from one sides only (crown-rivet) high stiffness in the structure and high velocity

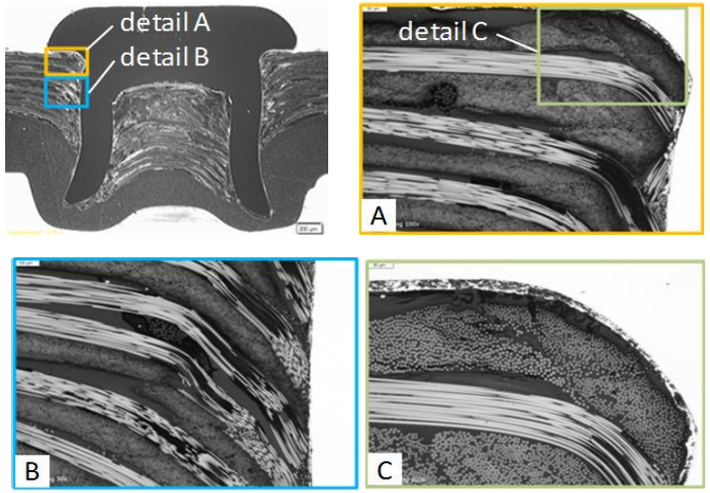

Micro section analysis

Virtual forecast

- Very good numerical predictability
- Process risks robustness analysis to estimate

Needs

- Rivet-friendly redesign
- corrosion protection

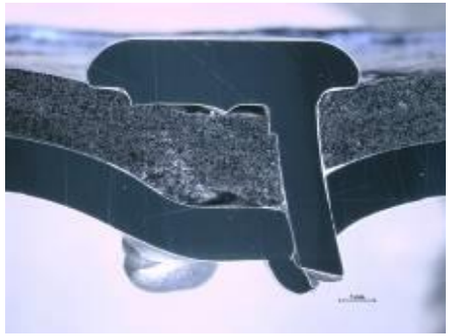

Crown Rivet /

Cross section with one side access

Dipl.-Ing. Carsten Lies

© Fraunhofer IWU

Dr. Reinhard Mauermann, division director joining department
Fraunhofer IWU Dresden; Tel.: 0049 351 4772-2400
reinhard.mauermann@iwu.fraunhofer.de

METAL/ CARBON COMPOSITES DEVELOPMENT, APPLICATIONS AND NEW BUSINESS OPPORTUNITIES – POWDER METALLURGICAL APPROACH

Th. Hipke[1]

[1] Fraunhofer Institute for Machine Tools and Forming Technology, Chemnitz

Thank you for your attention

Contact: E-Mail: Thomas.Hipke@iwu.fraunhofer.de (head of department)

Dipl.-Ing. Carsten Lies

© Fraunhofer IWU

The contents of this presentation may not be copied and/or distributed without permission of the author! Please note references at the end of the presentation!

CELLULAR METALS

Part I – Processes of manufacturing

© Fraunhofer IWU
Prof. Neugebauer

The contents of this presentation may not be copied and/or distributed without permission of the author! Please note references at the end of the presentation!

CONTENT

- Species of cellular metals and structures
- Cellular metals and structures
  - Open-cellular foams/structures
  - Closed-cellular foams
  - Hollow sphere structures
  - Fiber structures
  - Wire structures
  - Porous paper

Archivierungsangaben

The contents of this presentation may not be copied and/or distributed without permission of the author! Please note references at the end of the presentation!

Species of cellular metals and structures

© Fraunhofer IWU
Prof. Neugebauer

The contents of this presentation may not be copied and/or distributed without permission of the author! Please note references at the end of the presentation!

Cellular metals and structures

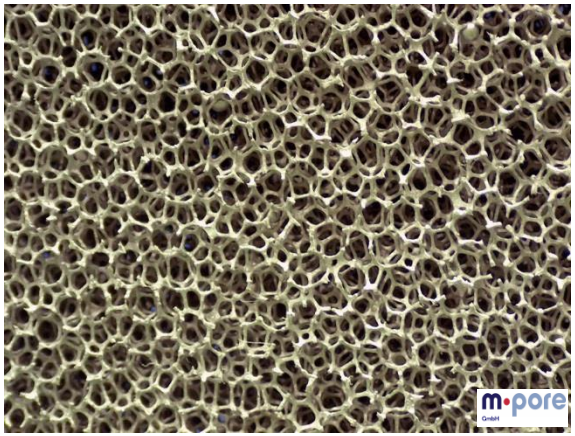

Open-cellular metal foam

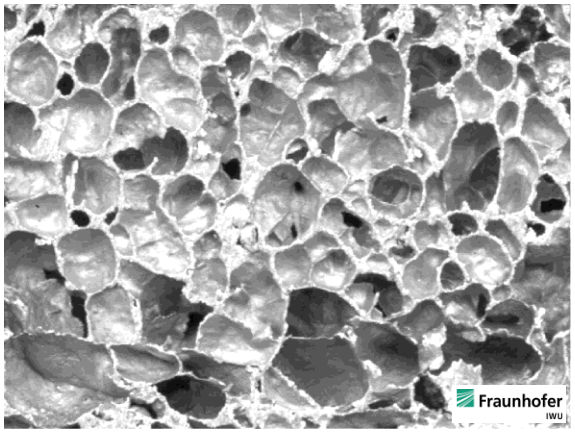

Closed-cellular metal foam

Hollow sphere structure

Fiber structure

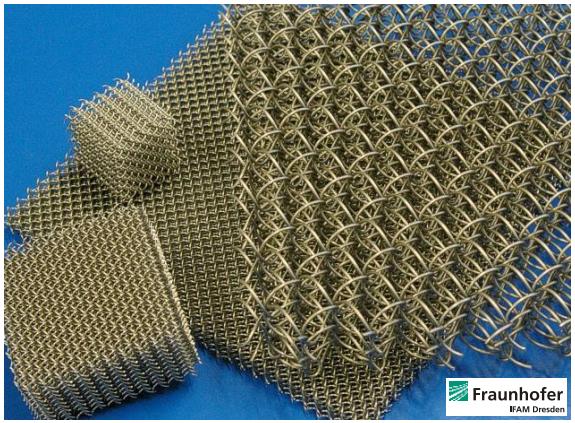

Wire structure

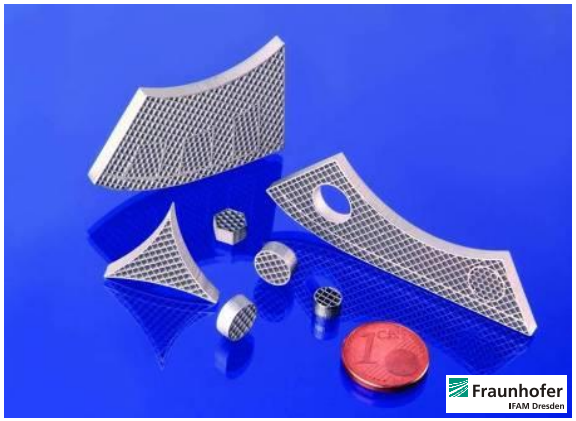

Direct typed metal structure

Archivierungsangaben

IWP WERKZEUGMASCHINEN UND PRODUKTIONSPROZESSE

Fraunhofer IWU

The contents of this presentation may not be copied and/or distributed without permission of the author! Please note references at the end of the presentation!

Manufacturer of cellular metals

At present 10 companies existing in Europe

- Covering a wide range of metals and alloys
  - Focus on aluminum alloys (6 x)
  - Fe-, Ni-based (2 x)
  - Mg-, Zn-based (2 x)
- Different types of cellular metals are manufactured

  Closed cell and open cell structures
- Wide range of geometries and products
  - Panels
  - 3-d net shape parts
  - Sandwich structures

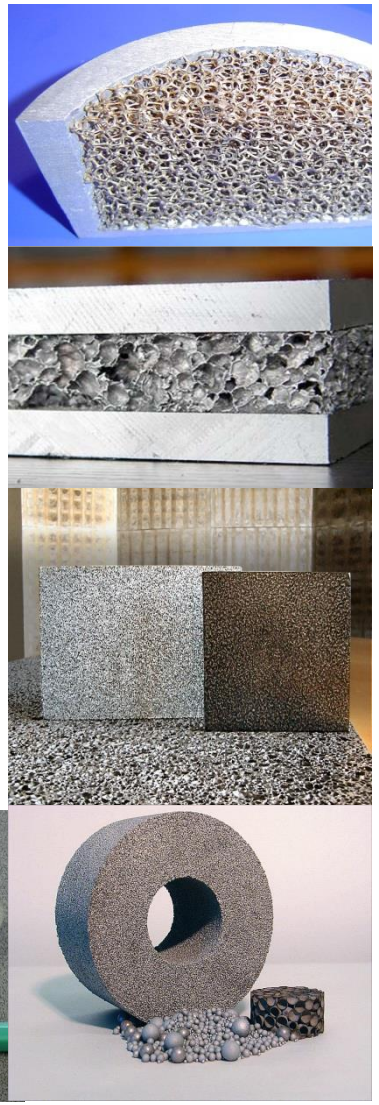

Archivierungsangaben

The contents of this presentation may not be copied and/or distributed without permission of the author! Please note references at the end of the presentation!

Cellular Metals

Stakeholder in Germany

Archivierungsangaben

IWP WERKZEUGMASCHINEN UND PRODUKTIONSPROZESSE

Fraunhofer IWU

The contents of this presentation may not be copied and/or distributed without permission of the author! Please note references at the end of the presentation!

Cellular metals and structures

© Fraunhofer IWU

The contents of this presentation may not be copied and/or distributed without permission of the author! Please note references at the end of the presentation!

Cellular Metals

Manufacturing Processes

Foaming	Forming	Replication	Generation
		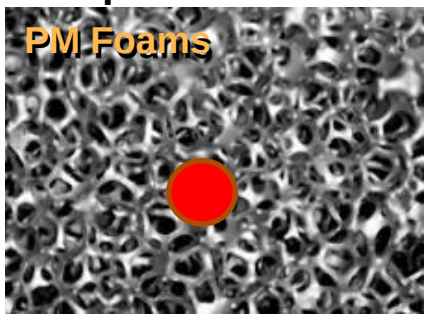	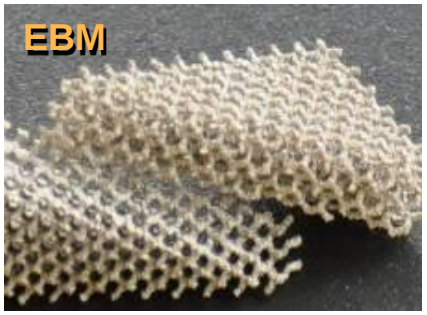
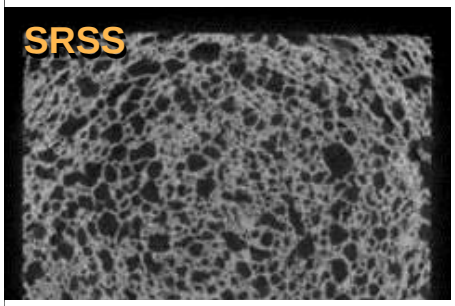		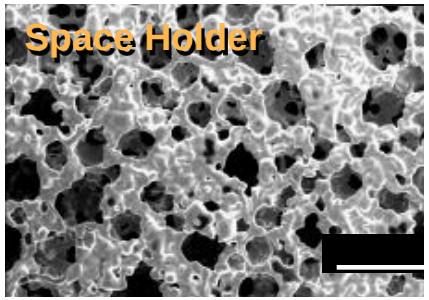	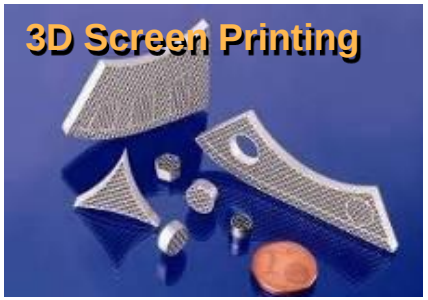
		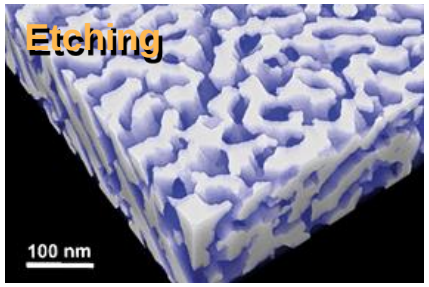	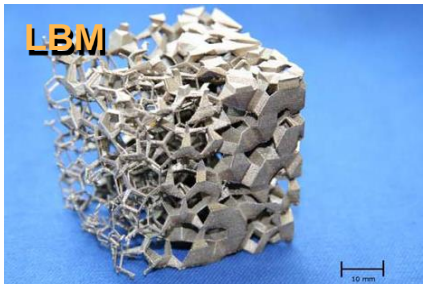

Archivierungsangaben

IWP WERKZEUGMASCHINEN UND PRODUKTIONSPROZESSE

Fraunhofer IWU

The contents of this presentation may not be copied and/or distributed without permission of the author! Please note references at the end of the presentation!

Open-cellular foams/structures

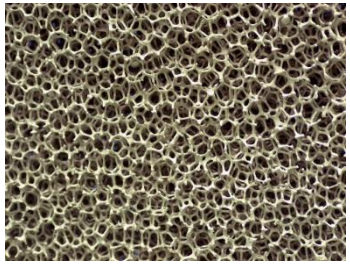

© Fraunhofer IWU
Prof. Neugebauer

The contents of this presentation may not be copied and/or distributed without permission of the author! Please note references at the end of the presentation!

Melt metallurgical process

Manufacturing

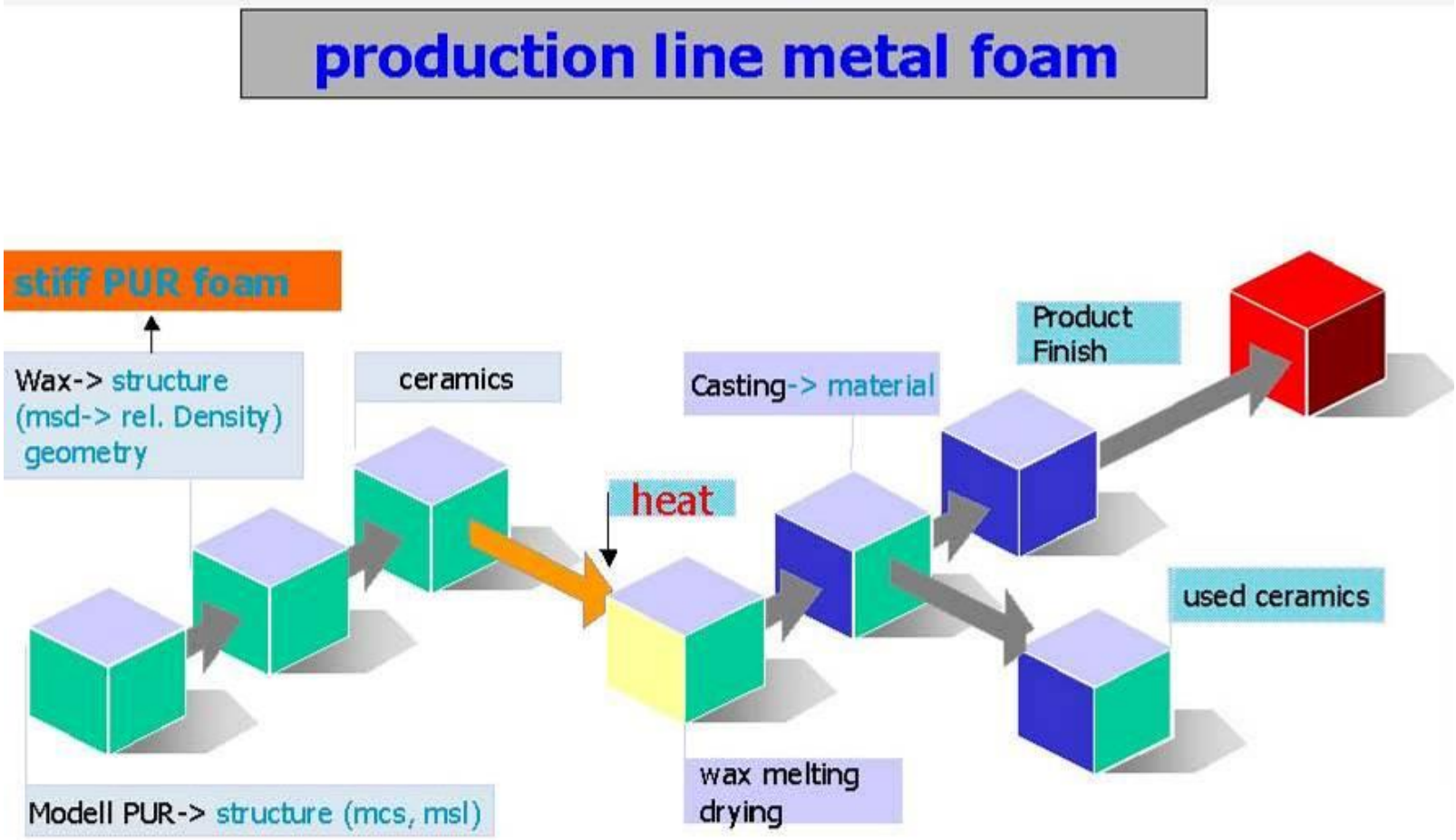

Archivierungsangaben

The contents of this presentation may not be copied and/or distributed without permission of the author! Please note references at the end of the presentation!

Melt metallurgical process

Semi-finished products

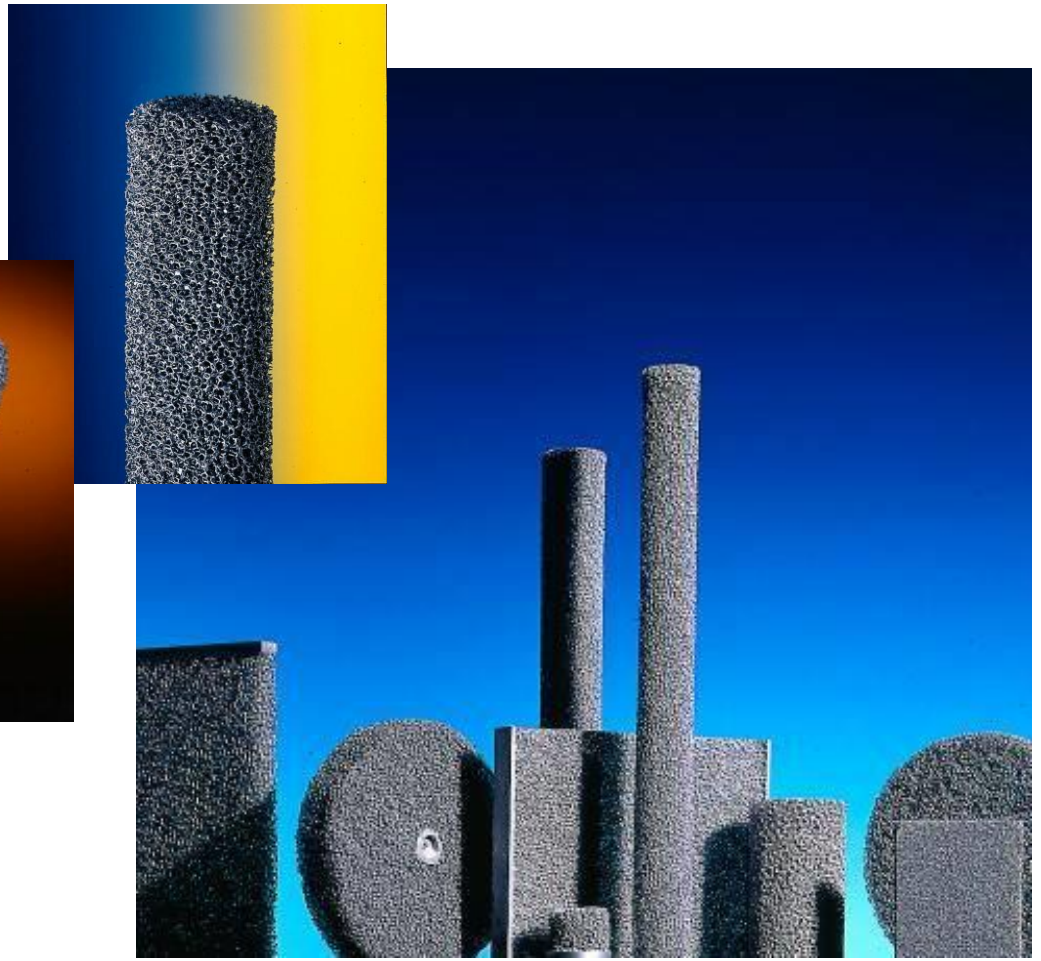

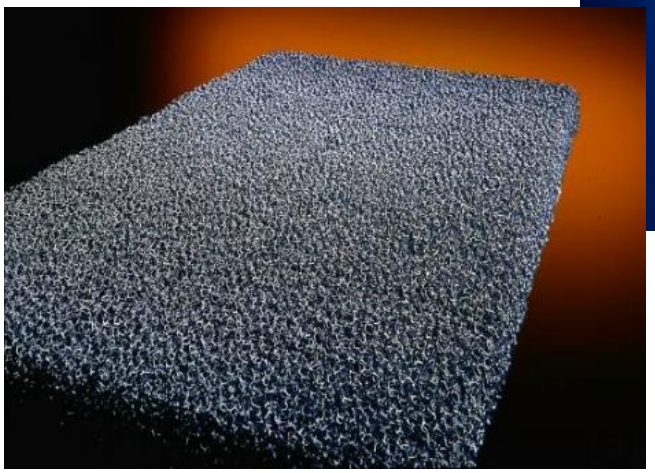

Archivierungsangaben

The contents of this presentation may not be copied and/or distributed without permission of the author! Please note references at the end of the presentation!

Sintering process

Manufacturing

- Molding composed of polymer foam
- Metal-powder-suspension

- Coating process of the ligaments of the polymer foam

- Drying
- Burning out of the PU-foam
- Sintering of the metals

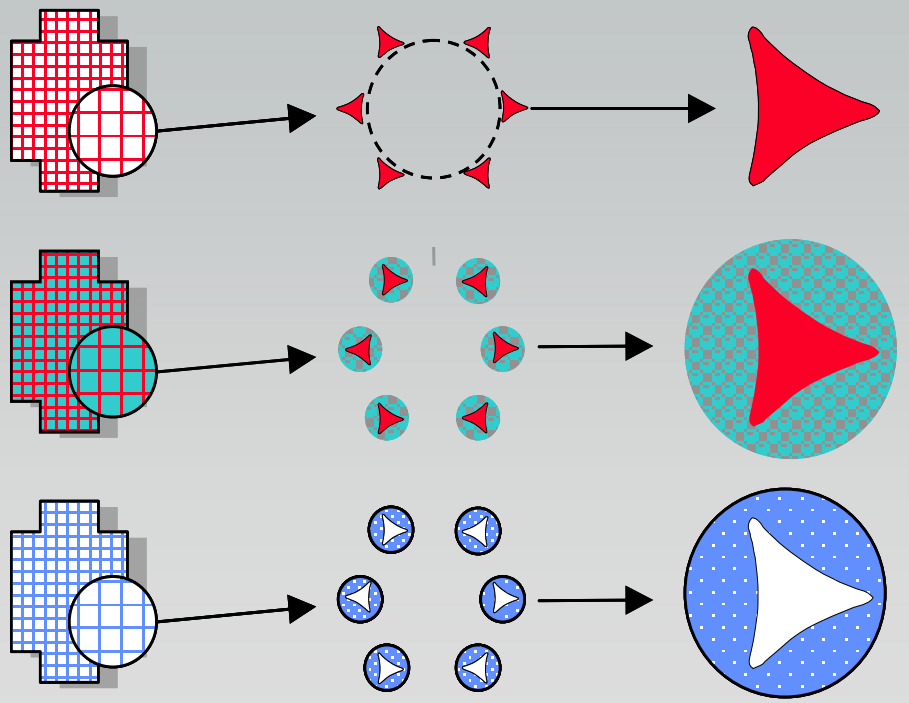

Archivierungsangaben

The contents of this presentation may not be copied and/or distributed without permission of the author! Please note references at the end of the presentation!

Sintering process

Possible pore sizes of powder-metallurgical foams

After ASTM D3576:
Number of pores per inch (ppi)

Pore size [ppi]	Pore size [mm]	Surface [m²/m³]
10	4.5 - 5.0	400
20	2.0 - 3.5	1100
30	1.8 - 2.0	1800
45	1.1 - 1.3	2800
60	0.7 - 0.8	3900
80	0.4 - 0.5	5300

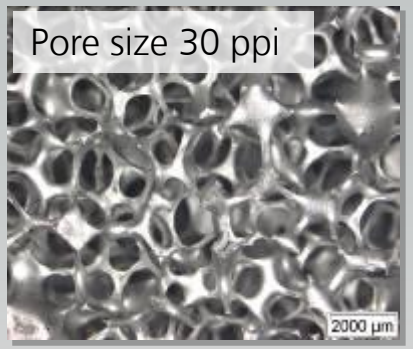

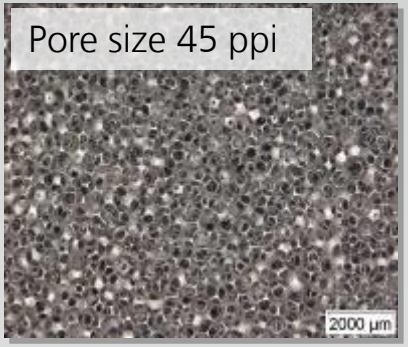

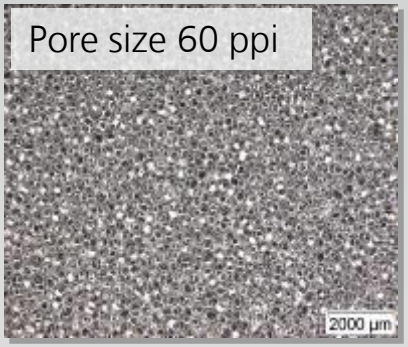

Archivierungsangaben

The contents of this presentation may not be copied and/or distributed without permission of the author! Please note references at the end of the presentation!

Sintering process

Semi-finished products

Archivierungsangaben

Fraunhofer IFAM Dresden

IWP Werkzeugmaschinen und Produktionsprozesse

Fraunhofer IWU

The contents of this presentation may not be copied and/or distributed without permission of the author! Please note references at the end of the presentation!

Properties

Open Cell Metal Foam

metal powder + binder + suspension additives + water

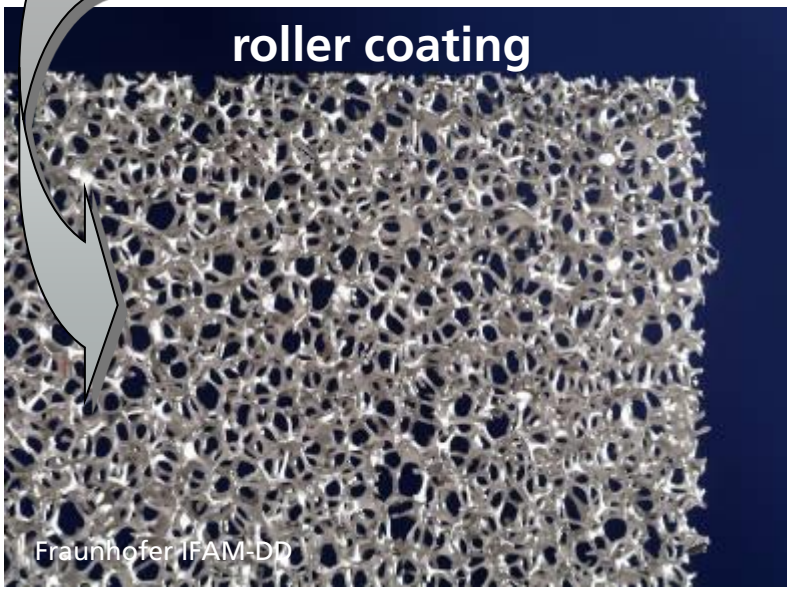

structural properties

density	5 - 30 % of basic material (adjustable)
cell sizes	0.4 – 5.0 mm
heat conductivity	ca. 1 – 5 % of basic material

adjustment of density by adjustment of coating mass

Archivierungsangaben

The contents of this presentation may not be copied and/or distributed without permission of the author! Please note references at the end of the presentation!

Properties

Open Cell Metal Foam

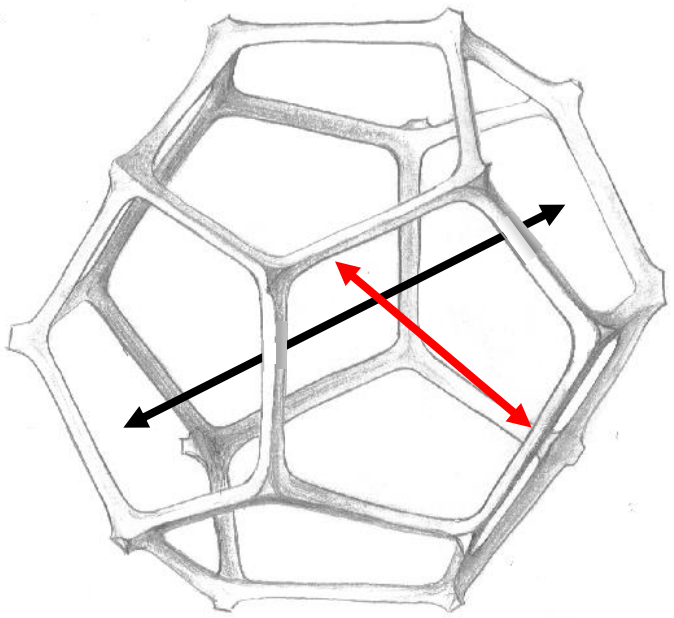

Structure

- Network of dodecahedron cells
- **cell size** = large diameter of cells
- **cell window** = small diameter of cells (appr. 1/3)
- Practically ideal porous organic structure

Cell size	cell width [mm]	surface [m²/m³]
ppi 10	4.5 - 5.0	400
ppi 20	2.0- 3.5	1100
ppi 30	1.8 - 2.0	1800
ppi 45	1.1 - 1.3	2800
ppi 60	0.7 - 0.8	3900
ppi 80	0.4 - 0.5	5300

Archivierungsangaben

The contents of this presentation may not be copied and/or distributed without permission of the author! Please note references at the end of the presentation!

Open porous metals

- Open porous structures made from aluminium, zinc, copper, steel
- Production e.g. by means of
  - Casting with place-holder structures
  - Sintering of Cu-electroplated textiles
  - Printing
- Composites possible (ceramics, zeolites, PCM,…)

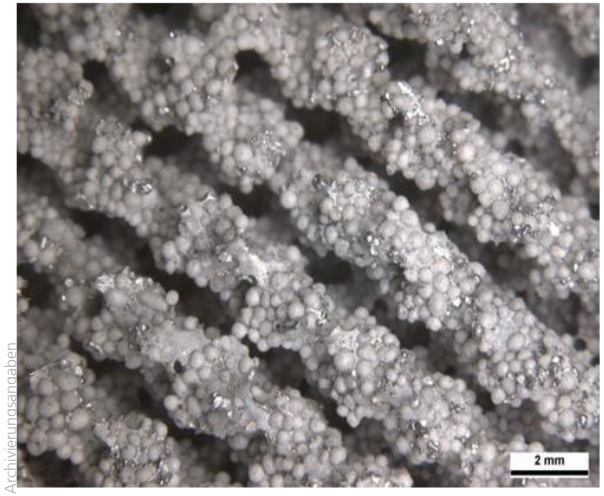

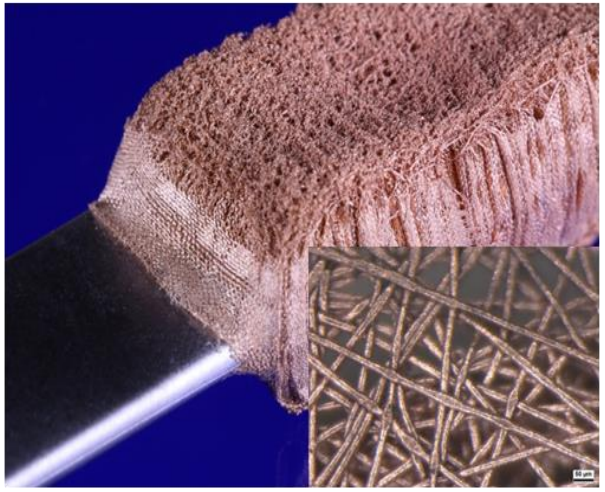

Archivierungsangaben

Joachim Baumeister, Fraunhofer Institute IFAM Bremen
Department of Powder Technology

Fraunhofer IFAM

The contents of this presentation may not be copied and/or distributed without permission of the author! Please note references at the end of the presentation!

Closed-cellular foams

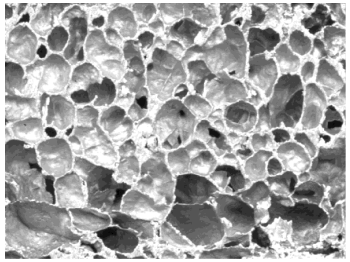

© Fraunhofer IWU
Prof. Neugebauer

The contents of this presentation may not be copied and/or distributed without permission of the author! Please note references at the end of the presentation!

Melt metallurgical process

Manufacturing

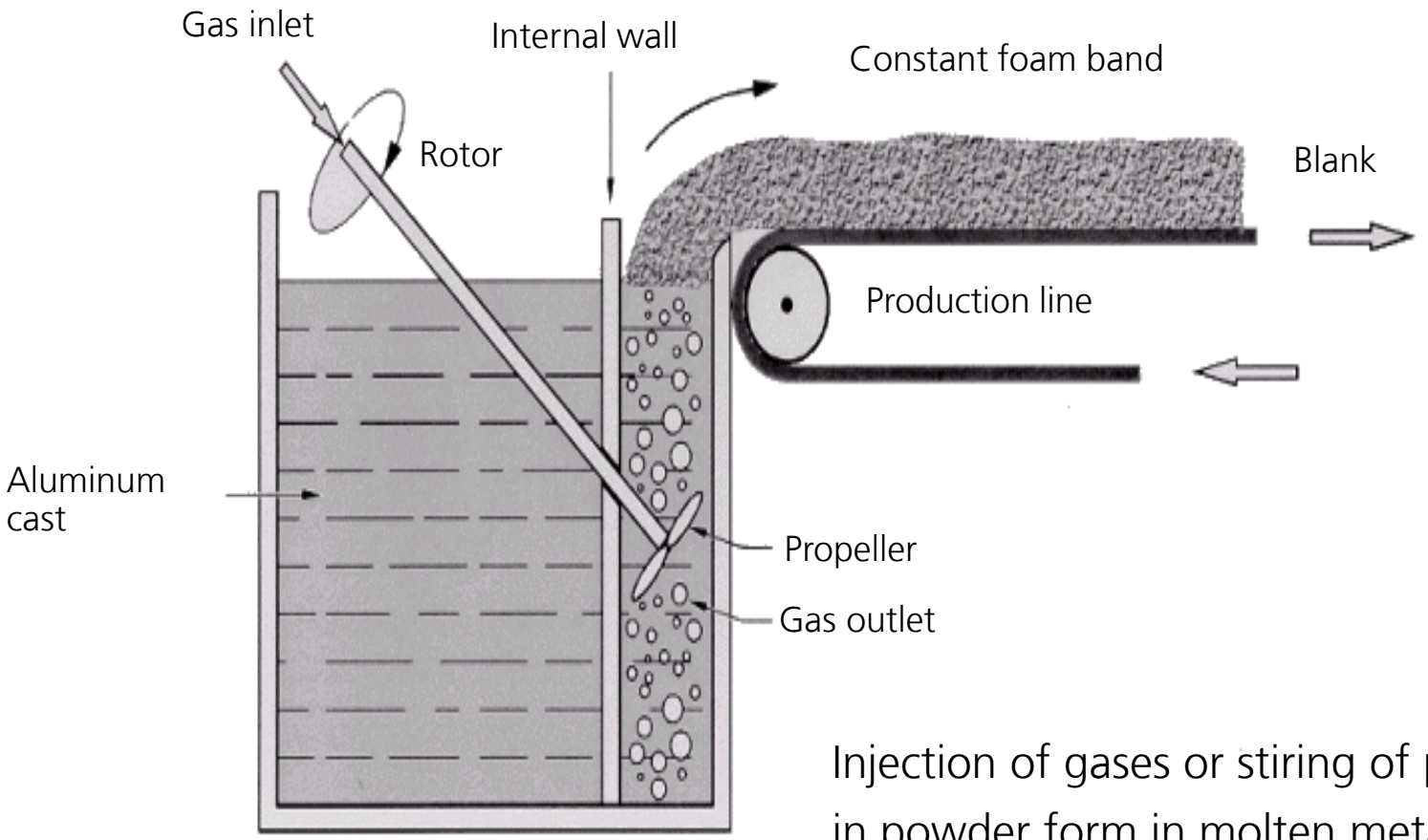

Injection of gases or stiring of propellants in powder form in molten metal.

Archivierungsangaben

The contents of this presentation may not be copied and/or distributed without permission of the author! Please note references at the end of the presentation!

Melt metallurgical process

Semi-finished products

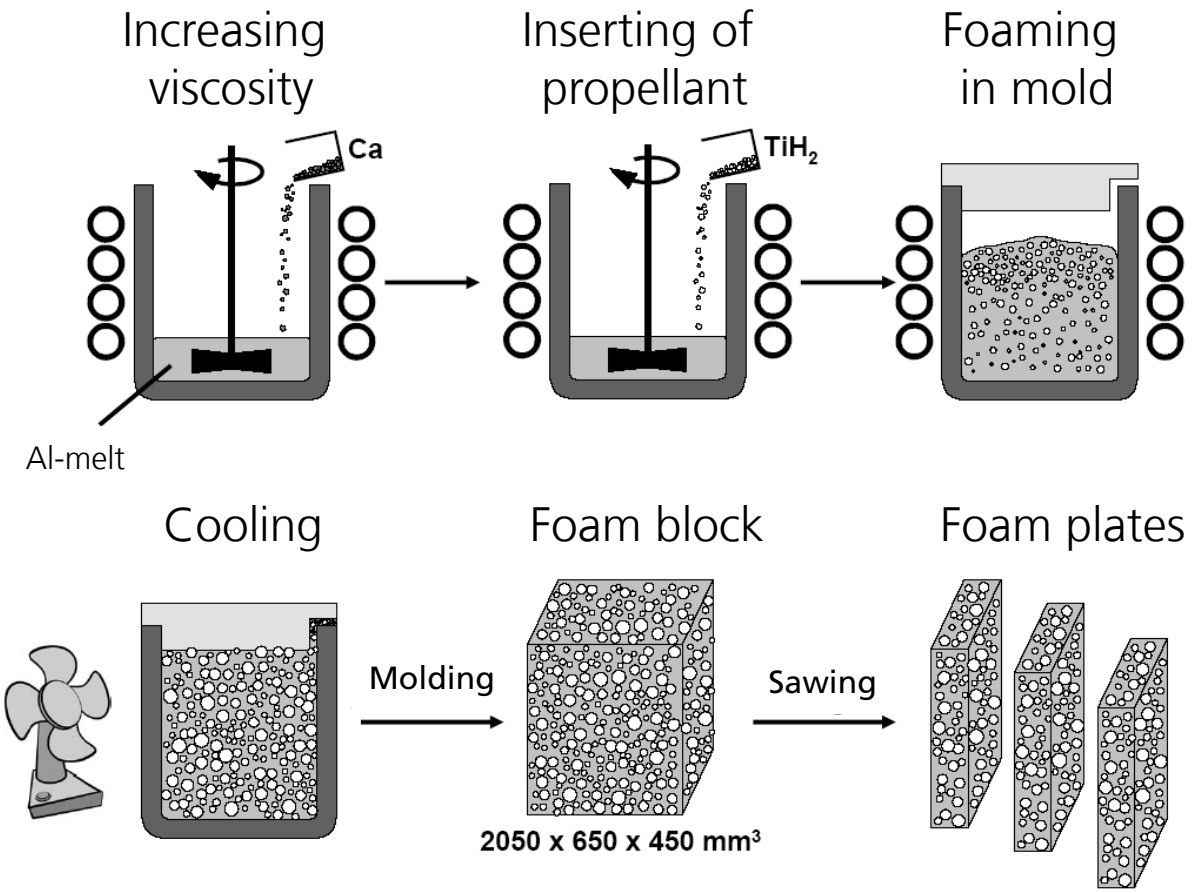

Archivierungsangaben

The contents of this presentation may not be copied and/or distributed without permission of the author! Please note references at the end of the presentation!

Powder metallurgical process

Manufacturing

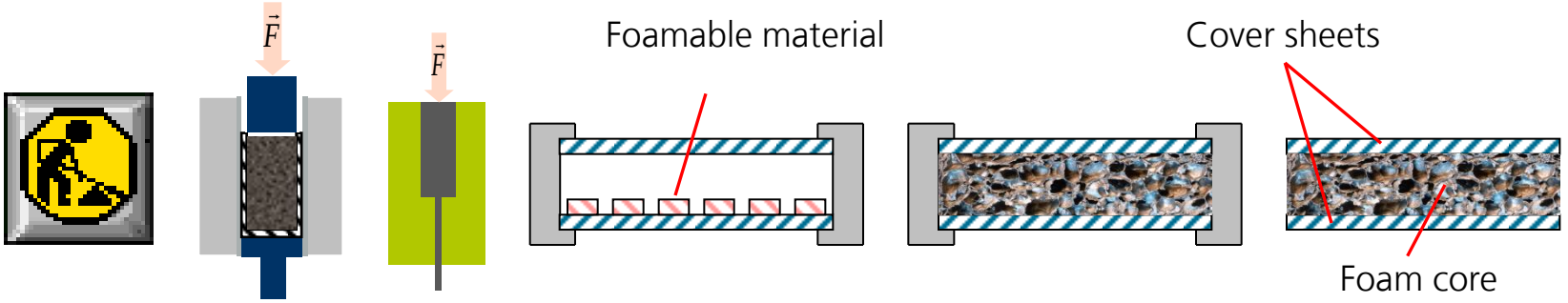

Mixing	Axial pressing	Pressing a rod	Input the precursor	Foaming	Cooling down

Foamable dimensions	➡	area:	1800 mm x 1400 mm
	➡	max. high:	50 mm
	➡	cover sheet thickness:	0,8 ... 10 mm

Archivierungsangaben

The contents of this presentation may not be copied and/or distributed without permission of the author! Please note references at the end of the presentation!

Powder metallurgical process

Foaming of aluminum

Foamable aluminum →

Infrared heating element →

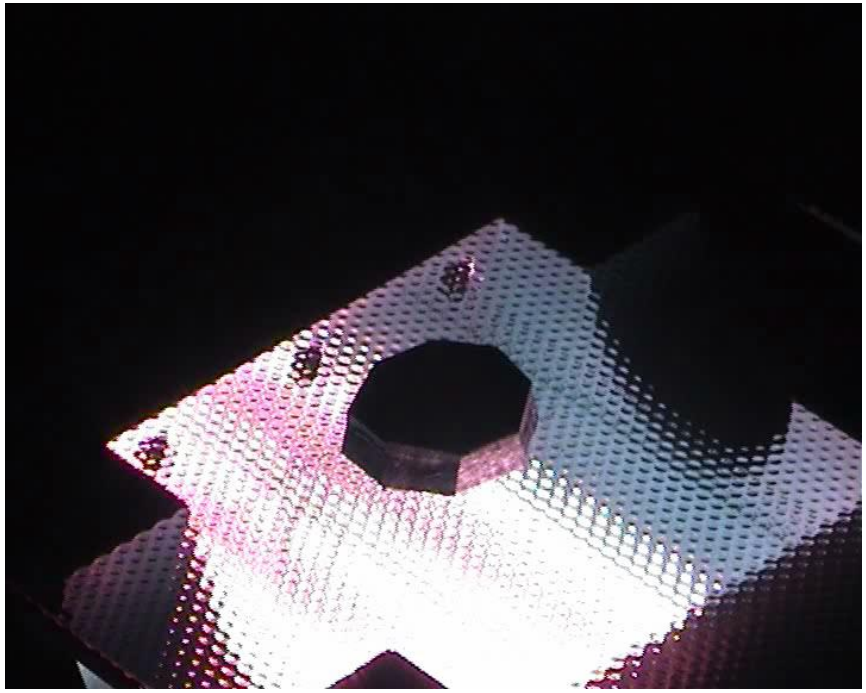

← Quartz plate

Foam process

Archivierungsangaben

The contents of this presentation may not be copied and/or distributed without permission of the author! Please note references at the end of the presentation!

Powder metallurgical process

Species of foam parts and semi-finished products

Species of parts

3-d foam parts	Sandwiches, plates	Foam filled tubes

Frequency of use

Rarely	Very often	Often

Archivierungsangaben

The contents of this presentation may not be copied and/or distributed without permission of the author! Please note references at the end of the presentation!

Powder metallurgical process

Possible combinations of materials

Future

	Foam	Steel profile + foamed out	Steel + Foam glued	Foam + Coating	Al profile + Foam glued	Al profile foamed out
Profile (also with inner tube.)						
Cross sections ≈ 200 x 250 s ≈ 1-15 mm			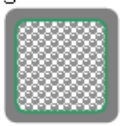			
up to 2400 mm long						Status: 100

	Foam	Steel foamed out	Steel + Foam glued	Foam + Coating	Al plate glued	Al plate foamed out
Sandwich			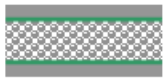		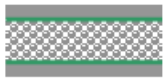	
1800 x 1400	1800 x 1400	2400 x 1600	1800 x 1400	2400 x 1600	Status: 2400 x 1100	

Steel = normal or stainless

Archivierungsangaben

The contents of this presentation may not be copied and/or distributed without permission of the author! Please note references at the end of the presentation!

Powder metallurgical process

Semi-finished products

Aluminum foam parts

Foamed out steel profiles up to 2000 mm

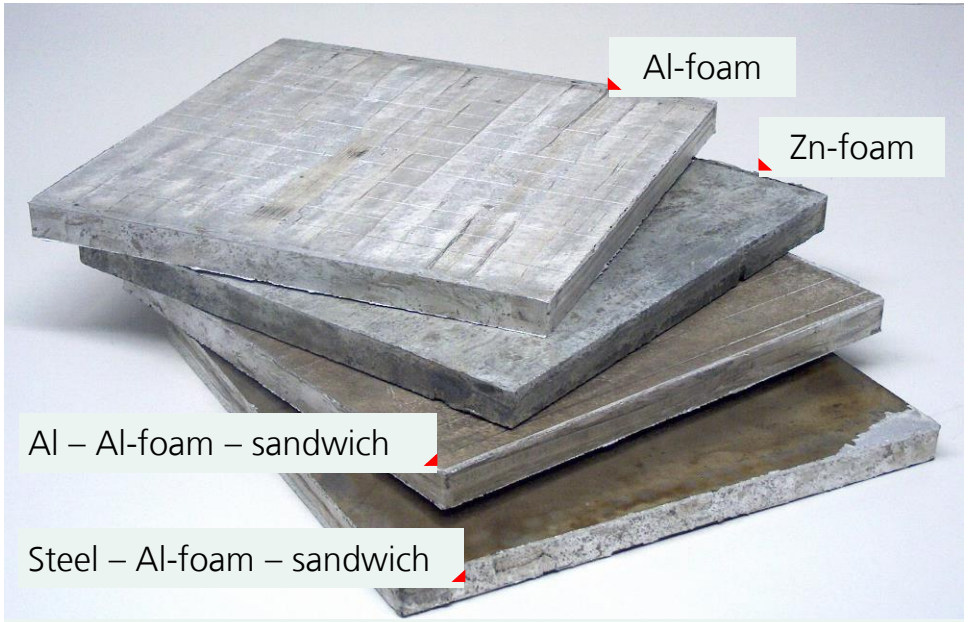

Metal foam plates and sandwich plates
up to 1800 mm x 1400 mm

Archivierungsangaben

The contents of this presentation may not be copied and/or distributed without permission of the author! Please note references at the end of the presentation!

Aluminum Foam Sandwich Structures

Technology: → Filling of premixed Al+TiH_2 powder into container

→ Compacting, rolling, cutting, deep drawing

→ Foaming

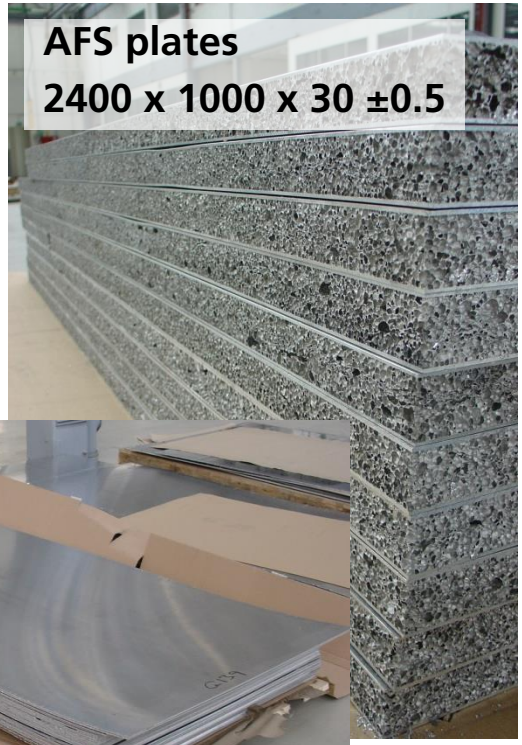

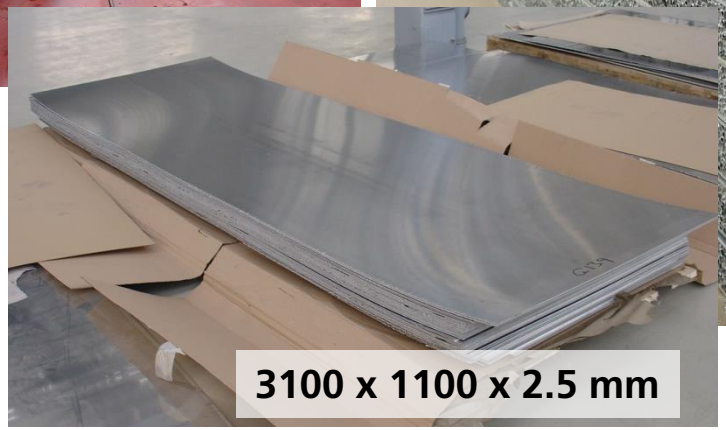

Properties AFS

E-Modulus: 18-21GPa

Comp. Strength: 4-8MPa

Tensile Strength: 120MPa

Therm. Cond.: 10-15 W/(m · K)

CTE: 25 · 10^{-6} 1/K

Archivierungsangaben

The contents of this presentation may not be copied and/or distributed without permission of the author! Please note references at the end of the presentation!

Low-pressure foam casting process (LPFC)

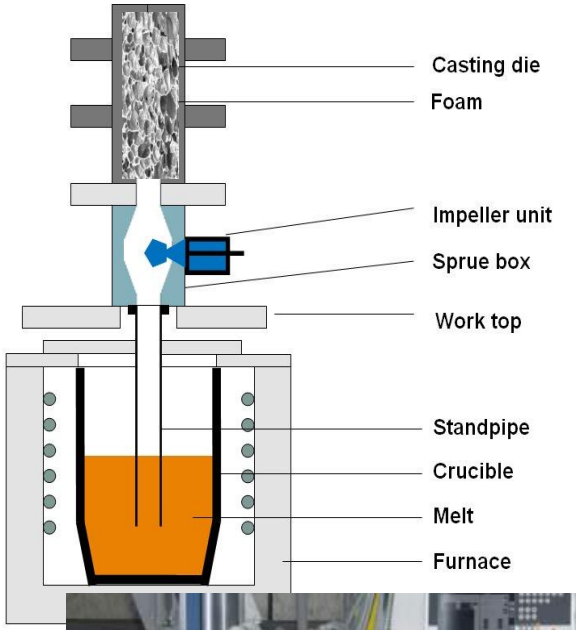

Technology:
- Partially injection of melt into the sprue box
- Stirring for melt foaming
- Injection to the casting die

Material:
- Al-MMC alloy

Properties:
- Density 0.3 - 1.0 g/cm³
- Variable wall thickness
- Homogeneous, closed-pore foam
- Complex geometries

+GF+

Archivierungsangaben

IWP WERKZEUGMASCHINEN UND PRODUKTIONSPROZESSE

Fraunhofer IWU

The contents of this presentation may not be copied and/or distributed without permission of the author! Please note references at the end of the presentation!

Low-pressure foam casting process (LPFC)

Progression of density in triple mold during a aluminum foam casting series using LPFC

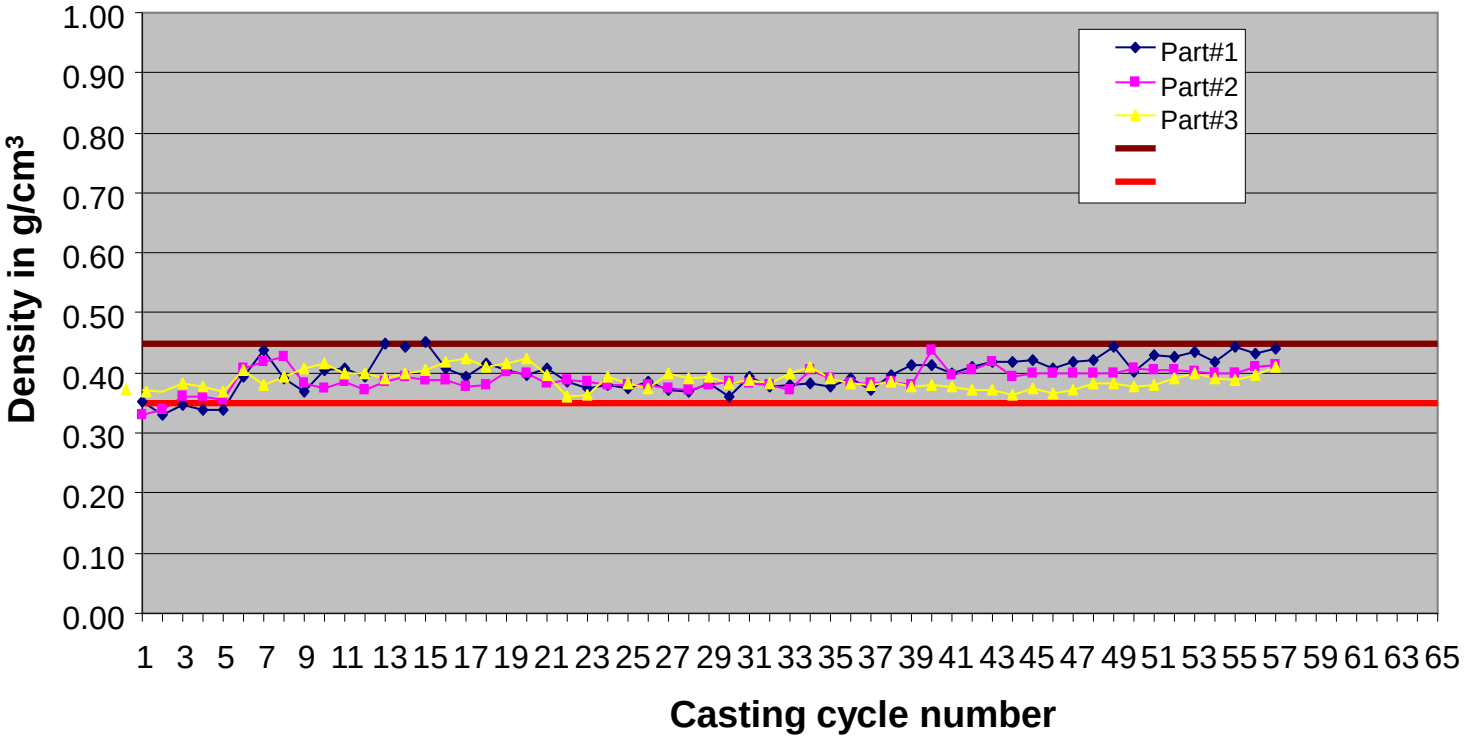

Archivierungsangaben

The contents of this presentation may not be copied and/or distributed without permission of the author! Please note references at the end of the presentation!

Idea of the Advanced Pore Morphology (APM) :

to separate the foaming step from the shaping step !!

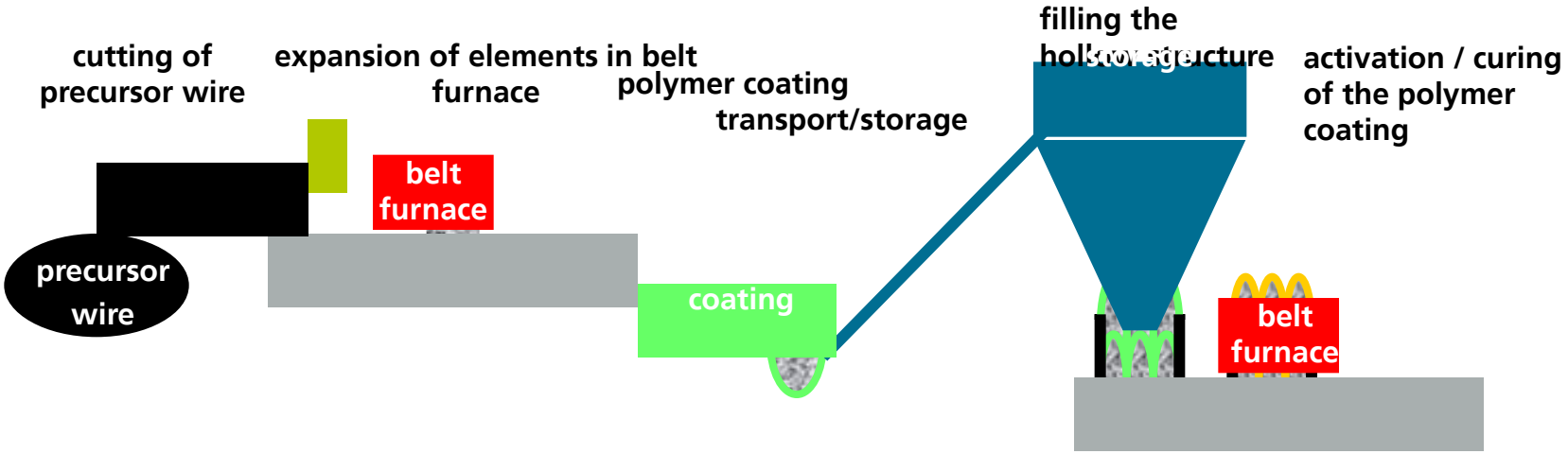

Archivierungsangaben

Joachim Baumeister, Fraunhofer Institute IFAM Bremen
Department of Powder Technology

Fraunhofer IFAM

The contents of this presentation may not be copied and/or distributed without permission of the author! Please note references at the end of the presentation!

Mechanical properties of APM hybrid foams

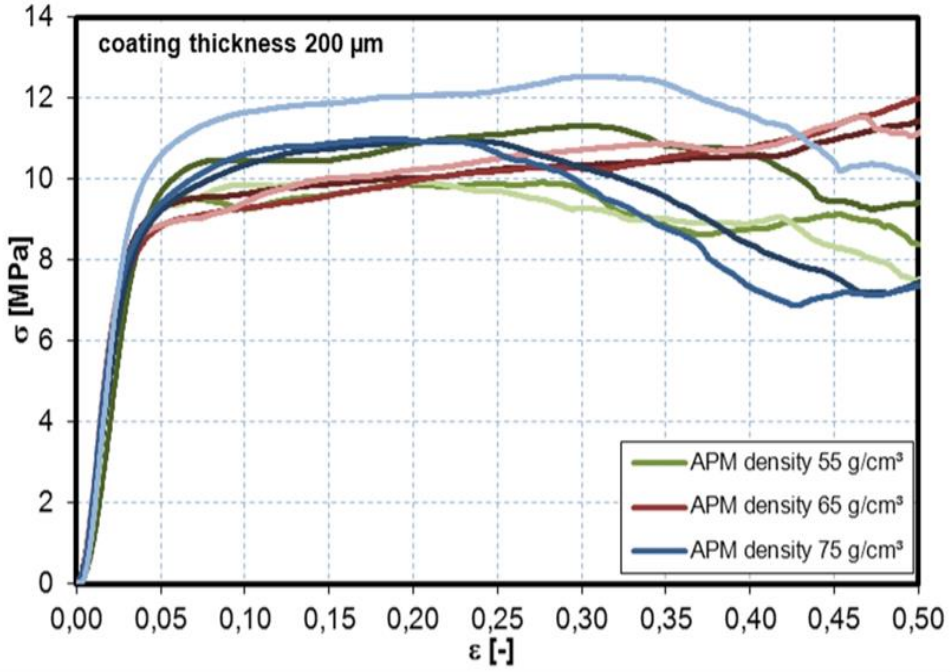

quasistatic tests ($d\varepsilon/dt \approx 0.004\ s^{-1}$)

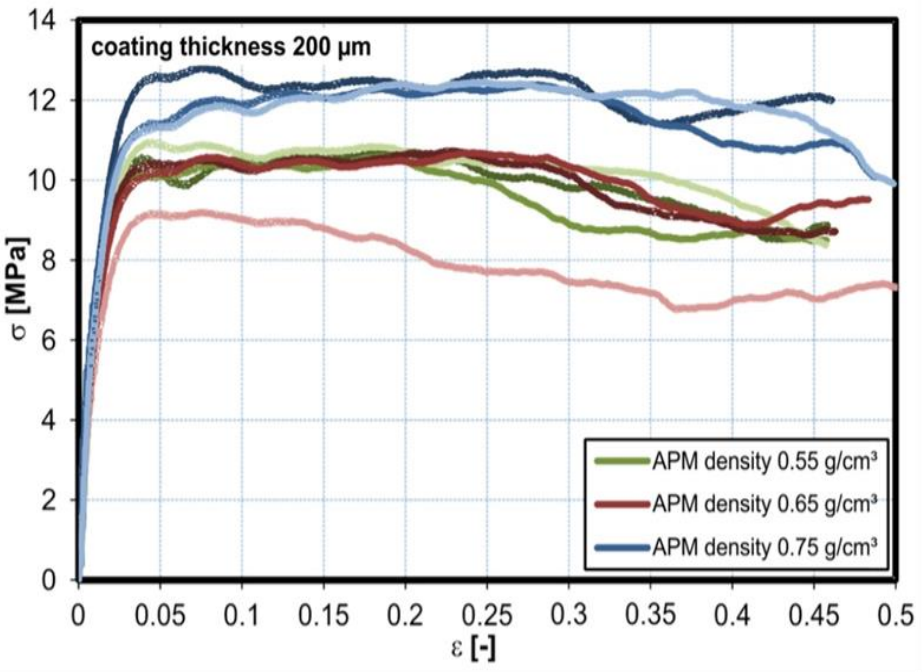

dynamic tests ($d\varepsilon/dt = 10\ s^{-1}$)

- ✓ strength similar to conventional aluminum foam of the same density
- ✓ no significant strain rate dependency of the properties

Archivierungsangaben

Joachim Baumeister, Fraunhofer Institute IFAM Bremen
Department of Powder Technology

Fraunhofer IFAM

The contents of this presentation may not be copied and/or distributed without permission of the author! Please note references at the end of the presentation!

APM Parts

APM foam parts

APM foam filled structures

APM sandwich structures

Archivierungsangaben

Joachim Baumeister, Fraunhofer Institute IFAM Bremen
Department of Powder Technology

Fraunhofer IFAM

The contents of this presentation may not be copied and/or distributed without permission of the author! Please note references at the end of the presentation!

Hollow sphere structures

© Fraunhofer IWU
Prof. Neugebauer

The contents of this presentation may not be copied and/or distributed without permission of the author! Please note references at the end of the presentation!

Production of metal green hollows

Fluid bed procedure

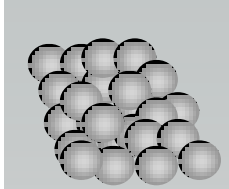

Polystyrene-granules

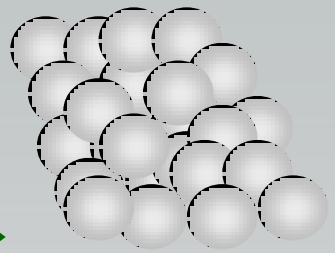

Pre-expanded EPS-spheres

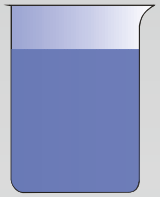

Metal powder-binder-suspension

Coating in fluid bed

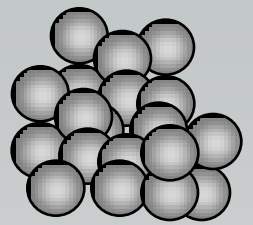

„Green spheres“

Archivierungsangaben

The contents of this presentation may not be copied and/or distributed without permission of the author! Please note references at the end of the presentation!

Production of metallic hollow sphere structures

Debinding and sintering from „green hollows“ to structures

„Green hollows“

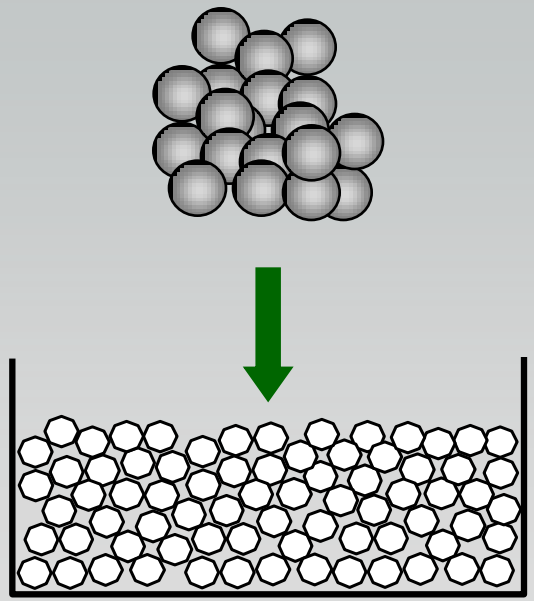

Molding → Green molded part

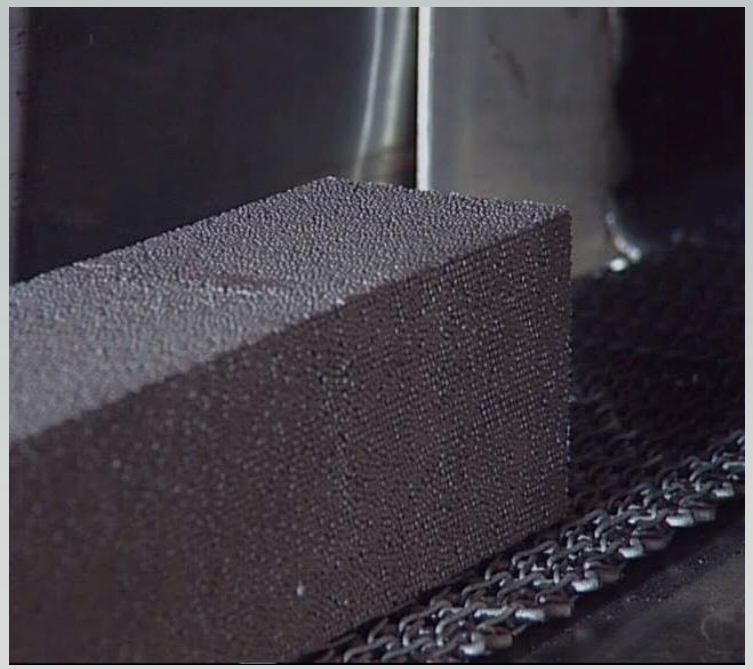

Heat treatment (debinding/sintering)

Archivierungsangaben

The contents of this presentation may not be copied and/or distributed without permission of the author! Please note references at the end of the presentation!

Production of metallic hollow sphere structures

Bonding, soldering, casting

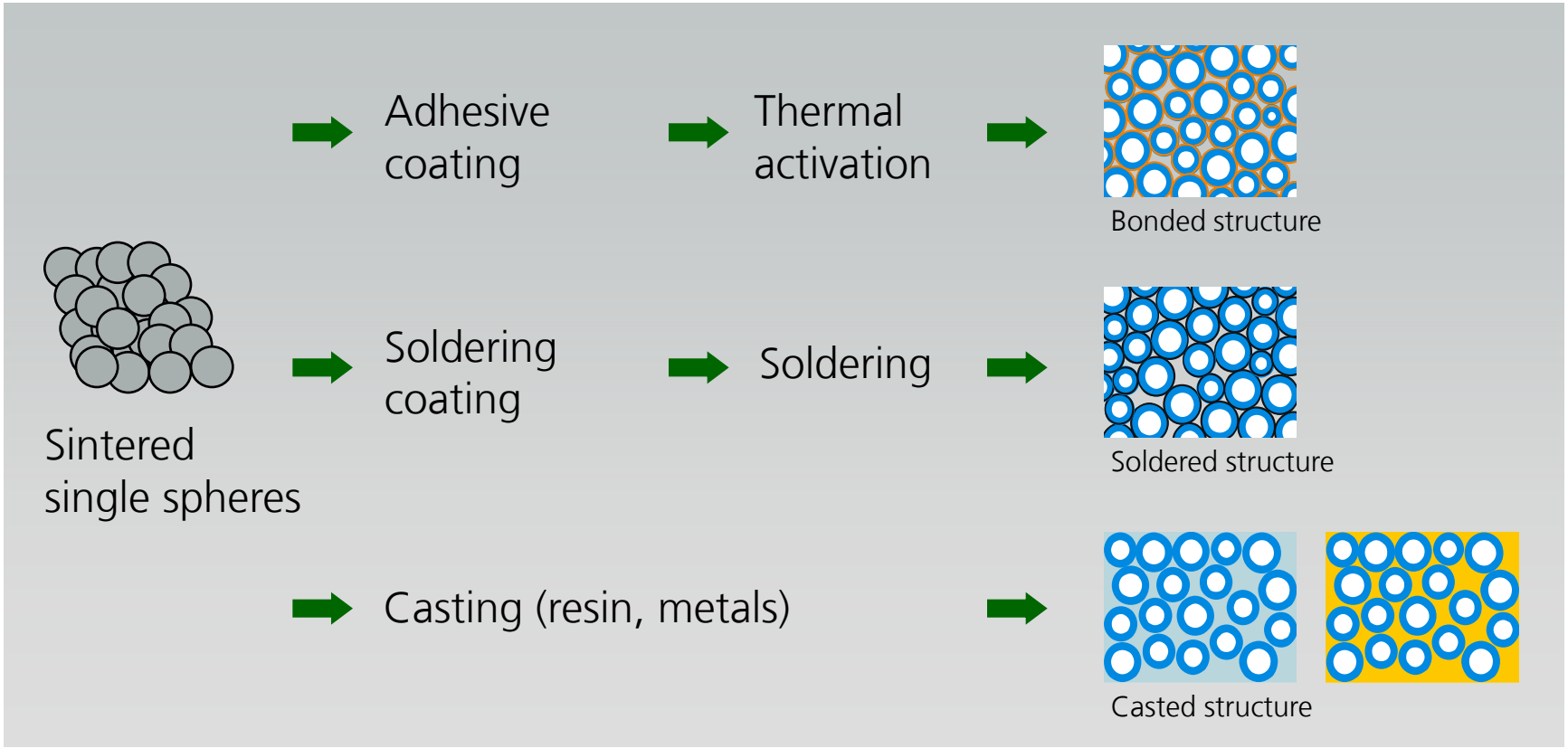

Archivierungsangaben

The contents of this presentation may not be copied and/or distributed without permission of the author! Please note references at the end of the presentation!

Properties

Hollow Metal Sphere Structures

Suspension: metal powder, binder + additive + water

Structural propertoes

density	5 - 30 % of basic material (adjustable)
porosity	75 – 96 %
cell size	0.4 – 5.0 mm
heat conductivity	ca. 1 – 5 % of basic material

adjustment of density by adjustment of coating mass

Archivierungsangaben

The contents of this presentation may not be copied and/or distributed without permission of the author! Please note references at the end of the presentation!

Production of metallic hollow sphere structures

Morphology of races

Diameter	D ≈	0.50 – 15 mm
Wall thickness	d ≈	0.02 – 1 mm
Density	ρ ≈	0.30 – 2 g/cm³

Morphology of races

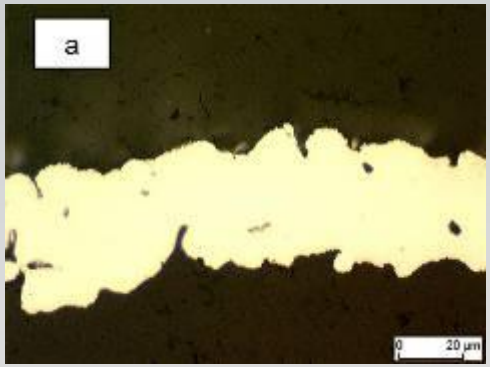

- Dense

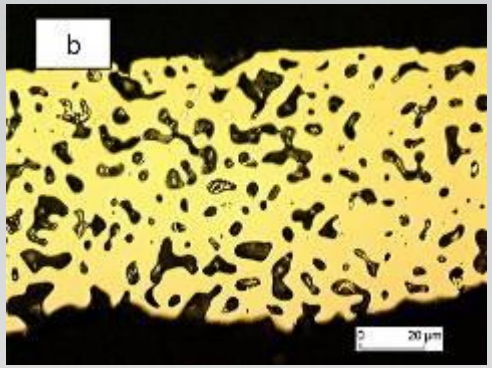

- Open porous

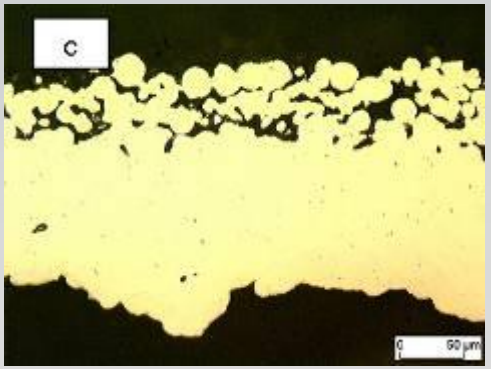

- Graded

Archivierungsangaben

The contents of this presentation may not be copied and/or distributed without permission of the author! Please note references at the end of the presentation!

Production of metallic hollow sphere structures

Semi-finished products

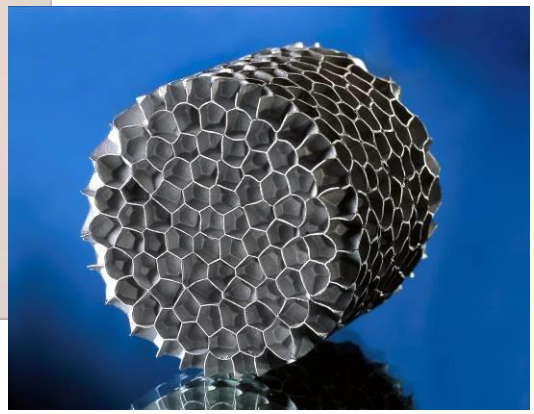

Fraunhofer IFAM Dresden

Archivierungsangaben

IWP Werkzeugmaschinen und Produktionsprozesse

Fraunhofer IWU

The contents of this presentation may not be copied and/or distributed without permission of the author! Please note references at the end of the presentation!

Properties

Hollow Metal Sphere Structures

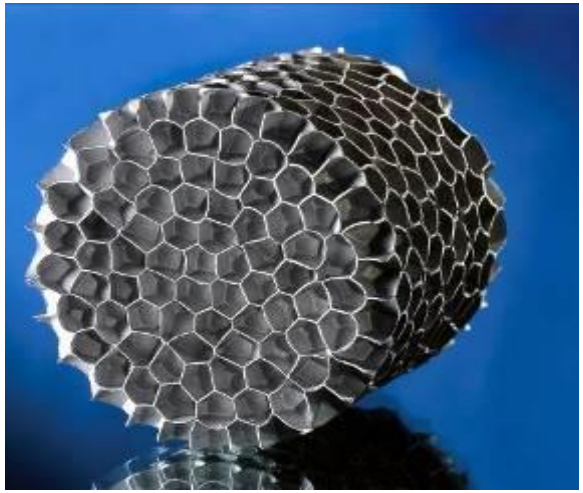

Closed cell honey comb
- high strength
- gas tight

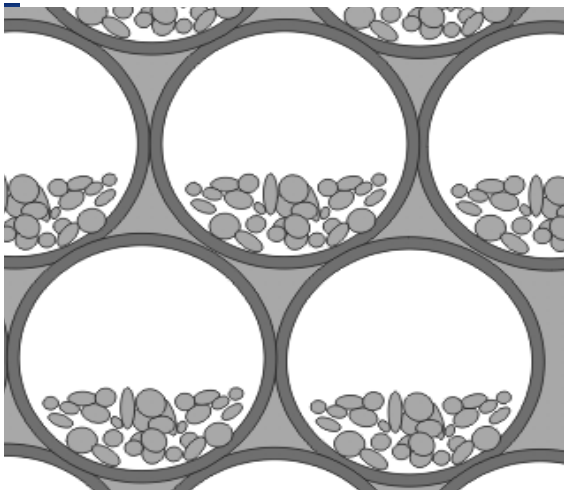

Particular filled structures
- high damping
- low mass

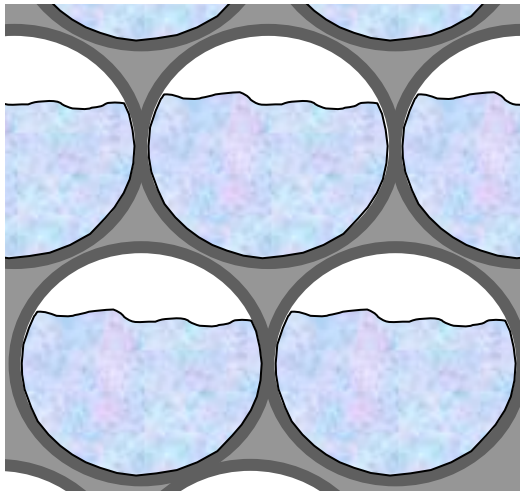

PCM-filled structures
- high thermal storage
- increased heat conductivity

Archivierungsangaben

The contents of this presentation may not be copied and/or distributed without permission of the author! Please note references at the end of the presentation!

Fiber structures

The contents of this presentation may not be copied and/or distributed without permission of the author! Please note references at the end of the presentation!

Melt extraction of metal fibers

Manufacturing

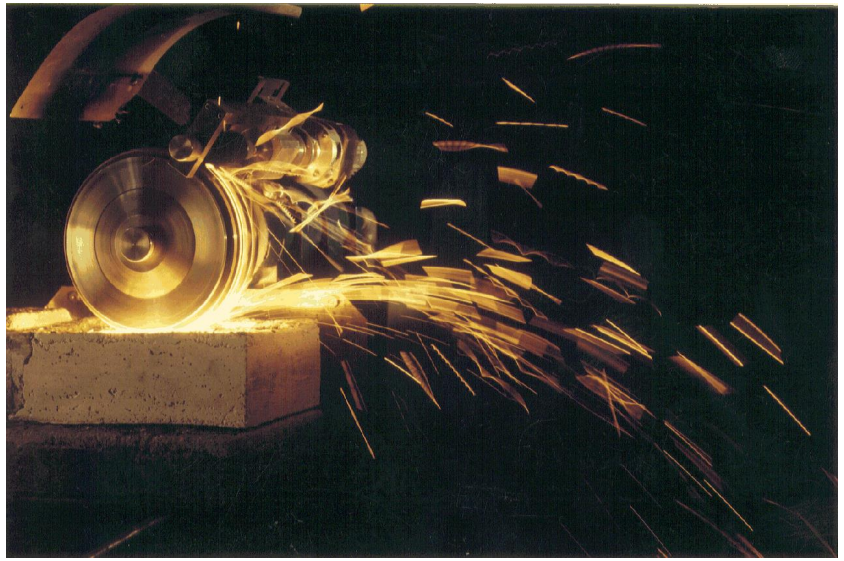

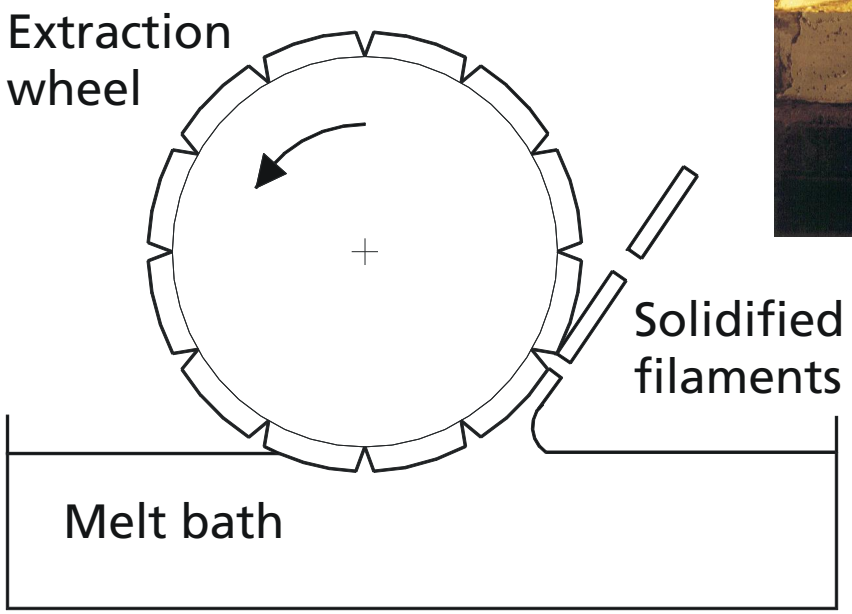

Archivierungsangaben

The contents of this presentation may not be copied and/or distributed without permission of the author! Please note references at the end of the presentation!

Production of chopped strand bonded fabrics

Dry laying technique for metallic chopped fibers

- Density stability: ± 5 %
- Dimension: 1000 x 2000 mm²

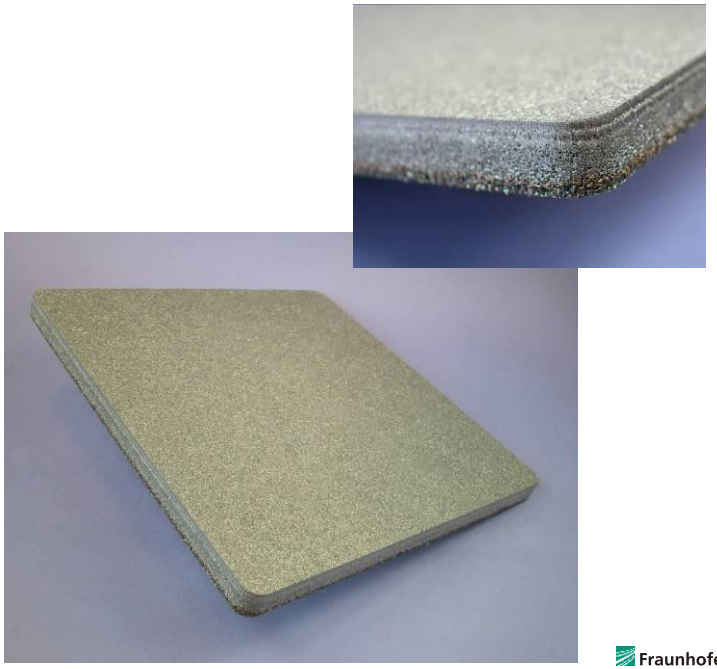

Fraunhofer IFAM Dresden

Archivierungsangaben

IWP Werkzeugmaschinen und Produktionsprozesse

Fraunhofer IWU

The contents of this presentation may not be copied and/or distributed without permission of the author! Please note references at the end of the presentation!

Production of chopped strand bonded fabrics

Continuous wet geomembrane - laying technique

Lab-wet geomembrane – laying plant (company PILL)

Laying of melt extracted chopped fiber

Archivierungsangaben

The contents of this presentation may not be copied and/or distributed without permission of the author! Please note references at the end of the presentation!

Materials

Fibre Production by Melt Extraction

Properties of Metal Fibres

- All common metals and alloys (Al, Mg, Cu, Fe, Ni, Ti, Au, Pt, etc.)
- Intermetallics (FeAl, NiAl, TiAl)
- Fiber diameters ranging from 50 to 250 µm
- Fiber length ranging from 3 to 50 mm

Archivierungsangaben

The contents of this presentation may not be copied and/or distributed without permission of the author! Please note references at the end of the presentation!

Production semi-finished parts with milled fibers

Sandwich with fiber core layer; fiber structures

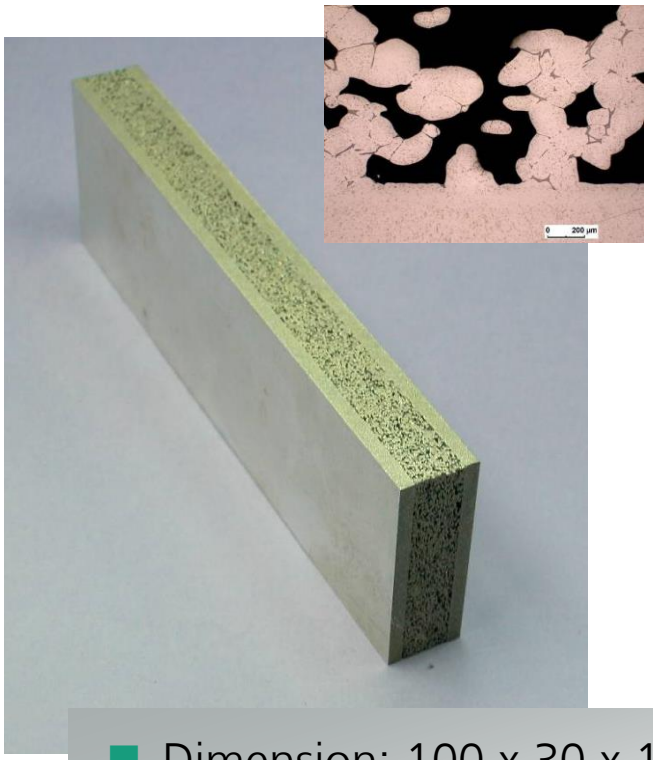

- Dimension: 100 x 30 x 11 mm^3
- Thickness of Al-cover sheet: 2 mm
- Al 6Cu 5Zn-fibers
- Metallurgical connection of cover sheets

Fraunhofer IFAM Dresden

Archivierungsangaben

IWP Werkzeugmaschinen und Produktionsprozesse

Fraunhofer IWU

The contents of this presentation may not be copied and/or distributed without permission of the author! Please note references at the end of the presentation!

Wire structures

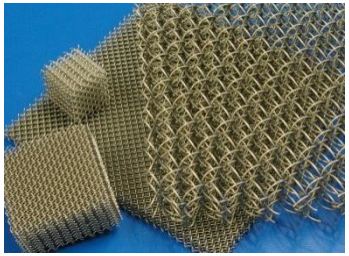

The contents of this presentation may not be copied and/or distributed without permission of the author! Please note references at the end of the presentation!

Technologies

3D Wire Structures

wire pay-off → leveller → forming → manufacturing of structures

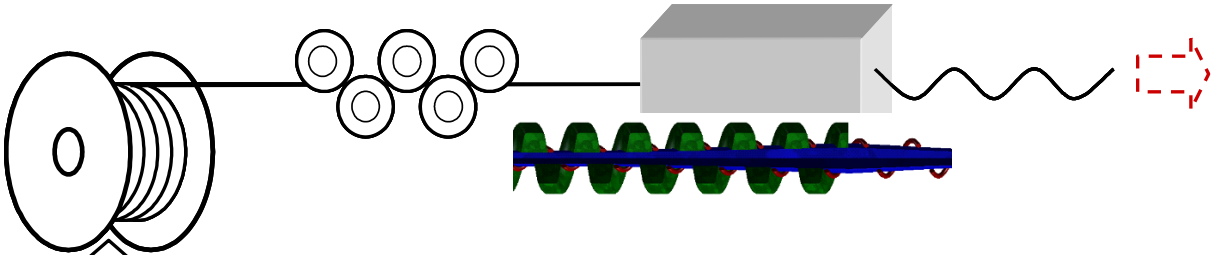

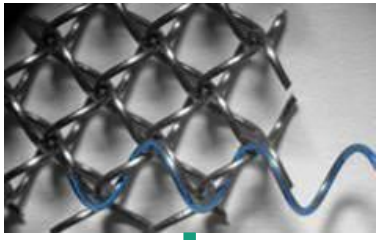

automated

manual

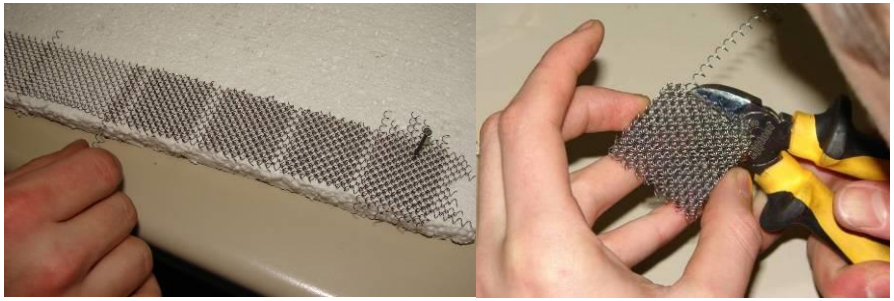

automated manufacturing test rig

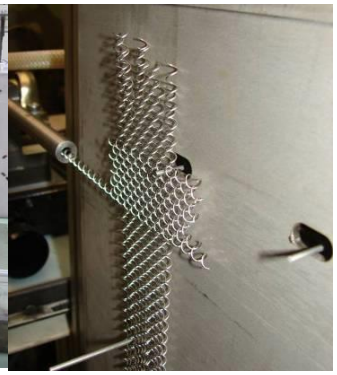

Archivierungsangaben

The contents of this presentation may not be copied and/or distributed without permission of the author! Please note references at the end of the presentation!

Wire structures

Manufacturing

- Anisotropic structures
- Wire diameter from 0.25 to 2.5 mm
- Cell widths from 1 to 20 mm
- Structure densities from 0.05 g/cm^3 possible
- Materials: steels, stainless steel, copper, aluminum, titanium

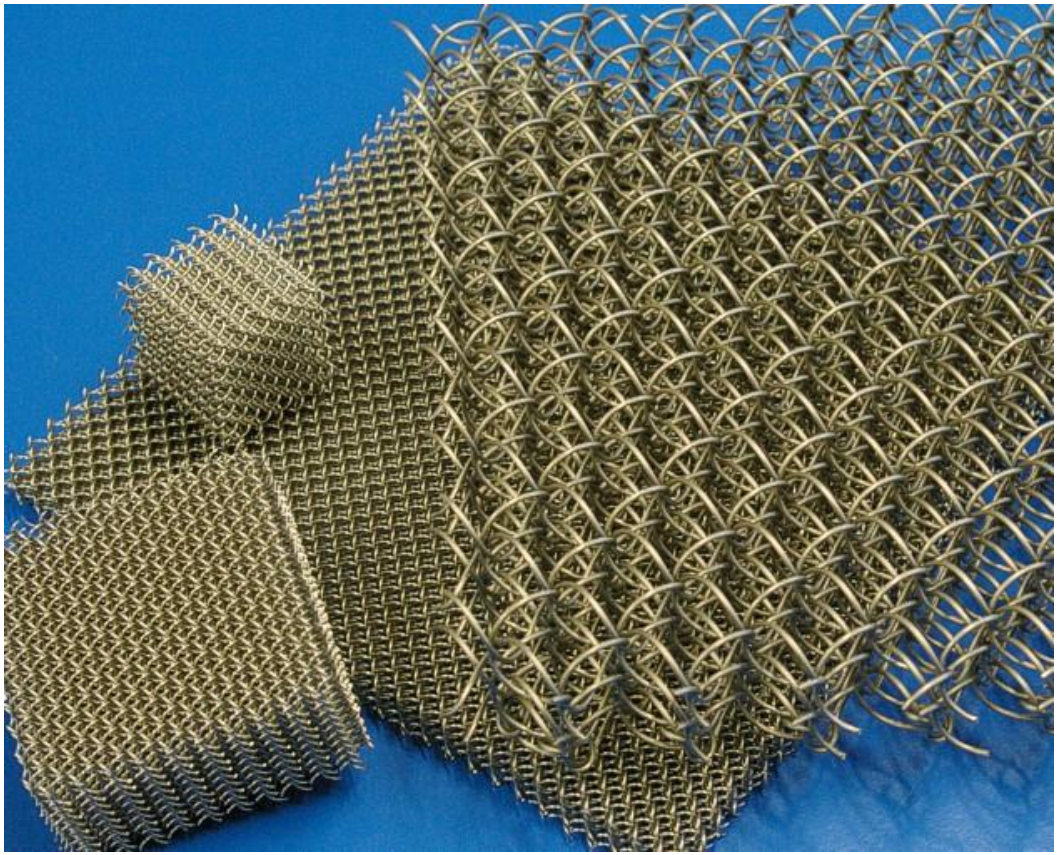

Archivierungsangaben

Fraunhofer IFAM Dresden

IWP Werkzeugmaschinen und Produktionsprozesse

Fraunhofer IWU

The contents of this presentation may not be copied and/or distributed without permission of the author! Please note references at the end of the presentation!

Wire structures

Manufacturing

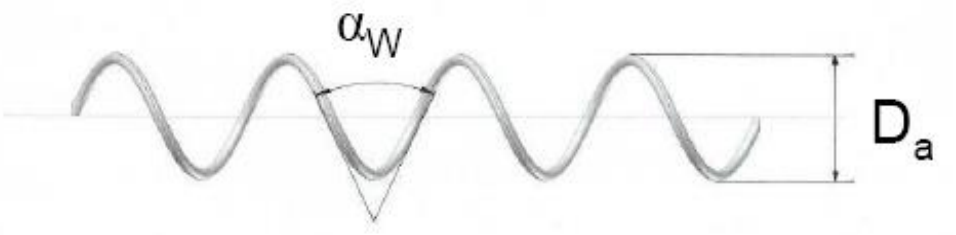

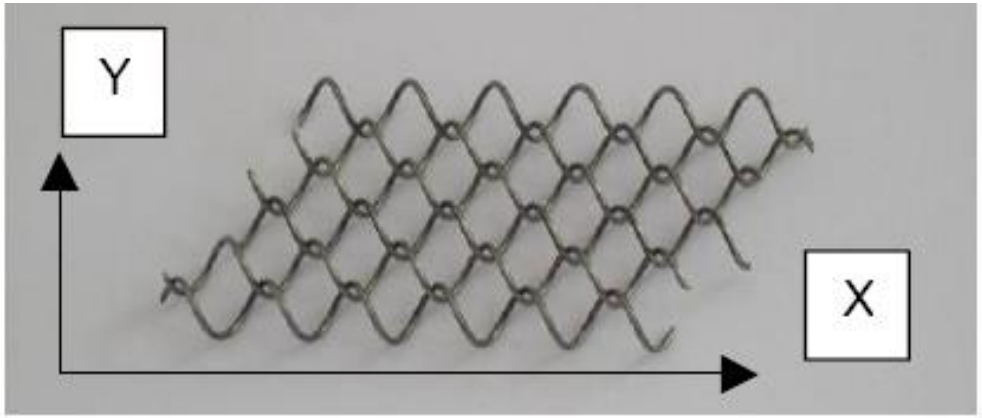

- Production in layers by interleaved turning of spiral beads
- Cross points are solded
- Stiffness and conductance adjustable

Fraunhofer IFAM Dresden

Archivierungsangaben

IWP Werkzeugmaschinen und Produktionsprozesse

Fraunhofer IWU

The contents of this presentation may not be copied and/or distributed without permission of the author! Please note references at the end of the presentation!

Properties

3D Wire Structures

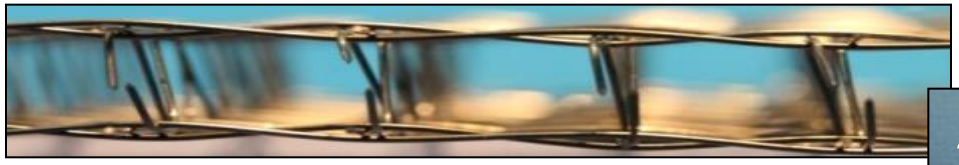

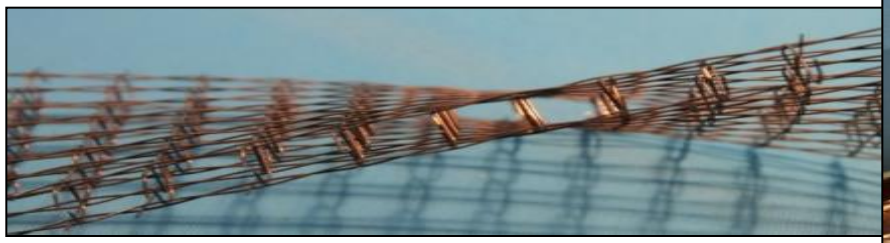

Archivierungsangaben

The contents of this presentation may not be copied and/or distributed without permission of the author! Please note references at the end of the presentation!

Wire structures

Manufacturing

- At the moment scales from ca. 150 x 150 x 150 mm^3 possible
- Automatic plant under construction with building area of 600 x 600 mm^2

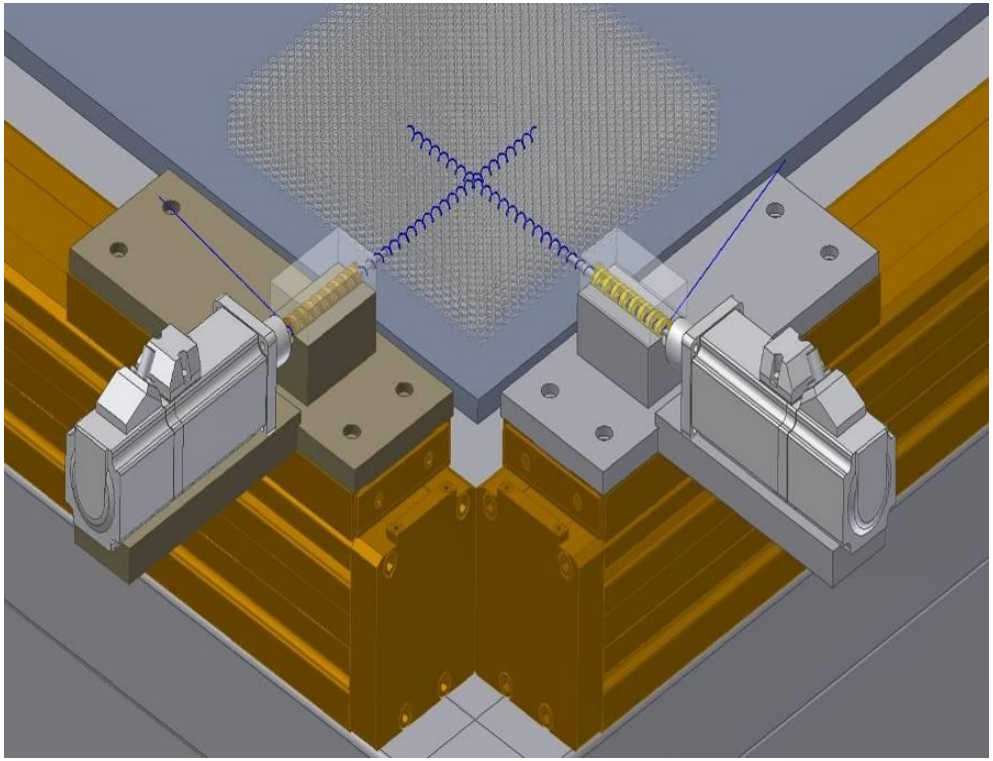

Archivierungsangaben

The contents of this presentation may not be copied and/or distributed without permission of the author! Please note references at the end of the presentation!

Technologies

Porous Metal Paper

Metal Paper
Paper Machine

Component production
Corrugation

Heat treatment
debinding/sintering

Technology from established mass production processes

Paper Manufacturing Process

Processing from corrugated board manufacturing industry

Sintering from metal injection moulding

Archivierungsangaben

PTS THE PAPER TECHNOLOGY SPECIALISTS

IWP WERKZEUGMASCHINEN UND PRODUKTIONSPROZESSE

Fraunhofer IWU

The contents of this presentation may not be copied and/or distributed without permission of the author! Please note references at the end of the presentation!

Properties

Porous Metal Paper

Porous Metal Paper - Microstructure after thermal treatment
(debinding and sintering)

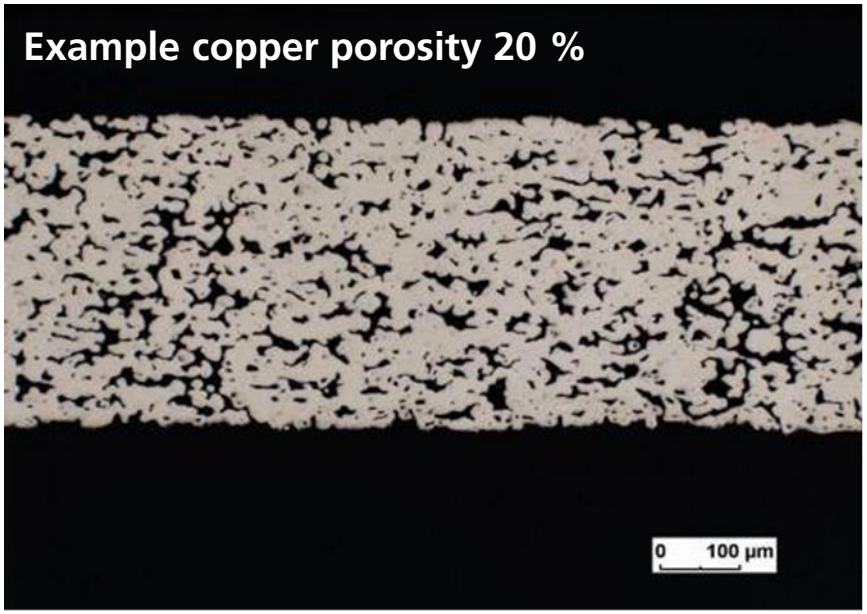

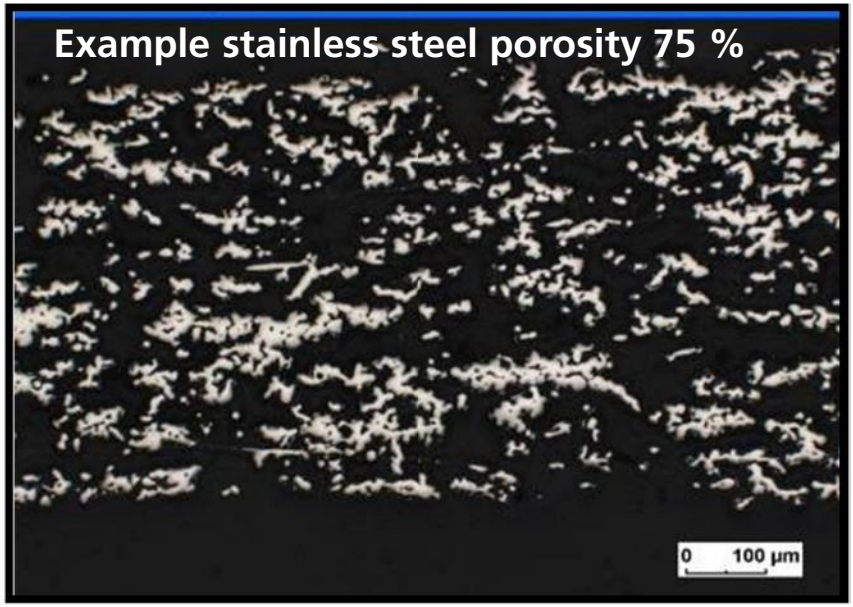

Variations with respect to pore size, morphology and porosity

Archivierungsangaben

The contents of this presentation may not be copied and/or distributed without permission of the author! Please note references at the end of the presentation!

Properties

Porous Metal Paper

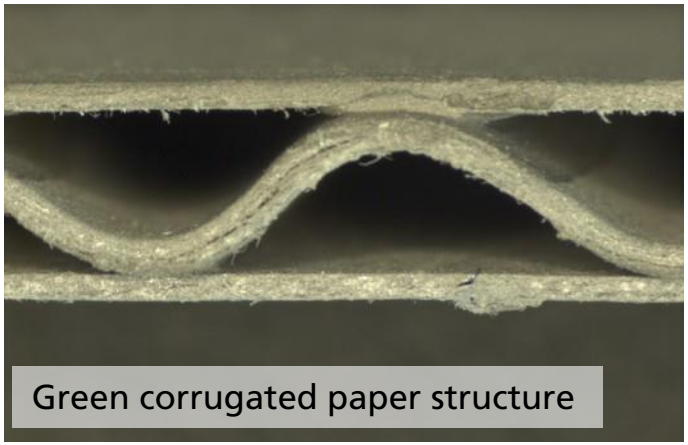

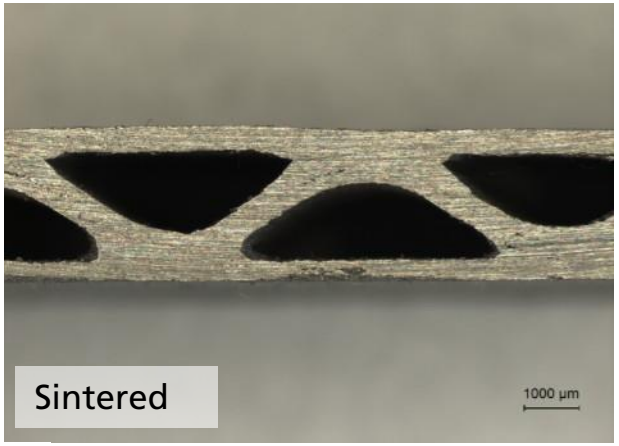

Archivierungsangaben

The contents of this presentation may not be copied and/or distributed without permission of the author! Please note references at the end of the presentation!

CELLULAR METALS

Part II – Properties and applications

© Fraunhofer IWU
Prof. Neugebauer

The contents of this presentation may not be copied and/or distributed without permission of the author! Please note references at the end of the presentation!

CONTENT

- Species of cellular metals and structures
- Properties and applications of cellular metals and structures
  - Open-cellular foams/structures
  - Closed-cellular foams
  - Fiber structures
  - Hollow sphere structures
  - Wire structures

Archivierungsangaben

The contents of this presentation may not be copied and/or distributed without permission of the author! Please note references at the end of the presentation!

Species of cellular metals and structures

© Fraunhofer IWU
Prof. Neugebauer

The contents of this presentation may not be copied and/or distributed without permission of the author! Please note references at the end of the presentation!

Cellular metals and structures

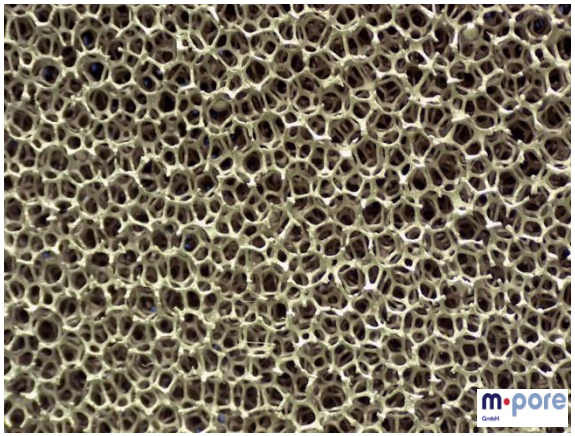

Open-cellular metal foam

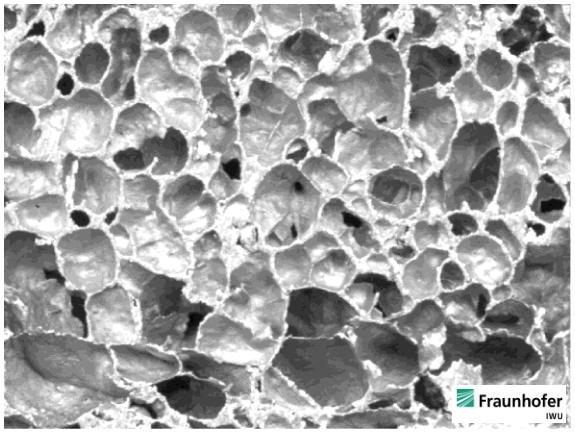

Closed-cellular metal foam

Hollow sphere structure

Fiber structure

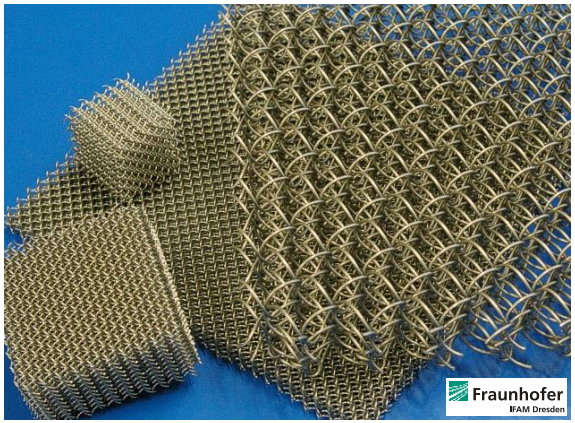

Wire structure

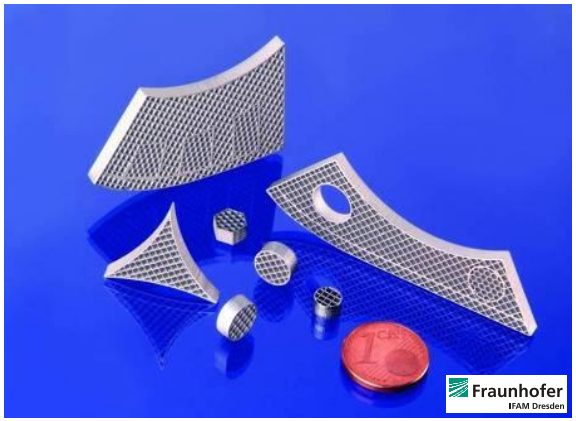

Direct typed metal structure

Archivierungsangaben

IWP WERKZEUGMASCHINEN UND PRODUKTIONSPROZESSE

Fraunhofer IWU

The contents of this presentation may not be copied and/or distributed without permission of the author! Please note references at the end of the presentation!

Advantages leading to market potential

Bending resistant

Lightweight

Vibration damping

Energy ansorbing

Recyclable

Radiation shielding

Heat resistant

Permeable

Archivierungsangaben

The contents of this presentation may not be copied and/or distributed without permission of the author! Please note references at the end of the presentation!

Applications of Cellular Metals

Compared to former time some new **real applications** coming up:

- Automotive (Alulight, Gleich) ➡ flame arresters (RECEMAT)
- Railway (IMMM, Gleich) ➡ biomaterials (Synthes)
- Machine tools (IWU, Gleich) ➡ silencers, chemical reactors (RECEMAT)
- Catalyzers (Evonic) ➡ design (Alulight, IWE, m-pore, Gleich)
- Heat exchanger (Mayser) ➡ consumer products (HZD)

First mass applications: > 100.000 pieces per annum

Steering-roll-housing based on Zinc by Havelländische Zink Druckguss GmbH

Mini crash absorber based on Aluminum by Alulight International GmbH

Component of a machine tool since 2004 by Fraunhofer IWU

Archivierungsangaben

The contents of this presentation may not be copied and/or distributed without permission of the author! Please note references at the end of the presentation!

Properties and applications of cellular metals and structures

© Fraunhofer IWU
Prof. Neugebauer

The contents of this presentation may not be copied and/or distributed without permission of the author! Please note references at the end of the presentation!

Open-cellular foams/structures

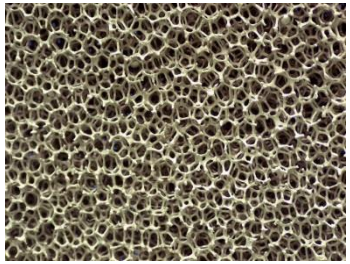

© Fraunhofer IWU
Prof. Neugebauer

The contents of this presentation may not be copied and/or distributed without permission of the author! Please note references at the end of the presentation!

Properties

General information

Materials	Fe-, Ni-, Co-, Ti-alloys, intermetallics
Structure geometry/ dimensions	Cell size 0.2 - 5 mm Cell wall thickness 20 µm - 1000 µm Plates, cylinders, tubes, net-shape-parts
Properties	- High permeability - Great specific surface - Well heat exchange ability - Well acoustic absorption - Calculable and repeatable

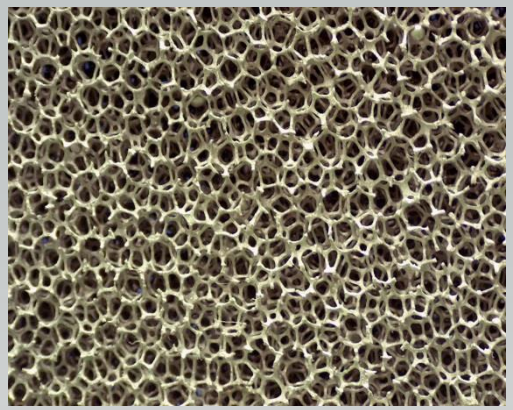

Archivierungsangaben

The contents of this presentation may not be copied and/or distributed without permission of the author! Please note references at the end of the presentation!

Properties

Selected properties – stream ability/permeability

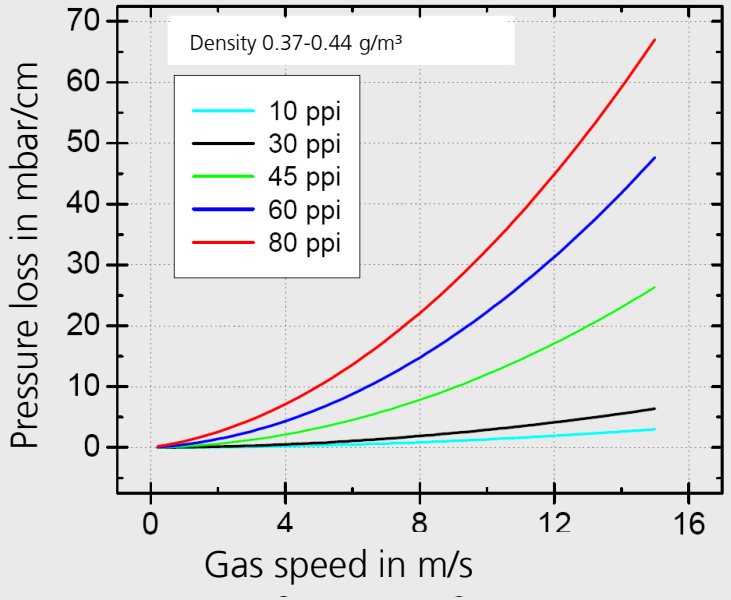

Pressure loss:

$$\frac{dp}{dl} = \frac{\mu_{gas}}{k_1} v + \frac{\rho_{gas}}{k_2} v^2$$

Cell width in [ppi]	Permeability k_1 in [m²]	Permeability k_2 in [m²]
10	$3.0 \cdot 10^{-7}$	110
30	$8.7 \cdot 10^{-8}$	230
45	$2.0 \cdot 10^{-8}$	950
60	$5.5 \cdot 10^{-9}$	1620
80	$2.2 \cdot 10^{-9}$	2080

Archivierungsangaben

The contents of this presentation may not be copied and/or distributed without permission of the author! Please note references at the end of the presentation!

Properties

Selected properties – pressure strength

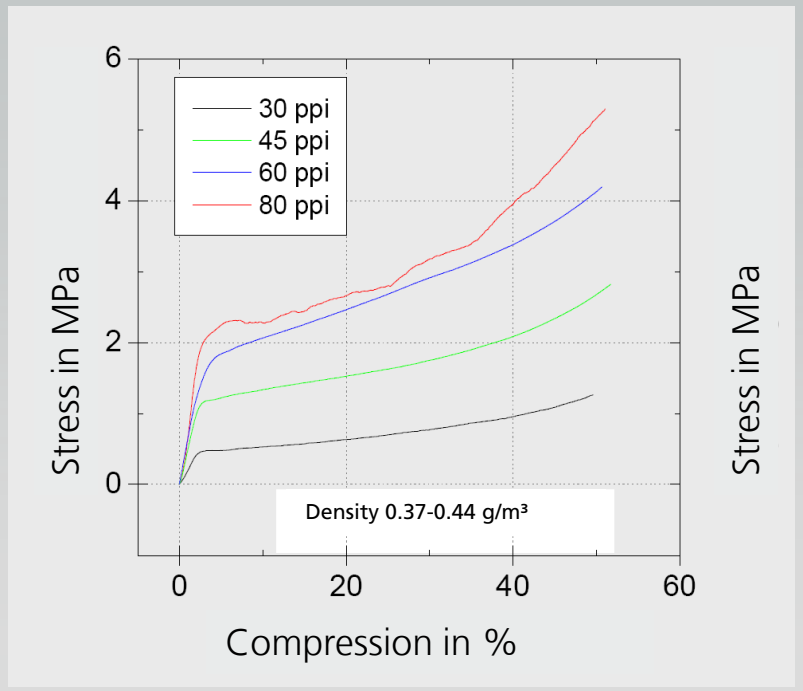

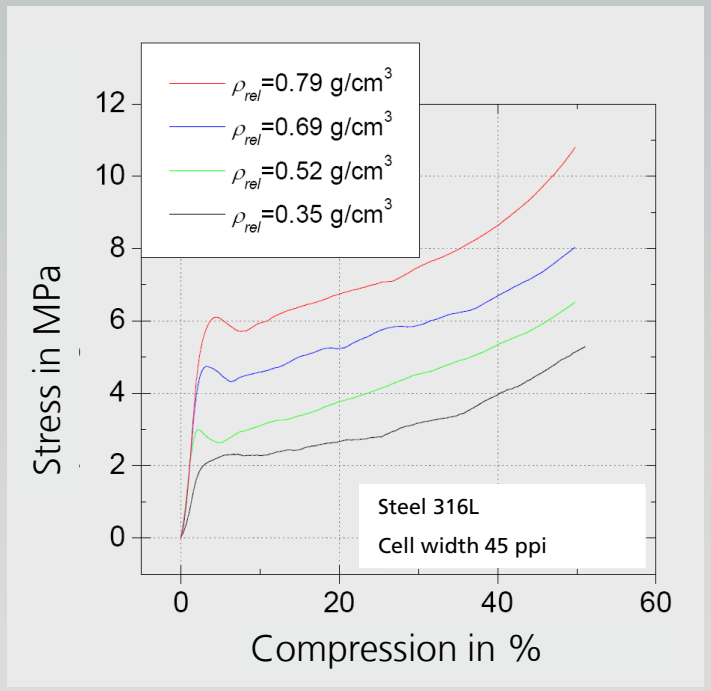

Archivierungsangaben

The contents of this presentation may not be copied and/or distributed without permission of the author! Please note references at the end of the presentation!

Properties

Selected properties – acoustics

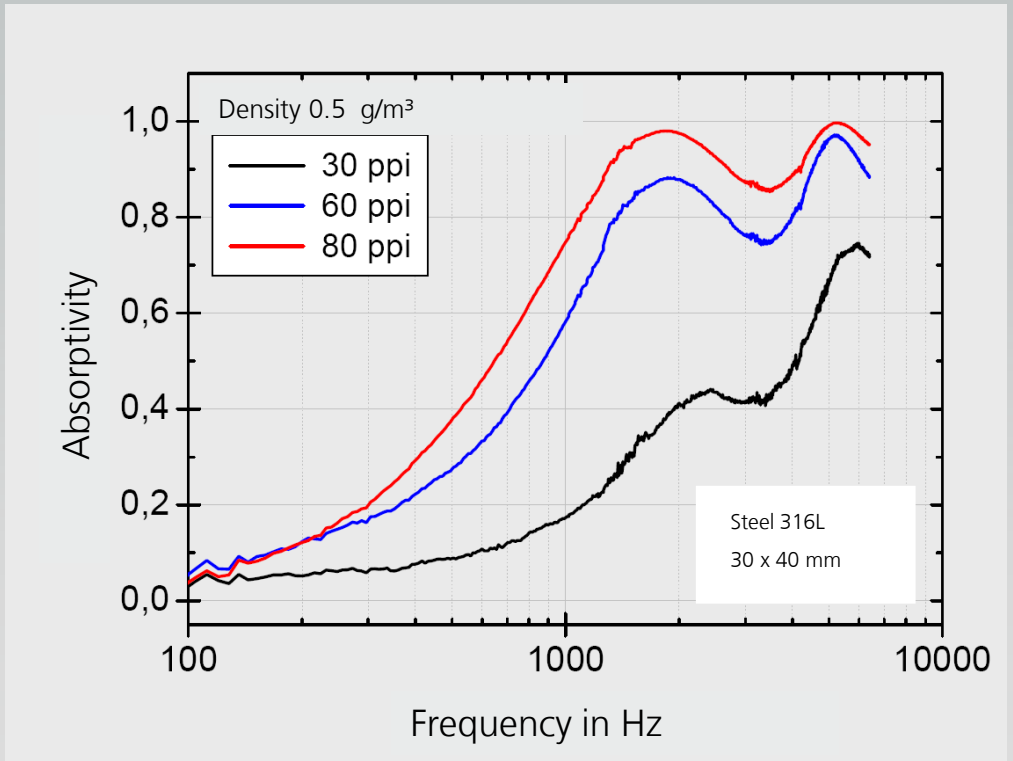

Archivierungsangaben

The contents of this presentation may not be copied and/or distributed without permission of the author! Please note references at the end of the presentation!

Open-cellular foams/structures

Use of permeability in filters and good thermal conductivity

Heat exchanger

Air inlet on computer housing

Computer processor cooler

Filter of exhaust hood

Archivierungsangaben

The contents of this presentation may not be copied and/or distributed without permission of the author! Please note references at the end of the presentation!

Open-cellular foams/structures

Use of visual attractivity and light scattering effects

Architectural applications such as trade fair stands and design elements

Lamps and advertisement signs (indirect lightning)

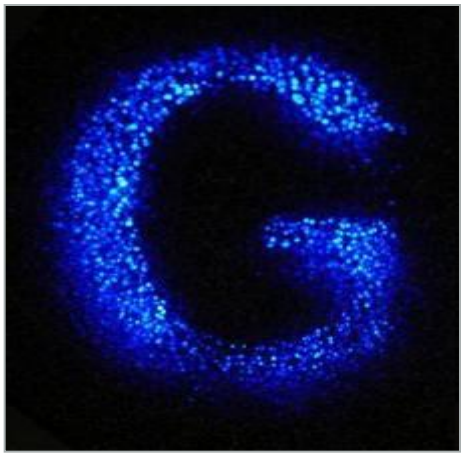

Archivierungsangaben

The contents of this presentation may not be copied and/or distributed without permission of the author! Please note references at the end of the presentation!

Metallic foams in DOC, DPF by INCOFOAM®HT

Coating of plain Nickel-foam with improved heat and corrosion resist

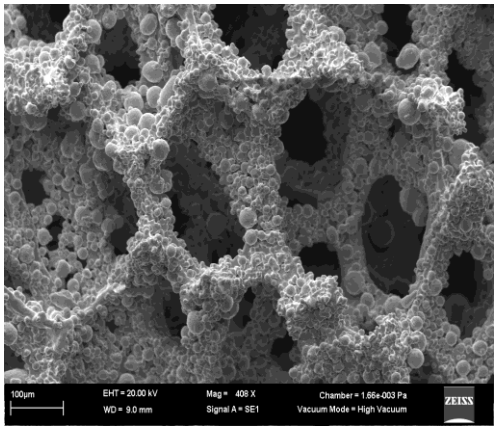

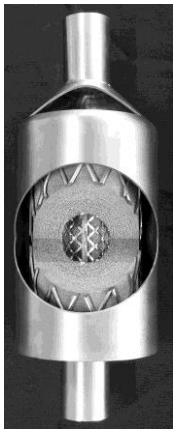

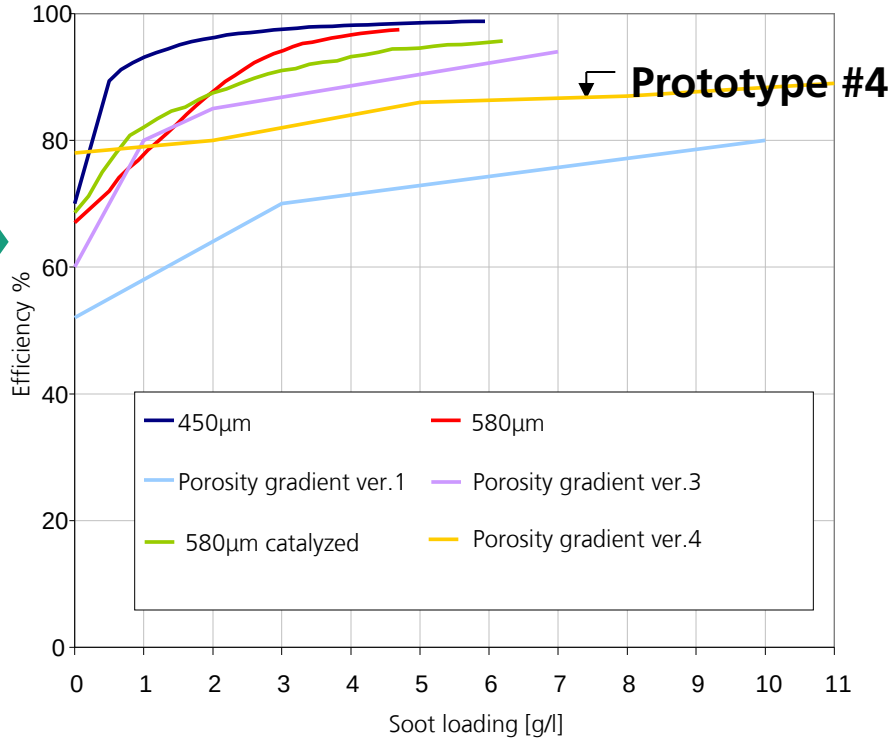

Results:

- → High volumetric efficiency (true tortuous path)
- → Excellent sound reduction properties
- → Temperature and corrosion resistance up to 1000 °C

Archivierungsangaben

The contents of this presentation may not be copied and/or distributed without permission of the author! Please note references at the end of the presentation!

Application

Latent storage device for climate control

Technology: Combination of open cell aluminum foam with phase change material

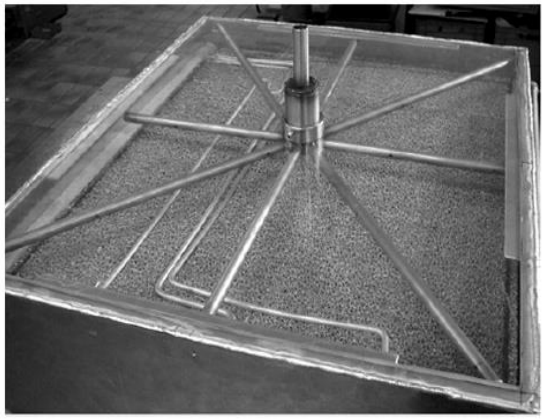

Latent storage system on ice basis for the mobile air conditioning. Discharge capacity of 6.2 kWh

Medium	Heat conductivity $\left[\frac{W}{m \cdot K}\right]$

	With metal foam	Without metal foam
H_2O	6.9	0.57
Ice	7.4	2.20
Paraffin RT6	7.0	0.2

Drawback Phase Change Material:

➡ **Low heat conductivity**

Results using open cell Al-foam:

→ Significant increase of the heat conductivity

→ Represent seed crystals and therefore avoiding super cooling and overheating

→ Flexibility in shape and design

m•pore

Archivierungsangaben

IWP WERKZEUGMASCHINEN UND PRODUKTIONSPROZESSE

Fraunhofer IWU

The contents of this presentation may not be copied and/or distributed without permission of the author! Please note references at the end of the presentation!

Applications

Adsorption Heat Accumulator

- Adsorber made of thin zeolite layers (SorTech AG, Germany) on highly heat conducting network with high specific surface area (5.000 to 25.000 m^2/m^3)
- Lab test samples reach a power density of 4 kW/l with cycling times in the range of a few minutes; target value for real-life adsorber including heat exchanger architecture is > 0.5 kW/l

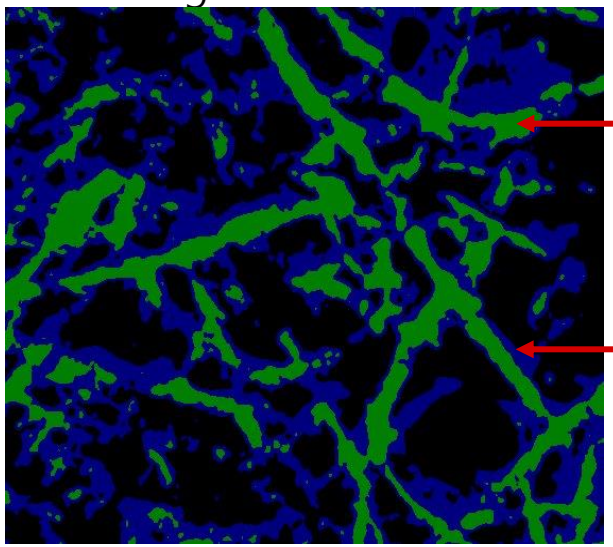

green: heat conducting AlCu5 fiber network

blue: zeolite layers

Tomography image courtesy of FhG ITWM

Archivierungsangaben

The contents of this presentation may not be copied and/or distributed without permission of the author! Please note references at the end of the presentation!

Open porous metals

- Possible application fields
  - Thermochemical energy storage
  - Heat exchanger
  - Condenser/Evaporator

cast Al/zeolite composite heat exchanger

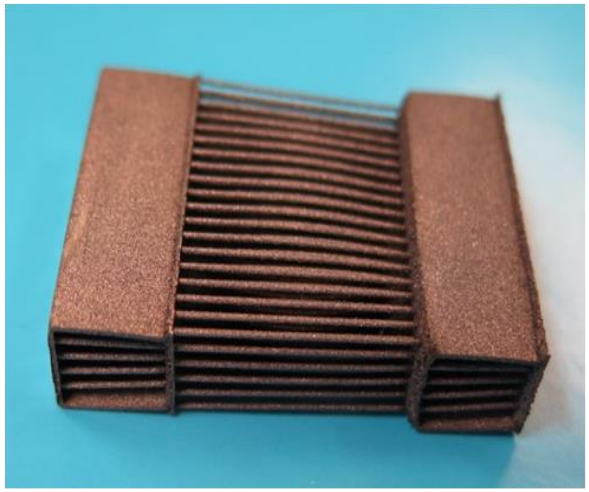

printed heat exchanger

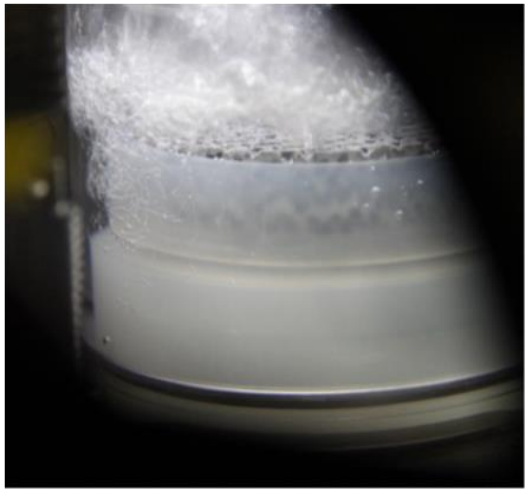

evaporator test

Aktivierungsenergien

Joachim Baumeister, Fraunhofer Institute IFAM Bremen
Department of Powder Technology

Fraunhofer IFAM

The contents of this presentation may not be copied and/or distributed without permission of the author! Please note references at the end of the presentation!

Open-cellular foams/structures

Use of open porous surface in medical equipment and implants

Bone structure

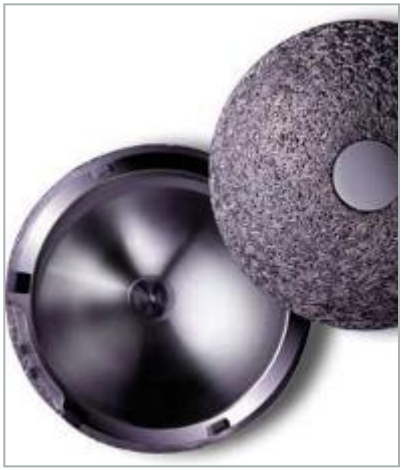

Bone structure

Interaction

Interaction

Metal foam

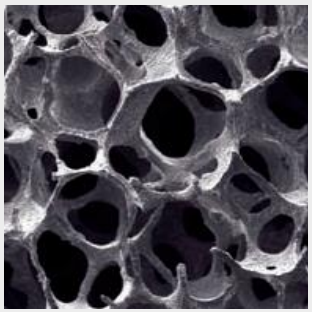

Metal foam

Archivierungsangaben

IWP WERKZEUGMASCHINEN UND PRODUKTIONSPROZESSE

Fraunhofer IWU

The contents of this presentation may not be copied and/or distributed without permission of the author! Please note references at the end of the presentation!

Applications

Synthetic Bone Replacement

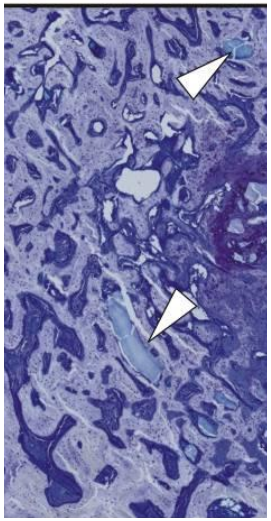
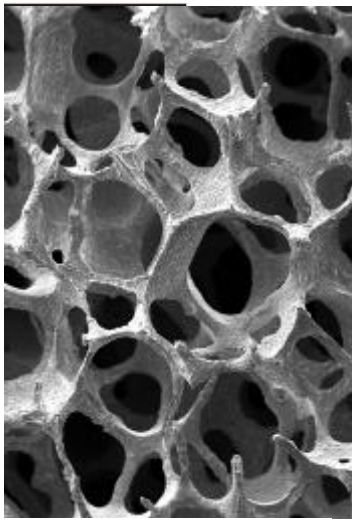
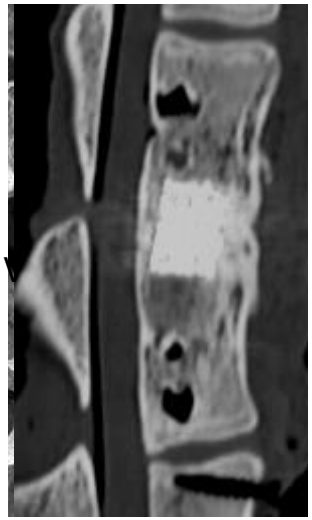
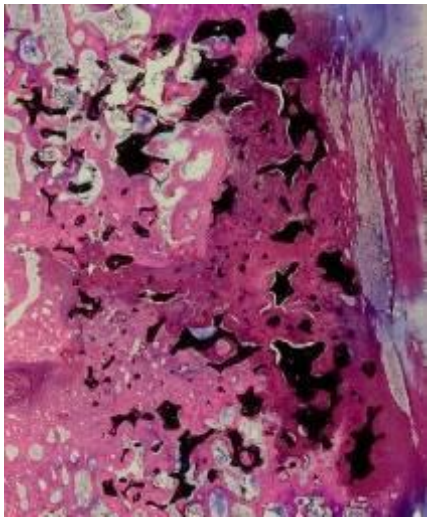
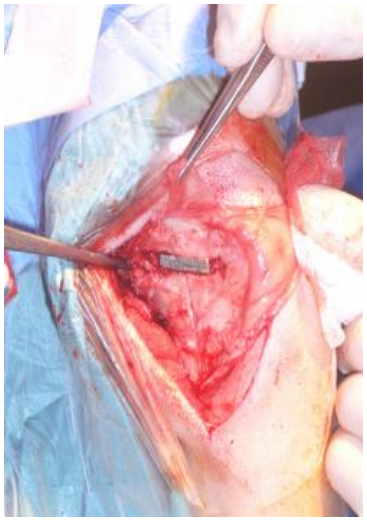

synthetic bone replacement

- Biomechanical adaption to bone properties
- Powder metallurgical technologies for manufacturing of cellular metals with adjustable stiffness
- interckonnecting pore structure
- osseointegration improves primary and secondary stability
- vascularisation needed for bone formation

Archivierungsangaben

CHARITÉ UNIVERSITÄTSMEDIZIN BERLIN
Medizinische Hochschule Hannover
LMU
IWP WERKZEUGMASCHINEN UND PRODUKTIONSPROZESSE
Fraunhofer IWU

The contents of this presentation may not be copied and/or distributed without permission of the author! Please note references at the end of the presentation!

Applications

Biodegradable Bone Replacement Implants

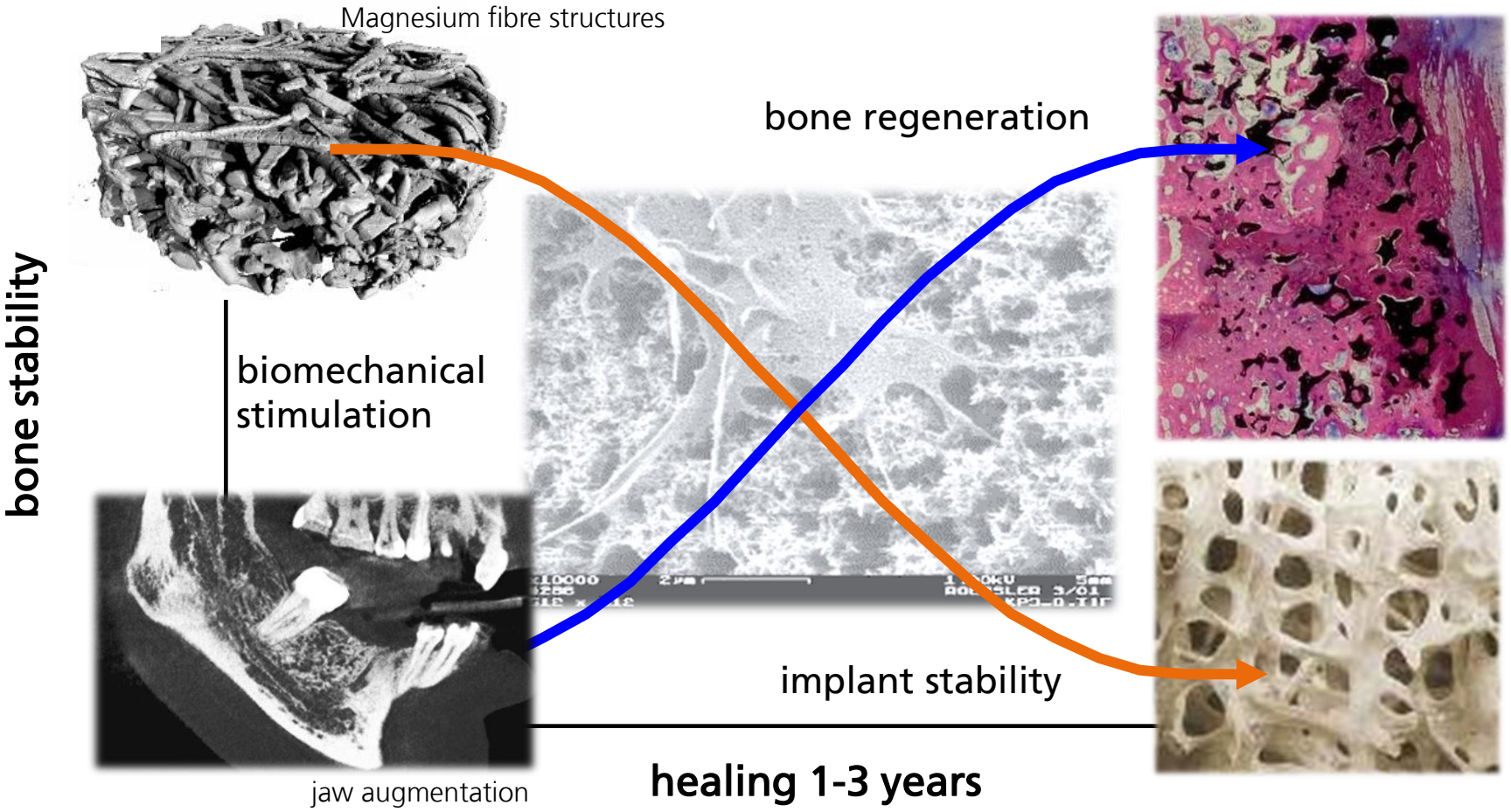

Archivierungsangaben

The contents of this presentation may not be copied and/or distributed without permission of the author! Please note references at the end of the presentation!

Closed-cellular foams

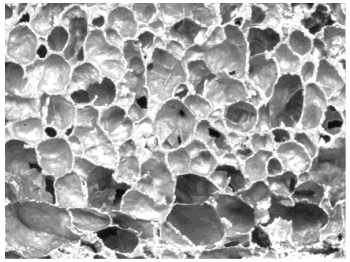

© Fraunhofer IWU
Prof. Neugebauer

The contents of this presentation may not be copied and/or distributed without permission of the author! Please note references at the end of the presentation!

Properties

Material parameters of aluminum foam

Density	**0,5 - 0,9 g/cm³**
Lateral contraction	**0,31 - 0,34**
Modulus of elasticity (0,7 g/m³)	**ca. 6300 N/mm²**
Pressure resistance (0,7 g/m³)	**ca. 15 N/mm²**
Heat conductance (0,7 g/m³)	**ca. 20 W/m·K**
Damping capacity of materials (0,7 g/m³)	**ca. $4{,}5 \cdot 10^{-3}$**

→ typical: 0.7 g/cm³

$KW_{Foam} = KW_{Solid} (r_{Foam}/r_{Solid})^n$ mit $n \approx 2$

Fulfils fire prevention requirements DIN 4102

Temperature resistance till ca. 500 °C

High energy absorption ability

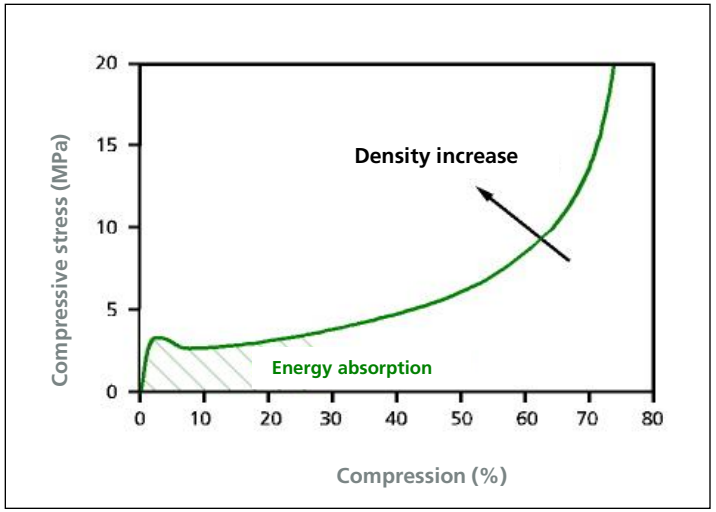

Fraunhofer IWU

Archivierungsangaben

IWP Werkzeugmaschinen und Produktionsprozesse

Fraunhofer IWU

The contents of this presentation may not be copied and/or distributed without permission of the author! Please note references at the end of the presentation!

Properties

Material characteristics of aluminum foam

Attributes	Unit	Al-Foam				
Density	g/cm³	0.5	0.6	0.7	0.8	0.9
Compressive strength	N/mm²	k. A.	7.9 (1) 12.7 (2)	k. A.	k. A.	k. A.
Tensile strength	N/mm²	k. A.	4.0 (1) 6.2 (2)	k. A.	k. A.	k. A.
Bending strength by 2.2 % expansion	N/mm²	k. A.	22-34 (1)	25-41 (1)	38-45 (1)	39-50 (1)
E-modulus	kN/mm²	3.5	4.7 4.9 (1) 4.5 (2)	6.0	7.5	9.1
Poisson's number	-	0.33				
Heat conductivity (0-300 °C)	W/(m·K)	12-20	16.7 (1)(3) 18.4 (1)(3)	19-36	k. A.	k. A.
Linear thermal expansion coefficient	10^{-6}/K	analog to the linear thermal expansion coefficient of the solid (Al: 23.9 by 0 °C)				
Specific heat capacity	kJ/(kg·K)	k. A.	0,88 (1) 0,92 (2)	k. A.	k. A.	k. A.

k. A. ... not specified (1) ... AlSi12 (2) ... AlMg1SiCu (not cured) (3) ... by RT

Archivierungsangaben

The contents of this presentation may not be copied and/or distributed without permission of the author! Please note references at the end of the presentation!

Properties

Lightweight construction potential of aluminum foam

Squared beam, set on both ends

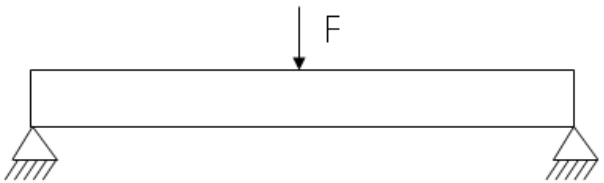

$$m = \frac{1}{2} \cdot \sqrt{\frac{F \cdot l^5}{f}} \cdot \frac{\rho}{\sqrt{E}}$$

constant

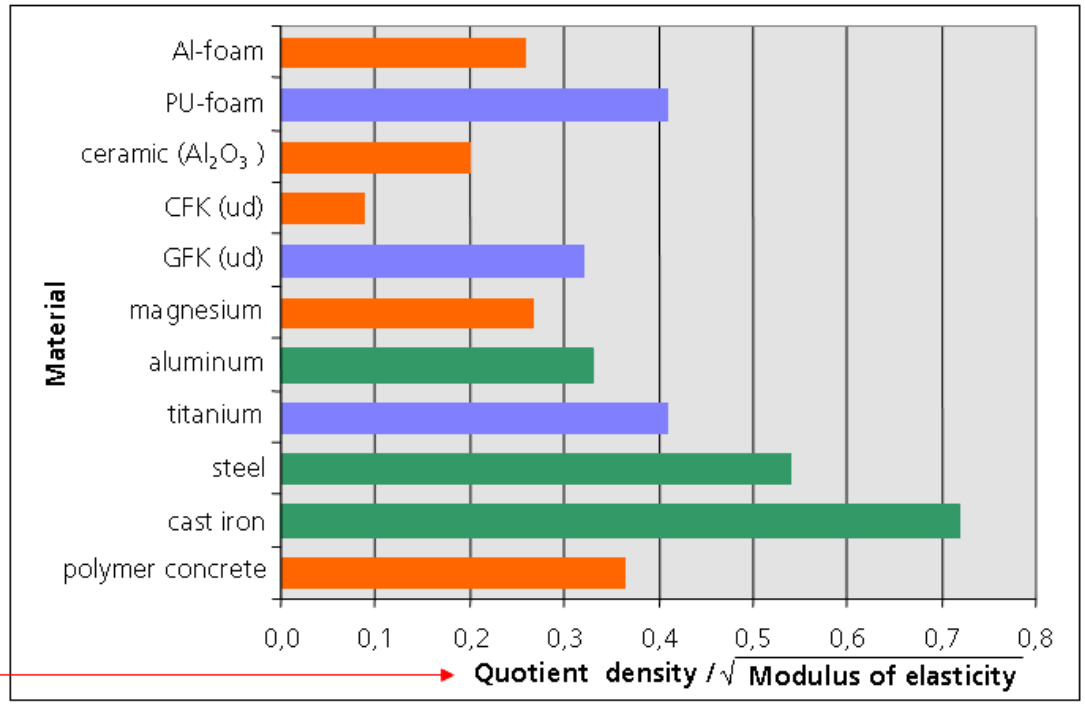

State of the art

Nearly non practical applications

Potential for lightweight construction

Fraunhofer IWU

Archivierungsangaben

IWP Werkzeugmaschinen und Produktionsprozesse

Fraunhofer IWU

The contents of this presentation may not be copied and/or distributed without permission of the author! Please note references at the end of the presentation!

Properties

Vibration damping potential of aluminum foam

$$\Lambda = \frac{\delta}{f_n} = \Pi \cdot d = \Pi \cdot D \cdot 2$$

D	...	damping	[-]
Λ	...	logarithmic decrement	[-]
δ	...	decay constant	[1/s]
f_n	...	natural frequency, number n	[Hz]
d	...	loss factor	[-]

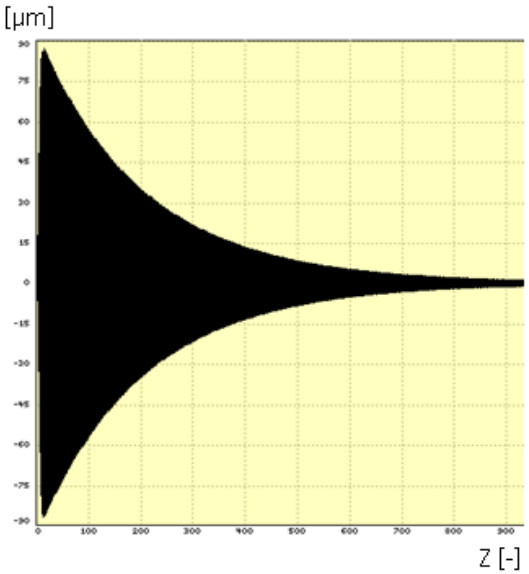

We distinguish between:

- damping of material,
- damping of friction,
- damping of displacement,
- heterodyne damping

"Structure damping" is the resulting damping of a component (structure)

Damping effects on vibrations and also:

- dimensional accuracy
- accuracy of path
- tool wear
- ...

Archivierungsangaben

The contents of this presentation may not be copied and/or distributed without permission of the author! Please note references at the end of the presentation!

AFS =

Aluminum foam-Sandwiches

Metallic bonding of aluminum foam with aluminum cover sheet

1 **2** **3** **4**

SAS =

Steel-Aluminum foam-Steel-Sandwiches

Metallic bonding of aluminum foam with steel cover sheet

钢板上铝泡沫的冶金接合

Archivierungsangaben

The contents of this presentation may not be copied and/or distributed without permission of the author! Please note references at the end of the presentation!

Closed-cellular foams

Light weight design slides in machine tools

Sandwiches with aluminum foam core and steel sheets

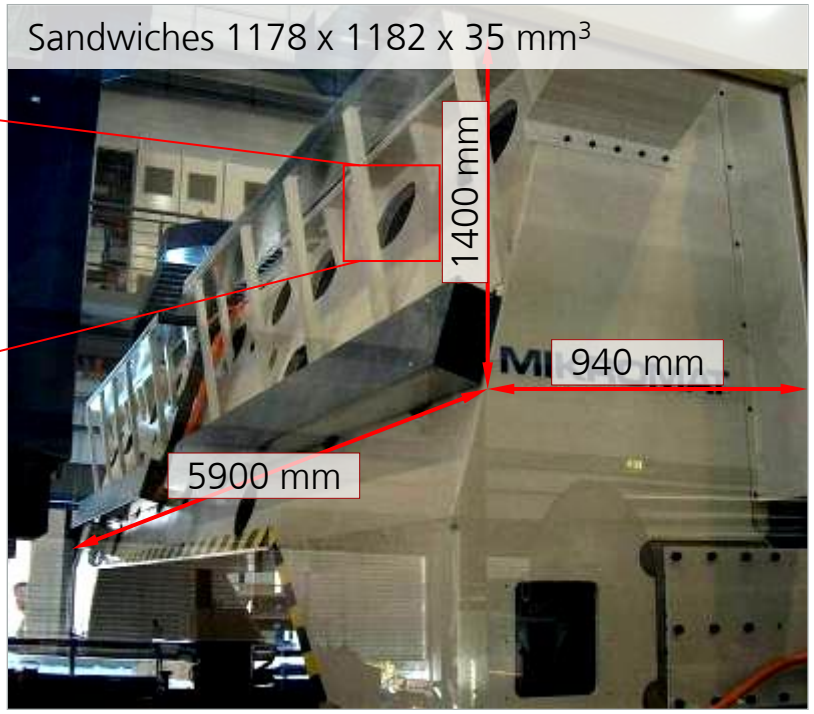

Fraunhofer IWU

Archivierungsangaben

IWP Werkzeugmaschinen und Produktionsprozesse

Fraunhofer IWU

The contents of this presentation may not be copied and/or distributed without permission of the author! Please note references at the end of the presentation!

Closed-cellular foams

Cross beam of a milling machine made of steel-foam sandwiches

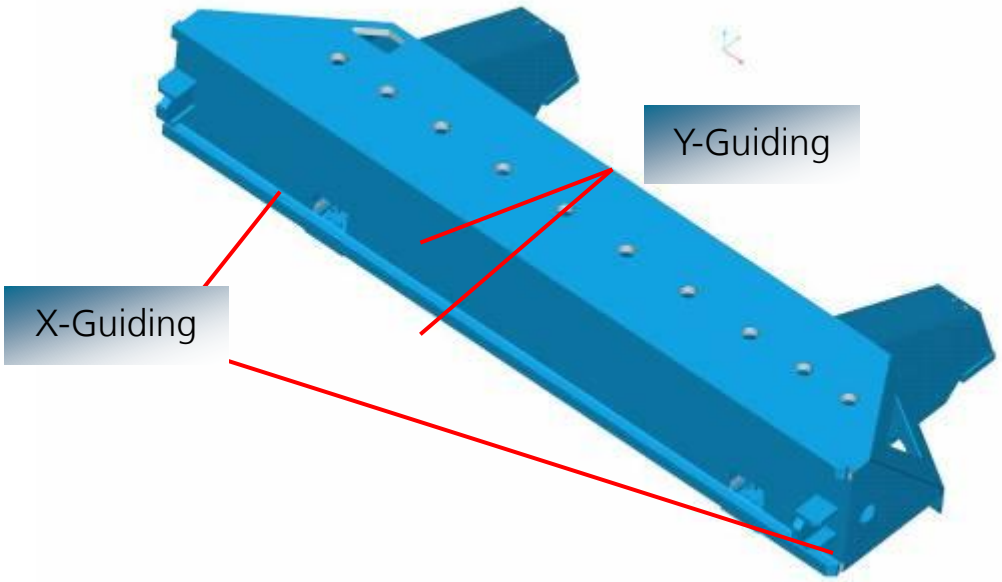

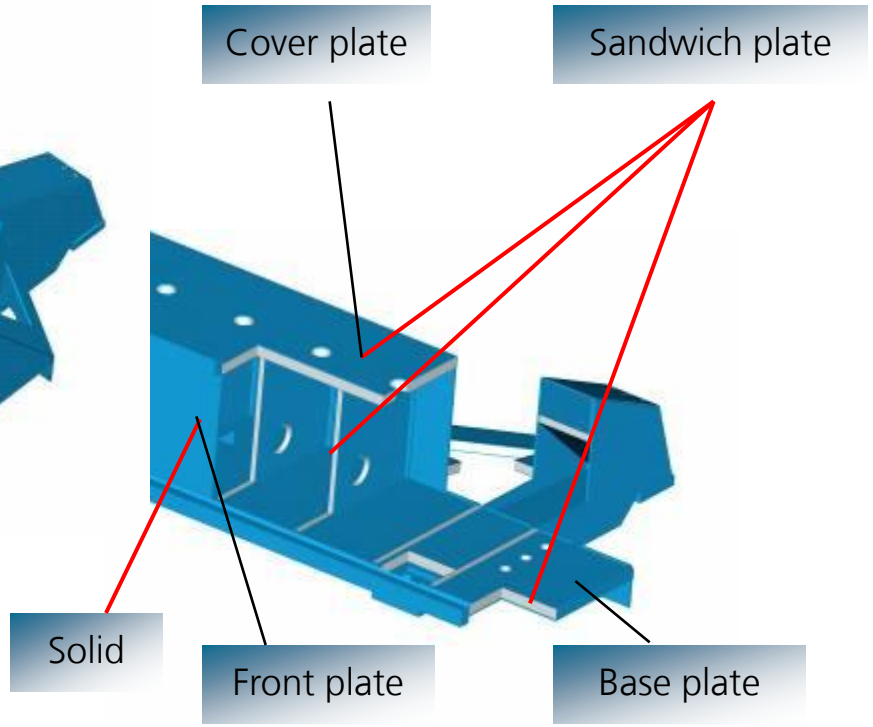

Change	
Mass	- 3 %
Stiffness	+ 21%
1. Natural frequency	+ 253%
Damping	+ 270%

Archivierungsangaben

The contents of this presentation may not be copied and/or distributed without permission of the author! Please note references at the end of the presentation!

Closed-cellular foams

Cross beam of a milling machine made of steel-foam sandwiches

Archivierungsangaben

The contents of this presentation may not be copied and/or distributed without permission of the author! Please note references at the end of the presentation!

Closed-cellular foams

Development of costs – examples of machine tools

Para-meter	Cross slide milling machine	Support	Crossbeam milling machine	Universal-slide milling machine
	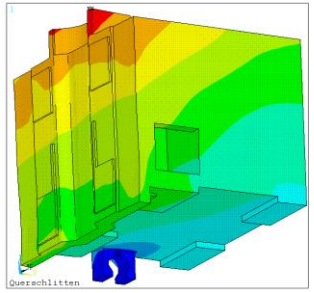	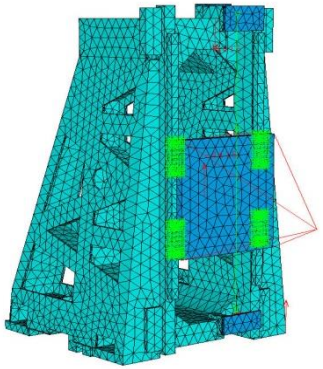	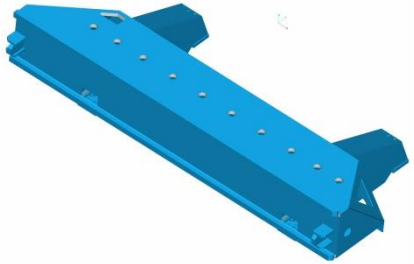	
Year	**1999**	**2002**	**2004**	**From 2004**
Δ m [%]	- 45 %	+ 4.5 %	- 3 %	-23 %
Δ S [%]	- 15 %	+ 12 %	+ 21 %	+ 4.6 %
Δ D [%]	720 %	380 %	270 %	not measured
Δ € [%]	380 %	180 %	170 %	140 %

m: Mass; **S**: Stiffness; **D**: Damping; **€**: Total charges

Archivierungsangaben

The contents of this presentation may not be copied and/or distributed without permission of the author! Please note references at the end of the presentation!

Closed-cellular foams

Architectural applications and design

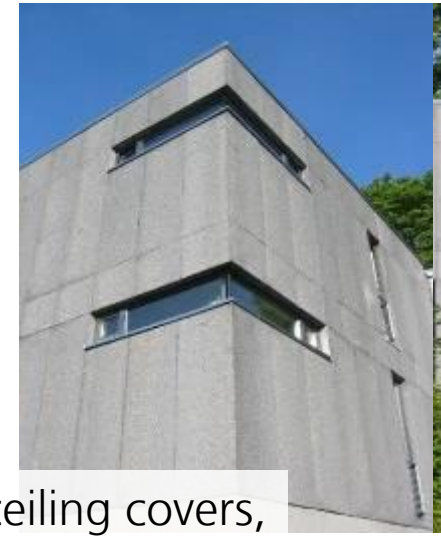

Wall and ceiling covers,
desks, chairs…

Archivierungsangaben

The contents of this presentation may not be copied and/or distributed without permission of the author! Please note references at the end of the presentation!

Closed-cellular foams

Architectural applications in ceiling and wall panels

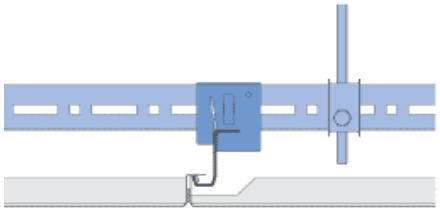

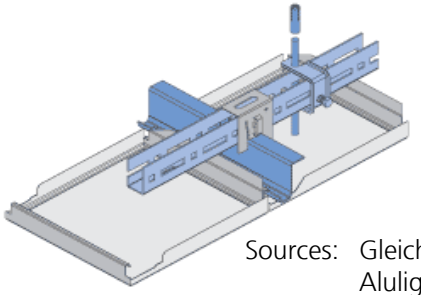

Sources: Gleich GmbH
Alulight GmbH

Archivierungsangaben

The contents of this presentation may not be copied and/or distributed without permission of the author! Please note references at the end of the presentation!

Application

Consumer goods based on Zinc-Foam → ZINCOPOR

Examples: **Steering-roll-housing** **doorknob**

Manufacturing: By modified Zinc-die casting

Properties: Porosity ≈ 30 – 55 %, tensile strength ≈ 30 - 150 MPa, yield strength ≈ 20 - 130 MPa

Advantages: Excellent surface finish, complex shapes available, material and cost saving (30%)

Status: Mass production for parts of vacuum cleaners > 100.000 parts/a

Archivierungsangaben

The contents of this presentation may not be copied and/or distributed without permission of the author! Please note references at the end of the presentation!

Closed-cellular foams

Crash absorber and elements of stiffening

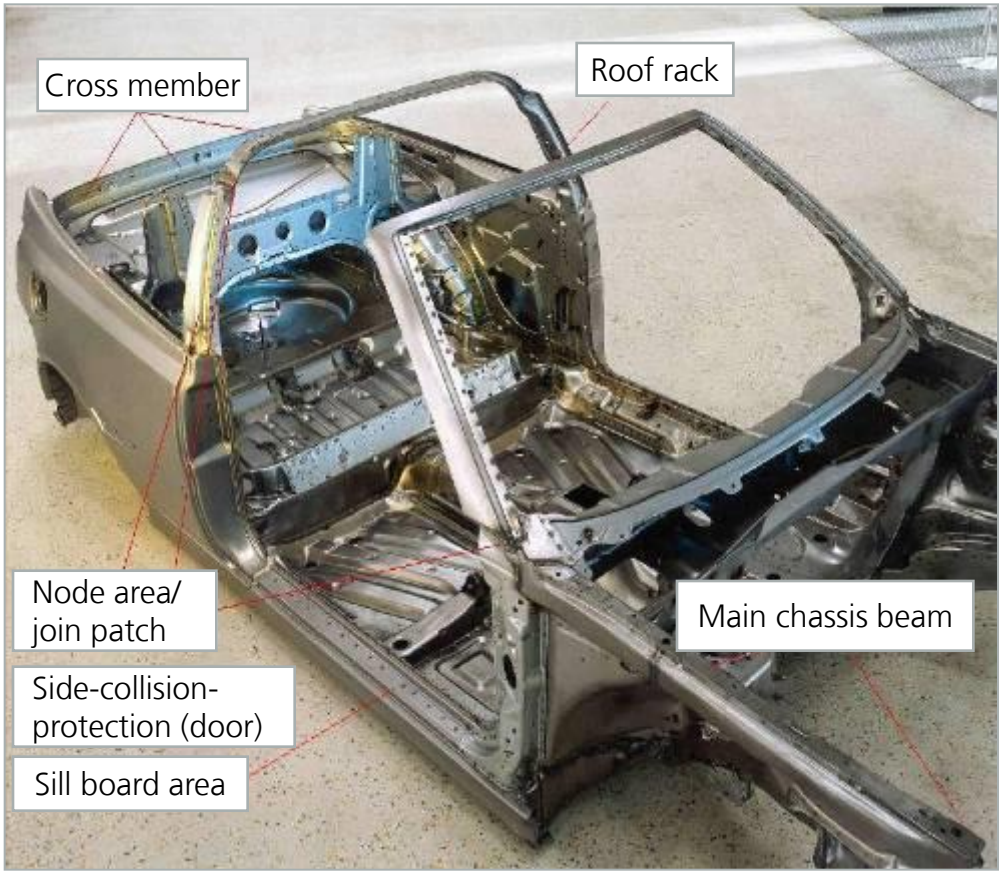

+ 10% torsion stiffness of the whole car body

Node area of D-pillar, stiffened by aluminum foam-cores

Foam-filled bumper

Sources: Volkswagen AG
Fraunhofer IWU

Archivierungsangaben

The contents of this presentation may not be copied and/or distributed without permission of the author! Please note references at the end of the presentation!

Closed-cellular foams

Crash absorber and elements of stiffening

200000 pieces / year

Metal foam crash absorber in a baggage net of Audi Q7.

Source: Alulight GmbH

3000 pieces / year

Reinforcing elements of metal foam in a side sill board of Ferrari Spider 430.

Source: Alulight

100 pieces / year

Lift arm holder of a telescope lift platform (telescope length: 25 m) of AFS

Source: alm GmbH

Archivierungsangaben

IWP WERKZEUGMASCHINEN UND PRODUKTIONSPROZESSE

Fraunhofer IWU

The contents of this presentation may not be copied and/or distributed without permission of the author! Please note references at the end of the presentation!

Closed-cellular foams

Crash absorber and elements of stiffening

Front hood

Crash box

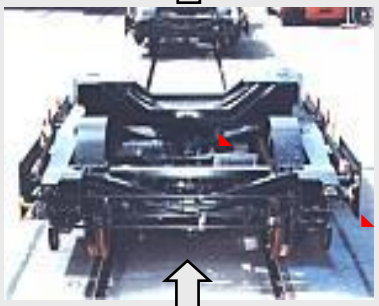

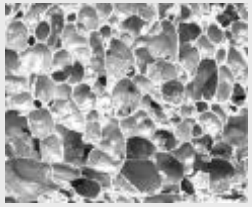

SIEMENS wilhelm schmitt

Archivierungsangaben

IWP WERKZEUGMASCHINEN UND PRODUKTIONSPROZESSE

Fraunhofer IWU

The contents of this presentation may not be copied and/or distributed without permission of the author! Please note references at the end of the presentation!

Quelle: www.siemens.com/press

Archivierungsangaben

The contents of this presentation may not be copied and/or distributed without permission of the author! Please note references at the end of the presentation!

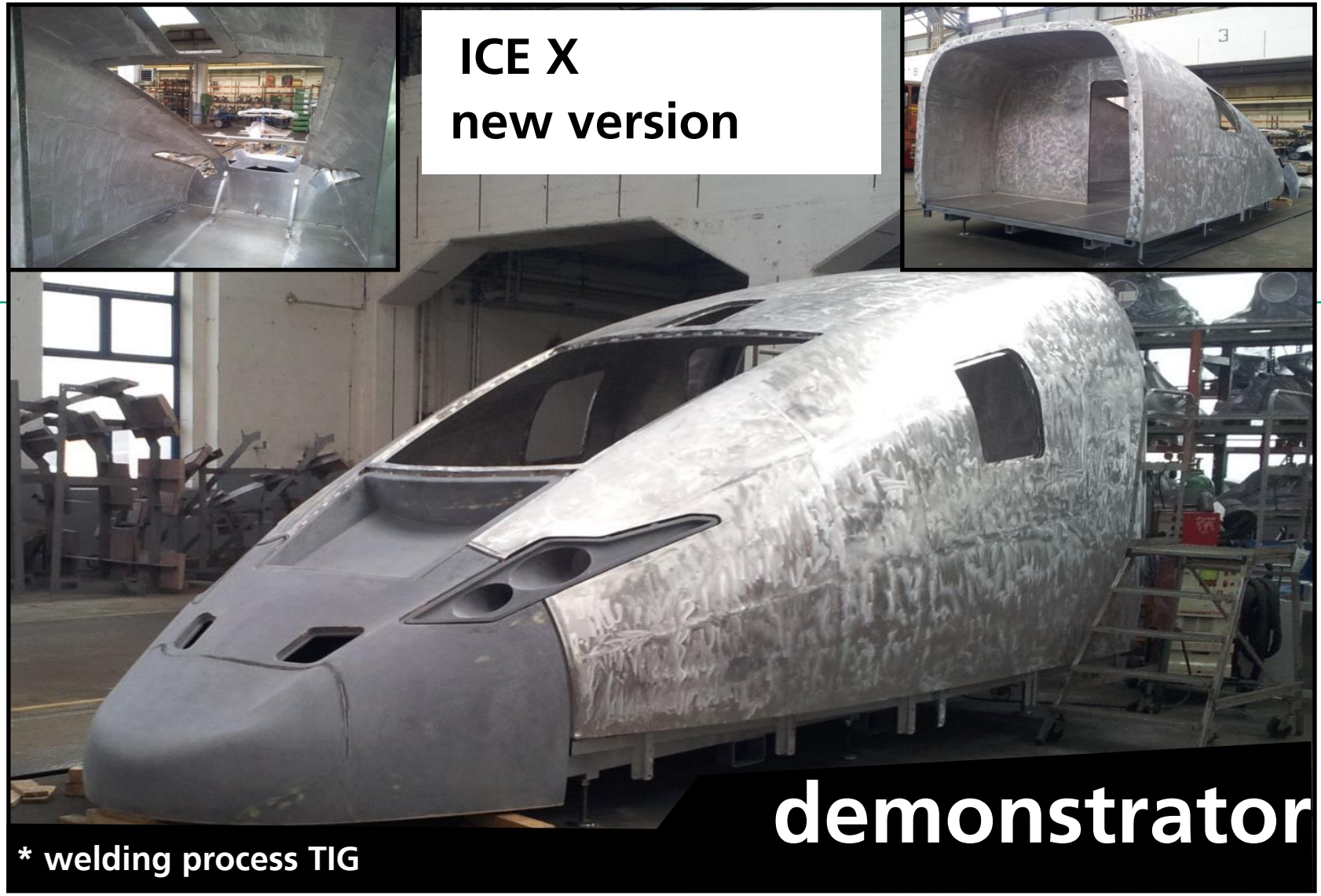

© Fraunhofer IWU
Prof. Neugebauer

The contents of this presentation may not be copied and/or distributed without permission of the author! Please note references at the end of the presentation!

Front cap of a high speed train

Comparison

ICE 3 D - Siemens

- bodywork: frame + outer shells
- Aluminum sheet 10 mm
- time-consuming positioning
- high tool expenses

Demonstrator - BlueS

- bodywork: sandwich, self-supporting
- Aluminum-Foam-Sandwich 30/2 mm
- reduced installation effort
- low tool expenses
- 20 % weight saving

Archivierungsangaben

The contents of this presentation may not be copied and/or distributed without permission of the author! Please note references at the end of the presentation!

© Fraunhofer IWU
Prof. Neugebauer

IWP WERKZEUGMASCHINEN UND PRODUKTIONSPROZESSE

Fraunhofer IWU

The contents of this presentation may not be copied and/or distributed without permission of the author! Please note references at the end of the presentation!

Subway floor

2008

Delivering of 21 plates

AFS 2400 x 1100 x 12

For a subway in Beijing

Archivierungsangaben

The contents of this presentation may not be copied and/or distributed without permission of the author! Please note references at the end of the presentation!

Subway floor

Core made from aluminum foam

Cover sheets made from aluminum

- 15-25 % lighter than wood at same stiffness or same deflection
- Same acoustic
- No absorption of water
- Not burnable / flammable
- No plastic / no adhesives
- Easy to recycle through melting

Archivierungsangaben

The contents of this presentation may not be copied and/or distributed without permission of the author! Please note references at the end of the presentation!

Durchschussversuche 透射试验

Optimaler Aufbau für die Prüffolge nach DIN EN 12417:
基于DIN EN 12417标准检测顺序的最佳结构
Aluminiumschaum-Sandwich (**3/15/3**) mit einer Kernlage aus Aluminiumschaum von 15mm, ein 3mm Stahlblech beschussseitig und ein 3mm Stahlblech benutzerseitig:
铝泡沫夹层（ **3/15/3** ）－带有一个15mm铝泡沫制成的芯层。射击方的一个3mm的钢板和用户方的一个3mm 钢板。

↑ Durchschussversuch bestanden 通过了透射试验

↑ Gesamtdicke des Aluminiumschaum-Sandwiches
铝泡沫夹层的总厚度: 21mm

↑ Gewicht des Aluminiumschaum-Sandwiches:
50,7kg/m² (19,3% leichter als 8mm Stahlblech)
铝泡沫夹层的重量： 50,7kg/m² （与8mm钢板存在19,3% 的差距）

↓ keine Kostenreduzierung, sondern Kostenerhöhung
不是削减、而是提高了成本

↓ Nachrüstbarkeit 可改装型

Beschussbild
射击图片:

Beschussseitig 射击方

Archivierungsangaben

The contents of this presentation may not be copied and/or distributed without permission of the author! Please note references at the end of the presentation!

Aluminiumschaum-Sandwich 铝泡沫夹层

- Automobil – Versuchsmuster 汽车－试验样品

Bauteil Bodengruppe 起落架部件

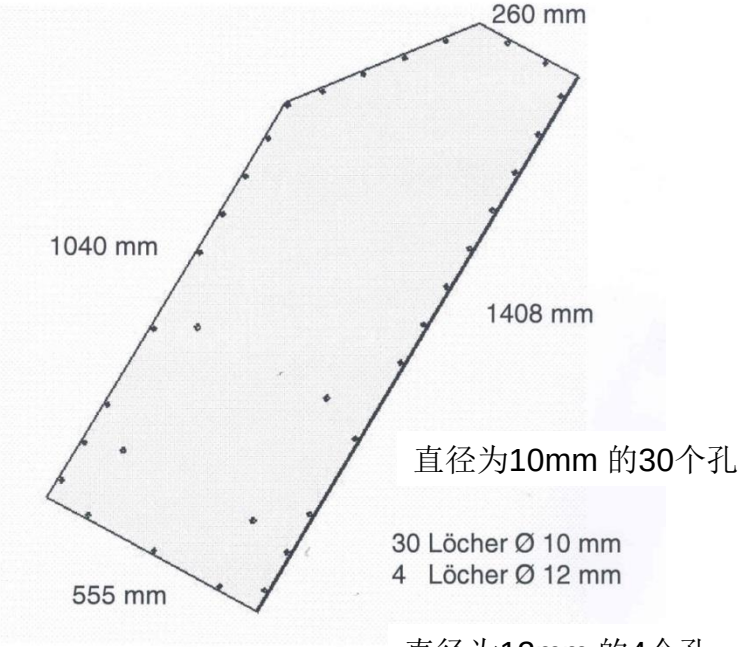

直径为10mm 的30个孔

直径为12mm 的4个孔

Demonstrator Schiebehubdach 高架遮阳顶棚的示例

Archivierungsangaben

The contents of this presentation may not be copied and/or distributed without permission of the author! Please note references at the end of the presentation!

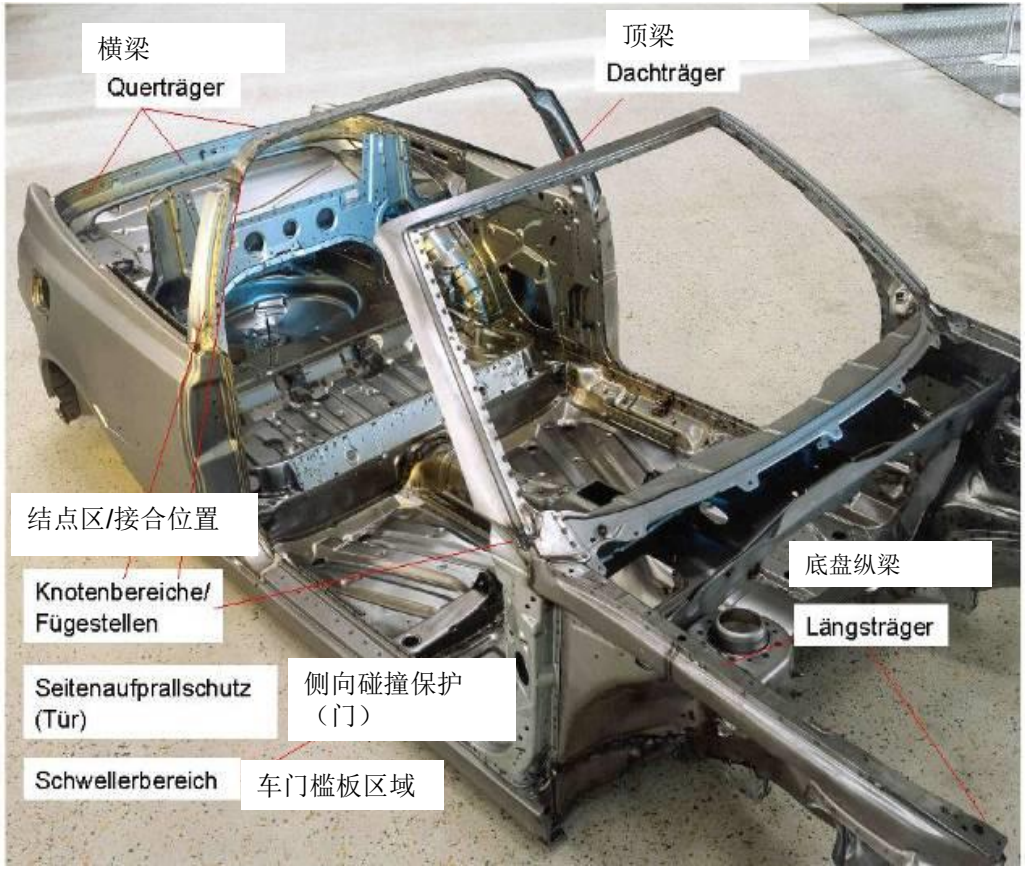

Crash-Elemente: 碰撞元件：

- Seitenaufprallschutz 侧向碰撞保护

-Längs- und Heckträger

-底盘纵梁和后端支梁

Versteifung 强化:

- Knotenbereiche 结点区

- flächige Elemente wie Dach, Motorhaube etc.

平面元件－诸如车顶、发动机罩，等。

- Querträger 横梁

Metall-Schaum
Anwendungsspektrum Karosserie
金属泡沫在车身的应用范围

Archivierungsangaben

The contents of this presentation may not be copied and/or distributed without permission of the author! Please note references at the end of the presentation!

„Knoten“-Versteifungen mit Aluminiumschaum 通过铝泡沫进行的“结点”强化

Ziel 目标
Erhöhung der Torsionssteifigkeit der Karosserie durch lokales Ausschäumen
通过局部的包装发泡来提高车身的扭转刚度

Prozesskette 流程链
Herstellung Schaumteile 制造泡沫部件

↓

Beschichten mit Terocore 使用Terocore（结构泡沫）进行涂漆

↓

Einlegen in den Knotenbereich (Rohbau)
嵌入结点区（车身本体）内

↓

Aufquellen des Klebers während der KTL- Behandlung
KTL表面处理期间粘合剂将膨胀

Ansätze für weitere Entwicklungen 后续技术开发的基本方案
- **Serienreife** für entwickelte Technologie erlangen (Grafitform, Einlegeteile, Terocore) oder
- **„Einspritzen“ von Metallschaum** in vorgefertigte Knotenbereiche der kalten Karosserie

为了将已开发技术投入成熟的批量生产，须在冷车身的预制结点区内采用（ Grafitform、插件、Terocore ）或注射金属泡沫。
→ neue Technologie 新技术! → Forschung notwendig 必备的研究

Potenzielle Einsatzbereiche 潜在的应用区域

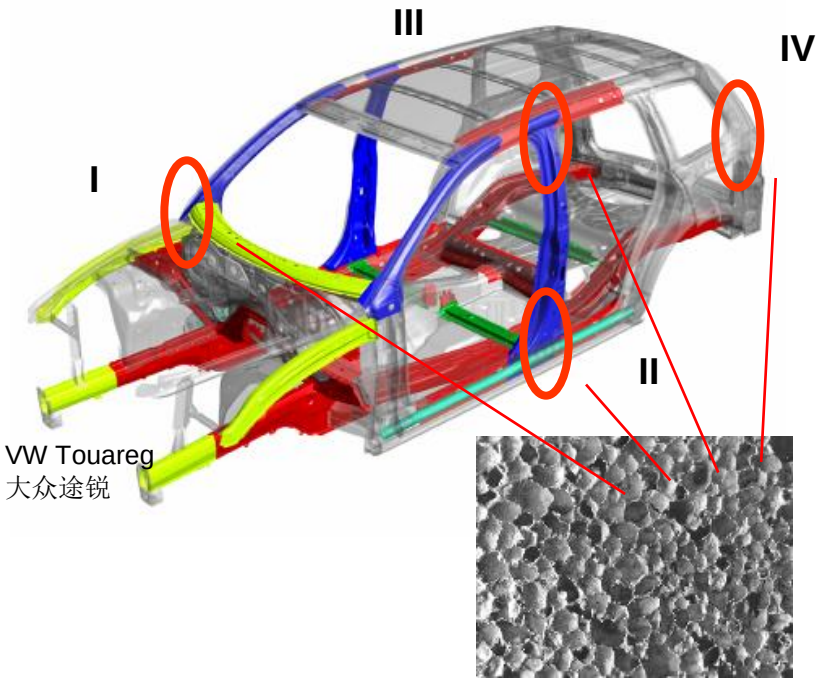

VW Touareg
大众途锐

Archivierungsangaben

The contents of this presentation may not be copied and/or distributed without permission of the author! Please note references at the end of the presentation!

Ship rudder

Old design

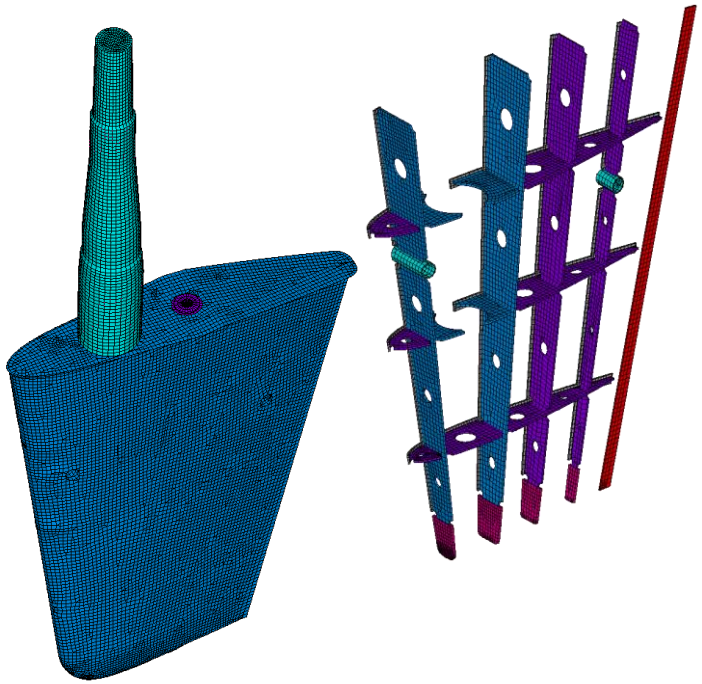

Many stringers

Much welding costs

Mass: 1176 kg

New design

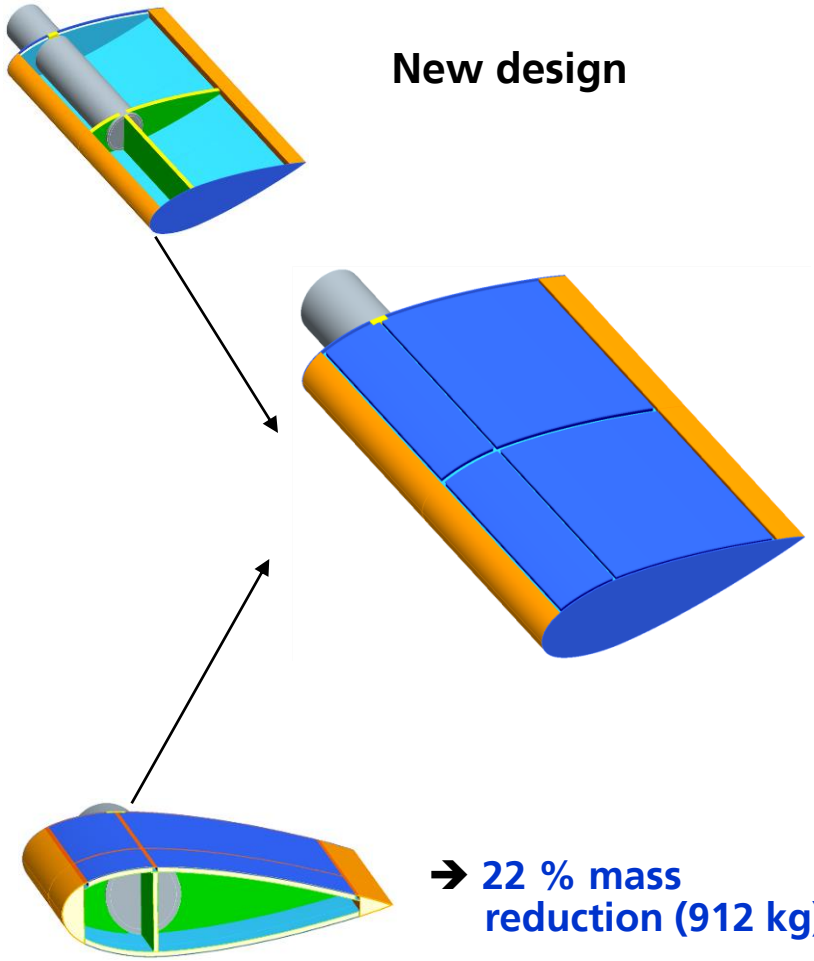

➔ 22 % mass reduction (912 kg)

➔ easier manufacturing

Archivierungsangaben

The contents of this presentation may not be copied and/or distributed without permission of the author! Please note references at the end of the presentation!

Ready for swimming!

Scale

1:1

2,6 m x
1,4 m x
0,5 m

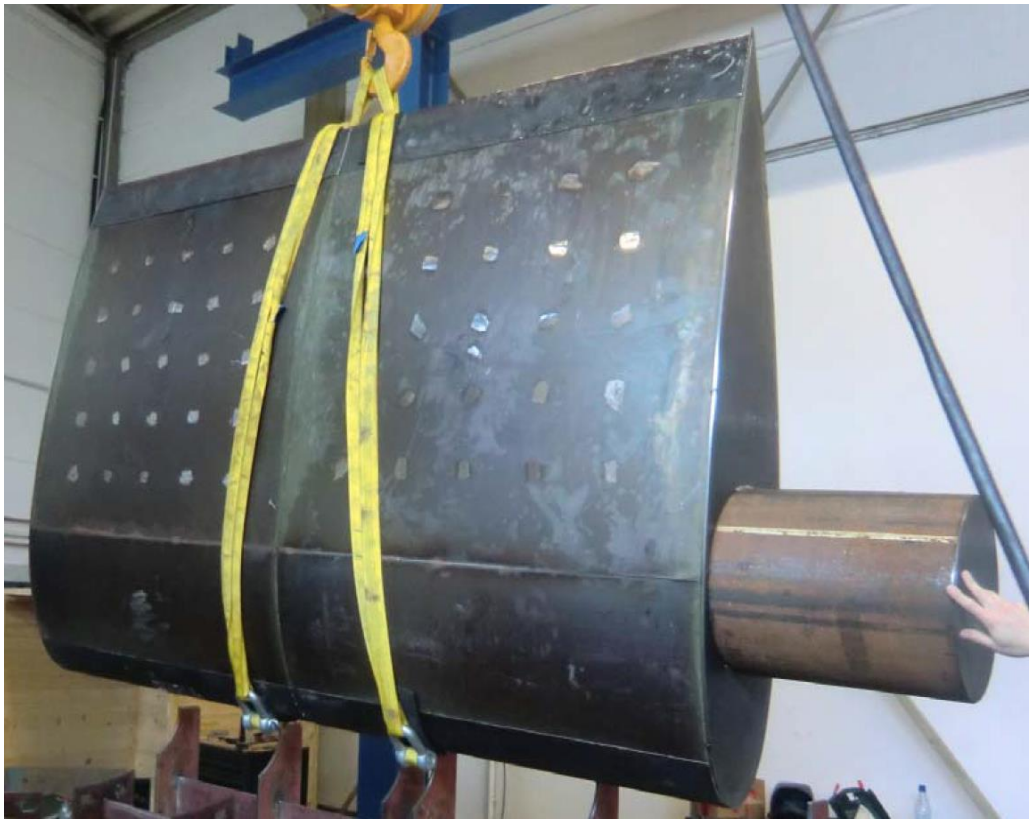

Archivierungsangaben

The contents of this presentation may not be copied and/or distributed without permission of the author! Please note references at the end of the presentation!

WATERTRUCK

- Containership with target 20% less mass than original!

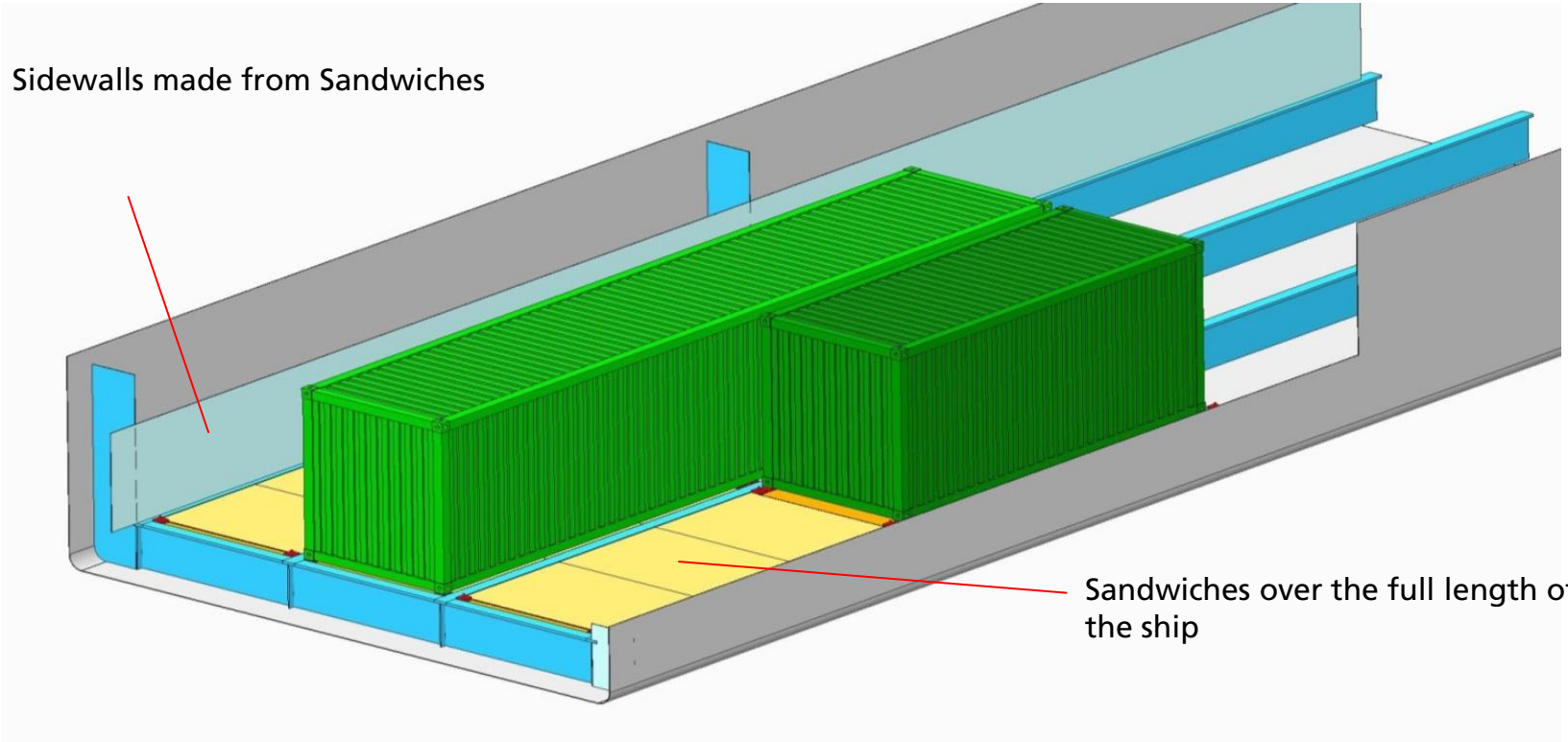

Archivierungsangaben

The contents of this presentation may not be copied and/or distributed without permission of the author! Please note references at the end of the presentation!

Applications in Shipbuilding

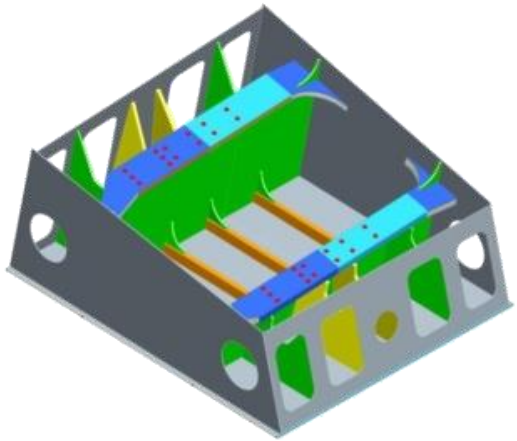

Gear base of a ship (2011)

Results:

- 20 % weight reduction (≈ 1,000 kg)
- Good vibration damping

Archivierungsangaben

The contents of this presentation may not be copied and/or distributed without permission of the author! Please note references at the end of the presentation!

MARTEC ERA-NET

ULIVES – Ultralight ice-going cargo vessels

Laufzeit: 01.03.2009 – 28.02.2012

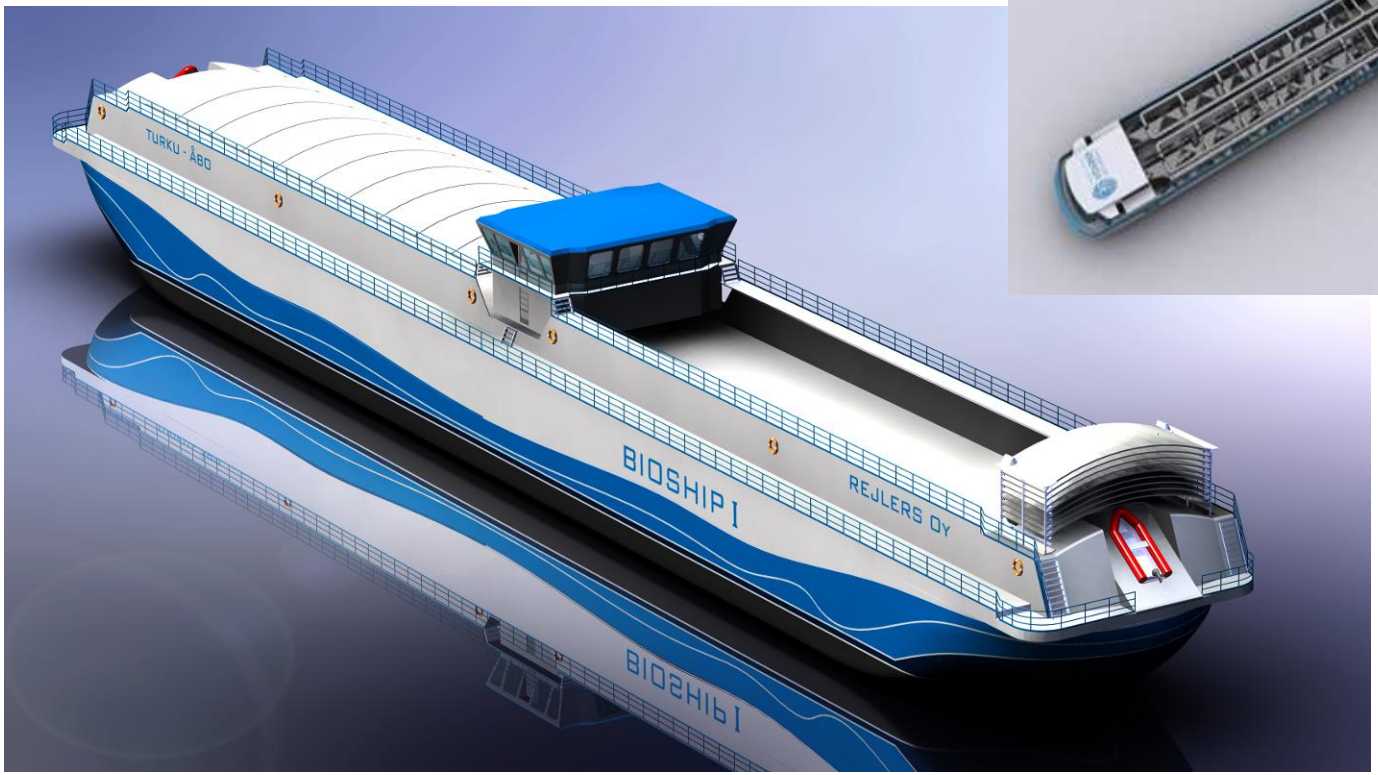

Archivierungsangaben

Applications
Shipbuilding

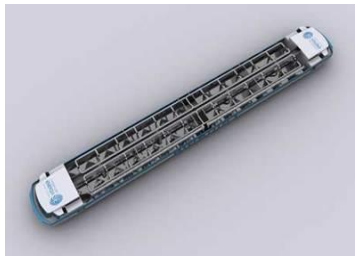

…wich with
…S

…ator ship segment

…tion about 25 %

Sar… …ets

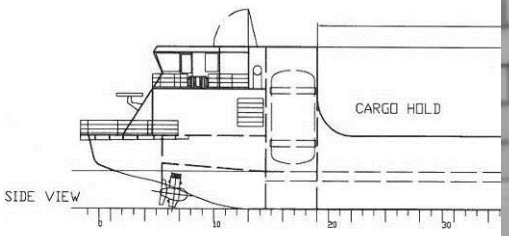

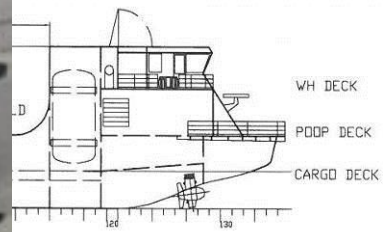

Archivierungsangaben

© Fraunhofer IWU
Prof. Neugebauer

Fraunhofer IWU

The contents of this presentation may not be copied and/or distributed without permission of the author! Please note references at the end of the presentation!

Changing the Model - Lightweight

mass potential:

ship's side_4 = 145kg (8mm Al)

ship's side_3 = 390kg (7mm Al)

ship's side_2 = 867kg (10mm St)

stringer – ship's side

L135x65 Aluminium = 194kg

→ Omission of the separate Stringer and integrate their function in the sandwiches

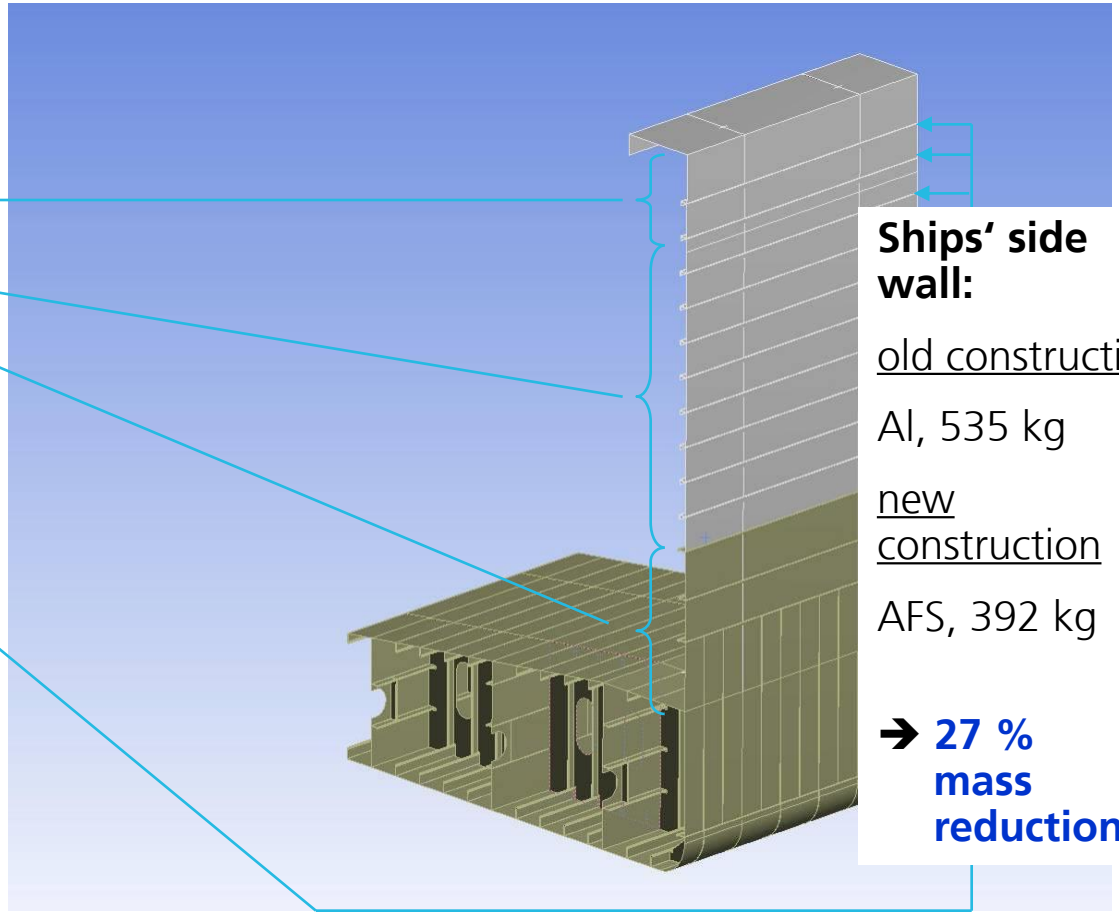

Ships' side wall:

old construction

Al, 535 kg

new construction

AFS, 392 kg

➔ 27 % mass reduction

Archivierungsangaben

The contents of this presentation may not be copied and/or distributed without permission of the author! Please note references at the end of the presentation!

Scale

1:4

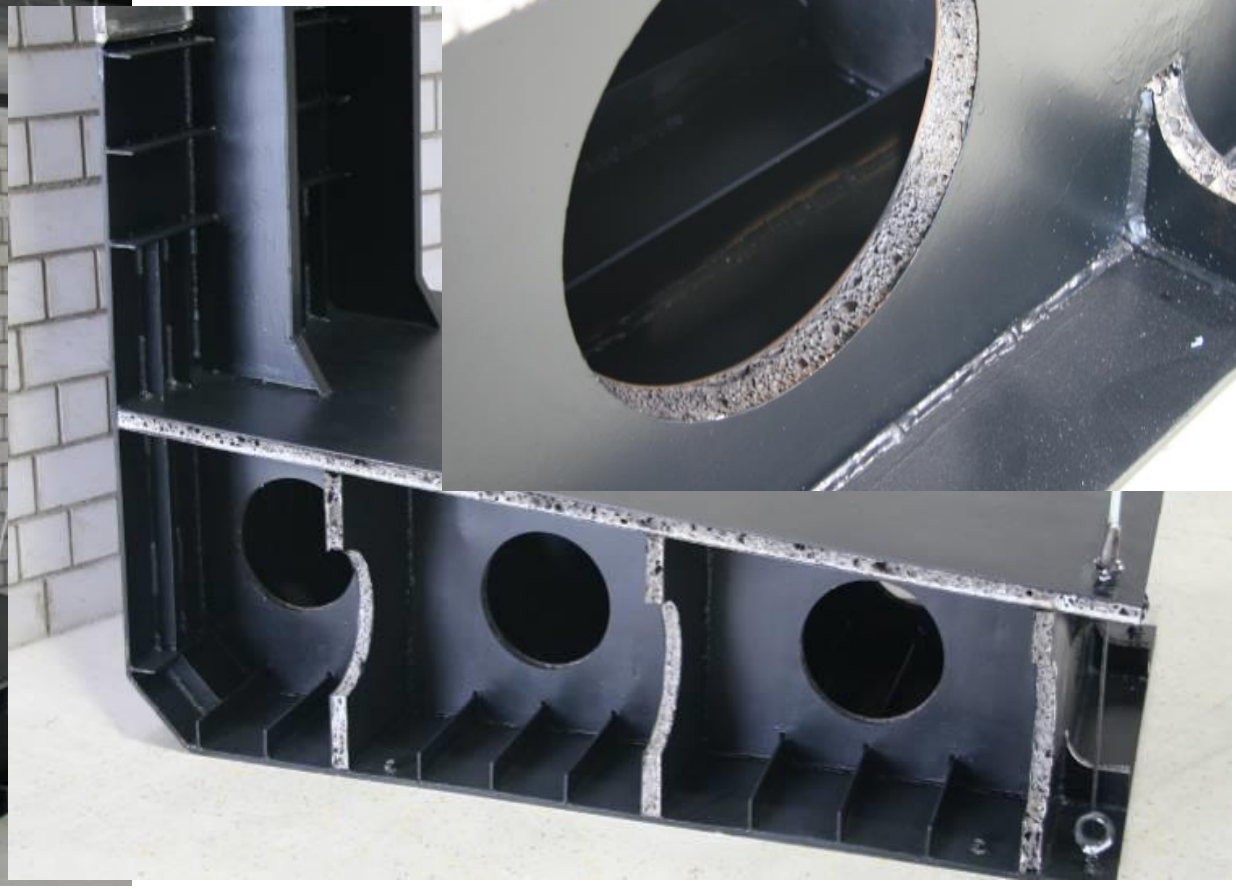

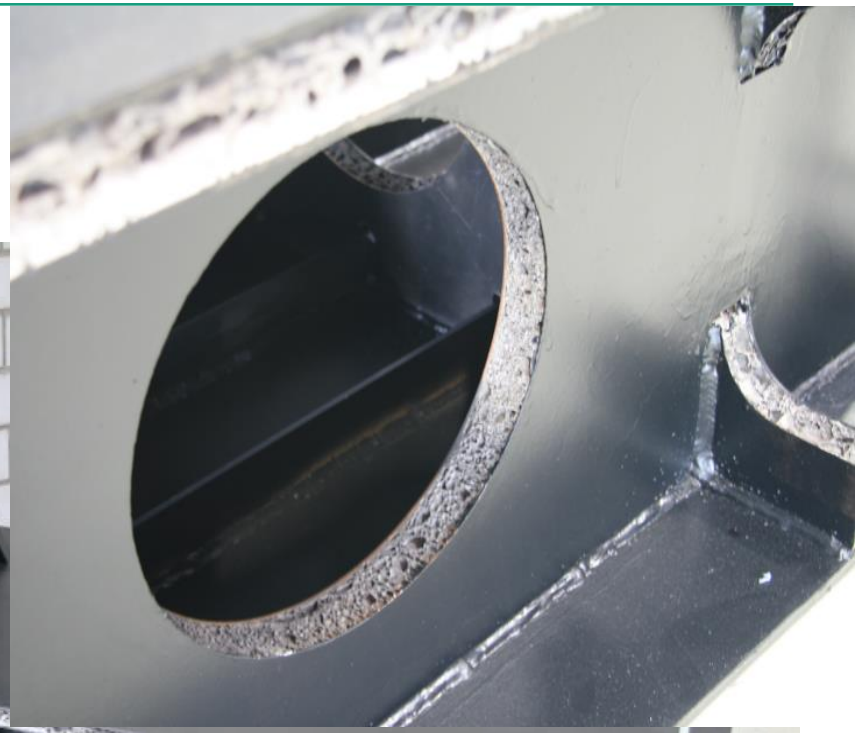

Archivierungsangaben

The contents of this presentation may not be copied and/or distributed without permission of the author! Please note references at the end of the presentation!

Metal foam sandwiches for shot protection

- Sandwich panels

  Steel/Aluminiumfoam/Steel

  sometimes covered by

  ceramics

- Breacking of the bullet, then energy absorption in the foam

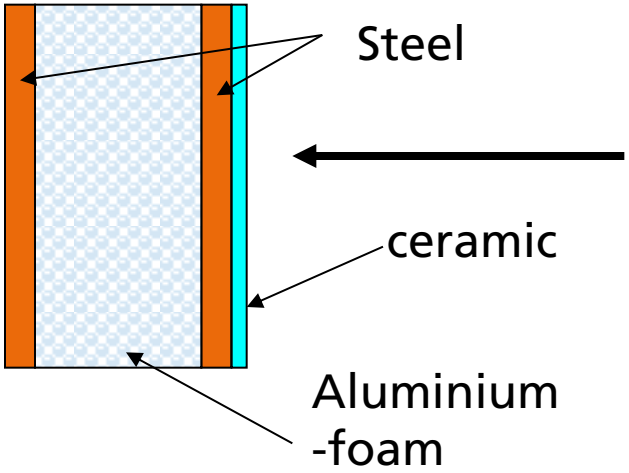

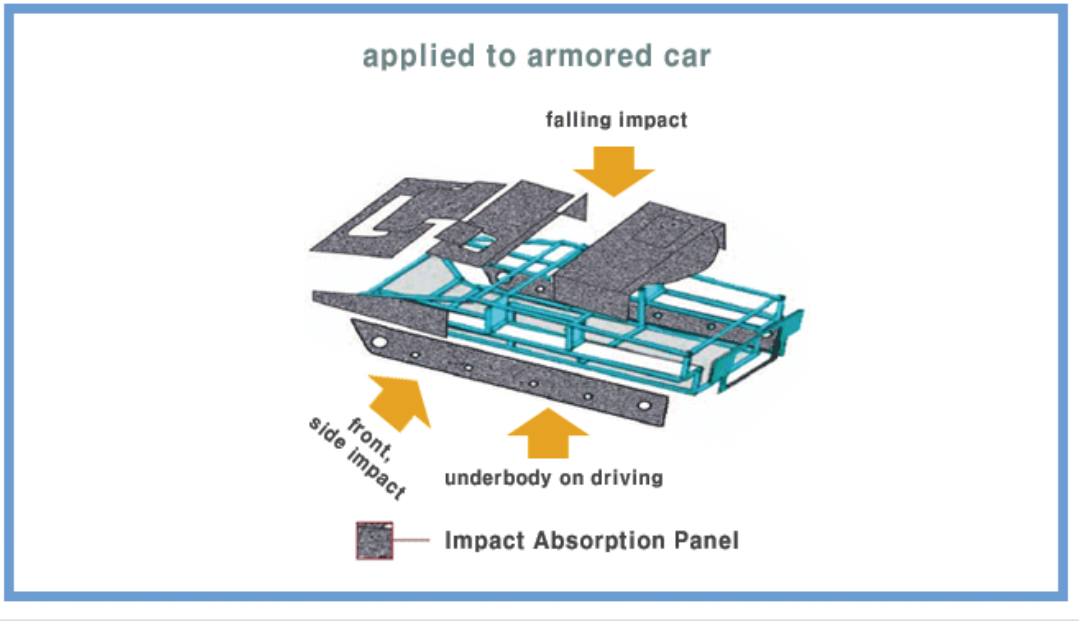

Archivierungsangaben

The contents of this presentation may not be copied and/or distributed without permission of the author! Please note references at the end of the presentation!

Metalfoam for protection against explosion and electromagnetic shielding

- Explosion protection

  Walls (f.e. buildings of the government), get an aluminium foam wall as a protecting cover, which can absorb the explosion energy.

- protection for electrical devices

  - small housing in cars and tanks
  - up to complete shielded rooms

Room complete made of metalfoam

Archivierungsangaben

IWP WERKZEUGMASCHINEN UND PRODUKTIONSPROZESSE

Fraunhofer IWU

Blast test

Images of the Third Blast Experiment

Third Blast Experiment Result

Reinforced concrete wall not protected by the Blast mitigation panel:

Serious crack generated

Reinforced concrete wall protected by the Blast mitigation panel:

Blast mitigation panel absorbs pressure and concrete unharmed

Third Blast Experiment Profile

- Date and Place: Aug. 5th, 2011 / OOO Test Site, ADD
- Purpose: Acceptance verification for military protection facilities on northwest islands (Explosion Generated Pressure Damage Evaluation of 200mm thick concrete wall)
- Conditions: 120 kg of TNT (5 m separation)

The contents of this presentation may not be copied and/or distributed without permission of the author! Please note references at the end of the presentation!

Hollow sphere structures

© Fraunhofer IWU
Prof. Neugebauer

The contents of this presentation may not be copied and/or distributed without permission of the author! Please note references at the end of the presentation!

Properties

General information

Materials	Nearly all verifiable materials (special: steels, super alloys, intermetallics)
Structure geometry/ dimensions	Cell size ca. 1.0 mm - 10 mm Cell wall thickness 20 µm - 1000 µm Density ca. 0.3 g/cm³ - 4 g/cm³ Plates, cylinders, tubes
Properties	- Heat- and sound absorbing - Energy absorbent - Mechanical and thermical solid - Calculable and repeatable

Archivierungsangaben

Fraunhofer IFAM Dresden

IWP Werkzeugmaschinen und Produktionsprozesse

Fraunhofer IWU

The contents of this presentation may not be copied and/or distributed without permission of the author! Please note references at the end of the presentation!

Properties

Energy absorption ability

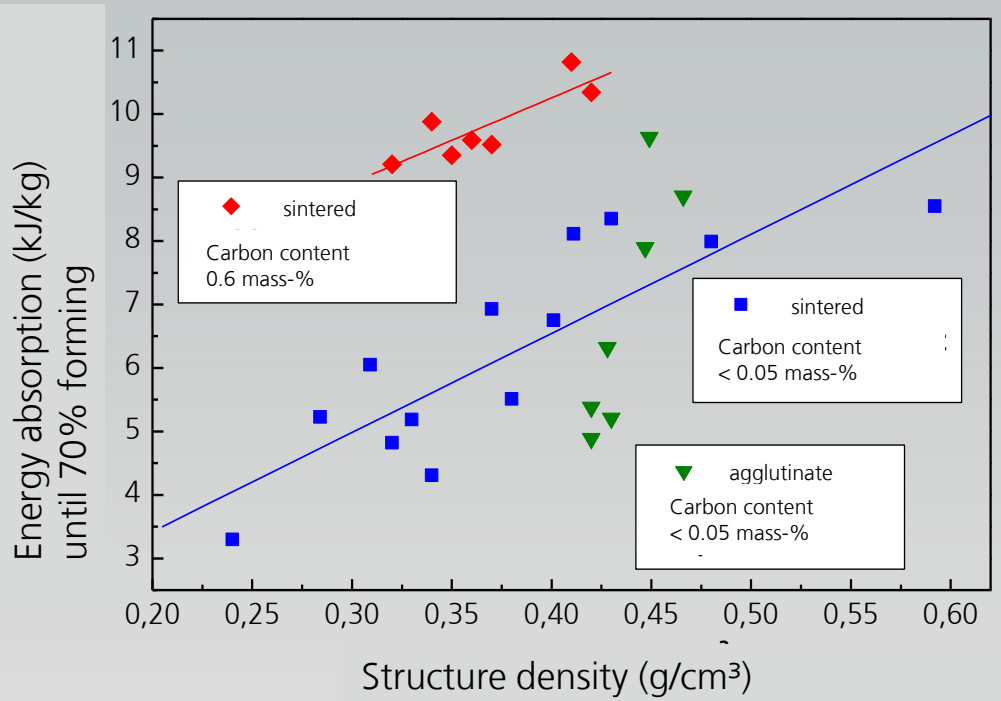

Hollow sphere structures composed of steel (0.6 % P) with different C-concentrations, Forming of 70 %

Archivierungsangaben

The contents of this presentation may not be copied and/or distributed without permission of the author! Please note references at the end of the presentation!

Properties

Thermal conductivity hollow ball structure with molybdenum

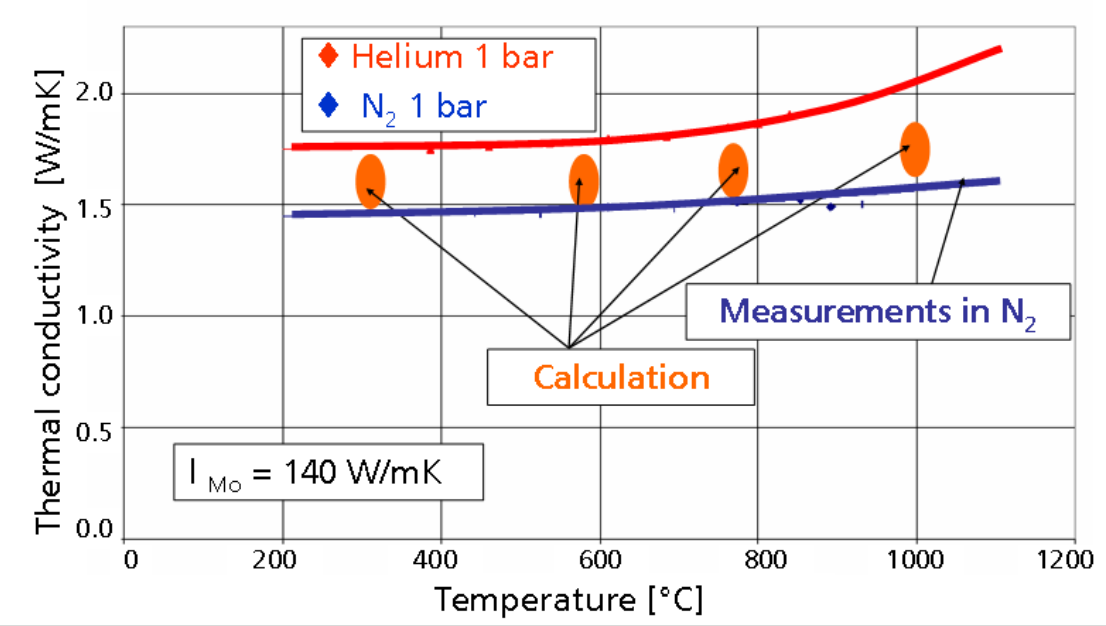

Good consistence of calculated und measured data!
The hollow ball structure has around 1 % thermal conductivity of massive material!

Archivierungsangaben

The contents of this presentation may not be copied and/or distributed without permission of the author! Please note references at the end of the presentation!

Hollow sphere structures

Silencer

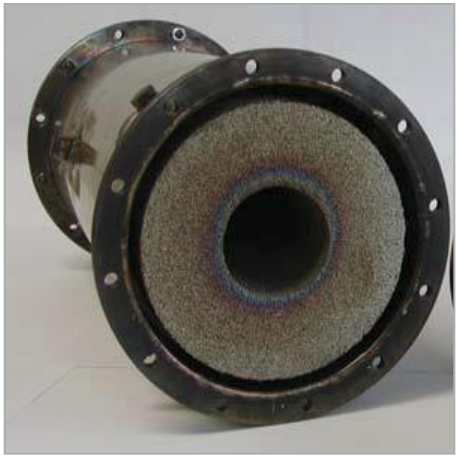

Hollow sphere enforced center pillar of a car

Archivierungsangaben

The contents of this presentation may not be copied and/or distributed without permission of the author! Please note references at the end of the presentation!

Hollow sphere structures

Muffler for exhaust systems of BMW 2.5 liter TD

Results:

- → Successful field tests up to 100.000 km
- → Sound can be tailored according the requirements
- → Overall weight saving up to 30 %!
- → Excellent additional thermal insulation

View of whole muffler hollow sphere structure

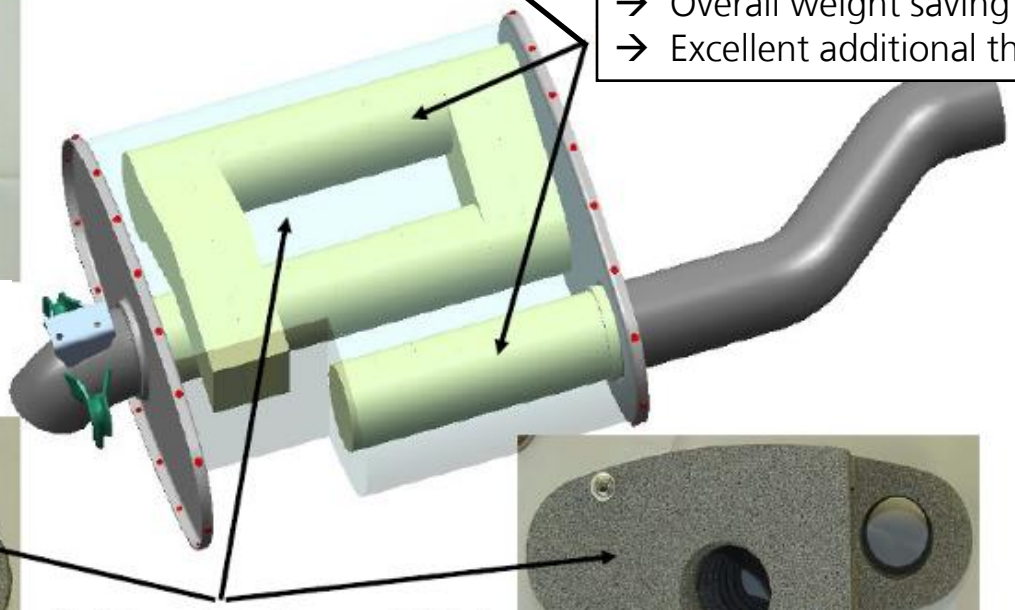

View inlet

Hollow spheres (316L)
∅ 2.8 mm; 0.3 g/cm³

View outlet

Archivierungsangaben

The contents of this presentation may not be copied and/or distributed without permission of the author! Please note references at the end of the presentation!

Applications

Lightweight Tools für manufacturing of EPS

Increase of energy efficiency of moulding machine
Objective

- Reduction of energy consumption for heating/cooling
- Increase of energy efficiency by 30 %
- Reduction of mass by 50 %

Strategy

- Reduction of thermal mass by use of cellular metals with low heat capacity
- Realization of nozzleless surfaces

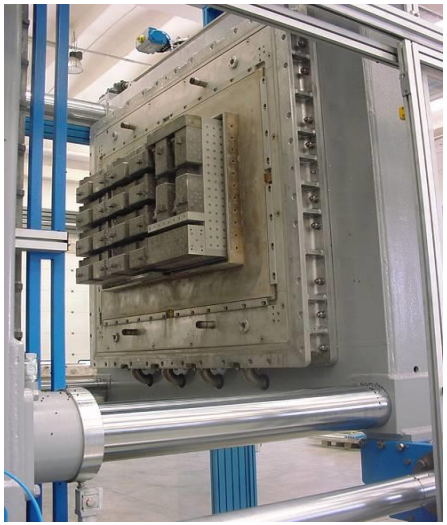

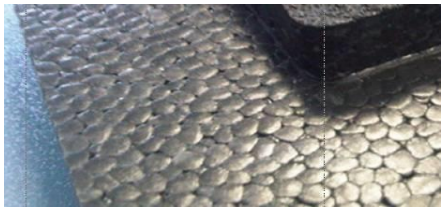

Archivierungsangaben

The contents of this presentation may not be copied and/or distributed without permission of the author! Please note references at the end of the presentation!

Applications

Crashbox

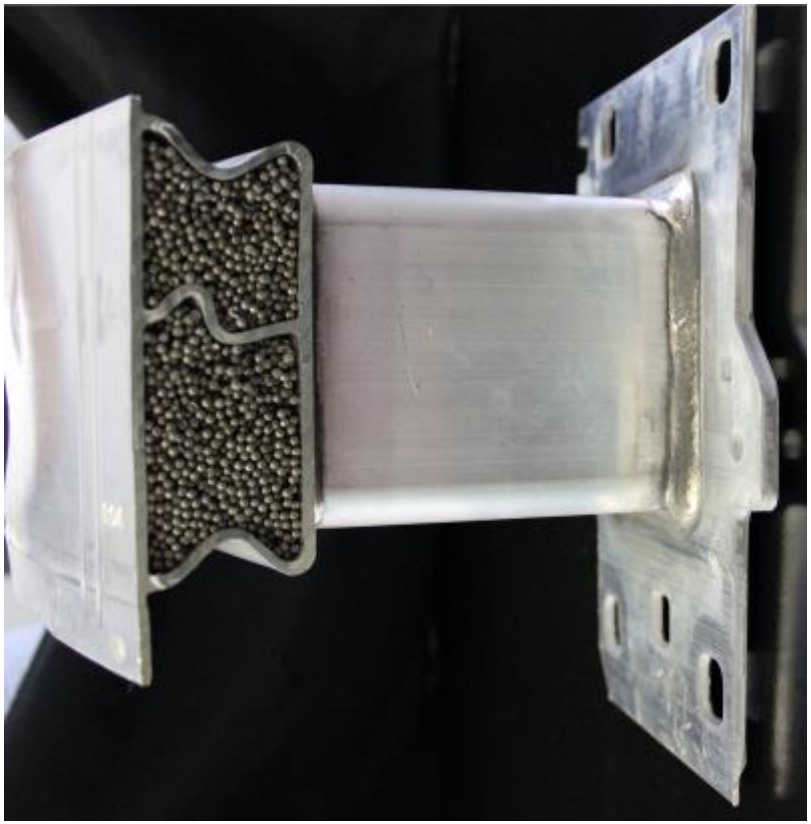

Cellular Metals in Crashbox

- Bonded hollow sphere structures
- Local increase of energy absorption capability
- lower wall thicknesses of profiles possible

Benefits

- lowered total mass
- lowered construction volume

Archivierungsangaben

The contents of this presentation may not be copied and/or distributed without permission of the author! Please note references at the end of the presentation!

Fiber structures

The contents of this presentation may not be copied and/or distributed without permission of the author! Please note references at the end of the presentation!

Properties

Metal Fibre Structures

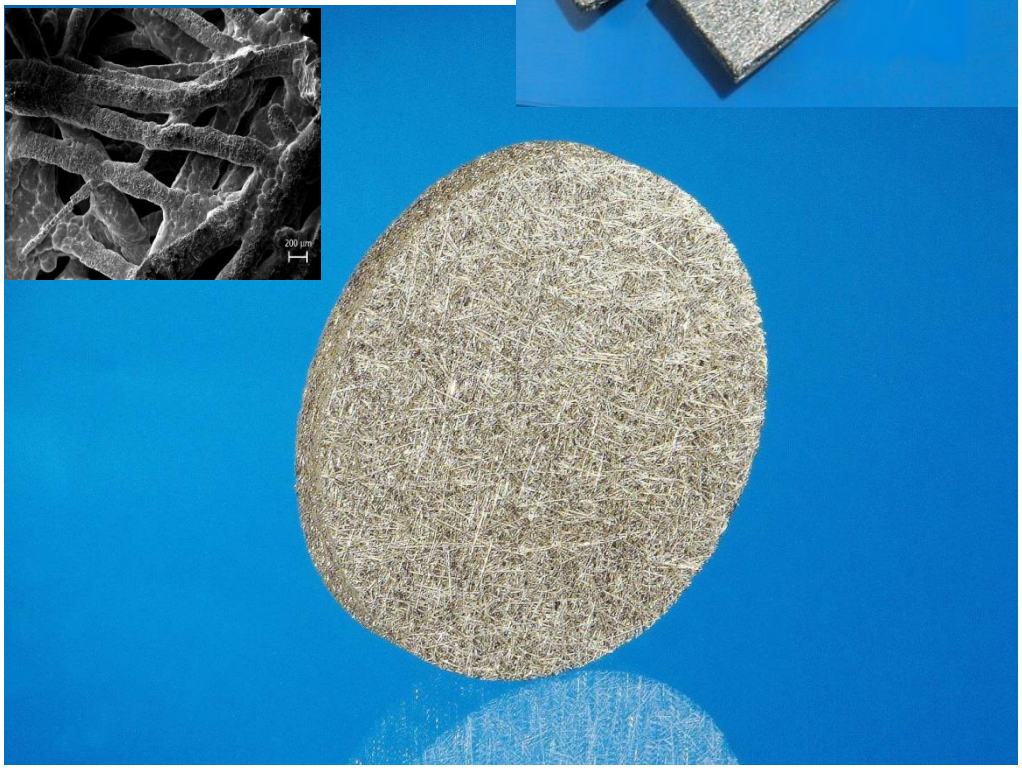

Properties of metal fibre structures

- sheets up to 600 x 1200 mm
- Rings with diameter up to 400 mm
- Open porosity 50 to 95 %
- pore sizes ca. 10 - 250 µm
- graded structures
- Materials: Al-, Mg-, Cu-, Fe, Ni-, Co-, Ti- basics

Archivierungsangaben

The contents of this presentation may not be copied and/or distributed without permission of the author! Please note references at the end of the presentation!

Properties

Selected properties

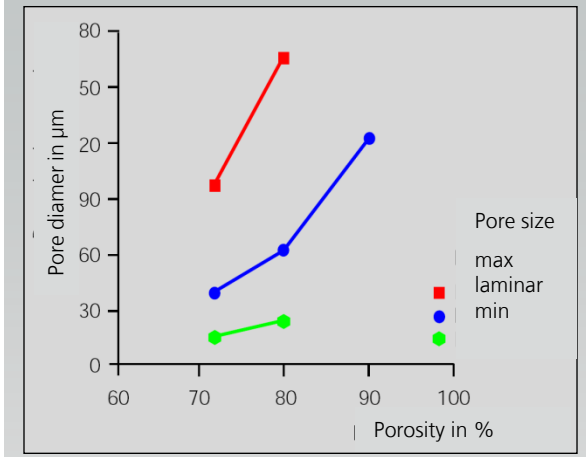

Minimal, maximal and median laminar diameter against porosity

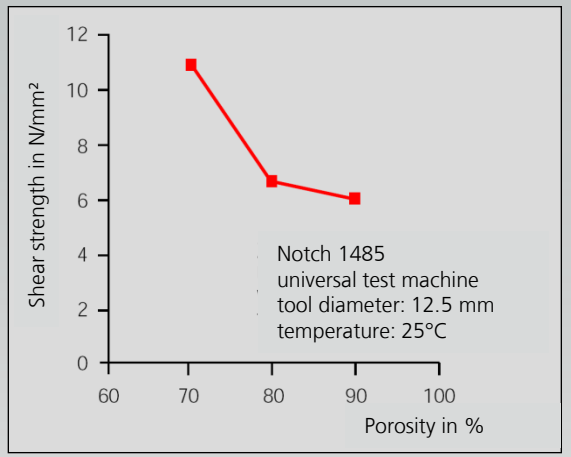

Shear strength against porosity

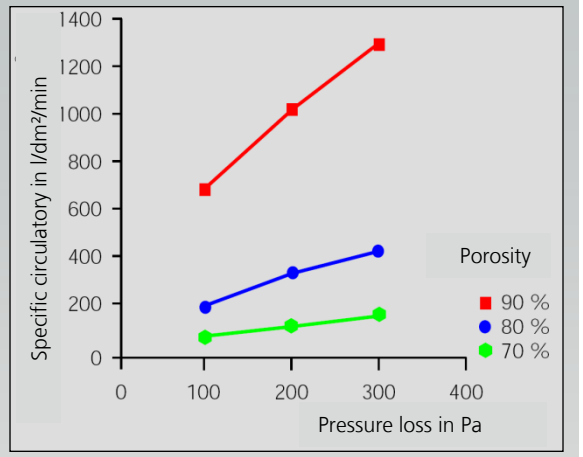

Specific circulatory over pressure loss against porosity

Archivierungsangaben

The contents of this presentation may not be copied and/or distributed without permission of the author! Please note references at the end of the presentation!

Fiber structures

Flame retarder, explosion control elements, filters, up to design elements, jewelry

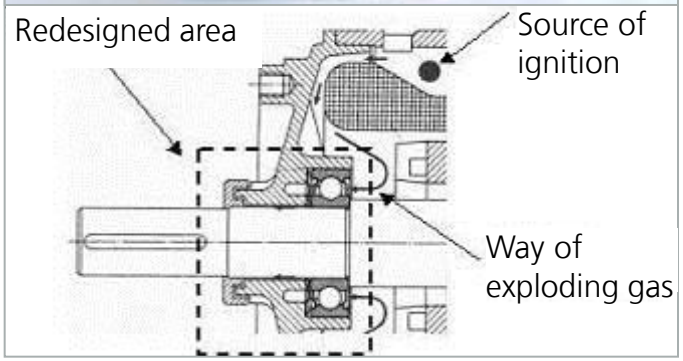

Archivierungsangaben

The contents of this presentation may not be copied and/or distributed without permission of the author! Please note references at the end of the presentation!

Fiber structures

Parts for heat generator

Surface burner (FeCrAl fibers), burner capacity 2 KW; oxidation resistant up to 1000 °C

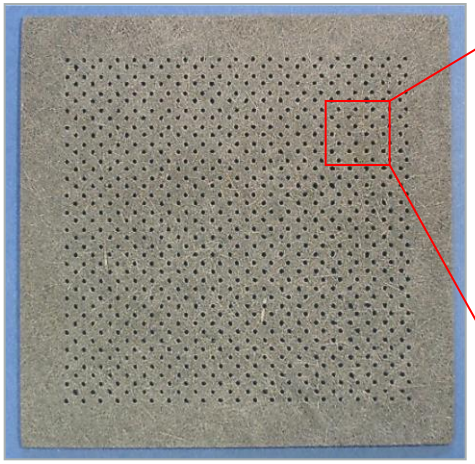

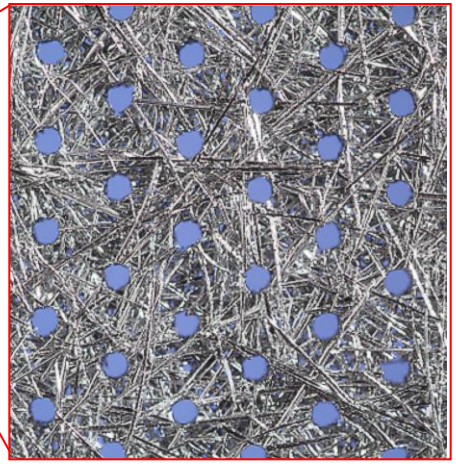

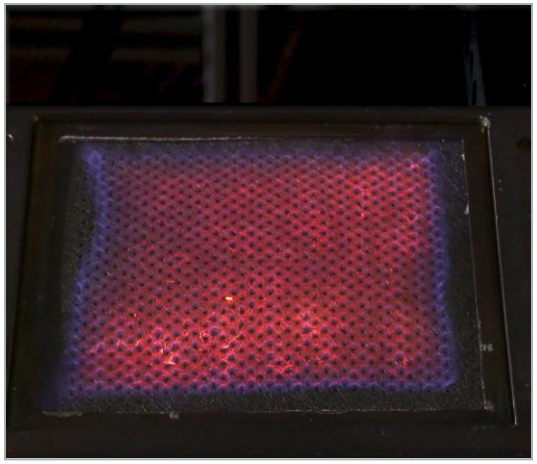

Archivierungsangaben

The contents of this presentation may not be copied and/or distributed without permission of the author! Please note references at the end of the presentation!

Applications

PCM filled metal fibre heat exchanger

Main features:

- Stack of sintered AlCu5 fiber plates 200 x 200 x 200 mm³ (porosity 80 %)
- Tubes mechanically widened
- Filling with paraffine RT 42
- Storage capacity ~ 0,4 kWh

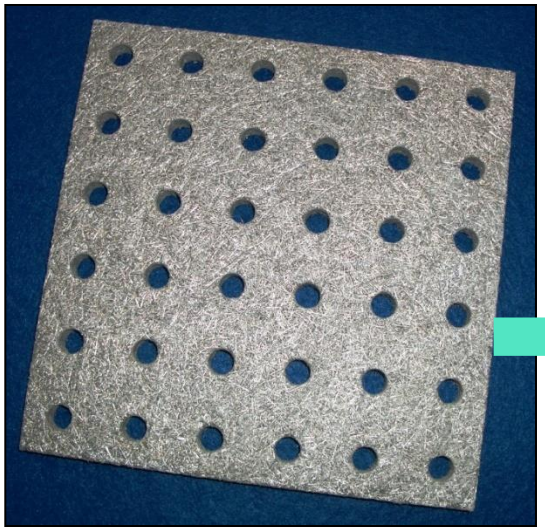

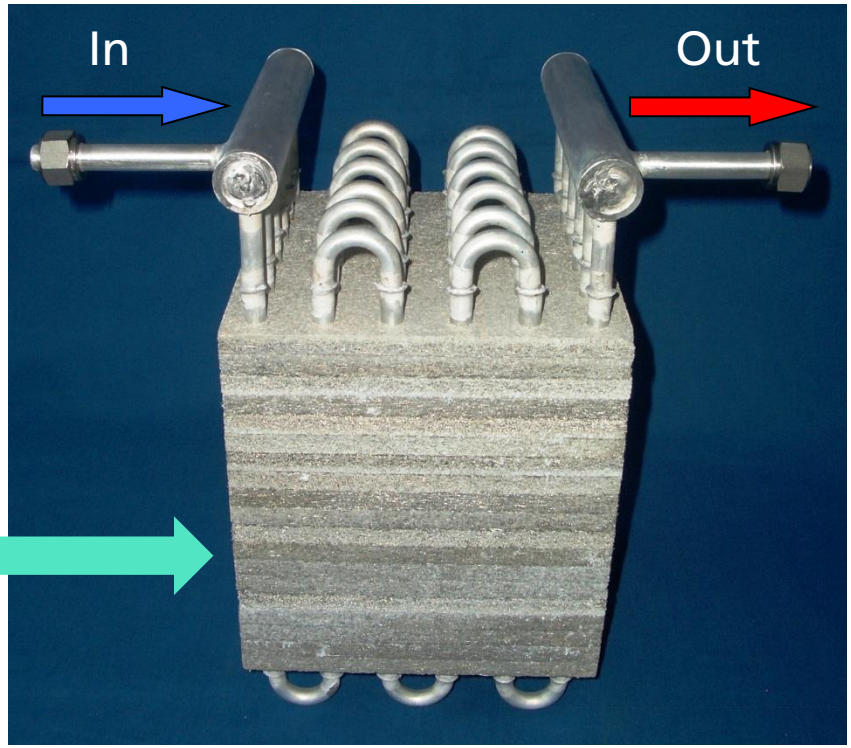

Archivierungsangaben

Bundesministerium für Wirtschaft und Energie
IWP Werkzeugmaschinen und Produktionsprozesse
Fraunhofer IWU

The contents of this presentation may not be copied and/or distributed without permission of the author! Please note references at the end of the presentation!

Wire structures

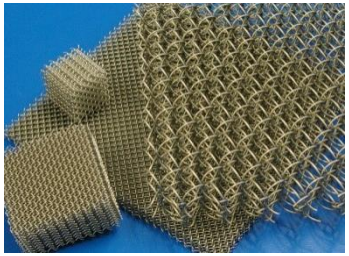

The contents of this presentation may not be copied and/or distributed without permission of the author! Please note references at the end of the presentation!

Properties

Cell structure and pressure resistence

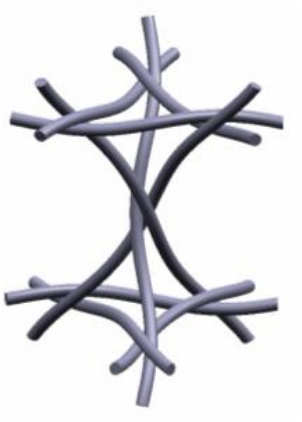

a) real wire structure

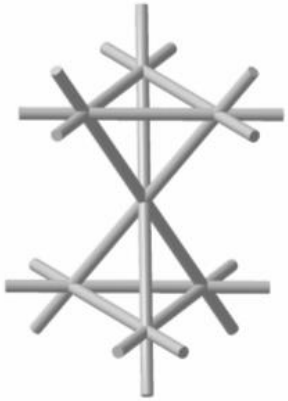

b) ideal Kagome-cell

Unit cells of 3-D-Kagome-structures

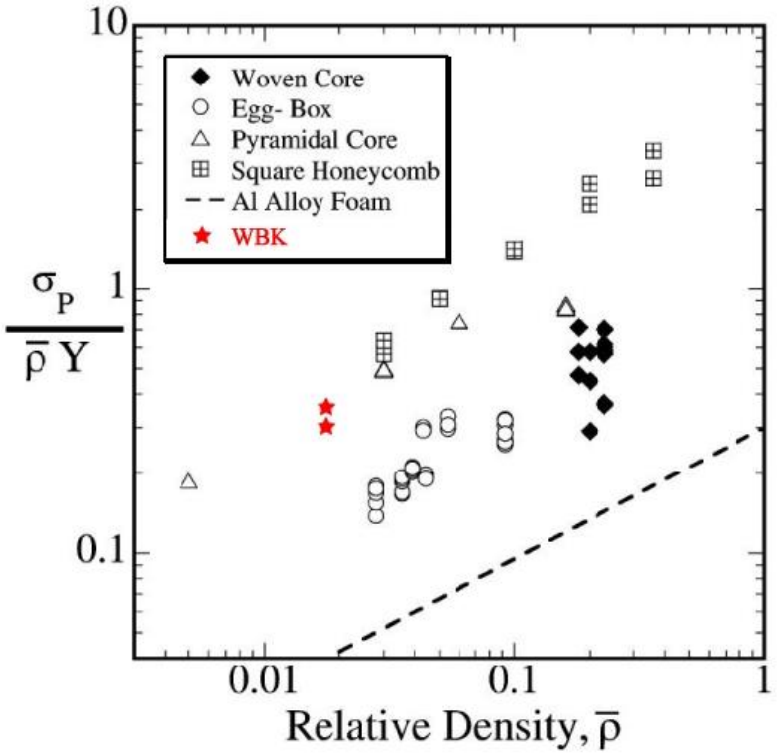

Pressure resistance normalized to the yield point of WBK-structures and others
Lightweight materials against relative density

Fraunhofer IFAM Dresden

Archivierungsangaben

IWP Werkzeugmaschinen und Produktionsprozesse

Fraunhofer IWU

The contents of this presentation may not be copied and/or distributed without permission of the author! Please note references at the end of the presentation!

Properties

Compression test of a Kagome-wire structure

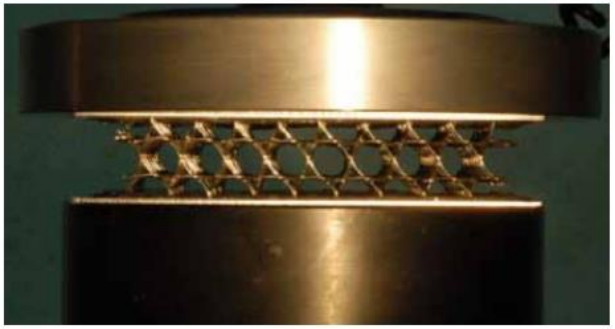

Experimetal setup

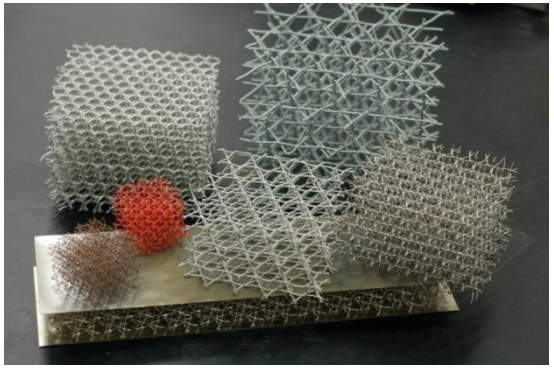

Kagome-wire structure composed of different materials (Al, Stahl, Cu) and a Kagome-sandwich-structure

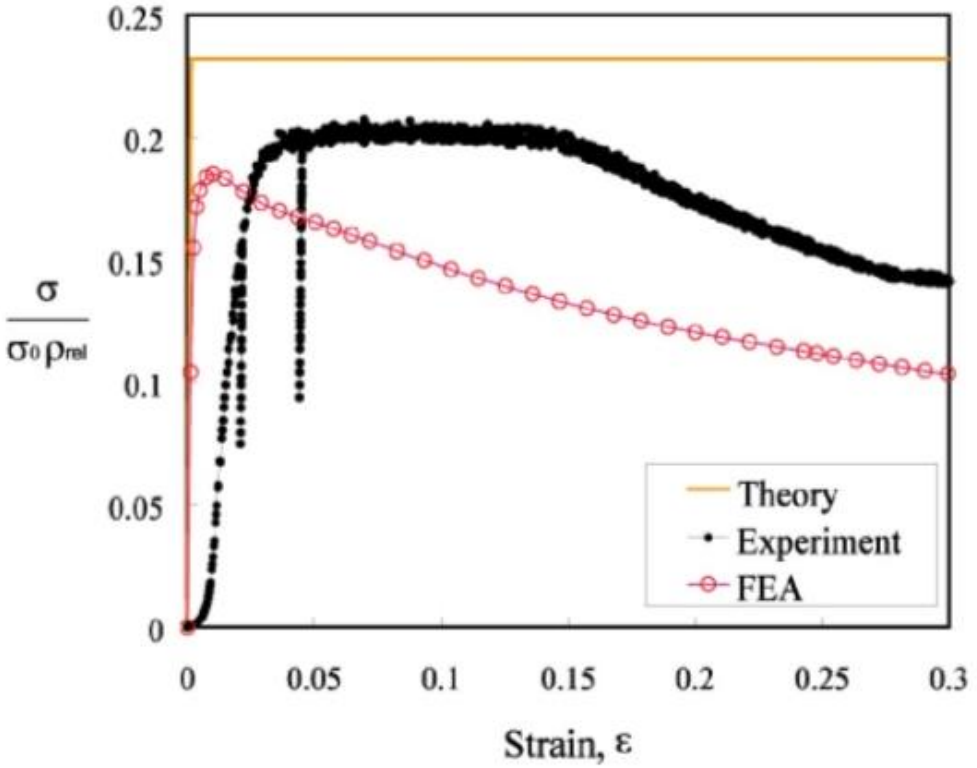

Archivierungsangaben

The contents of this presentation may not be copied and/or distributed without permission of the author! Please note references at the end of the presentation!

Properties

Bending strength of a Kagome-wire structure

Bending strength of a Kagome-wire structure (stainless steel 1.4401, structure density 0.1g/cm^3)

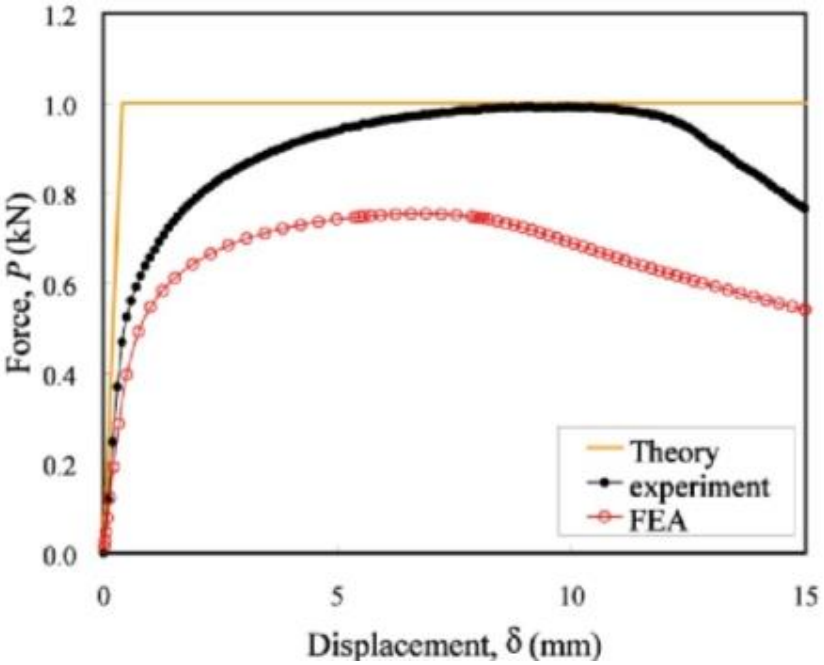

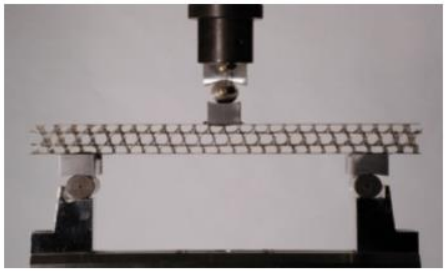

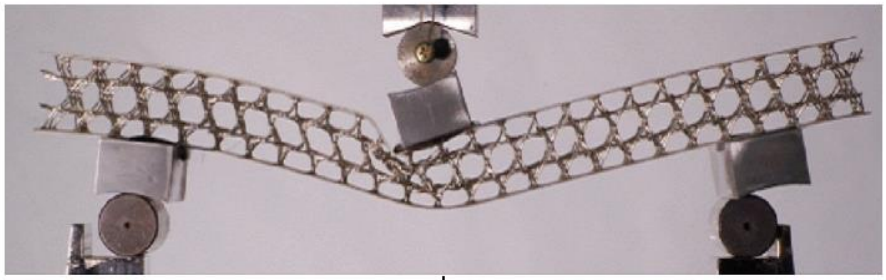

Breadboard

Archivierungsangaben

The contents of this presentation may not be copied and/or distributed without permission of the author! Please note references at the end of the presentation!

Wire structures

Possible applications: filters, heat exchangers, enforcement of other materials

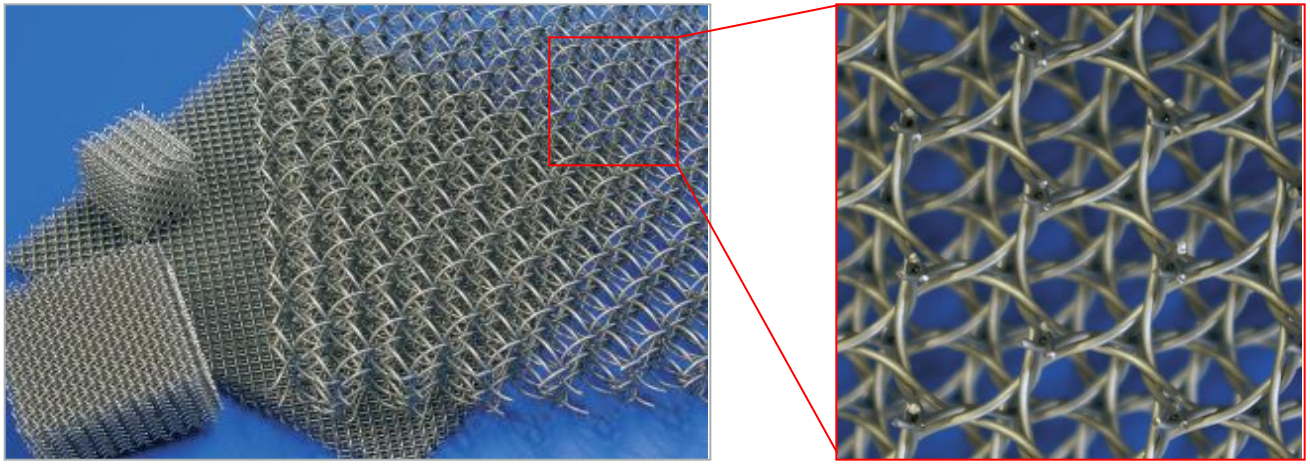

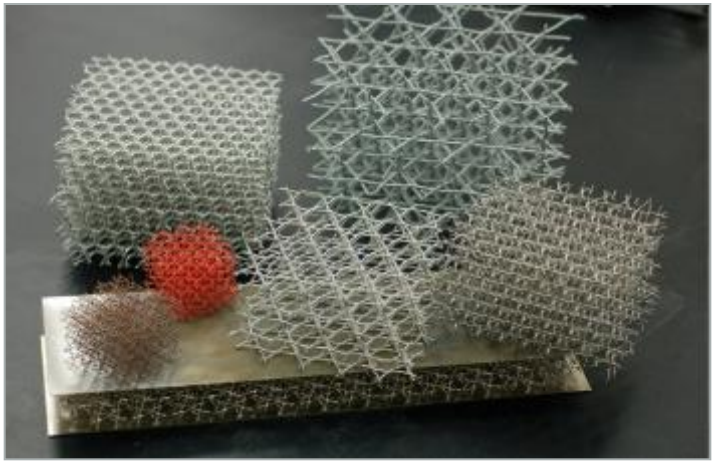

Archivierungsangaben

Fraunhofer IFAM Dresden

IWP Werkzeugmaschinen und Produktionsprozesse

Fraunhofer IWU

The contents of this presentation may not be copied and/or distributed without permission of the author! Please note references at the end of the presentation!

CELLULAR METALS

Part III – Design and computation

© Fraunhofer IWU
Prof. Neugebauer

The contents of this presentation may not be copied and/or distributed without permission of the author! Please note references at the end of the presentation!

CONTENT

- Principles for design
  - In general
  - Sandwich design
- Design-sample: Frame of a HSC-milling machine
- Methods for computation
  - Dimensioning of sandwiches
  - FEM

Archivierungsangaben

The contents of this presentation may not be copied and/or distributed without permission of the author! Please note references at the end of the presentation!

Principles for design

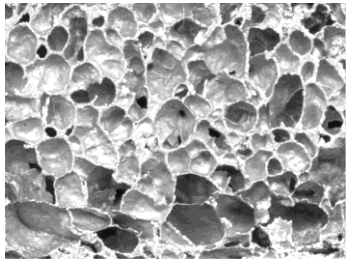

© Fraunhofer IWU

The contents of this presentation may not be copied and/or distributed without permission of the author! Please note references at the end of the presentation!

In general – Foam parts

- Foaming process = heat treatment
- Foaming process = time-dependent process with a max. time frame of heating
- The geometry of the foamed components should be constantly heated

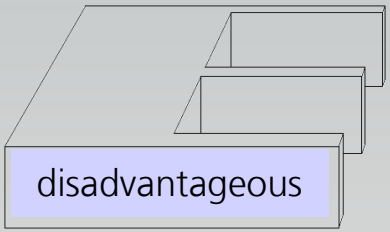

Disadvantageous component proportions

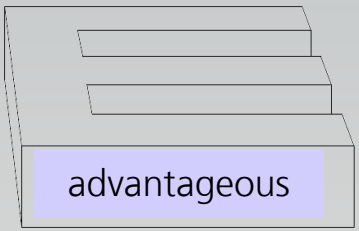

Advantageous component proportions

3-d aluminum foam parts

- Lower thickness limit of foamable precursor material is approx. 0.8 mm

  ➡ Thinner material is not homogeneous foamable

- Currently the upper limit of foam thickness is approx. 180 mm
- In principle any geometry which is producible by casting could also be produced by foaming

Archivierungsangaben

The contents of this presentation may not be copied and/or distributed without permission of the author! Please note references at the end of the presentation!

In general – Steel foam compounds

- Semi-finished products for construction of welding components or individual parts are:
  - steel – aluminum foam – sandwiches
  - foam-filled profiles
- For simply replacing steel walls:
  The mass of 1 mm steel sheet corresponds to approx.11 mm aluminum foam of the density 0.7 g/cm³!

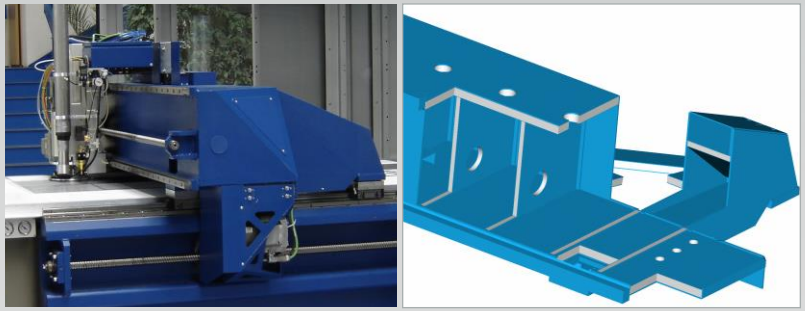

Cross beam of a milling machine, sandwich construction

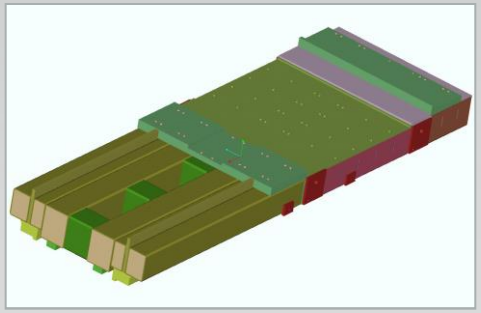

X-slide of a machining centre with foam-filled steel profiles

Basic design principle

Filigree, thin walled steel structure with foam-filled volumes or foam sandwiches!

Archivierungsangaben

The contents of this presentation may not be copied and/or distributed without permission of the author! Please note references at the end of the presentation!

Sandwich-joints

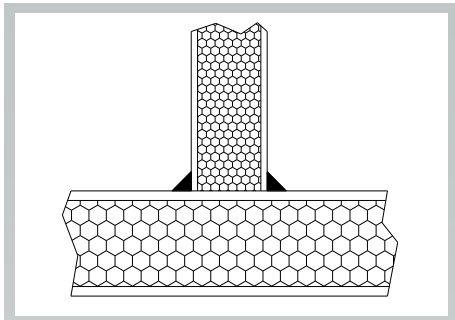

Sandwich-T-joint

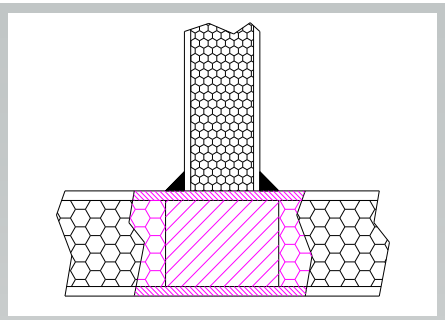

Sandwich-T-joint with insert to stiffening the compression

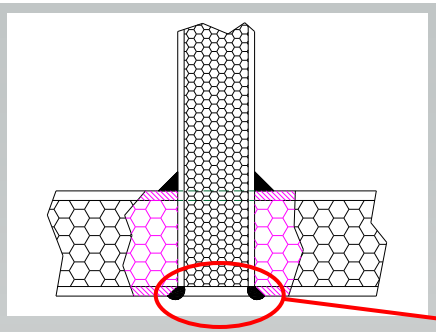

Sandwich-T-joint with fish joint to the lower cover plate for tension stiffening

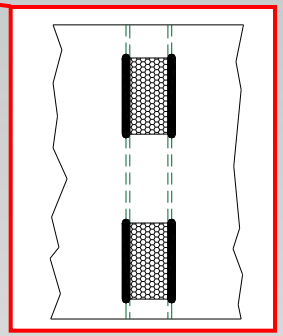

Fish joint

(View from below)

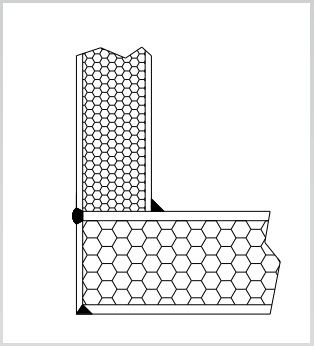

Sandwich-angle-joint: Welding of the second cover plate via notches

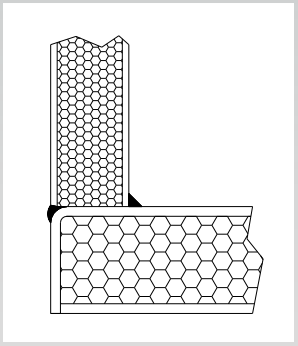

Sandwich-angle-joint: Lower cover plate as pan with top cover achieved

IMPORTANT:

The sandwiches should be welded with both cover plates, for utilization their potentials!

Archivierungsangaben

The contents of this presentation may not be copied and/or distributed without permission of the author! Please note references at the end of the presentation!

Design-sample:
Frame of a HSC-milling machine

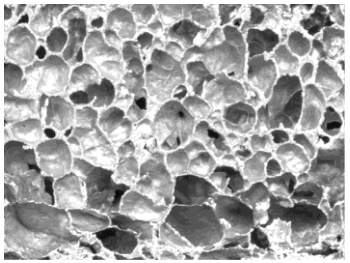

© Fraunhofer IWU
Prof. Neugebauer

The contents of this presentation may not be copied and/or distributed without permission of the author! Please note references at the end of the presentation!

Steps of development

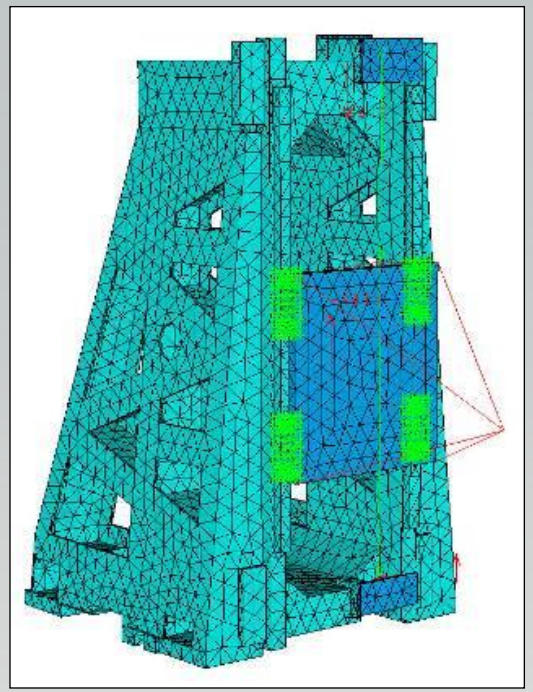

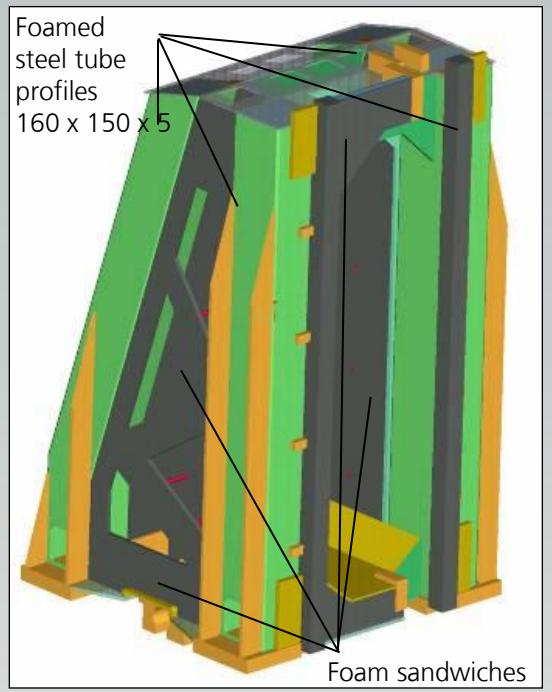

1. FEM-analysis previous construction

2. New design of steel-aluminum foam frame construction

3. FEM-analysis of new construction

4. Gradual improvement of new construction

5. Manufacturing of the final construction

6. Experimental determination of properties

→ Problem of former construction: Vibrations → Expectation: Increase of damping factor 4-5 fold

Fraunhofer IFAM Dresden

Archivierungsangaben

IWP Werkzeugmaschinen und Produktionsprozesse

Fraunhofer IWU

The contents of this presentation may not be copied and/or distributed without permission of the author! Please note references at the end of the presentation!

FEM-Analysis of new construction, iterative improvement

Changing of light weight construction- factors by several direction of forces

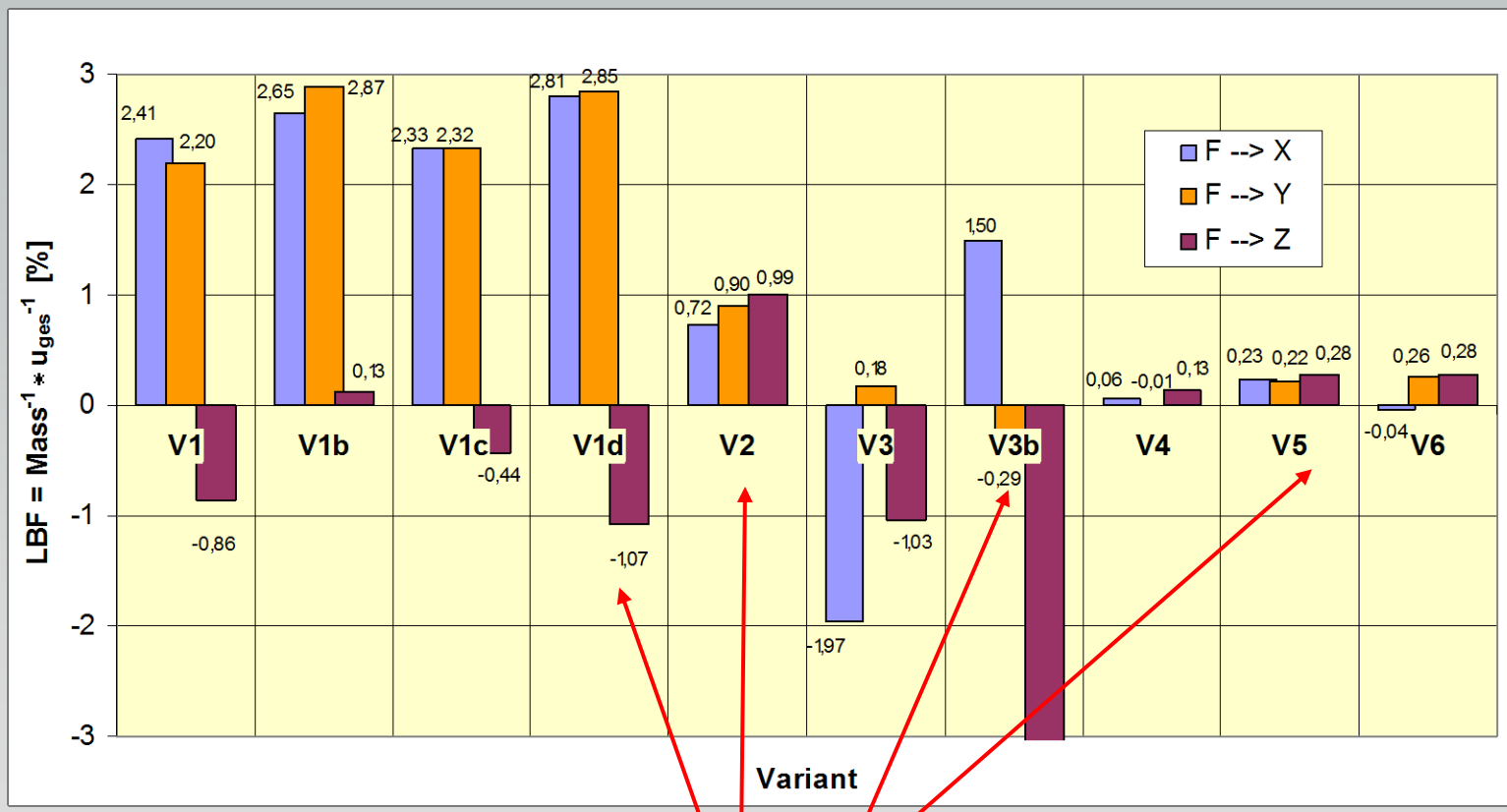

Archivierungsangaben

The contents of this presentation may not be copied and/or distributed without permission of the author! Please note references at the end of the presentation!

Properties of final construction compared to the original

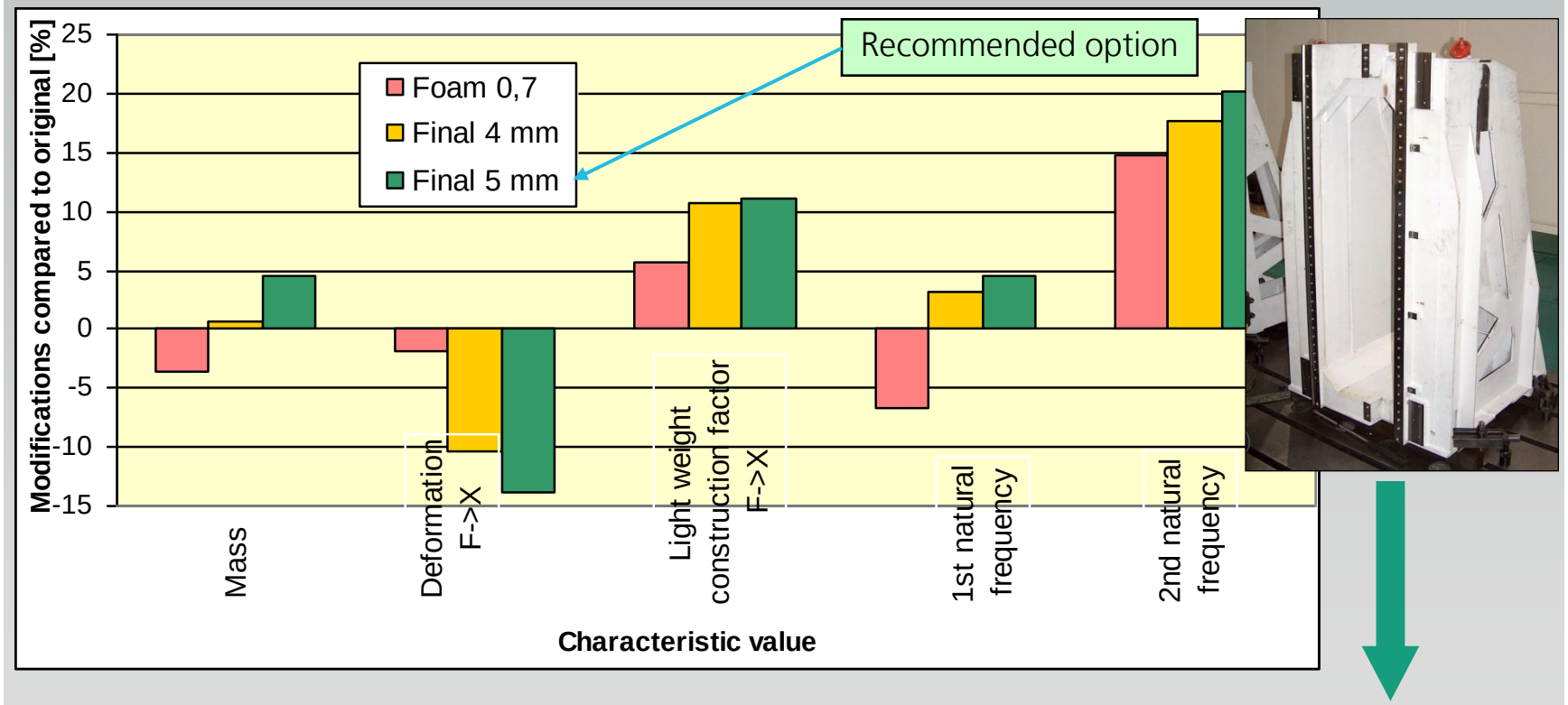

Increase of damping compared to the original : 385 % !

Archivierungsangaben

The contents of this presentation may not be copied and/or distributed without permission of the author! Please note references at the end of the presentation!

Methods for computation

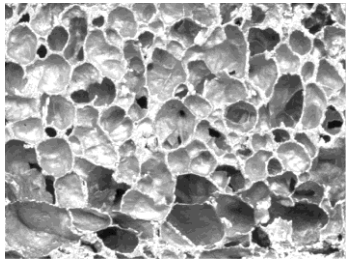

© Fraunhofer IWU
Prof. Neugebauer

The contents of this presentation may not be copied and/or distributed without permission of the author! Please note references at the end of the presentation!

Dimensioning of sandwiches

Optimal layer construction

Calculation regulation for optimal layer construction under prevention of plasticity in cover plates

Sandwich body will be described by:

b = Width sandwich
r_B = Density plate
M_B = Max. bending moment
t = Plate thickness
r_K = Density core
h = Distance plate middle levels
l = Length sandwich

Origin equations:

$$J = \frac{b \cdot t \cdot h^2}{2} \qquad \sigma = \frac{M_B \cdot (h + t)}{J \cdot 2}$$

mass sandwich:

$$m = l \cdot b \cdot \left[2 \cdot t \cdot r_B + (h - t) \cdot r_K \right]$$

Ratio t/h depends only on Density:

$$V_{opt} = \frac{t}{h} = 2 \cdot \frac{\rho_K}{\left(2 \cdot \rho_B - \rho_K + \sqrt{4 \cdot \rho_B^2 + 12 \cdot \rho_B \cdot \rho_K - 7 \cdot \rho_K^2} \right)}$$

Aim: Optimal ratio of mass/stiffness!

The optimal mass/stiffness – ratio of a steel – aluminum foam (foam-density 0.6 g/cm³) Sandwich is t/h = 0.037 (this means 1 mm steel coversheets with a 28 mm foam core)!

Archivierungsangaben

The contents of this presentation may not be copied and/or distributed without permission of the author! Please note references at the end of the presentation!

Dimensioning of sandwiches

Catalogue mechanical properties

Bending of sandwich due to a line load (different layer construction and foam densities)

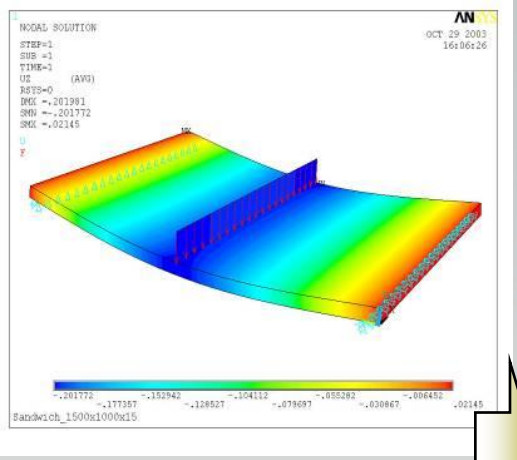

Gained parameter from FEM

Sandwich	Dimension	Lenght mm	Width mm	sigma zul.	E modulus St 37
		1500	1000	240	210000

Results of ANSYS-simulation

Height sandwich mm	Thickness Steel plate mm	Foam density g/cm³	E modulus foam N/mm²	Total volume kg	Max bending mm via self-weight	Max stress intensity N/mm² via self-weight	Max bending mm/1000N	Max stress intensity (N/mm²)/1000N	Max permissible line load kN	Light weight construction factor
10	1	0,50	3500	29,55	1,0650	5,49	5,883	38,76	6,050	5,752328
10	1	0,60	4900	30,75	1,069	5,55	5,701	37,17	6,308	5,704319
10	1	0,70	6000	31,95	1,0814	5,64	5,569	36,1	6,492	5,620202
10	1	0,90	9100	34,35	1,0837	5,7	5,233	33,56	6,982	5,563172
15	1	0,50	3500	33,30	0,5043	3,86	2,462	24,18	9,766	12,197413
15	2	0,50	3500	55,3	0,5088	3,84	1,4885	15,53	15,207	12,148594
15	3	0,50	3500	77,4	0,56	4,2	1,1695	12,66	18,626	11,047368
15	1	0,60	4900	35,25	0,4736	3,65	2,388	23,26	10,161	11,879730
15	2	0,60	4900	57	0,4719	3,59	1,4637	15,02	15,740	11,985967
15	3	0,60	4900	78,75	0,5161	3,9	1,1555	12,32	19,164	10,989539

Archivierungsangaben

The contents of this presentation may not be copied and/or distributed without permission of the author! Please note references at the end of the presentation!

FEM

Procedure

In general: Cellular metals modeled as isotropic and homogenized material

Modeling sandwiches: (2 variants)

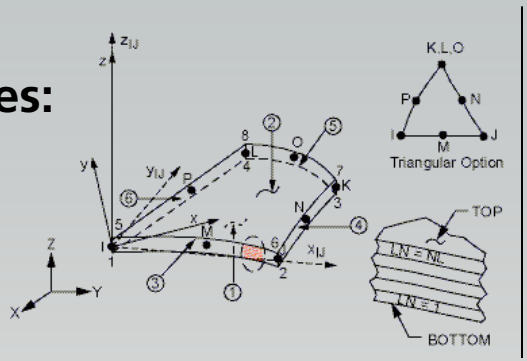

Layered SHELLs

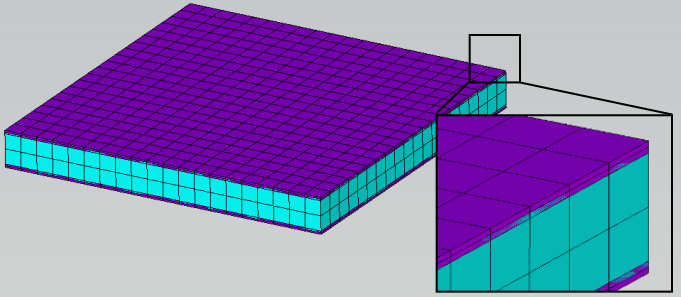

Foam core: SOLIDs, Coversheets: SHELLs

Modeling compact parts:

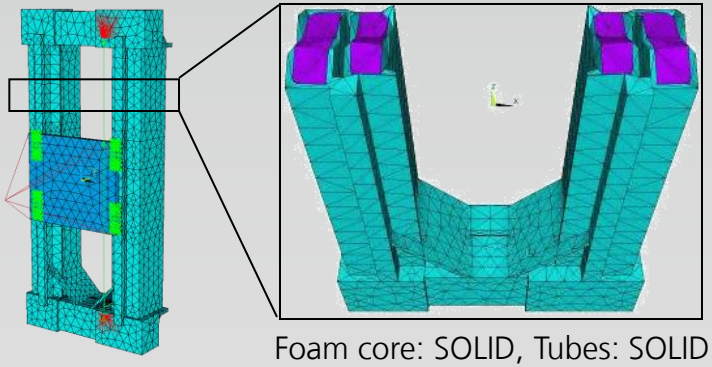

Foam core: SOLID, Tubes: SOLID

Archivierungsangaben

The contents of this presentation may not be copied and/or distributed without permission of the author! Please note references at the end of the presentation!

FEM

Procedure at the example of a foam filled double steel cantilever beam

STEP 1 → **STEP 2** → **STEP 3**

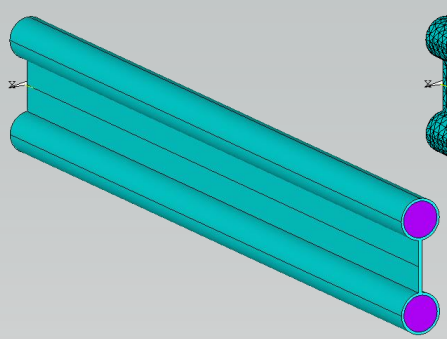

Import 3-d CAD-model:
Assembly with 3 parts
(volumes)

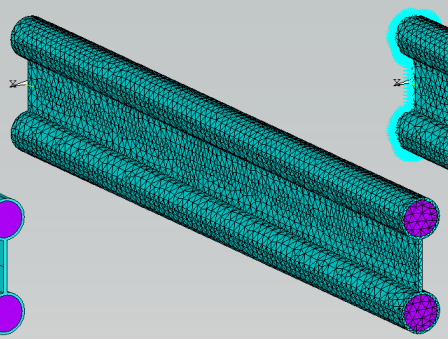

Generating FEM-Model:
10-Node Solid-Elements
Material 1: steel (cyan)
Material 2: aluminum foam (magenta)

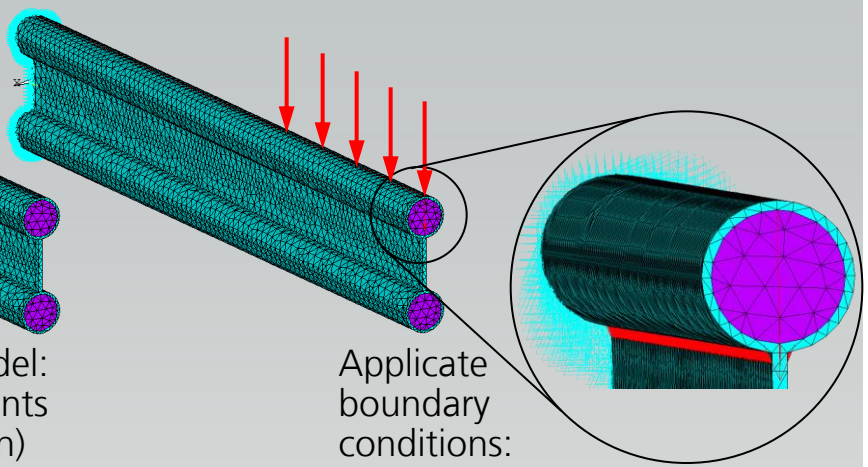

Applicate
boundary
conditions:
fixing, forces

→ **STEP 4**

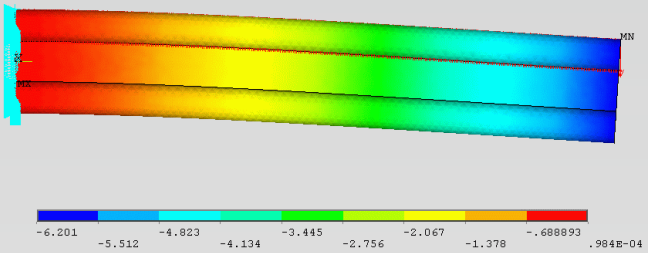

Post processing:
plotting stress, deformation etc.

Archivierungsangaben

The contents of this presentation may not be copied and/or distributed without permission of the author! Please note references at the end of the presentation!

FEM
Damping

Structure damping

Damping:

- Material parameter, which is necessary as input parameter by the FEM-Analysis
- Always addicted to the geometry

➡ **The damping of metal foam-compound structures can not be calculated reliable by the help of the FEM.**

Archivierungsangaben

The contents of this presentation may not be copied and/or distributed without permission of the author! Please note references at the end of the presentation!

CELLULAR METALS

Part IV – Standardization

© Fraunhofer IWU

The contents of this presentation may not be copied and/or distributed without permission of the author! Please note references at the end of the presentation!

Standardization

© Fraunhofer IWU
Prof. Neugebauer

The contents of this presentation may not be copied and/or distributed without permission of the author! Please note references at the end of the presentation!

Standardization – the base for database

Detection of standardized material parameters

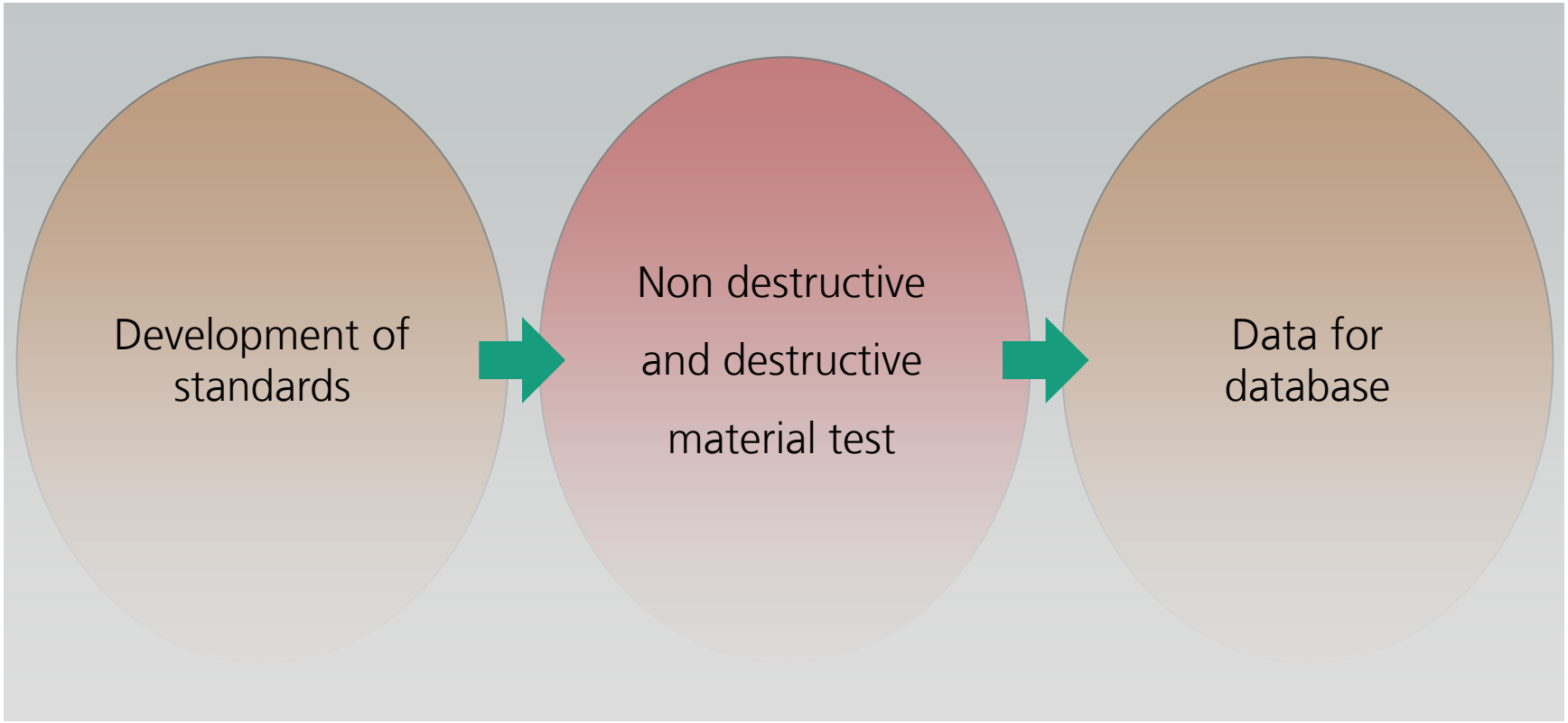

Archivierungsangaben

The contents of this presentation may not be copied and/or distributed without permission of the author! Please note references at the end of the presentation!

Standardization of compression testing for cellular metals

Compression testing of cellular metals

Engineering design requires
standardization of mechanical testing

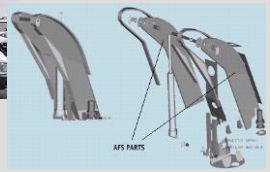

Archivierungsangaben

The contents of this presentation may not be copied and/or distributed without permission of the author! Please note references at the end of the presentation!

Standardization of compression testing for cellular metals

Parameters of compression testing

- Standard is applicable to cellular metals of a porosity larger than 50 %
- Testing System equipped with calibrated load cell and extensometer
- Parallel steel plates (min. 60 HRC) lubricated by graphite
- Specimens of round or rectangular cross section containing at least 10 pores in each spatial direction
- Length to diameter (or edge length) ratio between 1.5 and 2

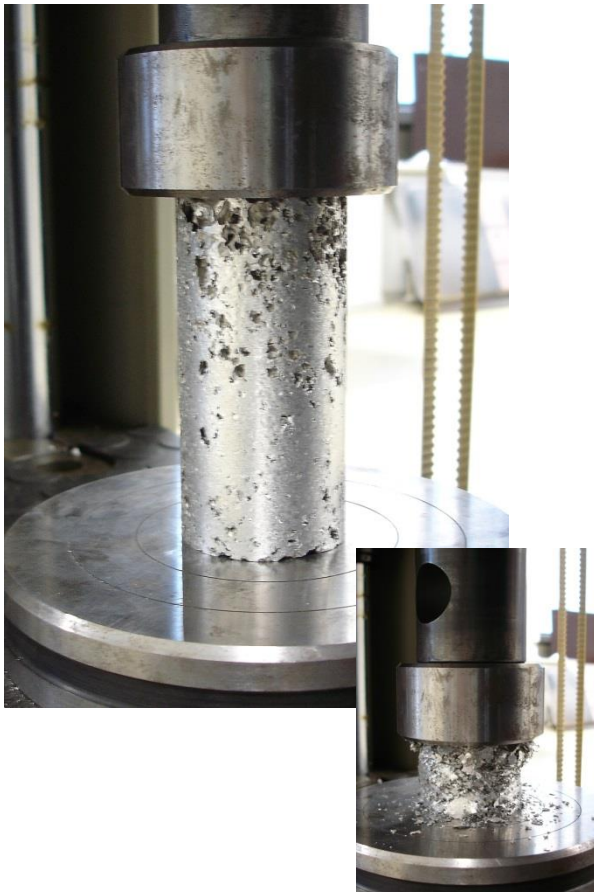

Archivierungsangaben

The contents of this presentation may not be copied and/or distributed without permission of the author! Please note references at the end of the presentation!

Standardization of compression testing for cellular metals

Definition of material's properties

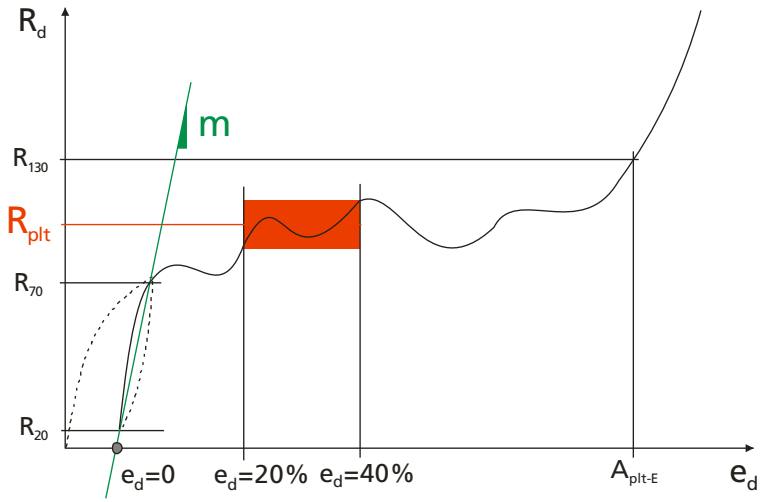

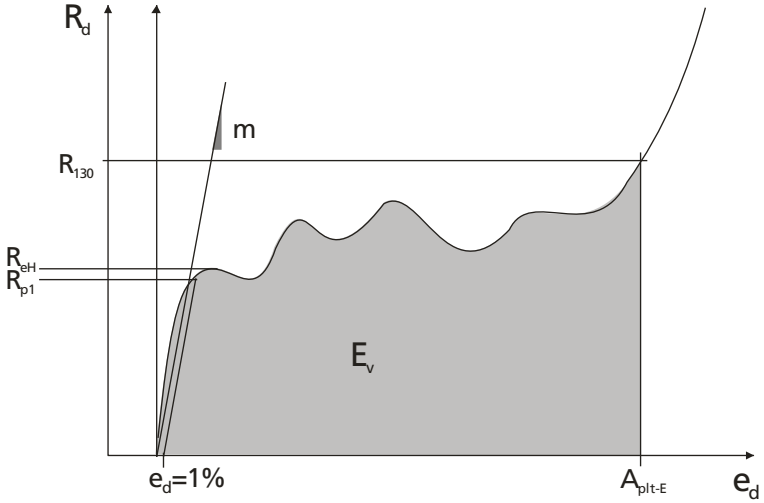

1. Plateau stress R_{plt} (mean value of the compressive stress in the range between e_d = 20 % and e_d = 40 %)
2. Slope of the quasi-elastic linear part of the compressive stress-strain diagram m
3. Compressive strain at the end of plateau regime A_{plt-E}
4. Specific energy absorption E_V

Archivierungsangaben

The contents of this presentation may not be copied and/or distributed without permission of the author! Please note references at the end of the presentation!

Standardization of compression testing for cellular metals

Compression testing procedure

1. Pre-test using a constant strain rate of $de/dt=10^{-2}\ s^{-1}$ to obtain an estimate value of the plateau stress R_{plt}
2. Determination of $R_{70} = 0.7\ R_{plt}$ and $R_{20} = 0.2\ R_{plt}$
3. Following compression tests start from a preload of $0.02\ R_{plt}$ using $de/dt=10^{-3}\ s^{-1}$ until reaching R_{70}
4. Unloading to R_{20} for determination of the equivalent Young's modulus m
5. Continuation of compression test until global densification begins (R130)
6. From a compressive strain of $e_d = 10\ \%$ the strain rate can be increased to $de/dt = 10^{-2}\ s^{-1}$

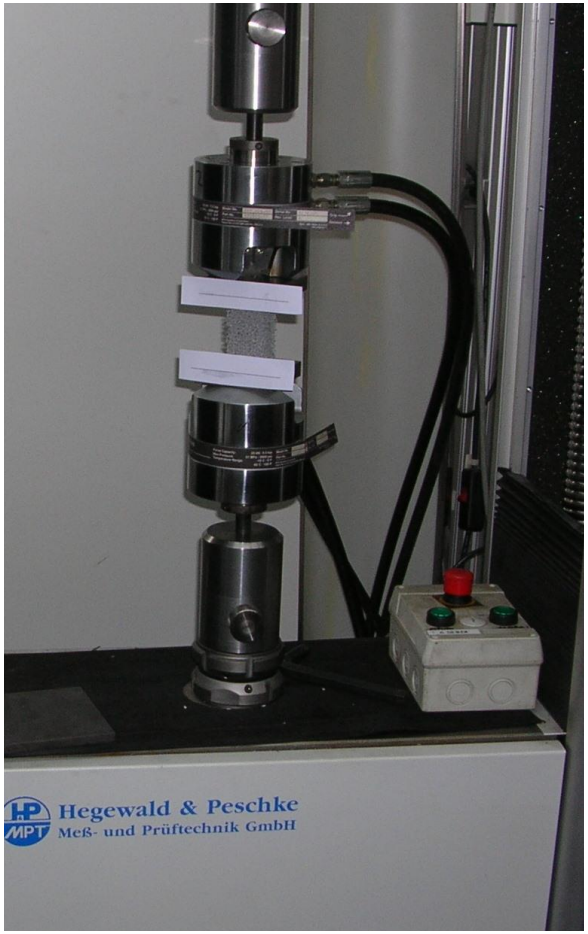

Archivierungsangaben

The contents of this presentation may not be copied and/or distributed without permission of the author! Please note references at the end of the presentation!

Standardization of compression testing for cellular metals

Experimental evaluation

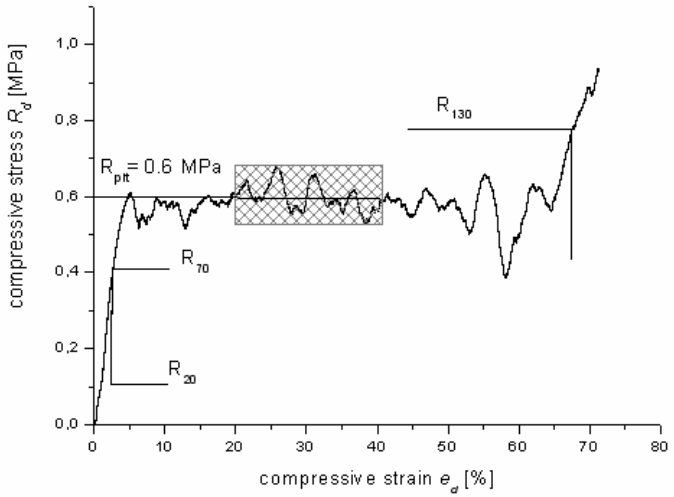

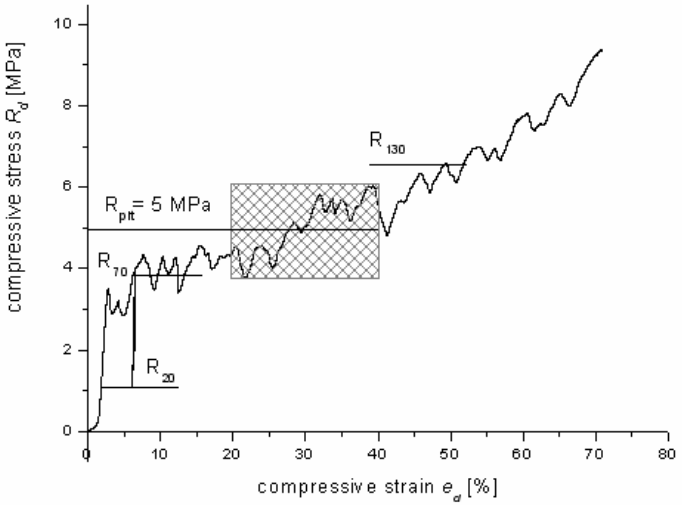

Open-cell aluminum foam

m-pore
10 ppi; density of 0.05

→ Distinct stress plateau

Determination of the material's properties according to the standard leads to reasonable values!

Closed-cell aluminum foam

Norsk Hydro
10 ppi; density of 0.12; stabilized by SiC

→ No distinct stress plateau

Unloading hysteresis at a compressive stress where damage has already occurred!

Archivierungsangaben

The contents of this presentation may not be copied and/or distributed without permission of the author! Please note references at the end of the presentation!

Standardization of compression testing for cellular metals

Example for compression testing of a hollow sphere structure

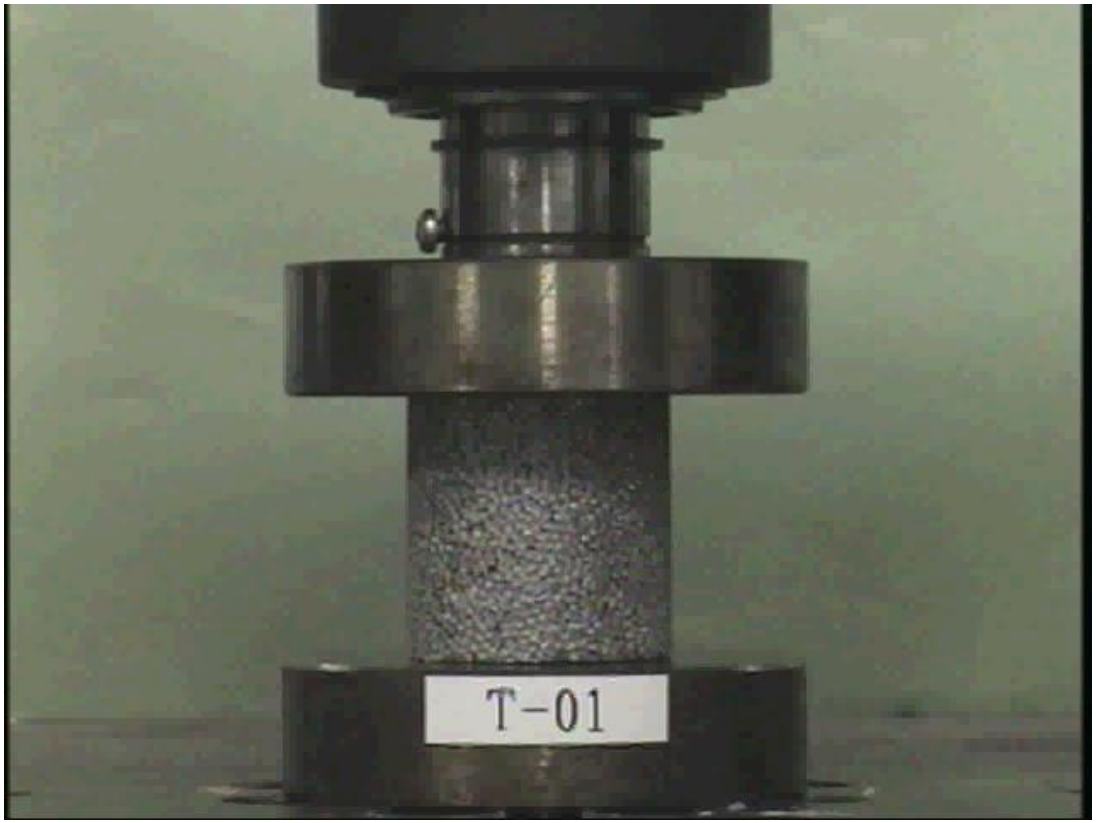

Archivierungsangaben

Fraunhofer IFAM Dresden

© Fraunhofer IWU

IWP Werkzeugmaschinen und Produktionsprozesse

Fraunhofer IWU

The contents of this presentation may not be copied and/or distributed without permission of the author! Please note references at the end of the presentation!

Standardization of compression testing for cellular metals

The standard “compression testing”

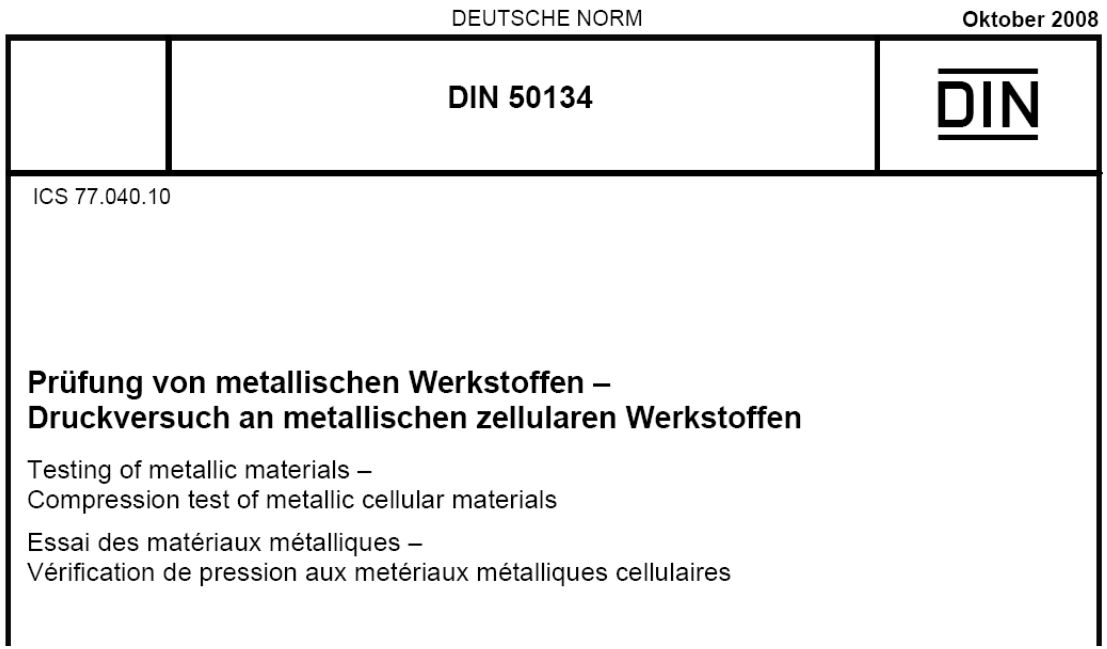

DEUTSCHE NORM Oktober 2008

DIN 50134

DIN

ICS 77.040.10

Prüfung von metallischen Werkstoffen –
Druckversuch an metallischen zellularen Werkstoffen

Testing of metallic materials –
Compression test of metallic cellular materials

Essai des matériaux métalliques –
Vérification de pression aux metériaux métalliques cellulaires

The standardization work was financially supported by Plansee AG, Glatt Systemtechnik GmbH, Alm GmbH, Alulight GmbH, IWU Chemnitz, IFAM Dresden and IFAM Bremen.

Archivierungsangaben

IWP Werkzeugmaschinen und Produktionsprozesse

Fraunhofer IWU

The contents of this presentation may not be copied and/or distributed without permission of the author! Please note references at the end of the presentation!

Standardization of compression testing for cellular metals

The standard “compression testing”

ISO 13314:2011(en)
Mechanical testing of metals — Ductility testing — Compression test for porous and cellular metals

Archivierungsangaben

The contents of this presentation may not be copied and/or distributed without permission of the author! Please note references at the end of the presentation!

CELLULAR METALS

Part V – Congresses, literature

© Fraunhofer IWU
Prof. Neugebauer

The contents of this presentation may not be copied and/or distributed without permission of the author! Please note references at the end of the presentation!

Congresses

© Fraunhofer IWU
Prof. Neugebauer

The contents of this presentation may not be copied and/or distributed without permission of the author! Please note references at the end of the presentation!

Congresses

Metfoam from 1999 to 2019 and 2011 to 2019

2011 Busan, Southkorea

2013 Raleigh, USA

2015 Barcelona, Spain

2017 Nanjing, China

2019 Detroit, USA

Archivierungsangaben

The contents of this presentation may not be copied and/or distributed without permission of the author! Please note references at the end of the presentation!

Congresses

Cellmet 2005 and 2008 later Cellmat 2010 to 2018

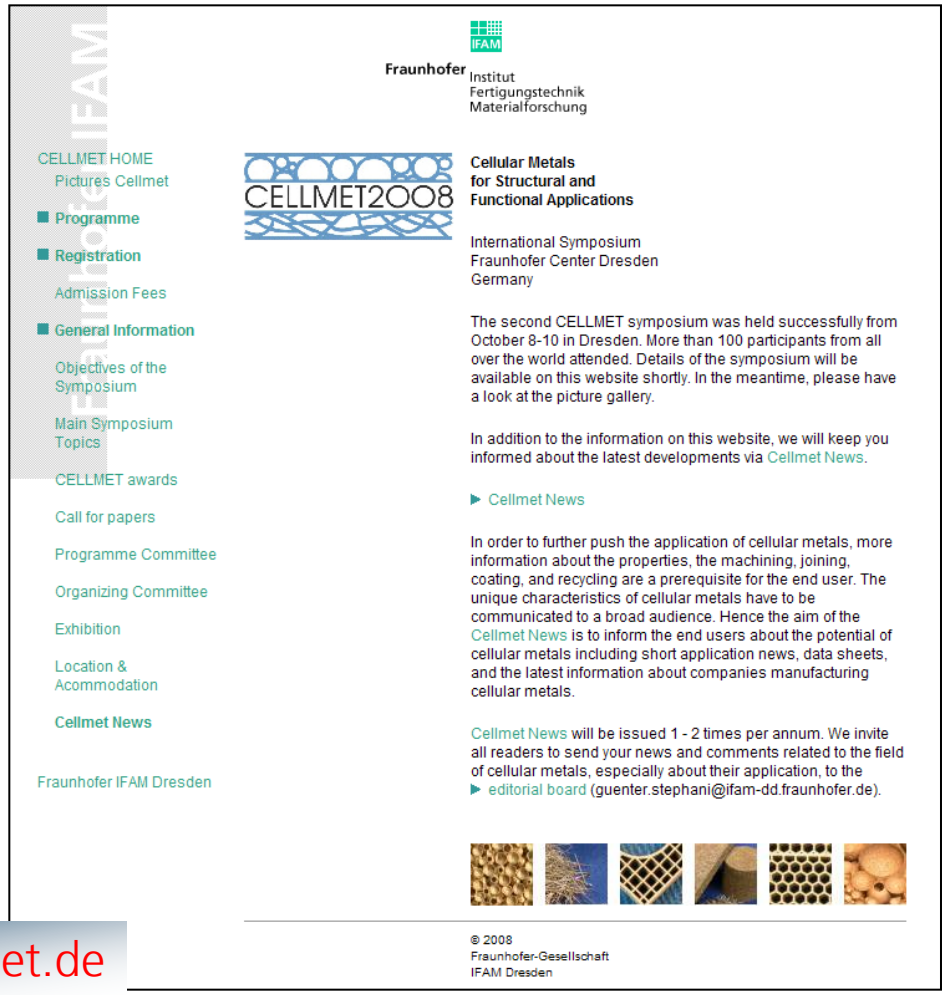

http://www.cellmet.de

Fraunhofer IFAM Dresden

Archivierungsangaben

IWP Werkzeugmaschinen und Produktionsprozesse

Fraunhofer IWU

The contents of this presentation may not be copied and/or distributed without permission of the author! Please note references at the end of the presentation!

Congresses

Cellmat

DGM Deutsche Gesellschaft für Materialkunde

Home • Contact • Membership • Coordination

The Conference • Programme • Proceedings • Conference Location • Exhibition • Registration

CELLMAT

Cellular Materials

CELLMAT2010

Now online:

- Call for Papers (PDF)

© Uni Karlsruhe (TH) IKM © Fraunhofer IFAM, Dresden © Fraunhofer IWU, Chemnitz

27 - 29 Oct 2010

Dresden, Germany

Copyright © 2010
Deutsche Gesellschaft für Materialkunde e.V.
Impressum

http://www.dgm.de/dgm/cellmat/

Fraunhofer IFAM Dresden

Archivierungsangaben

IWP Werkzeugmaschinen und Produktionsprozesse

Fraunhofer IWU

The contents of this presentation may not be copied and/or distributed without permission of the author! Please note references at the end of the presentation!

Congresses

Cellmat

http://www.dgm.de/dgm/cellmat/

Archivierungsangaben

The contents of this presentation may not be copied and/or distributed without permission of the author! Please note references at the end of the presentation!

Literature

The contents of this presentation may not be copied and/or distributed without permission of the author! Please note references at the end of the presentation!

Literature

Specialist book “Taschenbuch für Aluminiumschäume“

Taschenbuch für Aluminiumschäume

Aluminium Verlag, 2007, 207 pages, EUR 81.00

For those who deal with aluminum foam
this new publication is a must have!

The „Taschenbuch der Aluminiumschäume“ offers:

- A roundup of all information belonging to the topic
- Illustration from production to application
- Systematic basic knowledge of construction methods, guidelines and production technologies

Archivierungsangaben

The contents of this presentation may not be copied and/or distributed without permission of the author! Please note references at the end of the presentation!

Literature

Specialist book “Taschenbuch für Aluminiumschäume“

Content

- Production
- Structure
- Mechanical characteristics
- Fracture mechanics
- Joining technology
- Machining procedures
- Methods of testing
- Metallography, corrosion
- Construction
- Applications
- Forecast and trends
- List of current and completed research projects

Archivierungsangaben

The contents of this presentation may not be copied and/or distributed without permission of the author! Please note references at the end of the presentation!

Literature

Congress literature – Metfoam

J. Banhart, M.F. Ashby, N. A. Fleck (Editors)
MetFoam **1999**, Metal Foams and Porous Metal Structures
June 14-16, 1999; 1st International Conference on Metal Foams and Porous Metal Structures; 2000; Bremen

J. Banhart, M.F. Ashby, N. A. Fleck (Editors)
MetFoam **2001**, Cellular Metals and Metal Foaming Technology
June 18-20, 2001, 2nd International Conference on Cellular Metals and Metal Foaming Technology; 2002; Bremen

J. Banhart (Editor)
MetFoam **2003**, Cellular Metals – Manufacture, Properties, Applications
June 23-25, 2003, 3rd International Conference on Cellular Metals and Metal Foaming Technology; 2004; Berlin; Verl. MIT; 2003

H. Nakajima (Editor)
MetFoam **2005**, Porous Metals and Metal Foaming Technology
September 21-23, 2005; 4th International Conference on Porous Metals on Metal Foaming Technology; 2006; Kyoto

L. P. Lefebvre, J. Banhart, D. C. Dunand
MetFoam **2007**, Porous Metals and Metallic Foams
September 5-7, 2007; 5th International Conference on Porous Metals and Metallic Foams; 2008; Montreal

MetFoam **2009**, Porous Metals and Metallic Foams
September 1-4, 2009; 6th International Conference on Porous Metals and Metallic Foams; Bratislava; 2009
Not yet published

Archivierungsangaben

The contents of this presentation may not be copied and/or distributed without permission of the author! Please note references at the end of the presentation!

Literature

Congress literature – Cellmet

G. Stephani, B. Kieback (Editors)
Cellmet **2005**, Cellular Metals for Structural and Functional Applications
May 18-20, 2005; International Symposium; 2005; Fraunhofer IFAM; Dresden

G. Stephani, B. Kieback (Editors)
Cellmet **2008**, Cellular Metals for Structural and Functional Applications
October 8-10, 2005; International Symposium; 2005; Fraunhofer IFAM; Dresden

Archivierungsangaben

The contents of this presentation may not be copied and/or distributed without permission of the author! Please note references at the end of the presentation!

Literature

Other literature – Cellmet-News

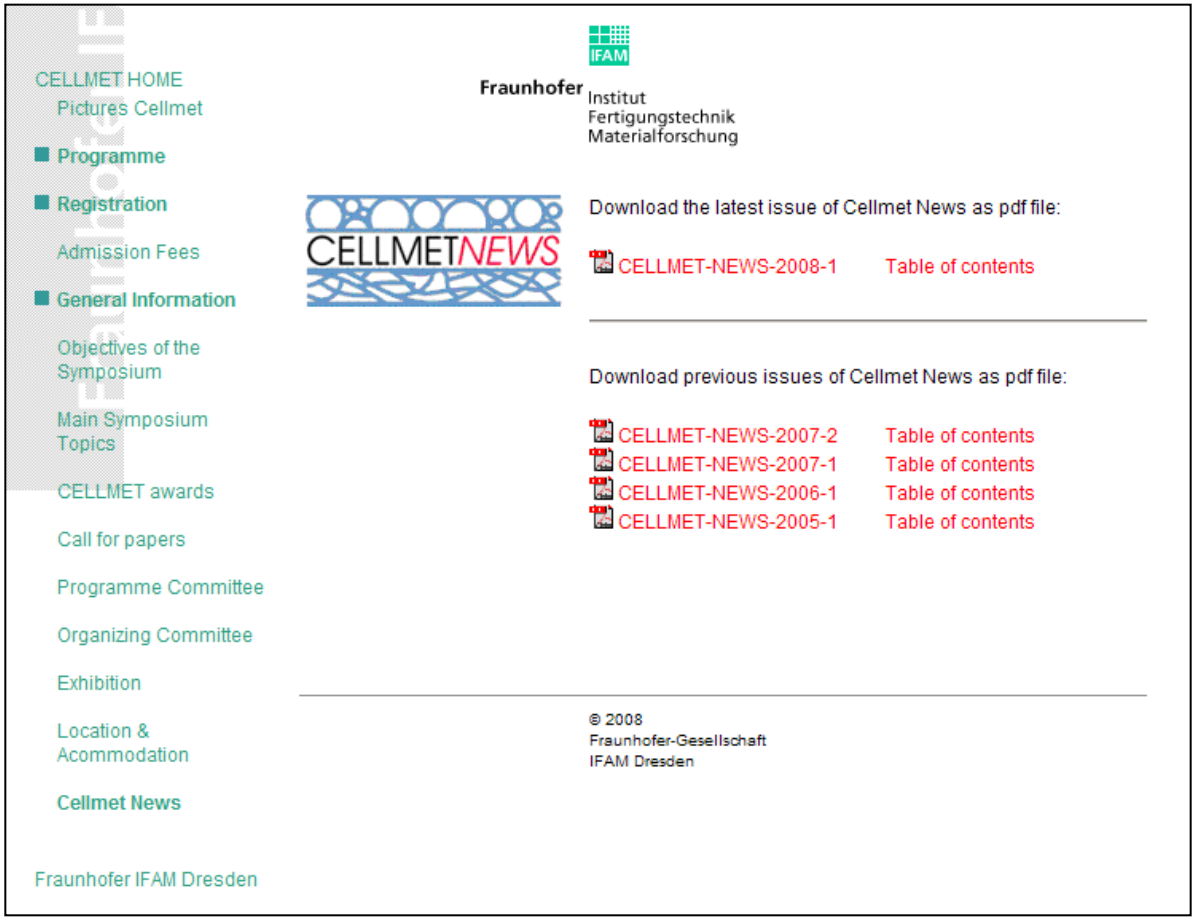

http://www.cellmet.de/news.html

Archivierungsangaben

The contents of this presentation may not be copied and/or distributed without permission of the author! Please note references at the end of the presentation!

CELLULAR METALS

Part VI – R&D-Activities containing cellular metals

© Fraunhofer IWU
Prof. Neugebauer

The contents of this presentation may not be copied and/or distributed without permission of the author! Please note references at the end of the presentation!

High melting alloys

Metal foams based on stainless steel and titanium

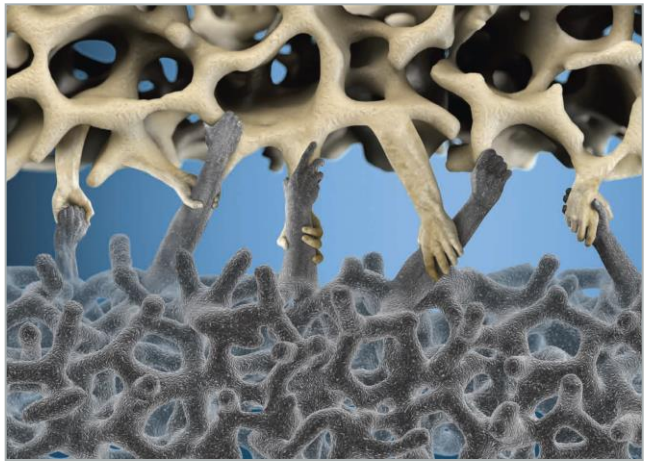

- High temperature applications
- Adjustable strength
- Biocompatible
- …

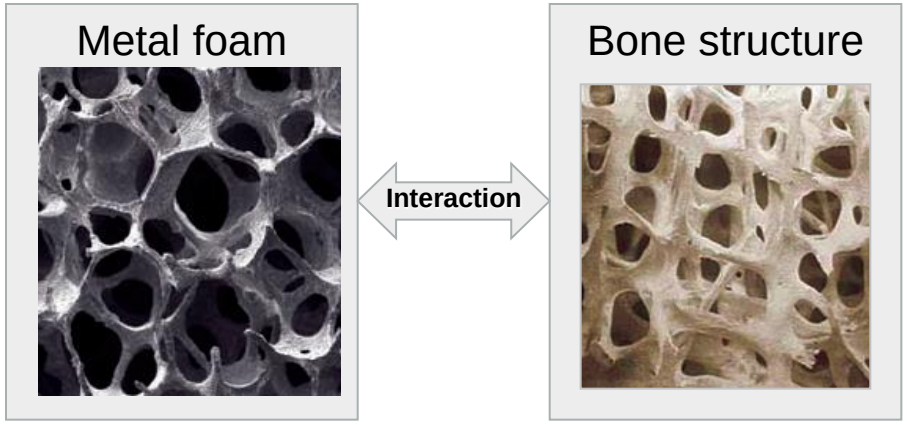

Archivierungsangaben

The contents of this presentation may not be copied and/or distributed without permission of the author! Please note references at the end of the presentation!

High porosity castings

Standard casting process for creating aimed porosity partitions

Main target: saving resources (material, energy)

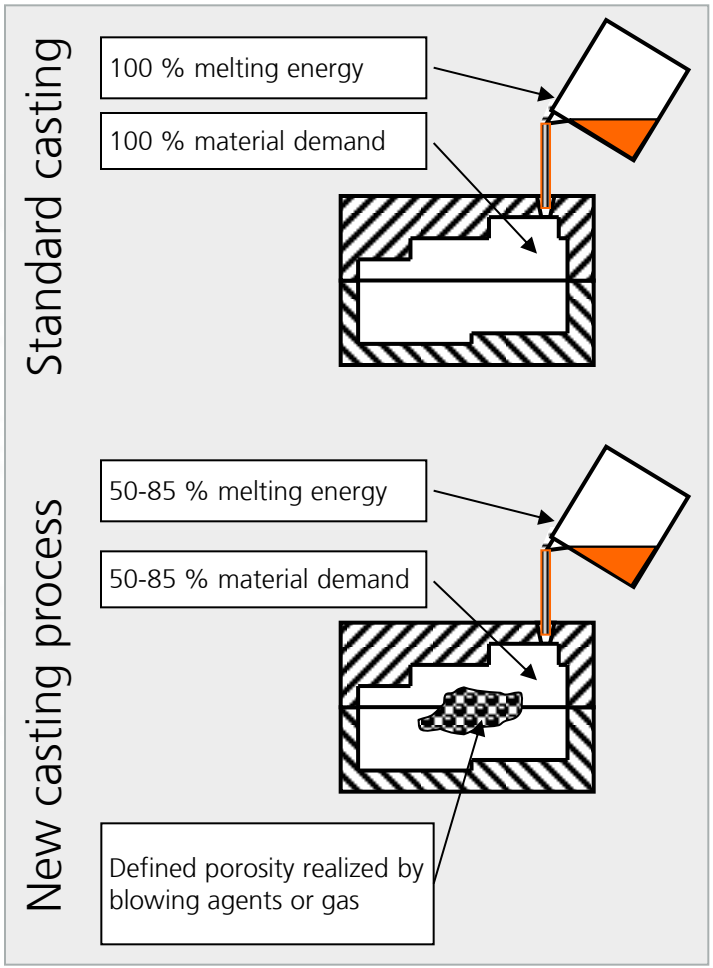

Archivierungsangaben

The contents of this presentation may not be copied and/or distributed without permission of the author! Please note references at the end of the presentation!

Hybrid construction

Combination of CFRP with aluminum foam

- Application for lighter and stiffer sandwich structures and profiles
- Vibration damping
- Crash absorber

Archivierungsangaben

The contents of this presentation may not be copied and/or distributed without permission of the author! Please note references at the end of the presentation!

Light weight construction-spot welding gun

Simulation, prototype construction and technical measurement examination of component properties

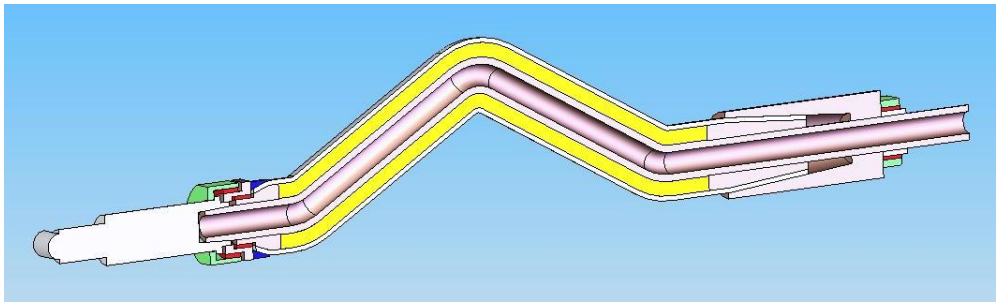

Simulation with failure criteria:

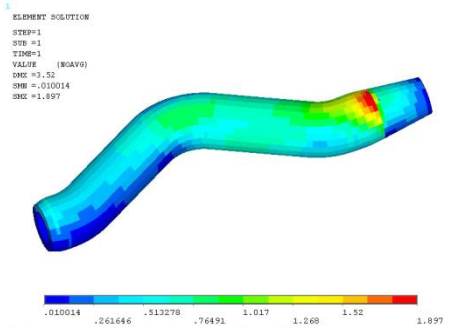

- Approx. 29 % reduction of mass compared to traditional steel construction
- Approx. 9 % increase of stiffness compared to traditional steel construction
- Great damping features

Archivierungsangaben

The contents of this presentation may not be copied and/or distributed without permission of the author! Please note references at the end of the presentation!

Increase of dynamic at the machine tool manufacture

Characteristics:

- CFRP-honeycombs-sandwich construction
- High dynamic moved: Acceleration till 2,5 g

Advantage compared to the steel-variant:

- Mass halved
- Stiffness of the components doubled
  - ➡ Increase of the dynamic stiffness about **factor 4**
  - ➡ Result: 70 % increase in productivity

Firm presentation of TRUMPF
(TruLaser 7040 NEU)

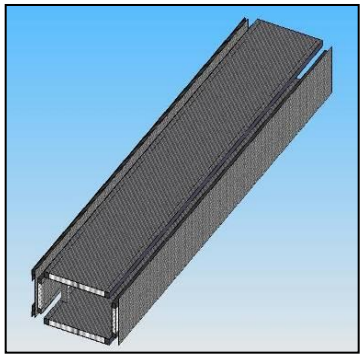

Simulative and metrological proof of the properties at the IWU

Demonstration of the first four natural frequencies

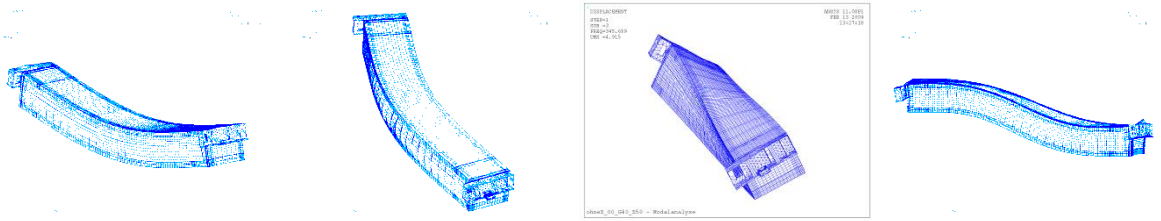

Archivierungsangaben

IWP WERKZEUGMASCHINEN UND PRODUKTIONSPROZESSE

Fraunhofer IWU

The contents of this presentation may not be copied and/or distributed without permission of the author! Please note references at the end of the presentation!

Alternative materials

Substitution of raw materials for the foaming process

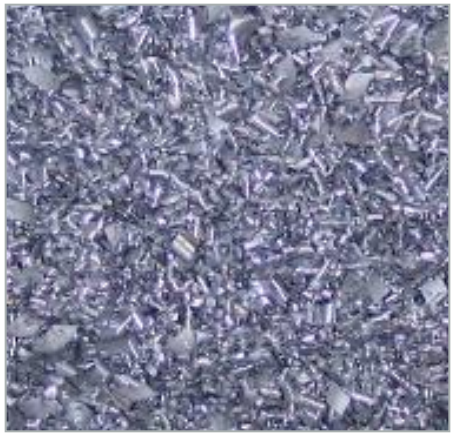

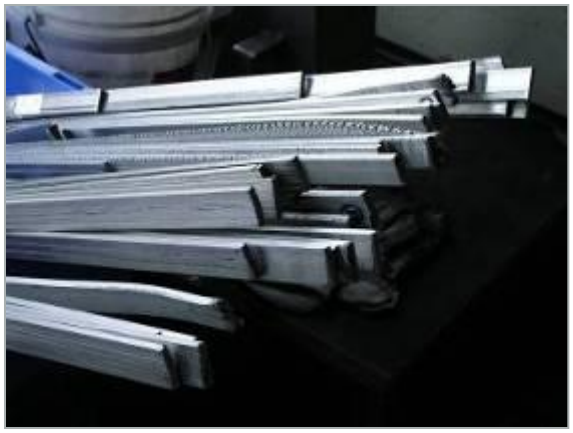

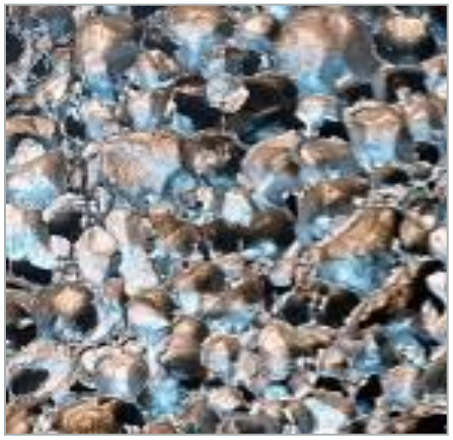

- Substitution of powder by recycled milling chips
- Substitution of currently used blowing agent
- Lowering the metal foam prices
- Recycling of material
- Protecting natural and energetic resources

Archivierungsangaben

The contents of this presentation may not be copied and/or distributed without permission of the author! Please note references at the end of the presentation!

Shortening of the process chain

Powder rolling

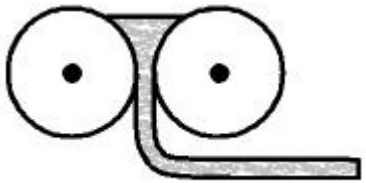

Mixing

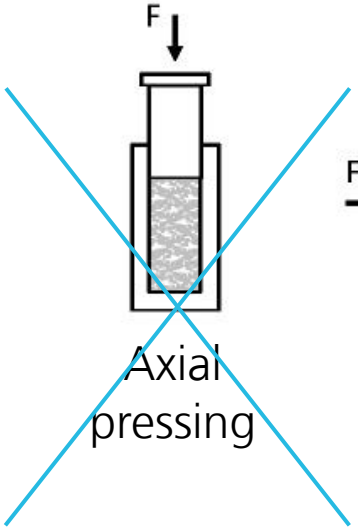

Axial pressing

Pressing a rod

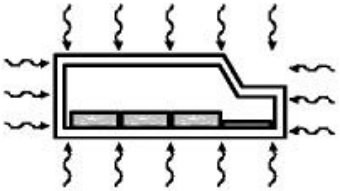

Input the precursor and Foaming

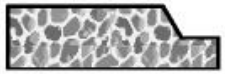

Foam part

Automated by modification!

PolyFoM®

Polymorphic Foamable Material

Direct filling of the powder mixture into the extrusion chamber

Archivierungsangaben

The contents of this presentation may not be copied and/or distributed without permission of the author! Please note references at the end of the presentation!

Aluminum - aluminum foam - composites

State of the art: Heating of precursor and covering material at the same time!

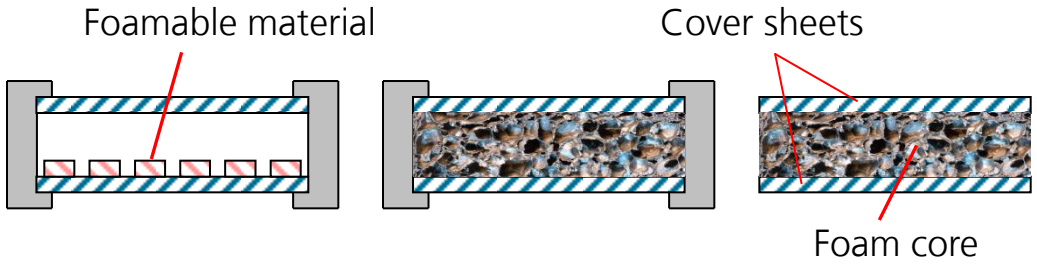

Problem/Risk: Melting of covering material → Loosing shape and properties

→ Process only possible for steel and thick-walled aluminum!

Alternative: Gluing → Manufacturing of a separate foam core and gluing into a profile!

Disadvantages

- Aging of the glue
- Restricted chemical/thermal stability
- Partial difficult joining possibilities

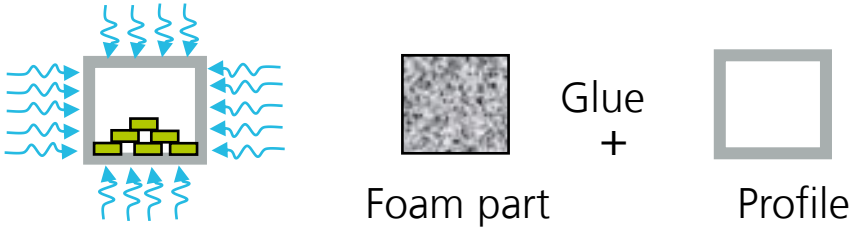

Archivierungsangaben

The contents of this presentation may not be copied and/or distributed without permission of the author! Please note references at the end of the presentation!

Aluminum - Aluminum Foam - Composites

Aim: Development and Manufacturing of thin-walled aluminum - aluminum foam - composites!

Approach:

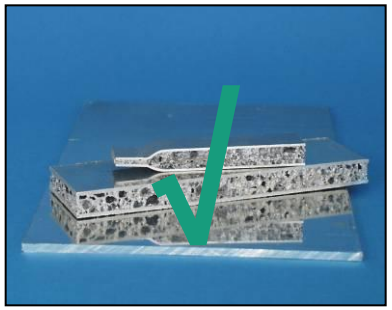

Sandwiches

- Thin-walled sandwiches realized by rolling process of precursor powder between aluminum cover sheets

Extrusion profiles (currently under development)

- Manufacturing of a composite material containing aluminum shell profile and precursor core material by extrusion in one step
- Foaming of the composite material (covering and precursor)

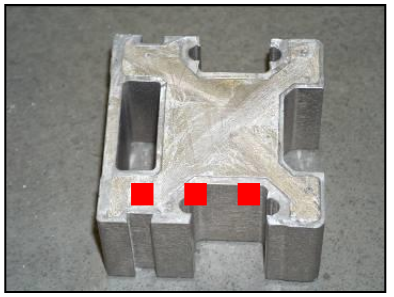

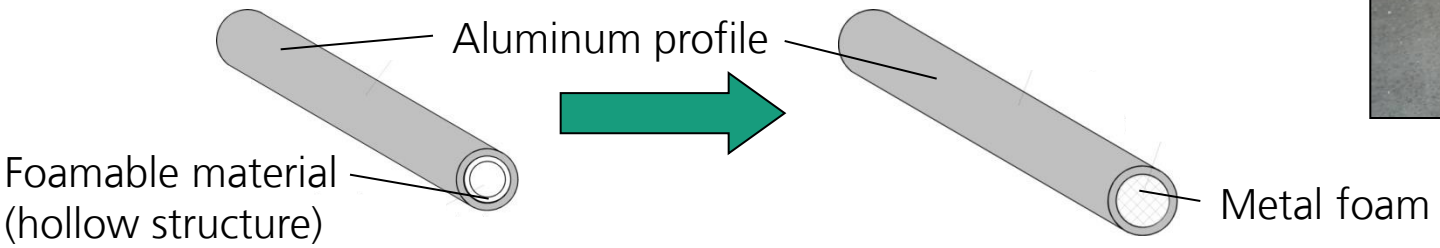

Archivierungsangaben

The contents of this presentation may not be copied and/or distributed without permission of the author! Please note references at the end of the presentation!

Further R&D activities

Manufacturing:

- Improvement of the homogeneity of aluminum foams and cost reduction!
- Complex cast Al-, Zn-foam parts,
- Sandwich structures
- Technology development for Ti-based foams
- New technologies (SEMB, screen printing, sinter paper, …)

Characterization: CT measurements becoming more importance

Modeling & Simulation: Strong activities during the last five years (heat transfer, acoustic absorption, mechanical properties, …)

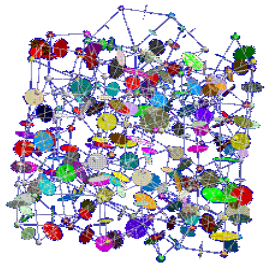

Archivierungsangaben

The contents of this presentation may not be copied and/or distributed without permission of the author! Please note references at the end of the presentation!

Low cost thixocast foamable aluminum precursor

Aim: Cost reduction Al-foam manufacturing

Technology:
- ➡ Precursor material produced from recycling chips (AlMg4.5Mn)
- ➡ Application of low-cost foaming agents $CaMg(CO_3)_2$; $CaCO_3$
- ➡ Conventional chip briquetting and subsequent thixocasting

Result: Complex shaped precursor material

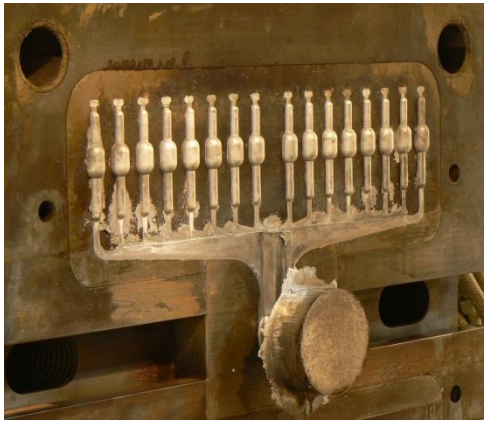

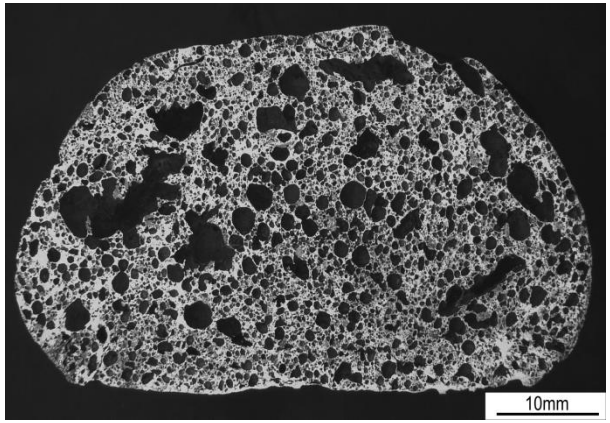

Archivierungsangaben

The contents of this presentation may not be copied and/or distributed without permission of the author! Please note references at the end of the presentation!

Syntactic micro-porous steel foams

Aim: Development of steel micro glass-bubble composites

Technology: Metal injection molding (MIM)

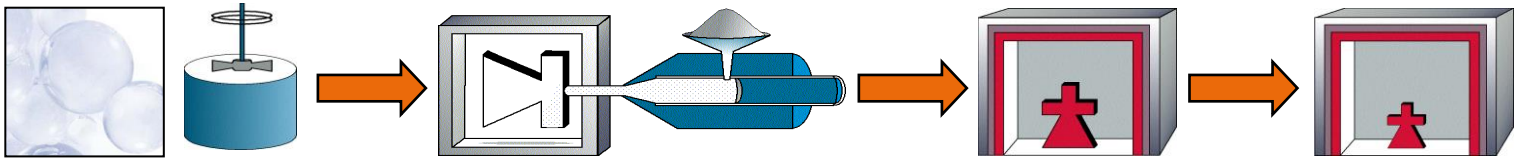

Materials:

- Fe, Fe-Ni, Fe-Cu-alloys
- Different glass bubble types
- Up to 10 wt% micro glass bubbles (∅ 50 - 500 µm)

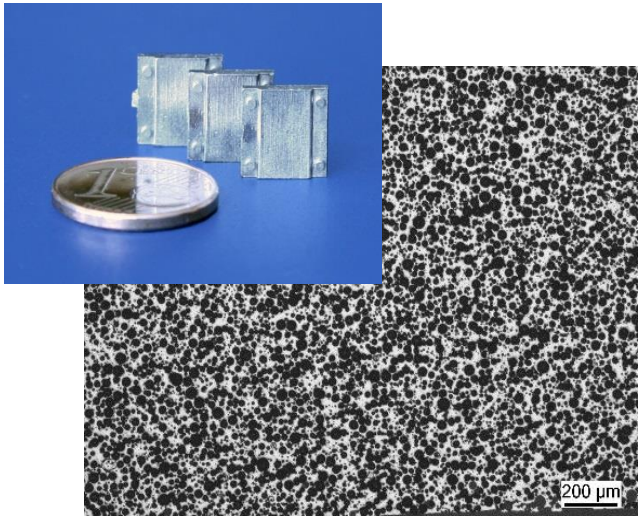

Target applications:

- Ultrasonic equipment
- Crash absorbers for high load densities

Fraunhofer IFAM Dresden

Archivierungsangaben

IWP Werkzeugmaschinen und Produktionsprozesse

Fraunhofer IWU

The contents of this presentation may not be copied and/or distributed without permission of the author! Please note references at the end of the presentation!

Magnesium integral foam with enhanced damping behavior

Technology: Magnesium injection molding with intergraded foaming process.

Results:

- Net shape parts with an excellent solid skin
- The foamed core has a graded pore structure between skin and core
- The internal friction of Mg-integral foam is 8x higher compared to compact material

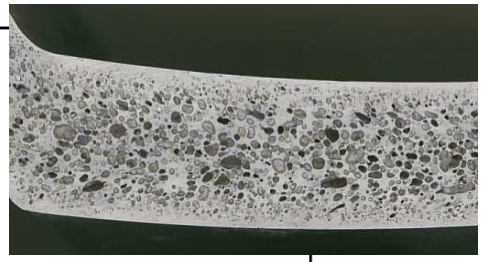

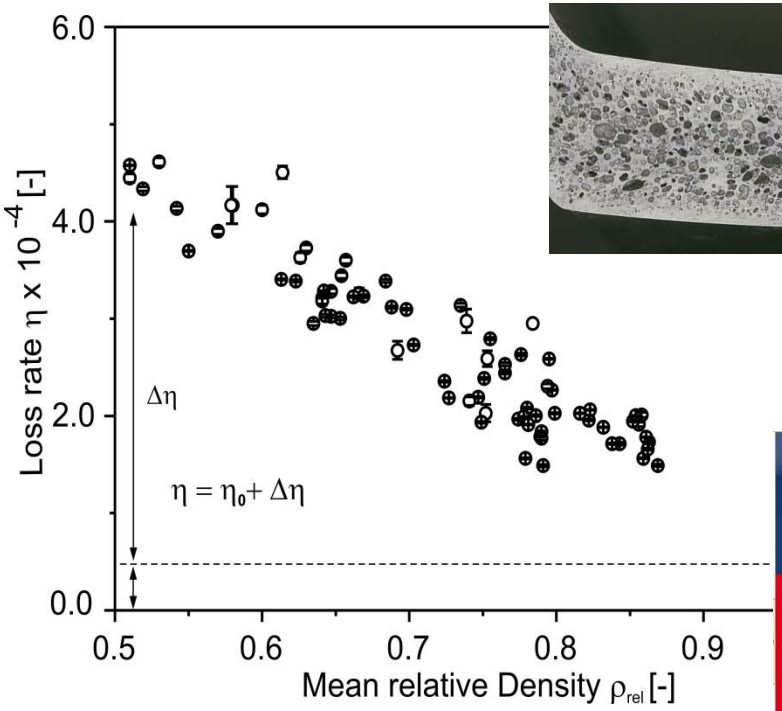

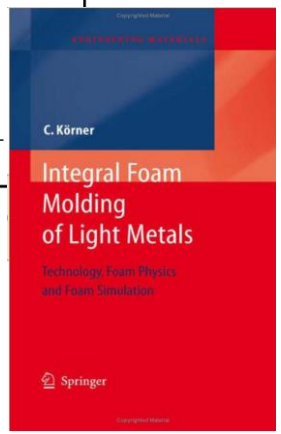

Archivierungsangaben

The contents of this presentation may not be copied and/or distributed without permission of the author! Please note references at the end of the presentation!

Machining of cellular metals and alloys

Aim: Designing of a technology database in machining including calculation model

Technologies: Laser beam and hydro-jet cutting, sink erosion, wire cutting, lathe-turning, milling, drilling including HSC machining, band sawing, diamond wire sawing

Results: Depended on the final requirements, like surface quality, dimension stability, process reliability, productivity and manufacturing costs

Optimized machining procedures with proposed parameters, including costs, have been evaluated.

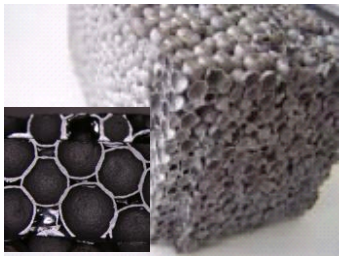

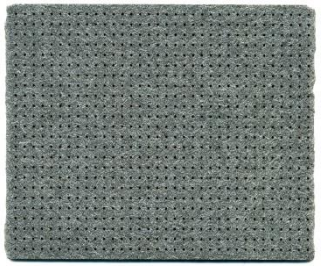

TECHNISCHE UNIVERSITÄT DRESDEN

Archivierungsangaben

IWP WERKZEUGMASCHINEN UND PRODUKTIONSPROZESSE

Fraunhofer IWU

The contents of this presentation may not be copied and/or distributed without permission of the author! Please note references at the end of the presentation!

Machining of cellular metals and alloys

Hydro-jet cutting

Objective: Making an HKS silencer element Ø 80.6mm x 70mm with inner drillings Ø 29.5mm; Ø 19.4mm; Ø 15.3mm; Ø 13 mm

Material: HKS plate X15CrNiSi25-20 (1.4841); sphere Ø ≈4mm

Machine: Trumatic WS 2500

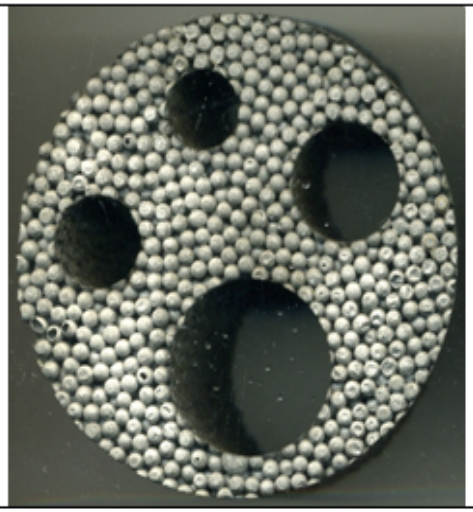

Pressure [bar]	Feed rate [m/min]	Main time [min]	Costs *) [€]
3000	0.2	2.5	4.68

*) hourly machine rate = 113 €/h

Hydro-jet cutting of a silencer element

Archivierungsangaben

The contents of this presentation may not be copied and/or distributed without permission of the author! Please note references at the end of the presentation!

Aluminum foaming in Space → microgravity experiments

Parabolic flight and sounding rocket experiments have been carried out to study the gravity influence during foaming

20 s microgravity

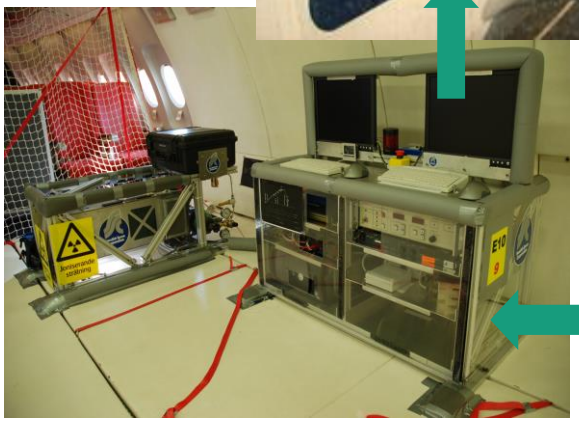

Experimental setup for the parabolic flight experiment

XRMON sounding rocket module <u>after</u> the flight

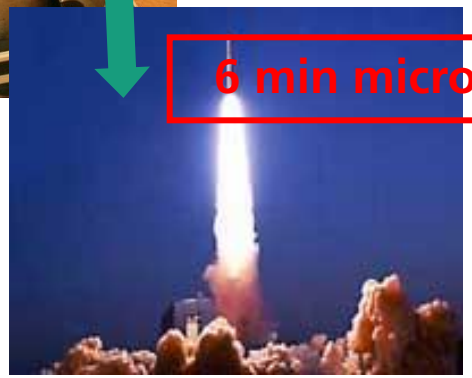

6 min microgravity

Archivierungsangaben

The contents of this presentation may not be copied and/or distributed without permission of the author! Please note references at the end of the presentation!

Aluminum foaming in Space – microgravity experiments

Material: Thixo AlSi6Cu4 + 0.6 wt%. TiH_2

Parabolic flight experiment

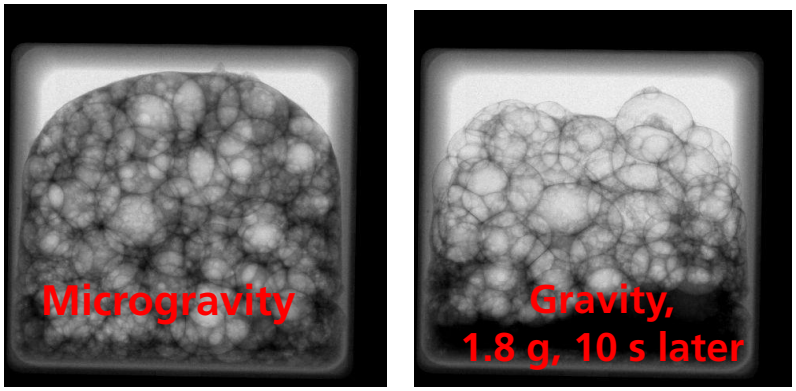

X-ray radiography investigations

Results:
- Homogeneous foaming
- Capillary force under micro-gravity stronger influence than drainage

Sounding rocket experiment MASER 11

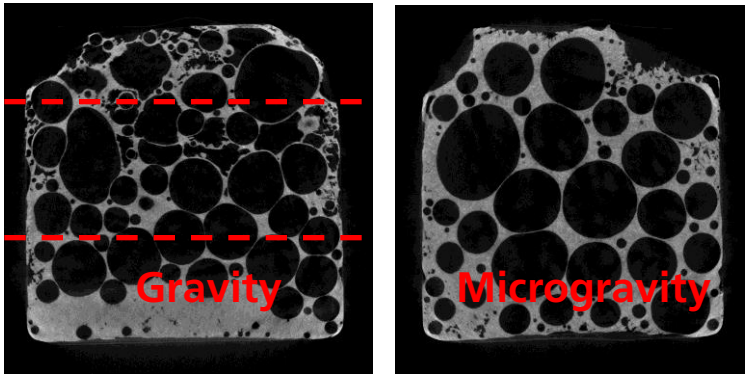

Tomographic reconstruction

Results:
- No change of the coalescence rate by microgravity
- Drainage can be avoided

Archivierungsangaben

The contents of this presentation may not be copied and/or distributed without permission of the author! Please note references at the end of the presentation!

CELLULAR METALS

Part A – Process chain at Fraunhofer IWU

© Fraunhofer IWU
Prof. Neugebauer

The contents of this presentation may not be copied and/or distributed without permission of the author! Please note references at the end of the presentation!

CONTENT

- Complete process chain of Fraunhofer IWU
- Draft/Construction
- Simulation
- Property Analysis

Archivierungsangaben

The contents of this presentation may not be copied and/or distributed without permission of the author! Please note references at the end of the presentation!

Complete process chain of Fraunhofer IWU

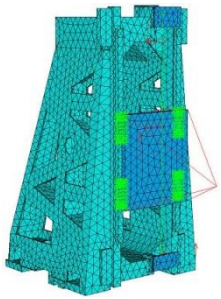

Mixing

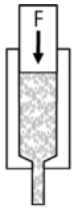

Extrusion

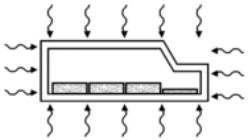

Charging/Foaming

Foam

Idea → Draft

Simulation → Construction

Production → Property analysis

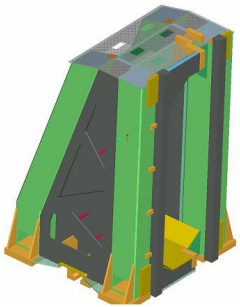

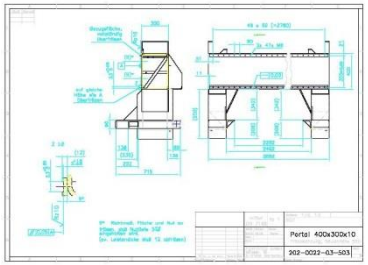

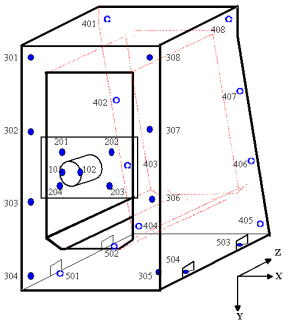

Archivierungsangaben

The contents of this presentation may not be copied and/or distributed without permission of the author! Please note references at the end of the presentation!

Draft/Construction

CAD (Draft & Construction):

- ProE Wildfire
- CATIA V5

Necessary parameters:

- Limits of the cross-section
- Permissible materials

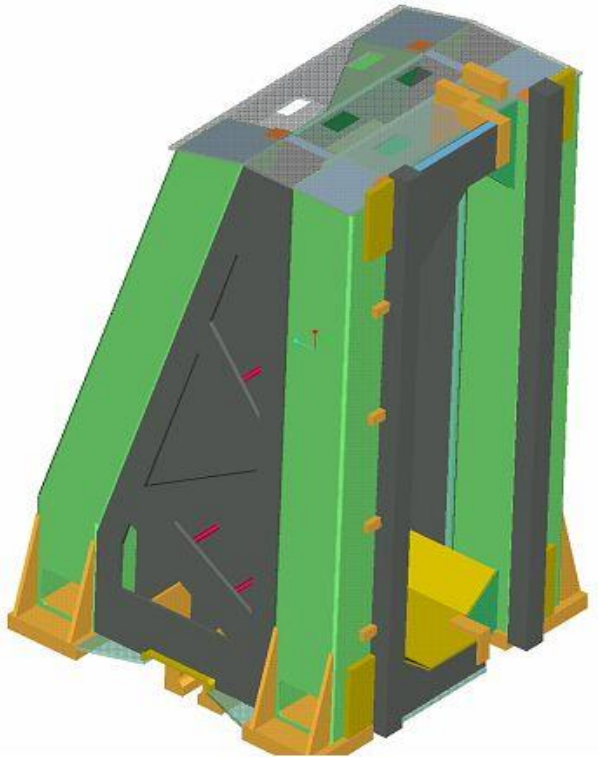

Archivierungsangaben

The contents of this presentation may not be copied and/or distributed without permission of the author! Please note references at the end of the presentation!

Simulation

Realization of Various analyses with ANSYS:

- Structure simulation
- Topology optimization
- Oscillation analysis (e. g. Modal Analysis)
- Thermal simulation

Necessary parameters:

- Loading conditions
- Bearing-constraints
- Permissible strains/deformations

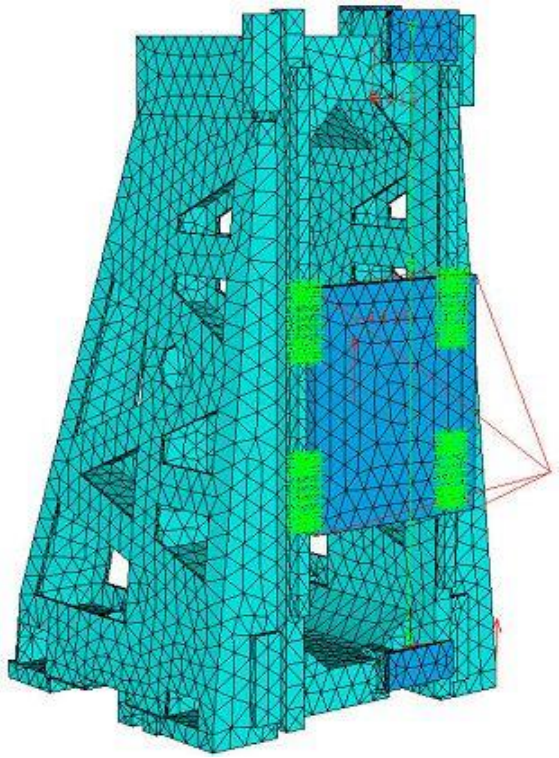

Archivierungsangaben

The contents of this presentation may not be copied and/or distributed without permission of the author! Please note references at the end of the presentation!

Property Analysis

Inspection of component properties:

- Tensile-, compression-, shearing-Tests
- Modal analysis
- Measurements of the components in installed and uninstalled state

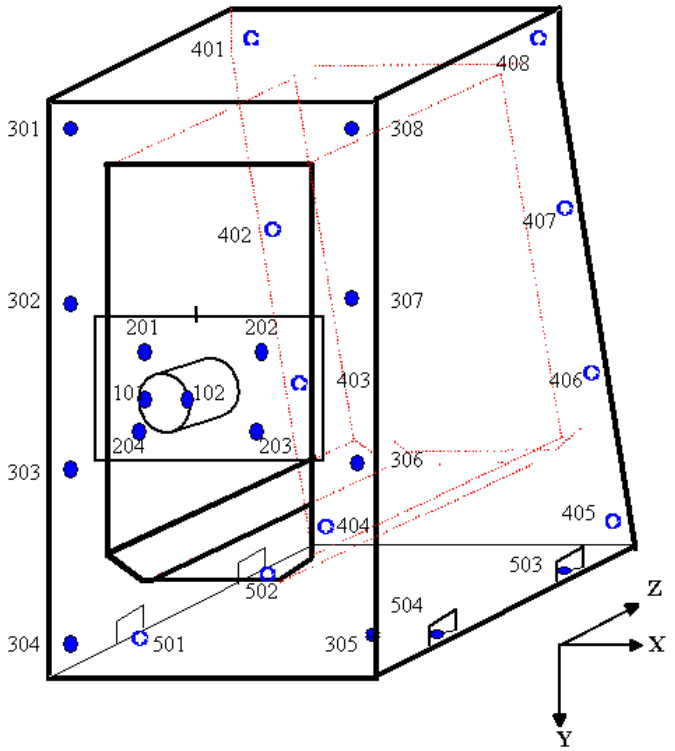

Archivierungsangaben

活動三

陶瓷基複合材料在高溫和效能要求環境下之用途研討會

由國立台灣大學材料科學與工程學系暨研究所特聘教授段維新教授主講

課程設計
Ceramic matrix composites for high temperature performance and applications

段維新

Jan. 30, 2018

for Hong Kong Productivity Council

From design, processing to the applications of ceramic matrix composites

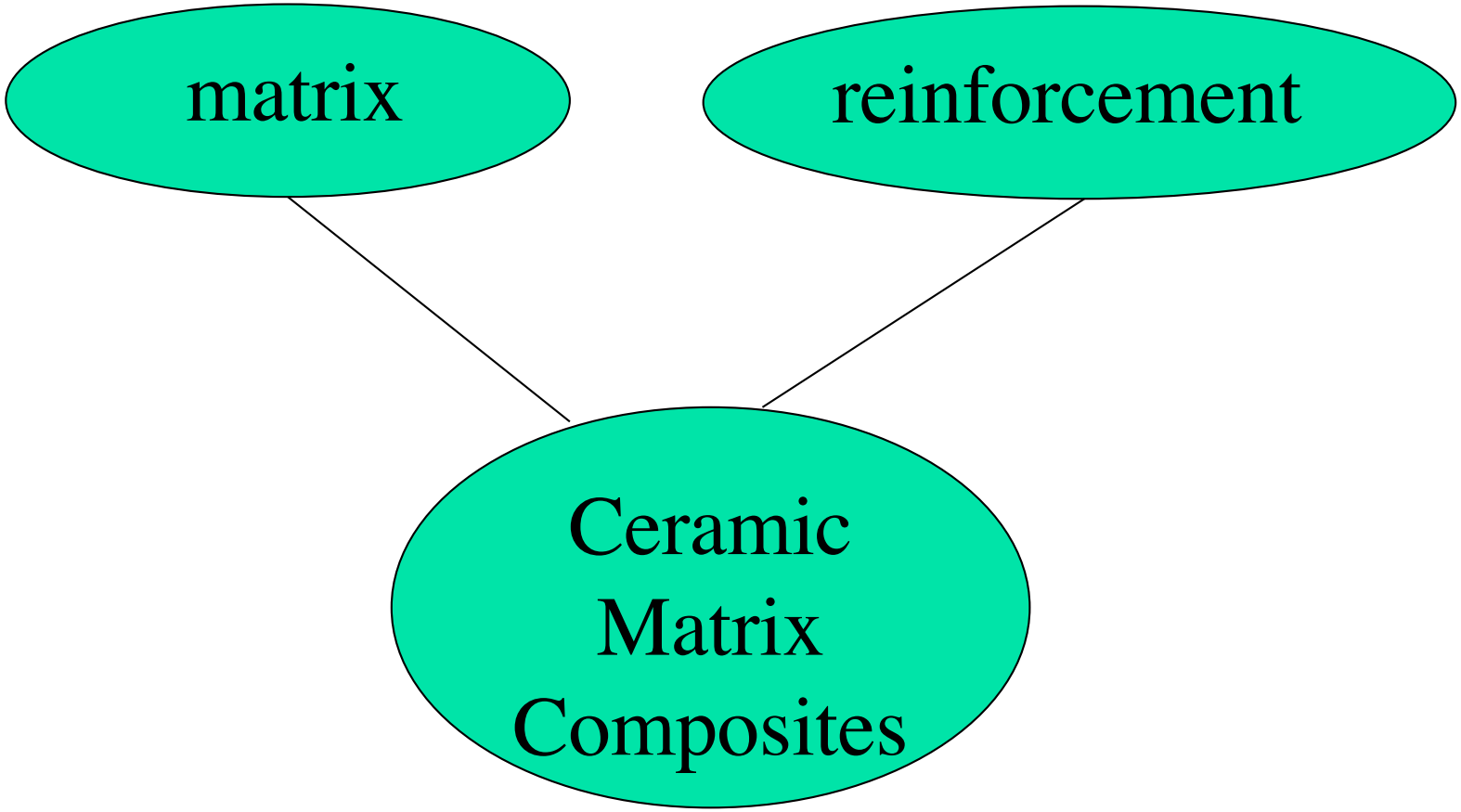

課程設計

- Unit 1, An overview
- Unit 2, Matrix & Reinforcement
- Unit 3, Design of CMC
- Unit 4, Processing
  - 4-a, Powder processing
  - 4-b, Novel processing
  - 4-c, Interface
- Unit 5, Properties
- Unit 6, Challenges & Future

課程設計

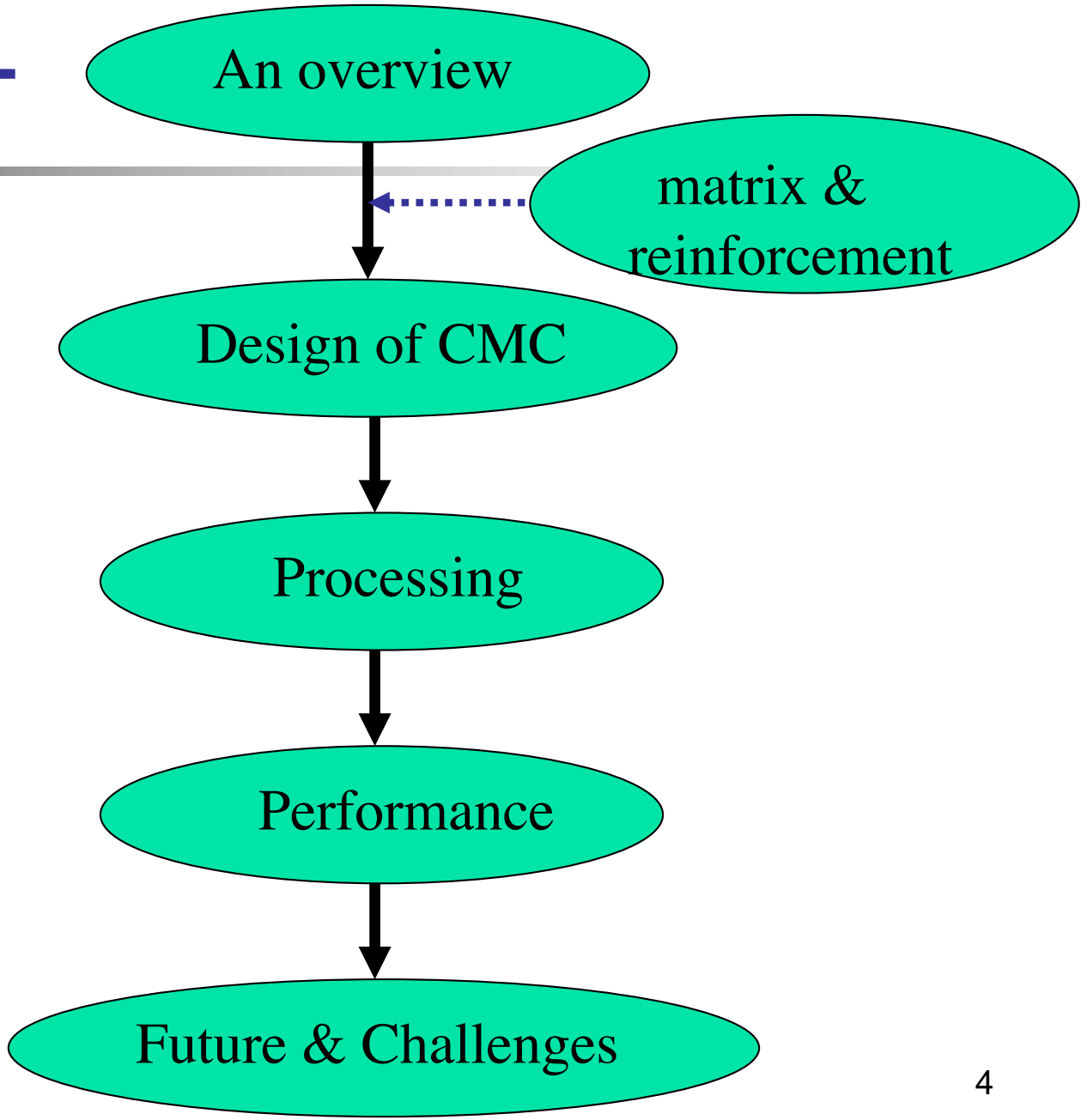
An overview
matrix & reinforcement
Design of CMC
Processing
Performance
Future & Challenges

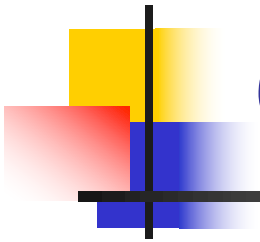

Objectives

- Basis for CMC
- Design of CMC
- Opportunities of CMC

References

- K. K. Chawla, Ceramic Matrix Composites, Chapman & Hall, London 1993

Unit One

Overview on Ceramic-Matrix Composites (CMC)

Definition of composites

For most ceramic-matrix composites (CMC), the ceramic is a continuous phase.

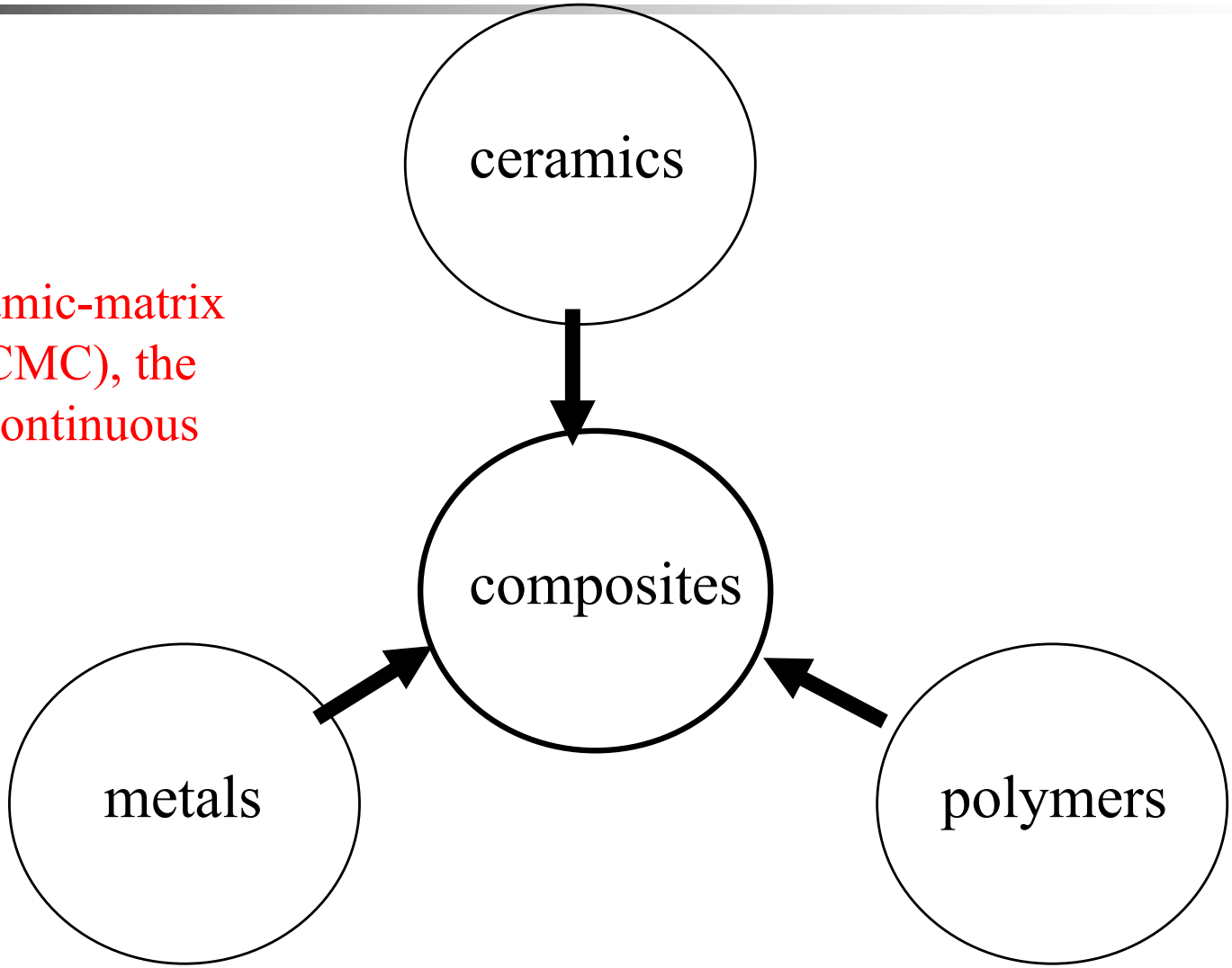

Scope

- Matrix
  - Ceramics
    - Ex.: Al_2O_3, ZrO_2, SiC, Si_3N_4, glass, etc.
- Reinforcements
  - Ceramic inclusions
    - Particulate, ex. SiC_p
    - Fiber (short or continuous), ex. SiC_f
    - Whisker, ex. SiC_w
    - Platelet, ex. $SiC_{platelet}$
  - Metallic inclusions
    - Particulate
    - Fiber
  - Polymeric inclusions, ex. Sea shell

Overview

- Problem & challenges of ceramics
- Engineering solution
- Academic background

Problems & Challenges

- What do we want from ceramics?
  - Reliability at room temperature
  - Reliability at high temperature
  - Low cost at any temperature

- Answers
  - Monolithic ceramics?
  - Ceramic matrix composites?

Monolithic ceramics

	Strength / MPs	Toughness / $MPam^{0.5}$	pro	con
Alumina	300~400	~3	Relative inexpensive	
Zirconia	600~1200	6~12		Degrade above 1000°C
Silicon nitride	1000 (max)	10 (max)		Oxidized at elevated temp
Silicon carbide	~500	~3	500 MPa @ 1400°C	Difficult to be sintered
glass	~100	~0.5	Low cost	Soften at elevated temp

Problems & Challenges

- Answers
  - Monolithic ceramics?
    - Not good enough!
  - Ceramic matrix composites

- What can we learn from Nature?
- What can we learn from the past?

What can we learn from Nature ?

- Most bio-materials are composites
  - Examples:
    - See shell

Sea shell

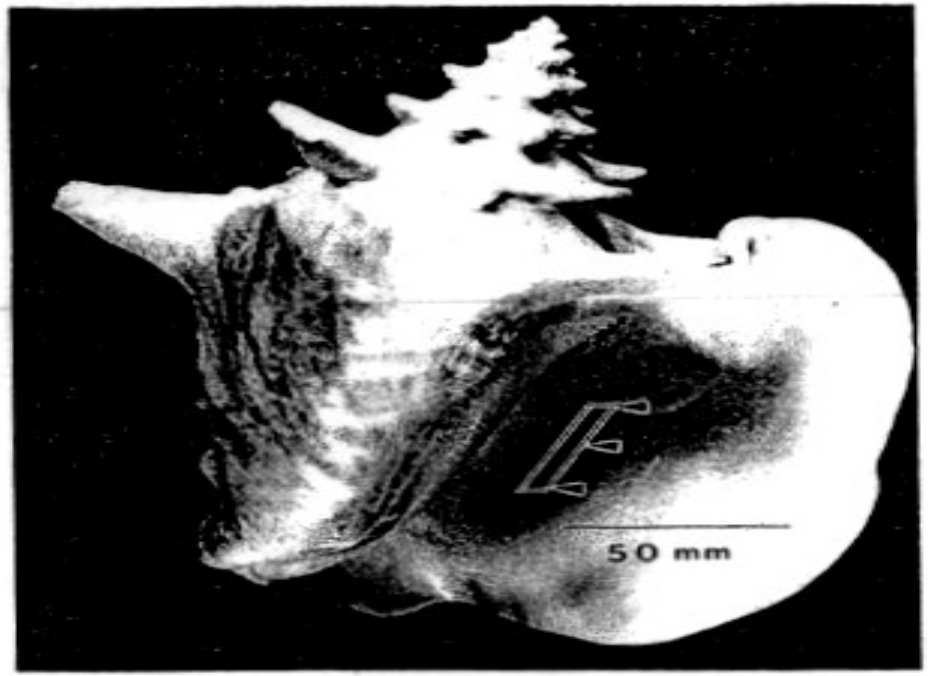

Fig. 1. Shell of *Strombus gigas*. The arrowed feature indicates the orientation and size of a typical specimen.

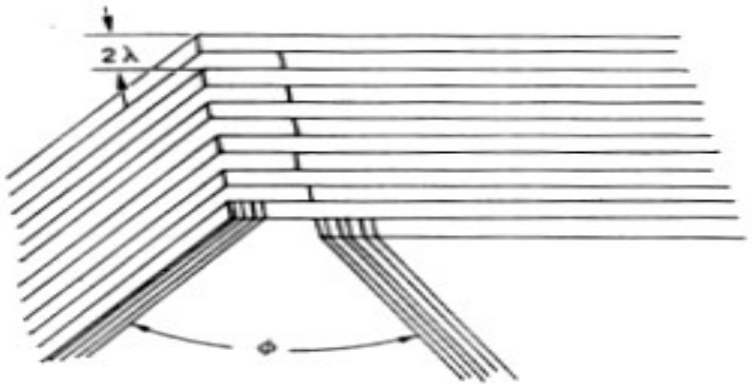

Fig. 2. Schematic line drawing of the crossed lamellar structure. First-order lamellae appear as plates. Second-order lamellae appear as laths within first-order lamellae, with the stacking sequence shown.

Ref: JACS, 1990

Strength of sea shell

Fig. 3. Low-magnification SEM photograph of the fracture surface of a four-point bend specimen. The surface loaded in tension is marked "a"

Flexural strength=100MPa

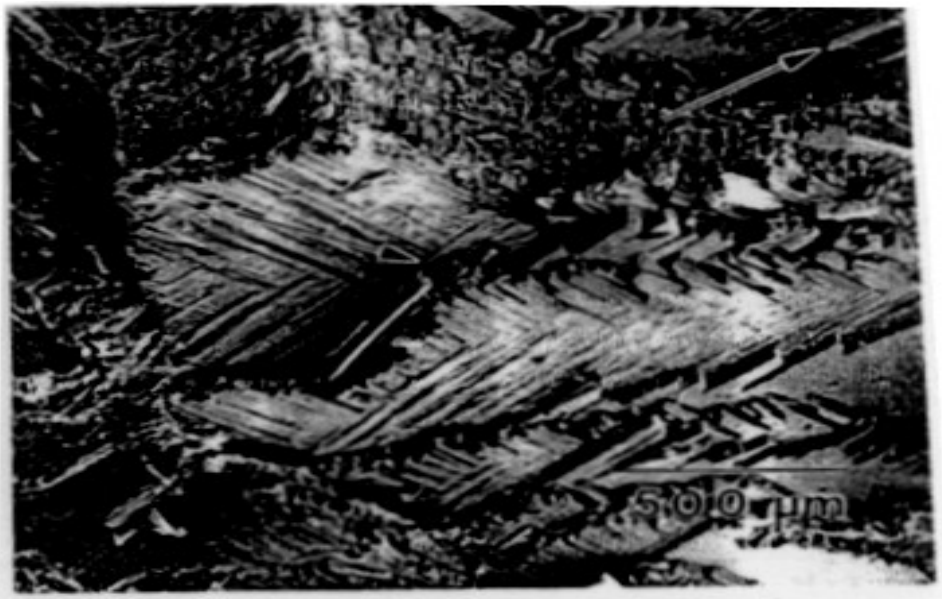

Fig. 4. SEM photograph of the same fracture surface as in Fi
Numerous examples of lath "pullout" are evident.

CMC Lab, NTU

Microstructure of sea shell

Ceramics in sea-shell:

$CaCO_3$ grains,

200nm x 100nm, amount~99%

polymer: protein

Ref: JACS, 80(7) cover (1997)

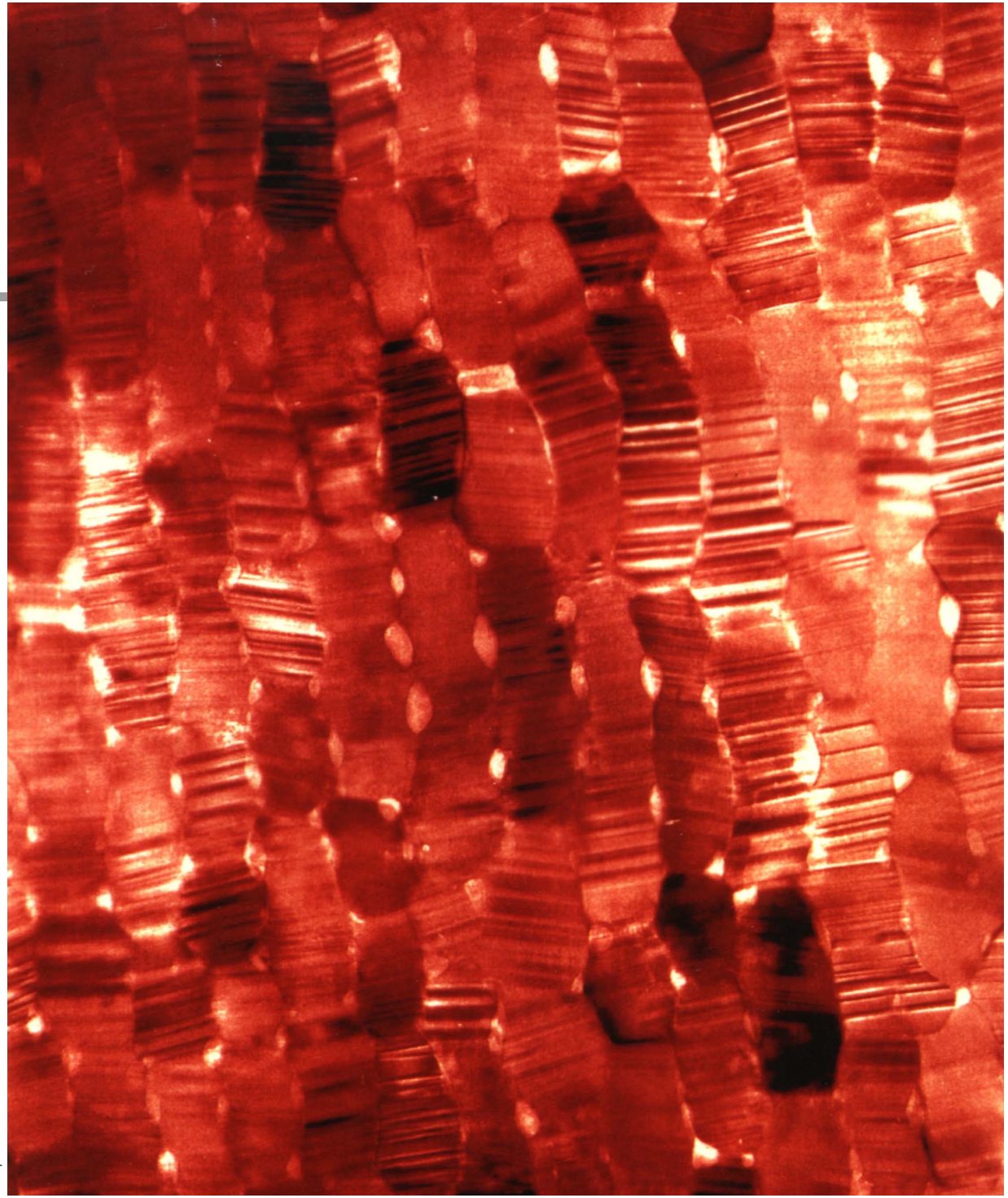

100 nm

CMC Lab, NTU

Learning from the Nature

Example: B_4C/Al

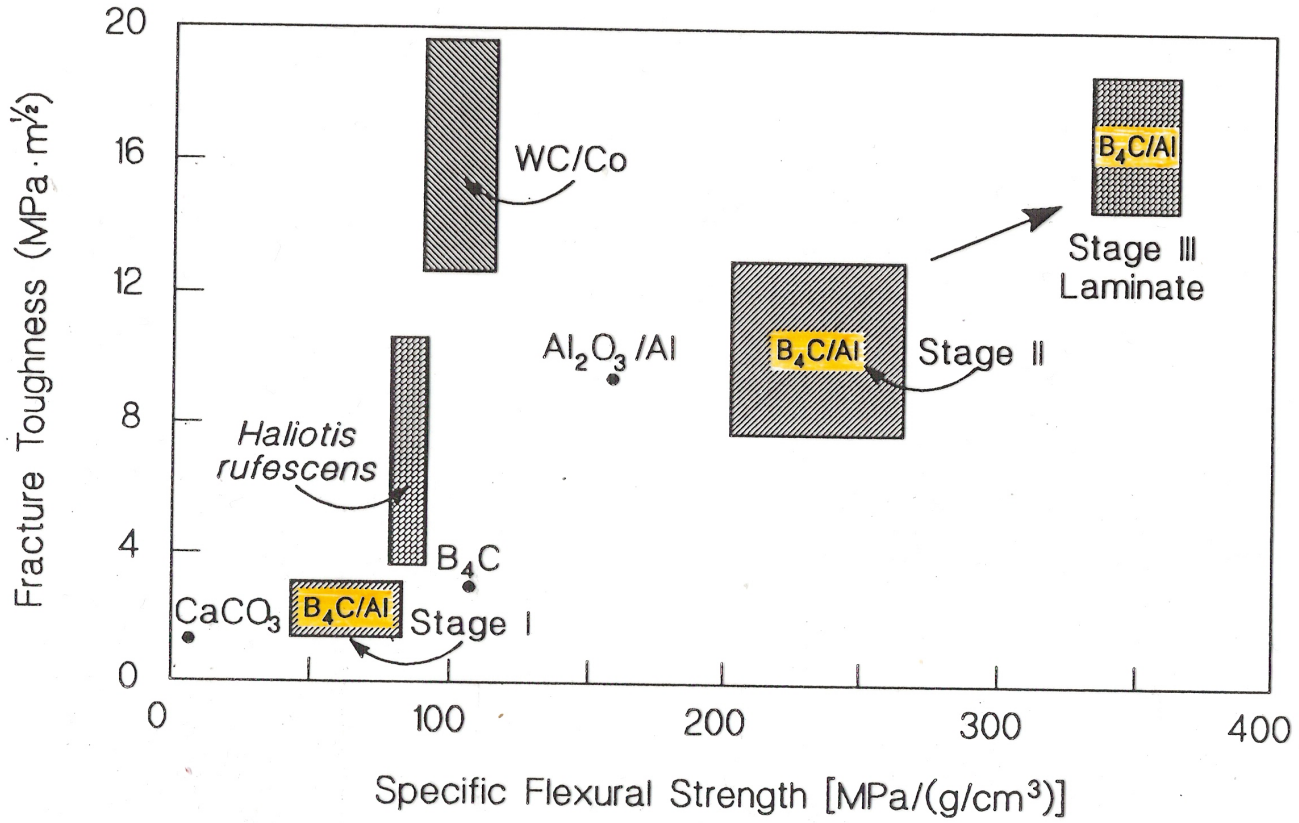

Ref: Aksay, ~1992

Figure 2. Mechanical properties of the nacre of red abalone (*Haliotis rufescens*) compared to synthetically produced ceramics and ceramic-based composites discussed in this paper. In *Stage I*, the processing of boron carbide/aluminum was done by hot pressing mixed powders. In *Stage II*, an infiltration technique was used to process an isotropic and interpenetrating phase composite. In *Stage III*, the lamination techniques described in this paper were used.

ref: Aksay, 1993

Features of bio-materials

- Delicate and complex microstructure
- Raw materials: very cheap
- Manufacture at low temperature: mostly at room temperature

Engineering solution

Microstructure complexity

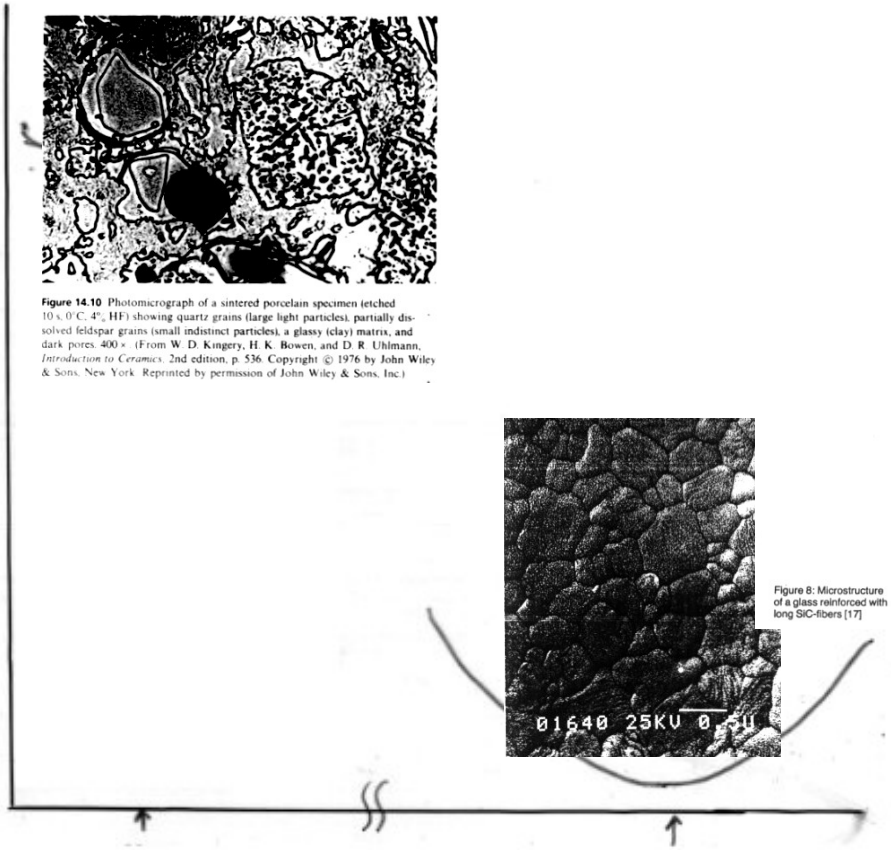

Composite

↓

Monolithic

↓

composite

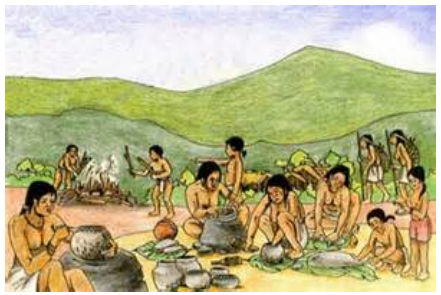

Stone age

New stone age

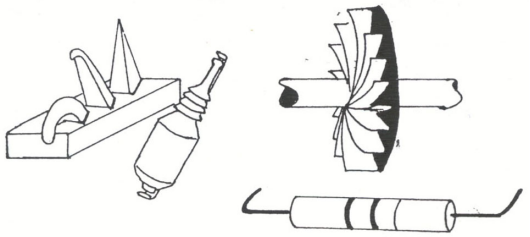

Example on CMC

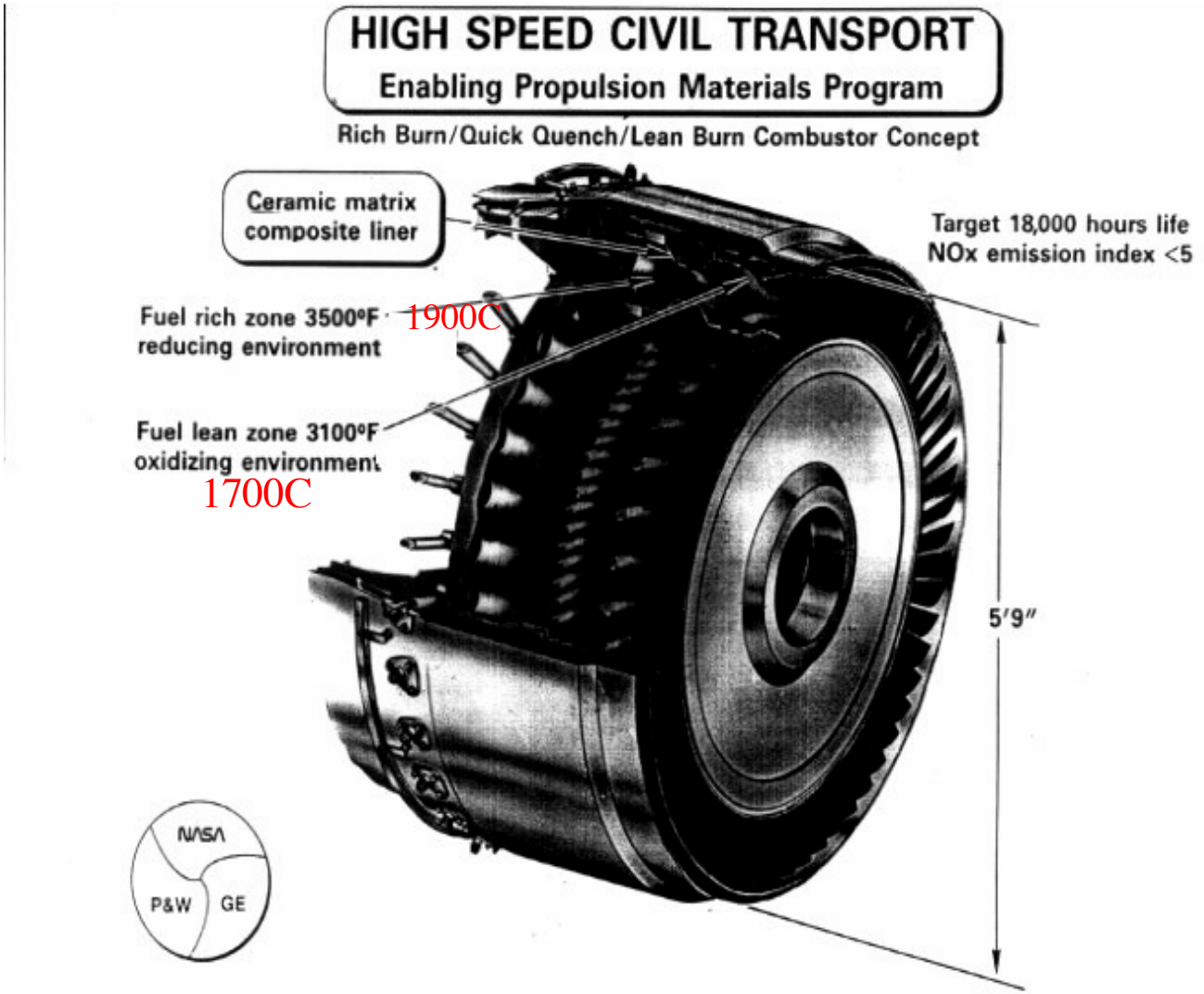

白皮書 @ 1992 for CMC

29 高性能陶瓷類複合材料

1. 技術製品之概要

陶瓷類複合材料將被使用於如噴射引擎零組件那樣的機械零組件，以代替耐熱性金屬。在氧化物、碳化物與氮化物系陶瓷中，混入陶瓷纖維予以強化，大幅提高其破壞韌性。此外，關於低價位的方面，由碳纖維等與不燃基質（玻璃、水泥等）所合成之不燃性、高彈性且高強度之輕量材料，將被使用於超高層建築結構材、大深度地下結構體、懸吊結構材等方面。

爲了使這種複合材料能夠與傳統的金屬材料一樣低廉地供應且輕便地使用，預測需要一段長期間的研究開發。

2. 邁向實用化之長期預測

若將實用化階段作爲100時，現在的研究開發之相對階段即爲10，而實用化之時期則被認爲是在2050年前後。

如果拿現在的研究開發作國際比較時，爲了渦輪機之節省能源而搶先開始研究之歐美，估計領先於日本。

One of the Objectives:
to improve the toughness of ceramics

Impossible to break!!!

or

Mission impossible!

CMC Lab, NTU

Why ceramic composites?

- Griffith law (for brittle solid)

$$\sigma_f = \frac{K_{IC}}{Y\sqrt{C}}$$

- The implications of Griffith law
  - C increase, σ_f decrease
    - Remove inhomogeneity
  - K_{IC} increase, σ_f increase
    - Adding inhomogeneity,
    - Correction of inhomogeneity

Why toughness so important?

- Examples :
  - K_{IC} for carbon steel ~ 100 $MPam^{0.5}$
  - K_{IC} for alumina ~ 3 $MPam^{0.5}$
  - When certain strength is required,
    - If the critical flaw size for steel is 5 mm, the critical flaw size allowed for alumina is only 5 μm.
    - But, the detection sensitivity of N.D.T. > critical flaw size of ceramics
- Critical issue for ceramics
  - To enhance the toughness of ceramics

What are the ceramics we want ?

- 1. Mechanical reliability at low temperature
  - Less strength scatter (process control)
  - Flaw tolerant

- 2. Microstructural stability at high temperature
  - Grain growth resistance (microstructural design)
  - Creep resistance

Reference: M. P. Harmer, H. M. Chan, G. A. Miller, “Unique opportunity for microstructural engineering with complex and laminar ceramic composites”, J. Am. Ceram. Soc., 75(7) 1715-28(1992)

- 3. Low cost at any temperature

Challenge:
strength scatter of ceramics

Example: Alumina

no.	fracture strength (MPa)	Estimated probability of failure, P=(n/N+1)
1	287	1/21
2	326	2/21
3	374	3/21
4	394	4/21
5	396	5/21
6	399	6/21
7	405	7/21
8	407	8/21
9	407	9/21
10	409	10/21
11	419	11/21
12	425	12/21
13	427	13/21
14	429	14/21
15	431	15/21
16	433	16/21
17	435	17/21
18	436	18/21
19	450	19/21
20	495	20/21

Challenge:
strength scatter of ceramics

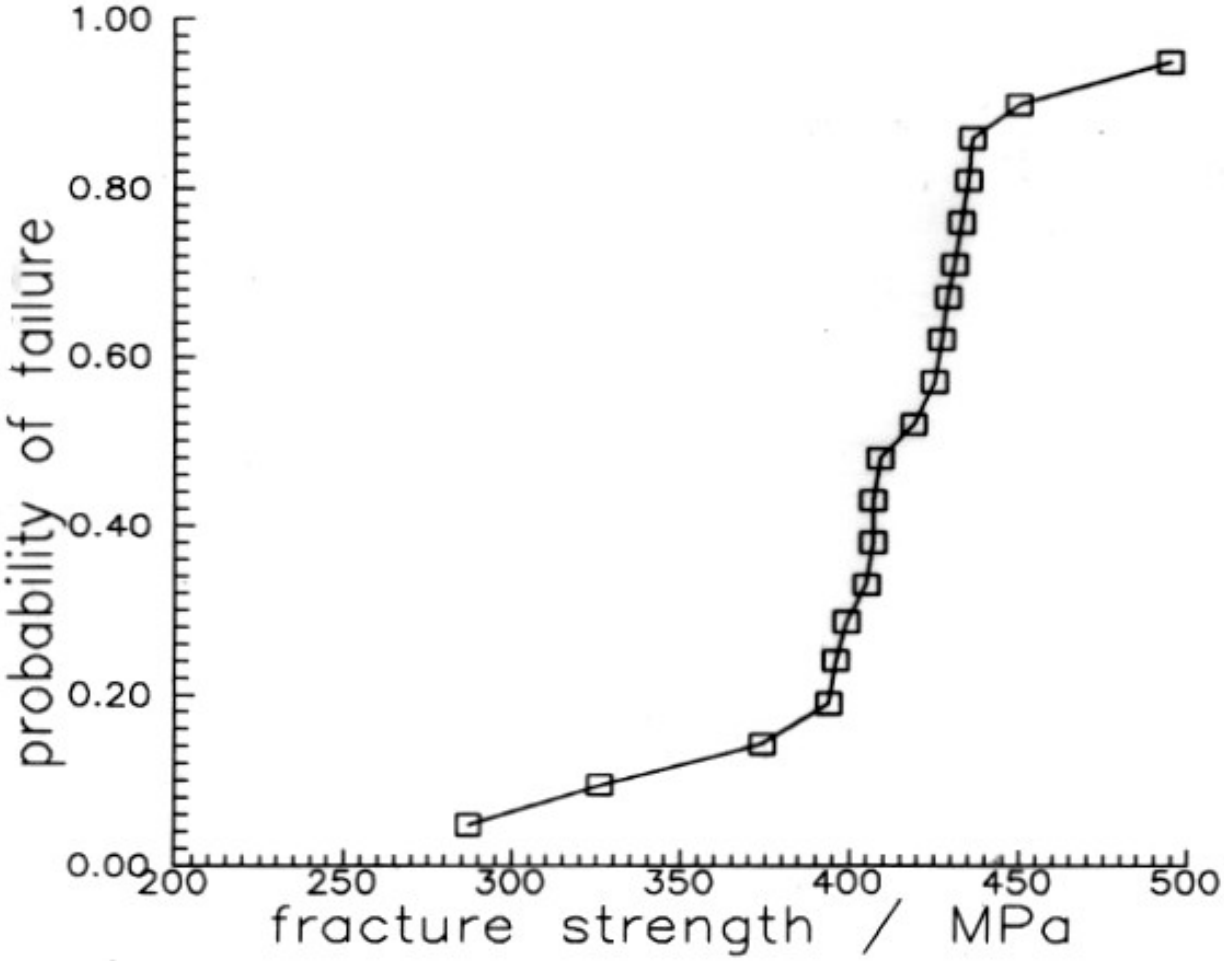

CMC Lab, NTU

Challenge:
strength scatter of ceramics

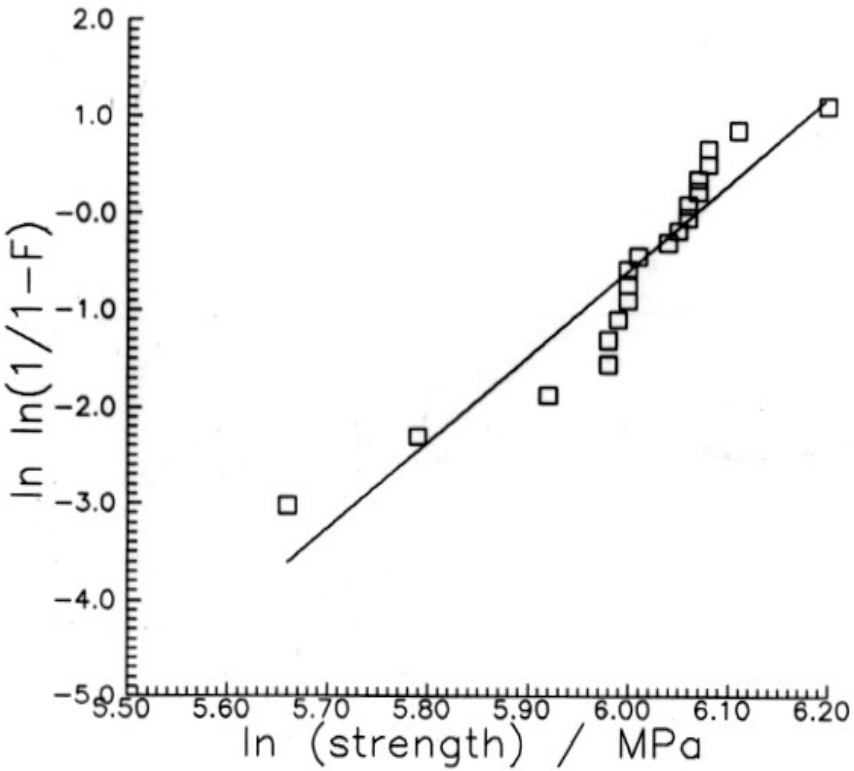

slope= Weibull modulus

m= 8.9

$\ln\ln(1/1-F) = 8.9(\ln\sigma_f)-53.8$

When F=0.1 σ_f=327MPa

F=0.01 σ_f=251MPa

F=0.001 σ_f=194MPa

Trend for the development of advanced ceramics

reliability

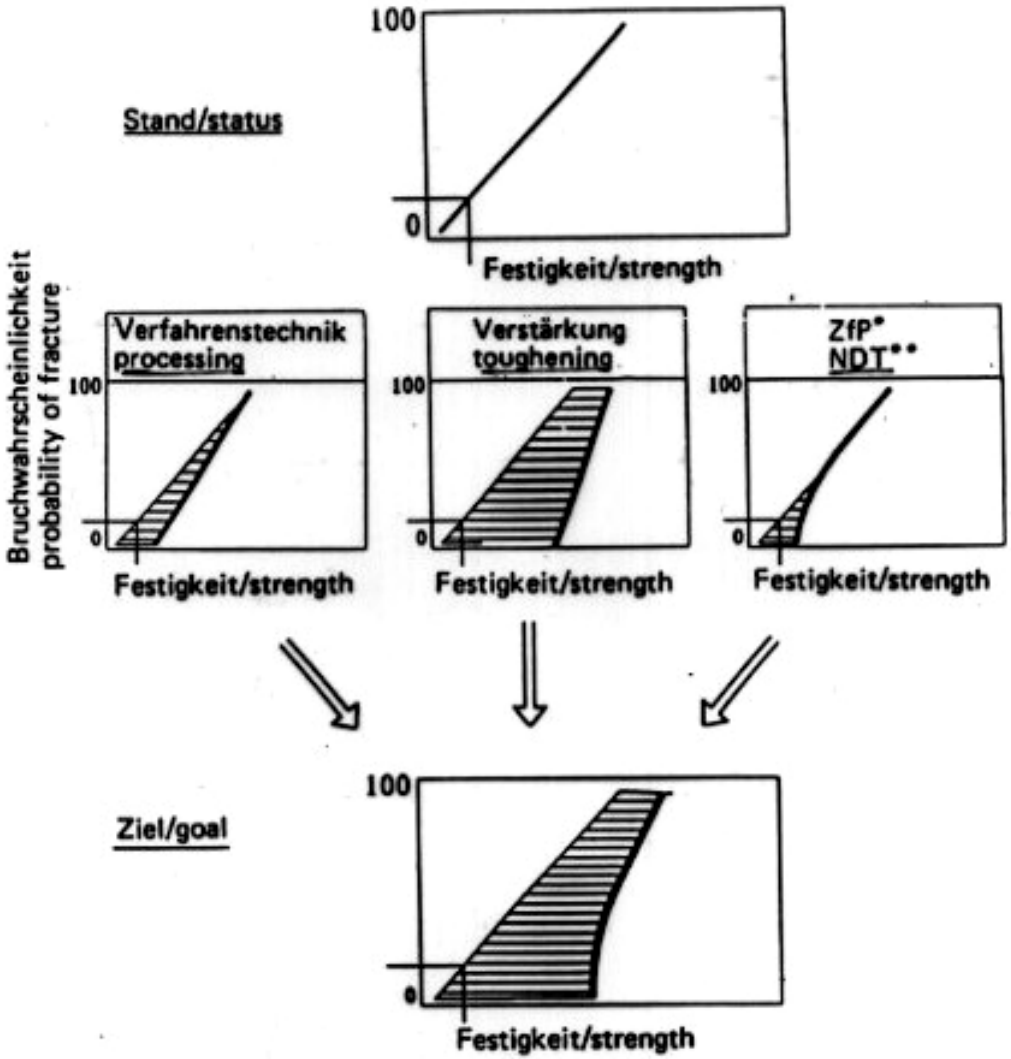

Mechanical reliability at low temperature- flaw tolerance

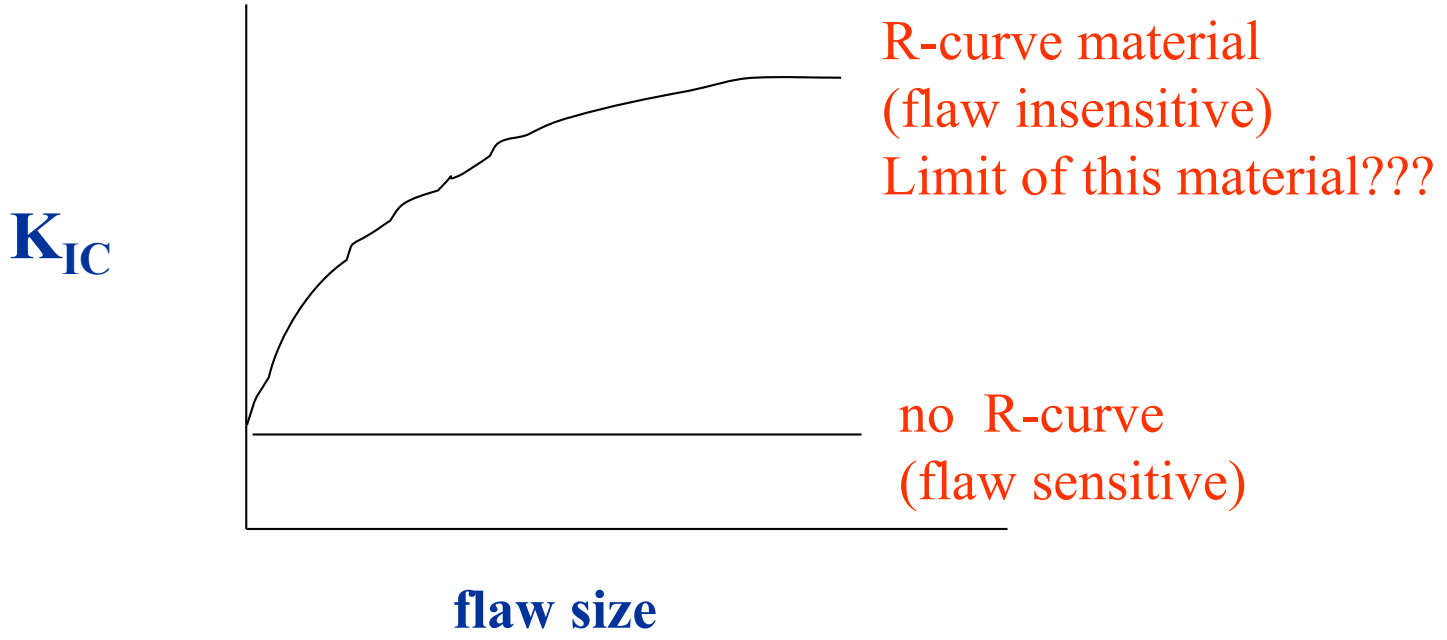

CMC Lab, NTU

Example: Al_2O_3

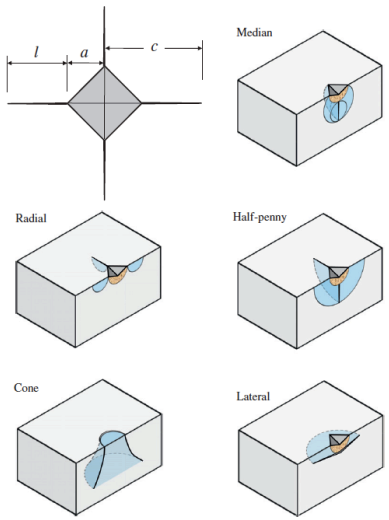

Fig. 1. Representative crack morphologies under indentation loading (after Ref. [2]). This study focuses on the evolution from median or radial cracks to ultimately half-penny cracks. These three crack systems can be described by the crack size c and the contact size a from the top surface.

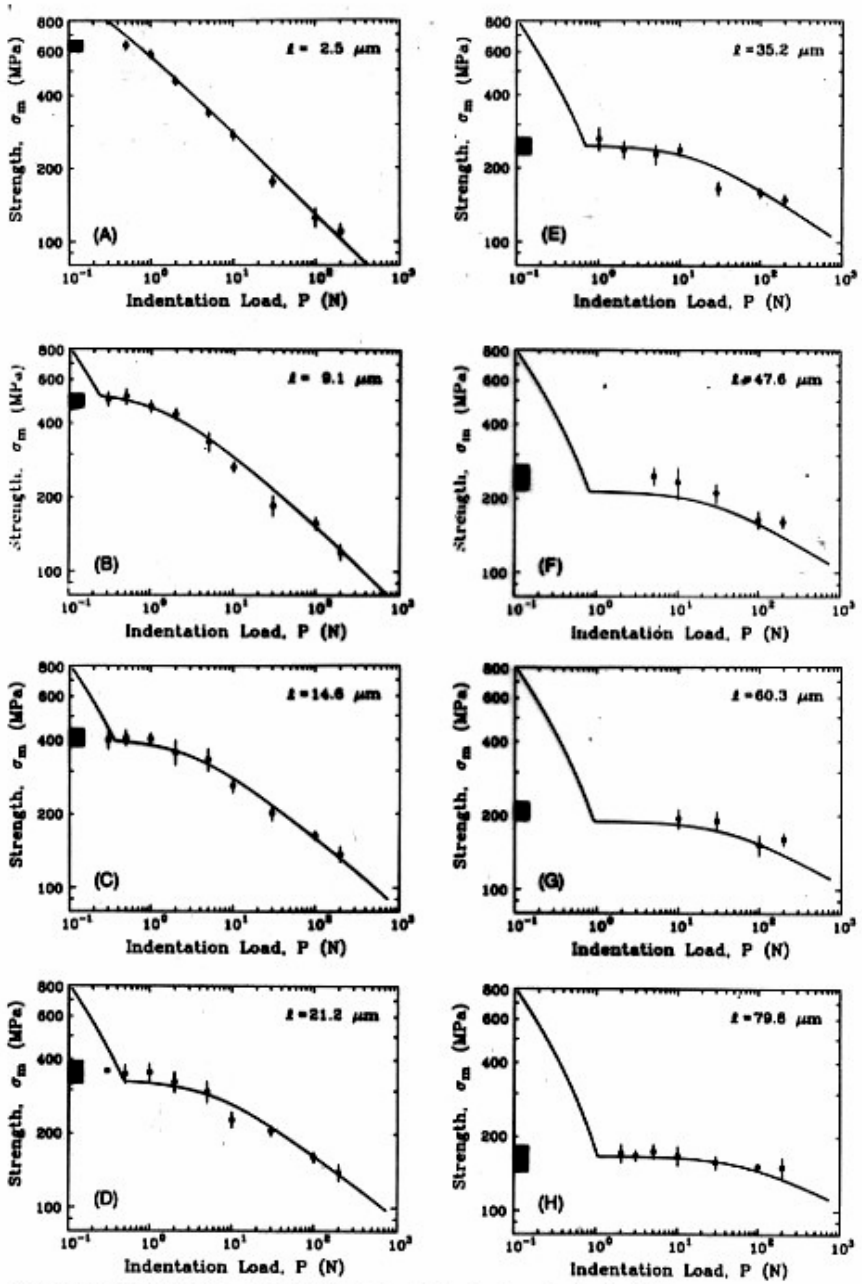

Fig. 4. Plots of inert strength σ_m, versus indentation load P, for aluminas of grain size (A) ℓ = 2.5 μm, (B) ℓ = 9.1 μm, (C) ℓ = 14.6 μm, (D) ℓ = 21.2 μm, (E) ℓ = 35.2 μm, (F) ℓ = 47.6 μm, (G) ℓ = 60.3 μm, and (H) ℓ = 79.8 μm. Curves are best fit from bridging model in Sections IV and V.

ref: P. Chantikul, S. J. Bennison, B.R. Lawn, 'Role of Grain Size in the Strength and R-curve Properties of Al_2O_3', J.A.C.S. 73(8), 2419, 1990

Mechanical reliability at low temperature- flaw tolerance

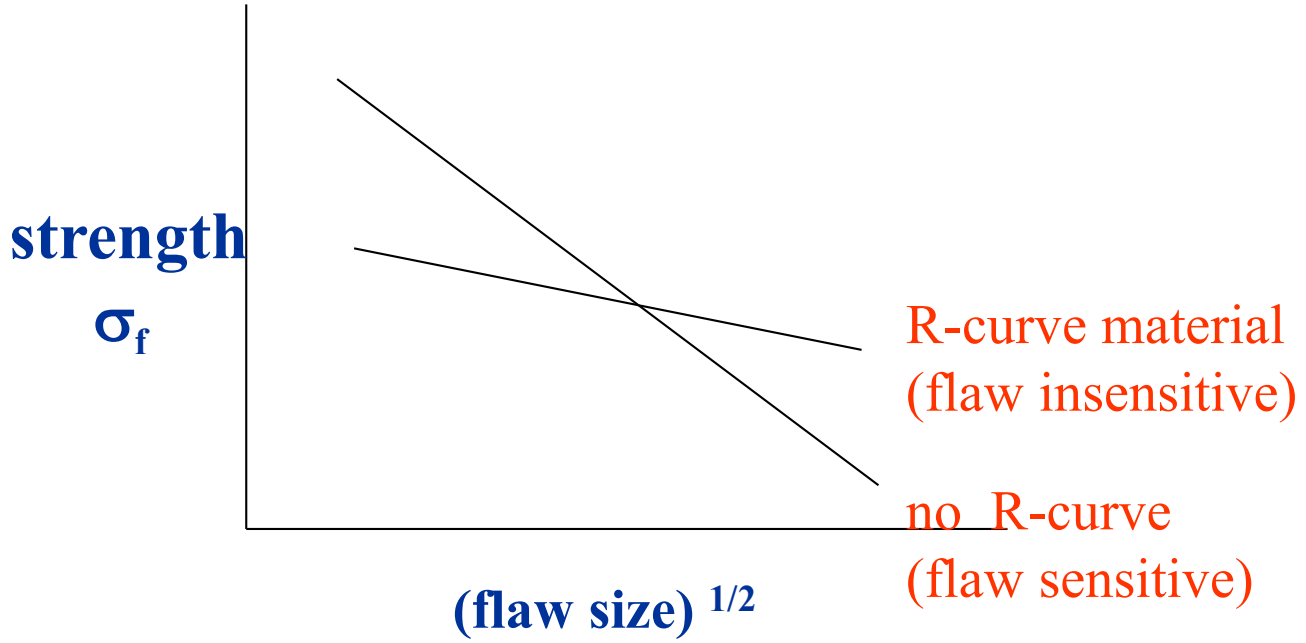

What are the ceramics we want ?

- 1. Mechanical reliability at low temperature
  - Less strength scatter (process control)
  - Flaw tolerant

- 2. Microstructural stability at high temperature
  - Grain growth resistance (microstructural design)
  - Creep resistance

Reference: M. P. Harmer, H. M. Chan, G. A. Miller, “Unique opportunity for microstructural engineering with complex and laminar ceramic composites”, J. Am. Ceram. Soc., 75(7) 1715-28(1992)

- 3. Low cost at any temperature

High-temperature stability

grain growth resistance - duplex microstructure

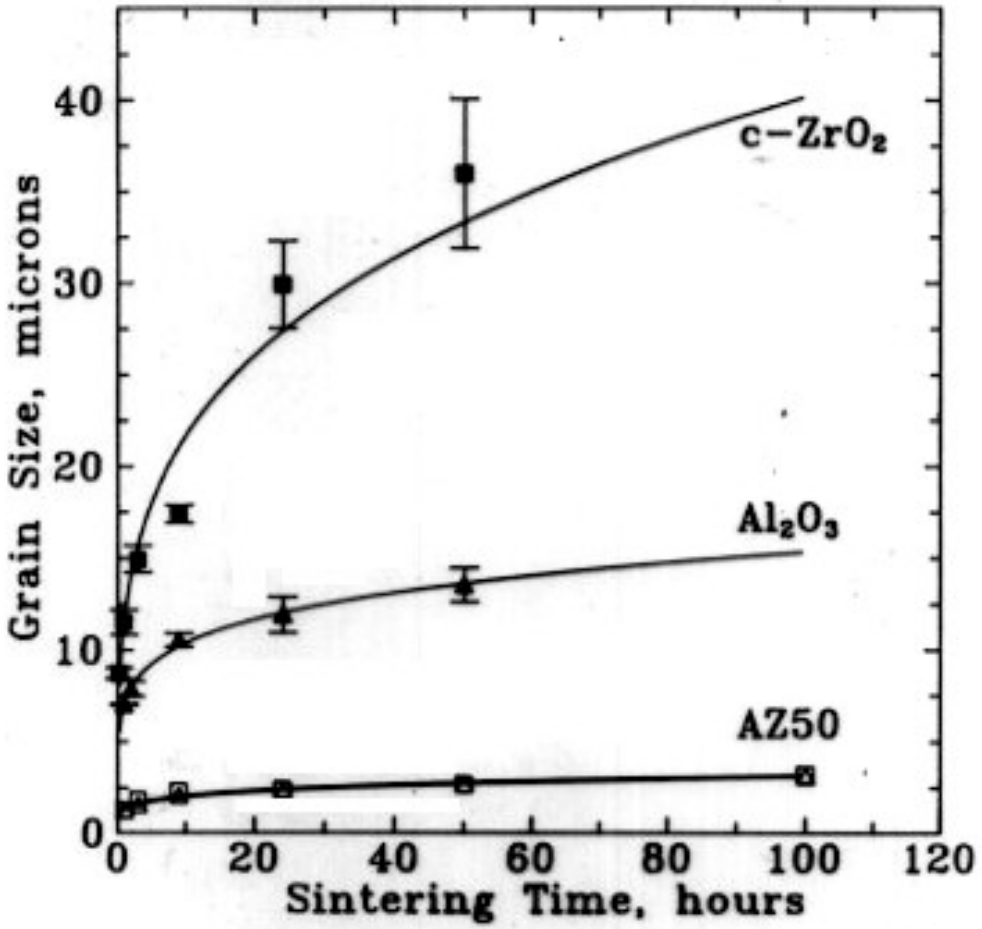

Fig. 1. Dependence of average grain size on sintering time at 1650°C for (■) single-phase c-ZrO_2, (▲) single-phase Al_2O_3, and AZ50 (△) Al_2O_3 and (□) c-ZrO_2.

Ref: French et al, JACS, 1990

Microstructure stability

c-ZrO2

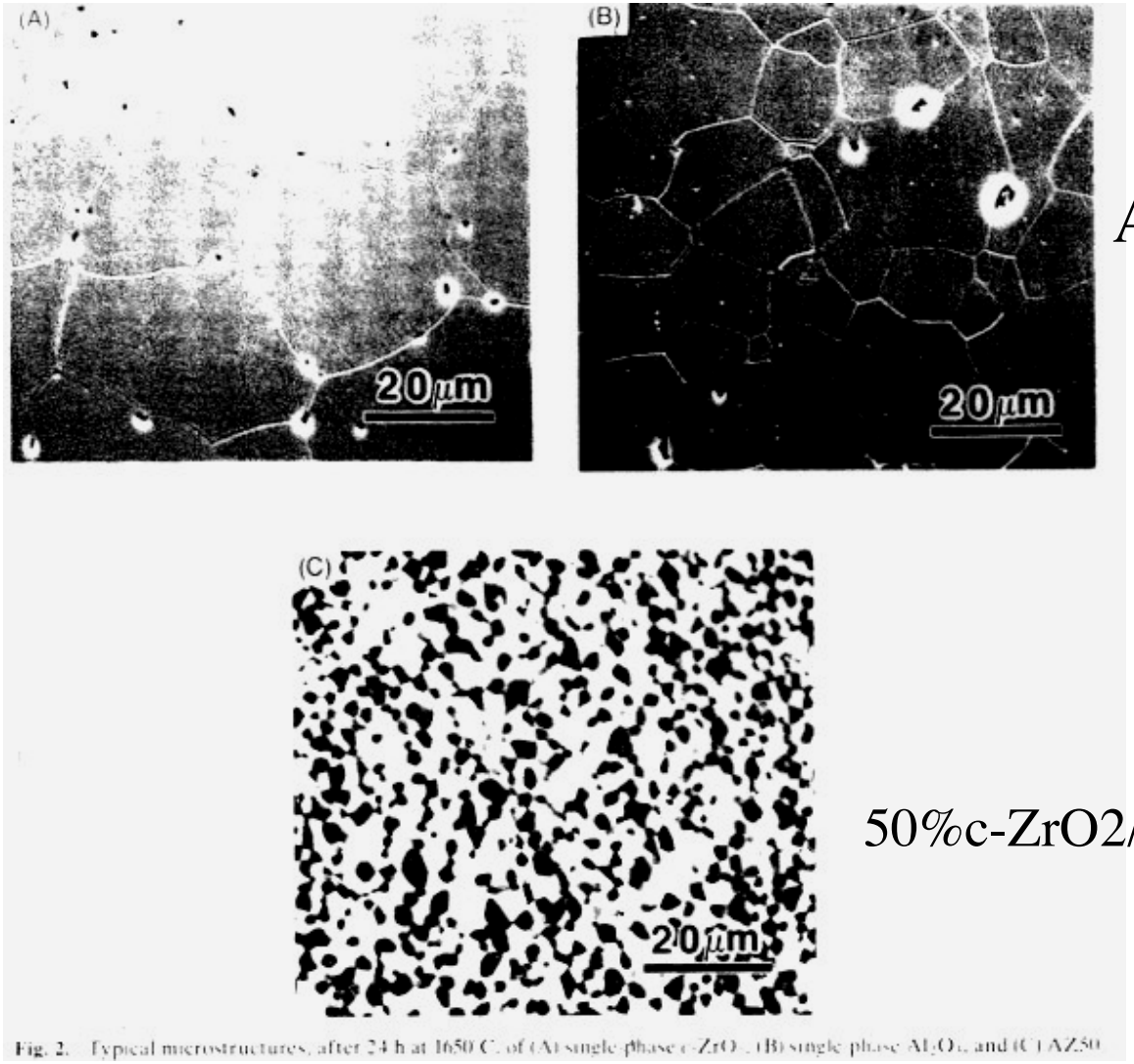

Al2O3

50%c-ZrO2/50%Al2O3

Desired ceramic

- Mechanical reliability at low temperature
- High temperature stability
  - $\Rightarrow$ Composites

CMC Lab, NTU

Overview

- Monolithic ceramics
  - Al_2O_3, ZrO_2, SiC, Si_3N_4, glass, etc.
  - Not good enough
- Most bio-materials are composites
- Engineering Ceramic-matrix composites
  - Al_2O_3/ZrO_2, Al_2O_3/SiC_w, SiC/SiC_f etc.
  - Promising
  - But, which one?

Unit 2, Matrix and Reinforcements for CMC

Matrix : ceramics

Reinforcements : ceramic fibres

: metallic fibres

: ceramic whiskers

: ceramic platelets

etc.

Ref: K. K. Chawla. ” Ceramic Matrix Composites,” Chapter 2,3,1993

Ceramic Matrices

Table 2.2 Physical and mechanical characteristics of some ceramic materials

	Density, ρ $(g\,cm^{-3})$	*Melting point* (°C)	*Young's modulus* E *(GPa)*	*Coefficient of thermal expansion,* α $(10^{-6}\,K^{-1})$	*Fracture toughness* K_{Ic} $(MPa\,m^{1/2})$
Al_2O_3	3.9	2050	380	7–8	1–3
SiC	3.2	–	420	4.5	2.2–3.4
Si_3N_4	3.1	–	310	3.1	2.5–3.5
MgO	3.6	2850	210	3.6	–
Mullite ($3Al_2O_3 \cdot 2SiO_2$)	3.2	1850	140	5.3	3.0–4.0
Borosilicate glass	2.3	–	60–70	3.5	0.5–2
Soda-lime	2.5	–	60–70	8.9	0.5–1

Ceramic Matrices

Table 2.4 Mechanical properties of glass-ceramics compared with some other materials

Material	*Flexural strength* (MPa)	*Young's modulus* (GPa)
Glass	55–70	70
Glass-ceramics	70–350	80–140
Al_2O_3	200–350	280–380
Steel	300–1400	210

Ceramic Reinforcements

Table 3.1 Some important ceramic reinforcements

Particle	*SiC, TiC, Al_2O_3*
Discontinuous Fibers	
(a) Whiskers	SiC, TiB_2, Al_2O_3
(b) Short fibers	Glass, Al_2O_3, SiC, ($Al_2O_3 + SiO_2$), vapor-grown carbon fibers
Continuous fibers	
Oxide	Al_2O_3, ($Al_2O_3 + SiO_2$), ZrO_2, silica-based glasses
Nonoxide	B, C, SiC, Si_3N_4, BN

Carbon nanotube (CNT)

Platelet

oxide Al_2O_3

nonoxide SiC, graphene

Inclusions (reinforcements)

Single Crystal
Silicon Carbide Whiskers

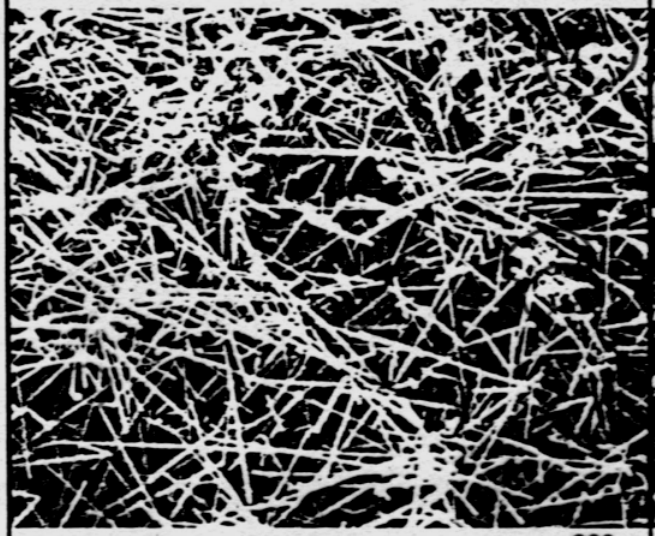

200x

- β Phase, Cubic Structure
- 0.5 to 3 μ Diameter
- 50 to 200 μ Length
- Low Particulate
- High Chemical Purity
- Easily Deagglomerated
- Available In Bulk Quantities

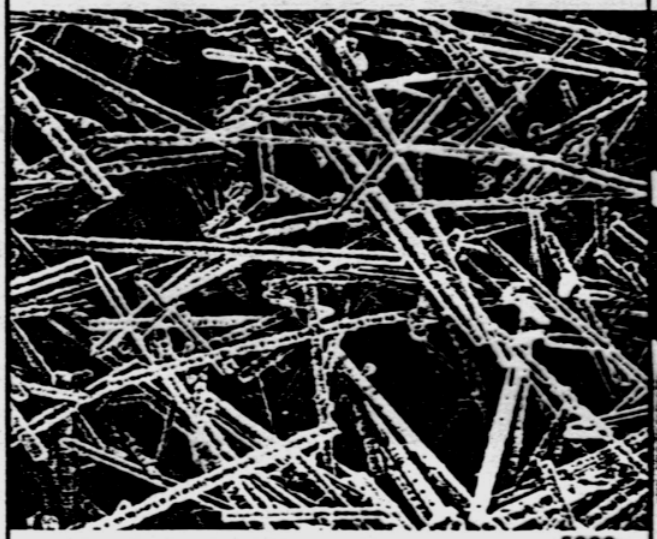

5000x

Single Crystal
Silicon Carbide Platelets

100x

- α Phase, Hexagonal Structure
- 10 to 10,000 μ Diameter
- 1 to 10 μ Thickness
- Free Flowing — No Agglomeration
- High Chemical Purity
- Available In Bulk Quantities

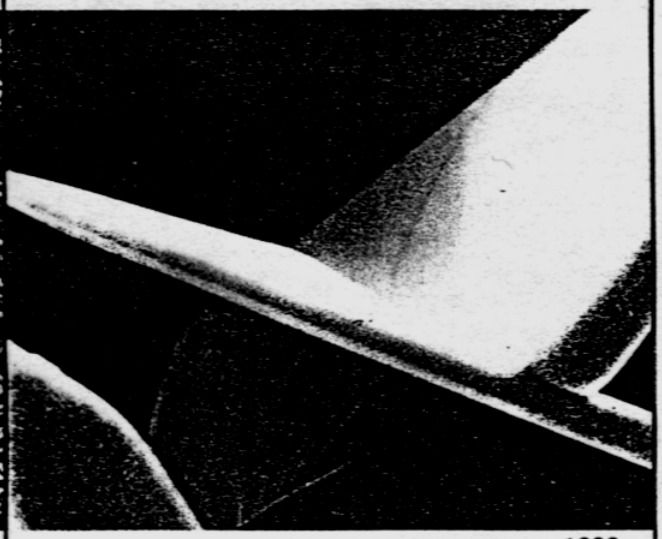

1000x

Particulate inclusions have to be removed first.

Toxicity of SiC whiskers

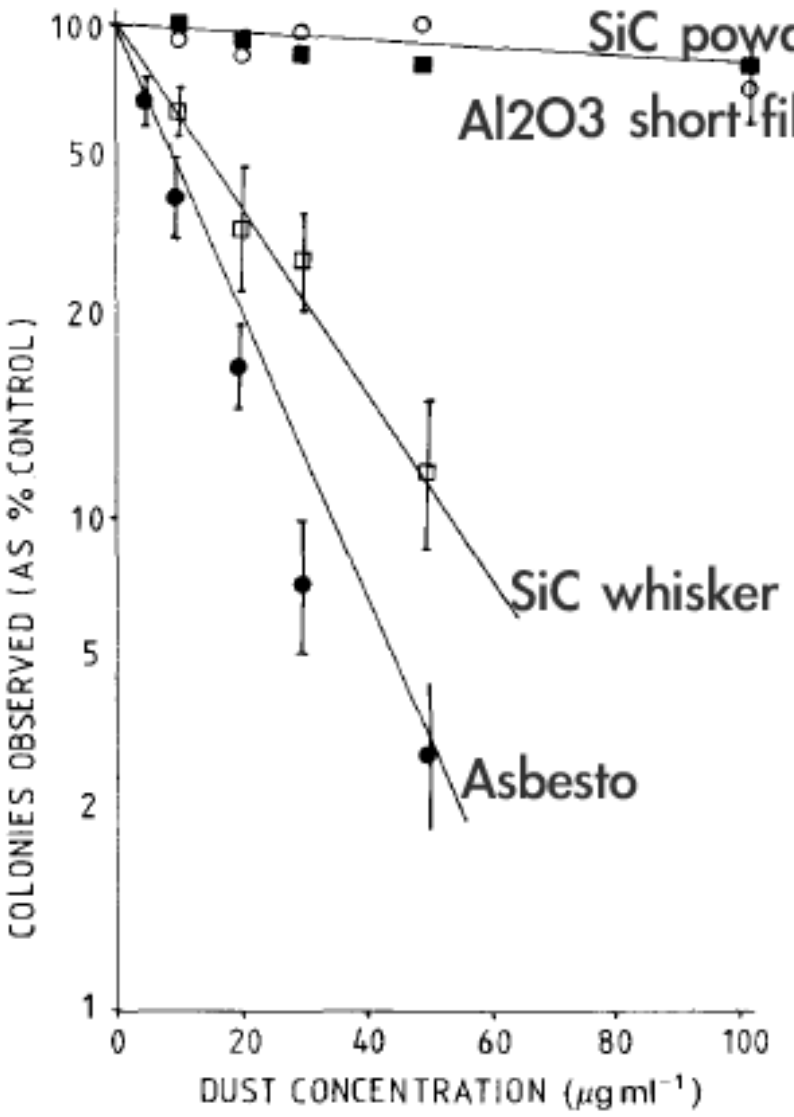

Figure 3 Cytotoxicity of SiC whiskers expressed as the percentage survival of cells in response to dust exposure. (■) Saffil, (●) UICC crocidolite, (○) SiC powder, (□) SiC whiskers.

SiC powder: ~0.4 um,

Al2O3 fiber: ϕ~1-7 um,

SiCw: ϕ=0.05 um,

Blue asbestos may cause mesothelioma！ ！ ！

惡性腫瘤

Ref:J. D. Birchall et al, J. Mater. Sci. Letter,1988.

Reinforcements-fibres

Shape does matter !

The strongest forms of all classes of materials are those that are fibrous in nature. Fibre reinforcement provides dramatic increases in stiffness and strength of polymers, enhanced high temperature properties in metals and improved toughness in ceramics.

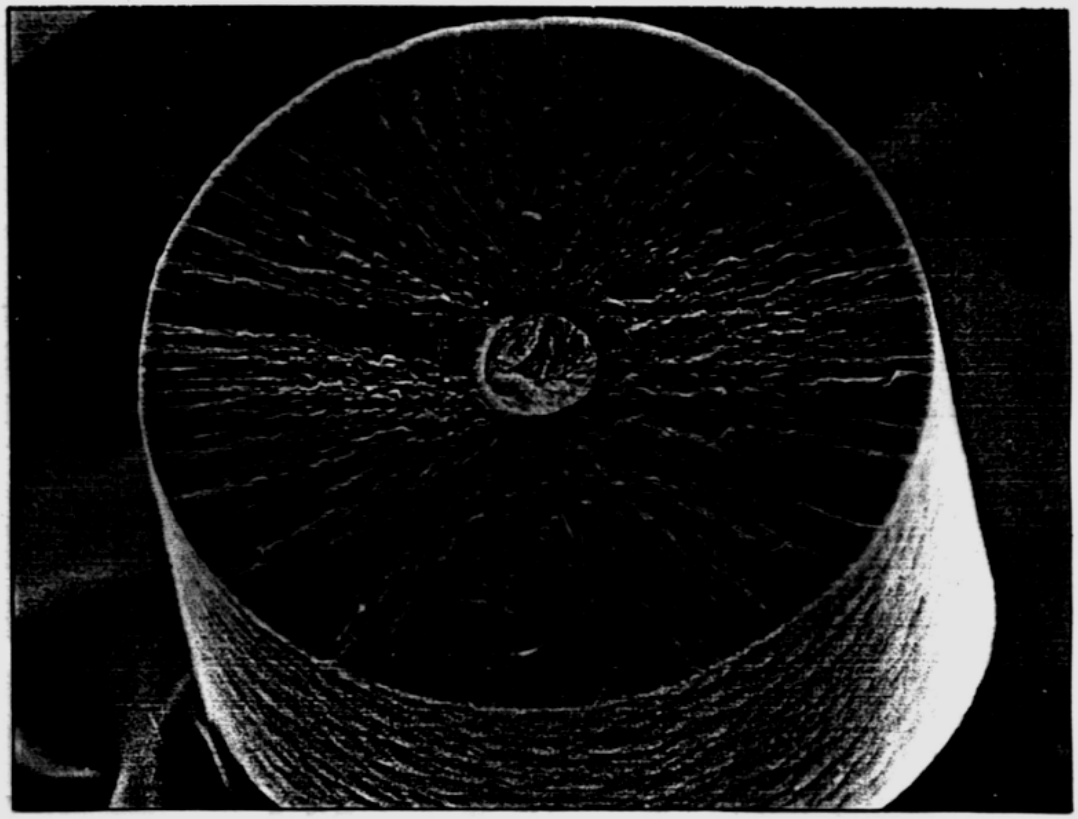

Figure 1 Scanning electron micrograph of a 100 μm diameter Sigma *silicon carbide fibre. This has been produced by chemical deposition of silicon carbide onto a heated tungsten wire. The 20 μm diameter wire can be clearly seen on the fracture surface, together with the radial substructure of the fibre. (Fibre supplied by Sigma, prior to acquisition by BP Composites; photomicrograph by D A Clarke) (×900)*

Ref:Mater. World , Jan,1993

Formation of fibre offers unique opportunity for structure alignment

Material: PE

K~0.1 W/mK

K=104 W/mK

LETTERS NATURE NANOTECHNOLOGY DOI: 10.1038/NNANO.2010.27

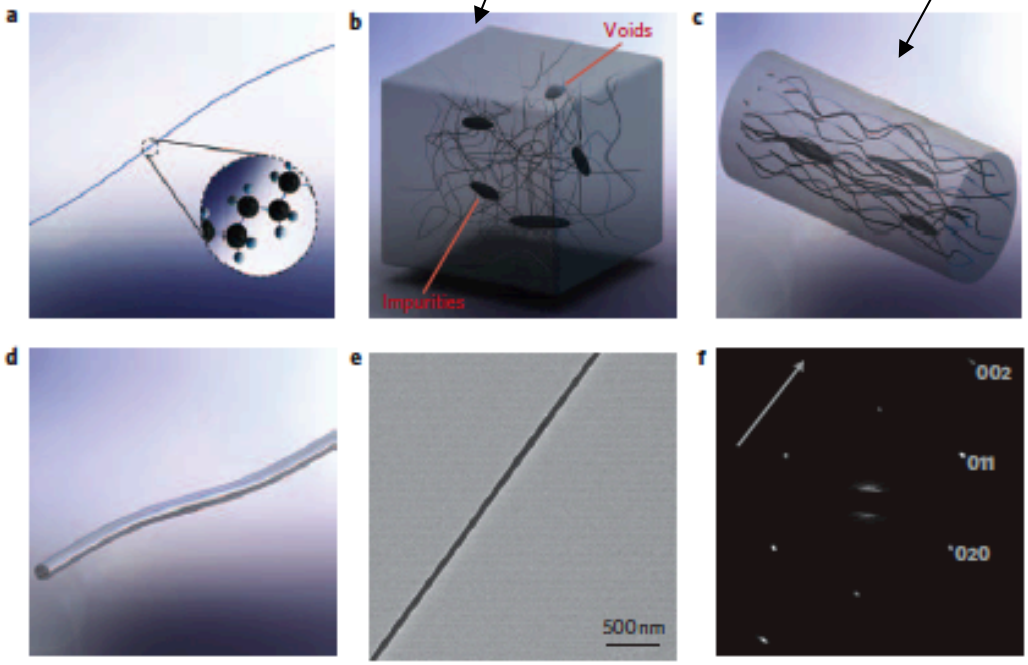

Figure 1 | Polyethylene chains and fibres. **a**, Illustration of one single molecular chain of polyethylene. The inset shows the chemical structure of polyethylene (carbon atoms are shown in black, hydrogen atoms in white). **b**, Bulk polyethylene containing chain ends, entanglements, voids and defects. **c**, Stretched polyethylene microfibre. **d**, 'Ideal' polyethylene nanofibre with perfectly aligned molecular chains. **e**, TEM image of an ultra-drawn polyethylene nanofibre. **f**, TEM diffraction image of the ultra-drawn polyethylene nanofibre. The arrow represents the drawing direction.

Ref: Shen et al, Nature nanotechnology, 2010

Oxide ceramic reinforcement-fibre(oxide)

CERAMIC REINFORCEMENTS

Table 3.2 Commercially available oxide ceramic reinforcements

Trade name	Manufacturer	Composition (%) Al_2O_3	ZrO_2	SiO_2	B_2O_3	Fe_2O
Continuous						
FP*	DuPont	>99				
PRD-166*	DuPont	85	15			
	Sumitomo	85		15		
	–	80		20		
Nextel 312	3M	62		24	14	
Nextel 440	3M	70		28	2	
Nextel 480	3M	70		28	2	
Nextel 550	3M	73		27		
Nextel 610	3M	>99		0.2–0.3		0.4–0.7
–	–		68	32		
Astroquartz	J.P. Stevens			99.95		
–	various			silica-based glass		
Saphikon	Saphikon			Al_2O_3 single crystal		
Discontinuous						
–	various			silica-based glass		
Saffil	ICI	96		4		
Fibermax	Carborundum	72		28		
Fiberfrax	Carborundum	52		48		

*Discontinued

Nonoxide ceramic reinforcement

Table 3.3 Commercially available nonoxide ceramic reinforcements

Composition	*Trade name*	*Manufacturer*
Continuous		
$SiC+O_2+C$	Nicalon	Nippon Carbon Co.
SiC*	SCS, Sigma	Textron Speciality Materials, BP
$SiC+Ti+C$	Tyranno	Ube Ind.
$SiC+Zr+C$	Tyranno	Ube Ind.
B	–	Textron Speciality Materials
C	–	various
Discontinuous		
SiC whiskers	–	Tateho
Si_3N_4 whiskers	–	–
SiC whiskers	Silar	Adv. Composite Materials Corp.
SiC whiskers	Tokawhisker	Tokai Carbon

*On tungsten or carbon substrate.

Fibre flexibility

$$\sim \frac{1}{MR}$$

M: bending moment

R: radius of curvature

$$\because \frac{M}{I} = \frac{E}{R}$$

I: moment of inertia

E: elastic modulus

$$I = \frac{d^4}{64}$$

$$\frac{1}{MR} = \frac{64}{Ed^4}$$

d: diameter

Oxide Fibre-Al_2O_3 fibre(3M)

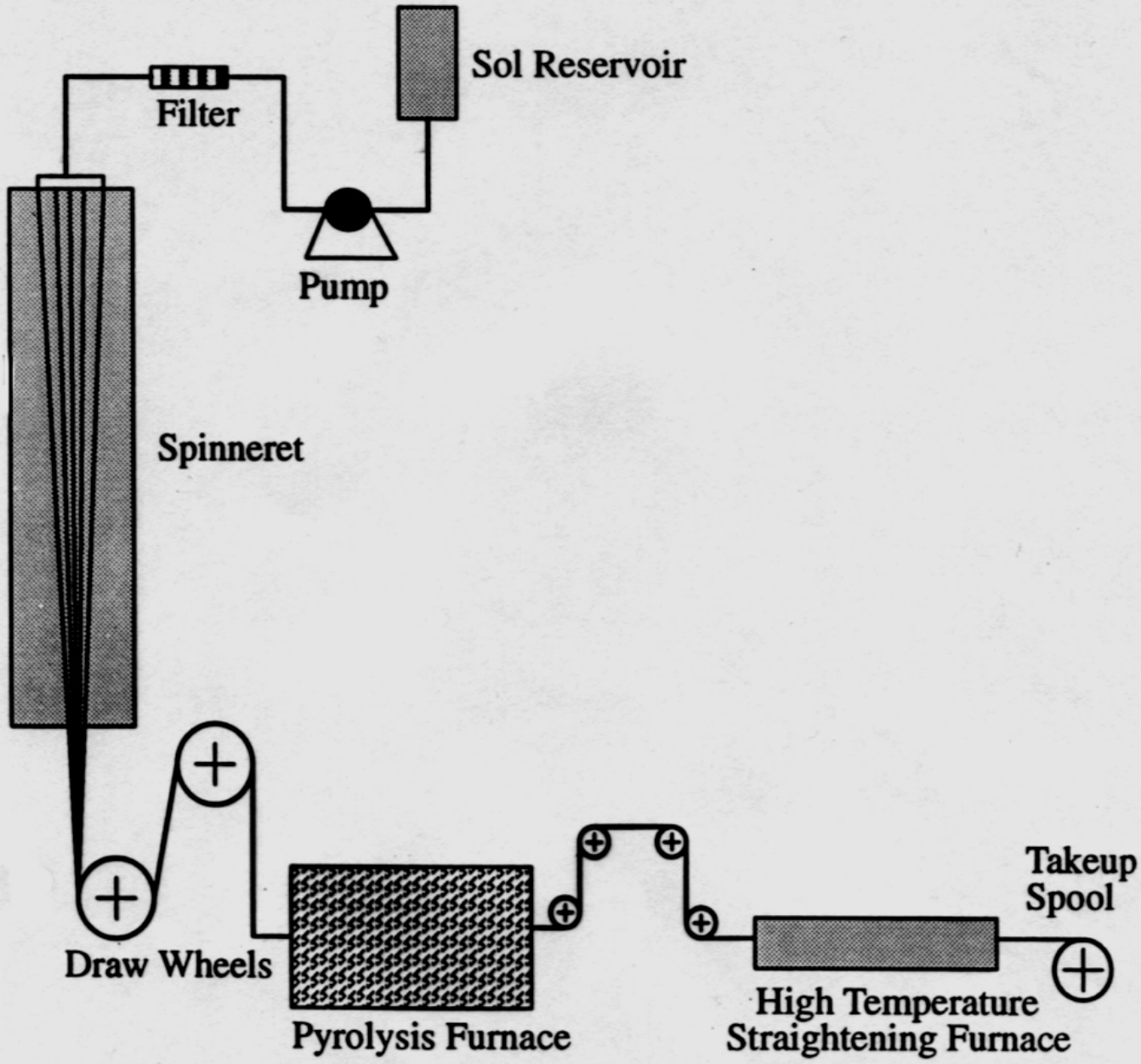

Fig. 3.25 3M process of making Al_2O_3 fiber.

Sol-gel process

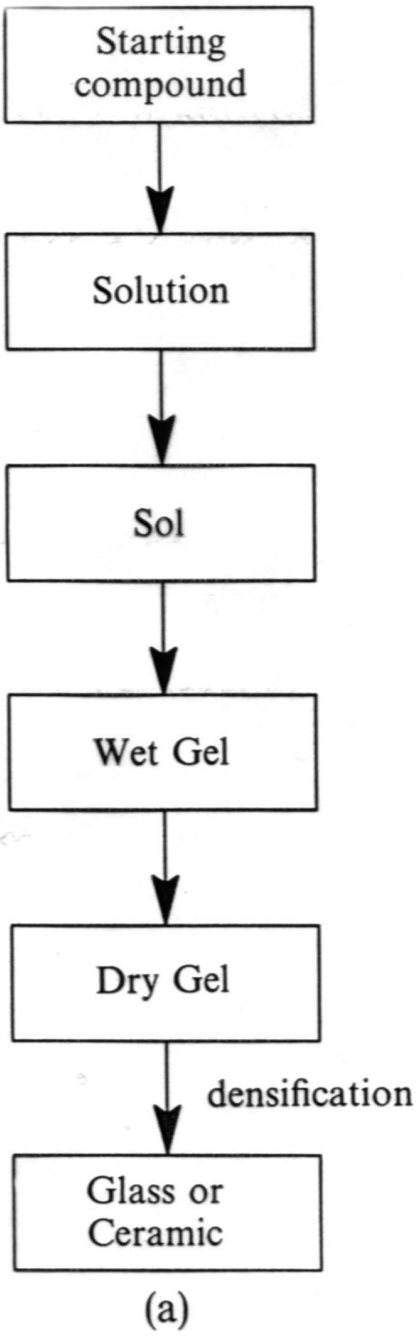

Fig. 2.6 The sol–gel process flow diagram; (b) microstructural changes occurring

sol gel

$$M(OR)_n + nH2O \longrightarrow M(OH)_n + nROH \quad \text{(hydrolyze)}$$

M:metal

R: alkyl group, ex. CH_3, C_2H_5 .....

$$M(OH)_n \longrightarrow MO_{n/2} + \frac{n}{2} H2O \quad \text{(pyrolysis)}$$

Sol-gel process

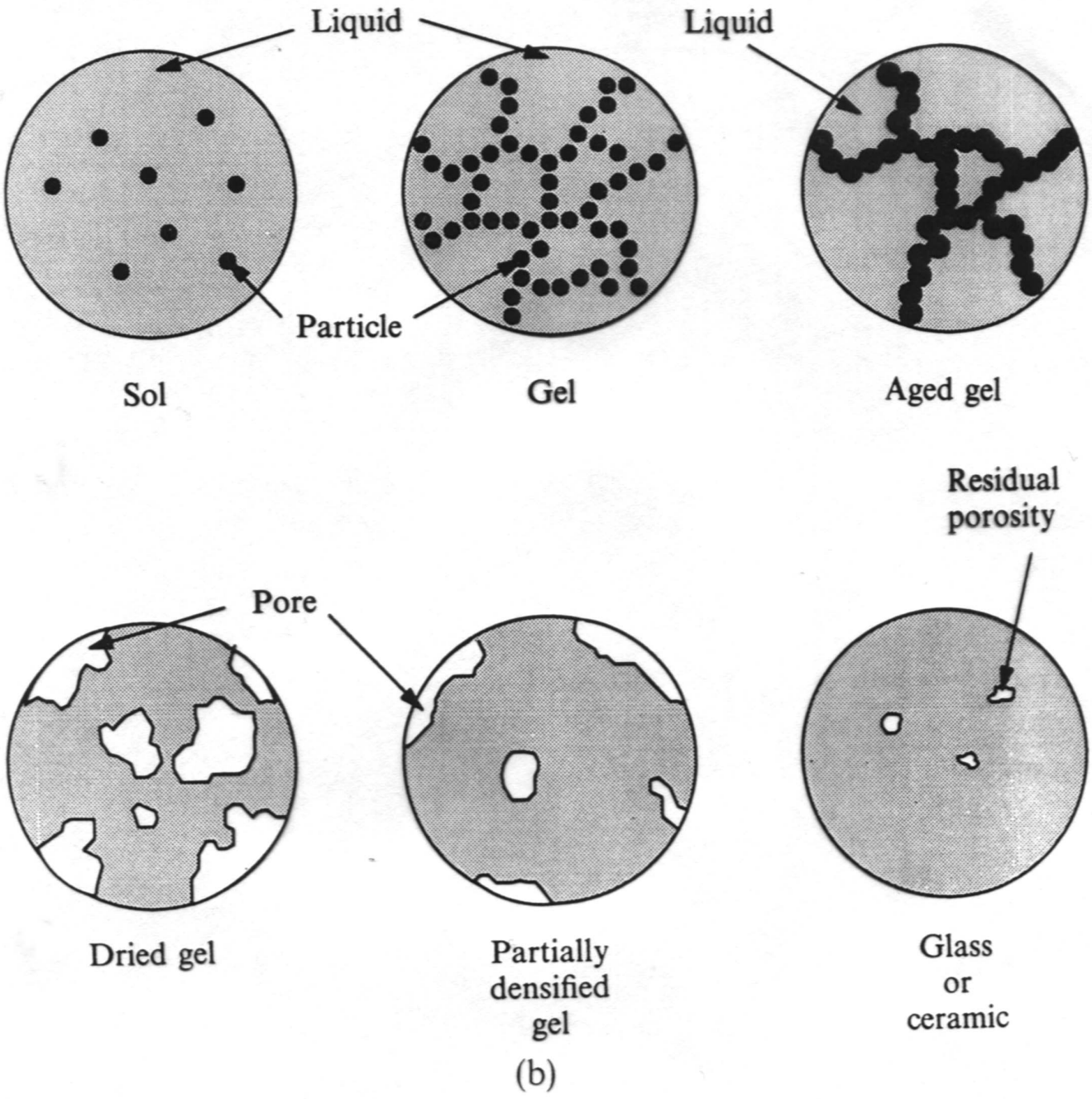

(b)

Sol-gel process

$M(OR)_n + nH_2O \rightarrow M(OH)_n + nROH$ (hydrolyzation)

- Gel is formed by chemical reaction

$M(OH)_n \rightarrow MO$ (oxide) + H_2O
(pyrolysis)

Example:

Si(OC2H5)4 + 4H2O → Si(OH)4 + 4 C2H5OH

Si(OH)4 → SiO2 + H2O

Si(OC2H5)4: tetraethyl orthosilicate, TEOS

The use of TEOS to produce SiO2 can date back to 1846. However, the drying time were in excess of a year to avoid the gels breaking into tiny pieces. No interest was given to this process that time. Until recently, the potential of this process is demonstrated in producing fibers, coating etc. Novel drying technique, such as critical-point drying, has also made this process to regain interest.

Ref: J.R. Jones, in Bioglass, An Introduction, Wiley, 2012

FP fibre (>99%Al2O3)

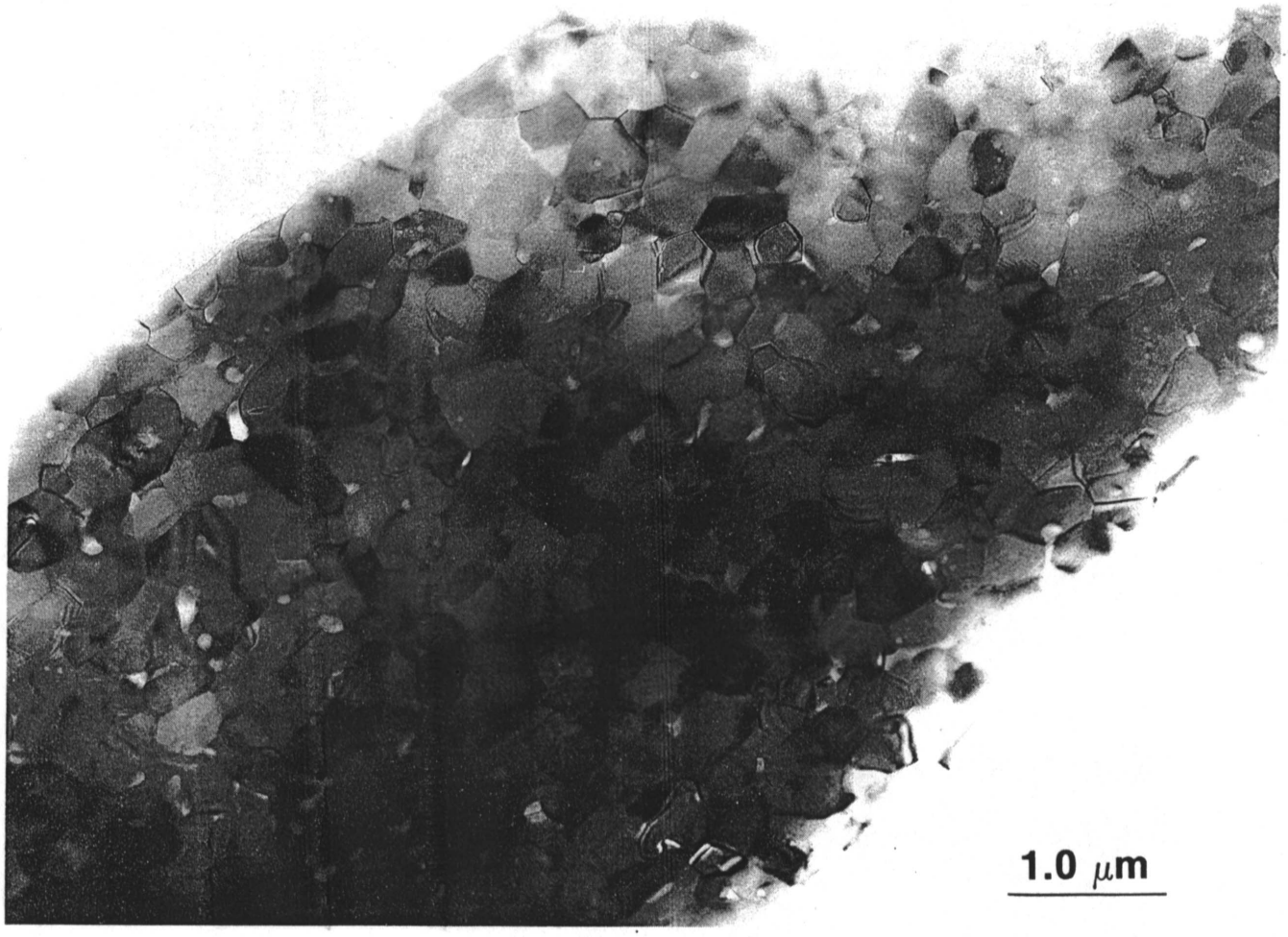

PRD-166 ($85\%Al_2O_3, 15\%ZrO_2$)

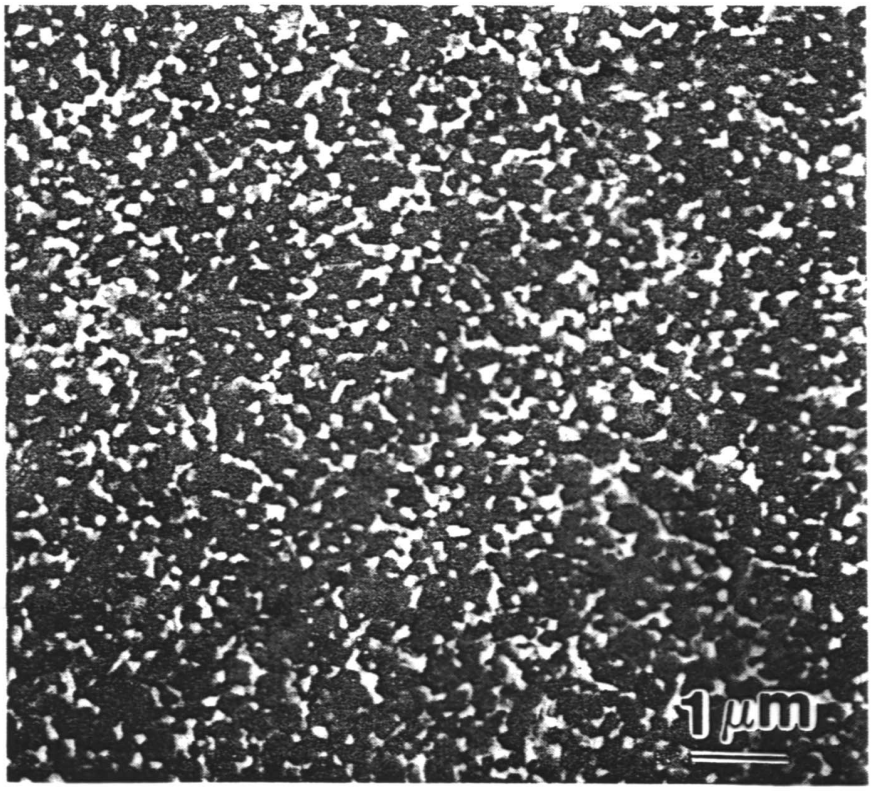

(a)

SEM

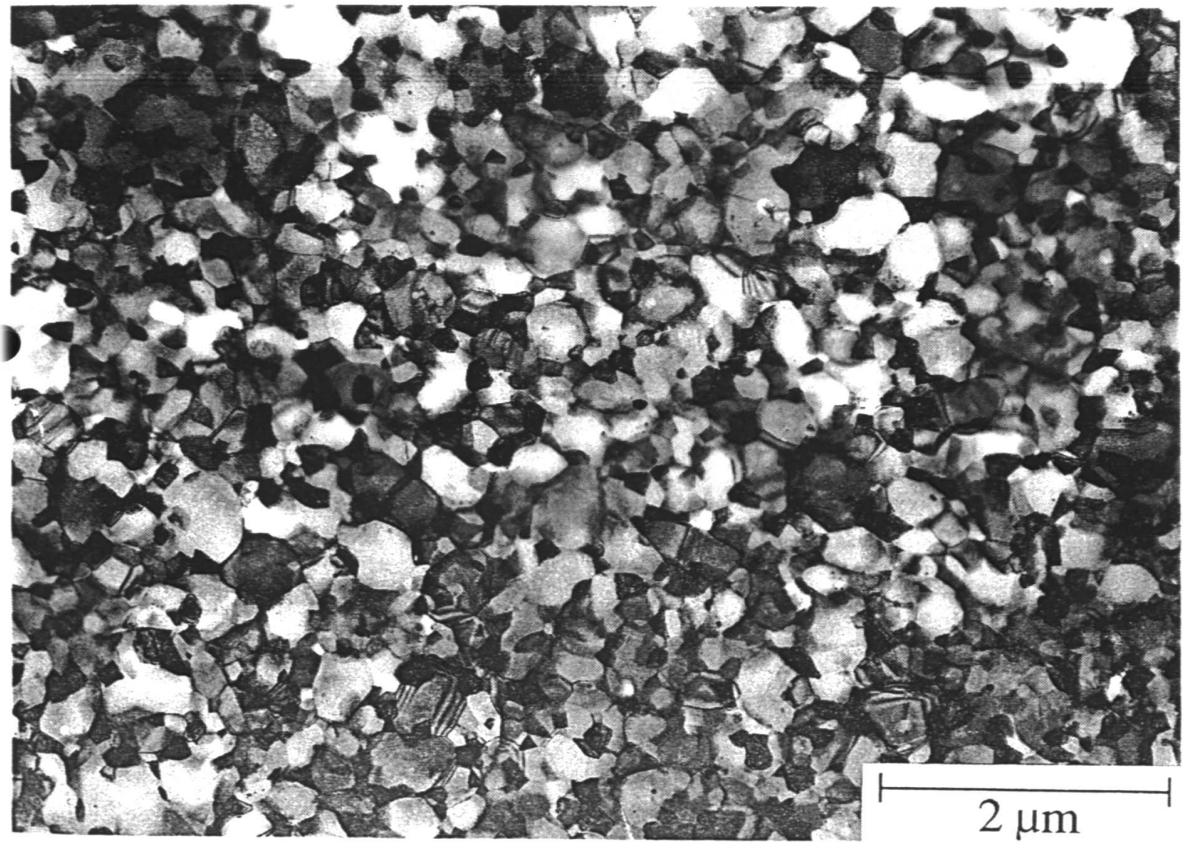

(b)

TEM

Fig. 3.24 (a) Microstructure of PRD-166 fiber as seen in a scanning electron microscope; (b) microstructure of PRD-166 fiber as seen in a transmission electron microscope. Zirconia particles (white) are mostly at grain boundary triple points (courtesy of S. Nourbaksh).

OXIDE FIBERS

Table 3.12 Properties of some oxide fibers

Fiber type	*Composition (wt%)*	*Diameter (μm)*	*Density ($g\,cm^{-3}$)*	*Tensile strength (MPa)*	*Young's modulus (GPa)*
3M					
Nextel 312	Al_2O_3-62, SiO_2-24, B_2O_3-14	10–12	2.7	1700	152
Nextel 440	Al_2O_3-70, SiO_2-28, B_2O_3-2	10–12	3.05	2000	186
Nextel 480	Al_2O_3-70, SiO_2-28, B_2O_3-2	10–12	3.05	2070	220
Nextel 550	Al_2O_3-73, SiO_2-27	10–12	3.03	2240	220
Nextel 610	Al_2O_3-99+, SiO_2-0.2–0.3, Fe_2O_3-0.4–0.7	10–12	3.75	1900	370
ICI					
Saffil	Al_2O_3-96, SiO_2-4	3	2.3	1000	100
Saphikon	Single crystal Al_2O_3	70–250	3.8	3100	380
Sumitomo	Al_2O_3-85, SiO_2-15	9	3.2	2600	250

Non-oxide fibre

SiC fibre

Non-oxide fiber

NONOXIDE FIBERS

CVD- process

CVD process

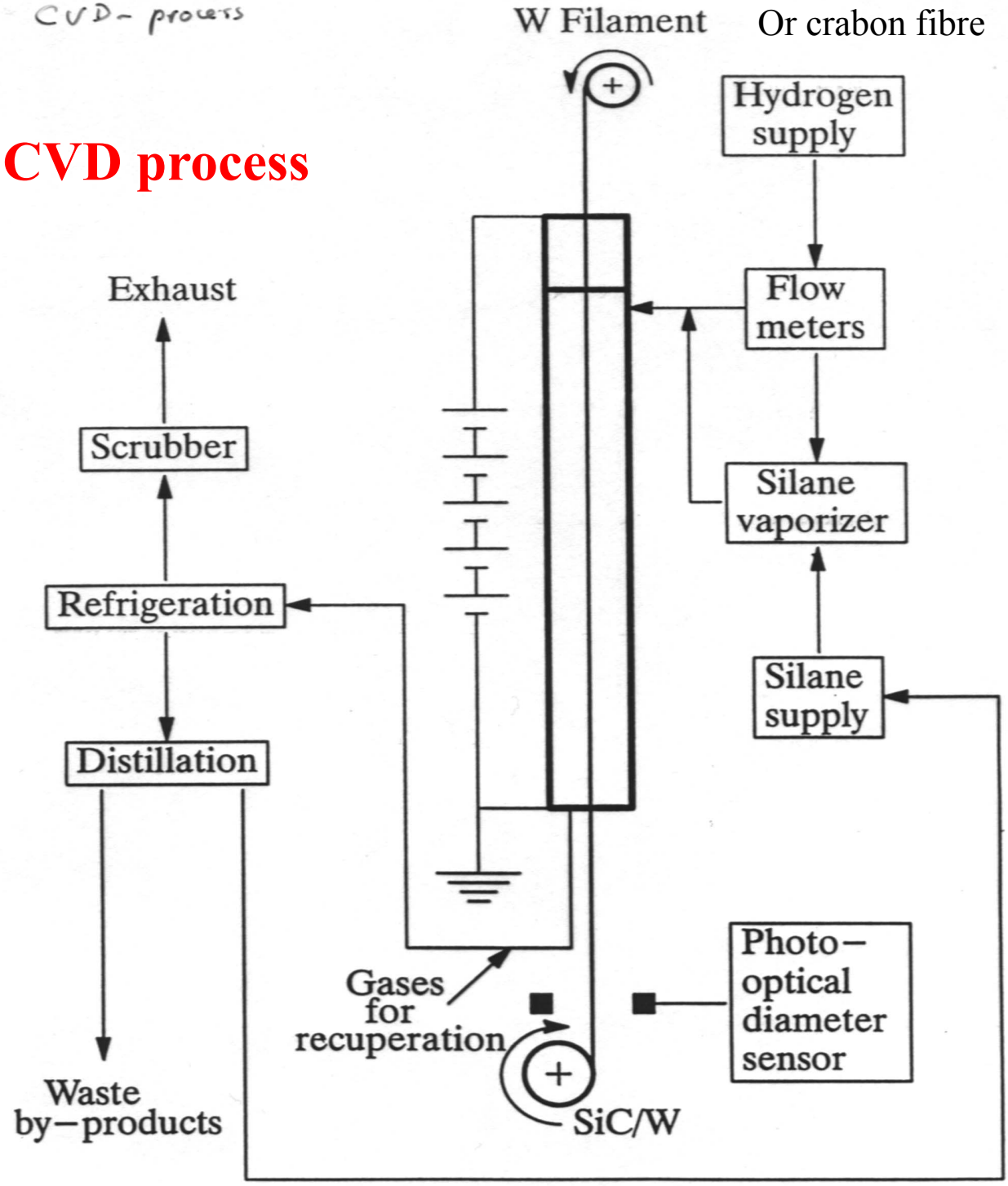

Fig. 3.34 A schematic of the BP process of making silicon carbide monofilament by CVD. The fiber has trade name of *sigma* fiber and the substrate is tungsten.

$$CH_3SiCl_{3\,(g)} \xrightarrow{H_2} SiC_{(s)} + 3HCl_{(g)}$$

Surface modified SiC fibre (SCS)

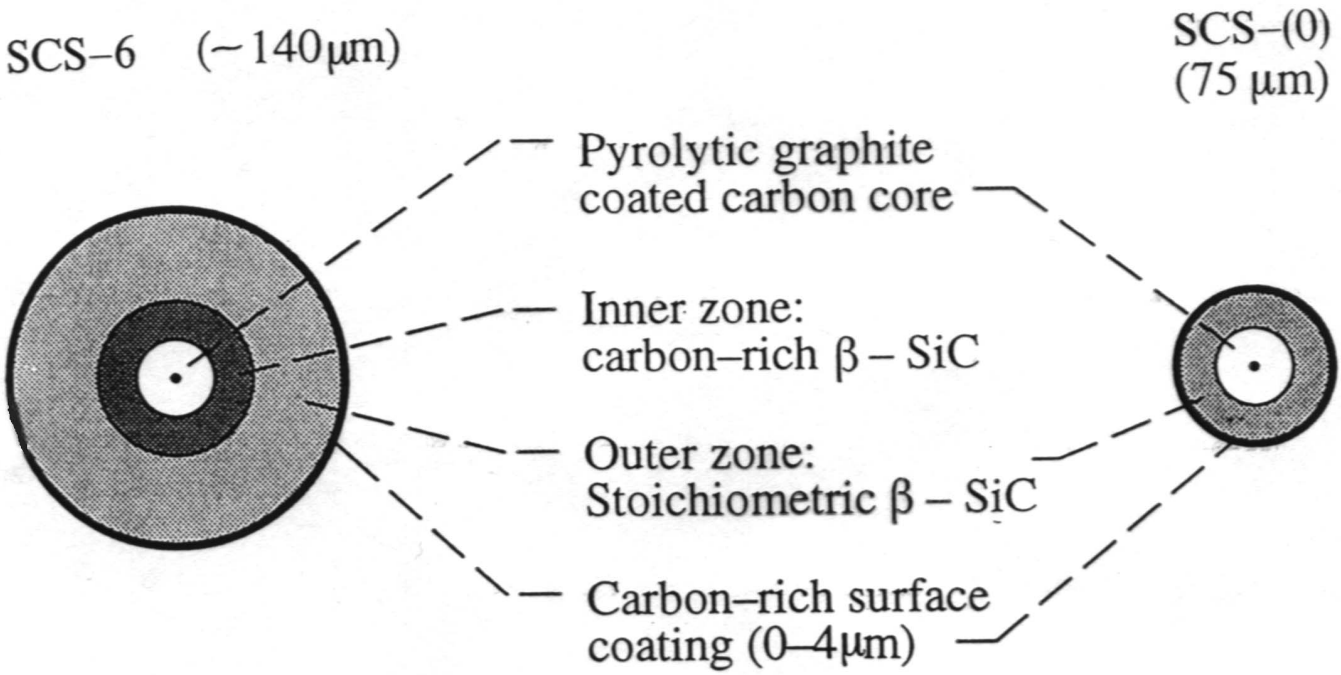

Table 3.14 Properties of CVD SiC (SCS-6) monofilament

Composition	*Diameter (μm)*	*Density ($g\ cm^{-3}$)*	*Tensile strength (MPa)*	*Young's moduus (GPa)*
β-SiC	140	3.3	3500	430

SCS-6

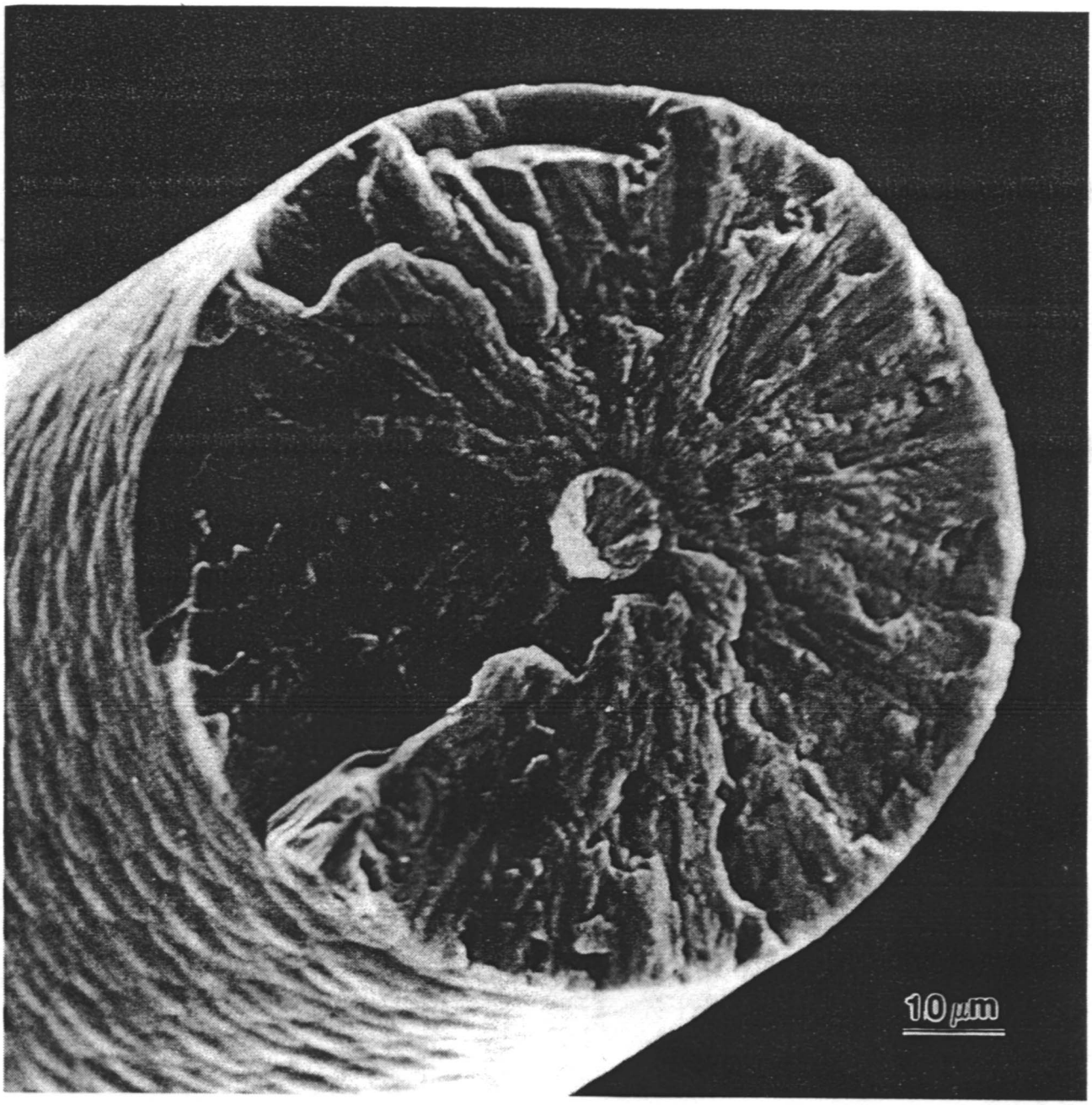

Fig. 3.36 Fracture surface of *sigma* CVD SiC fiber showing brittle fracture (courtesy of BP).

Non-oxide fibre by polymer route

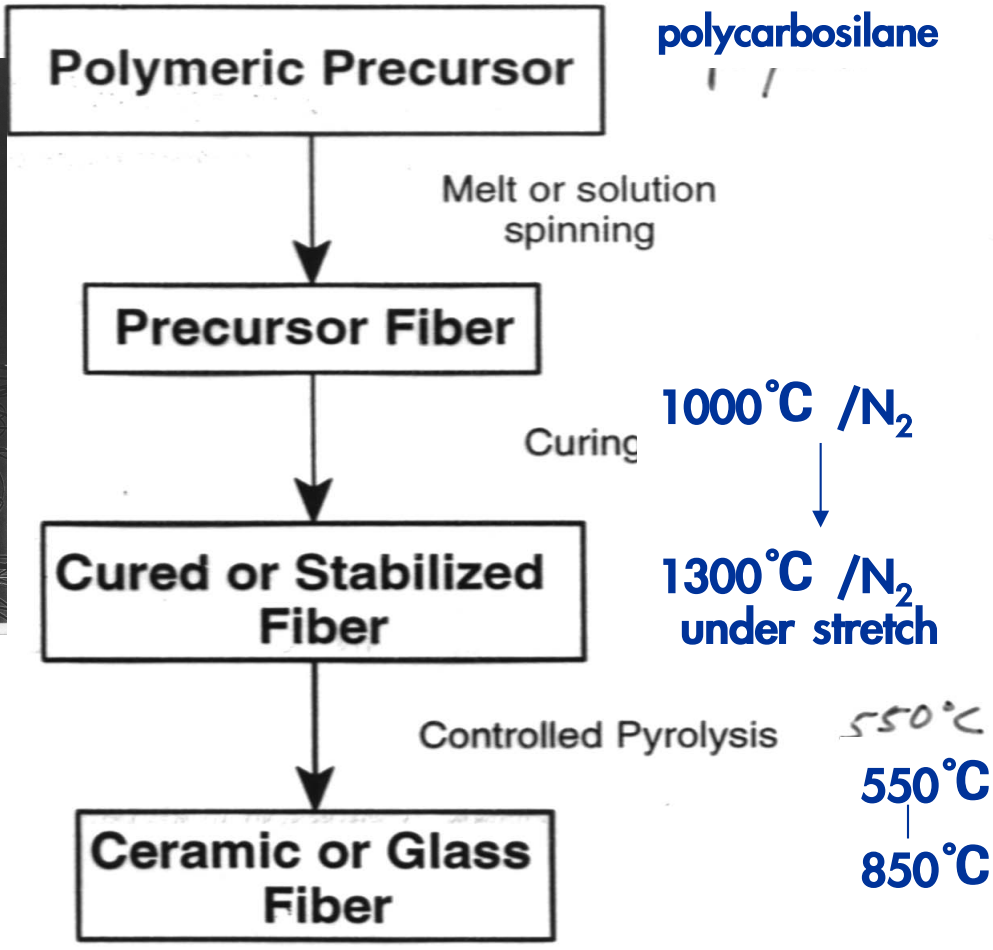

Fig. 3.37 Various steps involved in processing nonoxide fibers via polymer route.

Nicalon SiC

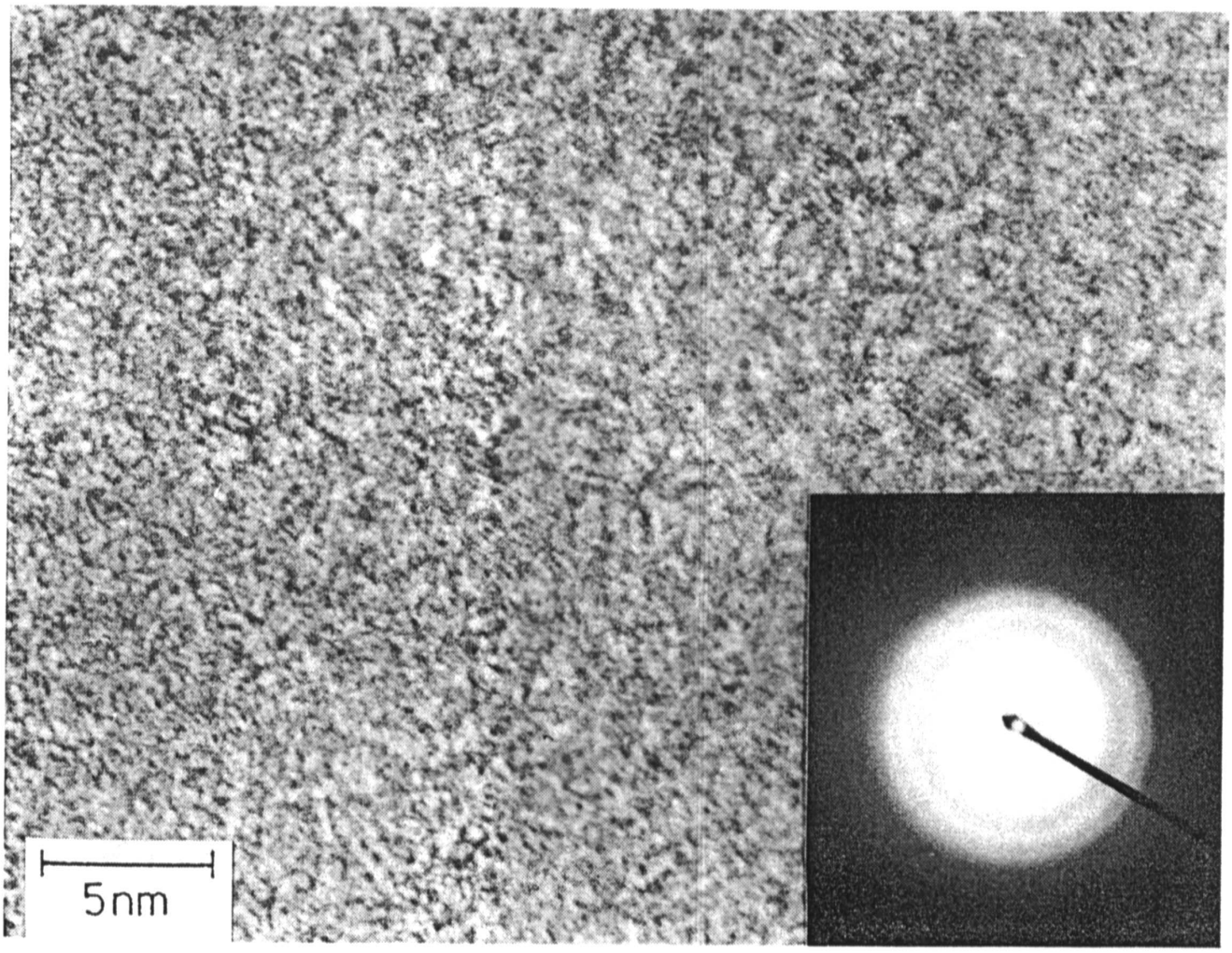

Fig. 3.39 High-resolution transmission electron micrograph of Nicalon-type SiC produced in a laboratory, indicating the amorphous nature of the SiC produced by the Yajima process (courtesy of K. Okamura).

Nicalon SiC

Journal of the American Ceramic Society—Jia et al.

Table I. Composition and Structure of As-Received Nicalon: NLP-201

	Elemental composition			Phase structure			
	Si	C	O	SiC	SiC_xO_y	SiO_2	
				Surface			
at.%	40	53	7	68	27	5	mol%
wt%	60	34	6	58	35	7	wt%
				$x = 2.4, y = 0.3$			
				Bulk*			
				68	30	-	mol%
				58	42	-	wt%
				$x = 2.0, y = 0.5$			

*The absence of SiO_2 in the bulk structure was pointed out by Laffon *et al.*[28] The molar and weight percentages of SiC_xO_y in the bulk were calculated assuming that the ratio Si:C:O remained the same in the surface and the core of the fiber.[18]

Ref: N. Jia, R. Bodet, R.E. Tressler," Effect of microstructural instability on the creep behavior of Si-C-O (Nicalon) Fibers in argon " , J.Amer. Ceram.Soc.,76(12)3051-60,(1993)

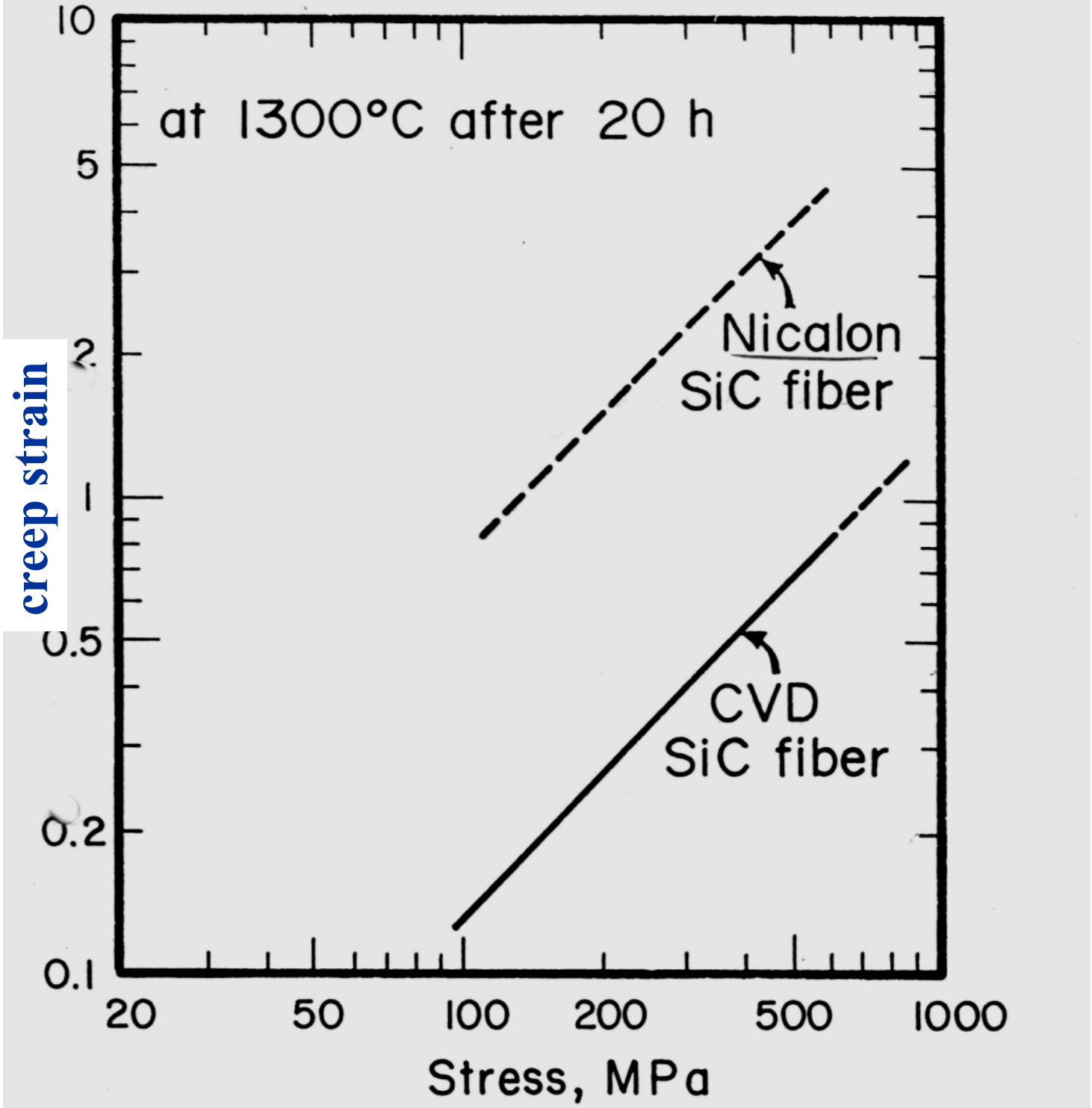

3.41 Comparison of the creep strain in Nicalon and CVD SiC fiber (after

3 generations of SiC fiber

TABLE III Details of manufacture, elemental composition and approximate cost of all three generations of SiC based fibres

	Trade mark	Manufacturer	Cross linking method	Approximate maximum production temperature	Elemental composition (wt%)	Density (g/cm^3)	Average diameter (μm)	Cost (US $/kg)
First Gen.	Nicalon 200	Nippon Carbon	Oxygen	1200°C	56Si + 32C + 12O	2.55	14	2000
	Tyranno LOX-M	Ube Ind.	Oxygen	1200°C	54Si + 32C +12O + 2Ti	2.48	11	1250
Second Gen.	Hi-Nicalon	Nippon Carbon	Electron irradiation	1300°C	62.5Si + 37C +O.5O	2.74	12	8000
	Tyranno LOX-E	Ube Ind.	Electron irradiation	1300°C	55Si + 37.5 +5.5O + 2Ti	2.39	11	N/A
	Tyranno ZM	Ube Ind.	Oxygen	1300°C	57Si + 34.5C + 7.5O + 1Zr	2.48	11	1500
	Tyranno ZE	Ube Ind.	Electron irradiation	1300°C	58.5Si + 38.5C + 2O + 1Zr	2.55	11	N/A
Third Gen.	Tyranno SA 1	Ube Ind.	Oxygen	>1700°C	68Si + 32C +0.6Al	3.02	11	N/A
	Tyranno SA 3	Ube Ind.	Oxygen	>1700°C	68Si + 32C +0.6Al	3.1	7.5	5000
	Sylramic	COI ceramics	Oxygen	>1700°C	67Si + 29C +0.8O + 2.3B +0.4N +2.1Ti	3.05	10	10000
	Sylramic iBN	COI Ceramics	Oxygen	>1700°C	N/A	3.05	10	>10000
	Hi-Nicalon Type-S	Nippon Carbon	Electron irradiation	>1500°C	69Si + 31C + 0.2O	3.05	12	13000

Ref: A. R. BUNSELL, A. PIANT, A review of the development of three generations of small diameter silicon carbide fibres, J MATER SCI 41 (2006) 823–839

SiC fiber-updated

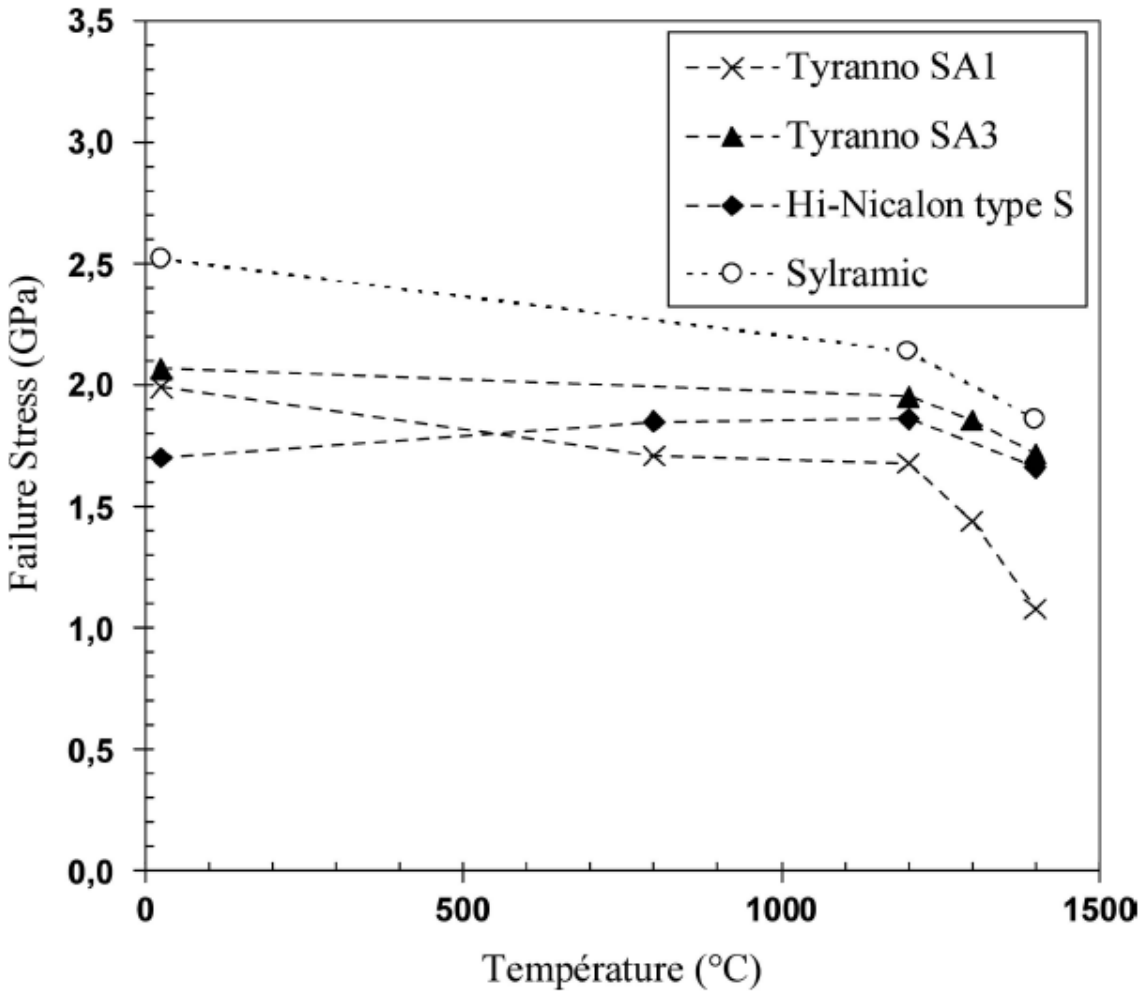

13 Strength as a function of temperature for third generation fibres with a 250 mm gauge length.

SiC fiber

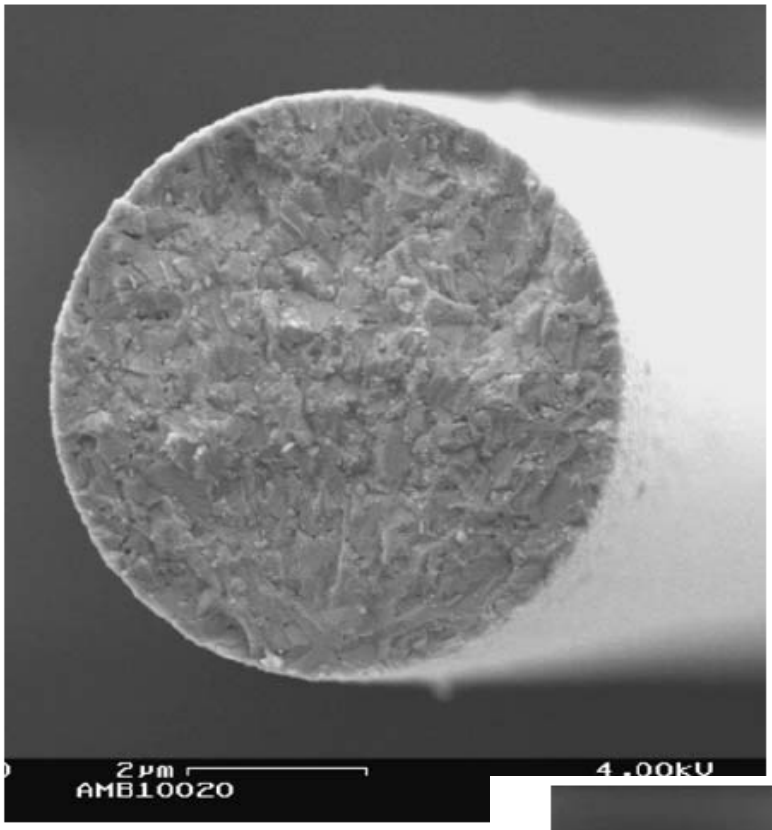

Figure 15 Fracture morphology of a Tyranno

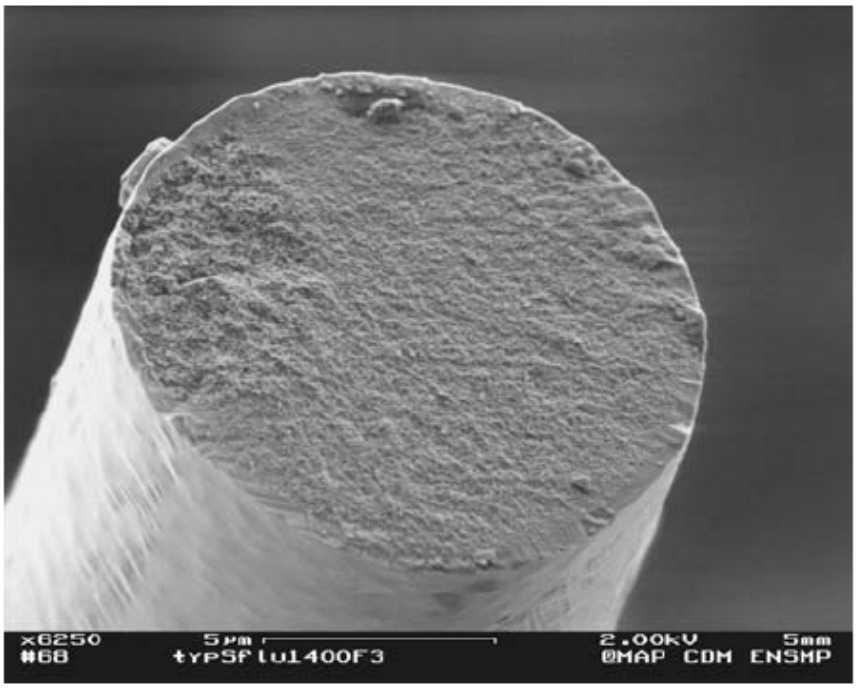

Figure 16 Fracture morphology of a Hi-Nicalon Type-S fibre broken at 1400°C.

Performance of ceramic fibres

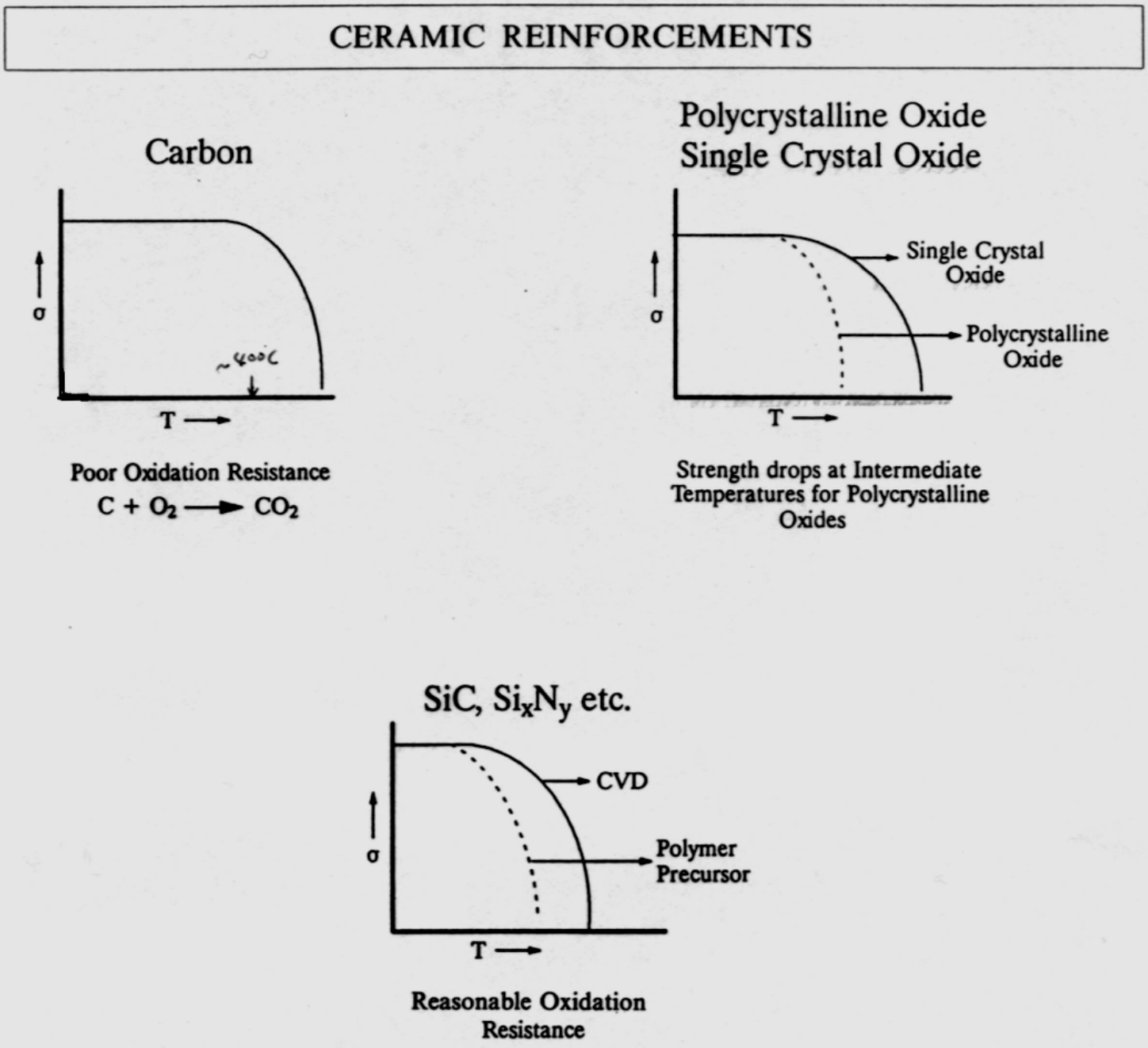

Fig. 3.45 Schematic of strength vs. temprature for some ceramic fibers.

Unit 3,
Design of CMC
& Material selection

- Design of CMC
  - Templates, biomimetic concept
  - Material selection

References :

1. M. F. Ashby, “Criteria for selecting the components of composites”, Acta Metall., 41(5) 1313-1335 (1993),

HKPC

Many Ceramic/Ceramic Composites have been developed in various Lab. Do these CMCs make any sense at all?

(CONTINUED)

MATRIX	DISPERSION PHASE	TYPES OF DISPERSION PHASE	PROCESSING	PROPERTY
Si_3N_4	Diamond	PARTICLE	UHP	TOUGHNESS
BN	Si_3N_4	"	CVD	TRANCELUCENT, REFRACTORY
cBN	TiN	"	UHP	HARDNESS
AlN	ZrO_2	"	HP	HARDNESS, TOUGHNESS
BN	TiN	"	CVD	HARDNESS, TOUGHNESS
SiC	SiC	FIBER	NS	TOUGHNESS
SiC	SiC	WHISKER	HP	TOUGHNESS
SiC	Al_2O_3	PARTICLE	HP	TOUGHNESS
SiC	TiC	"	HP	STRENGTH, ELECTRICAL CONDUCTIVITY
"	ZrC	"	"	"
"	WC	"	"	"
"	ZrB_2	"	"	"
"	TiB_2	"	"	"
"	HfB_2	"	"	"
"	NbB_2	"	"	"
"	TaB_2	"	"	"
TiC	TiB_2	PARTICLE	HP	HARDNESS, STRENGTH, ELECTRICAL CONDUCTIVITY
β-Sialon	SiC	PARTICLE	HP	STRENGTH, TOUGHNESS
ZrB_2	SiC			
$MoSi_2$	SiC	WHISKER	HP	STRENGTH, TOUGHLNESS
TiB_2	ZrO_2	PARTICLE	HP	" "
$CaZrO_3$	B-Ca_2SiO_4	"	NS	" "
$3Al_2O_3 \cdot 2SiO_2$	ZrO_2	"	NS, HP	" "
SiC	BeO	"	HP	THERMAL CONDUCTIVITY
SiC	V_2O_5			ELECTRICAL CONDUCTIVITY
AlN	BN	PARTICLE	HP	STRENGTH, THERMAL CONDUCTIVITY
TaN	ZrB_2-ZrN	PARTICLE	HP	HARDNESS, STRENGTH, ANTI-ABRASION
TaN	ZrB_2-WC	PARTICLE	HP	SAME ABOVE
ZrO_2 (Y_2O_3)	SiC	WHISKER	HP	TOUGHNESS, REFRACTORY

NOTE: NS; NORMAL SINTERING, HP; HOT PRESS, HIP; HOT ISOSTATIC PRESS, UHP; ULTRA HIGH PRESSURE, CVD; CHEMICAL VAPOR DIPOSITION

Old methodology: trial & error

Example: To improve the thermal conductivity of PP

Table 1
Selected properties of filler materials

	Magnetite (Fe_3O_4)	Barite ($BaSO_4$)	Talc ($Mg_3[Si_4O_{10}][OH]_2$)	Strontium ferrite ($SrFe_{12}O_{19}$)	Copper (Cu)	Glass fibres
Thermal conductivity (W/(m K))	a: 4.61 ± 0.42 a: **5.10** λ_{11} : 9.7	⊥ : 2.07 ± 0.02 ∥: 2.92 ± 0.07 a: **1.72** ± 0.04	⊥ : 1.76 ± 0.00 ∥: **10.69** ± 1.35 a: 2.97 a: 3.00 ± 0.10 a: 6.10 ± 0.90	>3	**401**	1.2–**1.5**
Ref.	[8]	[8]	[8]	[9]	[10]	[11]
Mean particle diameter (μm)	9	1.5	2.0	1.5	15	11
Particle shape	Irregular	Irregular	Platelet		Irregular	Fibre
Density (g/cm^3)	5.1	4.48	2.78	5.11	8.94	2.58

'a' denotes measurements on monomineralic aggregates. Directions of anisotropy are specified by the thermal conductivity tensor (λ_{11}, λ_{22}, λ_{33}), where λ_{33} is parallel to the crystal's optical c-axis, and the optical c-axis lies within the plane defined by λ_{11} and λ_{22} or by the thermal conductivity components normal or parallel to the direction of maximum thermal conductivity (⊥ , ∥).

Ref: Weidenfeller et al., 2004

Old methodology: trial & error

Example: To improve the thermal conductivity of PP

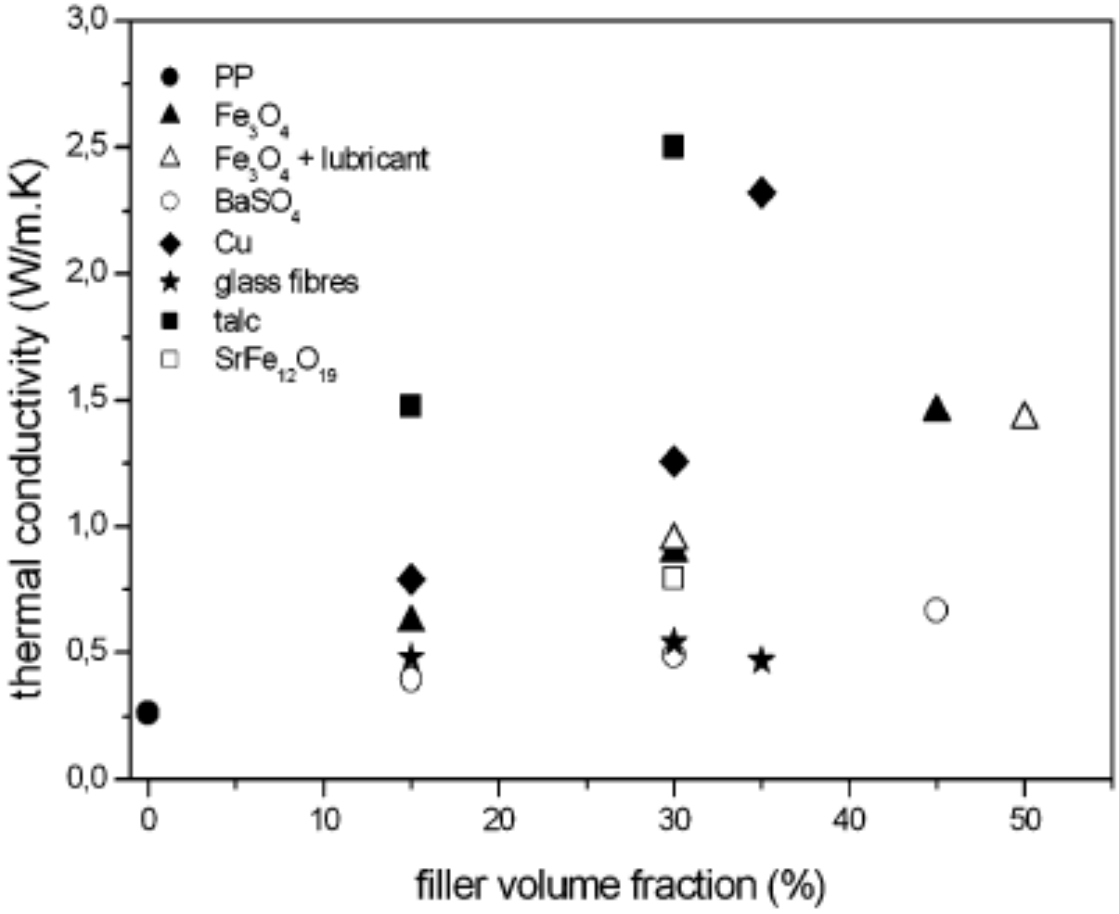

Fig. 1. Thermal conductivity of injection-moulded polypropylene-particle-composites with different fillers and various filler fractions.

Ref: Weidenfeller et al., 2004

Are there any templates for the design of CMC ?

Biomimetic
仿生

- Good example on microstructure can be imported from the biological systems - biomimetic.

Definition of Biomimetic (仿生)

- Biomimetics (also known as biomimicry, or bionical creativity engineering) is the application of biological methods and systems found in nature to the study and design of engineering systems and modern technology. (Ref: Wikipedia)

Start of biomimetic

Around 1990 a neologism crept into materials science. I have not been able to track down who used it first, but the *Chemical Abstracts* search under the keywords 'biomimesis' or 'biomimetic materials' shows the earliest citations to be by N. Herron in 1992. The total papers under 'biomimesis' are only five and under 'biomimetic materials' are 11; yet 'biomimetic' gets 1573 citations, which shows how complex database searching is.

Ref: R. Roy, TRIP, 3, 350, 1995

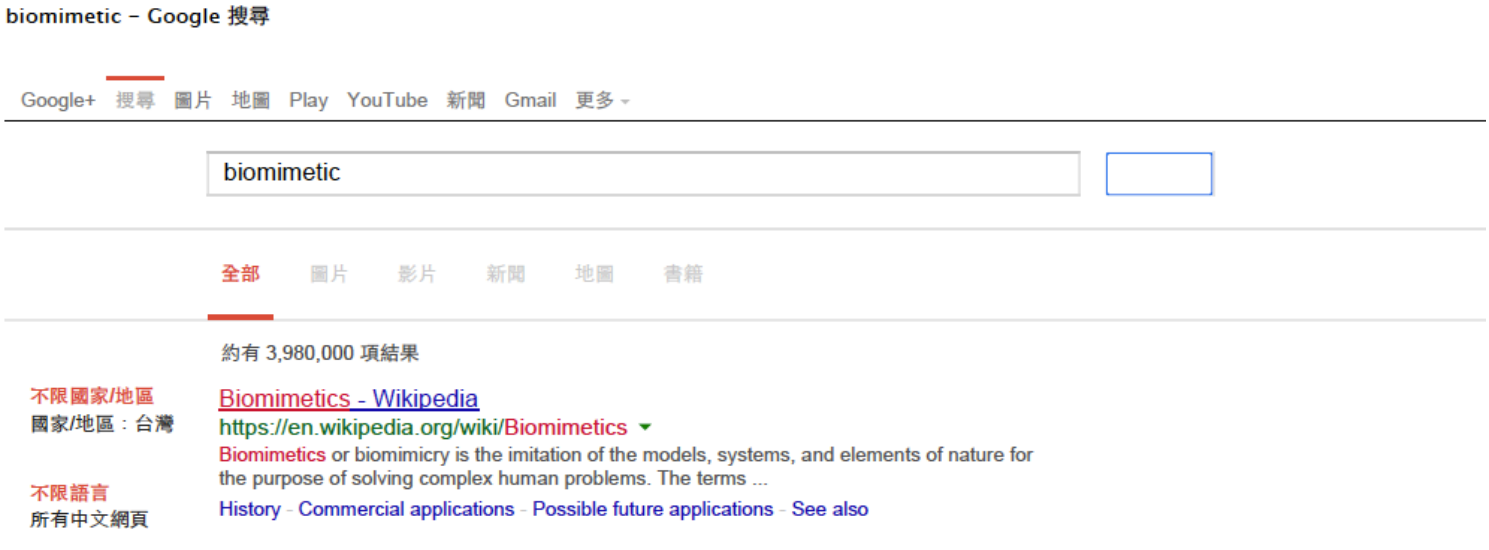

Is there a rule for materials selections?

Design sequence of composites

Performance indices

↓

Materials selection charts

↓

Properties bounds for composites

↓

Composite design

Ref: Ashby, 1993

Performance indices

examples : simple cases

- buoyancy : density, ρ
- stiffest beam : elastic modulus, E
- pendulum : thermal expansion, α

examples : a slightly complex cases

- lightest beam with specified stiffness : E/ρ
- energy storing capacity (spring) : σ_f^2/E
- minimum thermal distortion (for precise device) : λ/α

note : σ_f : strength
λ : thermal conductivity
precise devices : hard drive,
telescope
atomic force microscope

Table 2. Some performance indices

Design requirement	Performance index, M
Light stiff tie (tensile member)	$M_1 = E/\rho$
Light stiff beam, torsion member or column	$M_2 = E^{1/2}/\rho$
Light stiff plate, loaded in bending or buckling	$M_3 = E^{1/3}/\rho$
Light strong tie (tensile member)	$M_4 = \sigma_f/\rho$
Light strong beam or torsion member	$M_5 = \sigma_f^{2/3}/\rho$
Light strong plate, loaded in bending	$M_6 = \sigma_f^{1/2}/\rho$
Fast fracture, load controlled	$M_7 = (EJ_{1c})^{1/2}$
Fast fracture, displacement controlled	$M_8 = (J_{1c}/E)^{1/2}$
Fast fracture, energy controlled	$M_9 = J_{1c}$
Minimum thermal distortion	$M_{10} = \lambda/\alpha$

Note: A more complete list can be found in Ref. [5], pp. 61–64.

Design sequence of composites

Performance indices

Materials selection charts

Properties bounds for composites

Composite design

Material selection charts

ex. Light stiff tie

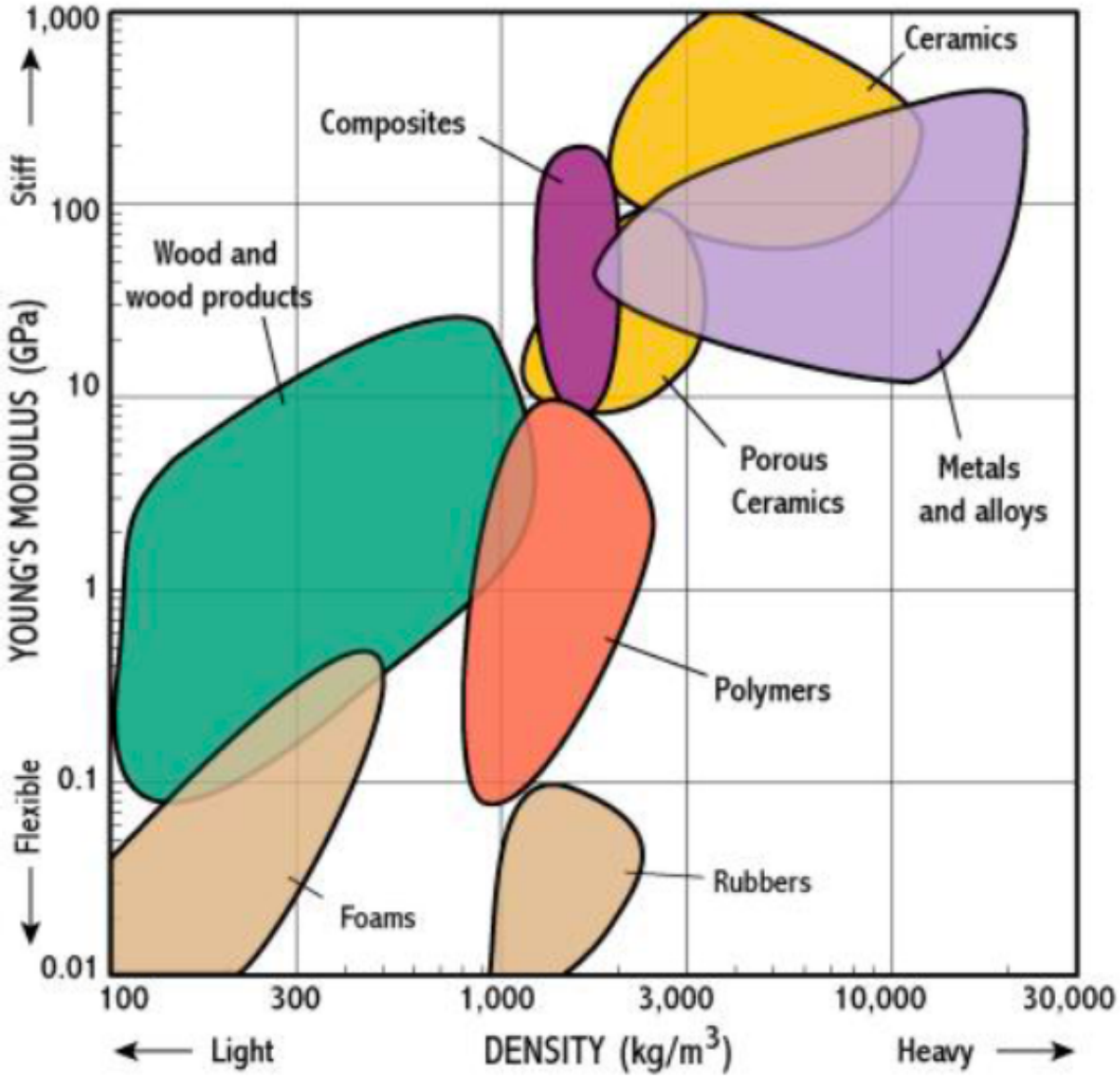

Material selection charts

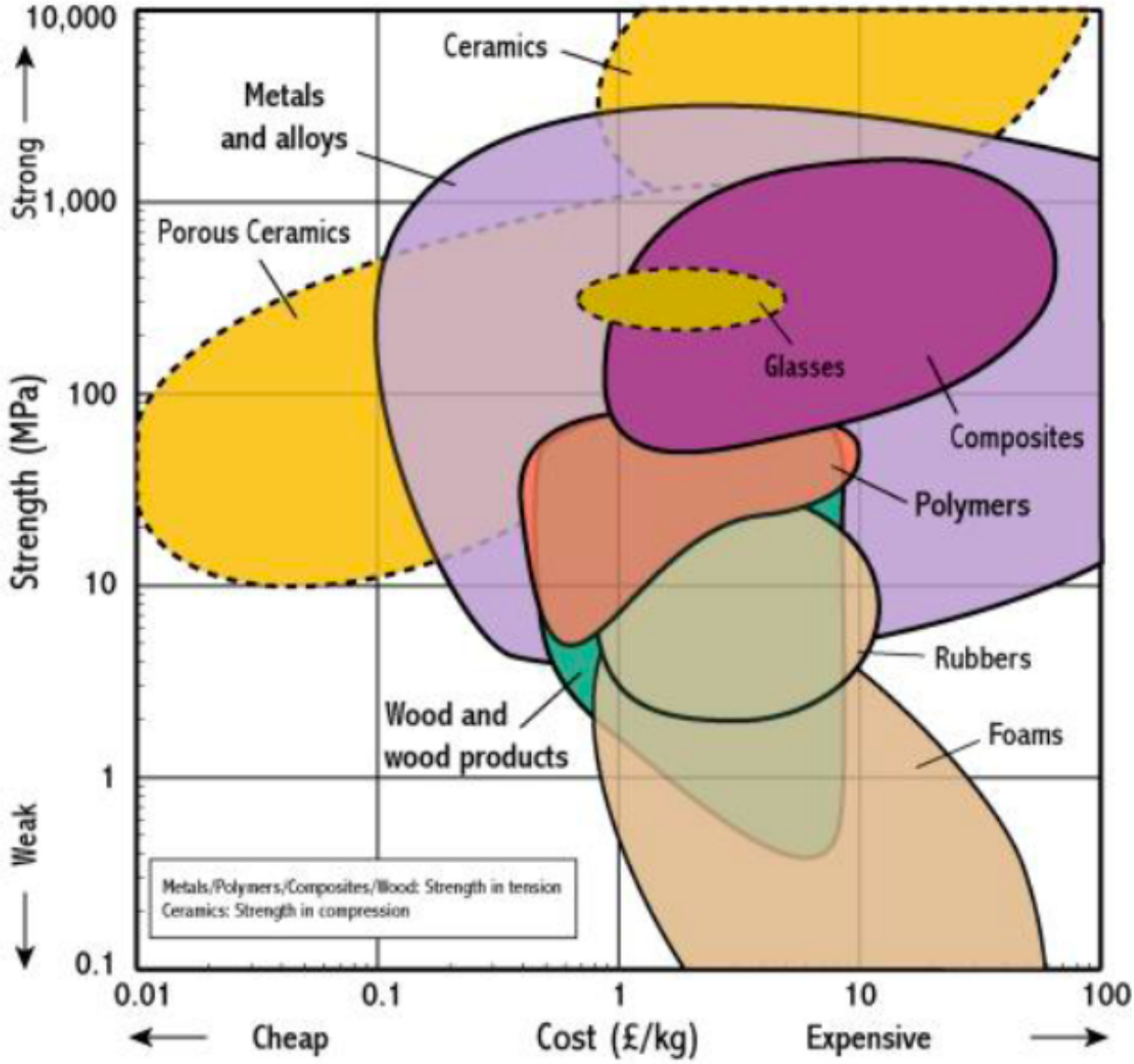

How to use material selection charts?

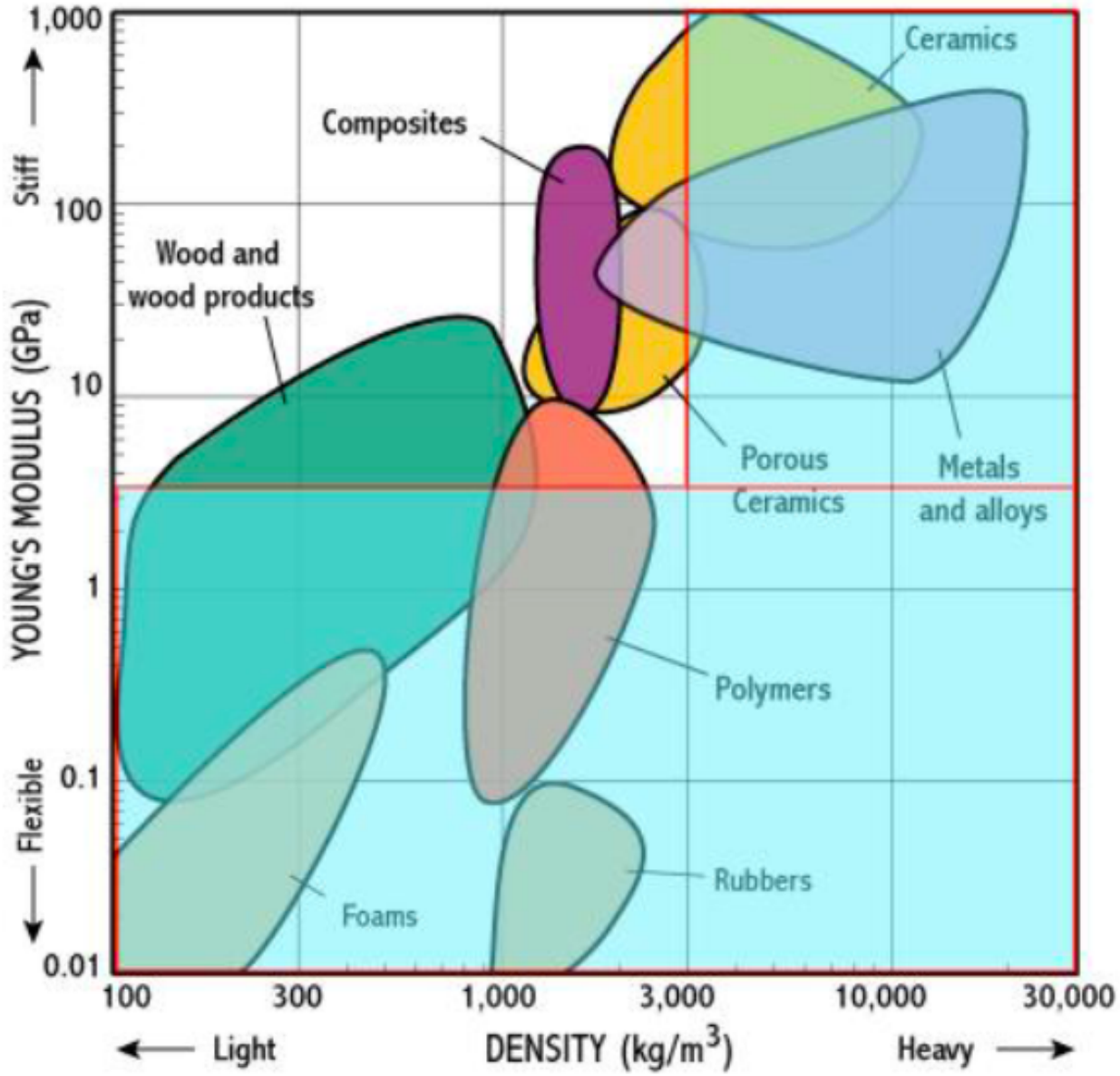

Design sequence of composites

Performance indices

Materials selection charts

Properties bounds for composites

Composite design

Properties bounds for composites

-- to define the envelop of properties accessible to a given composite system

assumptions :

a. fully dense composites
b. macro-composites (atomistic and dislocation mechanics can be ignored)
c. geometry independent

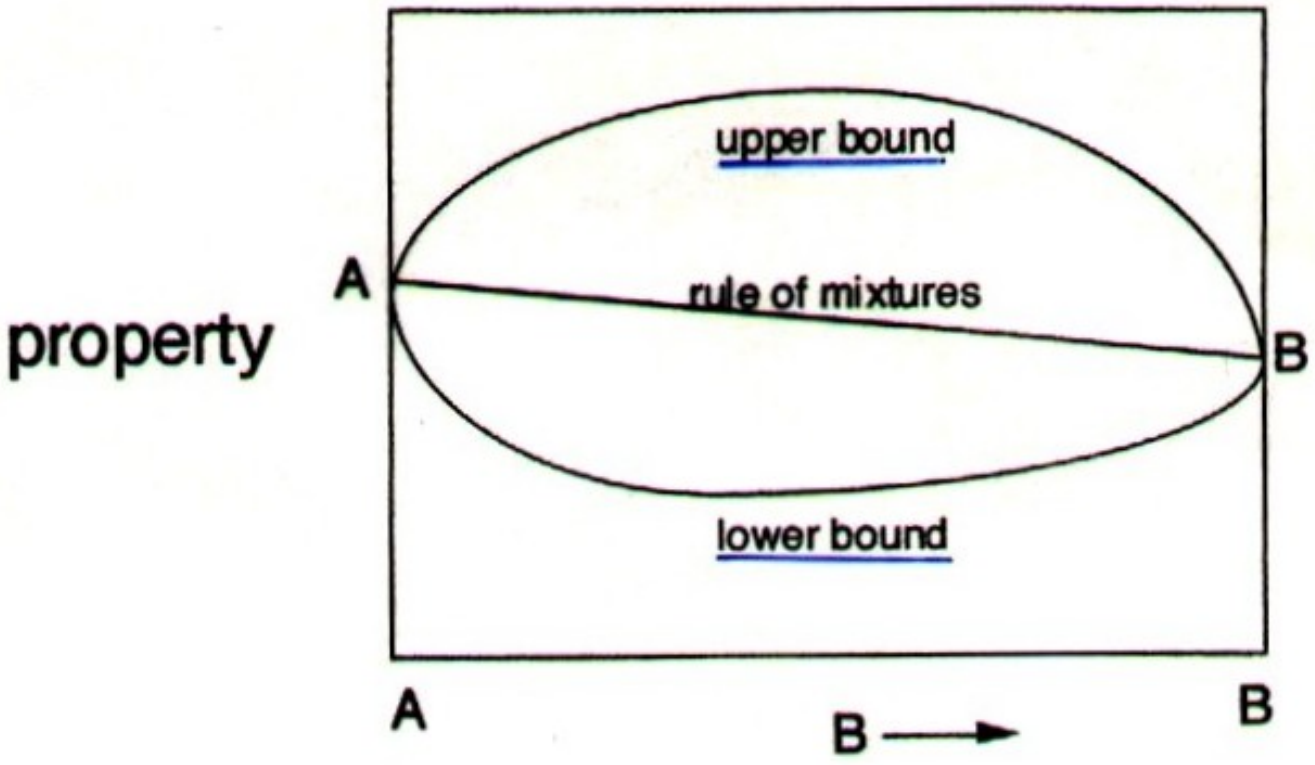

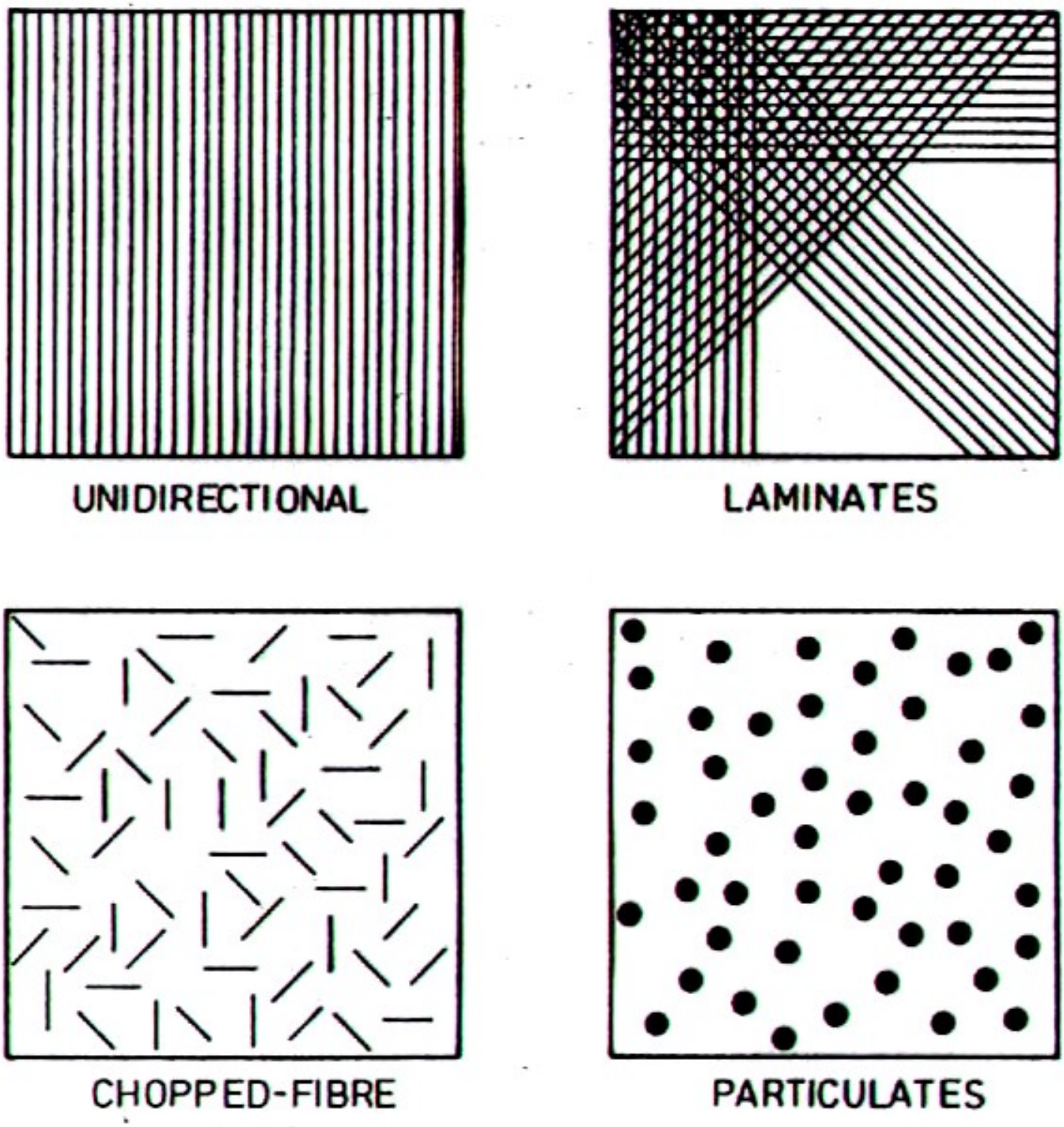

Fig. 2. Schematic of composites: unidirectional fibrous composite, laminated composite, chopped-fibre composite, and particulate composite. Bounds and limits, assembled in Section 4, bracket the properties of all of these.

Density & Elastic modulus

Assumng no reactions between matrix and reinforcement

$$\rho = F\,\rho_r + (1\text{-}F)\,\rho_m$$

r : reinforcement
m : matrix
f : volume fraction

rule of mixtures

<u>modulus</u>

$$E_u = F\,E_r + (1\text{-}F)\,E_m$$

u : upper bound

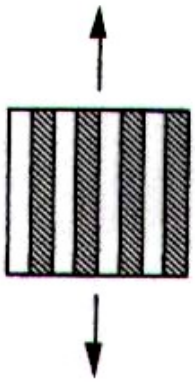

$$E_l = (E_m\,E_r)/\,[F\,E_m + (1\text{-}F)\,E_r]$$

l : lower bound

$$\frac{1}{E_l} = \frac{1-F}{E_m} + \frac{F}{E_f}$$

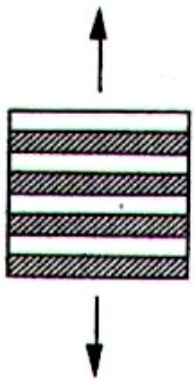

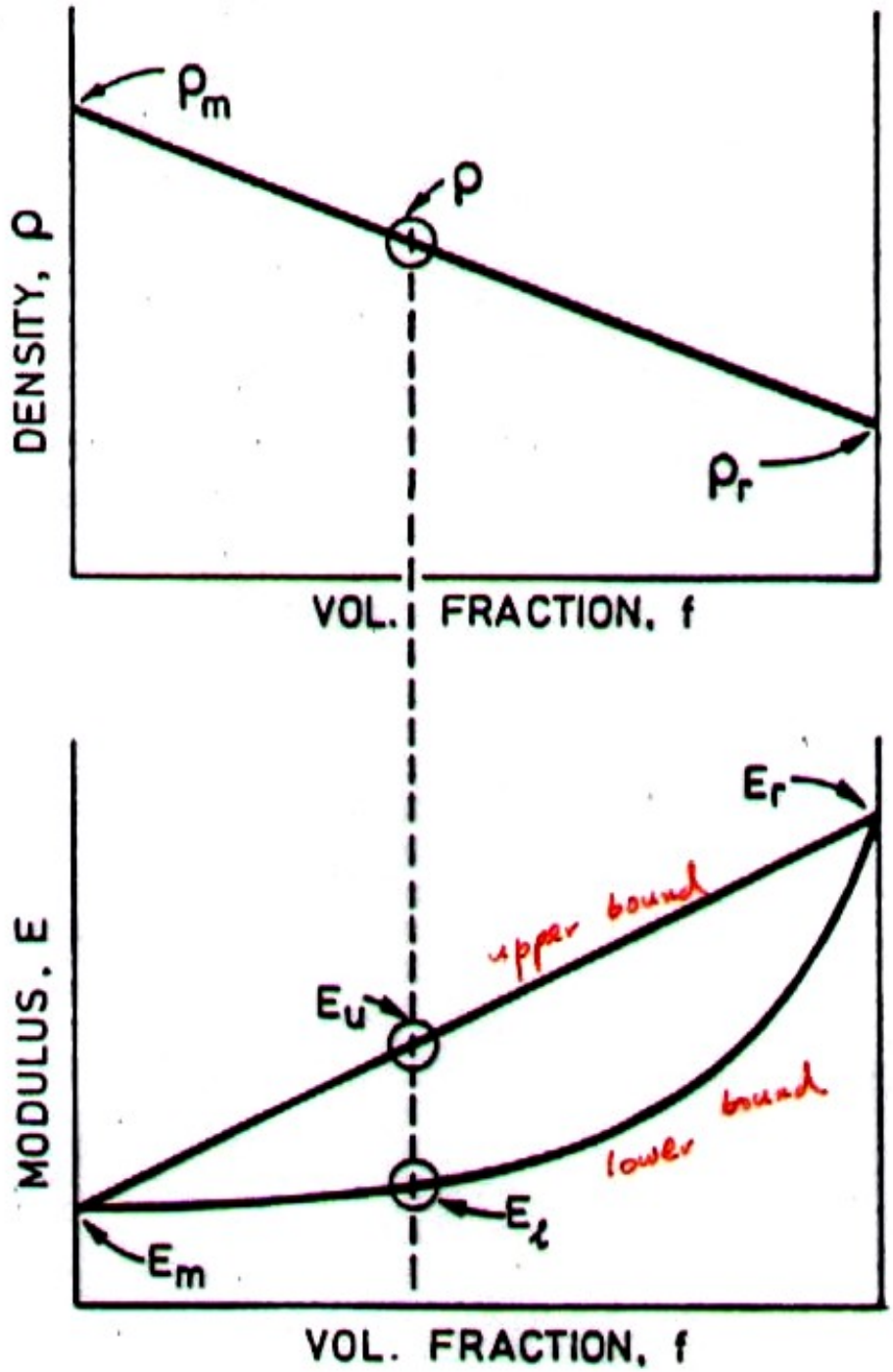

$\rho = f\,\rho_r + (1-f)\,\rho_m$

$E_u = F\,E_r + (1-F)E_m$

$1/E_l = (1-F)/E_m + F/E_r$

Fig. 6. For a given density, there exist two values of modulus: an upper bound, derived from equation (4), and a lower bound, from equation (5).

Hardness

For hardness, the upper bound, H_u, is obtained by applying the rule of mixtures [Ashby],

$$H_u = F\,H_i + (1-F)\,H_m \qquad (1)$$

where F is the volume fraction, H_i and H_m the hardness of inclusion and of matrix, respectively. The lower bound, H_l, is

$$H_l = \frac{H_i\,H_m}{F\,H_m + (1-F)\,H_i} \qquad (2)$$

$$1/H_l = (1-F)/H_m + F/H_i$$

Strength

The composite is strongest if both constituents reach their failure state at the same time. Thus the upper bound, σ_u, can be estimated with the rule of mixtures [Ashby]

$$\sigma_u = F\,\sigma_i + (1-F)\,\sigma_m \qquad (3)$$

where σ_i and σ_m are the strength of inclusion and of matrix, respectively. The lower bound, σ_l, is estimated for the worst case as[Ashby],

$$\sigma_l = \sigma_m \left[1 + \frac{F^{0.5}}{16\,(1-F^{0.5})}\right] \qquad (4)$$

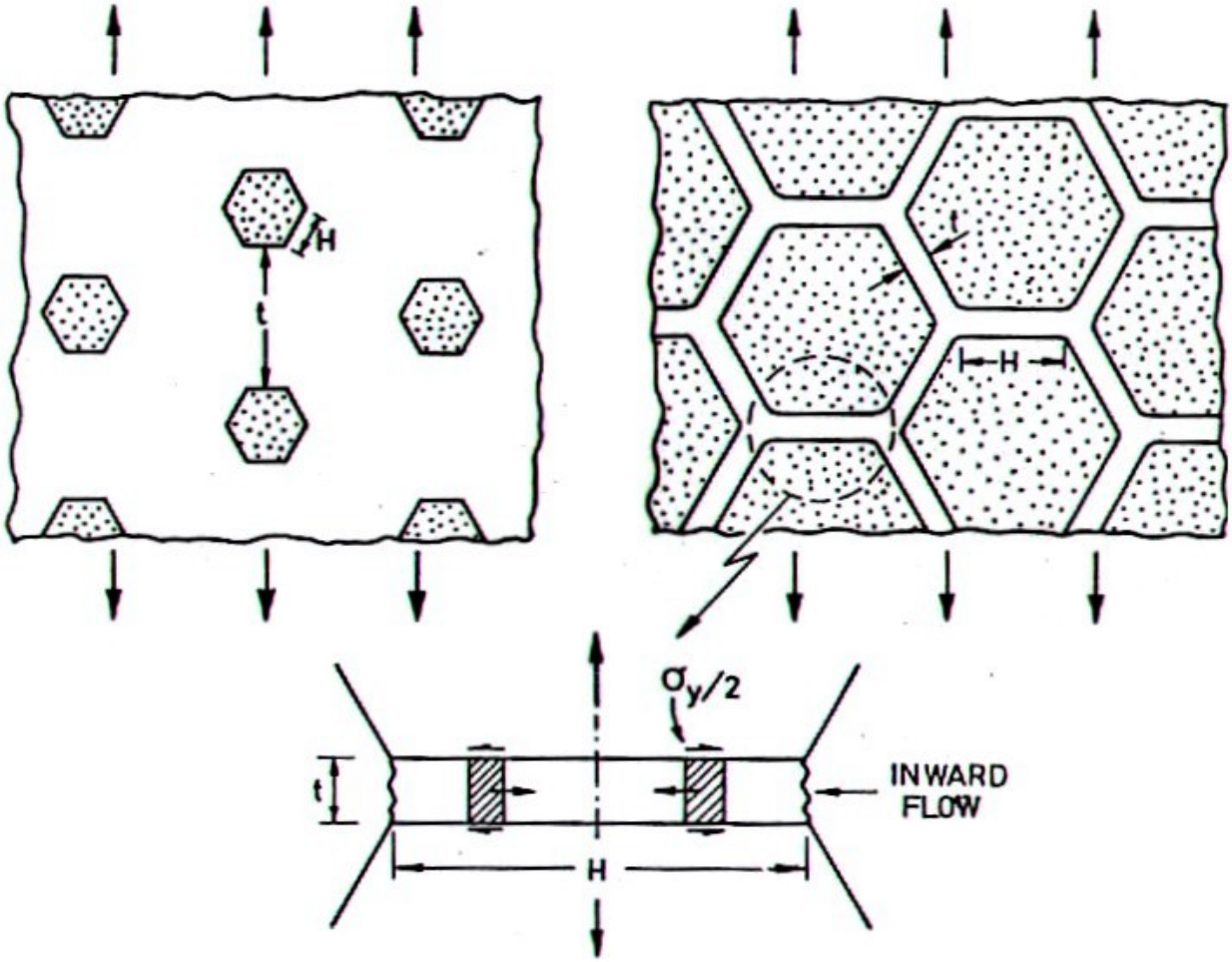

Fig. B1. The basis of the lower-limit calculation of strength. Plastic constraint of the softer phase by the harder one raises the stress required for general plasticity in the softer phase.

toughness

The upper and lower bounds for the toughness are also estimated from the best case and worst case [Ashby], respectively. The lower bound, $(J_{IC})_l$, is

$$(J_{IC})_l = (J_{IC})_m \left[\frac{(1 + 2F)^{0.5}}{1 - F^{0.5}}\right] \qquad (5)$$

where $(J_{IC})_m$ is the toughness of matrix. The upper bound, $(J_{IC})_u$, is

$$(J_{IC})_u = F\,(J_{IC})_i + (1-F)(J_{IC})_m + \left[\frac{F(1-F)E_i}{40}\right]^2 \frac{\pi a^*}{E_u} \qquad (6)$$

where $2a^*$ is the length of the maximum acceptable crack in the component, 2 mm is used in the calculations. E_i is the elastic modulus of inclusion, Eu is the upper bound of elastic modulus which can be estimated with the rule of mixtures.[Ashby] The first and the second terms on the right of eq.(6) are the contribution provided by the inclusion and by the matrix, respectively. The last term is the plastic deformation energy absorbed by the bridged inclusion. Fracture toughness, K_{IC}, can be related to J as

$$K_{IC} = (E J)^{0.5} \qquad (7)$$

Worst case

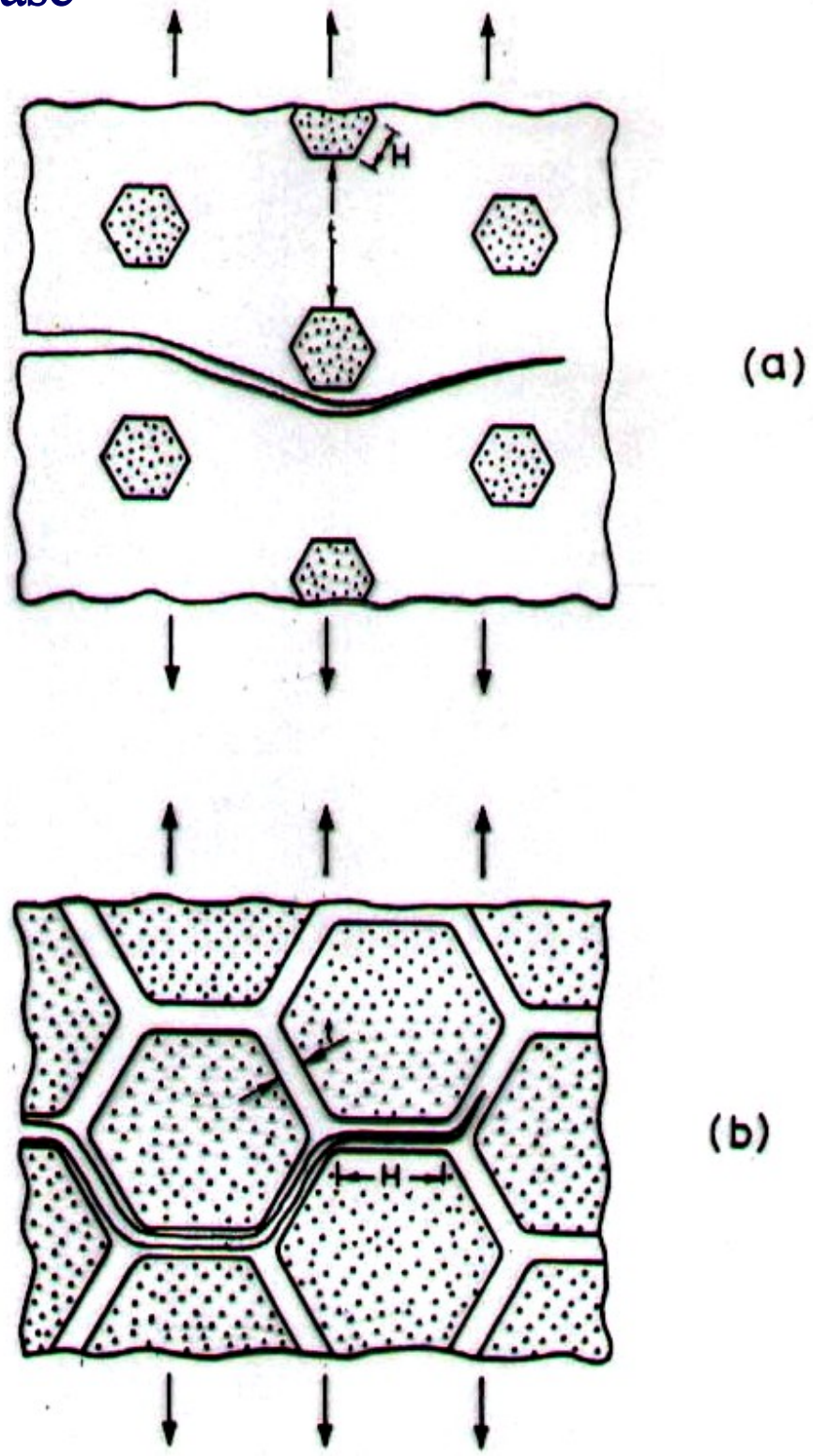

Fig. B2. The basis of the lower-limit estimate for toughness. The crack propagates entirely in the phase of lower toughness. The apparent toughness increases slowly with volume fraction because of increasing area, and because of an

Best case

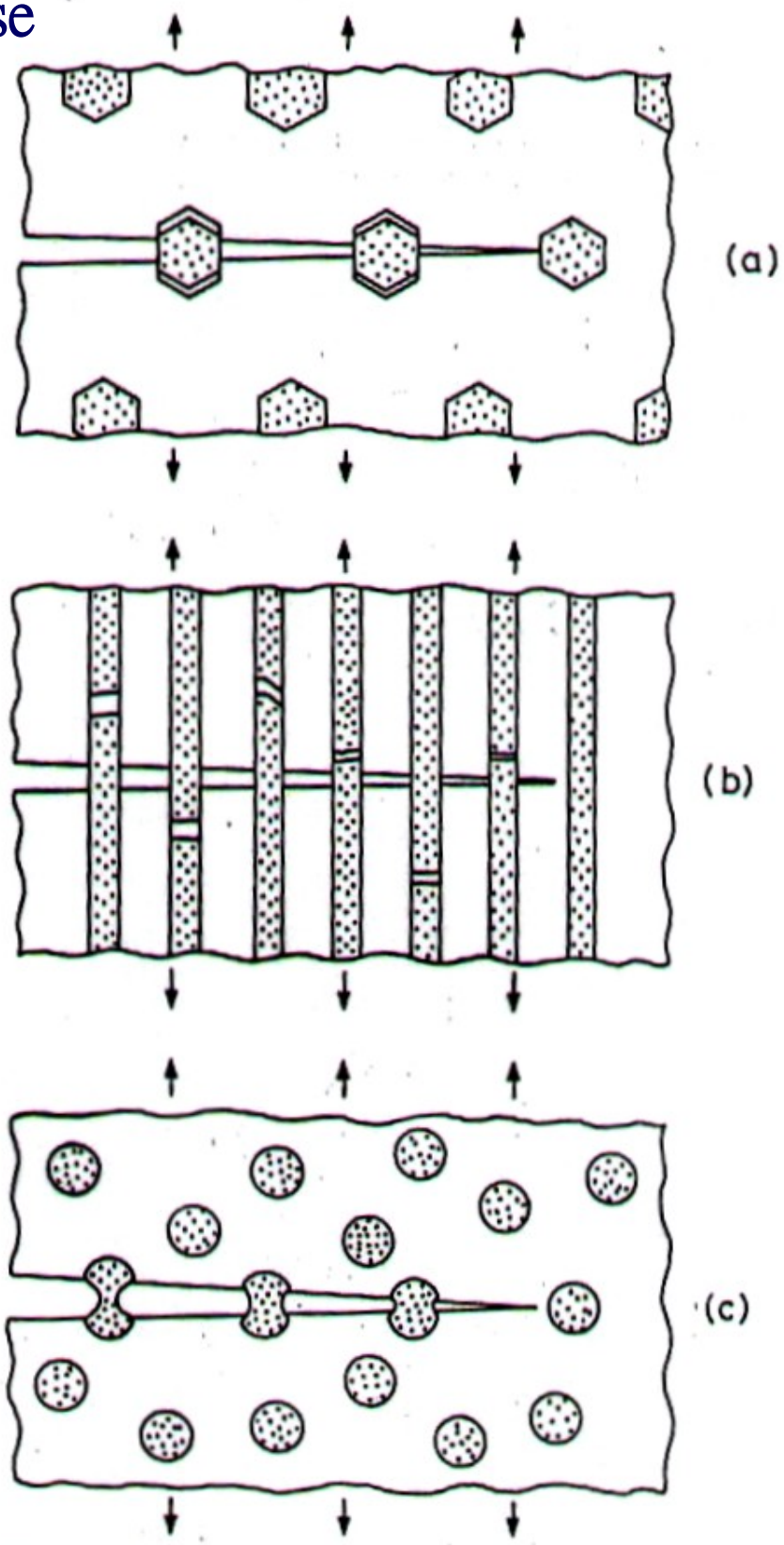

Fig. B3. The basis of the upper-limit estimate for toughness. The crack, propagating in the continuous phase is bridged by ligaments of the discontinuous one. Work of pull-out or

Design sequence of composites

Performance indices

Materials selection charts

Properties bounds for composites

Composite design

Composite Design
for stiffness at minimum weight

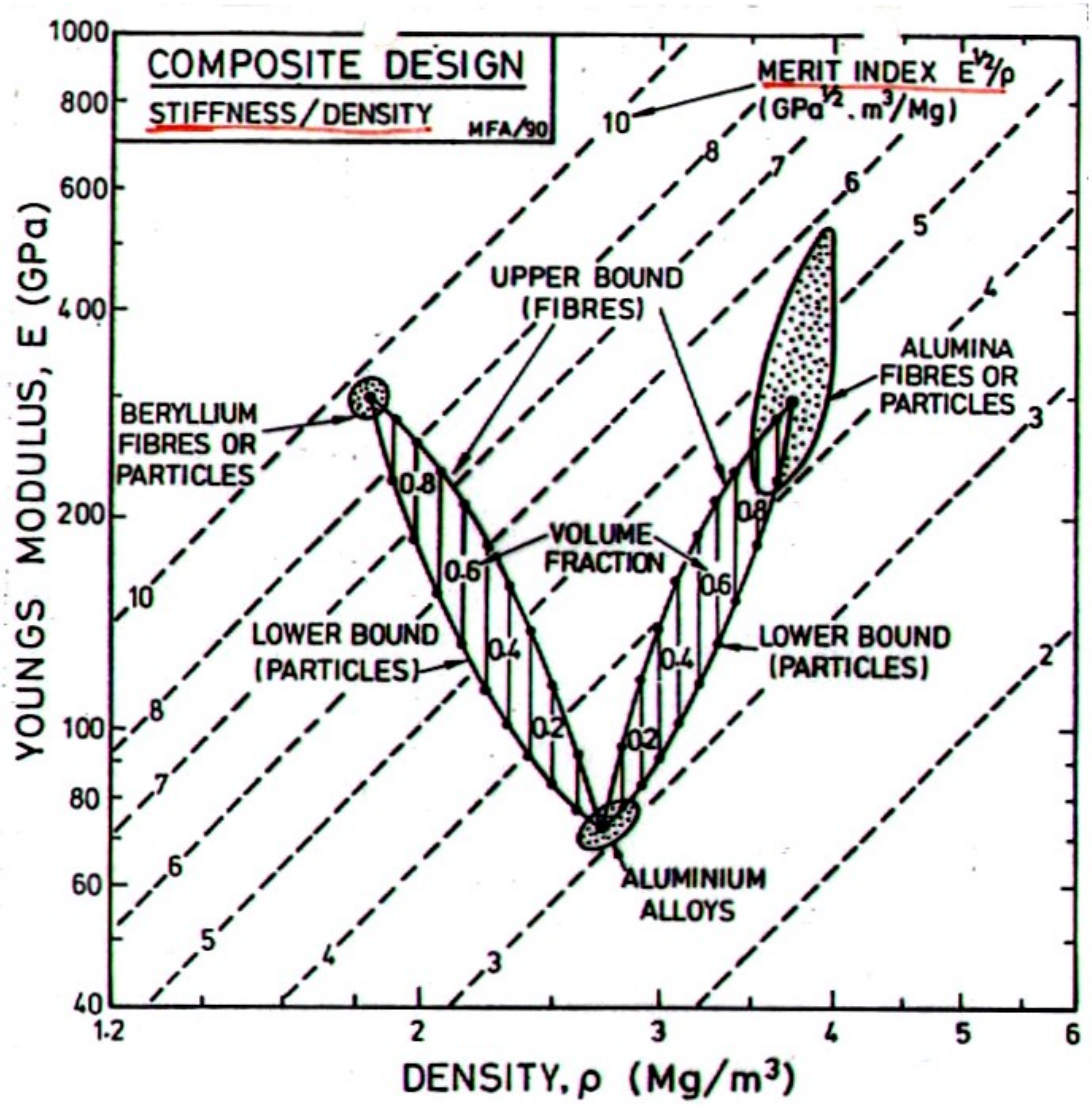

Fig. 5. A small part of modulus-density space, showing aluminium alloys, beryllium and alumina. The moduli of Al–Be and Al–Al_2O_3 composites are bracketted by the bounds described by equations (3)–(5). The Al–Be composite offers much greater grains in M_2 than the Al–Al_2O_3 composite.

Example:Al-Al2O3

Al-Be

At F=0.4

Al-0.4Al2O3 M_2=3.5-4

Al-0.4Be M_2=4.7-4.9

Example

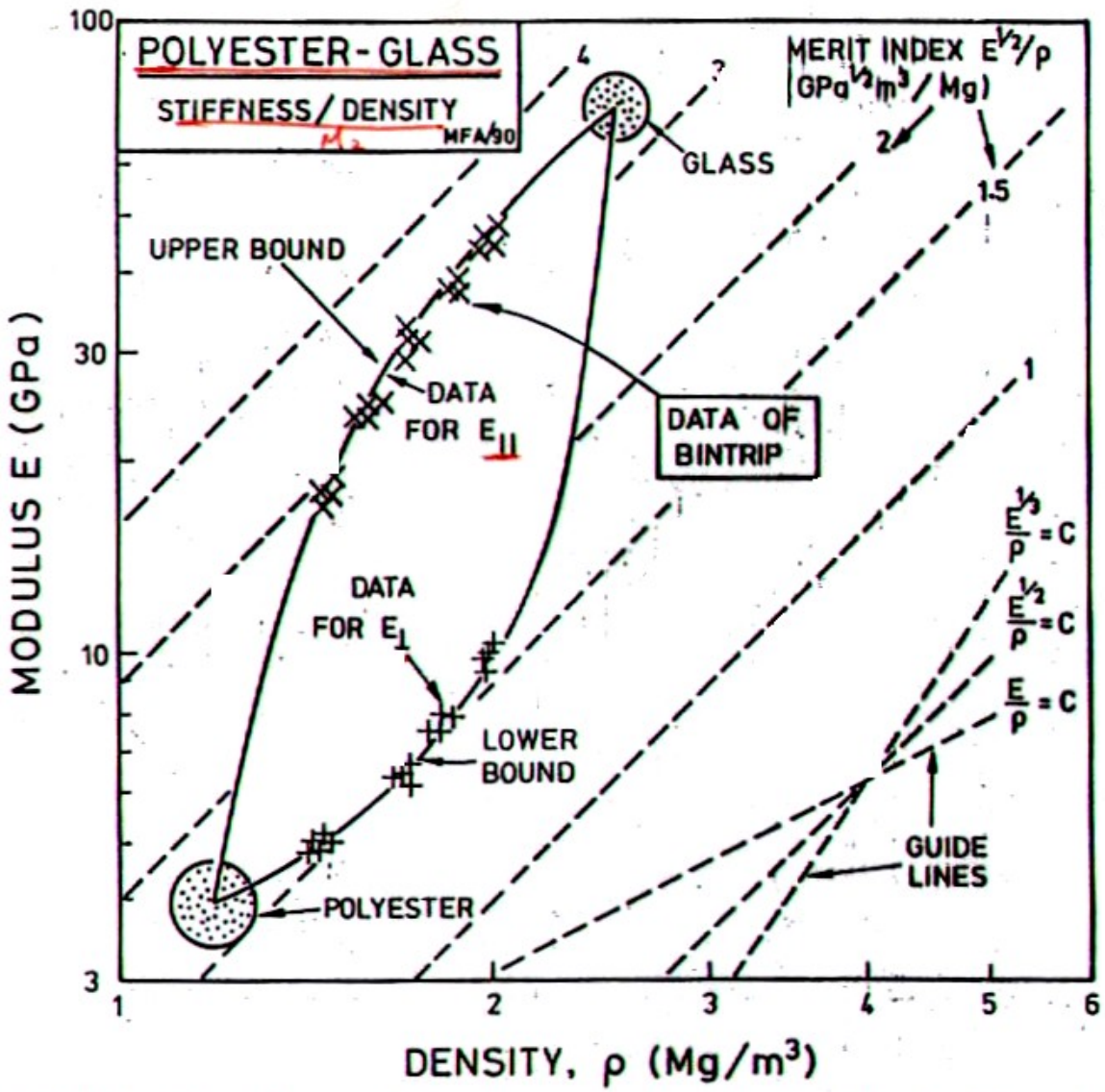

Fig. 7. Data for Young's modulus, parallel and perpendicular to the fibre direction, for a unidirectional polyester–glass composite. The data, from Bintrup [25], lie on the two bounds.

E_{11}:longitudinal model

$E_{\perp}$:tranverse model

Example

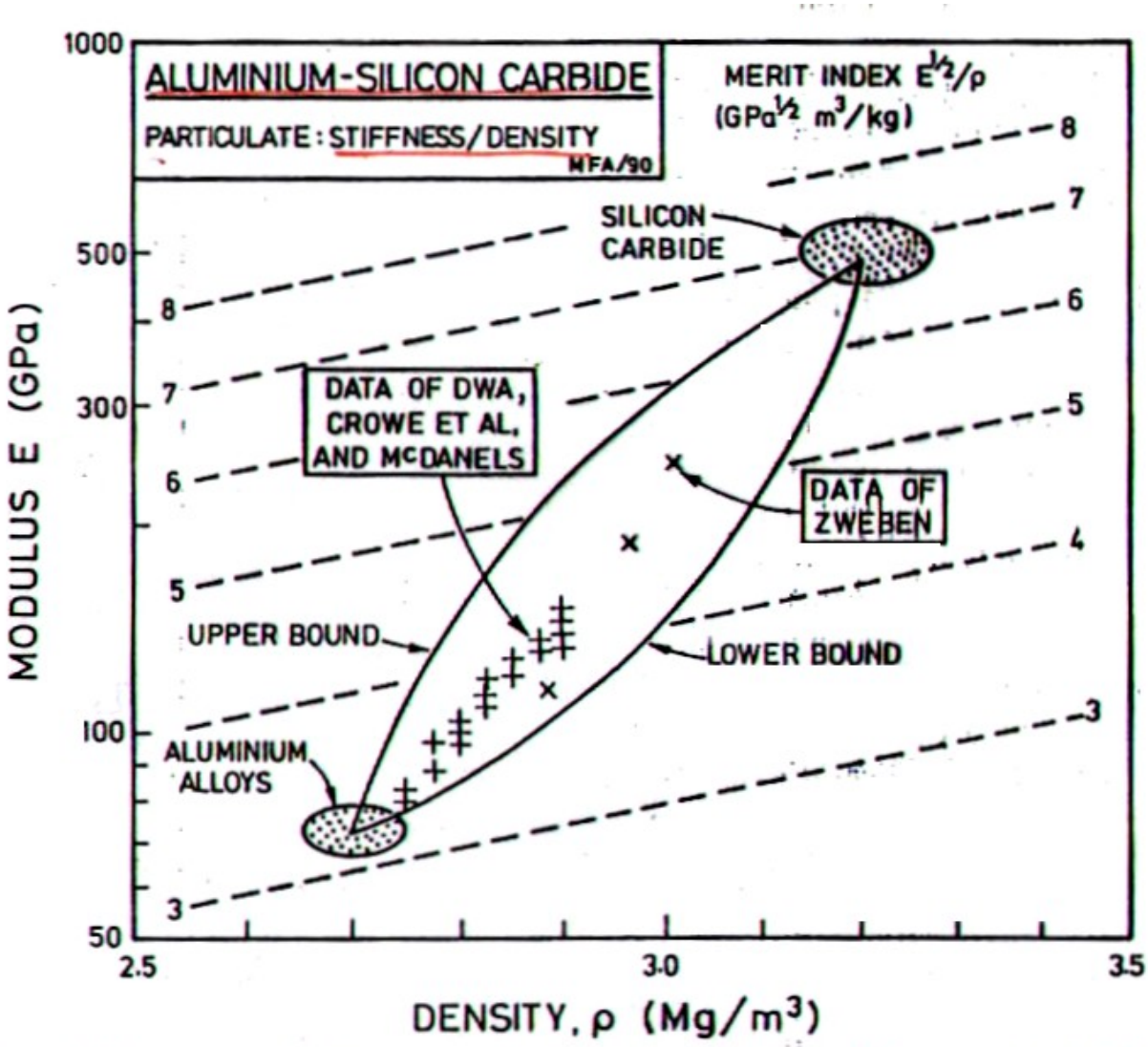

Fig. 8. Data for Young's modulus for a particulate aluminium–silicon carbide composite. The data, from Crowe *et al.* [26], McDanels [27], DWA [28] and Zweben [29], lie between the bounds.

Example:Al-SiC

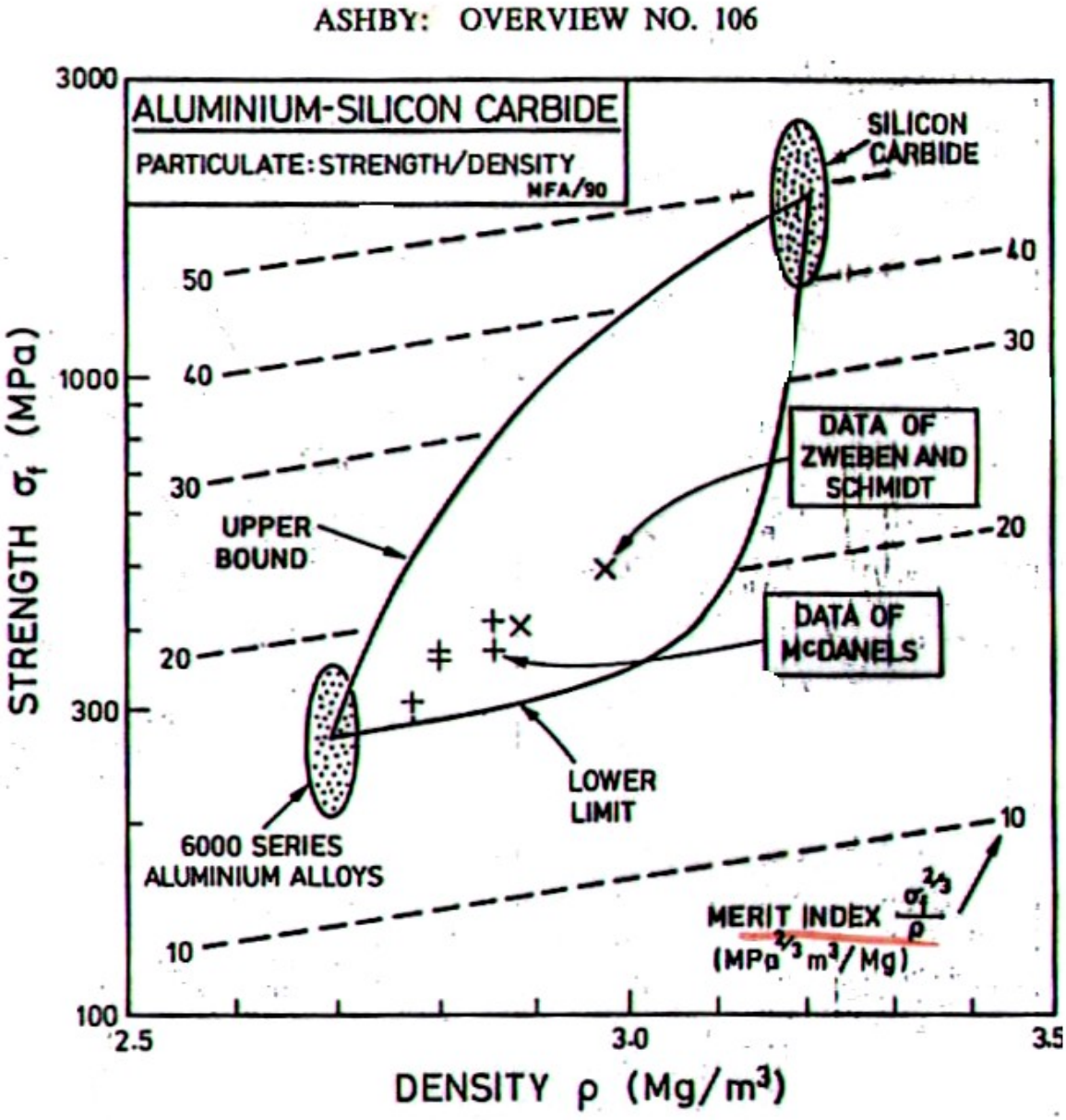

Fig. 11. Data for the yield strength of 6061 aluminium alloy reinforced with particulate SiC. The data from McDanels [27] and Zweben and Schmidt [30] are enclosed by the limits.

Composite design for specific thermal properties

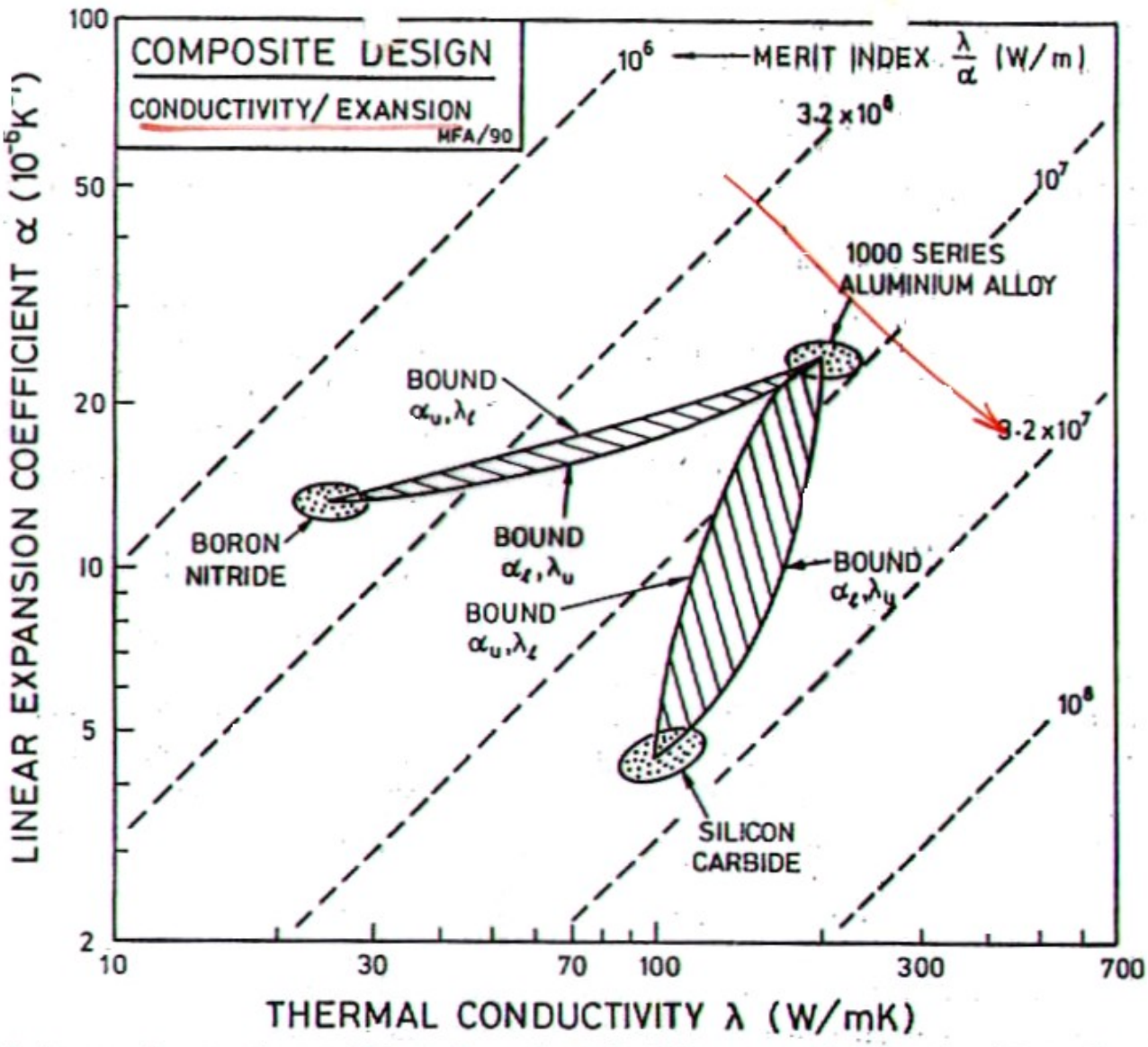

Fig. 14. A part of expansion coefficient–thermal conductivity space, showing aluminium alloys, boron nitride and silicon carbide. The properties of Al–BN and Al–SiC composites are bracketed by the bounds described by equations (9)–(12). The Al–SiC composites have better values of the merit index M_{10} (which increases towards the bottom right) than the Al–BN composites.

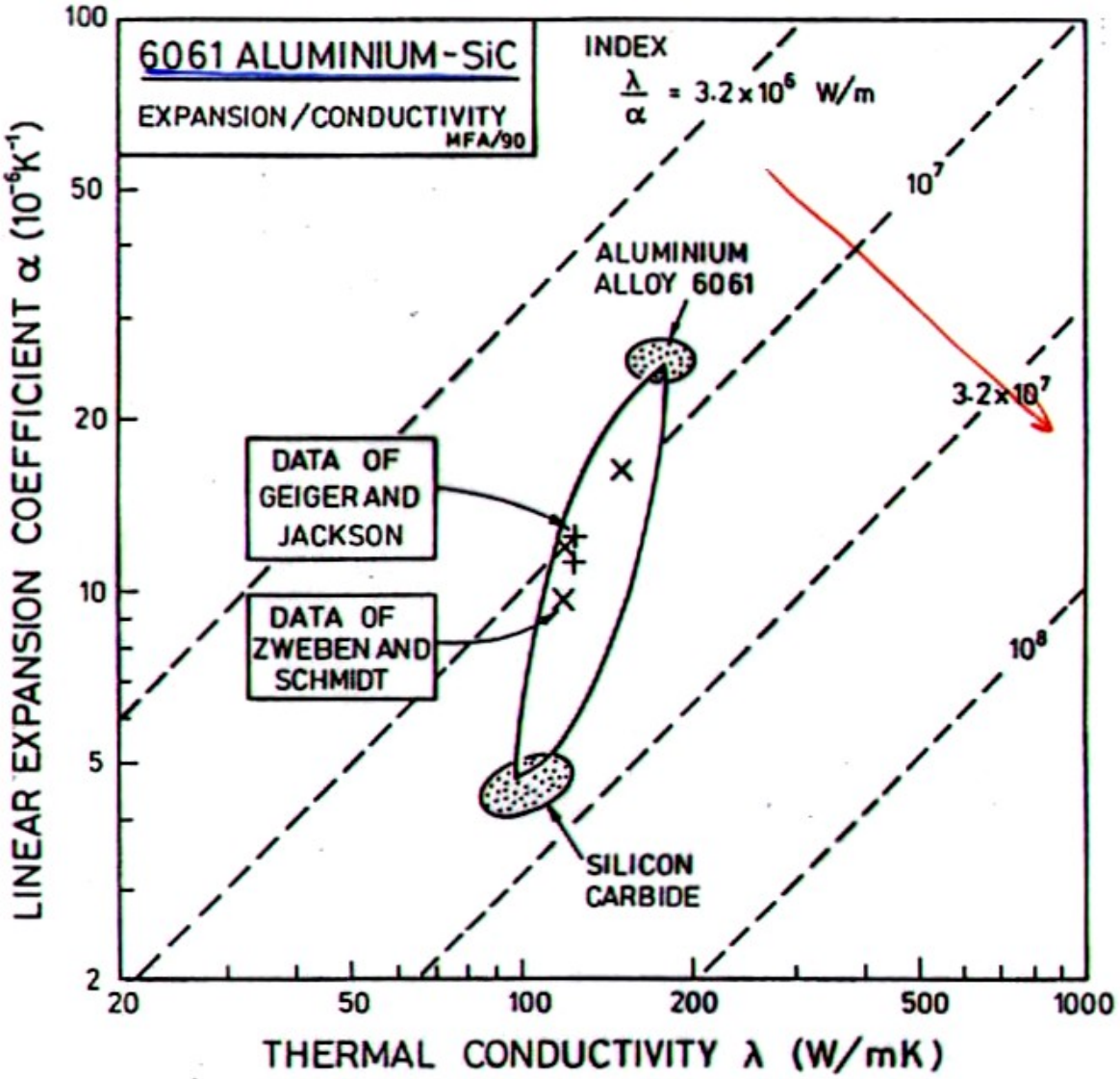

Fig. 15. Data for the thermal expansion and conductivity of 6061 aluminium reinforced with particulate silicon carbide. The data, from Geiger and Jackson [32] and Zweben and Schmidt [30] lie within the bounds.

Application:
Example 1: Mg-based composite (light, stiff structure)

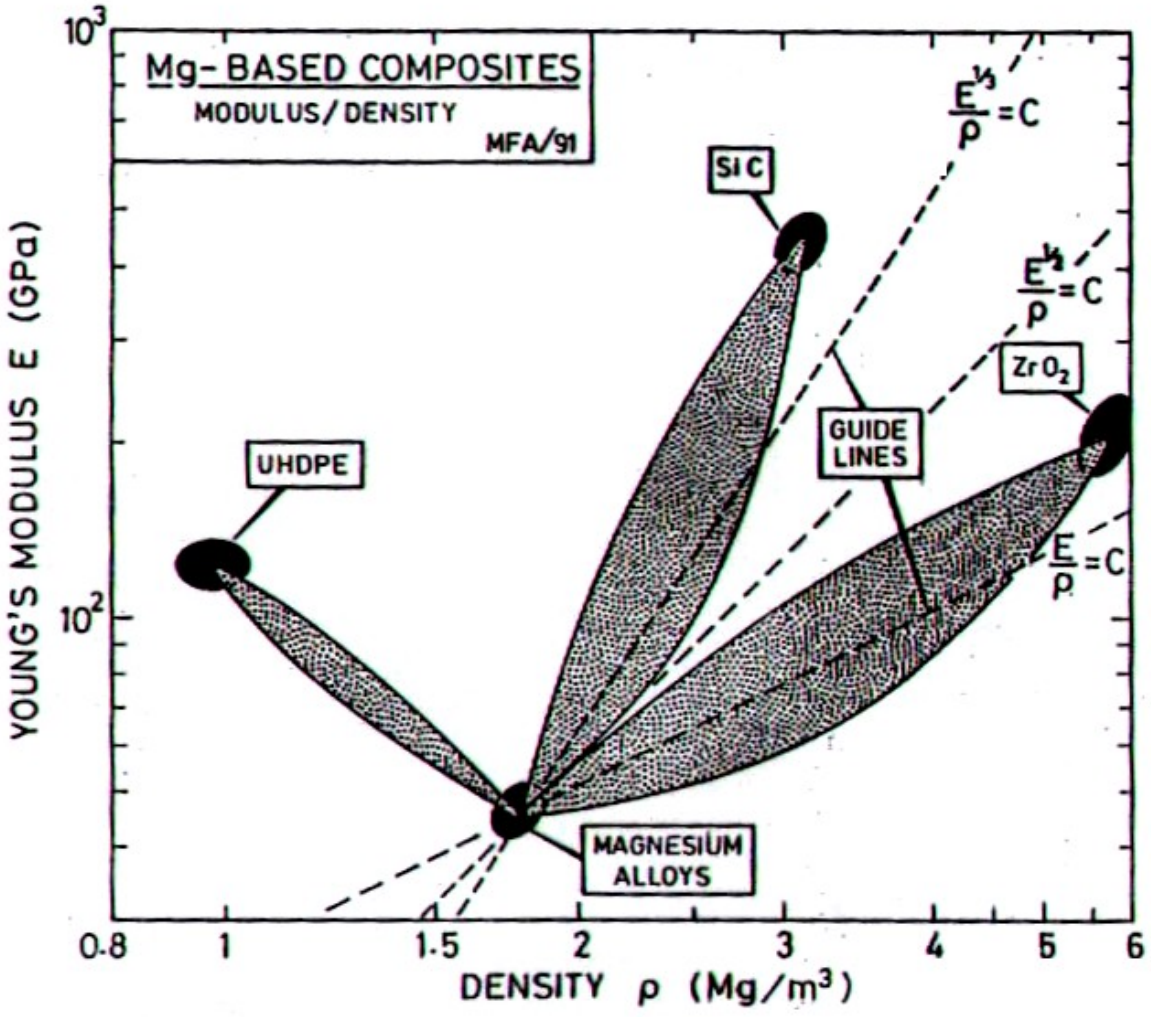

Fig. 21. Part of the E–ρ diagram, illustrating the potential of three magnesium-based composites. The property envelopes are constructed from the bounds of equations (3)–(5).

Example: Mg matrix composite for minimum thermal distortion

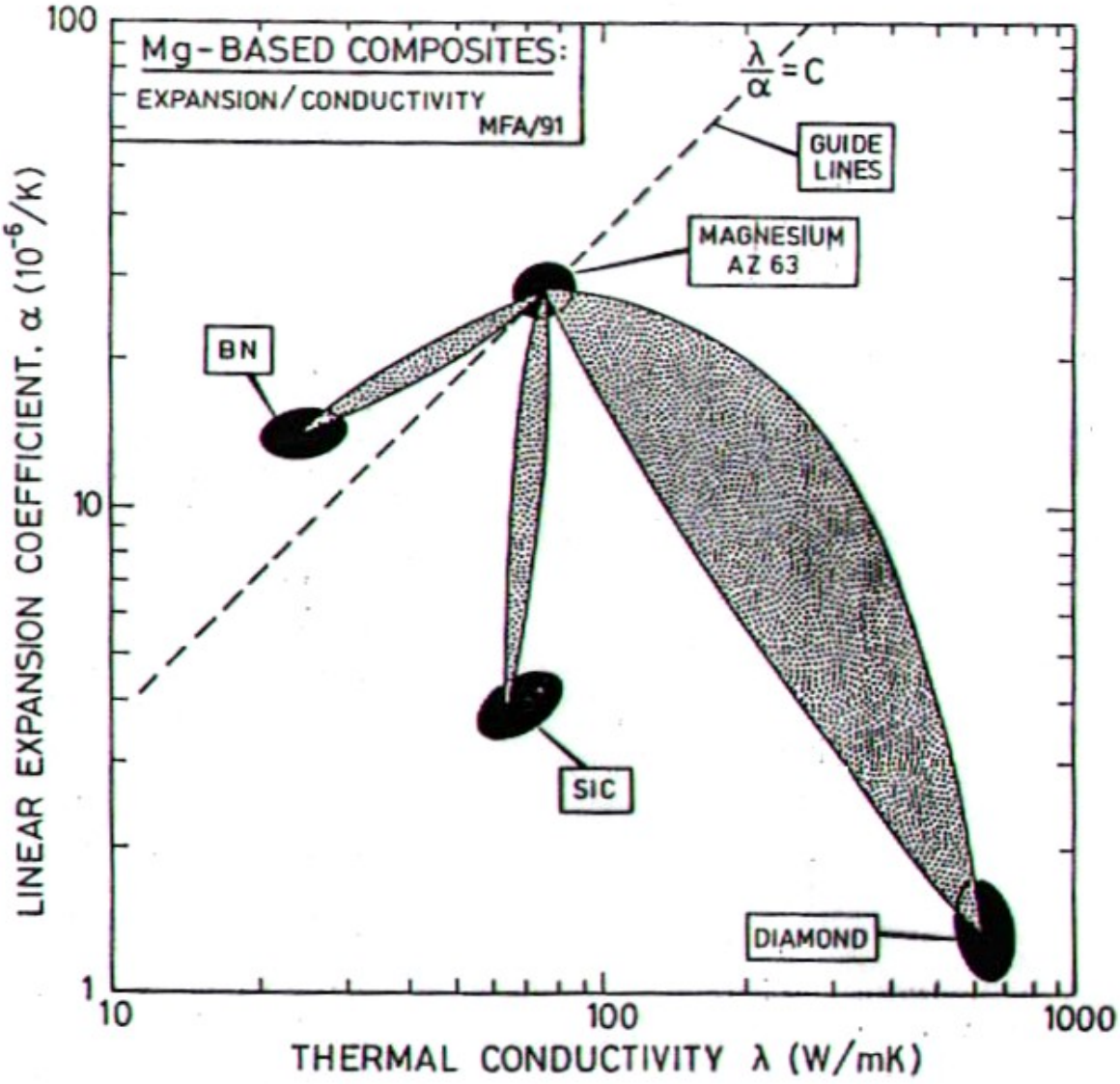

Fig. 24. Part of the α–λ diagram, illustrating the development of magnesium-based composites to resi thermal distortion. The property envelopes are constructed from the bounds of equations (9)–(12).

Another Important Application:
Finding the best uses for new composites

Table 3. Comparison of the performance of three alloys

Property	Aluminium (2124)	Al–SiC_p (20%)	Al–lithium (8090)
Density, ρ (Mg/m^3)	2.80	2.88 (+3%)	2.55 (−9%)
Modulus, E (GPa)	73	100 (+37%)	70 (0%)
Strength, σ_f (MPa)	425	510 (+20%)	475 (+12%)
T-expansion, α (10^{-6}/K)	24	10 (−58%)	25 (+4%)
T-conductivity, λ (W/mK)	150	130 (−13%)	144 (−4%)
M_1 GPa/(Mg/m^3)	26.1	34.7 (+33%)	27.5 (+5%)
M_2 $GPa^{1/2}$/(Mg/m^3)	3.05	3.47 (+14%)	3.28 (+8%)
M_3 $GPa^{1/3}$/(Mg/m^3)	1.49	1.61 (+8%)	1.62 (+8%)
M_4 MPa/(Mg/m^3)	151	177 (+17%)	186 (+23%)
M_5 $MPa^{2/3}$/(Mg/m^3)	20.2	22.1 (+10%)	23.9 (+18%)
M_6 $MPa^{1/2}$/(Mg/m^3)	7.36	7.84 (+7%)	8.55 (+16%)
M_{10} 10^6 W/m	6.25	13 (+108%)	5.76 (−8%)

The application for composite with high M_{10} index: precision devices (hard disk drives, gyroscope, telescope)

Prof. Ashby

Materials Selection

Materials and Design

Mike Ashby, Kara Johnson

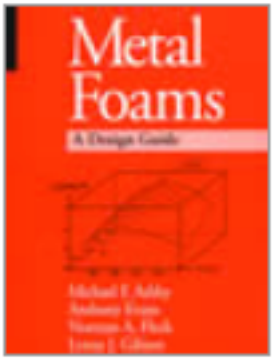

Metal Foams - A Design Guide

Professor Michael Ashby, Anthony Evans, Norman A Fleck, Lorna J Gibson, John W Hutchinson, Haydn N G Wadley

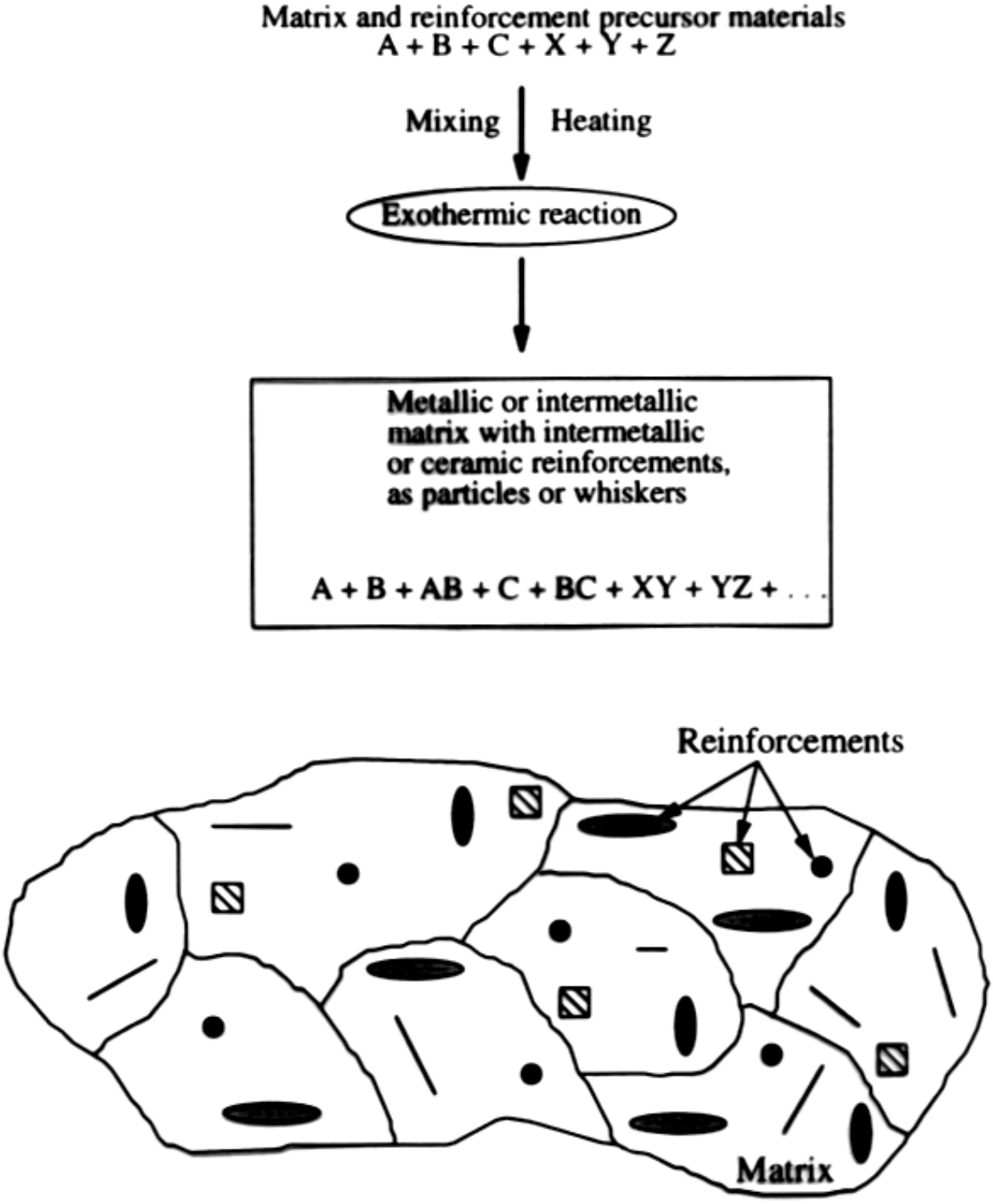

Fig. 4.17 Schematic of the XD™ process and the type of microstructure obtained (after [46]).

Unit 4-a

Processing -

Powder processing

Contents

- Powder processing vs. mechanical properties
  - Traditional powder processing
  - Powder mixing + hot pressing
  - Powder mixing + pressureless sintering
  - Powder mixing + HIP
- Examples
  - Al_2O_3/SiC_w, Si_3N_4/SiC_w, $TZP/Al_2O_{3platelet}$, $RBSN/SiC_{platelet}$, SiC/ZrB_2, $glass/SiC_f$
- Difficulties

Al_2O_3/SiCw composites – the 1st report

Al_2O_3 SiC_w

mixing

Hot-pressing

(2000C, 28-69MPa)

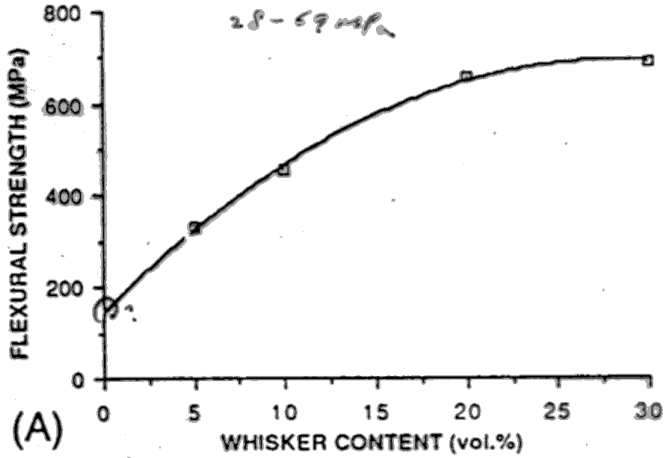

Fig. 1. Both flexural strength (A) and fractur
addition of SiC whiskers. Data are for hot-pres

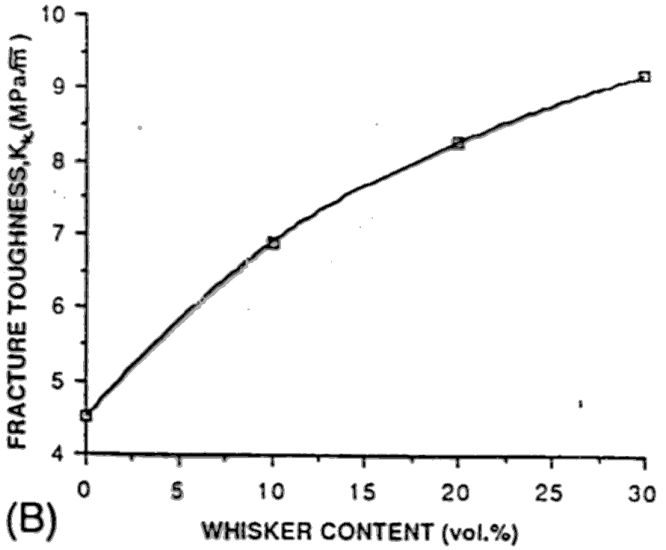

e toughness (B) of Al_2O_3 are increased with
sed composites.

Ref: Wei&Becher, Am. Ceram. Soc. Bull., 64(2) 298(1985)

Pressureless sintering of Al_2O_3/SiC_w composites

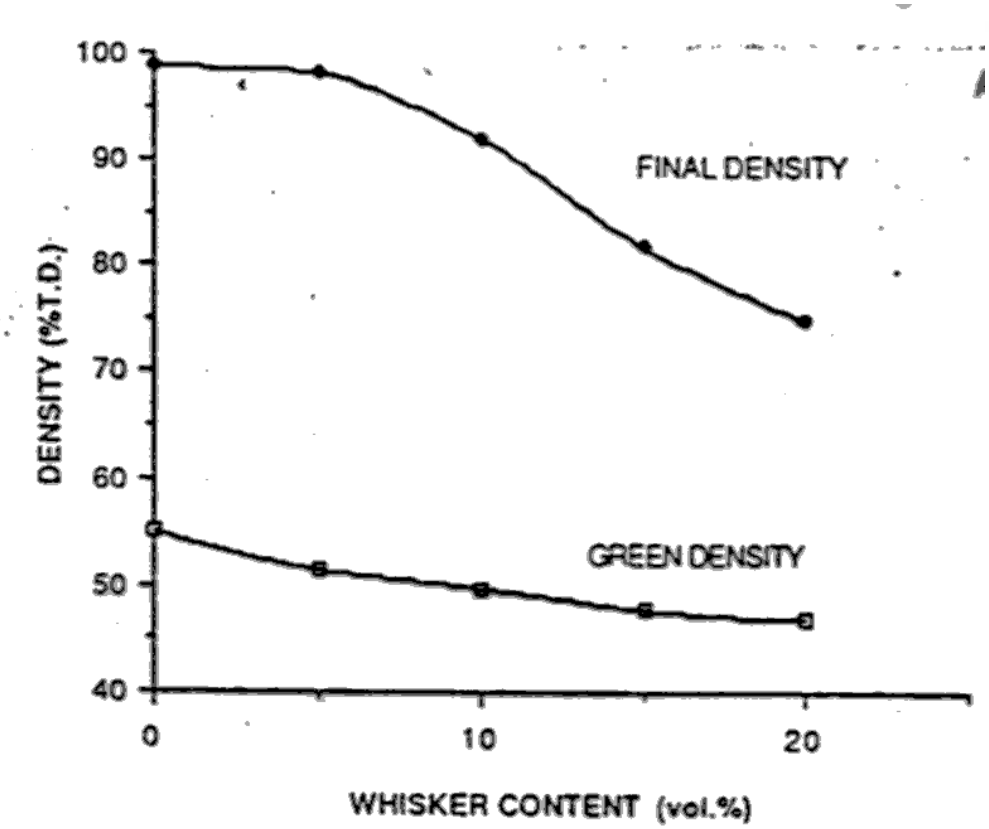

Fig. 2. Effect of SiC whiskers on densification of Al_2O_3 matrix composites using Baikowski CR-10 alumina, 2 wt% Y_2O_3, 0.5 wt% MgO, and no whisker aspect ratio modification

Ref: Tieg&Becher, Am. Ceram. Soc. Bull., 66, 339(1987)

Pressureless Sintering of composites

ZnO/SiC

SiC--12 μ m

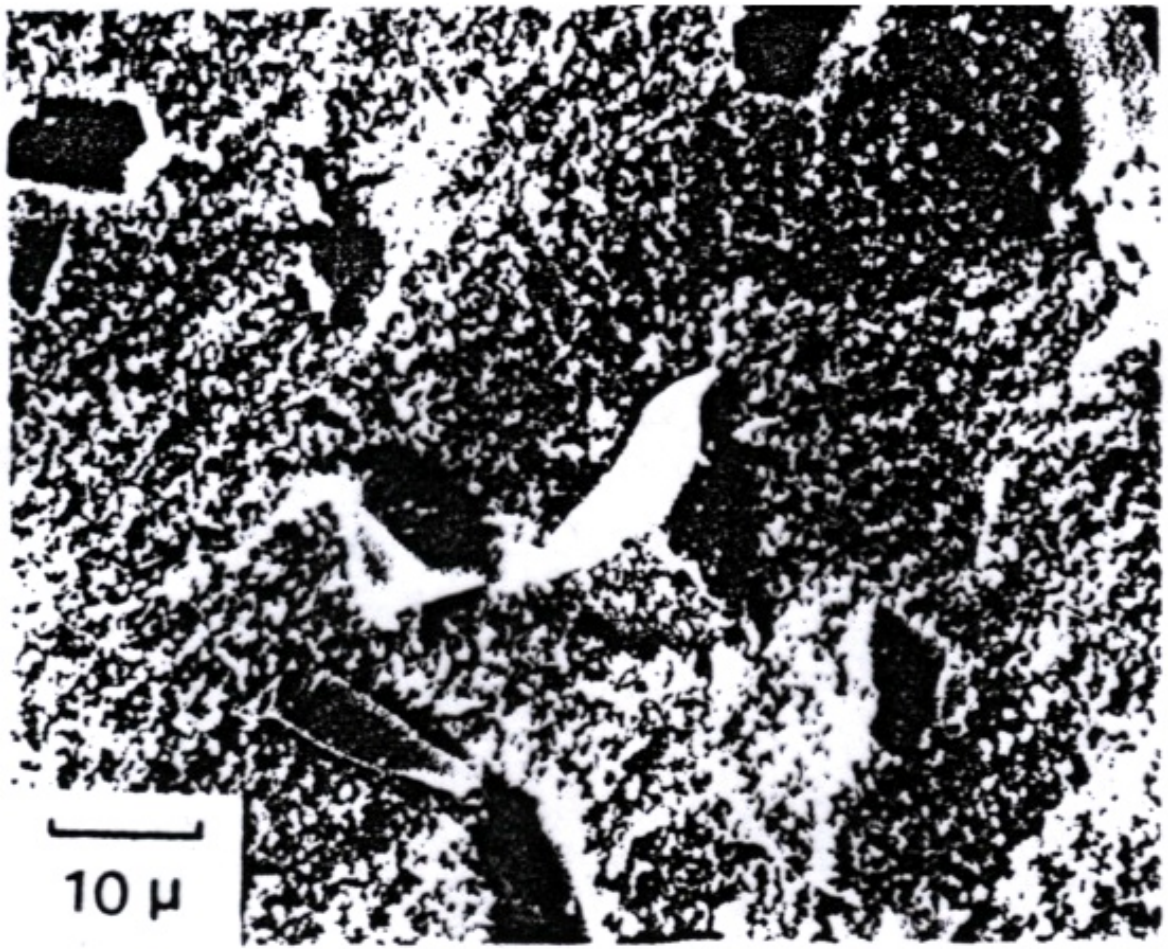

XBB 852-1420

Pressureless Sintering of composites

ex. ZnO+SiC,700^{0}C

De Jonghe, Acta Met, 34, 1467, 1986

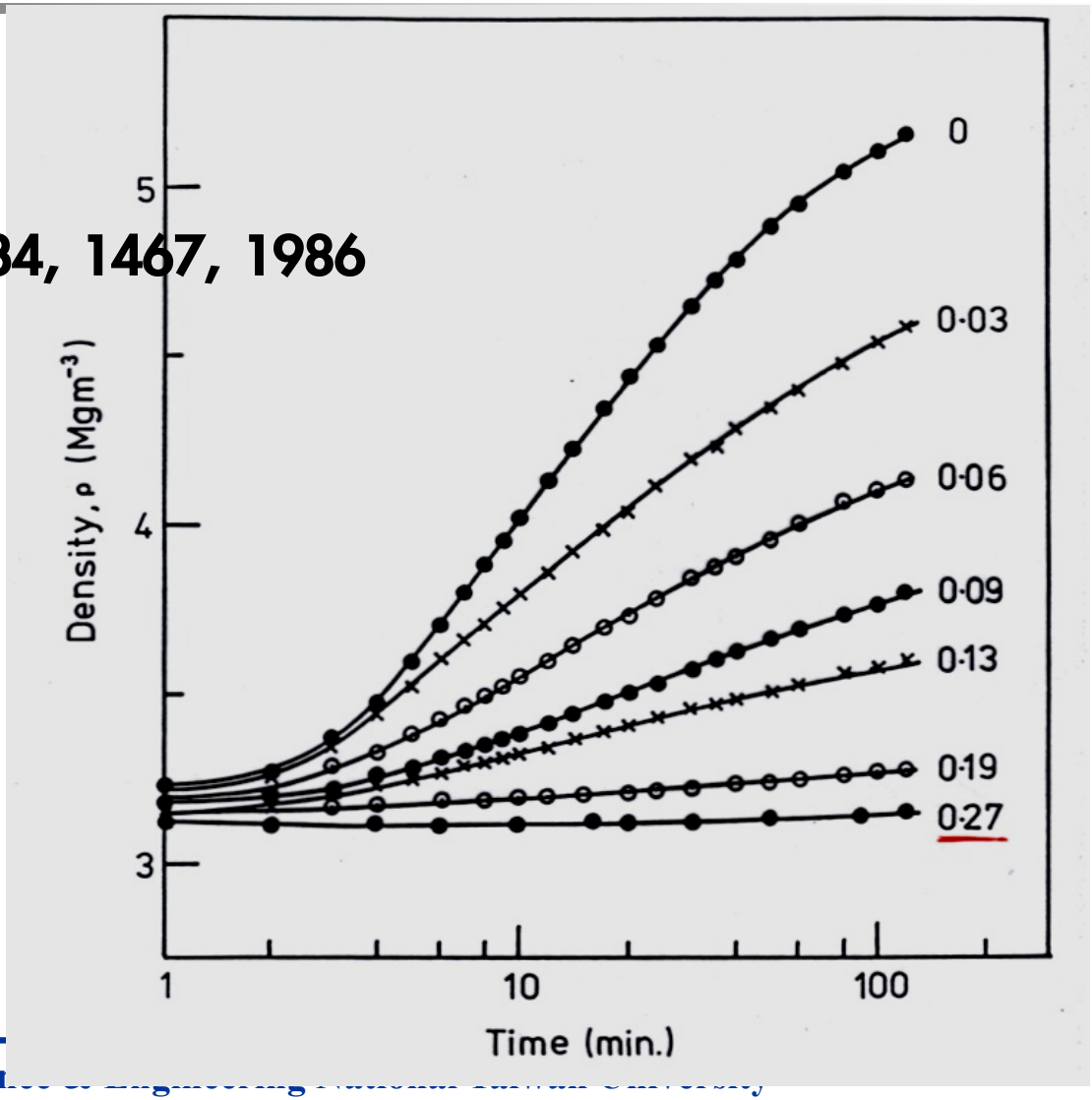

Si_3N_4/SiC_w composites

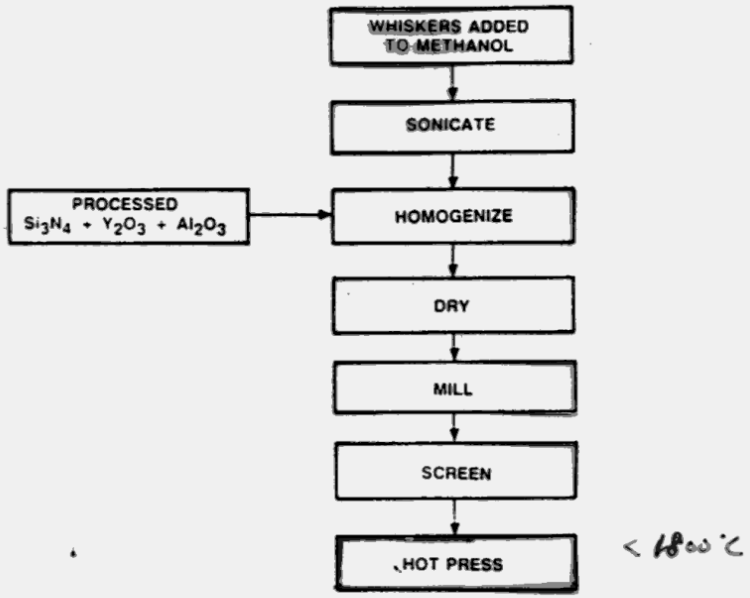

Fig. 1. Si_3N_4-SiC whisker composite process flow sheet.

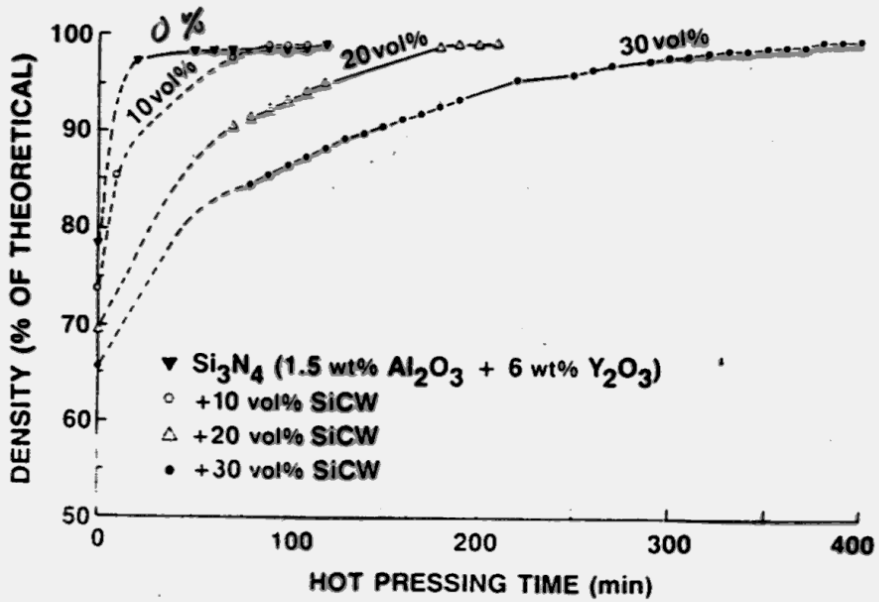

Fig. 2. Densification of Si_3N_4-based ceramics.

Ref: Buljian et al., Am. Ceram. Soc. Bull., 66, 347, 1987

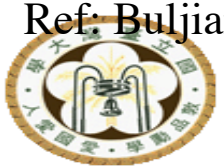

Si_3N_4/SiC_w composites

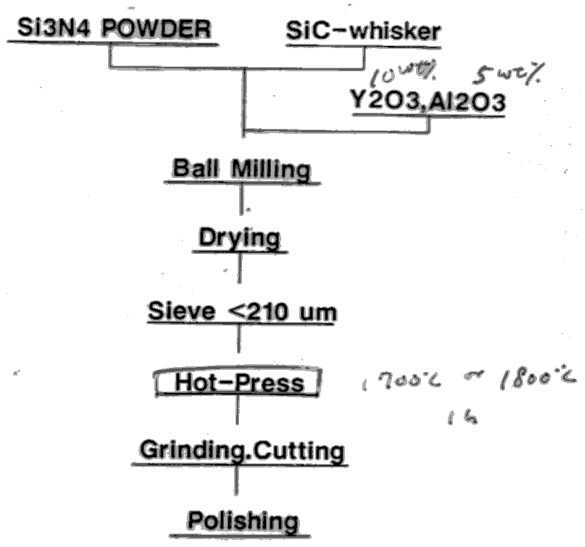

Fig. 1. Process for fabrication of SiC-whisker/SN composites.

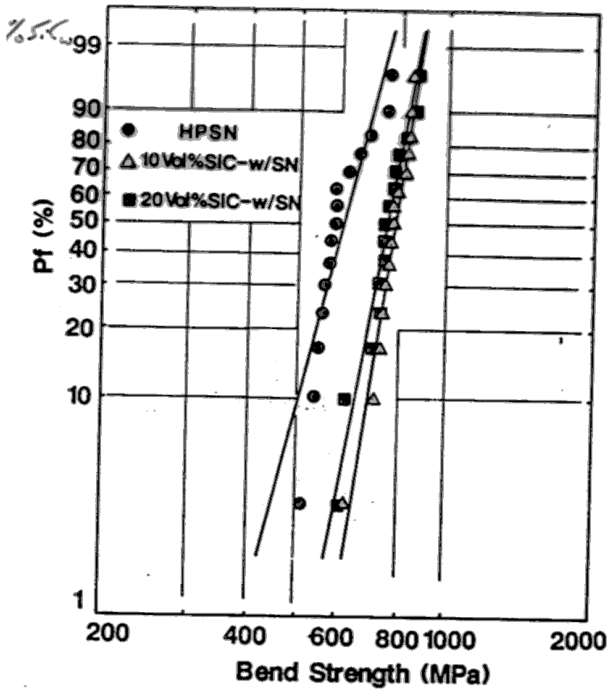

Ref: Akimune et al, J. Am. Ceram. Soc., 72, 791, 1989

Mechanical properties of Si_3N_4/SiC_w composites

	HP-Si_3N_4	HP-Si_3N_4/10%SiC_w
Strength / MPa	610	776
Toughness / $MPam^{0.5}$	4.7	5.8
Weibull modulus	9.3	15.7

Si_3N_4/SiC_w composites

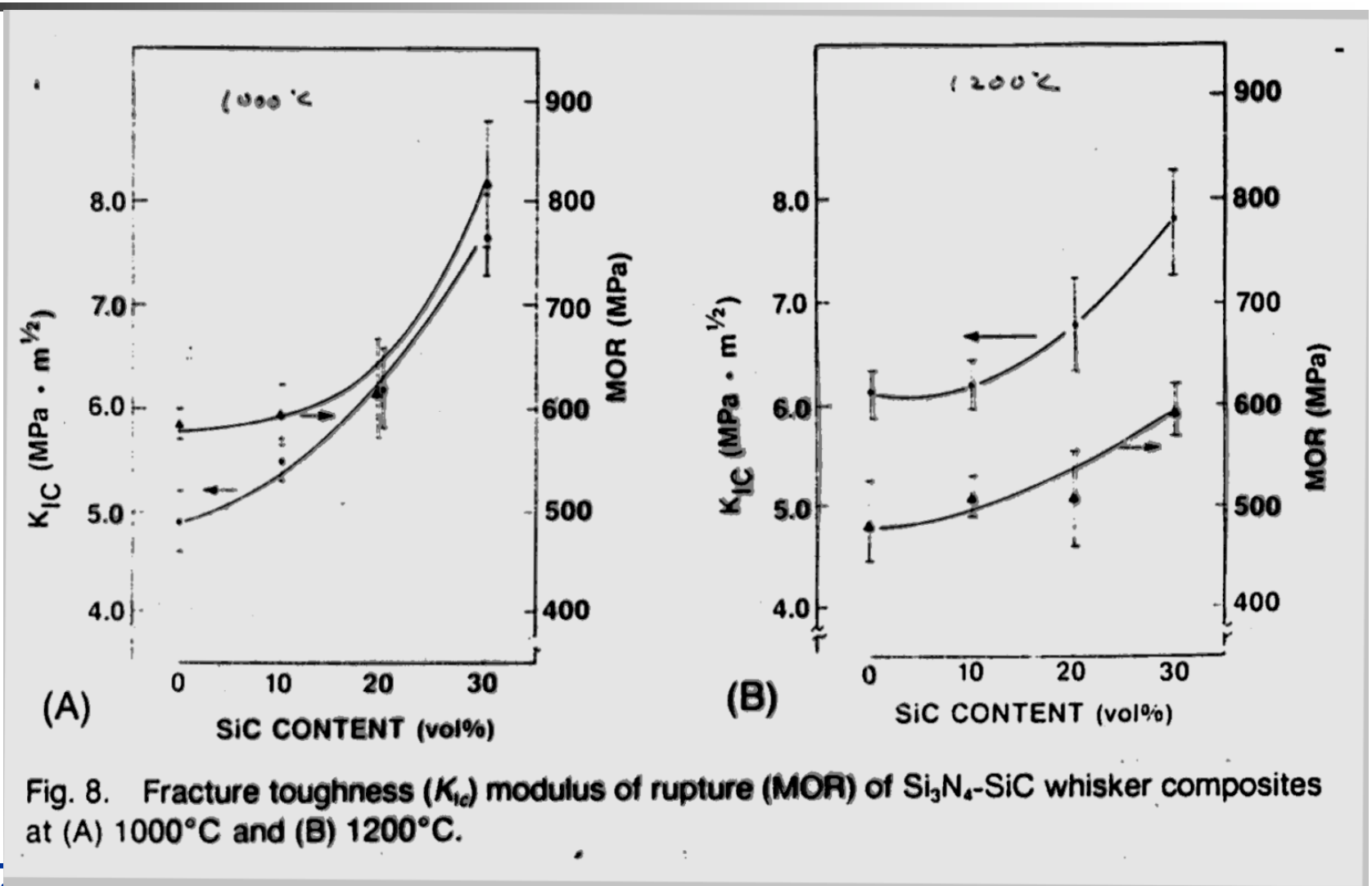

Fig. 8. Fracture toughness (K_{Ic}) modulus of rupture (MOR) of Si_3N_4-SiC whisker composites at (A) 1000°C and (B) 1200°C.

Difficulties involved in the manufacturing of CMC (powder processing)

- Mixing
- Hazardous substance: SiC_w
- Densification limit
- Relative instability of many reinforcements

Difficulty in mixing

Example: glass+SiC_w

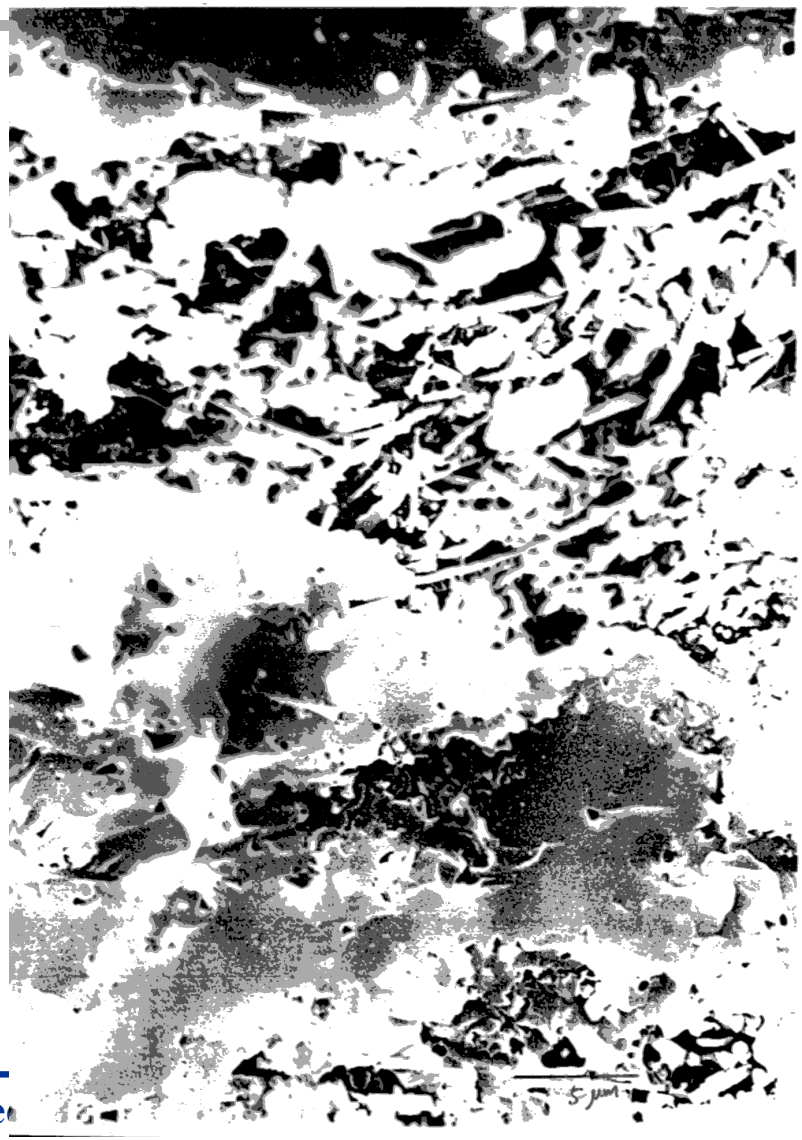

Toxicity of SiC whisker

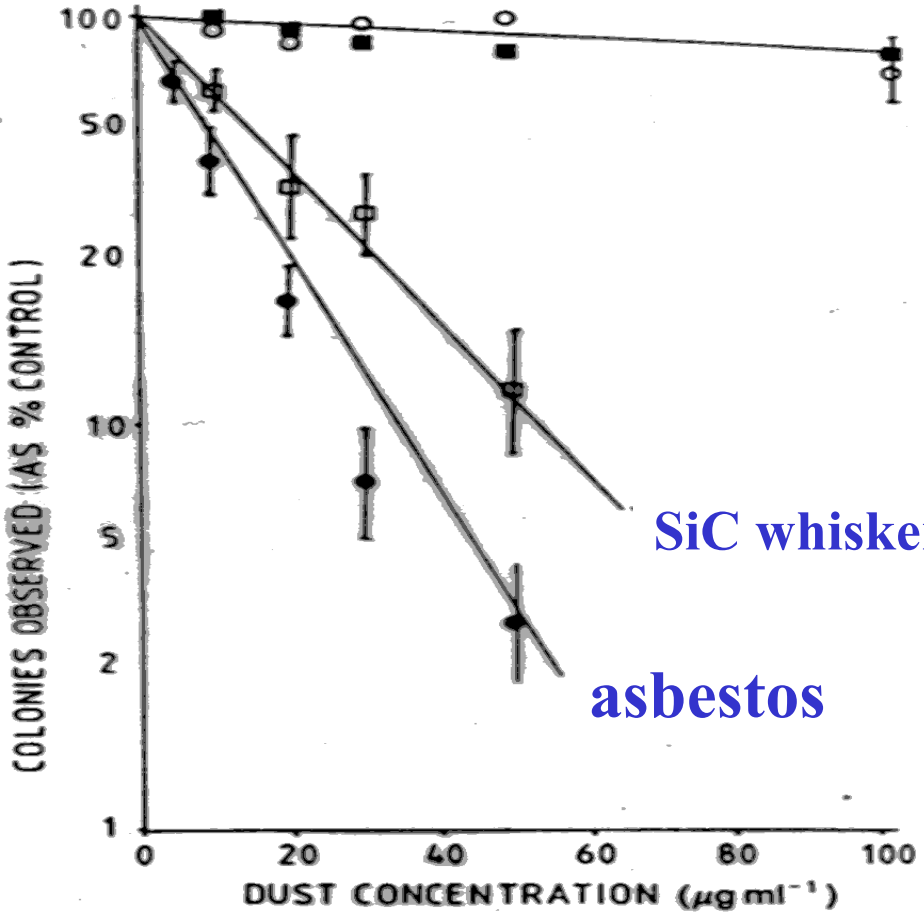

Al_2O_3 fibre

SiC powder Φ: 0.4 μm

SiC whisker, Φ : 0.05μ m

asbestos

Figure 3 Cytotoxicity of SiC whiskers expressed as the percentage survival of cells in response to dust exposure. (■) Saffil, (●) UICC crocidolite, (○) SiC powder, (□) SiC whiskers.

alternatives

- Whisker with larger diameter
- Platelet

- However, whisker addition can provide only **marginal** enhancement on toughness!!!

Thermal degradation of Nicalon™ SiC fibre

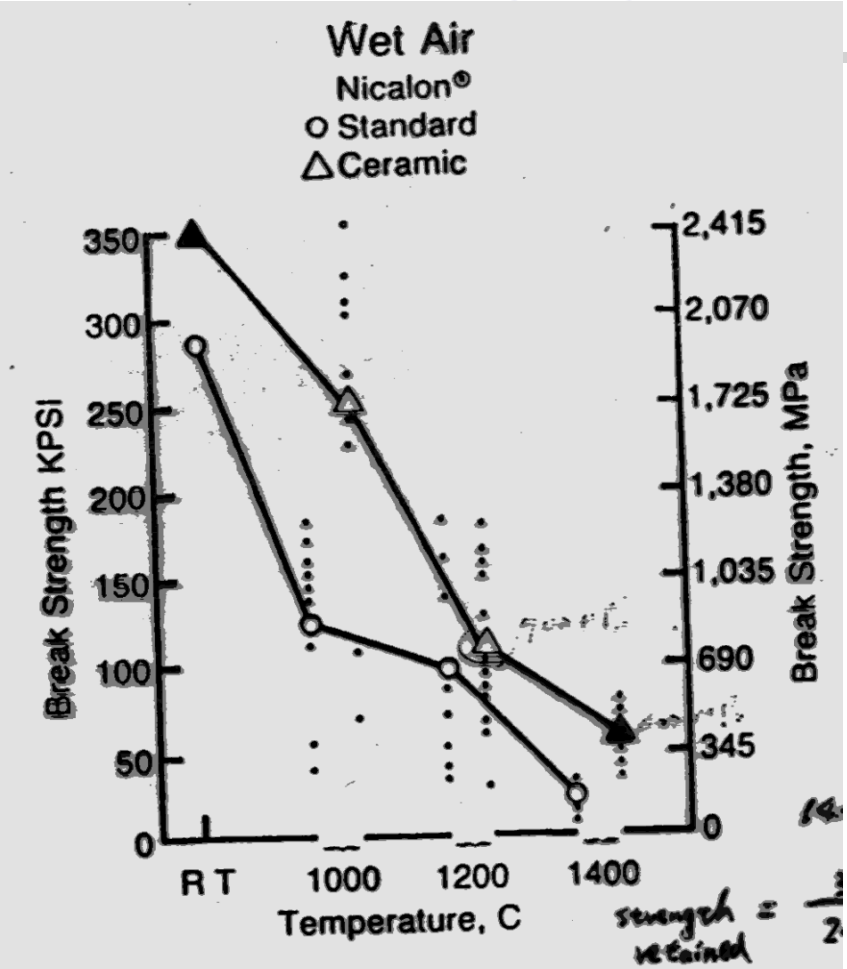

Fig. 4. Variation of fiber tensile strength with temperature after heat treatments in flowing wet air furnace environment (12 h soak).

After 1400C/12h,
retained strength=
350/2415=15%

Ref:T.J. Clak,R.M. Arons,J.B. Stamatoff,"Thermal Degadation of Nicalon™ SiC Fibres ",Ceam. Eng. Sci., Proc.,6 (7-8) 576-88(1985)

Difficulties involved in the manufacturing of CMC (powder processing)

- Densification limit
- Relative instability of many reinforcements

- Strategies
  - Avoid matrix shrinkage etc.
  - Avoid high temperature processing

- $\Rightarrow$ Reaction-based processing methods

Unit 4-b
Novel Processing

Contents

- Liquid (melt) infiltration

- Chemical vapor infiltration (CVI)
- Sol-gel process

Reference: K. K. Chawla, Ceramic Matrix Composites, Chapter 4.

Slurry infiltration process (or slurry impregnation process)

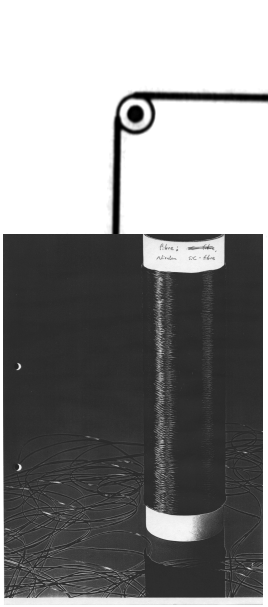

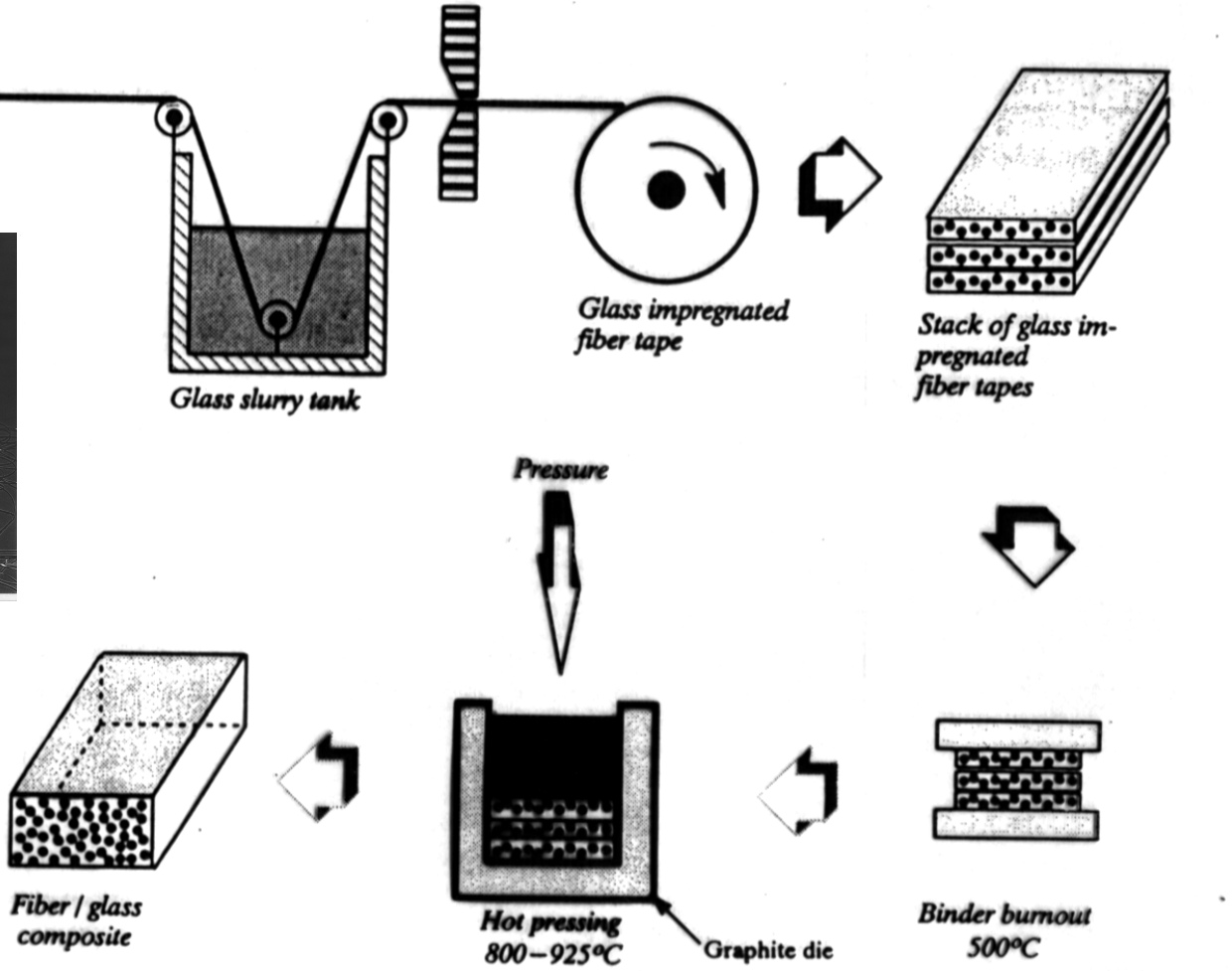

Fig. 4.1 A schematic of the slurry infiltration process of making a fiber-reinforced glass and glass-ceramic composite.

slurry: glass powder + solvent +binder + dispersant

Ref:D. M. Dawson, R. F. Preston,A. Purser,” Fabrication and Materials Evaluation of High Performance Aligned Ceramic Fibre-reinforced ,Glass-Matrix Composites ” ,Ceram. Eng. Sci. Poc. 8(7-8)815-21,1987

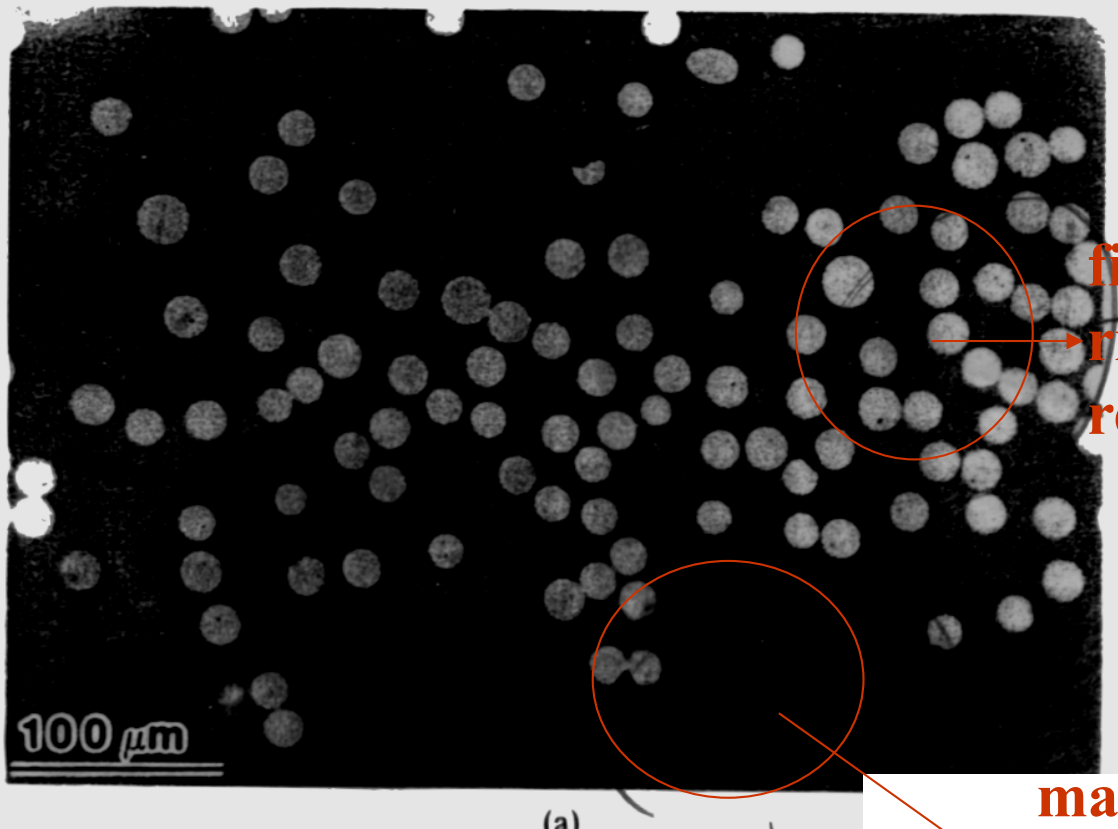

fibre rich region

matrix rich region

(a)

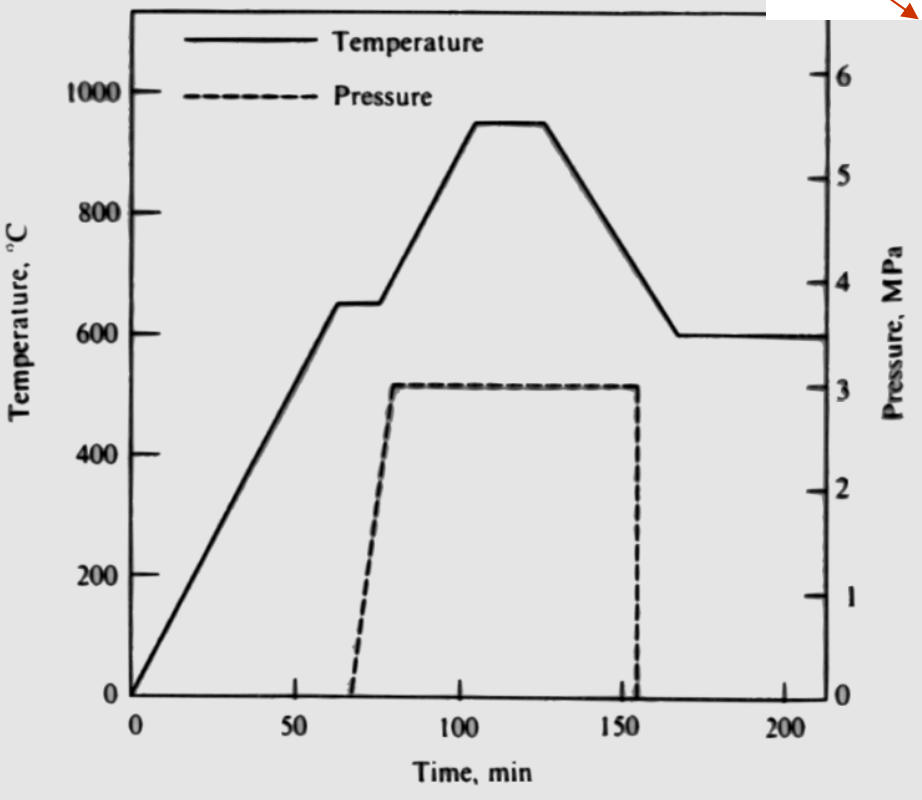

(b)

Fig. 4.2 (a) An optical micrograph of a cross-section of a unidirectional alumina fiber/glass matrix composite made by slurry infiltration; (b) the pressure and temperature schedule used during hot pressing of this composite.

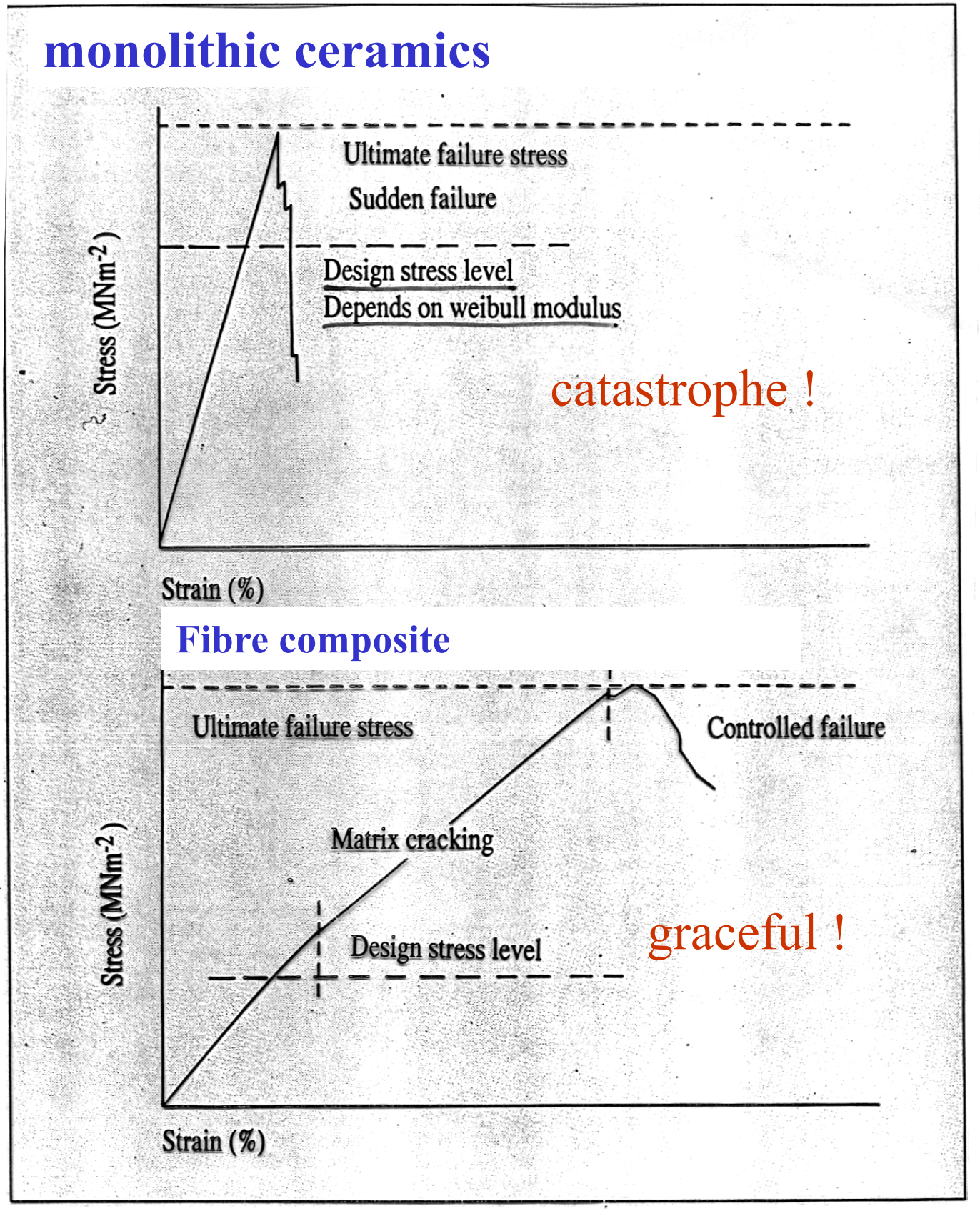

Figure 2 Comparison of stress–strain curves for monolithic, toughened ceramics (top) and fibre reinforced ceramics (bottom)

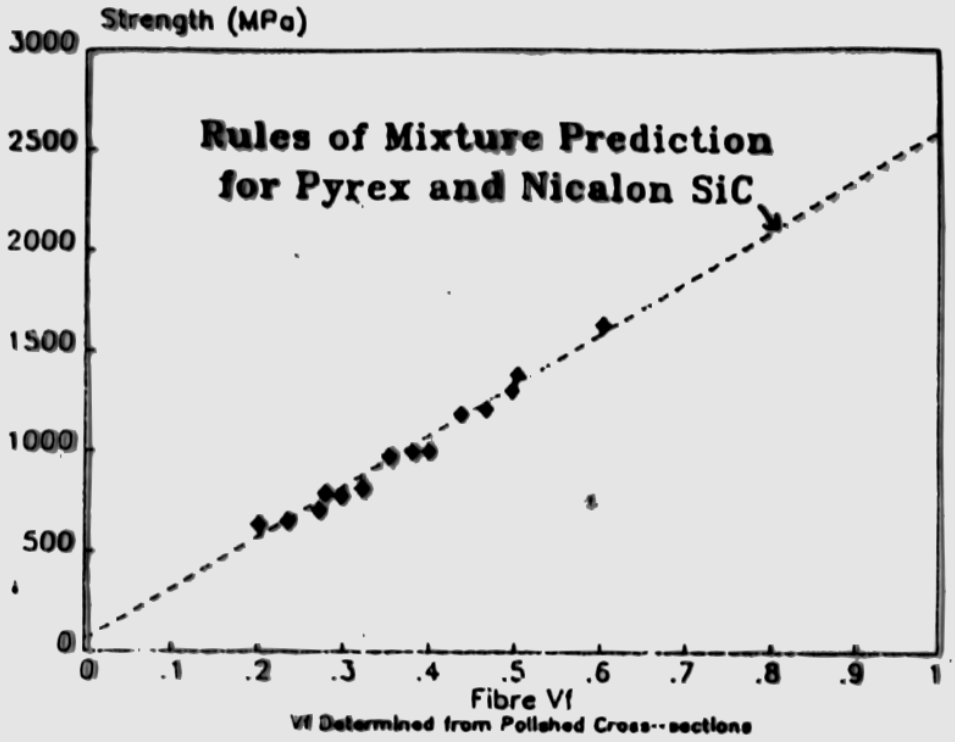

Fig. 2. Composite strength as a function of fiber volume fraction in tensile face.

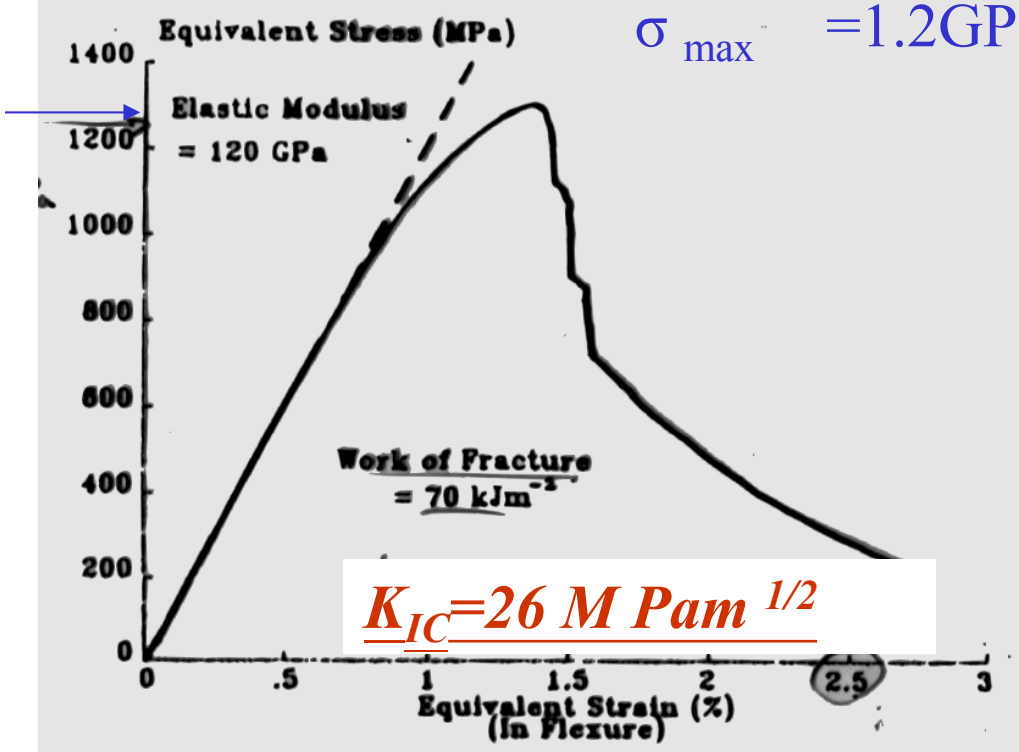

σ_{max} =1.2GPa

K_{IC}=26 M Pam $^{1/2}$

Fig. 3. Typical load/extension behavior of Nicalon SiC/Pyrex composite.

Fig 4 Nicalon SiC Pyrex composite tested to and beyond failure (strain = 2.5%). Note extensive fiber bridging

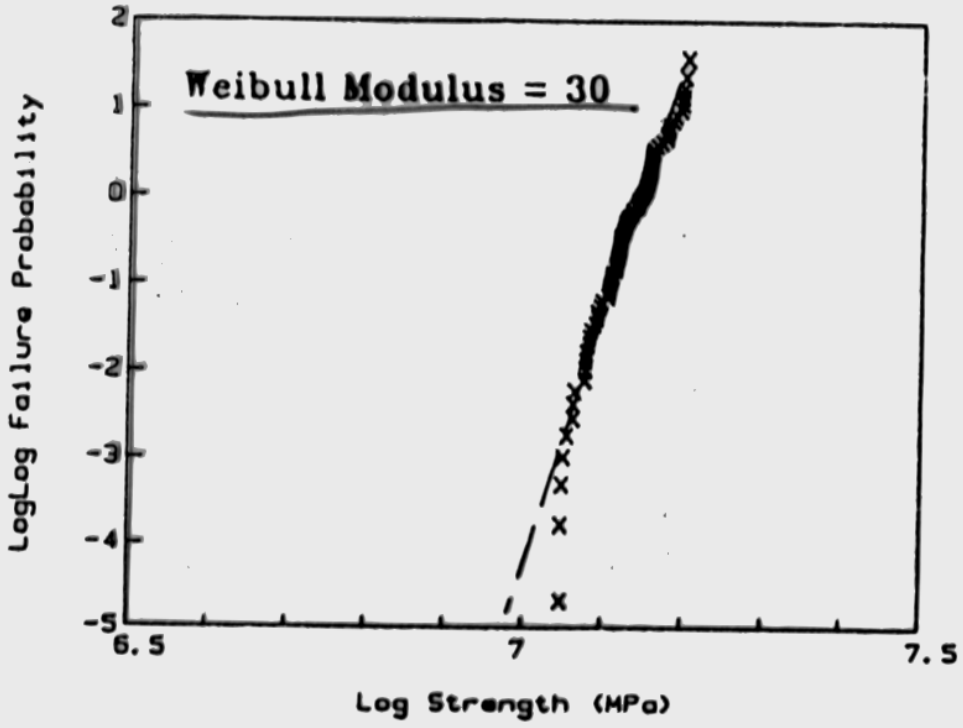

Fig. 5 Weibull analysis of the flexural strength of Nicalon SiC/Pyrex composite (Vf = 0.49, mean strength = 1.25 GPa).

Liquid infiltration

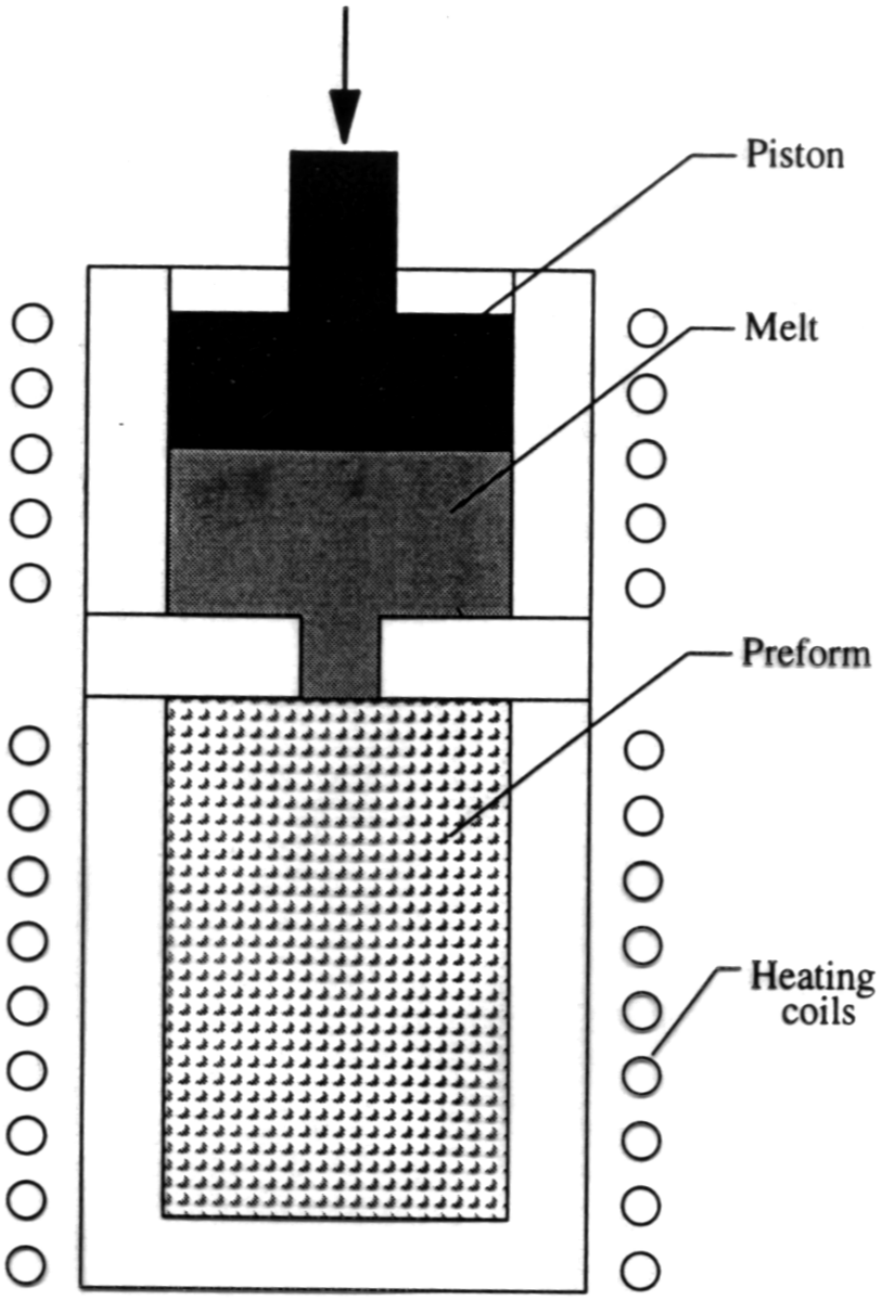

Fig. 4.6 A schematic of the melt infiltration process.

Example: C/C composite

C/C composite

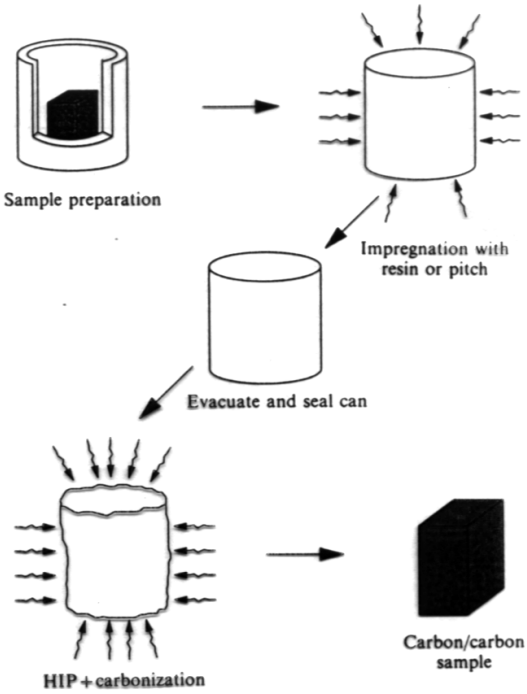

(a)

(b)

Fig. 4.7 (a) Schematic of a process for making carbon/carbon composites by liquid infiltration; (b) a two-dimensional carbon/carbon composite made by liquid infiltration of a resin, followed by charring of resin to carbon (courtesy of K. Upadhya).

- **Chemical vapour infiltration (CVI)**

deposit the matrix phase within a porous preform by chemical vapour deposition (CVD)

1000~1200℃ ,10~100 torr

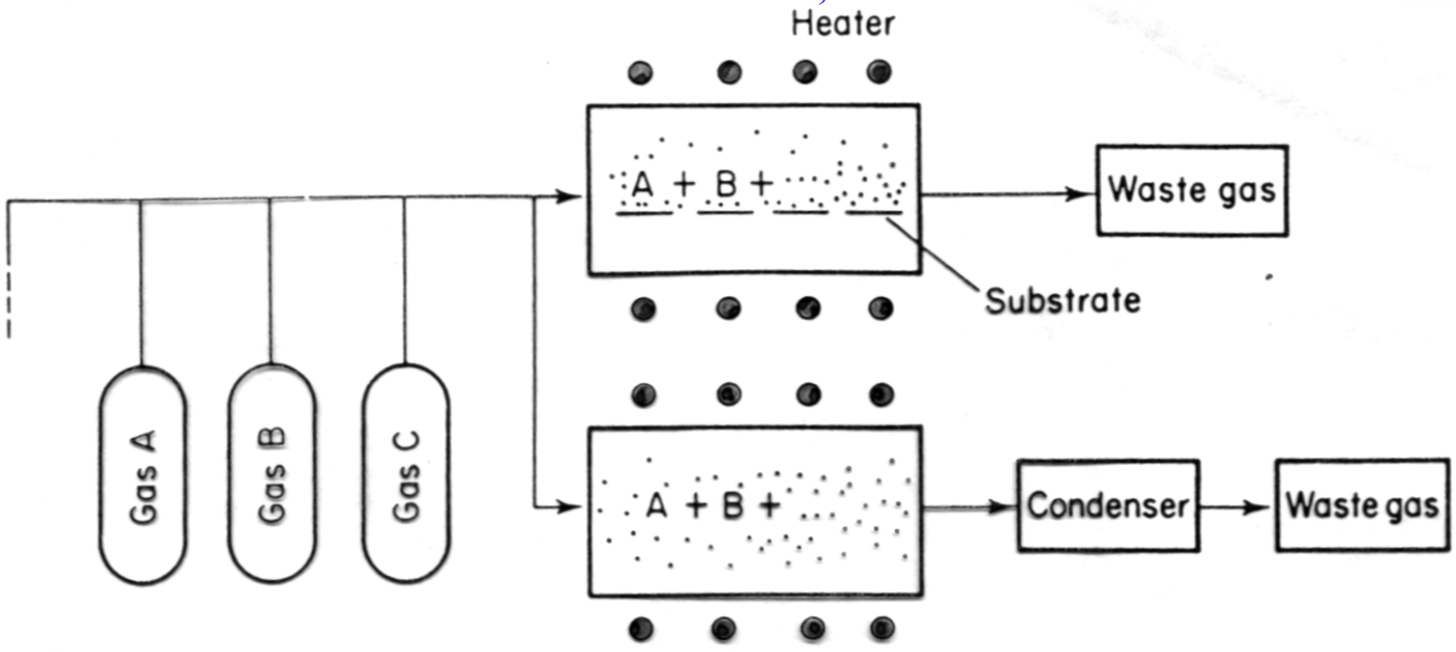

Fig. 1.23 CVD outline

For SiC,

precursor: methyltrichlorosilane (MTCS)

Advantages:

Ability to manipulate

- **the stoichiometry**
- **the crystal structure**
- **the crystal orientation**
- **the morphology of the deposit**
- **the purity**

- **operated at low temperature**
- **no matrix shrinkage**

Isothermal CVI

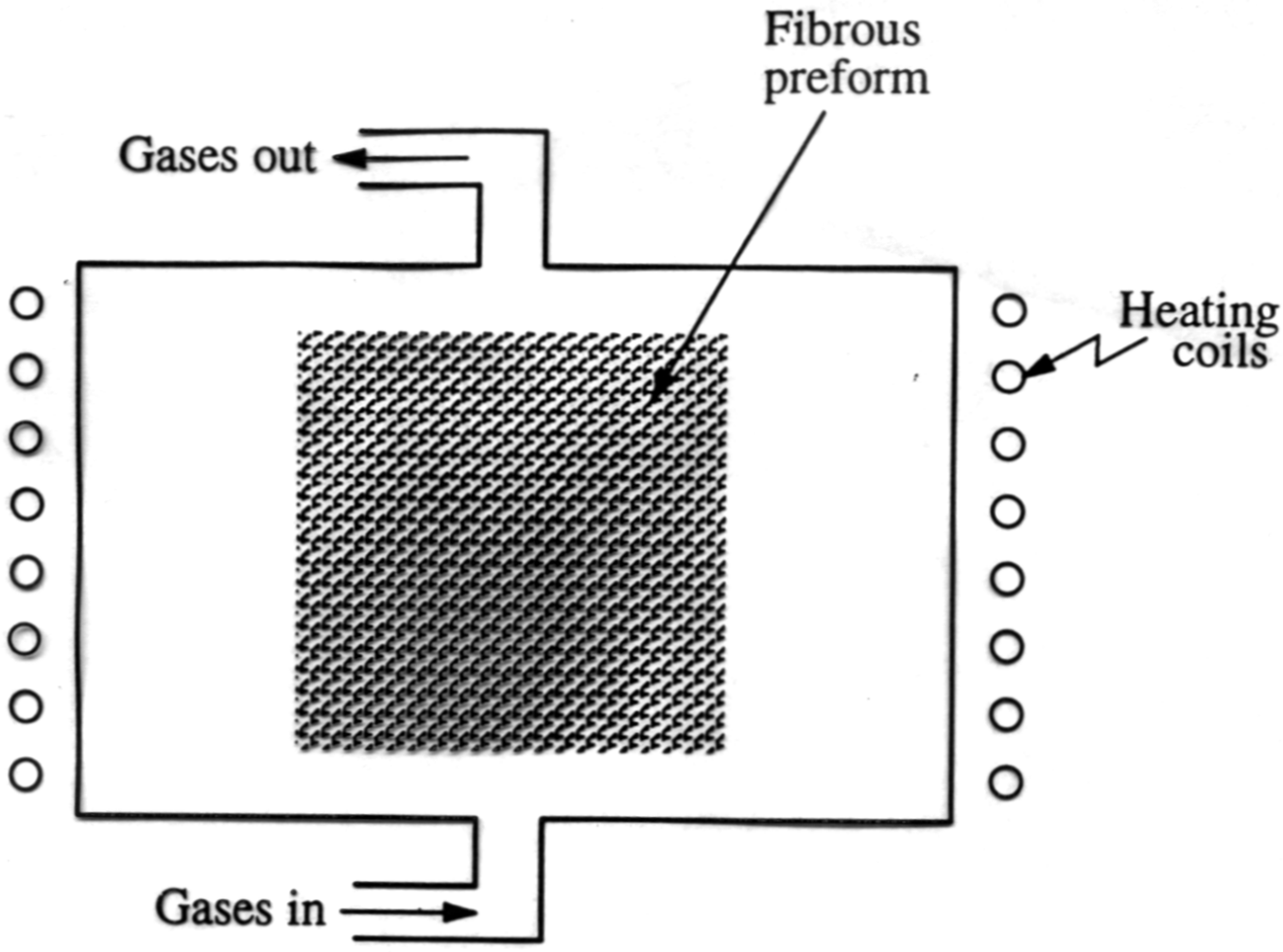

Fig. 4.13 An isothermal chemical vapor impregnation (ICVI) reactor in its simplest form.

SiC / SiC_f

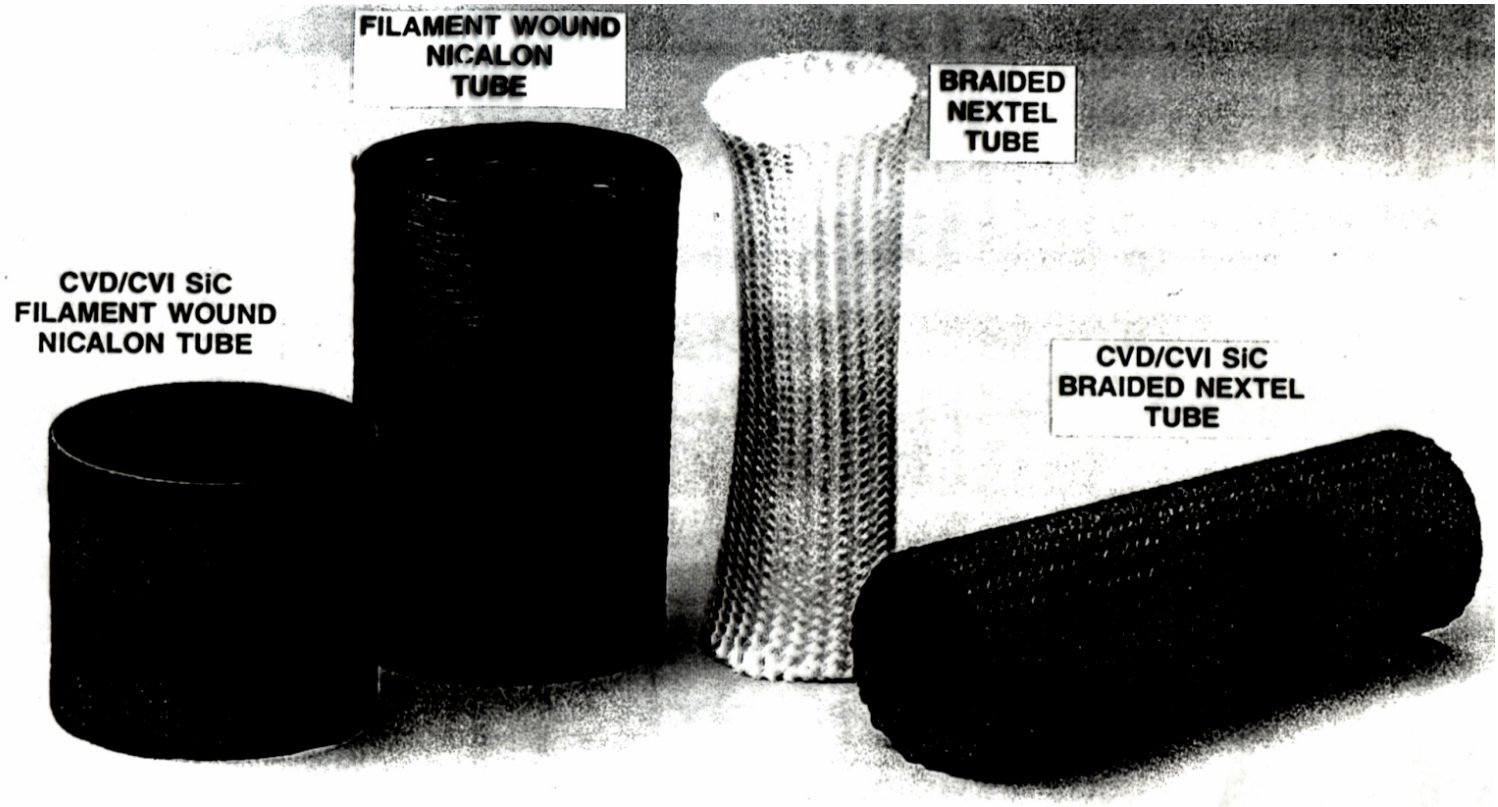

Fig. 4.12 A filament-wound Nicalon tube and a braided Nextel tube before CVI and after CVI (courtesy of P. Reagan, Thermo Electron Corporation).

microstructure

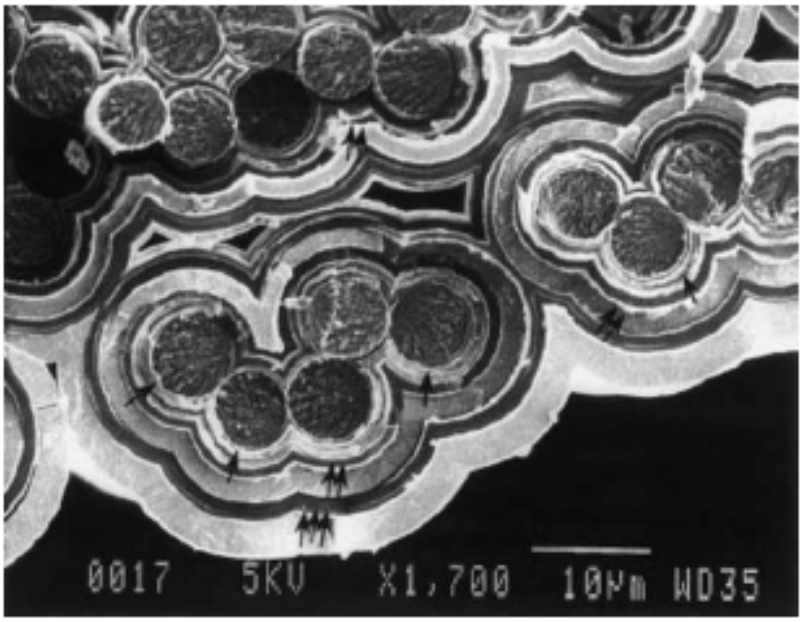

Fig. 6. Multilayered self-healing matrix deposited by I-CVI; each elementary sequence contains crack layers forming fluid oxide phases by the crack network. Such sequence a (simple arrow), group of fibers (d arrow), according to Lamouroux et

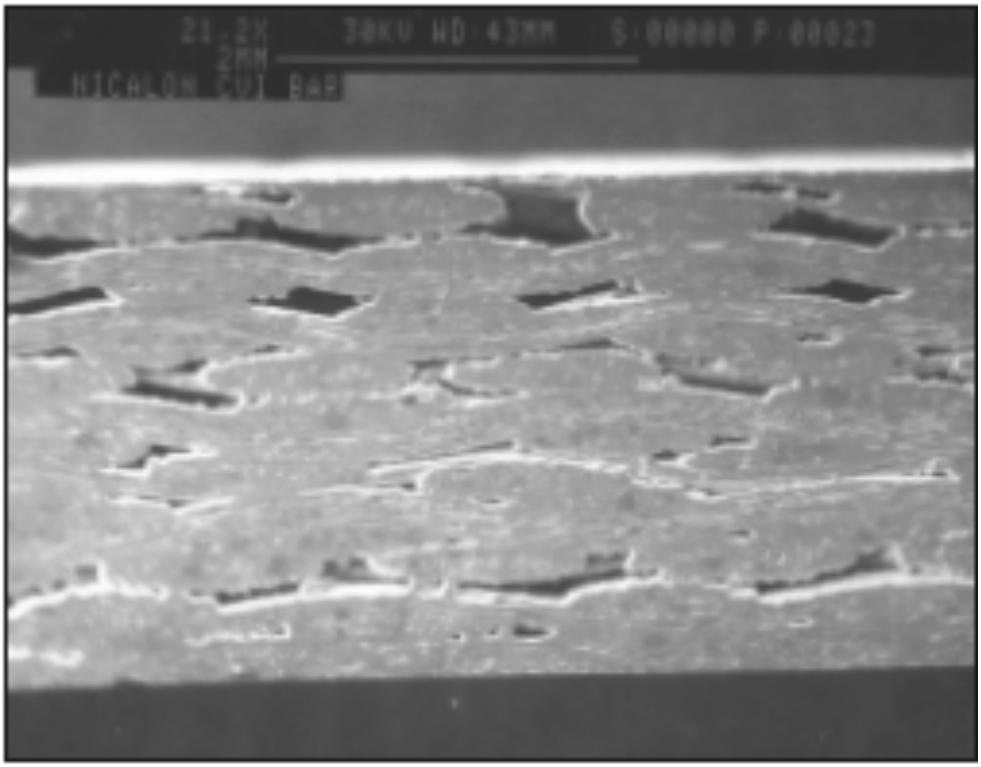

Fig. 4. Nicalon-fiber plate densified using CVI, showing interbundle porosity.

Cost

Table 1 Comparison of certain materials

	Cost [£/kg]	K_{Ic} [MPa $\sqrt{m}$]	W_f[Jm^{-2}]
Al_2O_3	20	3,5	30
Al_2O_3/TiC particles	80	4,5	40
Al_2O_3/SiC whiskers	220	9,0	160
SiC/SiC fibres (by chemical vapour infiltration)	5240	30,0	~104
Aluminium (dural)	2	100	~105

Disadvantages

- expensive, corrosive, toxic, explosive reactants.

  Ex.SiH_4 ,$SiCl_4$

- slow deposit rate

  Ex. Several mm takes 2 weeks to several month

- difficult to achieve uniform penetration

  → density gradient (especially when sample thickness > 3mm)

  → External surface has to be removed in order to “open up” the pore channels

Mechanical performance for SiC/SiC_f composite

$(\sigma_f)_{max}$= 450 MPa, up to 1400℃

$(K_{IC})_{max}$= 25 $MPam^{1/2}$, up to 1400℃

(Note: porosity = 15% to 25 %)

but fatigue resistance is poor !!!

Ref : P. J. Lamicq, G.A. Bernhart, M.M. Dauchier, J.G. Mace, "SiC/SiC Composite Ceramics", Amer. Ceram. Soc. Bull.,65(2) 336-38 (1986)
French group

Improved CVI (thermal gradient / forced flow process) —Oak Ridge National Lab.

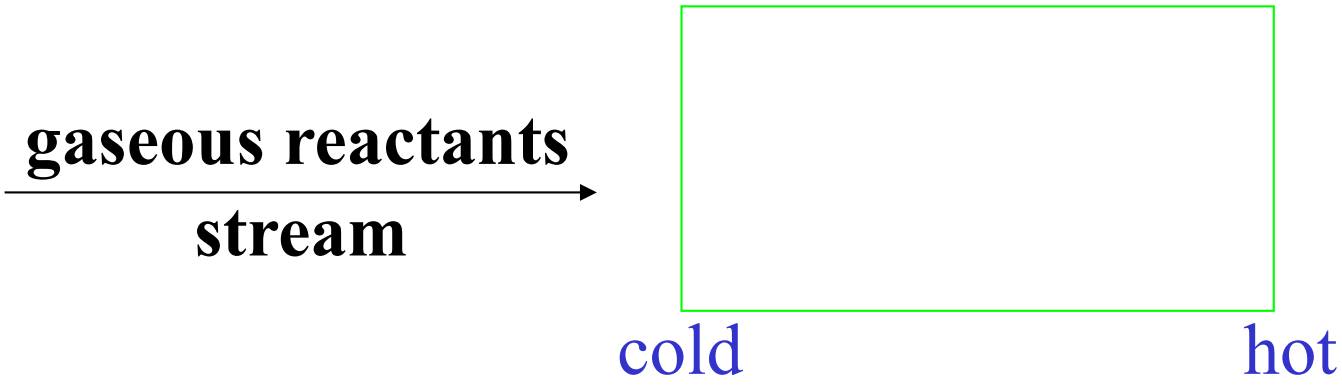

product thickness : 25 mm (within 24 hrs)

disadvantage : for plate and cones

Improved CVI (pulsed CVI)

Forced CVI

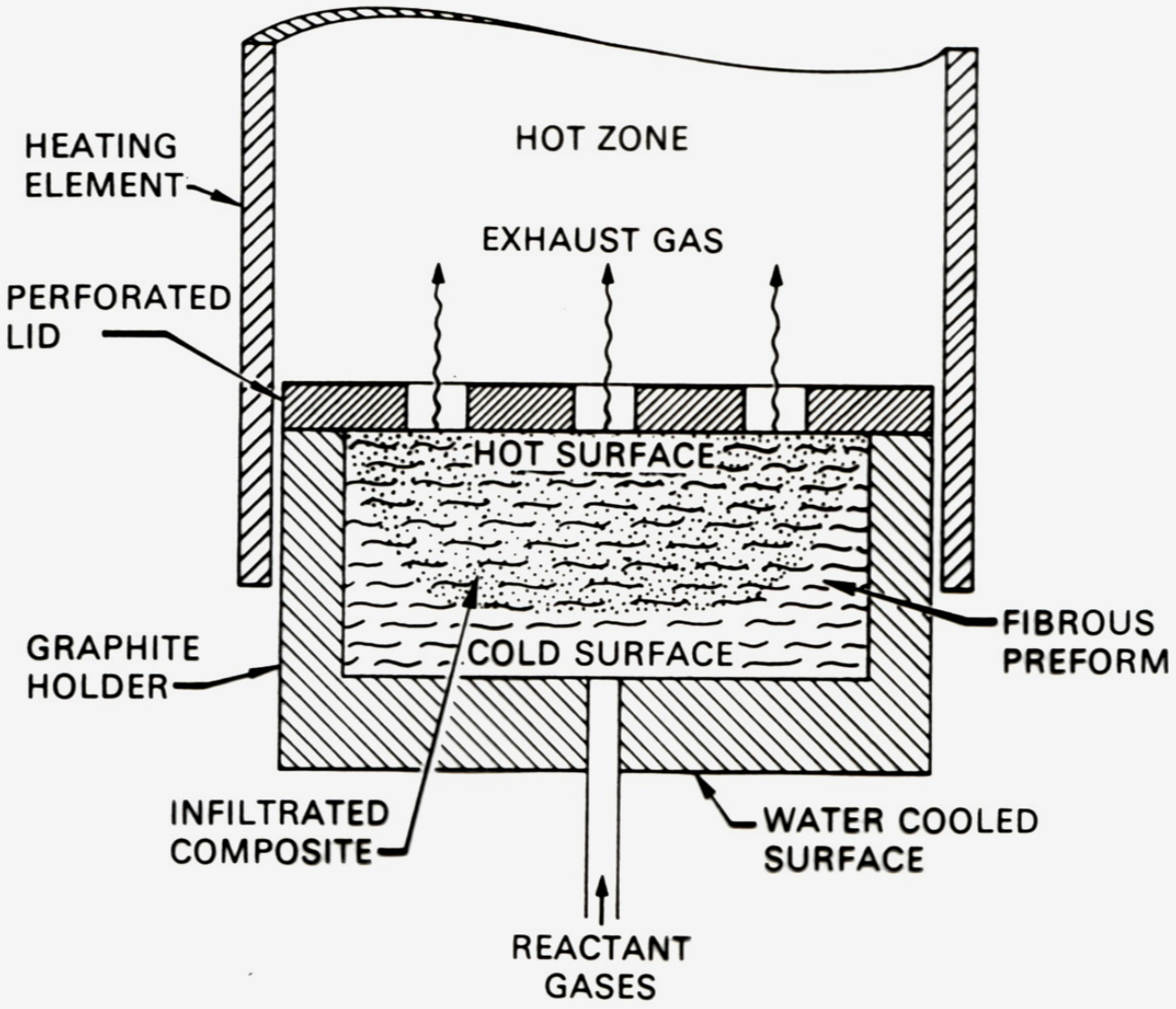

Fig. 4.14 A forced chemical vapor impregnation (FCVI) process combining thermal gradient and pressure gradient approaches (courtesy of R. Lowden, Oak Ridge National Laboratory).

Unit 4-c, processing Interface

Interface

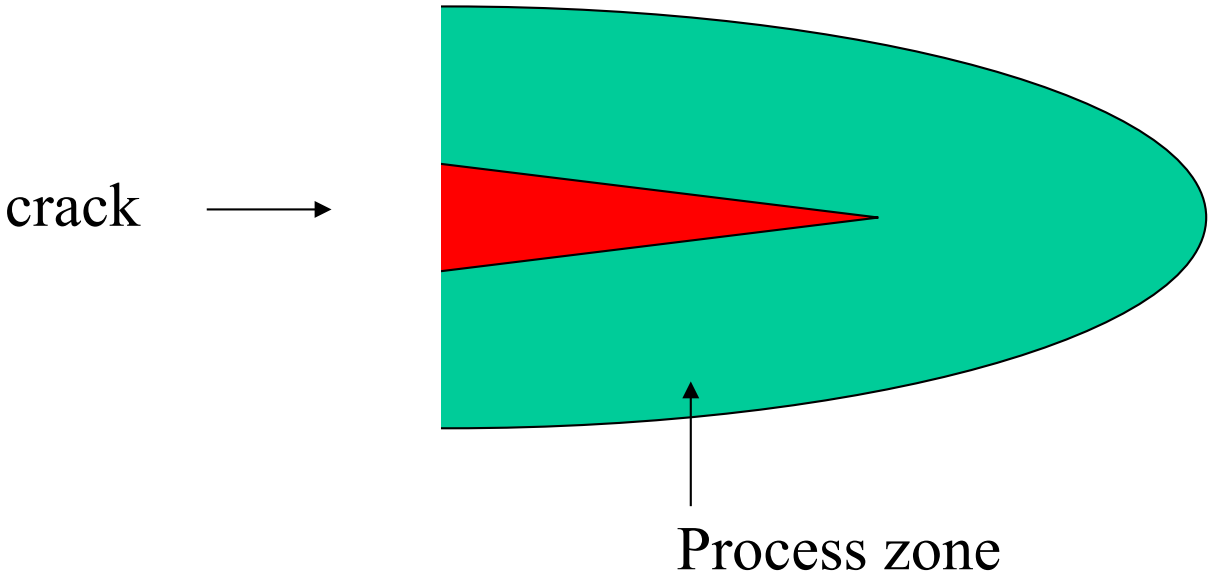

Fracture toughness:

the resistance to the propagation of crack

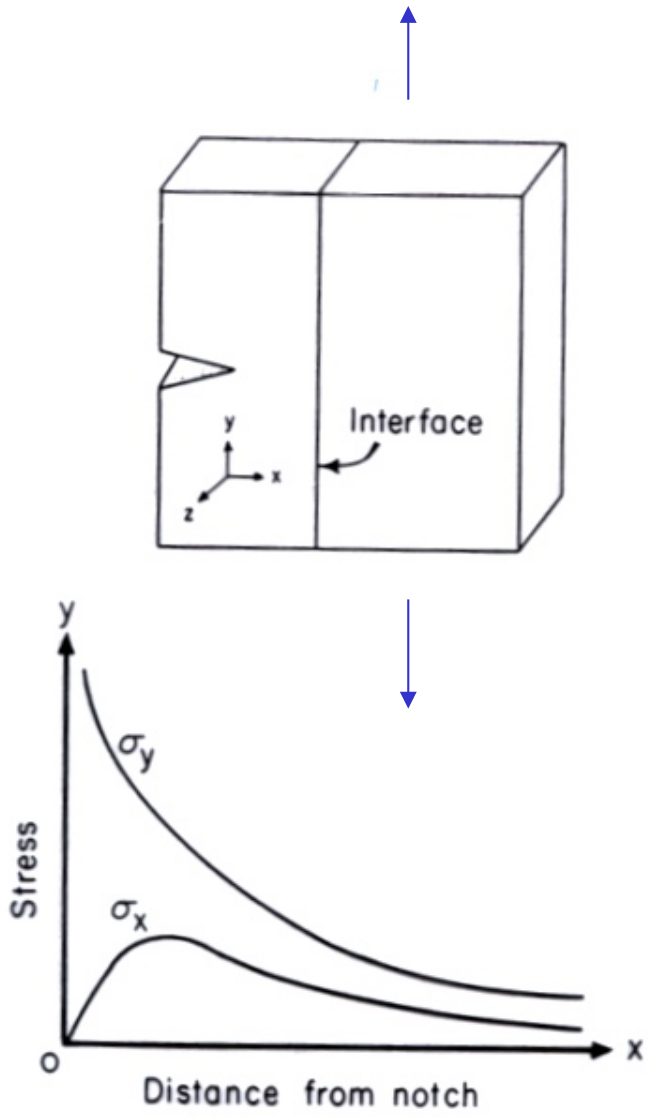

Fig. 5.7 Schematic of stress distribution at a crack tip (after [2]).

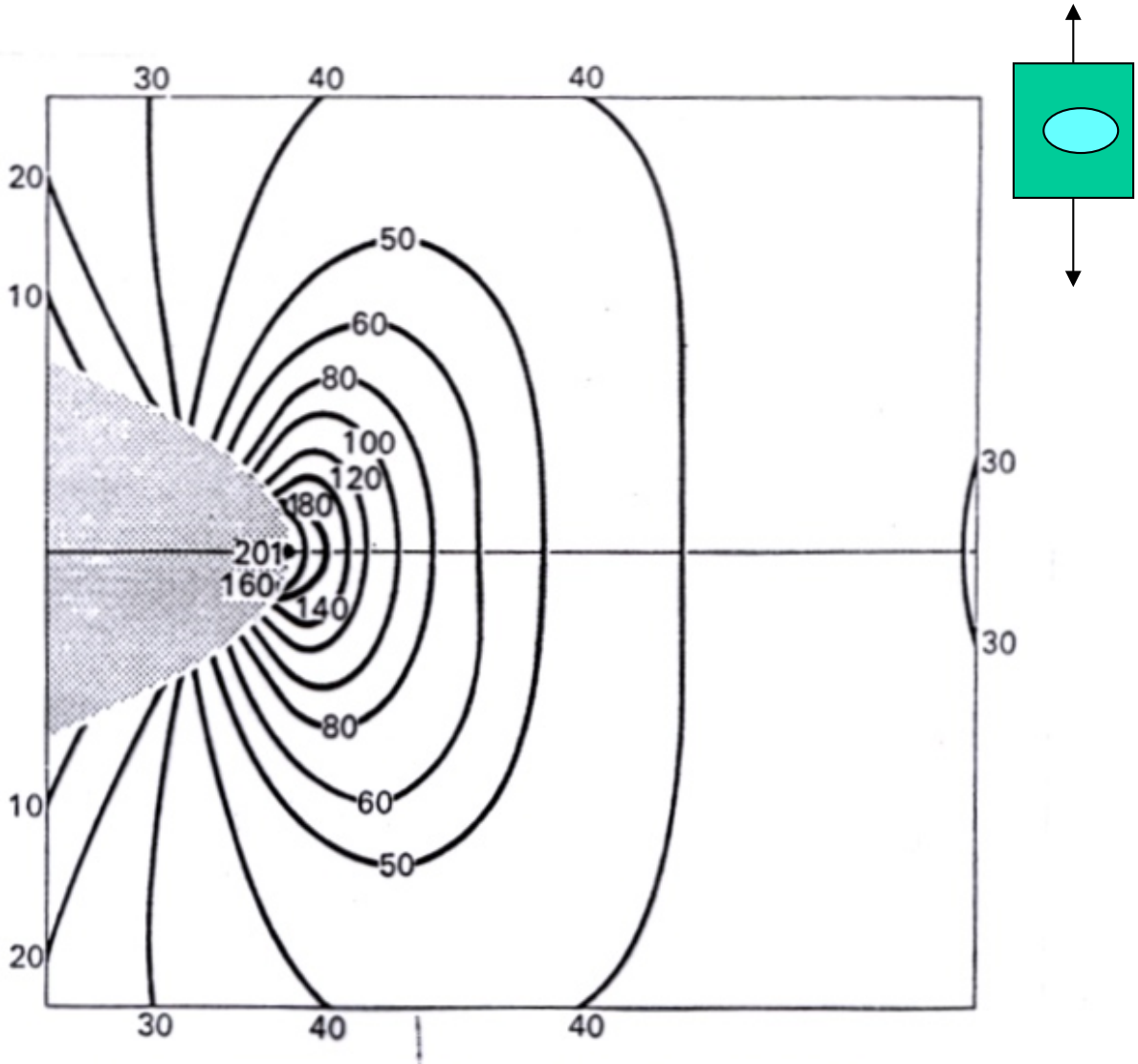

Figure 3. Stress system close to the tip of an elliptical crack. This is a map of the stress concentrations for stresses at *right-angles* to the plane of the crack, that is, parallel to the applied load. The shaded area represents the crack tip – that is, empty space. The curved lines are contours of equal stress concentration. The figures indicate the number of times by which the local stress is increased as compared with the mean stress remote from the crack. The maximum concentration of stress is about 200. The actual values of the stress concentration will, of course, vary with the length of the crack but the relative proportions remain constant.

Ref:J.E. Grodon:The New Science of Strong Material, Penguin Books Ltd, Harmondsworth, 2nd ed., 1976

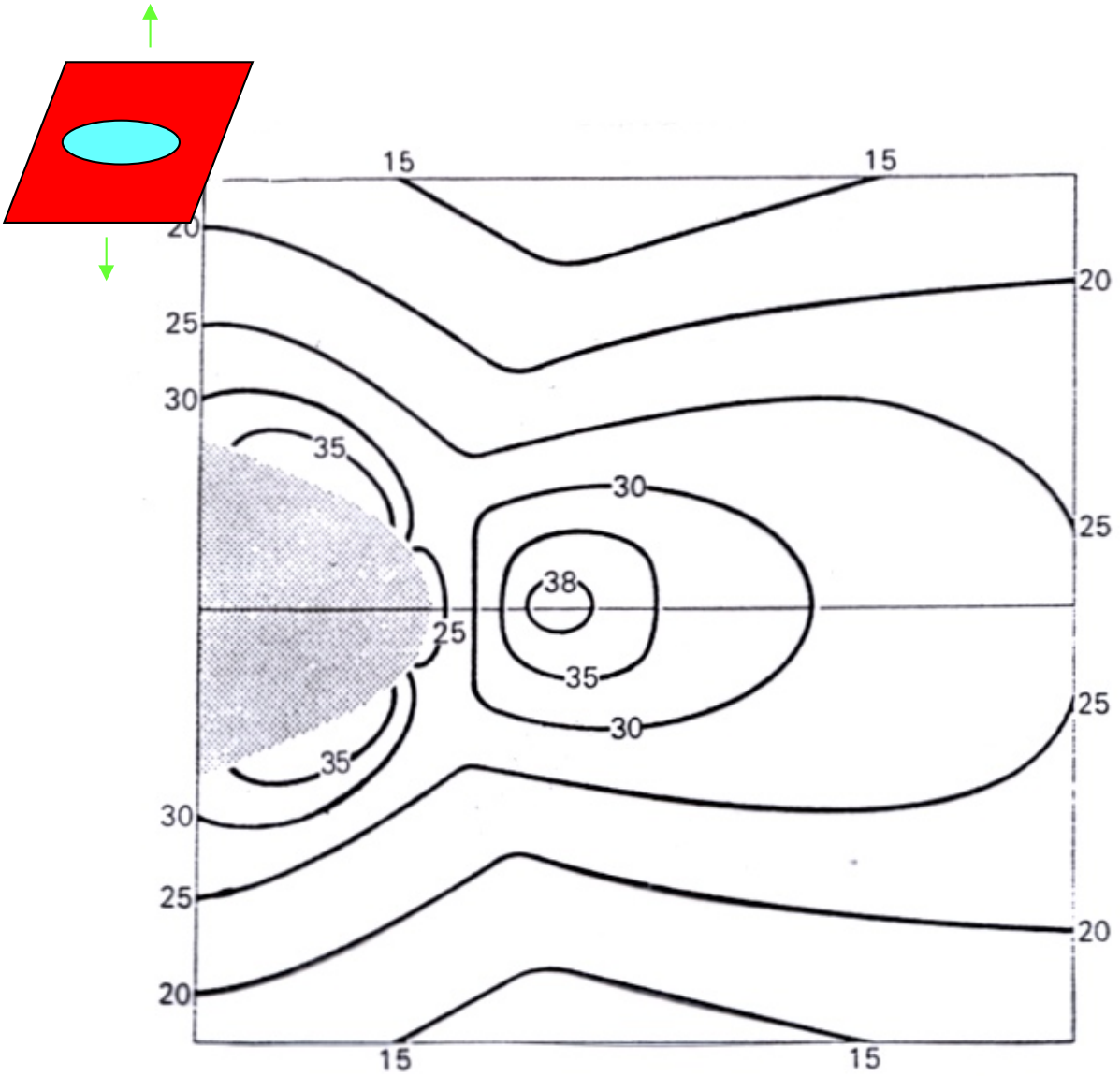

Figure 4. Stress system close to the tip of an elliptical crack. This is a map of the stresses *parallel* to the plane of the crack, that is, at right-angles to the applied loading. For this case the maximum stress concentration is about 40, i.e. one-fifth of that in Figure 3.

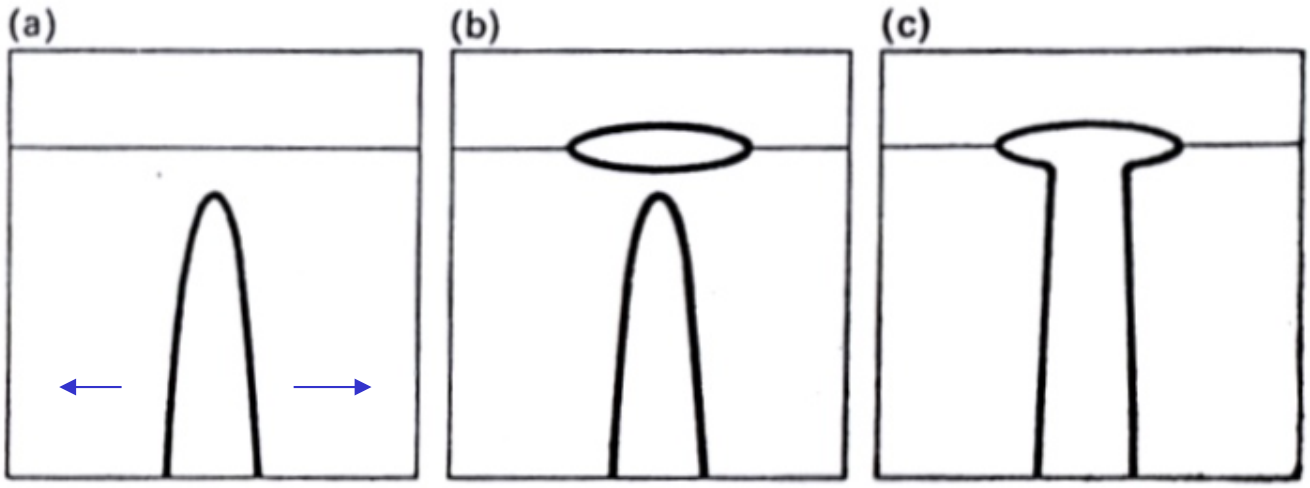

Figure 5. Cook-Gordon mechanism for stopping cracks at a weak interface.
(a) Crack approaches a weak interface.
(b) Interface breaks ahead of main crack.
(c) T-shaped crack-stopper. In practice the crack is usually diverted, as in Plate 11.

Role of interface in CMCs

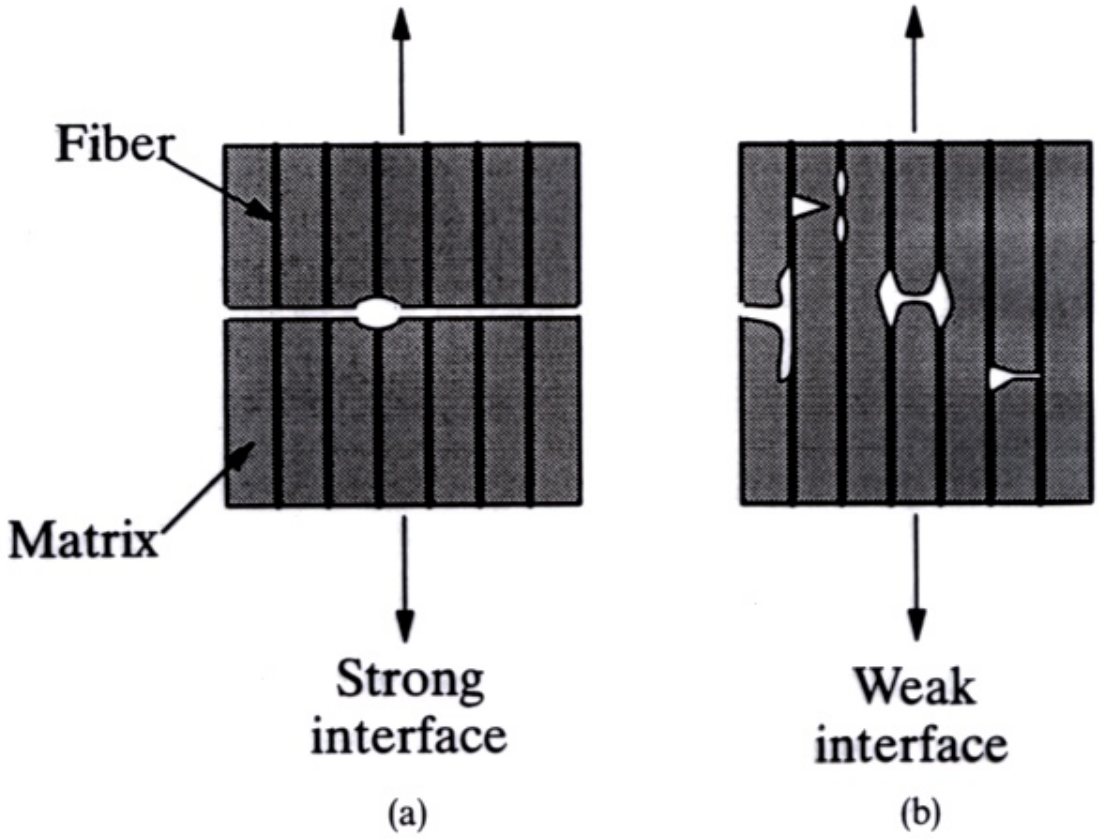

Fig. 5.6 Failure of a CMC as a function of interfacial bond strength: (a) strong interfacial bond; (b) weak interfacial bond.

Weak interface

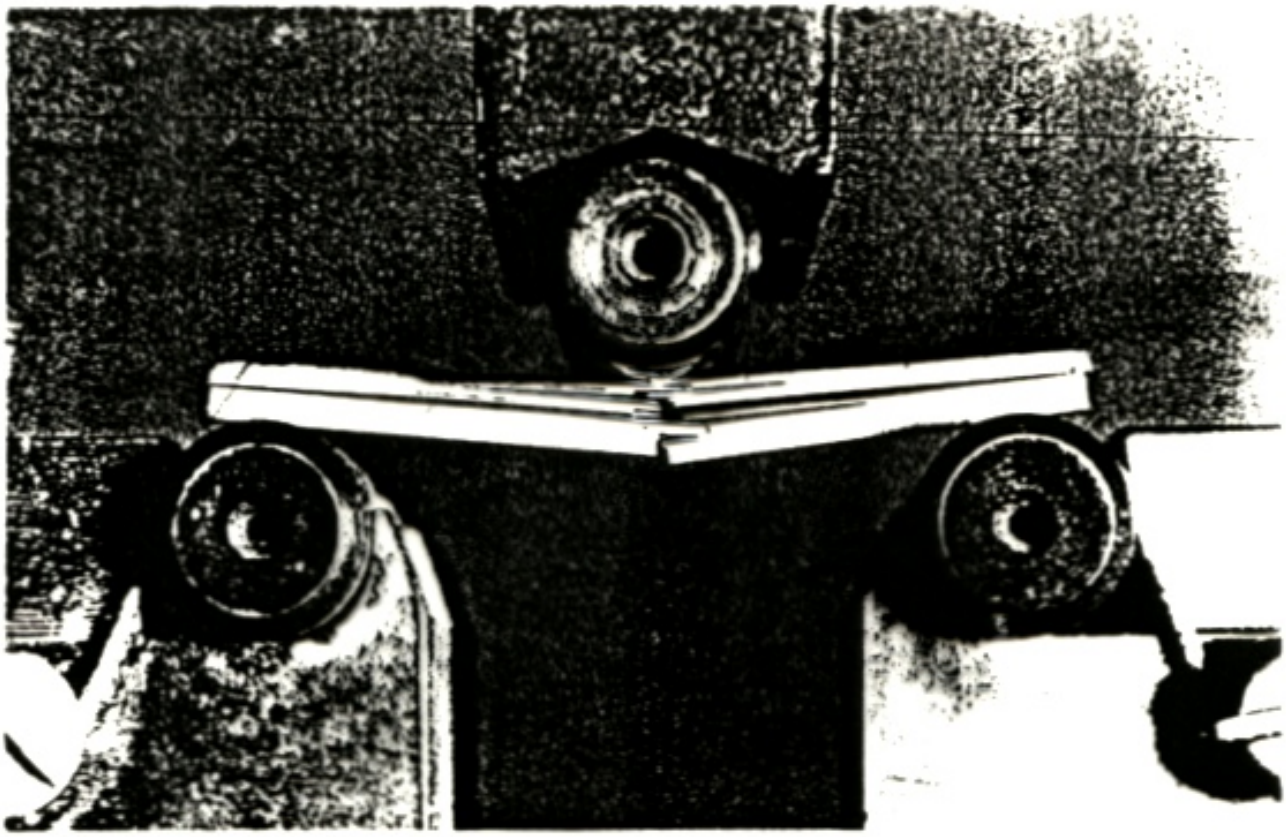

Fig. 1 A laminated SiC sample after crackgrowth with the extensive delamination that gives rise to the toughness

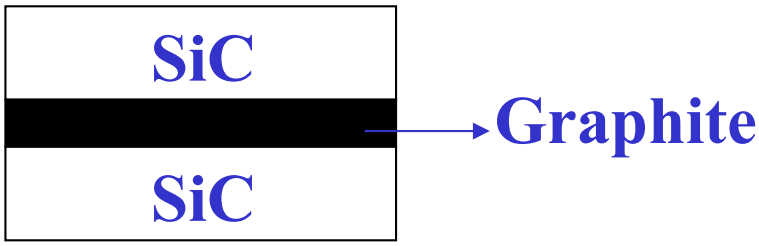

Ref: Clegg et al, Nature, 1990

Type of bonding

mechanical bonding

chemical bonding

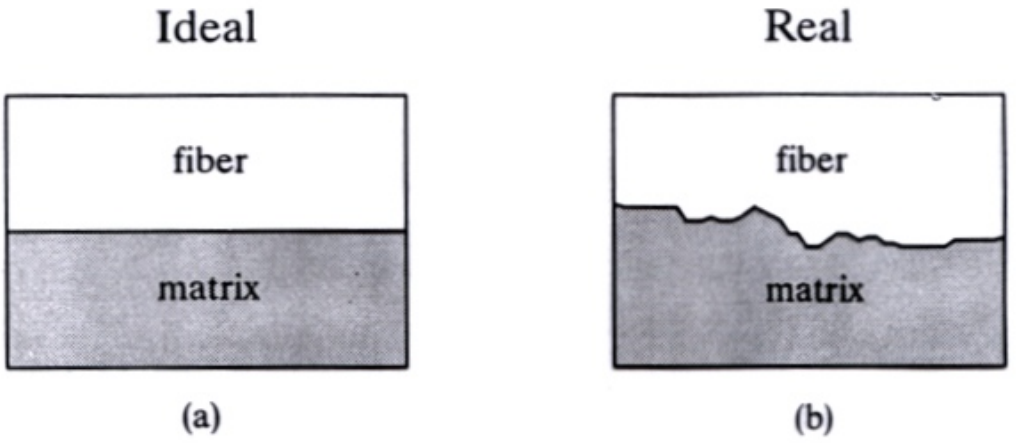

Mechanical interlocking

Fig. 5.4 (a) An ideal, smooth interface; (b) a real, rough interface.

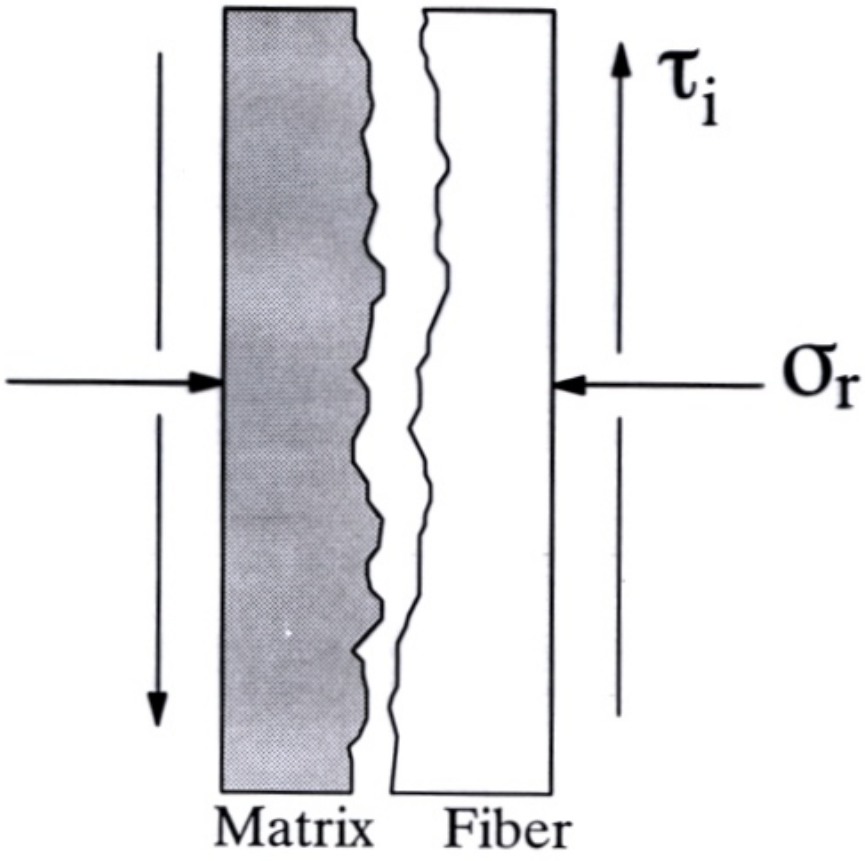

Fig. 5.5 A frictional or mechanical interface with transverse gripping forces.

Design on interface
Example:
$Al_2O_3/Y_3Al_5O_{12}$

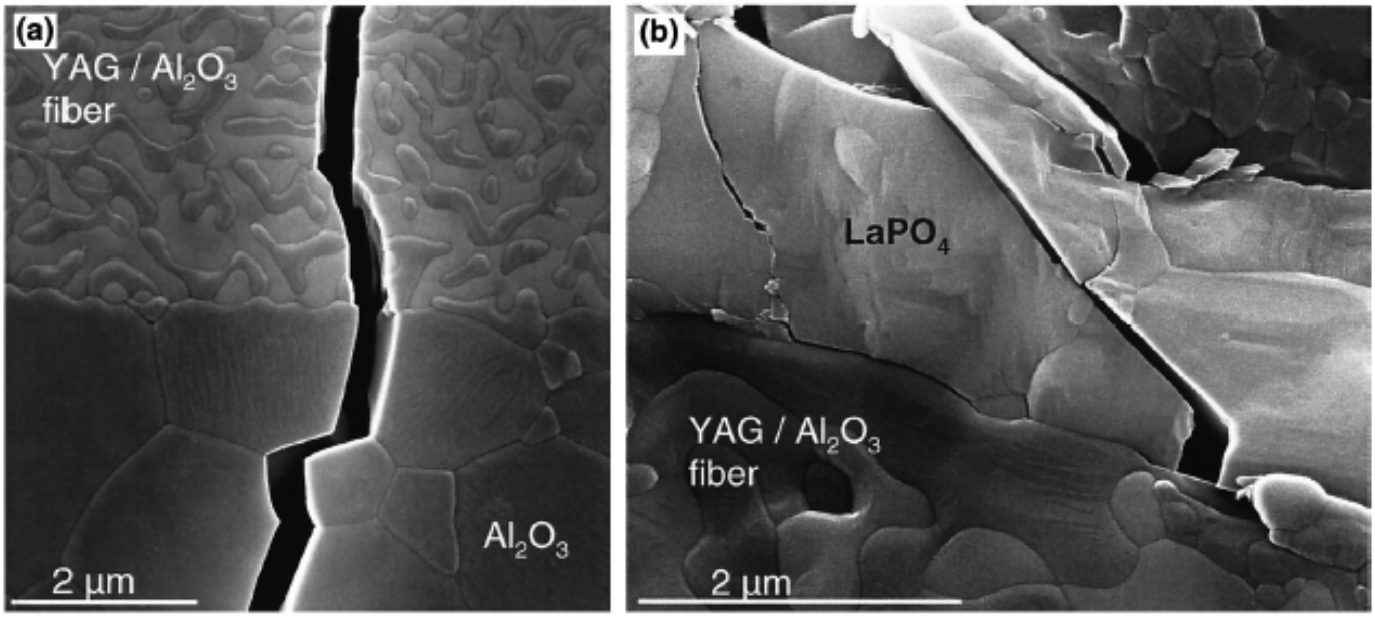

LaPO4: La-monazite

Ref: Davis et al., J.A.C.S., 86, 305, 2003

Example:
Al2O3/mullite

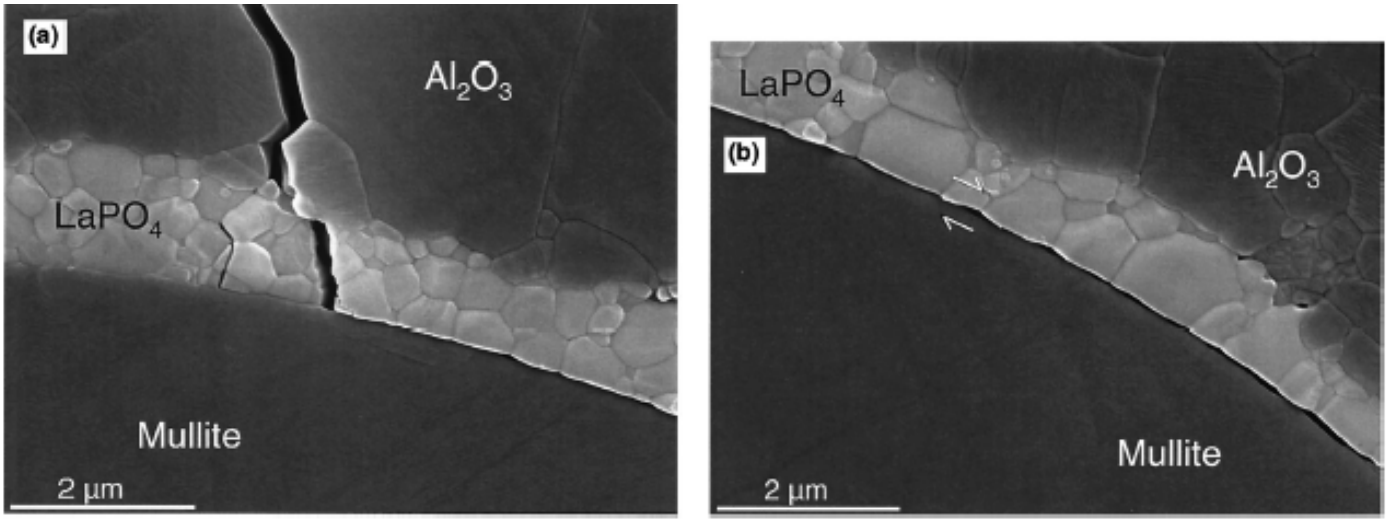

Fig. 4. SEM micrographs showing interaction of indentation crack with single-crystal mullite fiber (coated with $LaPO_4$, in alumina matrix): (a) intersection of indentation crack with interface and debonding (indentation located above region shown); (b) same fiber as in (a) but showing region further to the right along the debonded interface (arrows indicate magnitude of sliding displacement across debond crack).

LaPO4: La-monazite

Ref: Davis et al., J.A.C.S., 86, 305, 2003

Interface for CMC

- The interface should be **strong** enough for the load transfer to take place.
- The interface should be **weak** enough to fail before the approaching of crack front.

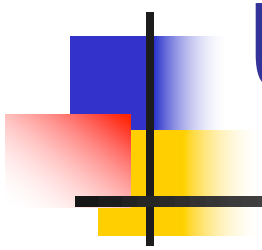

Unit 5

Properties of CMC

Crack propagation (mixed mode)

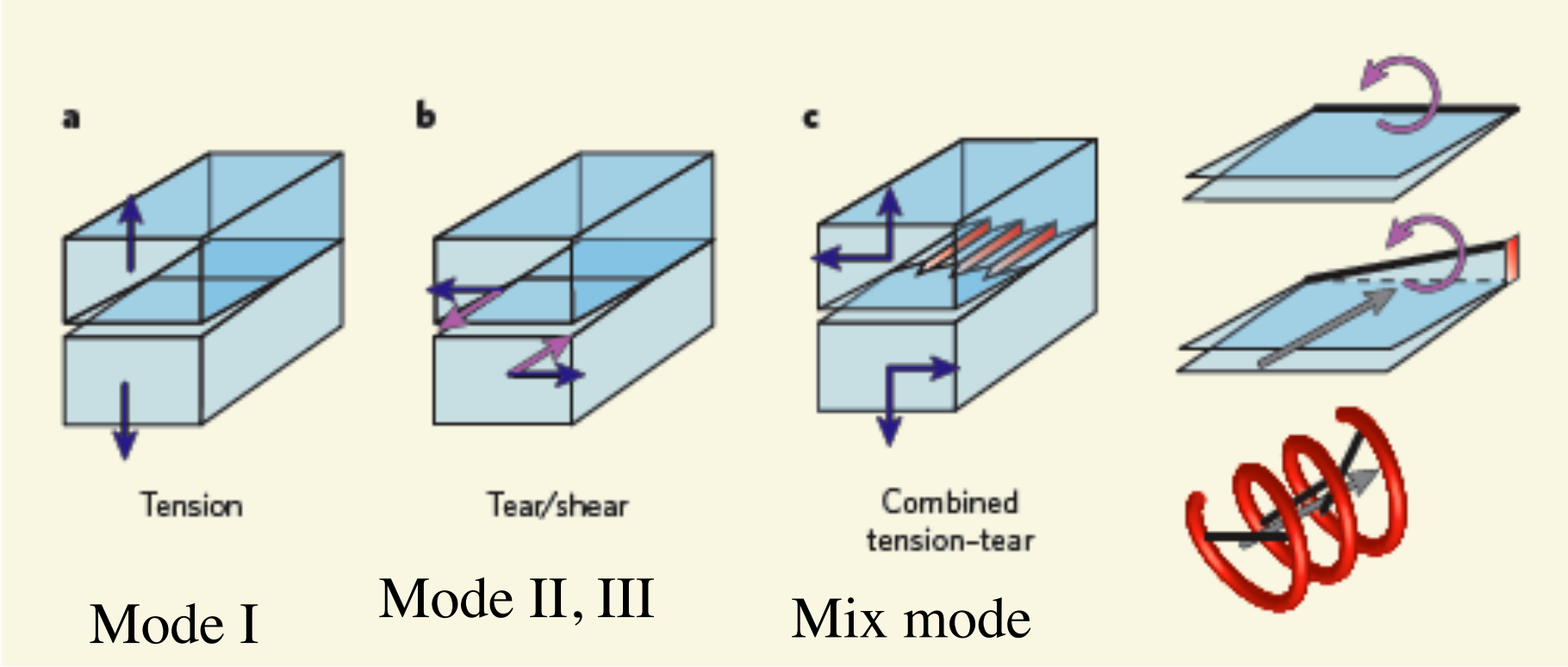

Figure 2 | Cracked specimen under different types of loading. **a**, Tension. **b**, Tear/shear (dark blue arrows for tear, pink arrows for shear). **c**, Combined tension–tear; under mixed tension–tear loading, an initially planar crack splits into several daughter cracks, or fracture 'lances' (red). This splitting is caused by a helical rotation of the crack front (thick black lines in right panel) around the principal direction of crack propagation (grey arrow). Pons and Karma's computational study[2] describes the three-dimensional details of crack-front evolution under such mixed tension–tear loading.

Ref: Buehler et al, Nature, 2010

Requirements on the mechanical properties of ceramics

- Strength
- Toughness
- Weibull modulus
- Crack-resistance (R-curve character)
- Creep resistance
- Thermal shock resistance

strength

Determination of mechanical properties

strength :

flexural strength,
MOR (modulus of rupture)

3-point bending

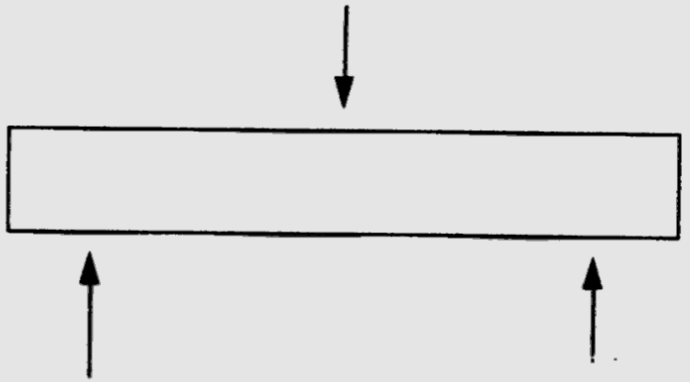

4-point bending

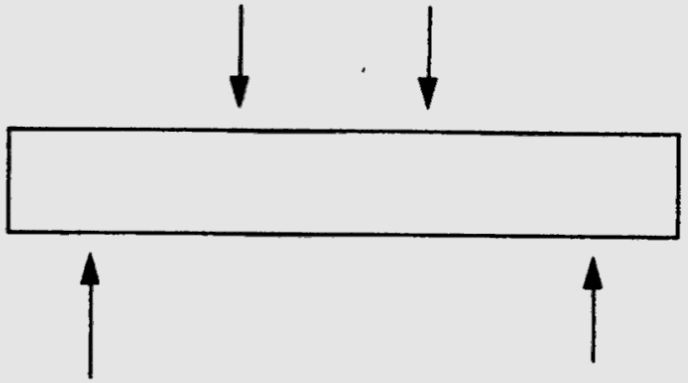

size : 3 x 4 x 36 mm or 3 x 4 x 44 mm

Griffith law

- For brittle material only

$$\sigma_f = \frac{K_{IC}}{\sqrt{SC}}$$

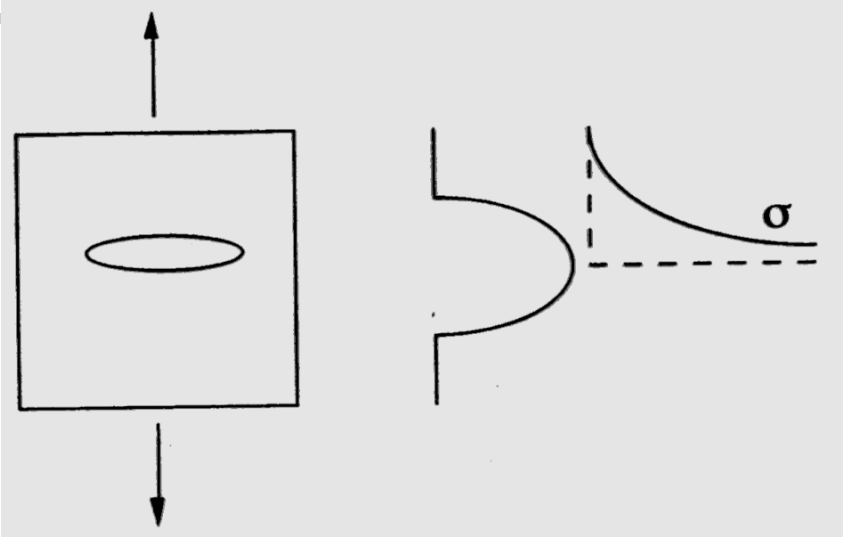

σ_f: strength

- K_{IC}: toughness
- S: shape factor, for spherical pore $S=\pi^{0.5}$
- C: flaw size

Calculation of toughness for SENB

- For 3-point bending
- For SENB

$$K_{IN} = \frac{3PL}{2wt^2}(\pi a)^{\frac{1}{2}} FIM(\alpha)$$

a: length of notch

$$\alpha = \frac{a}{t}$$

$$FIM(\alpha) = 1.122 - 1.121\alpha + 3.74\alpha^2 + 3.837\alpha^3 - 19.05\alpha^4 + 22.55\alpha^5$$

$$a = 1.4mm$$

$$FIM(\alpha) = 1.26$$

$$\sqrt{S} = (\pi)^{\frac{1}{2}} FIM(\alpha) = 2.23$$

$$S = 4.99$$

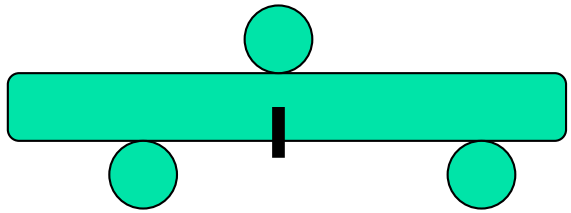

toughness

fracture toughness, K_{IC}

$$\sigma_f = K_{IC} / (S\ C)^{0.5}$$

measurement

Standards:

1. Single edge notched beam (SENB)
2. Single edge pre-crack beam (SEPB)

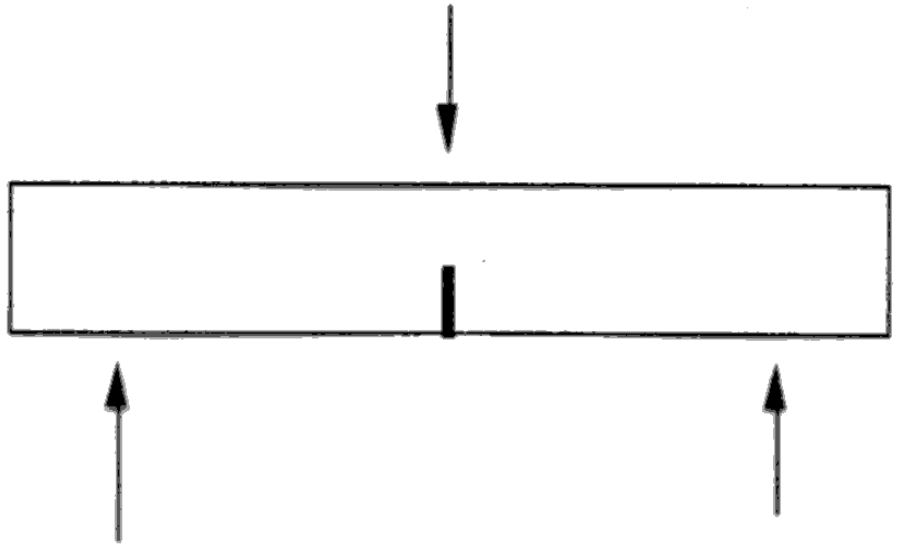

C>>Cintrinsic

Indentation technique

Establishment of standard testing technique: round robin

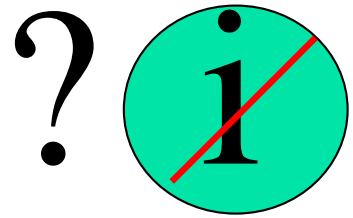

H. Miyazaki et al. / Ceramics International 36 (2010) 899–907

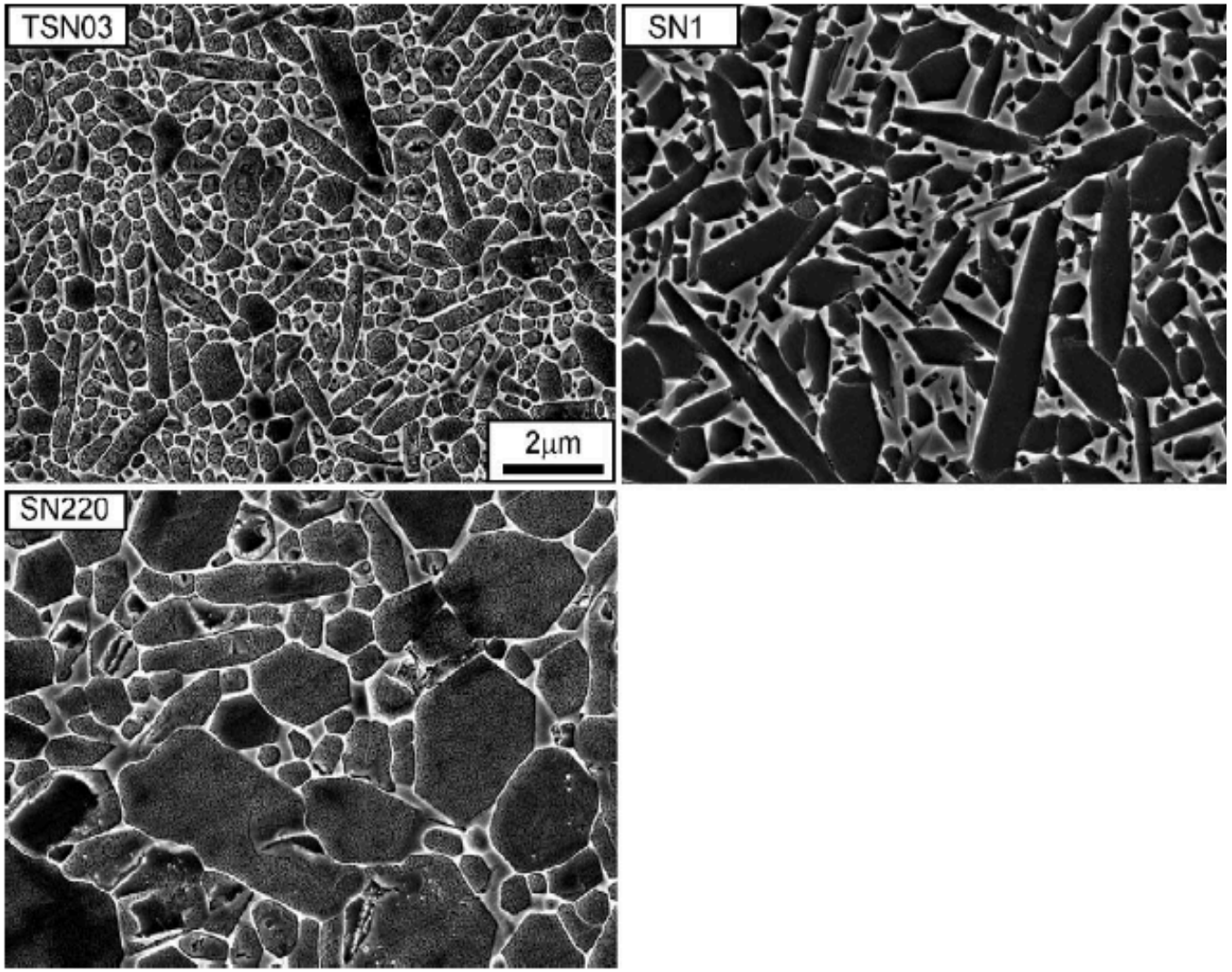

Fig. 1. SEM micrographs of the polished and etched surfaces of silicon nitride ceramics.

Miyazaki, H., Yoshizawa, Y., Hirao, K., Ohji, T. (2010). "Indentation fracture resistance test round robin on silicon nitride ceramics." Ceram. Inter. 36: 899-907.

Indentation technique

Establishment of standard testing technique: round robin

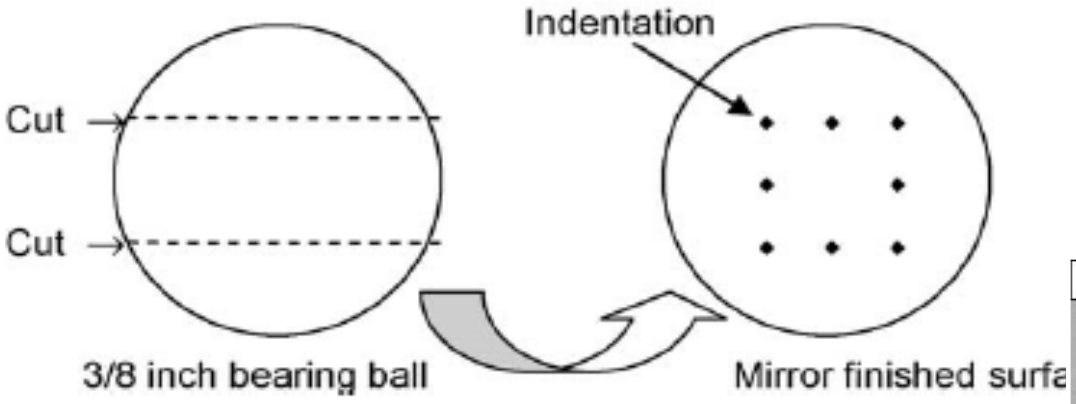

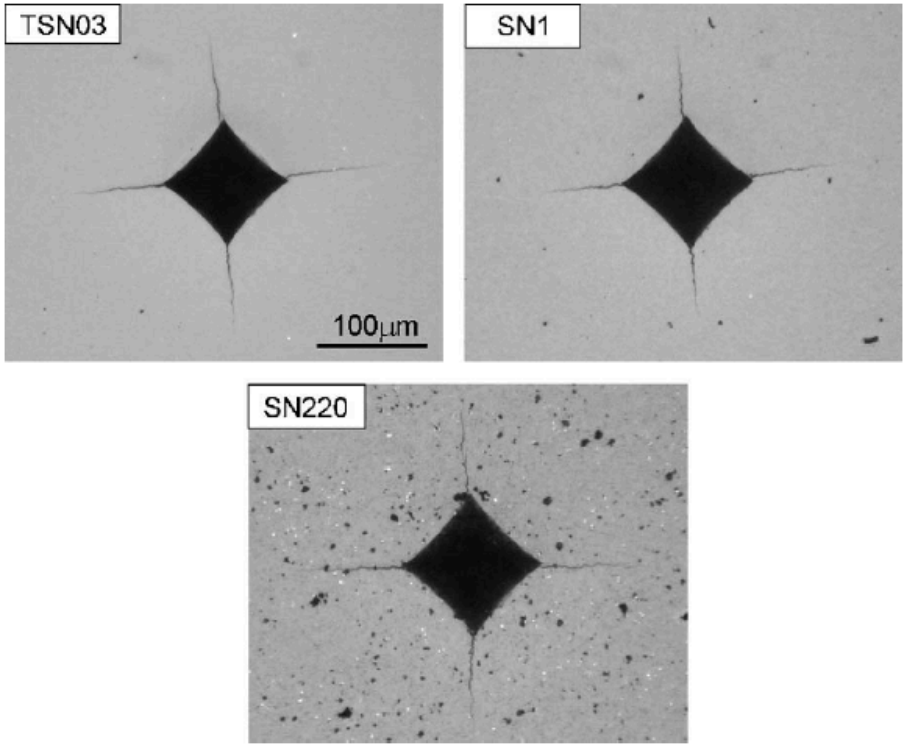

Fig. 3. Optical microscope photos of indentations at 98 N.

Miyazaki, H., Yoshizawa, Y., Hirao, K., Ohji, T. (2010). "Indentation fracture resistance test round robin on silicon nitride ceramics." Ceram. Inter. 36: 899-907.

Indentation technique

Establishment of standard testing technique: round robin

Table 1
List of participants.

Country	Laboratory
Ireland	University of Limerick
Korea	Korea Institute of Materials Science
U.S.A.	Oak Ridge National Laboratory
Japan	Ceramics Maker
	National Institute of Advanced Industrial Science and Technology (AIST)
	Yokohama National University

Observer	Indentation load (N)	Labs	Total indent.	Average (MPa $m^{1/2}$)	Repeatability (within-lab)		Reproducibility (between-labs)	
					Std. Dev. (MPa $m^{1/2}$)	COV (%)[a]	Std. Dev. (MPa $m^{1/2}$)	COV (%)[a]
Each lab	98	6	42	6.68	0.19	2.9	0.43	6.4
Each lab	196	6	38	6.87	0.12	1.8	0.28	4.1
Each lab	294	3	20	6.86	0.13	2.0	0.32	4.7
AIST	98	5	35	6.50	0.11	1.6	0.23	3.5
AIST	196	5	40	6.83	0.11	1.6	0.17	2.4
AIST	294	2	8	6.79	0.19	2.9	0.20	2.9

[a] Coefficient of variance.

Indentation technique

Establishment of standard testing technique: round robin

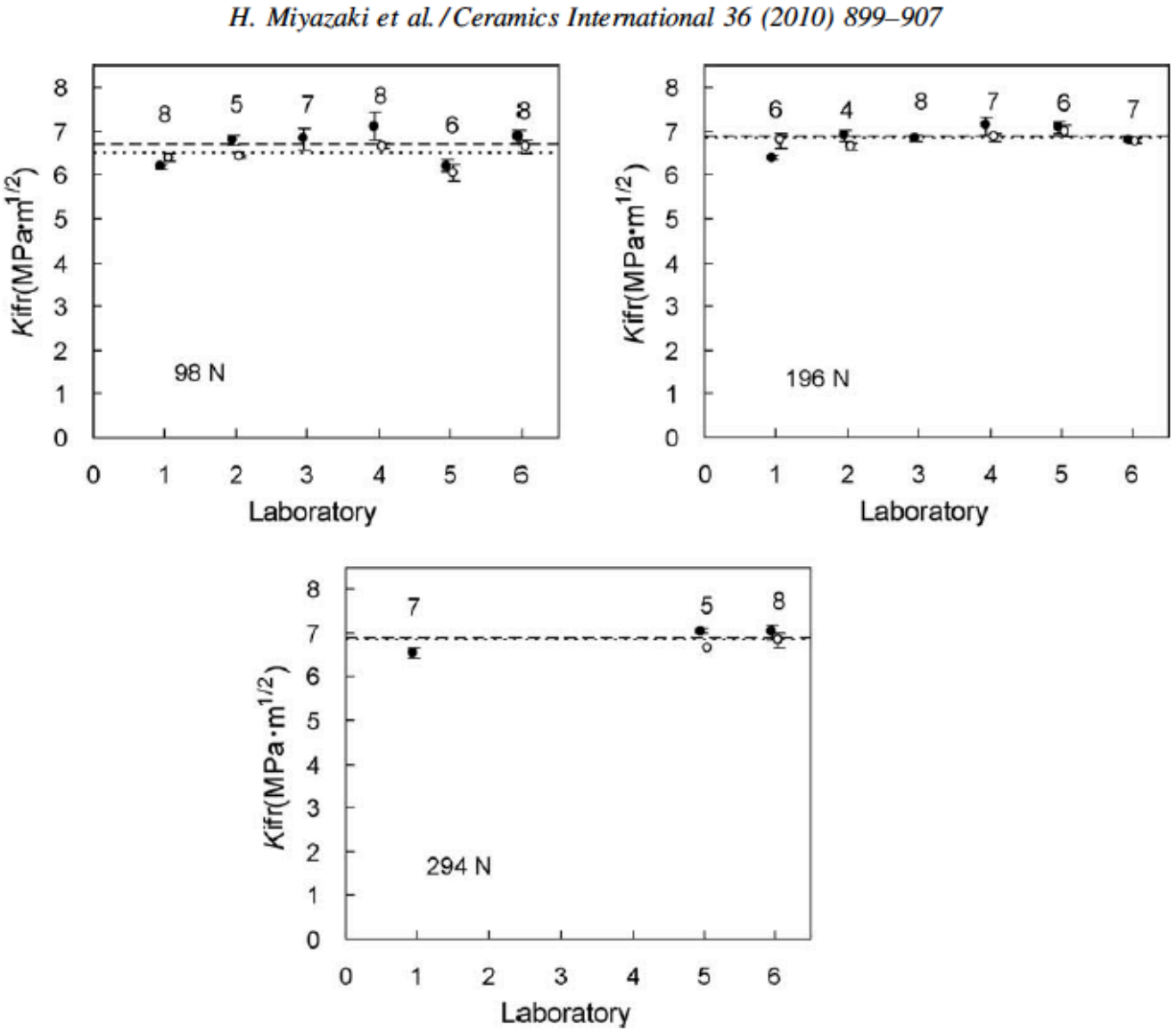

Miyazaki, H., Yoshizawa, Y., Hirao, K., Ohji, T. (2010). "Indentation fracture resistance test round robin on silicon nitride ceramics." Ceram. Inter. 36: 899-907.

Weibull statistics (weakest-link theory)

$$F = 1 - \exp[\int_V -(\frac{\sigma}{\sigma_o^x})^m dV]$$

- F: probability of failure
- V: volume
- σ: strength
- σ_o^x: the characteristic strength per unit volume, 63.3% probability of failure
- m: Weibull modulus

$$\ln\ln\frac{1}{1-F} = m\ln\sigma - m\ln\sigma_o^x + C$$

Weibull modulus, m

Survival probability,
lnln[1/(1-F)]

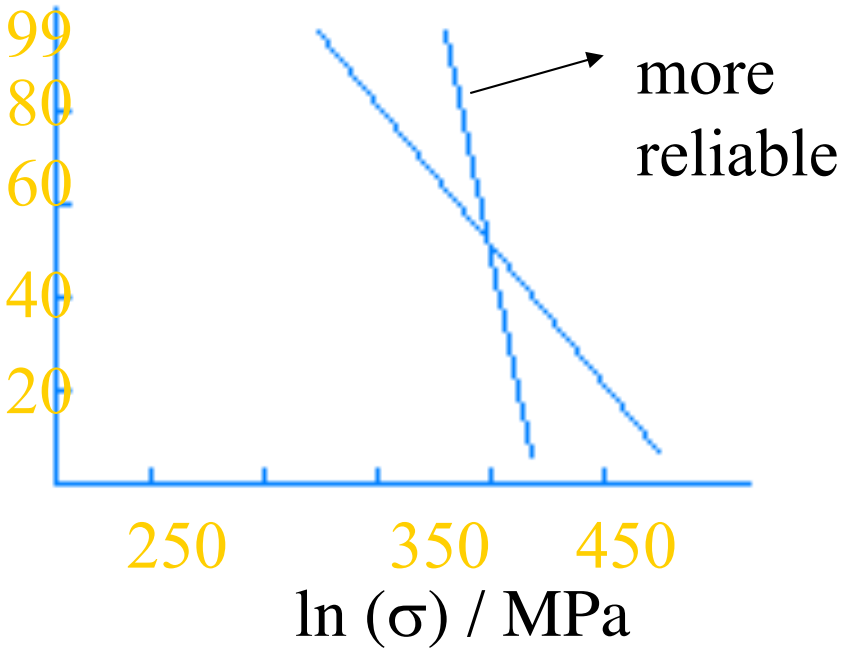

- slope= Weibull modulus
- Weibull modulus ⇑, reliability ⇑

R-curve behaviour

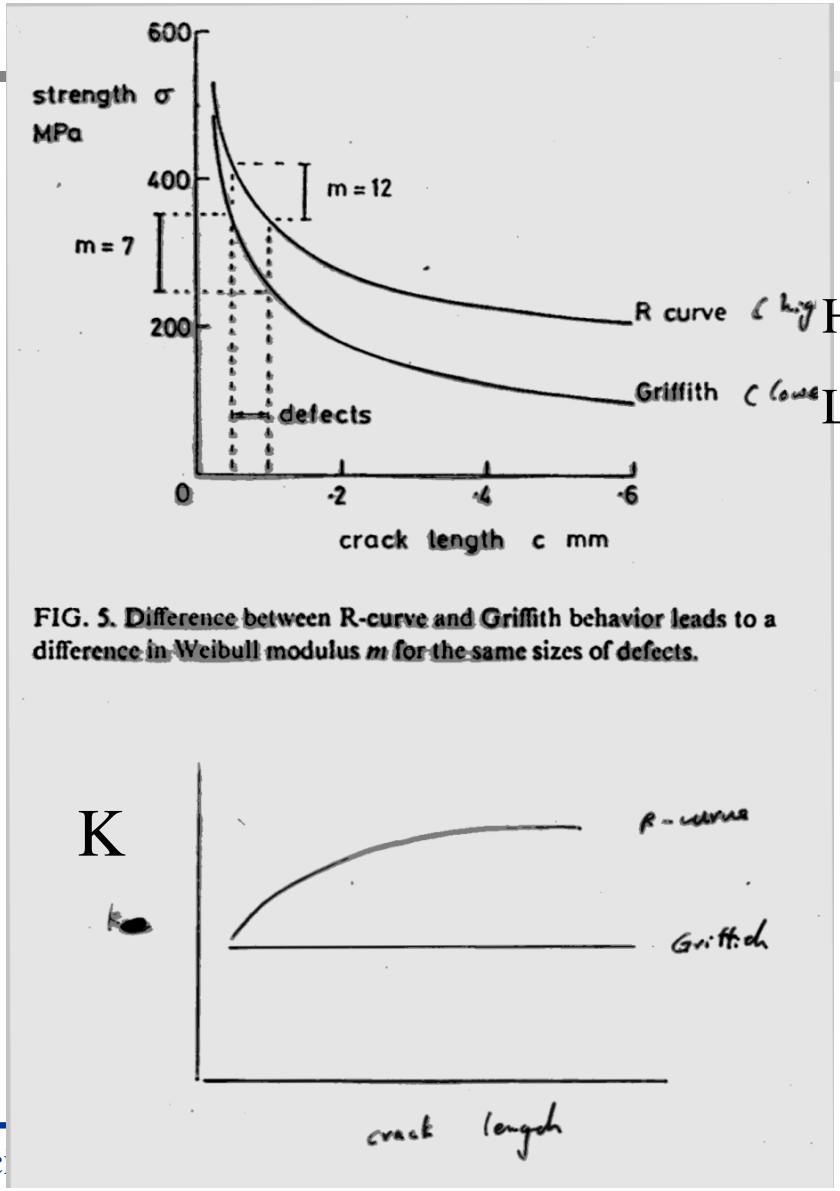

FIG. 5. Difference between R-curve and Griffith behavior leads to a difference in Weibull modulus *m* for the same sizes of defects.

Higher Weibull modulus

Lower Weibull modulus

Unit 6
Challenges and Future

- Major challenges
  - Cost, Cost, Cost…….

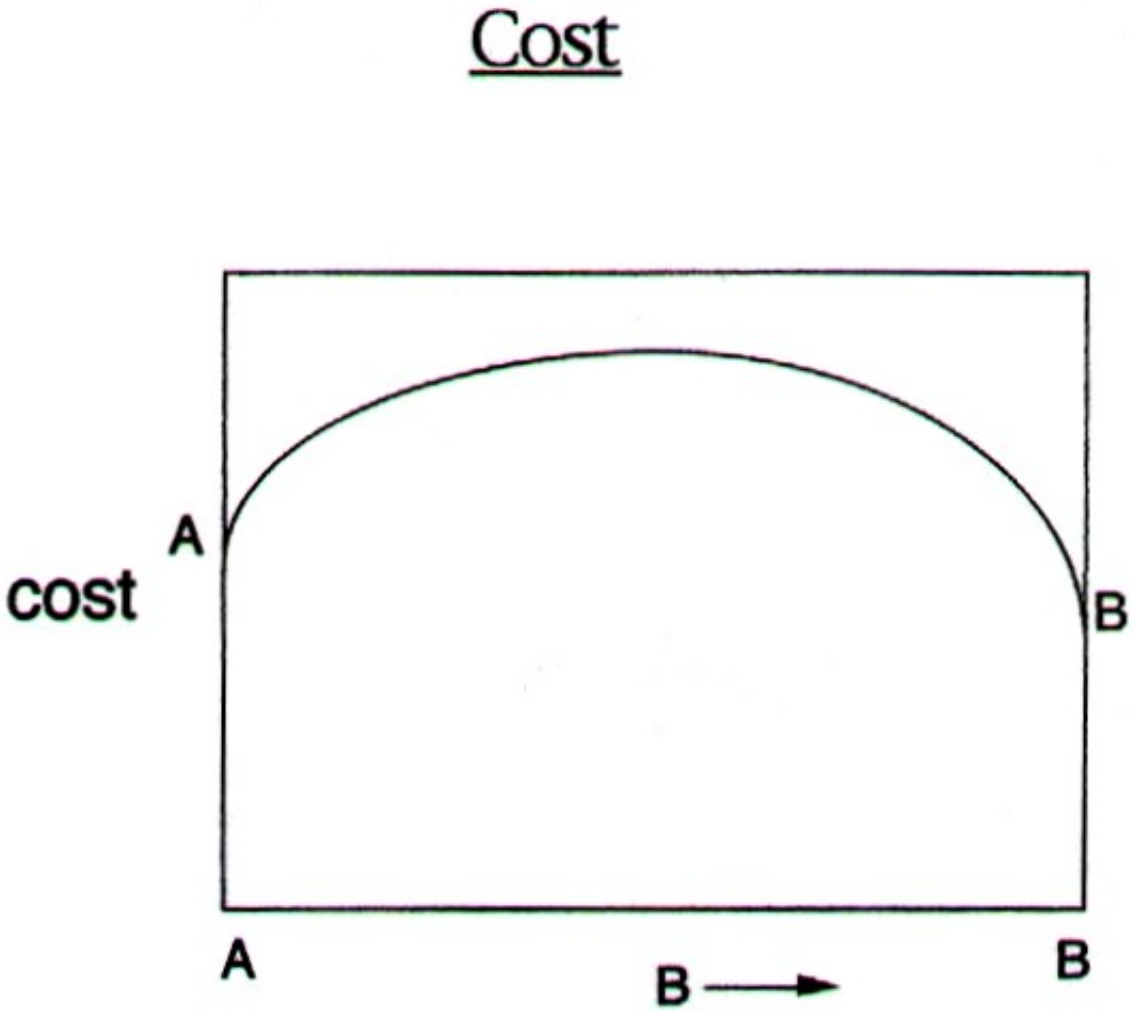

⇒ If the composite values are no better than those of existing materials, there is little point in making it.

*Comparison
example: SiC/SiC composite

	Composite	
Parameter	CVI-based	Melt-infiltrated
Cost	Highest	Midrange
Maximum component thickness	<1.5 cm	2–4 cm
Maximum use temperature	1700°C air, ~2000°C inert	1380°C†
Reactivity with metals, ceramics	High during processing, hot HCl damages most materials	High, silicon reacts with most metals and ceramics above 900°C

W. J. Sherwood, Am. Ceram. Soc. Bull., 2003

- Challenges
  - Cost
  - Application: a cost issue
- Examples
  - CVI, SiC/SiC_f
    - 幻象戰機
  - Melt-infiltration, SiC/SiC_f
    - Boeing, Airbus

Milestone for the application of CMC

- Aircraft components
  - Example: SiC/SiC composite for gas turbine engine
  - Example: GE takes CMC to air @ 2016
- Auto brakes
- Electronic packages
- Etc.

GE 9X from GE Aviation

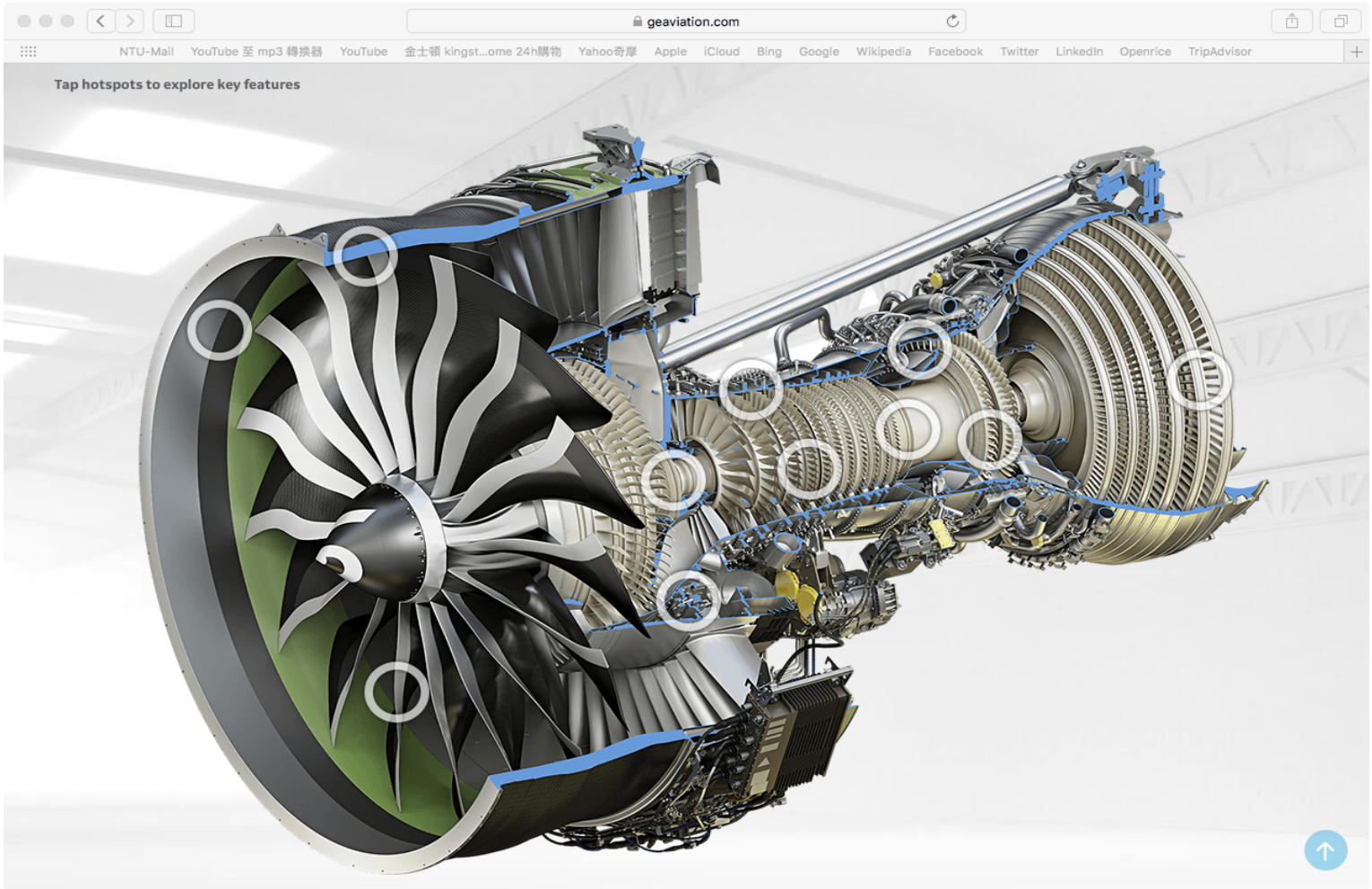

CMC for engine

- Advantages
  - Light, 1/3 that of Ni alloy
  - Withstand higher temperature, higher efficiency
  - Little, or no cooling, higher efficiency
  - Lower fuel burn
  - Lower emission

Engine components

Fig. 7. After-burner parts in a military aerojet engine already fabricated with SiC-matrix composites, according to Christin [19]: (a) exhaust cone, (b) outer flap, (c) inner flap, (d) flame holder.

Naslain, Composite Science and Technology, 2004

Engine components

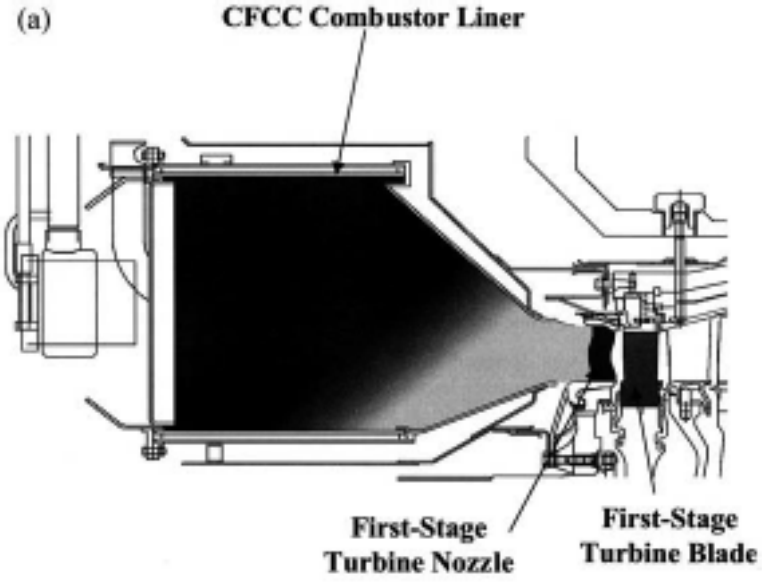

(b)

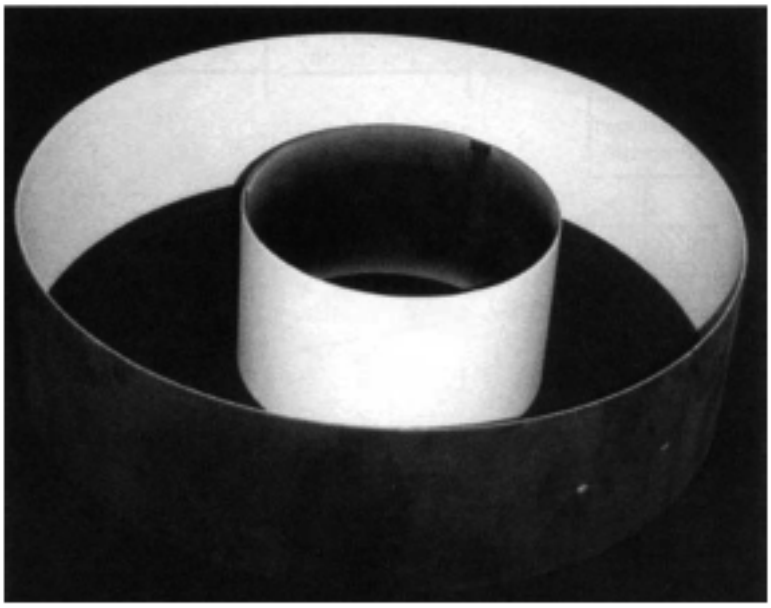

Fig. 8. SiC/SiC liners of a stationary gas turbine of cogeneration (a) chematic of the hot section and (b) combustor ceramic liners, from Miriyala et al. [64].

Naslain, Composite Science and Technology, 2004

HTCMC for engine

1. Melt infiltration SiC/SiC composites (HiPerComp) are attractive for high temperature application in gas turbines.

low matrix porosity,
high thermal conductivity,
high interlaminar strength,
superior oxidation strength

2. Feasibility of fabricating a wide variety of composites demonstrated.

Conclusions from HTCMC

3. Several successful field engine tests
   small engine shroud >1,000 h
   small engine combustor > 12,000 h
   large engine partial shroud set > 5,000 h
   Large engine full shroud set > 1,100 h
   and continuing

4. Anticipated engine performance benefit of CMC shroud system has been validated.

5. Remaining hurdles to commercialization include CMC material cost and demonstration of full component life.

applications

Fig. 8. Carbon-fiber polymer-derived SiC-matrix brake components.

W. J. Sherwood, Am. Ceram. Soc. Bull., 2003

applications

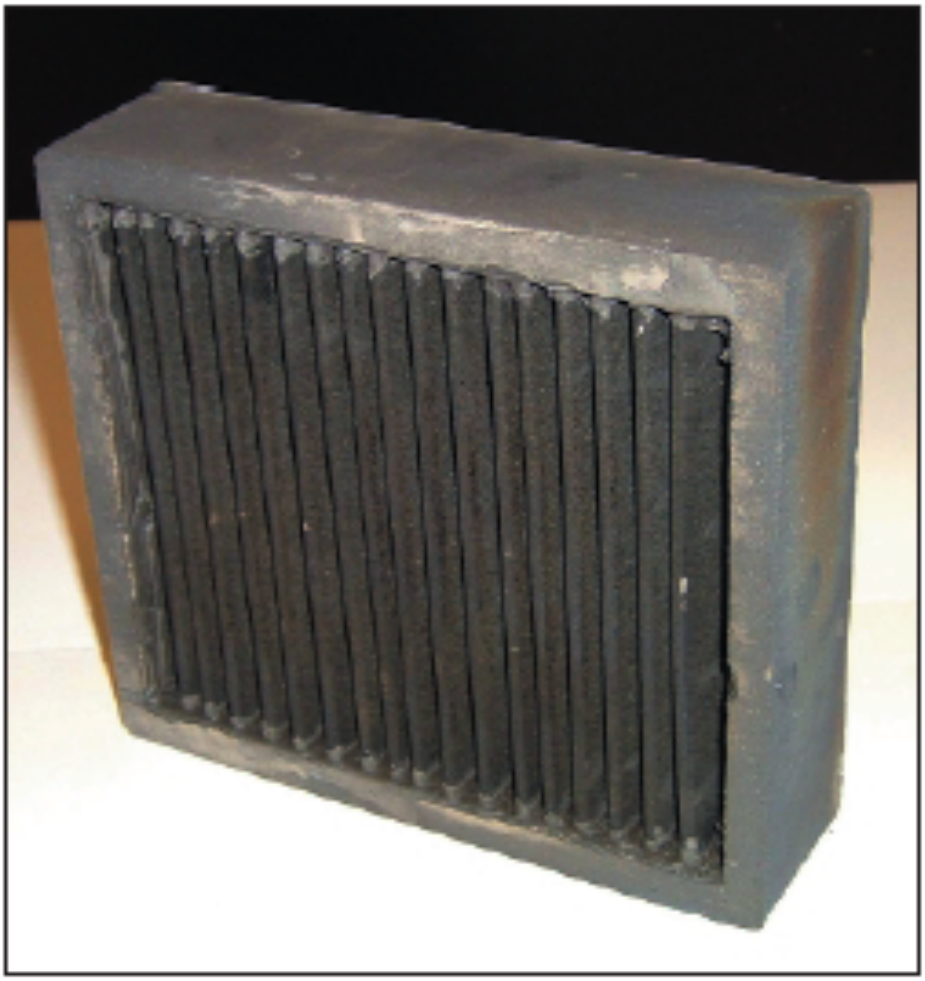

Fig. 9. Diesel filter section with the filter media and frame densified using ceramic-forming polymers.

W. J. Sherwood, Am. Ceram. Soc. Bull., 2003

applications

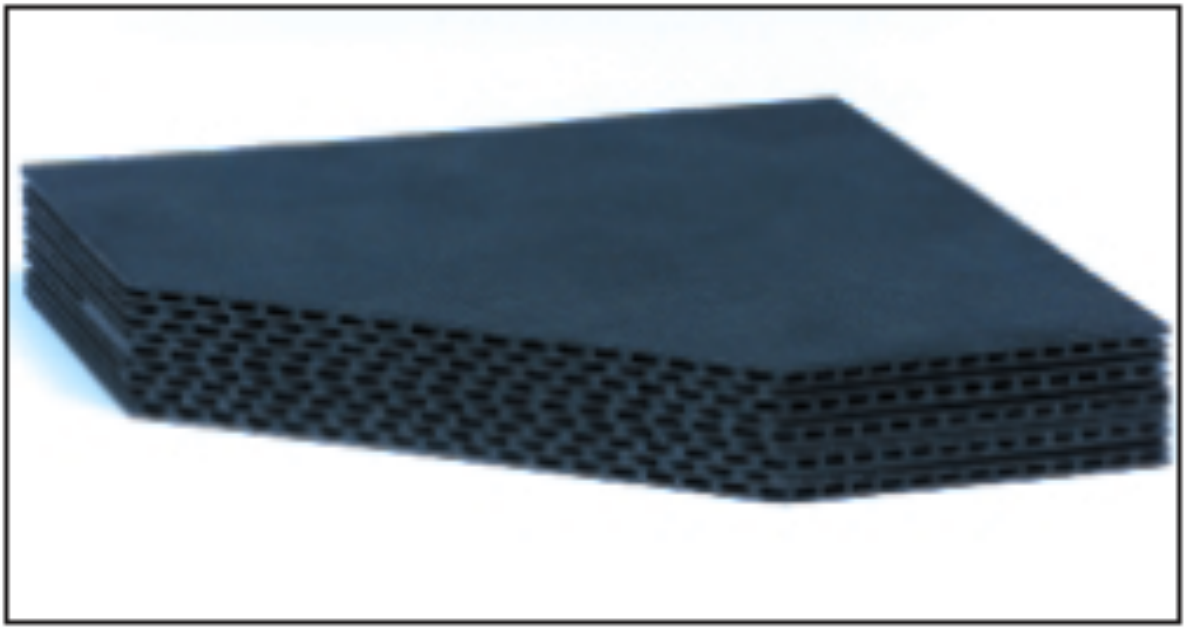

Fig. 10. Carbon cloth–SiC crossflow heat exchanger.

W. J. Sherwood, Am. Ceram. Soc. Bull., 2003

Example: SiC/diamond super-hard material

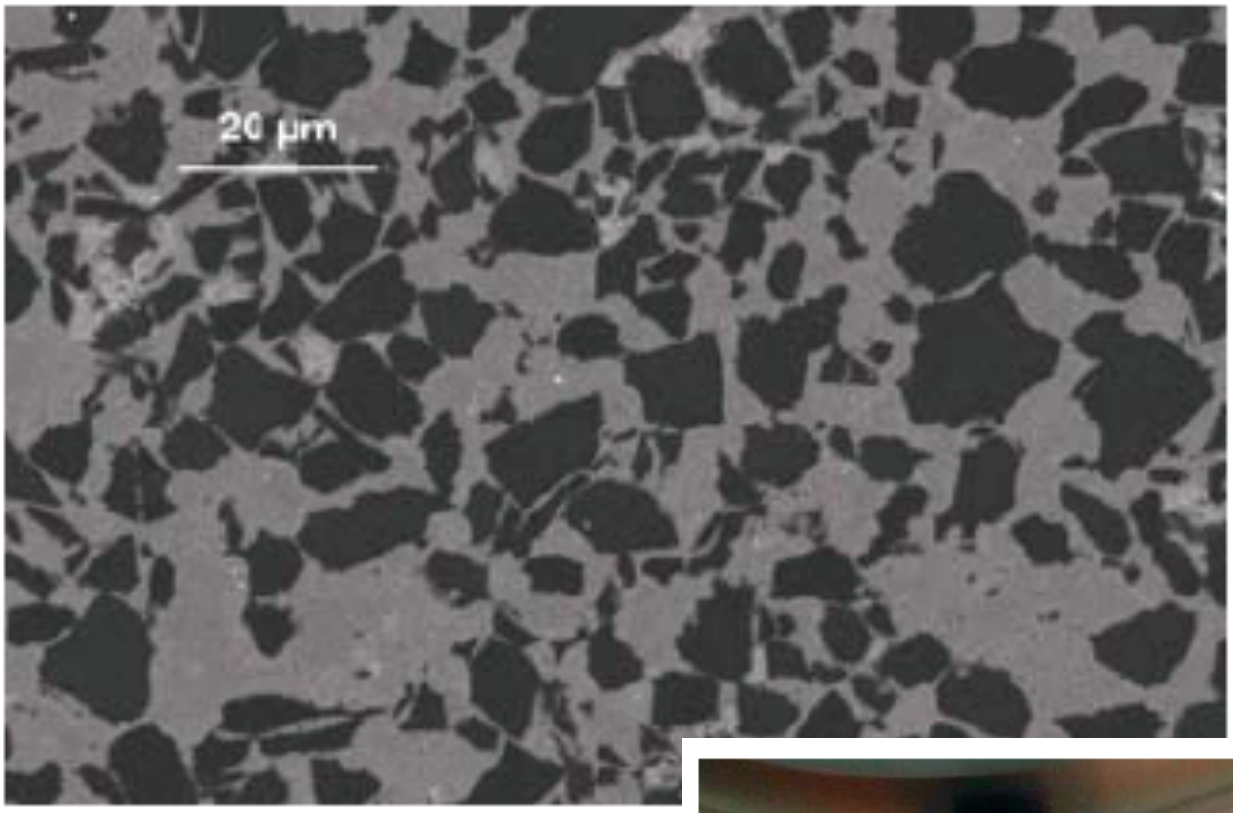

Microstructure of SiC/diamond

Si3N4

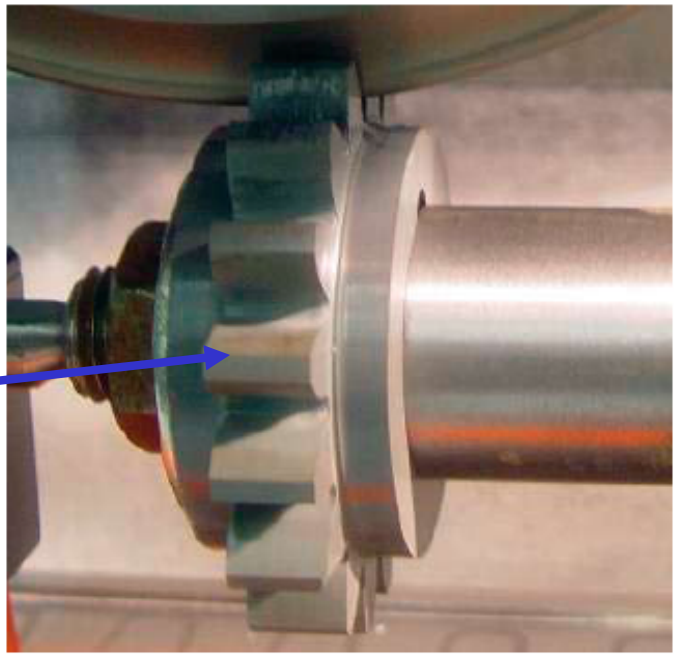

Manufacturing of ceramic gears made of Si_3N_4: Two opposed tooth flanks are grinded using formed grinding wheels. To increase the bearing capacity of the gear the tooth flanks are subsequently shot-peened.

Ref: Advancera Newletter, 2009

Example: C/SiC Clutch

can be machined by electrical discharge machining. So, detailed geometries can be realized which are required for silicon carbide extruded bodies for filter applications.

Porsche Ceramic Composite Clutch (PCCC) and C-SiC sample. (Source: Fraunhofer IPK)

Example: Al_2O_3/SiC_w composites

ARtuff® ceramic composites are the first commercially available ceramic composite materials manufactured from a high-purity aluminum oxide matrix reinforced with silicon carbide whiskers. ARtuff ceramic composites are characterized by extreme hardness, outstanding compressive strength and rigidity, combined with greatly improved toughness.

ARtuff Products Outperform

ARtuff ceramic composites are versatile materials for broad-based applications under the most severe operating conditions.

Typical applications in industry would include deep draw tooling, seal rings, valves and seats, pump components and extrusion dies – areas requiring the ultimate resistance to wear/erosion from abrasion and the ability to withstand thermal or chemical attack. For the chemical and food processing industries ARtuff composites provide superior erosion and corrosion resistance in environments that must be free of contamination.

Exceptional Resistance to Erosion

ARtuff has excellent high temperature properties and is nearly inert, thus it resists chemical erosion, electromechanical wear and abrasion. Finished products made of ARtuff ceramic composites are far superior to similar products made of metal, tungsten carbide or conventional ceramics. An ARtuff ceramic valve in a high pressure slurry pump increased the pumps service life 45 times over the stainless steel valve ARtuff replaced.

Greatly Enhanced Fracture Toughness

Production products such as seals, bearings, dies, etc., have greatly improved toughness and are far less likely to chip. ARtuff ceramic products can be installed using conventional installation techniques without breakage or chipping, allowing assemblies to be serviced and placed back in production faster. ARtuff ceramic composites are over 200% tougher than the best high alumina ceramics.

High Thermal Shock Resistance

ARtuff ceramic materials CC7000 and CC6000 exhibit no strength degradation when thermally shocked from 1000°C to room temperature and are ten times more resistant to thermal shock than conventional ceramics. This feature allows ARtuff products to be used in high temperature operations either under continuous or intermittent cycles which produce wide variations in temperature, and allows steam cleaning of assemblies with no damage to the ARtuff composite components.

Excellent Machinability, Design and Performance Predictability

Components fabricated from ARtuff composites can be designed with unprecedented performance predictability. ARtuff ceramics have outstanding compressive strength and rigidity; diamond is the only naturally occuring substance which exceeds ARtuff composite hardness.

ARtuff products can be designed and machined to extremely close tolerances due to its dimensional stability and toughness.

Future

- Automobile

- Consumables

Thank you for your attention

Contact information
tuan@ntu.edu.tw

活動四

低成本金屬部件局補強專門接合技術研討會

由德國弗勞恩霍夫物料及光束技術研究所主管恩斯・史丹夫博士主講

Seminar on tailoring joining technology for low cost localized performance enhancement of metal parts

13. February 2018, Hong Kong

Dr. Jens Standfuss
Fraunhofer Institute for Material and Beam Technology

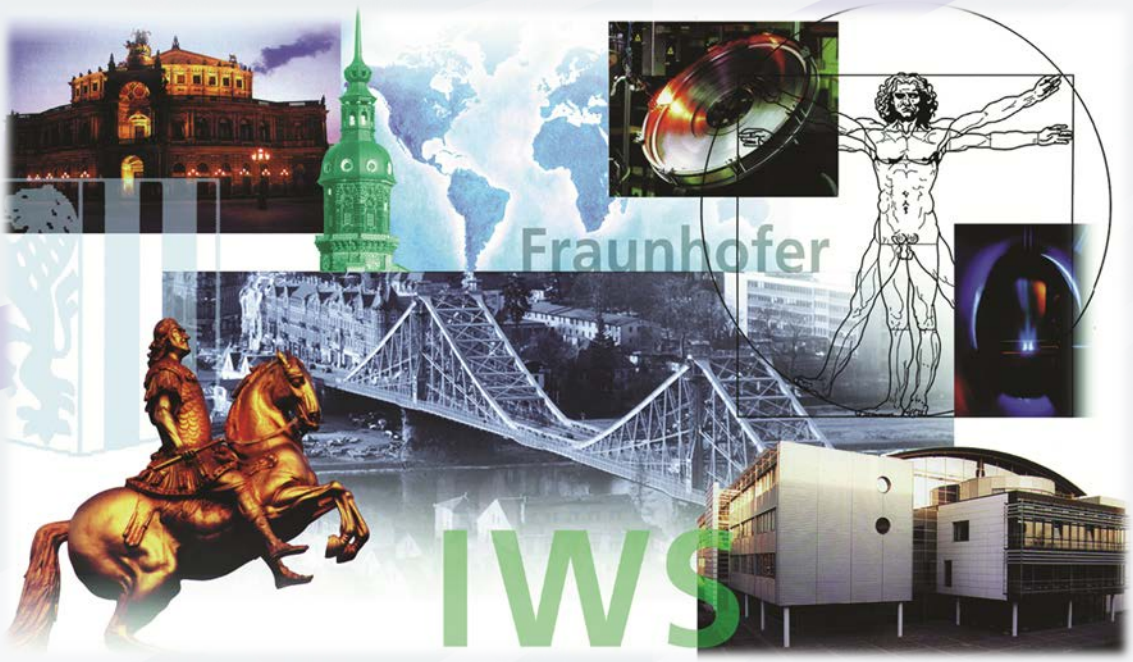

© Fraunhofer IWS

Content

Content	Chapter
Introduction	
The Fraunhofer Gesellschaft	01
Fraunhofer Institute for Material and Beam Technology IWS	02
Seminar topics	03
Laser Beam Welding	
Basics	04
Laser multi pass welding	05
Laser beam welding with high frequent beam oscillation	06
Laser beam welding of high reflective materials	07
Laser beam welding of powertrain components	08
Laser induction roll plating	09
Special Joining Technologies	
Magnetic pulse joining	10
Friction stir welding	11
Joining with reactive multi layers	12
Bonding and Composite technology	
Electrical-conductive bonding	13
Thermal direct joining of thermoplastic to metal	14
Mechanical Joining	
Enhanced mechanical connection by laser interference patterning	15

© Fraunhofer IWS

THE FRAUNHOFER-GESELLSCHAFT
WHO WE ARE

© Fraunhofer

Fraunhofer

Joseph von Fraunhofer (1787 – 1826)

- **Researcher**
  Discovery of “Fraunhofer Lines“ in the solar spectrum
- **Inventor**
  New methods of lens processing
- **Entrepreneur**
  Head of royal glass factory

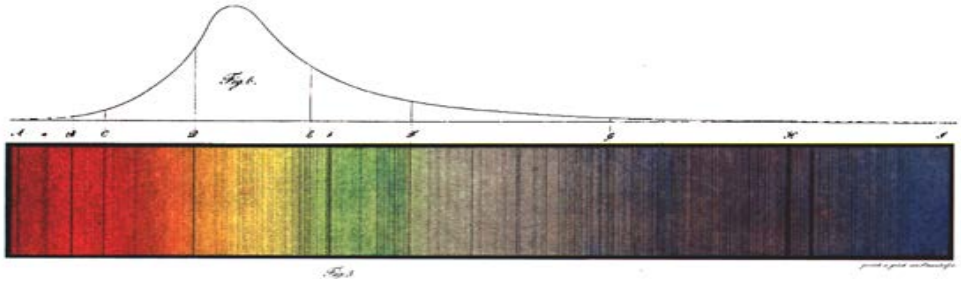

© Fraunhofer

Fraunhofer

The Fraunhofer-Gesellschaft – Europe's Largest Organization for Applied Research

Headquarters in Munich

- Founded in 1949 in Munich
- 69 institutes and research units in Germany
- More than 24,500 employees
- Annual budget is about € 2.1 billion, partially public founded
- Representative offices, research units, and subsidiaries worldwide

© Fraunhofer

The Fraunhofer-Gesellschaft in Germany

- 69 institutes and research units
- 24,500 staff

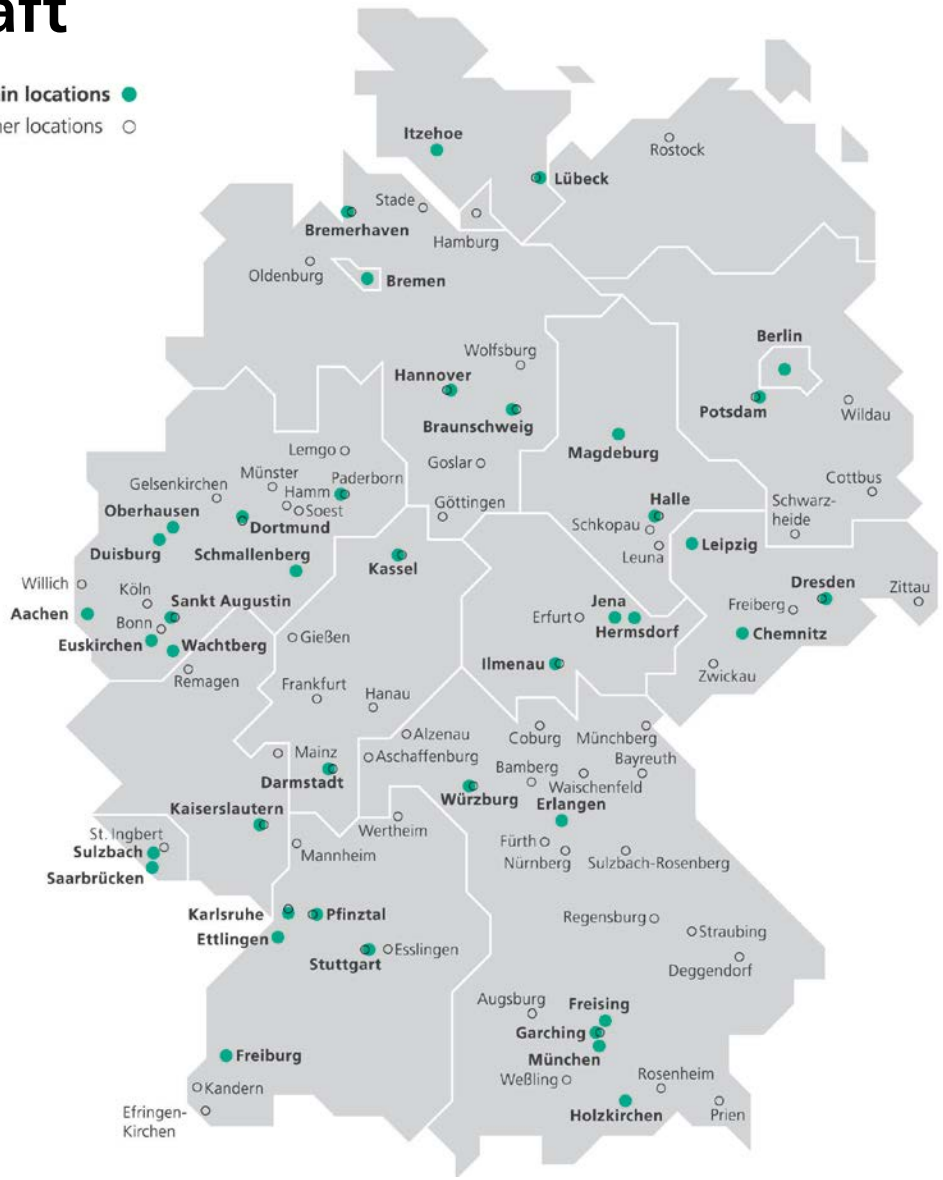

© Fraunhofer

Fraunhofer

Fraunhofer Fields of Research

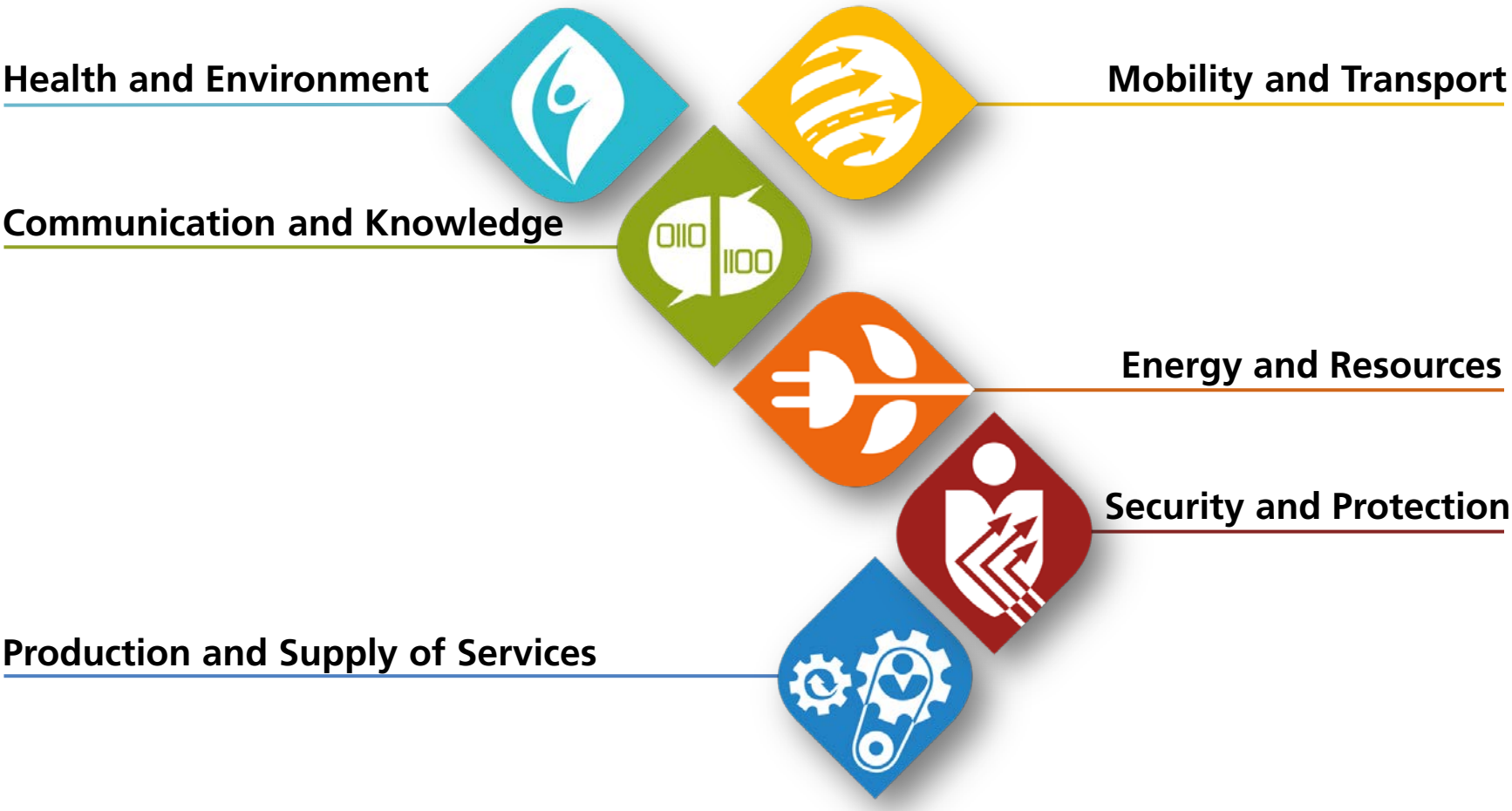

© Fraunhofer

Fraunhofer

Fraunhofer Groups

- Foster a joint presence on the R&D market
- Help defining the Fraunhofer business policy
- Implementing the organizational and funding principles of the Fraunhofer model

- Defense and Security VVS
- ICT
- Innovation Research
- Life Sciences
- Light & Surfaces
- Materials and Components
- Microelectronics
- Production

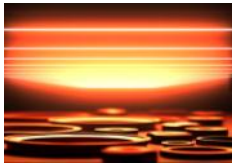

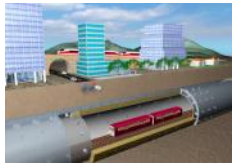

https://www.fraunhofer.de/en/institutes/institutes-and-research-establishments-in-germany/fraunhofer-groups.html

© Fraunhofer

Fraunhofer

Fraunhofer Alliances

- Facilitating customer access to the services and research areas
- Common points of contact
- Coordination of the development of appropriate solutions

Adaptronics

Additive Manufacturing

Advancer

Ambient Assisted Living

AutoMOBILE Production

Battery

Big Data

Building Innovation

Cleaning Technology

Cloud Computing

Digital Media

Embedded Systems

Energy

Food Chain Management

Lightweight Structures

Nanotechnology

Photocatalysis

Polymer Surfaces

Simulation

Space

Technical Textiles

Traffic and Transportation

Vision

Water Systems (SysWasser)

https://www.fraunhofer.de/en/institutes/institutes-and-research-establishments-in-germany/fraunhofer-alliances.html

© Fraunhofer

THE FRAUNHOFER-GESELLSCHAFT

BUSINESS MODEL, PATENTS
POSITION IN THE GERMAN RESEARCH LANDSCAPE

Research in Germany
Land of Ideas

© Fraunhofer

Fraunhofer

The German Research Landscape

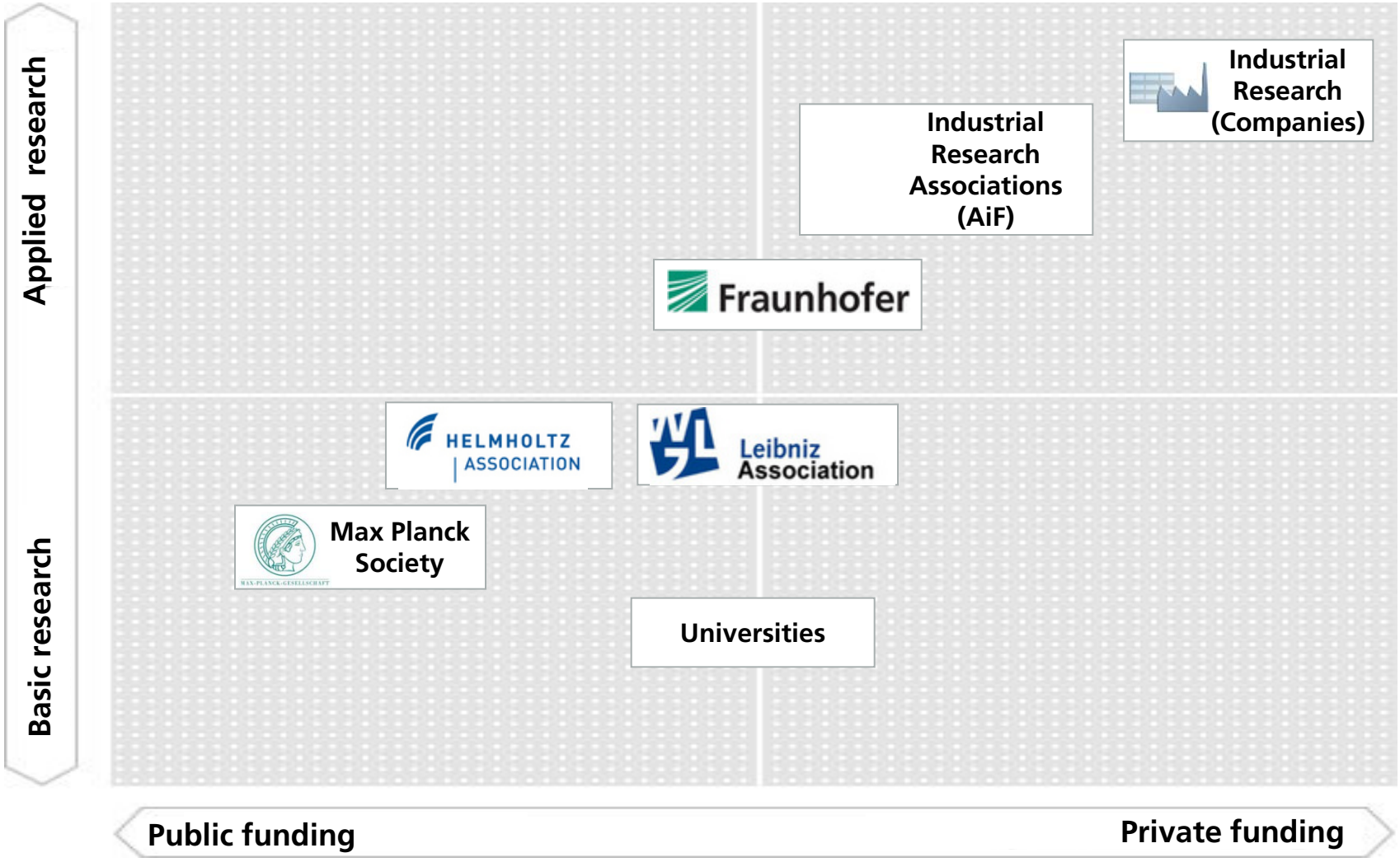

Source: BMBF Germany (simplified)

© Fraunhofer

Fraunhofer

Fraunhofer Research and Business Models

Contract Research

- Applied research and development for industry
- On specific requests of our customers, exclusive

Joint Research

- Forefront and applied research (demonstrators)
- Funded by European Union and national funding bodies

Fraunhofer Forefront Research

- Setting new standards, technologies (prototypes)

Patent / Technology / Product Licensing

- Worldwide, preferably non-exclusive

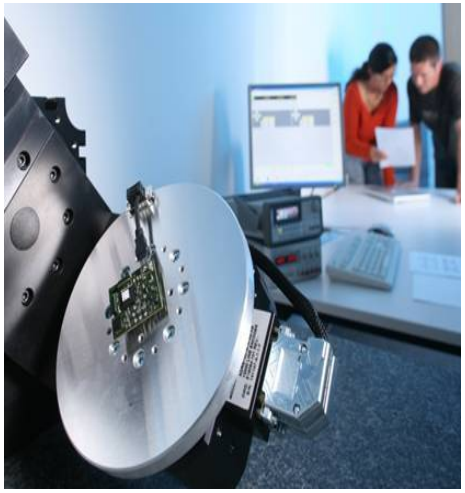

© Fraunhofer

Contract Research Revenue

(in € million)

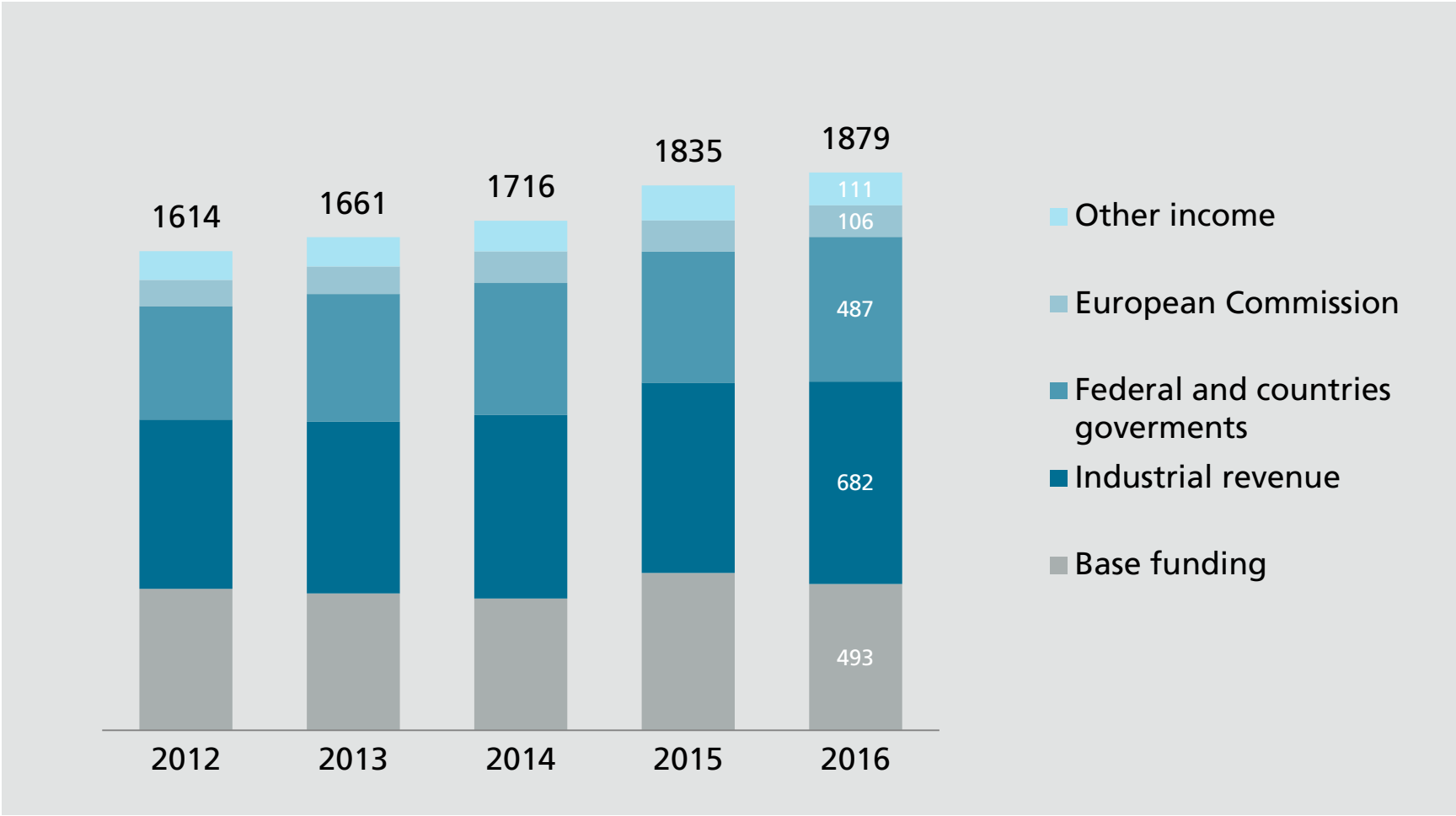

© Fraunhofer

Fraunhofer

THE FRAUNHOFER-GESELLSCHAFT
INTERNATIONAL ACTIVITIES

© Fraunhofer

Fraunhofer

Fraunhofer Worldwide

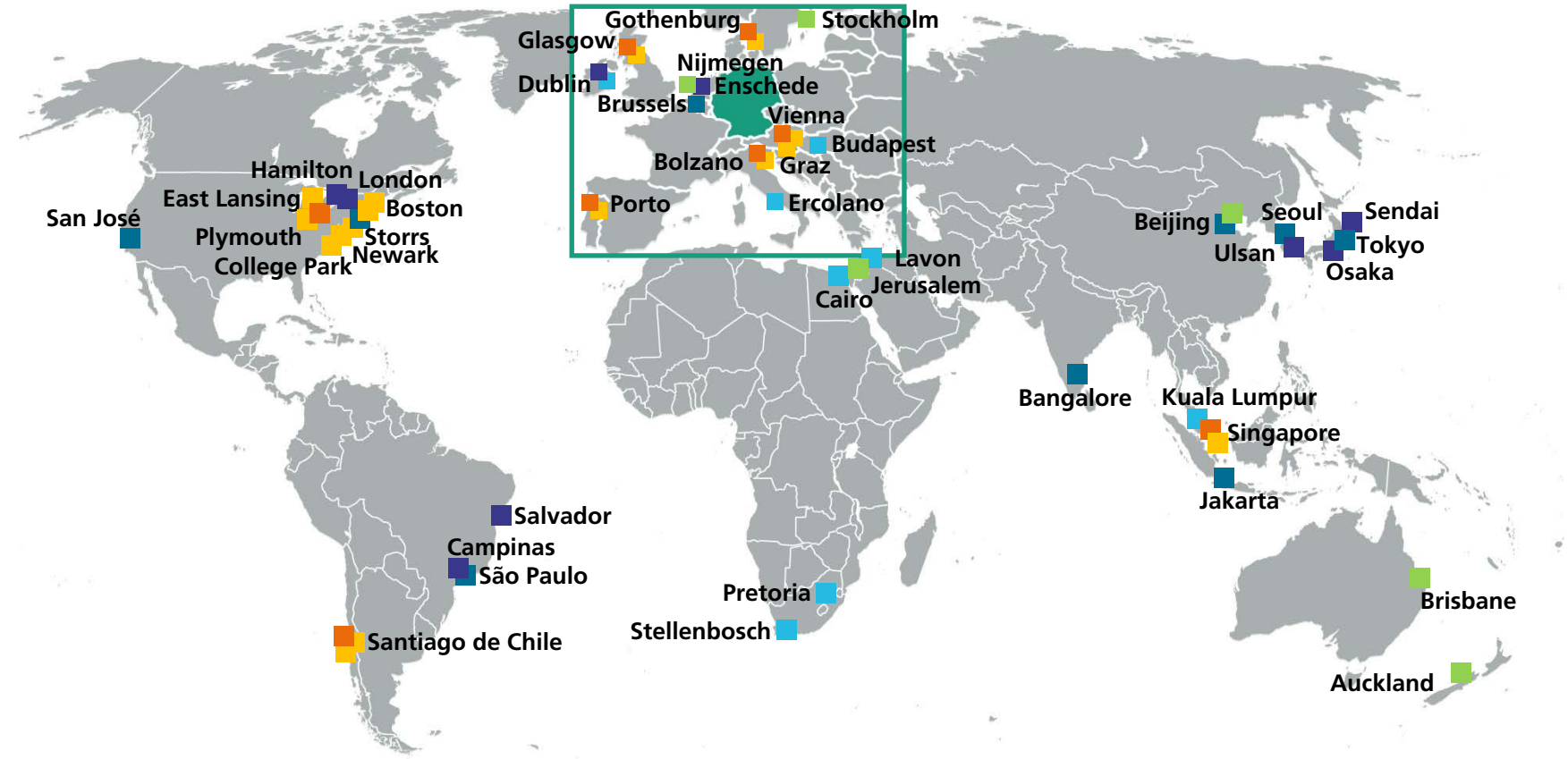

- Subsidiary
- Center
- Project Center
- ICON / Scientific Cooperation
- Representative / Marketing Office
- Senior Advisor

© Fraunhofer

Fraunhofer

Fraunhofer Subsidiarys and Center in Europe

- Fraunhofer Austria Research
  - Production- and Logistic Management, Vienna
  - Visual Computing, Graz
- Fraunhofer Italia Research
  - Fraunhofer Innovation Engineering Center IEC, Bolzano
- Fraunhofer Portugal Research
  - Fraunhofer Center for Assistive Information and Communication Solutions AICOS, Porto
- Fraunhofer Chalmers Centrum
  - Fraunhofer Chalmers Research Center for Industrial Mathematics FCC, Gothenburg
- Fraunhofer UK Research
  - Fraunhofer Centre for Applied Photonics CAP, Glasgow

© Fraunhofer

Fraunhofer

Other Fraunhofer Locations in Europe

- Fraunhofer EU Office Brussels
- Fraunhofer Senior Advisor Ireland & UK, Dublin
  Prof. Gerry Byrne
- Fraunhofer Senior Advisor Hungary, Budapest
  Prof. László Monostori
- Fraunhofer Senior Advisor Italia, Ercolano
  Prof. Luigi Nicolais
- Fraunhofer Project Center for Embedded Bioanalytical Systems, Dublin
- Fraunhofer Project Center for Design and Production Engineering for Complex High-Tech Systems, Enschede

© Fraunhofer

Fraunhofer

Fraunhofer USA, Inc.
First Overseas Subsidiary, Established in 1994

Laser Application CLA

Manufacturing Innovation CMI

Sustainable Energy Systems CSE

Energy Innovation CEI

Molecular Biotechnology CMB

Experimental Software Engineering CESE

Coatings and Diamond Technologies CCD

Digital Media Technologies DMT

© Fraunhofer

Fraunhofer

Fraunhofer in South America

- Fundación Fraunhofer Chile Research
  - Fraunhofer Center for Systems Biotechnology CSB, Santiago de Chile
  - Fraunhofer Center for Solar Energy Technology CSET
- Fraunhofer Project Center on Software and Systems Engineering, Salvador
- Fraunhofer Project Center for Innovations in Food and Bioresources, Campinas
- Fraunhofer Liaison Office, Dr. Ronald Dauscha, São Paulo

© Fraunhofer

Fraunhofer

Fraunhofer Senior Advisors in Middle East, North and South Africa

- Fraunhofer Senior Advisor Israel
  Prof. Dr. Raphael Wertheim

- Fraunhofer Senior Advisor Egypt
  Dr. Mona El Tobgui

Fraunhofer Senior Advisors South Africa

- Pretoria
  Prof. Dr. Oliver Damm
- Stellenbosch
  Prof. Dr. Dimiter Dimitrov

© Fraunhofer

Fraunhofer

Fraunhofer Representative Offices and Senior Advisor in Asia

- Representative Office Japan
  Hideya Miki
- Representative Office Korea
  Dr. Byeungkwan Park
- Representative Office Beijing
  N.N.
- Representative Office India
  Anandi Iyer
- Representative Office Indonesia
  Dr. Kesawa Narayana
- Senior Advisor Malaysia
  Dr. Ahmad B. Ibrahim

© Fraunhofer

Fraunhofer

Fraunhofer Activities in Asia

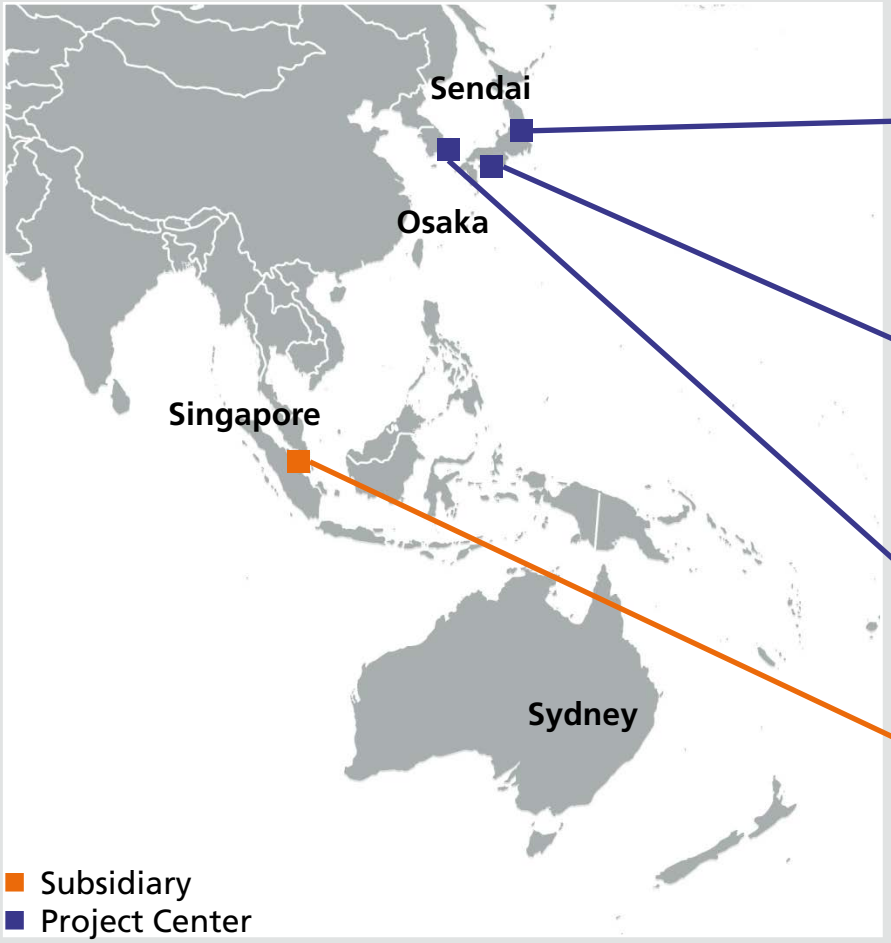

- Fraunhofer Project Center for NEMS/MEMS Devices and Manufacturing Technologies Tohoku University
- Fraunhofer Project Center for Electroactive Polymers National Institute of Advanced Industrial Science and Technology AIST
- Fraunhofer Project Center for Composites Research Ulsan National Institute of Science and Technology
- Fraunhofer Center for Interactive Digital Media (IDM) Nanyang Technological University NTU

© Fraunhofer

Fraunhofer

International Revenues by Regions

(in € million)

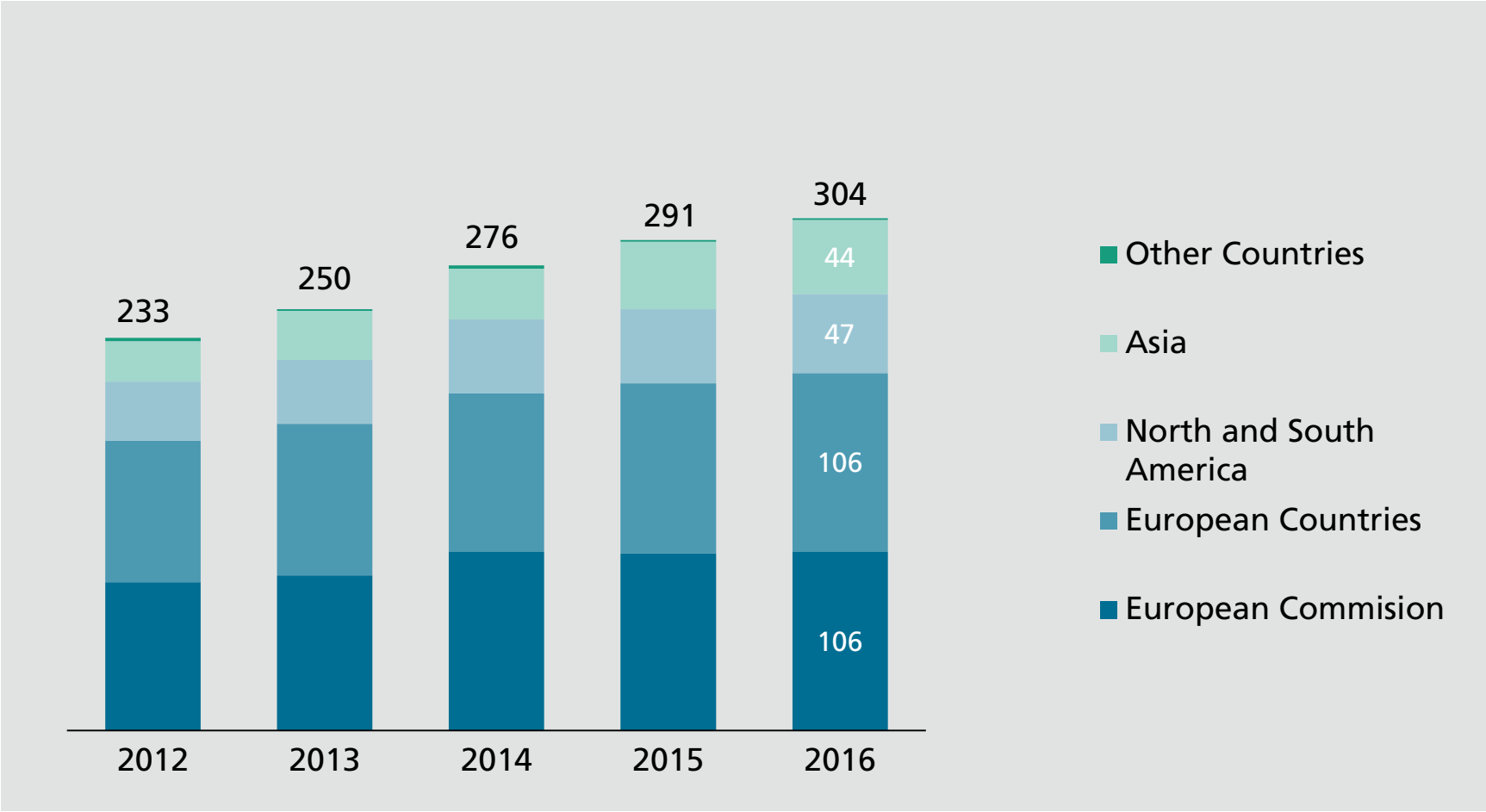

© Fraunhofer

Fraunhofer

International Revenue 2016 by Countries – Top 20

without EU-Commission, preliminary (in € million)

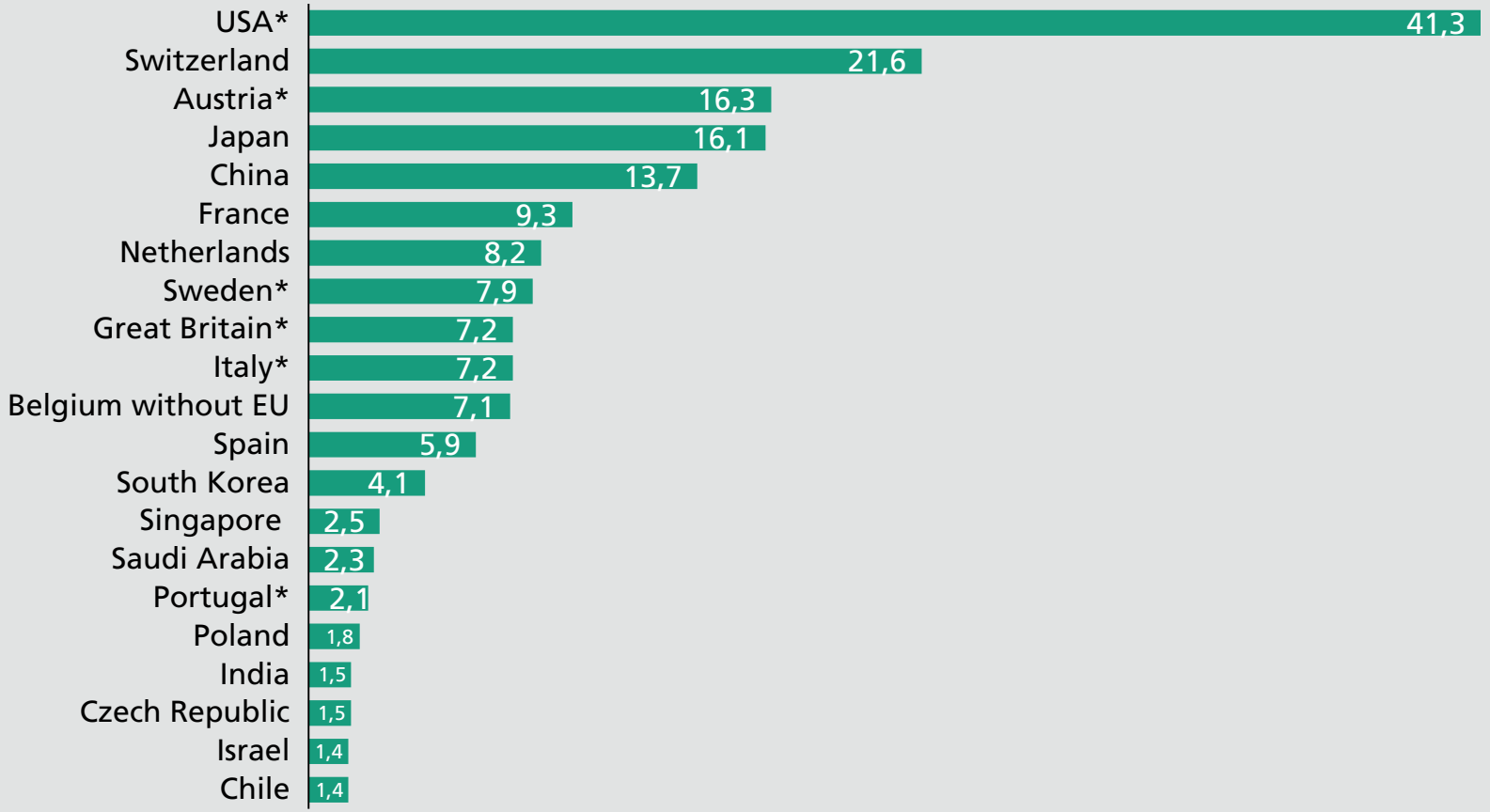

*** of which Fh-USA: 18,9 Mio €, Fh-Schweden: 3,5 Mio € , Fh-Austria: 2,5 Mio €, Fh-UK: 1,3 Mio €, Fh-Portugal: 1,4 Mio €, Fh-Chile: 1,0 Mio.€, Fh-Italia: 0,5 Mio €**

© Fraunhofer

Fraunhofer

Content

Content	Chapter
Introduction	
The Fraunhofer Gesellschaft	01
Fraunhofer Institute for Material and Beam Technology IWS	02
Seminar topics	03
Laser Beam Welding	
Basics	04
Laser multi pass welding	05
Laser beam welding with high frequent beam oscillation	06
Laser beam welding of high reflective materials	07
Laser beam welding of powertrain components	08
Laser induction roll plating	09
Special Joining Technologies	
Magnetic pulse joining	10
Friction stir welding	11
Joining with reactive multi layers	12
Bonding and Composite technology	
Electrical-conductive bonding	13
Thermal direct joining of thermoplastic to metal	14
Mechanical Joining	
Enhanced mechanical connection by laser interference patterning	15

© Fraunhofer IWS

Fraunhofer Institute Center Dresden

Fraunhofer FEP
Institute for Organic Electronics, Electron and Beam and Plasma Technology

Fraunhofer IKTS
Institute for Ceramic Technologies and Systems

Fraunhofer IWS
Institute for Material and Beam Technology

Fraunhofer IFAM
Institute for Manufacturing Technology and Advanced Materials, Branch Dresden

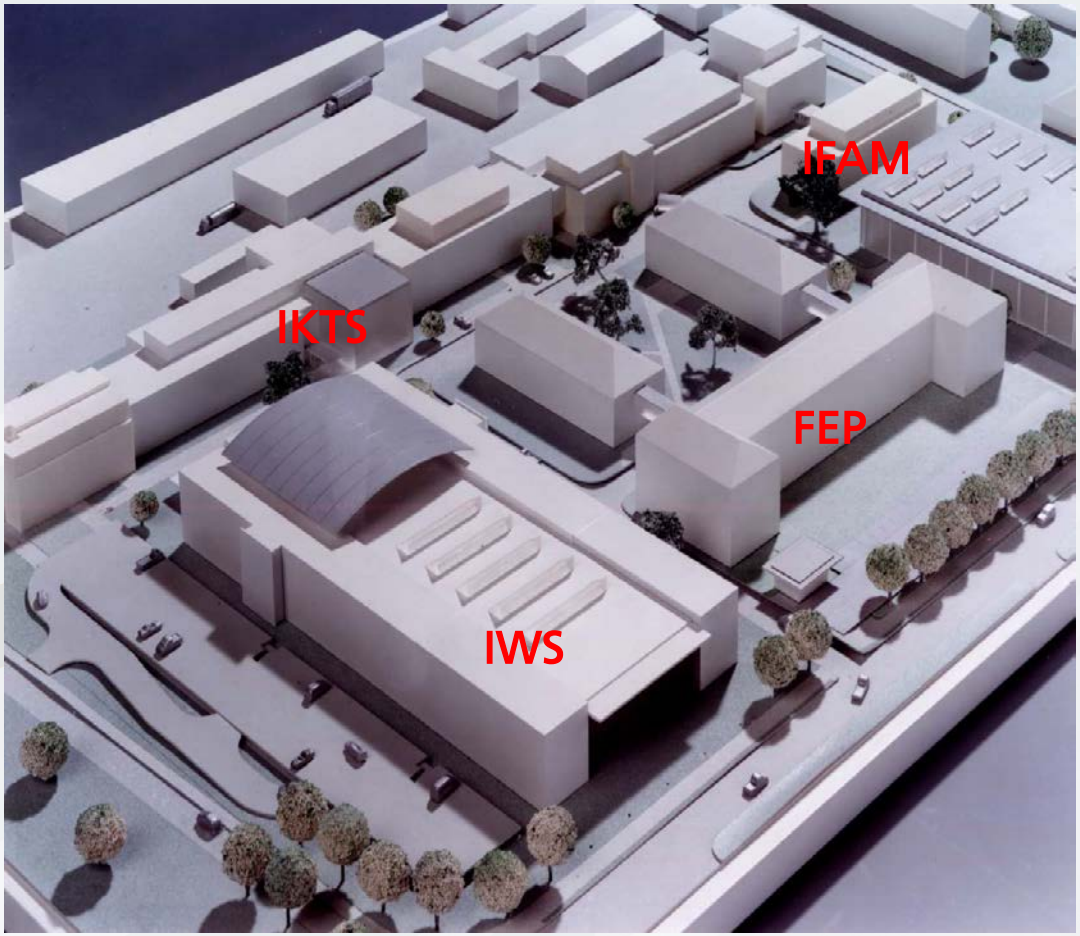

© Fraunhofer IWS

Fraunhofer IWS Dresden

Range of Services:

We offer contracts for work and services including the following topics:

- Consultations
- Feasibility studies
- Conducting of R&D work
- Technology developments
- Process tests (applications)
- System development together with our partners
- Setup and running of pilot plants
- Materials and component testing
- Failure analysis

As well as the education of:

- Scientists
- Engineers
- Maschine operators and
- Laboratory technicians

© Fraunhofer IWS

Fraunhofer Institute for Material and Beam Technology IWS

Short profile:

Permanent staff:	231
Guest researcher:	37
Research assistants:	152
Apprentices:	9
Budget:	28,0 Mio. €
Investment:	3,0 Mio. €
Industrial revenue:	42,7 %
Basic funding:	29,7 %

January 2017

www.iws.fraunhofer.de

© Fraunhofer IWS

Fraunhofer IWS Dresden

Fraunhofer Institute for Material and Beam Technology IWS

Equipment:

- CO_2-laser up to 8 kW
- Fiber laser up to 8 kW
- Disc laser up to 8 kW
- Nd:YAG-laser up to 4 kW
- Diode laser up to 20 kW
- Processing plants
- Robot systems
- SLM plants
- PVD coating plant
- CVD coating plant
- Plasma and induction heater
- Equipment for materials testing
- Metallography, TEM, REM, etc.

© Fraunhofer IWS

Fraunhofer Institute for Material and Beam Technology IWS

Business Units

Laser Materials Processing

Ablation and Cutting

Microtechnology

Joining

Surface Engineering and Coatings

Thermal Surface Technology

PVD and Nanotechnology

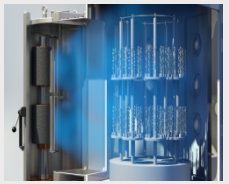
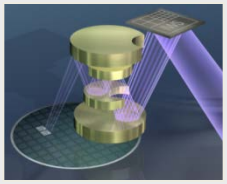

Additive Manufacturing and Printing

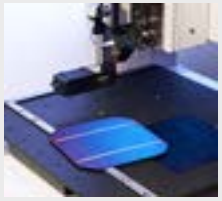

Chemical Surface and Reaction Technology

Field of Expertise: Materials Characterization and Testing

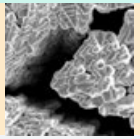

PVD and Nanotechnology

The business unit at a glance

- Fabrication of highly precise multilayer systems
  - EUV and x-ray optics
  - Fabrication of reactive multilayers for high-precision joining tasks
- Deposition of super hard, low-friction carbon films (Diamor®) by laser-arc-processes
- Deposition of nitride based hard coatings and metal functional coatings
- Development of process-specific modules and system technology for PVD coating technology

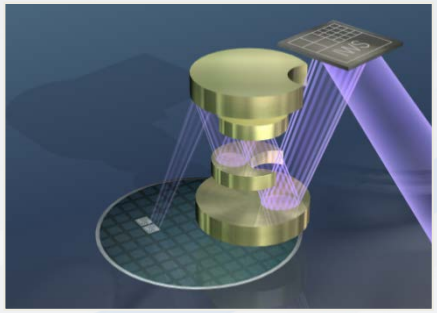

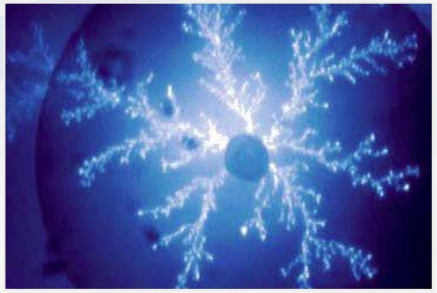

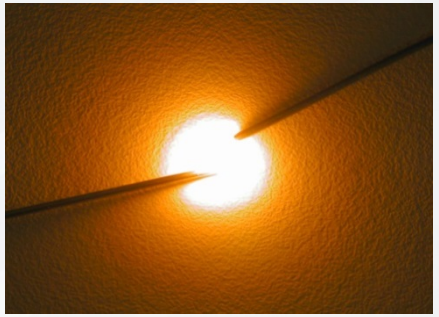

© Fraunhofer IWS

Microtechnology

The business unit at a glance

- Laser microprocessing
  - Manufacturing of micro parts and structures
  - Ablation and technical cleaning
  - Drilling (i.a. laser)
- Surface functionalization
  - Laser interference structuring for tribological, optical and biological functions
- Micro/bio system technology
  - Design, simulation of micro systems
  - Lab-on-a-Chip-systems for medical diagnostics
- Systems for micro materials processing
  - Laser micro processing with ultra short pulsed and short pulsed lasers
  - Laser interference structuring systems
  - R2R device

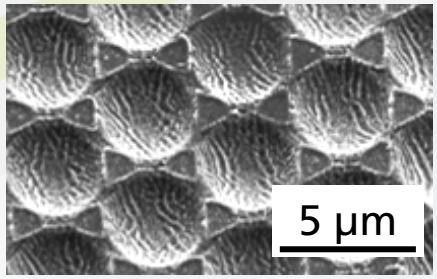

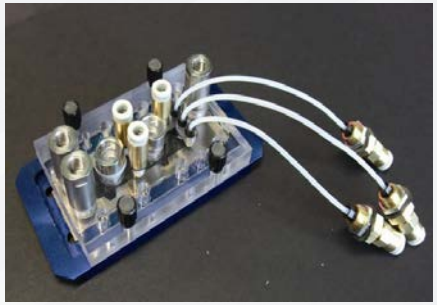

© Fraunhofer IWS

Ablation and Cutting

The business unit at a glance

- Laser cutting and ablation
- Process control and system technology
- Laser high speed cutting
  - Cycle-time minimized cutting
  - Remote processing
- Cutting and structuring of electrical sheets
- Process design and analysis
  - Modeling, simulation and statistical test planning (DOE)

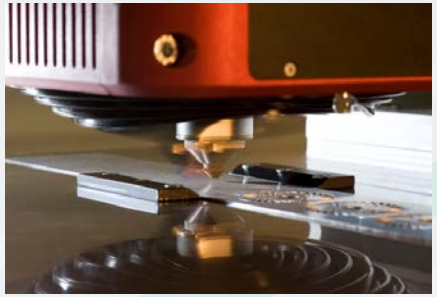

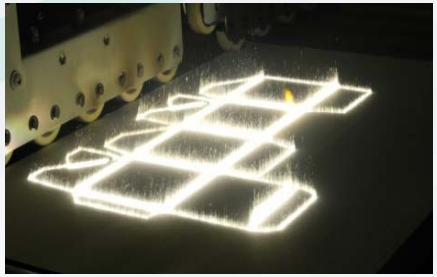

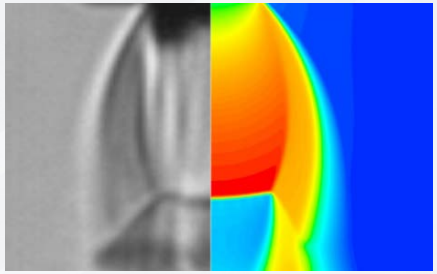

© Fraunhofer IWS

Chemical Surface and Reaction Technology

The business unit at a glance

- Coating and etching processes for
  - photovoltaics, corrosion protection and electrode materials
- Plasma sources and prototype systems for atmosheric processing
- Process monitoring for
  - gas, particle, surface and film analysis
- Chemical surface technologies for surface functionalization
- Battery technolgy

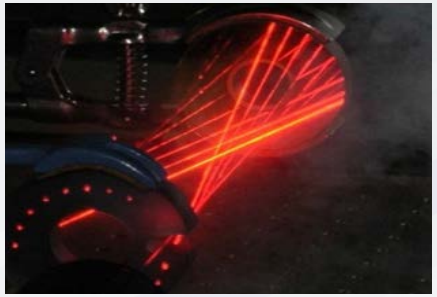

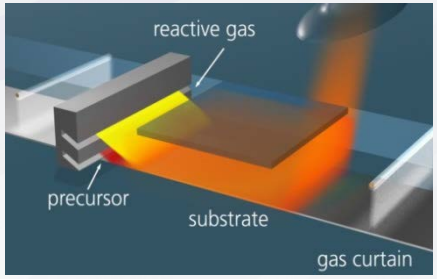

© Fraunhofer IWS

Additive Manufacturing and Printing

The business unit at a glance

- Additive manufacturing
  - Laser powder cladding and buildup welding of metals and multi material systems
- Material and process development for printing of thermoelectrics and functional materials
- Imaging and data bases for complex additive-manufactured components and Industry 4.0

© Fraunhofer IWS

Thermal Surface Technology

The business unit at a glance

- Laser buildup welding with powders and wires
  - Processes, materials and system technology
- Mechanical-thermal surface treatment
  - Laser hardening, plating
  - Process, system and plant engineering
- Thermal spraying with powders and suspensions
  - System technology and functional coating systems

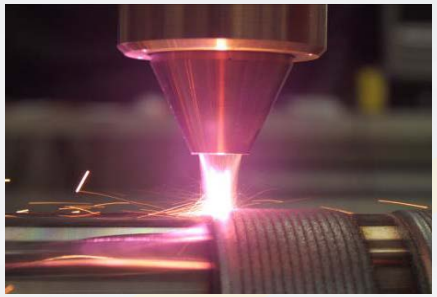

© Fraunhofer IWS

Joining

The business unit at a glance

- Laser beam welding
  - Laser-multi-pass welding und hybrid welding
  - Material combinations, cracks sensitive alloys
    Laser remote welding and systems
  - Large-scale components
- Special joining technology
  - Friction stir welding
  - Magnetic pulse joining
- Bonding and composite technology
  - Laser- and plasma surface treatment
  - Metal- polymer joining
- Component design
  - Process- and load adapted component design
  - light weight design with laser based technologies

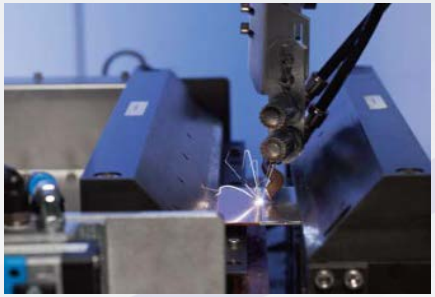

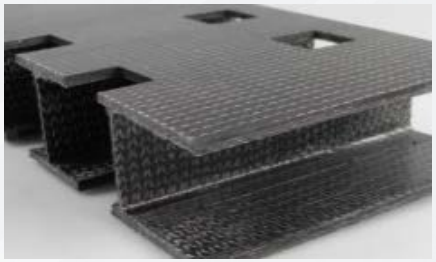

© Fraunhofer IWS

Content

Content	Chapter
Introduction	
The Fraunhofer Gesellschaft	01
Fraunhofer Institute for Material and Beam Technology IWS	02
Seminar topics	03
Laser Beam Welding	
Basics	04
Laser multi pass welding	05
Laser beam welding with high frequent beam oscillation	06
Laser beam welding of high reflective materials	07
Laser beam welding of powertrain components	08
Laser induction roll plating	09
Special Joining Technologies	
Magnetic pulse joining	10
Friction stir welding	11
Joining with reactive multi layers	12
Bonding and Composite technology	
Electrical-conductive bonding	13
Thermal direct joining of thermoplastic to metal	14
Mechanical Joining	
Enhanced mechanical connection by laser interference patterning	15

© Fraunhofer IWS

Terms and classification

.. Everything should be well structured and classificate

DIN - Deutsche Institut für Normung e. V.
(founded 1917)

- **DIN 8580 Manufacturing Processes**
- **DIN 8583 Joining Processes**

© Fraunhofer IWS

Tailoring joining technology for low cost localized performance enhancement of metal parts

DIN 8580

Fertigungsverfahren
Manufacturing processes

Urformen **Forming**	Umformen **Shaping**	Trennen **Separating**	Fügen **Joining**	Beschichten **Coating**	Stoffeigen-schaften ändern **Change material properties**

© Fraunhofer IWS

Tailoring joining technology for low cost localized performance enhancement of metal parts

DIN 8583

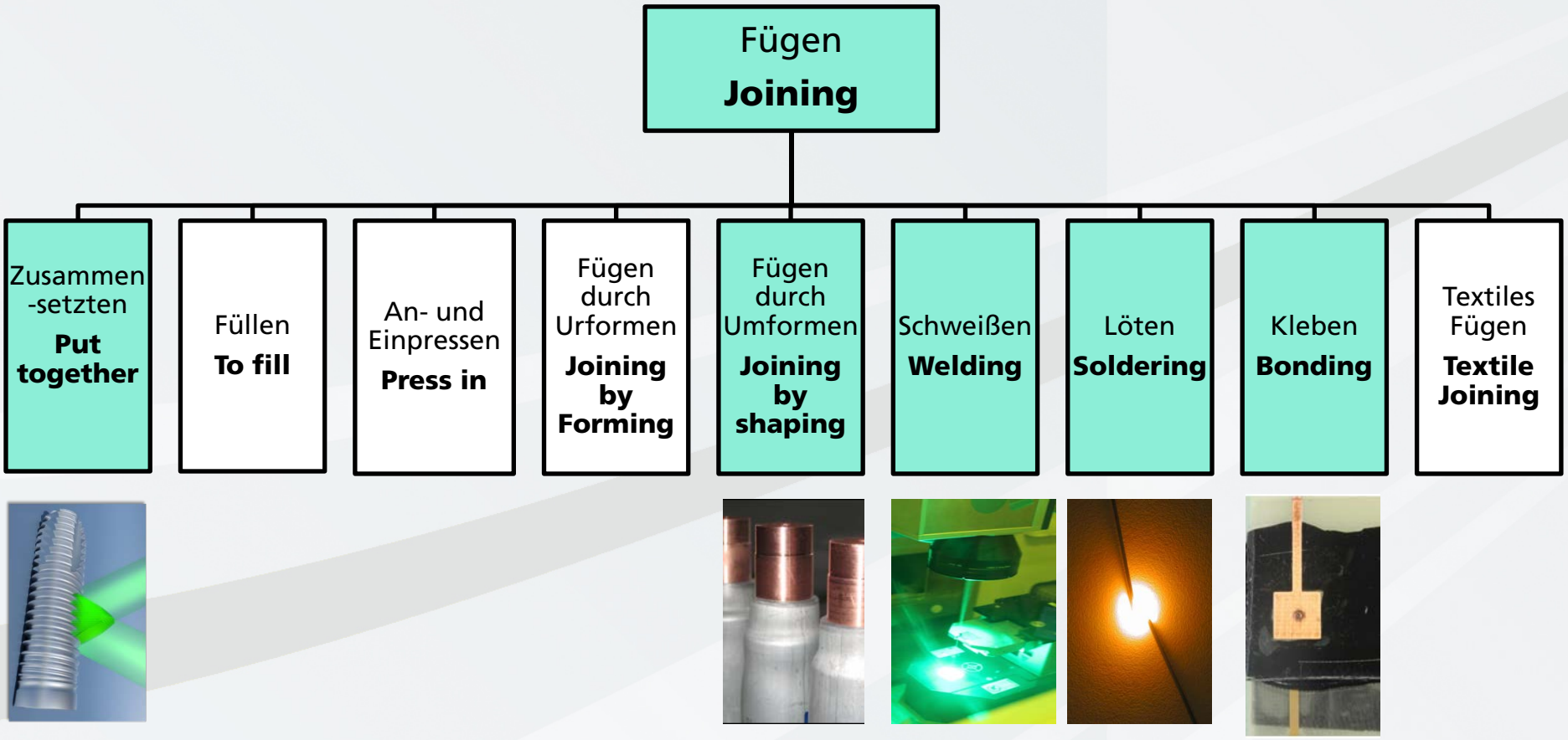

© Fraunhofer IWS

Tailoring joining technology for low cost localized performance enhancement of metal parts

Topics

Tailored joining technology
Laser multi pass welding
Laser beam welding with high frequent beam oscillation
Laser beam welding of high reflective materials
Laser beam welding of powertrain components
Laser induction roll plating
Magnetic pulse joining
Friction stir welding
Joining with reactive multi layers
Electrical-conductive bonding
Thermal direct joining of thermoplastic to metal
Enhanced mechanical connection by laser interference patterning

Industrial sector & application
Automotive parts
Tooling
Medical devices
Aviation parts
High end consumer products
Power generation parts
High power electronic & E-mobility
Micro-connection technology

© Fraunhofer IWS

Content

Content	Chapter
Introduction	
The Fraunhofer Gesellschaft	01
Fraunhofer Institute for Material and Beam Technology IWS	02
Seminar topics	03
Laser Beam Welding	
Basics	04
Laser multi pass welding	05
Laser beam welding with high frequent beam oscillation	06
Laser beam welding of high reflective materials	07
Laser beam welding of powertrain components	08
Laser induction roll plating	09
Special Joining Technologies	
Magnetic pulse joining	10
Friction stir welding	11
Joining with reactive multi layers	12
Bonding and Composite technology	
Electrical-conductive bonding	13
Thermal direct joining of thermoplastic to metal	14
Mechanical Joining	
Enhanced mechanical connection by laser interference patterning	15

© Fraunhofer IWS

LASER

Light
Amplification by
Stimulated
Emission of
Radiation

© Fraunhofer IWS

LASER

Light
Amplification by
Stimulated
Emission of
Radiation

1960	first pulsed laser effect in Rubin-FKL demonstrated (Mr. Maiman, USA)
1961	first Nd-glass-laser
1964	first cw CO_2-laser
1965	first application of laser for drilling of diamants (Herziger, D)
1969	first machine tool for the drilling of watch jewel (Herziger, D)
1978	first laser cutting machine in a company
1995	first high power diode laser for hardening applications
2002	first high power fiber laser for welding applications

© Fraunhofer IWS

Principal and effect of the Focussing

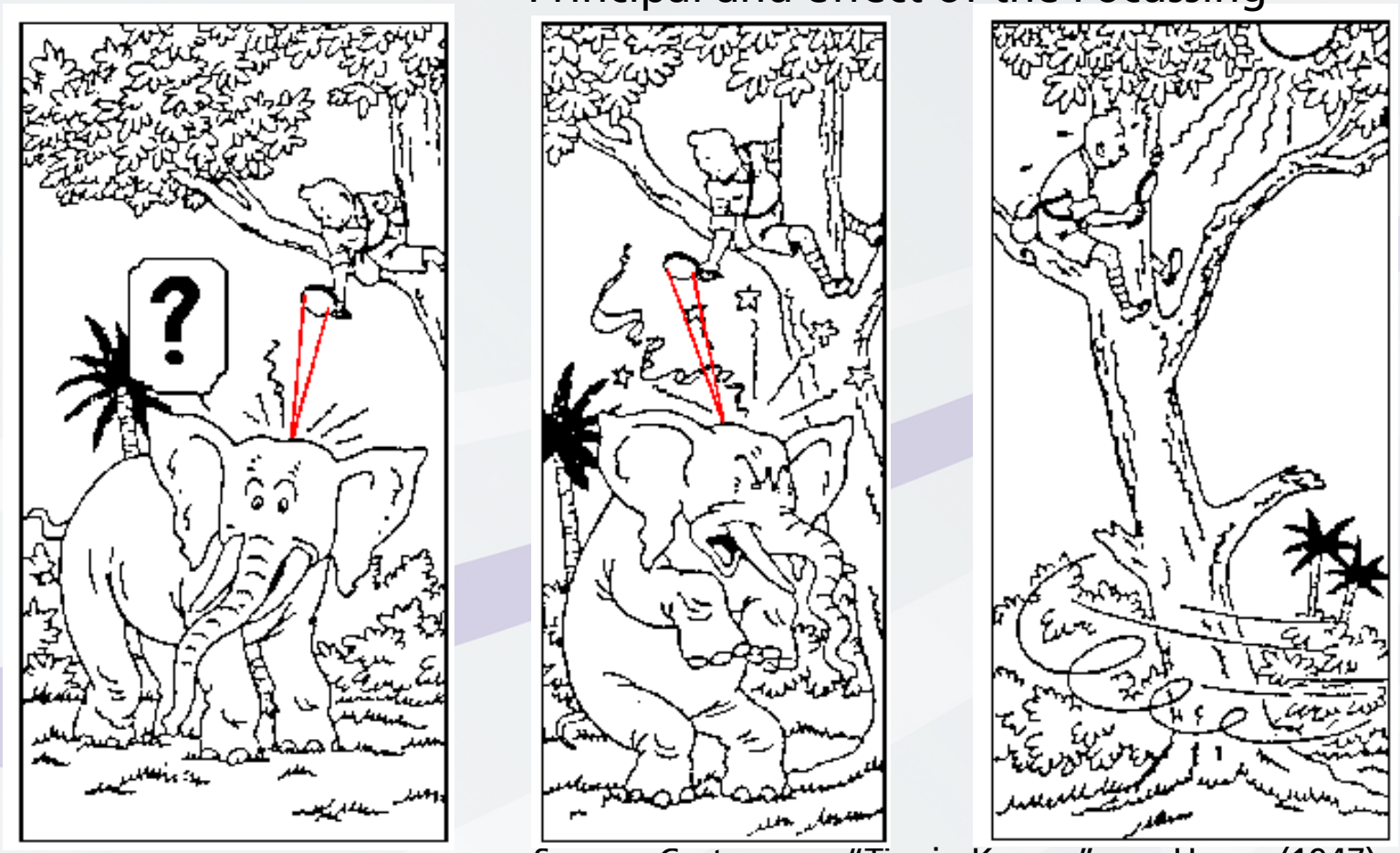

Source: Casterman, “Tim in Kongo” von Herge (1947)

© Fraunhofer IWS

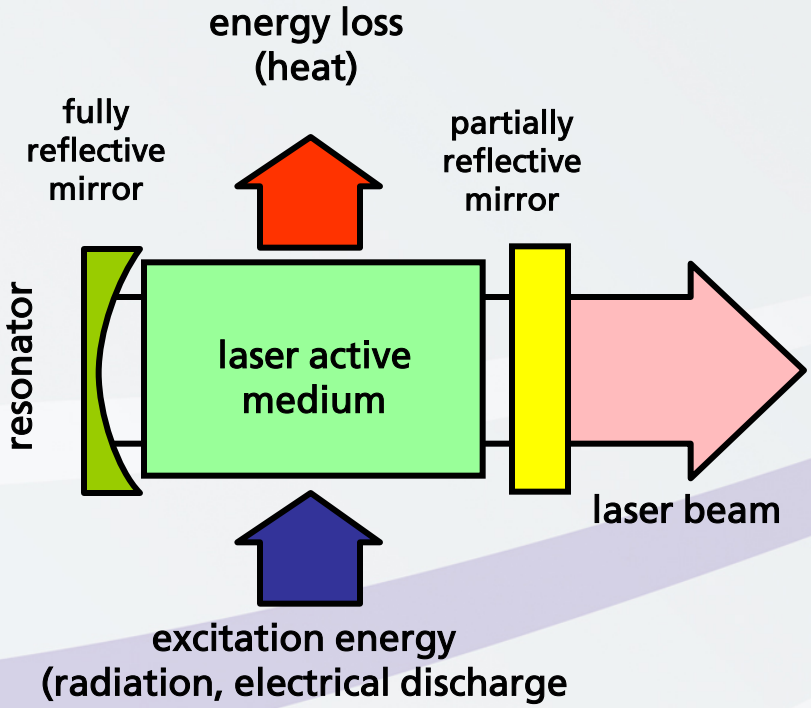

laser actives medium	excitation (energy supply)	resonator
e.g. solid state material, gas, organic dye in liquid solution, semiconductor, plasma, metal vapor	e.g. flashlamps, elect. discharge (dc or rf), pumping laser, electronic accelerator	stable/instable, with/without frequency selective components

properties of the laser

wavelength, power, beam quality, efficiency, operation mode, design manufacturing costs, lifespan

© Fraunhofer IWS

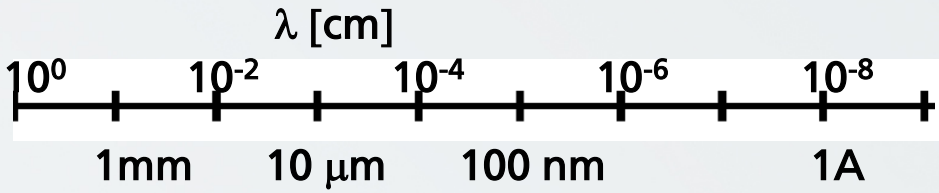

wavelength $\lambda = c_0 / \nu$

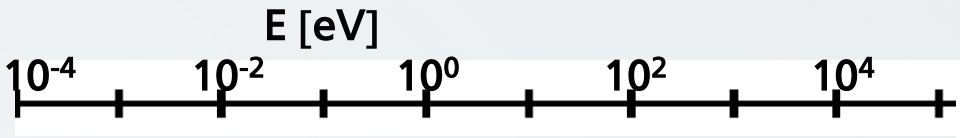

photon energy $E = h \nu$

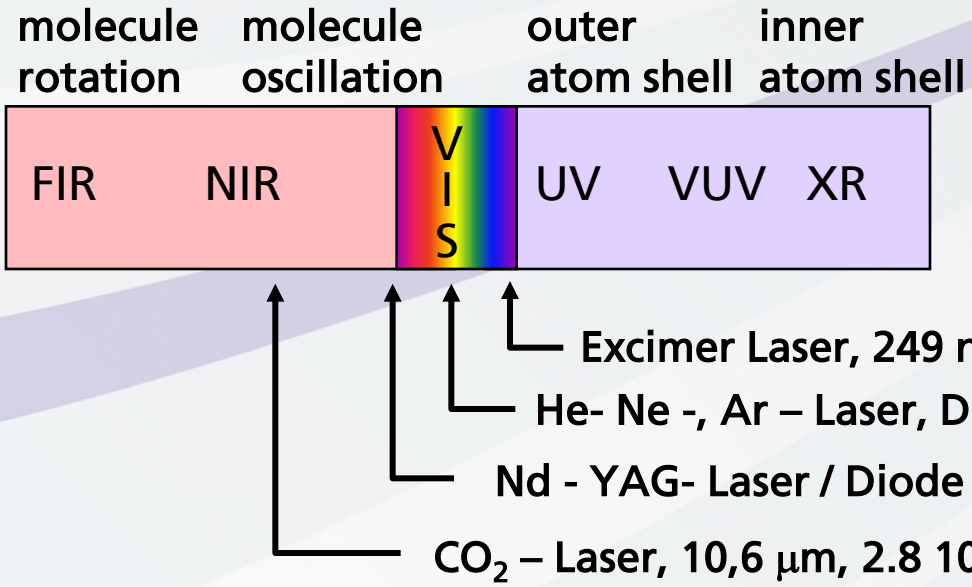

© Fraunhofer IWS

Absorption behavior vs. wavelength for metals

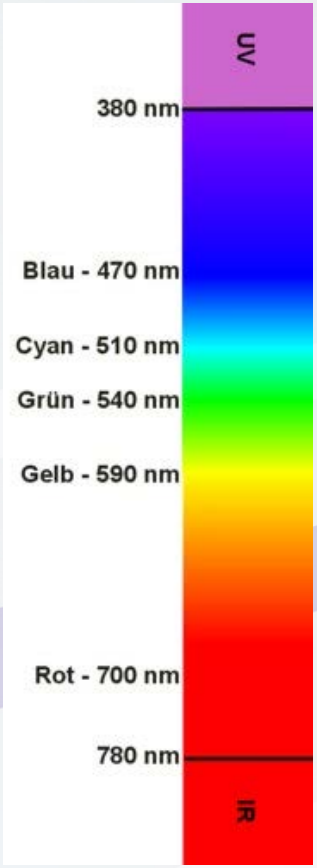

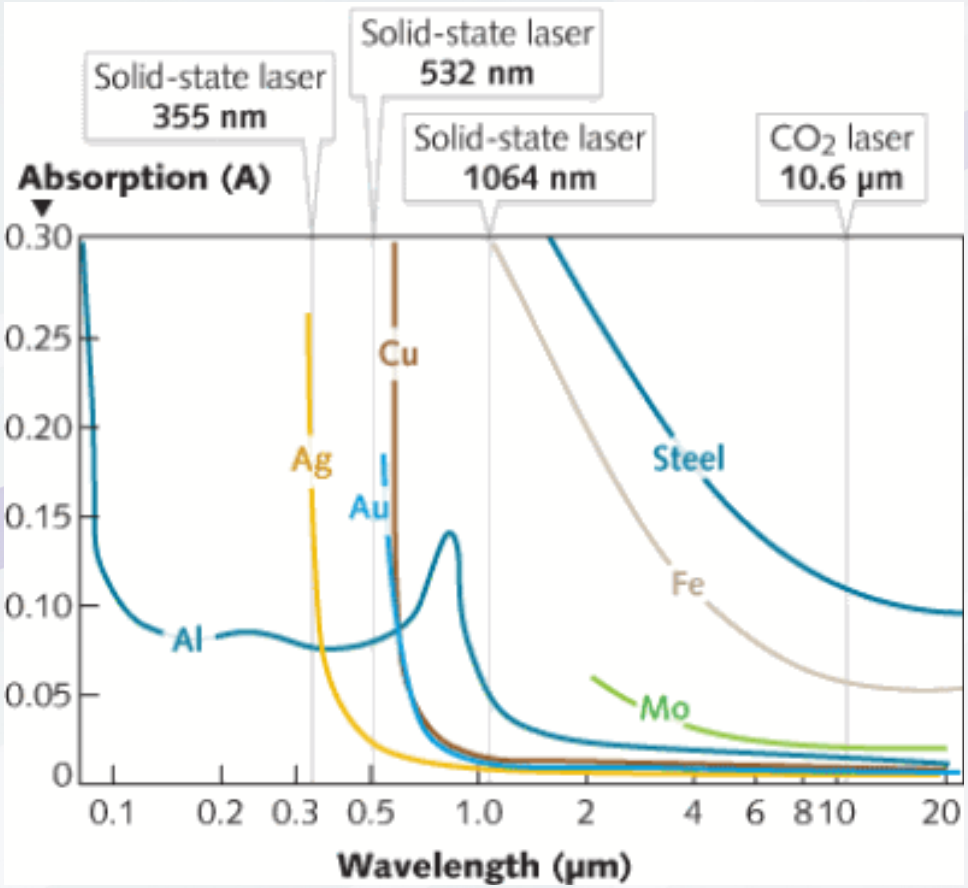

© Fraunhofer IWS

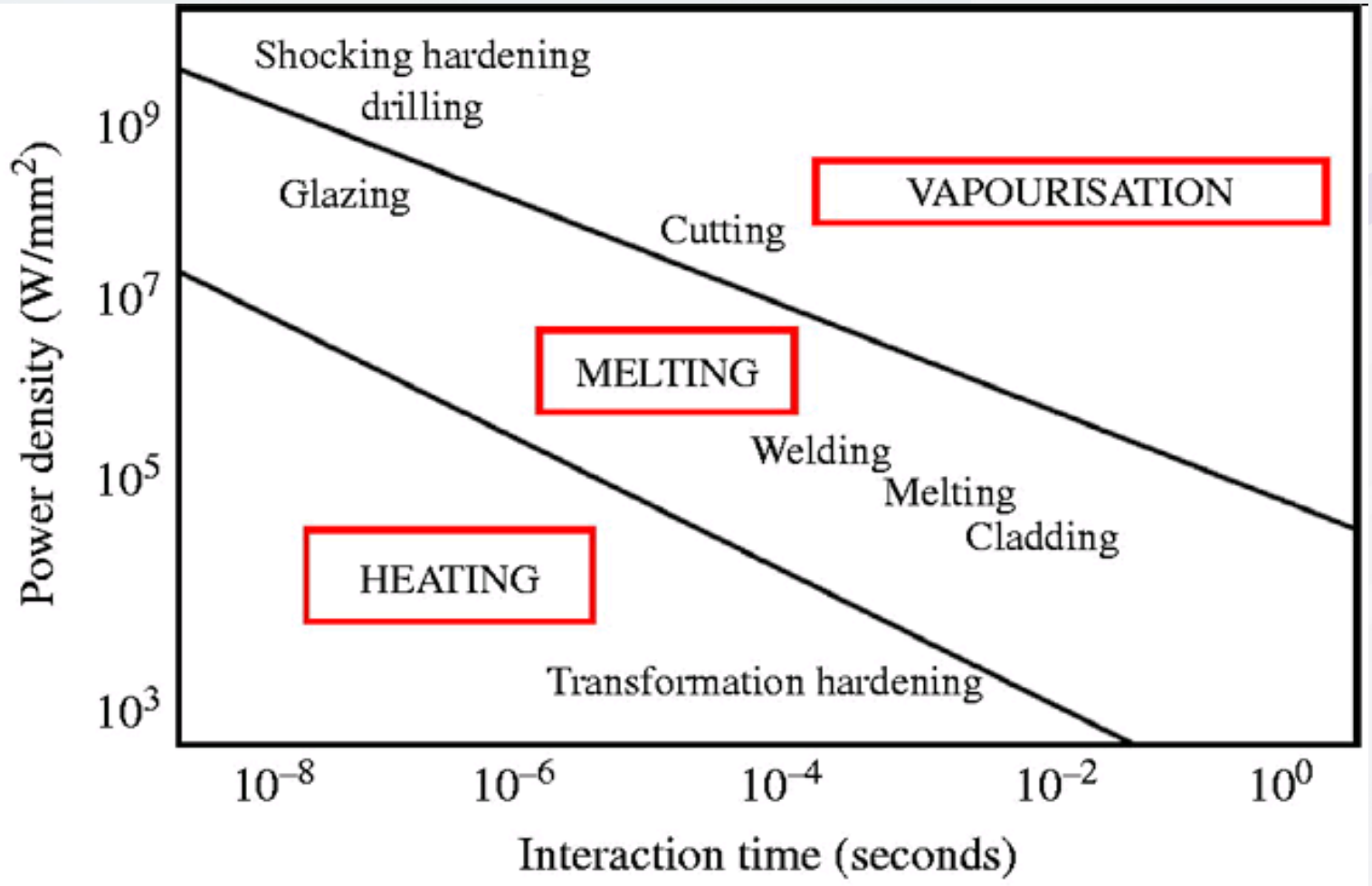

© Fraunhofer IWS

Laser heat conduction welding

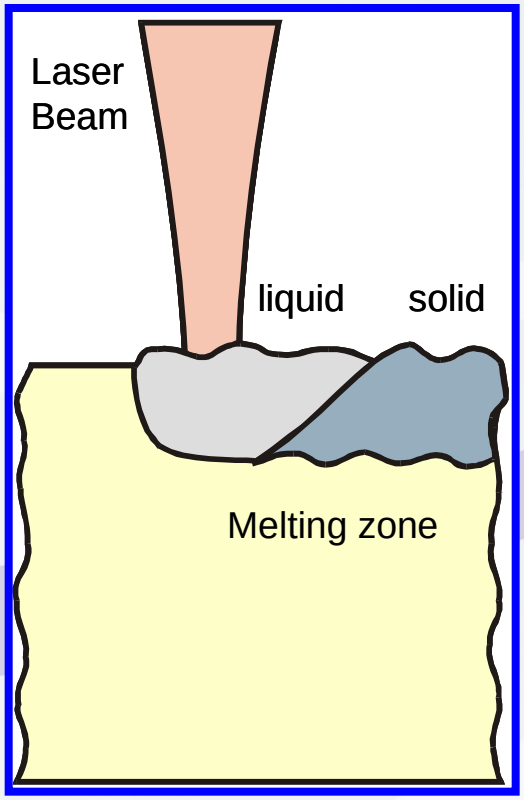

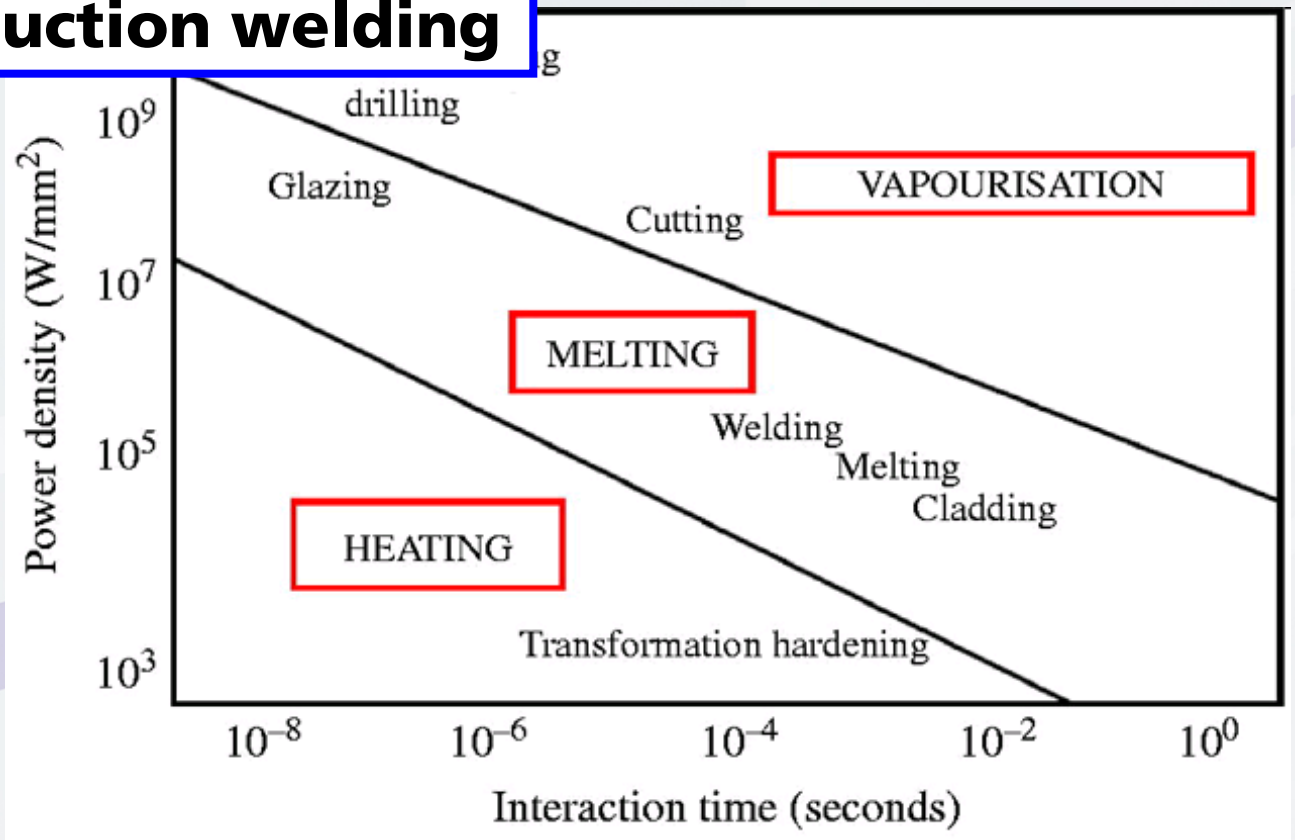

Source: GSI Group Inc.

© Fraunhofer IWS

Working principle laser heat conduction welding (I):

- **Mechanism**
  - Melting of surface
  - Melt pool convection determined welding depth
  - Reason for convection: Gradient of surface tension
- **Properties**
  - Aspect ration (wide-depth) app. 10 : 1 …1 : 2
  - Smooth melt pool
  - Less or no splatter
  - Low welding depth
  - low welding speed
  - High reflexion of laser power

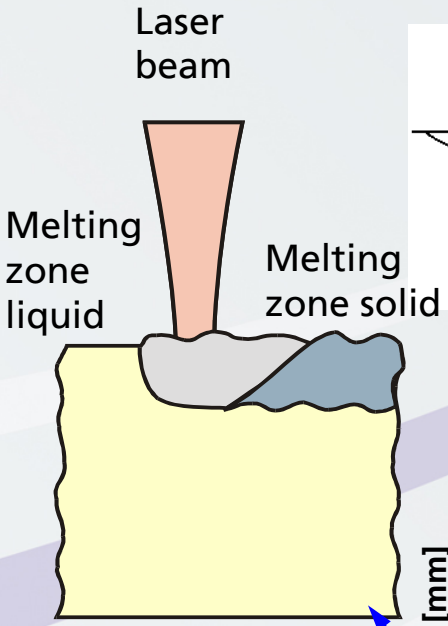

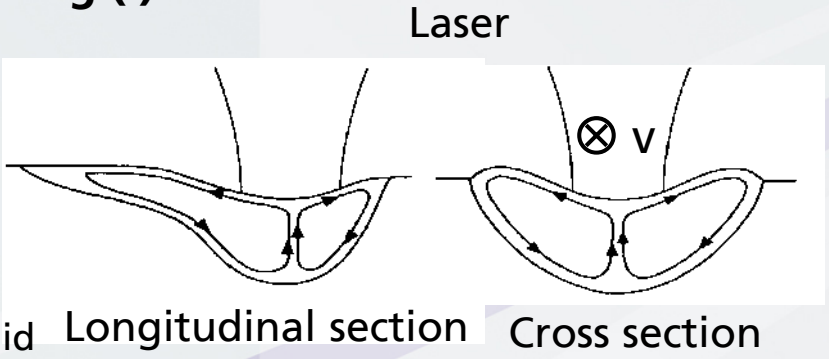

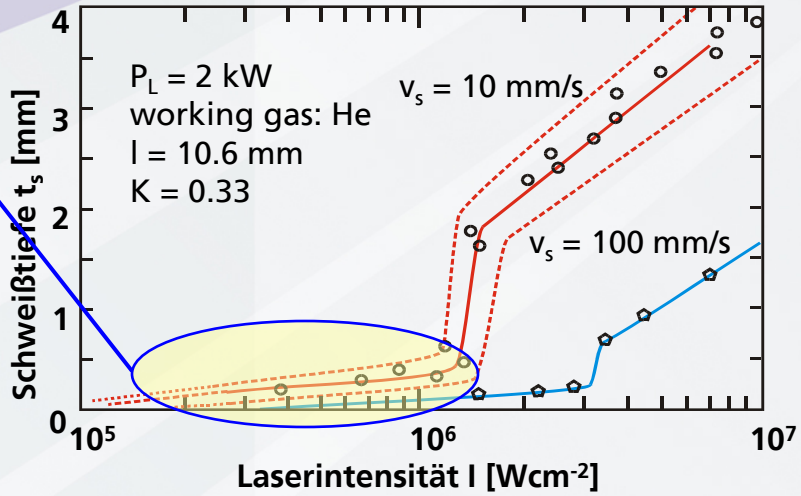

© Fraunhofer IWS

Working principle laser heat conduction welding (II):

Application

- Thin sheet metal e. g.
  - heat exchanger
  - fillet weld
  - small parts
  - fuel cells

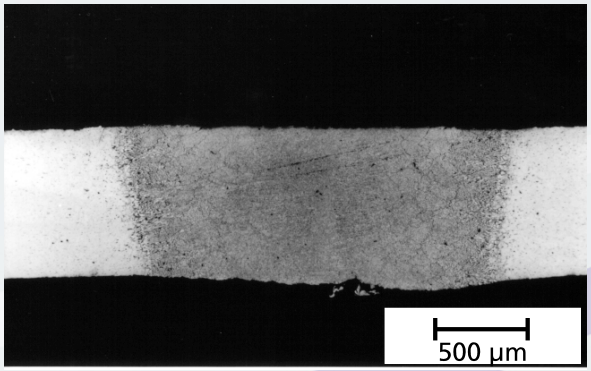

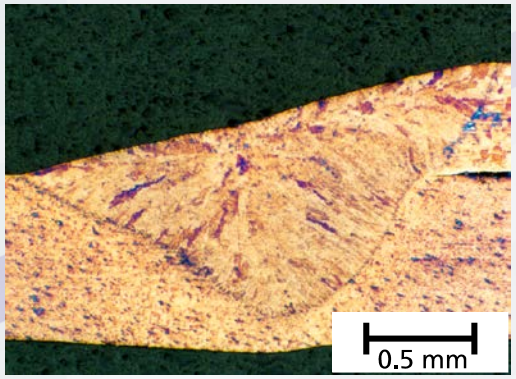

Advantages

- tight, no pores
- Good surface quality
- Less distortion compared to conventional Arc welding
- Low variation of welding depth
- Low requirements to edge preparation

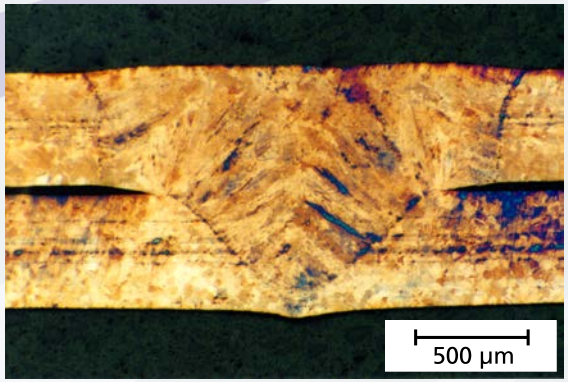

© Fraunhofer IWS

Laser deep penetration welding

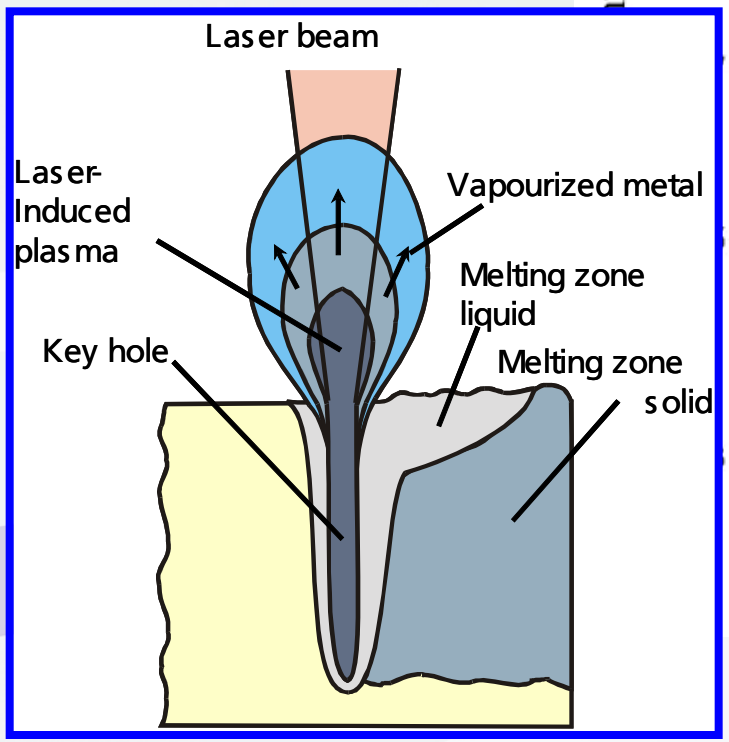

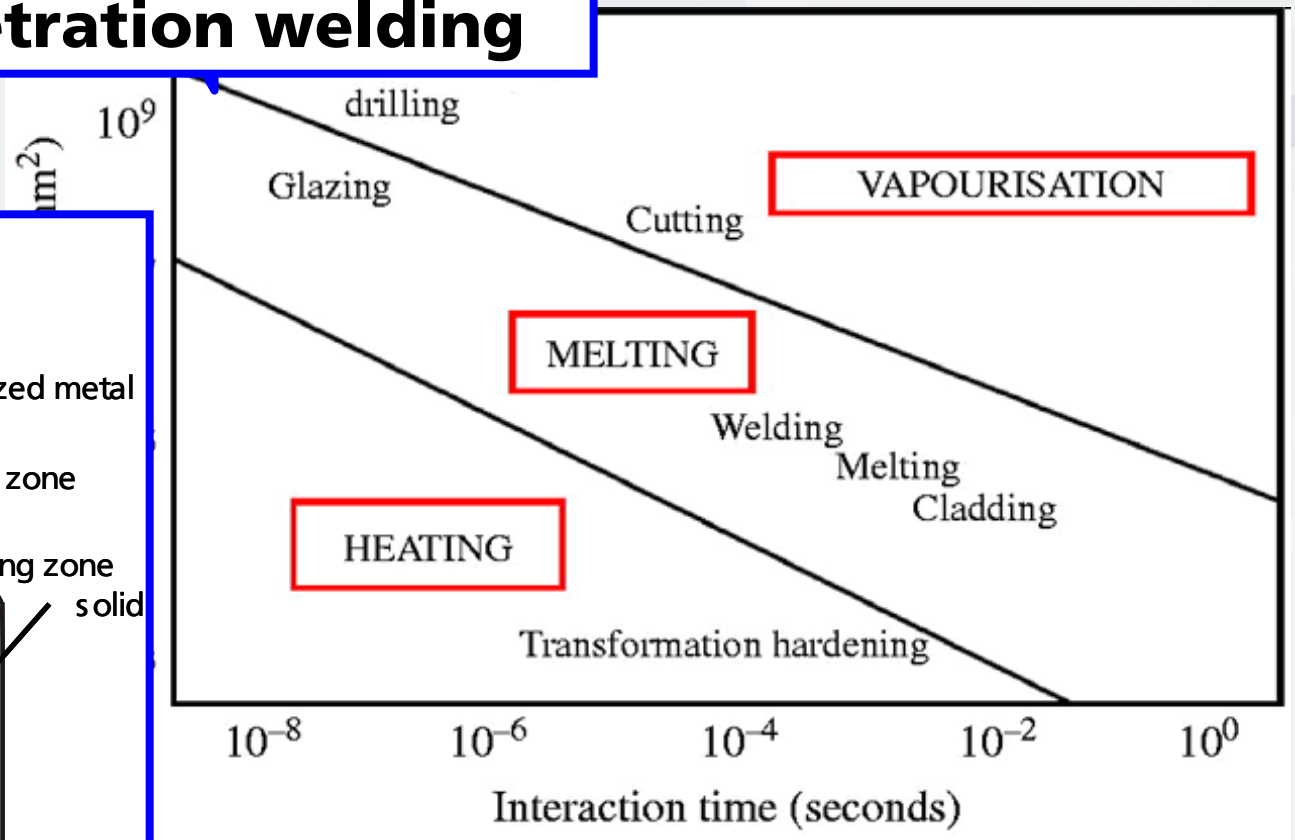

Source: GSI Group Inc.

© Fraunhofer IWS

Working principle laser deep penetration welding (I):

- **Mechanism**
  - Vaporization limit exceeded
  - Expansion of vapor channel in depth (Key-hole)
- **Properties**
  - High welding depth (up to ca. 20 mm)
  - Slight weld seams
  - Low line energy
  - Low distortion
  - High absorption of laser power → high welding speed

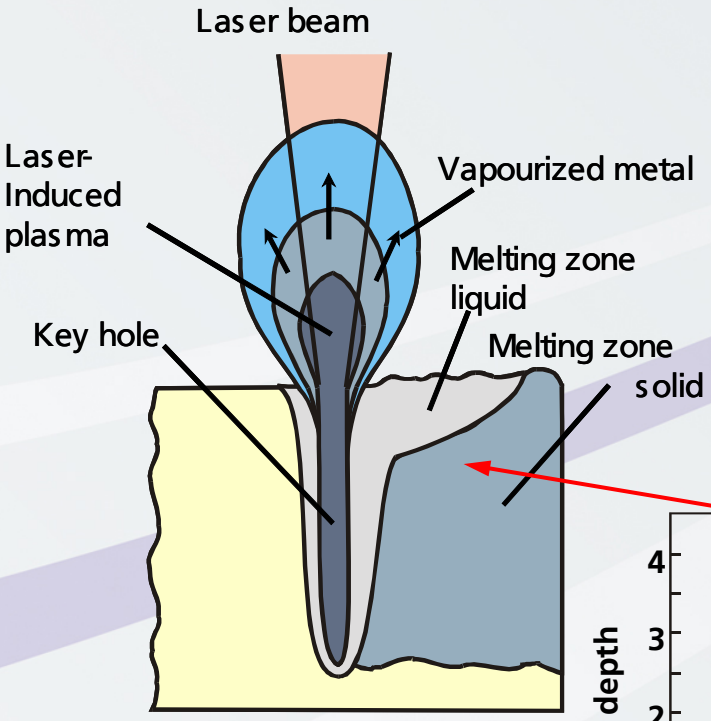

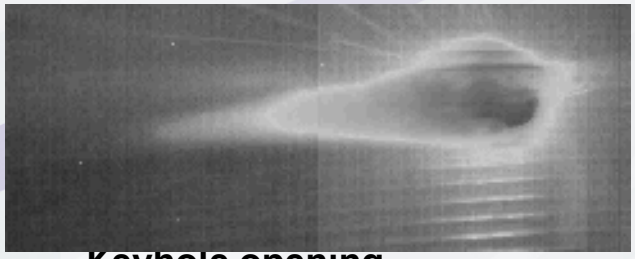

Keyhole opening Video

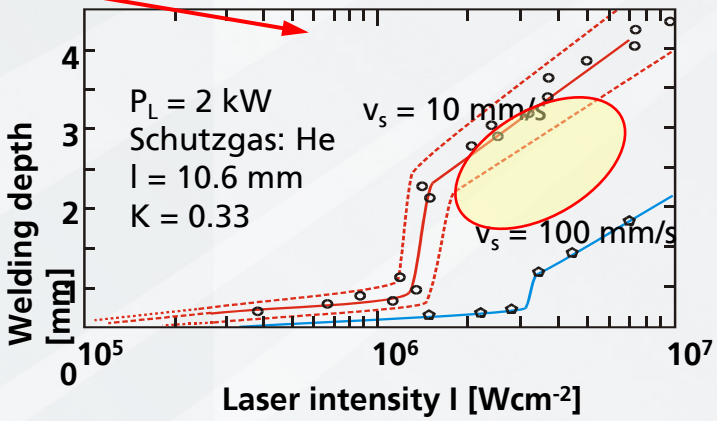

© Fraunhofer IWS

Working principle laser deep penetration welding (II):

Mechanism

- Vaporization limit exceeded
- Expansion of vapor channel in depth (Key-hole)

Properties

- High welding depth (up to ca. 20 mm)
- Slight weld seams
- Low line energy
- Low distortion
- High absorption of laser power → high welding speed

Melt pool convection

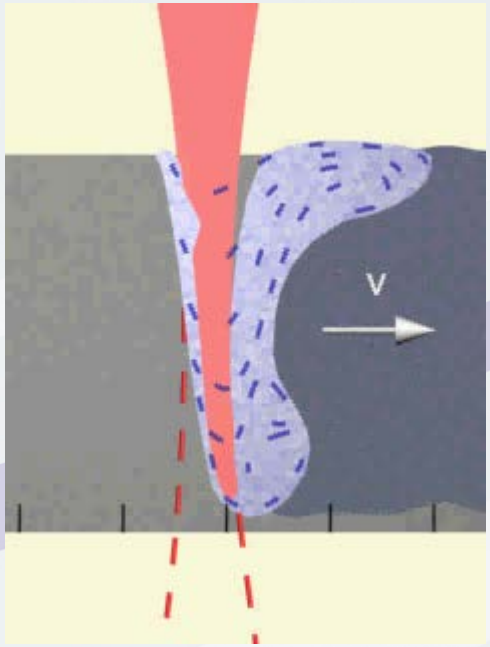

Video

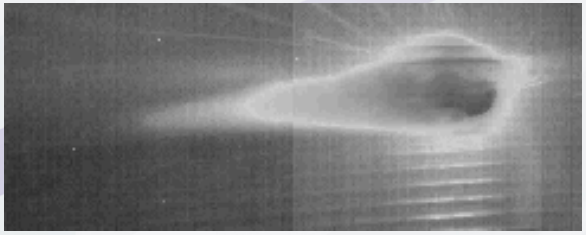

Keyhole opening

Video

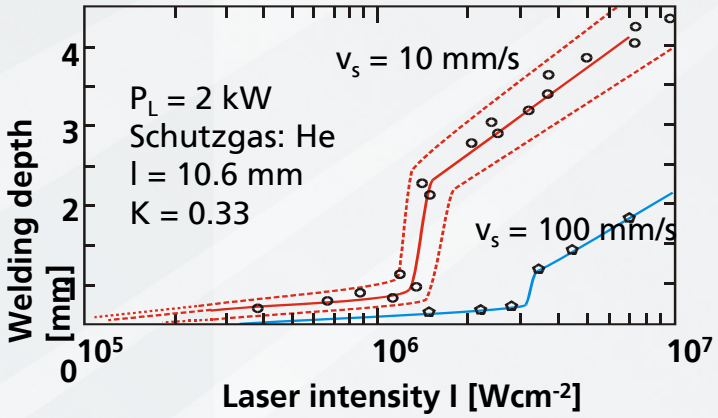

© Fraunhofer IWS

Working principle of CO_2-slab-laser

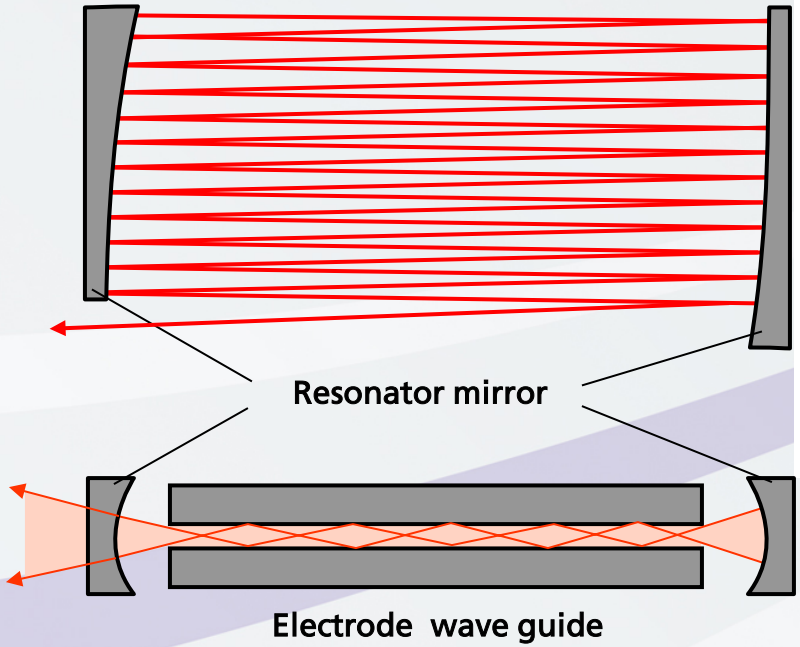

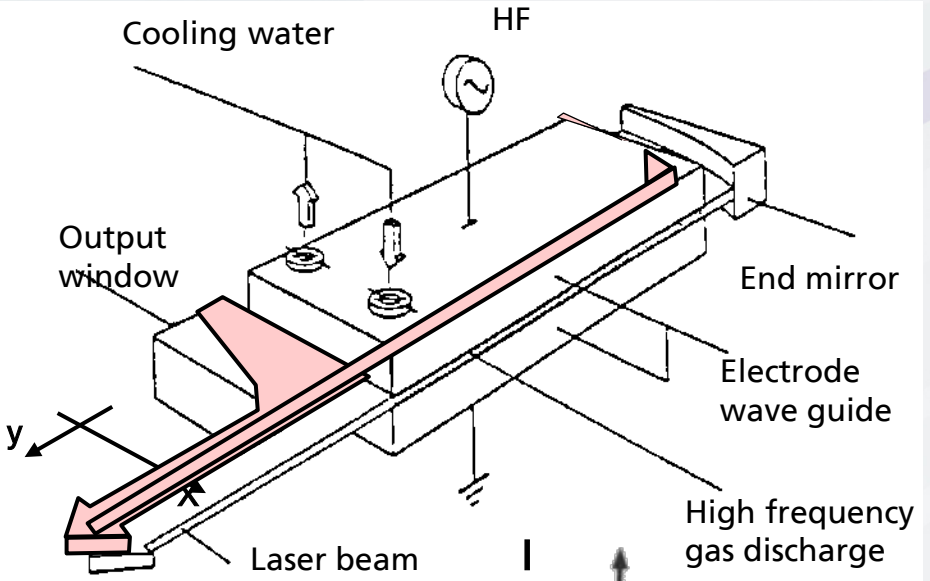

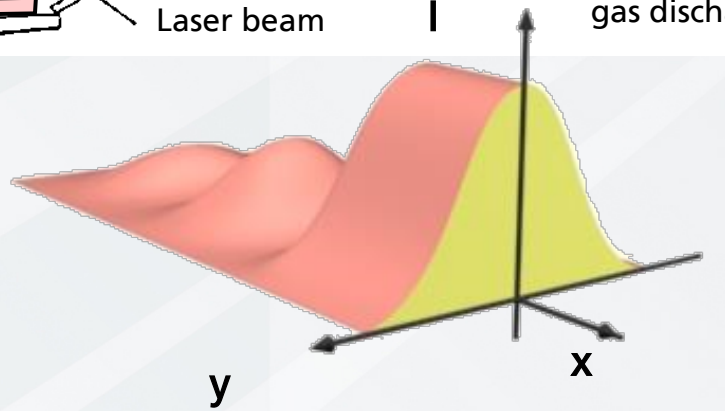

© Fraunhofer IWS

Working principle of disk Laser

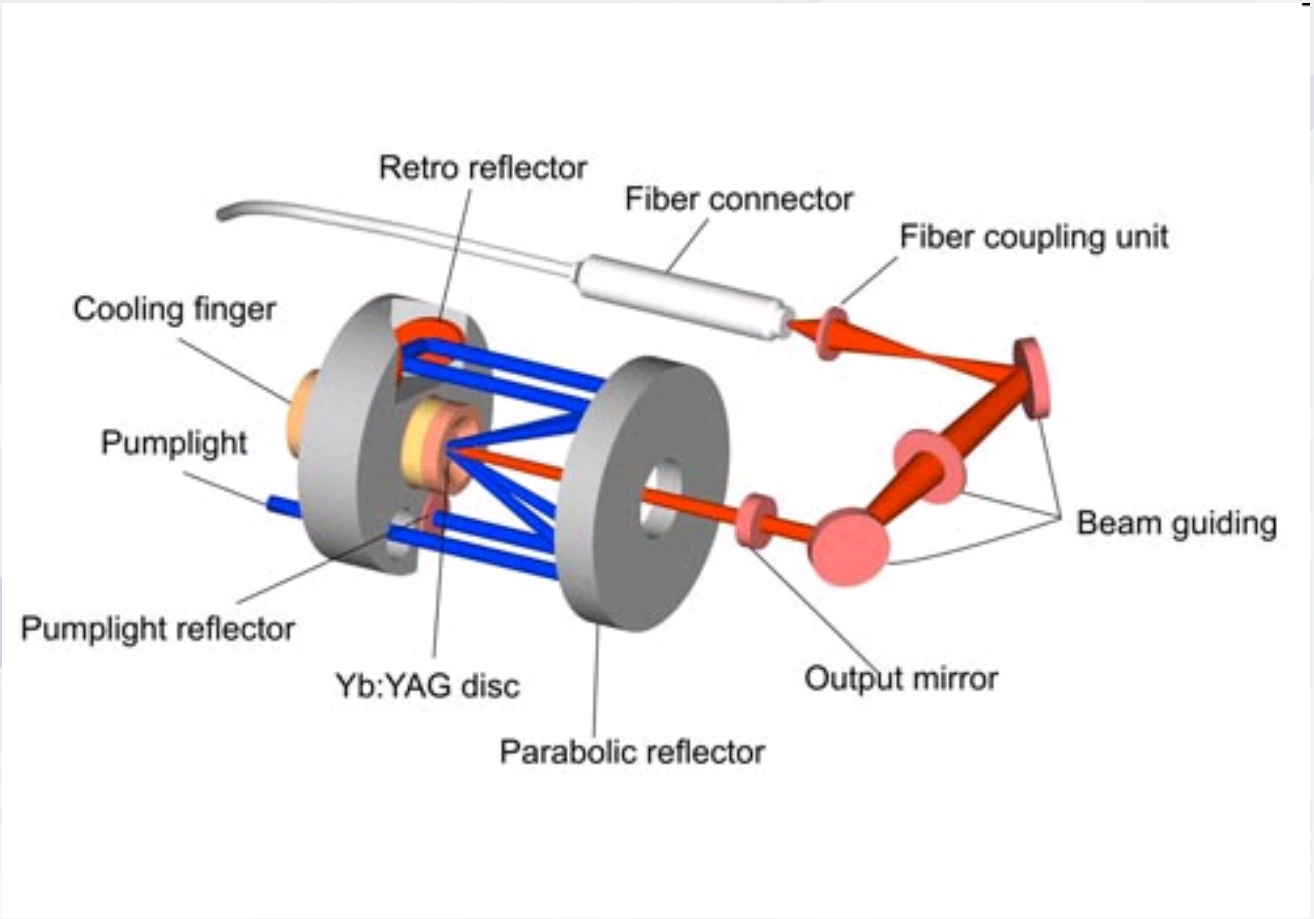

© Fraunhofer IWS

Working principle fiber coupled high power diode laser

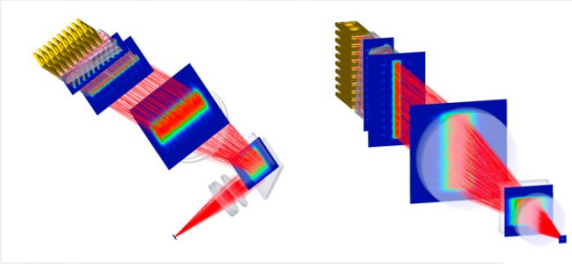

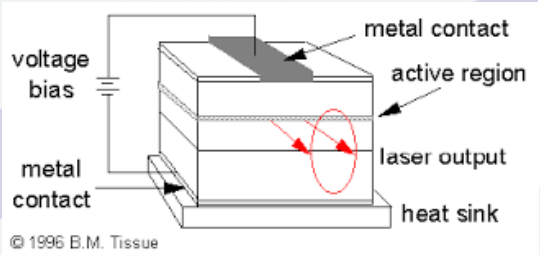

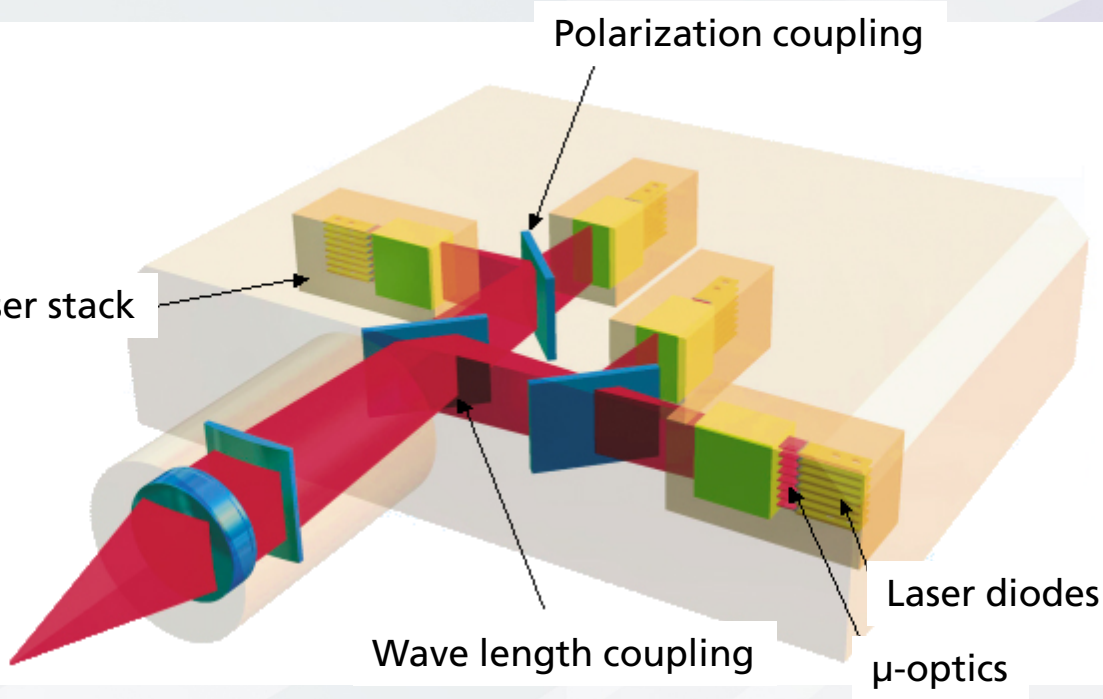

© Fraunhofer IWS

Working principle of Fiber laser

Principle of active fiber

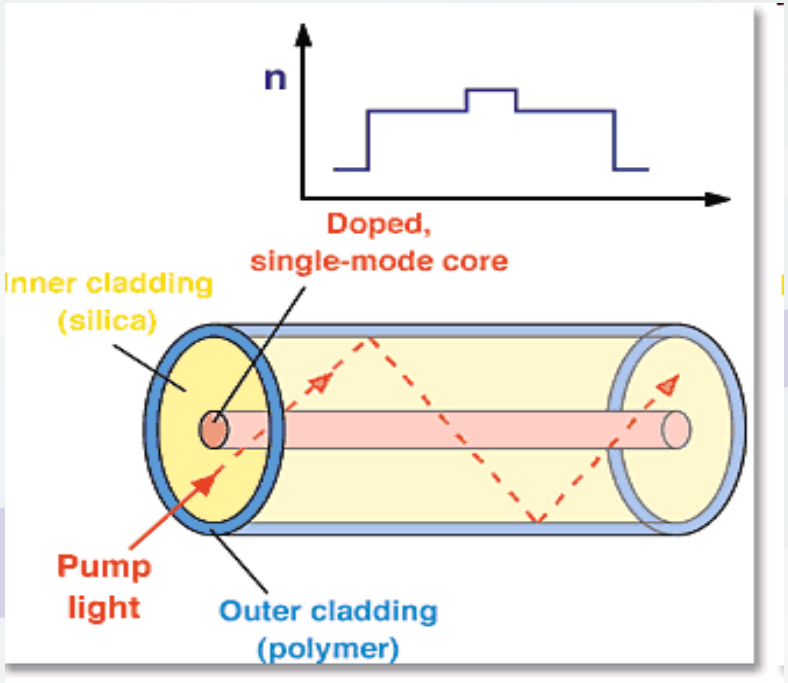

Principle

1. Pump diodes
2. Active fiber
3. Beam Switch
4. Passive fiber

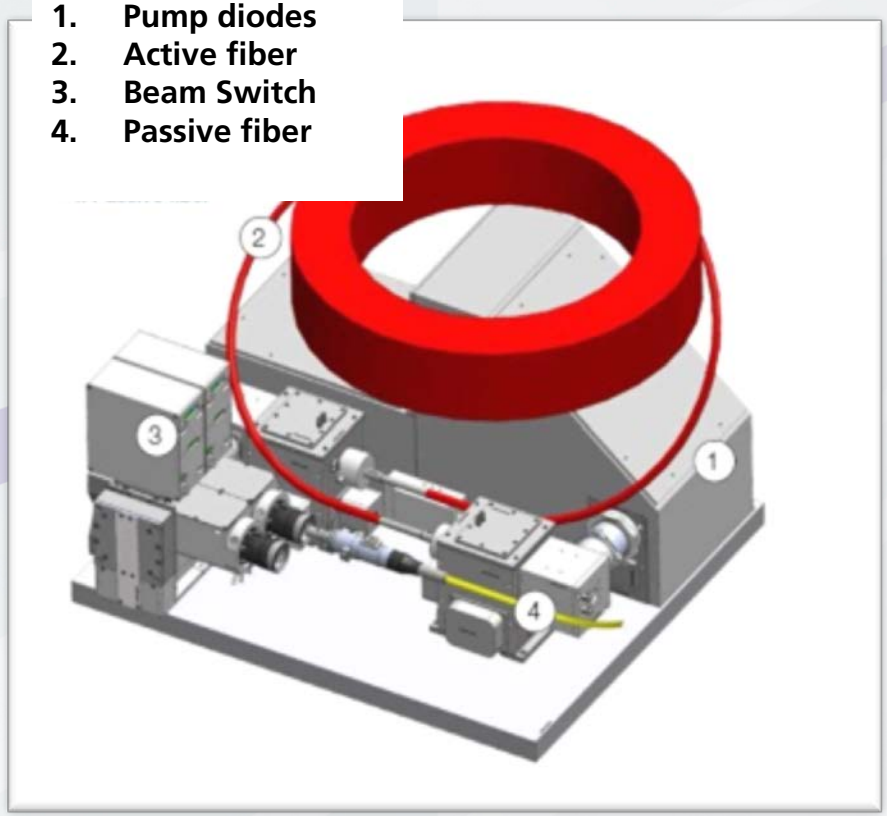

© Fraunhofer IWS

High power Laser source

Hugh amount of different laser source on the market – Are they quite differences, what is behind the “black” box?

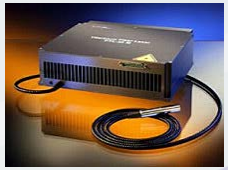

© Fraunhofer IWS

Comparison of modern laser sources

Laser \ Para-meter	Pics	Power [kW]	Wave length [µm]	Beam Quality BPP [mm*mrad]	Typical Spot size* [µm]	Electrical-optical ratio [%]
CO_2-Laser / CO_2-Slab		1,5…20 / 1,5… 8	10,6	3,5	150	~ 8
Diode pumped Nd:YAG-Laser		ca. 1…4,5	1,06	12	300	~ 3
Fiber laser Multimode		1…20 (50)	1,07	2-12 4-12**	65-300 130-600	~ 27
Fiber laser Single mode		1…4 (5)	1,07	0,35 2**	17-50 50-100	~ 27
Disc laser		1…6	1,03	2-12	65-300	> 20
Fiber coupled High power diode laser		1…10	0,9 … 1,03	20-150	200-1500	~ 40

* For app.. 150mm focal length
** after working fiber

© Fraunhofer IWS

Content

Content	Chapter
Introduction	
The Fraunhofer Gesellschaft	01
Fraunhofer Institute for Material and Beam Technology IWS	02
Seminar topics	03
Laser Beam Welding	
Basics	04
Laser multi pass welding	05
Laser beam welding with high frequent beam oscillation	06
Laser beam welding of high reflective materials	07
Laser beam welding of powertrain components	08
Laser induction roll plating	09
Special Joining Technologies	
Magnetic pulse joining	10
Friction stir welding	11
Joining with reactive multi layers	12
Bonding and Composite technology	
Electrical-conductive bonding	13
Thermal direct joining of thermoplastic to metal	14
Mechanical Joining	
Enhanced mechanical connection by laser interference patterning	15

© Fraunhofer IWS

Laser-Multi-Pass-Narrow-Gap-Welding

Motivation:

- welding depth up 50 mm with moderate laser power (up to 5 kW)
- potential application fields:
  - energy sector
  - Al-tanks for liquid gas transportation
  - ship and railway vehicle manufacturing
- Improved weld seam properties:
  - avoiding hot cracks in the weld root
  - controlling strength undermatching

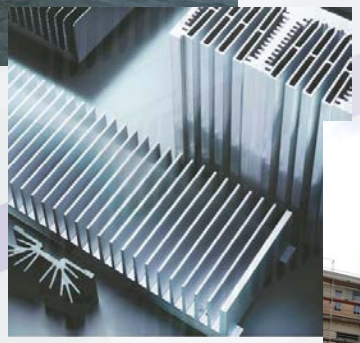

© Junior Kühlkörper GmbH

© Liebherr GmbH

Objectives:

- MPNG-welding for crack sensitive alloys
- reduction of laser investment costs
- expanding application fields
- providing mobile laser-machine solutions

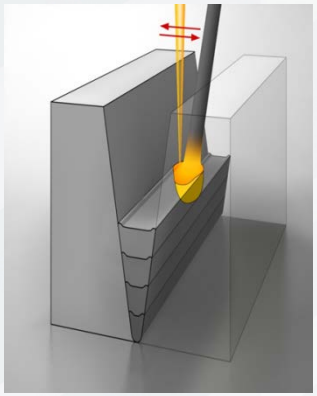

State of the art – conventional welding

Submerged arc welding (SAW)
converter assembly

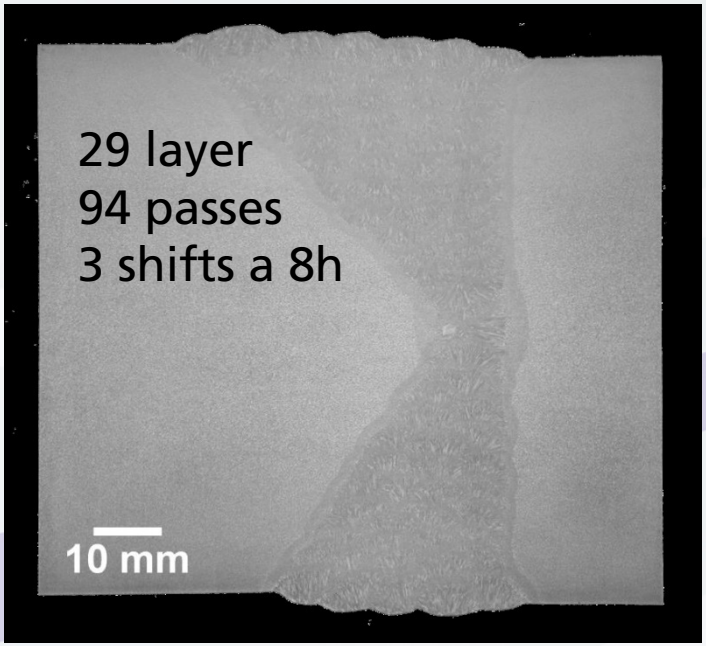

A. Weidig: „Fertigung von Konverterplattformen – Nordic Yards“ 6. Rostocker Schweißtage, 12.11.2013

Submerged arc welding (SAW)
ship's hull final assembly

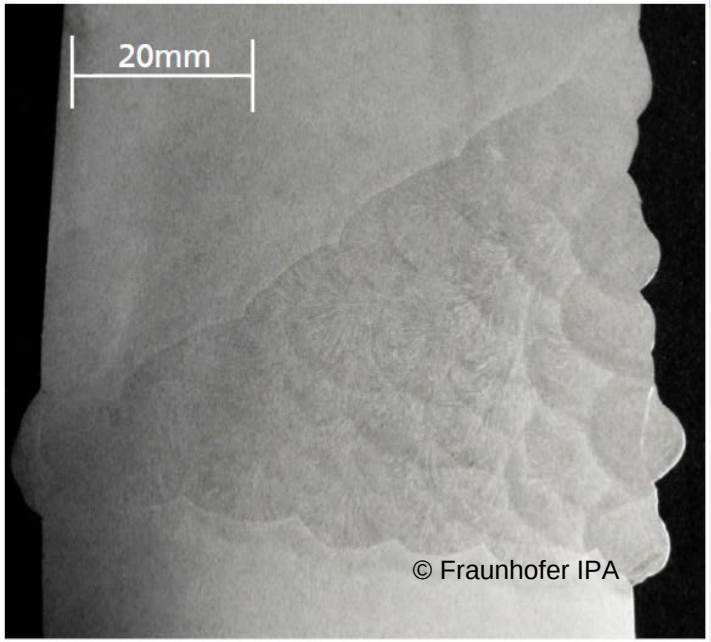

A. Gericke: „Wirtschaftliches UP-Quer-Schweißen an größeren Blechdicken in der Offshorestruktur –und Schiffskörperendmontage “ GST Essen, 19.09.2013

- ship’s hull assembly, manual and semi-automated processes
- on- and offshore welding applications

© Fraunhofer IWS

Laser-Multi-Pass-Narrow-Gap-Welding

State of the art – conventional welding

STEEL

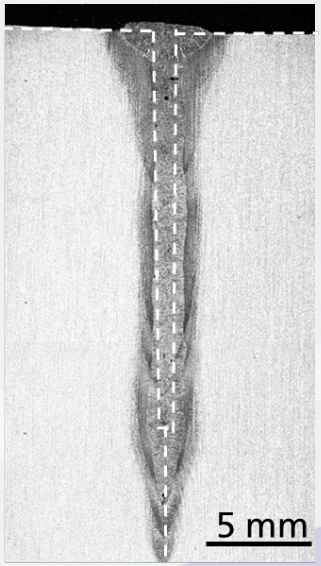

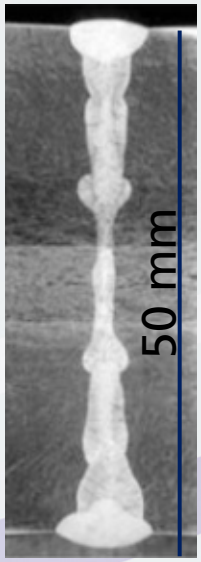

ICALEO Proc.

2001 *Jokinen, T. et al.*

2007 *Goebel, G. et al.*

2011 *Zang, X. et al.*

- strong activities for reactor pressure vessel application
- repair of fatigue-critical parts of gas turbines

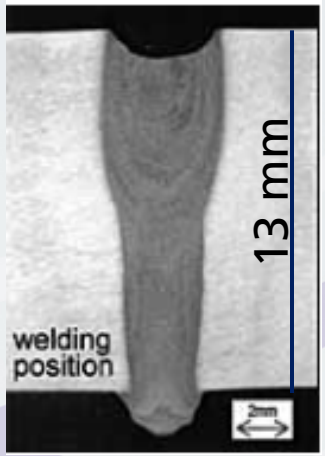

INALCO Proc.

2007

Verhaeghe, G.

ALUMINUM

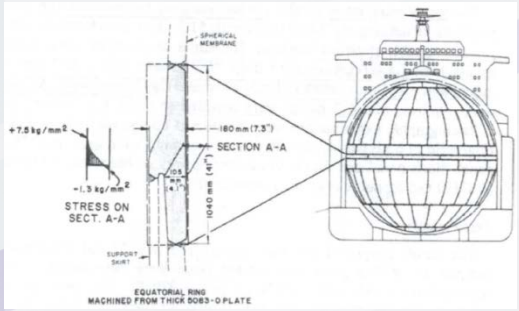

5083 Al-plate up to 100 mm conventional welding

ASTM Proc. STP 579

1974

- conventional welding for LNG spherical tank applications
- only thick plates of 50xx Al-alloys crack free weldable - no application for hot crack sensitive Al-alloys

© Fraunhofer IWS

Laser-Multi-Pass-Narrow-Gap-Welding

Technology approach for MPNG-welding

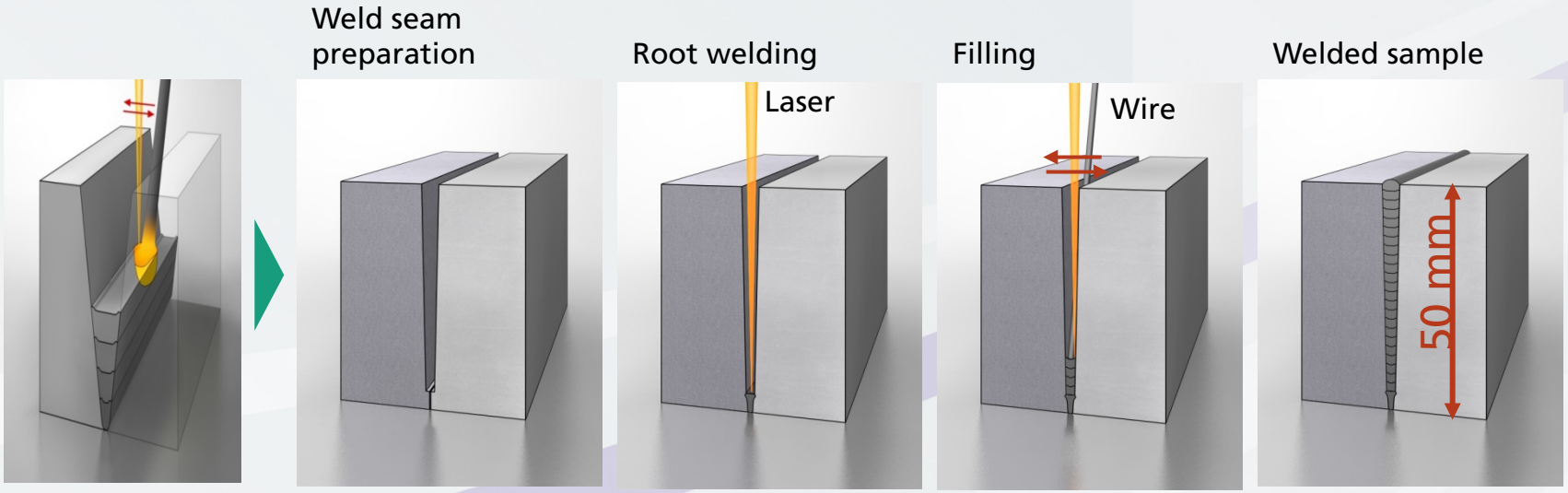

- high element content across the weld seam expected (especially in the root)
- low laser power for up to 50 mm tick plates possible
- groove angle can be reduced to less than 3 °
- high total intensity reduces reflection, good connection between weld metal and groove flanks

© Fraunhofer IWS

Technology approach for MPNG-welding

Equipment and set-up overview

Laser sources

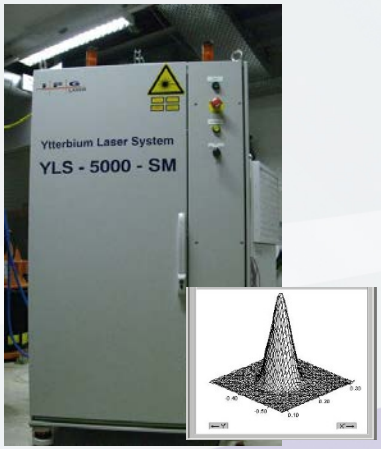

- Gauß-Mode
- SPP: 0,4 mm mrad
- ∅ 30 µm Faser
- $f_{Koll.}$=200, f_{Fokus}=500
- $\varnothing_{Fokus}$ ca. 90 µm

- Top-Hat
- SPP: 2,2 mm mrad
- ∅ 50 µm Faser
- $f_{Koll.}$=120, f_{Fokus}=500
- $\varnothing_{Fokus}$ ca. 220 µm

Experimental welding head

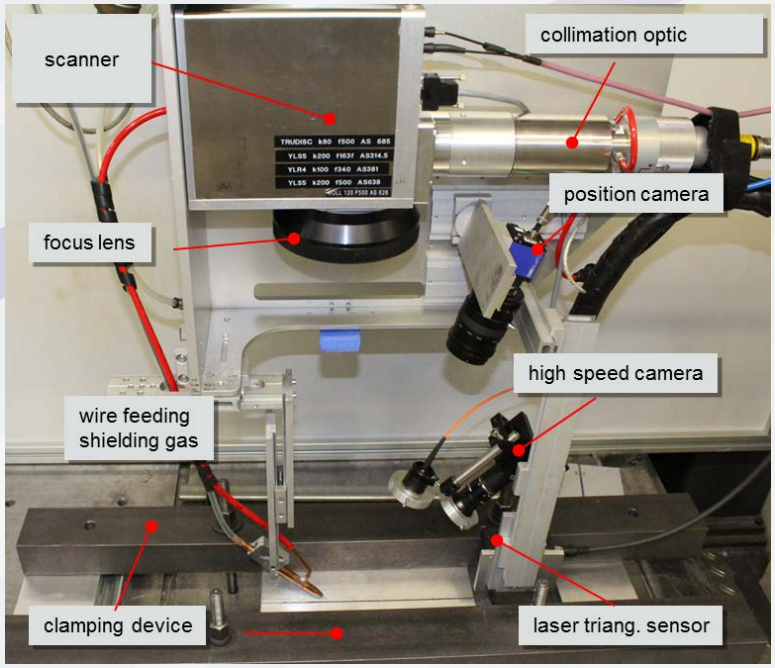

© Fraunhofer IWS

Laser-Multi-Pass-Narrow-Gap-Welding

Test on mild steel

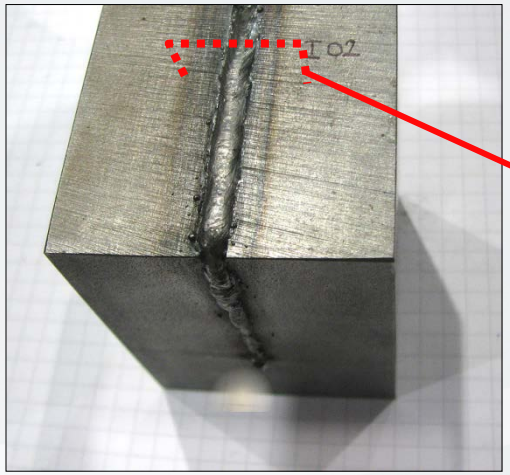

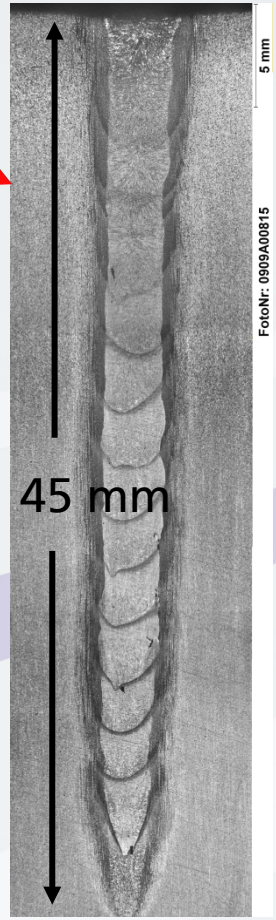

Parameters:

D. fiber core = 50 µm
Material: mild steel
groove α = 4°
Laser power = 4 kW
v per pass = 0,4 m/min
v_{WIRE} = 7 m/min
Pass count = 15

Test on stainless steel

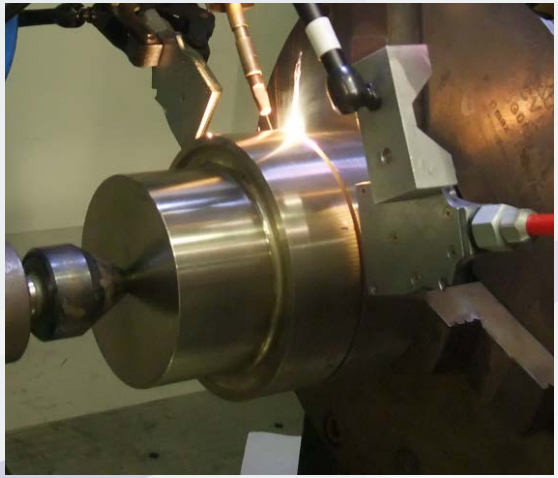

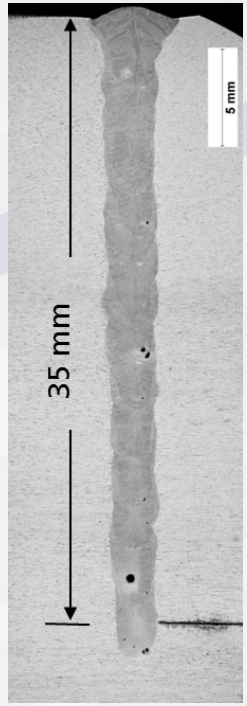

Parameters:

Wall-thickness = 35 mm
Material: 1.4301 (V2A)
groove α = 0°, width= 2 mm
Laser power = 2,5 kW
v per pass = 0,5 m/min
v_{WIRE} = 3,5 m/min
Pass count = 13

© Fraunhofer IWS

Laser-Multi-Pass-Narrow-Gap-Welding

Reworking of gas turbine rotor shaft

Motivation

- extending lifespan – certain gas turbines are reworked in critical areas
- a possible solution is turning of a fatigue critical area and re-insert stiffness bars ABOVE the turned groove

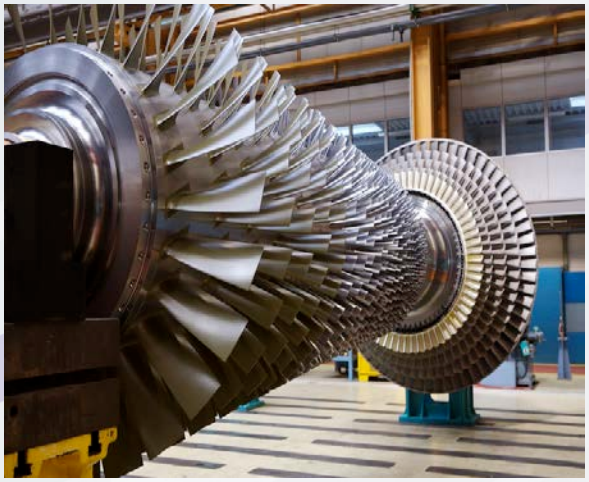

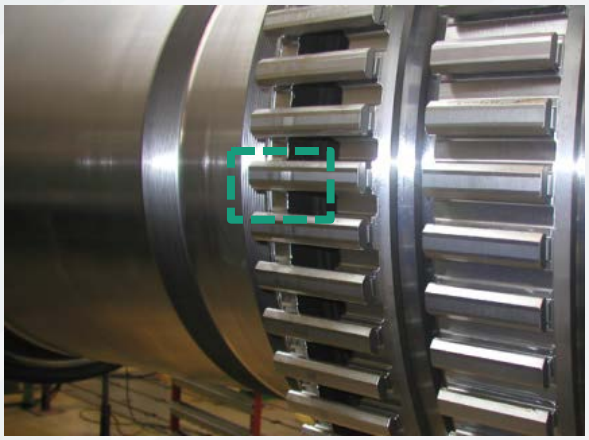

Challenges

- cold crack sensitive material
- distortion and rework should be minimized
- precise edge preparation required

© Fraunhofer IWS

Laser-Multi-Pass-Narrow-Gap-Welding

Reworking of gas turbine rotor shaft

Concept for Welding and Machining

- Use of Pentapod parallel kinematic machine
- Stationary or mobile machine

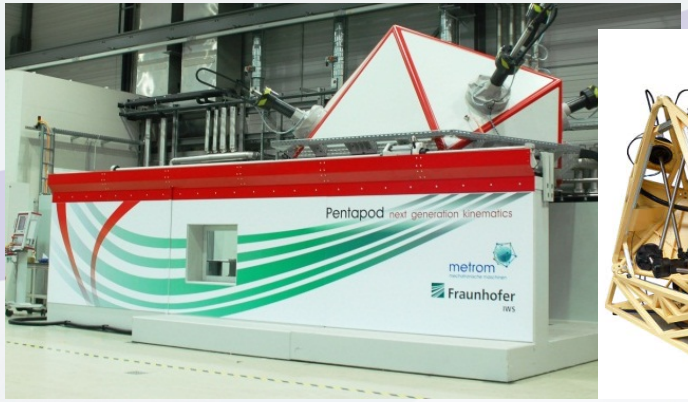

lab sample

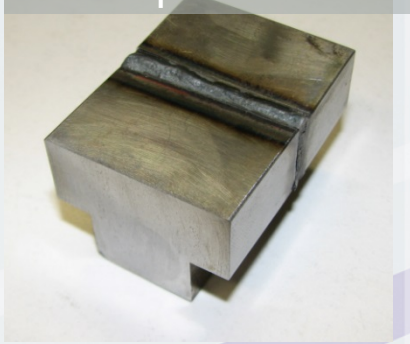

demonstrator

Edge praparation

finishing

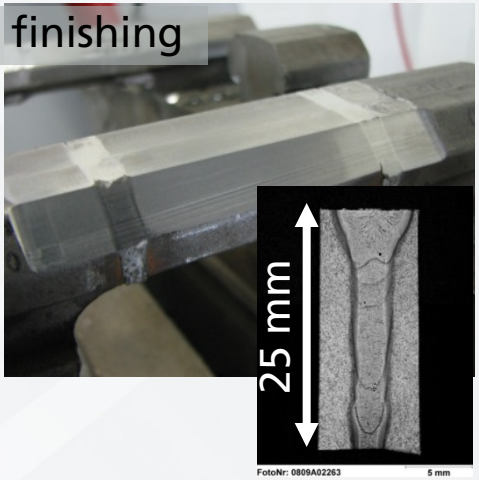

Motivation and Challenges for Aluminum

- high specific strength
- large application field for light weight construction (aircraft fuselage-, and space technology)
- strong request on effective joining techniques

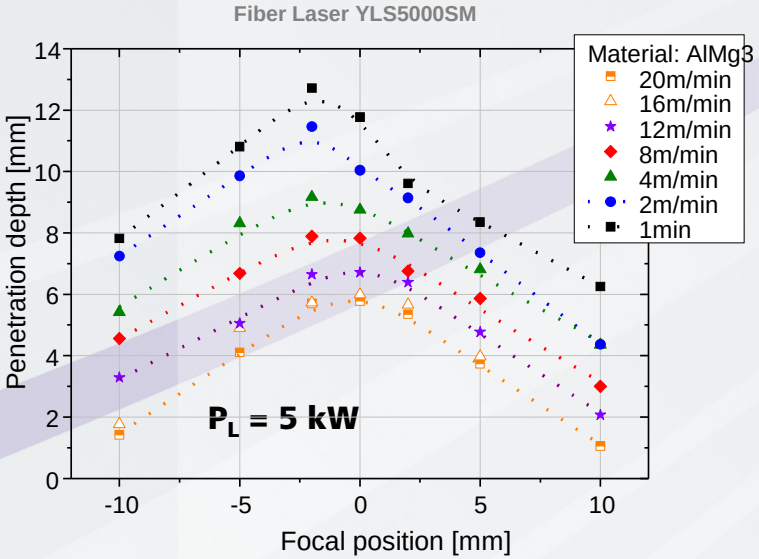

- penetration depth at 5 kW max. 6 to 12 mm
- For 6xxx low Si-content in the weld root → hot cracks
- increasing strength-undermatching for high strength aluminium alloys
- Very low melt pool viscosity
- physical properties of aluminium

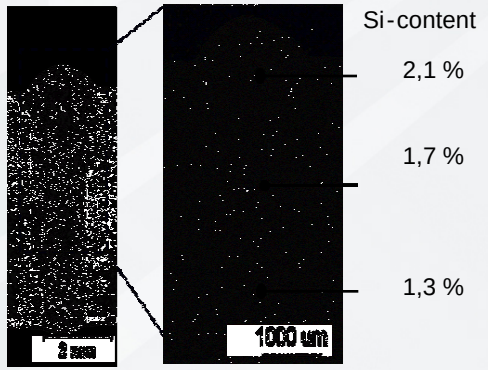

© Fraunhofer IWS

Laser-Multi-Pass-Narrow-Gap-Welding

Process development for hot crack sensitive Al-6082

Groove preparation:

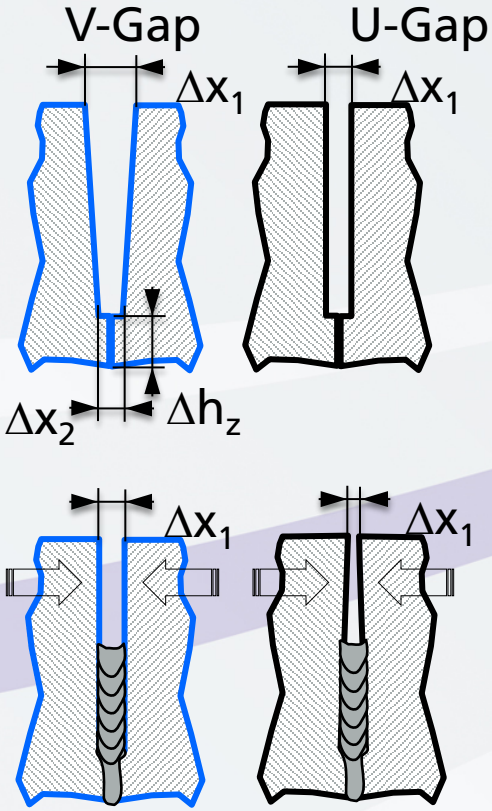

Influence on scan frequency:

f_{Scan} = 200 Hz f_{Scan} = 700 Hz

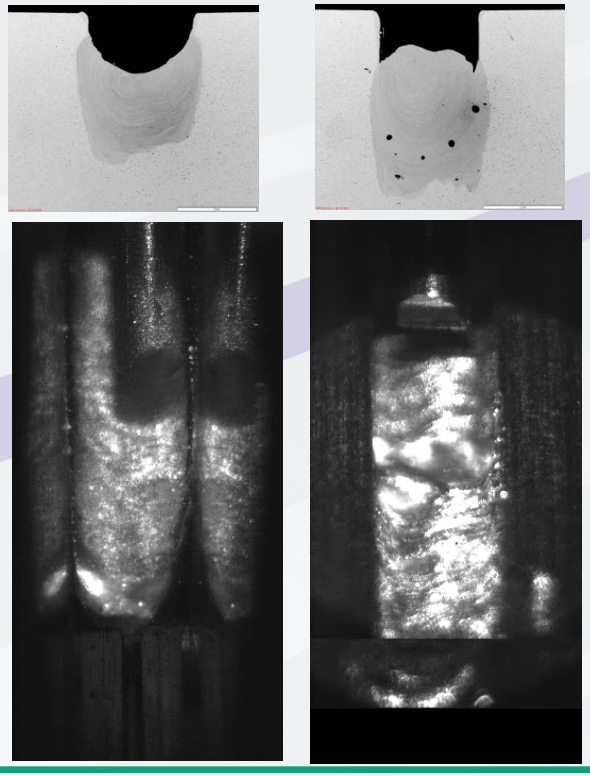

Efficiency improvement:

up to 1,5 mm up to 3,5 mm

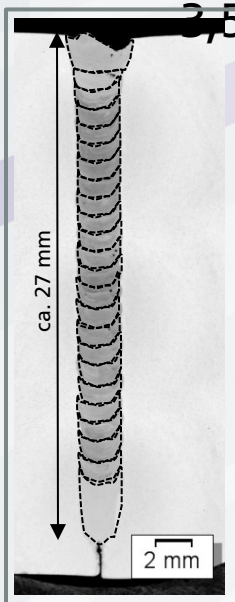

V_{weld} / V_{WIRE} = 1

$\varnothing_{Spot}$ = 210 µm

f_{scan} = 350 Hz

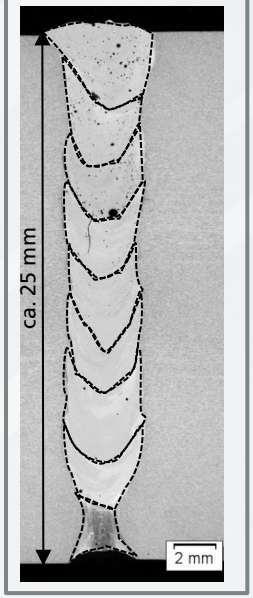

V_{weld} / V_{WIRE} = 3

$\varnothing_{Spot}$ = 600 µm

f_{scan} = 100 Hz

© Fraunhofer IWS

Laser-Multi-Pass-Narrow-Gap-Welding

Process chain (video)

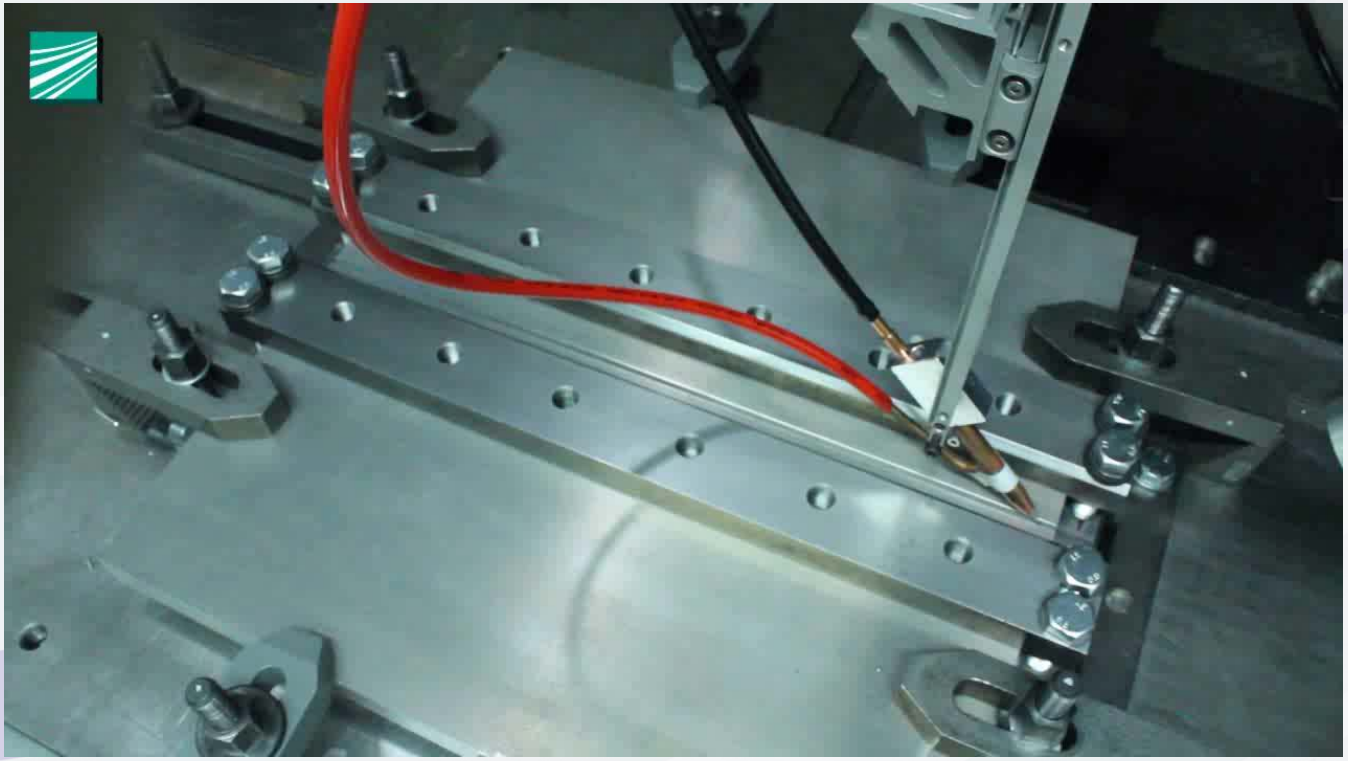

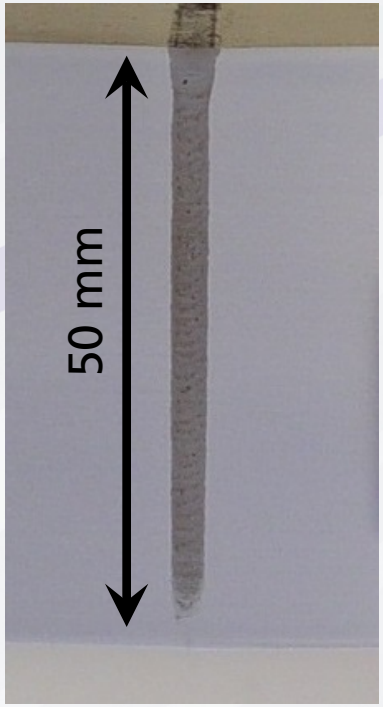

Homogeneous welding process, independent of the amount of passes.

© Fraunhofer IWS

Laser-Multi-Pass-Narrow-Gap-Welding

Weld seam properties for AA6082

30 kW MM fiber laser	30 kW MM fiber laser	30 kW MM fiber laser	2 kW SM fiber laser
Welding in full material	Welding in full material	Welding in full material	V-Groove 3,5 mm gap at top 0 mm at root
V_{wire}= 2m/min	V_{wire}= 6m/min	V_{wire}= 10m/min	V_{wire}= 1m/min
Si-content in %	Si-content in %	Si-content in %	Si-content in %
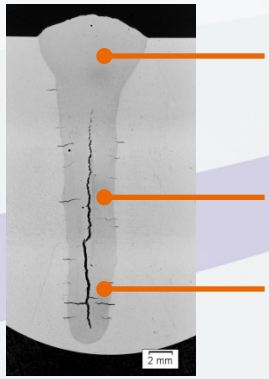	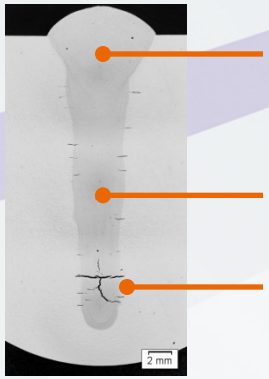	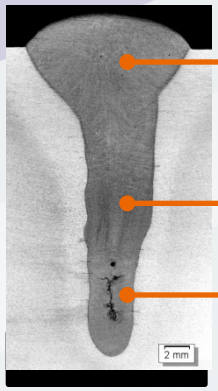	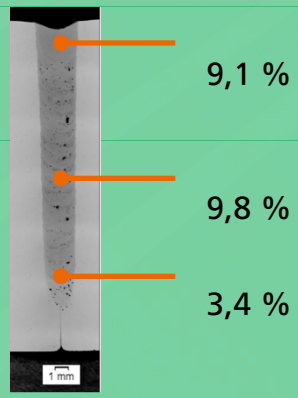

© Fraunhofer IWS

Laser-Multi-Pass-Narrow-Gap-Welding

Weld seam properties for AA6082

	[/]	Base material	MPNG welded sample T6 LBW	MPNG welded sample T6 LBW T6
$R_{p0,2}$	MPa	321	294	316
R_m	MPa	340	306	323
A	%	18,7	< 1	< 1,5

Base material strong necking

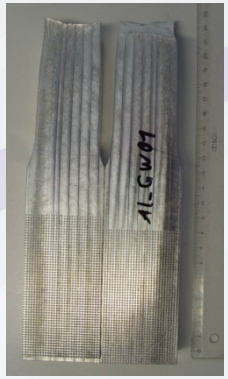

MPNG – sample no necking

Strength level of welds 95% .. 98% of base material!

MPNG-Welding for Aluminium

- low laser power – extreme deep weld seams → high aspect ratio
- reduced distorsion with increase of sheet thickness

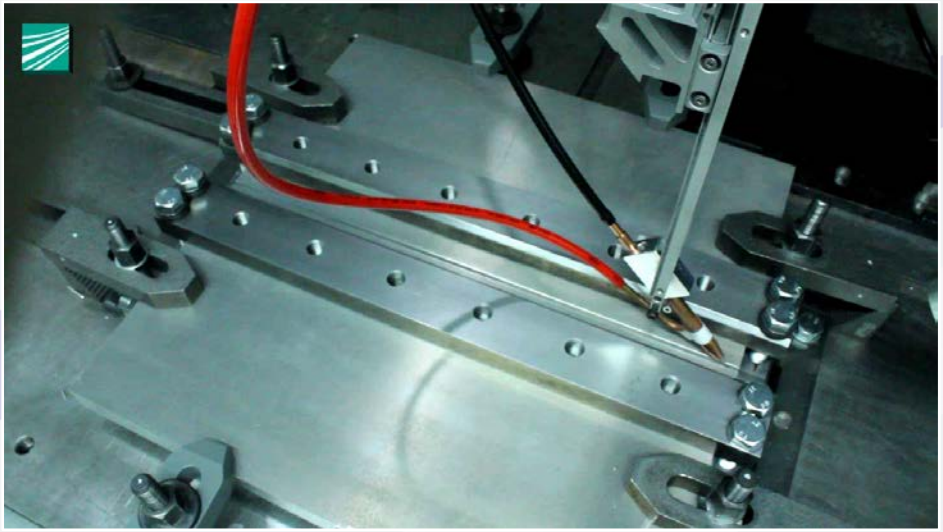

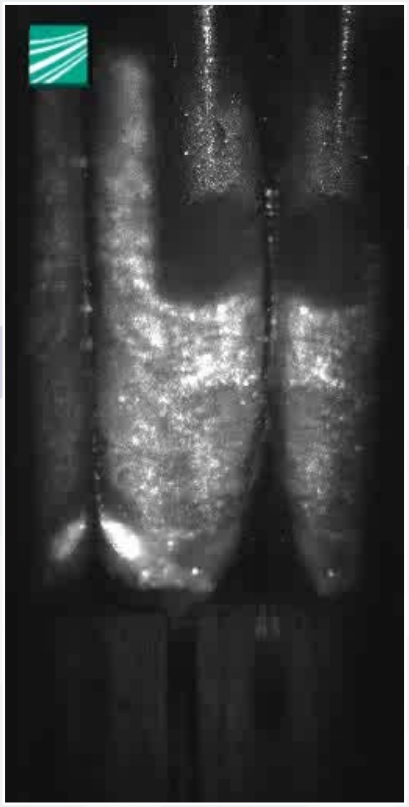

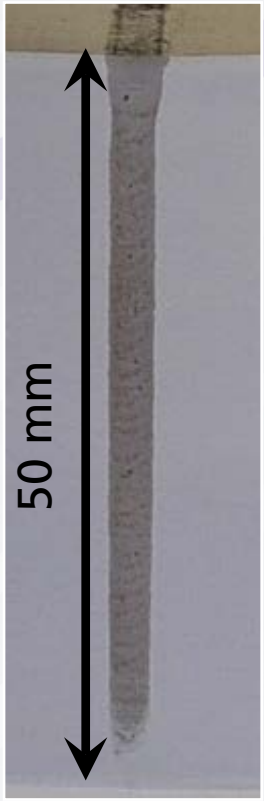

© Fraunhofer IWS

Laser Multi Pass Welding of thick sheets

MPNG-Welding

- low laser power – extreme deep weld seams → high aspect ratio
- available for steel and aluminum
- high weld seam stability, no dropping of melt liquid as usual for high power laser application
- high weld seam quality, low porosity
- low component distortion

Fiber-Laser

aluminium

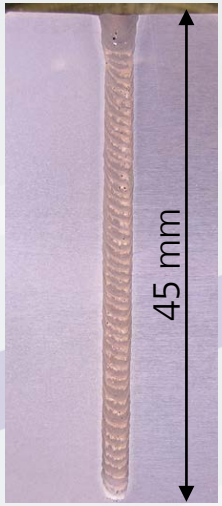

mild steel

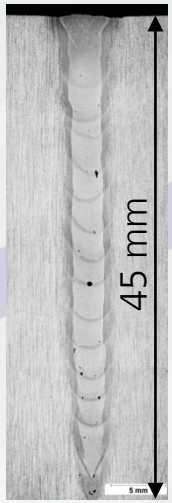

Diode-Laser

mild steel

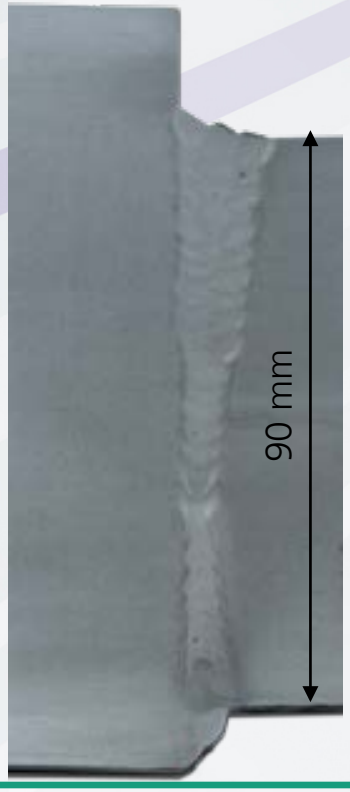

© Fraunhofer IWS

Content

Content	Chapter
Introduction	
The Fraunhofer Gesellschaft	01
Fraunhofer Institute for Material and Beam Technology IWS	02
Seminar topics	03
Laser Beam Welding	
Basics	04
Laser multi pass welding	05
Laser beam welding with high frequent beam oscillation	06
Laser beam welding of high reflective materials	07
Laser beam welding of powertrain components	08
Laser induction roll plating	09
Special Joining Technologies	
Magnetic pulse joining	10
Friction stir welding	11
Joining with reactive multi layers	12
Bonding and Composite technology	
Electrical-conductive bonding	13
Thermal direct joining of thermoplastic to metal	14
Mechanical Joining	
Enhanced mechanical connection by laser interference patterning	15

© Fraunhofer IWS

Laser beam welding with high frequent beam oscillation

Example:
High quality laser beam welding of light weight aluminium die cast material

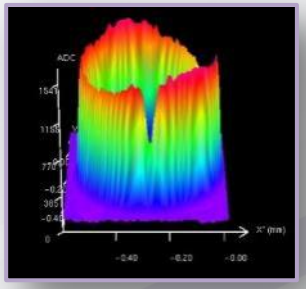

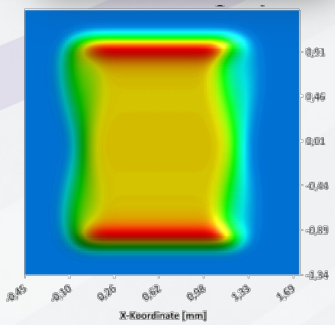

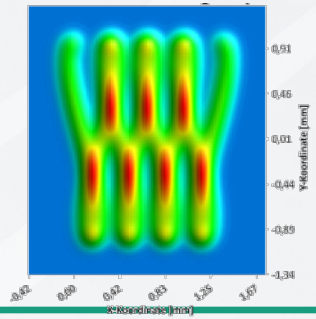

© Fraunhofer IWS

Laser beam welding with high frequent beam oscillation

Challenges for laser material processing:

- highly demanding specifications (material, properties and costs)
- stable, reproducible parameter und process windows required
- excellent product quality has to be ensured → strong demand on effective welding processes

Problem:

- laser beam welding with a static beam reaches boundaries
  → missing process solution
- Al-die cast material shows limitation regarding welding
  → limited quality pores, blow outs, leakage of weld seam

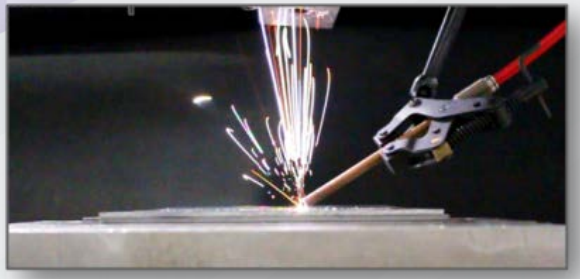

Approach:

- laser beam welding with high frequency beam oscillation

© Fraunhofer IWS

Laser beam welding with high frequent beam oscillation

Conventional strategies in beam shaping:

- static beam shaping (twin spot) / static power modulation
  - complex optics systems
  - limited variability
- filler wire replacing ejected material

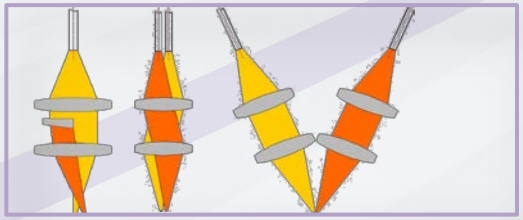

Quelle: W. Gref, IFSW Stuttgart

Problem:

- low market penetration of those technologies
- electron beam welding as an expensive alternative

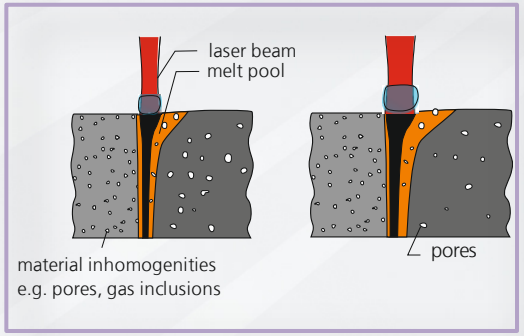

Solution:

- Laser beam welding with high frequency scanner and power modulation by special beam sources

© Fraunhofer IWS

Laser beam welding with high frequent beam oscillation

Solution approach

Novel process strategies:

- instead of large static spots (400 µm) → small spots + HF-scanning
- dynamic, high frequency 2D-beam oscillation → Lissajous-Figures
  - galvanometer scanner with frequencies of kHz level
- keyhole-stability + adapted melt pool dynamic → stabile processes → power modulation

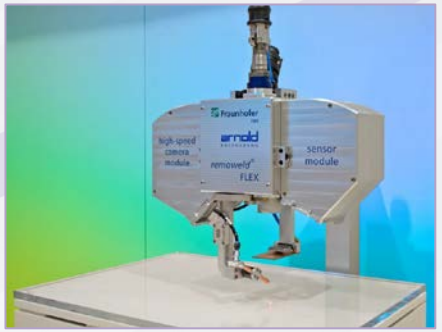

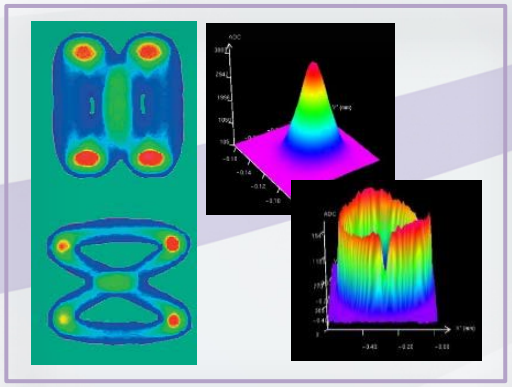

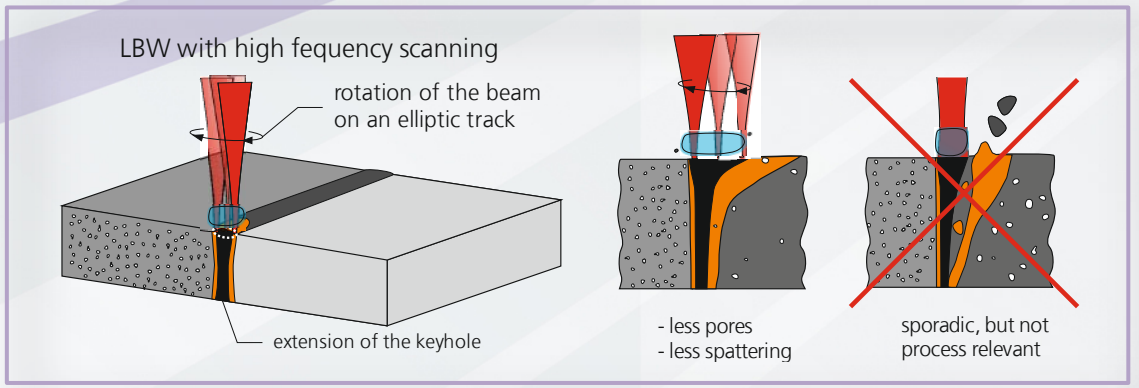

© Fraunhofer IWS

Effect of high frequency beam manipulation on the process:

- reduction of spatter for standard Al-wrought materials
  - reduction of process turbulences with increasing frequency
  - homogeneous welding process by moderate power
- stabilization of the keyhole → homogenization of melt pool fluctuations
- avoidance of non steady keyhole-situation

static beam	high dynamic beam oscillation
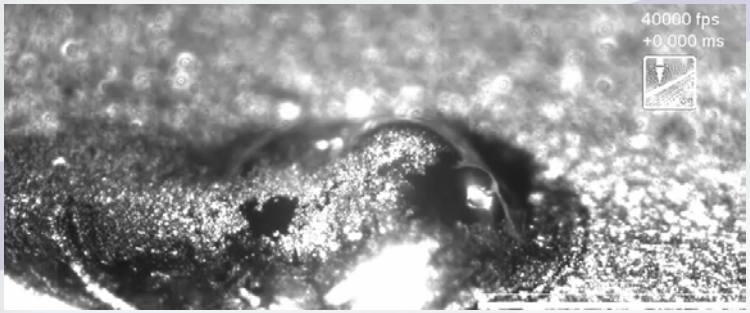	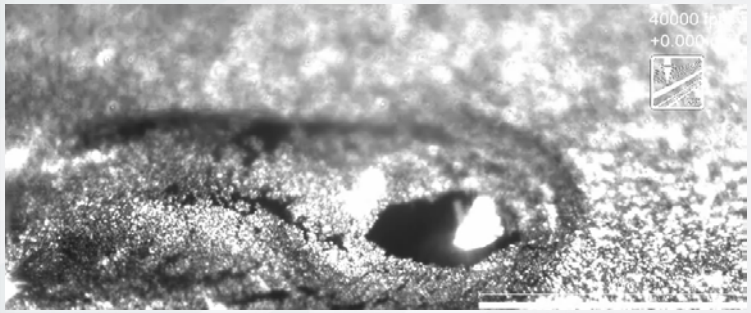

© Fraunhofer IWS

Laser beam welding with high frequent beam oscillation

Al-die cast laser welding

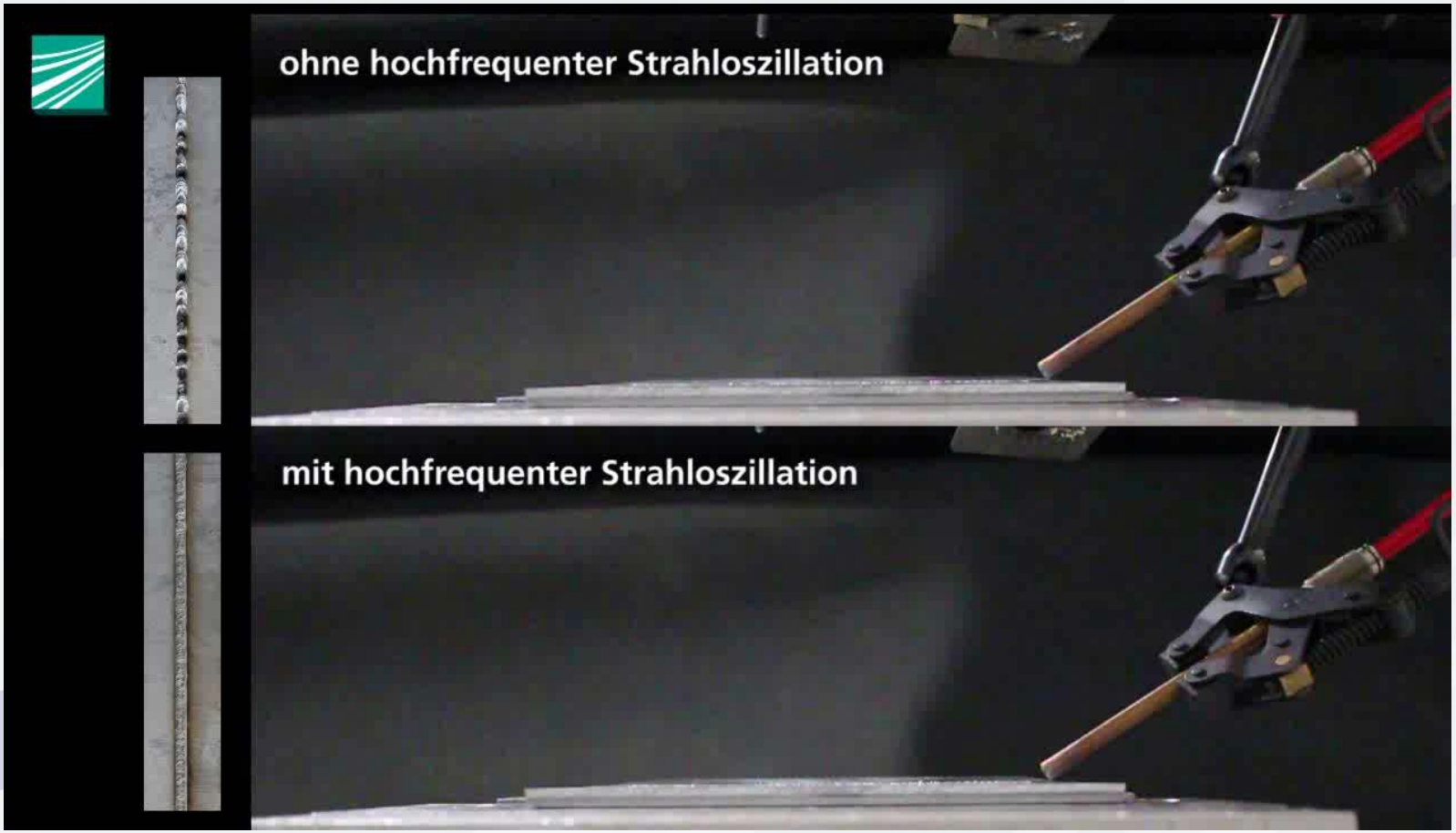

© Fraunhofer IWS

Calculation of energy deposition; effect of parameter

Explanation for calculation:

- fast approximation of parameter by using:

$$W_X = \frac{2 * \text{welding speed}}{\text{beam diameter} * \text{oscillation frequency}}$$

$W_X < 1$ homogeneous energy deposition

$W_X > 1$ in homogeneous energy deposition

- visualization of laser beam movement path
- display of laser beam & energy distribution
- adaption of energy intensity by oscillation- and power modulation parameter available

$$W_X = \frac{\Delta X}{r} = \frac{v_S}{f \cdot r}$$

f...Oszillationsfrequenz
r...Strahlradius
v_S...Vorschubgeschwindigkeit

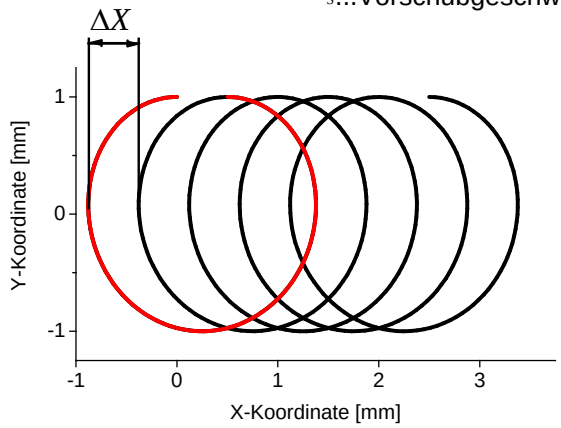

© Fraunhofer IWS

Calculation of energy deposition; effect of parameter

scan figure:

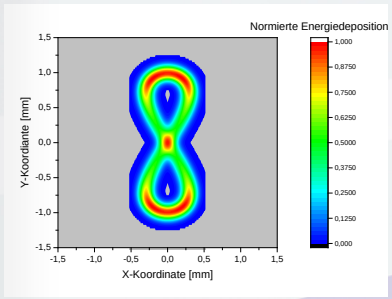

energy distribution at constant laser power

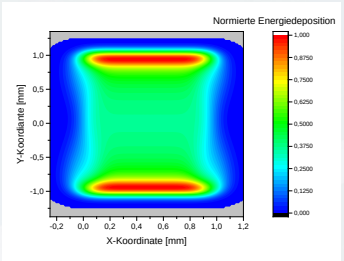

W_X=0,16

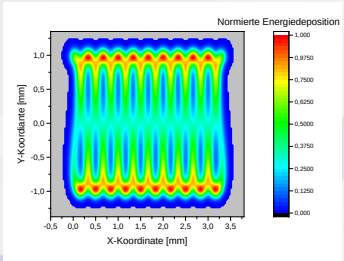

W_X=2,22

phase displacement power modulation

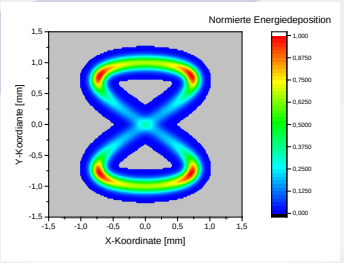

phase displacement: 45°

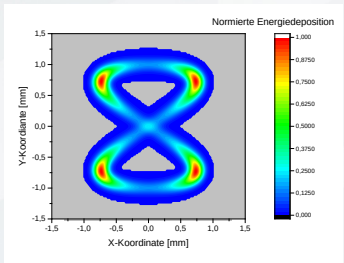

phase displacement: 270°

© Fraunhofer IWS

Influence of frequency to the energy distribution

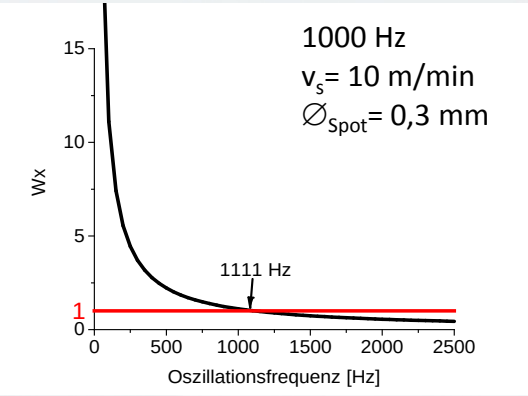

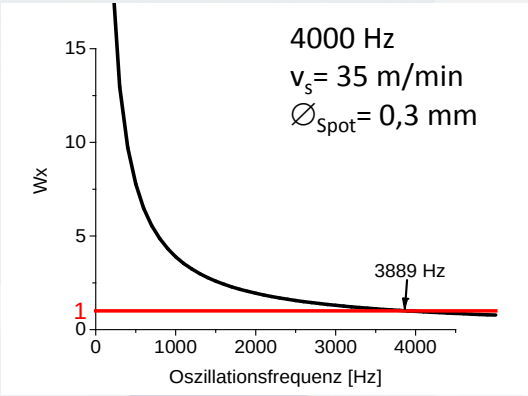

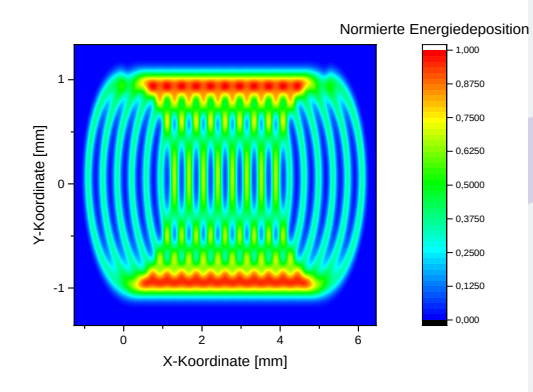

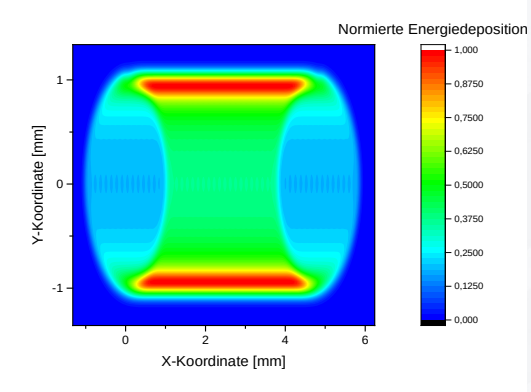

© Fraunhofer IWS

Influence of frequency to the energy distribution

Sand watch: Amplitude X: 0,3 mm; Y: 0,8 mm; Frequency: 300 Hz;
⋈ speed: 2 m/min; beam diameter: 36 µm

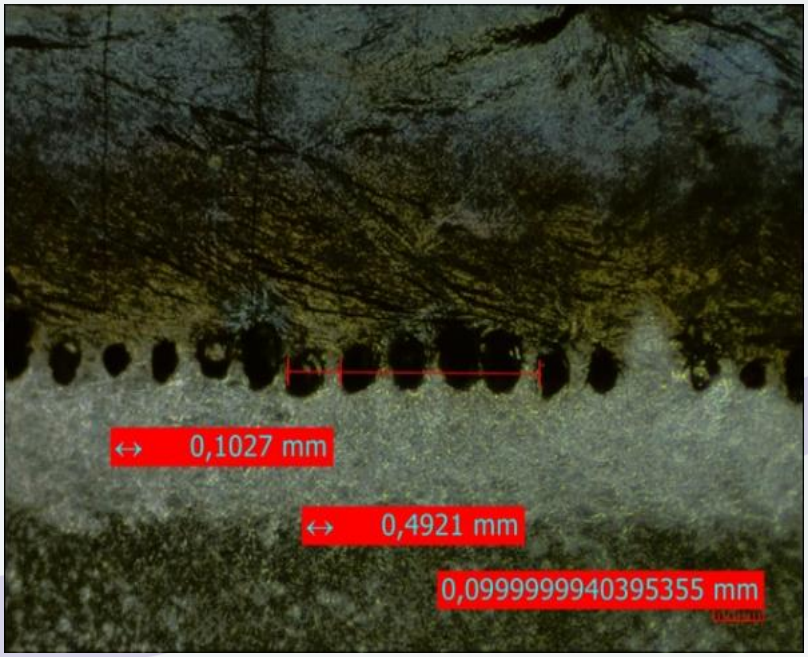

Figure: weld seam, distance between the holes: 0,1 mm

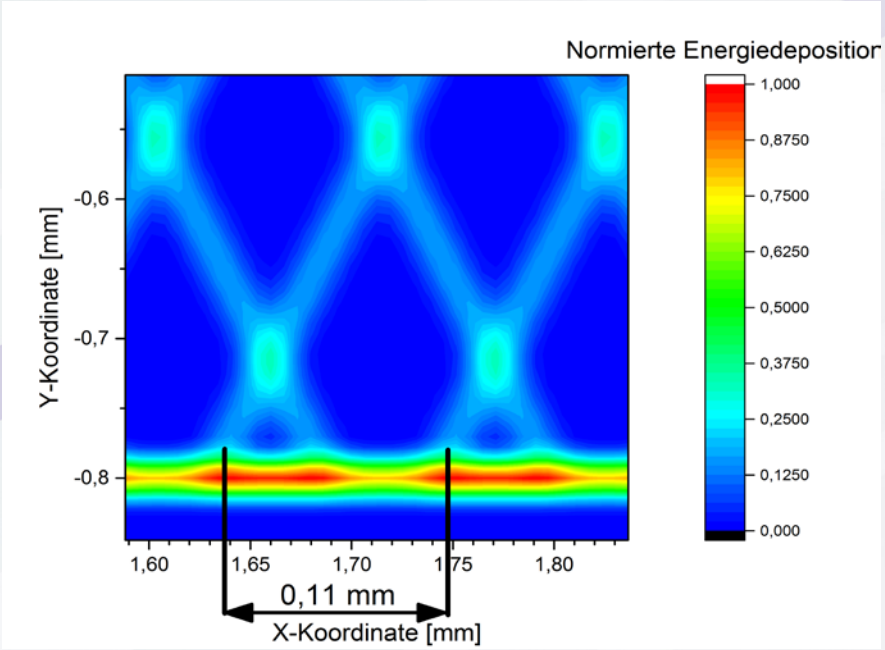

Figure: calculation, distance between the peak energy power: 0,1 mm

Conclusion: Calculated peak equal to the measured distance

© Fraunhofer IWS

Laser beam welding with high frequent beam oscillation

Potential Applications

Task:

- LBW automotive components, heat exchanger, electro mobility
- Al-die cast vs. Al-extrusions or Al-wrought material
- Goal: handling concept and industrial application and potential technology transfer

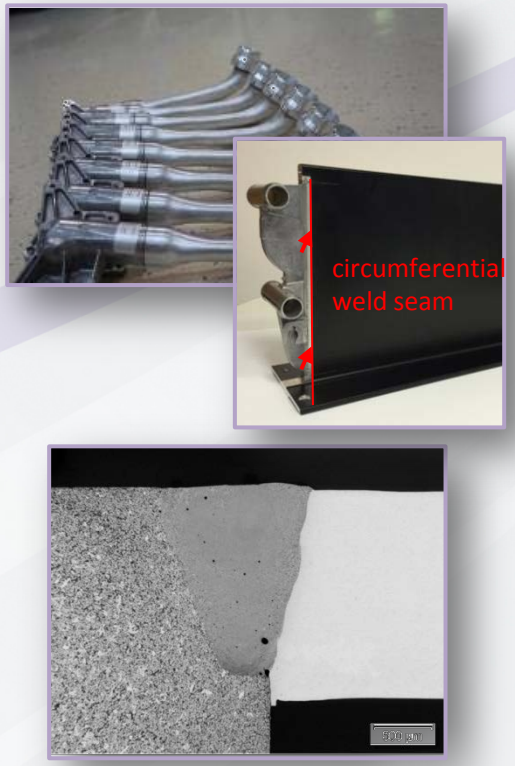

Solution:

- high frequency beam oscillation with SM-Fiber Laser

Result:

- pressure tight weld seams at high process stability

© Fraunhofer IWS

Laser beam welding with high frequent beam oscillation

Potential Applications

Task:

- LBW of small pressure vessels
- Al-tube vs. flux contaminated Al-lid
- Goal: obtaining high weld seam quality, pressure tight weld seam

Solution:

- high frequency beam oscillation with SM-Fiber Laser

Result:

- pressure tight weld seams at high process stability

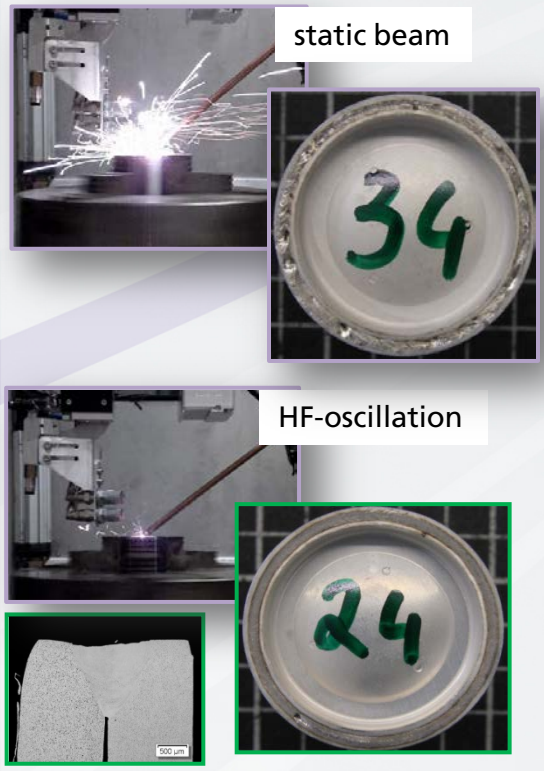

© Fraunhofer IWS

Laser beam welding with high frequent beam oscillation

Conclusion:

- Laser beam welding of Al-die cast material with brilliant laser beam sources and high frequency oscillation is now available for:
  - pressure tight weld seams without thermal component distortion
  - fast, efficient and reproducible welding processes,

- laser beam welding with high frequency beam oscillation (kHz) and beam modulation enables:
  - strongly expanded parameter field and therefore new possibilities of process development
  - quality enhancement by avoidance of spatter, pore reduction and homogeneous weld seam geometry

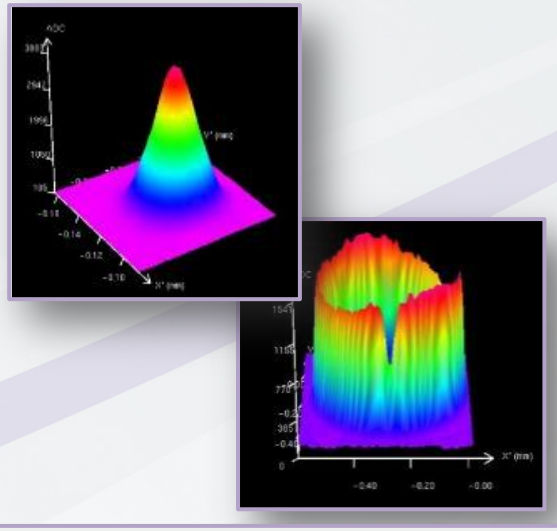

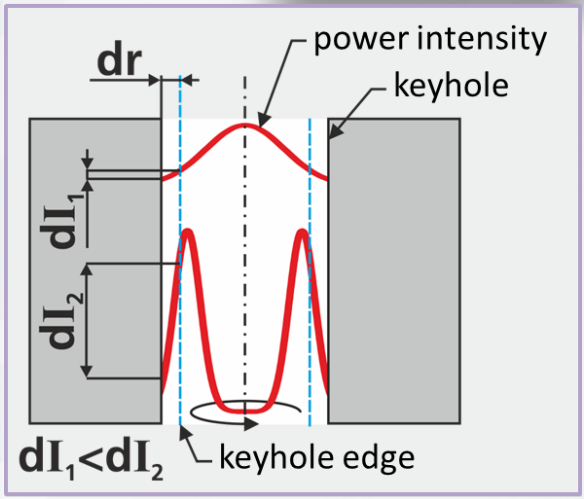

© Fraunhofer IWS

Content

Content	Chapter
Introduction	
The Fraunhofer Gesellschaft	01
Fraunhofer Institute for Material and Beam Technology IWS	02
Seminar topics	03
Laser Beam Welding	
Basics	04
Laser multi pass welding	05
Laser beam welding with high frequent beam oscillation	06
Laser beam welding of high reflective materials	07
Laser beam welding of powertrain components	08
Laser induction roll plating	09
Special Joining Technologies	
Magnetic pulse joining	10
Friction stir welding	11
Joining with reactive multi layers	12
Bonding and Composite technology	
Electrical-conductive bonding	13
Thermal direct joining of thermoplastic to metal	14
Mechanical Joining	
Enhanced mechanical connection by laser interference patterning	15

© Fraunhofer IWS

Laser beam welding of high reflective materials – influence of laser wave length

Influence of Laser Wave Length
„green“ vs. „infrared“

- Laser source and experimental setup
- Laser welding of copper and stainless steel
- Absorption and process behavior,
- Process efficiency and potential, preferred application

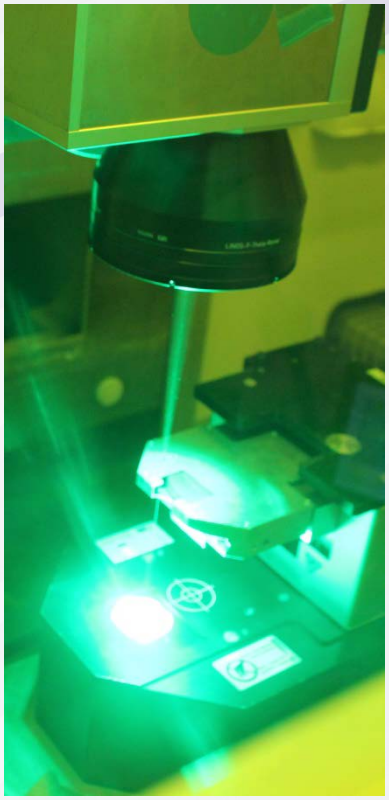

© Fraunhofer IWS

Laser beam welding of high reflective materials

ENGINE
stator / rotor;
cable connection;
Cu-Cu-, Al-Cu-joints

battery cell crash box, Al-St-joints

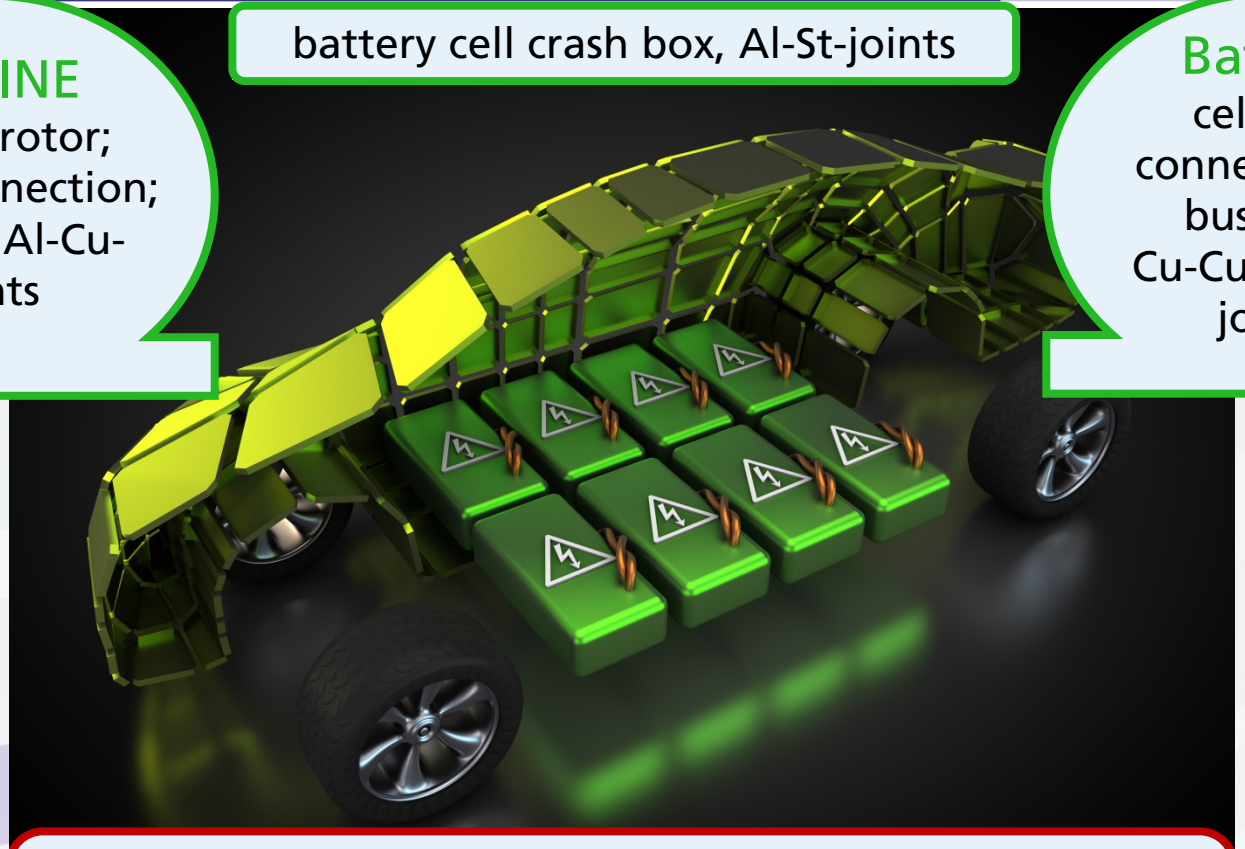

Battery
cell foil connections;
bus bars;
Cu-Cu-, Al-Cu-joints

Challenges

joining methods, metallurgical aspects (IM), productivity, costs, availability, quality

© Fraunhofer IWS

Wave length - „green“ vs. „Infrared“

Copper

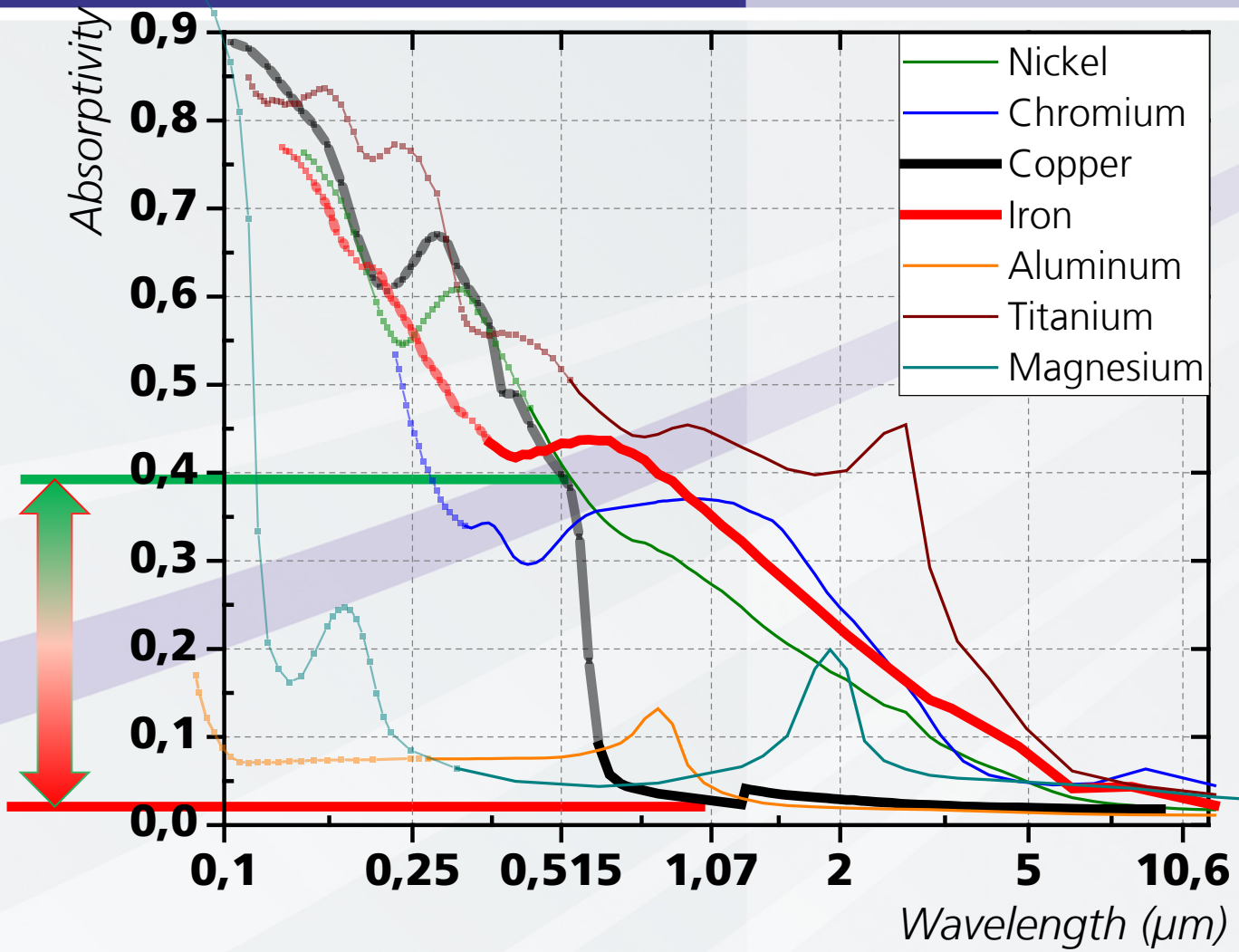

© Fraunhofer IWS

Wave length - „green“ vs. „Infrared“

Steel

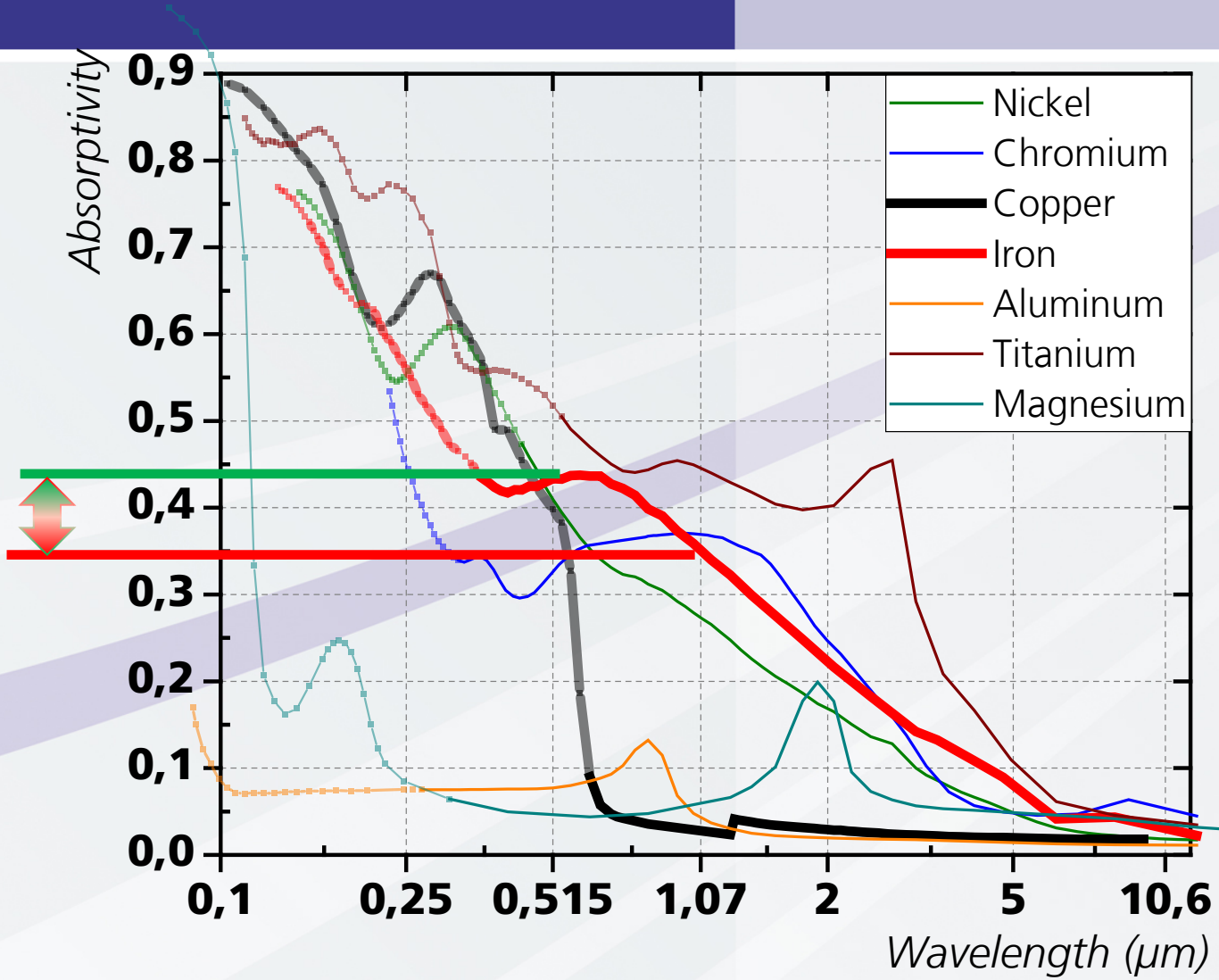

© Fraunhofer IWS

Laser beam welding – used sources

TRUMPF Trudisk 1020 (Prototype)

Max. Power	1000 W
Wave length	515 nm
Delivery fiber	50 µm
BBP / M^2	2,80 / 8,3

IPGYLR4000

Max. Power	4000 W
Wave length	1070 nm
Delivery fiber	50 µm
BBP / M^2	2,00 / 5,8

IPG YLS5000 SM

Max. Power	5000 W
Wave length	1070 nm
Delivery fiber	30 µm
BBP / M^2	0,40 / 1,3

© Fraunhofer IWS

Laser beam welding – used sources

TRUMPF Trudisk 1020

$\varnothing_{Focus,\ measured}$ = 96 µm

IPG YLR4000

$\varnothing_{Focus,\ measured}$ = 114 µm

IPG YLS5000

$\varnothing_{Focus,\ measured}$ = 101 µm

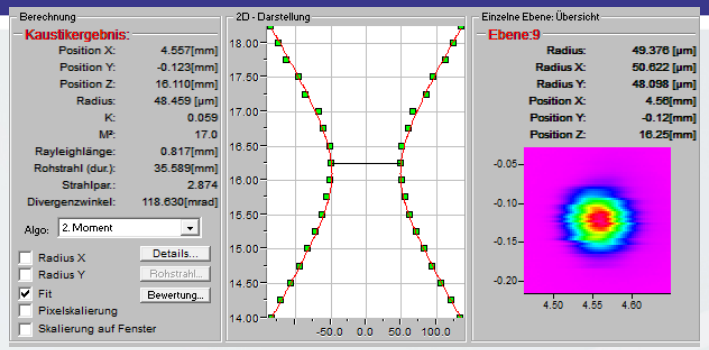

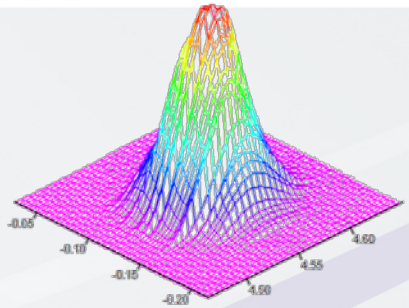

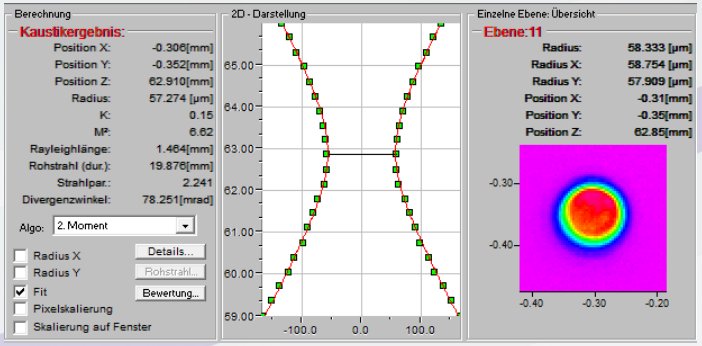

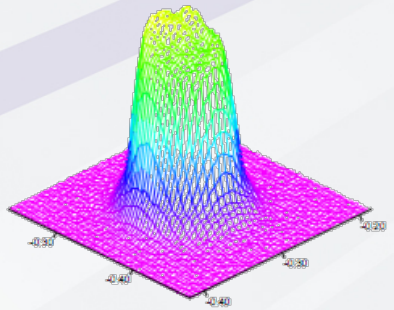

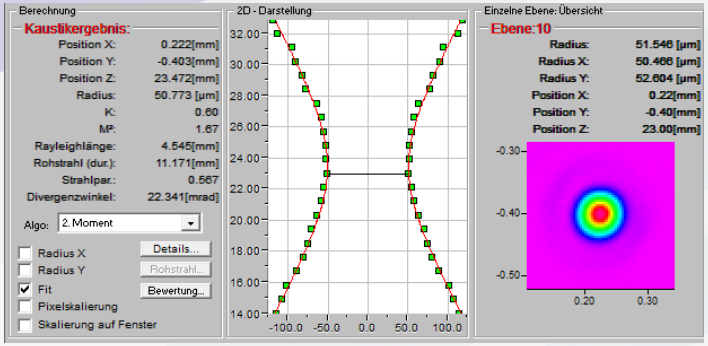

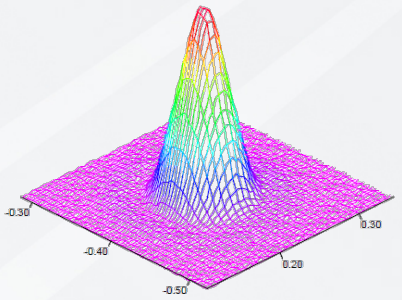

© Fraunhofer IWS

Laser welding with Disk laser @ 515 nm

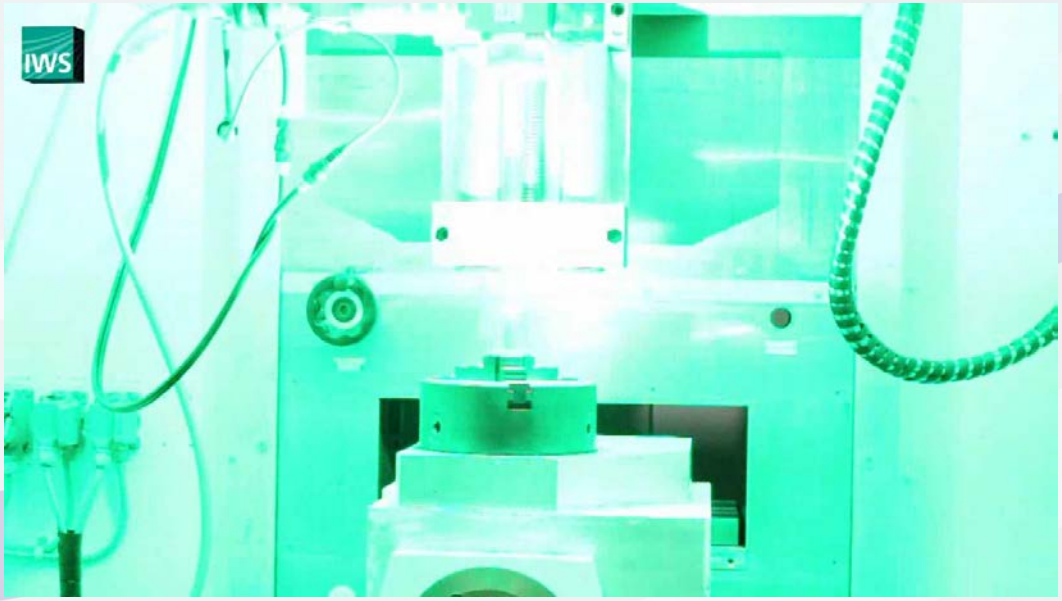

© Fraunhofer IWS

Laser beam welding of high reflective materials
Pretest

Disk laser with 515 nm

$\varnothing_{Focus,\ measured}$ = 96 µm

- Stable welding process on copper up to 400 W
- Penetration depth for used welding speed > 1.0 mm

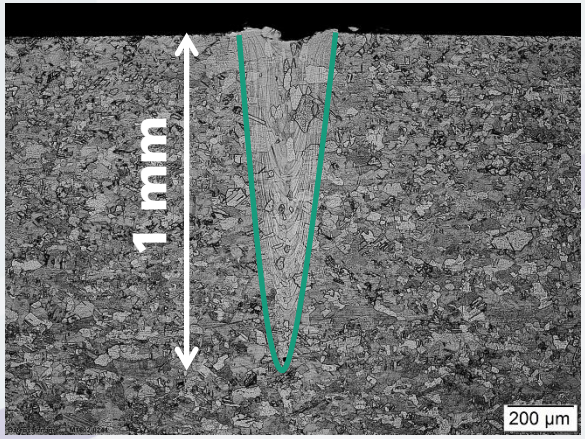

P_L = 700 W, v_S = 0,5 m/min

Worst case: polished copper

- For 1000 W @ 515 nm stable deep penetration welding
- For 1000W @ 1040 nm (single mode fiber laser) no stable welding process possible ($\varnothing_{Focus,\ measured}$ = 101 µm)

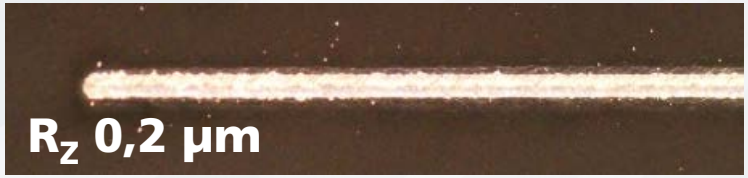

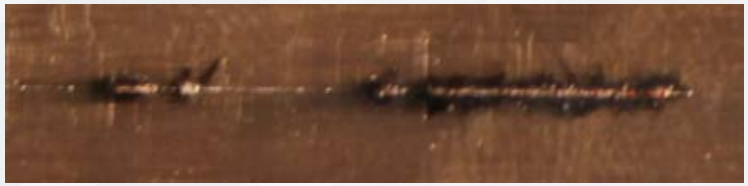

© Fraunhofer IWS

Experimental set up

- TRUDISK1020 with 515 nm and YLR4000 with 1070 nm
- Comparable optical configuration
  - Fiber diameter = 50µm
  - Collimation = 200 mm
  - Focusing = 200 mm
  - Laser power = 1000 W

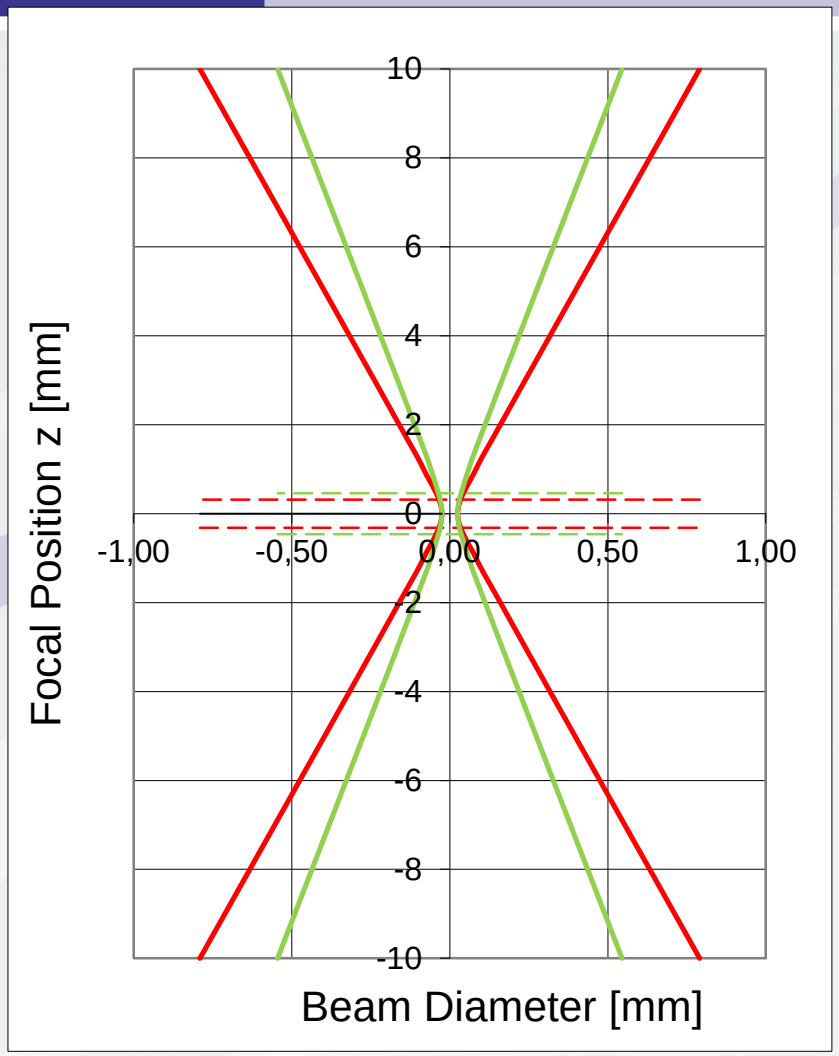

© Fraunhofer IWS

Laser beam welding of high reflective materials

Experimental set up

- Bead-on-plate welds on stainless steel and copper
  - Welding speed = 2 m/min,
  - Shielding gas Argon
  - Variation of focal position from -20mm … +20mm
  - Tilt angle 10°
- metallographic cross section
  - Weld seam shape
  - penetration depth & seam width on surface
  - molten area

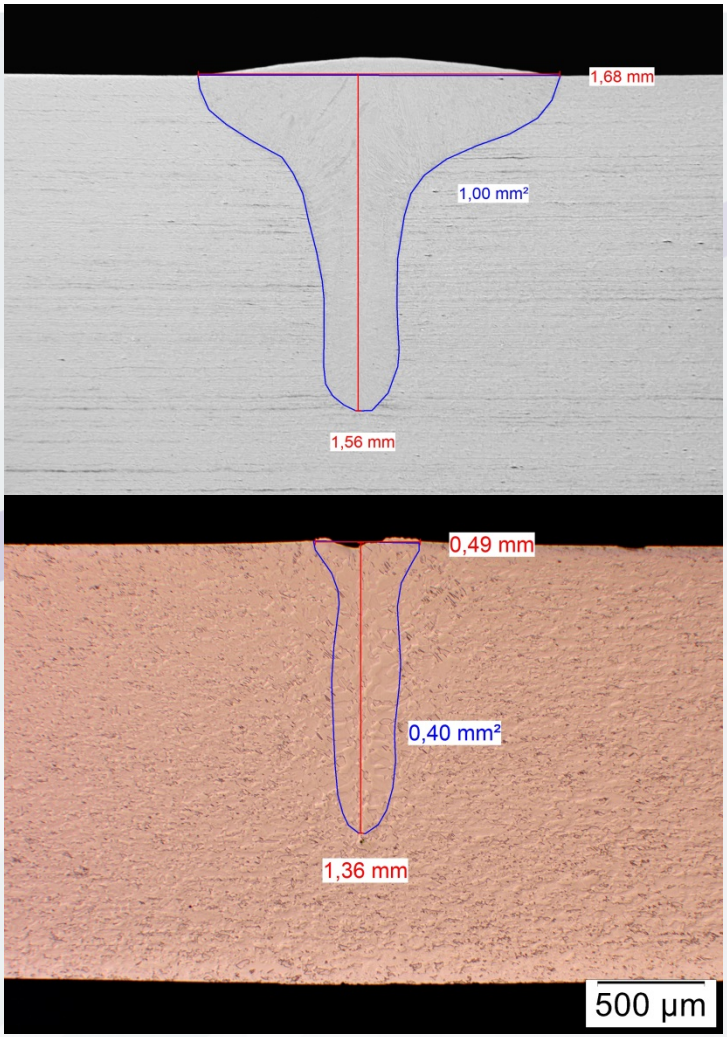

© Fraunhofer IWS

Laser beam welding of high reflective materials

Experimental results on copper

- Extreme small process window for welding with 1070 nm
- Significant higher penetration depth and process window for 515 nm

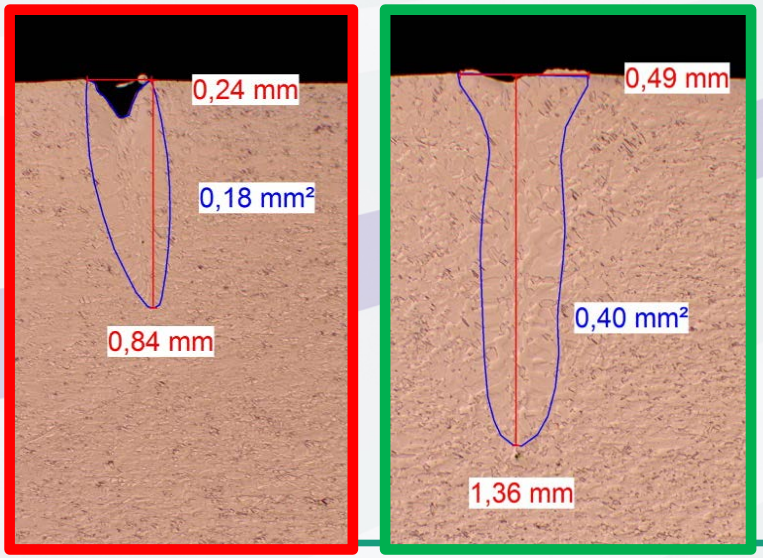

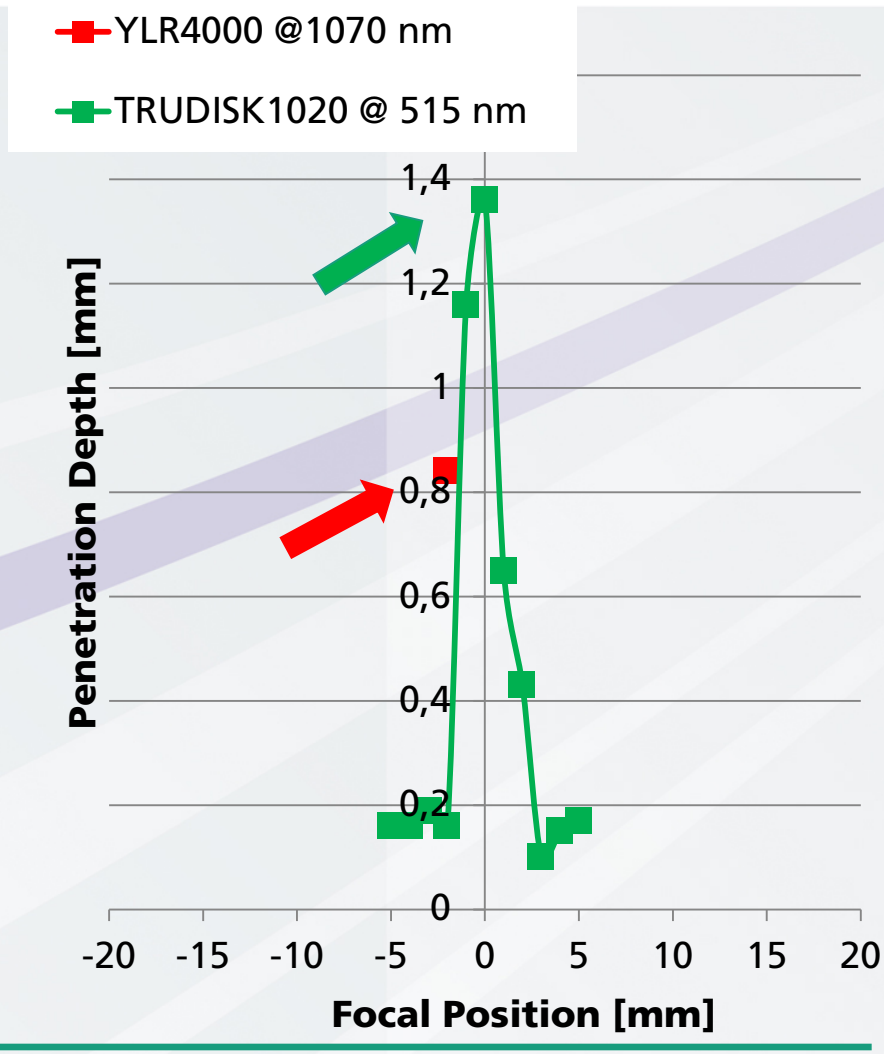

© Fraunhofer IWS

Experimental results on copper

- Extreme small process window for welding with 1070 nm
- Significant higher penetration depth and process window for 515 nm
- For 515 nm heat conduction welding of copper possible

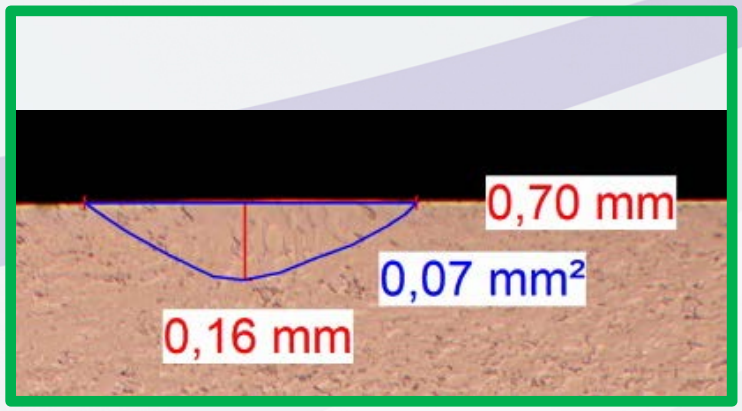

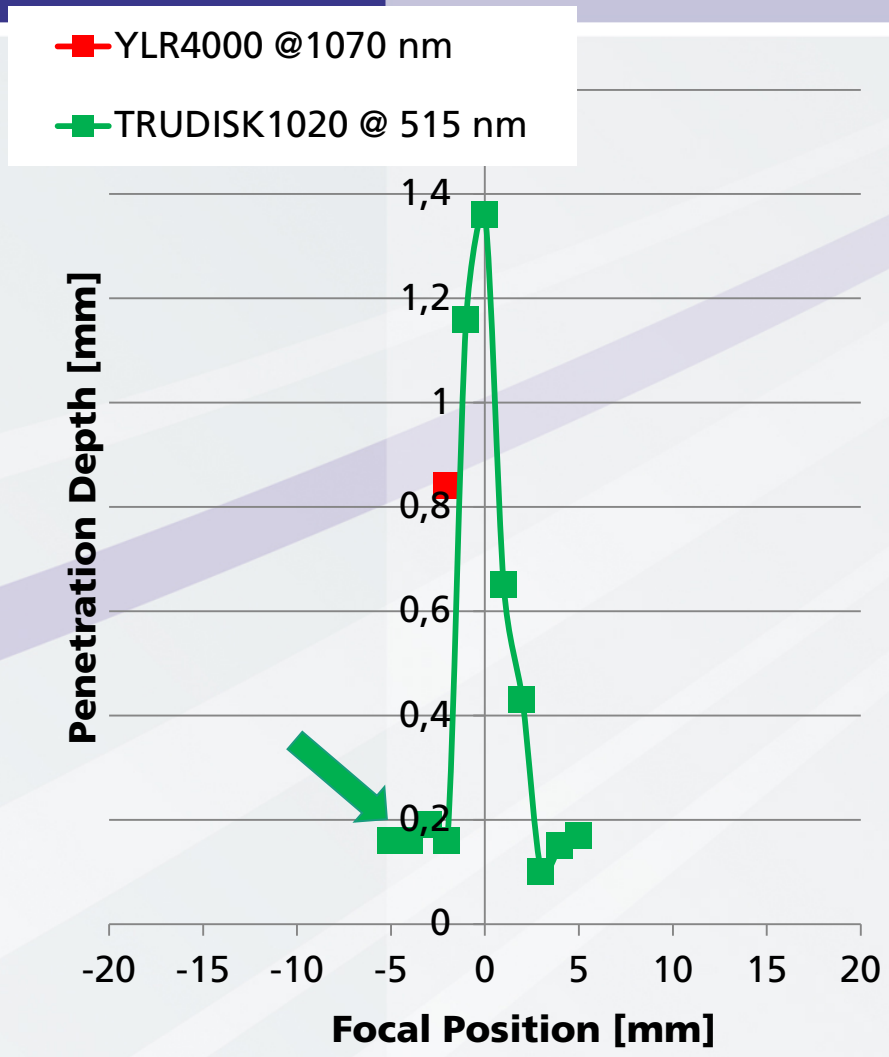

© Fraunhofer IWS

Experimental results on stainless steel

1) Penetration depth

- Highest penetration depth for both laser when focus below surface
- Slightly higher penetration depth for 515 nm

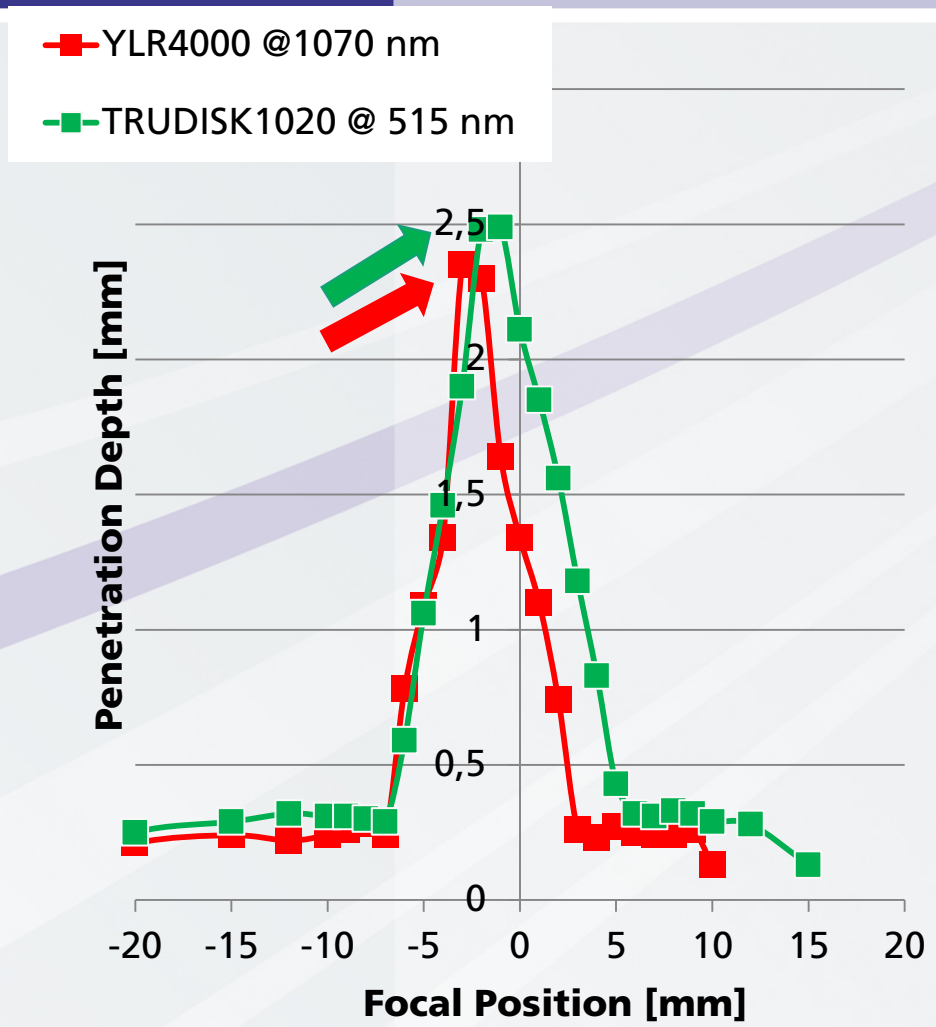

© Fraunhofer IWS

Experimental results on stainless steel

2) Seam width and shape

- Outside optimal focal position (highest penetration depth) higher seam width for 515 nm

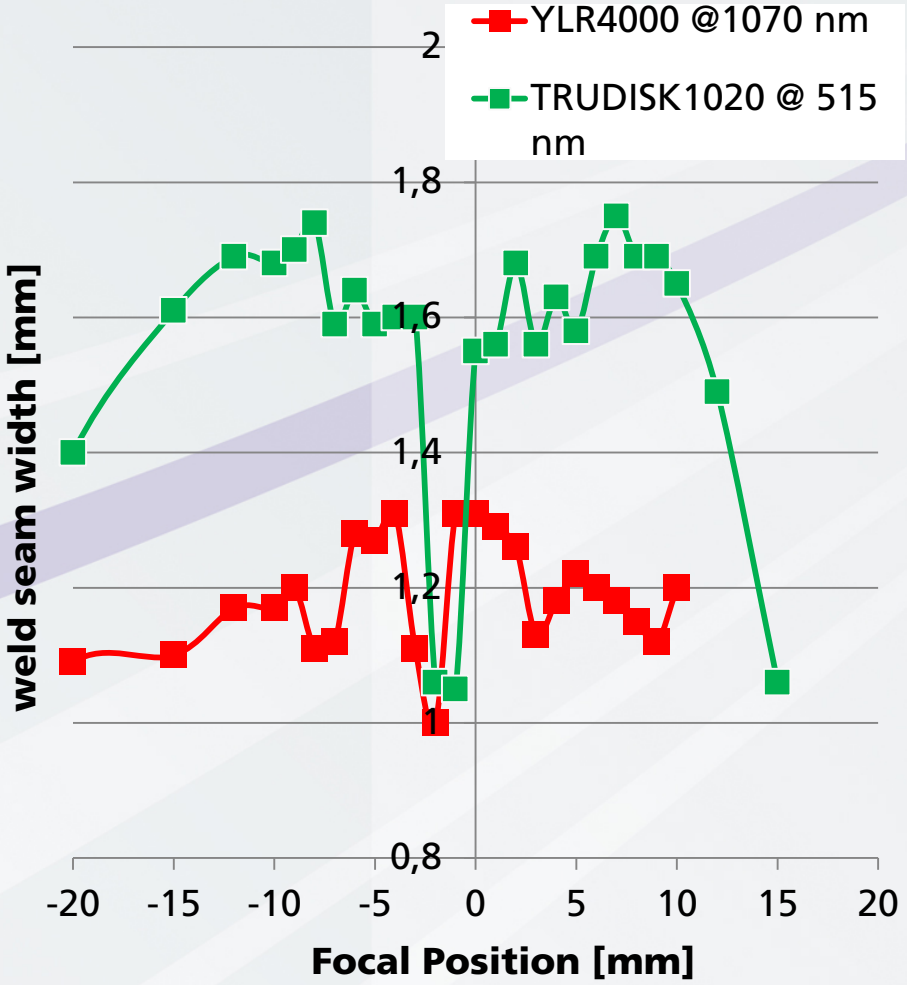

© Fraunhofer IWS

Laser beam welding of high reflective materials

Experimental results on stainless steel

2) Seam width and shape

- Outside focus in region with lower intensity higher seam width for 515 nm
- Mushroom shaped seam at deep penetration mode for both laser

➢ **Better absorption and less reflection of laser radiation at border area of laser beam @ 515 nm**

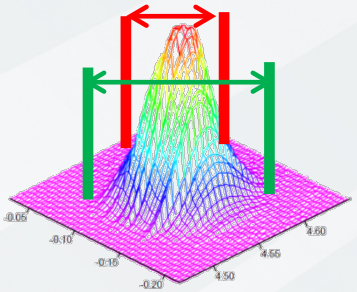

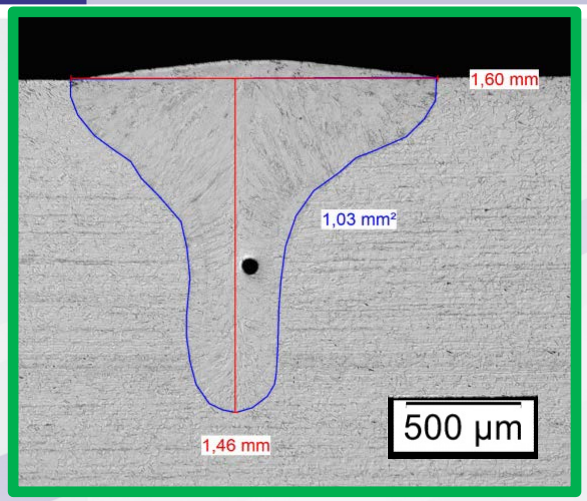

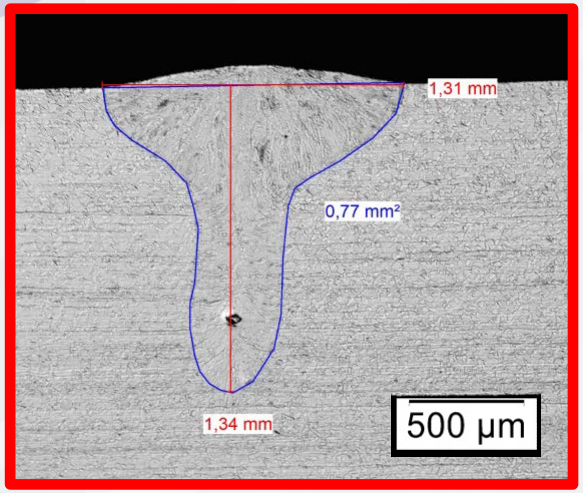

$\varnothing_{\text{spot size, surface}}$ ~300 µm

© Fraunhofer IWS

Comparison – Molten area per line energy

(parameter set with maximum penetration)

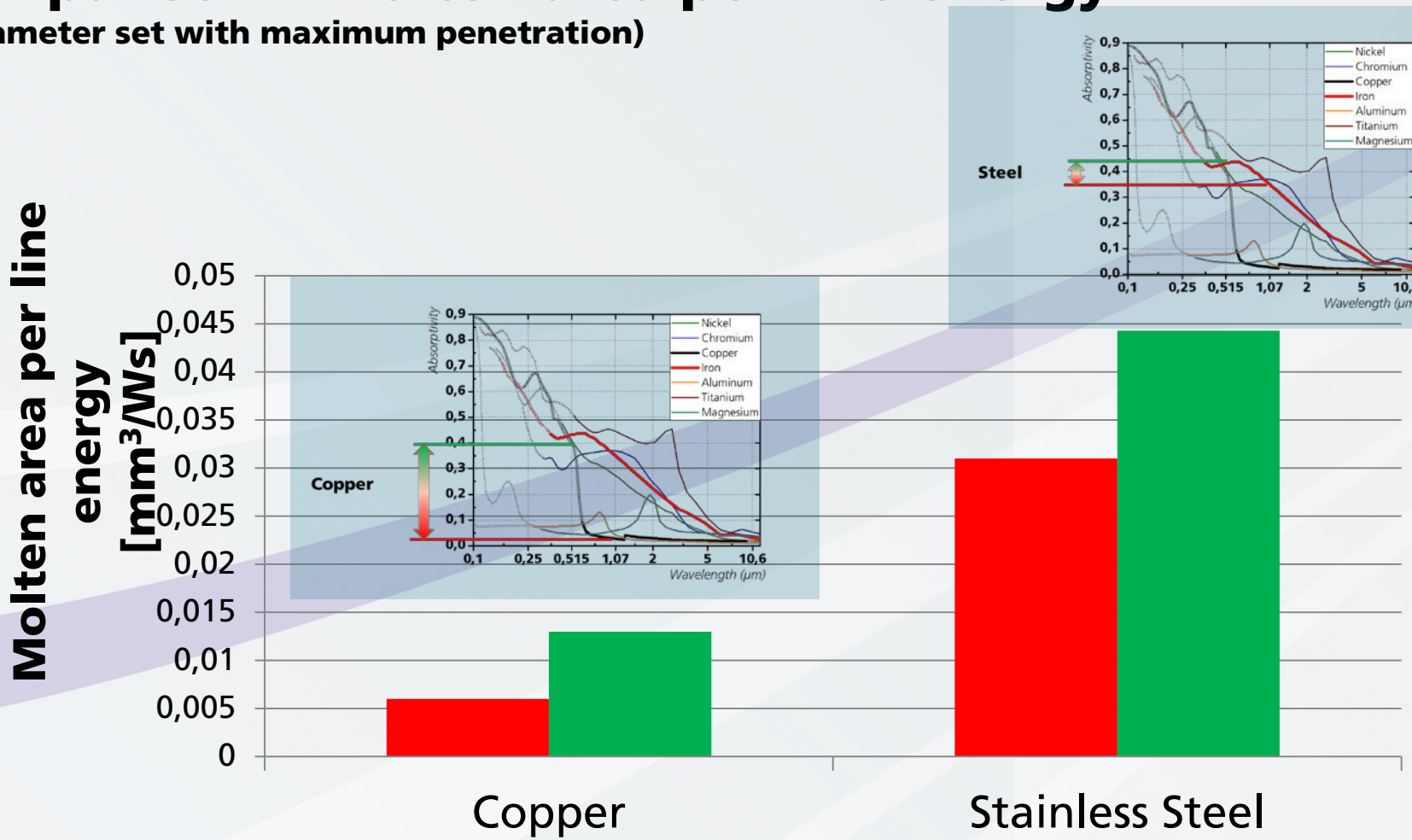

© Fraunhofer IWS

Examples for LBW copper with 1kW cw-laser @ 515 nm

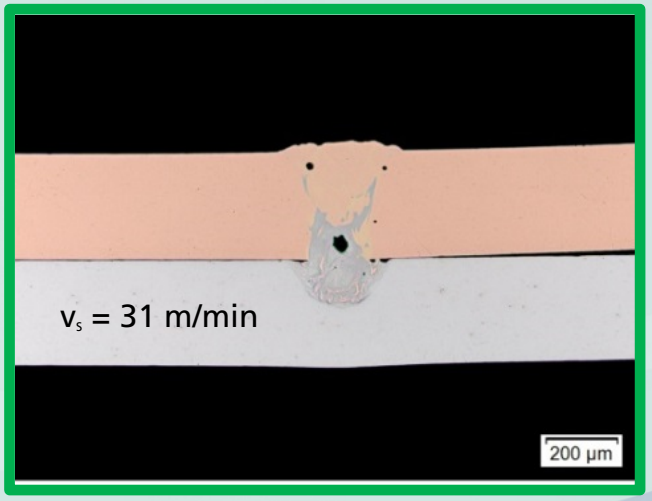

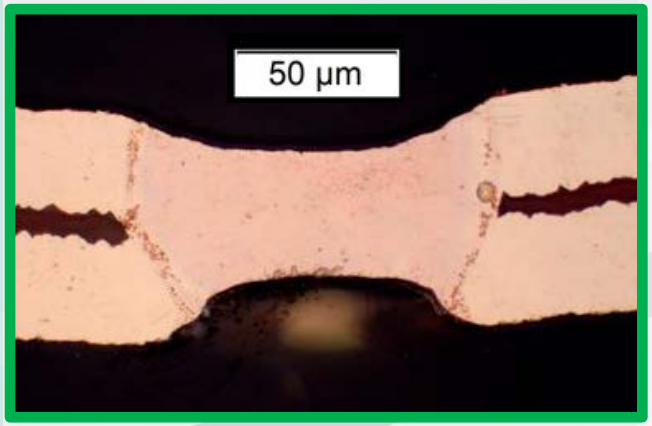

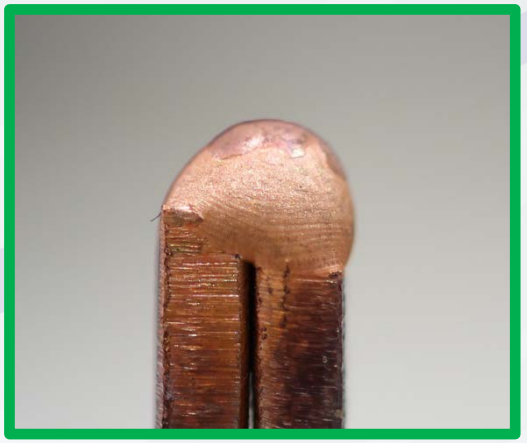

Battery contacts

- Copper as cover sheet possible
- Significant wider contact area compared to IR with Al as cover sheet

Foils

- Copper to copper

Contacts

- High current contacts like 2x4 mm² with less spatter

© Fraunhofer IWS

Laser beam welding of battery cell contacts

Case 1: Aluminum to copper in overlap (0.3 mm / 0.3 mm)

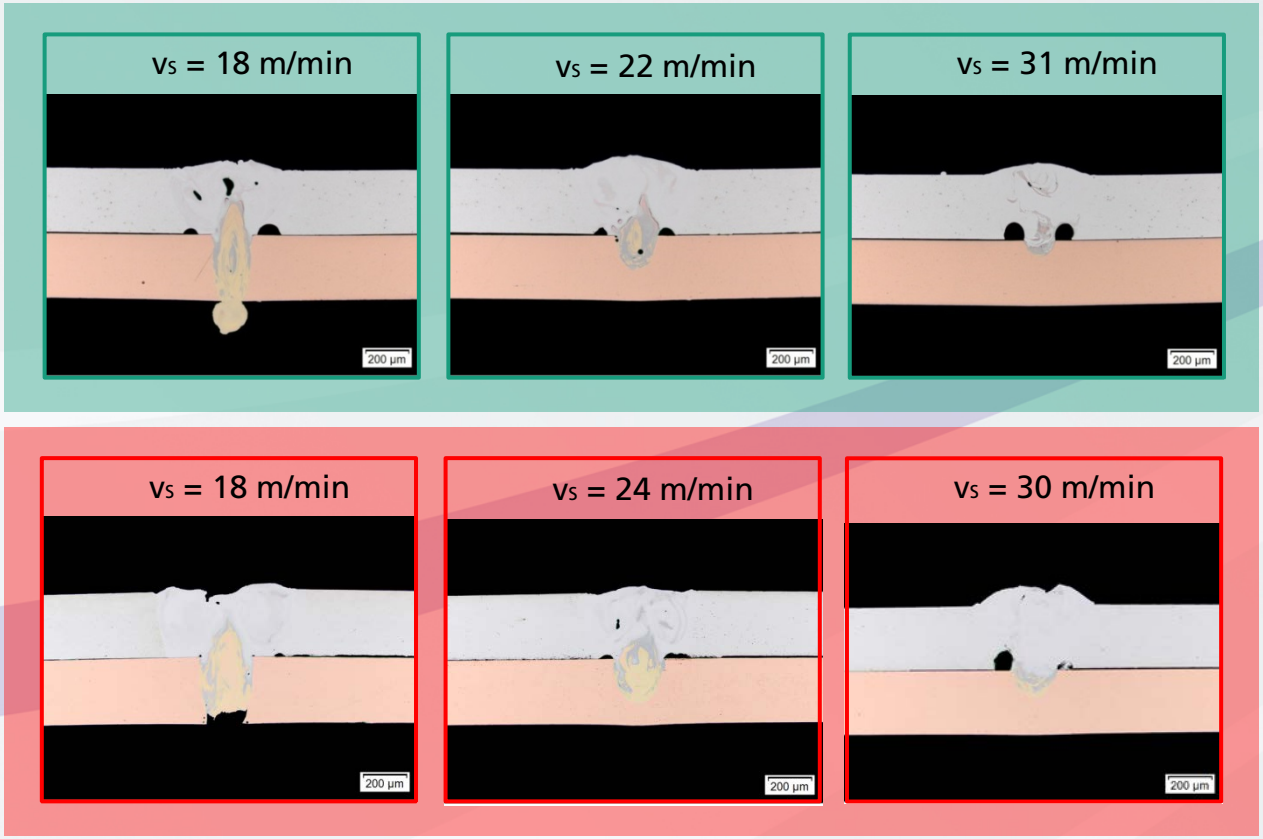

- For common used configuration Al to Cu no significant influence of wave length to welding behavior
- For nearly all parameter sets pores in overlap occurred

© Fraunhofer IWS

Laser beam welding of battery cell contacts

Case 2: Copper to Aluminum in overlap (0.3 mm / 0.3 mm)

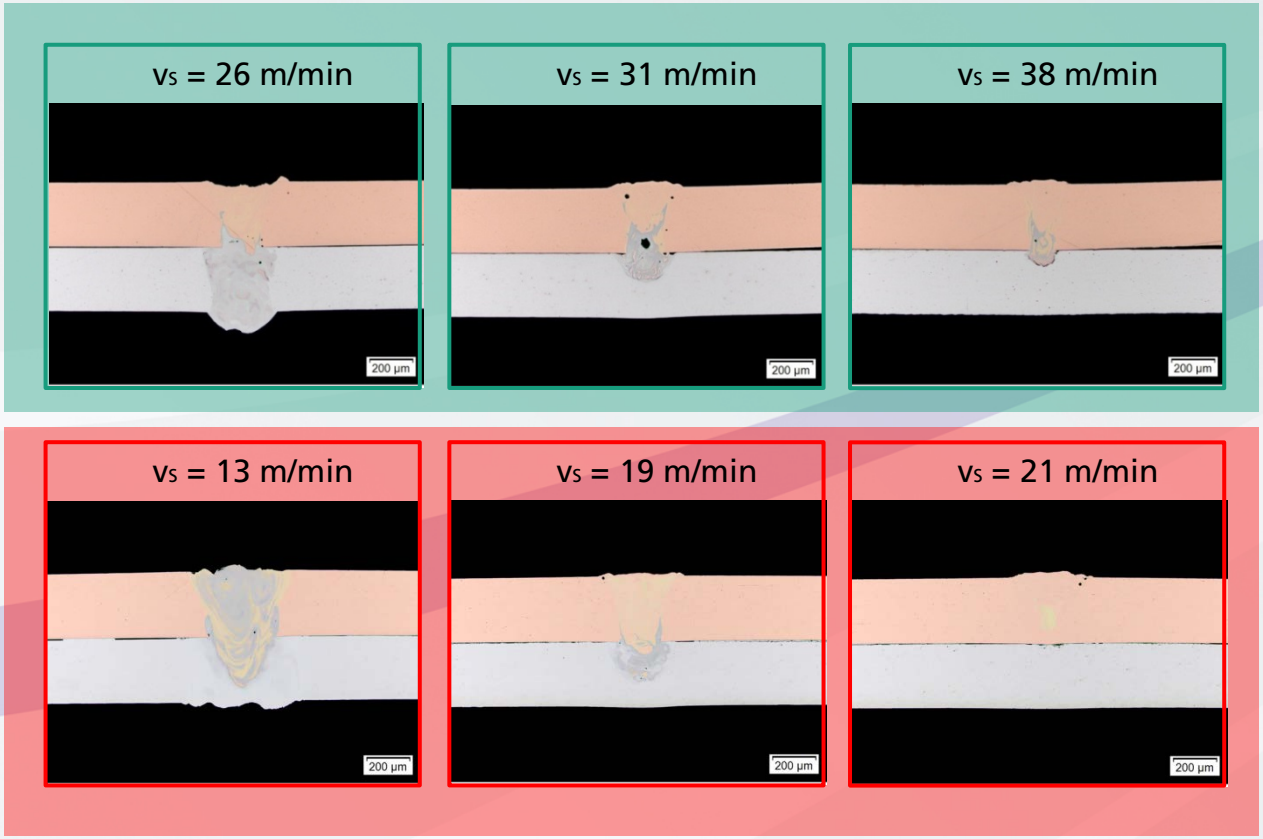

- For configuration Cu to Al significant higher welding speed with 515nm wave length
- Nearly no porosity for all parameters in overlap
- Better weld quality leads to higher shear strength for configuration Cu to Al compared to Al to Cu

© Fraunhofer IWS

Laser beam welding of battery cell contacts

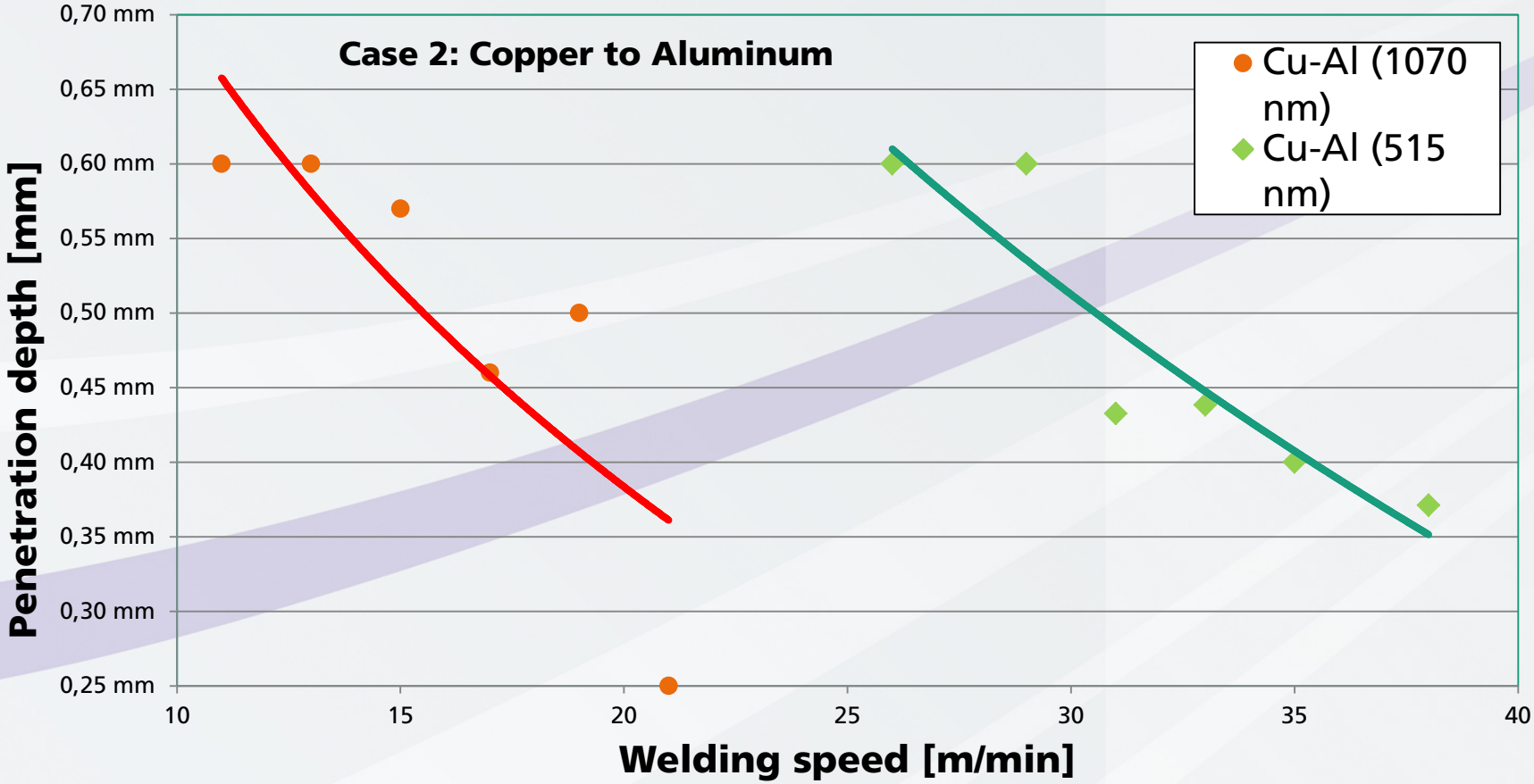

© Fraunhofer IWS

Laser beam welding of battery cell contacts

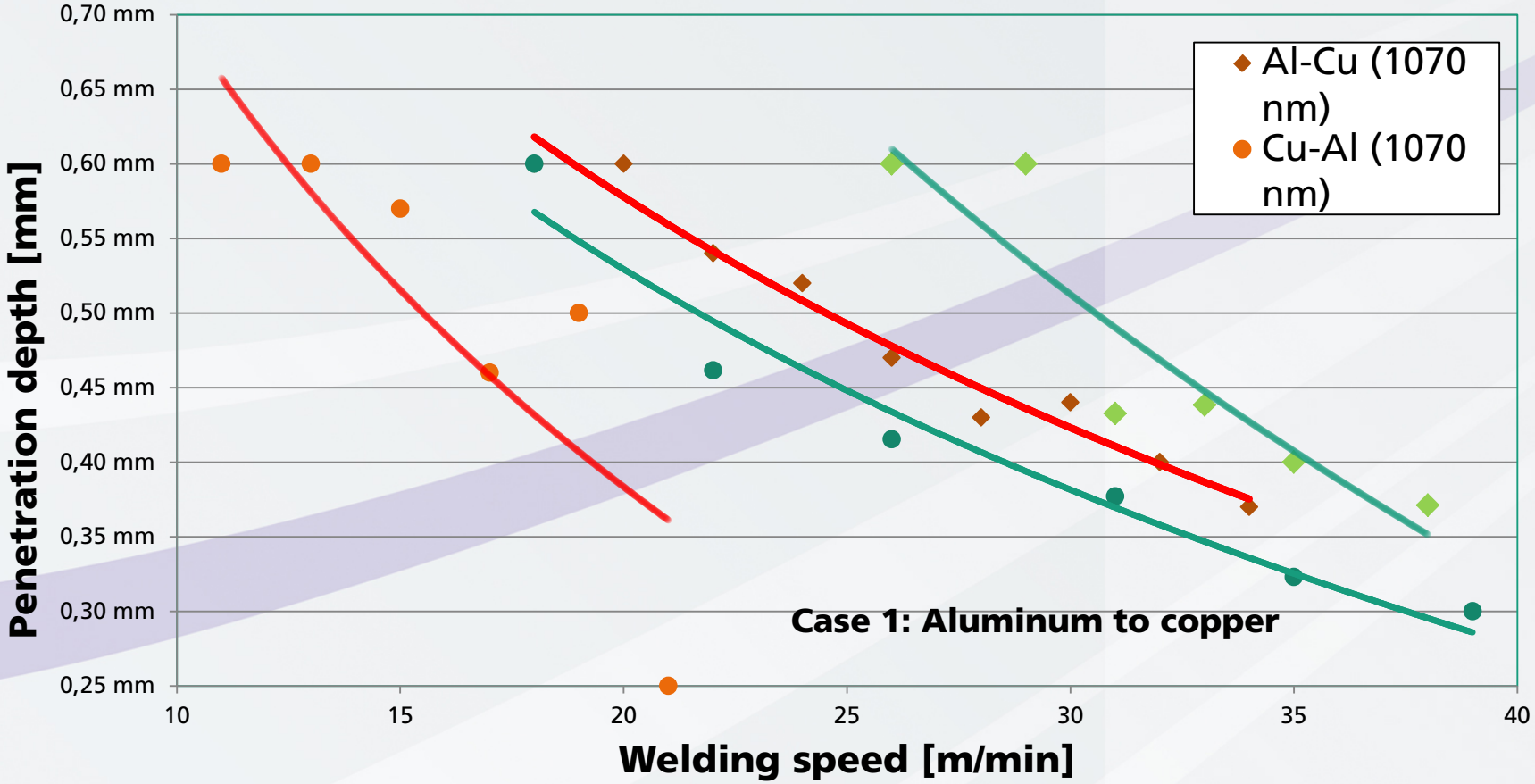

© Fraunhofer IWS

Summary and Conclusions

- Laser with wave length of 515 nm shows better absorption behavior at copper and stainless steel compared to IR laser
- Stable laser welding processes of copper with 515 nm at low power level (200...1000 W)
- Further advantages with respect of process efficiency for 515 nm particularly for heat conduction welding mode expected
  - Laser beam brazing
  - "powder" processes like cladding and additive manufacturing
- Future shows diode laser concepts in blue

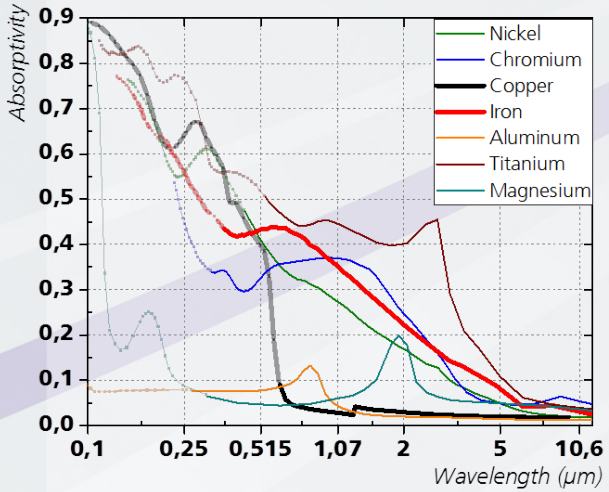

© Fraunhofer IWS

Content

Content	Chapter
Introduction	
The Fraunhofer Gesellschaft	01
Fraunhofer Institute for Material and Beam Technology IWS	02
Seminar topics	03
Laser Beam Welding	
Basics	04
Laser multi pass welding	05
Laser beam welding with high frequent beam oscillation	06
Laser beam welding of high reflective materials	07
Laser beam welding of powertrain components	08
Laser induction roll plating	09
Special Joining Technologies	
Magnetic pulse joining	10
Friction stir welding	11
Joining with reactive multi layers	12
Bonding and Composite technology	
Electrical-conductive bonding	13
Thermal direct joining of thermoplastic to metal	14
Mechanical Joining	
Enhanced mechanical connection by laser interference patterning	15

© Fraunhofer IWS

Novel developments for laser beam welding of power train components

© Fraunhofer IWS

Market situation of power train components

- Rising number and complexity of drive components:
  - Transmissions (7 … 10 - speed)
  - E-mobility components and hybrid modules
  - Differential gears and axles
- Increasing torque moments
- Decreasing dimensions / weight

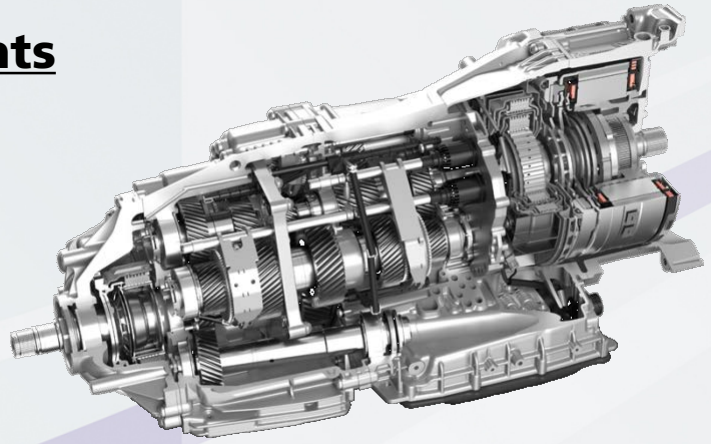

8-speed-automatic transmission [ZF]

Differential gear [Pagenstecher]

Challenges of laser beam welding

- **Increasing weld seam load**
- **Difficult to weld material combinations**

© Fraunhofer IWS

Development of laser beam welding in power train sector

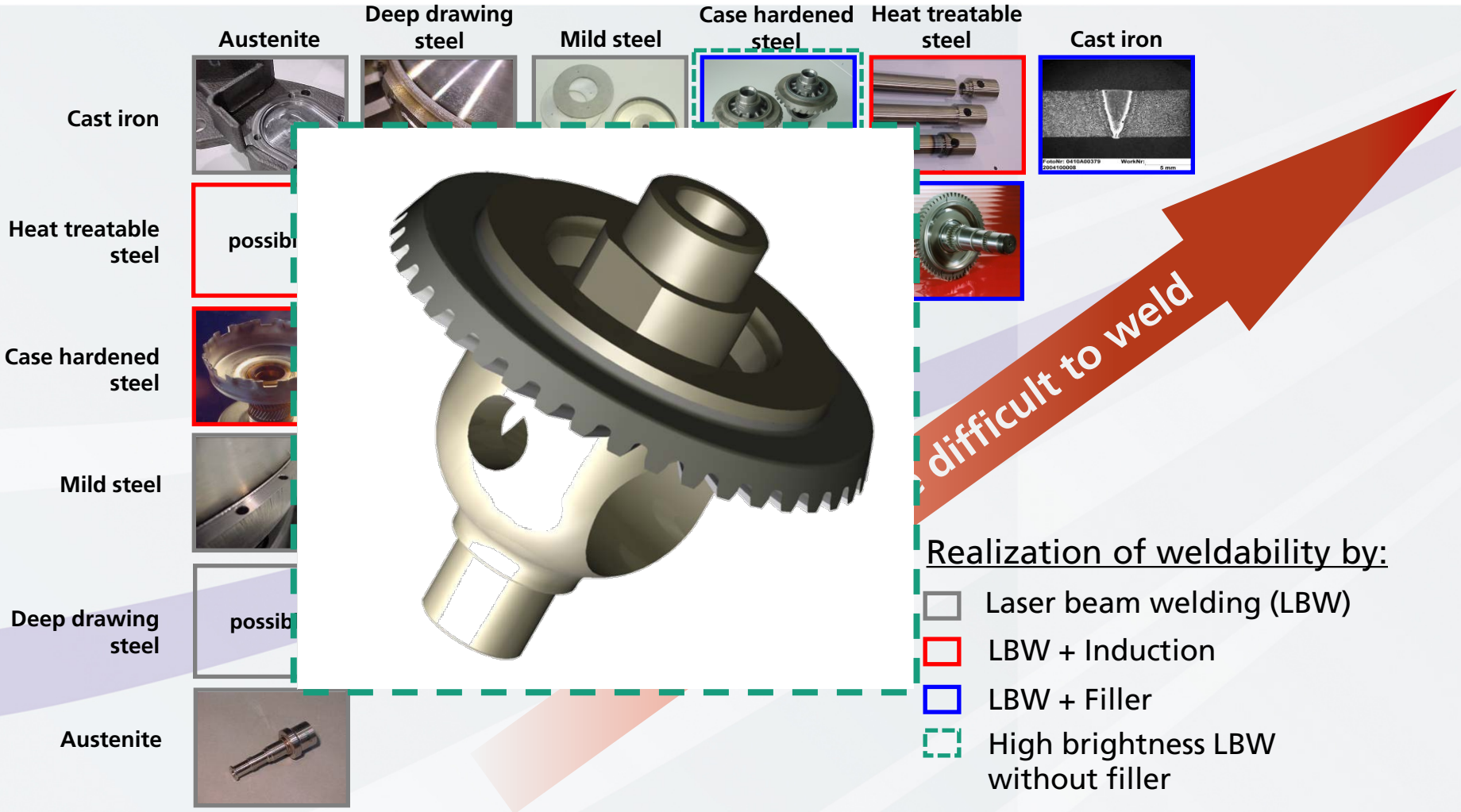

© Fraunhofer IWS

Example: Differential gear welding

Welding task

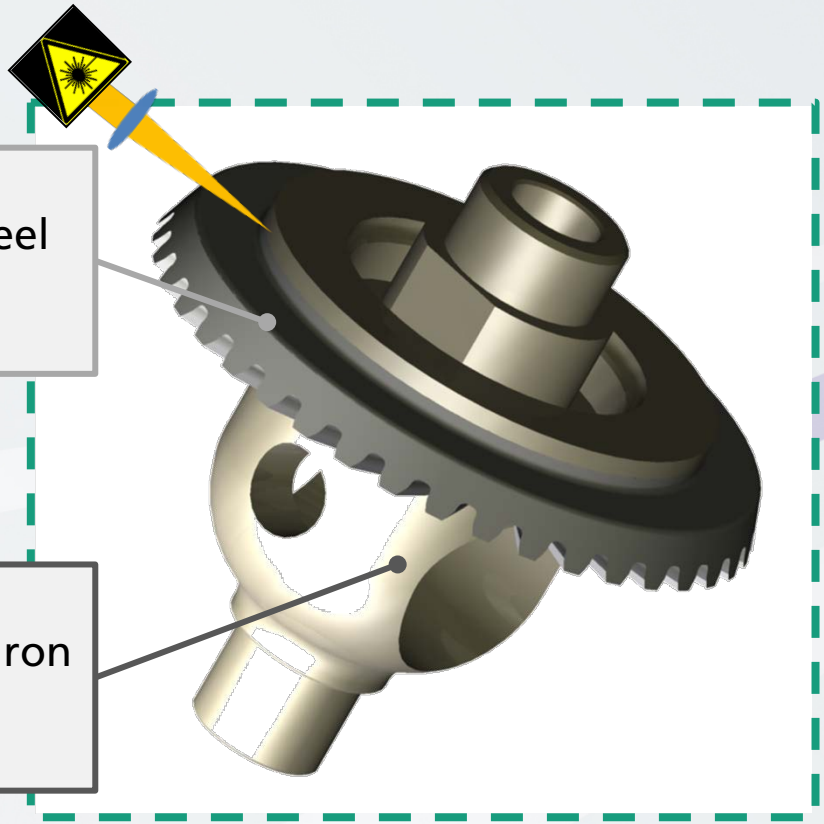

Crown wheel:
Case hardened steel
e.g. 16MnCr5
(0,16 % C)

Housing:
Ductile cast iron
e.g. GJS600
(ca. 3,5 % C)

Weldability:

Very high C-content

Extremely high seam hardening (martensite, ledeburite)

- **Cold crack risk**

Solution:

- **Ductile weld metal**
- **Minimization of brittle ledeburite formation in HAZ of cast iron**

© Fraunhofer IWS

Differential gear welding – development of welding process

Welding time ▼ / seam width ▼ / material degradation ▼

v_s = 1,5 m/min

CO_2-Laser + filler wire

Ind. production (GER) since 1999

v_s = 2,0 m/min

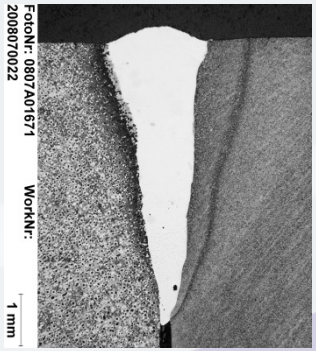

CO_2-Laser + filler foil

Ind. production (GER) since 2003

v_s = 3,0 m/min

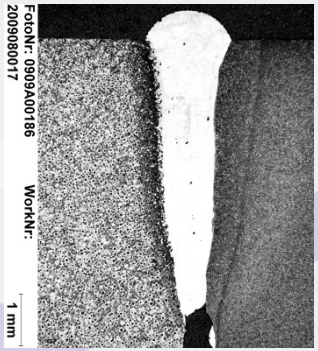

CO_2-Laser without wire

Laboratory since 2009

v_s = 4,5 m/min

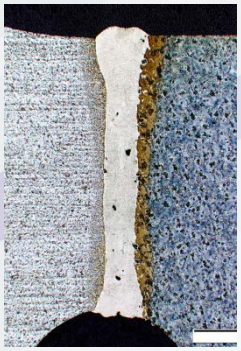

Disc Laser without wire

Ind. production (GER) since 2010

v_s > 4,5 m/min

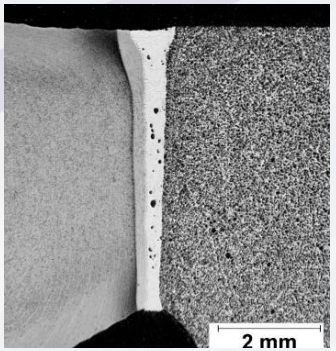

Fiber Laser without wire

Laboratory since 2006

Process window ▼ / requirements for positioning ▲

© Fraunhofer IWS

Differential gear welding – Comparison of welding processes

CO_2-laser + filler wire (Ni-base)		Disk laser without filler	
Source:	CO_2 Laser	Source:	Disk Laser
Spot diam.:	600 µm	Spot diam.:	200 µm
Power:	ca. 4 kW	Power:	ca. 4 kW
Speed:	1,5 m/min	Speed:	4,5 m/min
Time:	19 s (without tack weld)	Time:	6 s (no tack welding)
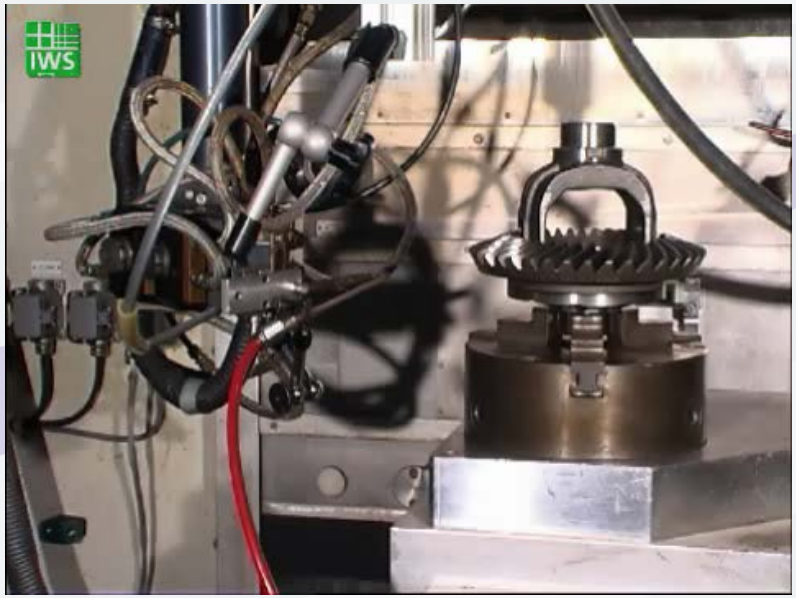		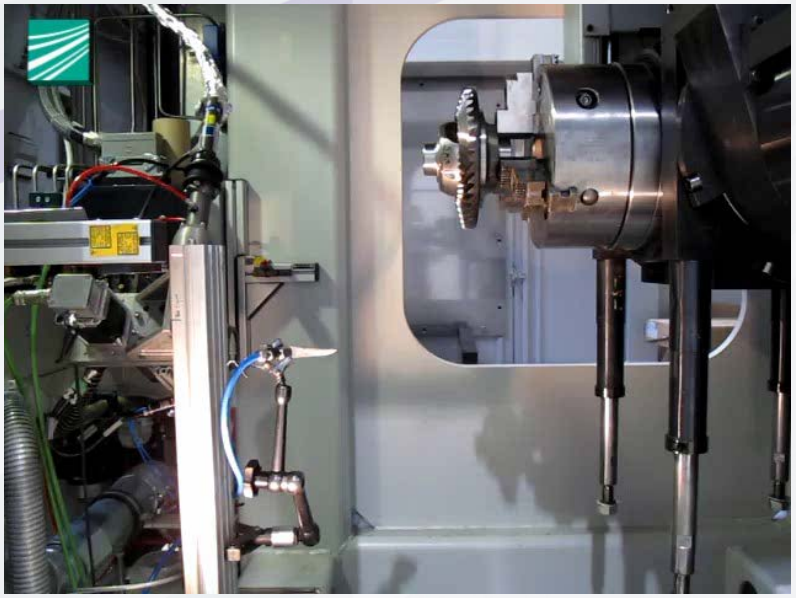	

© Fraunhofer IWS

Differential gear welding – Comparison of welding processes

CO_2-laser + filler wire (Ni-base)

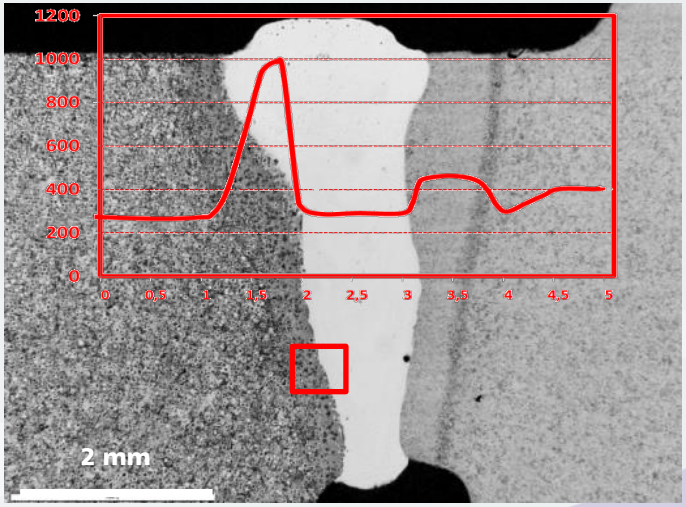

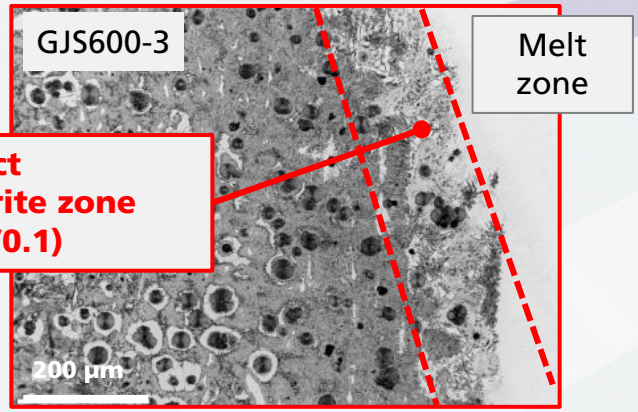

Disk laser without filler

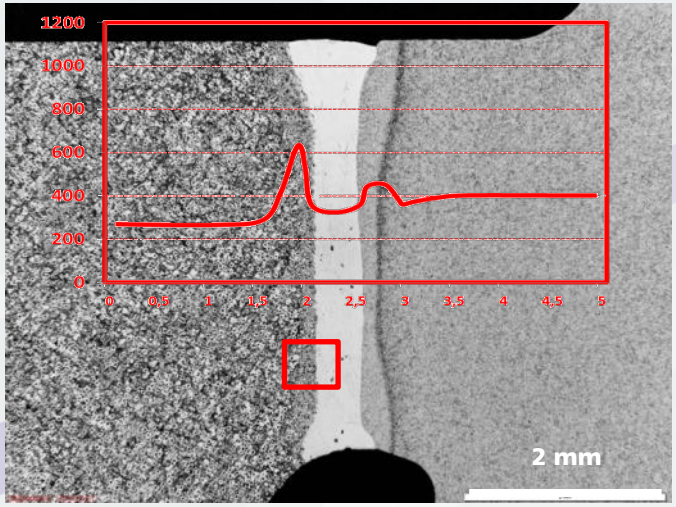

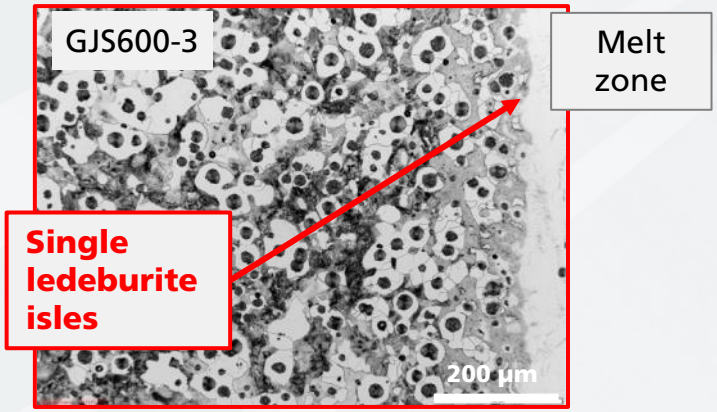

© Fraunhofer IWS

Differential gear welding – welding without filler wire

16MnCr5
(0,16 % C)

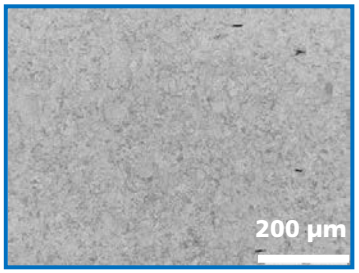

Weld metal
(1,8 % C)

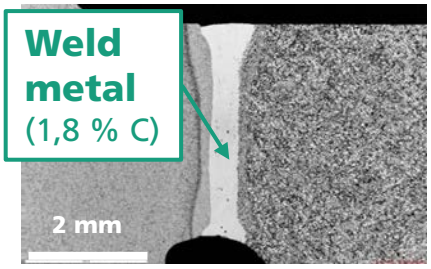

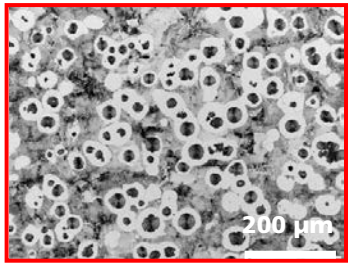

GJS600
(3,5 % C)

Good weldability.

Good weldability.
Ductile retained austenite

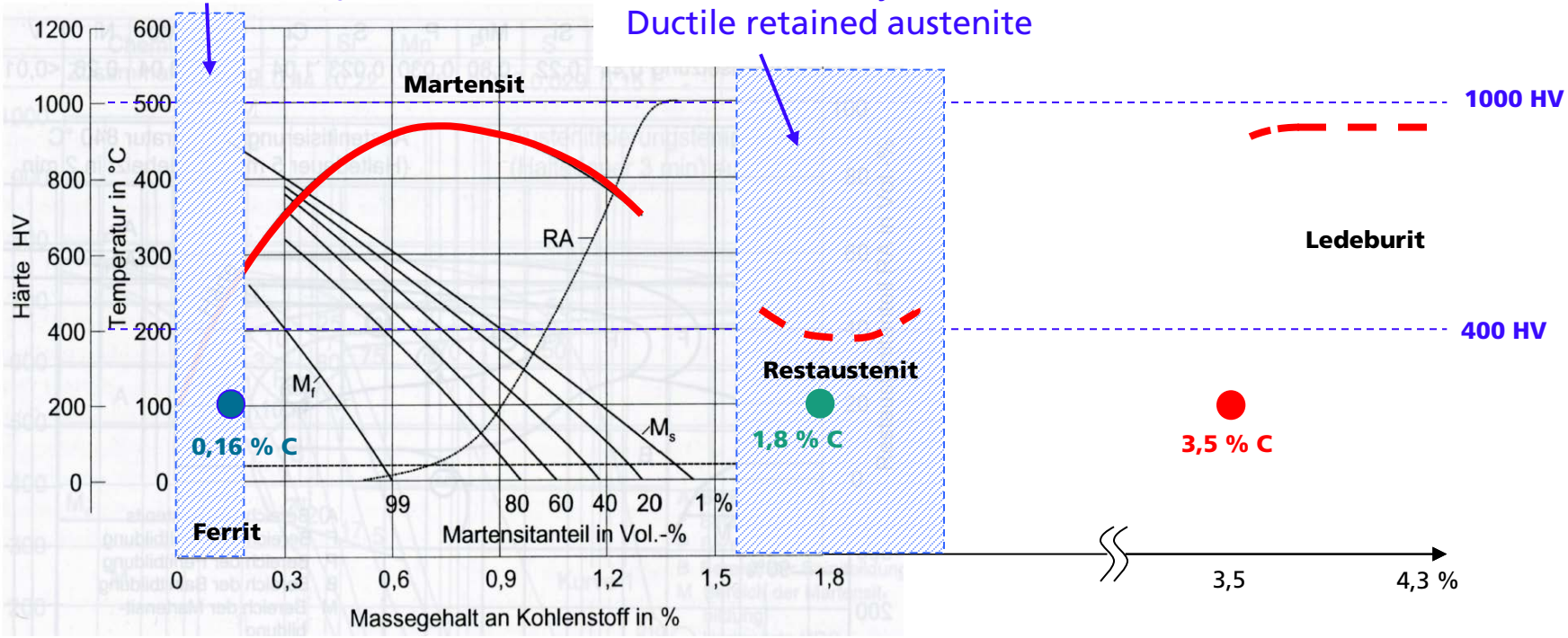

© Fraunhofer IWS

Differential gear welding – Comparison of welding processes

Advantages of laser welding without filler

Increase of welding process efficiency :

- No filler material
- Short welding time
- Low heat input

Microstructure and properties:

- Low HAZ width
- Nearly prevention of brittle ledeburite formation

Weld seam stresses:

- Reduced residual stresses
- Low distortion

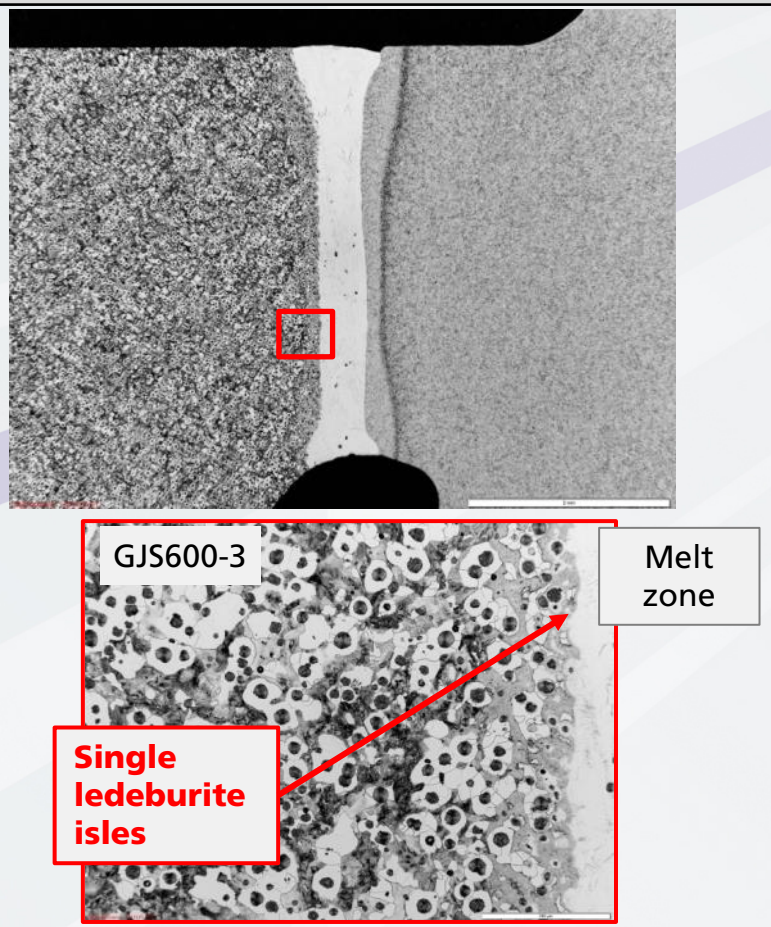

© Fraunhofer IWS

Proof of weld seam strength

FEM-simulation

Simplified test part

F_x, F_y, F_z

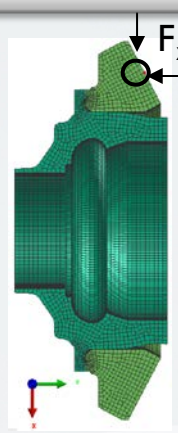

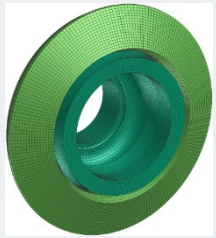

Adjustment of weld seam stress situation

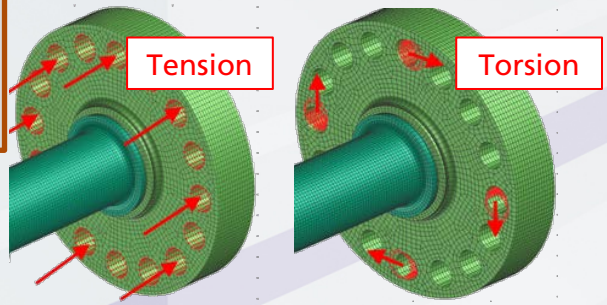

FEM-model

Test parts

Optimized component design

Component tests

Optimized component + welding process

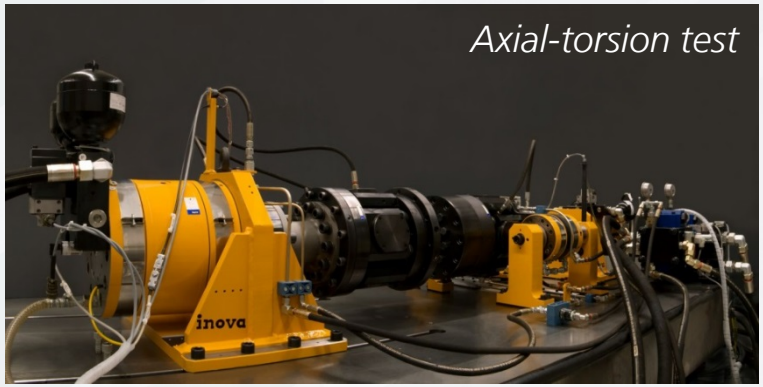

Axial-torsion test

© Fraunhofer IWS

Proof of weld seam strength

Component test under combined load:

- Cyclic torsion–axial test (M_t = ±8 kNm, F_{max} = ±40 kN, f_{max}= 50 Hz), free variation of load values
- ➢ Determination of S-N-Curves and fracture behavior
- ➢ Recalculation of weld seam strength

Torsion-axial test machine

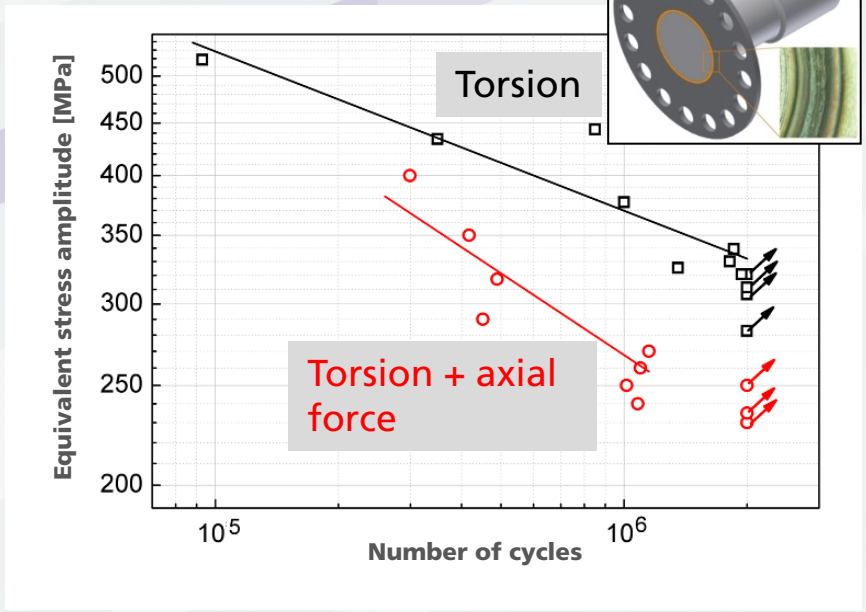

S-N curves of axial weld part

© Fraunhofer IWS

Conclusions

- Laser beam welding of power train components is commonly used in industrial production
- Welding with high brightness laser sources and without filler wire open new potential:
  - welding process efficiency increase
  - weld seam microstructure enhancement
  - weld seam stress condition improvement
- Real part weld seam strength can be determined by transformation of stress conditions to simplified component test

© Fraunhofer IWS

Content

Content	Chapter
Introduction	
The Fraunhofer Gesellschaft	01
Fraunhofer Institute for Material and Beam Technology IWS	02
Seminar topics	03
Laser Beam Welding	
Basics	04
Laser multi pass welding	05
Laser beam welding with high frequent beam oscillation	06
Laser beam welding of high reflective materials	07
Laser beam welding of powertrain components	08
Laser induction roll plating	09
Special Joining Technologies	
Magnetic pulse joining	10
Friction stir welding	11
Joining with reactive multi layers	12
Bonding and Composite technology	
Electrical-conductive bonding	13
Thermal direct joining of thermoplastic to metal	14
Mechanical Joining	
Enhanced mechanical connection by laser interference patterning	15

© Fraunhofer IWS

Laser induction roll plating / bonding

Topics

- **Motivation: Light weight design aspects**
- **Fabrication of bimetalic strips and –wires with the laser roll bonding process**
- **Aluminium to steel for automotive BIW components**
- **Aluminium to copper for electro mobility**

© Fraunhofer IWS

Weight saving potential by multi-material design

Example: Numerical study of generic front door (stiffness analysis)

Steel door (Reference)	**Approach A:** Outer panel: Aluminium	**Approach B:** Inner panel: Steel-Al Outer panel: Aluminium
Steel (all components) t = 1 mm	Aluminium (outer panel) t = 1 mm	Aluminium (outer panel) t = 1 mm
$m_{Door,Ref}$ = **16,59 kg**	$m_{Door,A}$ = **12,97 kg**	$m_{Door,B}$ = **8,81 kg**
ΔZ_{max} = **1,25 mm**	ΔZ_{max} = **1,25 mm**	ΔZ_{max} = **1,31 mm**

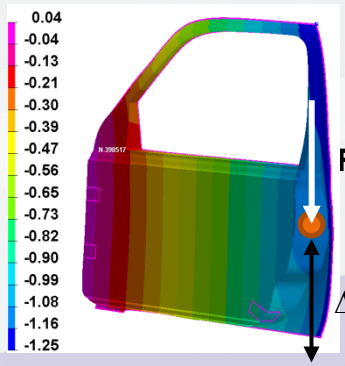

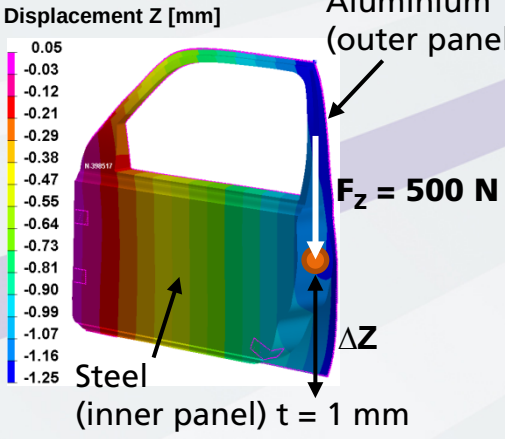

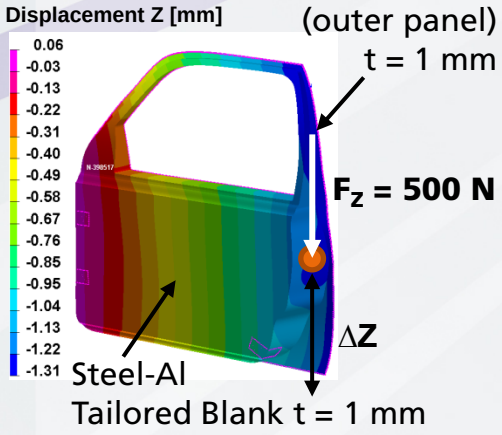

© Fraunhofer IWS

Weight saving potential by multi-material design

Example: Numerical study of generic front door (stiffness analysis)

How to get an Al-Steel-tailored welded blank?

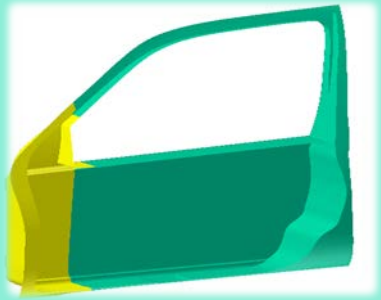

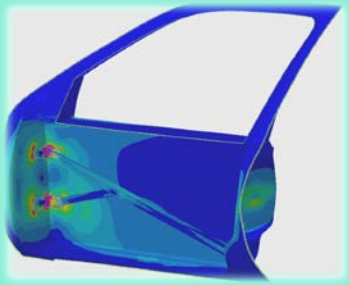

Approach B:
Inner panel: Steel-Al
Outer panel: Aluminium

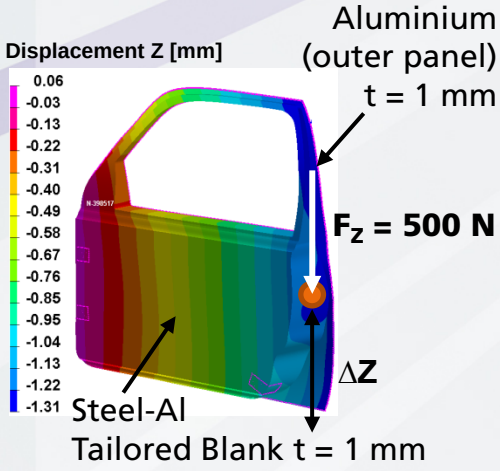

$m_{Door,B}$ = **8,81 kg**

ΔZ_{max} = **1,31 mm**

© Fraunhofer IWS

Al-Steel-tailored welded blank

Possible process chain

Laser induction roll plating

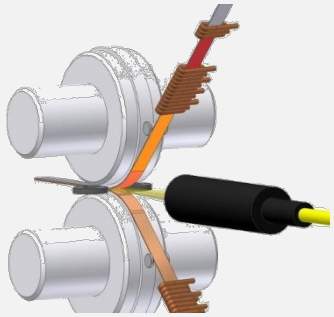

Bi-metal strip

Transition Joint

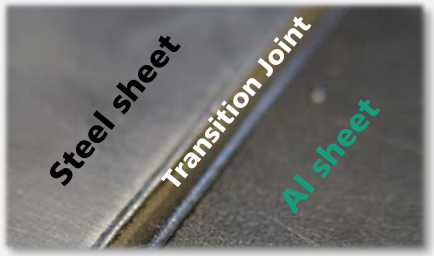

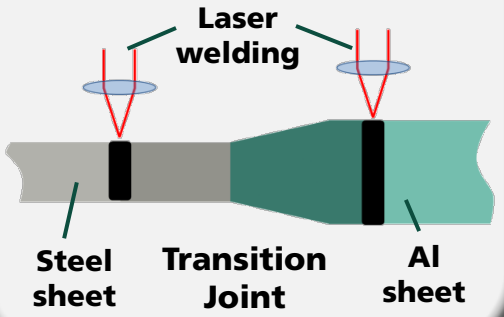

Hybrid parts

© Fraunhofer IWS

Fraunhofer IWS Dresden

Principle of laser roll bonding

Laser induction roll plating (LIRP)

- Efficient joining technique for not weldable material combinations
- Hot roll plating procedure (2 x induction + laser beam)
- Material adapted temperature control

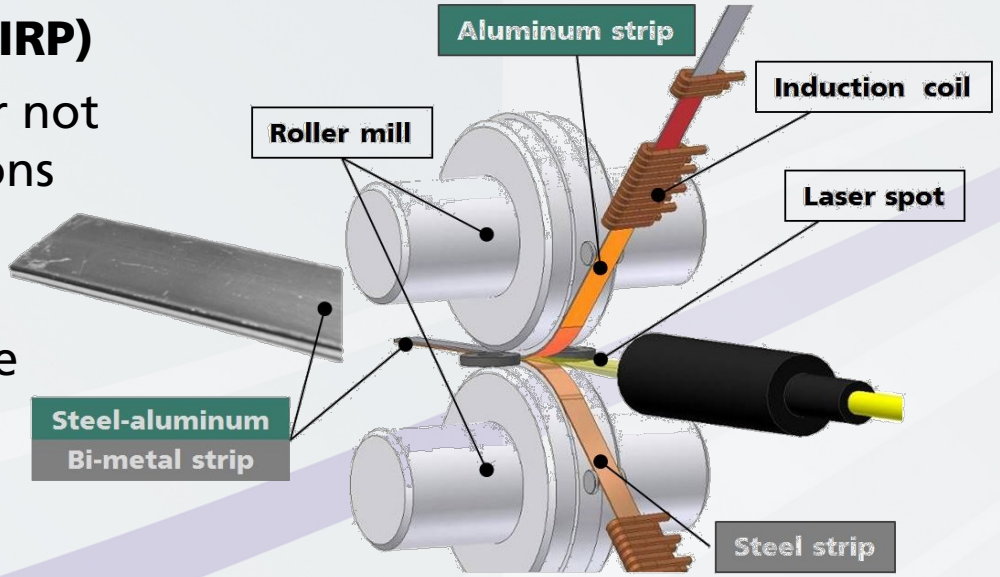

IWS patent
EP 2090395A2

Set-up for LIRP

Steel-aluminum bi-metal strip

- Control of intermetallic phase formation
- High strength
- Excellent formability

Twisted steel-aluminum strip

© Fraunhofer IWS

Fraunhofer IWS Dresden

Principle of laser roll bonding

→ Immediatly bevore the nip a laser heats both joining surfaces

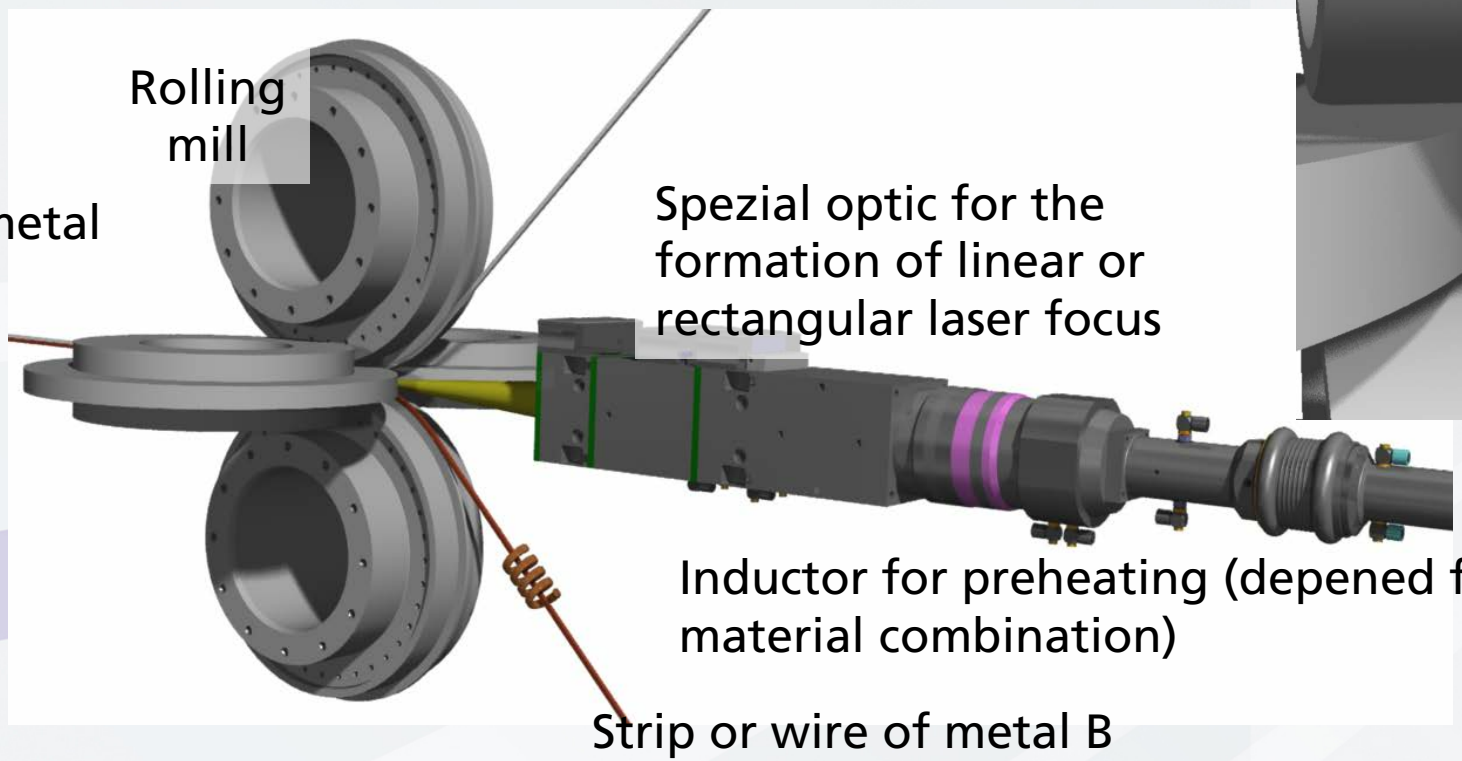

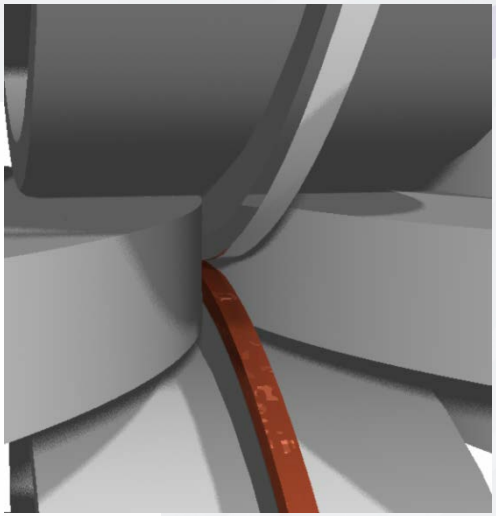

© Fraunhofer IWS

Fraunhofer IWS Dresden

Principle of laser roll bonding-system

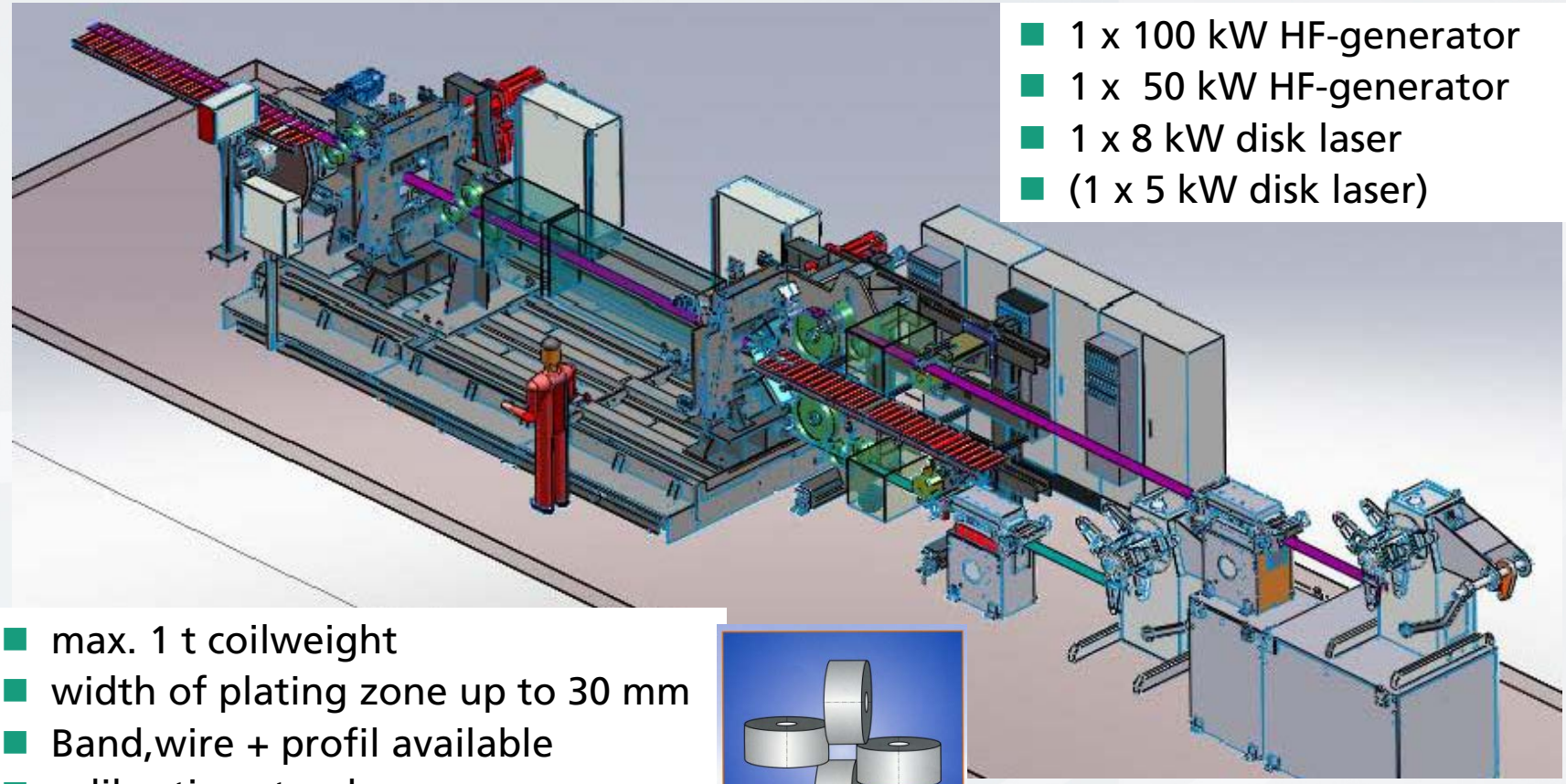

- 1 x 100 kW HF-generator
- 1 x 50 kW HF-generator
- 1 x 8 kW disk laser
- (1 x 5 kW disk laser)

- max. 1 t coilweight
- width of plating zone up to 30 mm
- Band,wire + profil available
- calibration stand

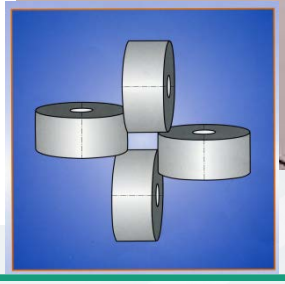

© Fraunhofer IWS

Fraunhofer IWS Dresden

Principle of laser roll bonding (animation)

© Fraunhofer IWS

Forms of laser roll bonded bimetals

Laser roll bonding

Homogene 100% overlap band platings

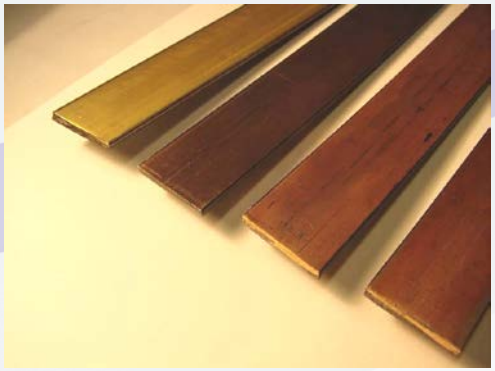

Partial overlap band platings

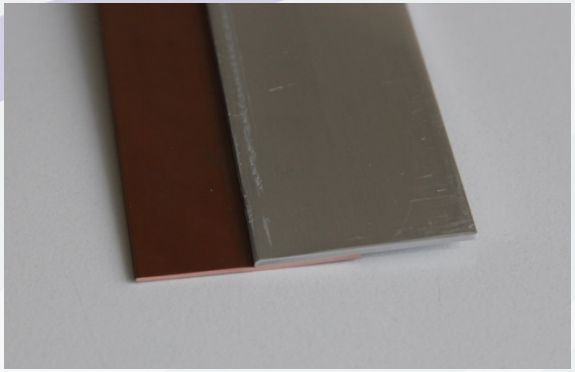

Homogene wire-like platings

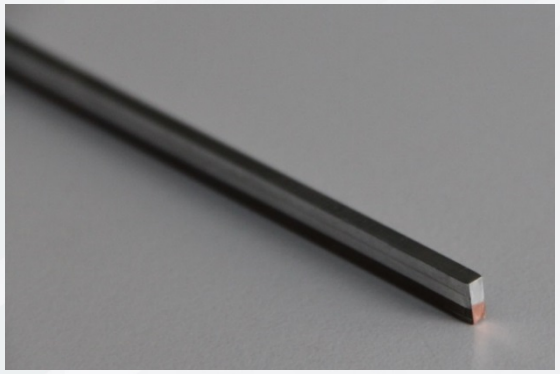

© Fraunhofer IWS

Processing of laser roll bonded bimetals

Good cold formability for calibrating

Swiveled by 90° to the rolling plane and rerolled to the final contour

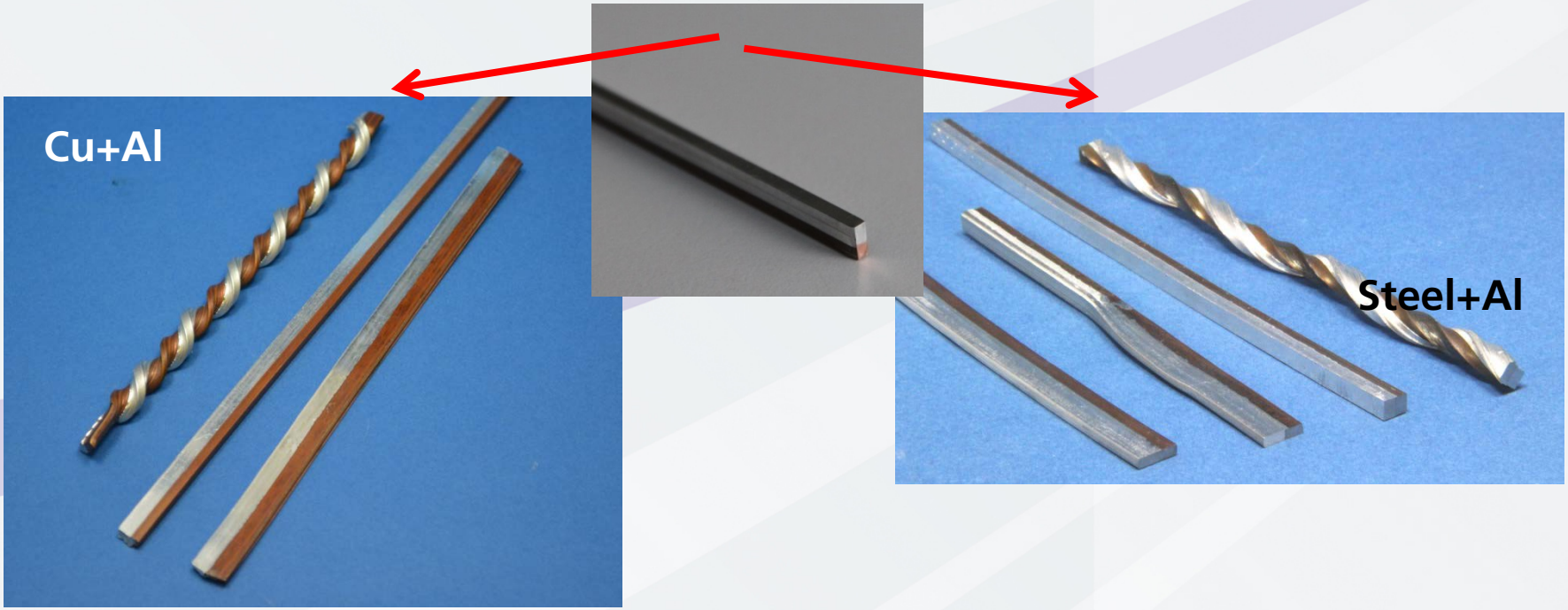

© Fraunhofer IWS

Combination AlMg3 - DT-S2CrMo1

Hardness characteristic

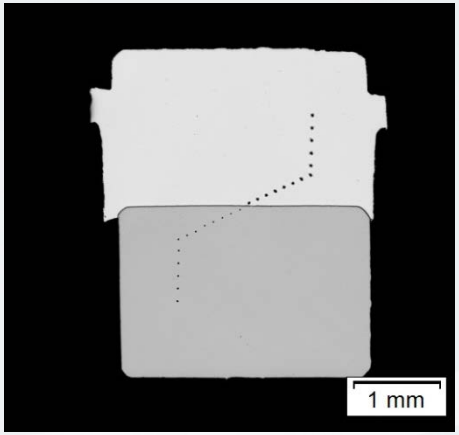

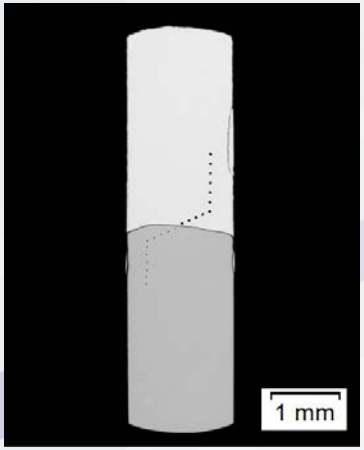

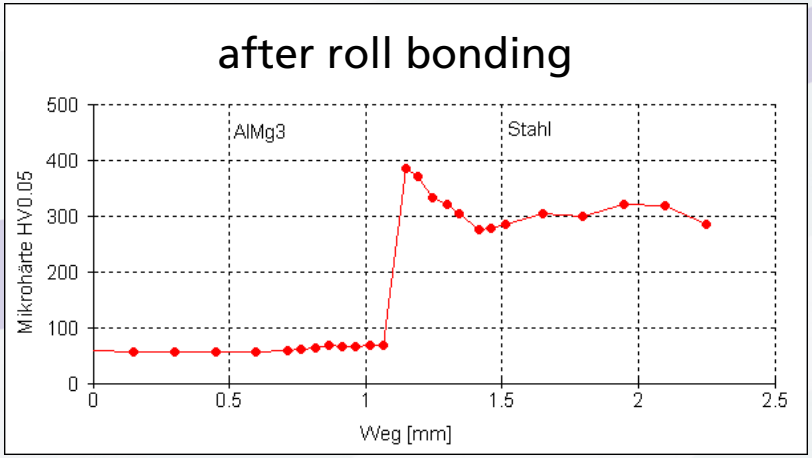

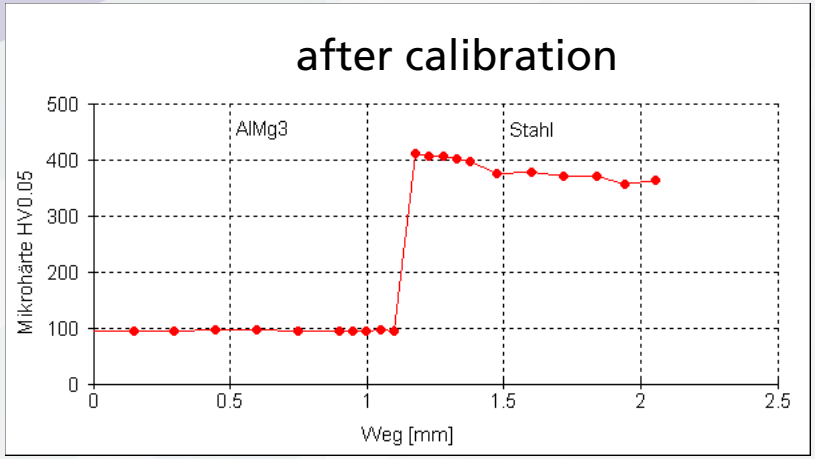

© Fraunhofer IWS

Fraunhofer IWS Dresden

Particularities of joining zones

Steel/AlSi12

Joining zone without macroscopic brittle intermetallic phases (< 3 µm)

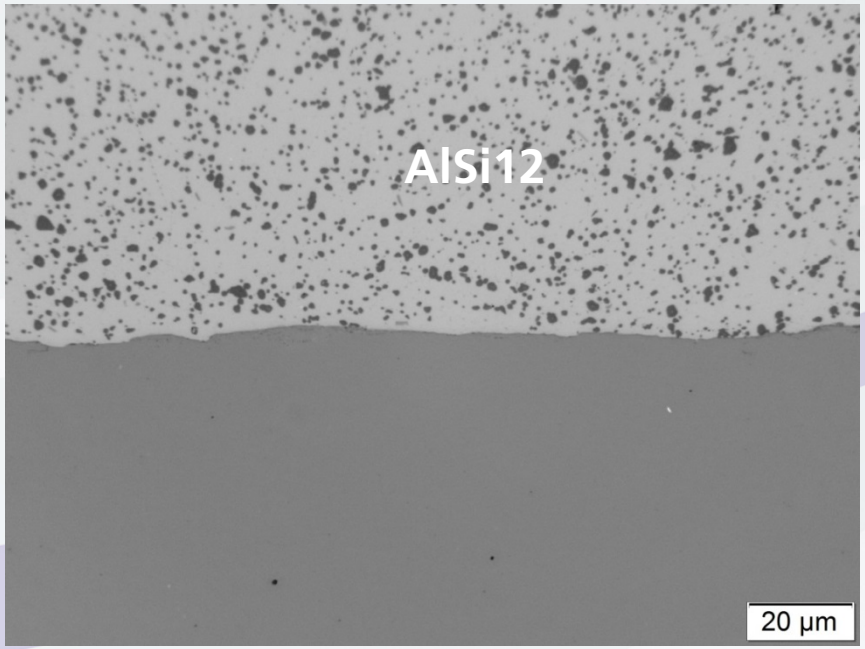

AlSi12- DT-S2CrMo1 (unetched), Joining zone without (visible) intermetallic phases hem

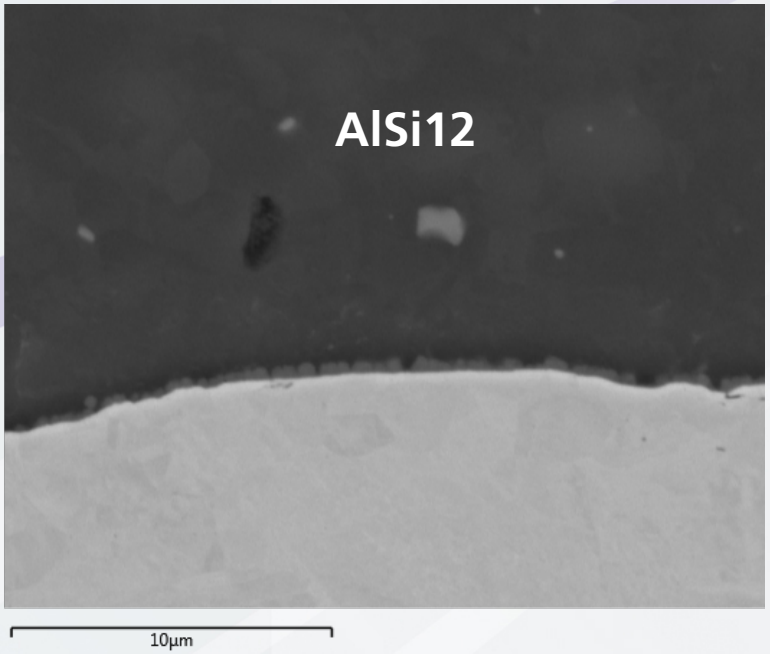

TEM-micrograph, with partial intermetallic phases hem

© Fraunhofer IWS

Fraunhofer IWS Dresden

Al-Steel-tailored welded blank

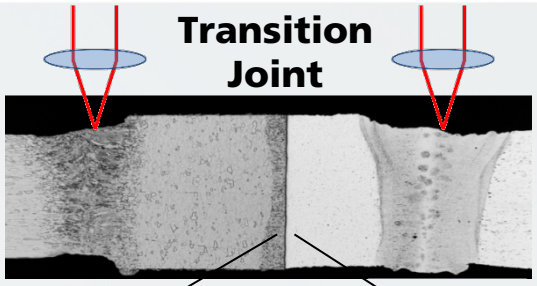

SEM of transition zone

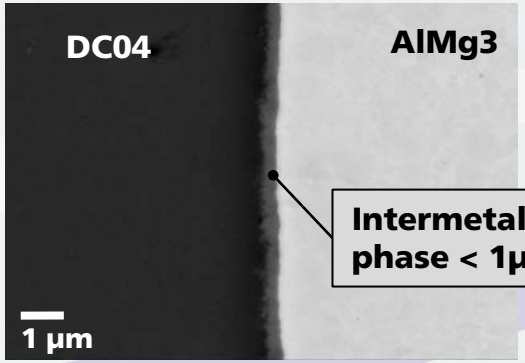

Laser welded hybrid tailored blank

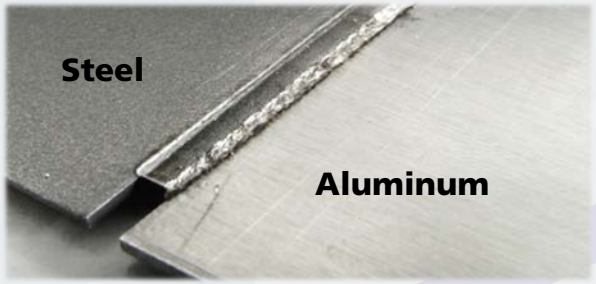

Transversal tensile test

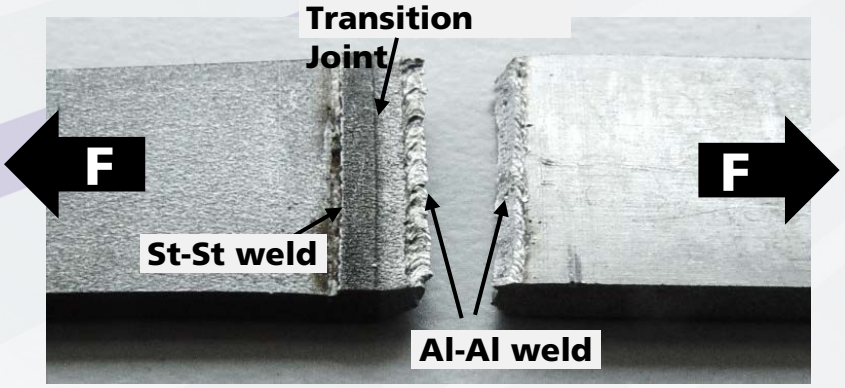

Joint characterization

- Uncritical thin intermetallic zone < 1µm
- No influence of welding heat or cataphoretic coating (tempering 180°C/30min)

⇨ Transition Joint with good formability!

© Fraunhofer IWS

Al-Steel-tailored welded blank

Deep drawing

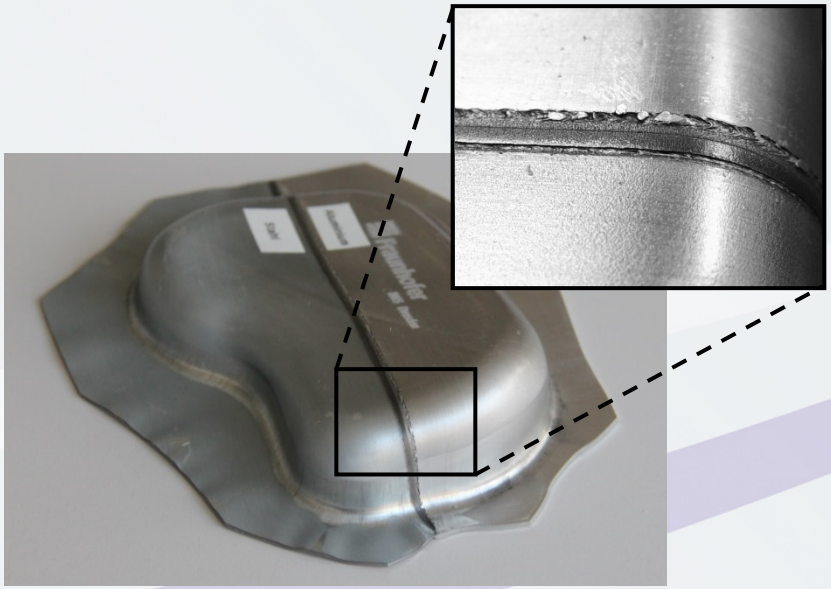

Die bending

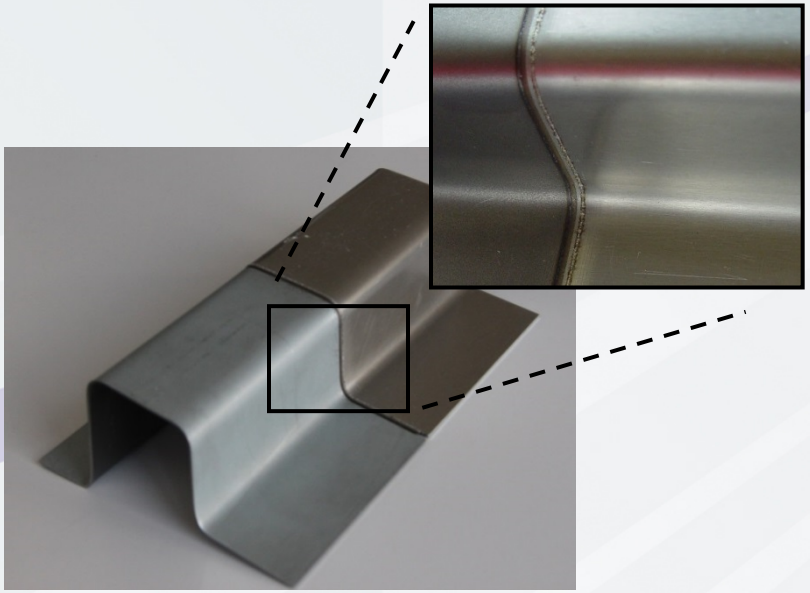

- No joining zone failure occurred
- Steel aluminum hybrid blanks now readily formable!

⇨ **Alternative solution for hybrid BIW components!**

[1] Cooperation with Fraunhofer IWU

© Fraunhofer IWS

Al-Steel-tailored welded blank

Corrosion behavior

Challenge

- Contact corrosion or bimetal corrosion at aluminum to steel joints

Conditions for contact corrosion in general

1) Two metals with different electro-chemical potential (in practice >100mV difference)
2) Electrical connection between both metals
3) Both surface wetted with the same electrolyte

Relevant electrochemical potentials for Zinc-coated steel with aluminum

Iron	(Fe)Fe^{2+}+ 2 e^-⇌ Fe	–0,41 V
	Fe3+ + e– ⇌ Fe2+	+0,77 V
Aluminium	(Al)Al^{3+}+ 3 e^-⇌ Al	–1,66 V
Zinc	(Zn)Zn^{2+}+ 2 e^-⇌ Zn	–0,76 V

Δ 1,25..2,43 mV

Δ 0,9 mV

heat protection shield (Al) with steel screw

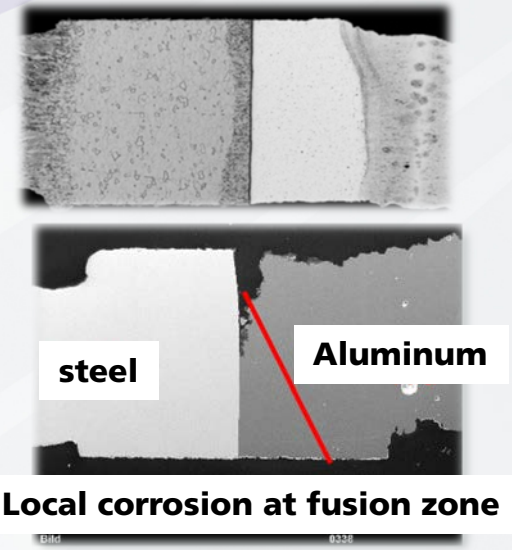

Local corrosion at fusion zone

© Fraunhofer IWS

Fraunhofer IWS Dresden

Al-Steel-tailored welded blank

Experimental setup

Test conditions and material

- Salt spray test according DIN EN ISO 9227
  - Steel HX380LAD+Z100MBO, 0,8 mm
  - Aluminum ECODAL608, 1,0 mm
  - Transition joint DC04/AlMg1

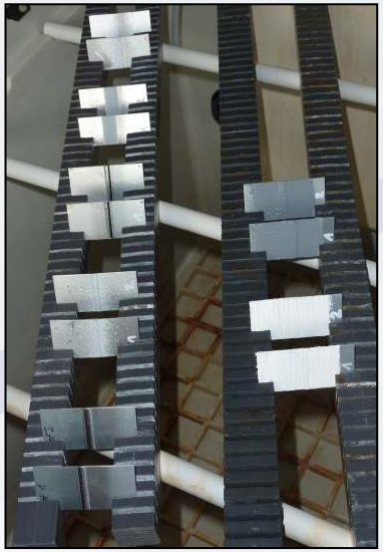

Local coating and protection

- Metallic coating with reduced electrochemical potential
  - wire arc spraying with aluminum and zinc
- Organic non-conductive coating
  - Polymere corrosion protective coating
  - PE band application

© Fraunhofer IWS

Al-Steel-tailored welded blank

Corrosion behavior
First results

Metallic coating with reduced electrochemical potential

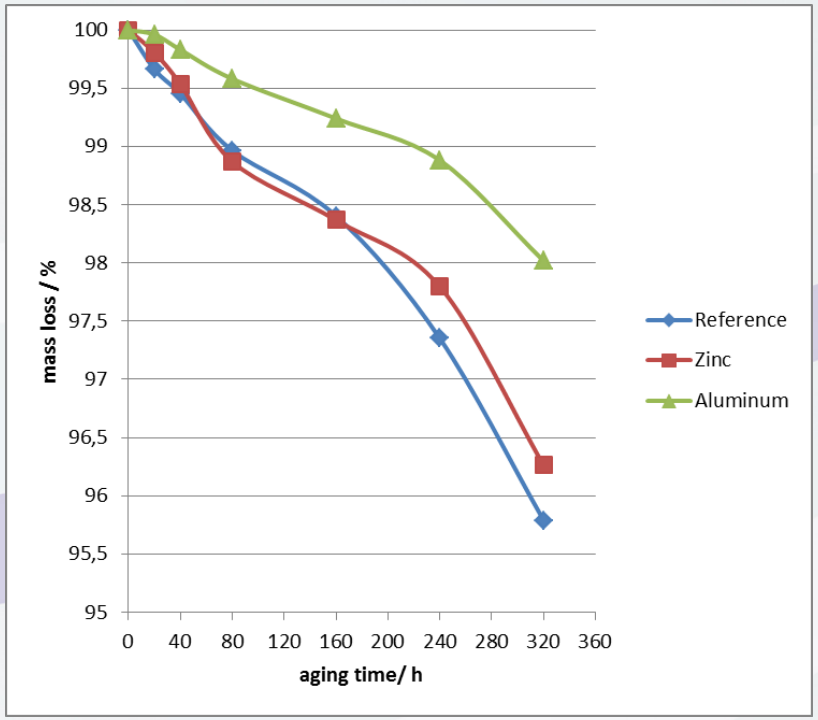

Organic non-conductive coating

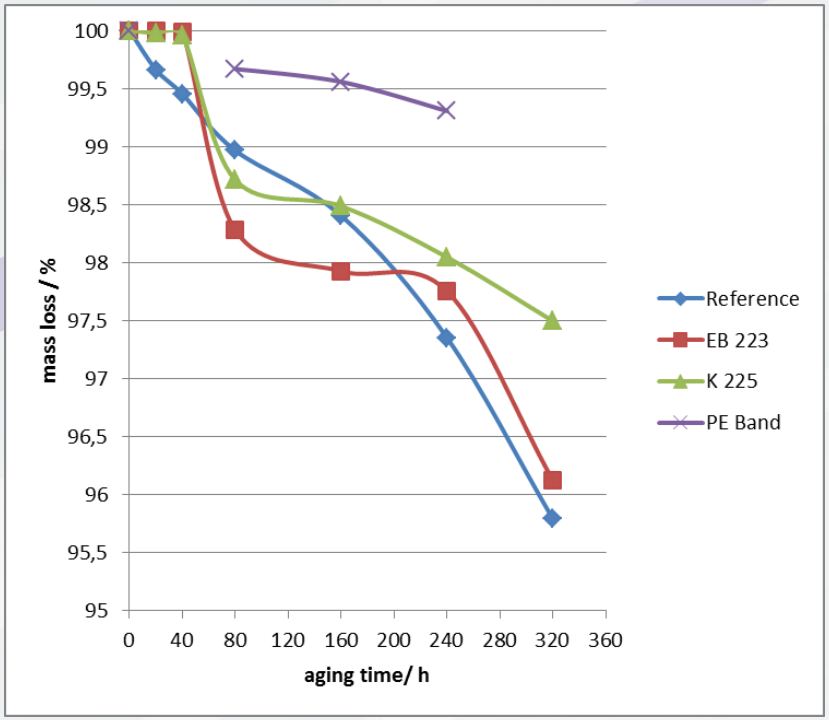

© Fraunhofer IWS

Fraunhofer IWS Dresden

Realized material combinations

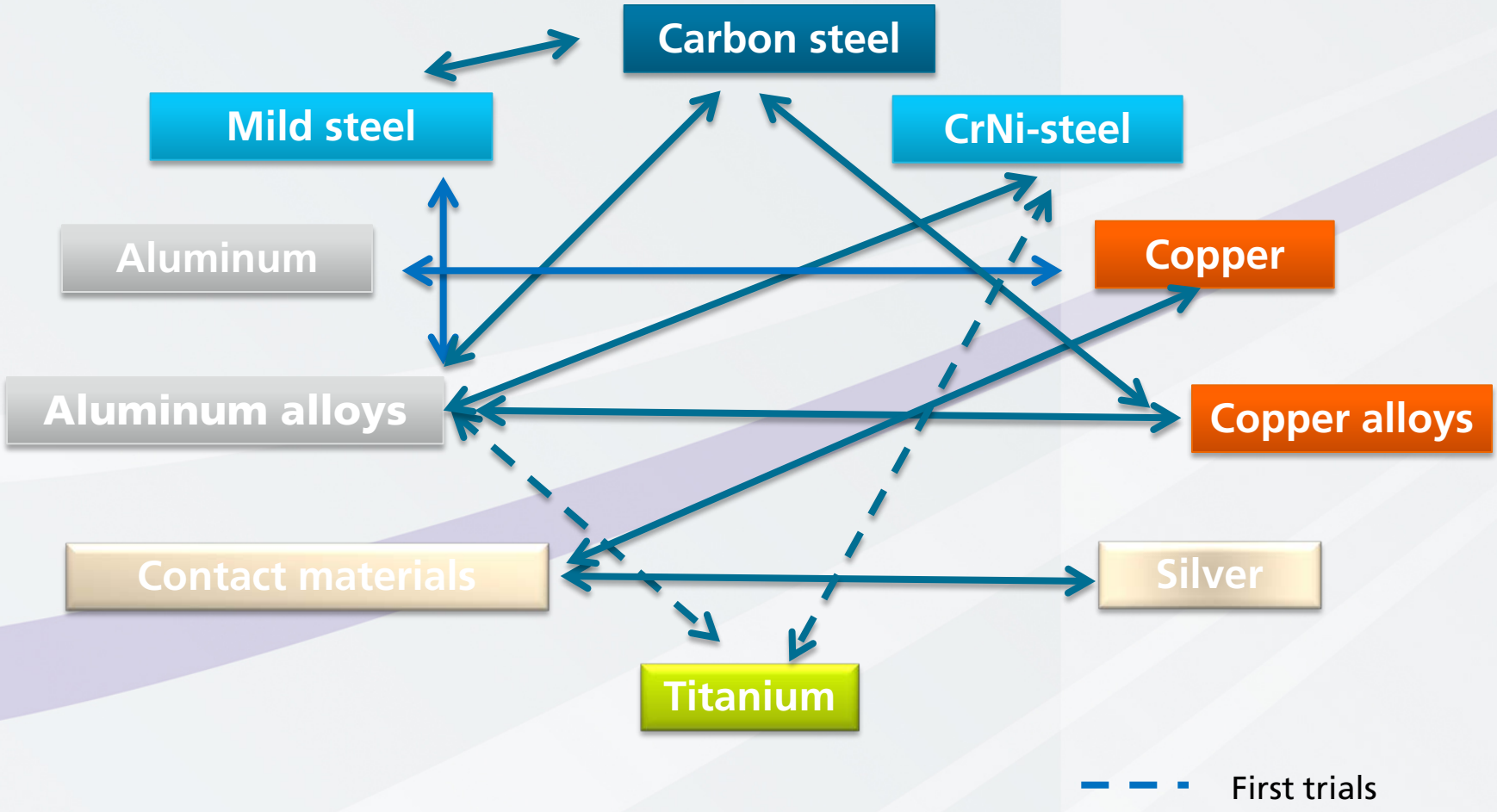

© Fraunhofer IWS

Particularities of joining zones

Cu/Al

- differently shaped joining zones (depending on geometry and alloy)
- Joining zone without or with hardly any brittle intermetallic phases hem

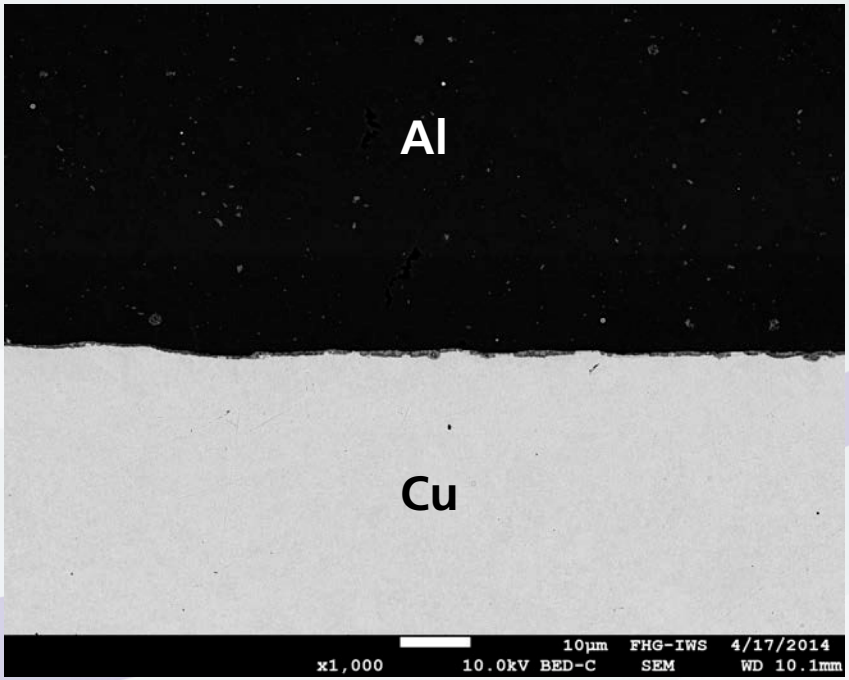

TEM-micrograph, Joining zone partial intermetallic phases hem (< 3 µm)

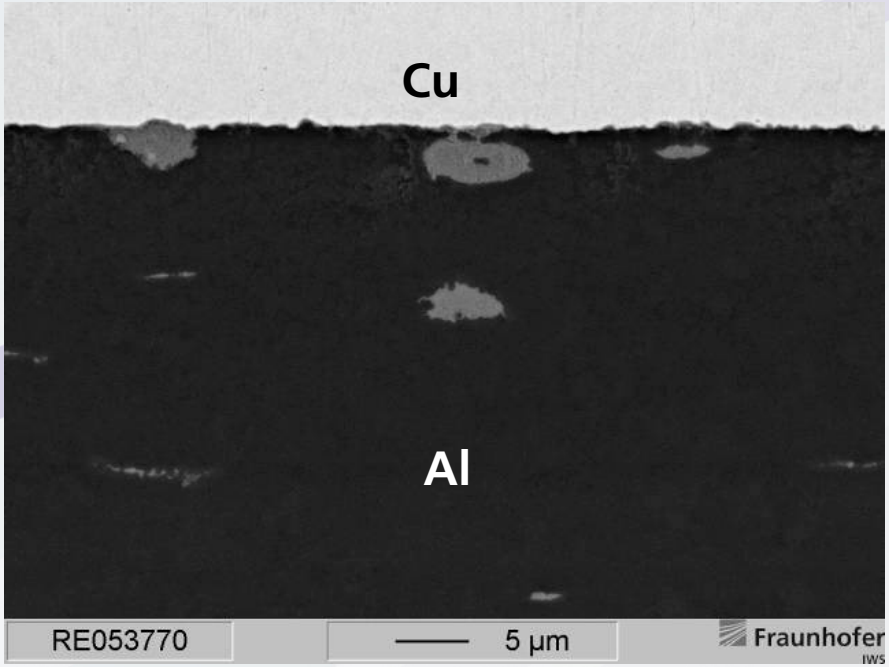

TEM-micrograph, local inclusions of melt droplets of the Cu surface without intermetallic phases hem

© Fraunhofer IWS

Fraunhofer IWS Dresden

Aluminum to Copper

Electro Mobility

- Long-term stable, high conductive connections

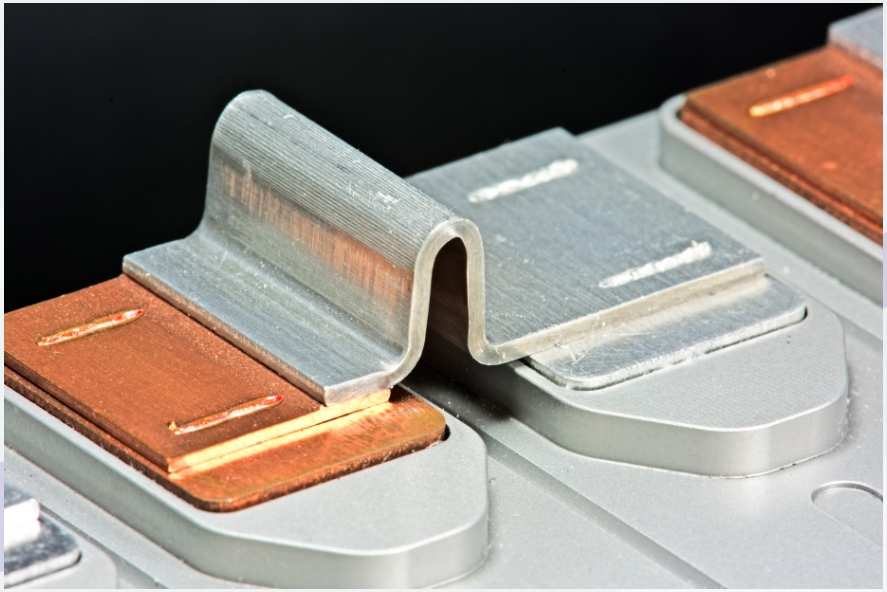

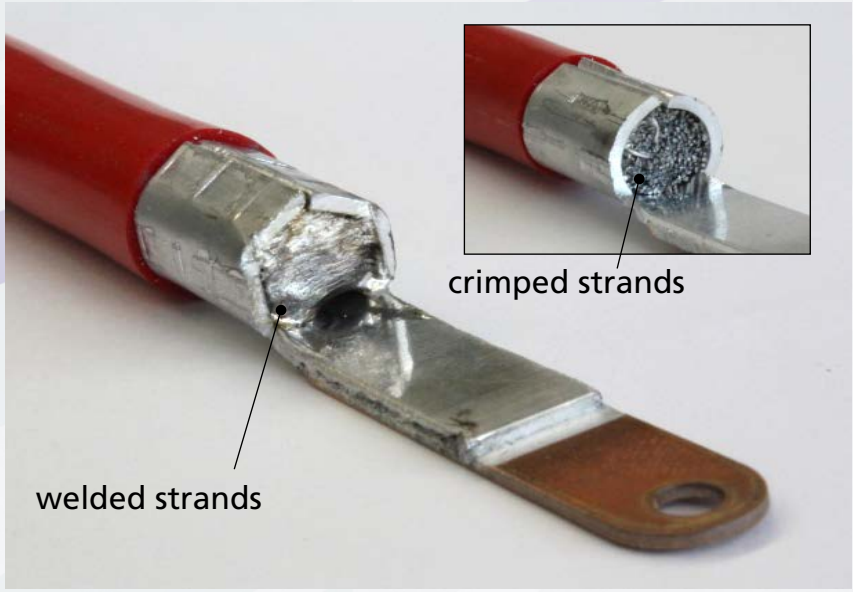

© Fraunhofer IWS

Fraunhofer IWS Dresden

Aluminum to Copper

Specific electric transition resistance of the joining area

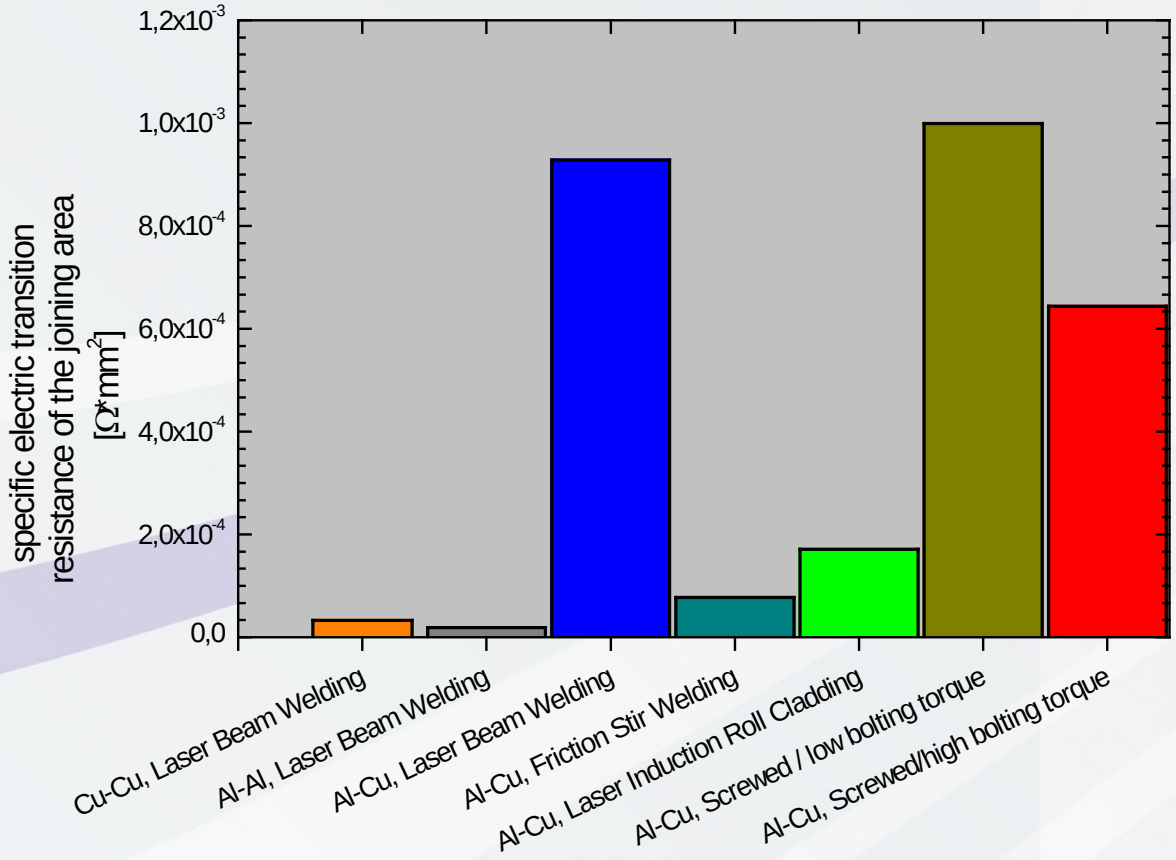

© Fraunhofer IWS

Fraunhofer IWS Dresden

Content

Content	Chapter
Introduction	
The Fraunhofer Gesellschaft	01
Fraunhofer Institute for Material and Beam Technology IWS	02
Seminar topics	03
Laser Beam Welding	
Basics	04
Laser multi pass welding	05
Laser beam welding with high frequent beam oscillation	06
Laser beam welding of high reflective materials	07
Laser beam welding of powertrain components	08
Laser induction roll plating	09
Special Joining Technologies	
Magnetic pulse joining	10
Friction stir welding	11
Joining with reactive multi layers	12
Bonding and Composite technology	
Electrical-conductive bonding	13
Thermal direct joining of thermoplastic to metal	14
Mechanical Joining	
Enhanced mechanical connection by laser interference patterning	15

© Fraunhofer IWS

Outline

1. Forming and welding with magnetic fields: advantages and applications
2. Important terminology
3. Physical background
4. Facilities at Fraunhofer IWS
5. Current research activities at Fraunhofer IWS

© Fraunhofer IWS

Forming and Welding with Magnetic Fields

Why Magnetic Pulse Joining?

- Magnetic pulse joining is an **impact** joining or welding technique used for sheets and tubes
- Features include:
  - Typical cylinder dimensions: ∅10 - 80 mm
  - Typical part thicknesses: 0,5 – 3 mm
  - Typical materials: copper, aluminum, steel, brass, etc.
  - Safe for industry
  - Energy efficient
  - Joining occurs in microseconds
  - Welding is solid state process → few intermetallic phases
  - Clean: no flux, no shielding gas and normally no surface preparation is necessary

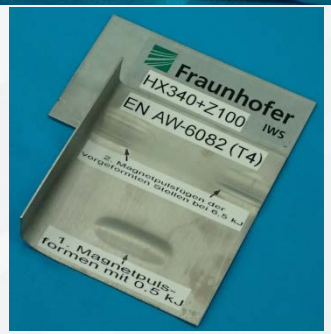

© Fraunhofer IWS

Forming and Welding with Magnetic Fields

How can Magnetic Pulse Technologies be Used?

- **Joining by crimping**
  - Cost-effective, fast, clean
- **Shaping**
  - Better shaping abilities
  - Reduction in wrinkling
  - Uses only one die
- **Welding**
  - Mixed materials possible
  - Fast and clean
- **Cutting**
  - High quality edges
  - Uses only one die

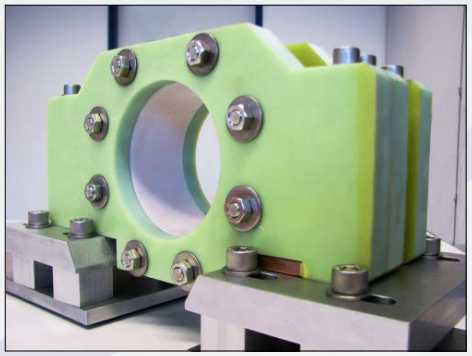

© Fraunhofer IWS

Forming and Welding with Magnetic Fields

Fields of Application

- **Lightweight design**
- **Joining/welding of mixed materials**

Automotive
- Power train components
- Drive shafts

Aerospace
- Al-connections
- Titanium connections

Medical
- Sealing of canisters

Facilities/ plant engineering
- Tube connections

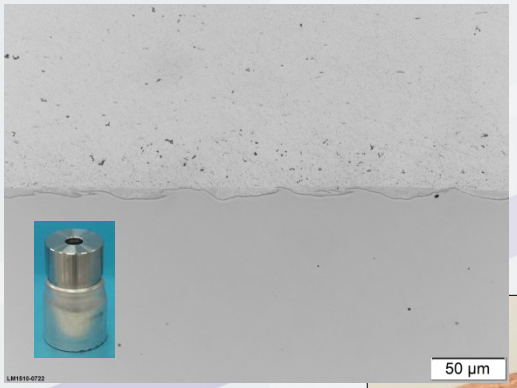

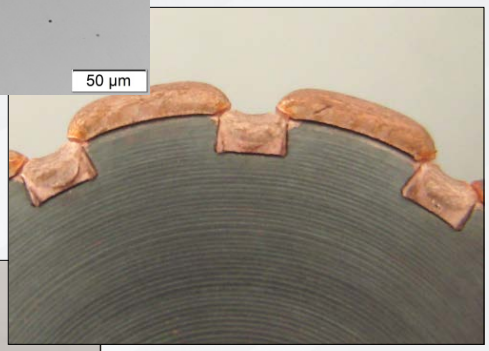

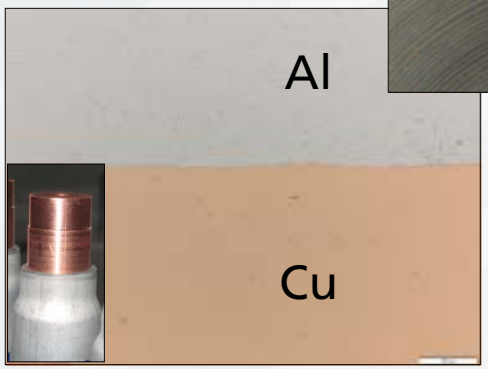

© Fraunhofer IWS

Forming and Welding with Magnetic Fields

Exemplary Application: Hybrid Drive Shafts

- Aluminum-tube (Ø 40 mm, thickness 2,5 mm)
- Steel-tube (Ø 33 mm, thickness 6,5 mm)

Metallurgical joints with a higher strength than the base material (aluminum) are achievable

© Fraunhofer IWS

Forming and Welding with Magnetic Fields

Exemplary Application: Hybrid Sheet Welding

Preformed Humps (for example electromagnetic or conventional formed)

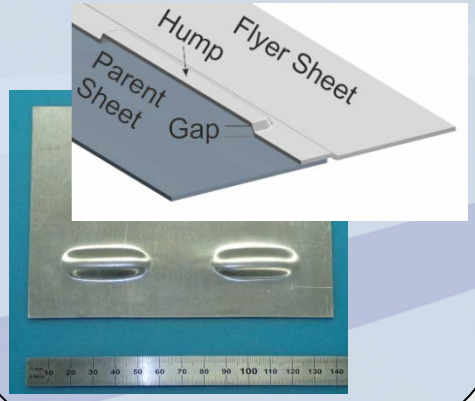

Positioning of both sheets next to the coil, joining of one hump after the other through electromagnetic forces

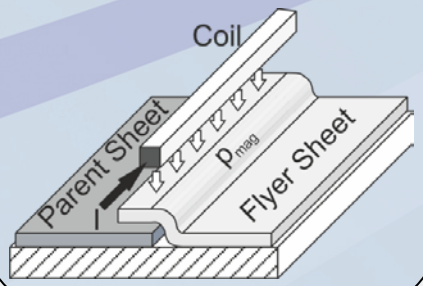

Multi-material line welding (2 x 40 mm)

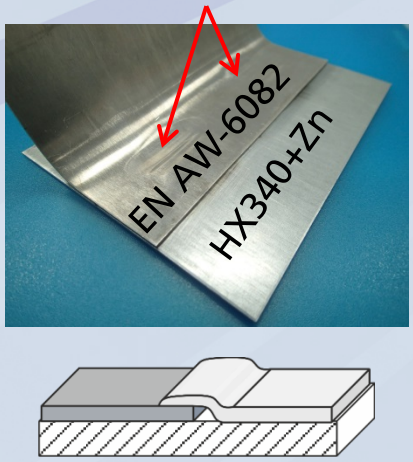

EN AW-6082 was successfully joined with HX340LAD, S355 and other steels

© Fraunhofer IWS

Terminology (Tubes)

Generator
- Discharges currents to coil

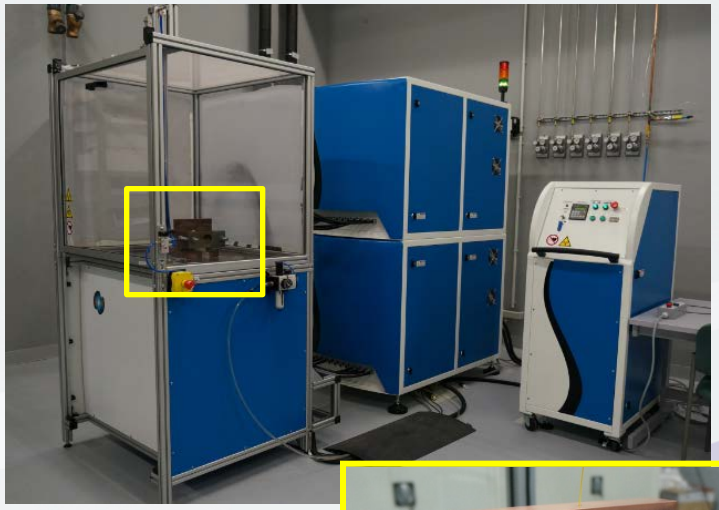

Flyer
- Outer workpiece
- Deforms, impacting anvil

Anvil
- Inner workpiece

Coil
- Transports current to piece or field shaper for deformation

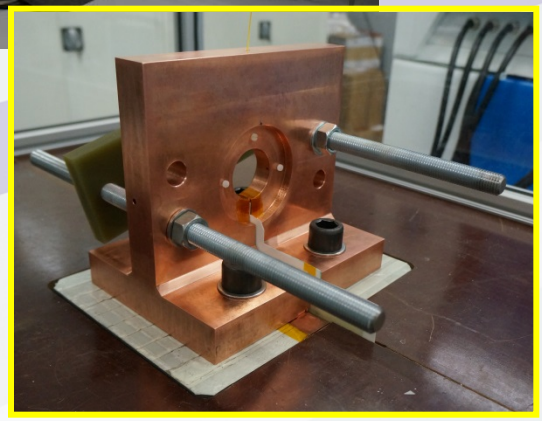

Field Shaper (optional)
- Concentrates field from coil
- Adapts coil geometry to workpiece
- Transports current for workpiece deformation

© Fraunhofer IWS

Terminology (Sheets)

Generator

- Discharges currents to coil

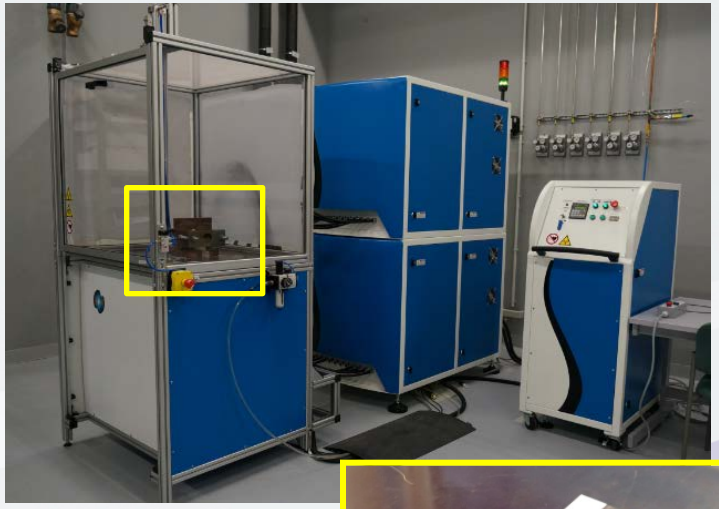

Coil

- Transports current to piece for deformation

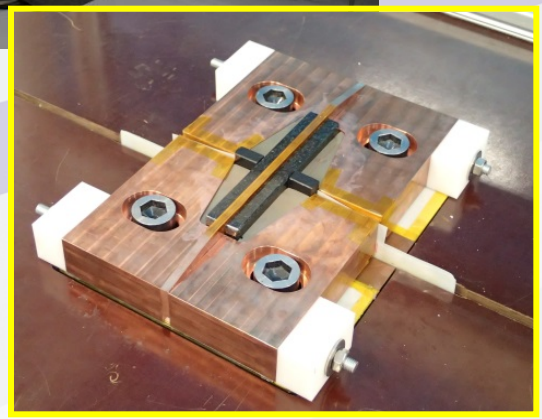

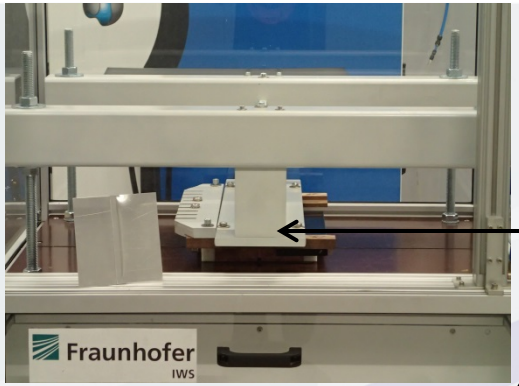

Backing

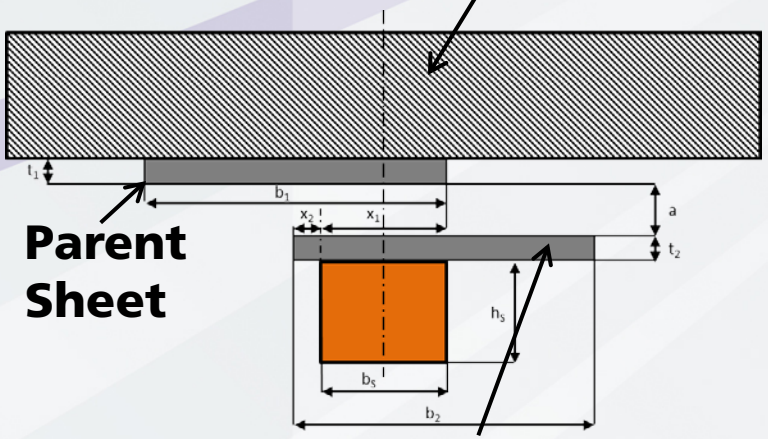

Parent Sheet

Flyer sheet

- Deforms, impacting parent sheet

© Fraunhofer IWS

Transient magnetic field generated by a coil

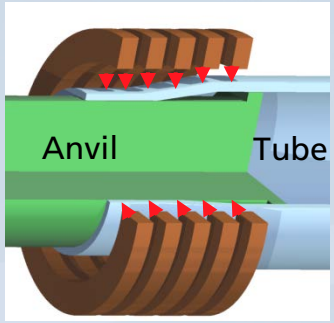

Outer workpiece is accelerated towards inner workpiece (by Lorentz forces)

Collision with high impact speeds (>200 m/s)

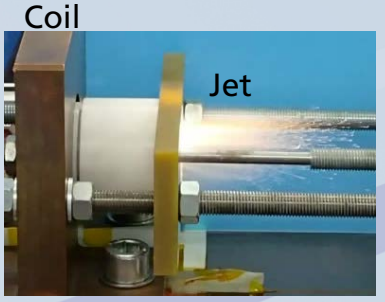

Shear at the workpiece surfaces creates a „Jet“

Cleaned metal surfaces and high collision pressure

Deformation and potential welding of partners

MPW is a solid state process and appropriate for hybrid metal joining with fewer intermetallic phases

© Fraunhofer IWS

Macroscopic Process (Coil)

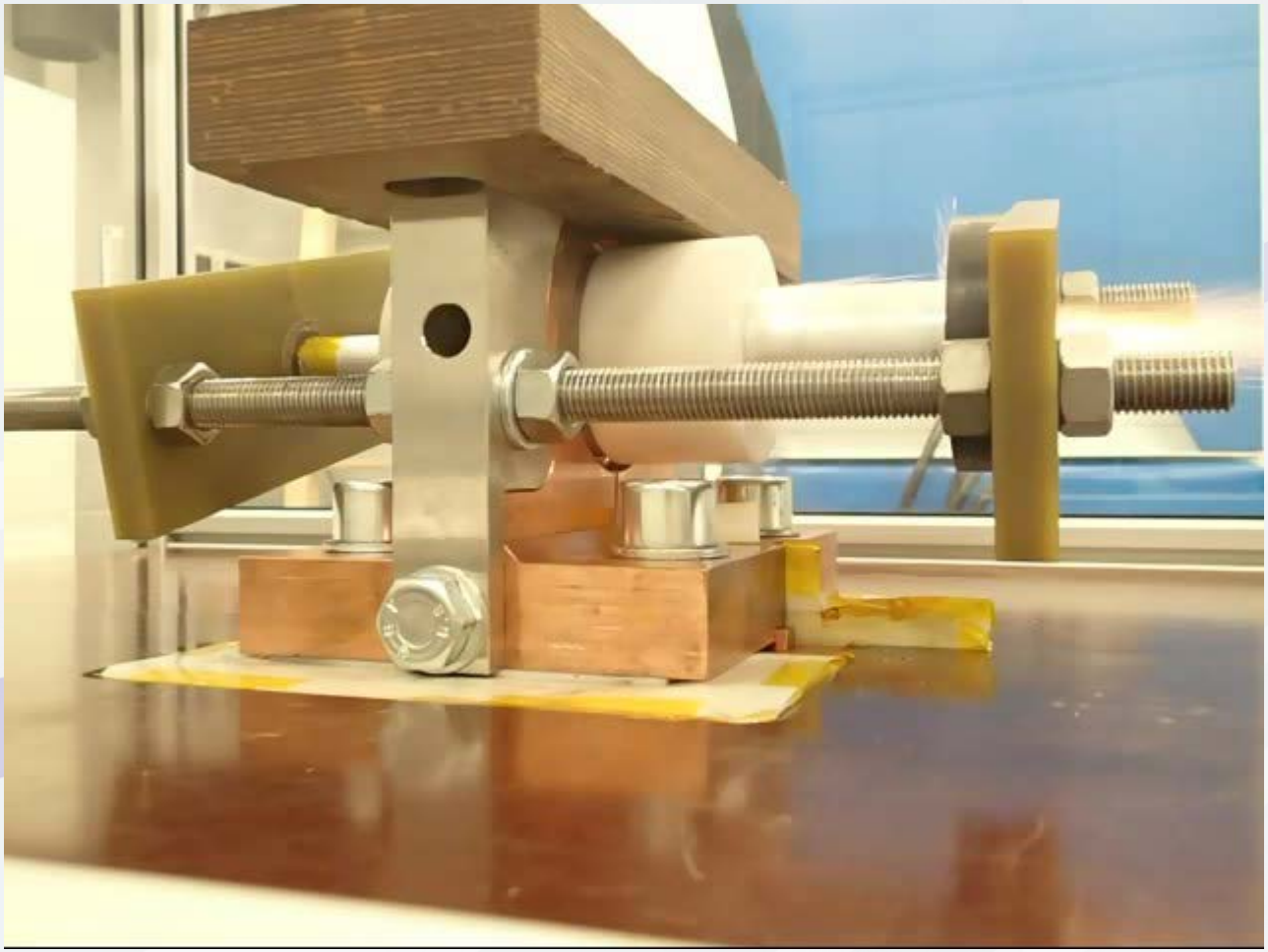

© Fraunhofer IWS

Deformation Induced by Lorentz Force

Current-carrying conductor (350 mA) in magnetic field oscillates a membrane

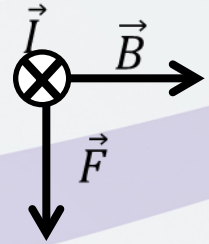

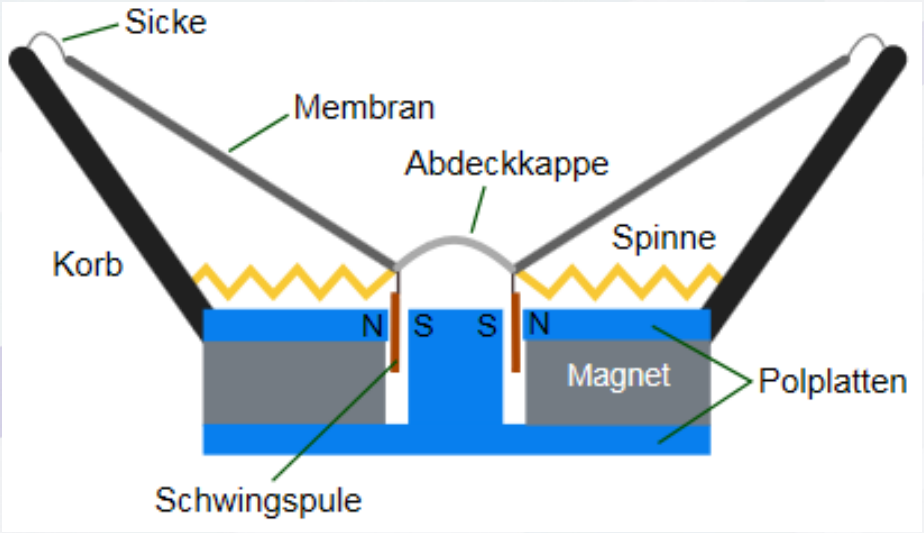

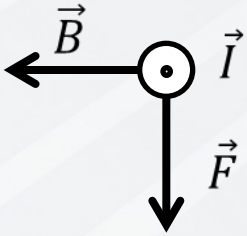

Source: Wikipedia („Lautsprecher“ 09.04.2015)

© Fraunhofer IWS

Deformation Induced by Lorentz Force

Current-carrying coil (approx. 350 kA) deforms metallic workpieces

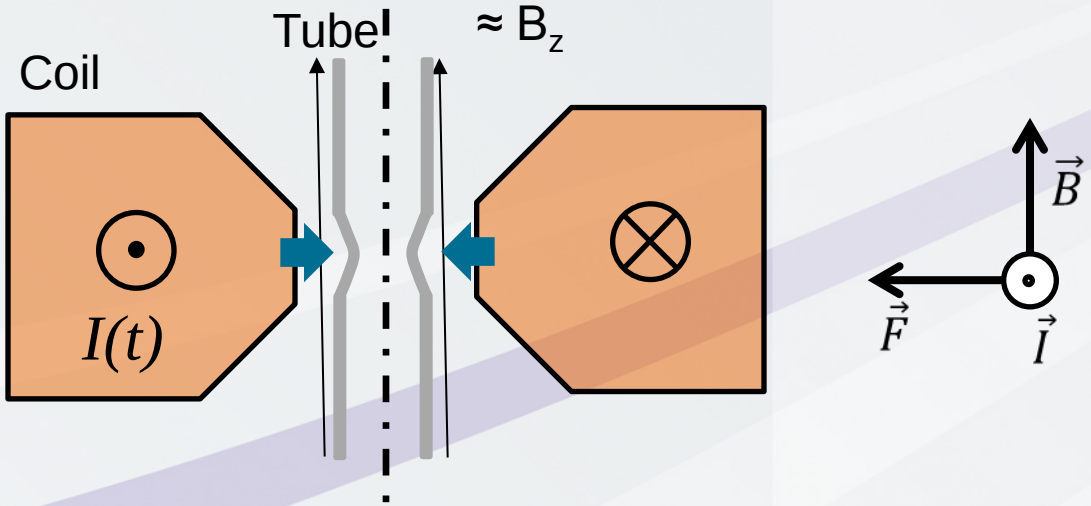

Magnetic pressure

$$p_{\mathrm{mag}} = \frac{B_z^2}{2\mu}$$

$\Rightarrow$

Tangential stress

$$\sigma_t = \frac{p_{\mathrm{mag}}}{2} \cdot \frac{d}{s}$$

$\Rightarrow$ Yield stress

© Fraunhofer IWS

Characterization of Joined Area

- Metallographic characterization of the joined area with cross sections in optical, scanning electron and transmission electron microscopy

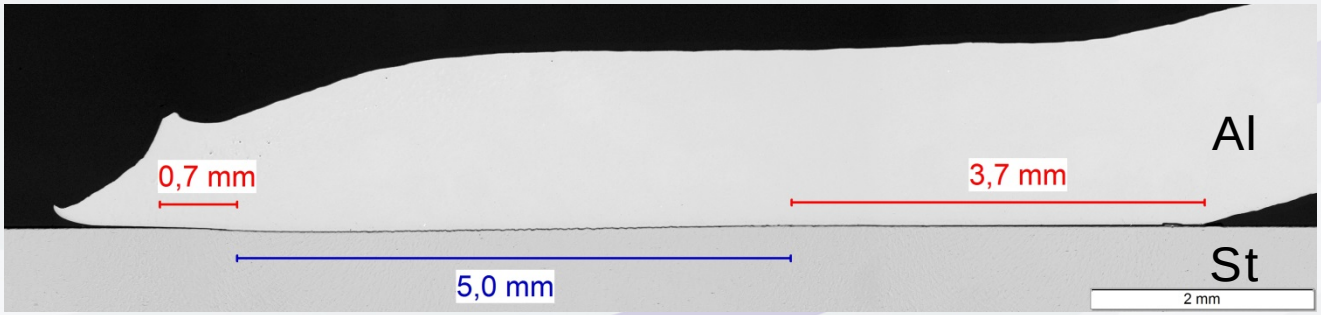

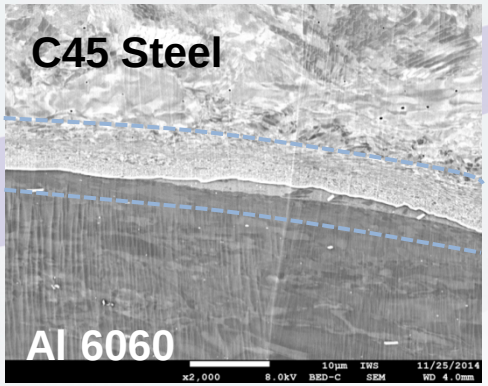

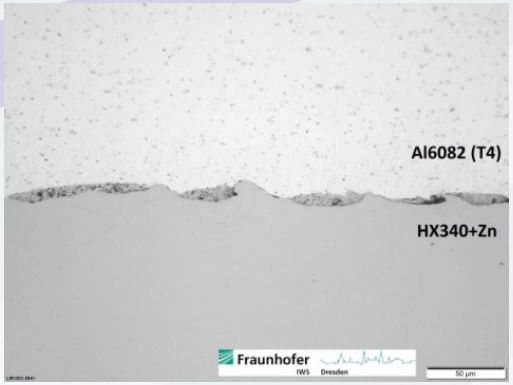

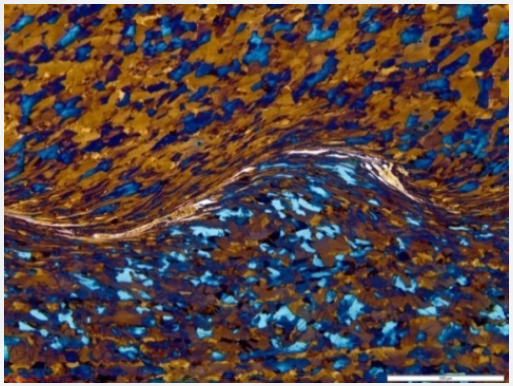

© Fraunhofer IWS

Magnetic Pulse Welding

Facilities at Fraunhofer IWS Lab

- *Industrial System:*
  - Built by BMAX in Toulouse, France
  - Maximum discharge energy: 32 kJ
  - Maximum voltage: 20 kV
  - Maximum current: 850 kA
  - Typical discharging frequency: 20 kHz

- *Prototype System:*
  - Built by Helmholtz-Zentrum Dresden-Rossendorf
  - Maximum discharge energy: 40 kJ
  - Maximum voltage: 24 kV
  - Maximum current: 400 kA
  - Typical discharging frequency: 8 kHz

© Fraunhofer IWS

Methods for Process Development: High Speed Photography

30 frames per second (fps)

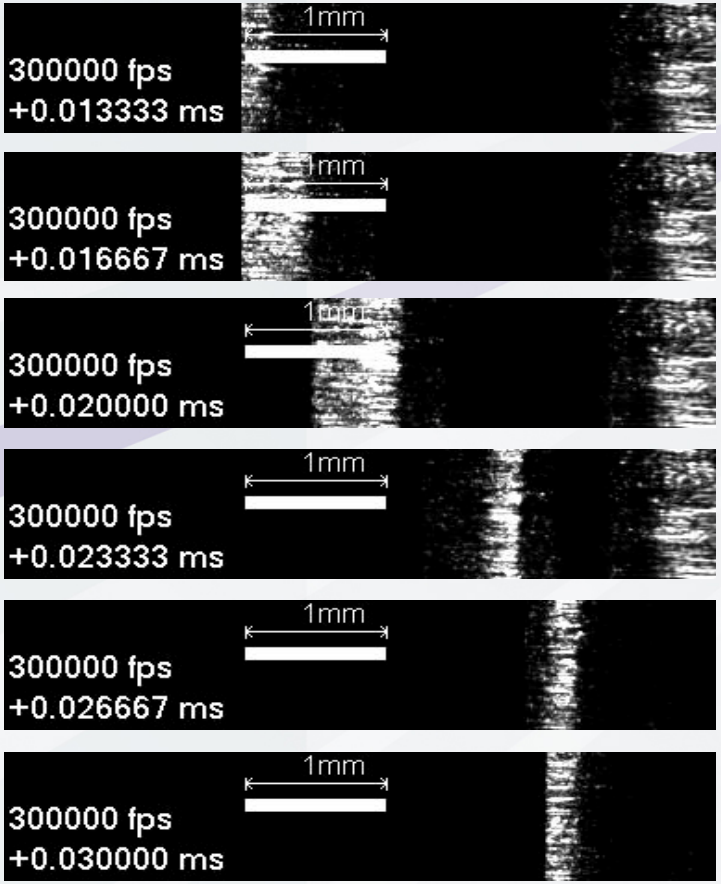

© Fraunhofer IWS

Photon Doppler Velocimetry for Process Control

Comparison of the Flyer-Deformation: PDV & Simulation

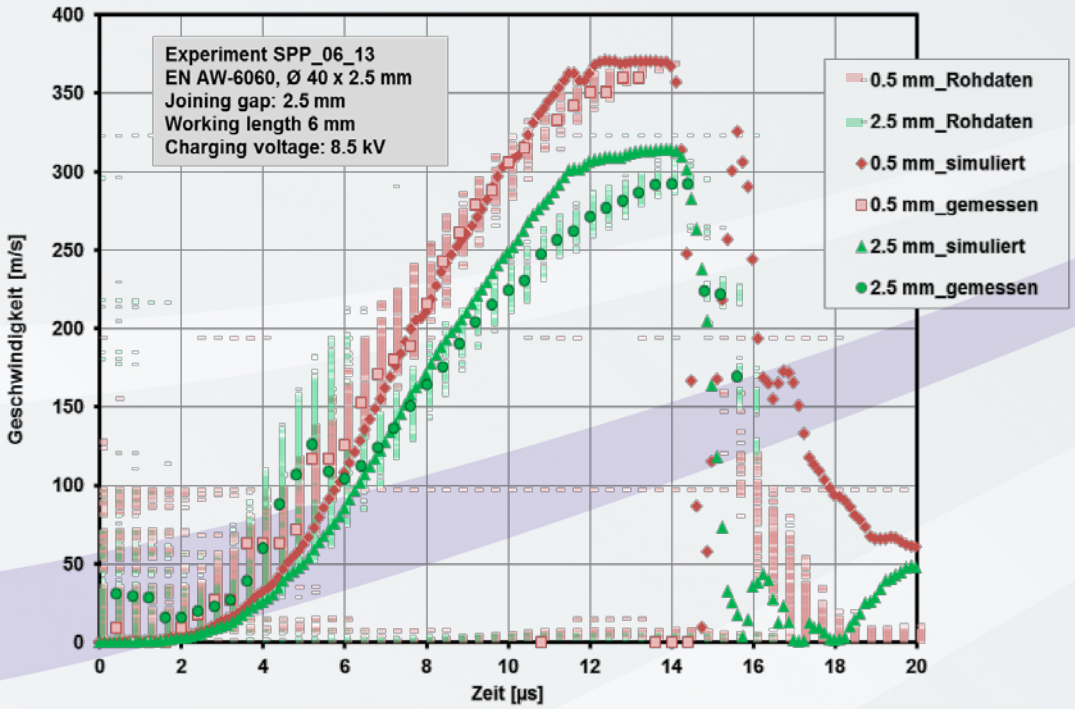

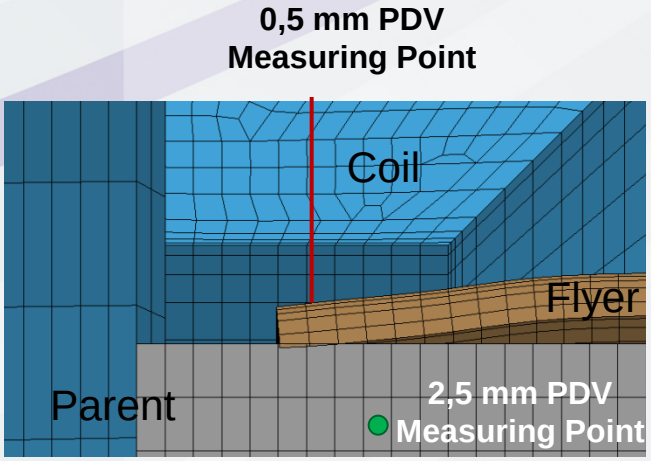

© Fraunhofer IWS

Development of Welding Windows

- Optimal angles between the workpieces is essential for jet creation and evacuation
- Welding windows are currently in development and may be used for parameter adjustment

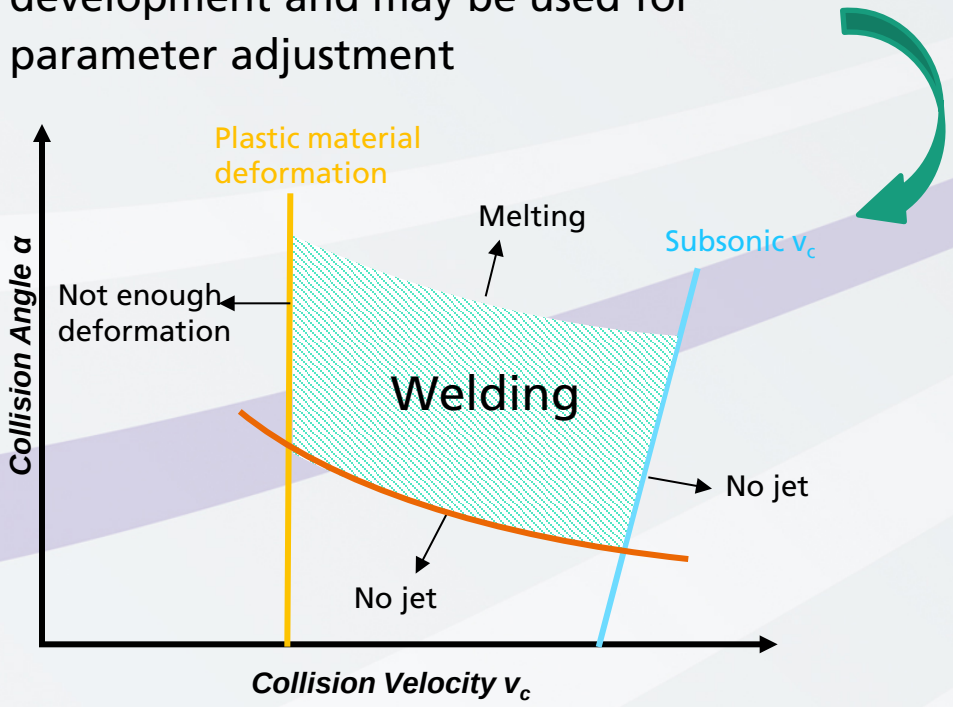

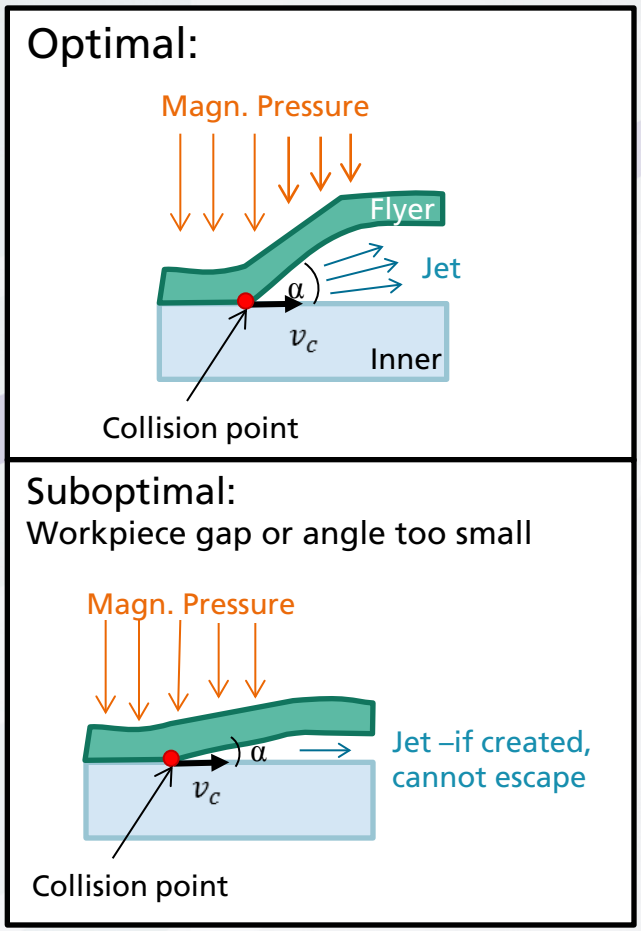

© Fraunhofer IWS

Development a Coil for Sheet Welding

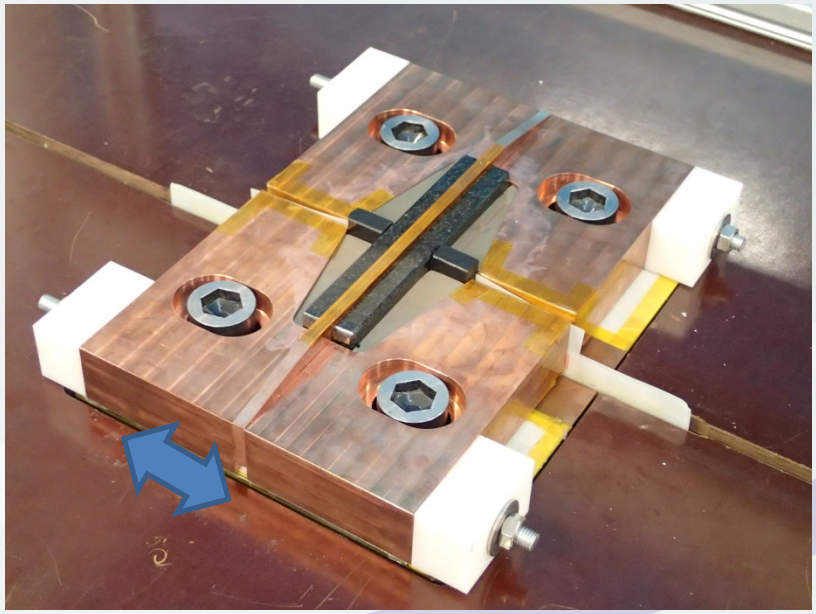

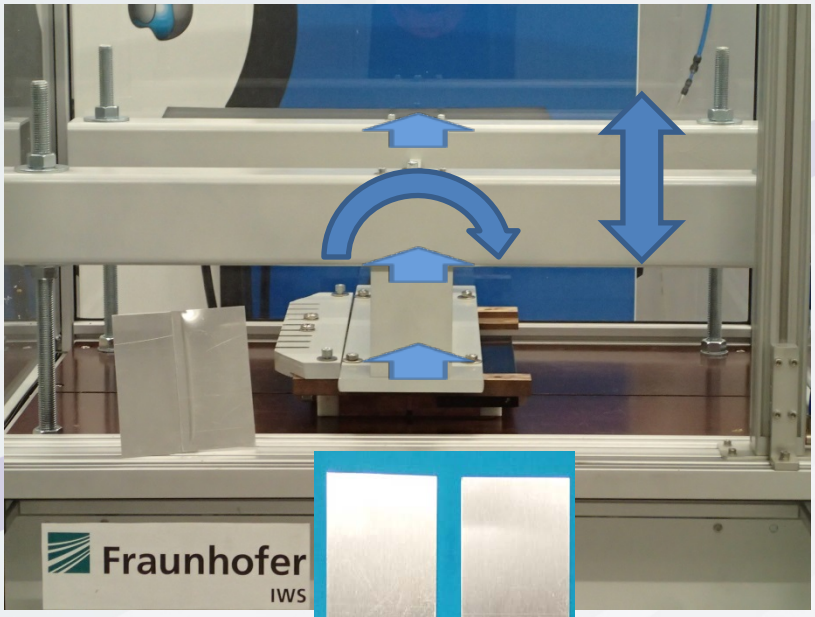

Suitable for (long-) sheet welding with various thicknesses

© Fraunhofer IWS

Simulation and Process Optimization

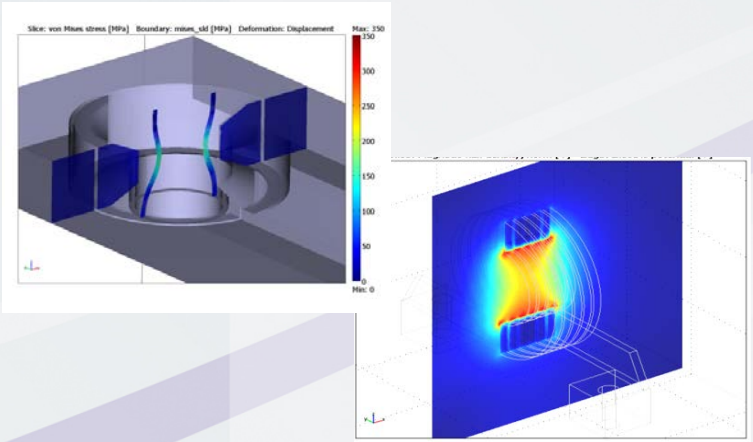

With Finite Element Methods

- Commercial FEM-tool: COMSOL Multiphysics
- Application: Design of coil geometries

With Analytical Calculations

- Complete analytical description of the RLC-circuit
- Fast and simple
- Prediction of relevant parameters
- Influence of geometrical changes are considered

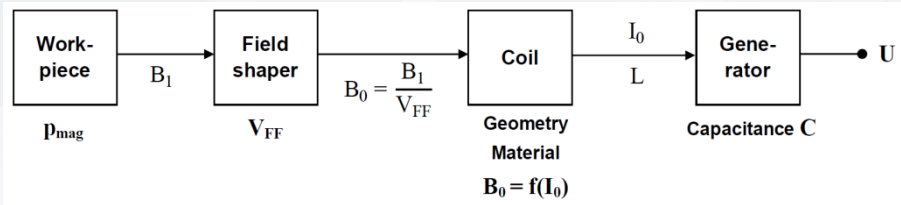

© Fraunhofer IWS

Our Service for You

- Development of solid state joining technologies for material combinations that are not suitable for fusion welding
- Consultation and preparation of feasibility studies
- Process development, concept studies
- Research & development in cooperation with partners from industry and also within public projects
- System developments in cooperation with our partners
- Industrialization

© Fraunhofer IWS

Content

Content	Chapter
Introduction	
The Fraunhofer Gesellschaft	01
Fraunhofer Institute for Material and Beam Technology IWS	02
Seminar topics	03
Laser Beam Welding	
Basics	04
Laser multi pass welding	05
Laser beam welding with high frequent beam oscillation	06
Laser beam welding of high reflective materials	07
Laser beam welding of powertrain components	08
Laser induction roll plating	09
Special Joining Technologies	
Magnetic pulse joining	10
Friction stir welding	11
Joining with reactive multi layers	12
Bonding and Composite technology	
Electrical-conductive bonding	13
Thermal direct joining of thermoplastic to metal	14
Mechanical Joining	
Enhanced mechanical connection by laser interference patterning	15

© Fraunhofer IWS

Content

- History
- FSW – how it works
- Potentials of the technique
- Equipment that is needed
- Process influencing factors
- Application examples
- Typical terms

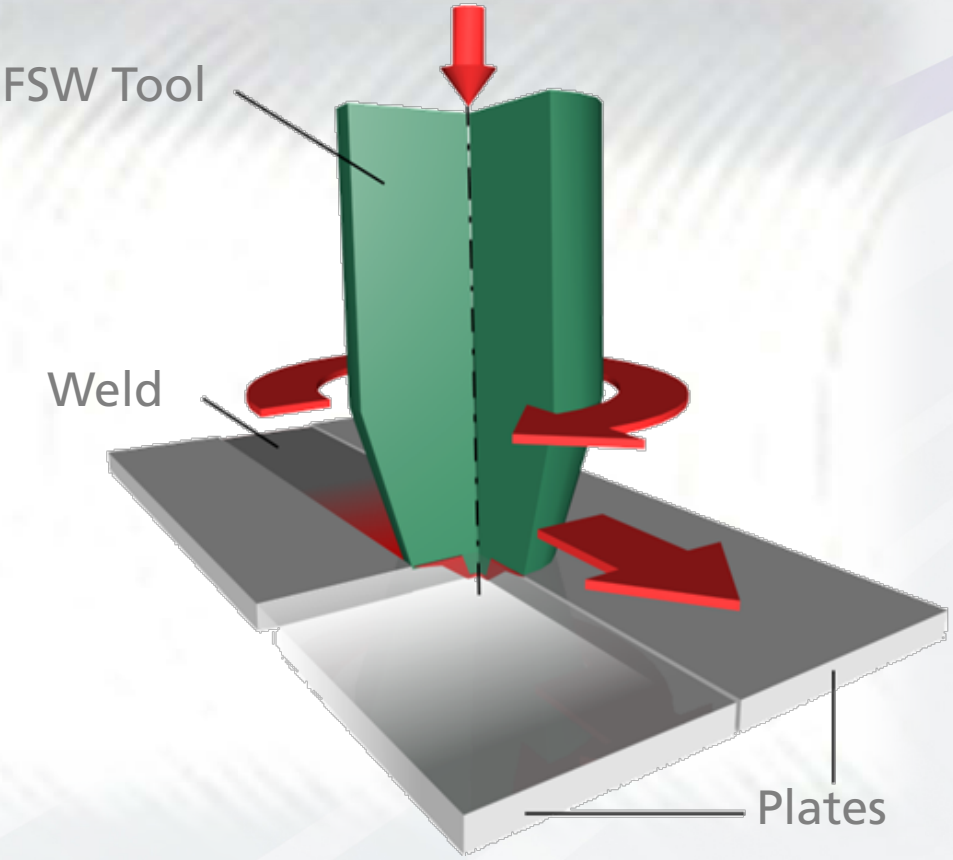

© Fraunhofer IWS

History and Patent Situation

- Invented in 1991 @ TWI (EP 0615480 B1) by Wayne Thomas
- Legacy patents ran out in 2015

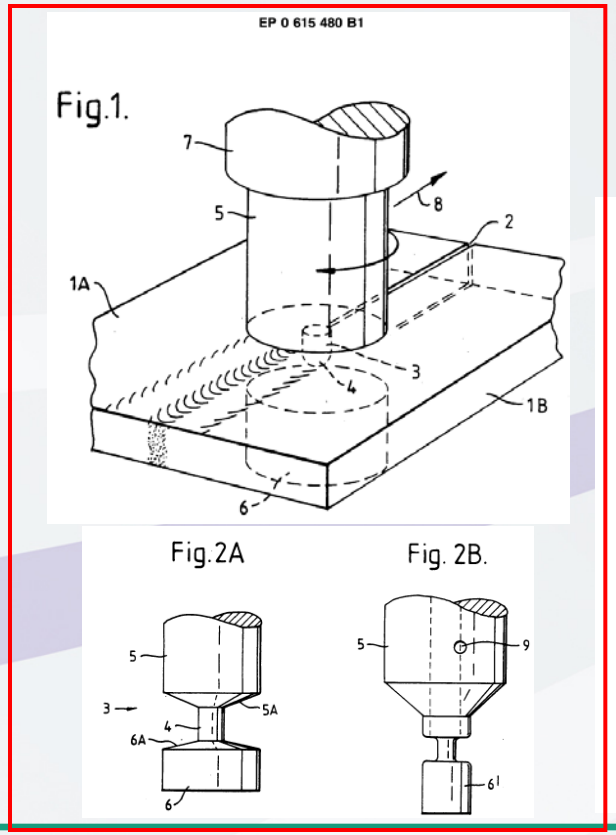

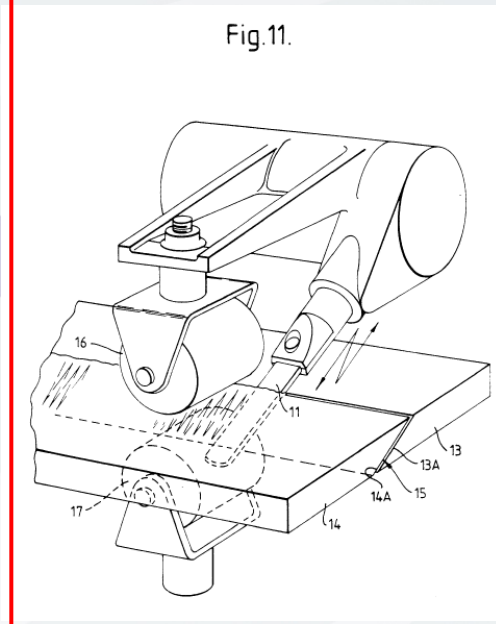

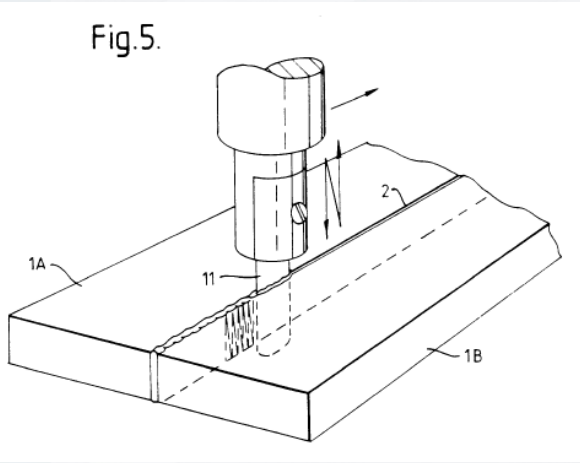

Source: Patent EP 0615480 B1

© Fraunhofer IWS

How it Works

- **Process principle:** creating metallic continuity by friction welding
- **Difference to classical friction welding:** a moving third element (tool) is creating friction between the parts to be joined
- The movement of the tool creates a line like weld

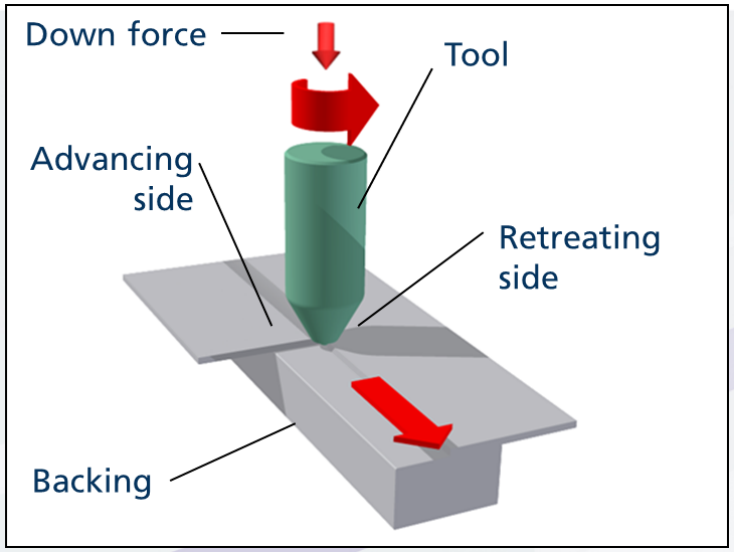

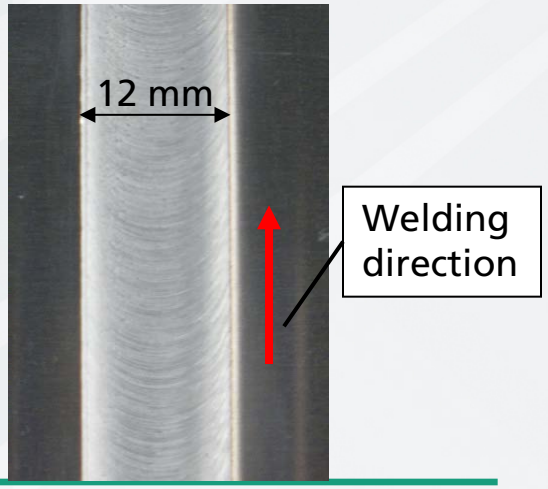

Exemplary weld surface:

© Fraunhofer IWS

- **Pro:**
  - No melting
  - Suitable for non-fusion-weldable materials
  - Dissimilar metals weldable
  - Large range of thicknesses weldable
  - Thermo-mechanically treated fine grained weld
  - No filler material needed

- **Contra:**
  - Relatively slow (v=0.5…2m/min typical)
  - Primarily suitable for aluminum
  - High process forces
  - Distortion > laser welds

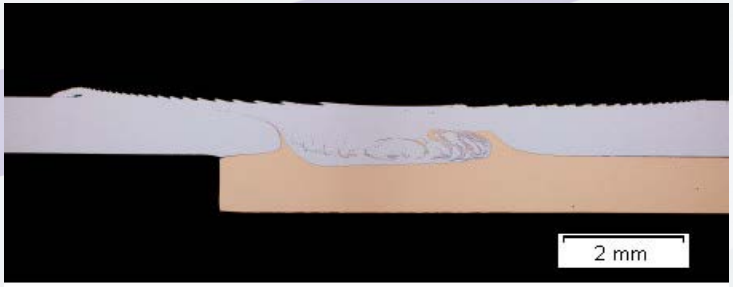

Cross section of an overlap weld (Al+Cu)

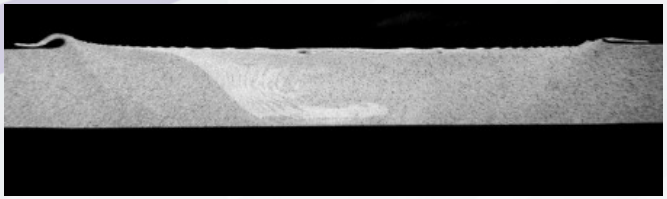
Cross section standard tool weld (Al)

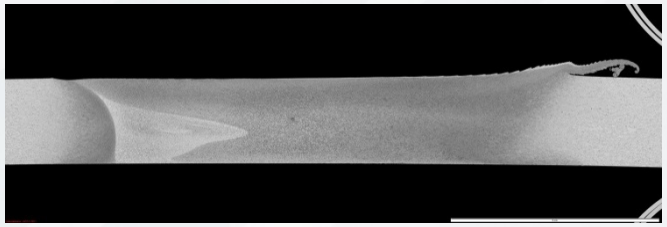
Cross section bobbin tool weld (Al)

© Fraunhofer IWS

Friction Stir Welding

Exemplary Applications

Nasa Satellite Fuel Tanks

Railway Carbody

Airbus A400M

SKB – Nuklear Waste Canister

Mazda RX-8

Eclipse 500

Ford GT

Mercedes SL

Telescopic Tube

Audi R8

Shipbuilding

MegaStir Tec., 1018 Steel (t = 20.0 mm)

Simmons Wheels, UT Alloy Works

© Fraunhofer IWS

- **Materials:**
  - Very good: most aluminum alloys, incl. cast aluminum
  - Average: copper, magnesium
  - Possible: softer steels, titanium alloys
- **Part and joint types:**
  - Plates/sheets (0.5… 10 mm)
  - Extrusion profiles
  - Al-cast housings
  - Butt- / overlap joints (seldom: T-joints)

© Fraunhofer IWS

Equipment needed

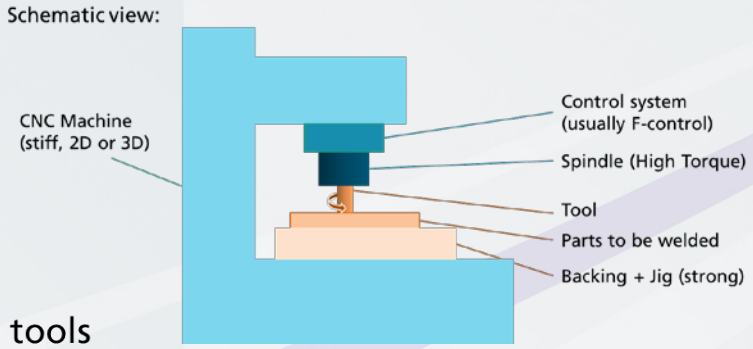

One sided tools

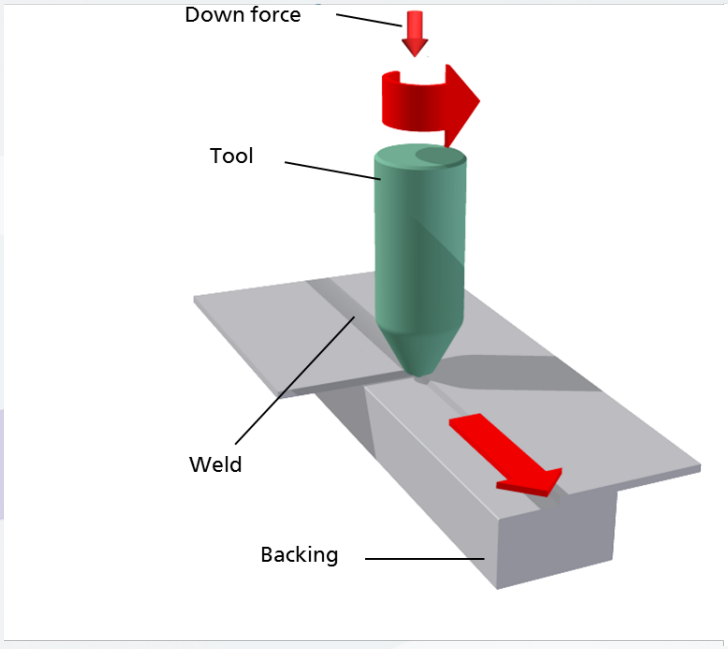

Double sided tools

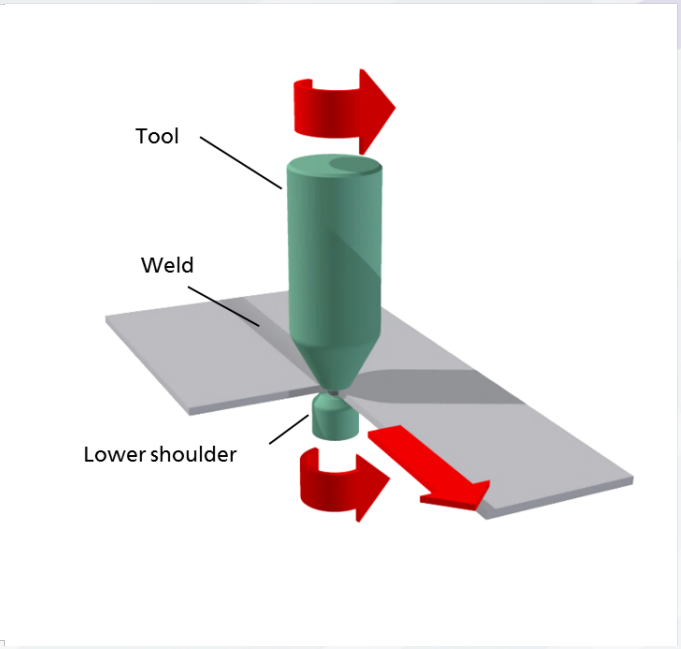

© Fraunhofer IWS

Equipment needed

One sided tools

- Fixed pin
  - "Classical" tools
    - Cone
    - Triflat
    - Other
  - Retractable pin t.
  - ΔN
- Moveable pin

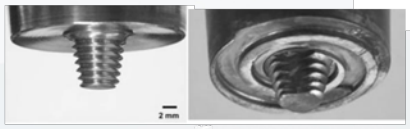

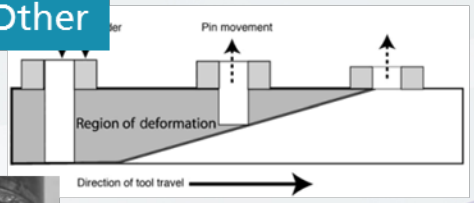

Source: Mishra, R.; Friction Stir Welding an Processing

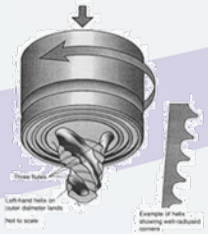

Source: Mishra, R.; Friction Stir Welding an Processing

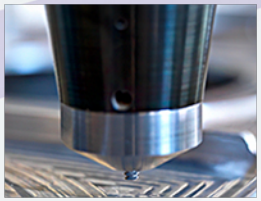

Source: EADS Apworks

Double sided tools

- Bobbin tools
  - Fixed
  - Adjustable
  - ΔN
- Multi-unit
  - "Tatsumaki"
  - Mirrored

Source: TWI

Source: J. Hilgert, Dissertation 2012

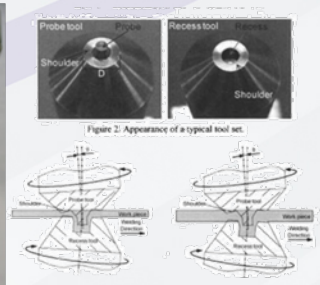

Source: Mishra, R.; Friction Stir Welding an Processing IV

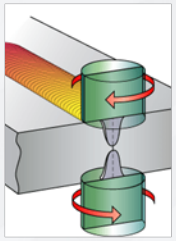

Source: TWI

© Fraunhofer IWS

Machine concepts

- Classical CNC Machines

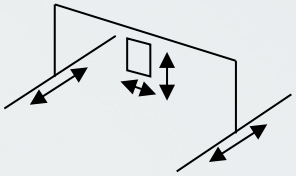

Source: MTI

Source: TWI

- Articulated Robots

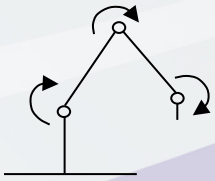

Source: EADS

- Parallel Kinematics

Tripod

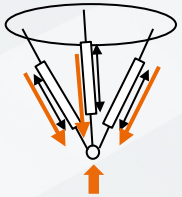

Source: PKM

Pentapod

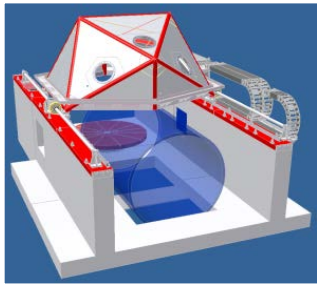

Hexapod

Source: Okuma

© Fraunhofer IWS

C-Frame Gantry Types

Serial kinematics machine type

+ High accuracy
+ High stiffness

- Large masses
- Low flexibility
- Gantry systems can be expensive

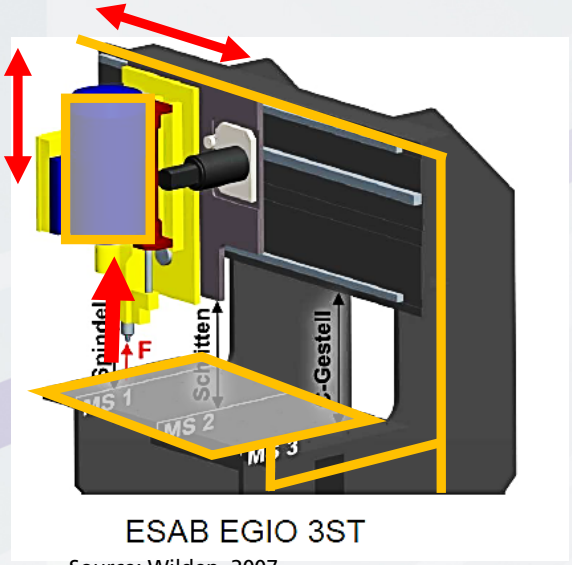

ESAB EGIO 3ST

Source: Wilden, 2007

Source: ESAB

© Fraunhofer IWS

Robotic system

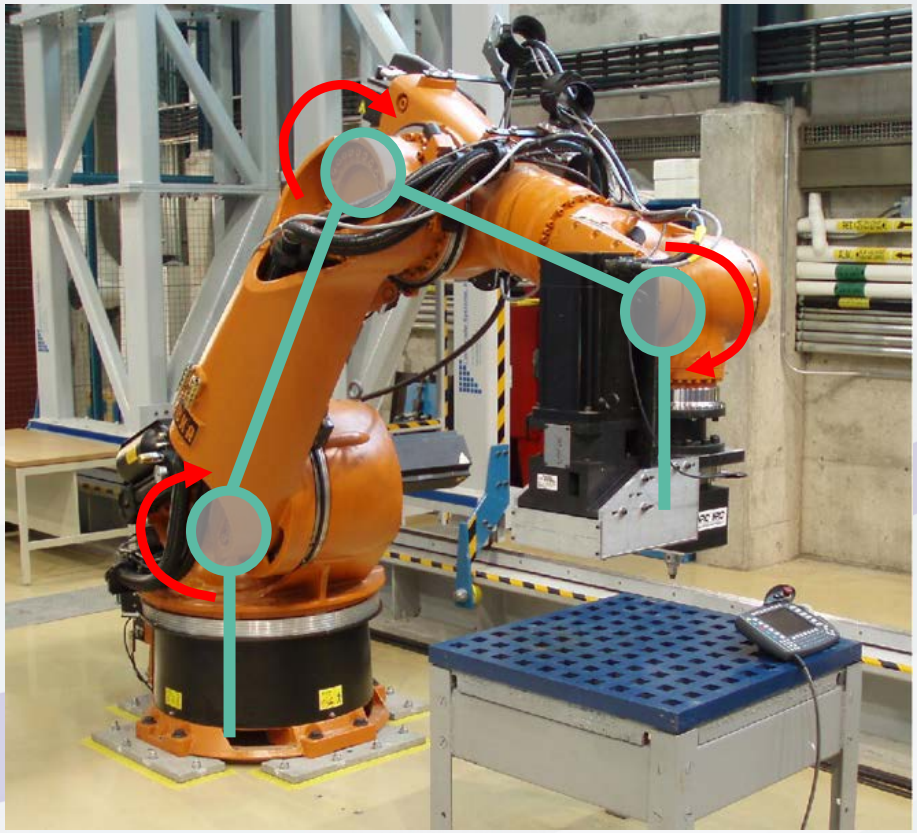

Source: Industrial Robot: An International Journal

Serial kinematics machine type

+ High flexibility
+ High dynamics
+ Low invest

- Low accuracy
- Low stiffness
- Robot with high payload needed

© Fraunhofer IWS

Parallel Kinematics

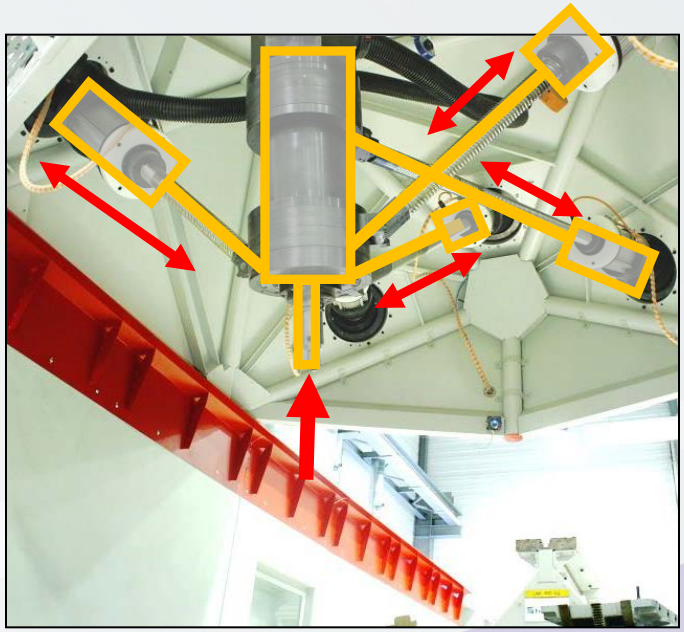

Pentapod at Fraunhofer IWS

Parallel kinematics machine type

+ High flexibility
+ High accuracy
+ Reasonable stiffness
+ Low masses → high dynamics

- Higher invest than robots

Pentapod:

- High flexibility
- High accuracy (0.05 mm)
- High Repeatability (0.03 mm)

- Outstanding space to working space ratio for parallel kinematics

© Fraunhofer IWS

The Pentapod PG2000:

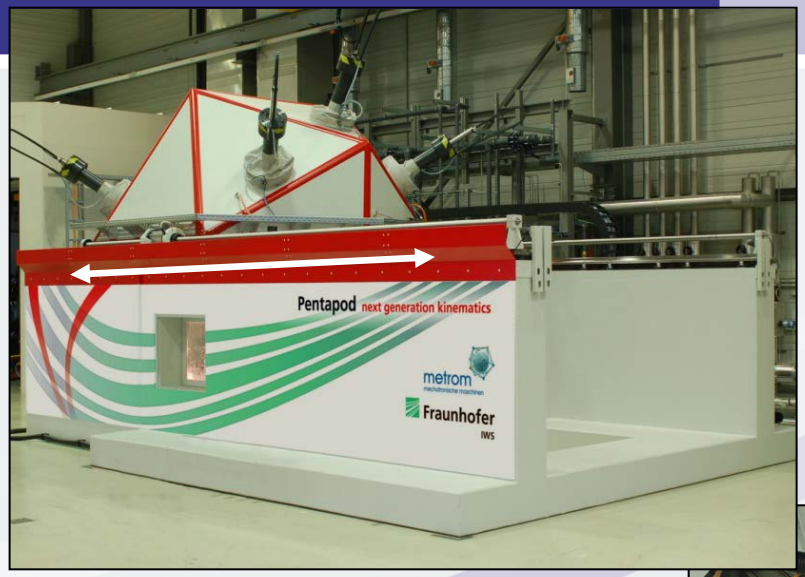

Pentapod at Fraunhofer IWS

Key Facts:

- 6 degrees of freedom
- Main spindle driven by 5 actuators
- Rotary table to achieve 3-D capability
- Linear movable hood
- Working space: 6.5 x 2.0 x 1.5 m³
- Payload: up to 12.0 kN

© Fraunhofer IWS

Control Algorithms

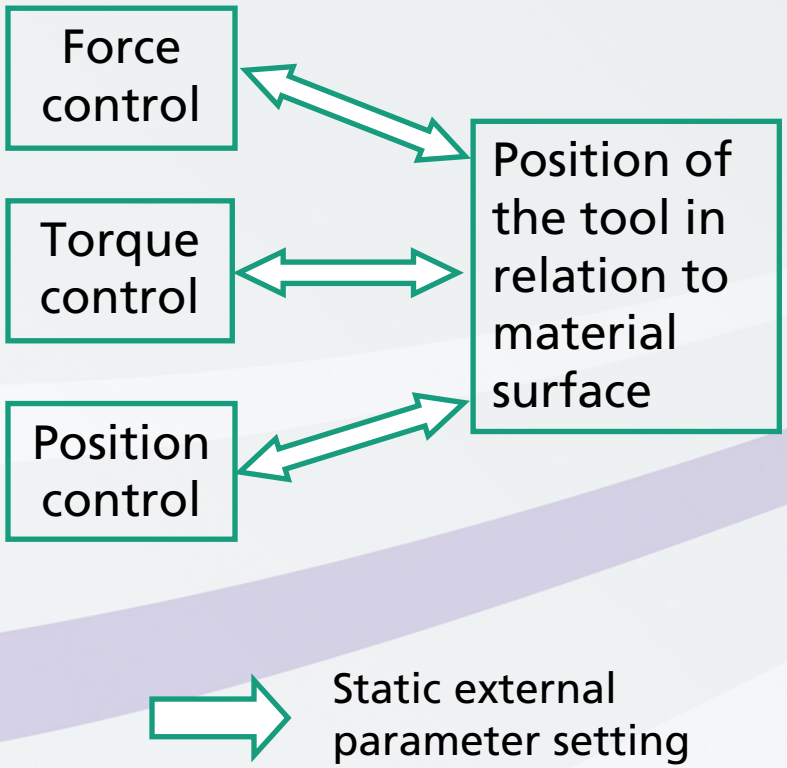

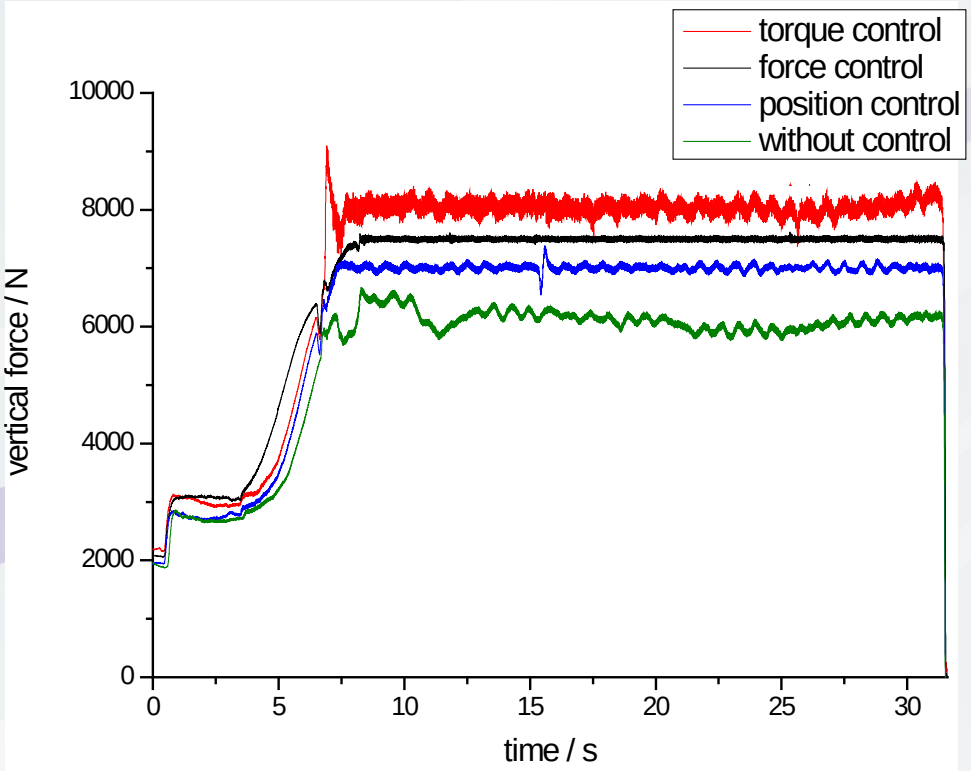

Resulting vertical forces of available control methods (EN AW-6082 T6 2.0 mm), feed rate 2.0 m/min

© Fraunhofer IWS

- Material (thermal softening behavior…)
- Tool geometry (controls mixing)
- Feed rate
- Rotation speed
- Z-Force

Weld defects:

- Lack of Penetration (LOP)
- Tunnel defects
- Large flash
- Melting

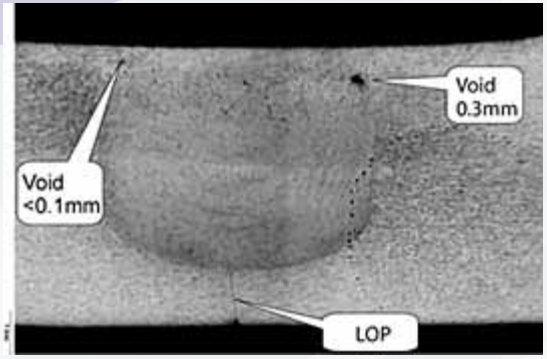

Source: TWI Global

Exemplary weld defect

© Fraunhofer IWS

Examples

Cylindrical test sample, EN AW-5754
feed rate: 0.2 m/min, radius: 25.0 mm

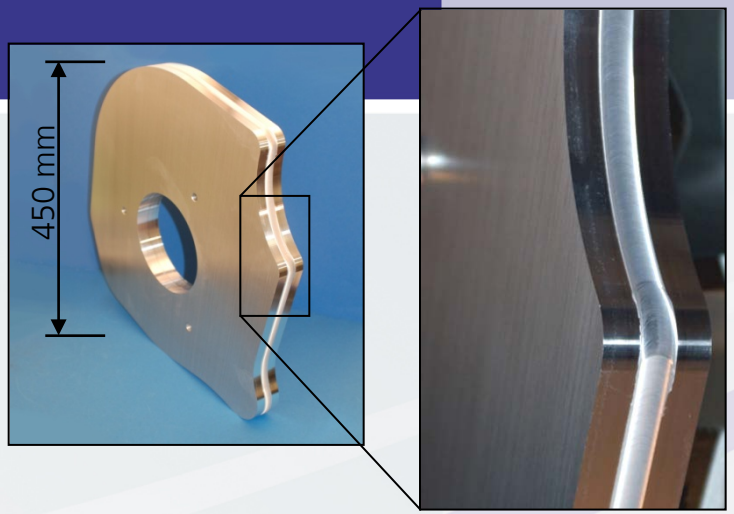

3D-structure FS-welded
EN AW-5754, feed rate: 0.25 m/min

Welded test carrier (scale 1:4)

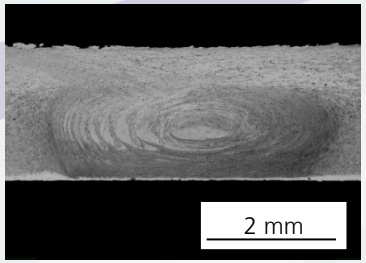

Cross section,
EN AW-2024 T351

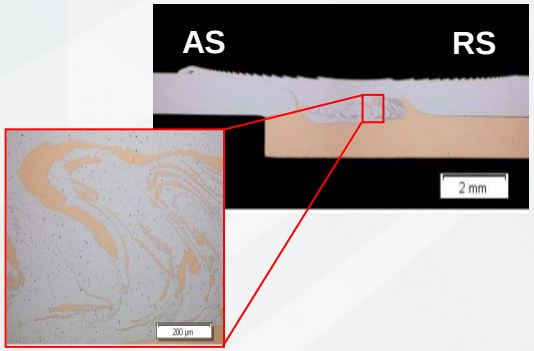

Mixed material joint cross section (Al-Cu)

© Fraunhofer IWS

TWB

3D welding

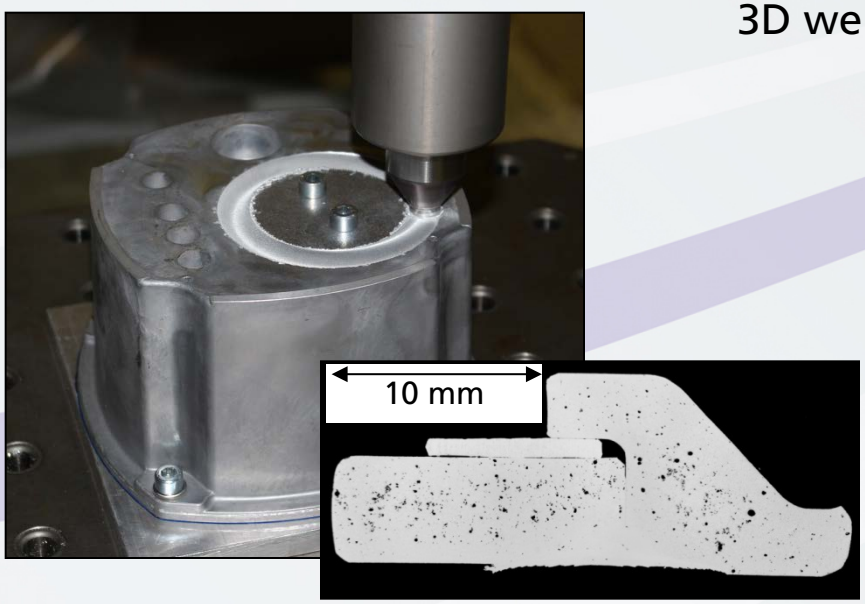

Al-diecast

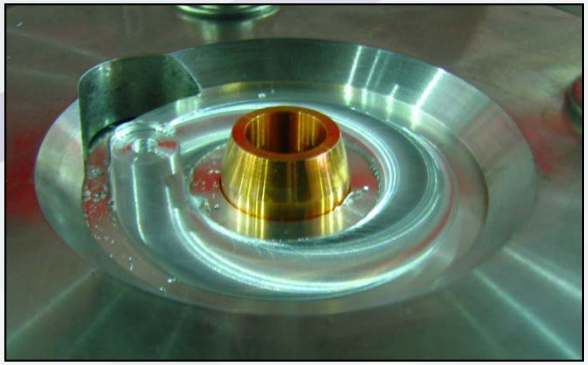

FSW Al/Cu

Longitudinal section

© Fraunhofer IWS

Content

Content	Chapter
Introduction	
The Fraunhofer Gesellschaft	01
Fraunhofer Institute for Material and Beam Technology IWS	02
Seminar topics	03
Laser Beam Welding	
Basics	04
Laser multi pass welding	05
Laser beam welding with high frequent beam oscillation	06
Laser beam welding of high reflective materials	07
Laser beam welding of powertrain components	08
Laser induction roll plating	09
Special Joining Technologies	
Magnetic pulse joining	10
Friction stir welding	11
Joining with reactive multi layers	12
Bonding and Composite technology	
Electrical-conductive bonding	13
Thermal direct joining of thermoplastic to metal	14
Mechanical Joining	
Enhanced mechanical connection by laser interference patterning	15

© Fraunhofer IWS

Tailoring joining technology for low cost localized performance enhancement of metal parts

Topics

Tailored joining technology
Laser multi pass welding
Laser beam welding with high frequent beam oscillation
Laser beam welding of high reflective materials
Laser beam welding of powertrain components
Laser induction roll plating
Magnetic pulse joining
Friction stir welding
Joining with reactive multi layers
Electrical-conductive bonding
Thermal direct joining of thermoplastic to metal
Enhanced mechanical connection by laser interference patterning

Industrial sector & application
Automotive parts
Tooling
Medical devices
Aviation parts
High end consumer products
Power generation parts
High power electronic & E-mobility
Micro-connection technology

© Fraunhofer IWS

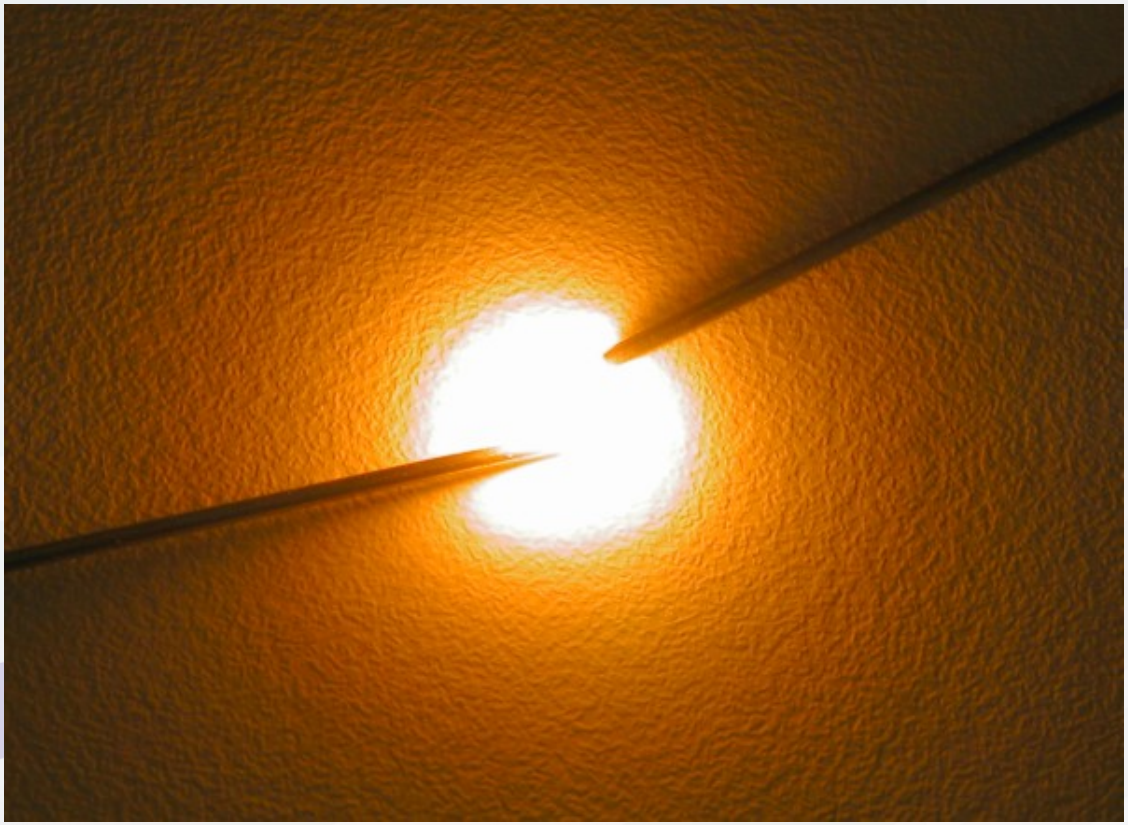

Ignition of a reactive foil by electrical spark

© Fraunhofer IWS

Joining with reactive multilayer systems (RMS)

1. Initial situation:
   - Conventional joining und welding processes generally heat up the joining components significantly
2. Problem:
   - Change of the material characteristic and the structure
   - Thermal stress of joining components with different thermal expansion coefficients
3. Approach:
   - A heat source, which could precisely insert in the joining zone and which have a very short process time
4. Solution:
   - Use of reactive nanometer multilayer systems (RMS)

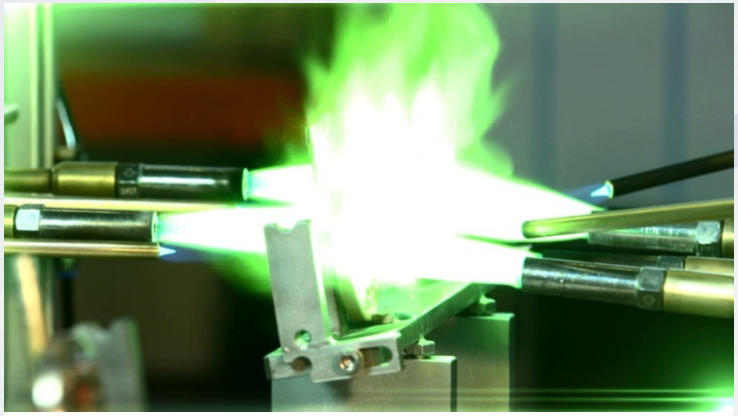

Torch brazing (Source: VDMA)

Soldering furnace (Source: Xerion)

© Fraunhofer IWS

Joining with reactive multilayer systems (RMS)

Reactive Multilayer Systems (RMS):

- Defined internal heat source
- Temporary and locally defined heat input
  - Temperature > 1000 °C
- Minimizing thermal deformation and stress
  - materials with different thermal expansion coefficient are joinable (e. g. metal and ceramic or polymer)
- Little deformation of the structure
  - Process time << 1 s
- High thermal and electrical conductivity
- No need for oxygen (possible under water/in vacuum)

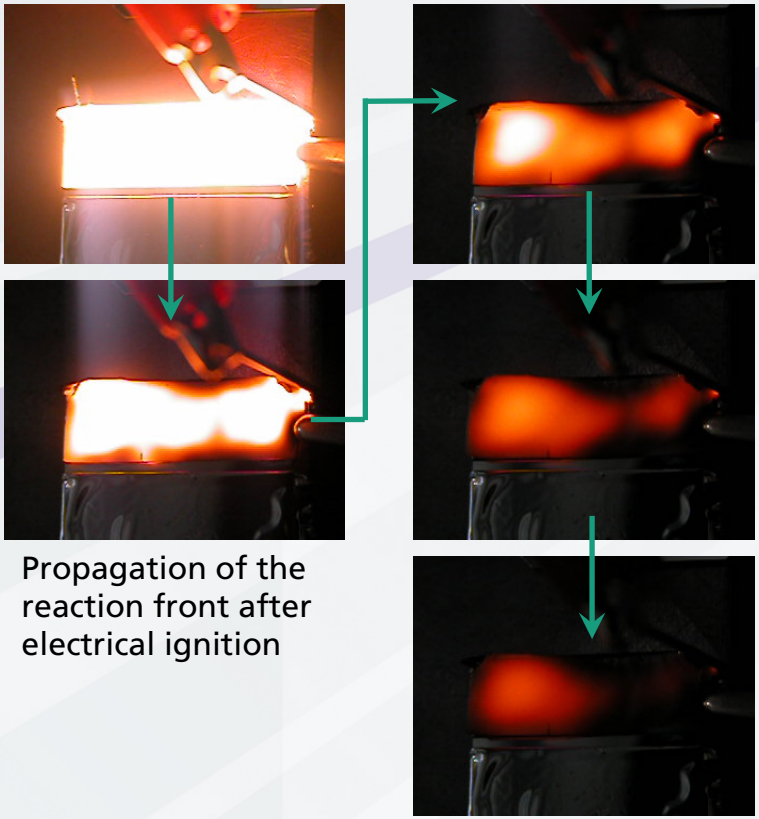

Propagation of the reaction front after electrical ignition

© Fraunhofer IWS

Intermetallic
„reacted“ state

Multilayer
„unreacted“ state

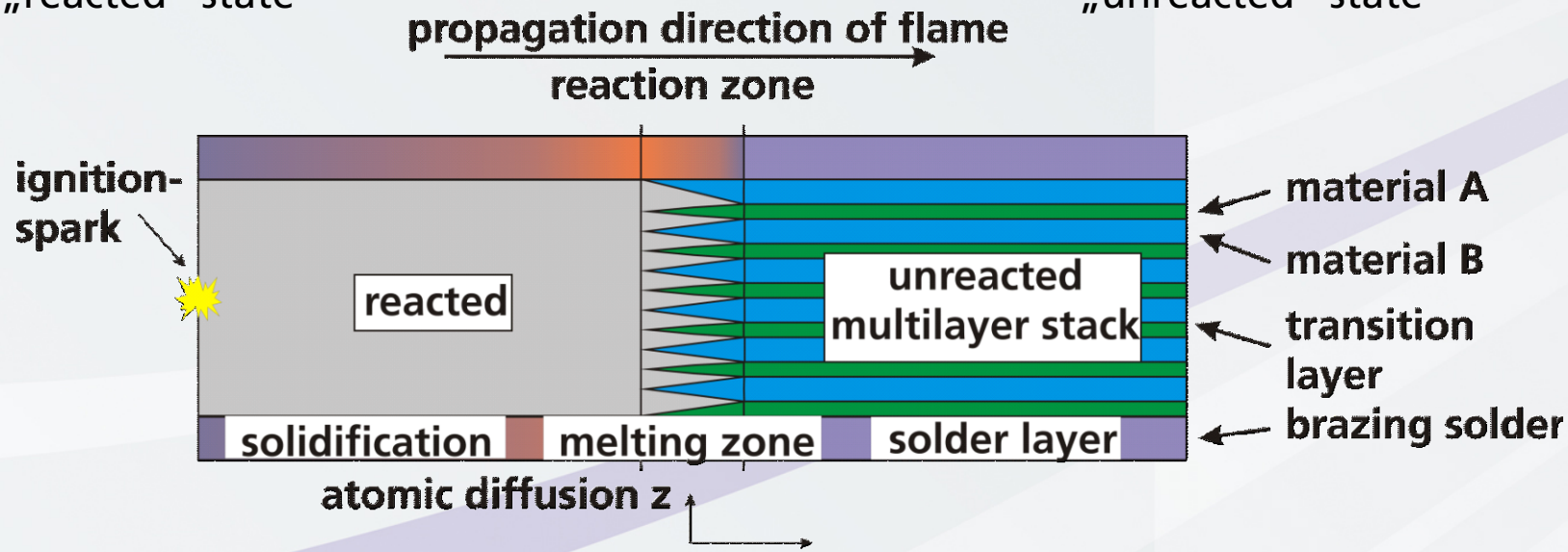

$$E_1 = E_2 + E_{reaction}$$

E_1

E_2

$E_{reaction}$

$$E_{reaction} \propto d_{Total}$$

The reaction does not need oxygen!
=> Application in vacuum and fluids is possible!

© Fraunhofer IWS

Joining with reactive multilayer systems (RMS)

- Vacuum production process: physical-vapor-deposition (PVD): magnetron-sputter-deposition (MSD)
- RMS geometry: five RMS-sheets á (430 x 220) mm² per deposition run
- Freestanding RMS foil and direct deposition on components available
- Structuring of RMS to complex geometry, for example with a cutter, punching or laser structuring

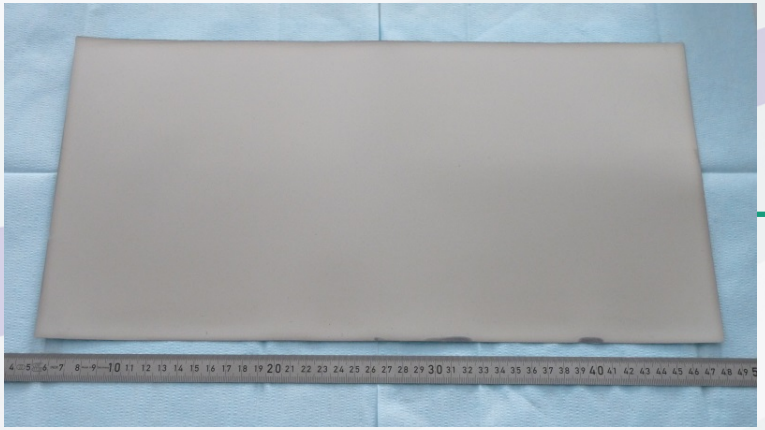

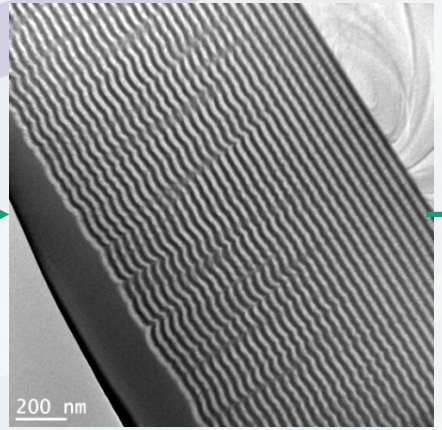

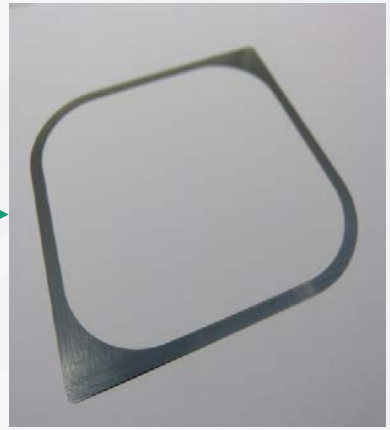

© Fraunhofer IWS

- Controllability of the released heat by designing the layer structure, choosing different material-combinations and their stoichiometric ratio
- Tailoring of the reaction temperature by designing the layer structure and choosing different material-combinations
- Tailoring of the reaction velocity by designing the layer structure, choosing different material-combination and their stoichiometric ratio

Reaction	redundant heat of formation	adiabatic reaction temperature
Ti + Al → TiAl	↓ increasing	1227 °C
Zr + Al → ZrAl		1480 °C
Ni + Al → NiAl		1639 °C
$5Ti + 3Si \rightarrow Ti_5Si_3$		2120 °C
$5Zr + 3Si \rightarrow Zr_5Si_3$		2250 °C
Pd +Al → PdAl		2380 °C

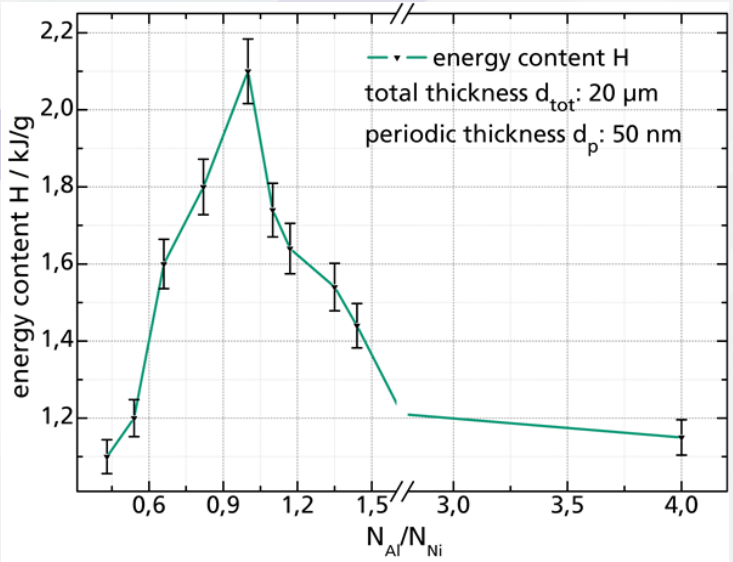

© Fraunhofer IWS

Joining with reactive multilayer systems (RMS)

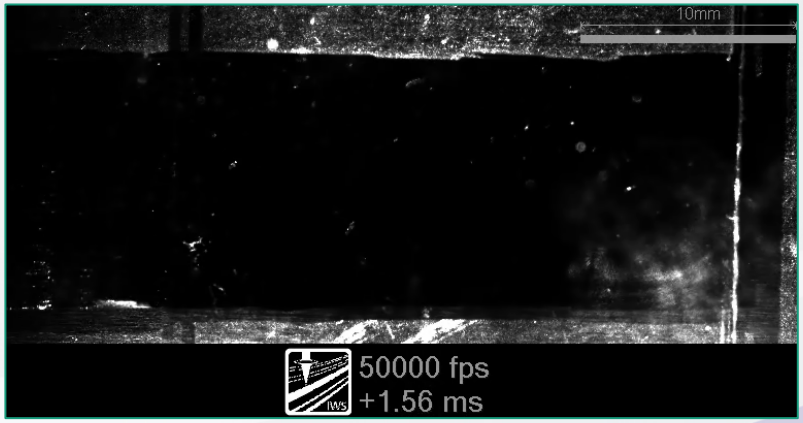

High speed camera video of a RMS reaction front

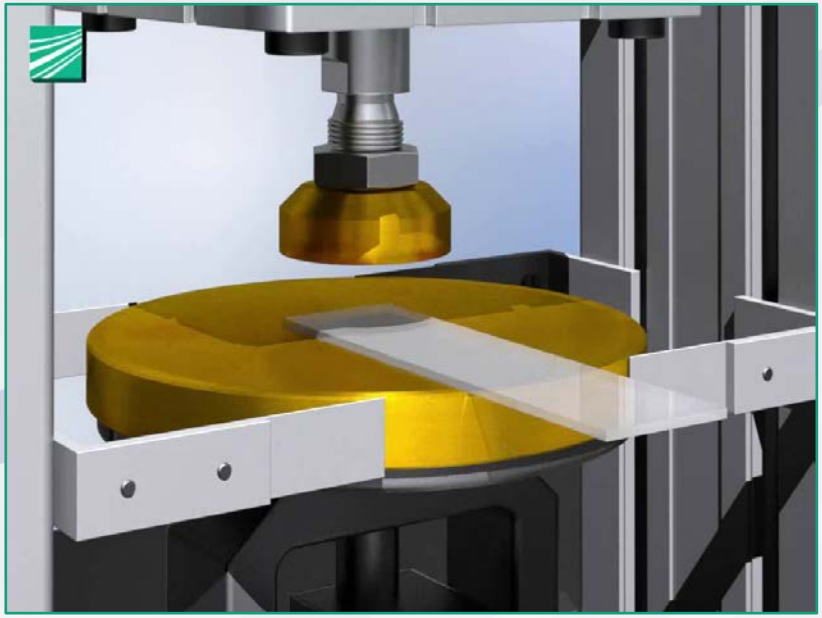

Animated RMS joining process

© Fraunhofer IWS

Joining with reactive multilayer systems (RMS)

- Similar and different materials are joinable e.g.: metal, steel, carbide, polymer, composites, glass, ceramic, diamond, silicon
- Tensile strength:
  - Thermoplastics up to 30 MPa
  - Soldering up to 30 MPa
  - Brazing solder up to 100 MPa

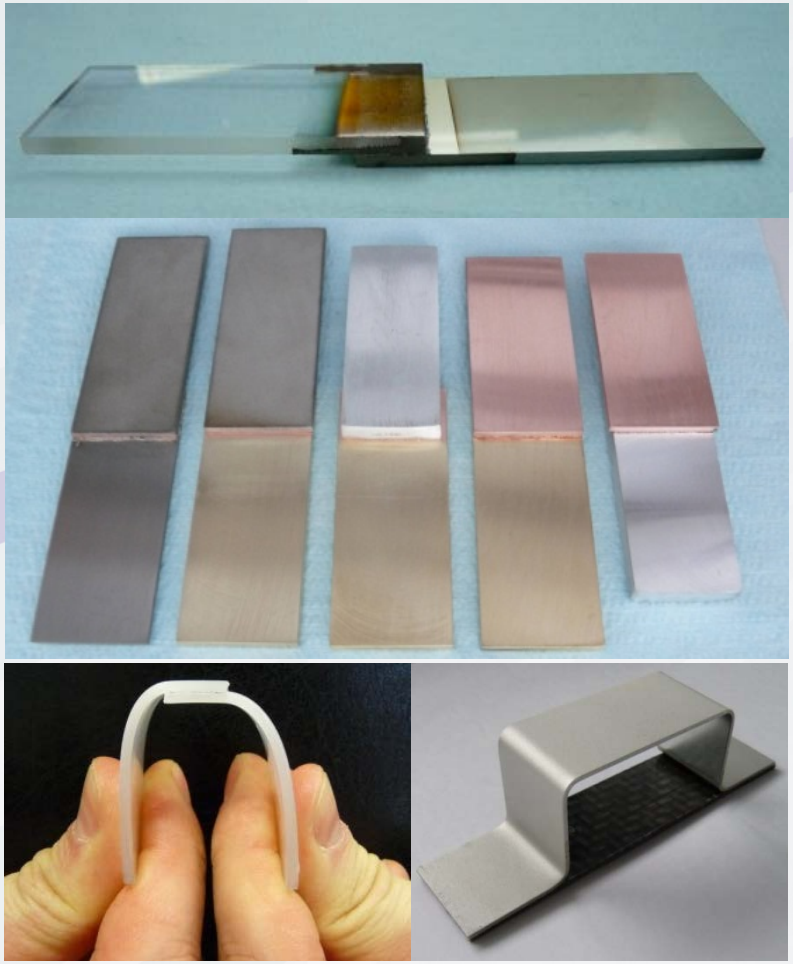

© Fraunhofer IWS

Joining with reactive multilayer systems (RMS)

Microsystems and Sensors:

- High conductive joint of a silicon based peltier element on a copper heatsink

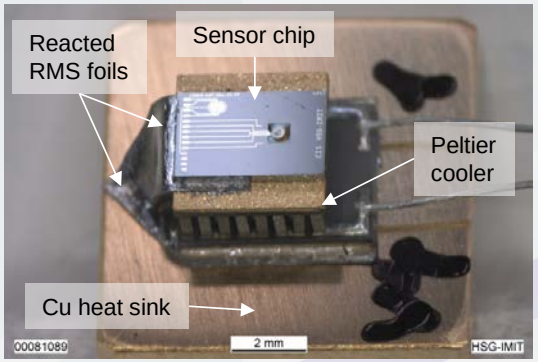

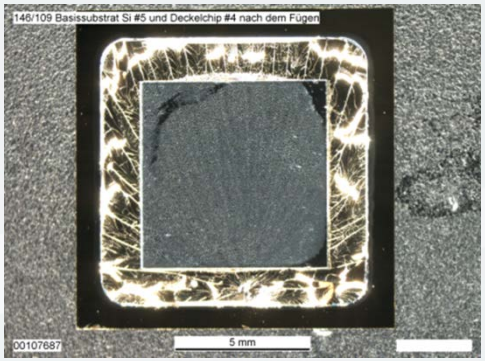

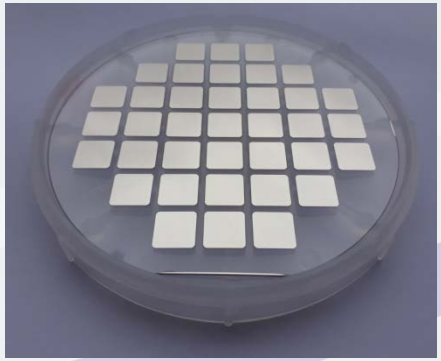

- Integrated high reactive RMS on pyrex (borsilicate wafer) as preform pads for joining of silicon based sensors on waferlevel

Automotive:

- Rubber seal of car door
- Housing cover
- Electrical connections in the field of e-mobility

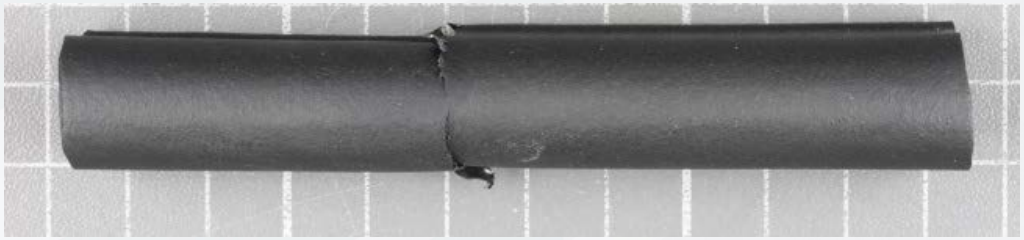

© Fraunhofer IWS

Content

Content	Chapter
Introduction	
The Fraunhofer Gesellschaft	01
Fraunhofer Institute for Material and Beam Technology IWS	02
Seminar topics	03
Laser Beam Welding	
Basics	04
Laser multi pass welding	05
Laser beam welding with high frequent beam oscillation	06
Laser beam welding of high reflective materials	07
Laser beam welding of powertrain components	08
Laser induction roll plating	09
Special Joining Technologies	
Magnetic pulse joining	10
Friction stir welding	11
Joining with reactive multi layers	12
Bonding and Composite technology	
Electrical-conductive bonding	13
Thermal direct joining of thermoplastic to metal	14
Mechanical Joining	
Enhanced mechanical connection by laser interference patterning	15

© Fraunhofer IWS

Tailoring joining technology for low cost localized performance enhancement of metal parts

Topics

Tailored joining technology
Laser multi pass welding
Laser beam welding with high frequent beam oscillation
Laser beam welding of high reflective materials
Laser beam welding of powertrain components
Laser induction roll plating
Magnetic pulse joining
Friction stir welding
Joining with reactive multi layers
Electrical-conductive bonding
Thermal direct joining of thermoplastic to metal
Enhanced mechanical connection by laser interference patterning

Industrial sector & application
Automotive parts
Tooling
Medical devices
Aviation parts
High end consumer products
Power generation parts
High power electronic & E-mobility
Micro-connection technology

© Fraunhofer IWS

Adhesive bonding process at IWS – ALL from a single source!

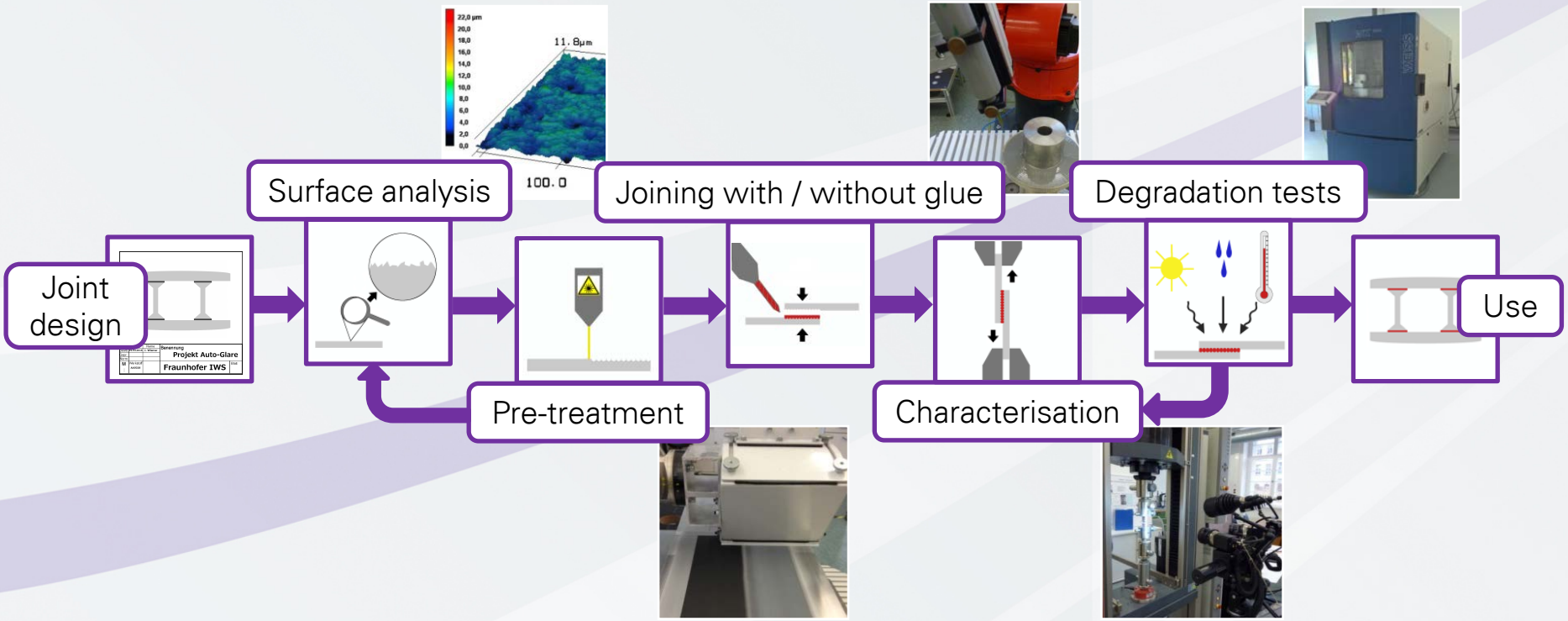

© Fraunhofer IWS

Adhesives with nanoscale fillers

Motivation

- Modification of conventional adhesives with nanoscale fillers
- Adjustment of material properites regarding to
  - Electrical values (isolating, anti-static discharge, electrical conductive)
  - Mechanical values (Shift of the elastic modulus, stress-strain-behaviour)
- Expert knowledge at the field of
  - Different allotropes of carbon (CNTs, CNHs, CB, GNP)
  - Ceramic particles (PMN-PT, $BaTiO_3$, $NaNbO_3$)
- Field of applications
  - Explosion prevention through the discharge of static loads
  - Full polymer dielectric elastomer actuators - artificial muscles

© Fraunhofer IWS

Electrical-conductive Adhesives

Technical basics

- Typical additives:
  - Metallic based additives
    - Silver, gold, …
  - carbon based additives

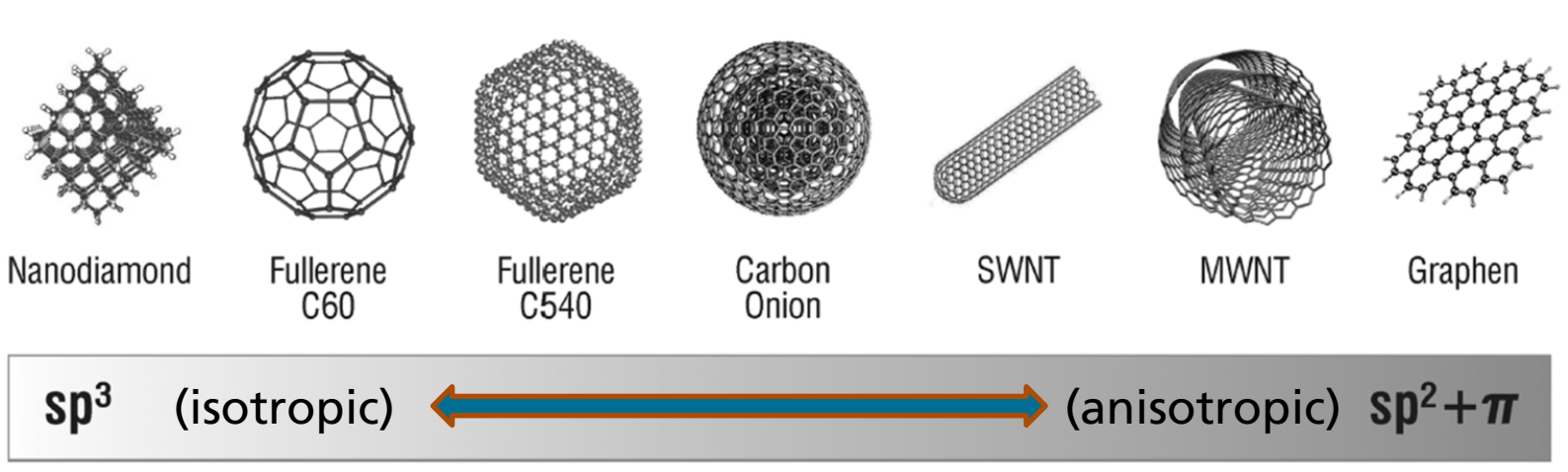

[Mauter, et. al.; Environ. Sci. Technol. (2008), 42: 5843–5859]

© Fraunhofer IWS

Electrical-conductive Adhesives

Technical basics

- Percolation theory

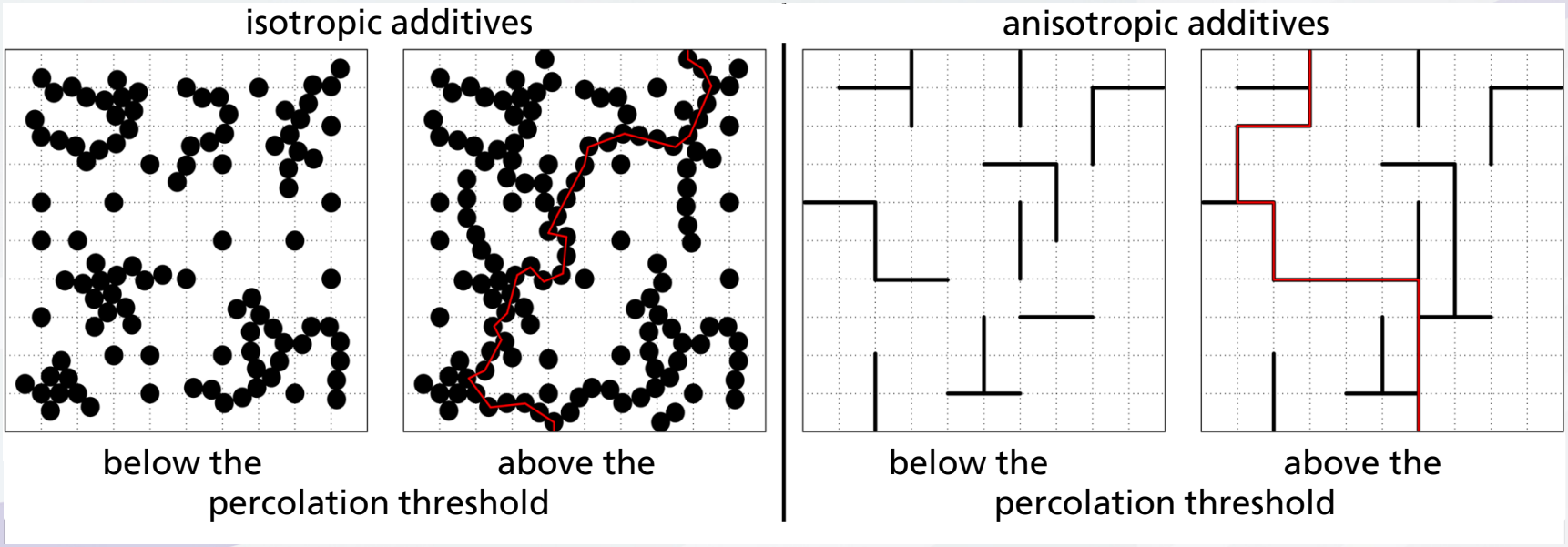

Homogenious dispersion of additives within adhesives
is essential to improves electrical conductivity

© Fraunhofer IWS

Electrical-conductive Adhesives

Technical basics

- Typical additives: metallic or carbon based additives

Additive	+	-
Silver	Excellent conductivity of the raw particles	High amount of particles High filler content necessary
Carbon black	Particle costs	
Graphite	Particle costs Comparatively huge particles	
Graphene	Minor thickness (monolayer)	
CNT´s	High aspect ratio Low filler content necessary	Significant increase of viscosity

© Fraunhofer IWS

Electrical-conductive Adhesives

Technical basics

- Adhesive modification

High pressure dispergator

Twin screw extruder

Sonotrode

Tripple roller

- Influence of bulk material properties:
  - Electrical values (isolating, anti-static discharge, electrical conductive)
  - Mechanical values (Shift of the elastic modulus, stress-strain-behaviour)

© Fraunhofer IWS

Electrical-conductive Adhesives

Application

- Modification of silicone

MWCNT…Multi walled Carbon Nanotube
SWCNT…Single walled Carbon Nanotube
CB…Carbon Black
CNH…Carbon Nanohorns
GP…Graphene Platelets

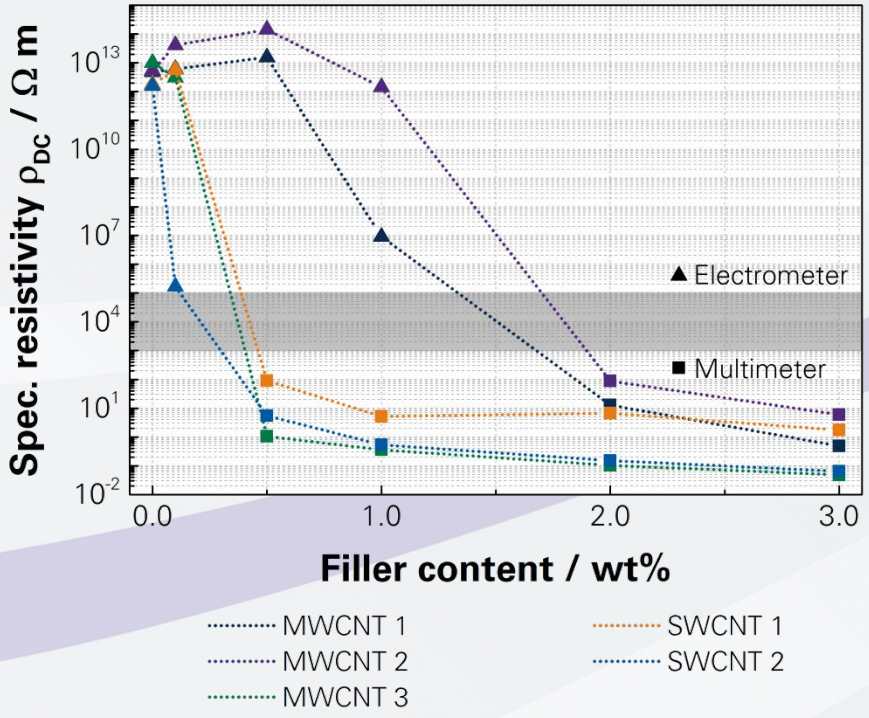

anisotropic additive

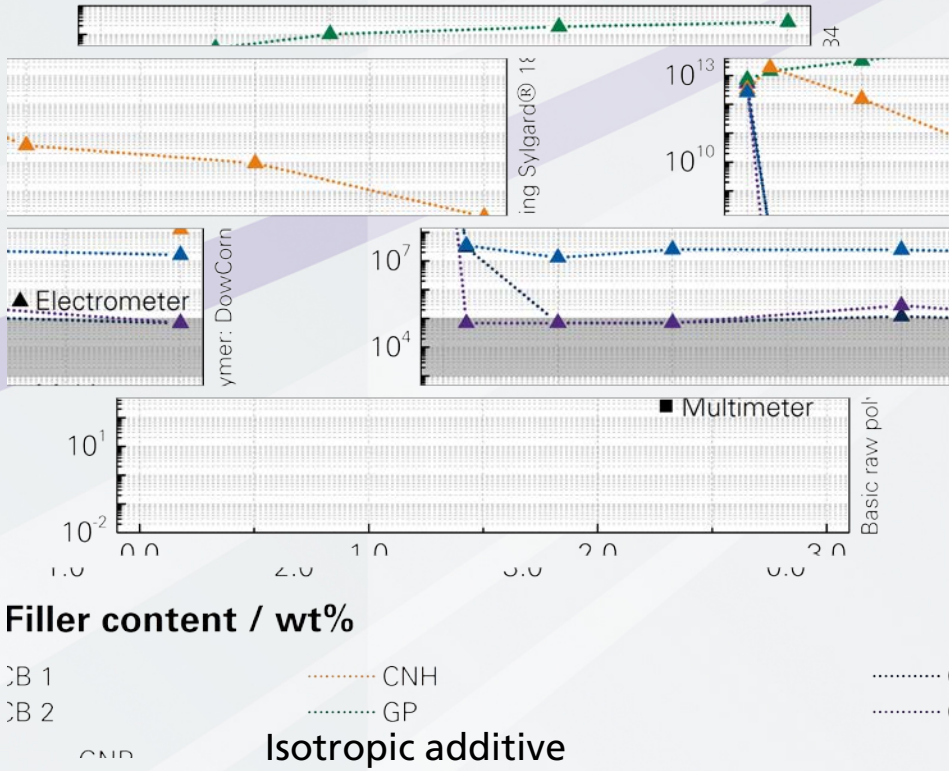

Isotropic additive

© Fraunhofer IWS

Fraunhofer IWS Dresden

Electrical-conductive Adhesives

Application

- Full polymer dielectric elastomer actuators - artificial muscles

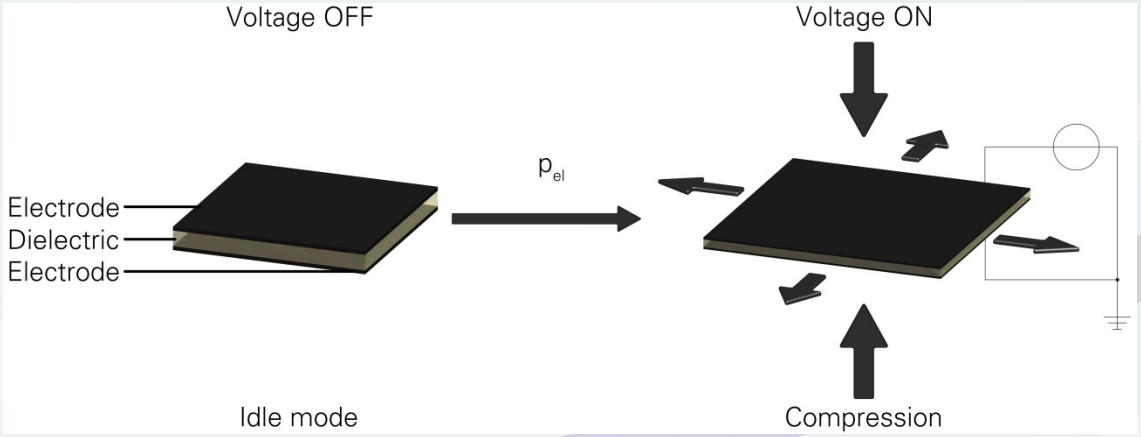

The polymeric electrodes (modified with CNTs) will be loaded with en electrical voltage, these will be attracted to each other and that causes a displacement of the incompressible dielectric layer by the electro-static pressure.

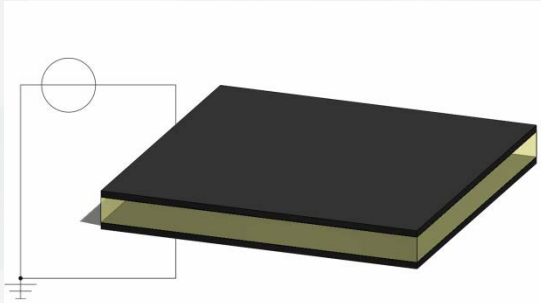

© Fraunhofer IWS

Electrical-conductive Adhesives

Application (Function integration)

- adding of nano and micro particles
- possible application in adhesives:
  - fast curing - adhesives in alternating inductive fields
  - electrical properties - conductivity, discharging and isolating
  - sealing, elastic and structural joints

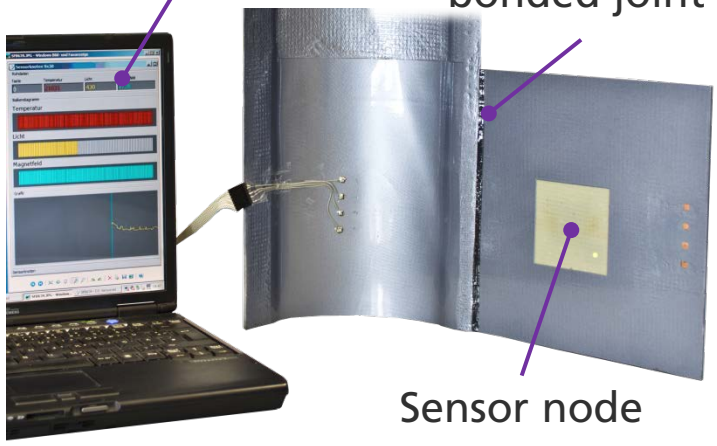

Conductive and structural joint (SFB 639)

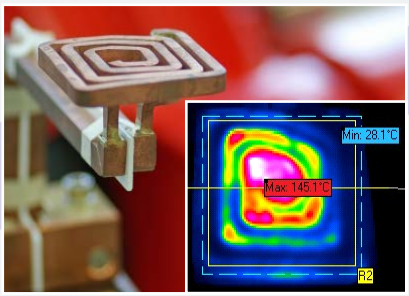

Inductor with heat distribution within the induction field

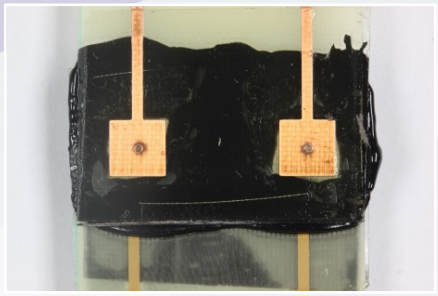

Conductive and structural joint

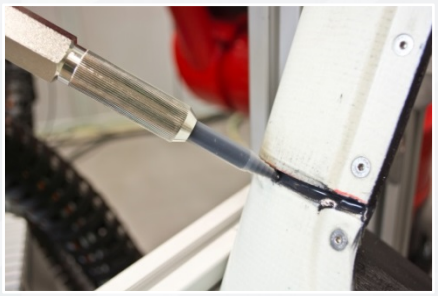

Automated adhesive application

© Fraunhofer IWS

Bonding and Composite Technology

Function integration in adhesives

- adding of nano and micro particles
- possible application in adhesives:
  - fast curing - adhesives in alternating inductive fields
  - electrical properties - conductivity, discharging and isolating
  - sealing, elastic and structural joints

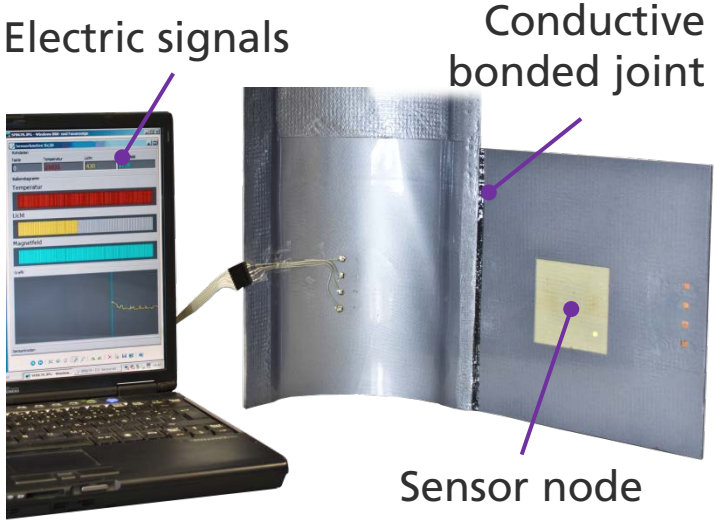

Conductive and structural joint (SFB 639)

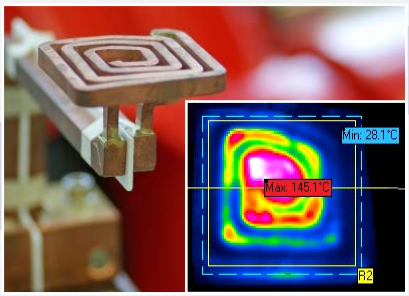

Inductor with heat distribution within the induction field

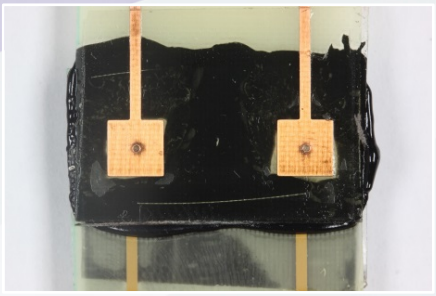

Conductive and structural joint

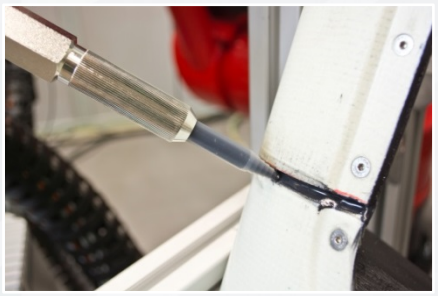

Automated adhesive application

© Fraunhofer IWS

Adhesives with ferromagnetic particles

Motivation

- Integration of ferromagnetic particles in adhesives to improve curing time by using inductive heating
  - Integration of particles by certain dispertion technologies
  - Using an inductive heating system to locally heat the adhesive

© Fraunhofer IWS

Adhesives with ferromagnetic particles

Technical basics

- Thermal curing via induction heating
  - Equipment: Hüttinger TrueHeat HF 3010
  - 11 kW, 400… 600 kHz, controlled via pyrometric sensor
  - Exchangeable liquid-cooled inductors

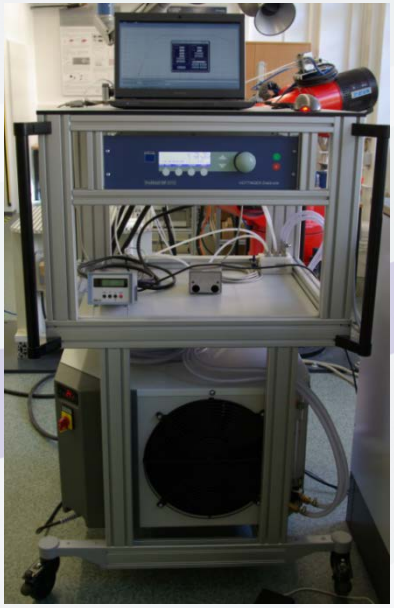

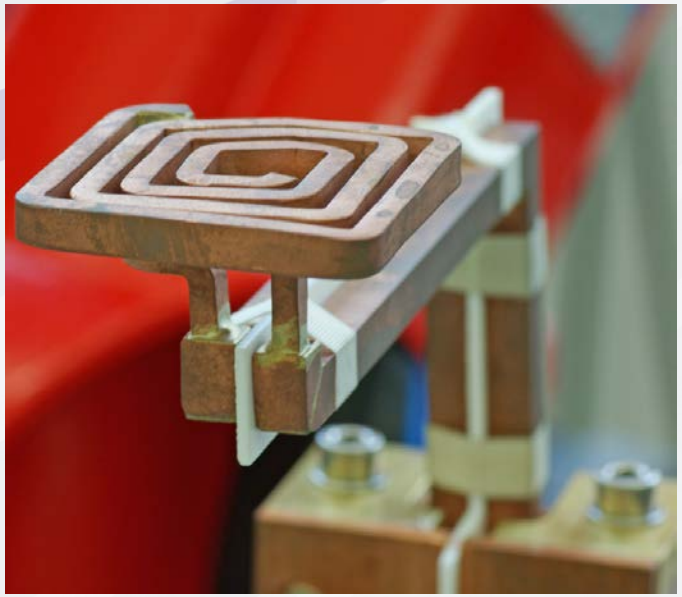

© Fraunhofer IWS

Adhesives with ferromagnetic particles

Technical basics

- Induction curing of NiCo-CFRP-lap-shear-samples
- Heating of the NiCo-sheet
- 20 s @ 210 °C

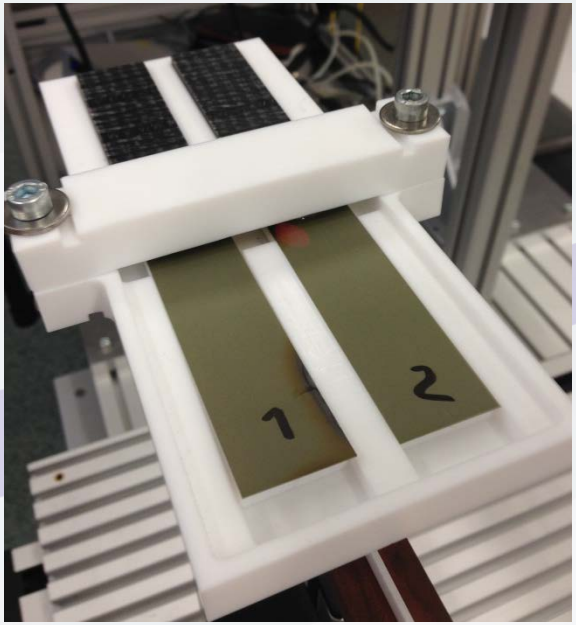

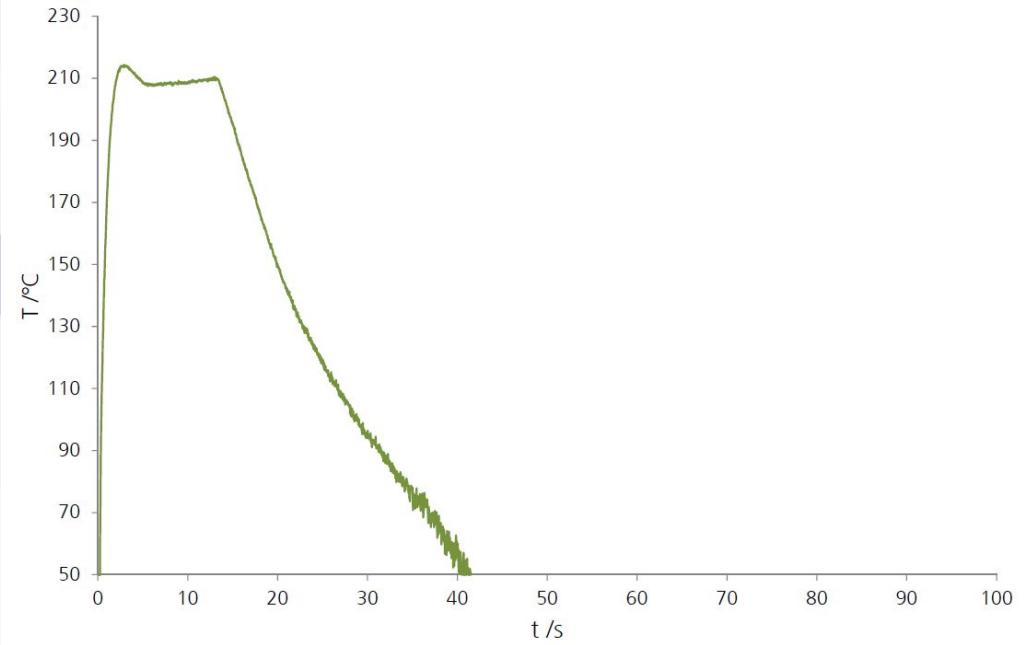

© Fraunhofer IWS

Adhesives with ferromagnetic particles

Technical basics

- Adhesive
  - 1C heat curing epoxy
  - MagSilica® 300 particles
    - Additive for accelerated curing
    - Iron oxide particles (~8µm) with a silica –cover
    - Dispersability: 5, 10, 15 and 20 wt%
- Accelerated curing by inductive heating
- Examples of application
  - Fixation of large area bonding zones and complex multi-body joints
  - Attachment of connecting elements

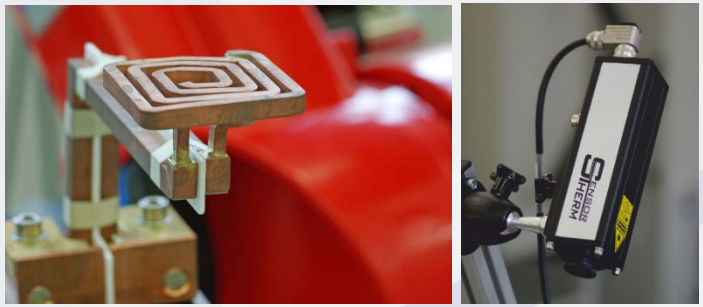

Rectangular inductor and pyrometer

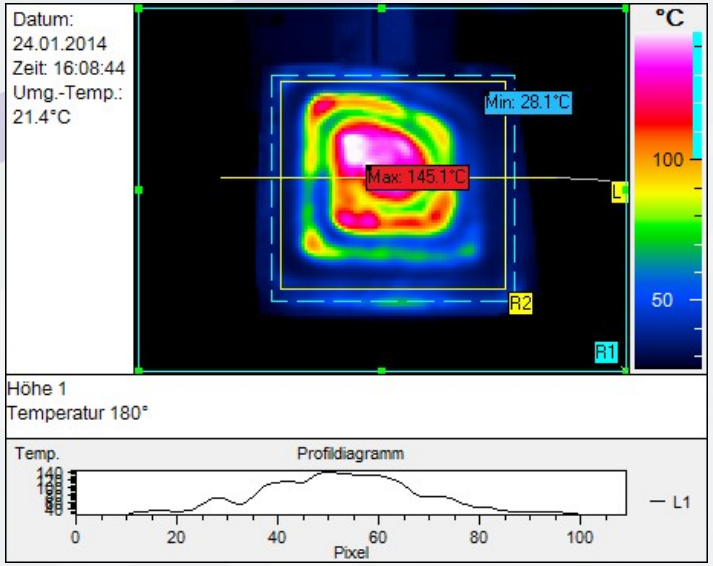

Heat distribution

© Fraunhofer IWS

Adhesives with ferromagnetic particles

Technical basics

- Test set-up
  - Tensile-shear tests on 4 mm thick samples (GF/PP)
  - Adhesive with 5 wt-% Magsilica
  - time and temperature controlled testing
- Results
  - Test setup avoids the destruction of the polymer
  - Comparable bonding strength can be achieved at 130 °C within 5 min

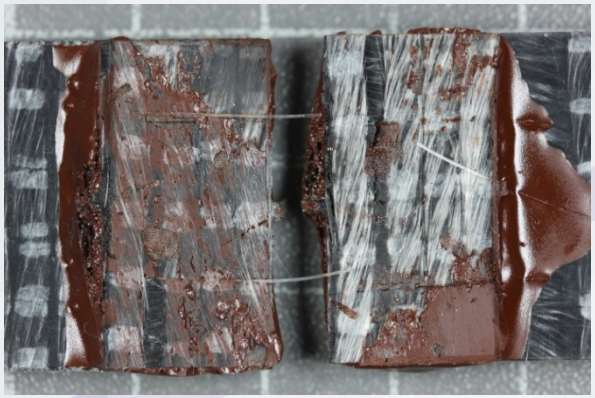

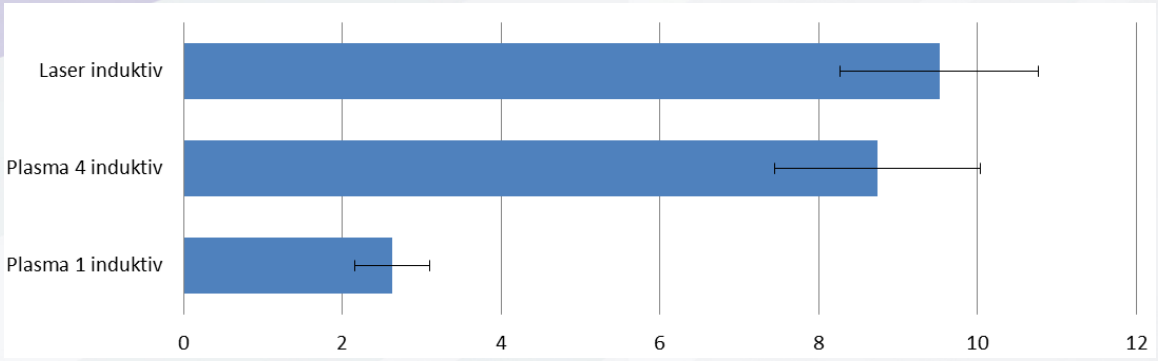

© Fraunhofer IWS

Content

Content	Chapter
Introduction	
The Fraunhofer Gesellschaft	01
Fraunhofer Institute for Material and Beam Technology IWS	02
Seminar topics	03
Laser Beam Welding	
Basics	04
Laser multi pass welding	05
Laser beam welding with high frequent beam oscillation	06
Laser beam welding of high reflective materials	07
Laser beam welding of powertrain components	08
Laser induction roll plating	09
Special Joining Technologies	
Magnetic pulse joining	10
Friction stir welding	11
Joining with reactive multi layers	12
Bonding and Composite technology	
Electrical-conductive bonding	13
Thermal direct joining of thermoplastic to metal	14
Mechanical Joining	
Enhanced mechanical connection by laser interference patterning	15

© Fraunhofer IWS

Composite use in structure?

- material costs
- Production costs
- Integration to metal structure

Trends

- local stiffening
- partial part exchange for „model upscaling“
- Interior integration

Task

- **Fast and productive joining of thermoplastic composites with metal**

© Fraunhofer IWS

Process chain

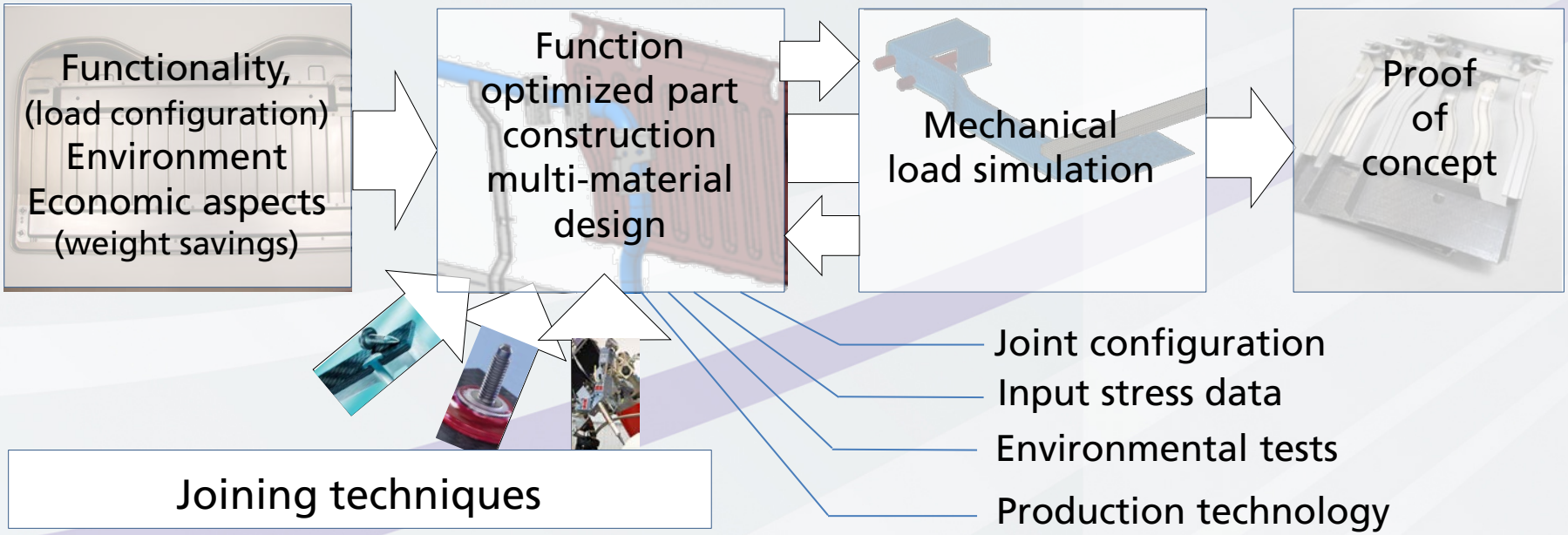

© Fraunhofer IWS

Thermal direct joining of thermoplastic to metal

Thermal direct joining

- Thermoplastics or hot melt required
- Short term heating by laser or induction
- Combination of adhesion bond + mechanical interlocking

Pre-treatment of metal surface !

Adhesive bonding

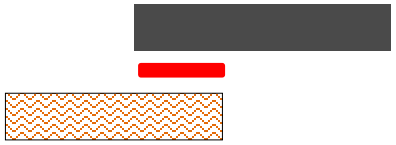

+ Strain and tolerance compensation
- Adhesive application
- Curing time

Thermal direct joining

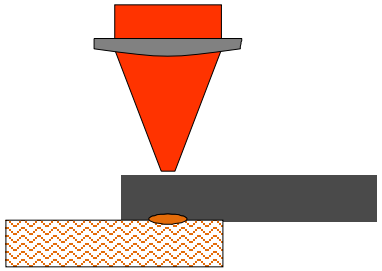

+ No additional material
+ Fast joining
- Residual stresses
- No tolerance compensation

© Fraunhofer IWS

Laser structuring with brilliant cw – fiber laser

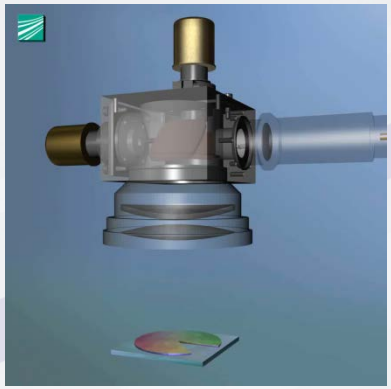

- High speed laser scanning (v > 10 m/s)
- Ablation efficiency: > 200mm²/s @ 2 kW laser power
- Ablation structure depends on composite composition

Function

- Surface extension
- Surface cleaning
- chemical surface modification
- Form-fit structures

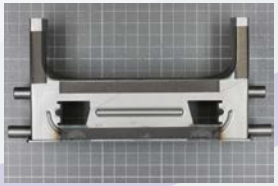

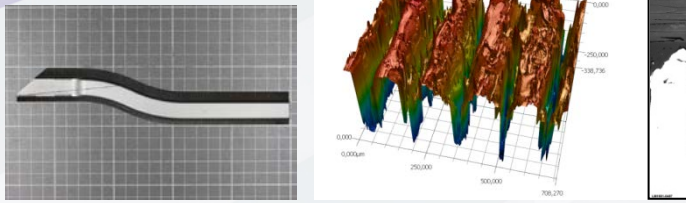

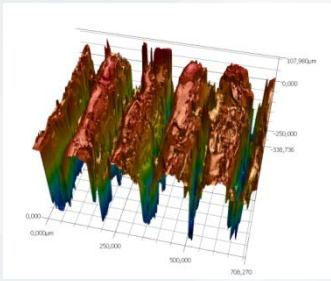

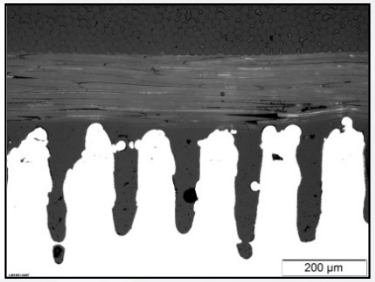

© Fraunhofer IWS

Thermal direct joining of thermoplastic to metal

Thermal direct joining by laser

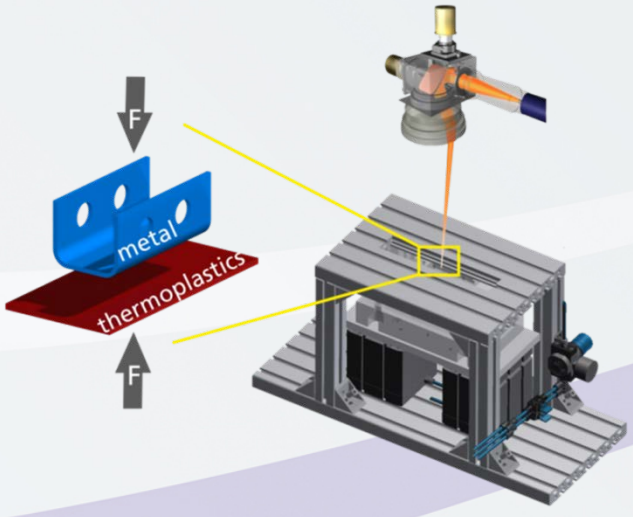

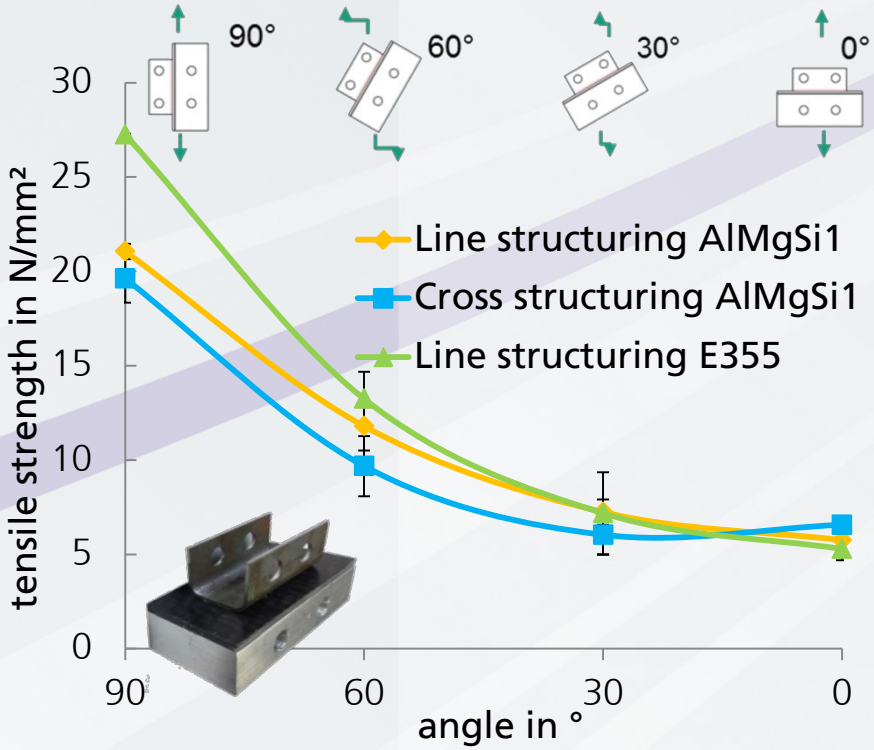

Input data for FEM simulation !

© Fraunhofer IWS

Thermal direct joining by induction

- Access from polymer side
- Fast heating
- Adapted inductor designs
- Simulation of energy coupling

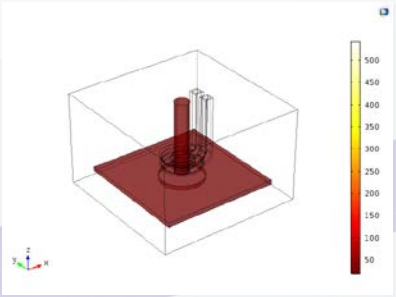

Pancake inductor with concentrator and ceramic ram

Without / with concentrator

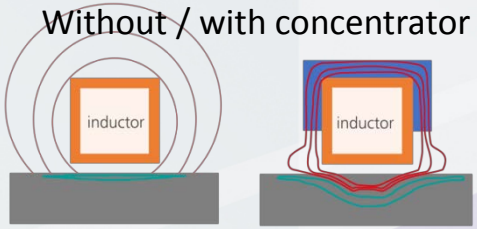

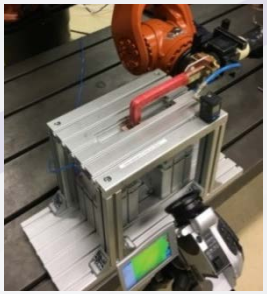

power	up to 60 kW
frequency	15 – 25 kHz
coupling distance	up to 5 mm
joining pressure	0,25 – 6 N/mm²

© Fraunhofer IWS

Thermal direct joining - summary

- Successful process development at coupon level
- Tensile strengths over 25 MPa
- Fast joining by laser and induction
- Strength decrease after 1000 h climate testing (up to 40%)
- Input data for FEM simulation

process	material	heating [sec.]	tensile strength [MPa]
laser	E355	3	25
	1.4301	8	25
	AA6082	3	> 20
induction	E355	4	> 20
	AA6082	3	> 20

Composite: Tepex® dynalite 102-RG600(x), 2 mm
Metal: variable, 1.5 mm
Pre-treatment: laser structuring
Testing conditions: DIN EN 1465

© Fraunhofer IWS

Design and simulation of structural part

- Technology demonstrator: middle arm-rest
- Design change:
  - Metallic weld structure → metal - composite hybrid part
- Demonstration of developed joining processes

Serial construction
MAL Daimler BR205
(carrying structure)

Design study 1

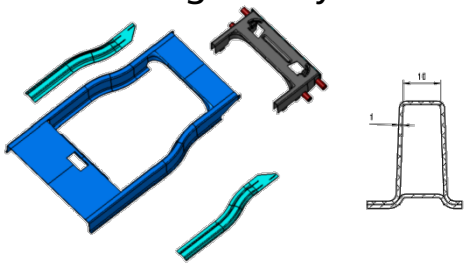

Outlook

Design study 2

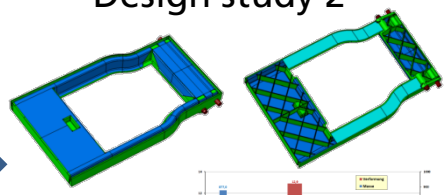

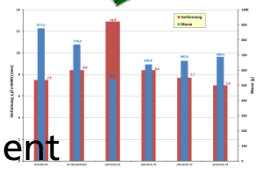

Further development

Design study 2

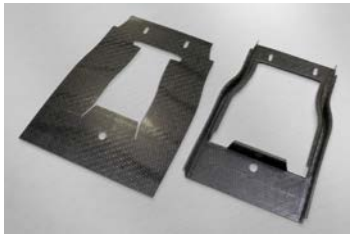

Tepex® dynalite 102-RG600(x)

Mild steel (E355)

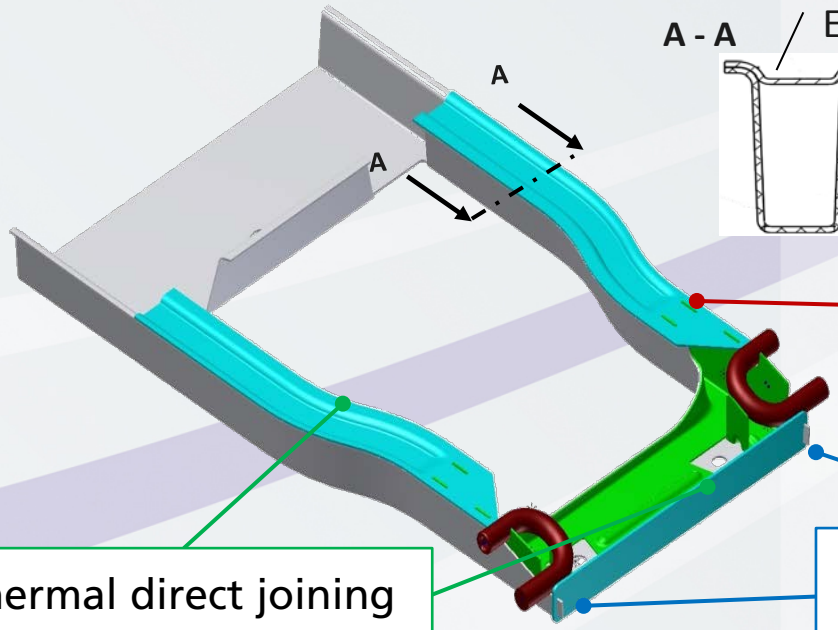

© Fraunhofer IWS

Design study 1: mechanical simulation in abaqus

- Level of detail 1: material=linear-elastic, joints=*TIE
- Level 2: material=linear-elastic, joints=*COHESIVE BEHAVIOR

→ calibration of simulation model by input data

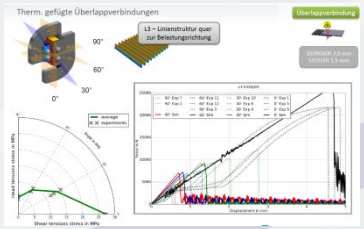

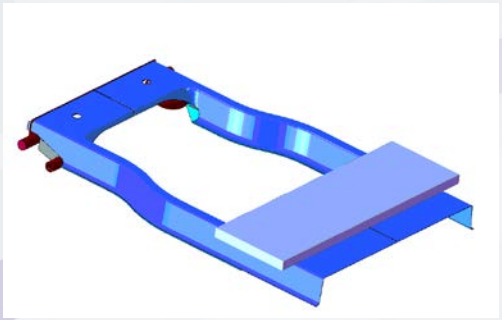

- Level of detail 3: material=MFGenYld+CrachFEM, joints=COHESIVE BEHAVIOR

→ Material tests with variable fiber orientation: compression-tension, shearing, bending…

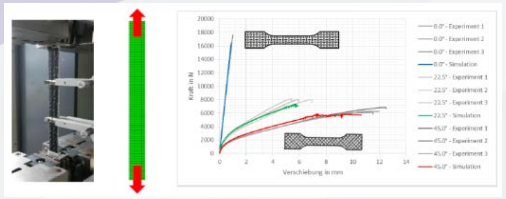

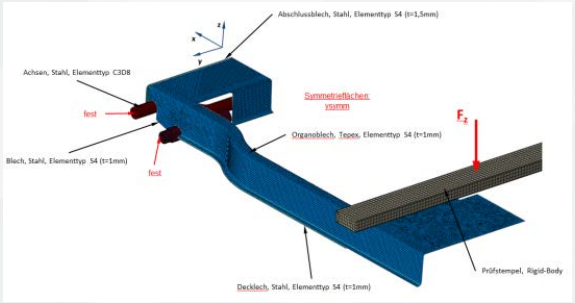

Proof of concept: demonstrator fabrication

Laser surface pre-treatment

Part fixing

Thermal direct joining

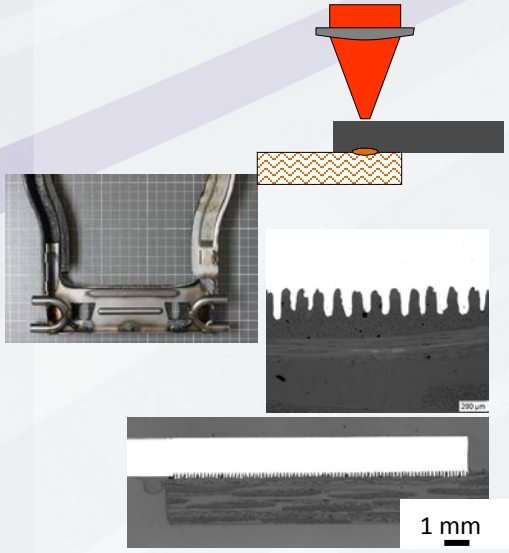

© Fraunhofer IWS

Multi-Remote Station *MuReA @ Fraunhofer IWS*

laser sources:

- 3 kW SM fiber laser
- 3,5 kW CO2 – laser
- 650 w CO_2 sealed-off laser

Laser beam movement by:

- Scanner optics, up to 15 m/s
- XY – table (1,5 x 1,5 m²), up to 100 m/min

- laser welding, heating, ablating
- Pre-treatment by laser and/or atmospheric pressure plasma
- Processing “on the fly”

© Fraunhofer IWS

Laser structuring

- CAD/CAM tool “DCAM”
- Programming of multi-lines and multi-cycles
- Postprocessor for scanner control

Laser power:	1,5 kW
Scanning speed:	5 m/s
Structure distance:	125 µm
cycles:	3

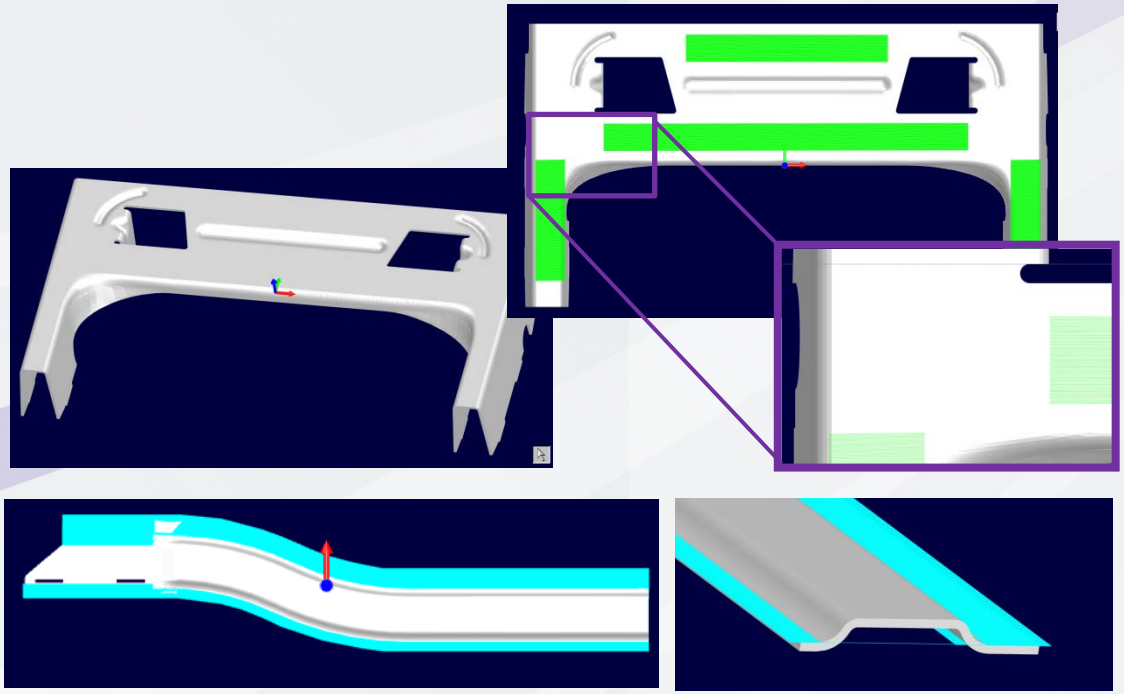

© Fraunhofer IWS

Laser structuring

- CAD/CAM tool “DCAM”
- Programming of multi-lines and multi-cycles
- Postprocessor for scanner control

Laser power:	1,5 kW
Scanning speed:	5 m/s
Structure distance:	125 µm
cycles:	3

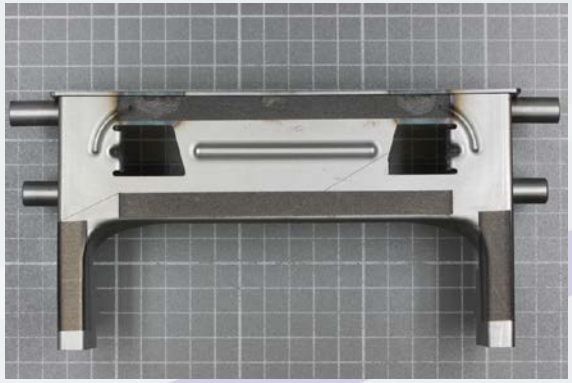

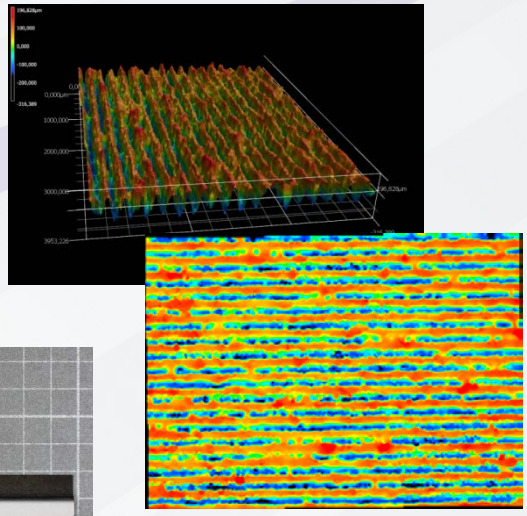

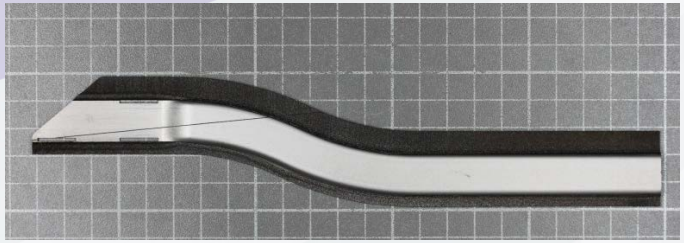

© Fraunhofer IWS

Laser assisted joining

- CAD/CAM tool “DCAM”
- Dynamic beam scanning for flexible heat input

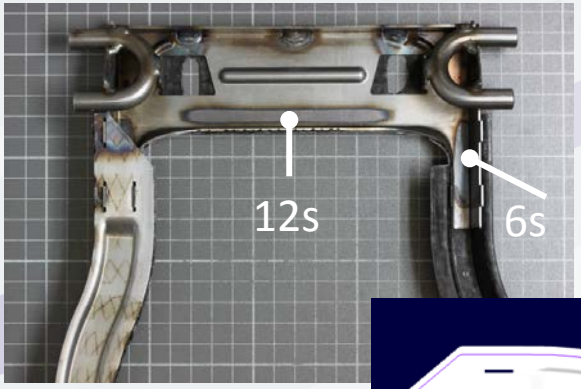

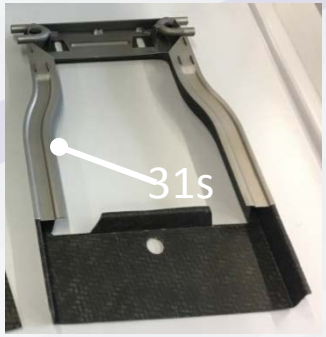

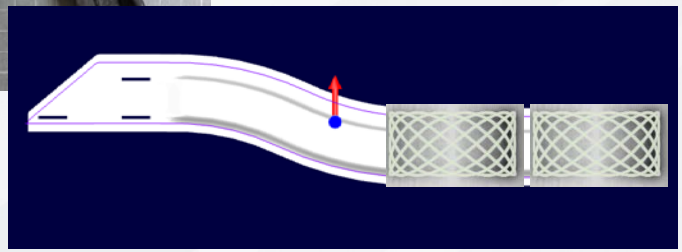

Laser power:	appr. 1 kW
Spot diameter:	appr. 5 mm
Heating time:	variable

© Fraunhofer IWS

SCHERDEL

Fraunhofer IWS Dresden

Mechanical testing

- Static load F_z= 400 N
- Static load F_z= 800 N

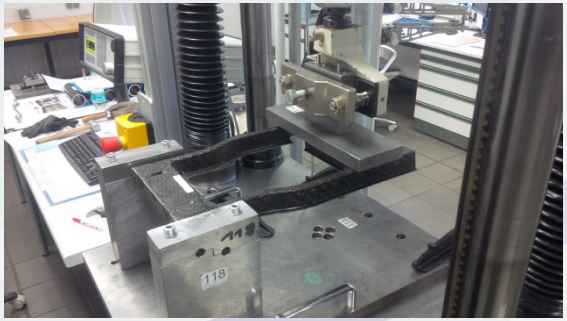

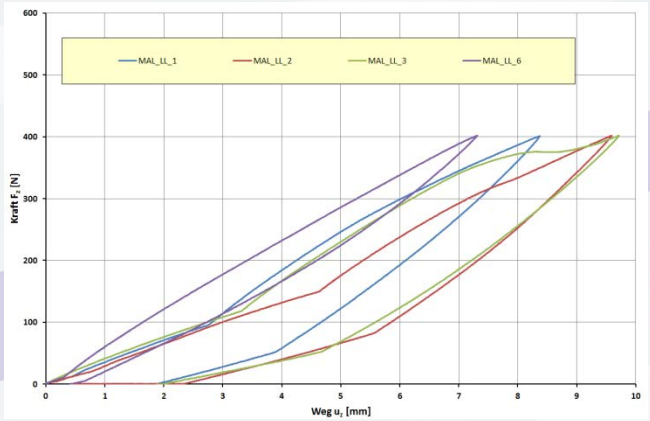

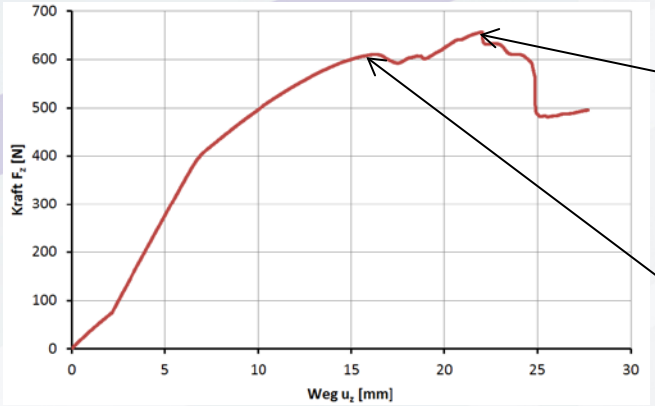

Failure images

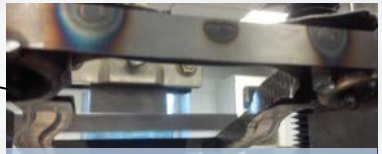

Overlap joint

Slot tab joint

© Fraunhofer IWS

Conclusion I

- Part simulation model with realistic material and joint data was developed
- Detailed characterisation of joint deformation properties needed
- Successful evaluation for load conditions of 400 N
- Stress parameter of coupon tests and demonstrator fabrication have to be validated to fit FEM and destructive testing

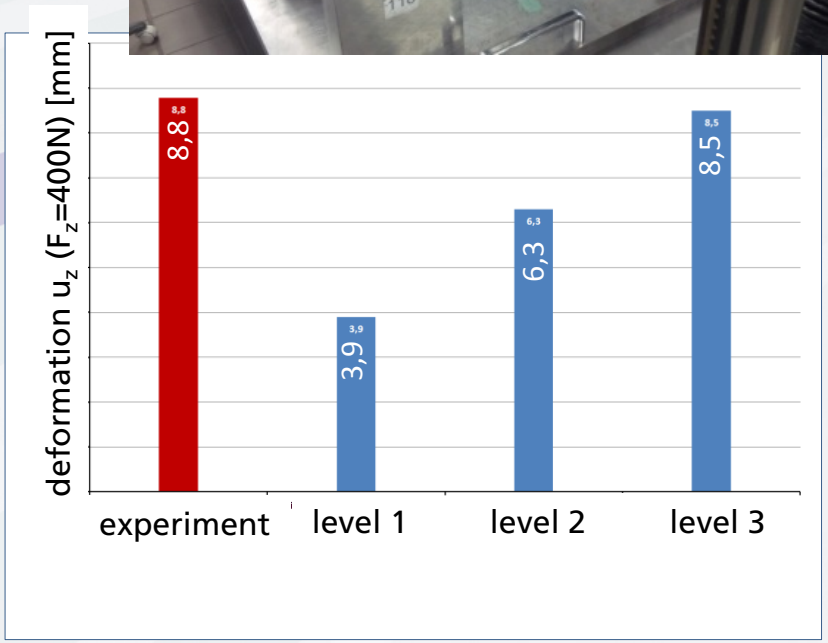

© Fraunhofer IWS

Conclusion II

- Thermal direct joining has potential to use in mass production (handling, process time, tolerances,..)
- Future demonstrator design (study 2) provide 30% weight saving and acceptable economic assessment
- Industrialisation concepts are under investiation

© Fraunhofer IWS

Content

Content	Chapter
Introduction	
The Fraunhofer Gesellschaft	01
Fraunhofer Institute for Material and Beam Technology IWS	02
Seminar topics	03
Laser Beam Welding	
Basics	04
Laser multi pass welding	05
Laser beam welding with high frequent beam oscillation	06
Laser beam welding of high reflective materials	07
Laser beam welding of powertrain components	08
Laser induction roll plating	09
Special Joining Technologies	
Magnetic pulse joining	10
Friction stir welding	11
Joining with reactive multi layers	12
Bonding and Composite technology	
Electrical-conductive bonding	13
Thermal direct joining of thermoplastic to metal	14
Mechanical Joining	
Enhanced mechanical connection by laser interference patterning	15

© Fraunhofer IWS

Tailoring joining technology for low cost localized performance enhancement of metal parts

Topics

Tailored joining technology
Laser multi pass welding
Laser beam welding with high frequent beam oscillation
Laser beam welding of high reflective materials
Laser beam welding of powertrain components
Laser induction roll plating
Magnetic pulse joining
Friction stir welding
Joining with reactive multi layers
Electrical-conductive bonding
Thermal direct joining of thermoplastic to metal
Enhanced mechanical connection by laser interference patterning

Industrial sector & application
Automotive parts
Tooling
Medical devices
Aviation parts
High end consumer products
Power generation parts
High power electronic & E-mobility
Micro-connection technology

© Fraunhofer IWS

Nano and microstructured surfaces for improved surface functions

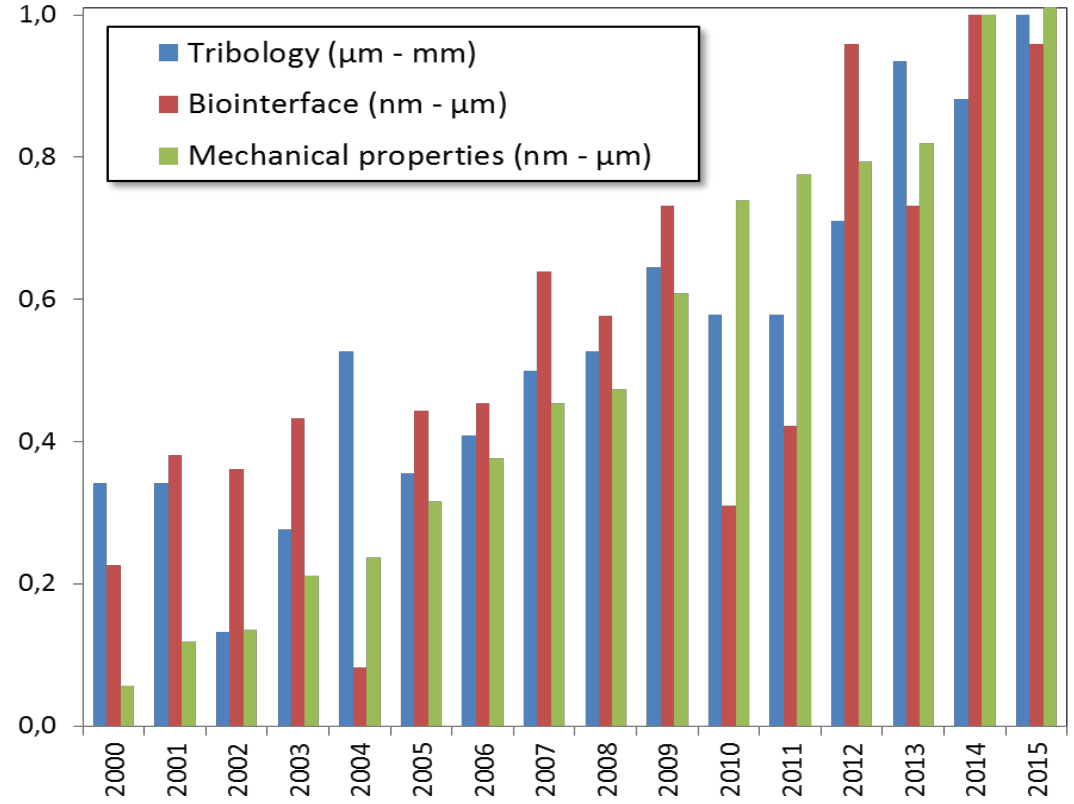

Tribology: 664 articles
Reduced friction & wear using structured surfaces
Feature sizes: µm – mm

Biointerface: 845 articles
Improved cell attachment, bacteria adhesion reduction, etc.
Feature sizes: sub-µm – µm

Mechanical properties:
3813 articles
Improved stiffness, hardness, etc.
Feature sizes: nm – µm

© Fraunhofer IWS

Enhanced mechanical connection by laser interference patterning

Surface structuring up to now only rough or slow…

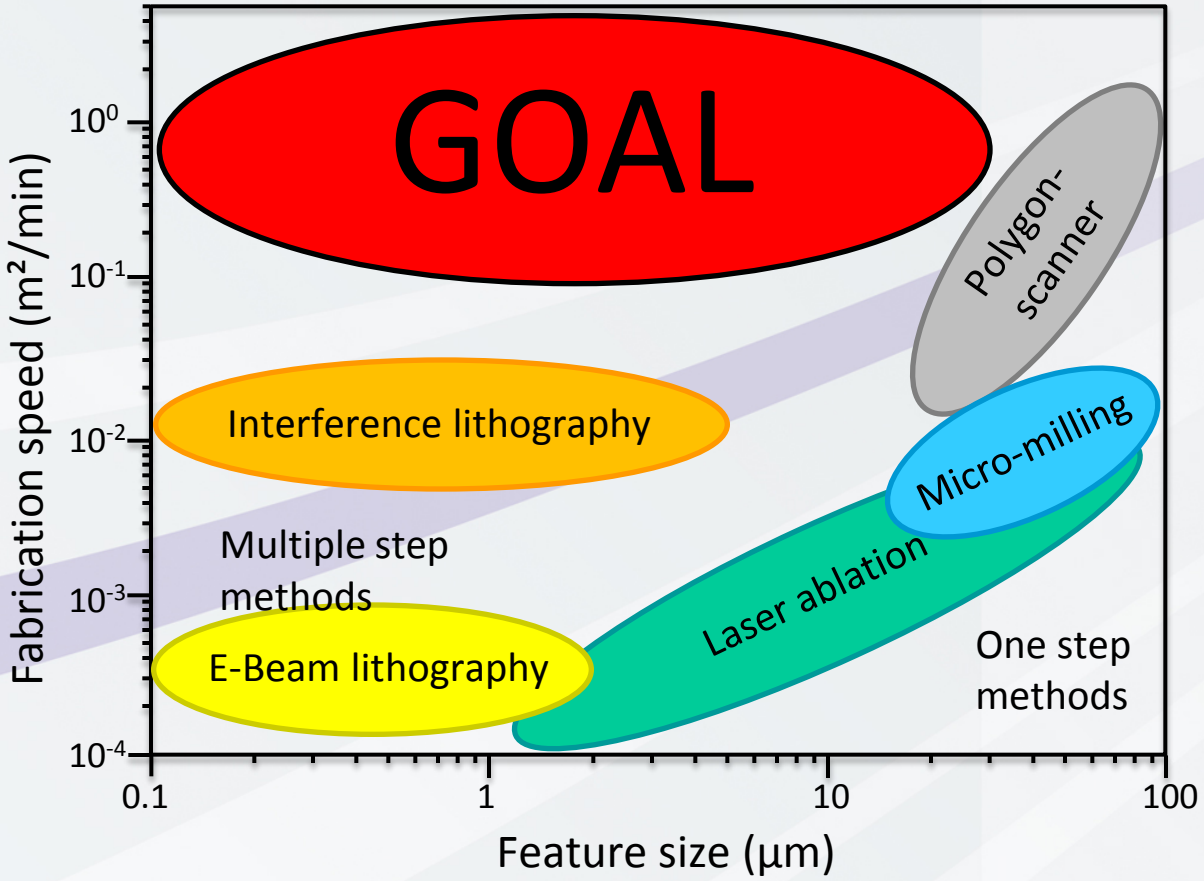

© Fraunhofer IWS

Enhanced mechanical connection by laser interference patterning

Direct Laser Interference Patterning (DLIP)- a new concept for direct laser structuring

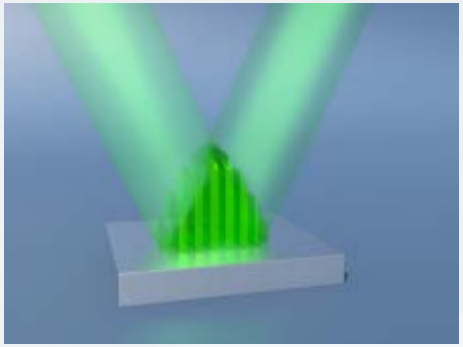

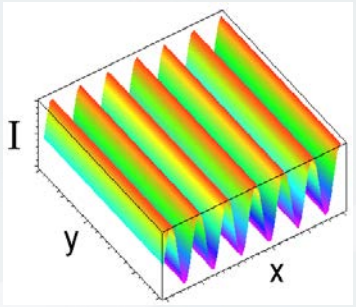

$$p = \frac{\lambda}{2\sin(\theta)}$$

- Resolution → λ
- Geometry → number and angle of beams, polarization, intensity
- Structuring process →local melting, ablation, reaction

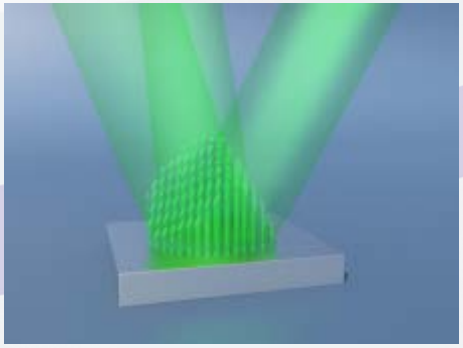

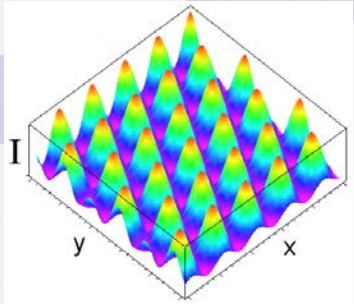

$$p = \frac{\lambda}{\sqrt{3}\sin(\theta)}$$

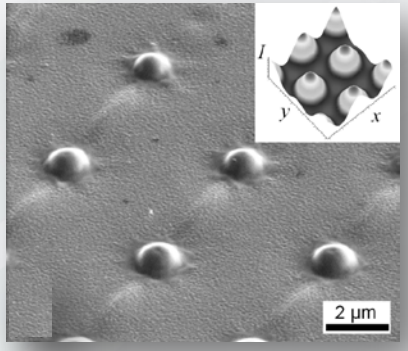

© Fraunhofer IWS

Enhanced mechanical connection by laser interference patterning

From LAB to FAB! - DLIP optical heads

Concept 1: High speed (2010)

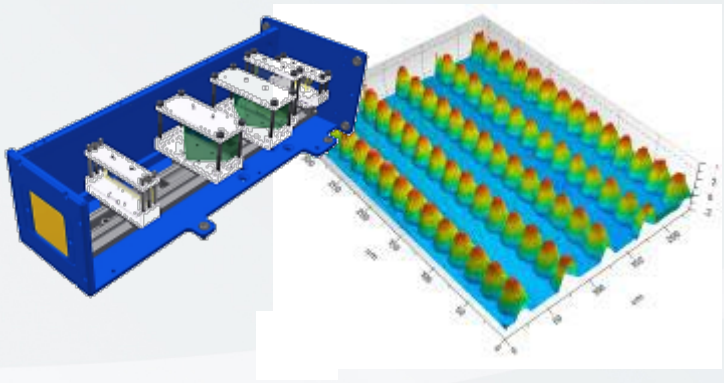

- Fabrication speed: **0.36 m²/min** for metals; **0.90 m²/min** on polymer

WORLD RECORD!

- Sub-beams shaped up to **300 mm**
- Geometry and size fixed
- Applicable with **ns**-pulsed Laser system (tested up to **200 W**)

Concept 2: High flexibility (2012)

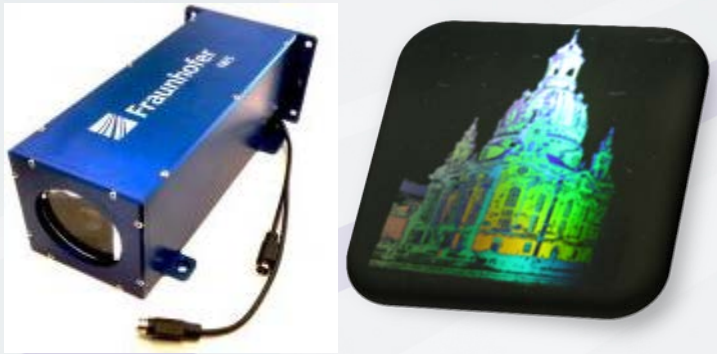

- Holographic pixels with **multiple geometry and size**
- Possible integration in existing laser writing systems
- For **ns** and **ps** laser systems operating in UV, VIS or IR wavelength

© Fraunhofer IWS

Enhanced mechanical connection by laser interference patterning

From LAB to FAB! - complete DLIP systems

- Resolution up to **1000 DPI** possible
- Processing of **3D** parts possible
- Possible feature sizes

  Metals > 1 µm (ns)

  Metals < 1 µm (ps)

  Polymers > 150 nm (ns, ps)

DLIP-µFAB System developed at Fraunhofer IWS. Processing area: 200 mm x 200 mm. Equipped with IR, Green or UV Laser system.

DLIP µFab

A. F. Lasagni, et al., Proc. of SPIE Vol. 9735 973515 (2016).

© Fraunhofer IWS

Enhanced mechanical connection by laser interference patterning

From LAB to FAB! - complete DLIP systems

- Up to **600 mm** length, **300 mm** diameter possible
- With **ns** and **ps** lasers and optical heads
- Resolution in sub-µm level possible (**300 nm feature size** with ps laser)
- Processing cost today: **30,000 – 200,000 €**
  with DLIP → 400 - 500 €

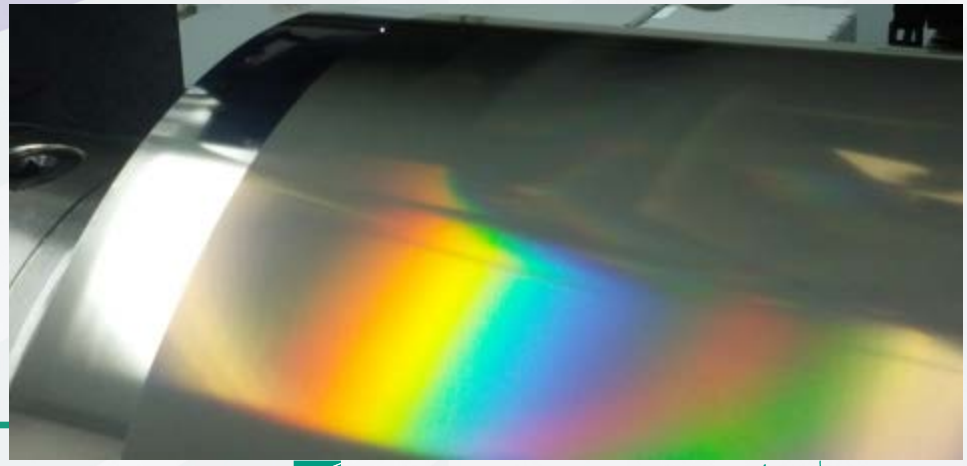

© Fraunhofer IWS

Enhanced mechanical connection by laser interference patterning

Strongly enhanced reliability required

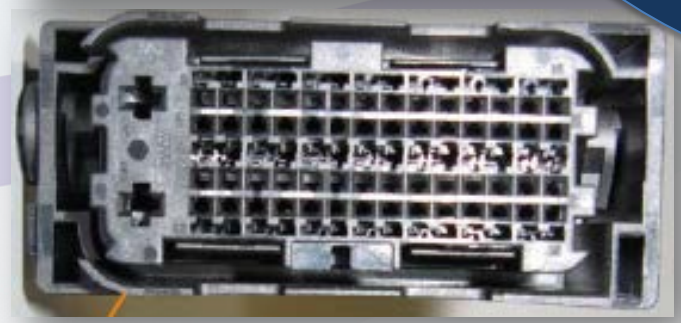

Car Breakdown Statistics

(ADAC Germany, 2014)

- **Electrical system: 46%**
- Motor management: 16%
- Engine: 7%
- Fuel system: 5%
- Air conditioning: 4%
- Miscellaneous 21%

kg
3100 m
1745

No. of electrical connectors: 2300

No. of contact housings: 671

→ + autonomous driving!

© Fraunhofer IWS

Enhanced mechanical connection by laser interference patterning

Reducing contact resistance by contact area patterning

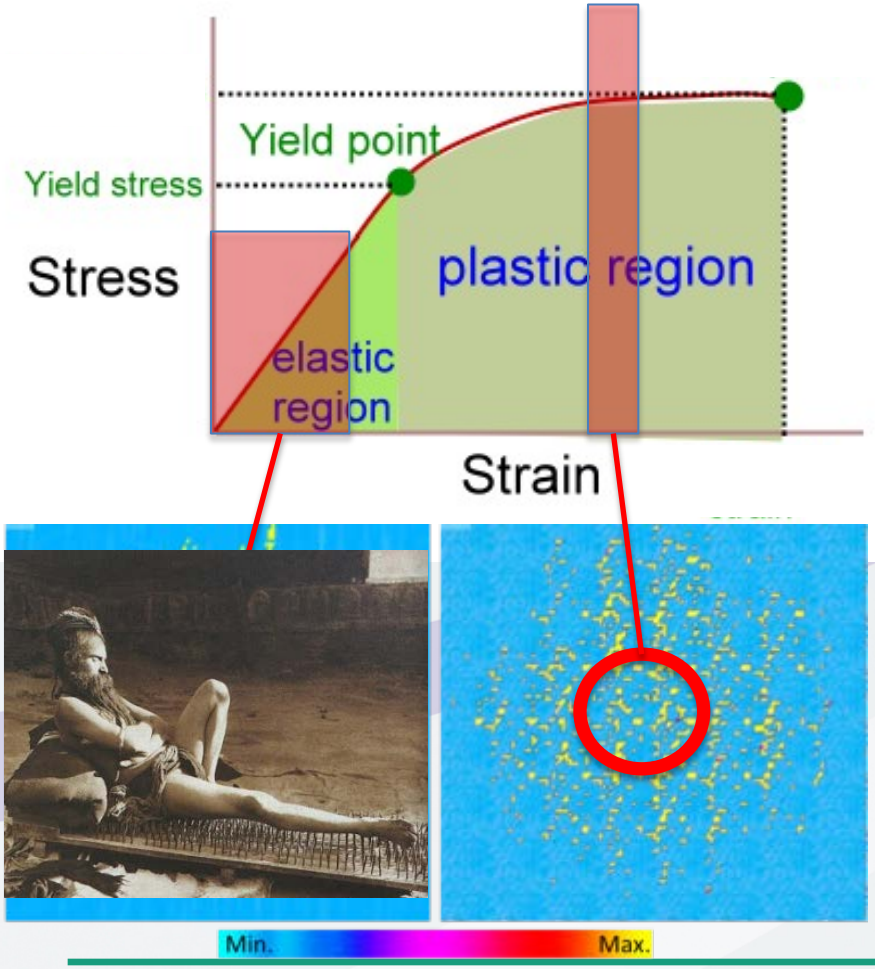

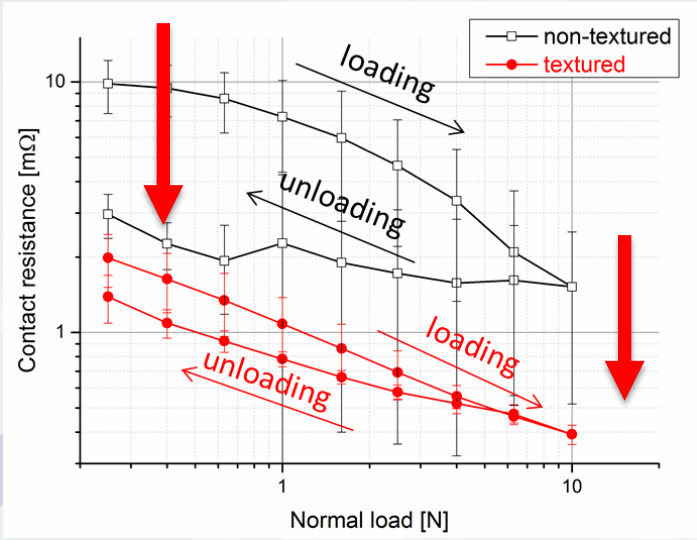

etal

- Contact pressure patterning
- Patterned oxide layer piercing
- Topographic particle trapping

Reliable contact resistance reduction: 80 %

© Fraunhofer IWS

Enhanced mechanical connection by laser interference patterning

Implementation into connector production line

Simultaneous two sided selective texturing
of pre plated or pre stamped strip material

High speed DLIP processing: **line speed 60 m/min (1 m/s)**
4266 connectors/min
ca. 40 sec / 1 Audi A8 (2300 connectors)

Cost DLIP processing: ca. 0.0001 Euro/contact
0.21 Euro /1 Audi A8
(calculated: 24/7, 100 contacts/min, 5 years…)

Timeline: 2016 – 2018 Design of pilot reel to reel line
2018 – 2021 **Start of production to deliver connector into automotive market**

© Fraunhofer IWS

Questions?

Contact:

Dr. Jens Standfuss

Business Unit Manager
JOINING
Fraunhofer Institute for Material and Beam Technology

Winterbergstrasse 28
01277 Dresden
Germany

Phone **+49 351 83391 3212**
Fax **+49 351 83391 3210**

jens.standfuss@iws.fraunhofer.de
www.iws.frainhofer.de

© Fraunhofer IWS

活動五

利用金屬基複合材料生產高韌度和強部件研討會

由國立台灣科技大學機械工程部黃崧任教授主講

Mg Metal-Matrix Composites (MMCs)

Song-Jeng Huang 黃崧任

TAIWAN TECH National Taiwan University of Science and Technology

Fabrication of Mg MMCs

(1) Melt-stirring technique
(2) Tube Extrusion of Mg MMCs
(3) Heat sink materials for LED

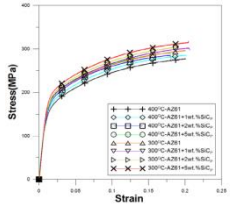

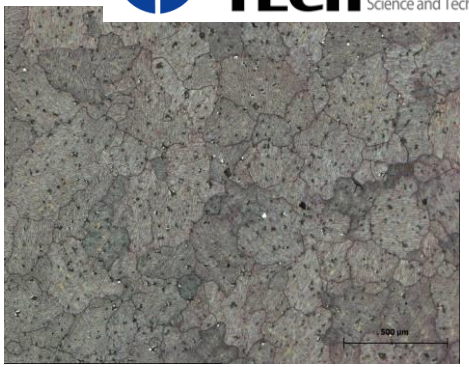

AZ91D/2wt%AlN-100X

[Acta Metallurgica Slovaca, Vol. 16, 2010]

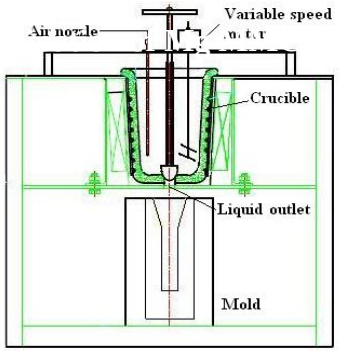

(1) Melt-stirring technique

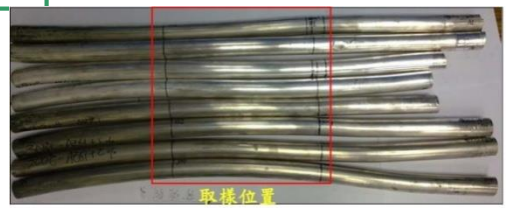

(2) Tube Extrusion of Mg MMCs

•**Best paper award** of 2011 annual conference of Taiwan Magnesium Association

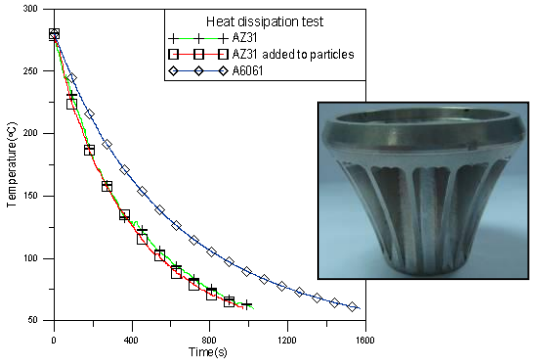

(3) Heat sink materials for LED

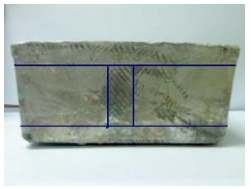

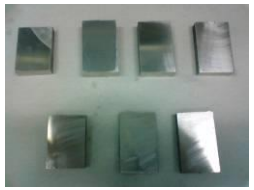

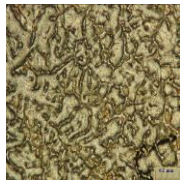

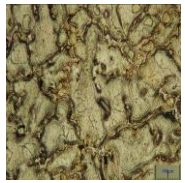

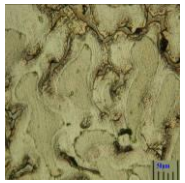

Mg MMCs

➢**In recent 5 years** (since 2009), SJ Huang obtained **24 project grants from MOST** and other organizations, and fruitfully published **22 journal papers and 40 conference papers**. Three of his invented **technologies have been transferred to 3 private Taiwanese companies.**

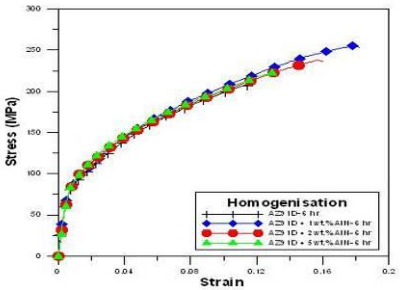

Mg Metal-Matrix Composites (MMCs)

Song-Jeng Huang 黃崧任

TAIWAN TECH National Taiwan University of Science and Technology

(4) ECAP

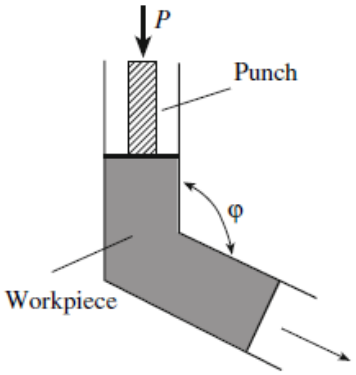

Diagram of performance of SPD using ECAP techn

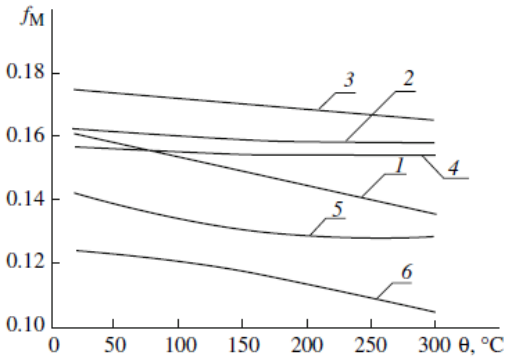

Fig. 7. Temperature dependences of the molecular component of the friction coefficient for studied alloys in the contact with steel R18: (*1*) AZ91D in the starting state, (*2*) AZ91D + SiC (S = 5 μm, C = 3%), (*3*) the same, S = 11 μm, C = 3%, (*4*) the same, S = 11 μm, C = 6%, (*5*) the same, S = 15 μm, C = 3%, and (*6*) AZ91D after two ECAP cycles.

Journal of Friction and Wear, Vol. 30, No.3. pp. 194-198 [NSC 95-2811-E-194-001 , NSC96-2923-E-194-001-MY3 (NSC-RFBR Taiwan-Russian Bilateral research project)]

Wear of Mg MMCs by severe plastic deformation (SPD)

(4) equal-channel angular pressing (ECAP)
(5) Wear of AZ91D MMCs
(6) Advanced Mg nano-MMCs reinforced by WS2 nanotubes

(6) Advanced Mg nano-MMCs reinforced by WS2 nanotubes

Best Paper Award in Composites of Colloquium of Metallurgy and Metallurgical Engineering CMME 2014 & 20th Anniversary of Acta Metallurgica Slovaca

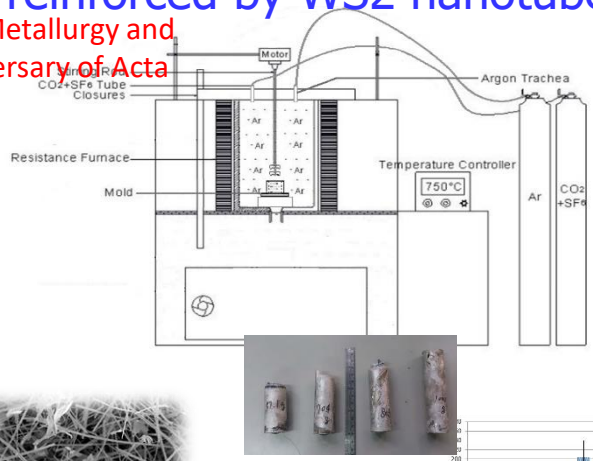

Mg-MMC ingots prepared at different temperatures

(5) Wear of MMCs

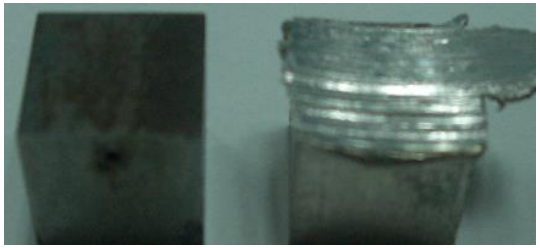

Outward appearance of AZ91D MMCs before and after wear test [Tribology Letters, 2010] [NSC95-2811–E–194–001]

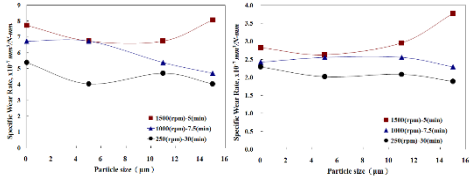

(a) (b)

Specific wear rate of MMCs with particle size of 3vol.% SiCp in AZ91D MMCs: loaded up to (a) 10N, (b) 50N. [Tribology Letters, 2010]

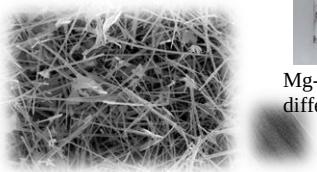

a. SEM image of an assortment of WS_2 nanotubes;
b. TEM image of a single WS_2 nanotube. Scale bar is 5 nm.

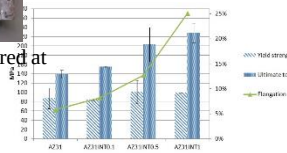

Summary of the mechanical testing of the different Mg-alloy samples.

Mg Metal-Matrix Composites (MMCs)

Song-Jeng Huang 黃崧任

TAIWAN TECH National Taiwan University of Science and Technology

Application of Mg MMCs

(7) Micro-arc Oxidation
(8) Magnesium hydrogen storage

(7) Micro-arc Oxidation

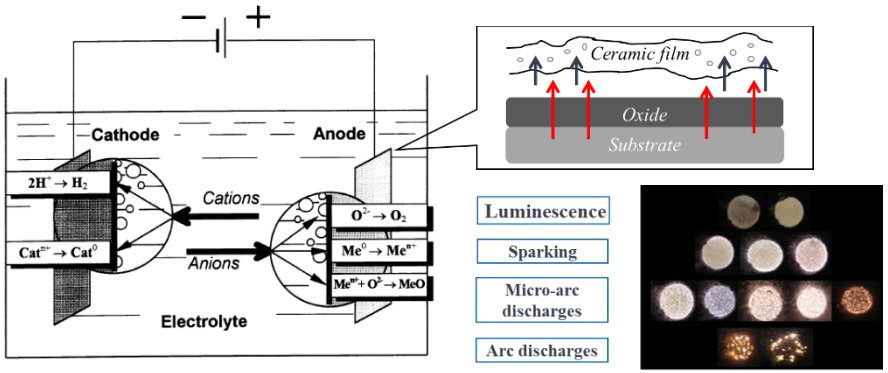

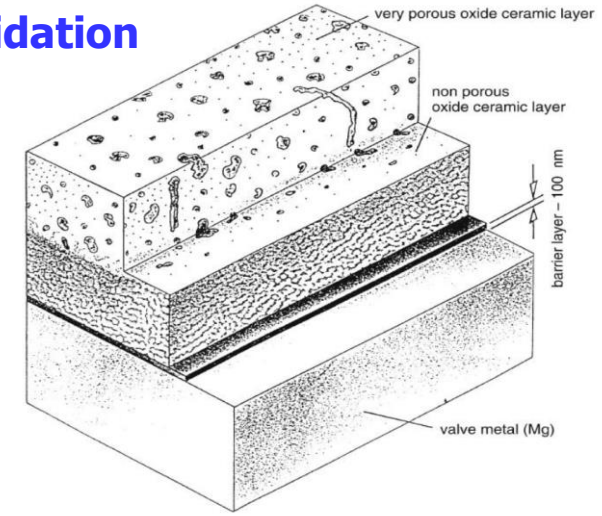

(8) Magnesium hydrogen storage

Advantage ：
- Light weight, resource-rich, low cost
- High hydrogen storage capacity (7.6 wt.%)

Disadvantages ：
- High thermodynamic stability
- Slow kinetic

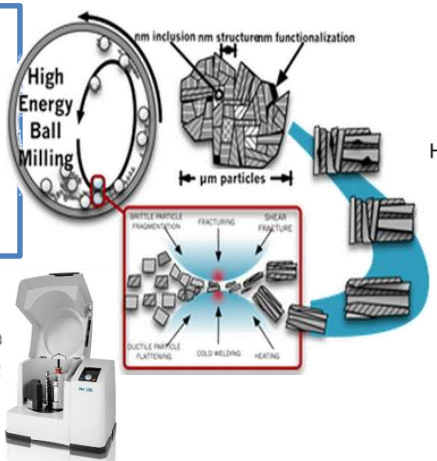

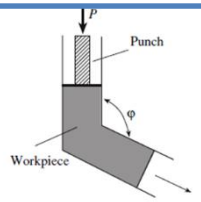

- Metal-Hydrogen system ：

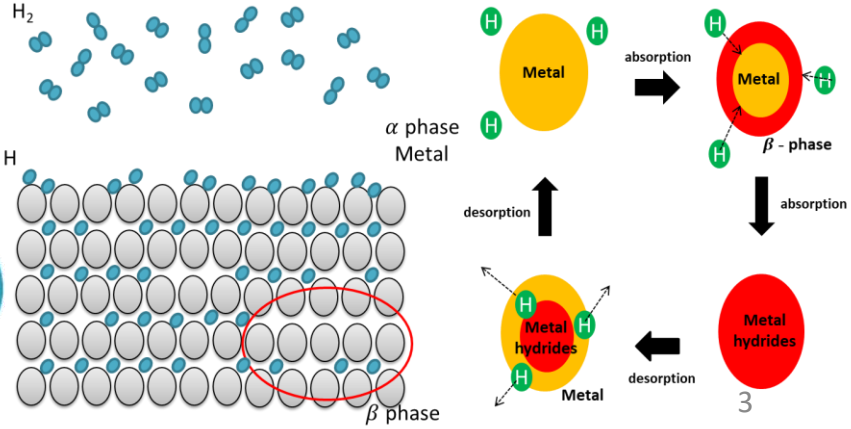

Blood Coagulation Bio-Chip System & Microbial Fuel Cell

Song-Jeng Huang 黃崧任

TAIWAN TECH National Taiwan University of Science and Technology

Blood Coagulation Bio-Chip System

(1) Absorptive of whole blood with each LED light

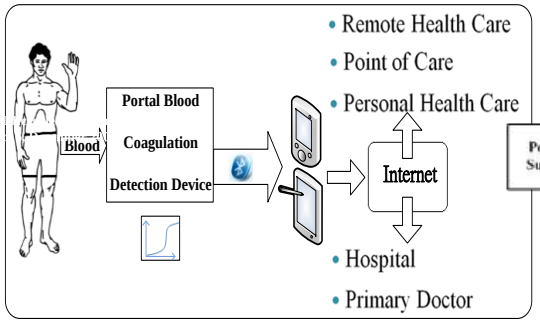

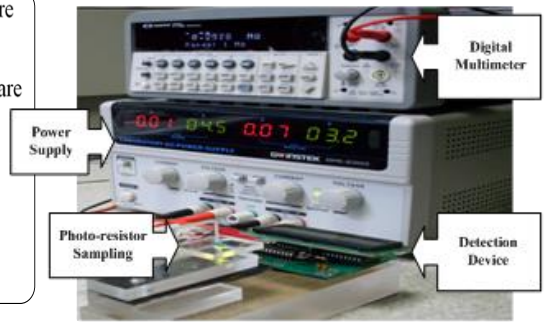

(1) Investigation of Micro Automated Blood Coagulation Analyzer BioChip Dalin Tzu Chi General Hospital 2004/02/01 ~ 2005/01/31

(2) The development of blood coagulation and allergen bio-chip system eChem Inc. Cooperation project 2009.08-2010.07

(3) Development of coagulation biochip and its applications MOST 99-2622-B-006 -002 -CC1, 2010.08-2012.07

(4) Optical based whole blood coagulatmet biochip: develpoment medical applications MOST 103-

(2) eChem Inc. project [98-]

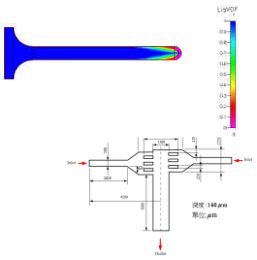

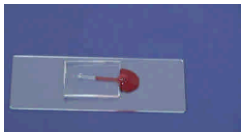

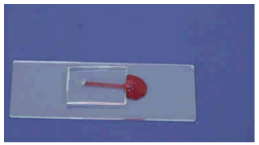

Bio-Chip

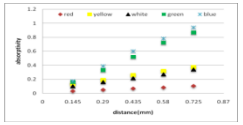

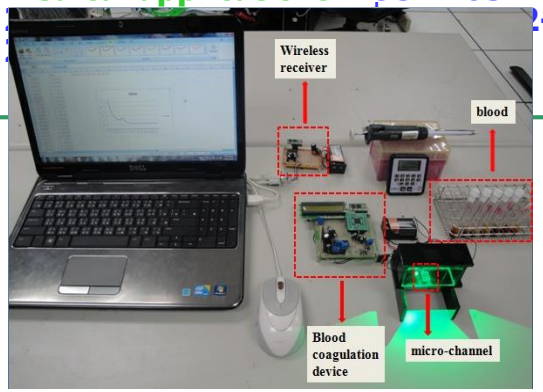

(3) Development of coagulation biochip and its applications(2/2) (NSC100-2622-B-006-005-CC1)

Excellent paper award of 2011 Annual Symposium on Biomedical Engineering and Technology of Taiwanese Society of Biomedical Engineering

Microbial Fuel Cell (MFC) and its metallic electrode

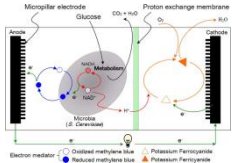

Source: Journal of Microelectromechanical Systems, vol. 17, no. 6, December 2008

Dental Implant Materials and Design

Song-Jeng Huang 黃崧任

TAIWAN TECH National Taiwan University of Science and Technology

Study of tribological and corrosion behavior of strain-hardened commercially pure titanium for medical applications with applied nanostructured diamond-like coating (MOST 104-2923-E-011 -003 -MY3)

CP Ti Grade 4 MAO Coating & Corrosion

UFG samples for corrosion

CG samples corrosion

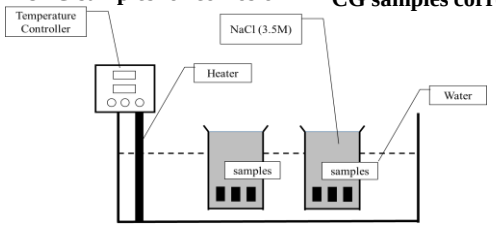

The schematic of the immersion test

		UFG	CG
Weight	before	8.524 g	8.274 g
	after	8.5195 g	8.2397 g
	remove corrosive	8.4663 g	8.1668 g
Corrosion area		0.05 < A ≤0.07	0.07 < A ≤ 0.10
RN		9.3	8.2

Experiment result for Immersion test

Titanium sample with MAO coating Technology

Design (CAD) and Simulation (FEM) of Dental Implant

Accepted for the 3rd International Conference on Precision Machinery and Manufacturing Technology (ICPMMT 2018),Auckland, New Zealand.

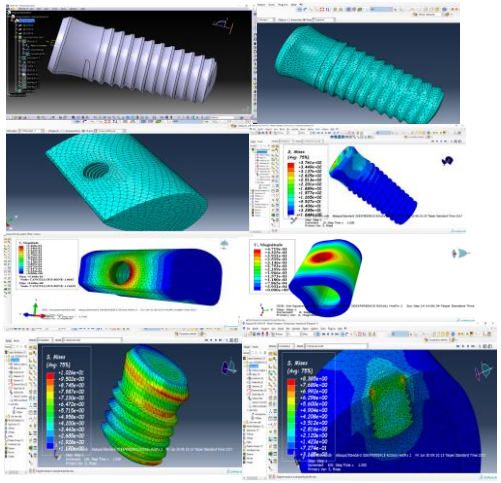

Long and Short Implant CAD/Simulation

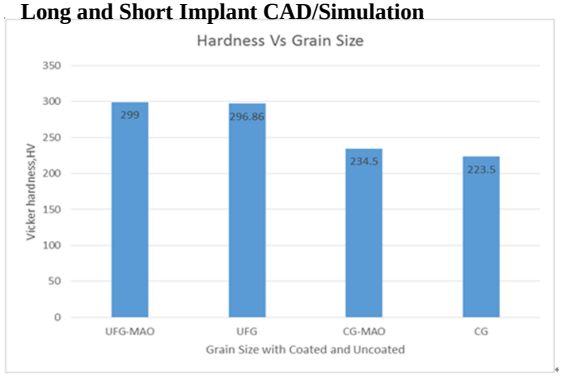

Micro-hardness Test Result

CP Ti Grade 4 Biocompatibility

Samples for Biocompatibility Test

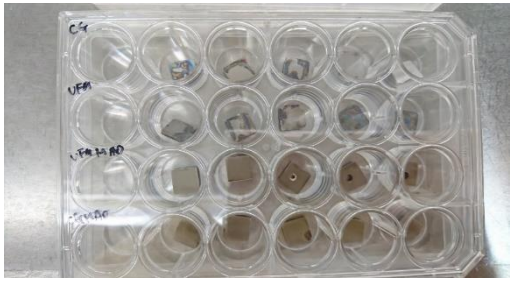

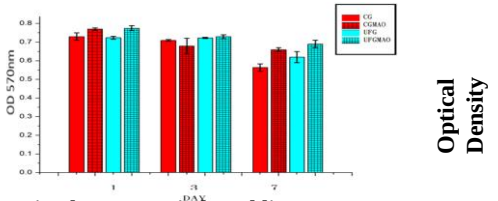

using human periodontal ligament Cell

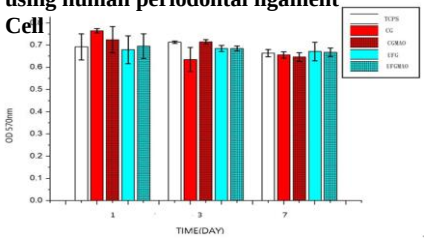

using Pulp Cell

Metal Matrix Composite Materials (MMCs)

Speaker

Professor Song-Jeng Huang

April, 2018

Types of Composite Materials

Introduction

Definitions

There are few definitions of composites that are.

1) A combination of a strong and weaker material.

2) A material composed of different parts.

3) A combination of two materials

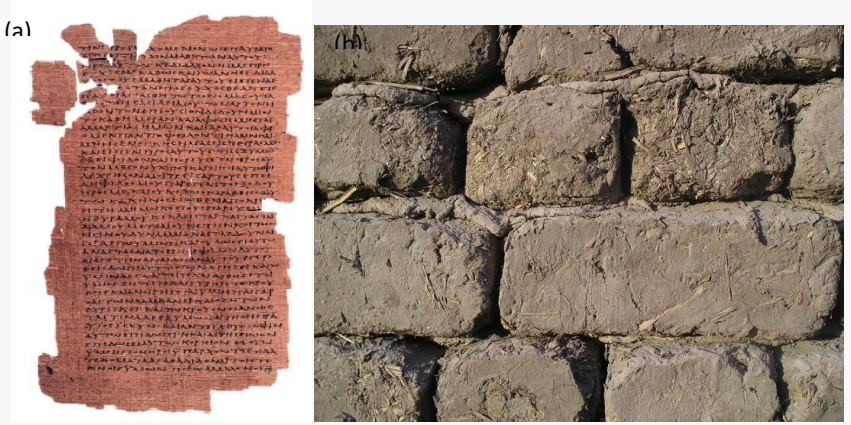

Fig. 1 (a) papyrus paper (b) bricks made from mud Egypt (Source: *https://www.flickr.com/photos/randall_niles/5075375173*)

*"A **composite** is a structural material that consists of two or more combined constituents that are combined at a macroscopic level and are not soluble in each other".*

…continued

Compositing technique is followed from ancient age.

The first production and man-made use of a fibrous composite material appears to be the ***papyrus paper*** *made by the Egyptians circa 4000 B.C.*

Egyptians use bamboo shoots and glued laminated wood to reinforcing ***mud walls*** *in 1500 B.C.*

According to the Book of Exodus ("do not give them ***straw for their bricks****, make them find their own straw"), this practice was used as early as1300 B.C.*

The first modern composite material was ***fiber glass****.*

Two or more chemically distinct materials which when combined have improved properties over the individual material.

The constituents retain their identities in the composites: that is they do not dissolve or otherwise merge completely into each other, although they act in concert.

…continued

Types of composites

On the basis of matrix phase, composites can be classified into

- Metal matrix composites (**MMCs**).
- Ceramic matrix composites (**CMCs**).
- Polymer matrix composites (**PMCs**).

The classifications according to types of reinforcement are

- Particulate composites (composed of particles).
- Fibrous composites (composed of fibers).
- Structural composites (composed of laminates).

…continued

Reinforced composites

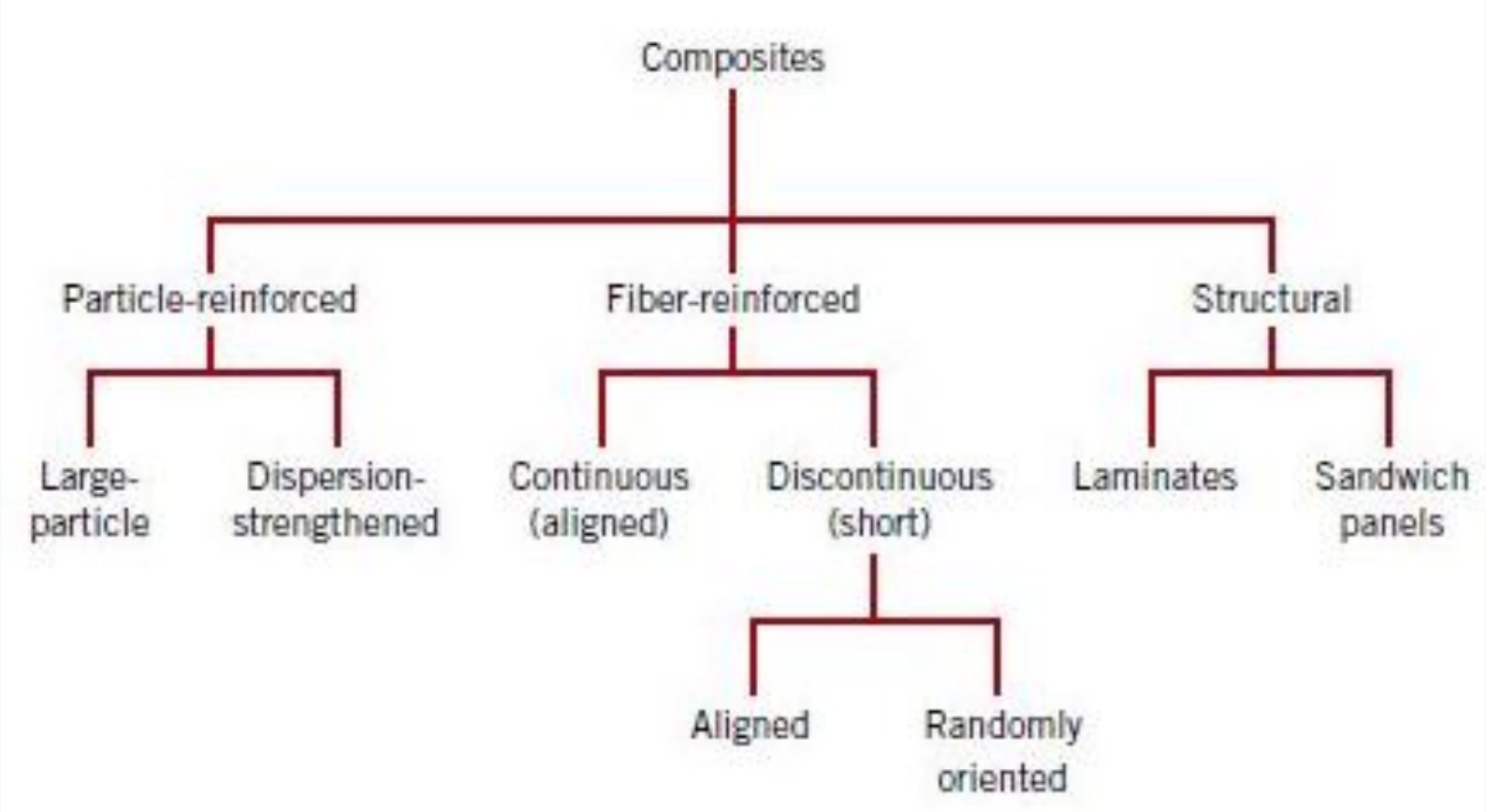

Classifications of composites based on reinforcement (Source: http://slideplayer.com/slide/5724175/)

…continued

Particulate composites

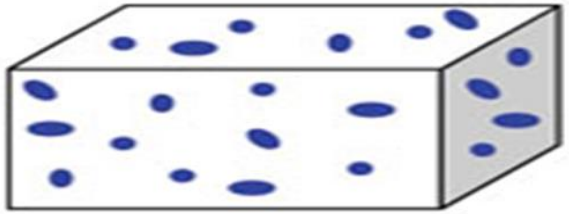

Source (https://www.slideshare.net/Albairaq/composites-rather-ford-group-mobile-heater-idm8)

Particulate Composites A composite that consists of tiny particles of one material embedded in another material.

The particulates can be very small particles (< 0.25 microns), chopped fibers (such as glass), platelets, hollow spheres, or new materials such as bucky balls or carbon nanotubes.

Particles are used to increase the modulus of the matrix, to decrease the permeability of the matrix, to decrease the ductility of the matrix and also used to produce inexpensive composites .

…continued

Fiber-reinforced composites

Fiber-reinforced composites are composed of

axial particulates embedded in a matrix material.

The objective of fiber-reinforced composites it to obtain a material

with *high specific strength* and *high specific modulus*.

Some common geometries for fiber-reinforced composites:

Aligned

Short Aligned

Random

…continued

Aligned

The fibers are longer than a critical length which is the minimum length necessary such that the entire load is transmitted from the matrix to the fibers.

Random

This is also called discrete, (or chopped) fibers. The strength will not be as high as with aligned fibers, however, the advantage is that the material will be isotropic and cheaper.

Short Aligned

The fibers are woven into a fabric which is layered with the matrix material to make a laminated structure.

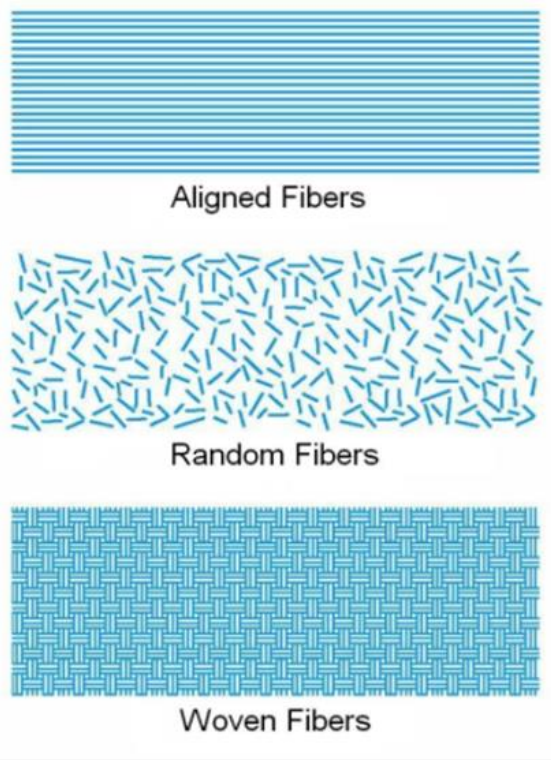

Source (composite Materials presented by BESSY JOHNY)

…continued

Structural Composites

- Laminated composite materials consist of stacks of layers, each layer usually composed by a matrix of polymeric material and fibers oriented in a specific direction.
- Laminated composites give the designer the ability to tailor the material according to the application and the structures formed by these materials present high stiffness/mass and strength/mass ratios.

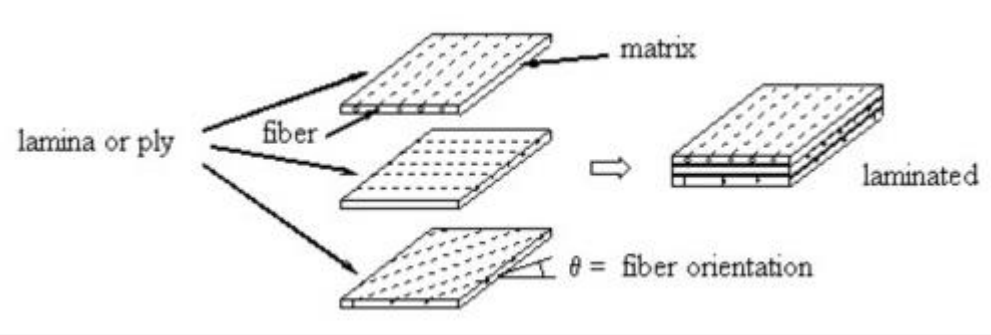

Source (Buckling Analysis of Laminar Composite Plates with Cutouts, Dilu RiswanaPublished 2016)

…continued

Matrix Composites

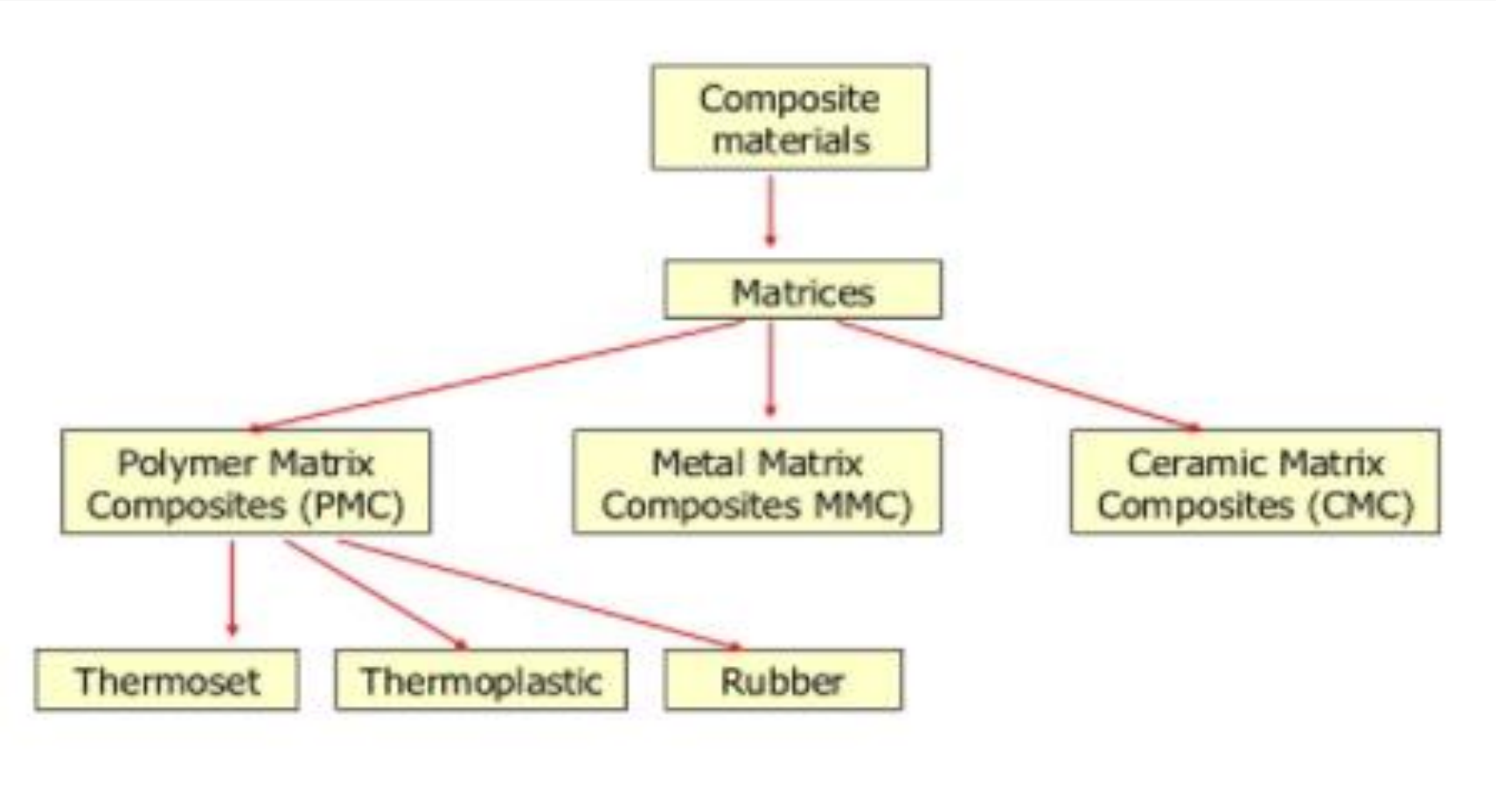

Classifications of composites on the basis of matrix type.

Source (https://www.slideshare.net/BKLR/polymer-matrix-composites)

…continued

Polymer Matrix Composites(PMC)

- Polymer Matrix Composite (PMC) is the material consisting of a polymer (resin) matrix combined with a fibrous reinforcing dispersed phase. Polymer Matrix Composites are very popular due to their low cost and simple fabrication methods.
- Thermoplastic polymers - Linear or branched polymers in which chains of molecules are not interconnected to one another.
- Thermosetting polymers - Polymers that are heavily cross-linked to produce a strong three dimensional network structure.
- Elastomers - These are polymers (thermoplastics or lightly cross-linked thermosets) that have an elastic deformation > 200%.

…continued

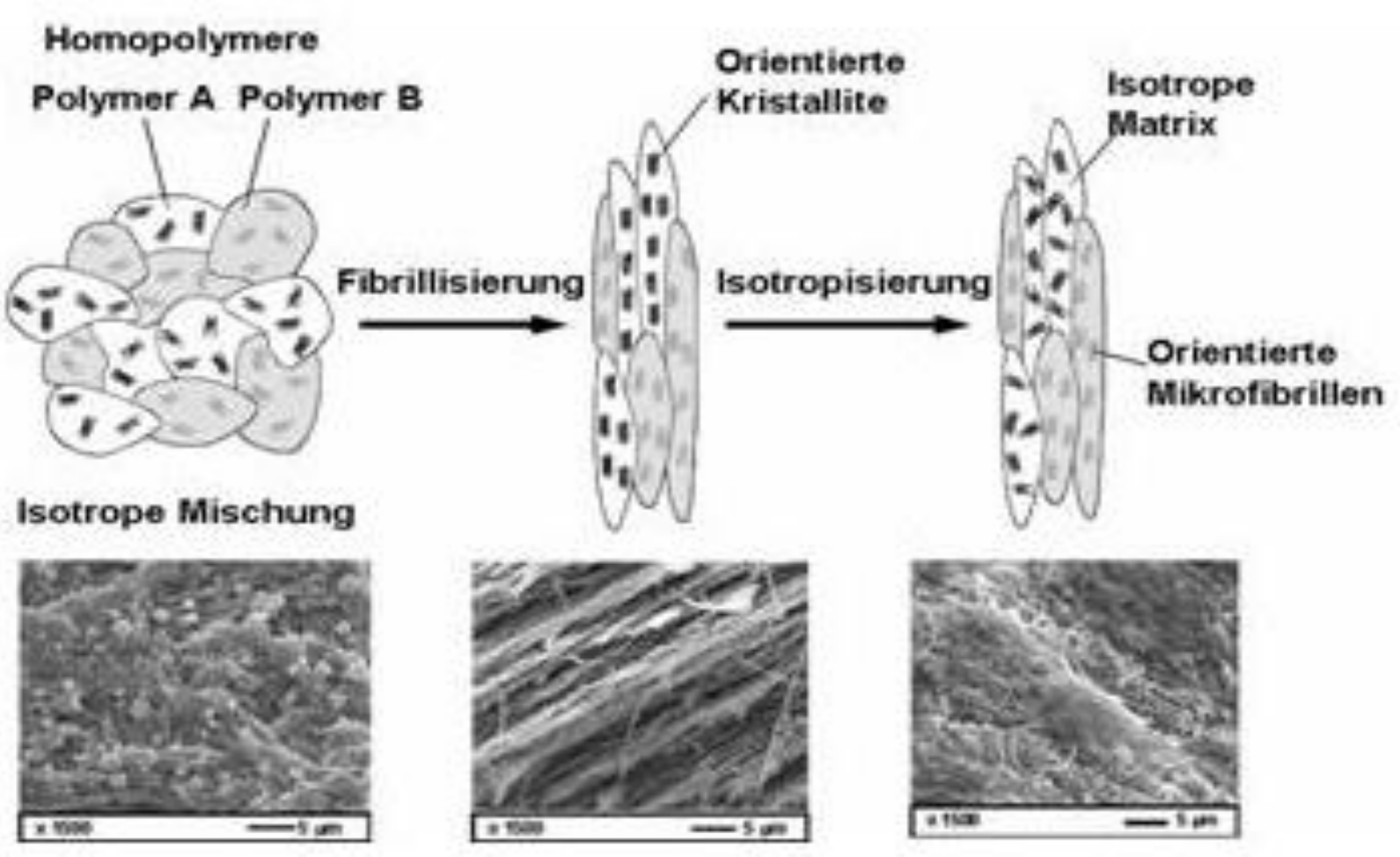

Polymer matrix composite structure and SEM image.

(Source: Everett, R., Metal matrix composites: processing and interfaces. 2012: Academic Press.)

…continued

Ceramic Matrix Composites

- Ceramic matrix composites (CMCs) are a subgroup of composite material as well as a subgroup of technical ceramic.
- They consist of ceramic fibers embedded in a ceramic matrix, thus forming a ceramic fiber reinforced ceramic (CFRC) material.

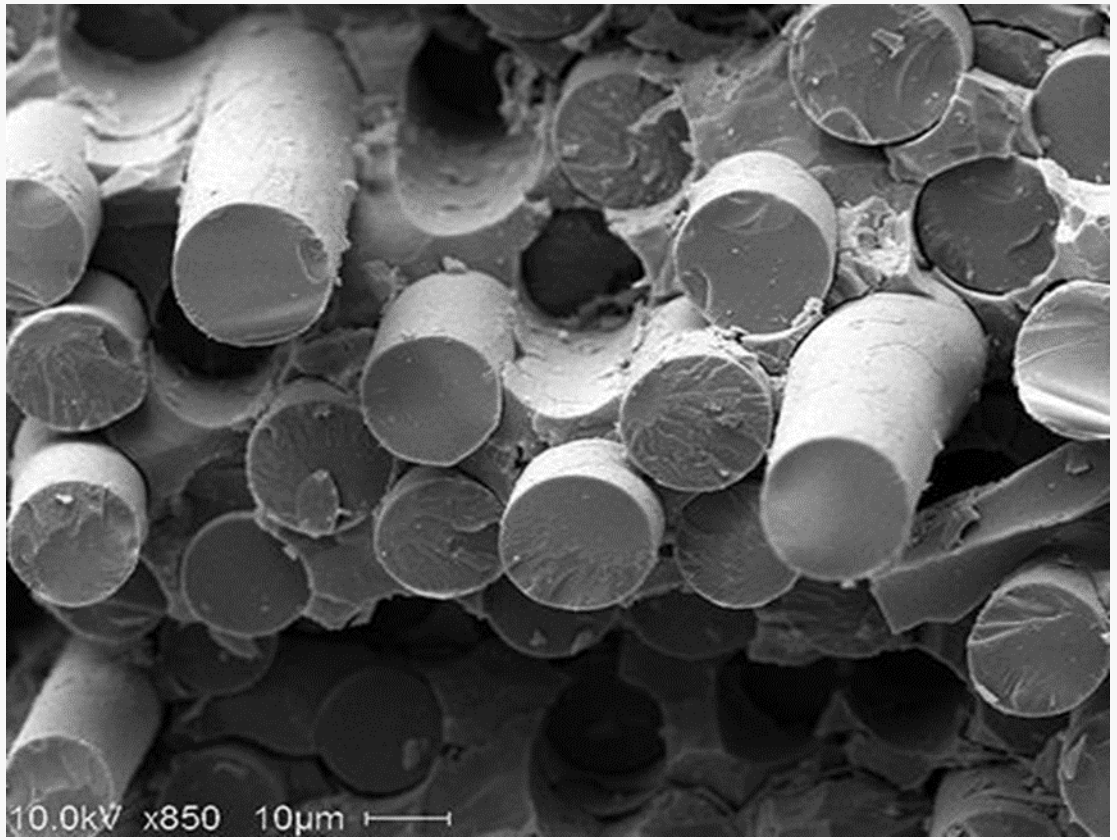

A photo micrograph (SEM) Shows the company's SiNC fiber in a CVI deposited SiC matrix

Source (https://www.compositesworld.com/articles/ceramic-matrix-composites-heat-up)

NTUST

Metal Matrix Composites

- A metal matrix composite (MMC) is composite material with at least two constituent parts, one being a metal.
- The other material may be a different metal or another material, such as a ceramic or organic compound.
- When at least three materials are present, it is called a hybrid composite.
- MMCs are made by dispersing a reinforcing material into a metal matrix. The reinforcement surface can be coated to prevent a chemical reaction with the matrix.
- For example, carbon fibers are commonly used in aluminum matrix to synthesize composites show.i.ng low density and high strength

…continued

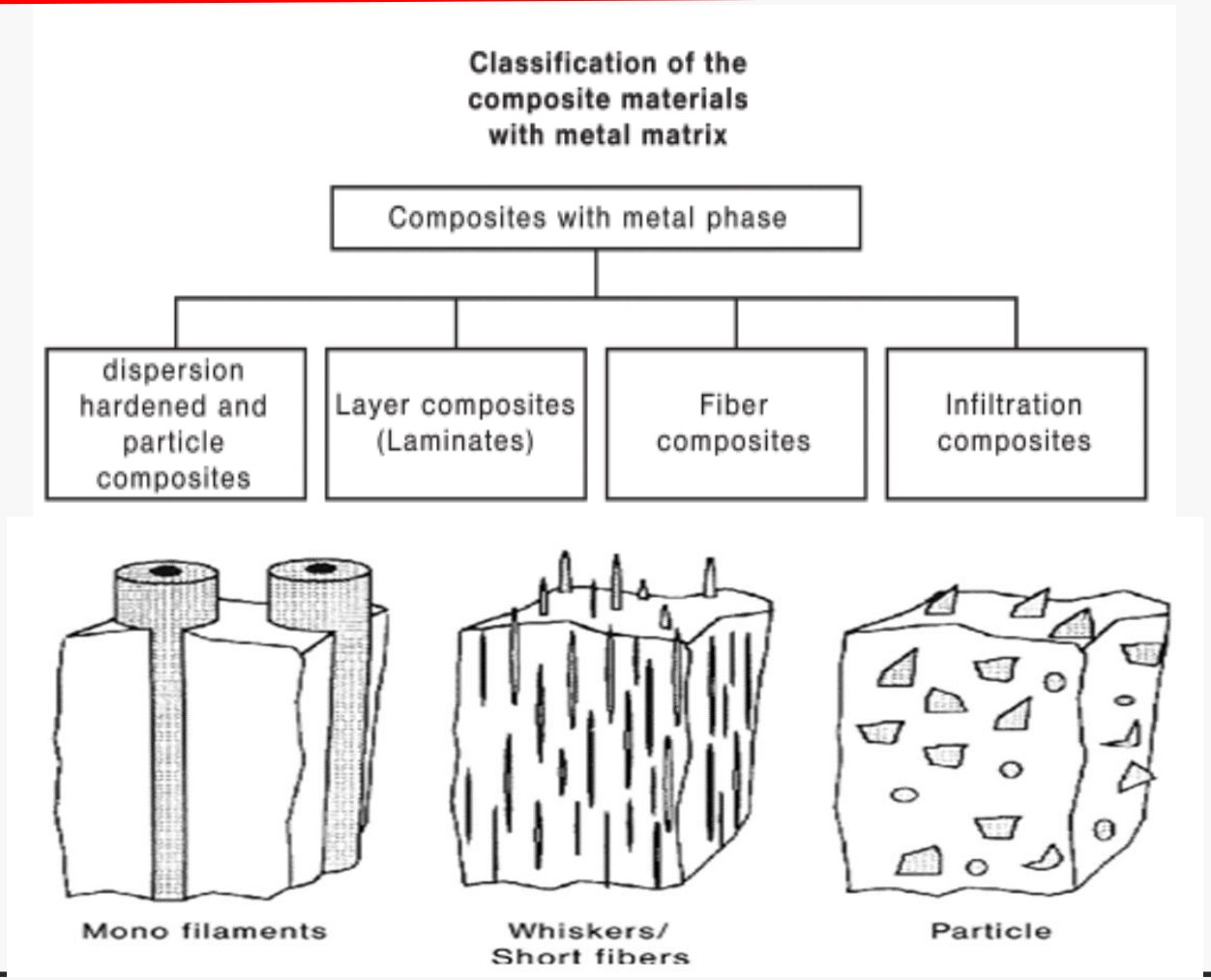

Fig shows the type of metal matrix composite and its schematic diagram.
(Basics of Metal Matrix Composites Karl Ulrich Kainer, page 4.)

Conclusion

Metal matrix composites gives a good degree of maturity that shows the expansion of their use.

To identify it's full ability or potential composites great attention support is needed in analysis.

The number of MMCs in use are in various stages of development: that are B/Al, B/ Ti, graphite/Al and super alloys reinforced with refractory metal.

The metal- metal system have high specific strength and moduli, toughness, desirable high-temperature properties.

The boron/ reinforced aluminum system is in very advanced level of development and properly data are sufficient for the design.

Design of Metal Matrix Composites

…continued

- Composite = reinforcement +matrix
- Properties of MMC =reinforcement properties + Matrix properties

  ≠ reinforcement properties ≠ Matrix properties

MMCs are designed for their greater potential for high specific strength, stiffness, enhanced wear resistance, and better high temperature properties compared to monolithic metals and alloys

Higher levels performance critically required in industrial applications can be achieved by specific matrix and reinforcement

…continued

Properties of interest in composite

- Elastic engineering properties,
- Coefficient of thermal expansion and
- Thermal conductivity,
- Yield strength,
- Hardening parameters.
- Thermomechanical loading

…continued

Designing Parameters

- Properties of interest (strength, conductivity, hardness etc.)
- Matrix properties (Al, Be, Mg, Ti, Fe, Ni, Co, and Ag)
- Reinforcement properties (SiC, Al_2O_3, B_4C, TiC, TiB_2, graphite etc.)
- Morphology of matrix and reinforcement (Continuous fiber, Chopped fiber or whisker, and Particles)
- Cost of materials and process
- Manufacturing Process

…continued

Metallurgical design and Materials Limitations

- Metallurgical design of MMC relies on intrinsic property matrix particles(whiskers/fibers/particles)
- MMC overcomes the specific metallurgical limitations of metallic and ceramic by blending their mutually exclusive property profiles.
- MMC design depends on desired property profile and application
- Suitable MMC are characterized intrinsic properties of Matrix and reinforcement.

…continued

Basic Concepts in MMC

- Any two materials can be combined to make a composite(may be different geometries)
- Three concepts are used:
- **Performance indices** which isolate the combination of material properties that maximize performance;
- **Materials-selection charts**, onto which both material properties and performance indices can be plotted; and
- **Use of bounds** to define the envelope of properties accessible to a given composite system

…continued

Indices of performances

It is a property or group of properties that measures the effectiveness of a material in performing a given function.

It is needed to maximize or minimize.

For Light, stiff beam, maximize E/ρ

For Heat conducting materials, maximize λ/α

…continued

Selection Charts

- The indices combine two or more properties which suggests construct charts on which one property is plotted against another in such a way that both the properties and their combinations can be examined.
- The index E/ρ appears on slope 1

and $E^{1/2}/\rho$ is on slope 2

- Possible upper and lower properties can estimated.

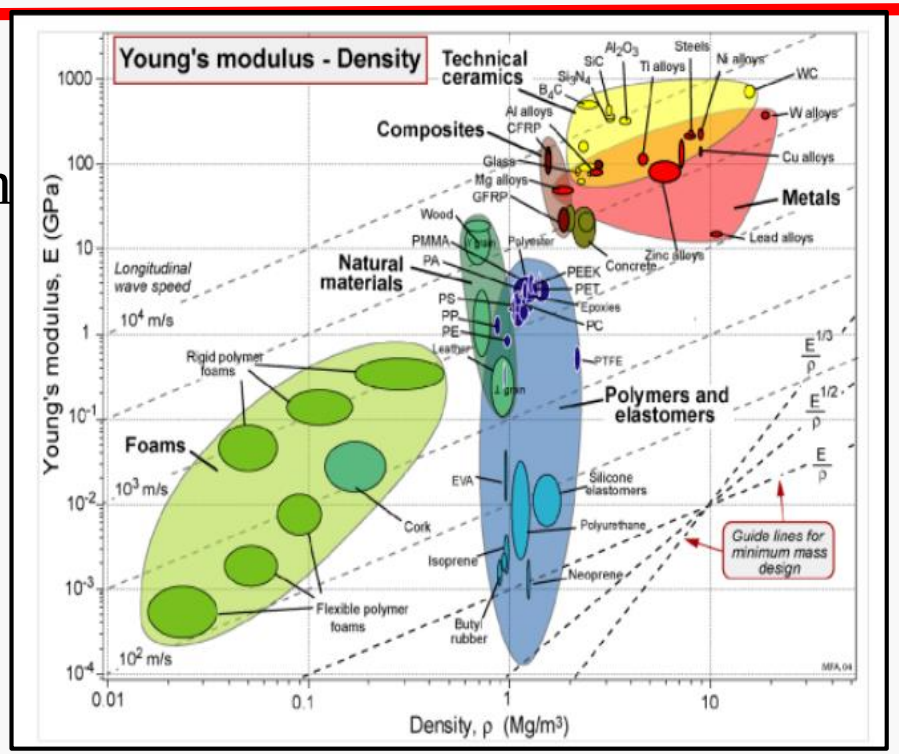

A schematic selection chart: modulus E is plotted against density ρ.(Source: http://slideplayer.com/slide/9162265/, date accessed, 30, March,2018)

…continued

Property Bounds

- The rigorous boundaries beyond which specific property can not exceeds or fall below.
- Some are calculated (density, specific heat, moduli, thermal expansion, thermal conductivity, diffusivity) and some are derived.

Table 1 Design limiting properties

Property	Symbol and usual units
Density	ρ (Mg m^{-3}
Young's modulus	E (GPA)
Strength	σ_f (MPa, sometimes GPa)
Toughness; or fracture toughness	J_{1c} (kJ m^{-2}); K_{1c}(MPa $m^{1/2}$)
Linear thermal expansion coefficient	α (K^{-1})
Specific heat	C_p (J $kg^{-1}K^{-1}$)
Thermal conductivity	λ (W $m^{-1}K^{-1}$)
Thermal diffusivity	a (m^2 s^{-1})

…continued

Property Bounds

Density

$\rho_r = f\rho_r + (1-f)\rho_m$

- ρ_r =Reinforcement
- ρ_m =matrix density
- F =Reinforcement fraction

Modulus

$E_r = fE_r + (1-f)E_m$

And

$$E_r = \frac{E_m E_r}{f E_{m+(1+f)E_r}}$$

E_r =Reinforcement Modulus

E_m =Matrix Modulus

…continued

Property Bounds

Strength

- The upper bound is,

$$(\sigma_f)_u = f(\sigma_f)_r + (1-f)(\sigma_f)_m$$

- lower bound is

$$(\sigma_f)_l = (\sigma_f)_m 1 + \frac{1}{16}\left(\frac{f^{1/2}}{1-f^{1/2}}\right)$$

Specific Heat

Specific heat can be described by

$$\rho C_p = f\rho_r (C_p)_r + (1-f)\rho_m (C_p)_m$$

…continued

Thermal Expansion Coefficient

- approximate lower bounds

$$\alpha_l = \frac{E_r \alpha f + E_m \alpha_m (1-f)}{E_r f + E_m (1-f)}$$

upper bound

$\alpha_u = f\alpha_r(1+\nu_r)+(1-f)\alpha_m(1+\nu_m)-\alpha_L[f\nu_r+(1-f)\nu_m]$

Thermal Conductivity

upper bound;

$\lambda_u = f\lambda_r+(1-f)\lambda_m$

Lower bound

$$\lambda_l = \frac{\lambda_r + 2\lambda_m - 2f(\lambda_m - \lambda_r)}{\lambda_r + 2\lambda_m + 2f(\lambda_m - \lambda_r)}$$

…continued

Composite Design for Stiffness at Minimum Weight

- beryllium (Be) or of alumina (Al_2O_3) incorporated composites are shown in example.
- Performance indices ($M=E^{1/2}/\rho$), the quantity we wish to maximize
- Upper and lower bounds for the modulus–density relationship can thus be plotted on chart using volume fraction *f* as a parameter
- longitudinal Fibrous reinforcement gives upper bound;
- Particulate reinforcement gives lower one.

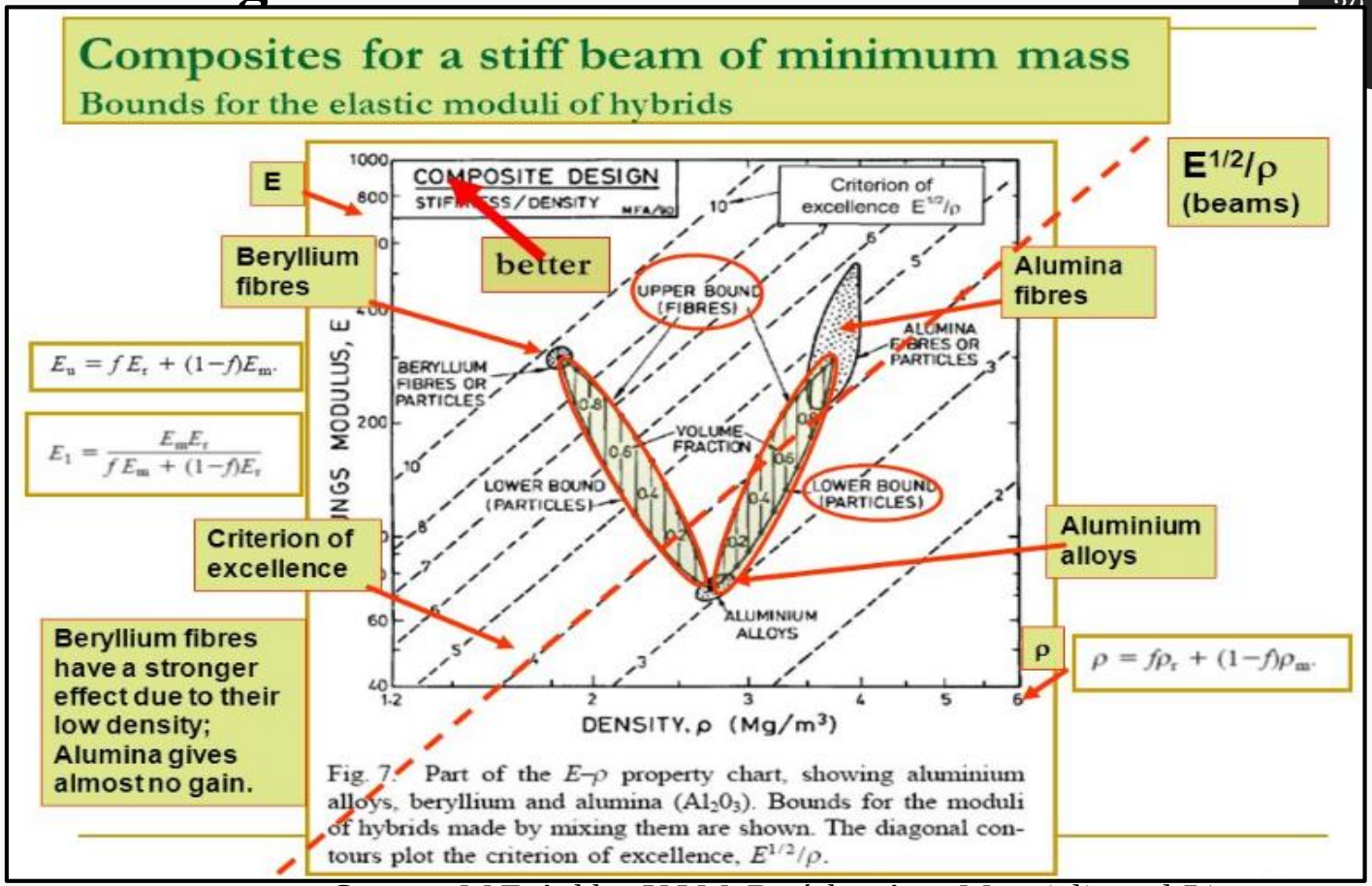

Fig. 7. Part of the E–ρ property chart, showing aluminium alloys, beryllium and alumina (Al_2O_3). Bounds for the moduli of hybrids made by mixing them are shown. The diagonal contours plot the criterion of excellence, $E^{1/2}/\rho$.

Source: M.F. Ashby, Y.J.M. Bre´chet,Acta Materialia, vol.51, pp.5801–5821, 2003)

…continued

Composite Design for Specific Thermal Properties

- Three groups of materials are shown, aluminum alloys, boron nitride (BN), and silicon carbide (SiC)
- Minimizing thermal distortion M=λ/α.(bound)
- The thermal properties of Al–BN and Al–SiC are bracketed by lines that show the bounding equations

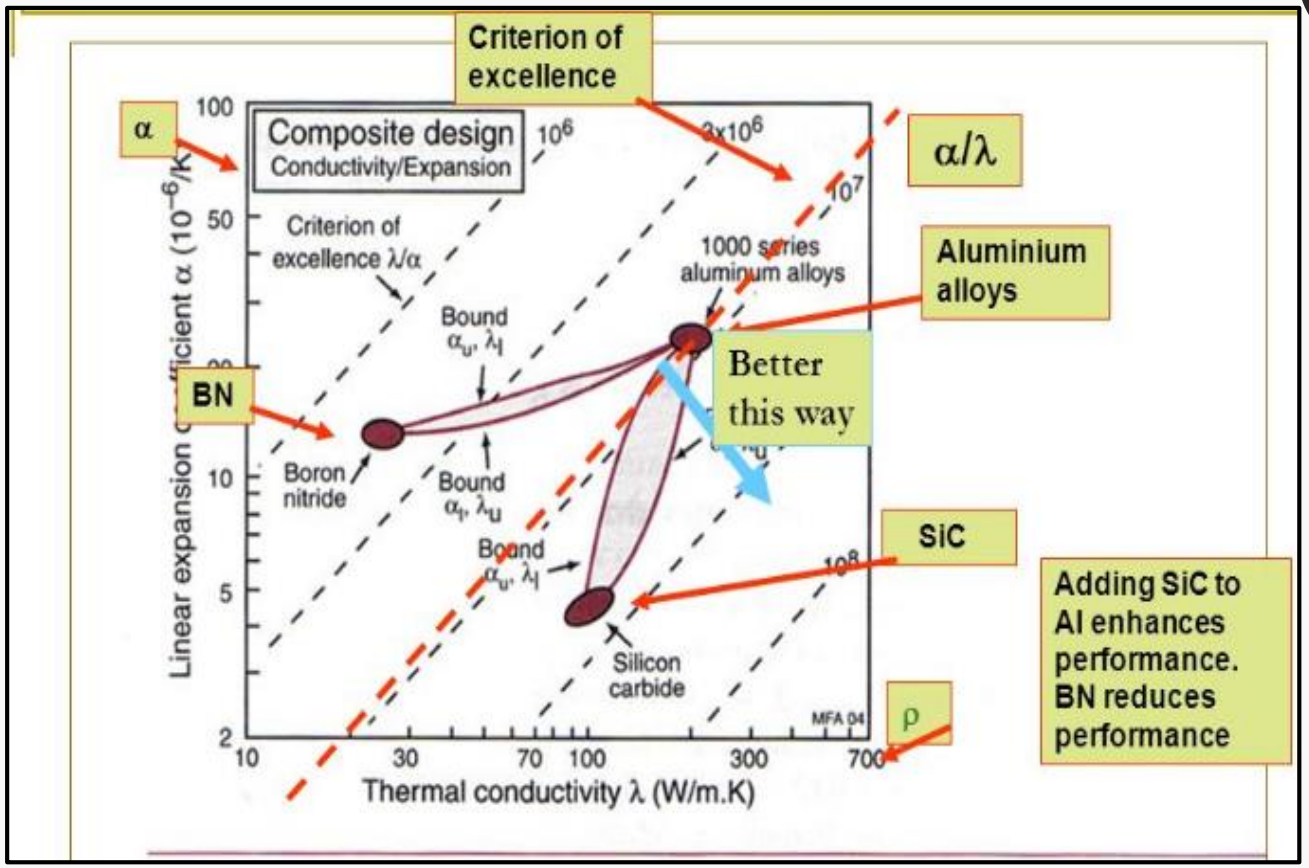

Source: M.F. Ashby, Y.J.M. Bre´chet,Acta Materialia, vol.51, pp.5801–5821, 2003)

Conclusion and summary

IT IS HELPFUL TO FIND STRENGTHS AND WEAKNESSES AND APPLICATIONS BEFORE PREPARATION.

DESIGN IS SERIAL PROCESS COMPRISING OF IDEAS OF PERFORMANCE INDICES, MATERIALS SELECTION CHARTS AND BOUNDS FOR PROPERTIES OF INTEREST.

THE PROCESS IS EXPLAINED BY TWO EXAMPLES.

Manufacturing Techniques of MMCs

Classification of manufacturing techniques of MMCs

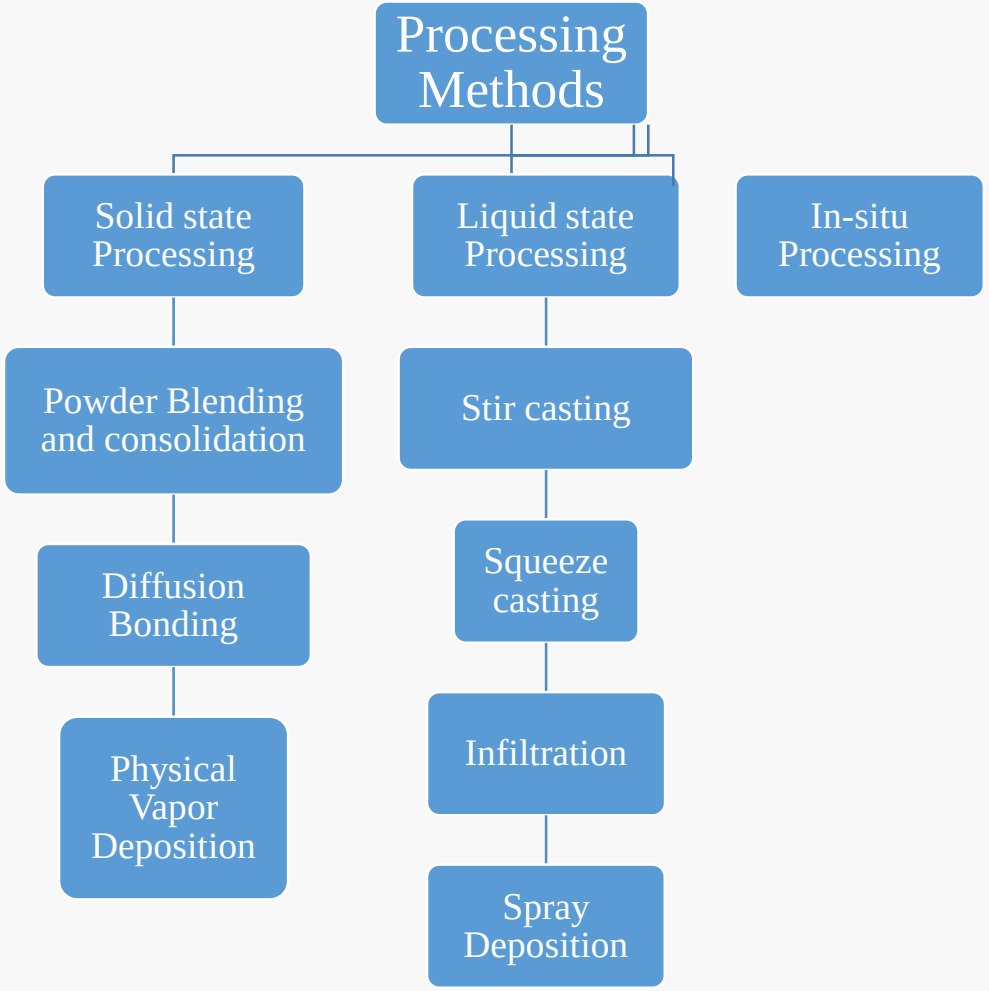

Fig. Classification of manufacturing techniques of MMCs, (Source: Trinh, S.N. and S. Sastry, Mechanical Engineering and Materials Science Independent Study, Vol. Paper 10, 2016)

Solid State Processing – Powder Blending and consolidation

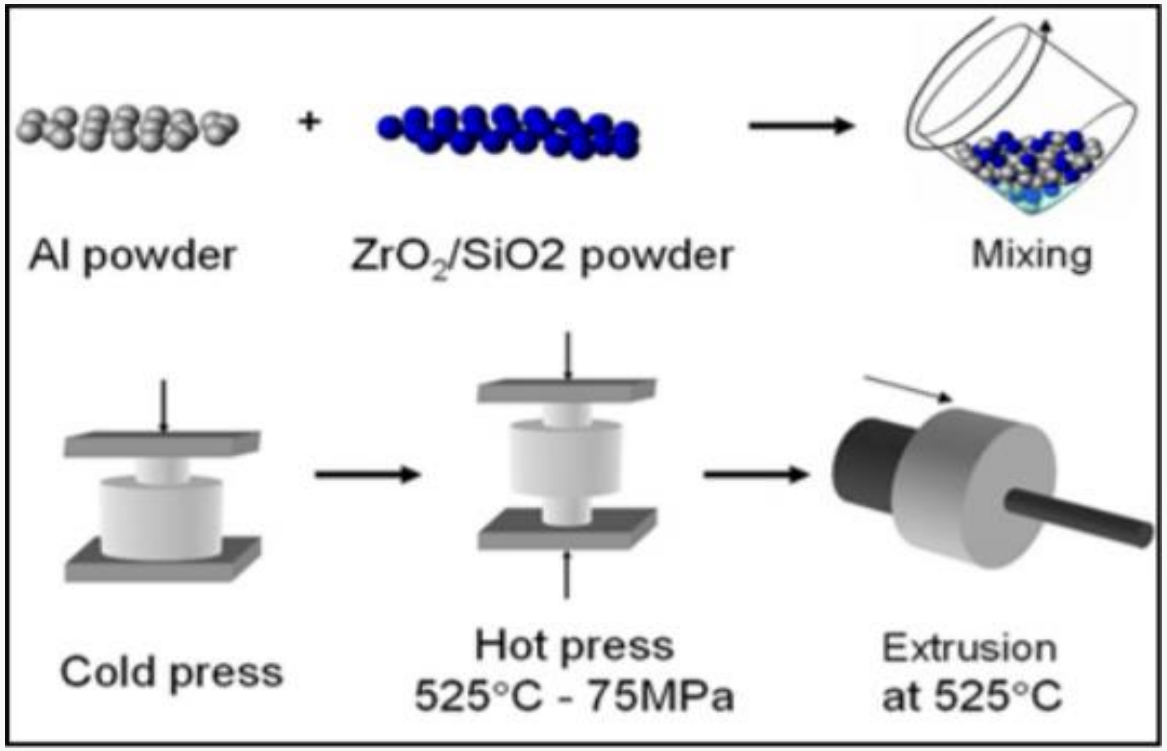

Fig. An example for powder metallurgy process (Source: Kandpal, B.C., J. Kumar, and H. Singh, International Journal of Research in Mechanical Engineering and Technology, Vol. 4, pp 27-32, 2014)

- This method is usually used for the processing of aluminum and magnesium metal matrix composites.
- Metal alloy powder is blended with ceramic whisker/short fiber/particles in dry condition or in liquid suspension. After blending, the mixture is further processed by cold compaction, canning, degassing, and high temperature consolidation to Strengthen MMC

…continued

Diffusion bonding

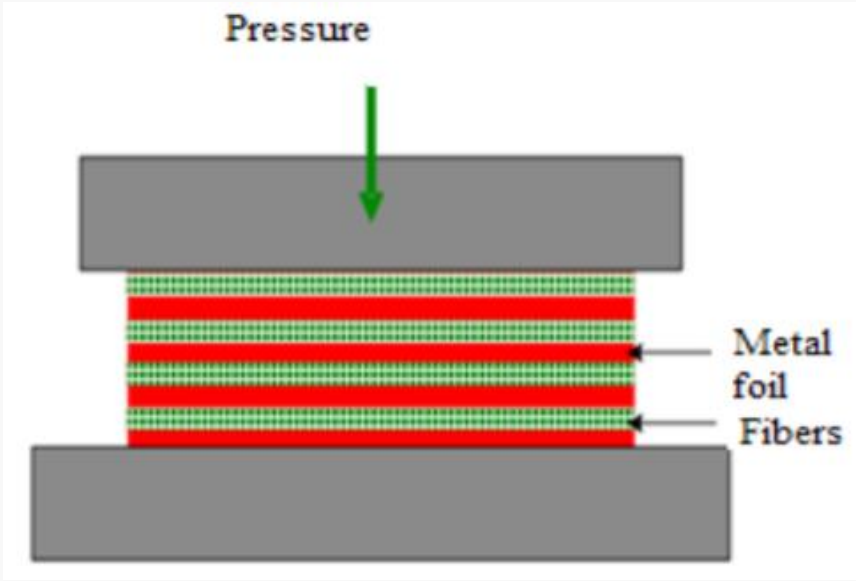

(Source: http://www.substech.com/dokuwiki/doku.php?id=solid_state_fabrication_of_metal_matrix_composites, Acc date 30, march, 2018)

Inter diffusion of atoms between clean metallic surfaces, in contact at an elevated temperature, leads to bonding.

Physical vapor Deposition

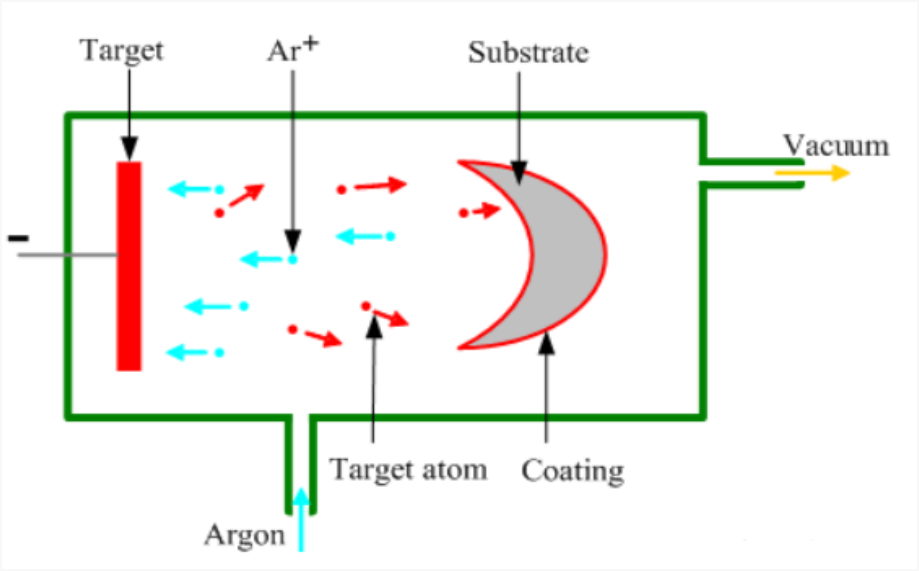

(Source:http://www.substech.com/dokuwiki/doku.php?id=vapor_deposition#physical_vapor_deposition_pvd, , Acc date 30, march, 2018)

This Process involving vaporization of the coating material in vacuum, transportation of the vapor to the substrate and condensation of the vapor on the substrate surface. Picture shows Sputtering process, a PVD method.

Liquid State Processing- Stir Casting

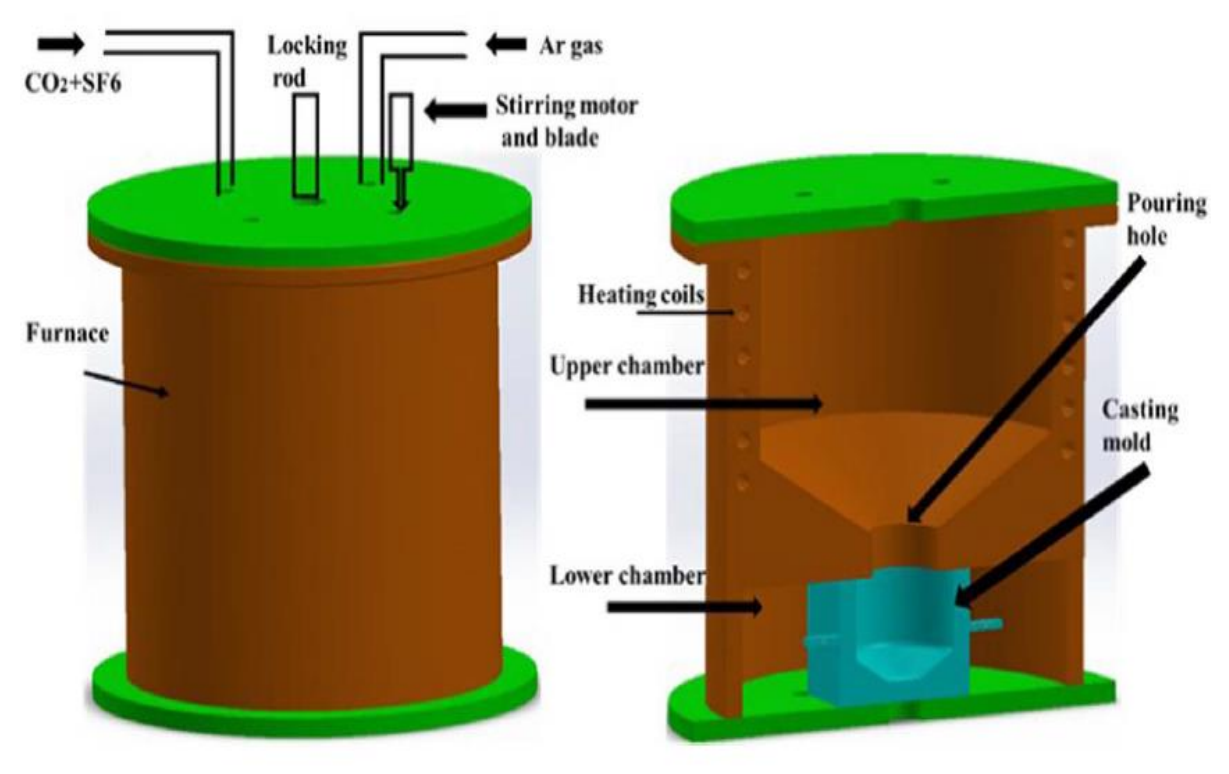

Fig. Stir casting process (Source: Huang, S.-J. and A.N. Ali, Materials Science and Engineering: A, Vol. 711, pp 670-682, 2018)

- Solid state process involves incorporation of dispersed phase into a molten matrix metal, followed by its solidification.
- Particulate reinforcements are mixed with liquid metal melt and the mixture then solidifies. Specifically, the pre-treated particles are inserted into the vortex of molten alloy, which is created by a rotating impeller.
- Advantage: low cost, short processing times and high fiber contents.
- Disadvantage: The reinforcements are not uniformly distributed and form sediments in the molten alloy.

Squeeze Casting

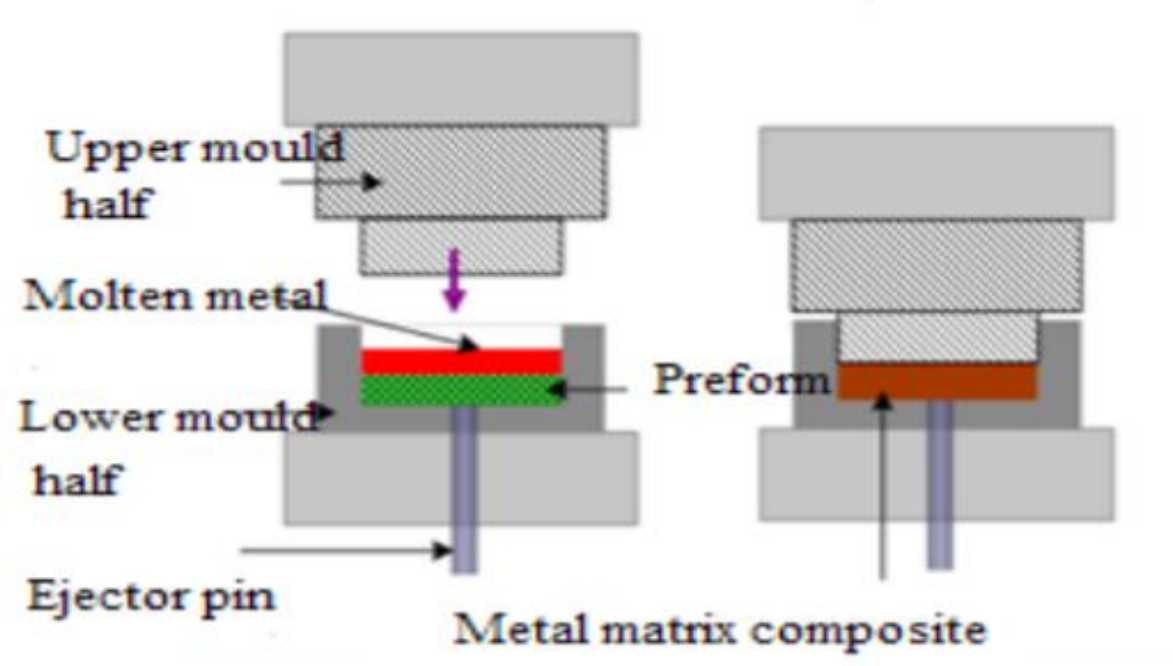

Fig. Squeeze casting, (Source:http://www.substech.com/dokuwiki/lib/exe/detail.php?id=liquid_state_fabrication_of_metal_matrix_composites&cache=cache&media=squeeze_casting_infiltration.png, Acc date 30, march, 2018)

- It is the combination of casting and Forging Process.
- This process can result in the highest Mechanical properties attainable in cast products.
- Molten metal is introduced into an open die. The dies are then closed so that the molten metal solidifies under pressure within the dies.
- Application: Squeeze casting is an economical, simple and convenient process. It has found extensive application in automotive industry in producing aluminium front steering knuckles, chassis frames, brackets or nodes. High capacity propellers for boat-engine.

Infiltration Process

- A preformed dispersed phase (ceramic particles, fibers, woven) is soaked in a molten matrix metal, which fills the space between the dispersed phase inclusions.
- Silica and metal-based mixtures are often employed as binder to retain the integrity and shape of the porous forms.

➢Gas Pressure Infiltration

➢Pressure die Infiltration

Gas Pressure Infiltration

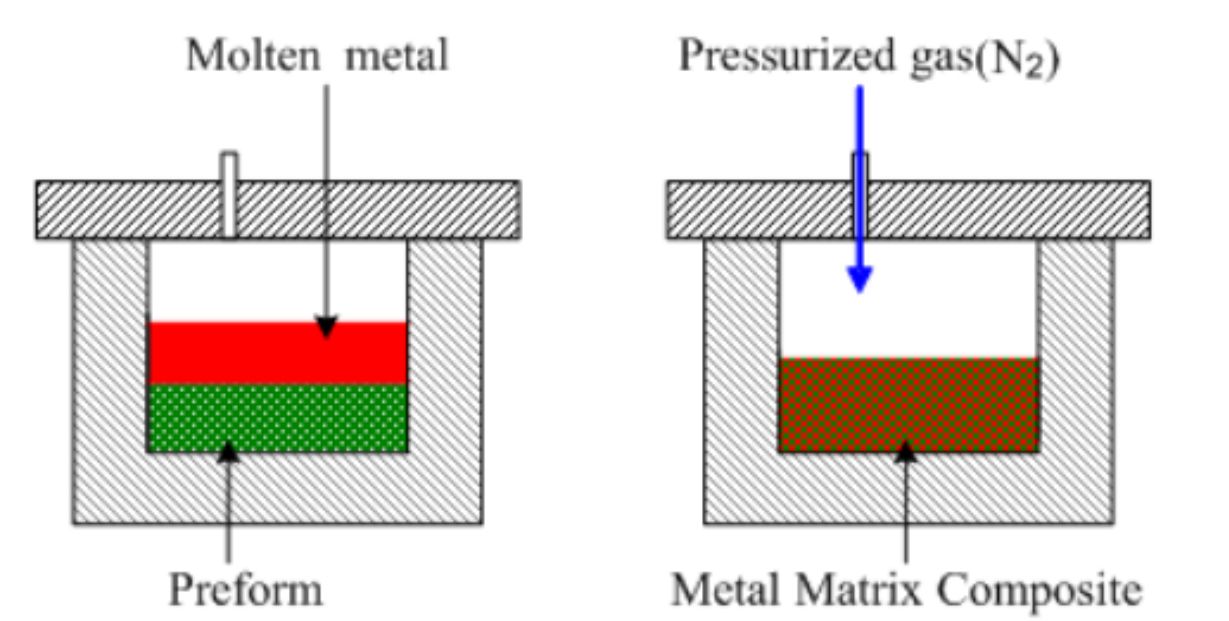

Fig. Gas Infiltration Process (Source:http://www.substech.com/dokuwiki/lib/exe/detail.php?id=liquid_state_fabrication_of_metal_matrix_composites&cache=cache&media=gas_pressure_infiltration.png, Acc date 30, march, 2018)

- Applying pressure on the molten metal and forcing it to penetrate into a preformed dispersed phase.
- Manufacturing large composite parts.
- The method allows using non-coated fibers due to short contact time of the fibers with the hot metal.
- Low damage of the fibers.

Pressure Die Infiltration

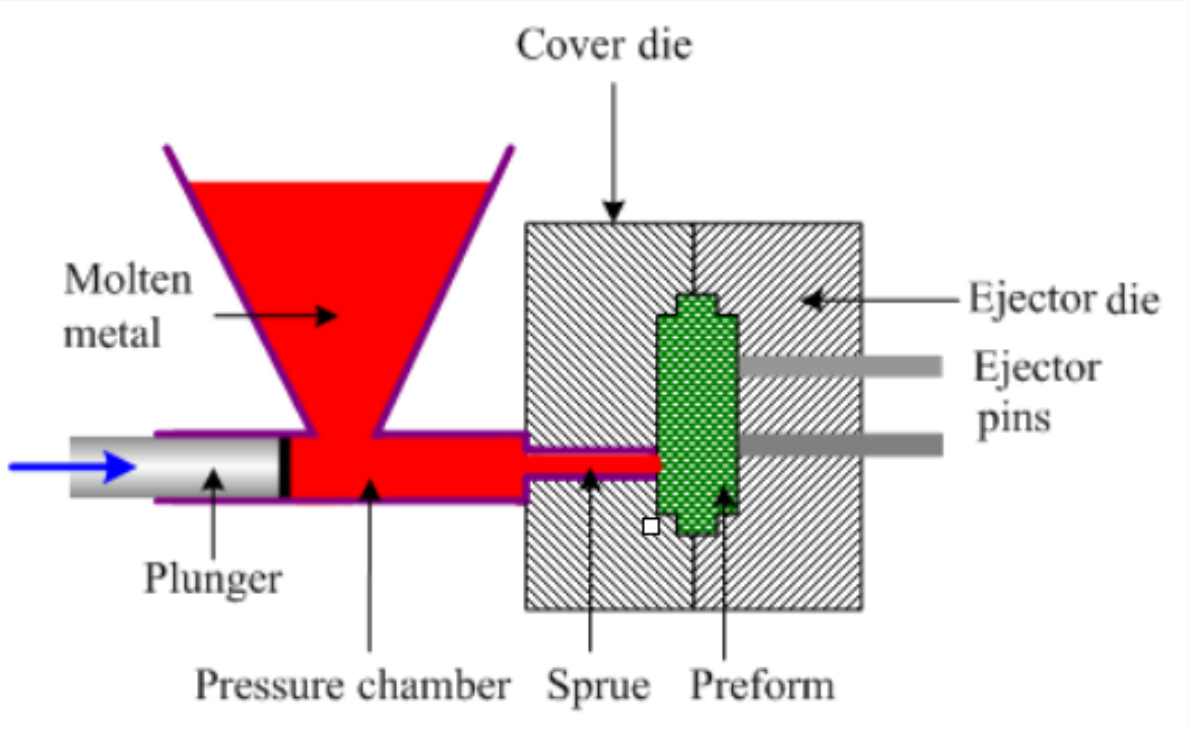

Fig. Pressure Die Infiltration (Source: http://www.substech.com/dokuwiki/lib/exe/detail.php?id=liquid_state_fabrication_of_metal_matrix_composites&cache=cache&media=pressure_die_infiltration.png, Acc date 30, march, 2018)

- Forced infiltration method.
- Preformed dispersed phase (particles, fibers) is placed into a die (mold) which is then filled with a molten metal entering the die through a sprue and penetrating into the preform under the pressure of a movable piston.

Spray Deposition

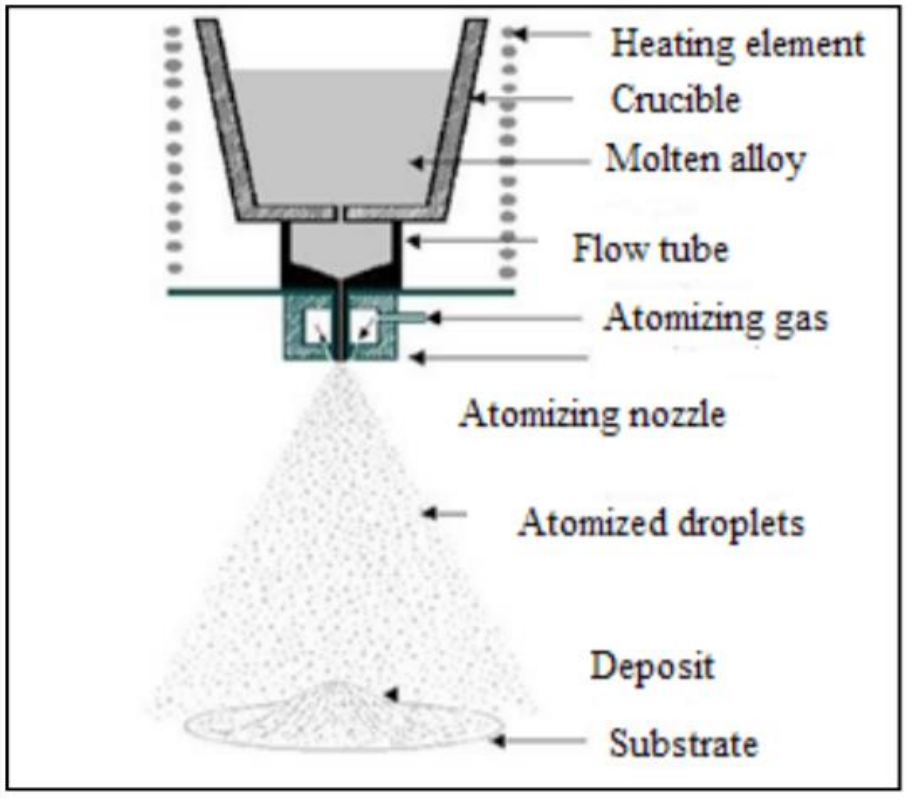

Fig. Spray Deposition (Source: Pawar, P. and A.A. Utpat, Procedia Materials Science, Vol. 6, pp 1150-1156, 2014)

- Osprey process: The droplet stream is produced from a molten bath.
- Thermal spray process: continuous feeding of cold metal into a zone of rapid heat injection
- The spray process has been extensively explored for the production of AMCs (Aluminium Matrix Composites) by injecting ceramic particle/whisker/short fibre into the spray.
- AMCs processed by spray deposition technique is relatively inexpensive with cost that is usually intermediate between stir cast and PM processes.

Chemical Vapor Deposition (CVD)

- In this process, the substrate is placed inside a reactor to which a number of gases are supplied. The fundamental principle of the process is that a chemical reaction takes place between the source gases. The product of that reaction is a solid material with condenses on all surfaces inside the reactor.

➢ **L**ow **P**ressure CVD (LPCVD)

➢ **P**lasma **E**nhanced CVD (PECVD)

Suitable for thin film with good step coverage

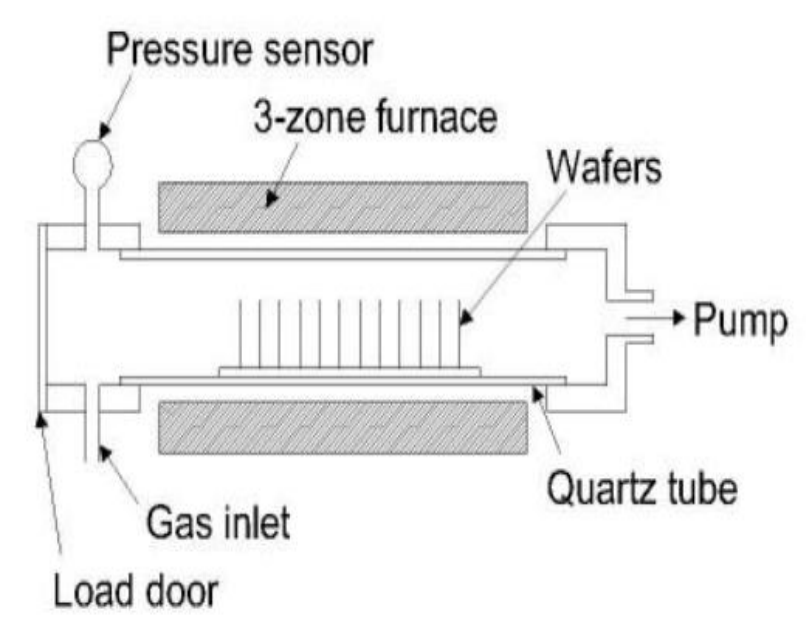

Fig. A Typical hot-wall LPCVD reactor (Source:https://www.memsnet.org/mems/processes/deposition.html, Acc date 30, march, 2018)

In-Situ Processing (Reactive processing)

- Different process fall in this category including liquid-gas, liquid-solid, liquid-liquid and mixed salt reactions.

- For Example , In a process the alloy of Al–Mg is placed on the top of ceramic preform in a crucible. The entire assembly is heated to a suitable temperature in the atmosphere of free flowing nitrogen bearing gas mixture.

- This method provides thermodynamic compatibility at the matrix reinforcement interface.

Research work in the Manufacturing of MMCs

- Last two decades Manufacturing of MMCs interests in high structural efficiency, excellent wear resistance, and attractive thermal and electrical characteristics in following fields.

➢Ground transportation (auto and rail)

➢Thermal management

➢Aerospace

➢Industrial

The future of advanced materials is related to systems solutions, economical manufacturing processing, diverse markets and new technologies.

Research work in the Manufacturing of MMCs

- A recent method Accumulative roll bonding (ARB) developed to produce particle reinforced metal matrix composites.
- In this method Aluminum matrix composite reinforced by submicron particulate alumina was successfully produced, the results of tensile and yield strength increasing by increasing the ARB cycles.
- Mechanical alloying (MA) technique- Aluminium-based metal matrix composite powders which enhances the powder production and eliminates the ball mills for blend steps.
- Squeeze casting technology provides elimination of porosity and shrinkage, 100% casting yield, attainment of greater part details, good surface finish, good dimensional accuracy, high strength to weight ratio, improved wear resistance, higher corrosion resistance, higher hardness, and resistance to high temperature, improved fatigue and better creep strength.

Research work in the Manufacturing of MMC - Continuous processing

NTUST

- Developed MMC wires with the diameter of 0.5-1.6 mm continuously by continuous pressure infiltration unit. Its Importance in high performance MMC wires for large scale commercial applications.

- Some Investigations going in developing metallic glasses with higher volume fraction to provide stronger and tougher materials.

Summary

- MMCs usually be light-weight metals like aluminum, magnesium, or titanium, and the reinforcements are usually ceramic particulates, whiskers, or fibers.
- Reinforcements – determining the property
- Al MMCs and Mg MMCs – many similarities used in Automobile and Aerospace industries.
- Ti MMCs- used in High Temperature properties.
- The main aim is to make these manufacturing processes more economical, productive and efficient.

Application of Metal Matrix Composites (MMCs)

Why MMCs? And Application areas

NTUST

- The high **strength-to weight ratio**, **enhanced mechanical and thermal properties** over conventional materials, improved **fatigue and creep characteristics, better wear resistance, and tailor ability** of properties make MMCs attractive in a variety of applications.
- Current MMC markets in the United States are primarily military. MMCs have potential for use in **aircraft structures, aircraft engines**, and **naval weapons systems**. Experimental MMC components were first developed for applications in **aircraft**, **jet engines**, **rockets**, and the **space shuttle**.

MMCs in different market sectors

- Applications in this segment include drive shafts, engine components, and brake components. The main constraint in the **transportation sector** is that it is an extremely cost-sensitive sector.

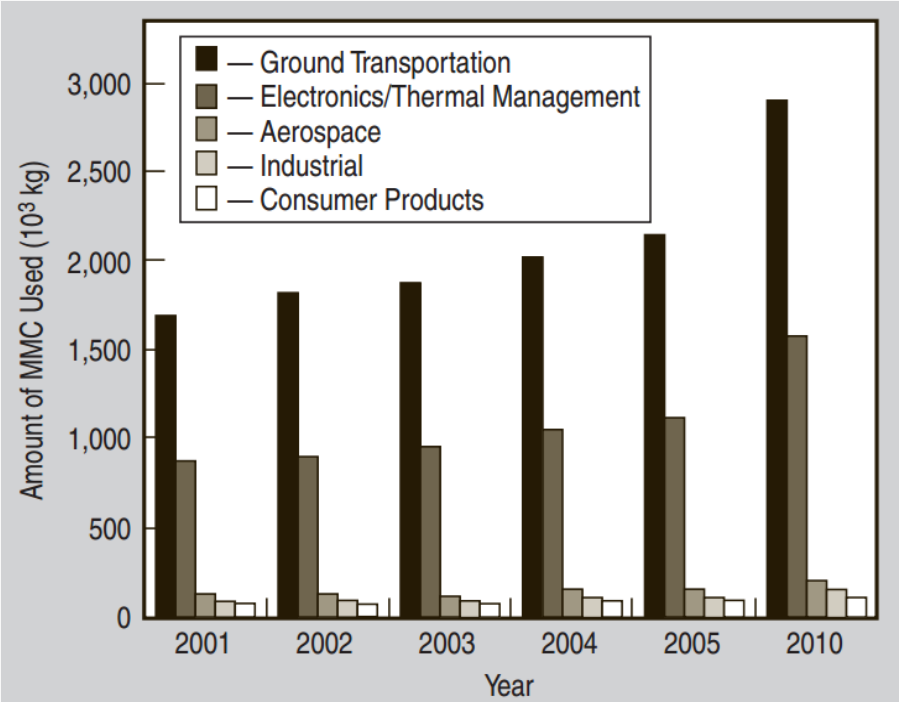

Fig. 25 The use of MMCs in different market sectors (adapted from a report by BCC, Inc.3)[**Source**:Chawla, N. and K. Chawla, JoM, **58**(11): p. 67-70, 2006].

Spacecraft Structural Application

Production space shuttle orbiter struts

- The high stiffness and compression strength and low density of **boron fiber-reinforced aluminum** led to its use in production space shuttle orbiter struts
- boron fiber-reinforced aluminum as MMCs material were used

continuous-fiber reinforced MMC B/Al tubular struts

Fig. 23 Mid-fuselage structure of Space Shuttle Orbiter showing boron-aluminum tubes. (Photo courtesy of U.S. Air Force/NASA) (**Source**:Kainer, K., WILEY-VCH. *2006*.)

Gr/Al composite is a high-gain antenna boom

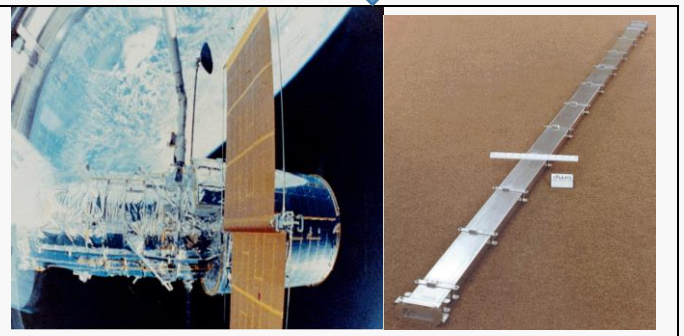

Fig. 24 The P100/6061 Al high-gain antenna wave guides/ boom for the Hubble Space Telescope (HST) shown (a-right) before integration in the HST, and (b-left) on the HST as it is deployed in low-earth orbit from the space shuttle orbiter (**Source**:Kainer, K., WILEY-VCH. *2006*.).

Automobile Engine application

- Metal-matrix composites are used in a variety of automotive applications. An early and successful engine application was selectively reinforced with aluminum pistons in the **Toyota diesel engine**.
- The conventional **diesel engine piston** has an **Al-Si casting alloy** with a crown made of a nickel cast iron. The main property requirement was **increased wear resistance** in this area.

…continued

- **Aluminum matrix materials reinforced** with **SiC** particles have also been used in **piston applications**, primarily in drag racing cars. In this case, the lower coefficient of thermal expansion of the MMC as compared to that of conventional aluminum allowed reduced clearances between the piston and cylinder wall, leading to improved performance.

Short fiber particulate reinforced aluminum matrix composite

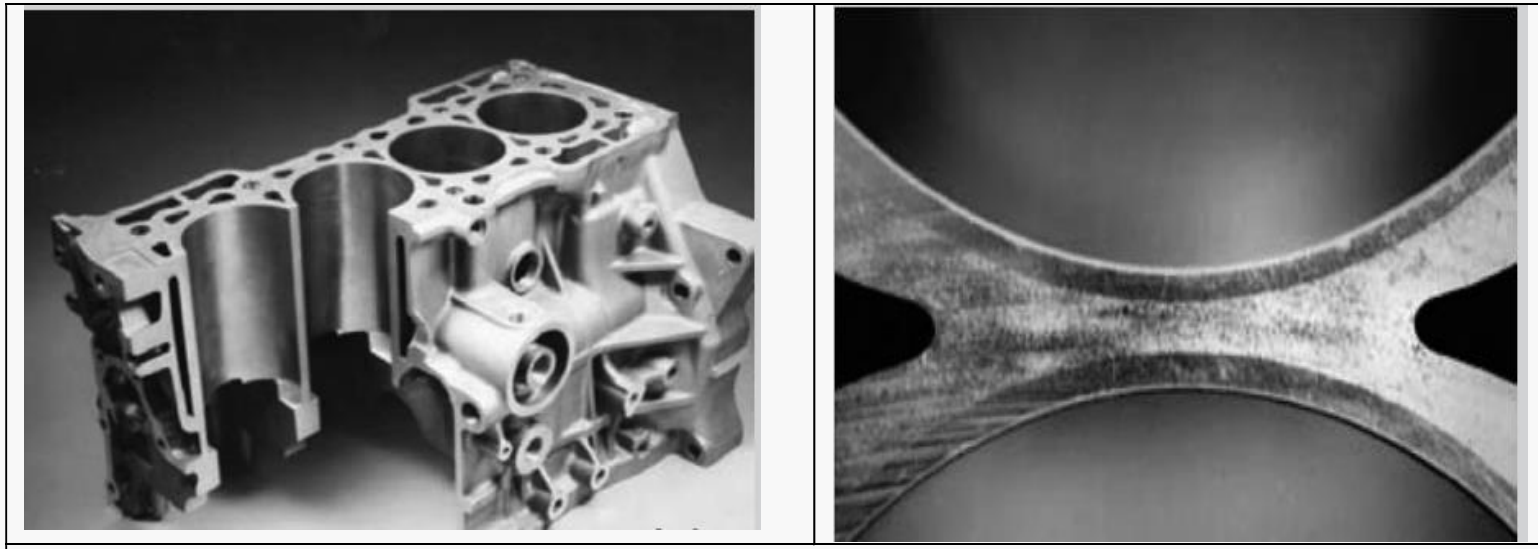

Fig. 26 A short fiber particulate reinforced aluminum matrix composite used as a cylinder liner in the Honda *Prelude* [parts (a) and (b) courtesy of D. Miracle]. The composite consisted of an Al-Si matrix with 12% Al2O3 for wear resistance, and 9% carbon for lubricity. (a) *Prelude* engine block, (b) magnified view of cylinder liner[**Source**:Chawla, N. and K. Chawla, JoM, **58**(11): p. 67-70, 2006].

NTUST

For driveshaft and brake drums and brake rotors

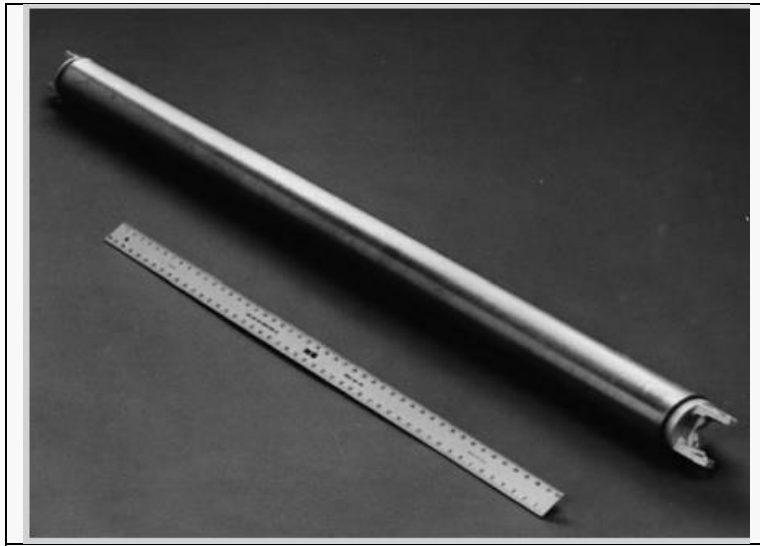

Fig. 27 A 6061/Al2O3/20p composite used as driveshaft in the *Corvette* (courtesy of D. Miracle). The composite exhibits a 36% increase in specific modulus over steel [**Source**:Chawla, N. and K. Chawla, JoM, **58**(11): p. 67-70, 2006].

Fig.28 Particulate MMCs for use in brake drums and brake rotors, as a replacement for cast iron (courtesy of D. Miracle). The high wear resistance and thermal conductivity coupled with 50–60% weight savings make MMCs quite attractive for this application [**Source**:Chawla, N. and K. Chawla, JoM, **58**(11): p. 67-70, 2006].

Passenger car engine and sinter forged MMC connecting rods

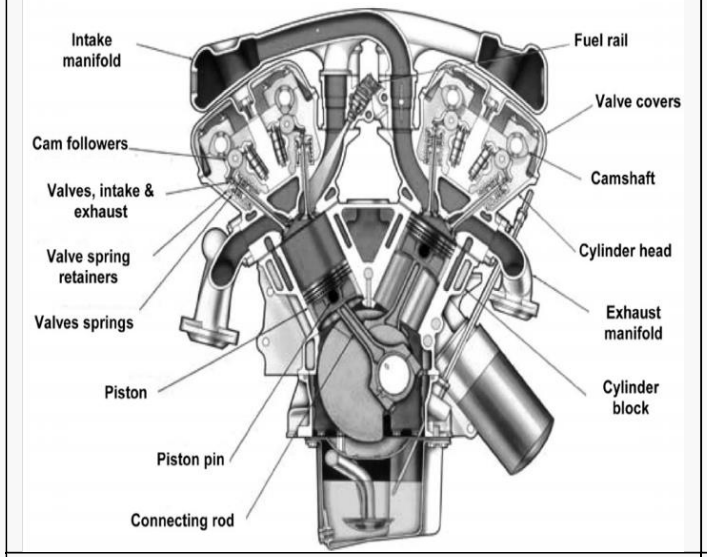

Fig. 29 A cross section of a passenger car engine showing the location of the connecting rod (courtesy of J. Allison) [**Source**: Chawla, N. and K. Chawla, JoM, **58**(11): p. 67-70, 2006].

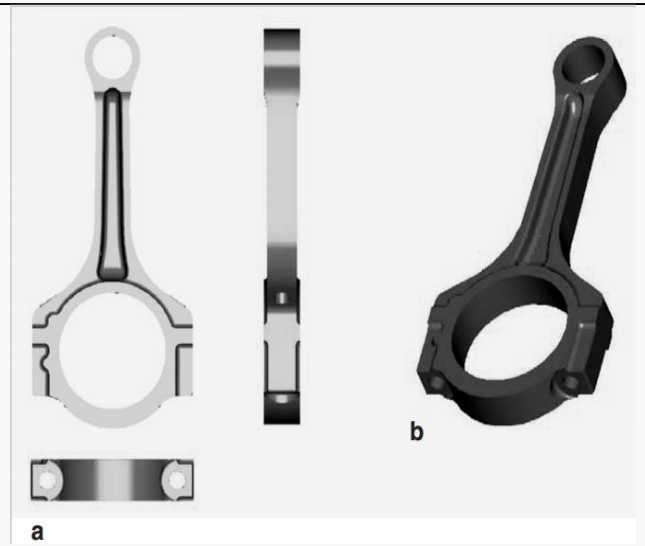

Fig. 30 Models of sinter forged MMC connecting rods: (a) two-dimensional view and (b) three-dimensional view (courtesy of F. Liu) [**Source**:Chawla, N. and K. Chawla, JoM, **58**(11): p. 67-70, 2006].

High speedway railroad Application

High speedway railroad coach bogie.

A selectively cast aluminum -matrix composite with SiC particles for this application.

The weight was reduced from 115 kg for a spheroidal graphite iron disk to 65 kg for the MMC disk, a weight savings of 43%.

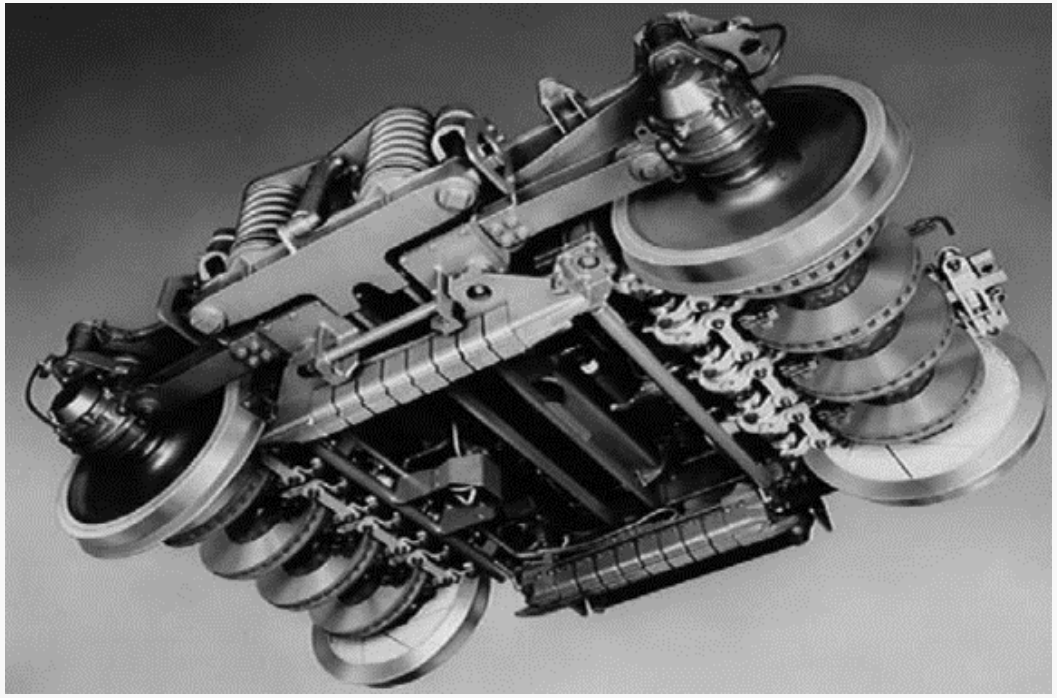

Fig. 31 High speedway railroad coach bogie with four brake disks produced by SAB Wabco (courtesy of H. Ruppert) [**Source**:Chawla, N. and K. Chawla, JoM, **58**(11): p. 67-70 2006].

…continued

- **Aluminum alloys reinforced** with **ceramic particulates** have significant potential for **structural applications** due to their **high specific strength and stiffness** as well as **low density.**
- These properties have made particle-reinforced metal matrix composites (MMCs) an attractive candidate for the use in **weight-sensitive and stiffness-critical components** in **aerospace, transportation and industrial sectors**.

…continued

- The driving force for **lightweight railway vehicles** has also prompted the use of **high performance MMCs**.
- A conventional brake system for a railway vehicle, consists of **four brake disks, calipers, hand brake, and electromagnetic track brake.**

Aerospace engine Application

- With increasing demand on fuel economy improvement and emission control, there is great deal of interest in using advanced materials to produce lightweight vehicles.
- Aerospace engine and airframe designers are constantly seeking lighter weight high strength materials to reduce weight and improve performance of power plants and aircraft.

NTUST

Potential engine applications for Ti MMCs

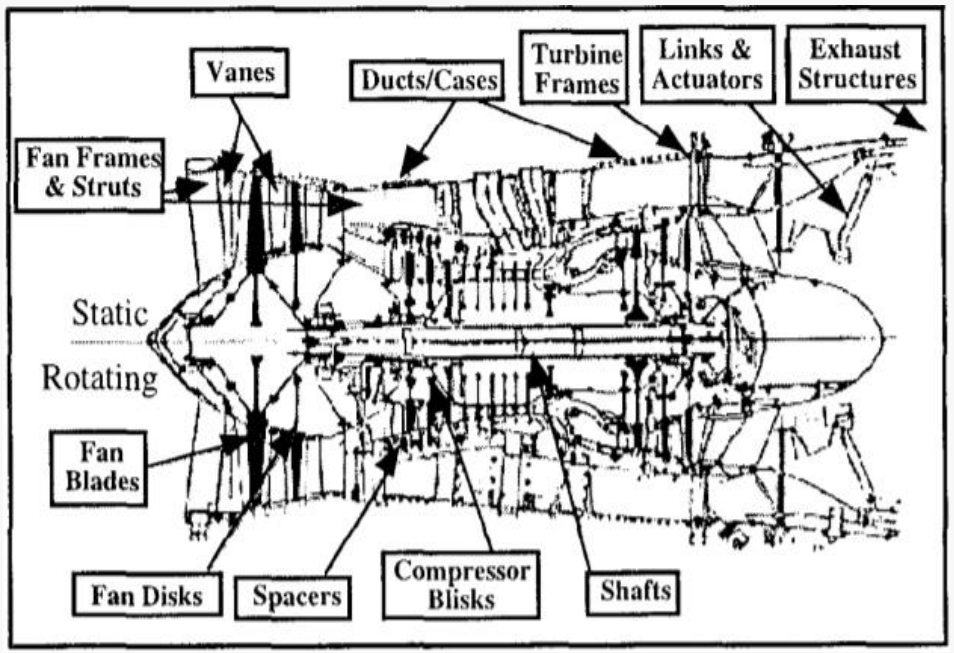

a)

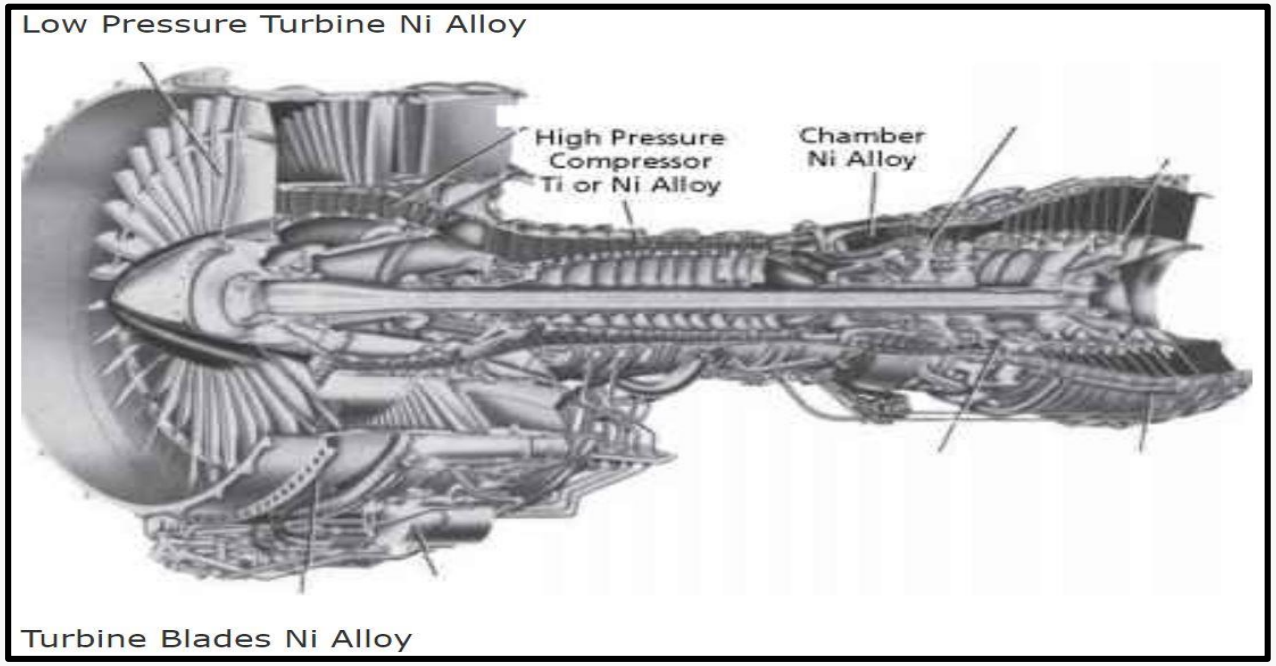

b)

Fig. 32. a) Potential engine applications for Ti MMCs and
b) Typical Material Distribution in Jet Engine (**Source**: Mahenderkar, N.K., T.R. Prabhu, and A. Kumar, *Nanocomposites Potential for Aero Applications*, p. 391-411, 2017).

Summary

- The use of Metal Matrix Composite in different advanced engineering application is a result of its low density, high strength to weight ratio, high toughness and impact strength, high elastic modulus, high surface durability, low sensitivity to thermal shock, good wear and fatigue resistance, high specific strength and stiffness, impact strength, and high surface durability.

Continued …

- MMCs are applicable in the area of automobile engine, aerospace engine components, ground transportation, industrial sectors, and spacecraft structural application.
- Generally, some of MMCs considered for potential applications contain **ceramic particles or short fibers** in a light alloy, such as **aluminum, magnesium and titanium**.

Case studies

…continued

Stir casting furnace and accessories.

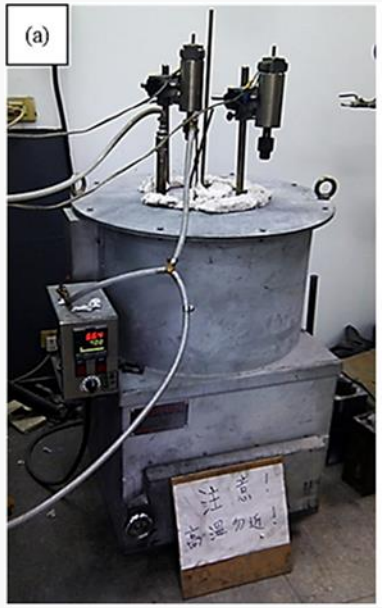

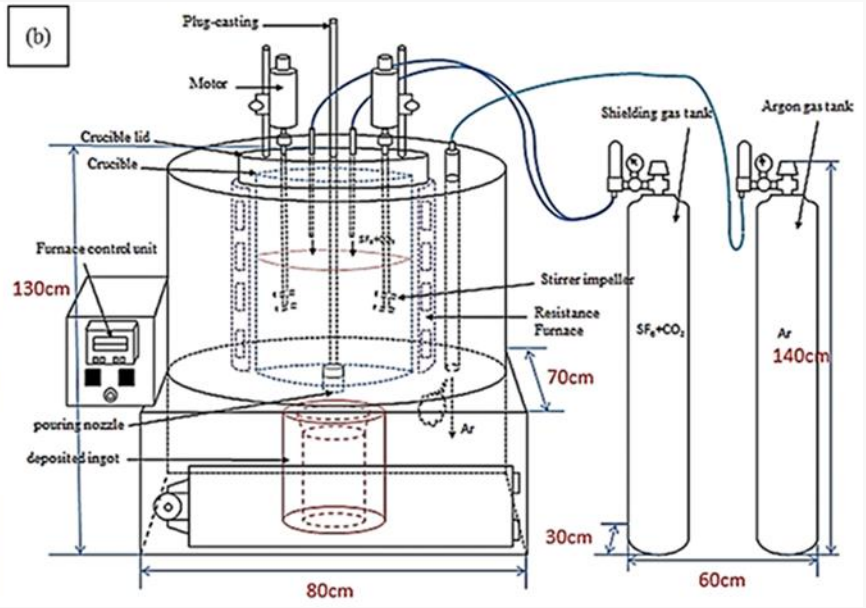

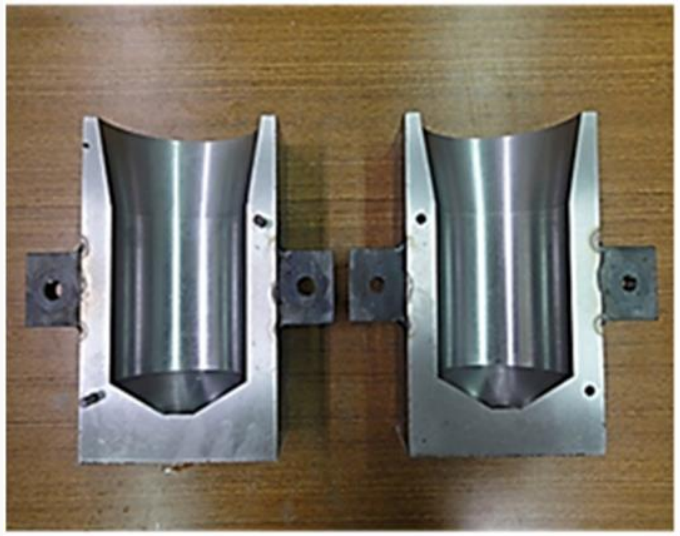

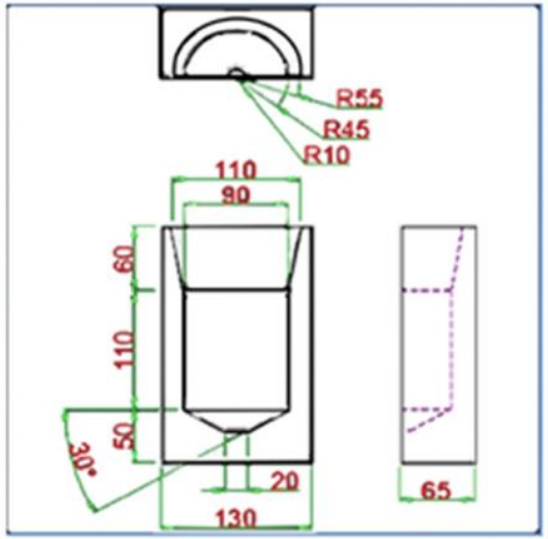

In our lab, the most common fabrication method of metal matrix composites is stir casting method.

…continued

High specific strength and wear resistance behaviour

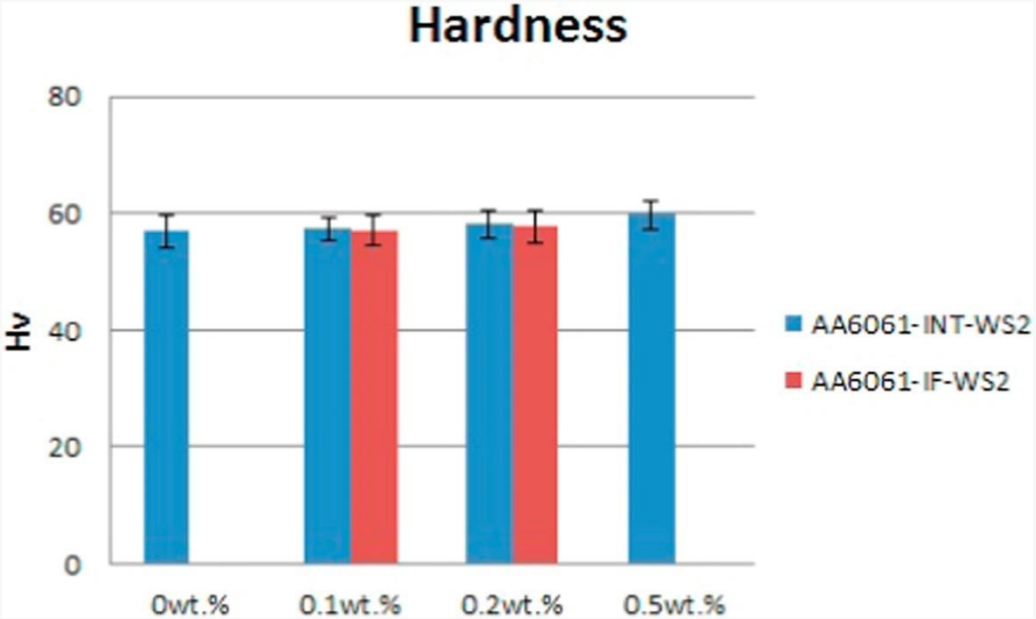

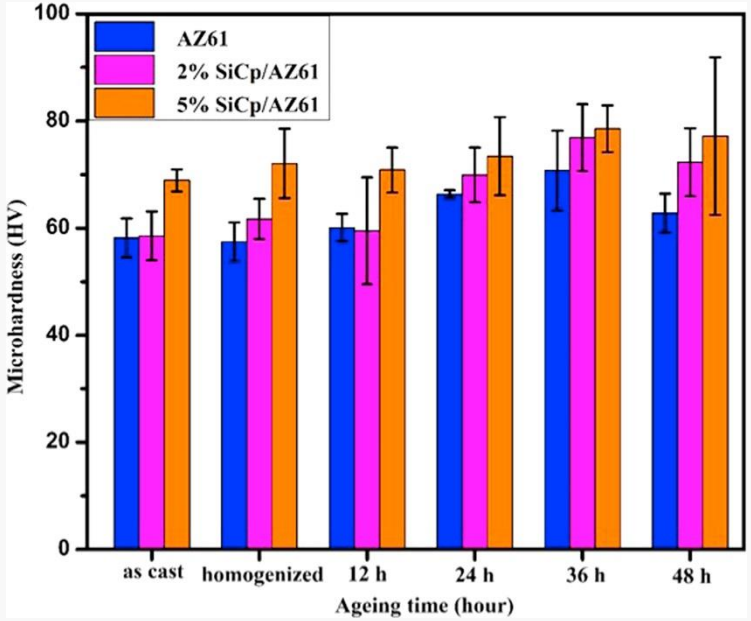

The main purpose of metal matrix composites is to balance the strength, weight and ductility properties of light weight (magnesium, aluminum) matrix materials and reinforcing hard particles.

…continued

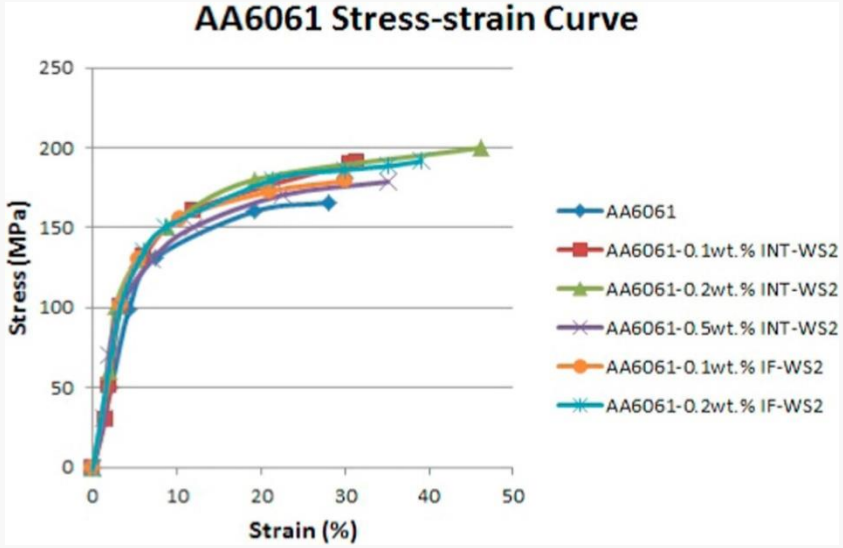
AA6061 Stress-strain Curve
Stress (MPa)
Strain (%)
0
50
100
150
200
250
0
10
20
30
40
50
AA6061
AA6061-0.1wt.% INT-WS2
AA6061-0.2wt.% INT-WS2
AA6061-0.5wt.% INT-WS2
AA6061-0.1wt.% IF-WS2
AA6061-0.2wt.% IF-WS2

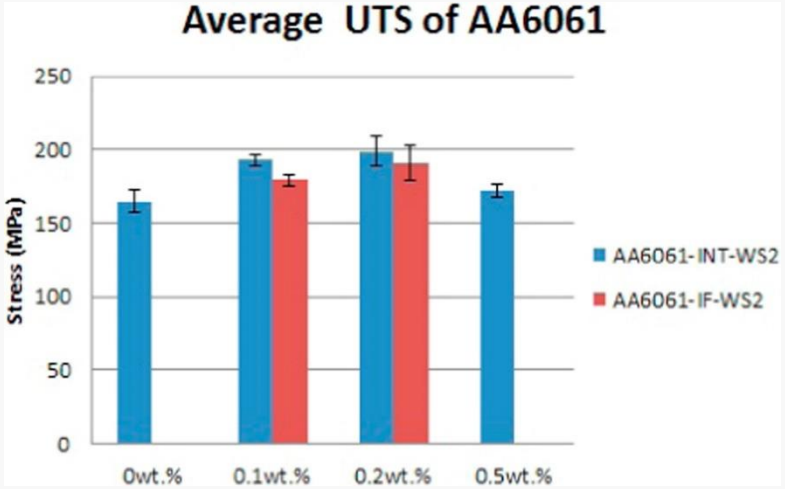
Average UTS of AA6061
Stress (MPa)
0
50
100
150
200
250
0wt.%
0.1wt.%
0.2wt.%
0.5wt.%
AA6061-INT-WS2
AA6061-IF-WS2

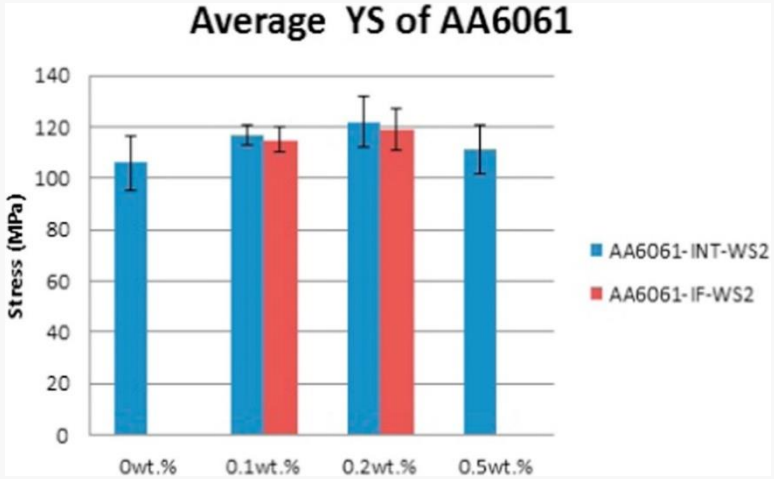
Average YS of AA6061
Stress (MPa)
0
20
40
60
80
100
120
140
0wt.%
0.1wt.%
0.2wt.%
0.5wt.%
AA6061-INT-WS2
AA6061-IF-WS2

…continued

a. **b.** **c.** **d.**

Fig. 39 SEM image of an assortment of WS_2 nanotubes; **b.** TEM image of a single WS_2 nanotube Scale bar is 5 nm **c.** Mg-MMC ingots prepared at different temperatures **d.** Summary of the mechanical testingof the different Mg-alloy samples

…continued

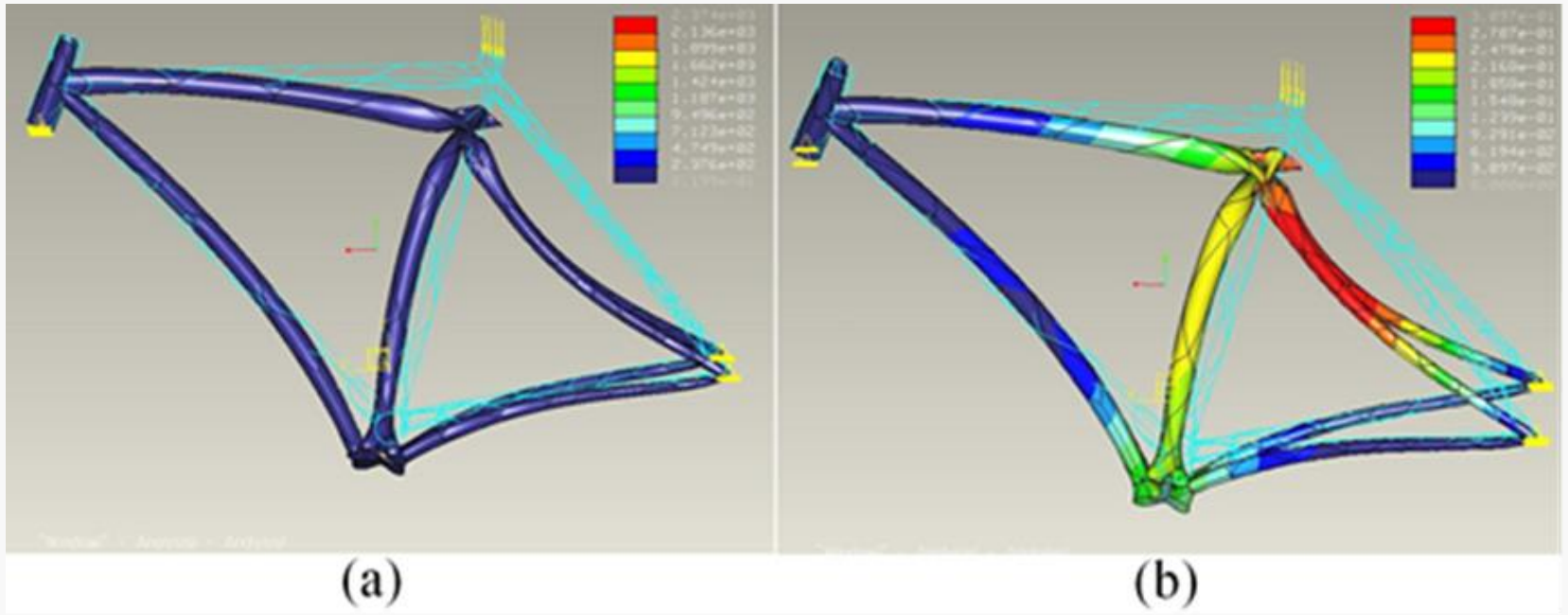

(a) Stress analysis and (b) displacement analysis of a bicycle frame.

Formability

In our lab equal channel angular pressing severe plastic deformation is used to produce different plastic stages of metal matrix composites.

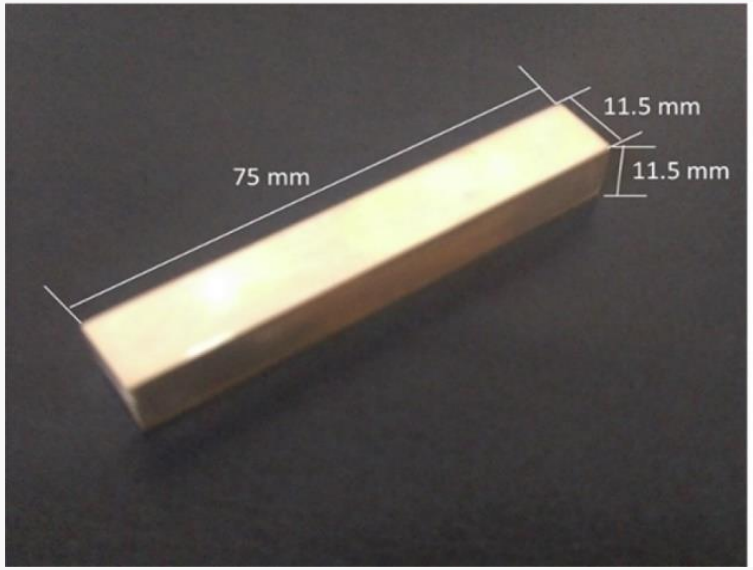

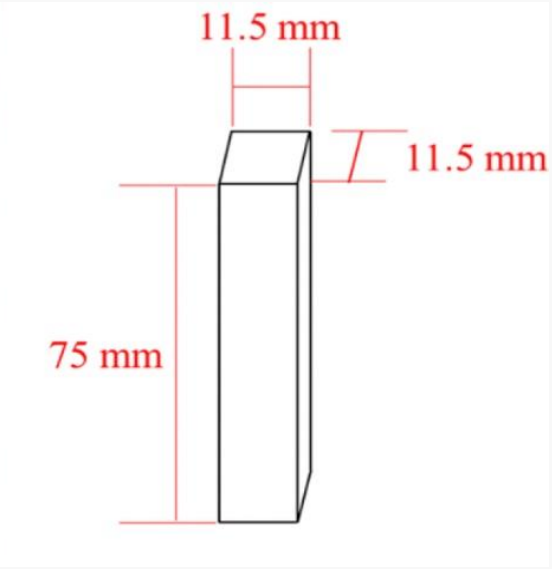

Billets of size 11.5 mm × 11.5 mm × 75 mm prepared for ECAP.

…continued

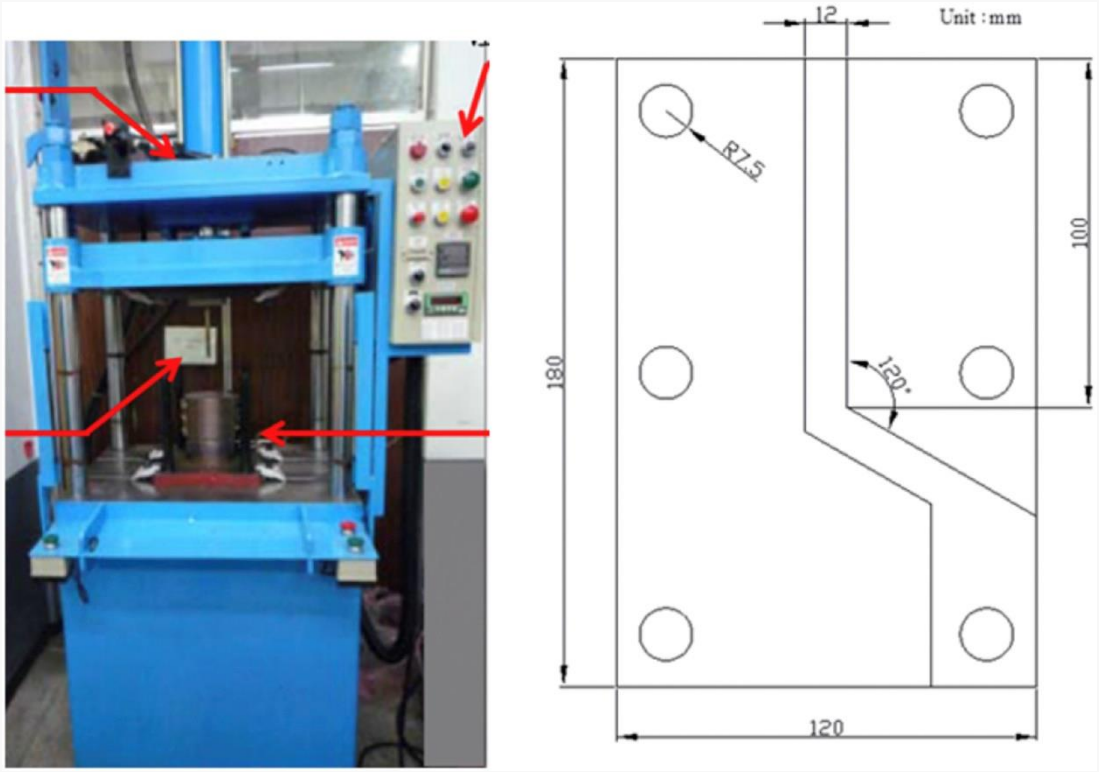

Scheme of the ECAP machine and its mold dimension.

…continued

Outer appearance of AZ61 after ECAP treatment of one, four, and eight passes (N: number of passes).

ECAPed AZ61 Magnesium Alloy. (a) 1 pass, (b) 2 pass and (c) 4 pass.

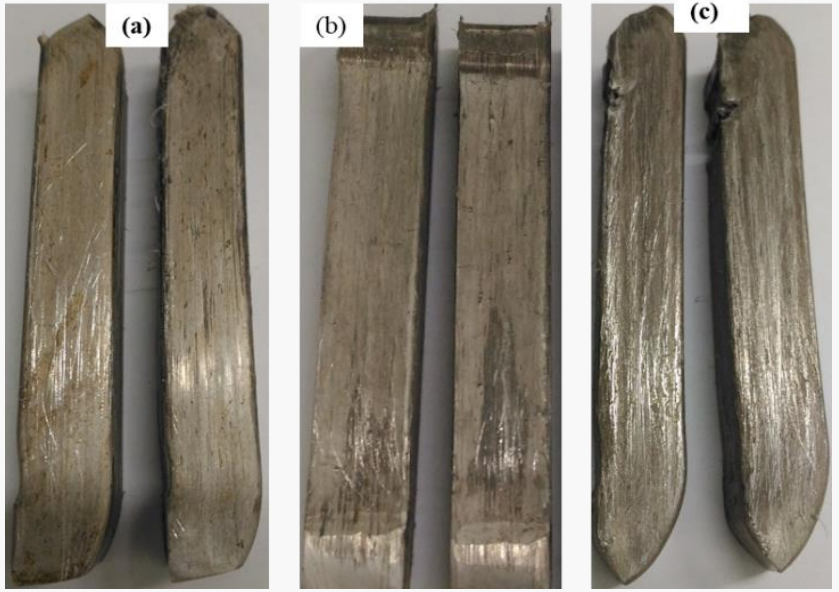

ECAped 2 wt% SiCp/AZ61 Mg MMCs. (a) 1 pass, (b) 2 pass and (c) 4 pass.

…continued

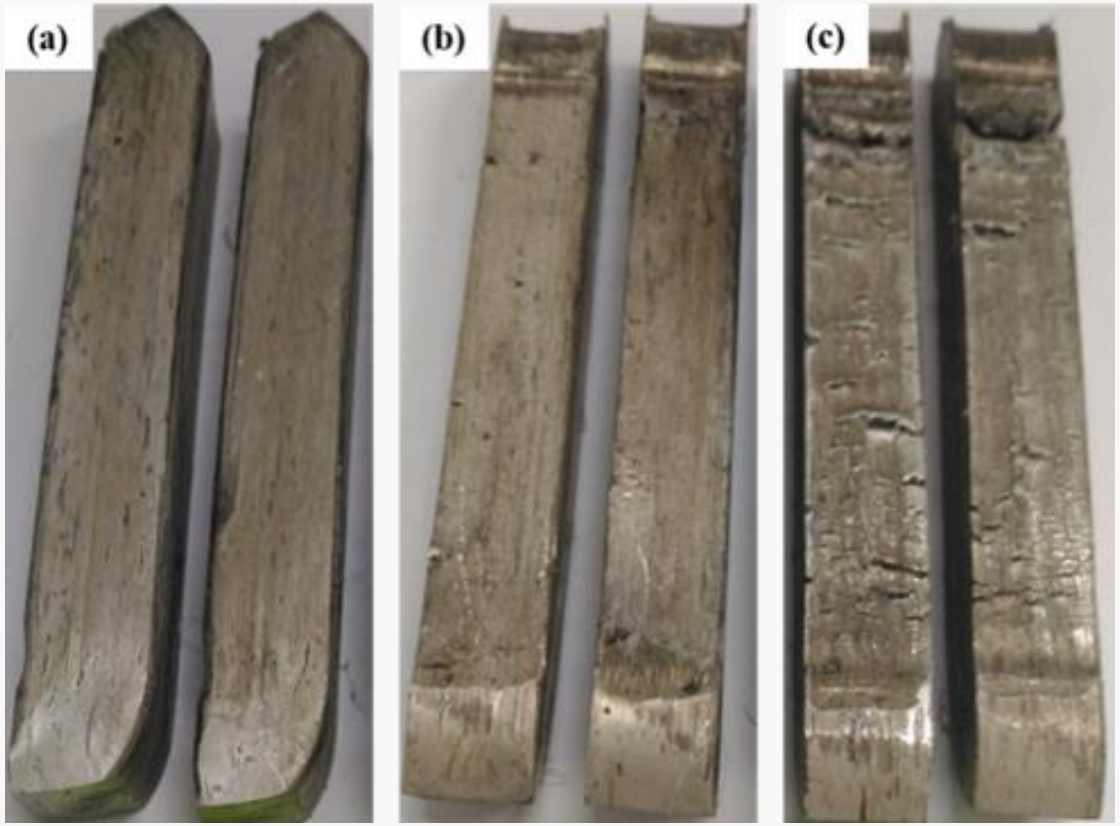

ECAPed 5 wt% SiCp/AZ61 Mg MMCs. (a) 1 pass, (b) 2 pass and (c) 4 pass.

…continued

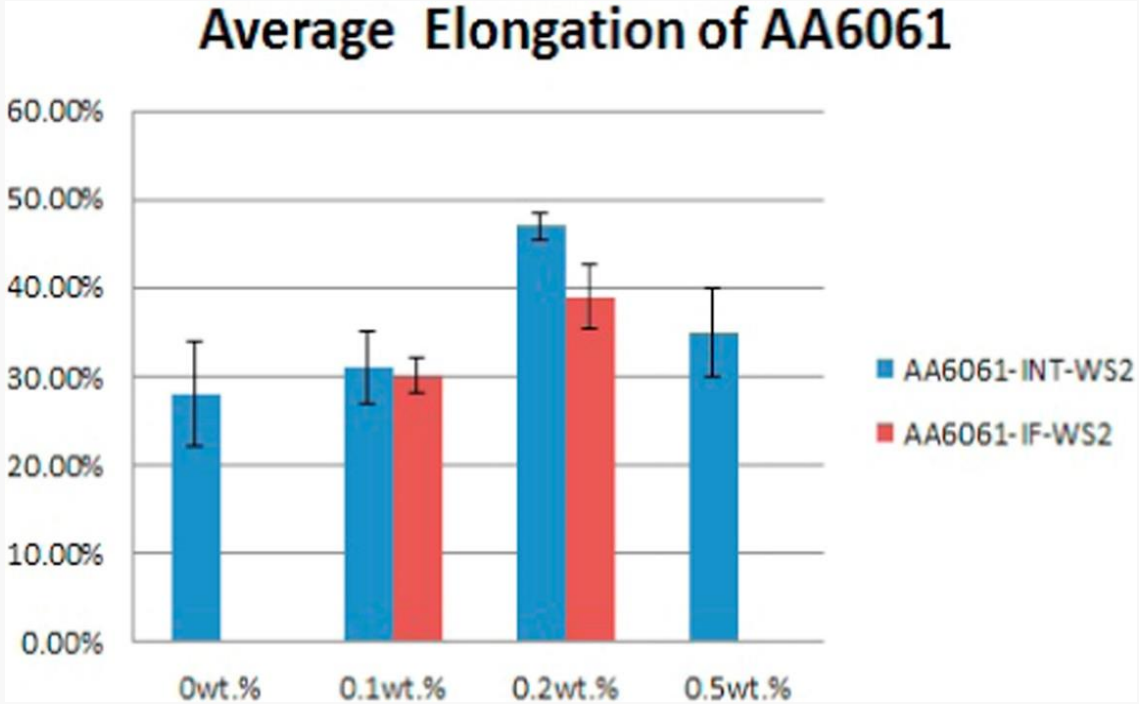

Elongation of AA6061/WS_2 INT MMCs and AA6061/WS_2 IF MMCs with different concentrations of the nanotubes/nanoparticles

…continued

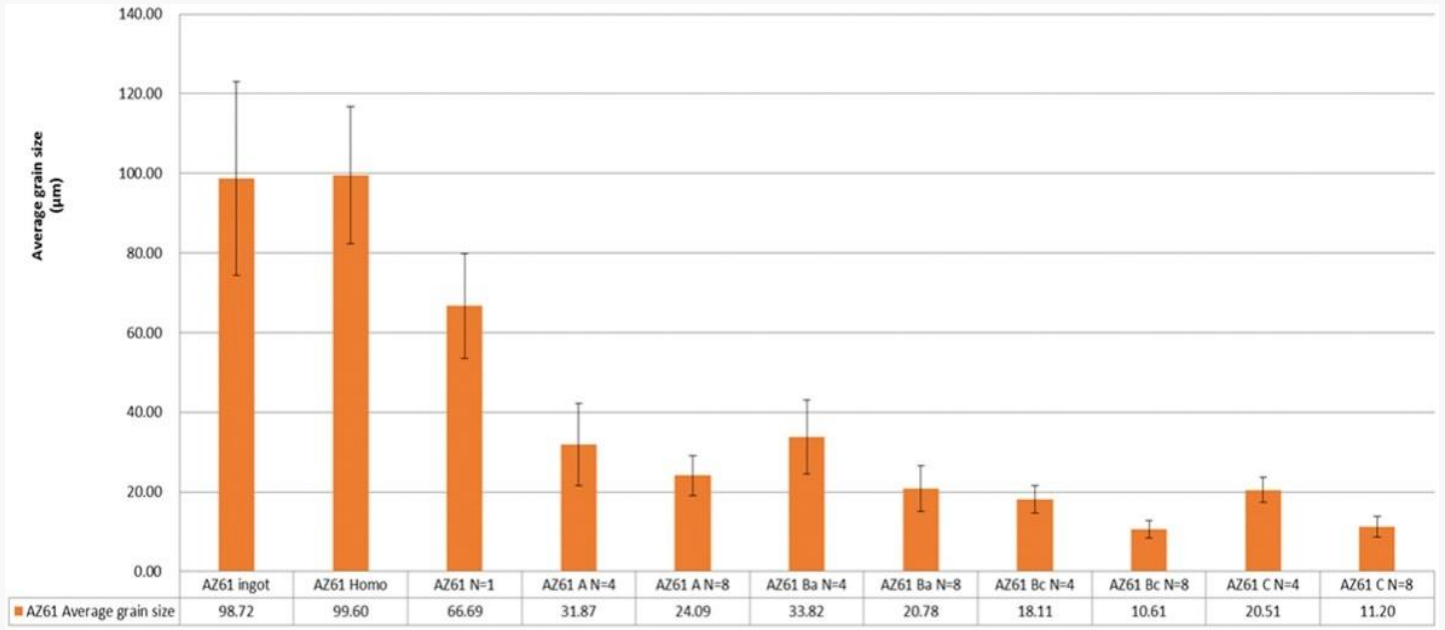

Average grain size of AZ61 as-cast (ingot), homogenized (Homo), and ECAP-treated with N = 1, 4, and 8 and route A, Ba, Bc, and C (N: number of passes).

…continued

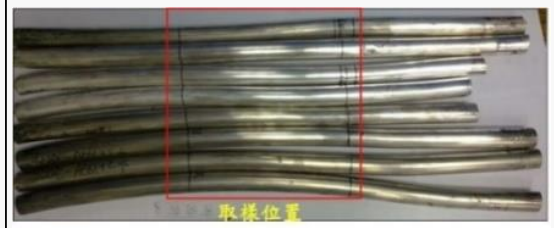

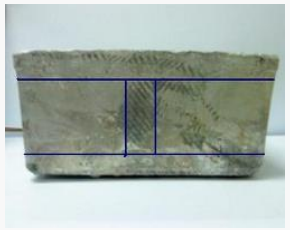

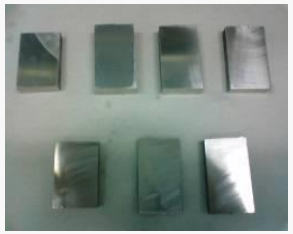

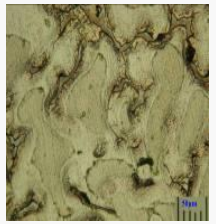

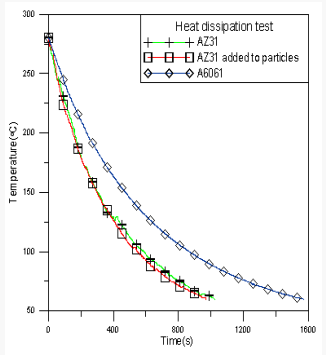

a **bc**

Fig. 49 a. Tube Extrusion of Mg MMCs **b.**Mg MMCs**c.**Heat sink materials for LED

…continued

Superior hydrogen storage efficiency

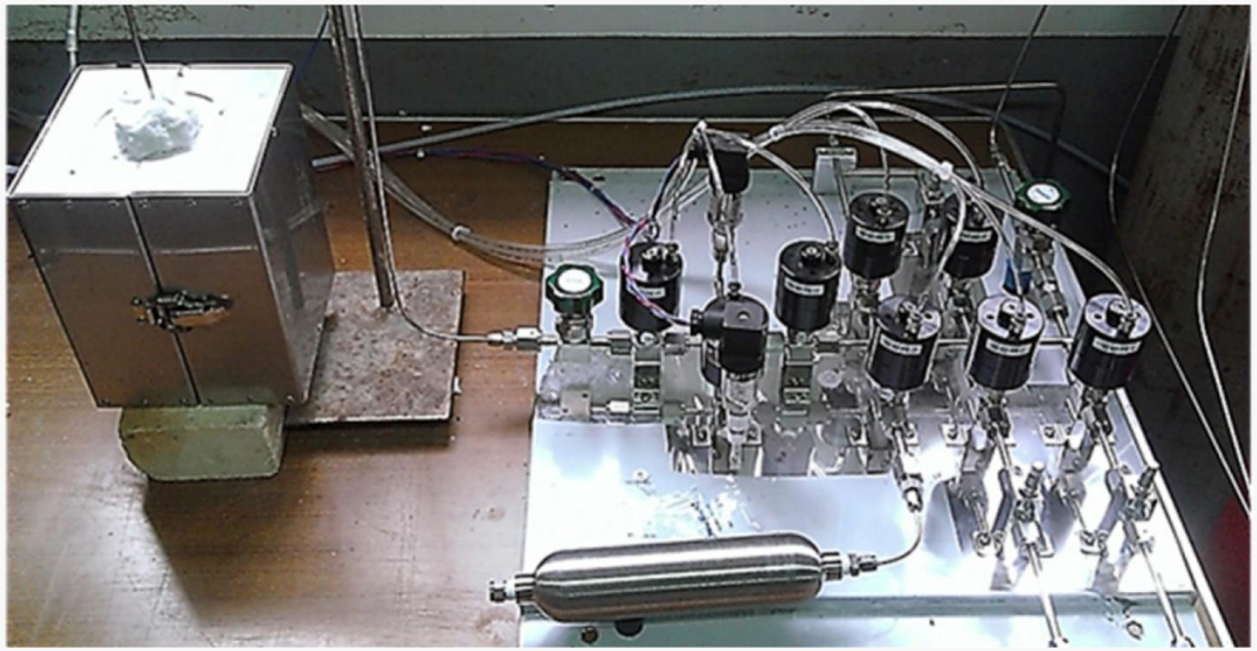

Sievert-type hydrogen measurement system

…continued

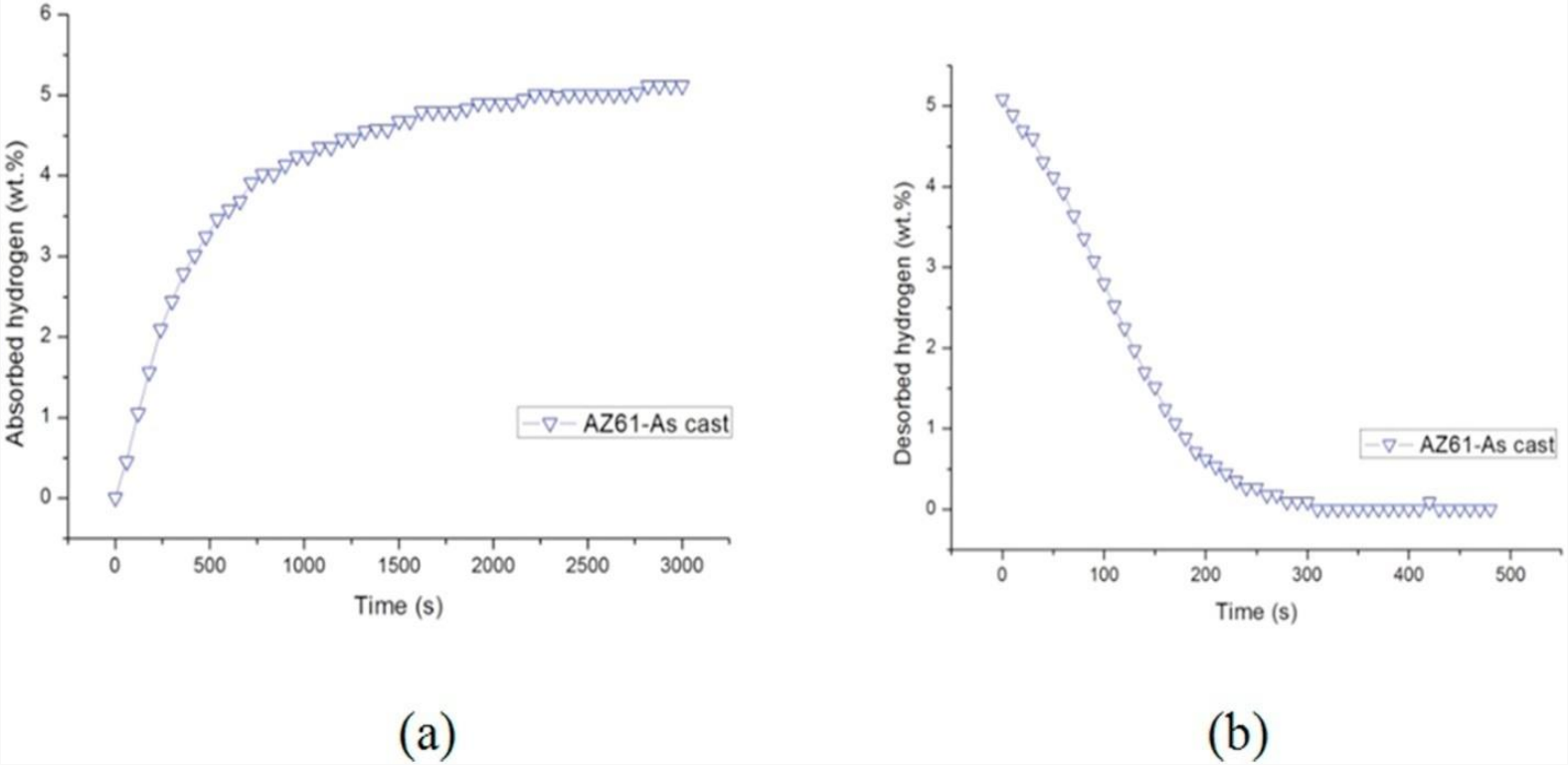

Kinetics of hydrogen (a) absorption and (b) desorption at 648 K in as-cast samples of AZ61.

…continued

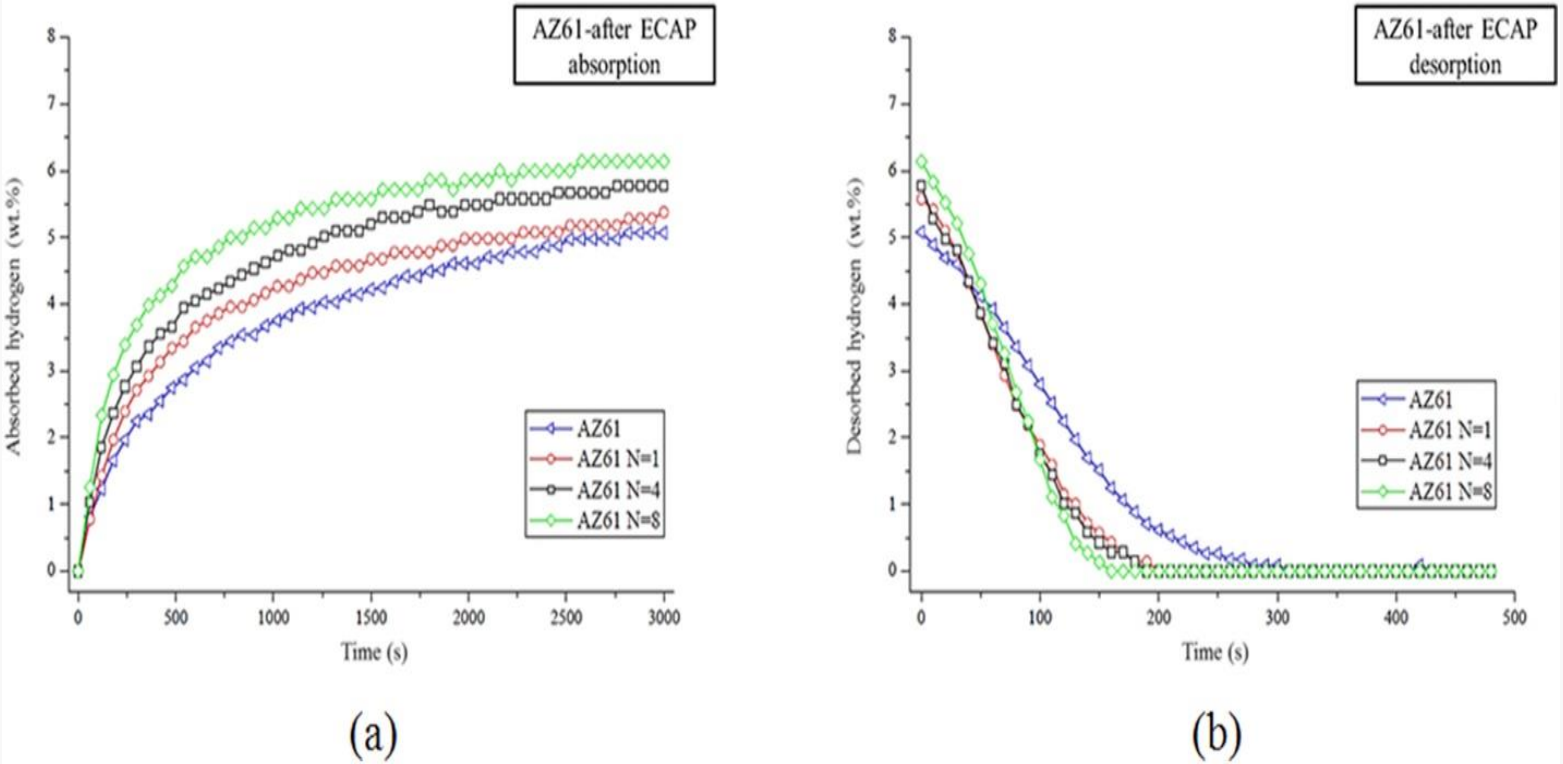

Kinetics curves of hydrogen (a) absorption and (b) desorption at 648 K in as-cast and ECAP-processed samples of AZ61.

…continued

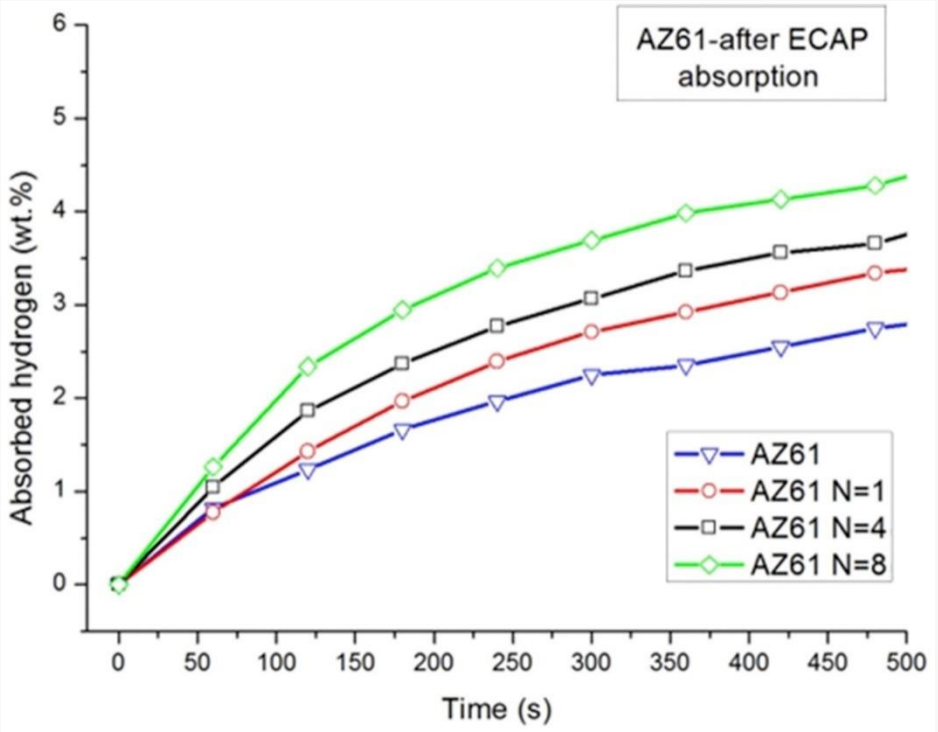

Kinetics curves of hydrogen absorption at first 500 s at 648 K in as-cast and ECAP-processed samples of AZ61.

Biocompatibility

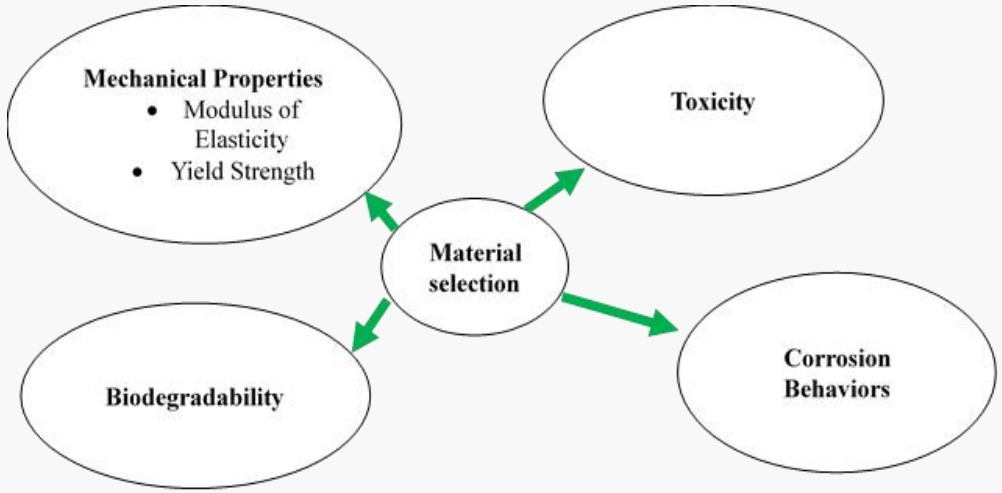

Materials selection processes and MMCs application areas.

…continued

CAD design and simulation of dental implant and bones (Cancellous and Cortical).

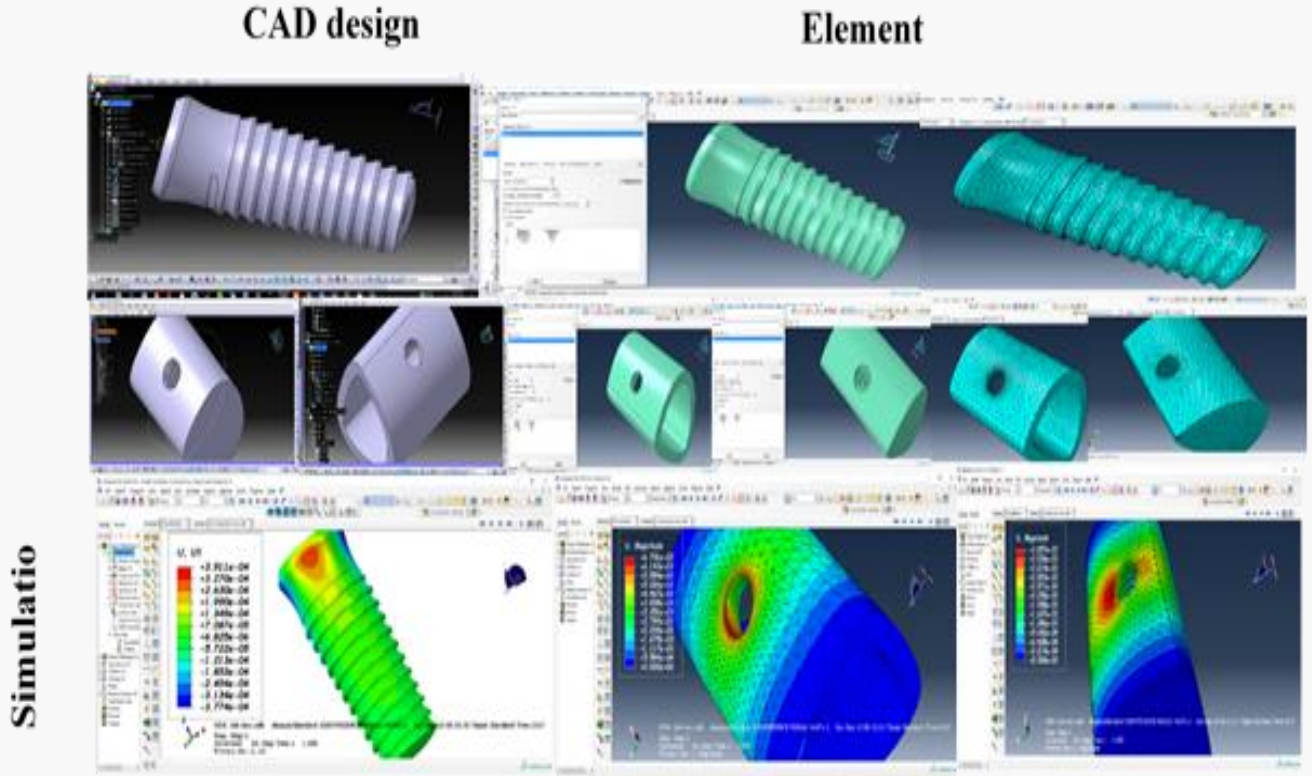

…continued

Standard Plus Short (SPS) Regular Neck(RN) Struatmann Implant

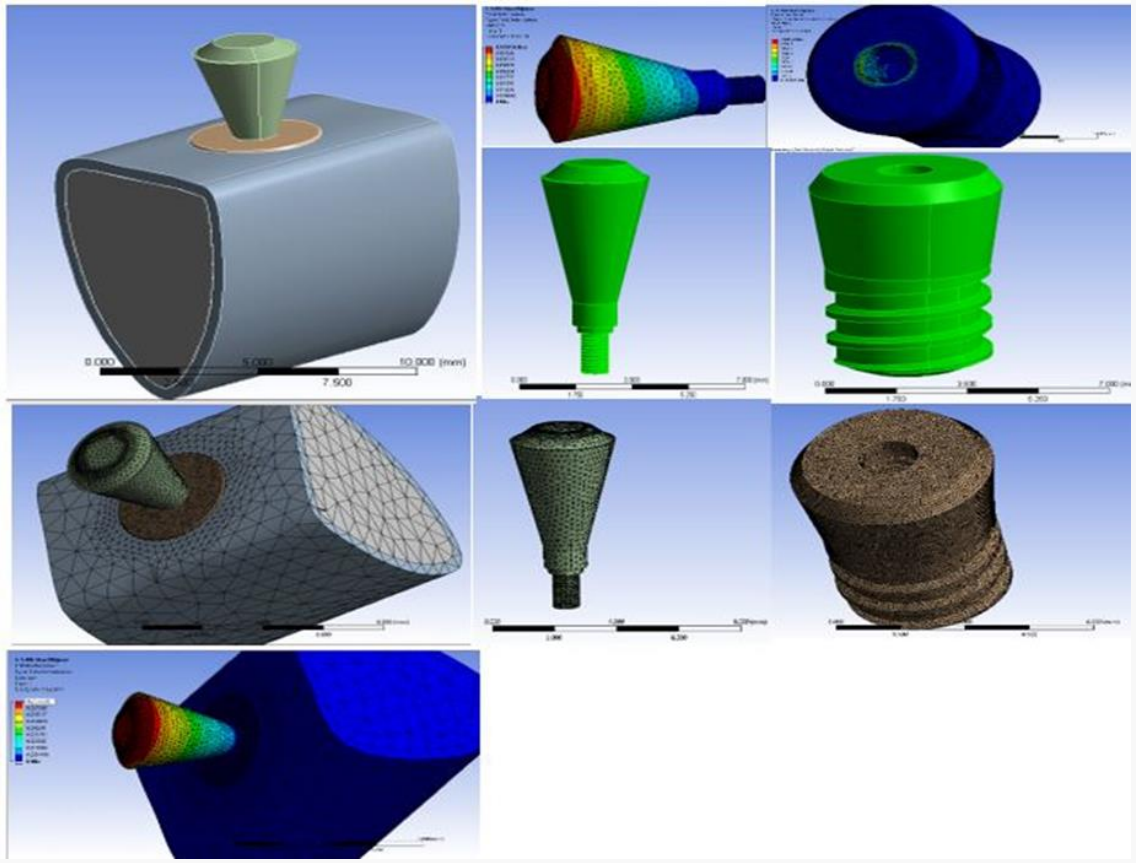

…continued

Standard Plus Short Struatmann Wide Neck (WN) implant

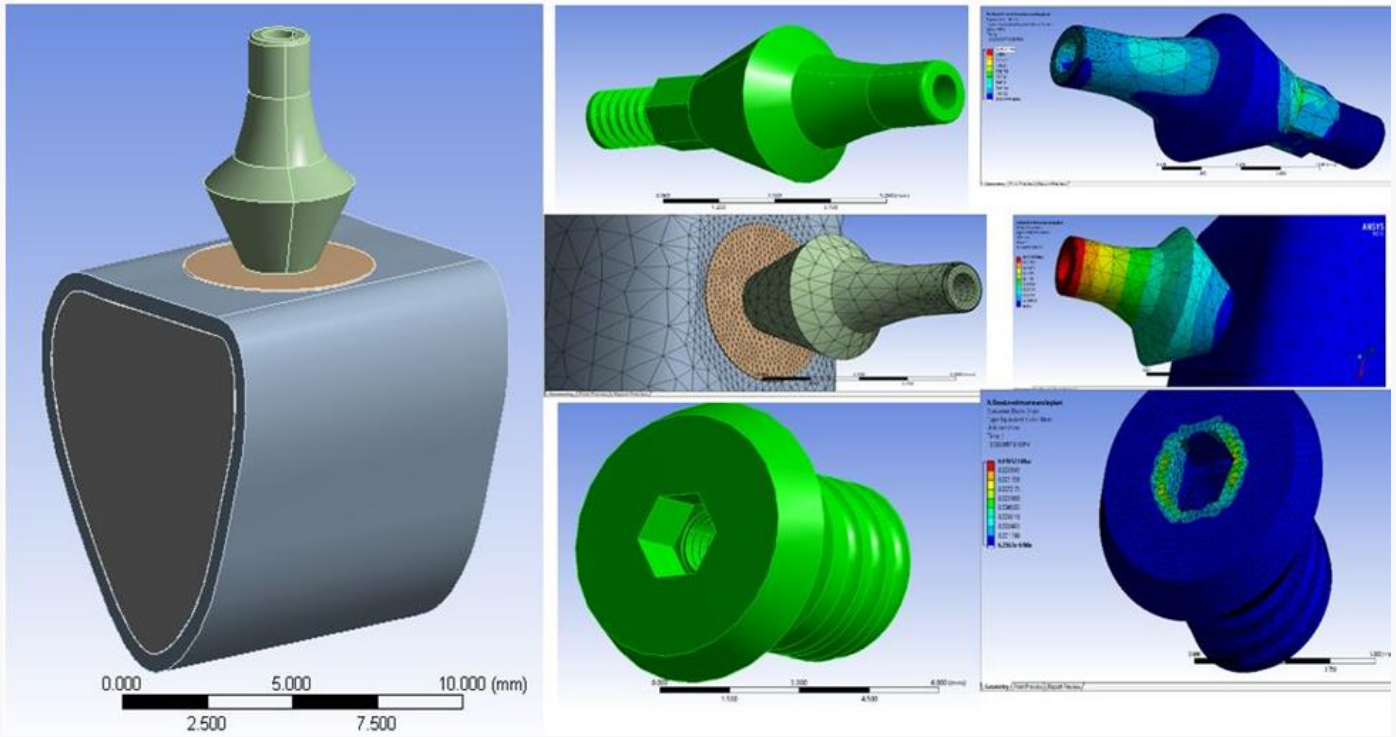

…continued

CAD design and simulation of dental implant and bones (Cancellous and Cortical).

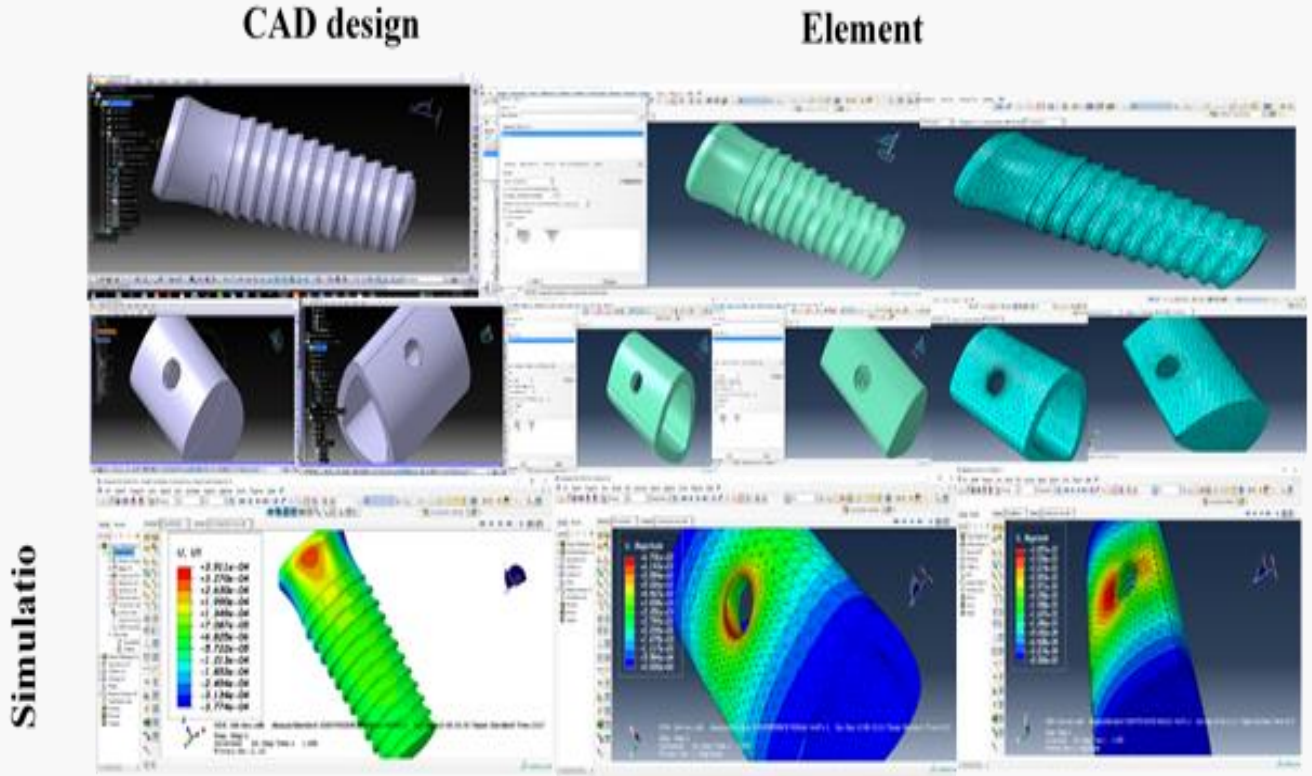

Mechanical behaviour enhancement

Mechanical Behavior Enhancement of AZ31/WS_2 and AZ61/WS_2 Magnesium Metal-Matrix Nanocomposites

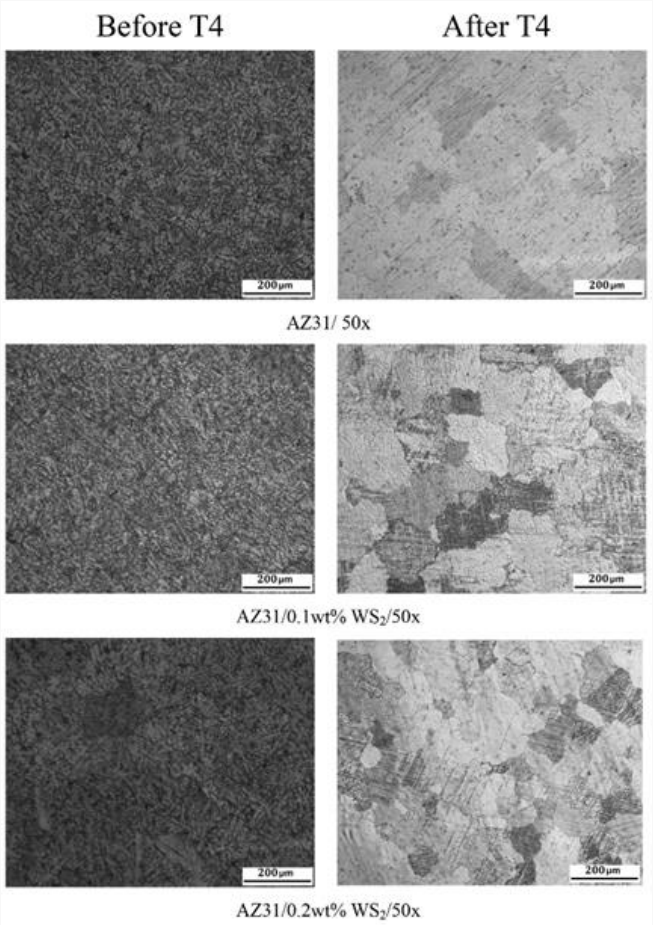

Comparison of AZ31 magnesium alloy castings before and after solution heat treatment (magnified 50).

…continued

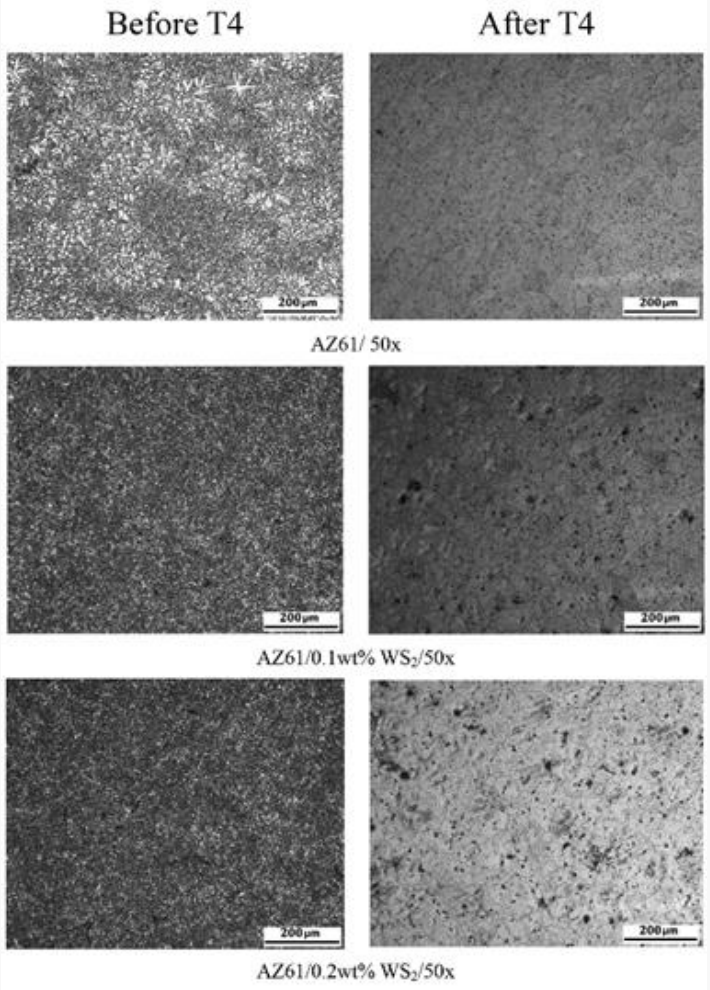

Comparison of AZ61 magnesium alloy castings before and after solution heat treatment (magnified 50).

…continued

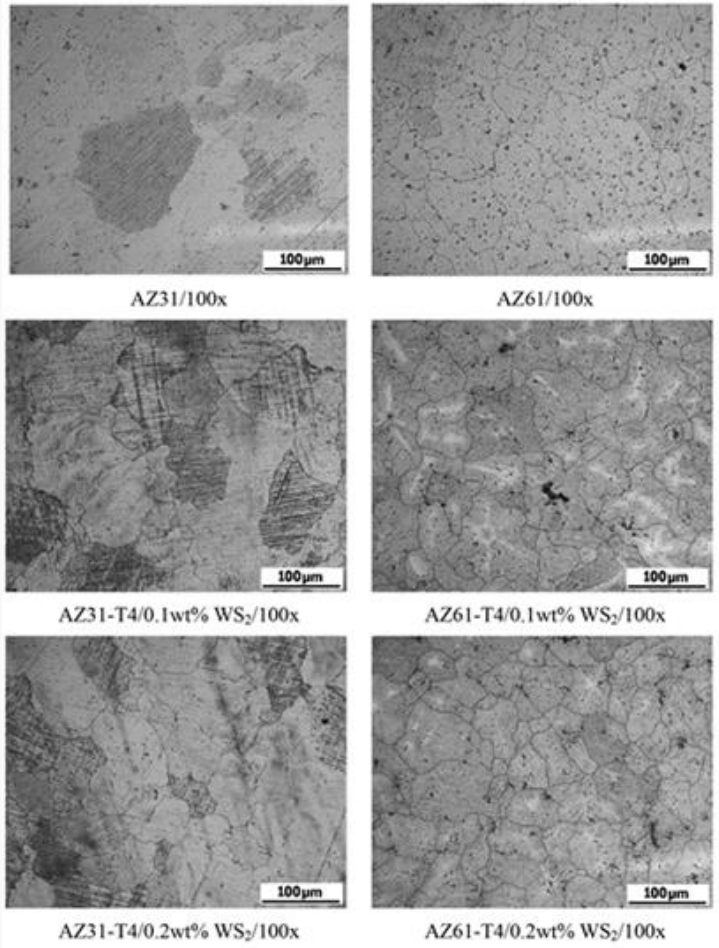

OM images of AZ31-T4 and AZ61-T4 with various weight percentages of WS2 (magnified 100).

…continued

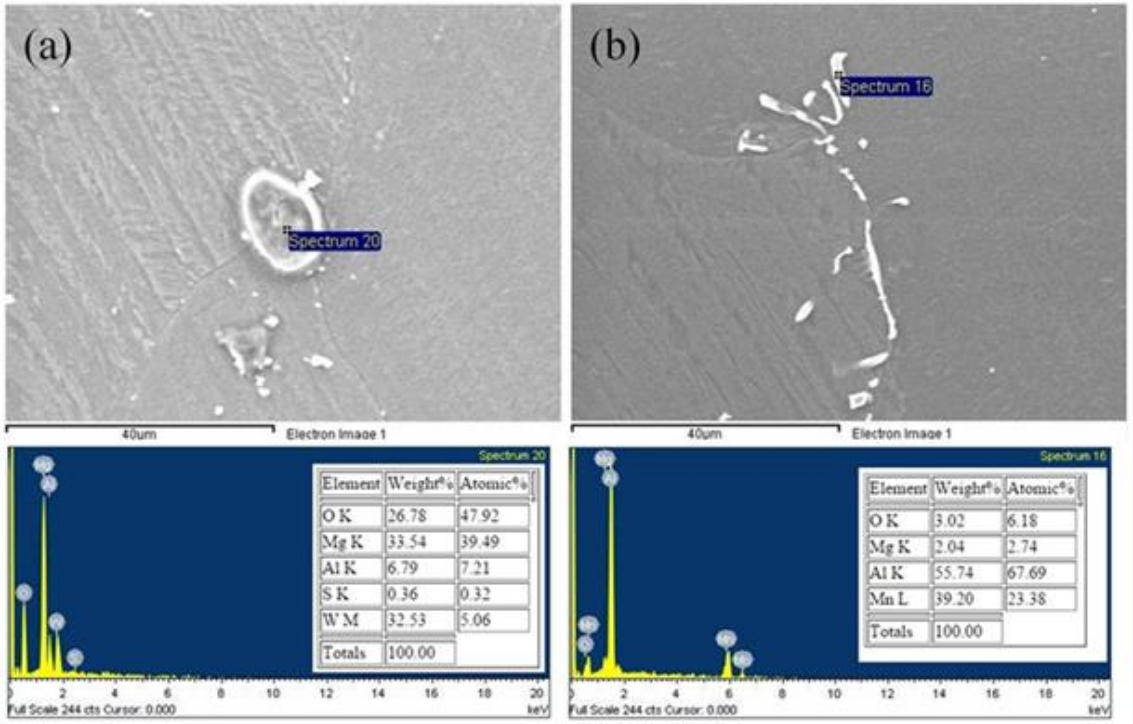

SEM micrographs and EDS with 0.2wt% WS2 ：(a) WS2 in AZ31. (b) AlMn in AZ61.

…continued

Vickers hardness of AZ31-T4 and AZ61-T4 with various contents of strengthening phase

	0 wt.% INT	0.1 wt.% CNT	0.1 wt.% INT	0.2 wt.% INT
AZ31-T4	51.0	52.3	54.3	55.9
AZ61-T4	55.4	57.8	58.3	58.6

Tensile test results of AZ31-T4 and AZ61-T4 with various contents of strengthening phase

	wt.%	Yielding stress (MPa)	Ultimate tensile stress (MPa)	Elongation (%)
AZ31-T4	0%	74.8	134.8	13.90
	0.1% CNT	75.4	141.0	13.92
	0.1% INT	85.7	171.7	23.42
	0.2% INT	87.2	208.2	25.74
AZ61-T4	0%	76.8	130.4	10.0
	0.1% CNT	79.3	141.4	14.98
	0.1% INT	79.8	157.3	19.08
	0.2% INT	85.4	188.7	19.62

…continued

Average elongation of AZ31-T4 and AZ61-T4 MMCs.

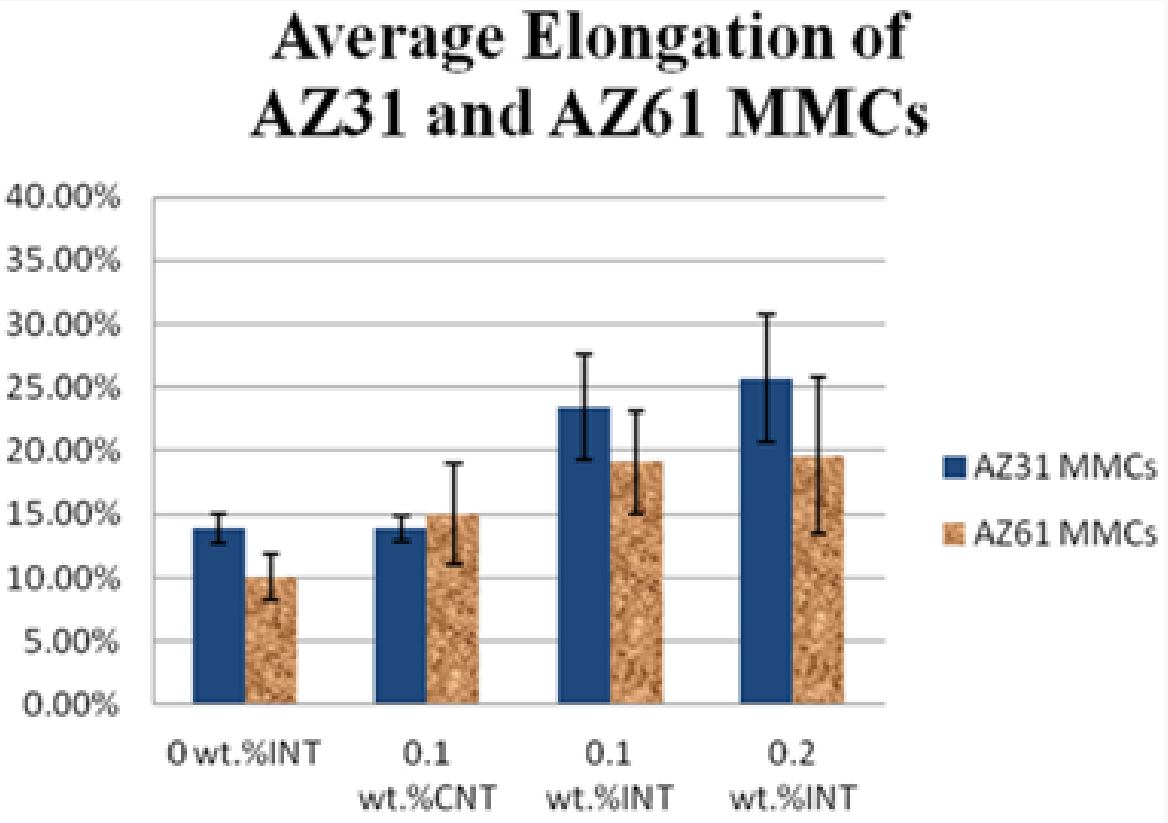

…continued

- Compared to pure metals, metal matrix composite materials are more suitable for structural and biomedical applications
- The corrosion and wear behaviour of metal matrix composites are also higher compared to pure metals and alloys
- The plastic deformation process of metal matrix composites is also similar to pure metals and alloys for a certain limit of reinforcement weight/volume percentages.
- Generally, mechanical behaviour of metal matrix composites depend on the weight/volume

percentage, type and size of reinforcing particles.

THANK YOU

MECHANICAL PROPERTIES ENHANCEMENT OF Mg/WS_2 INORGANIC NANOTUBES METAL MATRIX COMPOSITES

- ✓ **Journal of Alloys and Compounds, Vol. 654, pp.15-22, 2016**
- ✓ **"METAL ALLOY COMPOSITES", USA Patent filed no. 62/169,094 (01 June 2016)/ PCT no. PCT/IL2016/050563 (08 Dec. 2016)**
- ✓ **ISBN 978-965-7632-16-1 p127-134**

Prof. **Song-Jeng Huang**[1*], Jheng-Yang Huang[1] and Prof. **Alla Zak**[2]

[1]*Department of Mechanical Engineering, National Taiwan University of Science and Technology, Taipei, Taiwan, R.O.C.*

[2]*Holon Institute of Technology, 52 Golomb Street, Holon 5810201,* ***Israel***

ICPMMT 2018 Auckland, New Zealand
20180204-08

TAIWAN TECH National Taiwan University of Science and Technology

מכון ויצמן למדע
WEIZMANN INSTITUTE OF SCIENCE

OUTLINE

Topic: Mechanical properties of Mg metal matrix composites enhanced by WS2 inorganic nanotubes

Song-Jeng Huang[a,b*], Jheng-Yang Huang1 [a] , Y. Feldman[c] and Reshef Tenne[b]

[Journal of Alloys and Compounds, Vol. 654, pp.15-22, 2016
"METAL ALLOY COMPOSITES", USA Patent filed no. 62/169,094 (01 June 2016)/ PCT no. PCT/IL2016/050563 (08 Dec. 2016)]

- **Introduction**
- **Experimental details**
  - Source materials
  - Fabrication of AZ31/INT WS_2 MMC nanocomposites
- **Results and discussion**
  - Mg-MMC Ingots preparation
  - XRD detection
  - Tensile test
  - Grain size refinement
- **Conclusion**

Introduction

- **Magnesium (Mg)** alloys are gaining more recognition as a lightest structural material for light-weight applications, due to their low density and high stiffness-to-weight ratio [1-2].

- In spite of this, Mg alloys have not been used for critical mechanical applications mainly due to their inferior mechanical properties compared to other engineering materials such as steel and aluminum.

- Hence, many researchers attempt to fabricate **Mg-based metal-matrix composites** (Mg MMCs) by varied methods to obtain light-weight materials with excellent mechanical properties.

Properties of some alloys and composites

	Hardness (Hv)	Tensile Strength (Mpa)	Elongation (%)	Density (g/cm^3)	Specific Strength	Price (NT$/Kg)
Steel: SS400	180	276	>25	**8.2**	**33.7**	20~25
Al alloy: 6061	105	125	20~30	**2.7**	**46.3**	120
Mg alloy: AZ31B	50	**170**	15	**1.77**	**96.0**	146
Mg alloy: AZ91D	65	**128**	3.6	**1.81**	**70.7**	146
Carbon Fiber Composite: T300		3600	< 3%	1.750	2057	1300

Introduction(cont.)

- Nanoparticles of inorganic layered compounds, like WS_2, MoS_2 and numerous others are known to fold into tubular (inorganic nanotube, INT) and quasi-spherical fullerene-like (IF) structures.

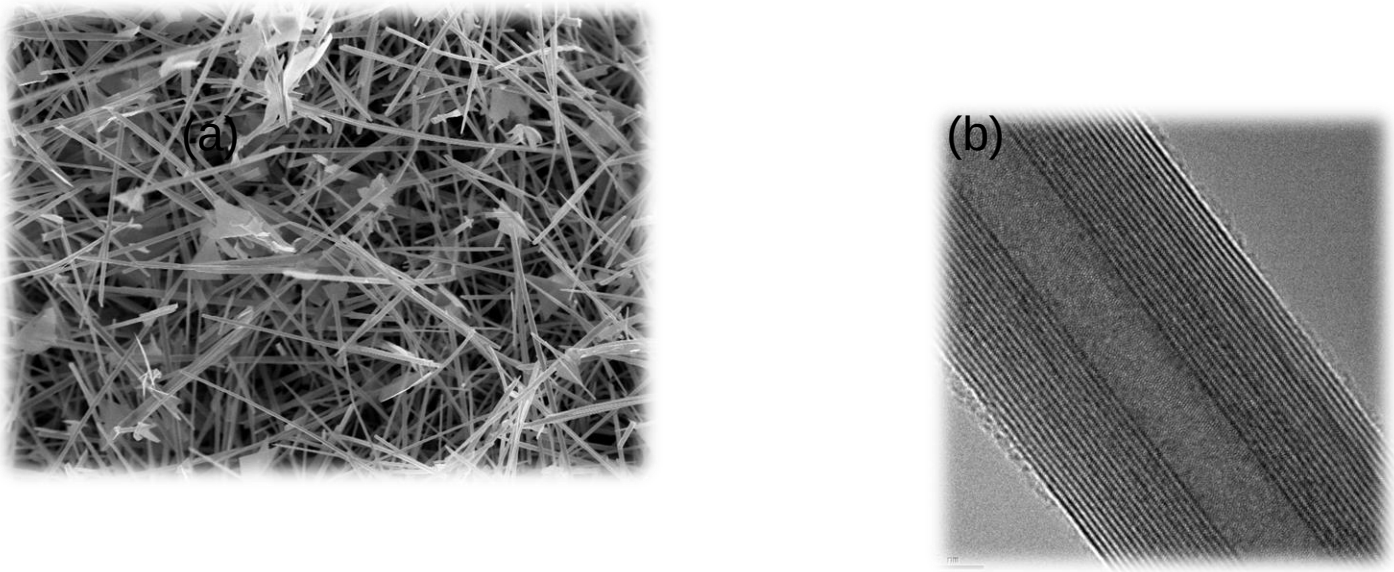

Fig .1 a. SEM image of an assortment of **WS_2 nanotubes**; **b**. TEM image of a single **WS2 nanotube**. Scale bar is 5 nm.

Introduction(cont.)

- Following extensive studies industrial grade **IF-WS_2** nanoparticles were successfully commercialized, primarily as additives to high-performance lubricants and greases ("NanoLub") and also in surface protective polymer films.

- The application of **IF-WS_2** nanoparticles for improving the tribological properties of polymer and metallic matrices has been demonstrated a while ago [3-5].

Introduction(cont.)

- The proposed new **INT-WS_2**-based Mg nanocomposites, which were prepared by melt-stirring with no further mechanical or chemical processing revealed stronger and tougher properties compared with the pure Mg alloy.

- Surprisingly, the present new Mg nanocomposites exhibit both increased tensile strength and elongation (strain), simultaneously.

Experimental details

◆ Materials

➢ The Mg-alloy studied in this work is AZ31 and AZ61 with ~3.0 and ~6.0 wt% aluminum- available commercially. Its chemical composition cited by the manufacturer is presented in Table 1.

Table 1. Chemical composition of AZ31 and AZ61

Elements	Al	Zn	Mn	Si	Fe	Cu	Ni	Mg
wt %	3.08/6.0	0.908	0.393	0.022	0.001	0.002	0.01	Balance

Experimental details

◆ Fabrication of AZ / INT-WS_2 MMCS' Ingots

- The fabrication of the **AZ31** MMCs containing 0.1, 0.2 0.5 and 1wt% INT-WS_2 and **AZ61** containing 0.1, 0.2 wt% INT-WS_2 was carried out using the melt-stirring technique.

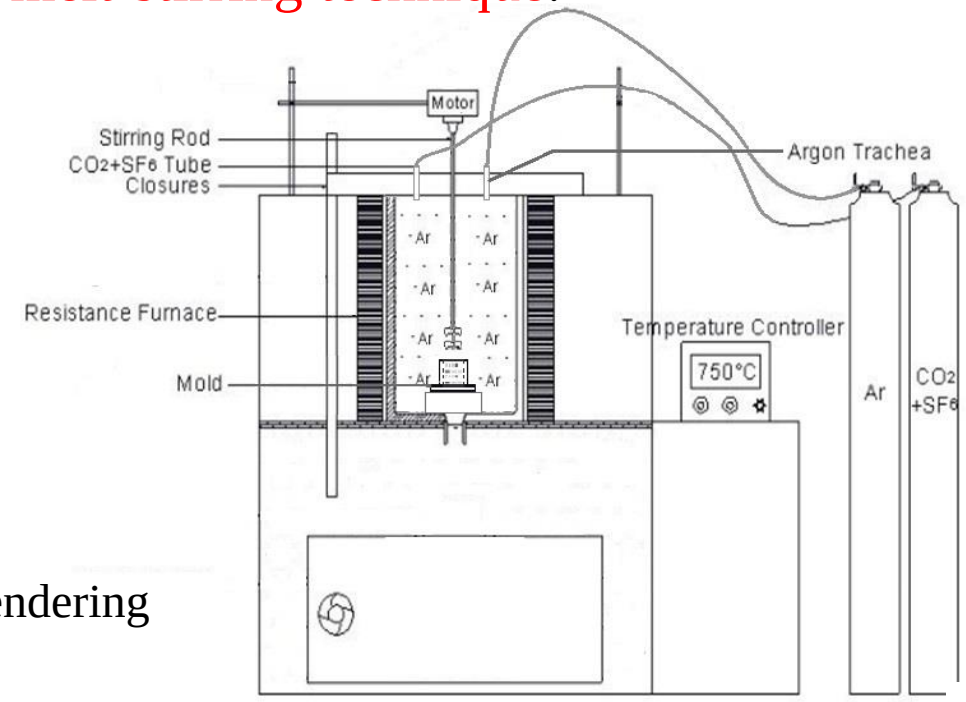

Fig 2. Schematic rendering of the reactor

◆ Fabrication of AZ31/INT-WS_2 MMCS' Ingots (cont.)

1. At first, The AZ31 or AZ61 and the WS_2 nanotubes were placed inside a stainless crucible and heated to 400°C in a resistance-heating furnace for 15 minutes; then a stirring vane was applied; meanwhile, CO_2 and SF_6 gasses were bubbled into the crucible to help mixing the melt.

2. After that, the melt was heated up to 600°C for 15 minutes. The crucible was further heated gradually up to 700-720°C, with the molten alloy being stirred with a vane operated at 350 rev/min for 3 minutes.

3. Finally, the composite melt was poured into a metallic mold.

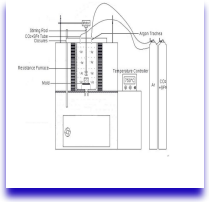

◆ Fabrication of AZ31/INT-WS_2 MMCS' Ingots (cont.)

4. Each composition, the Mg MMCs containing nanotubes with weight fraction of 0.1-1 , was repeated at least three times.

5. Due to the small size of the crucible, the **blade** propeller led to vortices and non-uniform mixing of the nanotubes in the Mg MMC. Therefore, the blade stirrer was replaced by a **rod** stirrer (b in Table 2).

Table 2.. Specimens used for this study and their notation

Notation	Matrix	wt% of INT-WS_2	Blade (*a*) or rod (*b*) stirring
AZ31-x*	AZ31	0	x=1&2 (*a*); 3&4 (*b*)
AZ31INT0.1-x	AZ31	0.1	x=1-3 (*a*)
AZ31INT0.5-x	AZ31	0.5	
AZ31INT1-x	AZ31	1	x=1-3 (*b*)
			x=1-3 (*b*)

Results and Discussion

◆ Mg-MMC Ingots preparation

- A picture of a few ingots obtained after the melt stirring in different temperatures is shown in Figure 3.

- Noticeably, the ingots which were prepared at temperatures of 700 °C and above looked more uniform compared to those prepared at lower temperatures.

Fig 3. Optical micrographs of four of the Mg-MMC ingots prepared at different temperatures

Results and Discussion

◆ AZ31INT0.5 XRD detection

- INT (002) plane at 13.91° (interlayer spacing of 6.36 Å) is shifted with respect to bulk 2H-WS_2.
- Slightly larger swelling of the interlayer spacing could be attributed to Mg intercalation between the WS_2 layers.
- This downshift represents a 2-3% expansion in the interlayer spacing and is attributed to relaxation of the strain in the nanotubes.

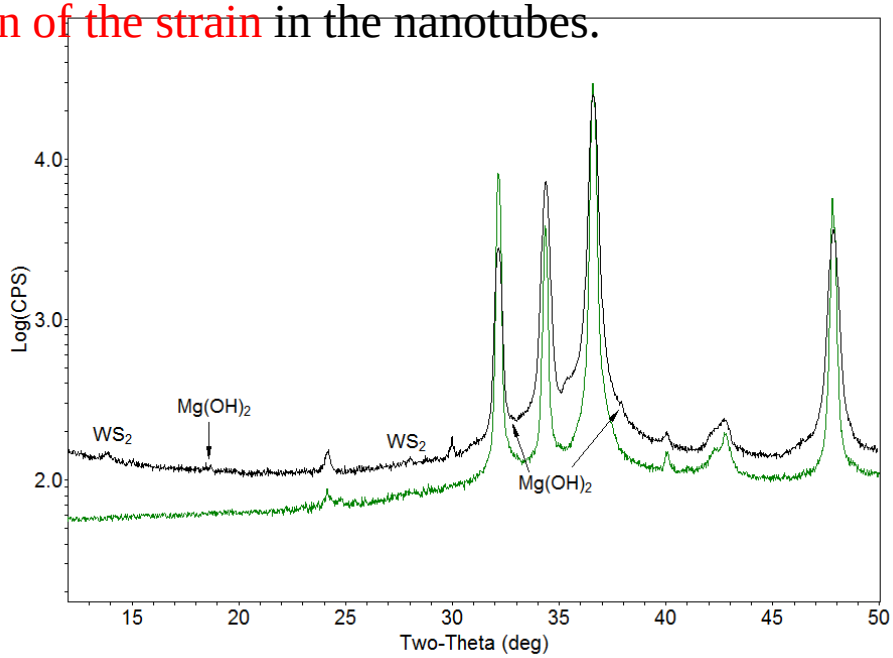

Fig 4. XRD patterns of the AZ31INT0.5-1 sample and a pristine Mg alloy (green)

◆ AZ31INT1 Tensile test

- Two obvious conclusions can be drawn from this figure:
  1. Scattering in the data.
  2. Minor effect on the stiffness and yield strength, but had a remarkable advantageous effect on the tensile strength and the strain .

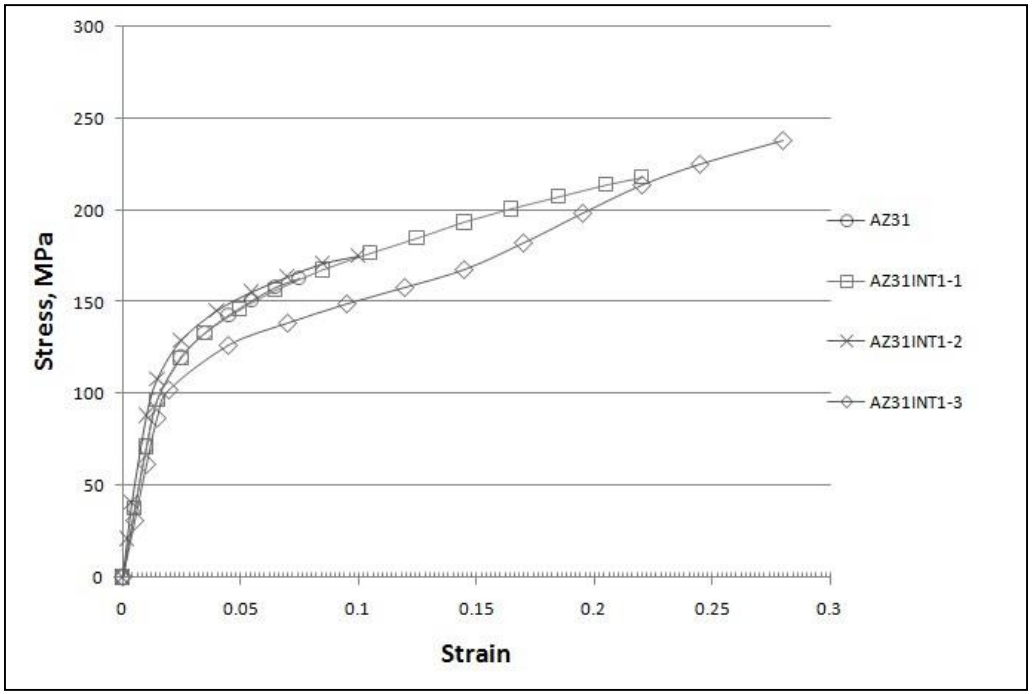

Fig 6. Stress-strain curve (tensile test) of the pure Mg-ZA31 alloy and the Mg MMC with 1 wt% nanotubes (AZ31INT1-x; x=1-3).

◆ AZ31INT Tensile test (cont.)

- The Mg-MMC with 1 wt% nanotubes exhibit appreciable improvements in the mechanical properties compared with the pristine alloy.

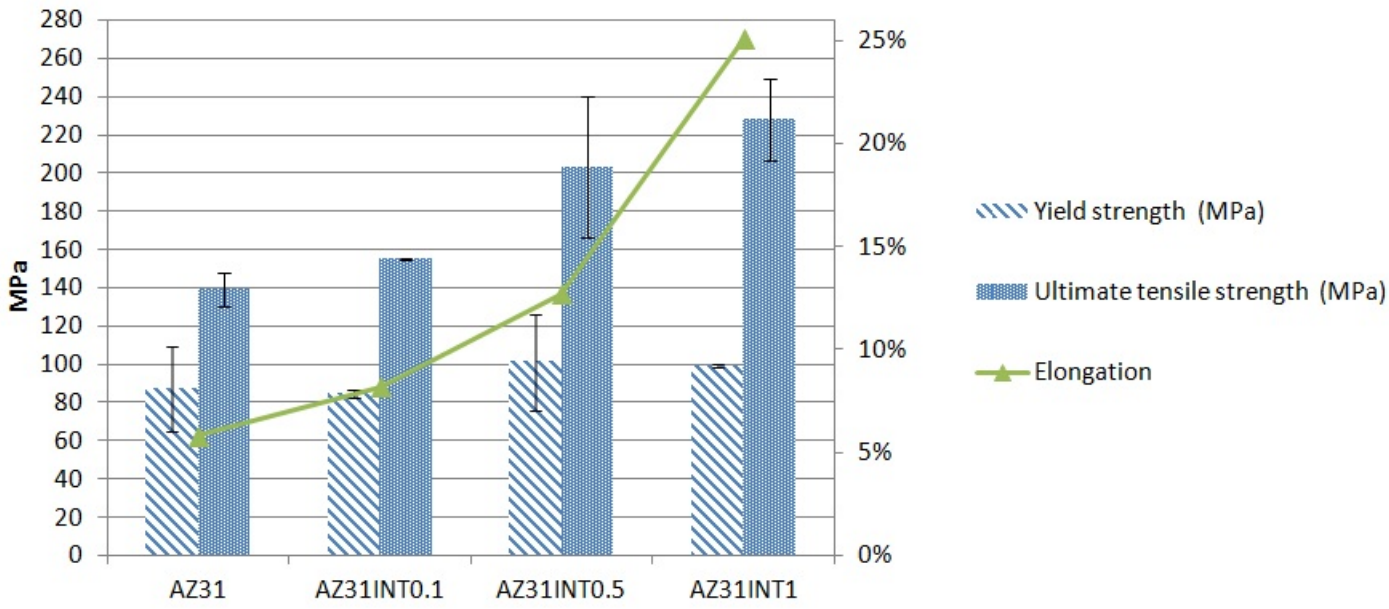

Fig 5. Summary of the mechanical testing of the different Mg-alloy samples.

Table S1. Mechanical properties of present nanocomposites and other nanocomposites

Notation	Specification	Yield strength , [MPa] (% change)	Ultimate tensile strength, [MPa] (% change)	Elongation (% change)
AZ31[a)]	**As-cast AZ31 Mg alloy**	84.3 (0)	136.0 (0)	5.3% (0)
AZ31**INT**0.5 [a)]	**AZ31 with 0.5 wt.% WS_2 nanotubes**	101.1 **(+20.0)**	203.0 **(+49.3)**	12.7% **(+139.6)**
AZ31**INT**1 [a)]	**AZ31 with 1 wt.% WS_2 nanotubes**	99.0 **(+17.4)**	227.7 **(+67.4)**	25.1% **(+373.6)**
AZ31**CNT**0.1 [e)]	**AZ31 with 0.1 wt.% CNT**	62.5 **(-25.6)**	104.8 **(-22.9)**	3.25% **(-38.7)**
AZ31**CNT**0.5 [e)]	**AZ31 with 0.5 wt.% CNT**	64.0 **(-24.1)**	114.4 **(-15.9)**	4.73% **(-10.8)**
Pure Mg [b)]	**Pure Mg**	47±3 (0)	120±4 (0)	12.3±1.1% (0)
Mg-1wt% SiC [b)]	**Pure Mg with 1 wt.% SiC nanoparticles**	67±4 **(+42.0)**	133±5 **(+10.8)**	6.3±0.8% **(-48.8)**
AZ91 [c)]	**As-cast AZ91 Mg alloy**	250 (0%)	350 (0%)	16.5% (0%)
AZ91MWCNT0.1 [c)]	**AZ91 with 0.1 wt.% CNT**	300 **(+20.0)**	415 **(+18.6)**	24.5% **(+48.5)**
AZ91 [d)]	**As-cast AZ91 Mg alloy**	135 (0)	210 (0)	6% (0)
AZ91MWCNT0.1 [d)]	**AZ91 with 0.7wt.% CNT + 0.3wt.%SiC**	210 **(+55)**	305 **(+45)**	9% **(+50)**

◆ Tensile test (cont.)

- A reproducible and significant improvement in the fracture toughness of the Mg-MMCs with addition of minute amounts of WS_2 nanotubes was confirmed.

Table 3. Fracture toughness of the pure AZ31 Mg-alloy and the INT-WS_2 (1 wt%)-Mg-alloy nanocomposites

	Toughness [MPa]	**% change**
AZ31-4	13.1	-
AZ31INT1-1	38.1	190
AZ31INT1-2	15.3	17
AZ31INT1-3	48.8	272
AZ31INT1-avg.	**34.1**	**160**

Results and Discussion

◆ AZ31INT1 Grain size refinement

➢ Primarily, the Hall-Petch mechanism [6], which relates the grain size to the fracture toughness of the matrix could be anticipated.

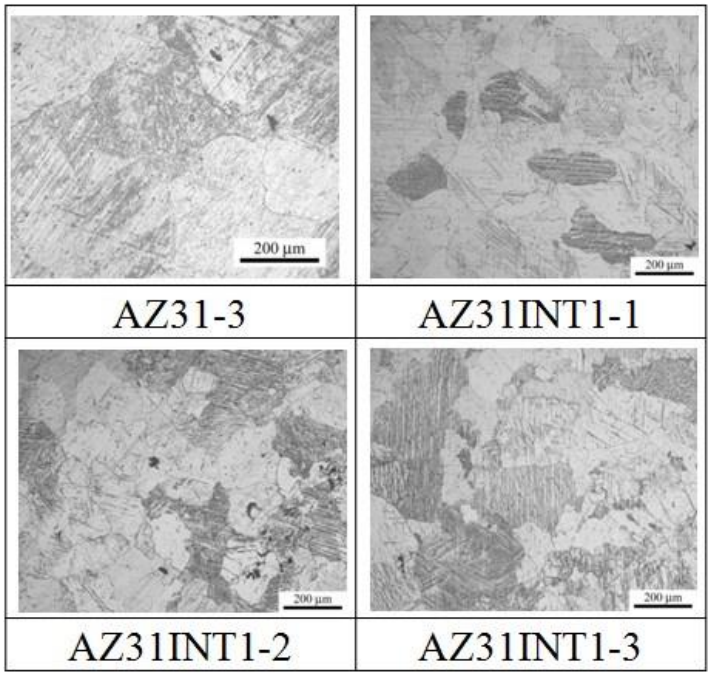

Fig 7. Metallography of the pure Mg alloy and the different Mg alloys formulated with 1 wt% INT-WS_2

Results and Discussion

◆ Grain size refinement (cont.)

- The nanotubes play the role of nucleation centers which lead to the diminution of the grain size of the MMC during solidification.

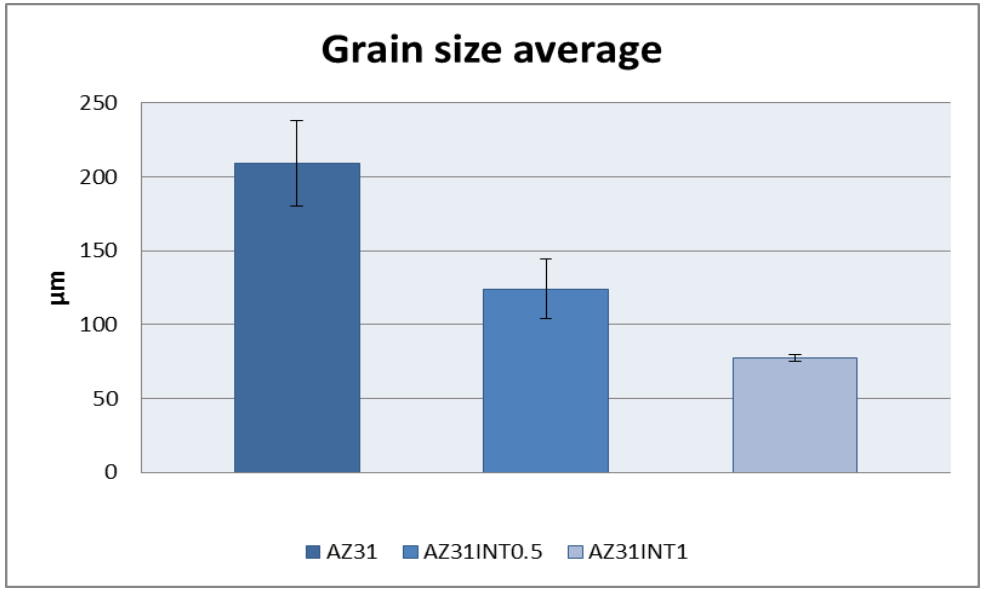

Fig 8. Comparison between the grain sizes of the pristine AZ31 Mg alloy and the MMC's with 0.5 and 1 wt% of WS_2 nanotubes.

Results and Discussion

◆ Reinforcement mechanisms of AZ31 0.1 wt% INT-WS2

➢ The greatest contribution for the reinforcement effect: dislocations density increasing at the nanotube-Mg-alloy matrix.

Table 4. Calculated contributions of the different mechanisms for the reinforcement of the AZ31 by 0.1 wt% INT-WS_2

Symbol	Description	Value [MPa]	Percentage of strengthening contribution
$\Delta\sigma_{Hall\text{-}Petch}$	enhancement of composite strength due to grain refining	6.4698	14.4%
$\Delta\sigma_{CTE}$	enhancement of composite strength due to dislocation density increase	31.2113	69.7%
$\Delta\sigma_{Orowan}$	enhancement of composite strength due to Orowan strengthening	7.0407	15.7%
$\Delta\sigma_{load}$	enhancement of composite strength due to load bearing	0.09834	0.2%

Contributions of the different mechanisms for the reinforcement

- Coefficient of thermal expansion difference effect[52]

$$\Delta\sigma_D = \sqrt{3}\beta G_m b\sqrt{\frac{12\left(T_{\text{process}} - T_{\text{test}}\right)(\alpha_m - \alpha_p)V_p}{b d_p}}$$

- Hall-Petch strengthening [53]

$$\Delta\sigma_{\text{Hall-Petch}} = k_y\left(d_m^{-1/2} - d_c^{-1/2}\right)$$

- Orowan strengthening [54]

$$\Delta\sigma_{\text{Orowan}} = \frac{0.13 G_m b}{d_p\left[\left(\frac{1}{2V_p}\right)^{1/3} - 1\right]}\ln\frac{d_p}{2b}$$

- Load bearing effect

$$\Delta\sigma_{\text{load}} = 0.5 V_p \sigma_{\text{ym}}$$

Table S2. Parameter for calculation of AZ31-0.1 wt% (WS_2)

Parameter	Description	Value	Reference/note
α_m	coefficient of thermal expansion of the matrix	27.9×10^{-6} $^oC^{-1}$	[1]
α_p	coefficient of thermal expansion of the nanoparticles	15.96×10^{-6} $^oC^{-1}$	[2]
β	dislocation strengthening coefficient	1.25	[3]
b	magnitude of the burgers vector	0.32 nm	[4]
d_c	average grain size in the composite sample	82.7 µm	experimentally determined
d_m	average grain size in the monolithic sample	227.9 µm	experimentally determined
d_p	nanoparticle diameter	100 nm	manufacture supplied average particle size
G_m	shear modulus of the matrix	16.7 GPa	calculation and experimentally determined
k_y	Hall-Petch material constant	0.0145MPa	calculation and experimentally determined
$T_{process}$	processing temperature	720 ^{o}C	-
T_{test}	testing temperature	25 ^{o}C	-
V_p	volume fraction of nanoparticles	0.000023	calculated from weight fraction
σ_{ym}	Yield stress of the matrix	84.3 MPa	experimentally determined

◆ Contribution of strengthening mechanisms in AZ31-T4 and AZ61-T4 (both with 0.2 wt.% WS2 INT addition)

Symbol	Enhancement of composite strength	AZ31		AZ61	
		Value (MPa)	strengthening contribution	Value (MPa)	strengthening contribution
$\Delta\sigma_{Hall\text{-}Petch}$	grain refining [17–18]	2.91	11.7%	0.69	3.0%
$\Delta\sigma_{CTE}$	dislocation density increase [19]	16.85	67.8%	16.85	74.5%
$\Delta\sigma_{Orowan}$	Orowan strengthening [20]	5.06	20.4%	5.06	22.4%
$\Delta\sigma_{load}$	load bearing	0.02	0.1%	0.02	0.1%

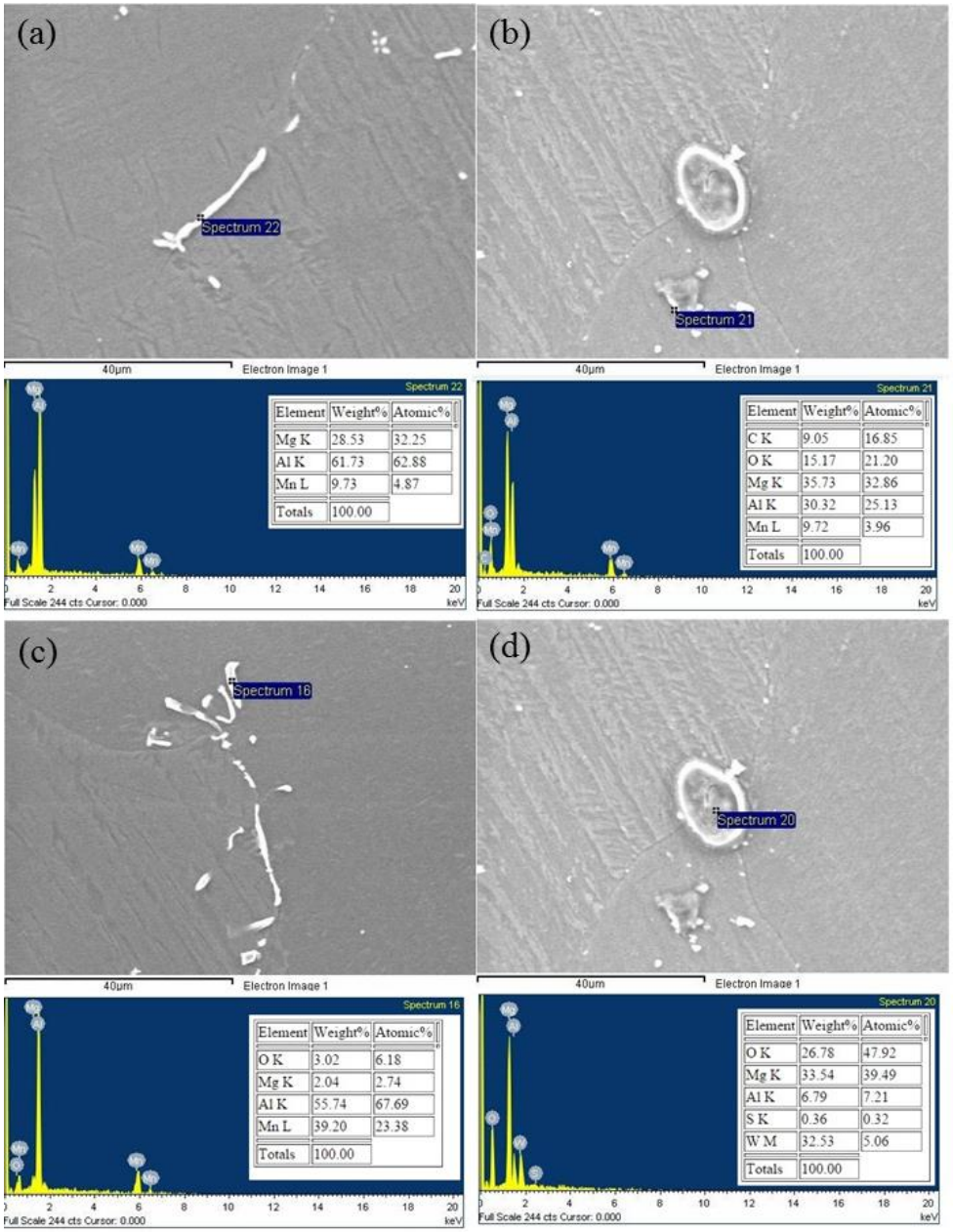

Fig. EDS with 0.2wt% WS2 ：(a) AZ61 β phase (Mg17Al12). (b) AZ31 β phase (Mg17Al12). (c) AlMn in AZ61. (d) WS2 in AZ31.

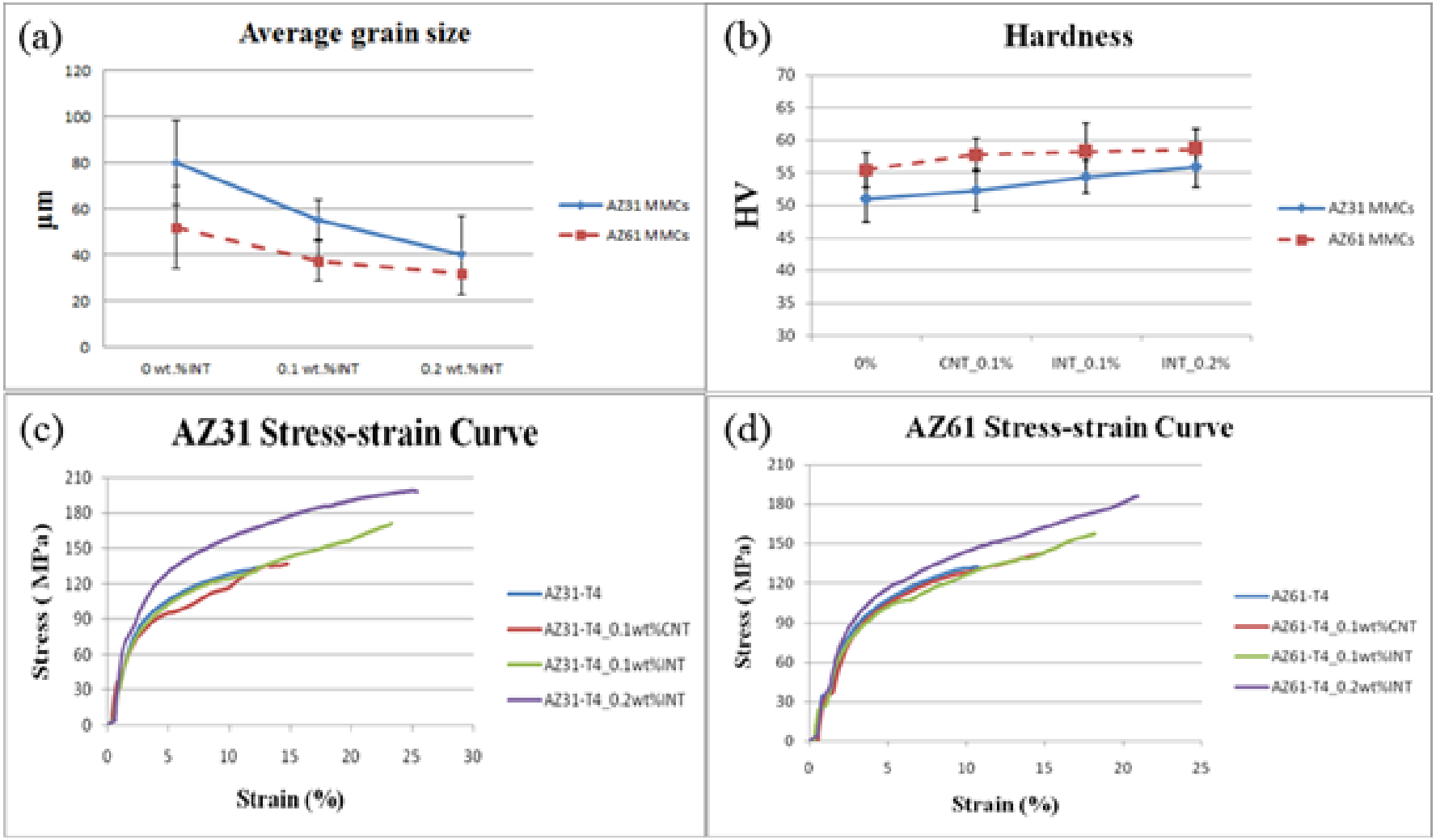

Fig. (a) Average grain size of AZ31-T4 and AZ61-T4(unit: µm) (b) Hardness of AZ31-T4 and AZ61-T4 (c) Stress-strain curve of AZ31-T4 and MMCs (d) Stress-strain graph of AZ61-T4 and MMCs with various contents of strengthening phase (note: INT represents INT-WS_2)

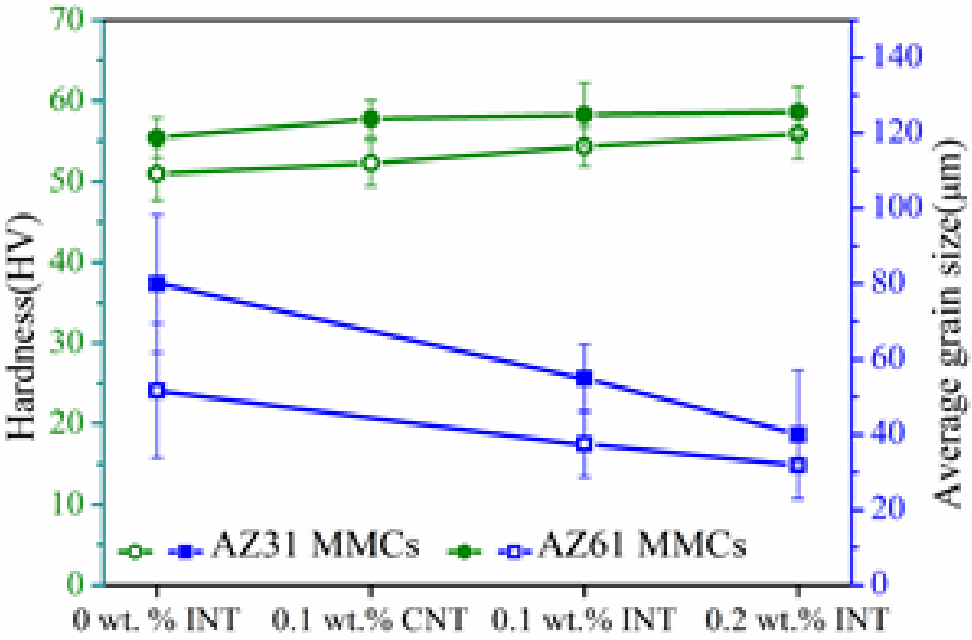

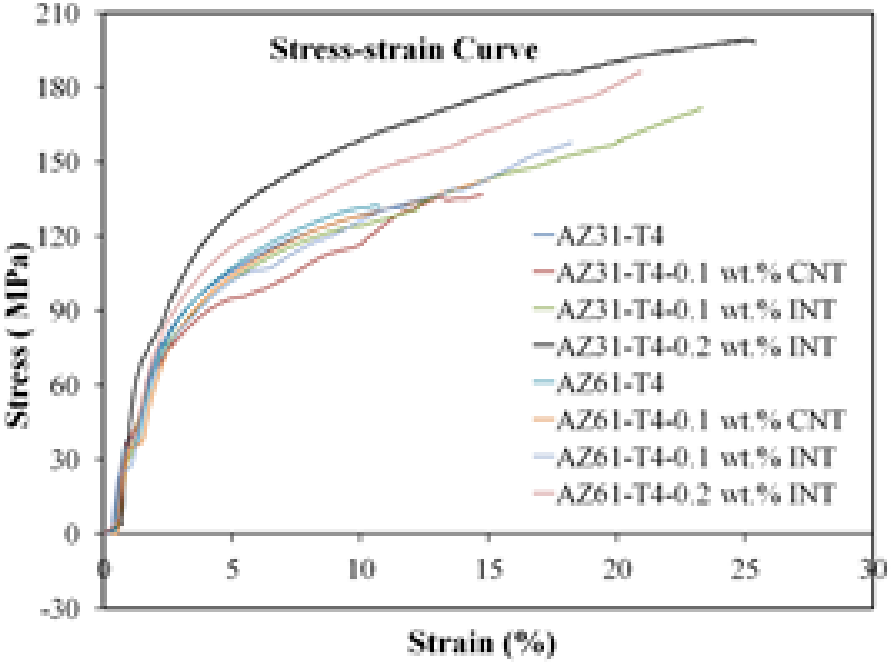

Fig. (a) Average grain size and Hardness curves of AZ31-T4 and AZ61-T4 (b) Stress-strain curve of AZ31-T4 and AZ61-T4 and MMCs with various contents of strengthening phase (note: INT represents INT-WS2)

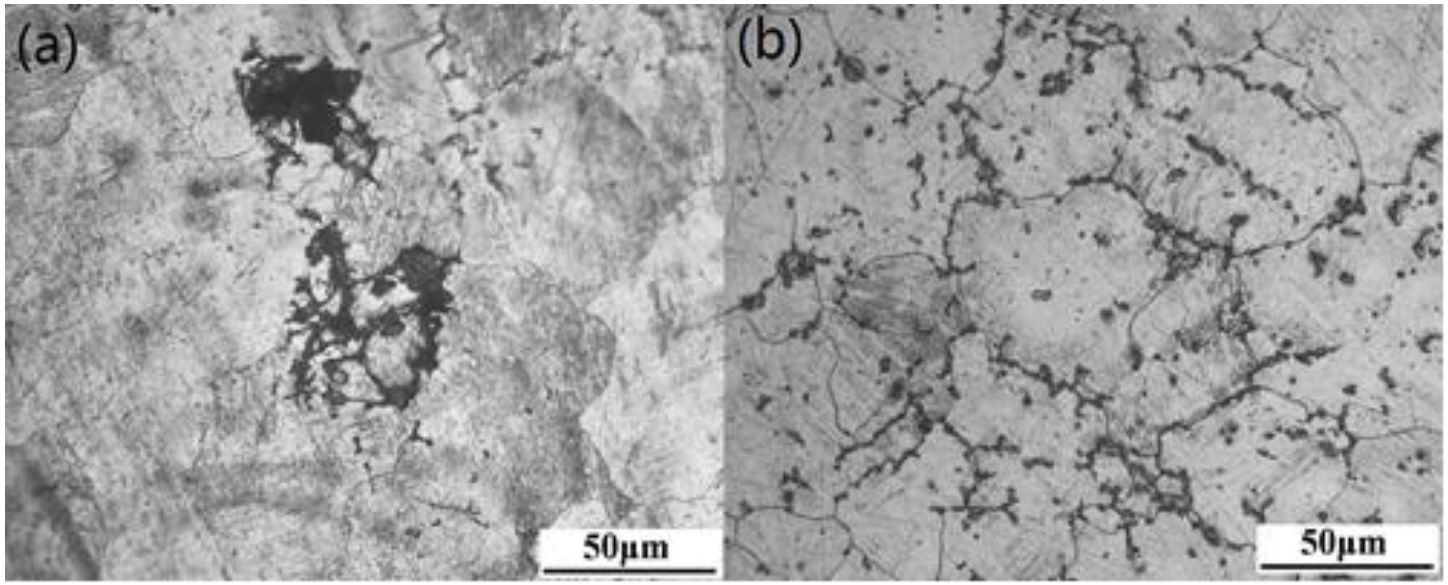

Fig. Defect of (a) AZ31-T4_0.1%CNT; (b) AZ61-T4_0.1%CNT (magnified 200x)

◆ Fabrication of AZxx/XX_p MMCS' Ingots (cont.)

- AZ61/SiC_p ingots with 80 mm in diameter and 140 mm height obtained by the melt-stirring process were machined to be tube billets with 25 mm inner and 64 mm outer diameters, respectively, and 50 mm height.

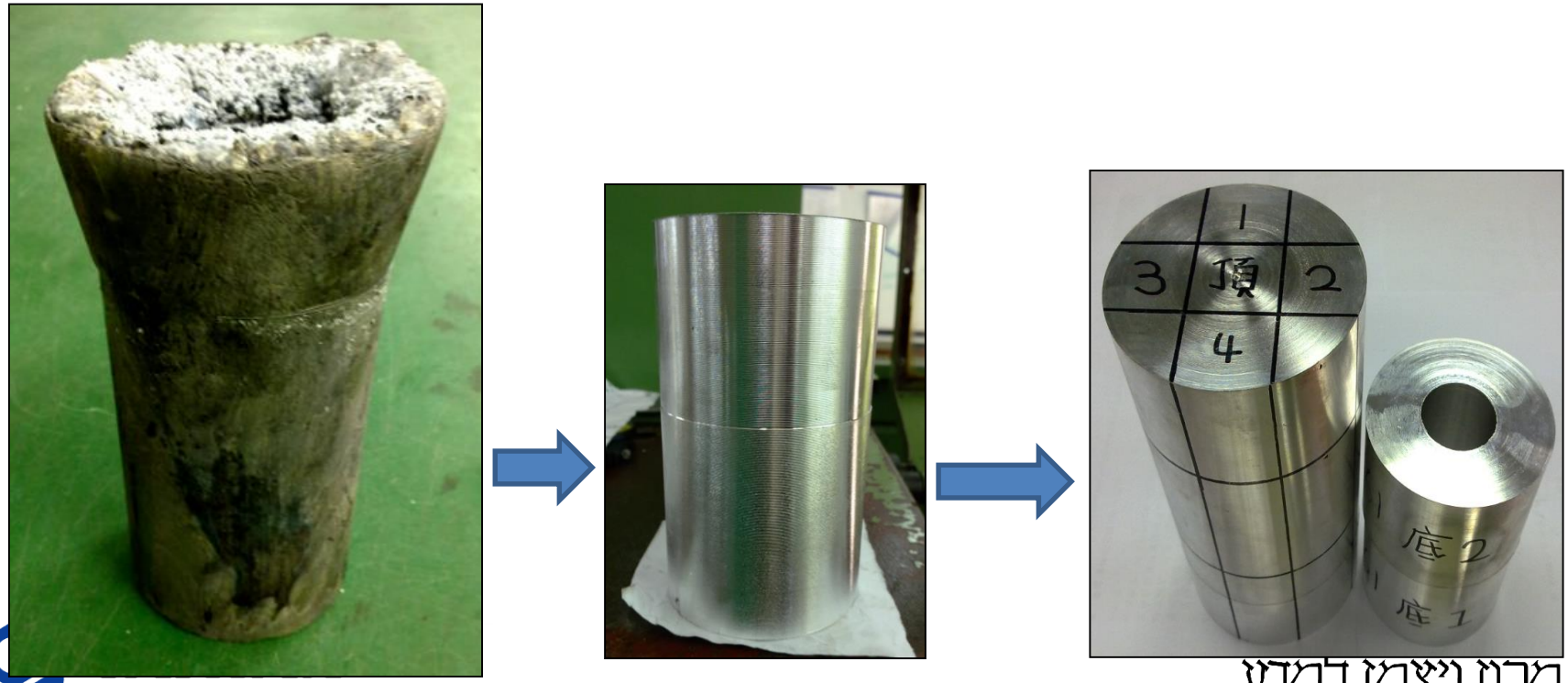

350 tons extruder of Prof. Y.-M. Hwang

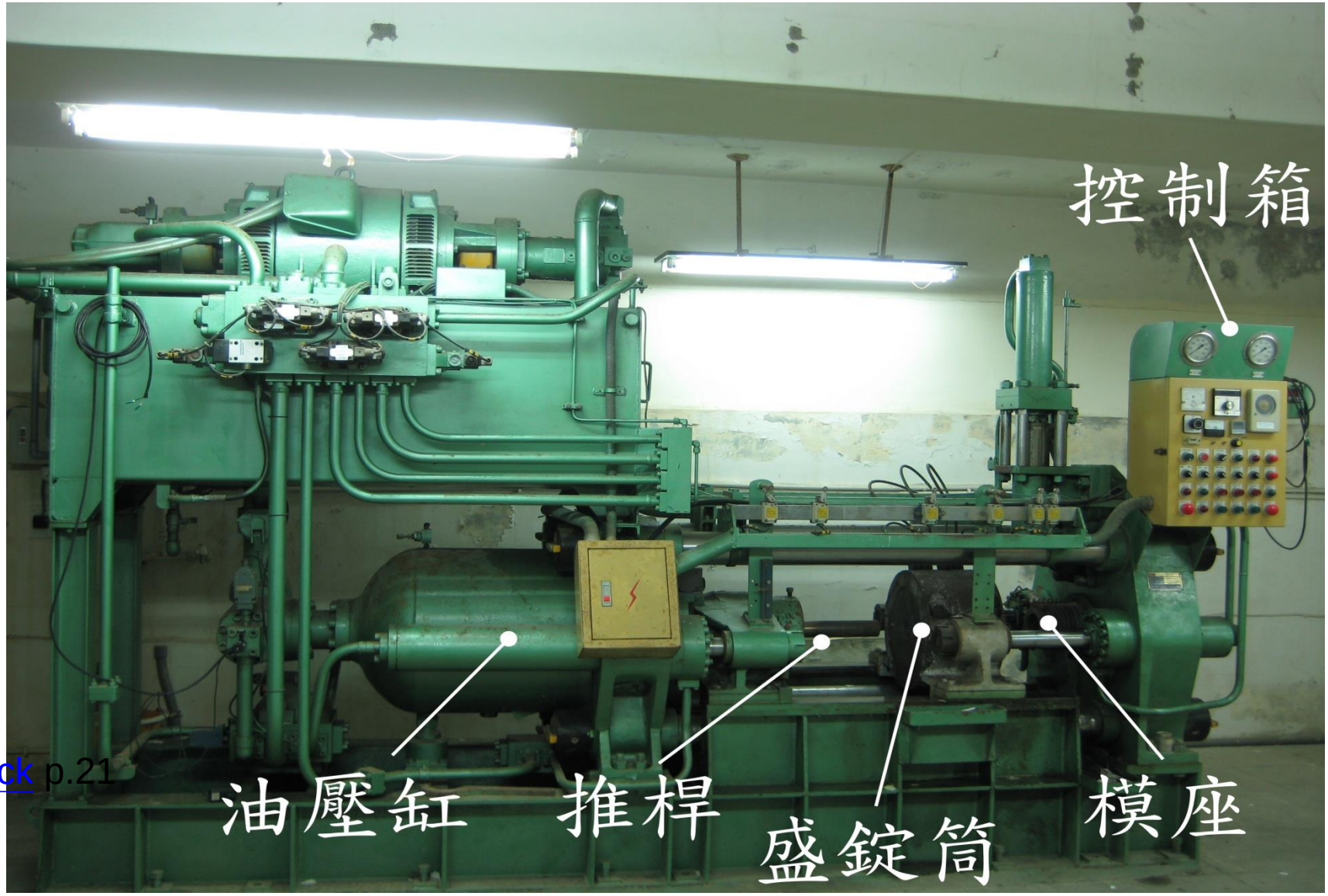

Back p.21

◆Hot Extrusion procedure of forming AZxx and AZxx/XX$_p$ MMCs' Tubes

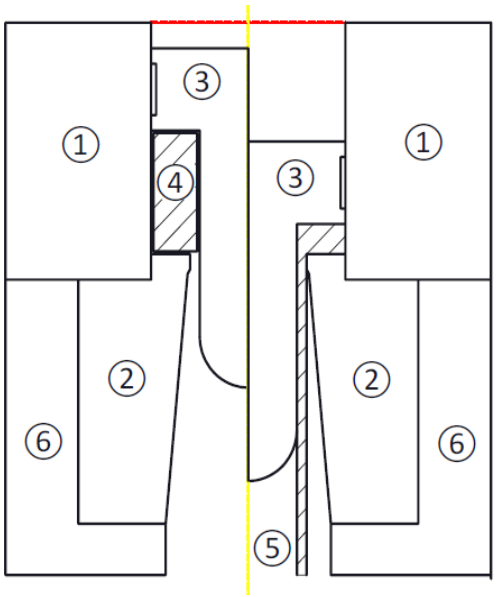

① Container
② Die
③ Ram and mandrel
④ Billet
⑤ Product
⑥ Die holder

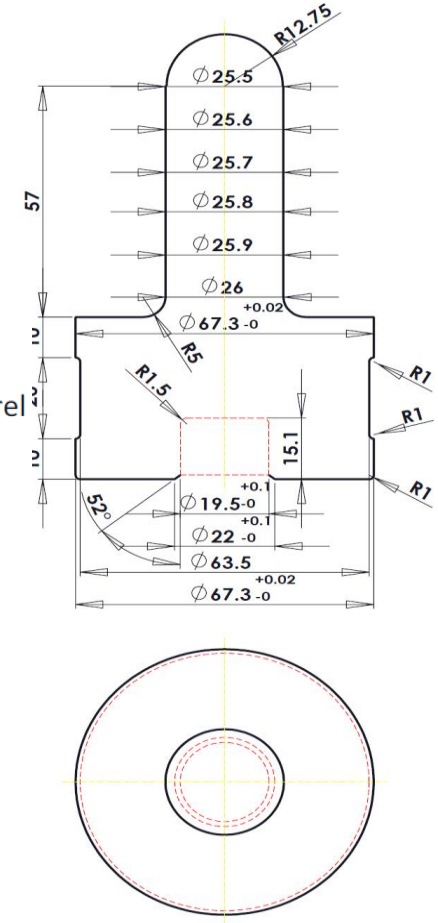

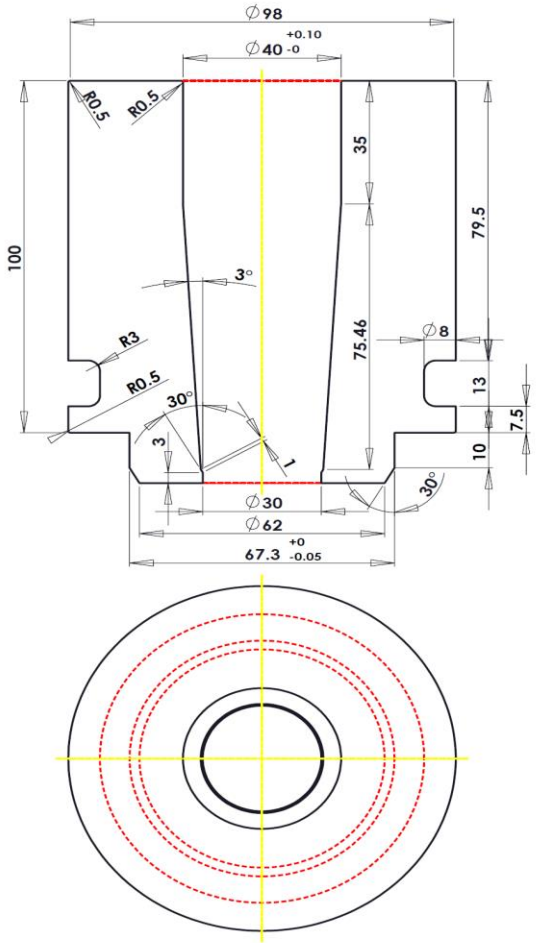

(a) Punch | (b) Die

Fig. 2 Extruder design

Back p.21

◆Hot Extrusion procedure of forming AZxx and AZxx/XX$_p$ MMCs' Tubes (cont.)

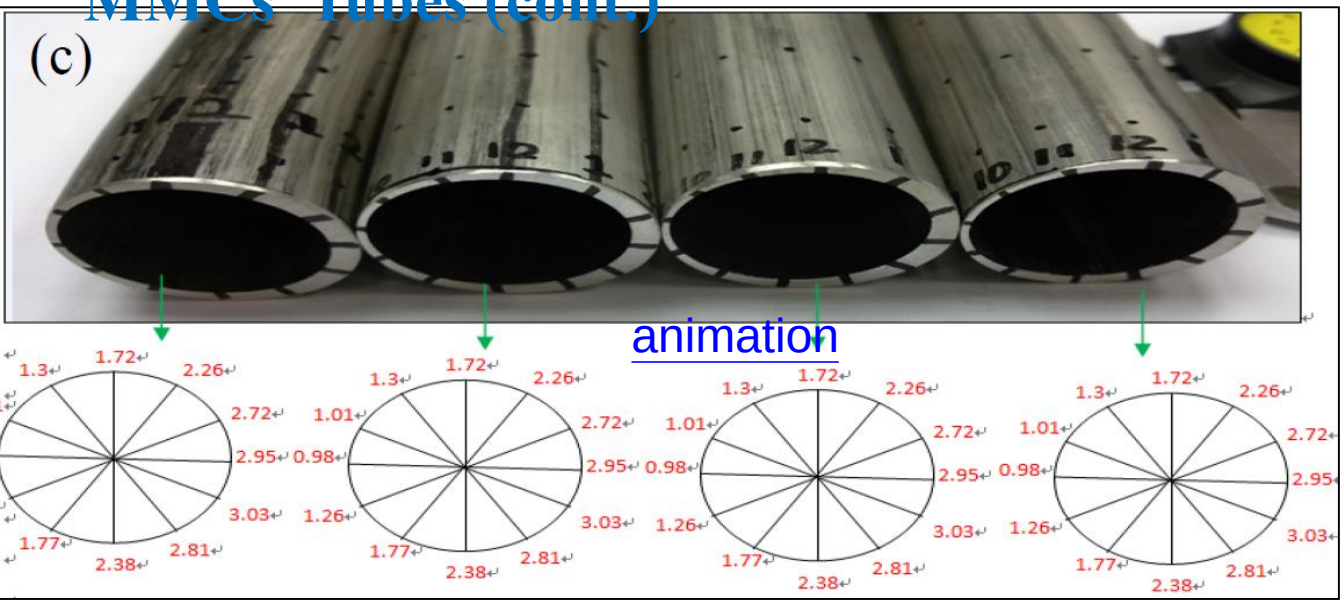

Explosion figures

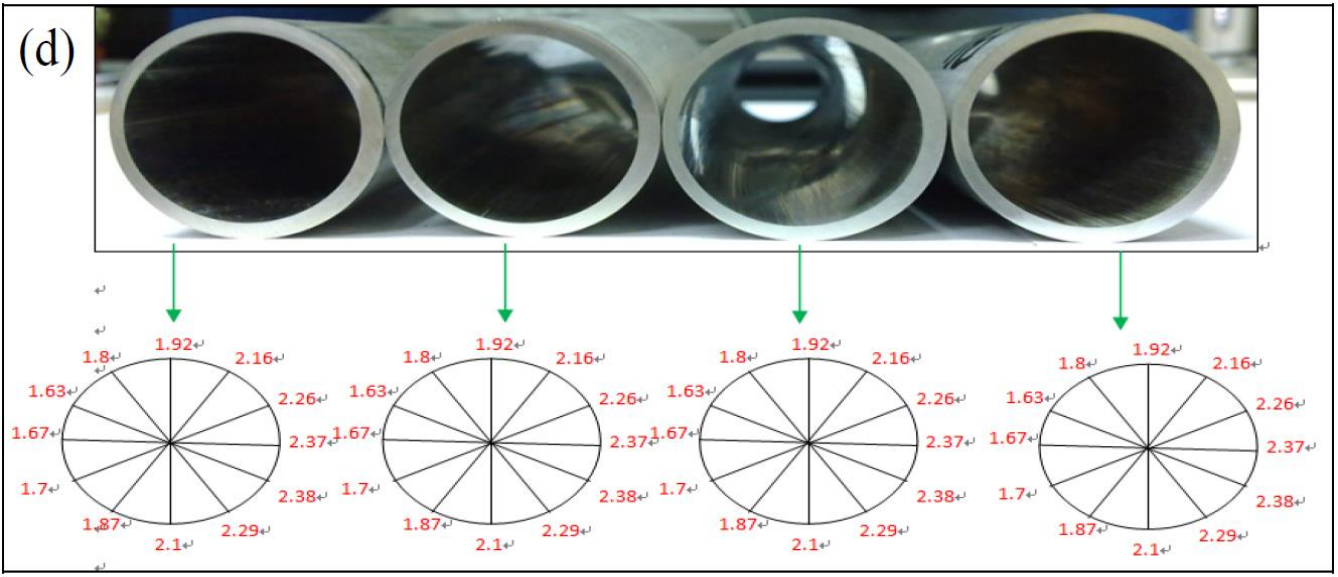

最厚2.38與最薄1.63，
相差0.75mm

Tubes for Bicycle Application

Break rig
Mg: 0.47 Kg

Stand pipe
Mg: 0.175 Kg
Al: 0.26 Kg

Weight decreasing 33%

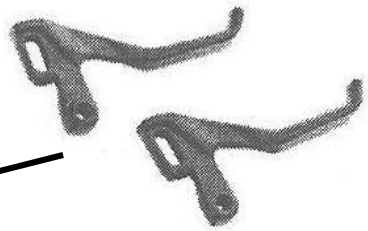

Break handle

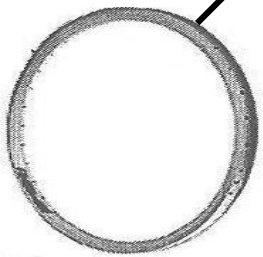

Wheel frame
Mg: 0.4 Kg
Al: 0.6 Kg

Decreasing 33%

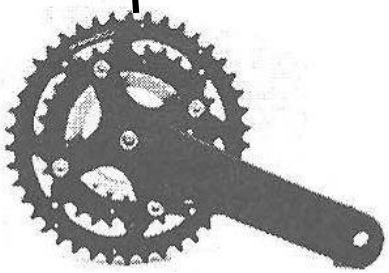

Crank

Pedal
Mg: 0.32 Kg

Fork mounting
Mg: 0.4 Kg

Casted parts for Airplane Application

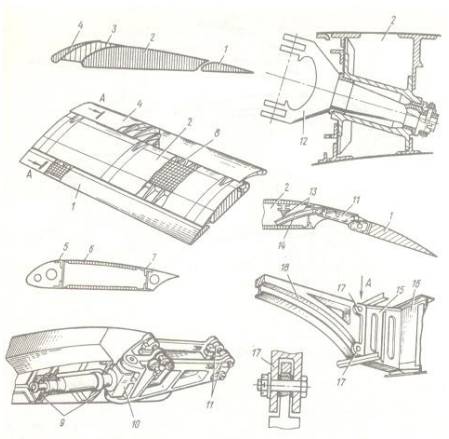

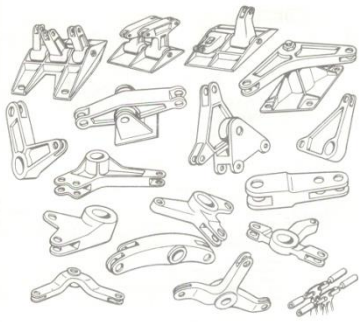

Source:

1. G. I. Zitomirskii, “Structure of Aircrafts”, Mashinostroenie, Moscow, 1996
2. http://www.skydynamics.com/Information/magnesium.htm

Conclusion

- Both the tensile strength of the AZ31alloy and its elongation (and consequently the fracture toughness) were largely improved.
- Significant improvement in the fracture toughness of the Mg-MMCs with addition of minute amounts of WS_2 nanotubes were obtained.

- Metallographic analysis of the alloys clearly showed that the thermal mismatch between the nanotubes and the Mg-alloy leads to the formation of numerous dislocations in the grain boundaries in the vicinity of the nanotube-matrix interface.

- These dislocations impede the progress of the crack under load.

Acknowledgements

- This research was supported by
  - the Israel Science Foundation and
  - the Israel National Nano-Initiative through the FTA program.
  - the Helen and Martin Kimmel Center for Nanoscale Science;
  - the Harold Perlman Foundation,
  - the Irving and Azelle Waltcher Foundation honoring Prof. M. Levy and
  - the Irving and Cherna Moskowitz Center for Nano and Bio-Nano Imaging.
  - In additional, the authors would like to acknowledge the support of the Ministry of Science and Technology of Taiwan for supporting this research through a grant (MOST-103-2918-I-011-003).

Acknowledgements

- **This research was supported by**
  - **In additional, the authors would like to acknowledge the support of the Ministry of Science and Technology of Taiwan for supporting this research through a grant (MOST-103-2918-I-011-003).**
  - **Group members of Micro- & Nano-Composite Materials Laboratory of Mechanical Engineering Dep. of TWIWAN TECH**

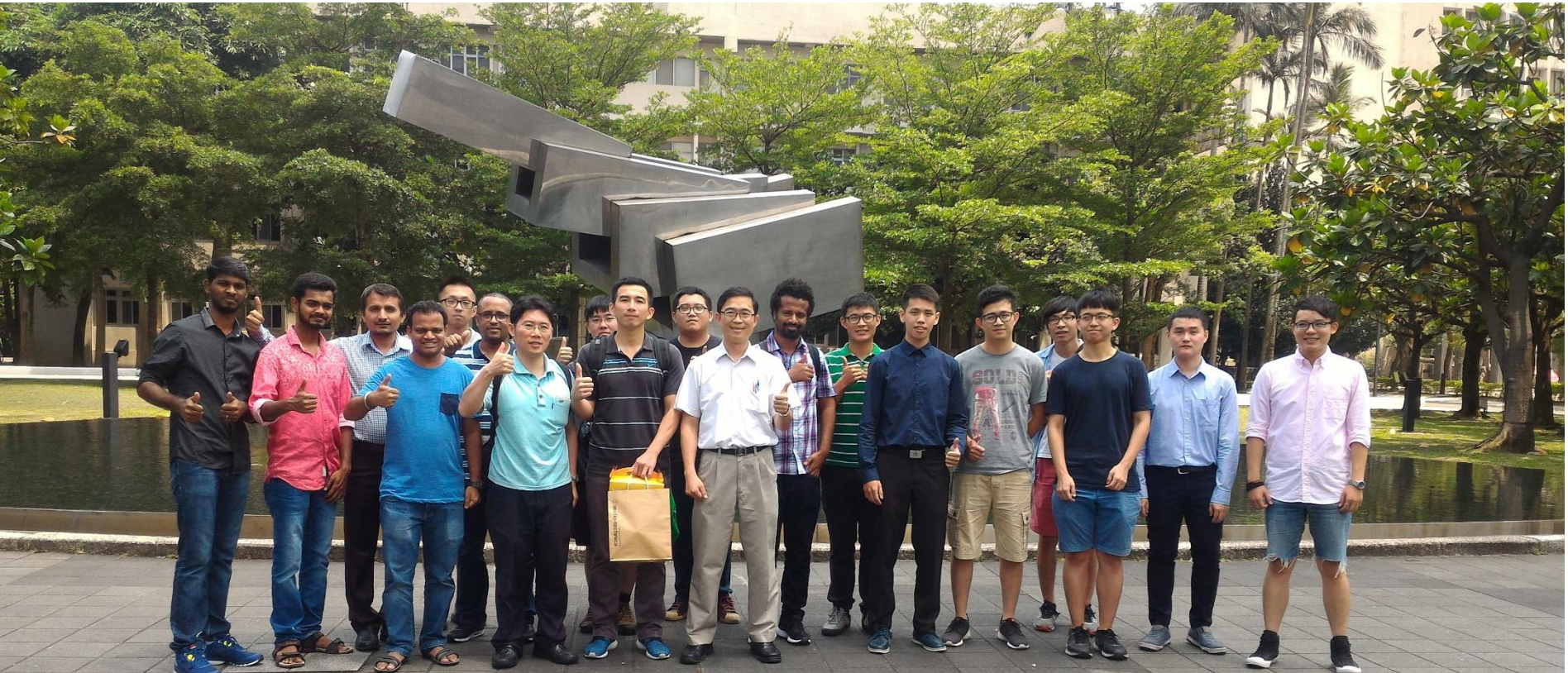

Department of Mechanical Engineering
National Taiwan University of Science and Technology
(TAIWAN TEC)

Thanks for attention!

Welcome to Taipei, TAIWAN!

Dr. Song-Jeng Huang: sgjghuang@mail.ntust.edu.tw

Taipei 101 building: 508 meter or 1,667 feet high.

MONGOLIA
CHINA
INDIA
BURMA
LAOS
THAILAND
VIETNAM
CAMBODIA
NORTH KOREA
SOUTH KOREA
NEPAL
BHUTAN
BANGLADESH
Ulaanbaatar
Urumqi
Beijing
Tianjin
Shenyang
Vladivostok
Pyongyang
Seoul
Lhasa
Xi'an
Nanjing
Wuhan
Chongqing
Changsha
Nanchang
Guiyang
Kunming
Nanning
Hanoi
Vientiane
Kathmandu
Thimphu
Kolkata (Calcutta)
Dhaka
Nagpur
Hyderabad
Rangoon
Chiang Mai
Bangkok
Phnom Penh
Ho Chi Minh City
Bangalore
Chennai (Madras)
Bay of Bengal
South China Sea
Manila
Taiwan

National Parks and National Scenic Areas

The Beauty of Taiwan
- FORMOSA
台 灣 之 美

阿里山日出雲海
A view of the sunrise and cloud sea
from Alishan National Scenic Area

阿里山登山火車
Forest Train in Alishan National Scenic Area
漫 步 在 雲 端
alishan.cyc.edu.tw

阿里山入口
The entrance of Alishan National Scenic Area

台北淡水河景觀 Danshuei River , Taipei

台北淡水河 Danshuei River, Taipei
台北 淡水河 / 齊桓林 攝影

野柳滑翔傘 The Para-Gliding in Yehliu

墾丁國家公園海邊
The Beachscape of Kenting National Park

台灣墾丁海邊
The beach in Kenting National Park

蘇花公路清水斷崖
Chingshuei Cliff of Coastal Mountains

S. J. Huang sgjghuang@mail.ntust.edu.tw

宜蘭蘇澳港
Suao Port, is situated in the northeast coast of Taiwan

Weizmann Institute of Science 2013-2014

Back to 以色列

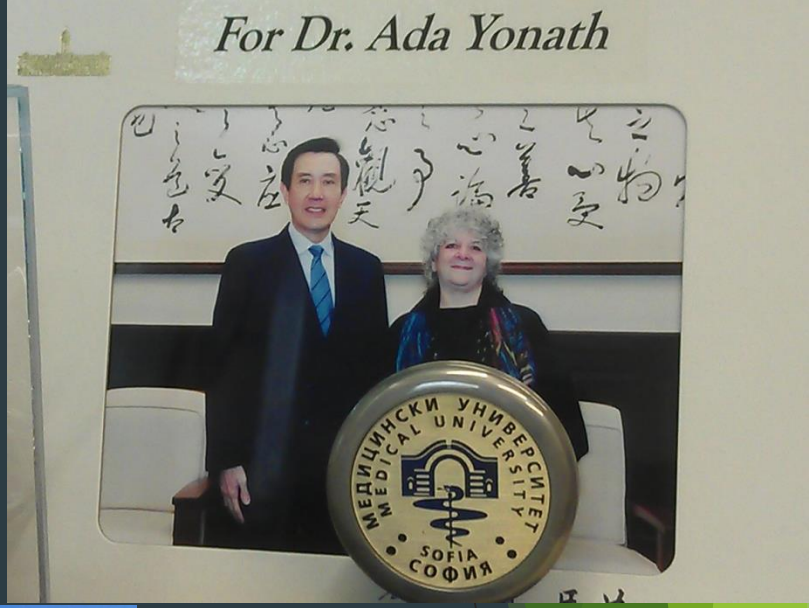

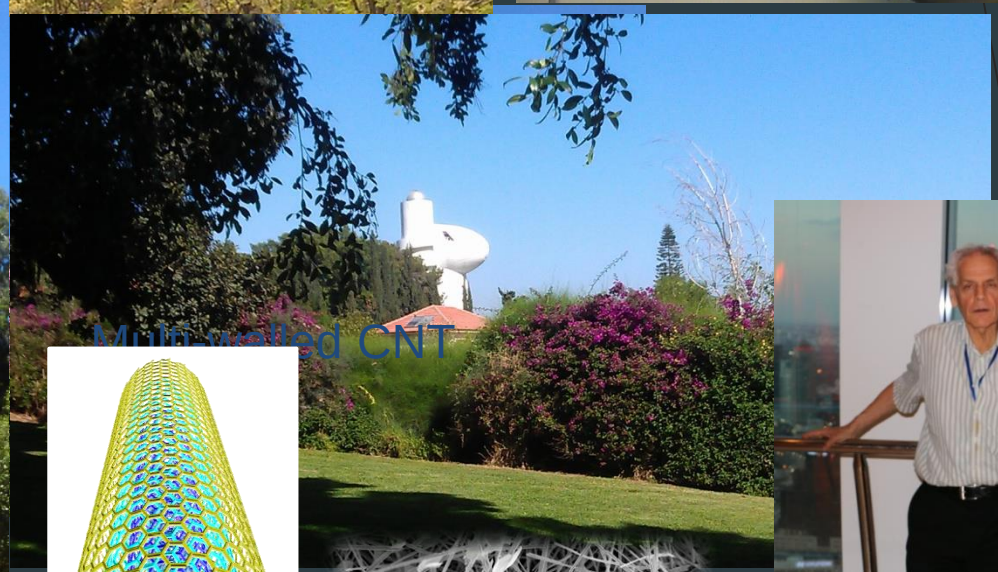

Multi-walled CNT

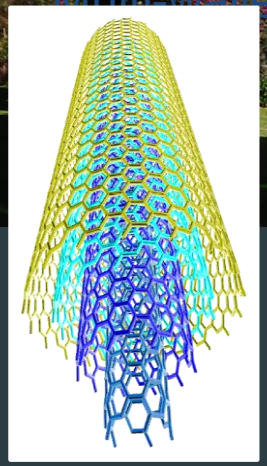

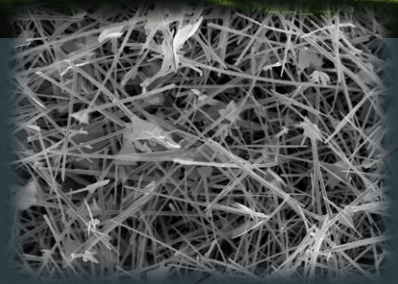

Metal Matrix Composites (MMCs) and Bio-composite

TAIWAN TECH National Taiwan University of Science and Technology

Fabrication of Mg MMCs

(1) Melt-stirring technique
(2) Tube Extrusion of Mg MMCs
(3) Heat sink materials for LED

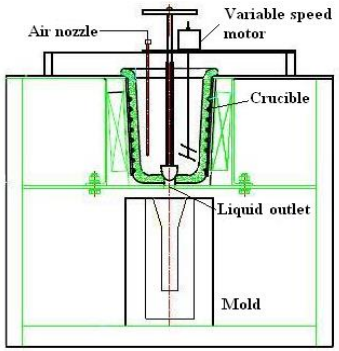

(1) Melt-stirring technique

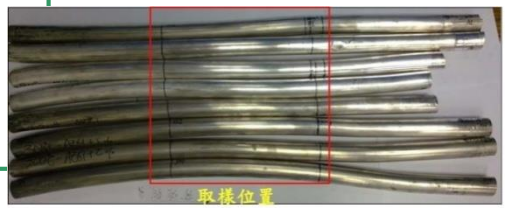

(2) Tube Extrusion of Mg MMCs
Best paper award of 2011 annual conference of Taiwan Magnesium Association

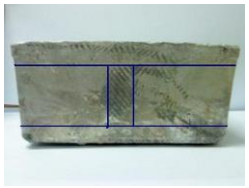

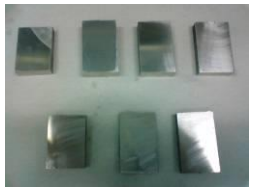

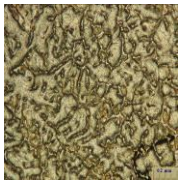

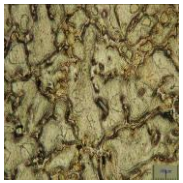

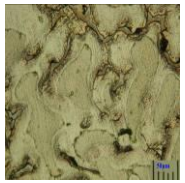

Mg MMCs

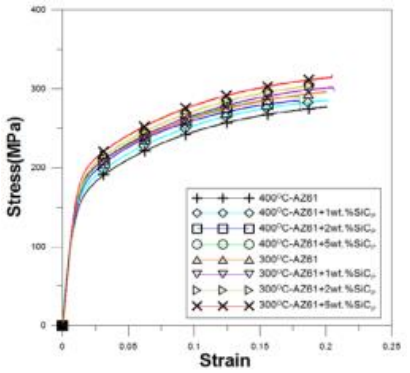

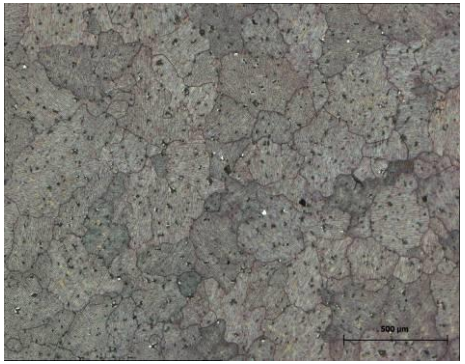

AZ91D/2wt%AlN-100X

[Acta Metallurgica Slovaca, Vol. 16, 2010]

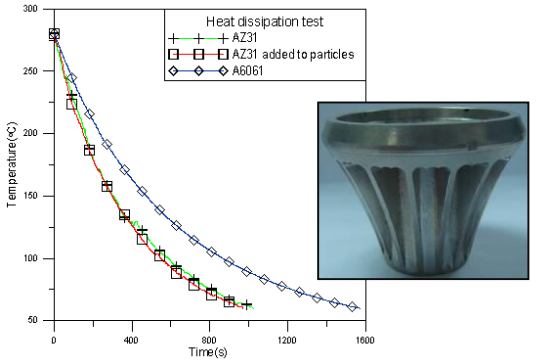

(3) Heat sink materials for LED

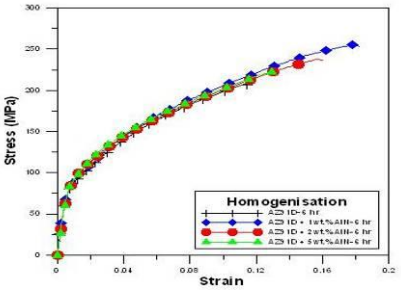

Metal Matrix Composites (MMC)

TAIWAN TECH National Taiwan University of Science and Technology

(4) ECAP

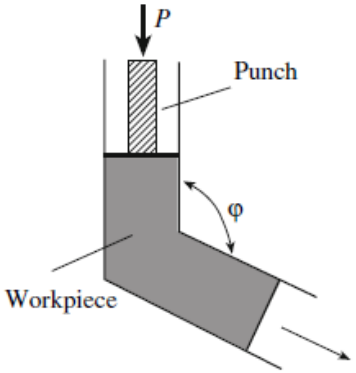

Diagram of performance of SPD using ECAP techn

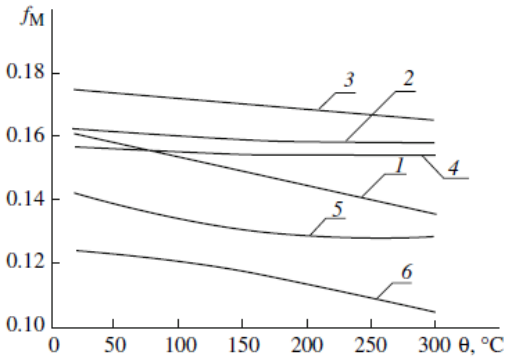

Fig. 7. Temperature dependences of the molecular component of the friction coefficient for studied alloys in the contact with steel R18: (*1*) AZ91D in the starting state, (*2*) AZ91D + SiC (S = 5 μm, C = 3%), (*3*) the same, S = 11 μm, C = 3%, (*4*) the same, S = 11 μm, C = 6%, (*5*) the same, S = 15 μm, C = 3%, and (*6*) AZ91D after two ECAP cycles.

Journal of Friction and Wear, Vol. 30 No.3. pp. 194-198 [NSC 95-2811-E-194-001 , NSC96-2923-E-194-001-MY3 (NSC-RFBR Taiwan-Russian Bilateral research project)]

Wear of Mg MMCs by severe plastic deformation (SPD)

(4) equal-channel angular pressing (ECAP)
(5) Wear of AZ91D MMCs

(5) Wear of MMCs

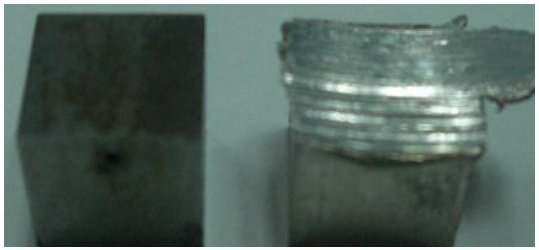

Outward appearance of AZ91D MMCs before and after wear test [Tribology Letters, 2010]
[NSC95-2811–E–194–001]

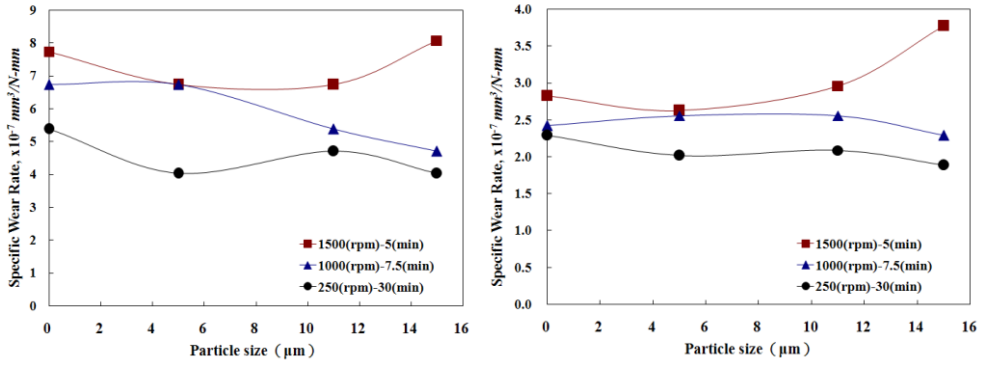

Specific wear rate of MMCs with particle size of 3vol.% SiCp in AZ91D MMCs: loaded up to (a) 10N, (b) 50N. [Tribology Letters, 2010]

Micro-arc Oxidation

- **Advantage**
  - **Enhancing surface hardness, wear resistance and anti-corrosion ability**
  - **Eco-friendly electrolyte**

- **Applications**
  - **Mobile phone**
  - **Aerospace industry**
  - **Semiconductor industry**
  - **Biomedical technology**
  - **Automotive industry**

Step 1

Valve metals are pro thin, self-healing, tigh adherent dielectric ox in naturally

Step 2

The weakest area of insu film will be gone through to the phenomenon of a discharge

Step 3

High temperatures and pressure formed in disc channels

Step 4

Electrolyte additives v participate in the react around the micro-arc discharge channels

Step 5

Then a new layer of oxide film is formed at the breakdown area

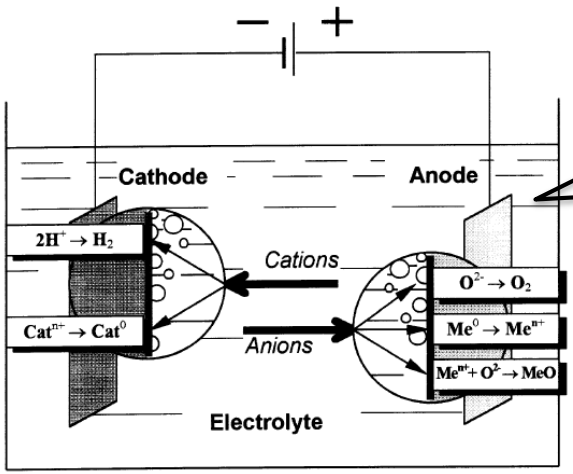

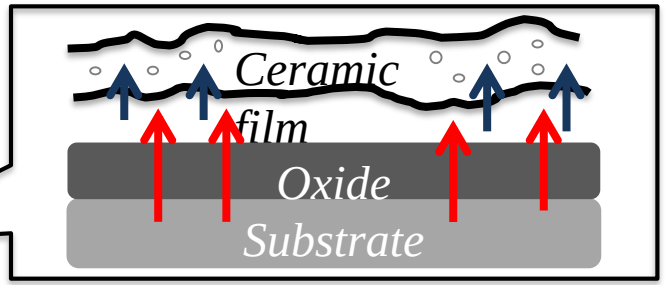

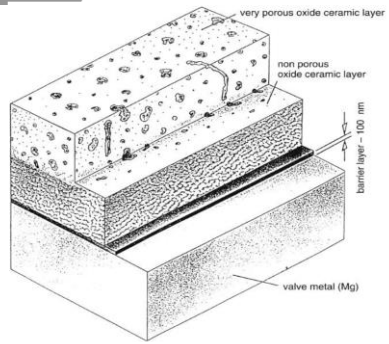

Luminescence

Sparking

Micro-arc discharges

Arc discharges

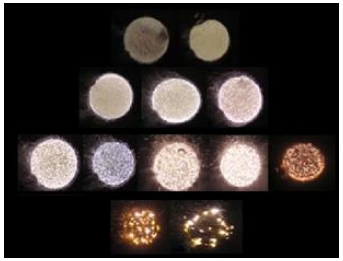

- **Commonly use electrolyte system**
  - **Silicate**
  - **Phosphate**
  - **Aluminate**

Metal hydrogen storage material

- **Magnesium hydrogen storage**：
  - **Advantage**：
    - Light weight, resource-rich, low cost
    - High hydrogen storage capacity (7.6 wt.%)
  - **Disadvantages**：
    - High thermodynamic stability
    - Slow kinetic

- Metal-Hydrogen system：

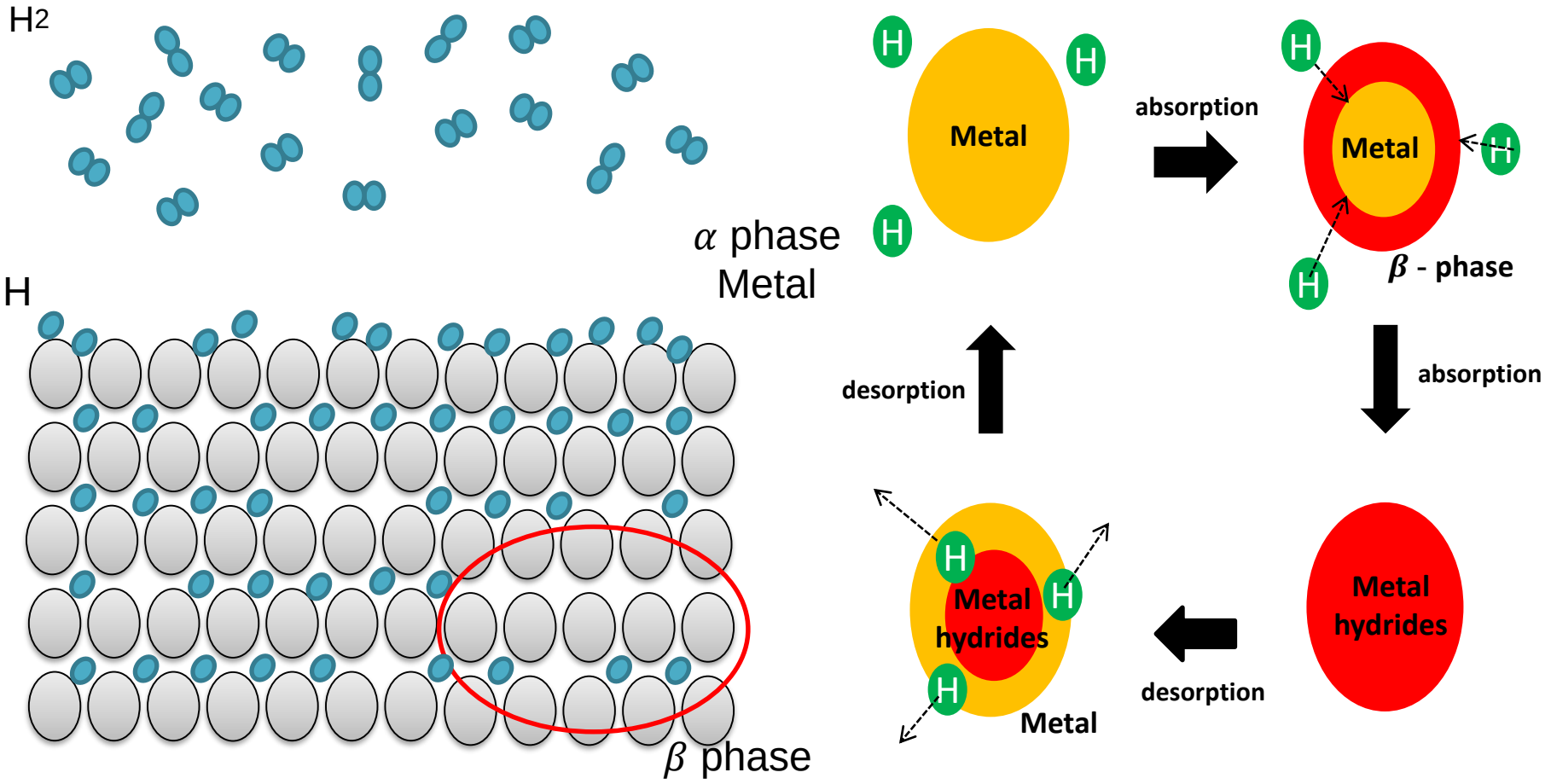

Bicycle Application

Break rig
Mg: 0.47 Kg

Stand pipe
Mg: 0.175 Kg
Al: 0.26 Kg
Weight decreasing 33%

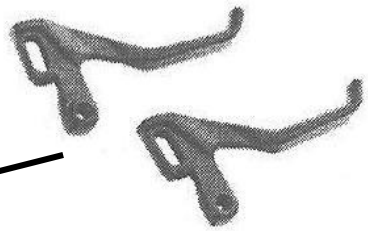

Break handle

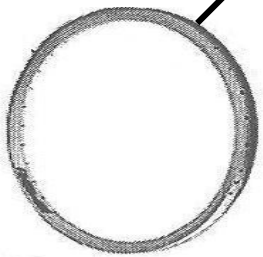

Wheel frame
Mg: 0.4 Kg
Al: 0.6 Kg
Decreasing 33%

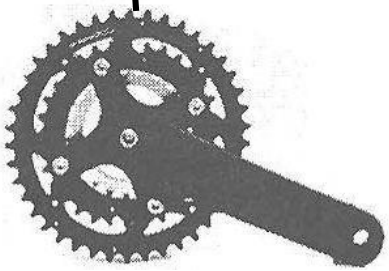

Crank

Pedal
Mg: 0.32 Kg

Fork mounting
Mg: 0.4 Kg

Leisure industry

Source: ITIS, Taiwan

Computer industry

- ASUS 2010: 10 in LCD, 1.8 cm thick, 1.1 kg

ASUS Mg alloy case Notebook
Source: ASUS, Taiwan

DELL Studio XPS **Source: DELL**

hTC one s
Source: hTC

Microsoft Surface Pro 2
Source: Microsoft

Car industry

Back frame of hatchback

Mg: 2.7 Kg

Al: 4.5 Kg

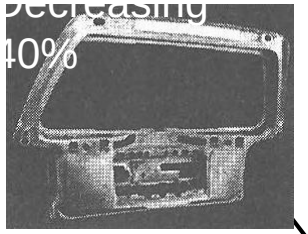

Frame of Hatchback

Mg: 2.69 Kg

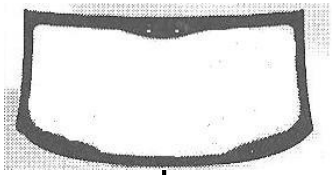

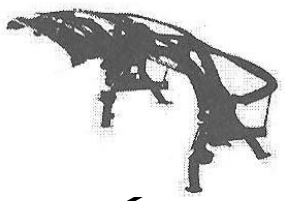

Movable roof

Mg:5.4~6.8 Kg

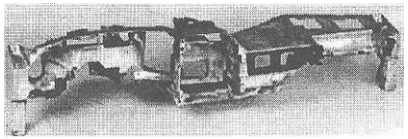

Instrument panel frame

Mg: 12 Kg

Steel: 18 Kg

Decreasing

33%

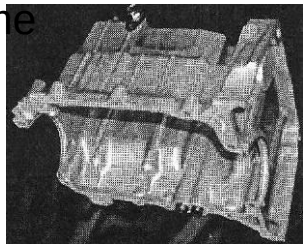

Bottom

shell of oil

Wheel frame

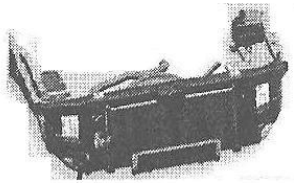

Front frame

Mg: 6.2 Kg

Steel: 15.2 Kg

Decreasing

60%

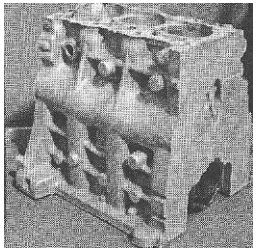

Cylinder body

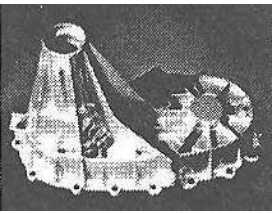

Shell of speed gear

Mg: 4.36 Kg

Steering Mg: 0.9 Kg

Steel: 1.4 Kg

Decreasing

33%

Seat frame

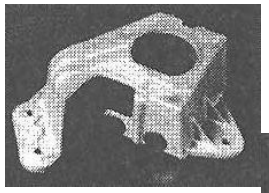

Cover of air-bag

Mg: 0.7 Kg

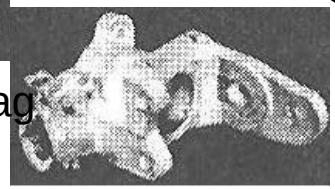

Shell 鎖架外殼

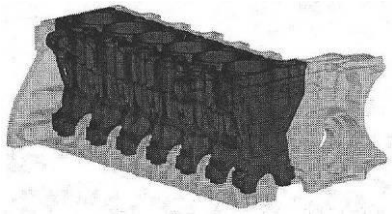

Crankcase

Source: MIRDC, Taiwan

TAIWAN TECH National Taiwan University of Science and Technology

Magnesium applications in Cars：

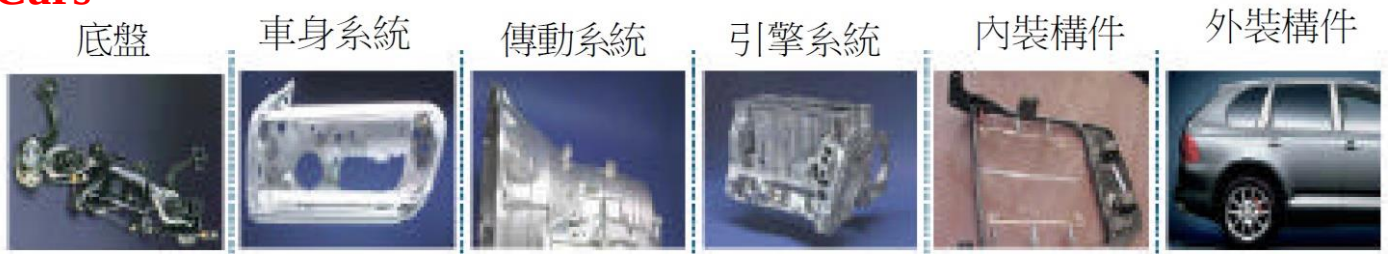

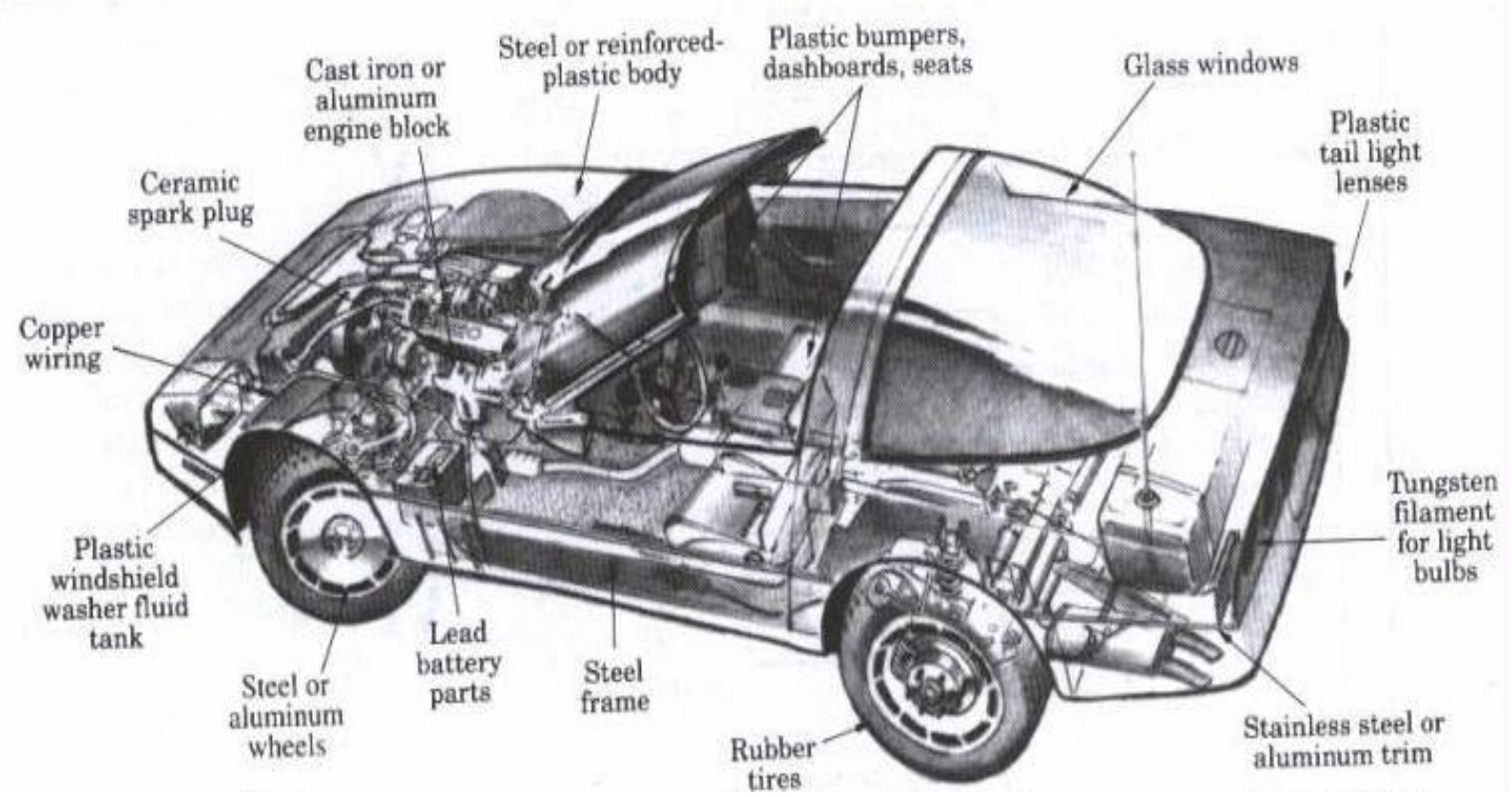

Engineering Materials used in automobile

Car industry

ew Mercedes E350 BlueTec (pictured) gets 9-speed 9G-TRONIC auto (July 24, 2013 By Cars UK)

Source: http://www.carsuk.net/mercedes-launch-new-9g-tronic-gearbox-on-e350-bluetec/#ixzz2jIu7oq00

China: 23 million automobiles made per year

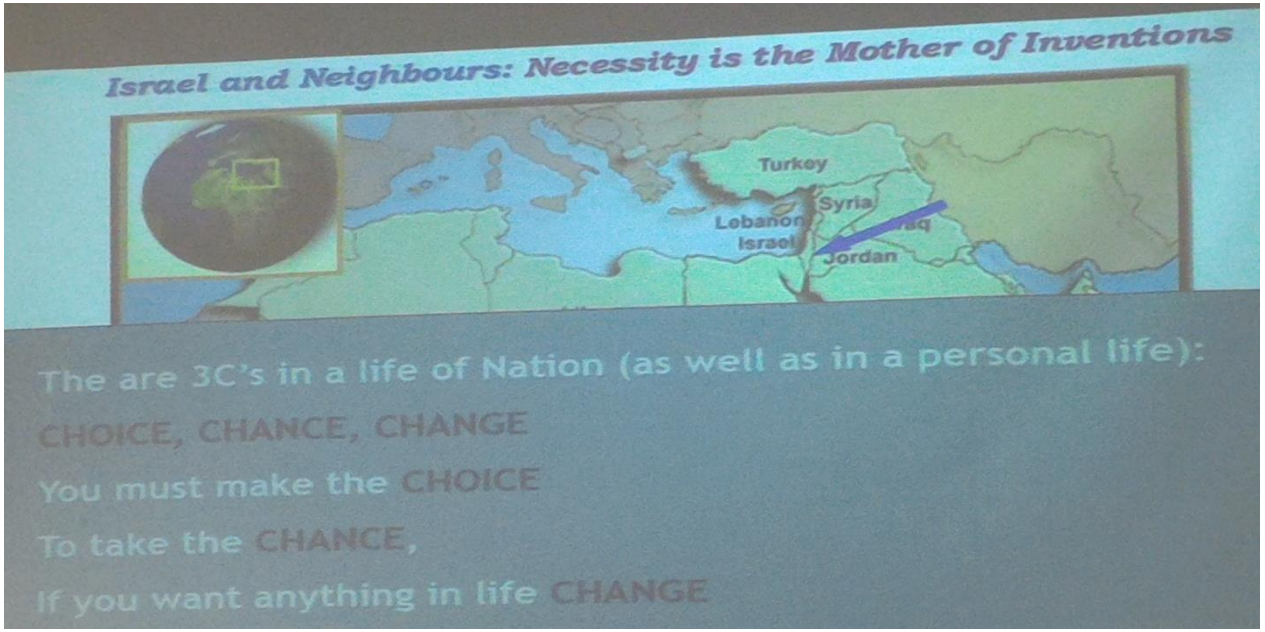

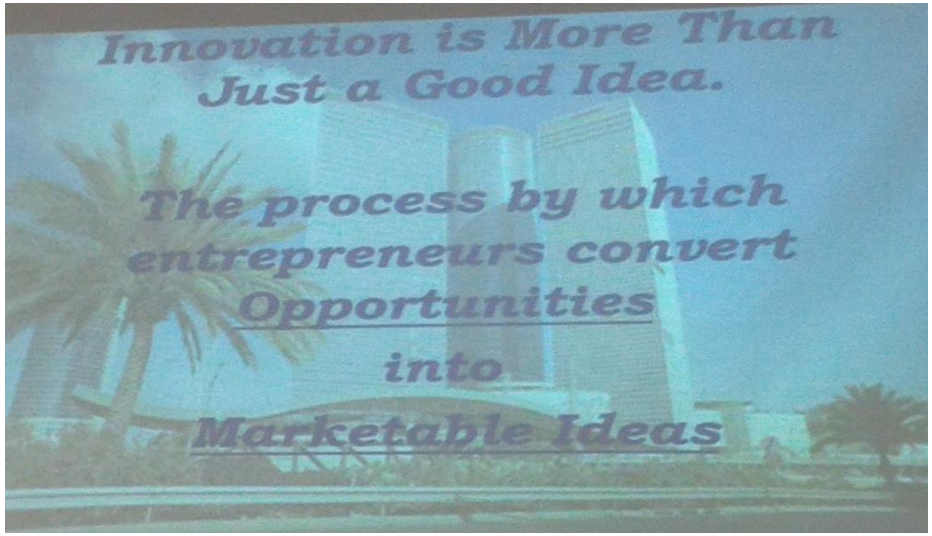

Source: E. Shkolnik "Israel: From Start-Up Nation to Exit Nation" 28 Aug. 2017

強化機制計算結果

- 根據Sanaty-Zadeh[55]的研究指出，當加工製程溫度處於室溫下，則Orowan的散佈強化影響會大於熱膨脹係數差異影響。

- 當製程溫度超過室溫的話，會隨著加工製程溫度的提高(~270℃)，強化機制的影響則會由熱膨脹係數差異影響大於Orowan的散佈強化影響。

- 主要是因為當溫度升高的時候，基材與顆粒之間熱膨脹係數不同，使得兩者之間產生大量的差排，導致差排密度增加，進而達到強化的效果。

Symbol	Description	Value	Percentage of strengthening contribution
$\Delta\sigma_D$	enhancement of composite strength due to dislocation density increase	159MPa	56%
$\Delta\sigma_{Hall\text{-}Petch}$	enhancement of composite strength due to grain refining	98MPa	34%
$\Delta\sigma_{orowan}$	enhancement of composite strength due to Orowan strengthening	28MPa	10%

鎂合金的強化機制

Hall-Petch關係式：

$$\sigma = \sigma_o + kd^{-1/2}$$

(σ為降伏強度； σ_o與k為常數； d為晶粒尺寸)

- 由此關係式可以得知當晶粒尺寸愈小時，材料降伏強度則會愈高。此外，晶粒細化可以抑止雙晶的形成，進而改善延性。
- 晶粒之間形成的晶界會阻擋差排的滑移，如透過TEM觀察通常能發現許多差排堆積在此處，當結晶材料晶粒越小伴隨的晶界數目越多，代表差排的滑移會更困難，因此材料的強度便會提升[7]。

鎂合金的強化機制

Orowan關係式：

- Orowan強化理論則用來解釋強化相達到奈米等級大小時所產生的強化效果，其強化機制主要是差排與奈米顆粒之間的交互作用，假設差排通過顆粒時不會造成被顆粒剪斷的現象，受力時差排線會繞過強化相顆粒並留下差排環[25]。

$$\sigma = (2Gb) / [6d \left(\frac{2\pi}{F}\right)^{\frac{1}{2}}]$$

(G為剪變模數；b為Burger's向量；d為顆粒尺寸；F為強化相之體積分率)

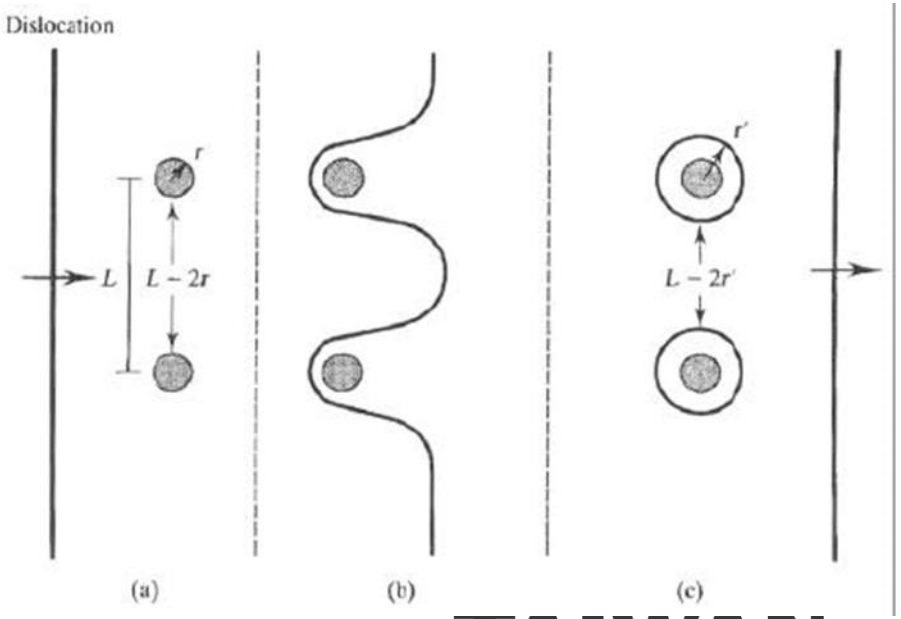

Reference

[1] P. G. Koppad, V. K. Singh, C. S. Ramesh, R. G. Koppad, K. T. Kashyap, in Advanced Carbon Materials and Technology (Anonymous), John Wiley & Sons, Inc.2014, 331-376.

[2] S. C. Tjong, Mater. Sci. Eng., R: Reports. 2013, 74(10), 281-350.

[3] L. Rapoport, O. Nepomnyashchy, R. Popovitz-Biro, Yu Volovik, B. Ittah, and R. Tenne, *Adv. Eng. Mater.,* 2004, **6,** 44.

[4] L. Rapoport, M. Lvovsky, I. Lapsker, V. Leshchinsky, Yu Volovik, Y. Feldman, A. Zak, and R. Tenne, *Adv. Eng. Mater*., 2001, **3,** 71-75.

[5] W. X. Chen, Z. D. Xu, R. Tenne, R. Rosenstveig, W. L. Chen, H. Y. Gan, J. P. Tu, *Adv. Eng. Mater.,* 2002, **4,** 686-690.

[6] N. Hansen, *Scr. Mater.,* 2004, **51,** 801-806.

Appendix I

Mechanisms for the reinforcement

Hall-Petch strengthening

$$\Delta\sigma_{\text{Hall-Petch}} = K_y\left(d_m^{-1/2} - d_c^{-1/2}\right)$$

Coefficient of thermal expansion difference effect

$$\Delta\sigma_{\text{CTE}} = \sqrt{3}\beta G_m b\sqrt{\frac{12V_p\left(\alpha_m - \alpha_p\right)\left(T_{process} - T_{test}\right)}{(1 - V_P)bd_p}}$$

Orowan strengthening

$$\Delta\sigma_{\text{Orowan}} = \frac{0.13G_m b}{d_p\left[\left(\frac{1}{2V_p}\right)^{1/3} - 1\right]}\ln\frac{d_p}{2b}$$

Load bearing effect

$$\Delta\sigma_{\text{load}} = 0.5V_p\sigma_{\text{ym}}$$

AZ31-1 wt% (WS2
Table S6. Parameter for calculation

Parameter	Description	Value	Reference/note
$\mathbf{d_c}$	average grain size in the composite sample	77.2 μm	experimentally determined
$\mathbf{d_m}$	average grain size in the monolithic sample	227.9 μm	experimentally determined
$\mathbf{d_p}$	nanoparticle diameter	100 nm	manufacture supplied average particle size
$\mathbf{V_p}$	volume fraction of nanoparticles	0.002333	calculated from weight fraction
$\boldsymbol{\sigma_{ym}}$	Yield stress of the matrix	84.3 MPa	experimentally determined

Table S7. Calculated contributions of the different mechanisms for the reinforcement of the AZ31 by 1 wt% INT-WS_2

Symbol	Description	Value [MPa]	Percentage of strengthening contribution
$\Delta\sigma_{\text{Hall-Petch}}$	enhancement of composite strength due to grain refining	6.4698	14.4%
$\Delta\sigma_{\text{CTE}}$	enhancement of composite strength due to dislocation density increase	31.2113	69.7%
$\Delta\sigma_{\text{Orowan}}$	enhancement of composite strength due to Orowan strengthening	7.0407	15.7%
$\Delta\sigma_{\text{load}}$	enhancement of composite strength due to load bearing	0.09834	0.2%

Bio-Medical Engineering

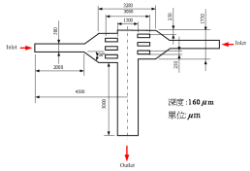

Bio-Chip

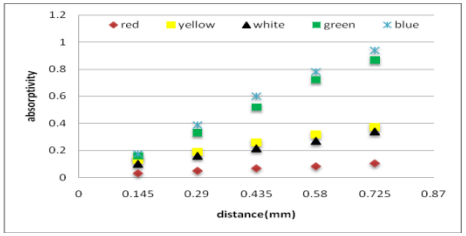

Blood Coagulation Bio-Chip System

(1) Absorptive of whole blood with each LED light
(2) eChem Inc. Cooperation project 2009.08-2010.07
(3) NSC 99-2622-B-006 -002 -CC1, 2010.08-2012.07

(1) Absorptive of whole blood with each LED light

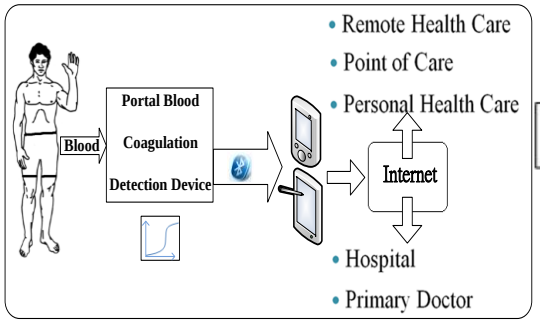

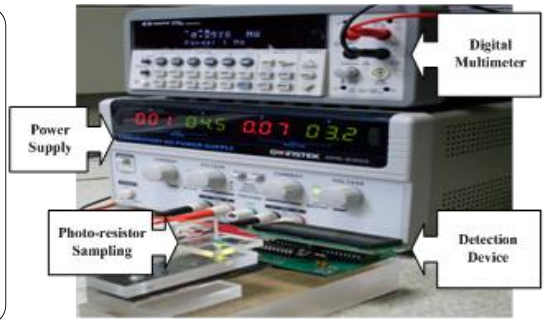

(2) eChem Inc. project [98-]

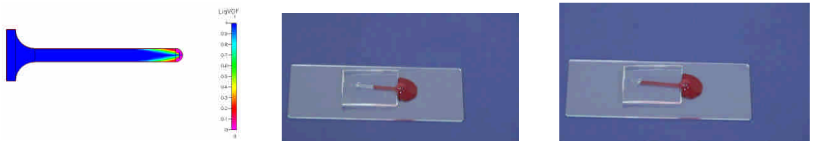

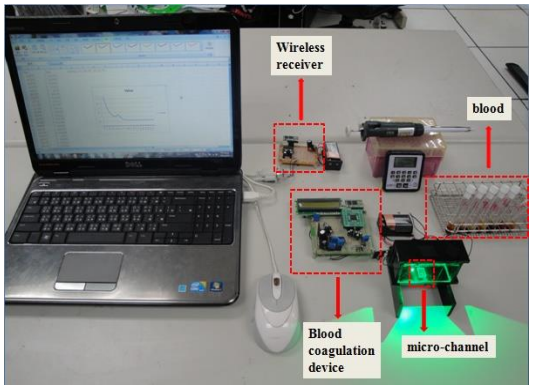

(3) Development of coagulation biochip and its applications(2/2) (NSC100-2622-B-006-005-CC1)

Excellent paper award of 2011 Annual Symposium on Biomedical Engineering and Technology of Taiwanese Society of Biomedical Engineering

Communications industry

Carbon fibres/magnesium metal matrix composite

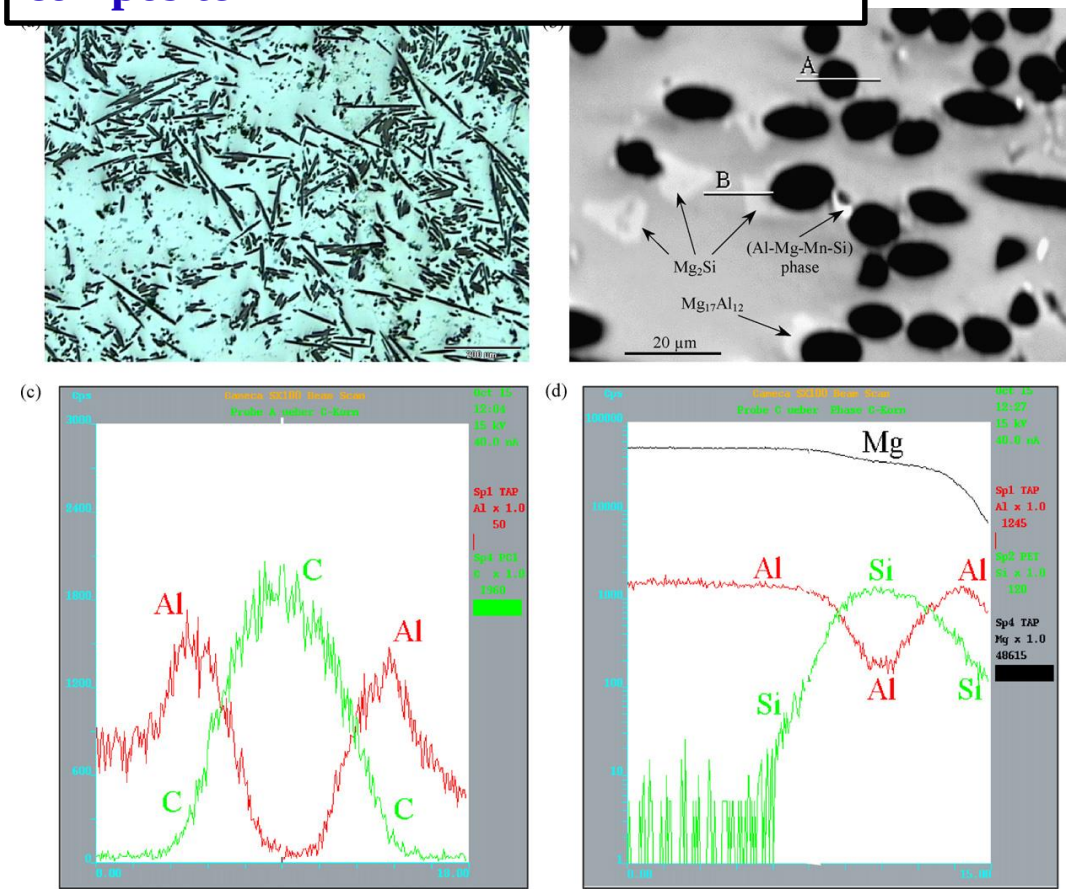

Fig. 7. Microstructure of C/AS41 Mg substrate, as-received: (a) optical micrograph for the horizontal plane, (b) SEM micrograph for the normal plane, (c) qualitative WDX-elemental scan along the "line A" shown in micrograph (b), and (d) semilogarithmic qualitative WDX-elemental scan along the "line B" shown in micrograph (b).

Corrosion behaviour **of carbon fibres/magnesium** metal matrix composite

Electrochimica Acta 54 (2009) 1597–1606

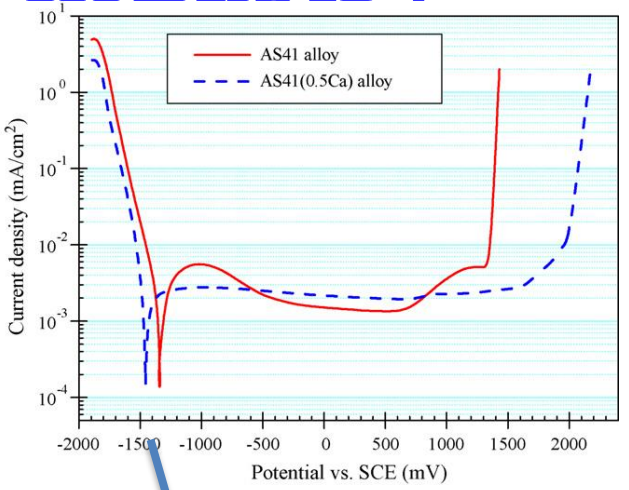

Fig. 1. Potentiodynamic polarisation diagrams for monolithic AS41 and AS41(0.5% Ca) Mg alloys in 100ppm NaCl solution; pH 12.

Corrosion behaviour of **carbon fibres/magnesium** metal matrix composite

Electrochimica Acta 54 (2009) 1597–1606

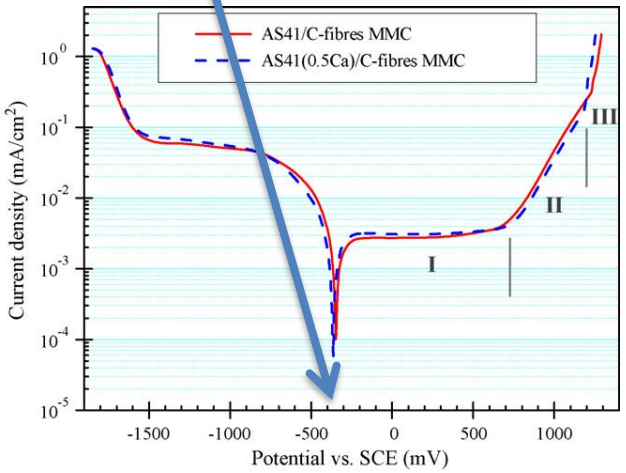

Fig. 2. Potentiodynamic polarisation diagrams for both **C**/AS41 and **C**/AS41(0.5% Ca) Mg MMCs in 100ppm NaCl solution; pH 12.

Electrochimica Acta 54 (2009) 1597–1606

Communications industry

Mg particle size (25, 53, 106, 180 μm) on the reactivity and superconducting properties of in situ **MgB2** **(Magnesium diboride)**

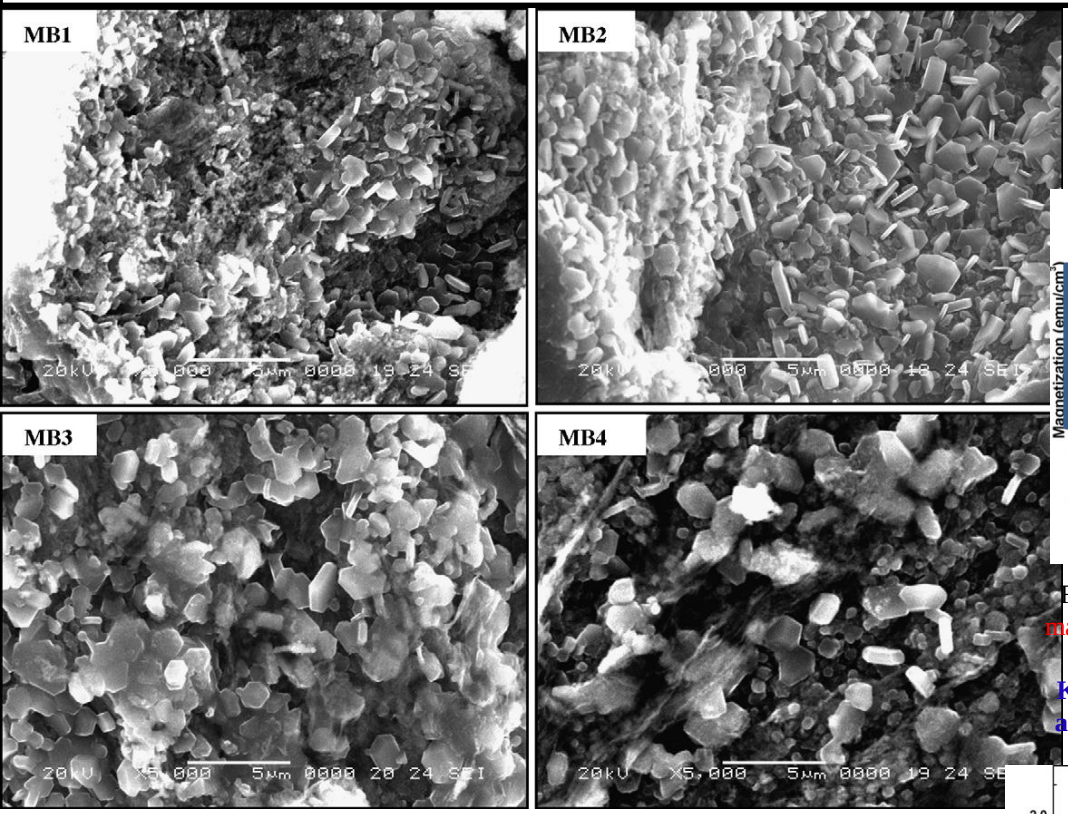

Fig. 2. SEM images of the samples
Influence of Mg particle size on the reactivity and superconducting properties of in situ MgB2
K. Vinod et al. / Journal of Alloys and Compounds 464 (2008) 33–37

Table 1
Volume percentage (vol.%) of MgB2, MgO and Mg in the samples

Sample	MgB2	MgO	Mg
MB1	97.40	2.60	0.00
MB2	98.04	1.44	0.52
MB3	93.83	1.12	5.05
MB4	93.08	1.04	5.87

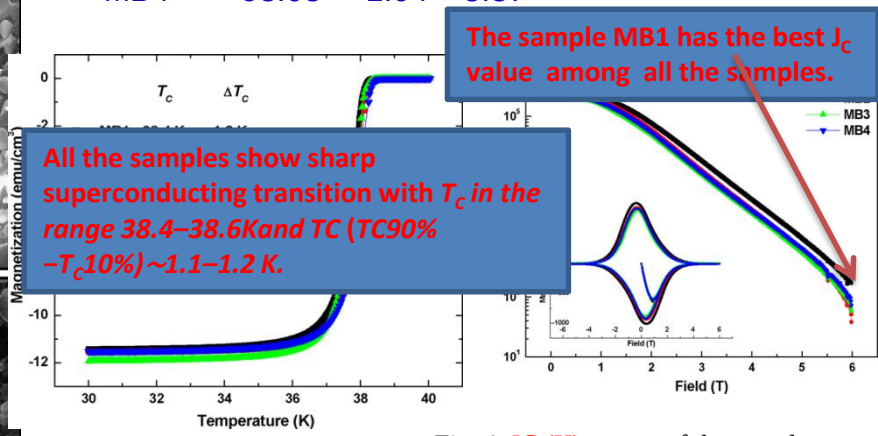

Fig. 3. Temperature dependence of magnetization (M–T) plots at 100 Oe of the samples.
K. Vinod et al. / Journal of Alloys and Compounds 464 (2008) 33–37

Fig. 4. JC (H) curves of the samples at 15 K. Figure inset shows the M–H plots of the samples.
K. Vinod et al. / Journal of Alloys and Compounds 464 (2008) 33–37

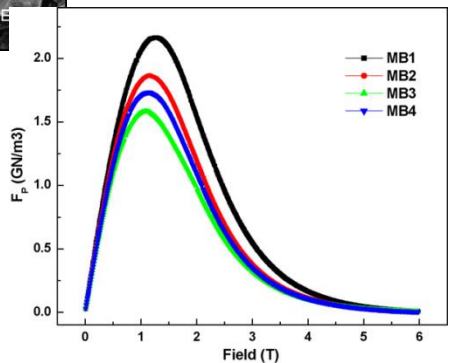

Fig. 5. Normalized flux pinning force density as a function of applied magnetic field for the samples.
K. Vinod et al. / Journal of Alloys and Compounds 464 (2008) 33–37

Consumer Electronics & Fuel Cell industry

Three different types of electroless nickel (EN)-phosphorus plating were applied on AZ31 wrought magnesium alloy.

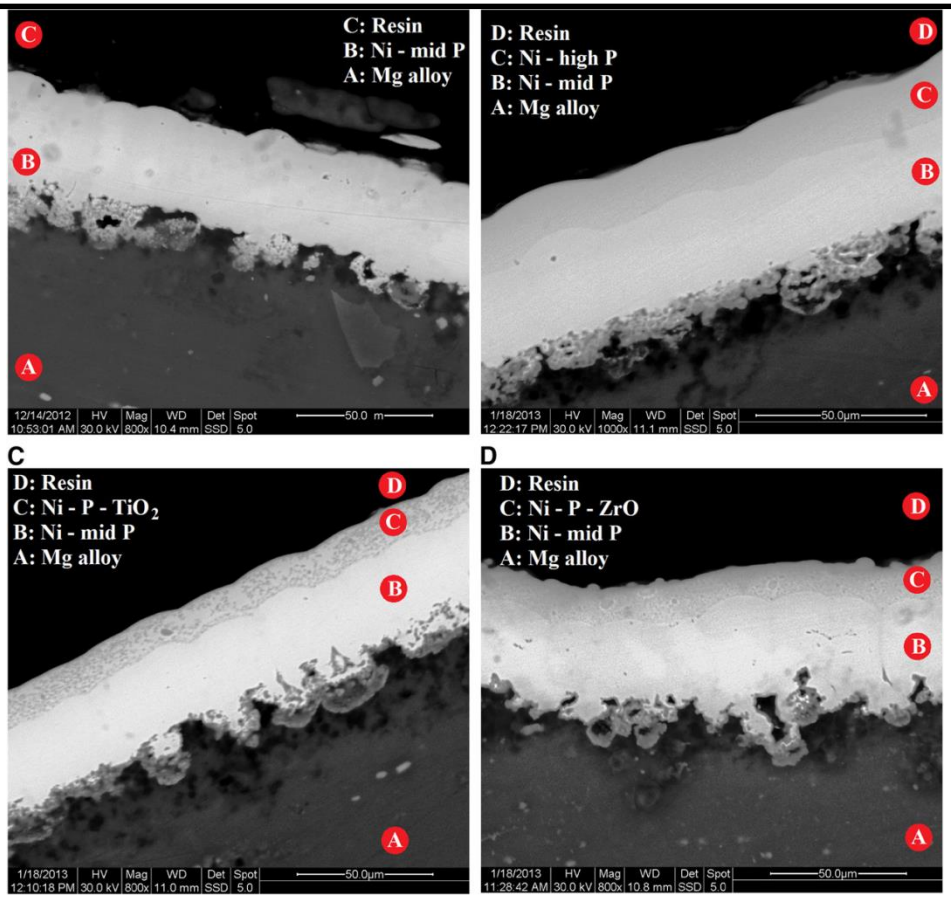

Fig. 3. SEM images of cross-sections of as-plated coupons, a) plain Ni-P coating, b) duplex Ni-P coating, c) duplex Ni-P-TiO2 coating, d) duplex Ni-P-ZrO2 coating. Ceramic microparticles appear as tiny grey dots.

Characterization and corrosion resistance of duplex electroless Ni-P composite coatings on magnesium alloy

E. Georgiza et al. / Surface & Coatings Technology 232 (2013) 432–439

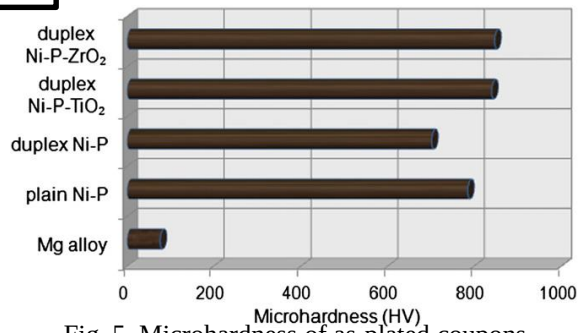

Fig. 5. Microhardness of as-plated coupons.

Characterization and corrosion resistance of duplex electroless Ni-P composite coatings on magnesium alloy

E. Georgiza et al. / Surface & Coatings Technology 232 (2013) 432–439

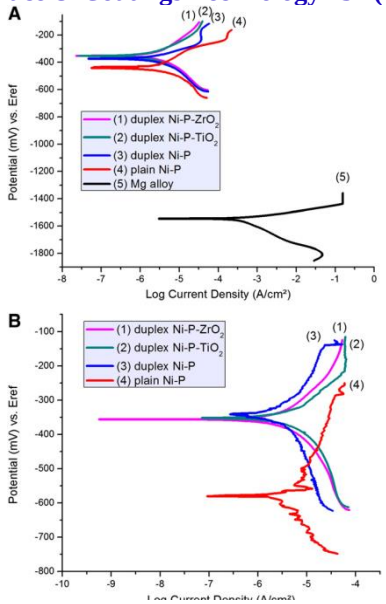

Fig. 6. Comparative polarization curves of a) as-plated coupons and substrate, coupons after heat treatment for 2 h at 200 ˚C.. **Georgiza et al. / Surface & Coa**

Technology 232 (2013) 432–439

Consumer Electronics & Fuel Cell industry

Corrosion resistance of thermally sprayed Al and Al/SiC coatings on pure Mg

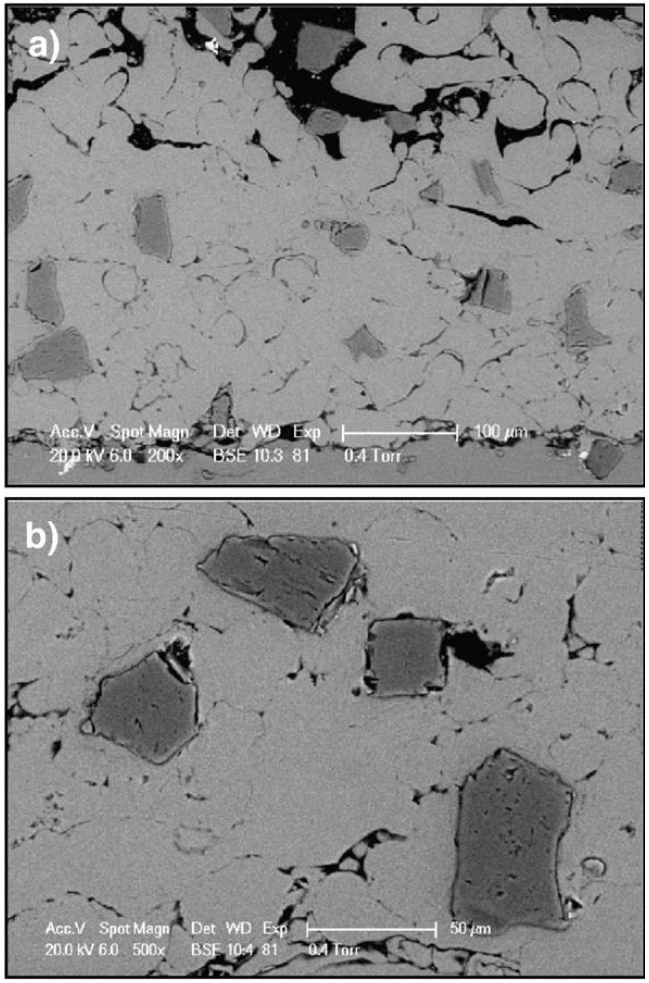

Fig. 4. Transversal section of the Al/SiC composite coating sprayed at 15 cm in two layers on Mg substrate: a) general view and b) detail of SiC particles.

Corrosion resistance of thermally sprayed Al and Al/SiC coatings on Mg

M. Campo et al. / Surface & Coatings Technology 203 (2009) 3224–3230

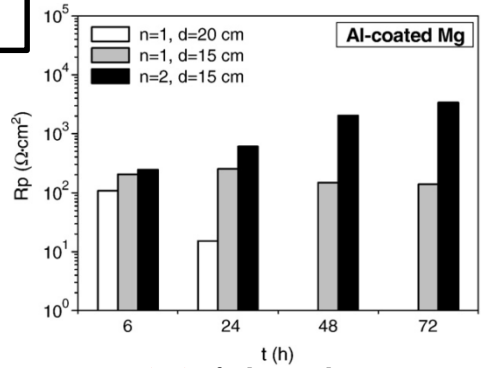

Fig. 3. Polarization resistance (Rp) of Al-coated Mg vs. immersion time in 3.5 wt.% NaCl solution as a function of spraying distance and number of layer deposited.

Corrosion resistance of thermally sprayed Al and Al/SiC coatings on Mg

M. Campo et al. / Surface & Coatings Technology 203 (2009) 3224–3230

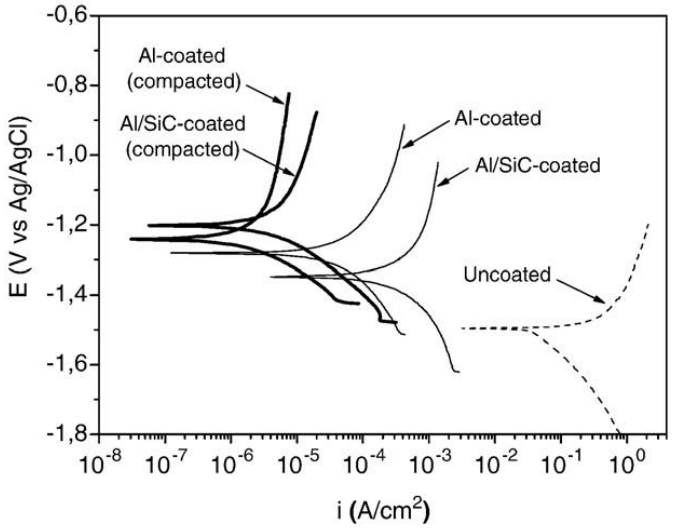

Fig. 6. Polarization curves of uncoated, and as-sprayed and compacted Al-coated a Al/SiC-coated magnesium after 1 h of immersion in 3.5 wt.% NaCl solution.

Corrosion resistance of thermally sprayed Al and Al/SiC coatings on Mg

M. Campo et al. / Surface & Coatings Technology 203 (2009) 3224–3230

Consumer Electronics & Fuel Cell industry

Hydrogenation behavior of high-energy ball milled amorphous Mg2Ni catalyzed by MWCNTs

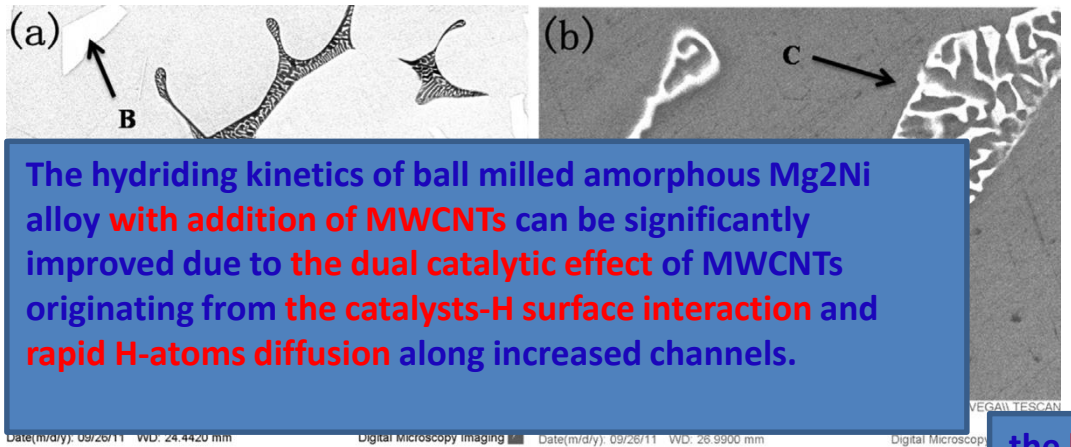

The hydriding kinetics of ball milled amorphous Mg2Ni alloy with addition of MWCNTs can be significantly improved due to the dual catalytic effect of MWCNTs originating from the catalysts-H surface interaction and rapid H-atoms diffusion along increased channels.

Fig. 2 e Scanning electron micrograph of the as-cast Mg2Ni alloy.

Hydrogenation behavior of high-energy ball milled amorphous Mg2Ni catalyzed by multi walled carbon nanotubes

Hou X, et al., International Journal of Hydrogen Energy (2013), http://dx.doi.org/10.1016/j.ijhydene.2013.09.053

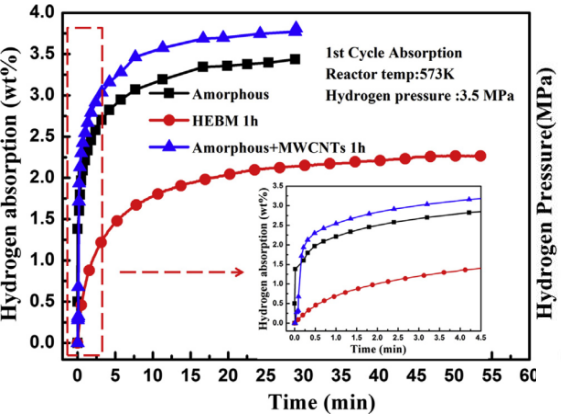

Fig. 6 Kinetics of hydrogen absorption for Mg2Ni alloys (Crystalline, Amorphous, Amorphous D WCNTs).

Hou X, et al., International Journal of Hydrogen Energy (2013),

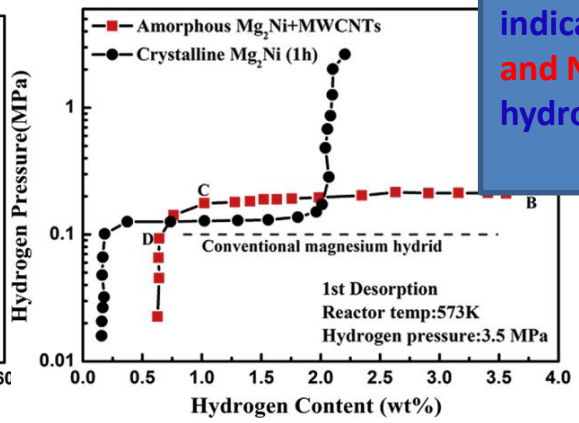

Fig. 7 P-C-T results for amorphous Mg2Ni alloy ball milled with MWCNTs for 1 h and crystalline Mg2Ni ball milled for 1 h at 573 K..

Hou X, et al., International Journal of Hydrogen Energy (2013),

Hydrogen storage properties of Mg-TM-La (TM : Ti, Fe, Ni) ternary composite powders

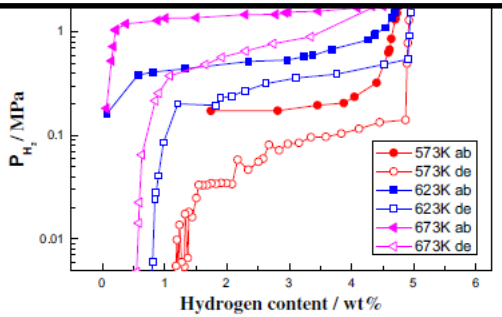

the hydrogenation enthalpies of Mg in Mg-TM-La powders were determined to be -68.7 kJ/mol H2 for the Mg-Ti-La powder, -72.9 kJ/ mol H2 for the Mg-Fe-La powder and -82.1 kJ/mol H2 for the Mg-Ni-La powder. These results indicated that minor addition of TM to Mg, especially Ti and Ni, can alter the thermodynamic properties of Mg for hydrogen storage.

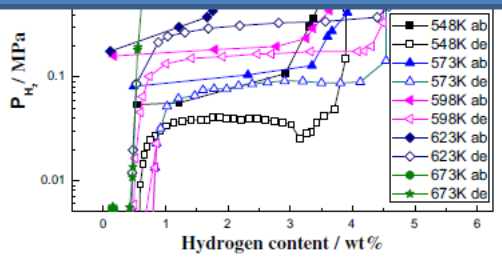

Fig. 5 PCT absorption and desorption curves at various temperatures for the Mg-Ti-La (a), Mg-Fe-La (b) and Mg-Ni-La (c) powd

Hydrogen storage properties of Mg-TM-La (TM [Ti, Fe, Ni) ternary compo powders prepared through arc plasma method

Jianxin Zou et al., i n t e r n a t i o n a l j ournal o f hydrogen energy 3 8 (2 0 1 3) 8 8 5

超镁合金复合材料

内容大纲

一.超镁合金材料

- 技术、产品应用

二. 团队

三.发展规划及商业模式

四. 市场定位及竞争优势

五. 资金需求

一.超镁合金材料

1-1 超镁合金概述
1-2 研发镁基复合材料之目的
1-3 各类合金材料性质比较
1-4 本公司产品型号
1-5 镁合金各种用途分类
1-6 全球市场应用说明
1-7 超镁合金应用领域

1-1 超镁合金概述

超镁合金是一種**金属基复合材料** (Metal Matrix Composites, MMCs)

- 增加材料特性

  结合两种以上不同的材料特性，增加单一材料的机械性质。

- 主要研发产品

  以重量轻的金属与合金加上强化材为主。

1-2 研发镁基复合材料之目的

1. 提高极限强度。
2. 增加降伏强度。
3. 延展性的提升。
4. 更好的硬度 。

机械性质	一般镁合金	超镁合金
极限强度 (MPa)	230-260	267-315
降伏强度 (MPa)	130-160	146-174
延展性 (%)	7-14	16-32
硬度 (HV)	55-65	68-85

1-3超镁合金與國內外各类合金材料性质之比较

合金类别 性质比较	钢材	钛合金	铝合金 (6061)	铝合金 (7005)	镁合金 (AZ80A)	**超镁合金 (MMCs)**	碳纤维复材 (T300)
比拉伸强度 (MPa · cm^3/g)	约33.7	211	115	180	210	**105~307.7**	2057
密度 (g/cm^3)	8.2	4.5	2.7	2.8	1.8	**1.81~1.95**	1.75
硬度 (HV)	180	223	105	120	75	**68~125~ 500 (MDO)**	
延展性 (%)	40	30	20	20	7	**16~32**	3
价格 (RMB$/Kg)	4~5	188	25	28	40	**22~30**	190

1-4 产品型号

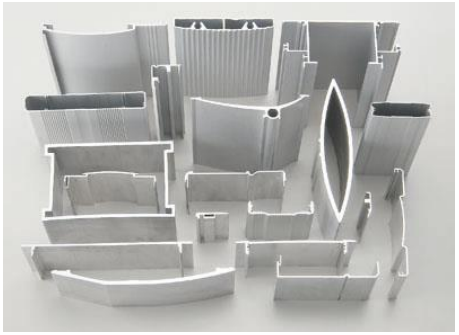

•AZ系列_**超镁合金**

合金系列	机械性质			
	极限强度 (MPa)	降伏强度 (MPa)	延展性 (%)	硬度 (Hv)
AZ61S1	305-317	135-145	15-19	68-75
AZ61S2	260-275	147-165	18-26	64-70

•AZ系列_國內外一般市面上镁合金

合金系列	机械性质			
	极限强度 (MPa)	降伏强度 (MPa)	延展性 (%)	硬度 (Hv)
AZ61	255-273	129-138	10-14	55-60

1-4 产品型号

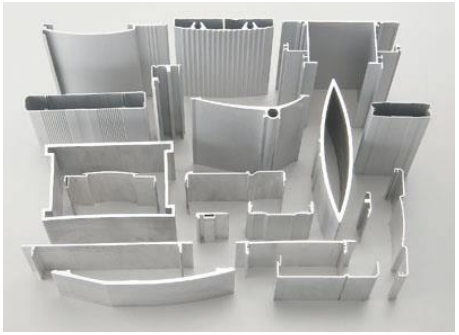

•AM系列_**超镁合金**

合金系列	机械性质			
	极限强度 (MPa)	降伏强度 (MPa)	延展性 (%)	硬度 (Hv)
AM60S1	240-285	138-170	27-35	67-78

•AM系列_國內外一般市面上镁合金

合金系列	机械性质			
	极限强度 (MPa)	降伏强度 (MPa)	延展性 (%)	硬度 (Hv)
AM60	230-241	126-133	7-13	59-65

1-4-1 专利与产品

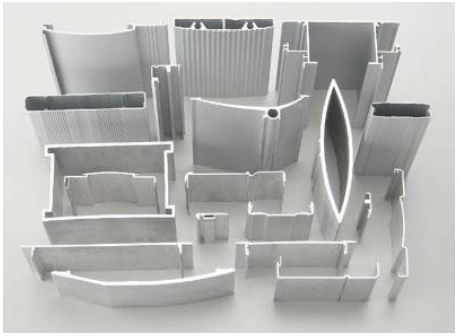

- 本公司首席顾问黄崧任教授专利项目 PATENTS
- **「具有微粒掺杂的镁合金复合材料」**,中华民国发明专利编号：I414612 (专利权期间: 2013/11/11 至2028/06/28). (许晖侃代理)
  发明人: 黄崧任、许晖侃、江堂豪
  专利权人: 许闳巨,许以暄,许佑杰,施淑姿,黄模森,林秋菊

  - 发明专利 (I)申请中：
  - 发明专利 (II)申请中：

1-5 镁合金各种用途分类

镁合金	用途
AZ31、AZ61	适用于挤制成形，其重量轻，并保有强度高及挤制性。 如：棒件、管材、散热片、脚踏车支架等。

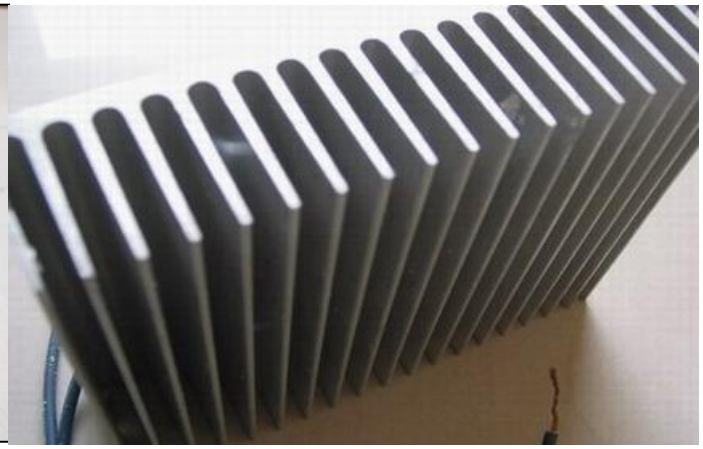

1-5 镁合金各种用途分类(cont.)

镁合金	用途
AZ91	最普遍使用的镁合金，拥有高强度及优良的铸造性能。 如：运动用品、计算机与手机外壳、手提工具、家庭用品等。
AM60	拥有卓越的延展性及减震特性。 如：汽车零件、方向盘、脚踏车前叉、支架等。

1-6 全球市场应用说明

运动用品

户外休闲用品

器材用品

航天用品

超镁合金

精密机械

3C用品外壳

医疗用品

交通工具

1-7 超镁合金应用领域

运动用品
溜冰鞋
自行车
慢跑机
钓具
登山用品
高尔夫球杆
滑板

户外休闲用品
旅行箱
露营用具
携带式桌椅
帐篷
挡风片

医疗用品
轮椅
担架
病床
点滴架

1-8 中国国内市场需求

随着人们环境保护意识的增强，**绿色产品**消费市场迅速壮大。2002年1～3月由中国环境新闻工作者协会主办的一项调查表明，中国公众的环境意识水平有了很大的提高，绝大多数受访人在购买商品时考虑各种与环保相关的因素，68%的受访人愿意政府为环境保护增税，65%的受访人为了环保，愿意购买比一般价格贵20%的商品。因此企业大量投资开发绿色产品，树立绿色形象，**镁合金作为21世纪最令人瞩目的绿色工程材料**，成为各国企业投资和研究的热点。

在镁合金产品开发应用的进程中，最先发展的成形加工技术是压铸，国内压铸业顺应国际趋势而迅速发展，大陆地区镁压铸工业的发展主要由**交通工具（汽车、摩托车、自行车、列车）**带动，台湾镁合金的发展由3C产品带动，正在向其它产品拓展，一些台湾的镁合金压铸工业转移至内地，也促进了镁合金的应用。

中国正进行汽车产品的结构调整，调整方向是**轿车**占汽车总量的比重增加，低排放、低污染、节能的绿色环保汽车替代非环保汽车。2005年轿车产量占总产量的比重从2000年的29.2%提高到35%以上，使各种车型的百公里油耗平均降低10%，近几年政府加大了**电动汽车的研发力度**，镁合金在国产汽车领域将得到广泛应用。

1-8 中国国内市场需求

中国大陆镁合金用量增长迅速，特别是内需应用镁合金压铸件的市场令人瞩目，交通工具产业镁合金用量2010年的需求量为**17.64万吨**，与2000年的用量**3400吨**相比，增幅达到51.9倍。

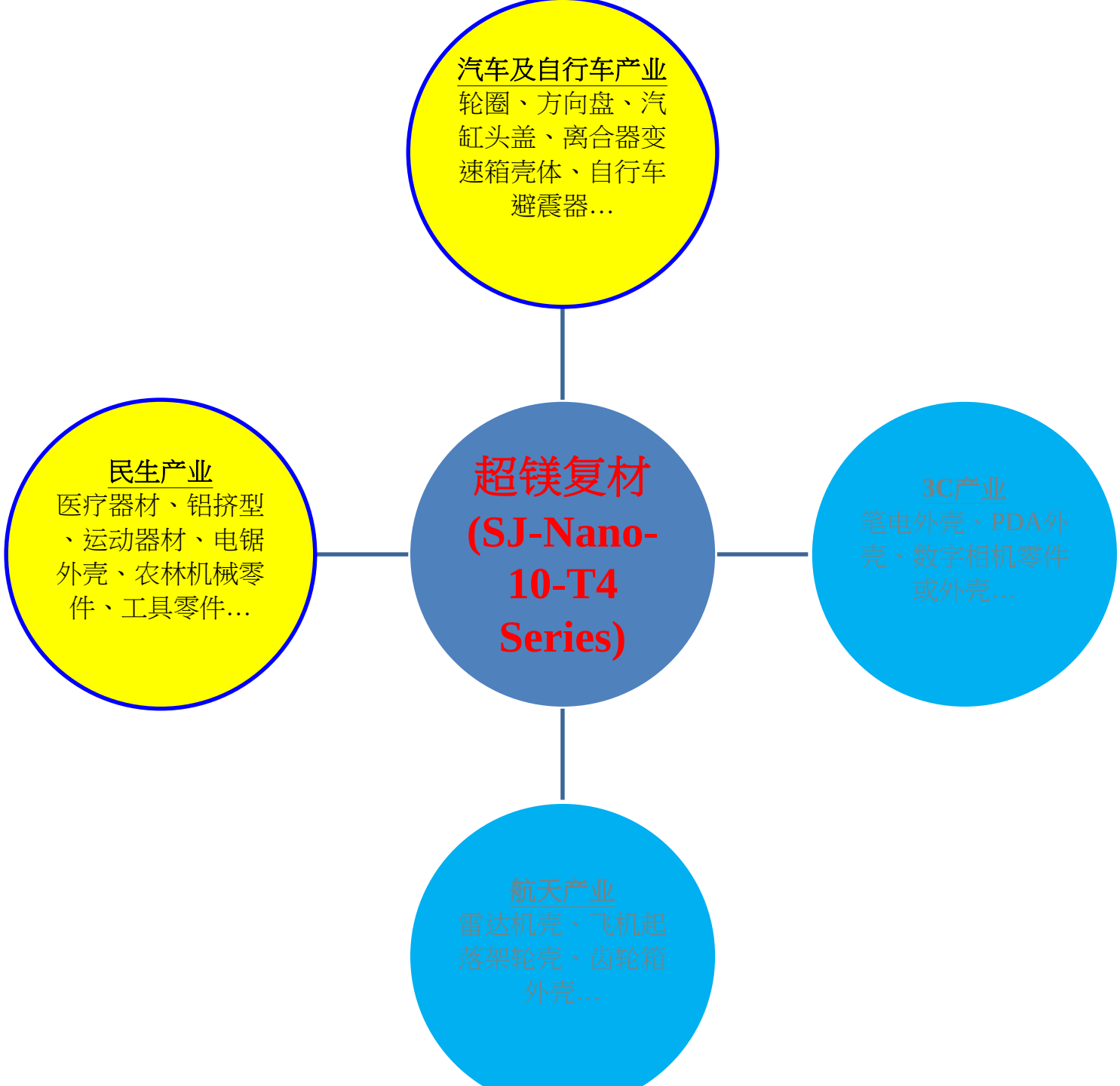
汽车及自行车产业
轮圈、方向盘、汽缸头盖、离合器变速箱壳体、自行车避震器…
民生产业
医疗器材、铝挤型、运动器材、电锯外壳、农林机械零件、工具零件…
超镁复材
(SJ-Nano-10-T4 Series)
3C产业
笔电外壳、PDA外壳、数字相机零件或外壳…
航天产业
雷达机壳、飞机起落架轮壳、齿轮箱外壳…

结论

- **提升强度、延展性**

  镁合金基材添加强化相，所制作出的镁合金复合材料，强度、硬度及塑变性皆有提升的效果。

- **维持质轻特性**

  添加强化相并不会影响密度，即能维持其质轻的特性。

- **开发7吋复材挤锭**

  目前正在开发，已进入最终试验阶段，以大量生产为目标，提供高质量之复材挤锭。

感谢您的参与及指教

活動六

應用液態金屬微量化產品、生成薄膜及改變功能研討會

由香港城市大學科學及工程學院特聘劉錦川教授主講

香港城市大學
City University of Hong Kong

Bulk Metallic Glasses (BMGs) and their mechanical behavior

Prof. C. T. Liu
University Distinguished Professor
Center for Advanced Structure Materials
City University of Hong Kong,

Hong Kong 生產局
April 12, 2018

Structural feature and deformation behavior of bulk metallic glasses (BMGs)

(晶态材料和大块非晶合金的变形)

•**Crystalline materials** (晶态材料) with long rang ordered structures contain the structural defect of dislocations (位错), and their plastic deformation proceeds with dislocation glide on slip planes

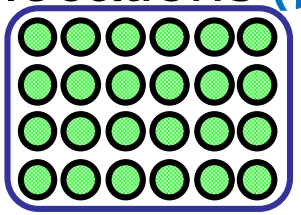

•**BMGs**(大块非晶)with amorphous (无定形)structures contain no dislocations, and their deformation proceeds with localized shears on shear bands (剪切带)

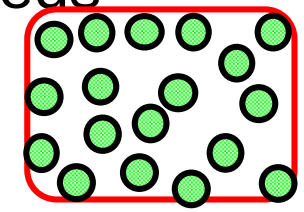

•Because of these fundamental differences, their deformation behaviors and mechanical properties are basically different (基于这些差别,两者的变形行为也截然不同)

Metallic glasses (MGs)/bulk metallic glasses (BMGs): Phase relationship (大块非晶合金的物相关系)

- **Crystalline alloys: (晶态合金)**

  Liquid state (液态) —Slow cooling 慢冷→ Crystalline state (晶态)

- **Metallic glasses (非晶合金，金属玻璃):**

  Liquid state (液态) —Fast cooling 快冷→ amorphous state (非晶态)

- **Bulk metallic glasses (大块非晶合金):**

  Metallic glasses with cross section ≥1 mm

  (非晶的截面尺寸≥1 mm的非晶合金)

Comparison of atomic arrangement in crystalline and amorphous materials

Crystalline metals: order

Metallic Glass: amorphous

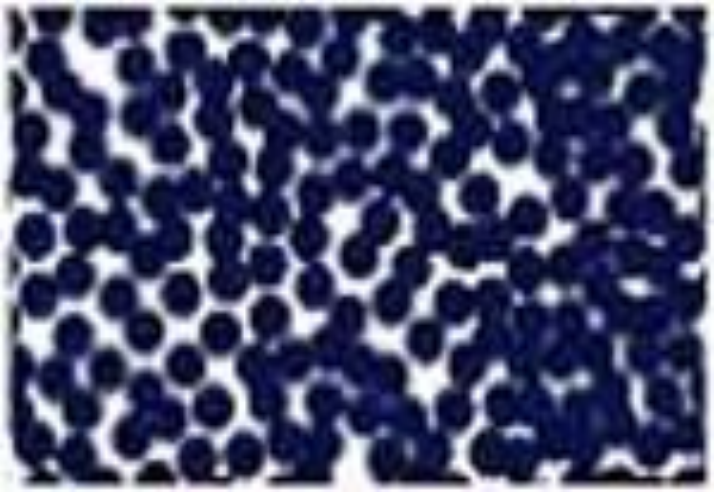

Cast BMG button having a mirror finish surface

Dimensional tolerance of glassy alloys

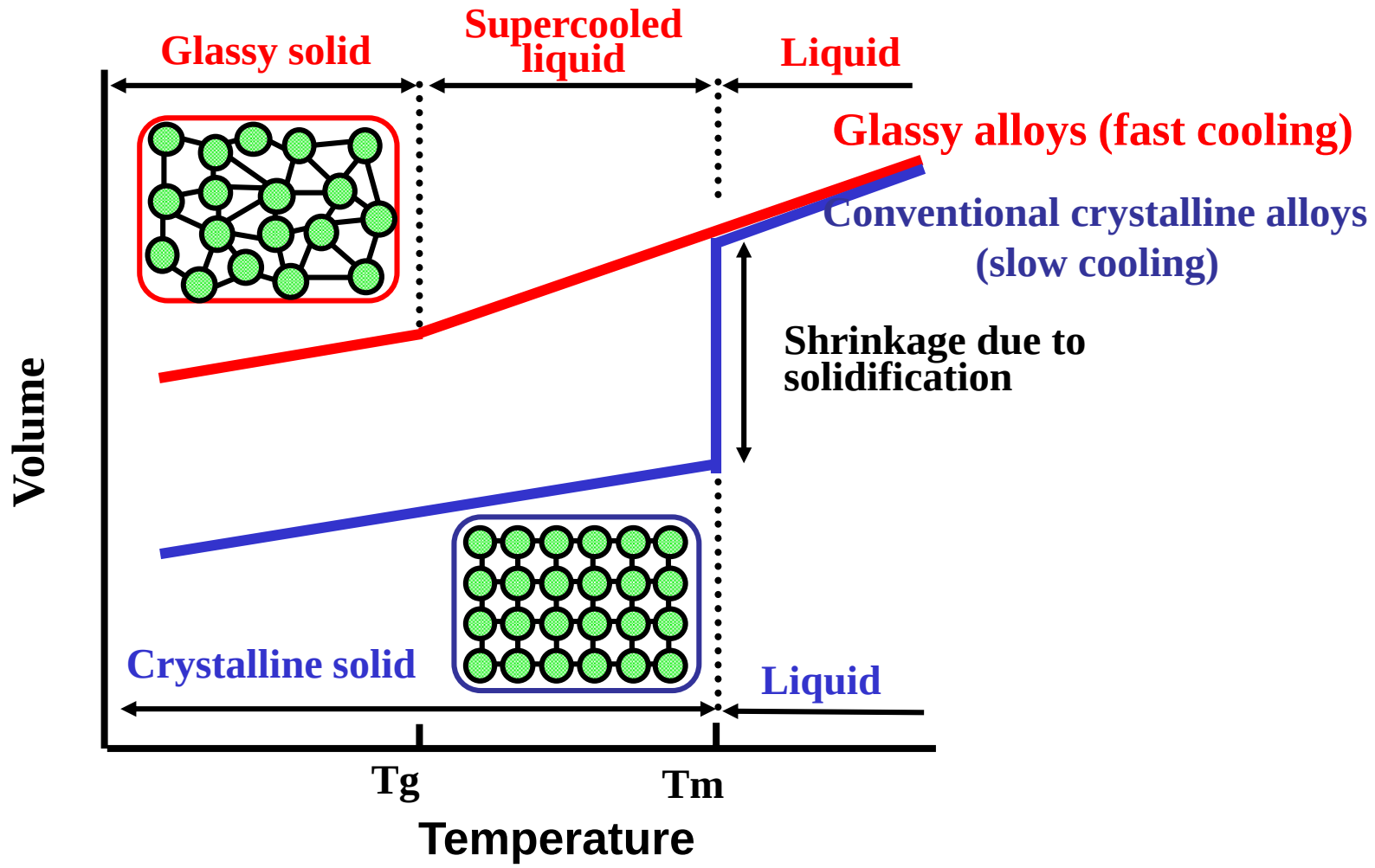

Superior dimensional precison is expected !

Successful synthesis and fabrication of Fe-based BMGs with ingots up to 12 mm diameter

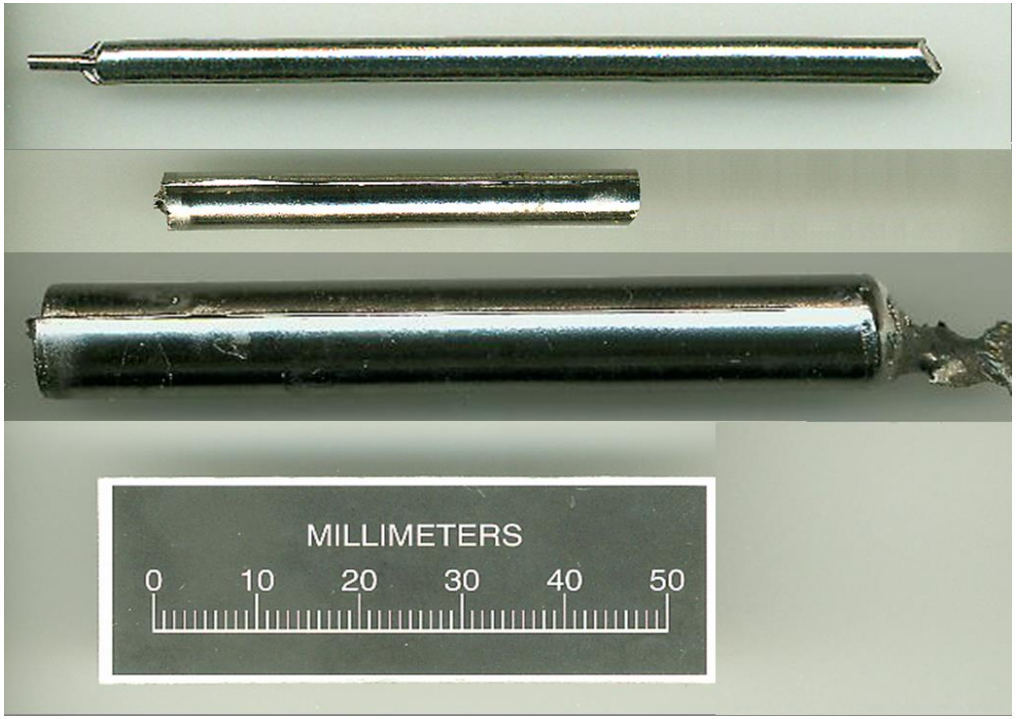

- **The Fe-based BMGs developed at ORNL show unusual mechanical properties (1220 DPH) and magnetic behavior (ferro, para, and anti-ferromagnetic and spin glass for many applications**

Unique properties of BMGs for **structural** uses
(应用: 大块非晶合金的独特性能)

- **Extremely strong and hard in cast conditions:**
  strength >2000 MPa, and hardness: >1000 DPH
  (铸态下超强超硬: 强度: >2000 MPa, 硬度: >1000 DPH)

- **Excellent formability above T_g in the supercooled liquid region: elongation > 10,000%**
  (在过冷液相区间,具有优异的成形性: 延伸率> 10,000%)

- **Liquid-to-liquid phase transformation during solidification, with a minimum shrinkage for super precision dimensional control**
  (凝固过程中,只有液相-过冷液相转变,收缩小,可以精密控制尺寸的 大小)

- **No microstructural roughness due to grain sizes & particles,** suitable for use as submicro- and nanoscale grating materials (不存在因晶粒尺寸或颗粒而引起的微观粗糙度，可作为亚微米和纳米尺度光栅材料)

BMGs show superplatic behavior at the supercooled liquid state

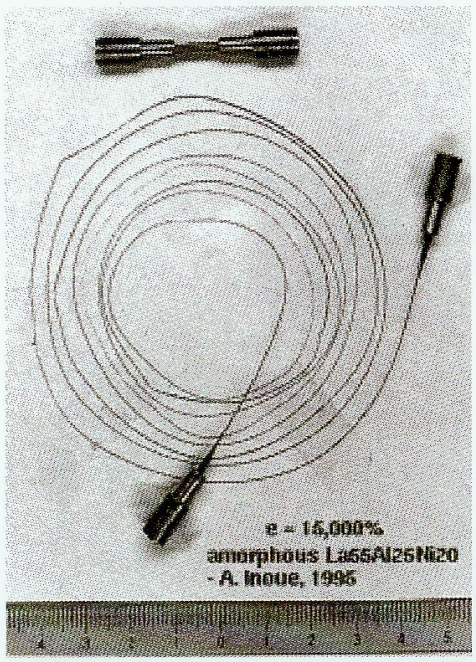

Excellent mechanical formability

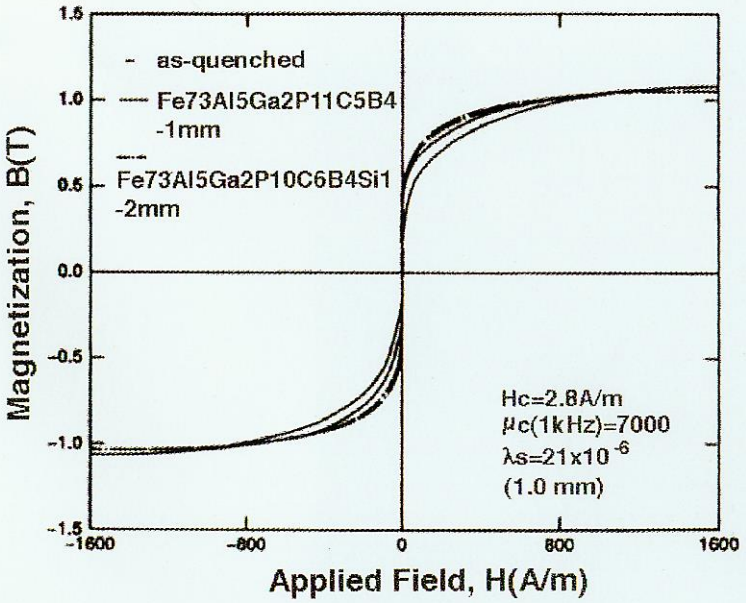

(Inoue *et al*, 1998)

Low energy loss

金属玻璃也可像普通玻璃一样“吹”出来！

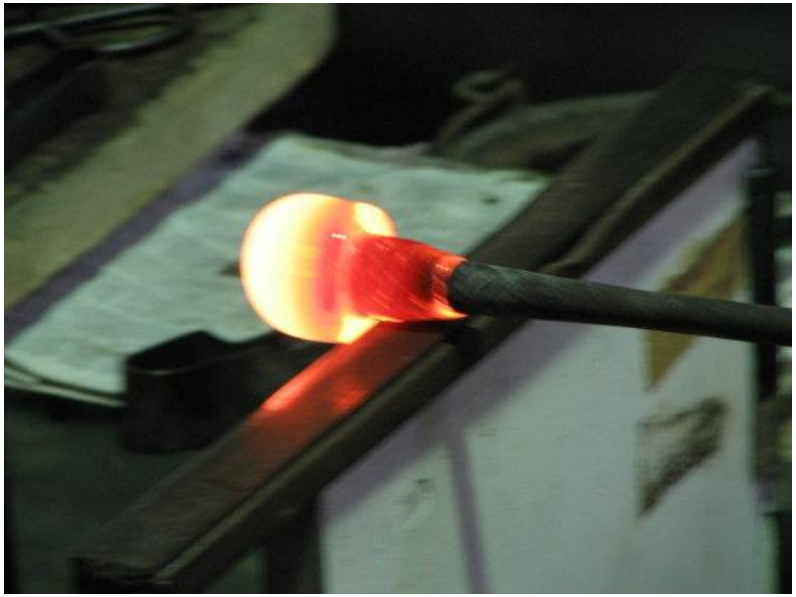

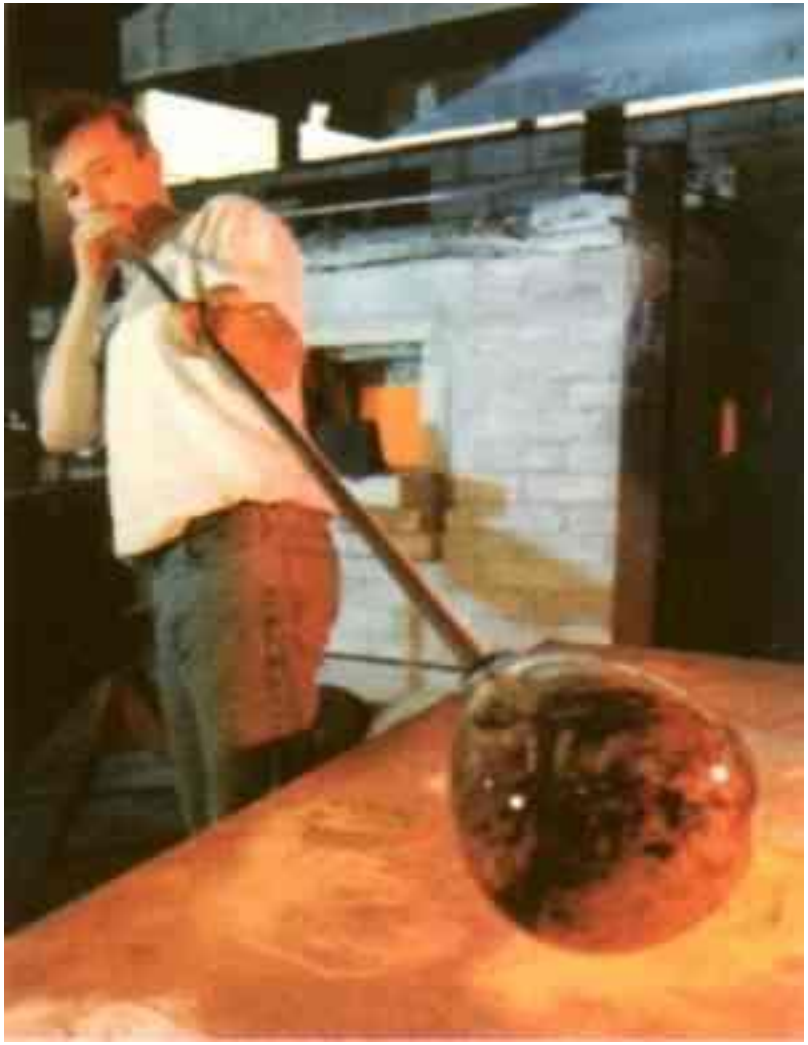

Comparison of stress-strain curves for crystalline & MG/BMG materials (晶态材料和大块非晶合金的变形)

Crystal (晶体)

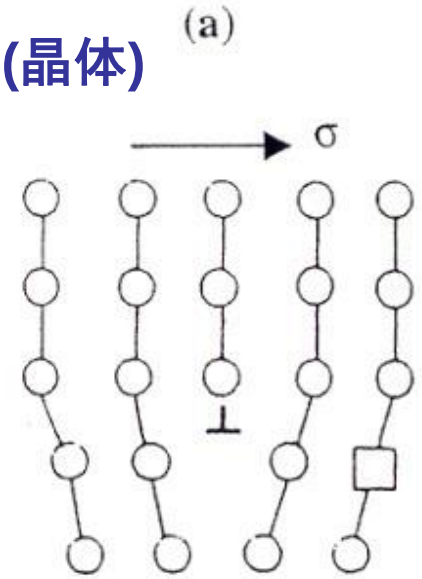

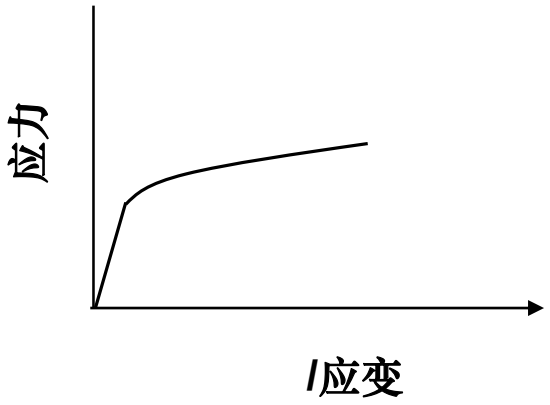

BMG (金属玻璃)

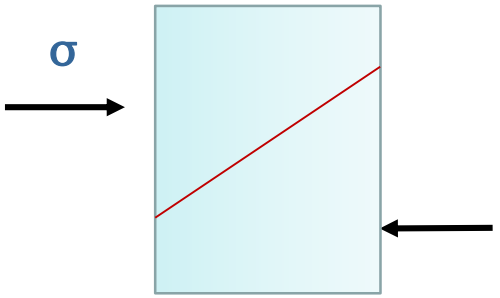

Shear band stable propagation

(剪切带稳定扩展)

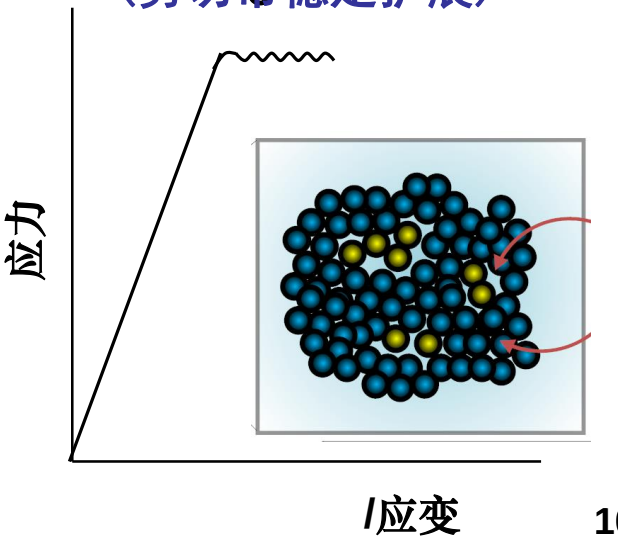

Mechanical property of Ni-based MGs

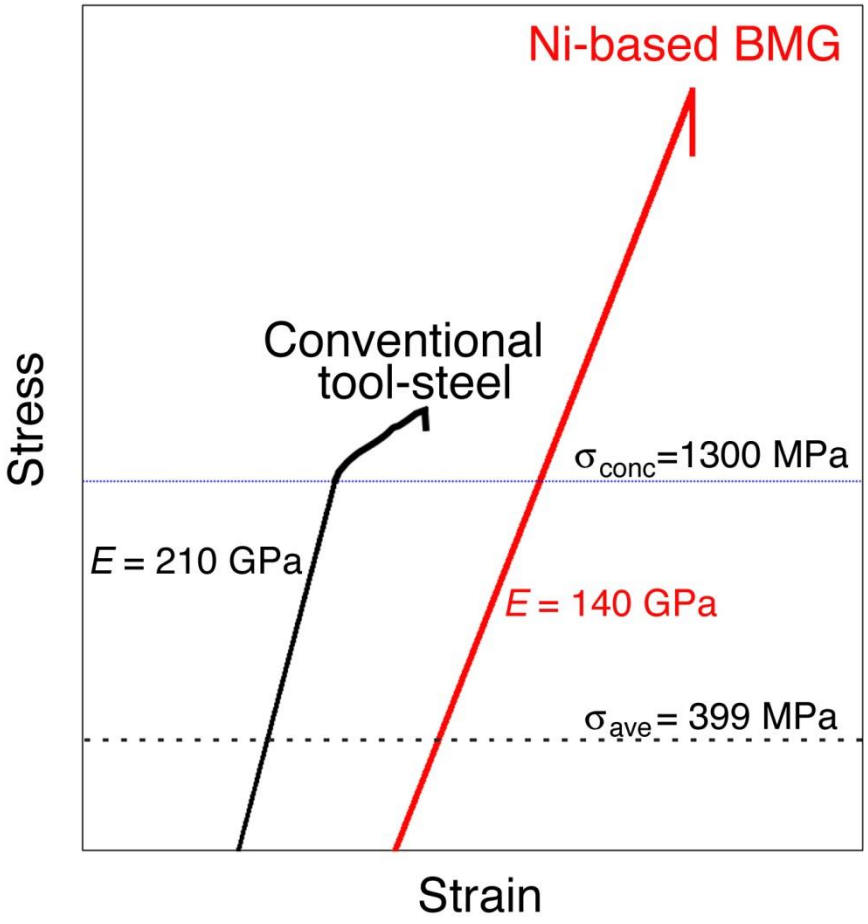

Actual stress at the roughness of the gear surface

↓

above 1300 MPa

Tool-steel

↓

Yielding & work hardening

↓

Abrasive wear

Ni-based BMG

↓

High strength & still elastic

↓

Recoverable !

Superior durability is expected !

金属玻璃的机械性能优势

强度

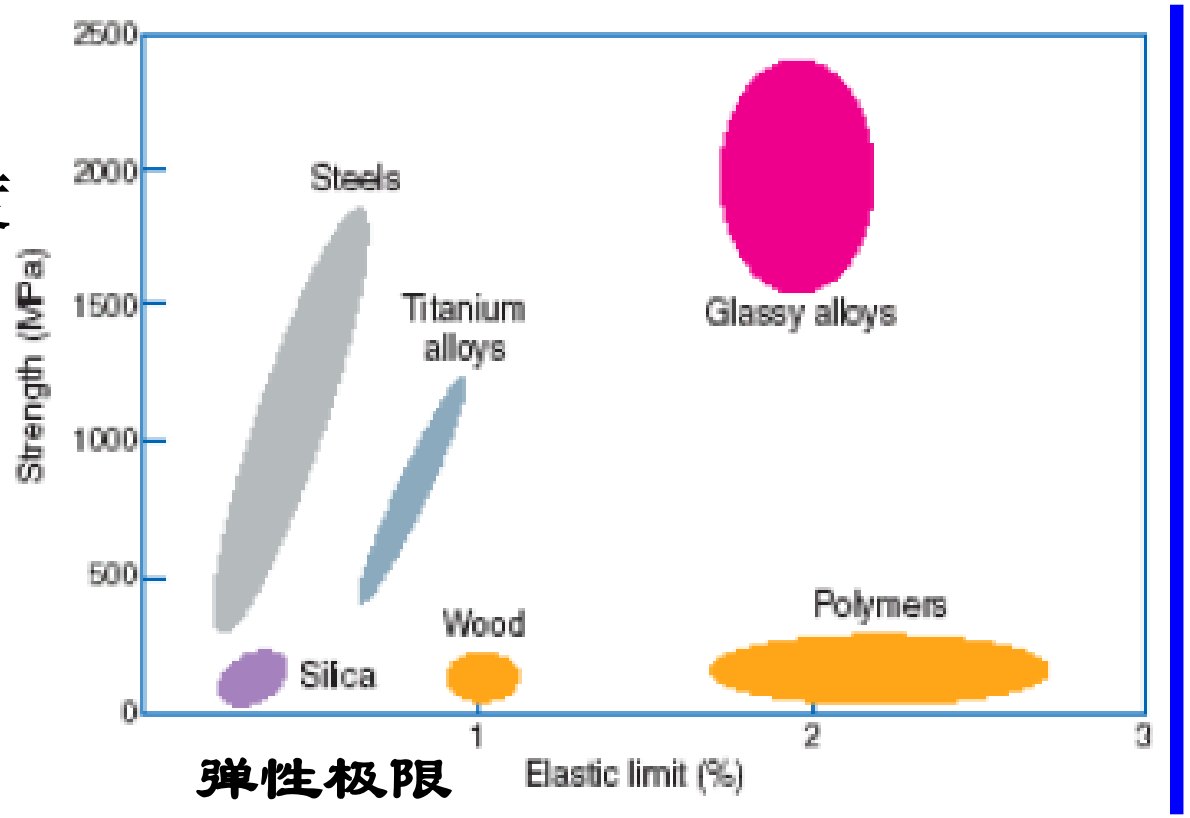

弹性极限

- 室温下金属玻璃具有橡胶般的弹性极限，但比金属的强度高出橡胶数倍

Structural Applications/結構应用

Vitreloy 1: Density=6.0 g/cm^3, yield strength=1.9 GPa, elastic limit=2%

Thermal Spray Coating
High hardness; excellent corrosion and wear resistance

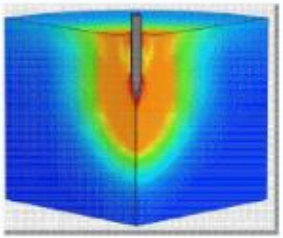

Penetration
Self-sharpening; shear banding

Defense and Space Exploration
High specific strength

Packaging and Consumer Products
Light weight; high strength; excellent wear resistance

Sporting & Automotive Products
Light weight; high strength; high elastic strain

•From Liquidmetal Technologies

优异的过冷液态精密成形性，可制备复杂形状的部件

日常生活用品

Micro-gear parts made of glassy alloys

非晶合金用于制备微齿轮部件

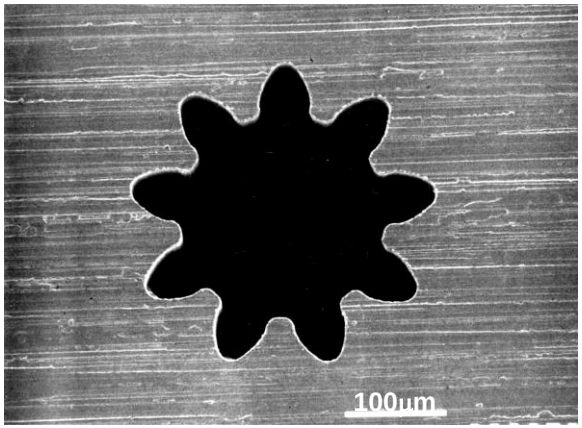

Super-precision gear mold 精密磨具

Only one casting process

一次铸造成型

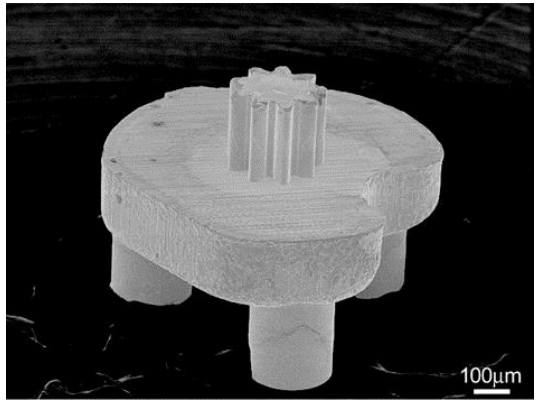

Super-precision gear parts 精密齿轮部件

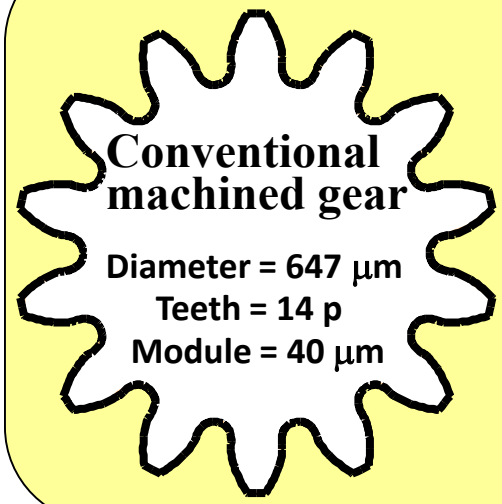

最新研制齿轮

Newly developed gear

Diameter = 288 μm

Teeth = 9 p

Module = 25 μm

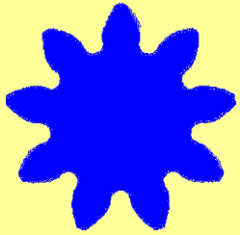

Human hair 头发

（d= 80 μm ）

Nishiyama et al, 2005

Expected applications of micromotors
微马达预期应用领域

Advanced medical Equipments
先进的医疗设备

Precision optics
精密光学

- Lenz drive
- Small camera

Micro-industries
微工业

- Micro-robots
- Measurements & Analytic equipments

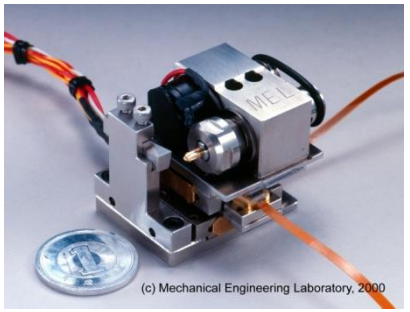

Micro-factory
微工厂

- Micro-lathe

Capsule endoscope
胶囊式内窥镜

Micro-pump 微观泵

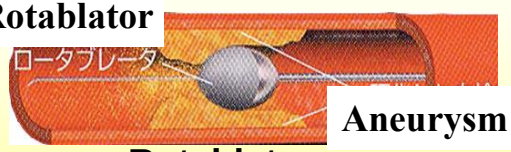

Rotablator
旋磨管

Catheter for thrombus removal
去除血栓的导管

Heterogeneous structural features in MGs as revealed by DAFM (dynamic atom force microscopy)

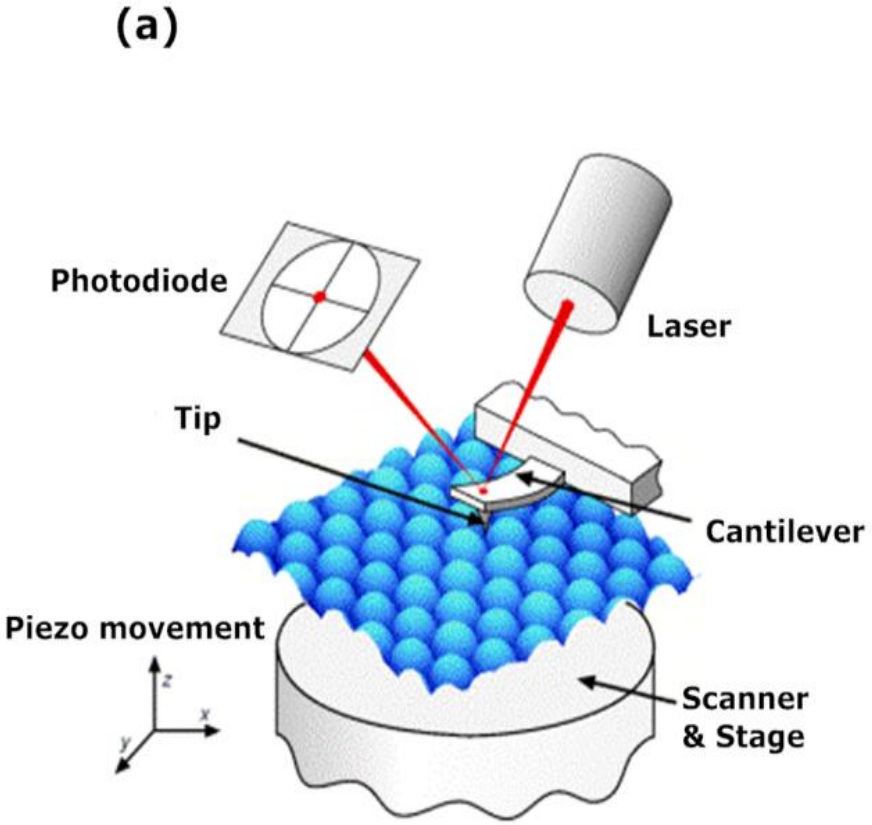

Schematic illustration of DAFM

(MW Chen et al., PRL 2011;
Yang et al., Acta Mater. 2012)

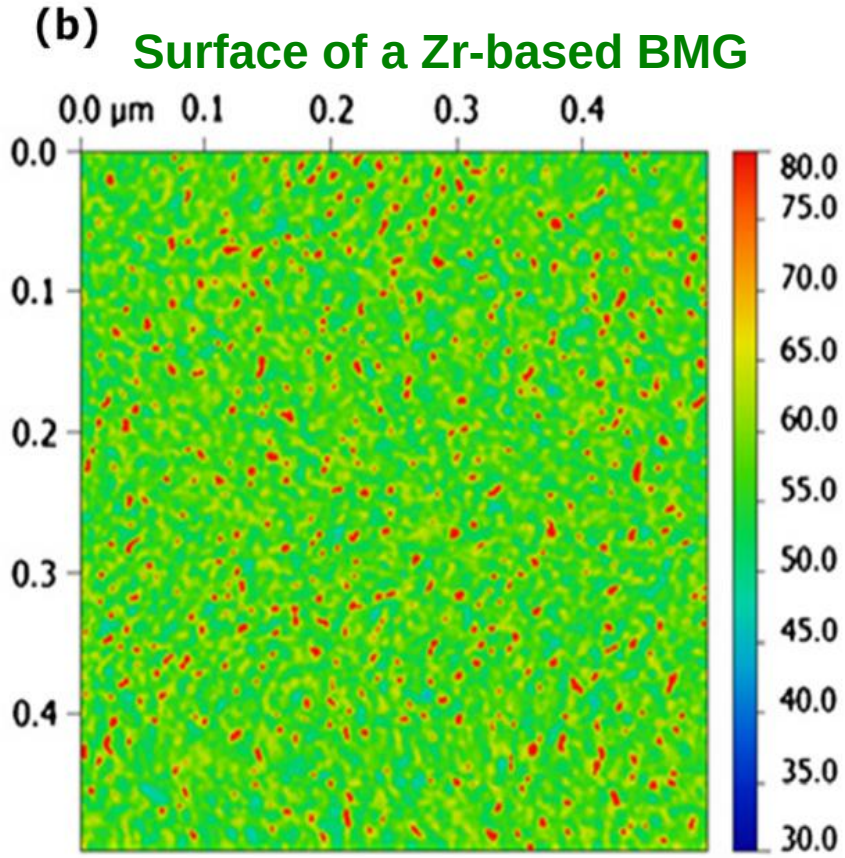

Nano-scale structural contrasts from energy dissipation obtained from phase-shift measurements

Evolution of LLZs and development of yielding and shear banding

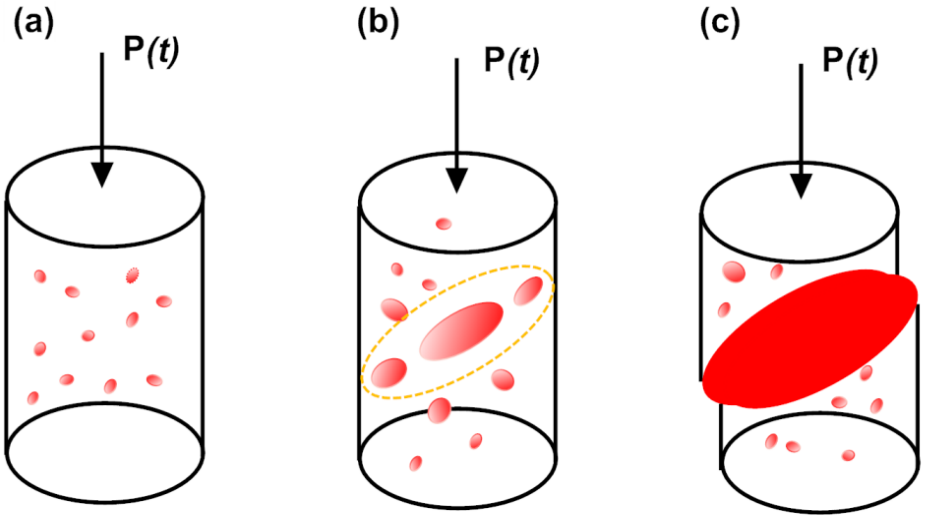

a) Under a stress, liquid-like zones are activated and start to grow up

b) Up to a critical point, LLZs would become elongated substantially along the direction of a shear plane, creating an instability condition

c) The liquid-like layer is formed and proceeds viscously by sliding along the shear plane

Comparison of shear bandings in BMGs with faults and earthquake in granular materials

BMG:
a major shear band

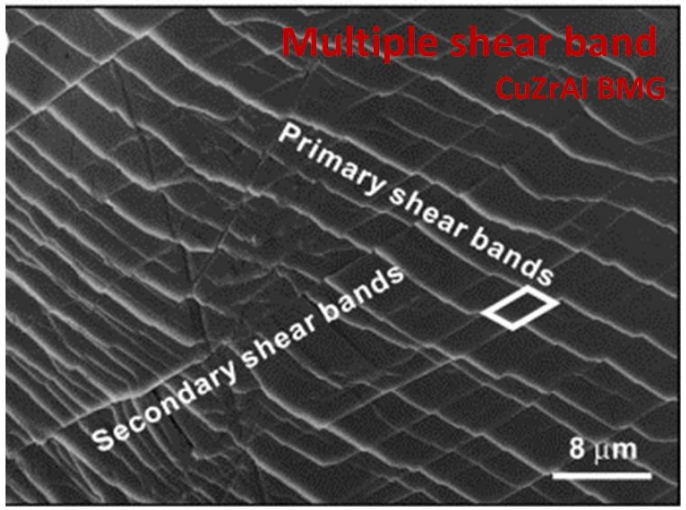

BMG:
multiple shear bands on a BMG surface

Granular material:
fault

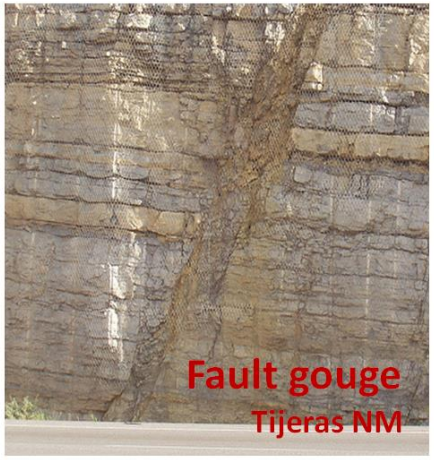

Granular material:
earthquake

- **Phenomenologically, the deformation dynamics in these amorphous materials may be considered to be similar**

Shear band developed in a layere

Sketch to show applied stress, atomic structures, viscosity & liquid-like-zone evolution in MGs

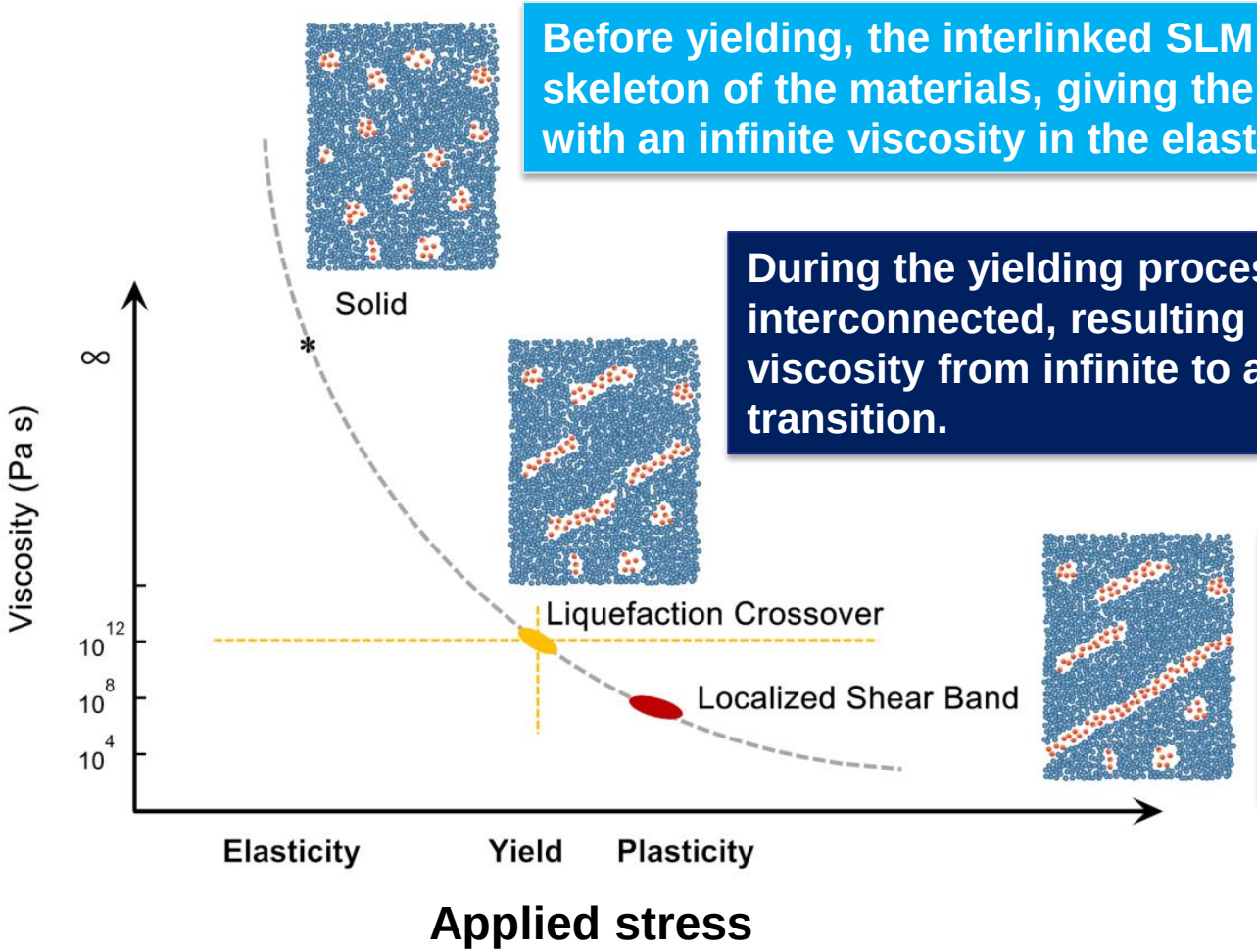

Before yielding, the interlinked SLM constitutes the skeleton of the materials, giving the solid performance with an infinite viscosity in the elastic range.

During the yielding process, stress makes the LLZs interconnected, resulting in dropping the flow viscosity from infinite to a value at level of glass transition.

To a percolation point, instability occurs and released energy softens a band region to a supercooled liquid state

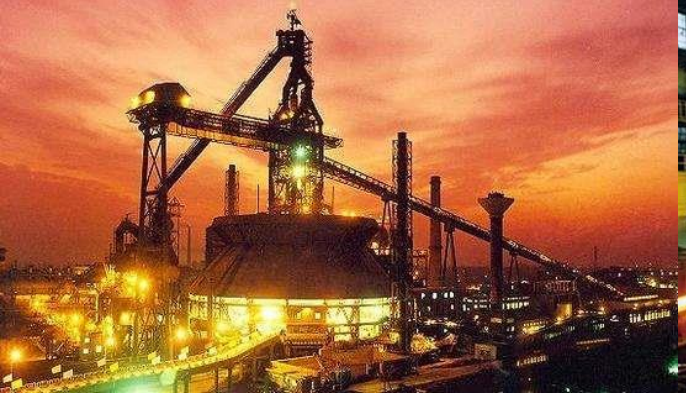

新一代铁基非晶軟磁合金的研发

刘锦川
大学杰出教授
理工学院
香港城市大学

生產局2018-4-12

Introduction of metallic glasses (MGs)

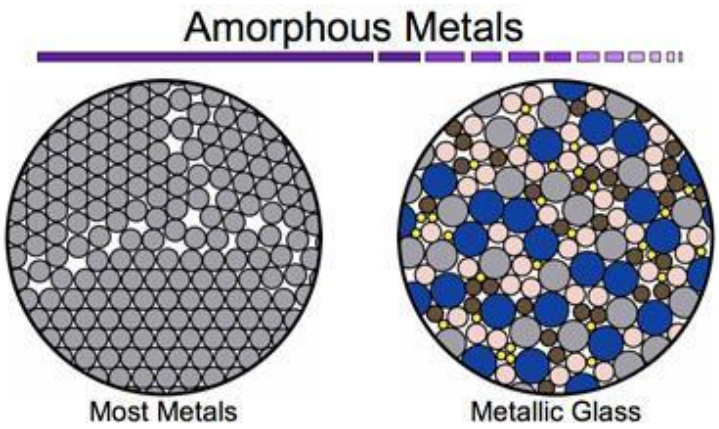

Unique properties:

- **Mechanic**
- **Magnetic: Fe-based MGs**
- **Chemical**
- **etc.**

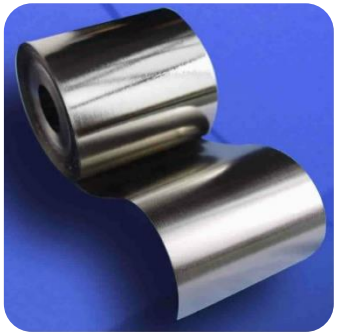

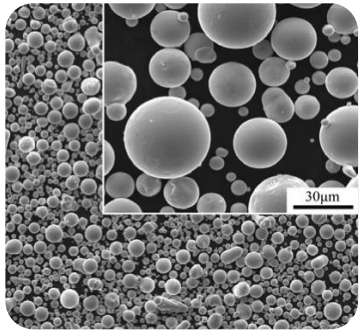

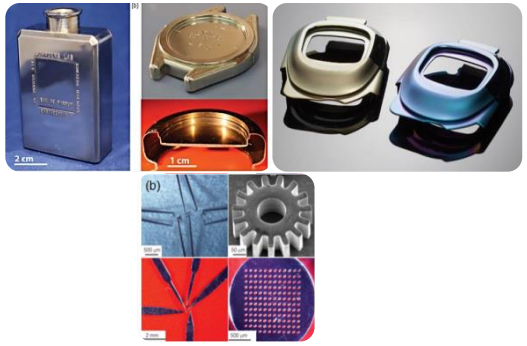

In general, the smaller the MG size, the better is its material quality and properties

- **Amorphicity**
- **Productivity**
- **Properties**
- **(Ductility, etc.)**

各种铁基软磁材料的微观结构与磁性能之关联

Fe-based Crystalline

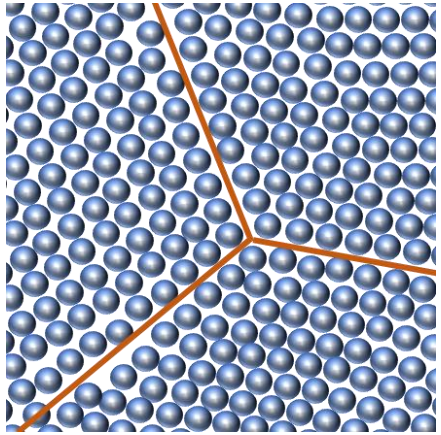

Bs 高, 磁導率低

Fe-based Amorphous

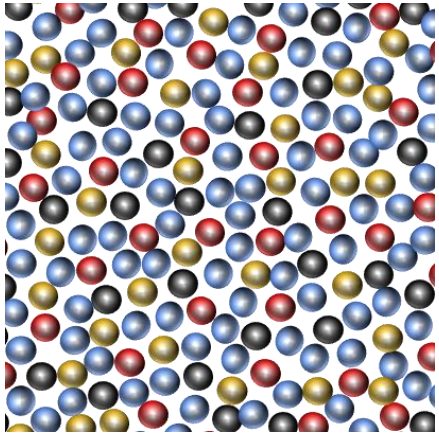

Bs 低, 磁導率高

Nanocrystalline

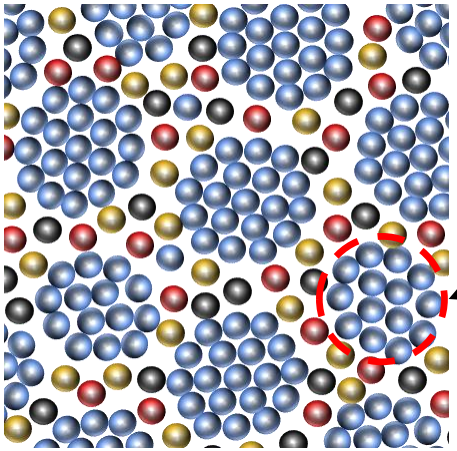

Magnetically coupled

Nano size (<<100 nm)

Bs and 磁導率?

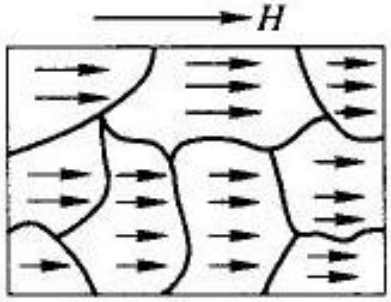

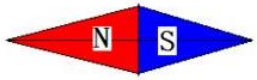

Soft magnet:
move & rotate easily

各种磁性材料性能之比較

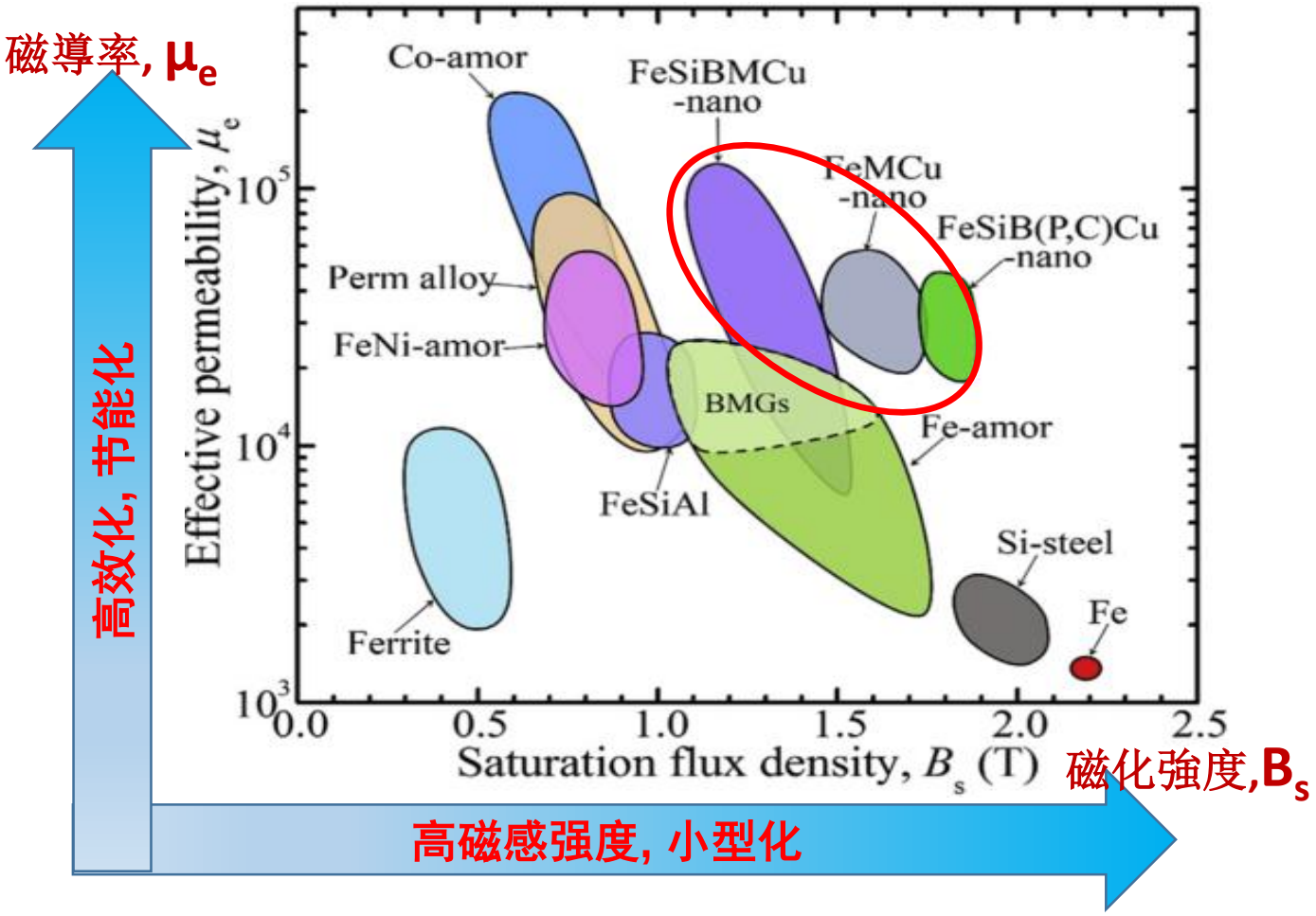

- 開发新一代鉄基磁性材料

Potential energy saving by using Fe-based MG ribbons to replace Si steels for energy applications

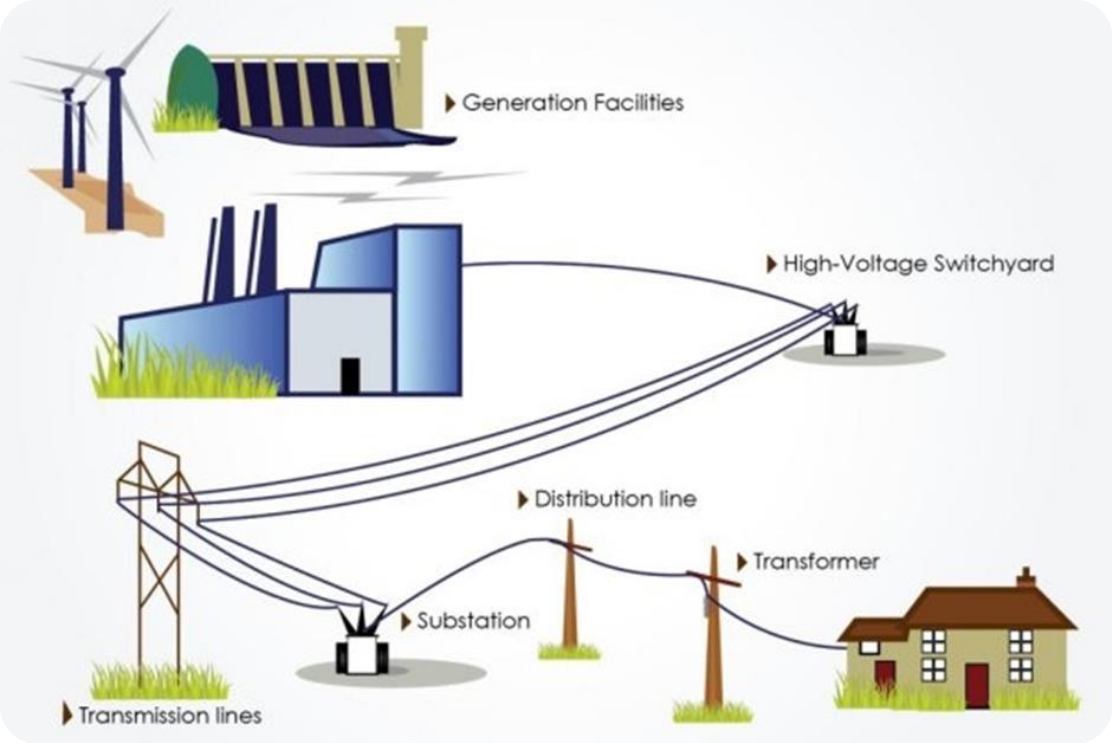

Electrical transformers

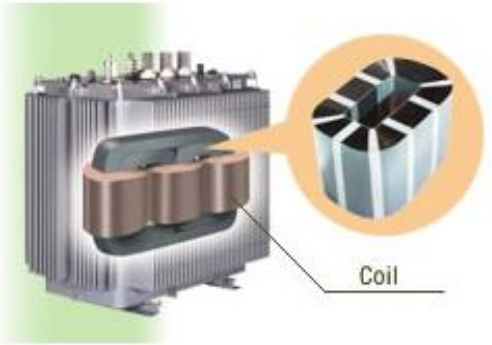

Motors

- **Total energy saving by using Fe-based MGs to substitute for Si steels**
  Transformers: ~2.5% Electric motors: ~6%
- **Total electrical energy saving: ~8% (440 billion kW, 4400亿千瓦 in China)**
  (due to the high permeability of MGs**)**

非晶软磁合金的节能减排效果：与硅钢对比

少能耗

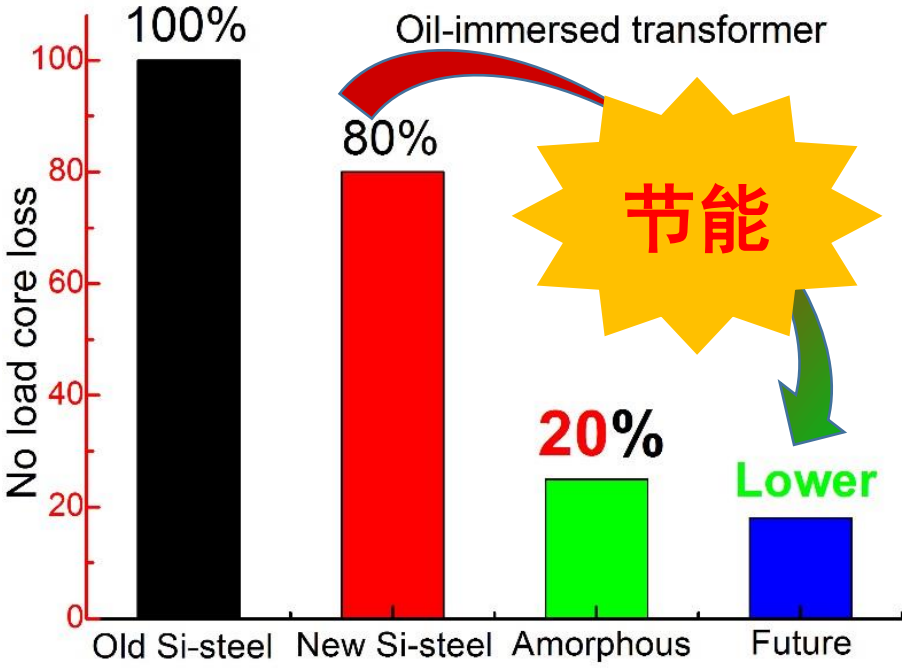

高功效

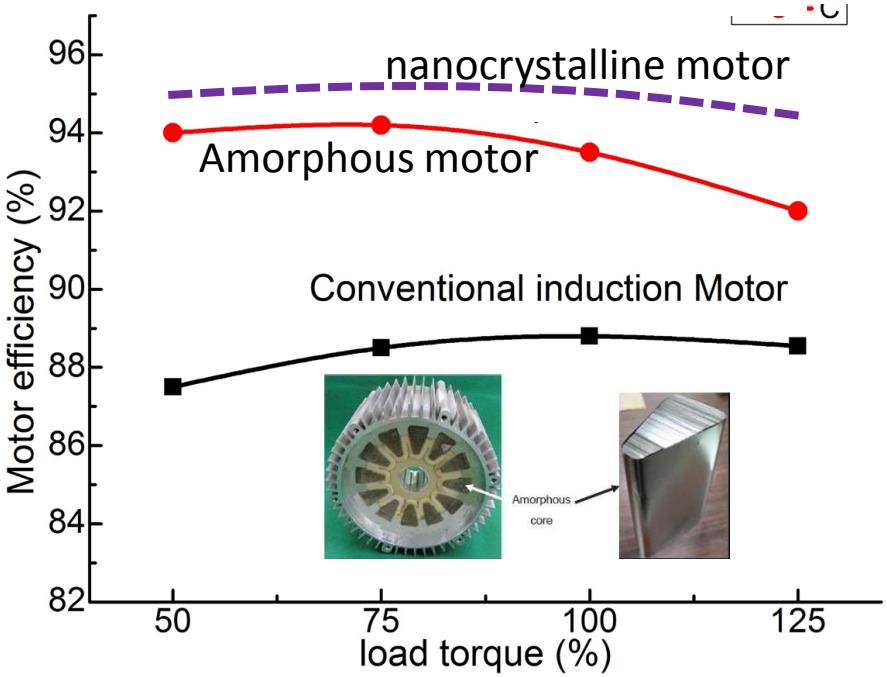

- 替代硅钢的节能效果：

  变压器: ~2.5%　　电机: ~6%

- 总节能效果:~8% (4400亿千瓦)

国家十三五計劃 (2015年~2020年)

- 国家能源局发布的《配电网建设改造行动计划》，提出“十三五”期间, 电网改造累计投资不低于1.7万亿元，年投资不低于3,000亿元

- 国家电工钢协会统计数据显示，中国每年生产和使用电工钢超过1千万吨，材料费用超过1000亿，相关电力电子产品市场远超过1万亿

非晶合金带材和硅钢带材的生产工艺对比

非晶带材生产线：高效节能

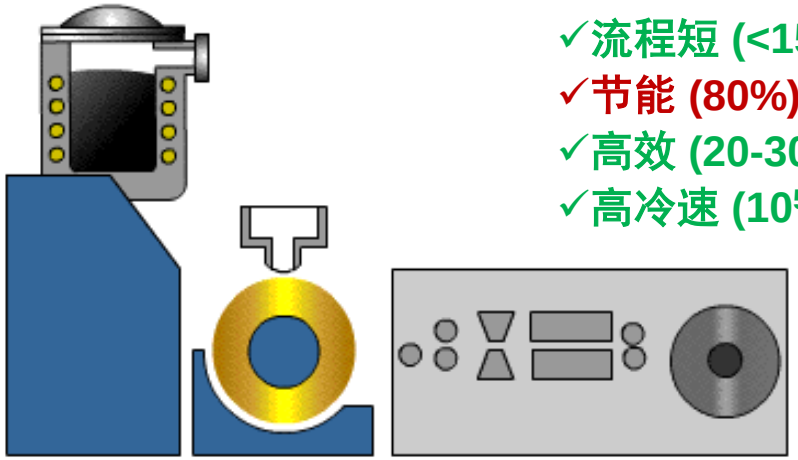

✓流程短 (<15 m)
✓节能 (80%)
✓高效 (20-30 m/s)
✓高冷速 (10^5 K/s)

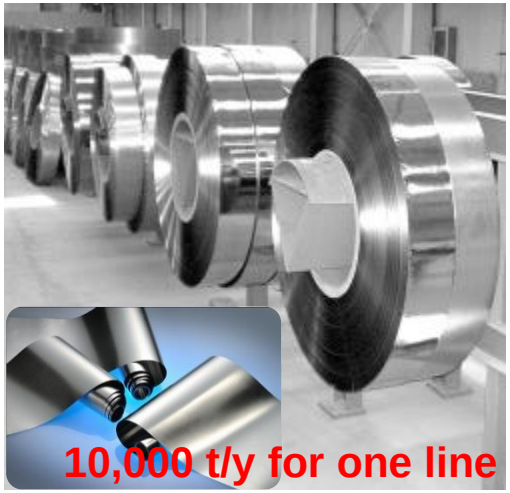

硅钢生产线：1-2 km

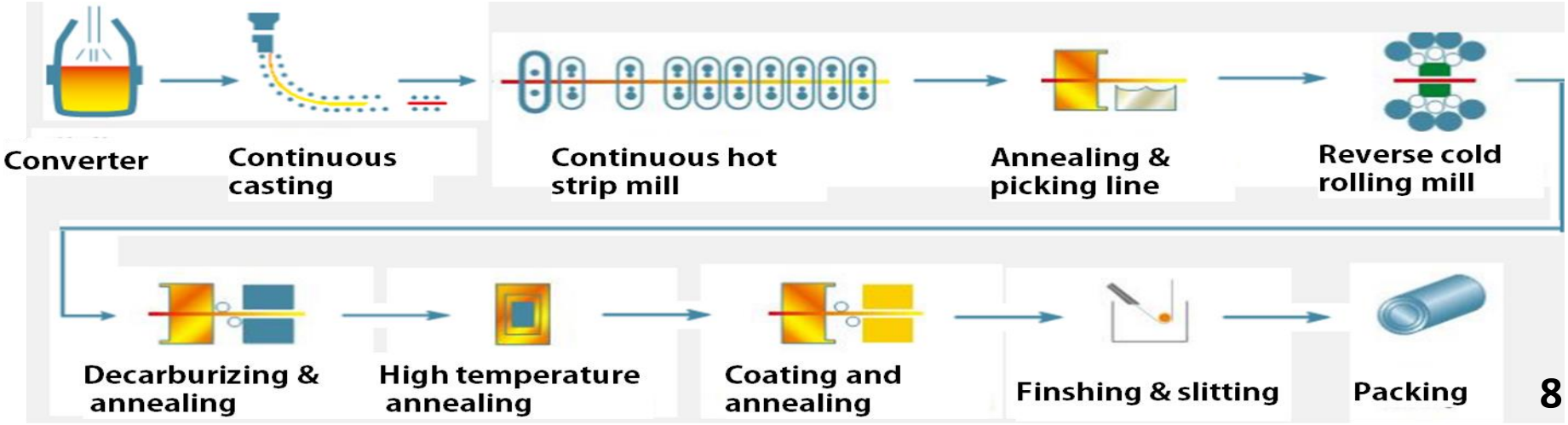

目前商业化非晶合金存在的问题一

性能对比: Bs低

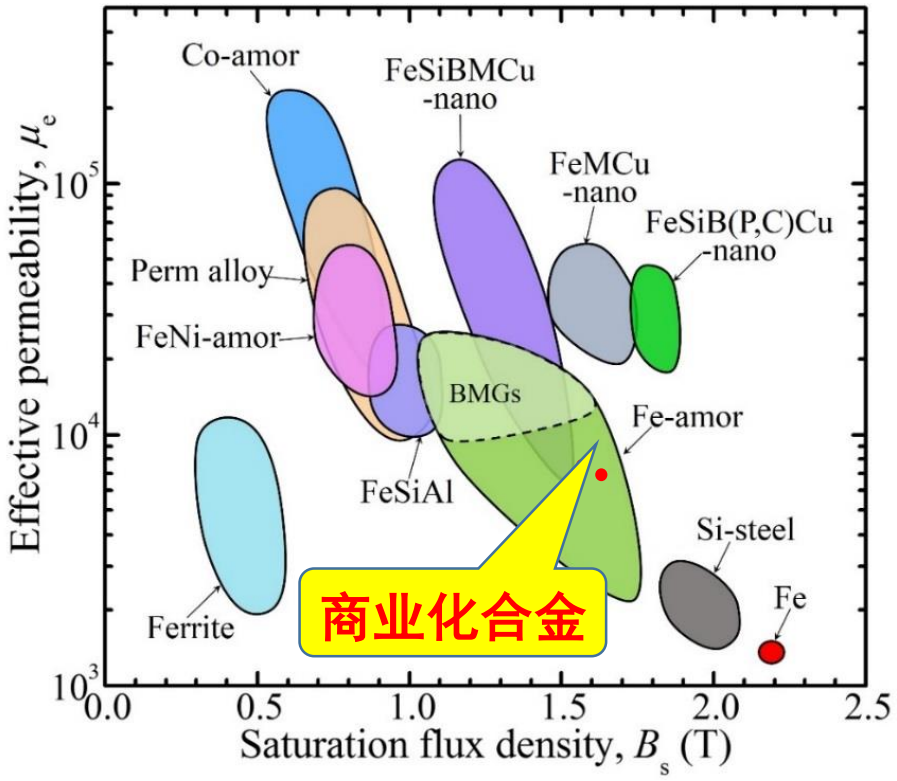

存在的问题

Bs低 ⟹ 体积大，噪音大

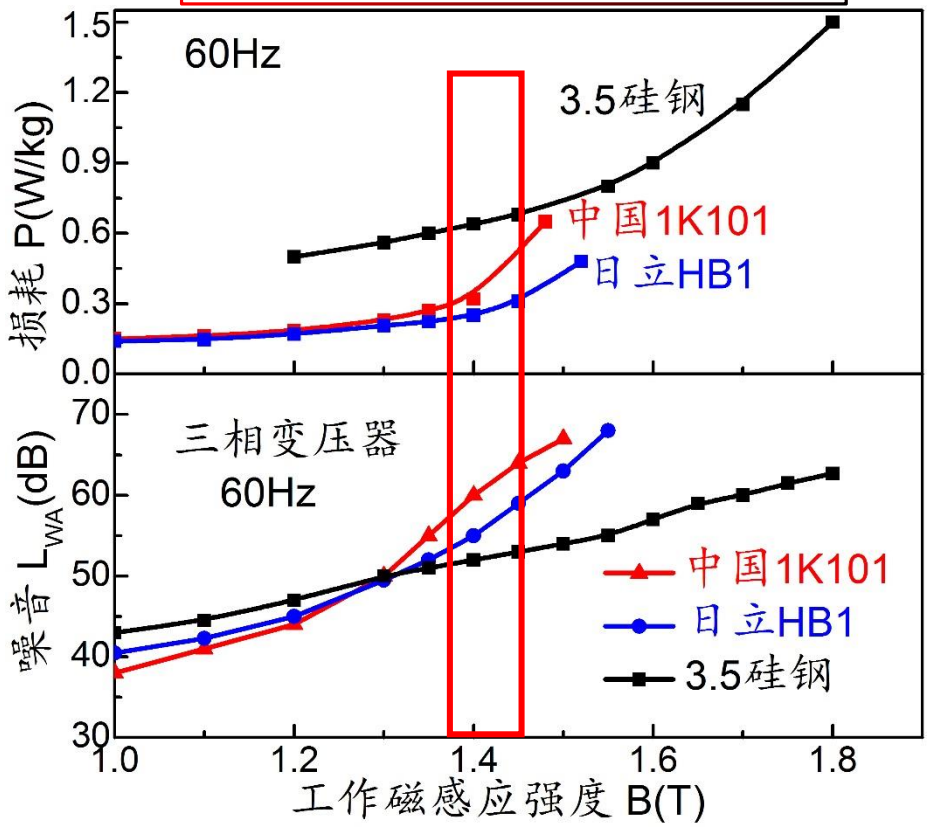

- 亟需开发优良的高Bs非晶和納米晶合金

目前商业化非晶合金存在的问题二

热处理后的脆性

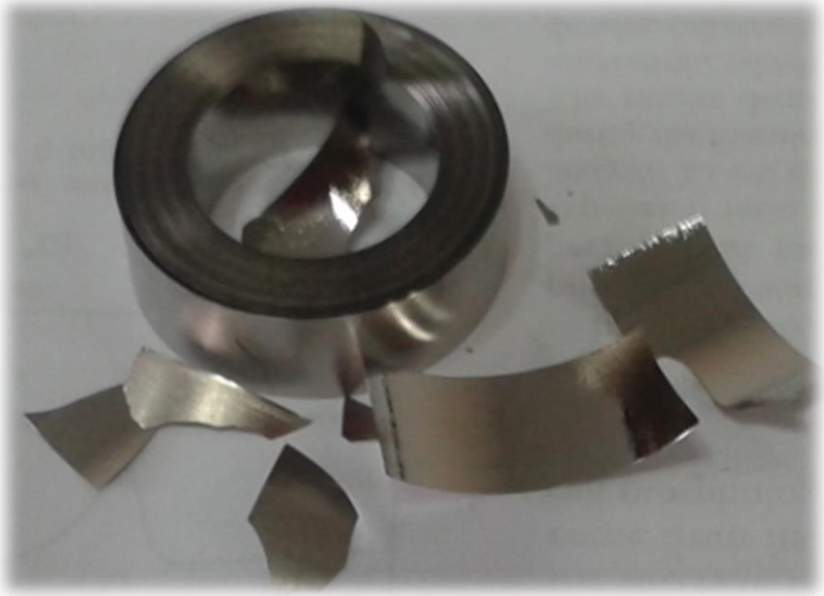

韧 ⟶ 脆

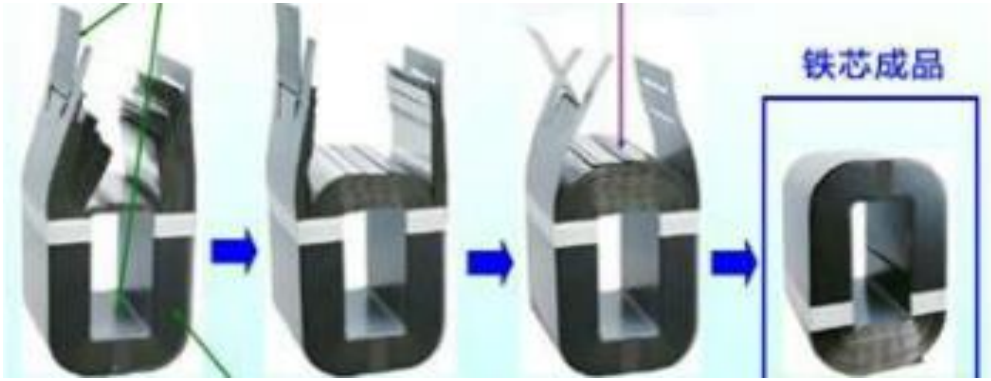

- 降低**加工效率**和**器件安全性**

开发高Bs非晶合金需要增加 glass forming ability (GFA)

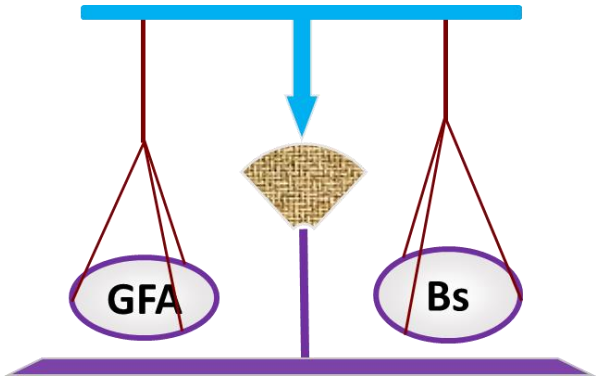

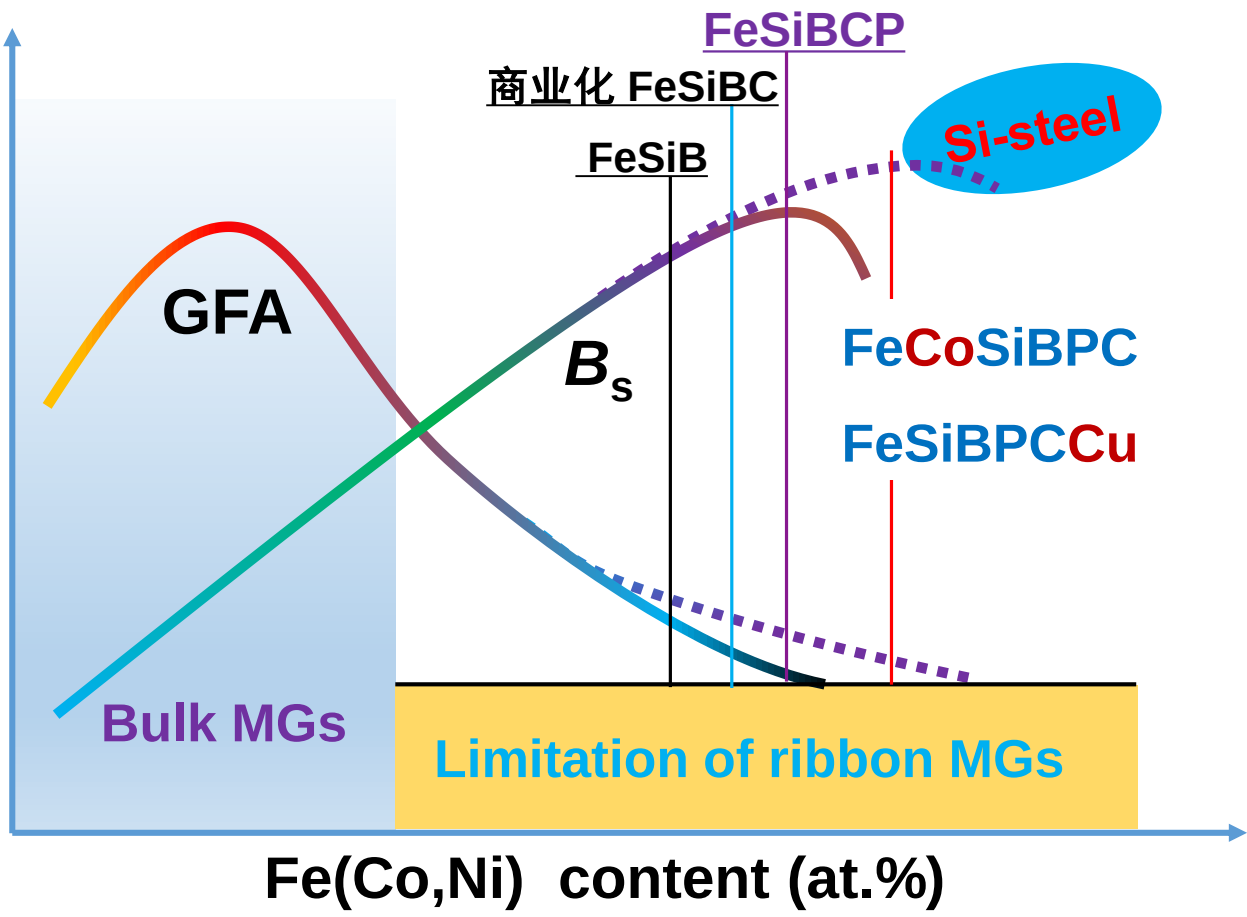

- ✓ 优化非晶形成元素含量，突破Fe含量极限，
- ✓ 添加Co元素，利用Fe和Co原子间的强力交换作用增加B_s
- ✓ 添加Cu 可纳米晶化，析出细密的α-Fe晶粒

1. 研发非晶合金中Fe含量与高硅钢中Fe含量的比较

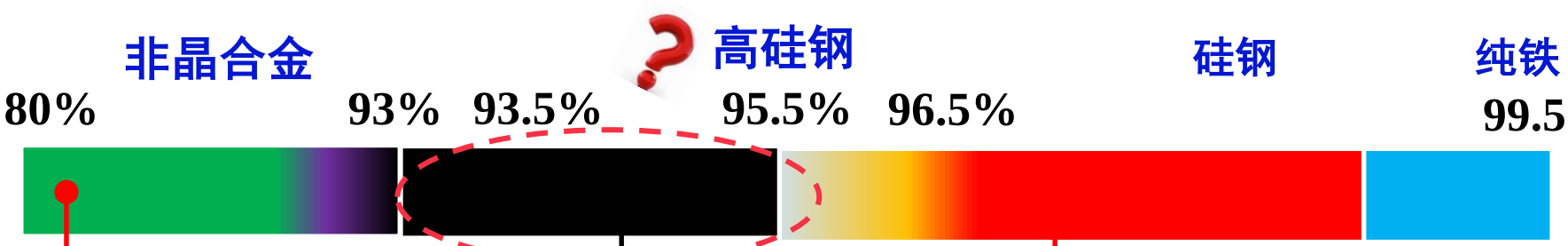

- ✓生产工艺简单
- ✓高磁导率
- ✓低矫顽力
- ✓高电阻率
- ✓低材料加工成本

- ✓ 高电阻率
- ✓ 低磁致伸缩系数
- ✓ 优异的软磁性能
- ✓ 低铁损
- ✓ 优良的频率特性

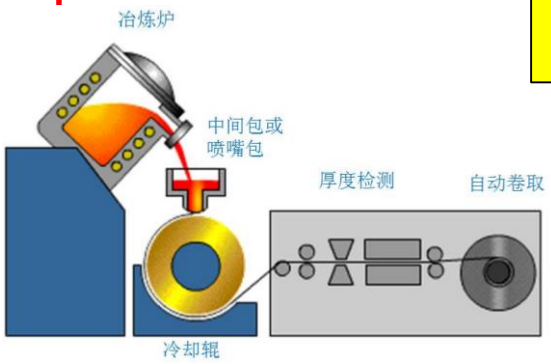

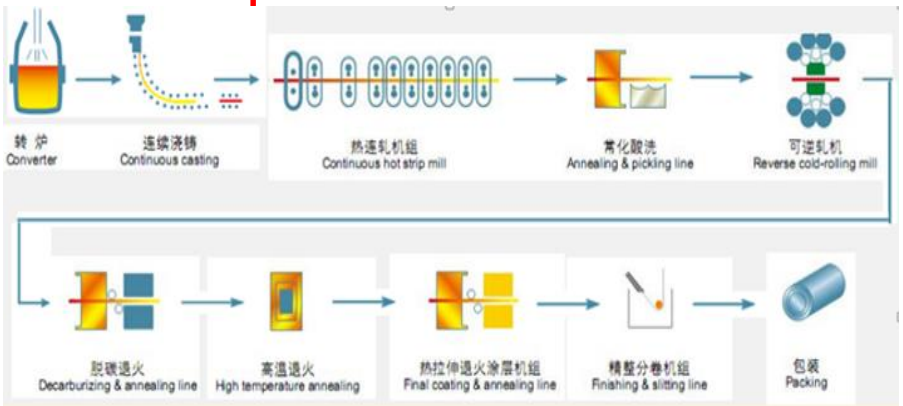

1. 目前新非晶合金中Fe的含量已接近高硅钢中Fe含量

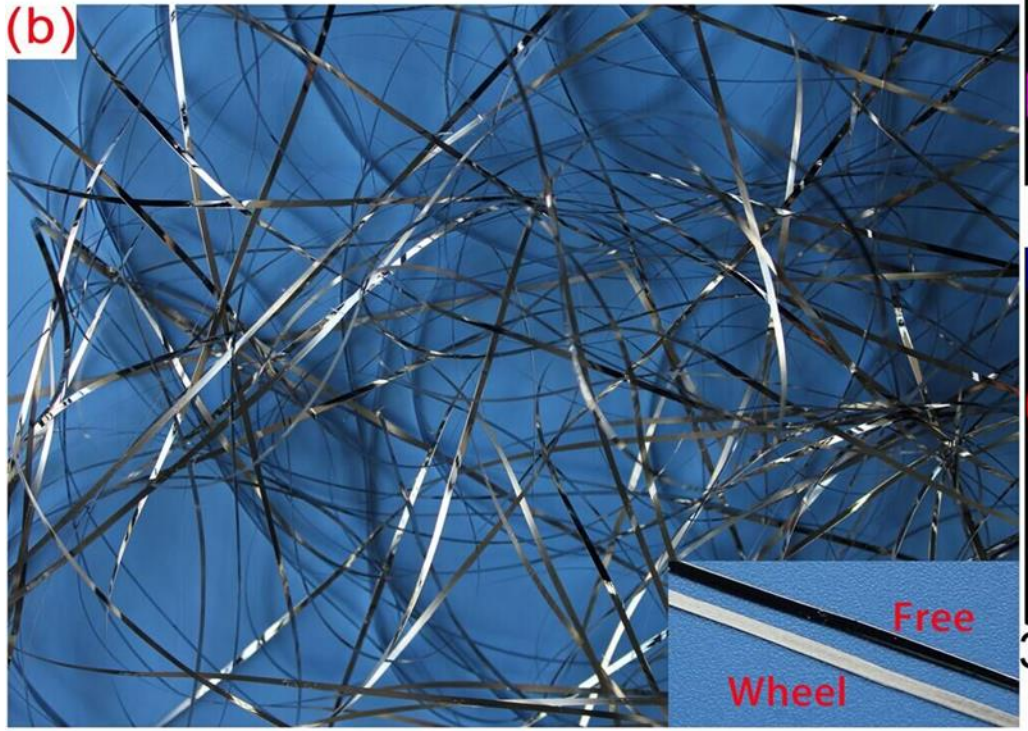

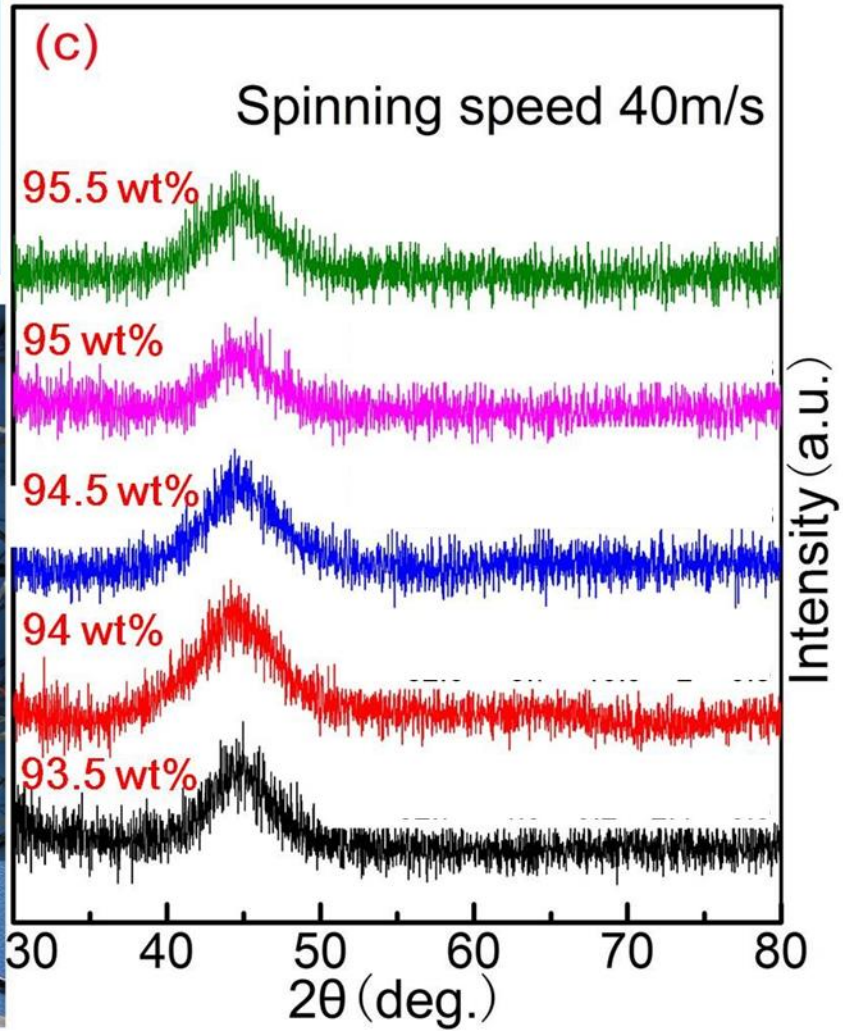

- 新非晶合金有优异的韧性和带材表面质量

1. 新高Fe非晶合金与高硅钢有相似的Fe含量

磁性能（磁导率）

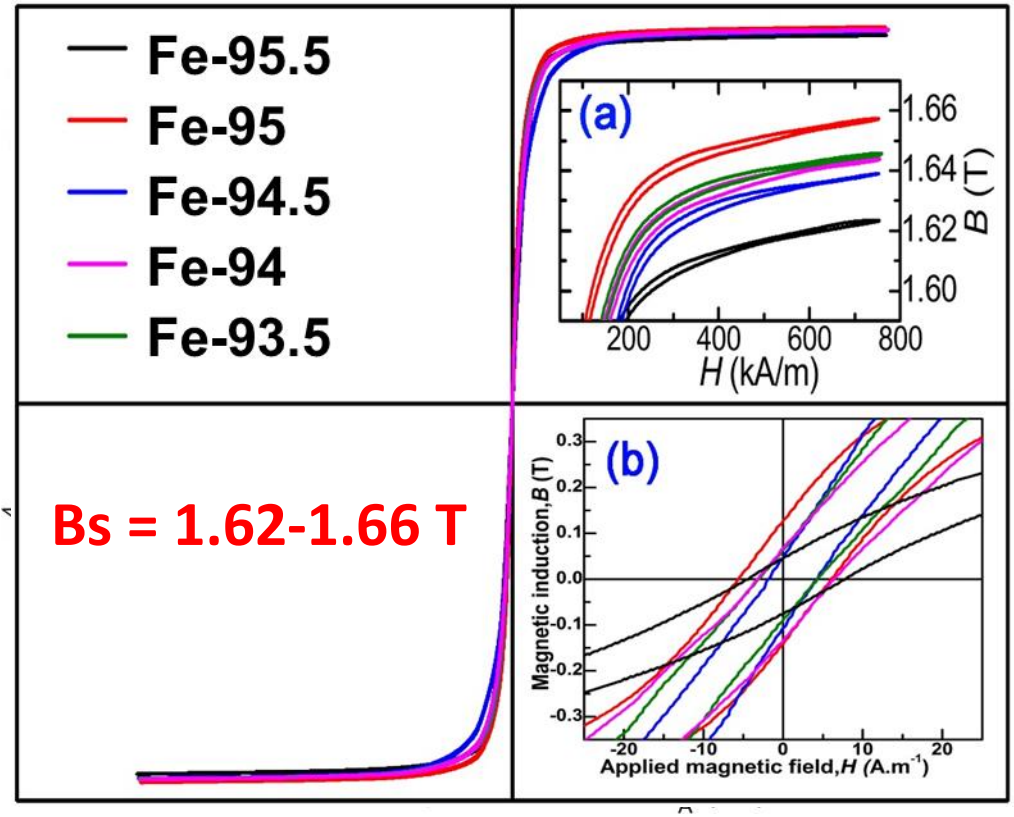

Bs = 1.62-1.66 T

韧性

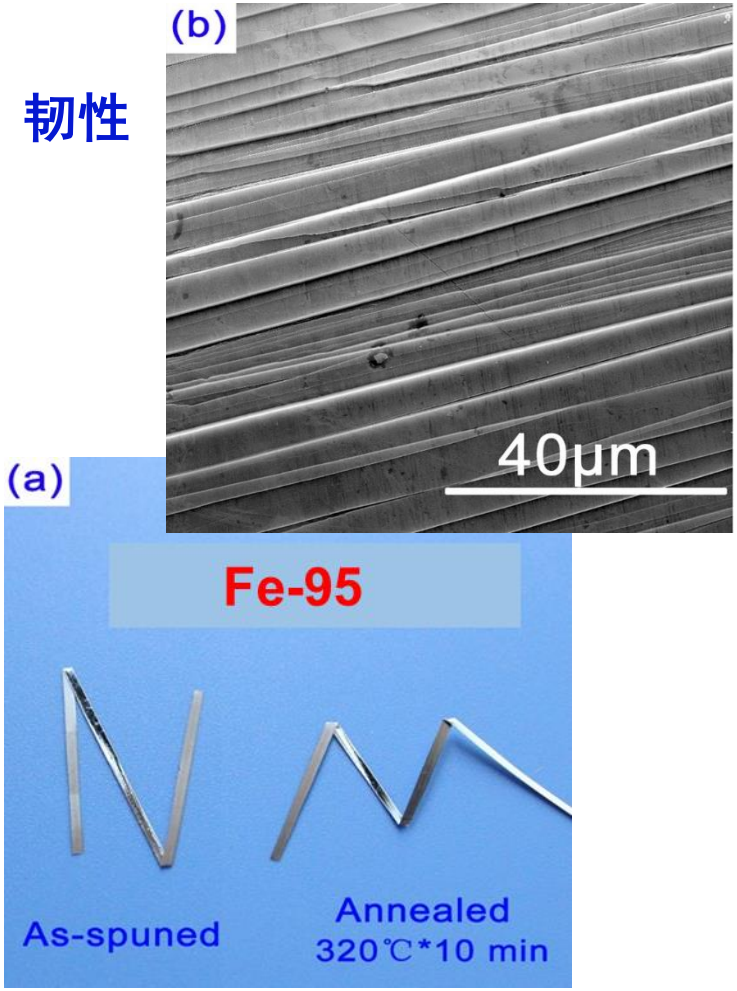

- 低热处理温度后磁性能优异，脆性问题被成功克服

2. 开发接近硅钢Bs的新非晶合金：需要加Co和特殊热处理

添加Co元素：

$Fe_{83-x}Co_xBPSiC$

新型热处理工艺：

Bs = 1.76 T

(*Hc* < 2 A/m)

μe = 13,000

AQ: As Quenched

NA: Normal Annealed

SA: Specially Annealed

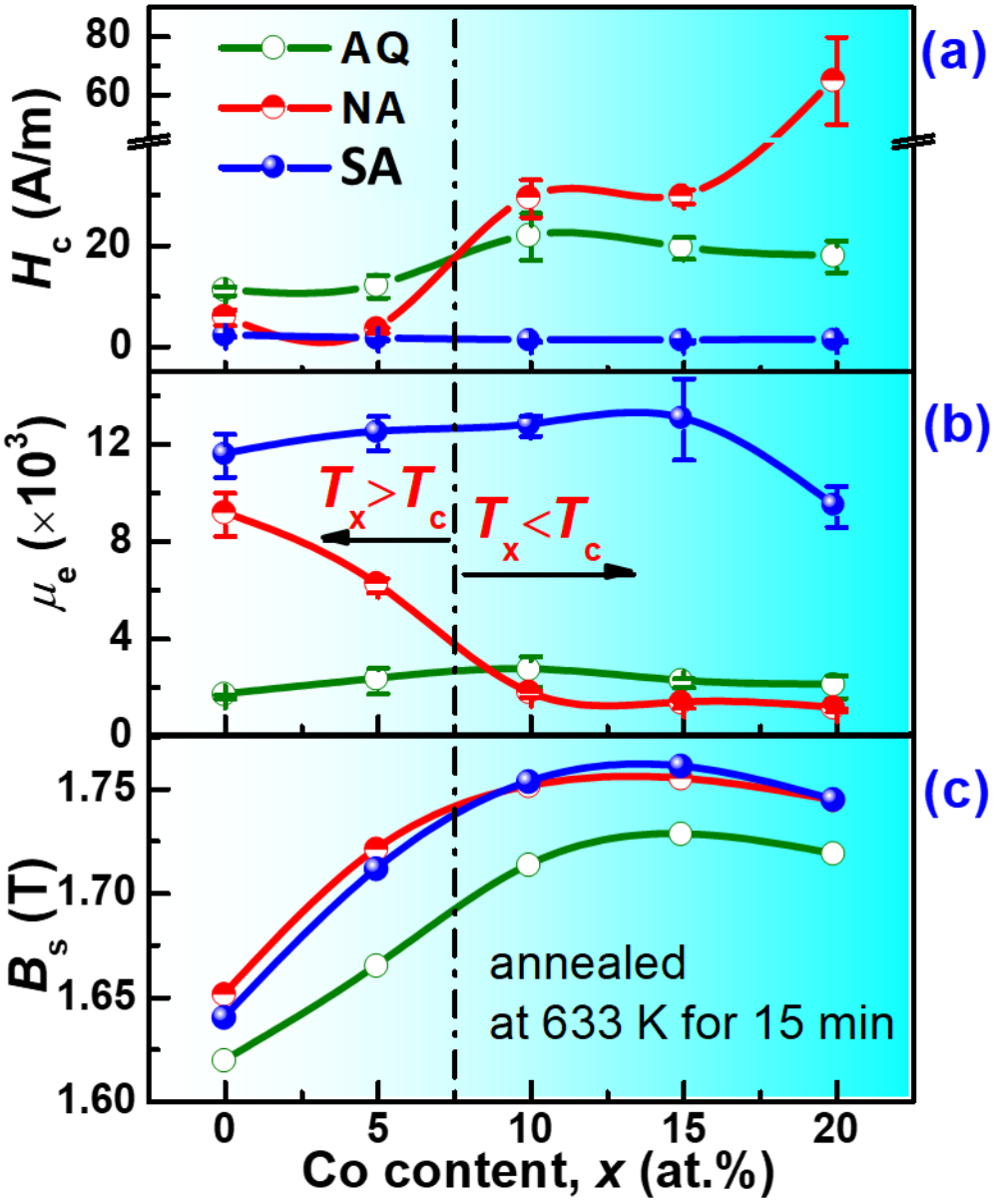

3. 开发高Bs低成本纳米晶合金：加Cu

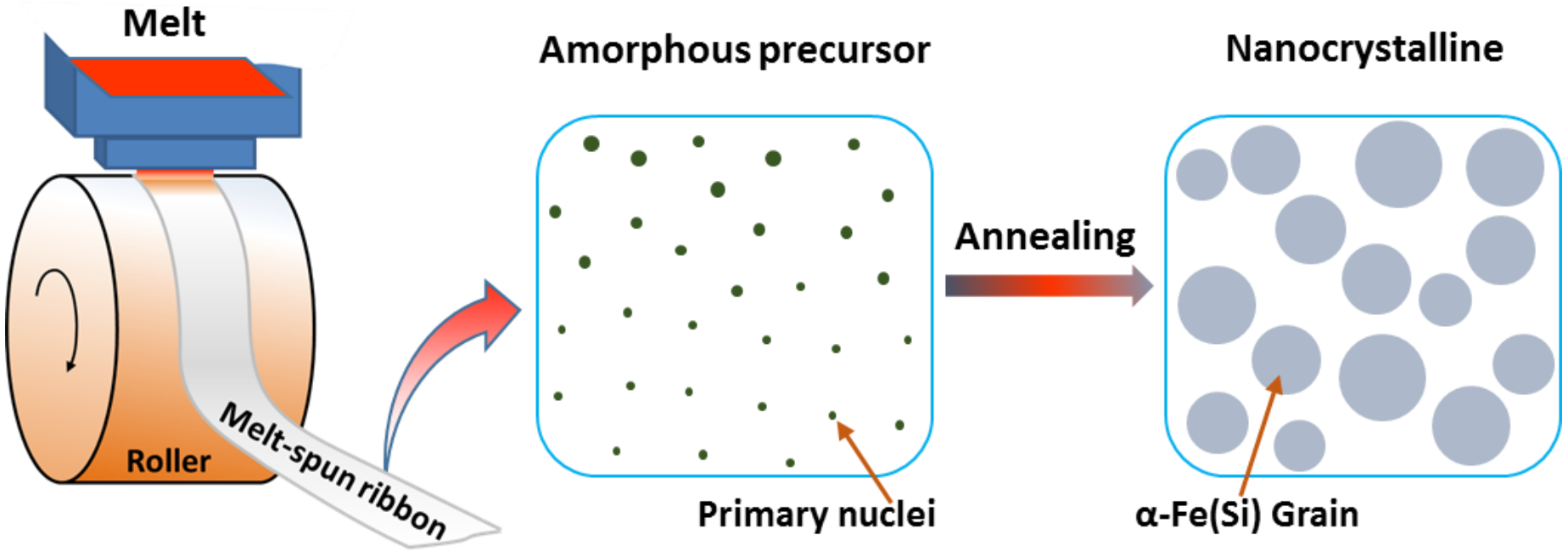

由於低非晶形成能力而造成截面均匀性較差

加Cu促进形核，改良非均匀性

3. 新型非晶成分设计：$Fe(Co)_{82-85}$ + (Si,B,C,P) + Cu

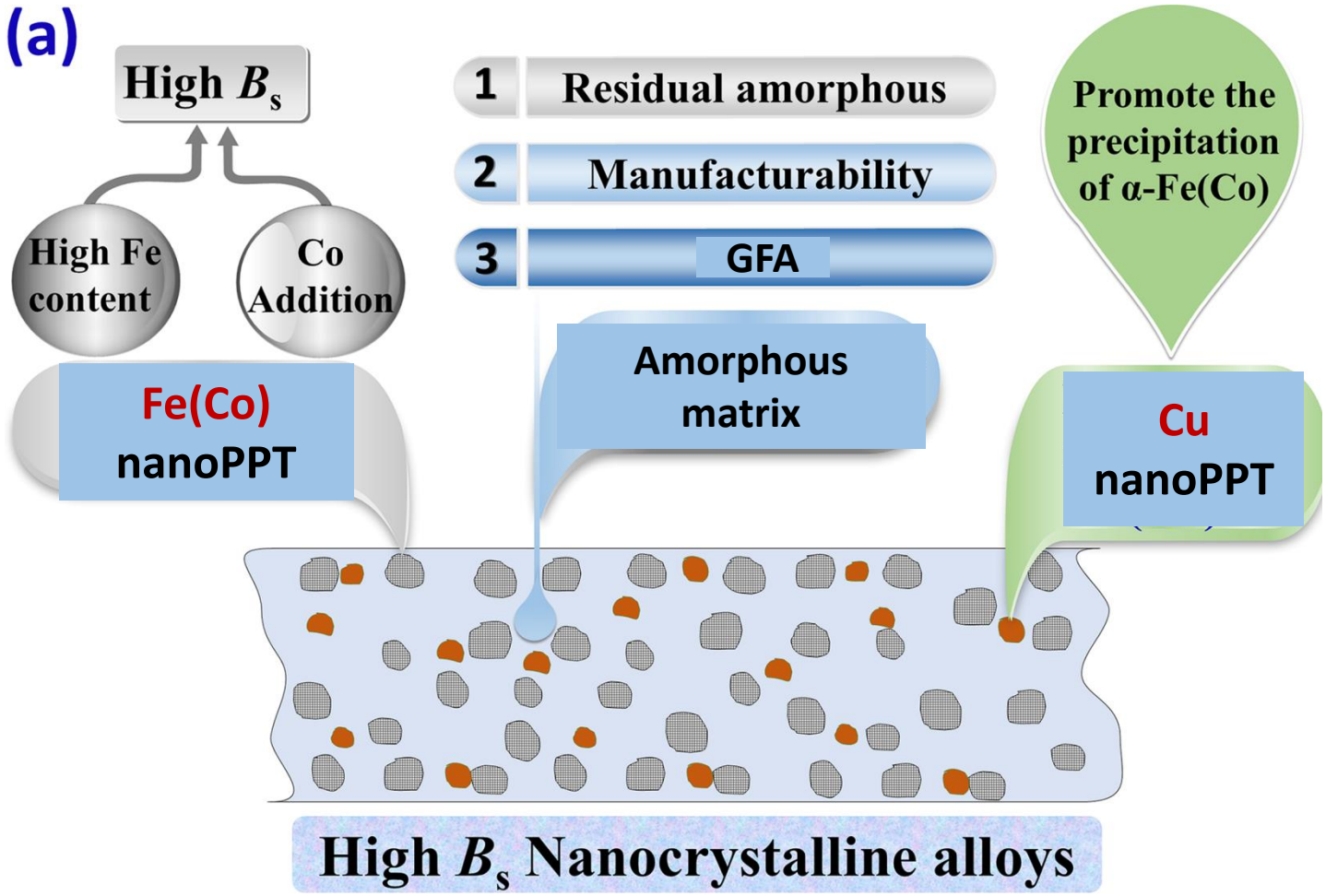

- 成功制备高Bs的纳米晶合金

4. 高Bs纳米晶合金开发：有优良磁性能

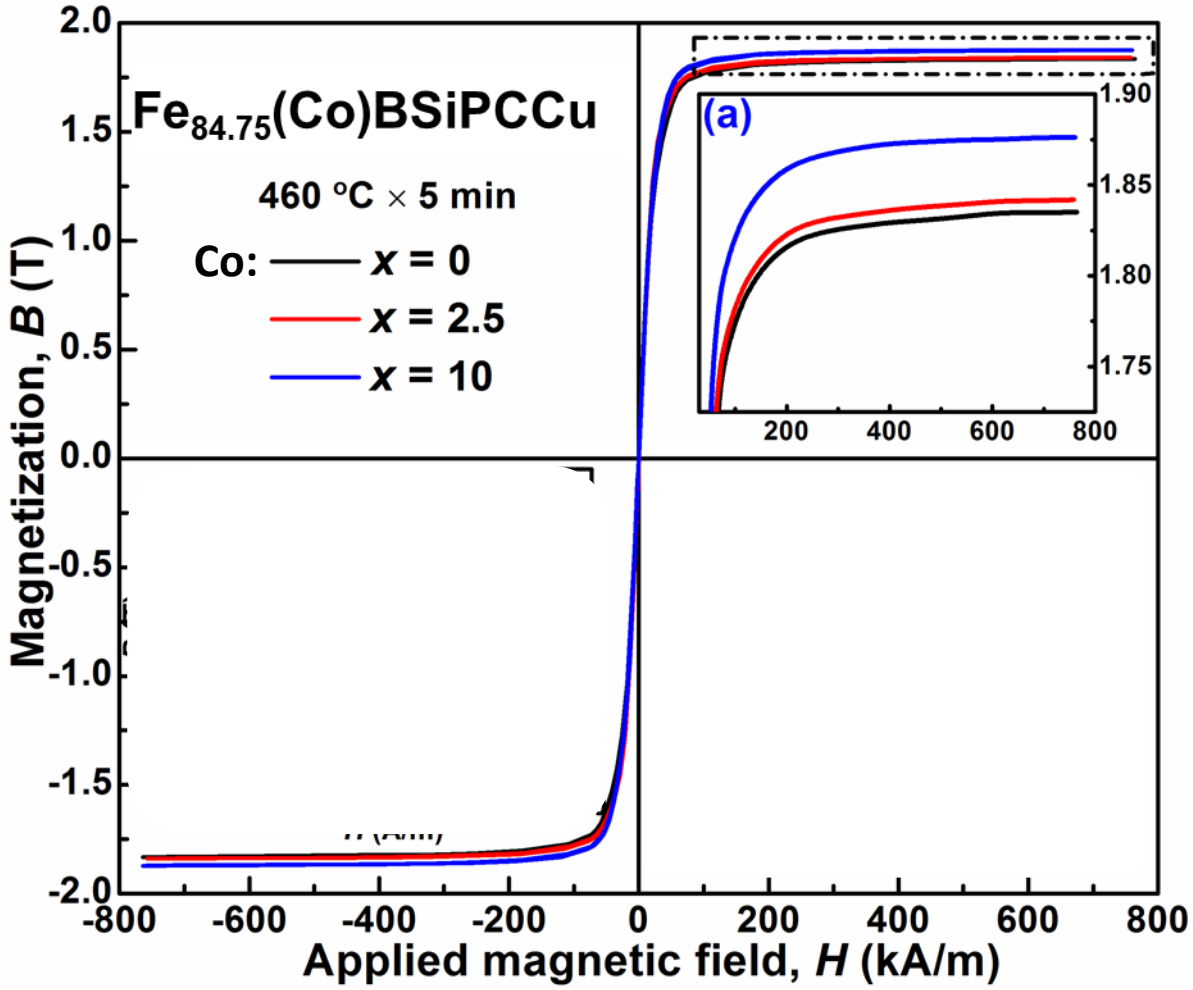

- 高 Bs > 1.83 T, 高 μe = 27,000 (低 Hc < 5 A/m)

5. 用低纯工业原料已成功制备出低價纳米晶合金

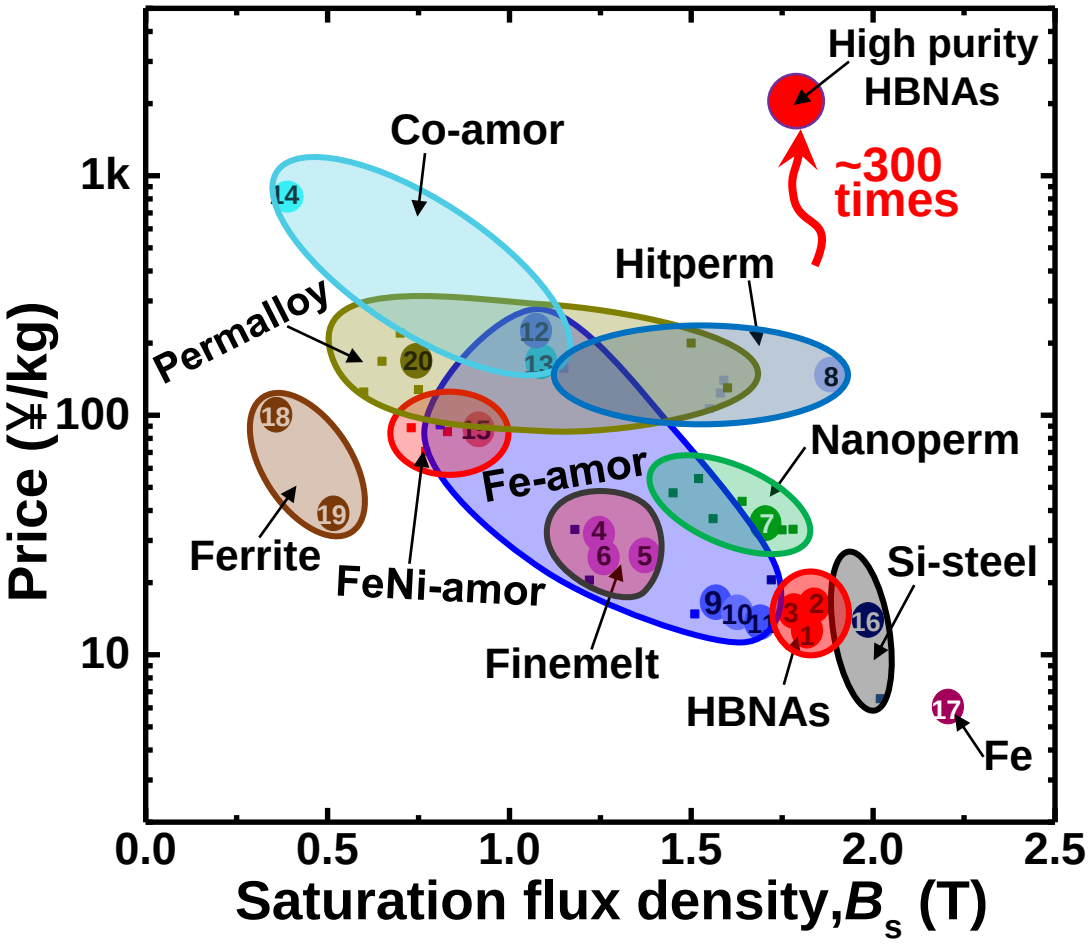

新纳米晶合金有

- 高 μe > 30,000
  (20 times higher than Si-steel)
- 成本与硅钢相当

HBNAs: High Bs Nano Alloys

- 新纳米晶合金有高性价比

结论:已經成功开发各种优质鉄基納米晶和非晶材料

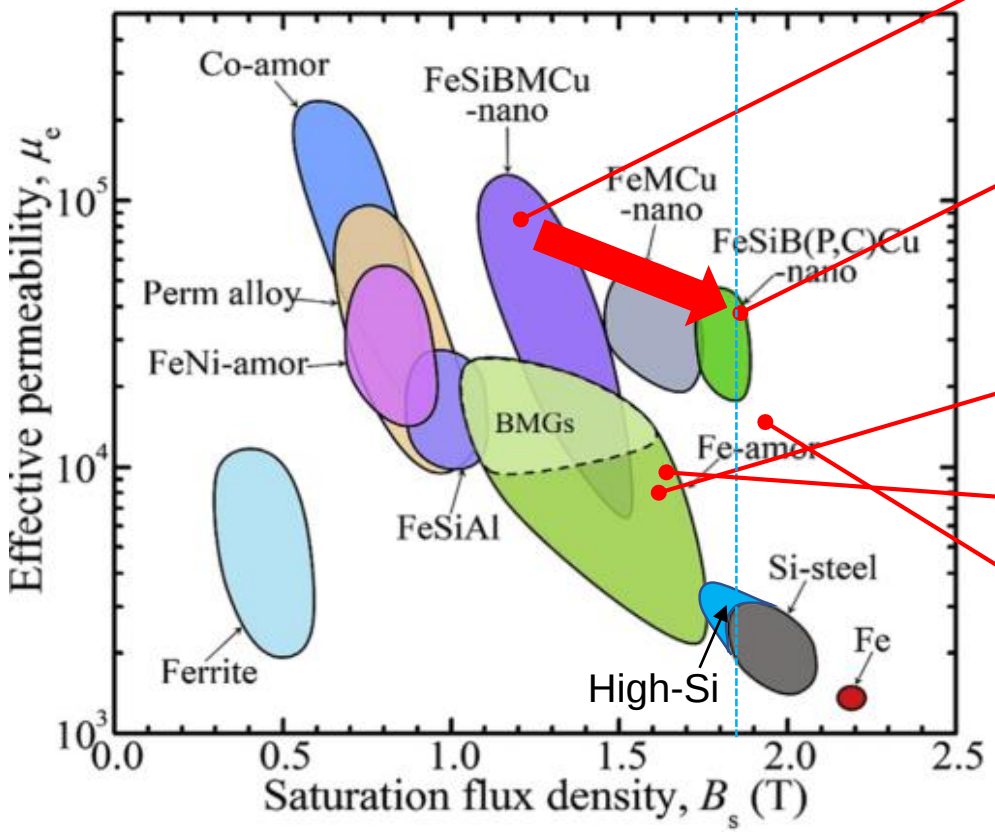

现有 纳 米 晶合金 $Fe_{73.5}SiBNbCu$
B_s = 1.24 T

$Fe_{82\text{-}85}SiBPCCu$
1.83 T

现有非晶 $Fe_{78}Si_9B_{13}$
1.56 T

高韧性FeSiBPC
1.62-1.66 T

$Fe_{67\text{-}70}Co_{15}SiBPC$
1.86 T

- 成功开发了高Bs≥1.83 T(Fe含量接近高硅硅钢),软磁性能优异的非晶和纳米晶合金
- 目前正在用工业原料制备，具有广泛的电机应用前景

但用工业原料也还有一些制造非晶带材问题

- 非晶形成能力较差的材料

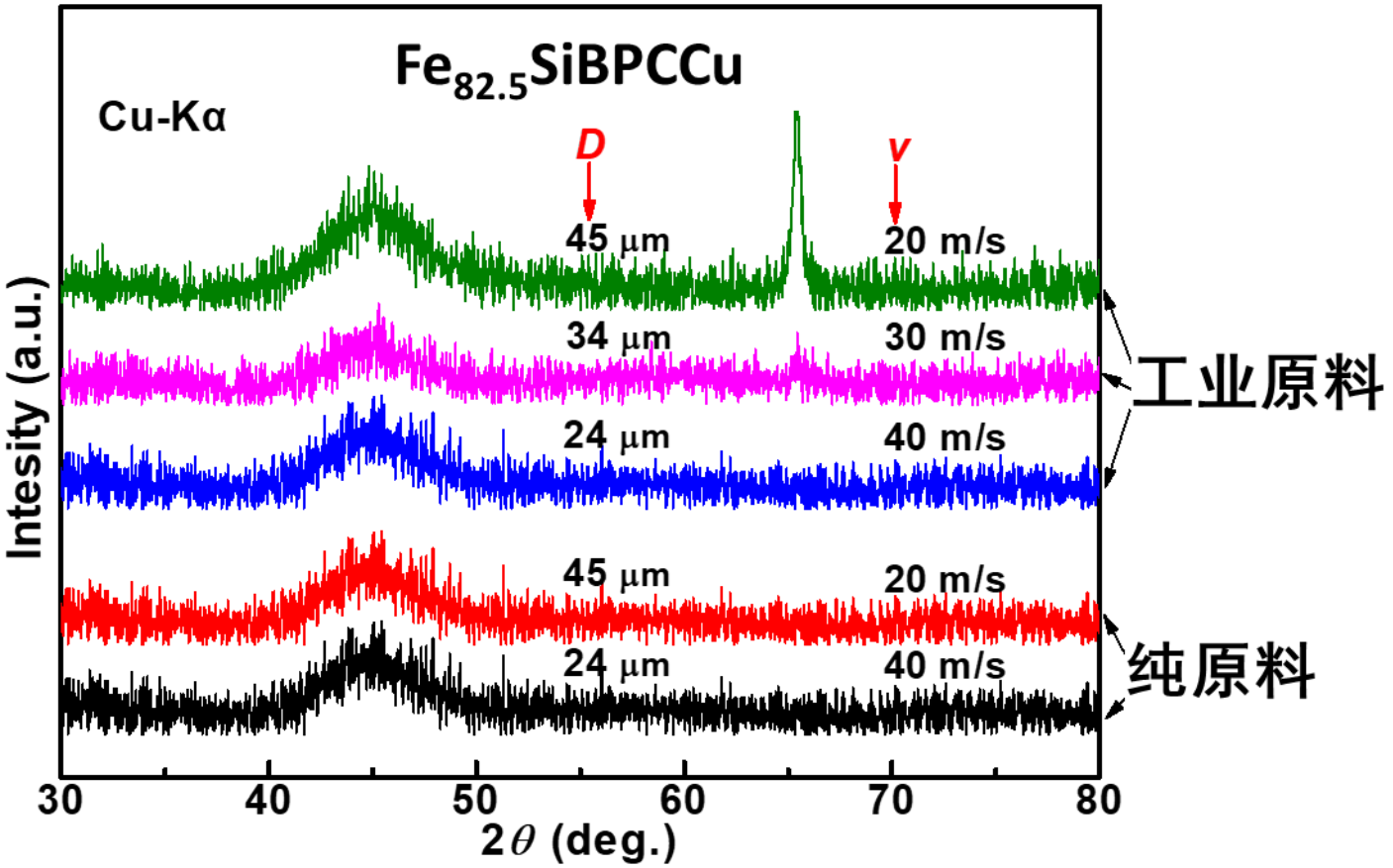

- 工业原料只能制备较薄的高Bs 非晶合金

Industrial processing of MG ribbons: Quite complex

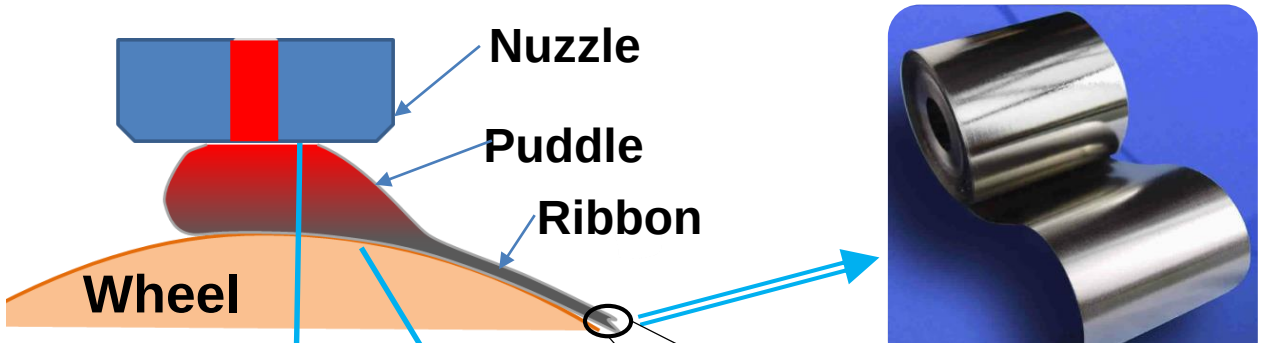

- Environmental-atmosphere effect
- Limited GFA of alloys
- Influence of material impurity
- Non-uniform microstructures
- Surface crystallization
- Pressure
- Temperature
- Wheel speed

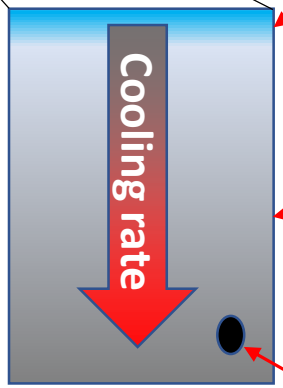

Ribbon cross section

Surface crystallization

Gradient microstructures

Impurity phases

Production of the new MG with $Fe_{83}C_1B_{11}Si_2P_3$

- $Fe_{83}C_1B_{11}Si_2P_3$: B_s = 1.67 T
- Good ductility after annealing

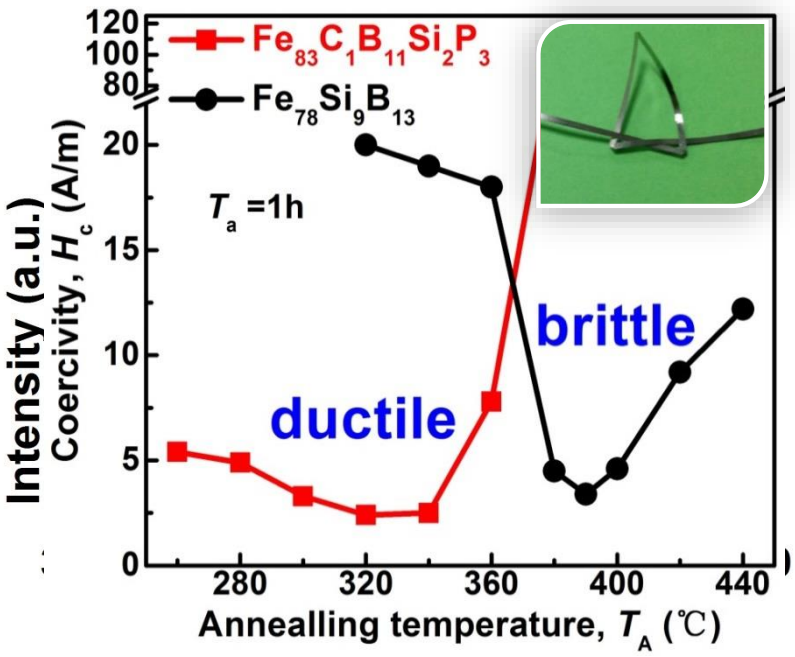

Wang, A. D., et al. (2015). J. Alloy. Compd. 630: 209-213

Industrial material: surface recrystallization

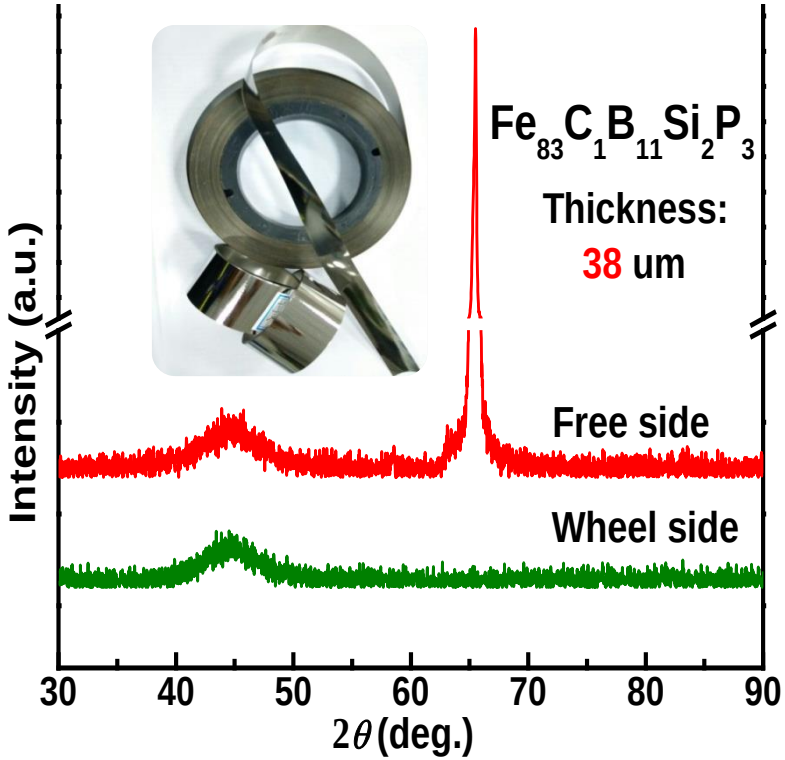

Pang, J., et al. (2017). J. Magn. Magn. Mater. 433: 35-41.

Laboratory production: ribbons are Okay

→

Industrial production: surface recrystallization (high coercivity)

Surface crystallization caused by material impurity

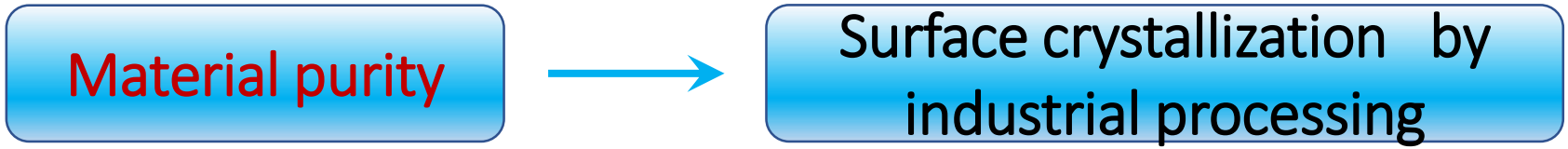

Detailed studies are thus required to resolve this surface-crystallization problem

- Detailed characterize microstructural features
- Understand impurity effects on surface crystallization
- Find feasible ways to resolve this production problem

Examination of surface crystallization by OM and SEM

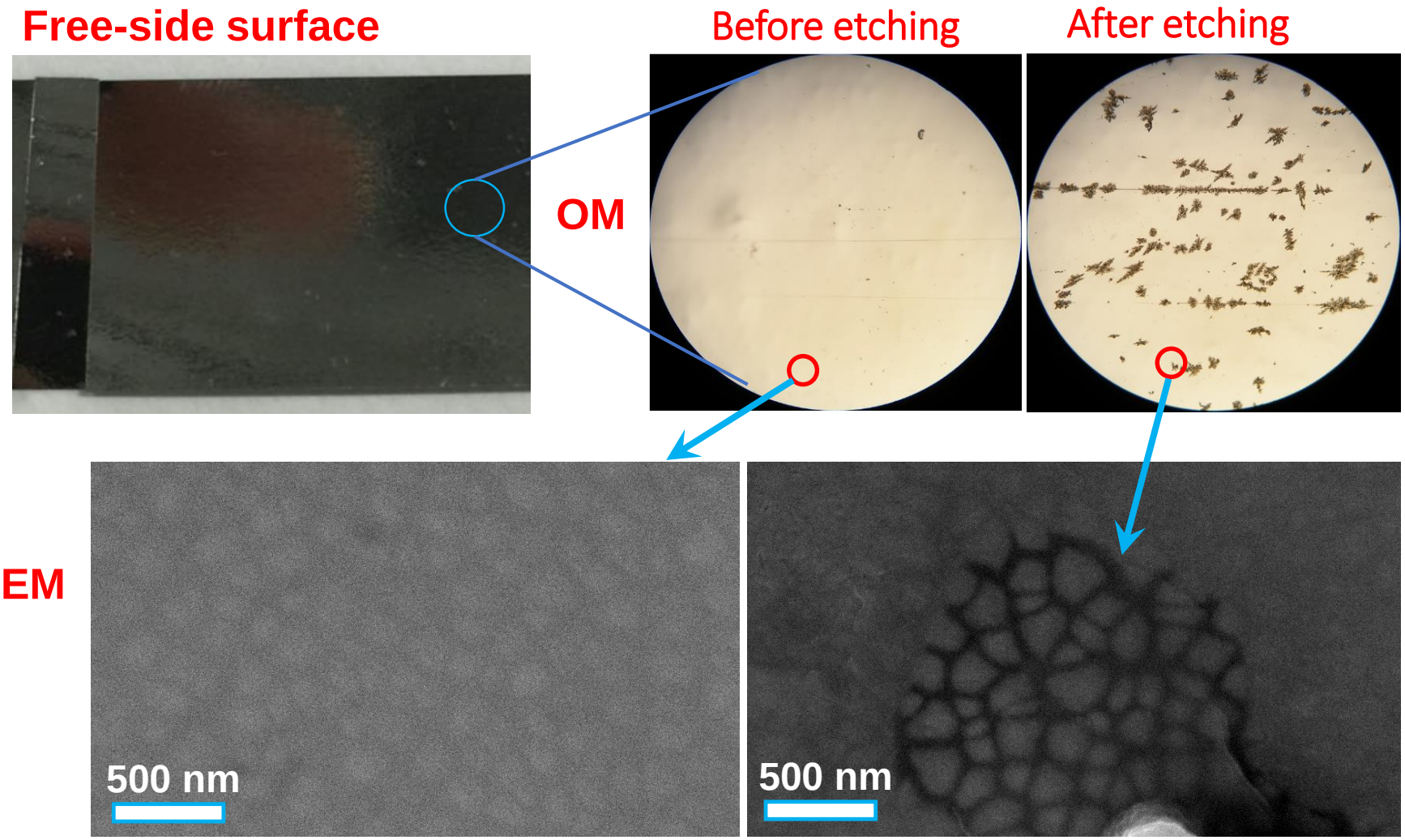

Measurement of the surface-layer thickness on ribbons

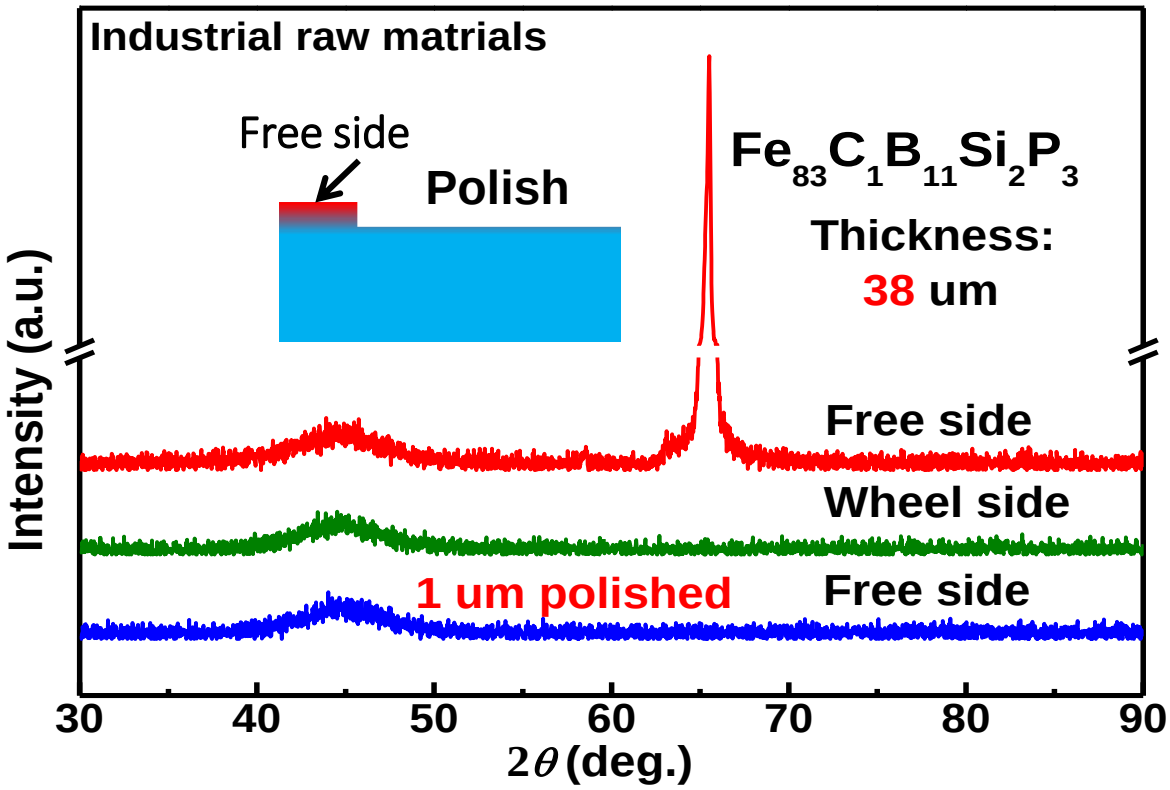

- **Surface-layer thickness: < 1 um**

Possible mechanism for forming oxide particles on surface

a) Oxides first formed on ribbon surface

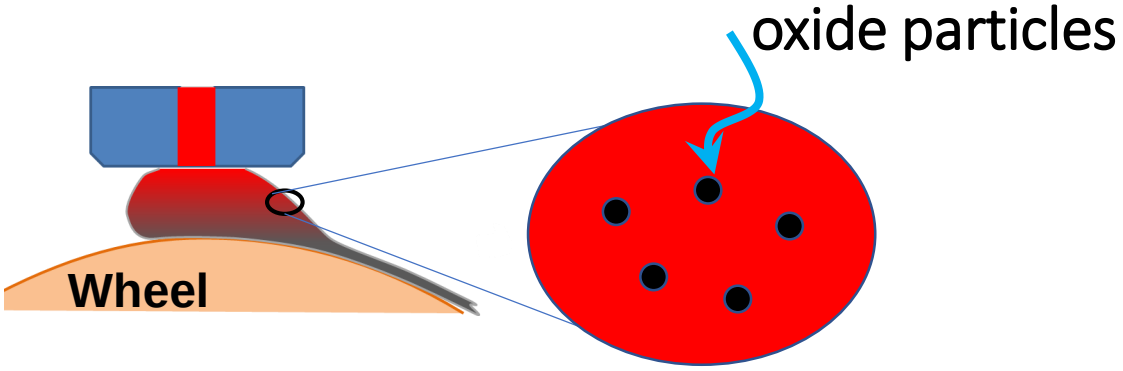

b) They then trigger formation of Fe crystals on ribbon surface